WASTE LOAD ALLOCATION SEMINAR NOTES

Prepared for

U.S. Environmental Protection Agency
Contract No. 68-01-5918

MANHATTAN COLLEGE
NEW YORK, N.Y.

WASTE LOAD ALLOCATION SEMINAR NOTES

Prepared for

U.S. Environmental Protection Agency
Contract No. 68-01-5918

MANHATTAN COLLEGE
NEW YORK, N.Y.

TABLE OF CONTENTS

Waste Load Allocation Seminar Notes

Chapter	Title	Page No.
1	Waste Load Allocation Principles	
	Principles and Issues of Waste Load Allocations	1-1
	Measures of Verification	1-26
2	Water Quality Analysis	
	One-Dimensional Time Varying Analysis of Streams and Rivers	2-1
	Time Variable Water Quality Models: Estuaries, Harbors and Off-Shore Waters	2-53
	Relationship Between Waste Load Variability and Water Quality Response	2-86
	Example of Time Variable D.O. Modeling: Upper Delaware River	2-97
	The Eutrophication Problem	2-108
	A Steady State Eutrophication Model for Lakes	2-155
	A Dynamic Model of Phytoplankton Populations in Natural Waters	2-169
	Simplified Phytoplankton Modeling for Streams	2-219
	Effect of Sinusoidal Load Variation on Stream Dissolved Oxygen Concentrations	2-246
3	Case Studies	
	The Wicomico Estuary-An Estuarine Eutrophication Example	3-1
	Examples of Sensitivity Analyses	3-36
	Rocky Fork Waste Load Allocation	3-61

TABLE OF CONTENTS (cont'd)

Chapter	Title	Page No.
4	Toxic Substances	
	Introduction and Basic Concepts	4-1
	Adsorption-Desorption	4-13
	Modeling Framework	4-29
	Lakes and Reservoirs	4-45
	Saginaw Bay-Solids and PCB Model	4-61
	Stream and River Models	4-90
	Application to PCBs in the Hudson River	4-99
	Applications - Toxic Substances in Streams	4-112
	Analysis of Completely Mixed Systems - Toxic Substances	4-135
	Ammonia Toxicity	4-160
	Toxics Concentrations in Streams	4-166
	Toxics Concentrations in Lakes	4-177
5	Waste Load Allocation Examples	
	Example Waste Load Allocation Analysis	5-1
	WLA Analysis - Initial Deficit, Benthal Demand, P-R	5-28
	A Methodology for Estimating Future Benthal Demands in Streams	5-38
6	Treatment Considerations	
	APPENDIX	
	Simplified Analytical Method for Determining NPDES Effluent Limitations for POTWs Discharging into Low-Flow Streams	A3

PRINCIPLES AND ISSUES OF WASTE LOAD ALLOCATIONS*

1. INTRODUCTION

A) Basic Principles

The central problem of water quality management is the assignment of allowable discharges to a water body so that a designated water use and quality standard is met using basic principles of cost benefit analysis. Figure 1 shows a representation of the overall waste load allocation (WLA) problem. There are several components to the problem, including the determination of desirable water use standards, the relationship between load and quality and projected conditions. It is generally not sufficient to simply make scientific engineering analysis of the effect of waste load input on water quality. The analysis framework must also include the economic impacts as well and in term must also recognize the socio-political constraints that are operative in the overall problem context. (see also Thomann, 1980).

The principle steps in the WLA process are summarized in Figure 2 as:

1) A designation of a desirable water use or uses, e.g. recreation, water supply, agriculture.
2) An evaluation of water quality criteria that will permit such uses,
3) The synthesis of the desirable water use and water quality criteria to a water quality standard promulgated by local State Interstate or Federal Agency,
4) An analysis of the cause-effect relationship between present an projected waste load inputs and water quality response through use of
   a) available field data or data from related areas and
   b) a calibrated and verified mathematical model.
   c) a simplified modeling analysis based on literature, other studies and engineering judgment
5) A sensitivity analysis and projection analysis of achieving water quality standard through various levels of waste load input,

* Robert V. Thomann

6) Determination of the "factor of safety" to be employed through, for example, a set aside of reserve waste load capacity,
7) For the residual load, an evaluation of the
   a) the individual costs to the discharges
   b) the regional cost to achieve the load and the concomitant benefits of the improved water quality standard
8) Given all of the above, a complete review of the feasibility of the designated water use and water quality standard
9) If both are satisfactory, a promulgation of the waste load allocation permitted for each discharger

A recent intent by the US EPA to provide guidance for review of advanced waste treatment illustrates several key points related to the WLA process (Federal Reg. 1980). The following definitions were offered and are generally followed throughout these notes:

1) Secondary treatment: Maximum monthly average BOD_5 and suspended solids = 30 mg/ℓ respectively, or 85% removal, if more stringent.
2) Advanced Waste Treatment (AWT): Maximum monthly average BOD_5 and suspended solids less than 10 mg/ℓ, respectively, and/or total nitrogen greater than 50% removal.
3) Advanced Secondary Treatment (AST): Intermediate between secondary and AWT.

Several factors are identified that determine the level of review of projects. The level of review, of course, implies a position on the part of the US EPA of the important issues that must be considered in a WLA.

The factors that determine the level of review are:

1) Incremental cost of the project: A capital cost of #3 million is considered as dividing line between projects requiring detailed analysis.
2) Local financial impact: The impact is considered significant if the total annual cost is greater than 1% for median income of less than $10,000, 1.5% for median income between $10,000-17,000 and 1.75% for median income greater than $17,000.

3) Inflationary impacts: The impact is considered significant if the incremental AST/AWT costs are greater than the delay cost due to an assumed inflation of 12%.

It should be noted that these factors are economic ones and reflect the concern that AST/AWT projects may have a significant economic effect and, as such, should be carefully evaluated.

The requirements for technical review include

1. Effluent limitations assessment: This assures the validity of state adopted, federally approved water quality standards and represents one level of technical review
2. Comprehensive evaluation: This evaluation may include
   a) effluent limitations assessment
   b) review of facility planning
   c) additional water quality analysis such as
      i) evaluation of established water quality standard
      ii) beneficial use designations
      iii) evaluation of water quality criteria

These requirements are expressions of the general WLA process shown in Figure 1.

B) Steps in Allocation Computation

In the determination of an allowable discharge, the principle framework is given by Figure 2. Within that framework, it is assumed that a calibrated and verified water quality model is available. At the very least, an assessment of the given river condition and a choice of modeling framework have been made. The steps of the WLA process at another level of detail then proceed as shown in Figure 3.

As shown in the steps of this Figure, there are several points at which iterations are required to provide a defensible WLA. For example, step #4, the determination of design conditions including flow and parameters should be re-evaluated after a preliminary allocation has been made (step #18). It should also be noted that the specifications or projections of flow and parameter conditions under the design event (step #4) is a most critical step and is a blend of engineering judgement and sensitivity analysis. In the steps outlined in Figure 3, there is no specific step included for integrating the cost/benefit factors of the allocation.

Aside from the broad guidance mentioned earlier and aside from more elaborate optimization schemes, it is assumed in Figure 3 that the final WLA is worth accomplishing in the light of the promulgated water quality standard.

From a broad perspective, there are several classes of issues resident in the WLA process as follows:

1) Water Quality Issues
2) Cost-Benefit Issues
3) Issues of evaluation of alternate control options

Some of the principal aspects of these issues are discussed below.

II. WATER QUALITY ISSUES

A. Introduction

Although Figure 1 shows schematically the WLA problem, there are several other issues that must be addressed. The basic question in WLA is "What is the permissible equitable discharge of residuals that will not exceed a water quality standard." Additional relevant questions then are:

1) What does "permissible" mean? Is "permissible" in terms of maximum daily load, 7 day average load or 30 day average load?
2) What does "exceed" mean? Does it mean "never" or 95% of the time and for all locations?
3) What are the design conditions to be used for the analysis?
4) How credible is the water quality model projection of expected responses due to the WLA, i.e. what is the "accuracy" of the model calculations and how should the level of the analysis be reflected, if at all, in the WLA?

From a water quality point of view, the basic relationship between waste load input and resulting response is given by a mathematical model of the water system. The development and applications of such a water quality model in the specific context of a waste load allocation involves a variety of considerations including the specifications of parameters and model conditions. However, the preceding questions raise some additional issues that are discussed below.

The water quality issued raised by these questions involve the following considerations:

1) Magnitude and temporal variations in waste loads
2) Specification of design hydrological conditions for the water system including considerations of the temporal variations in river flows
3) Water quality standard specifications including the temporal variability of water quality
4) Modeling relationships between temporal variations in waste load, flow and quality
5) Measures of credibility and performance of the water quality model

B. Waste Loads and Variability

1. Introduction. It should be recognized in any WLA analysis that effluents from waste treatment plants can vary significantly over time. Although average values of various constituents can be specified and can often be used in a WLA, the temporal variability of the load needs to be incorporated either directly or indirectly into the analysis. A variety of sources provide estimates of the average concentrations of sewage and the expected concentrations after various treatment steps (e.g. Metcalf and Eddy, 1972; Thomann, 1972; Mueller and Anderson, 1979). Some examples of temporal variations in effluent quality are shown in Figure 4.

As indicated in Figure 4(a) and (b), there may be significant diurnal variation in both flow and quality constituent, in this case, ammonia. In streams that are dominated by the effluent, these variations may be reflected in downstream water quality. Figure 4(c) shows the variation in BOD loading (lb/day) from a primary effluent. Inspection and also analysis of this time series indicates a significant seven day oscillation or periodicity in the effluent. Figure 4(d) shows the variation in the final effluent BOD loading from an activated sludge plant and indicates a strong seasonal increase in load. In this particular case, the marked increase in the late summer is due to an additional load from a seasonal canning industry that discharges to the municipal system. These examples indicate the variability that is normally present in all effluents and that should be recognized in a WLA.

2. Analysis of Variations in Load

a. Basic statistics - Several simple measures can be used to qualtify temporal load variations. These measures include

i) Central tendency measures - e.g. mean, median, geometric mean

ii) Dispersion measures - e.g. standard deviation, variance, coefficient of variation

The mean concentration $\bar{c}$ if given by

$$\bar{c} = \frac{\Sigma c_i}{N} \tag{1}$$

where c_i is the individual concentration values and N is the number of data points. The geometric mean, representing the mean of the logarithms of the data is sometimes useful where the underlying distribution of the data is log normal. The geometric mean is given by

$$\bar{c}_g = \frac{\Pi c_i}{N} \tag{2}$$

The estimate of the variance of the concentration s_c^2 is

$$s_c^2 = \frac{\Sigma(c_i - \bar{c})^2}{N - 1} \tag{3}$$

and the standard deviation s_c is then easily obtained. The coefficient of variation is a measure of the variation relative to the mean and is given by

$$cv = \frac{s_c}{\bar{c}} \tag{4}$$

Table 1 (Thomann, 1970) shows some of these measures of variability. The data from this very limited sample show the tendency for the coefficient of variation to increase with increasing degrees of treatment. It can also be noted that the cv of the flow is significantly less than that of the BOD concentration.

TABLE 1. STATISTICAL VARIATION FOR EIGHT PLANTS
(From Thomann, 1970)

Plant Number	Mean flow, in millions of gallons per day	CV flow[a]	Mean influent BOD, in milligrams per liter[b]	CV influent BOD	Mean primary effluent BOD, in milligrams per liter	CV primary effluent BOD	Mean secondary effluent BOD, in milligrams per liter	CV secondary effluent BOD, in milligrams per liter	Remarks
1	2.5	0.21	183	0.26	128	0.21	23	0.50	N.J. Sec. Plt.-Little industrial waste
2	6.5	0.32	125	0.27	100	0.23	14	0.82	Conn. Sec. Plt.-Little industrial waste
3	17.5	0.17	275	0.27	205	0.27	35	1.07	Ill. Sec. Plt.-Moderate industry; operating problems
4	60.6	0.19	453	0.26	319	0.39	59	0.79	Cal. Sec. Plt.-Heavy industry; seasonal canning load
5	100.7	0.15	180	0.25	94	0.28	-	-	Penn. Pri. Plt.-Moderate to heavy industrial waste
6	102.2	0.21	260	0.33	202	0.34	-	-	Ohio Pri. Plt.-Moderate to heavy industrial waste
7	107.1	0.27	163	0.30	116	0.27	-	-	Penn. Pri. Plt.-Moderate industrial waste
8	140.2	0.14	215	0.17	-	-	57	0.22	Penn. Sec. Plt.-Moderate to heavy industrial waste

[a] CV = coefficient of variation = $s/\bar{x}$.

[b] All BOD values for 5-day period.

b. Frequency distributions of effluent quality - Another representation of the variation in effluent quality can be obtained by plotting a frequency distribution of the concentration or flow. This is obtained by simply arranging the data in ascending order and assigning an estimated frequency of m/N + 1 where m is the number representing the position of the ranked concentration and N is the total number of data points. A distribution plot of concentration vs frequency scaled to a normal density function can then be prepared. Figure 5(a) shows a typical distribution, in this case for the Westernport Treatment Plant located in the North Branch of the Potomac River at Luke, Md. The data are for one month of daily composited samples. From the frequency distribution, one can determine the median effluent concentration (50%) as well as the 5% exceedance level. As shown, 95% of the time the effluent concentration is equal to or less than about 70 mg BOD/ℓ for this plant. Therefore, 5% of the time the concentration is expected to be greater than 70 mg BOD/ℓ.

Figure 5(b) shows frequency distributions for different averaging of the effluent BOD i.e., 7 day average and 30 day average. These averaging periods are often of use in assigning load allocations for systems that are not responsive to daily oscillations in load. Estuaries, large deep rivers and lakes would be such water bodies.

If the 95th percentile is used as a measure of the upper bound or maximum concentration, then relationships can be derived between this upper bound and the mean values. This has been done by Roper et al. (1979) for 12 months of operational data gathered from 10 secondary and 9 AWT plants. Only secondary plants that had mean effluent BOD_5 of 30 mg/ℓ or less were included in order to provide an analysis consistent with "typical" secondary effluent. Figure 6 from their work is particularly useful. This Figure relates the effluent arithmetic mean BOD_5 or total suspended solids (TSS) to the equivalent 95th percentile levels. Therefore, if the long term design concentration of BOD_5 is 10 mg/ℓ then

a) monthly average 95th percentile concentration is 17 mg/ℓ

b) weekly average 95th percentile concentration is 19 mg/ℓ

and c) daily average 95th percentile concentration is 22.5 mg/ℓ

Note that the 95th percentile daily level is more than twice the long term average.

In a WLA, one would work backward from the water quality analysis of the stream to obtain the 95% concentration level. A typical requirement might then be "the effluent concentration shall not exceed 20 mg/ℓ BOD_5 more than 5% of the time based on a monthly average" (Roper et al. 1979 provides a procedure for estimating other percentile concentrations). This would make the notion of a "maximum" monthly average as previously defined more rigorous. In this case, "maximum" is considered to be defined by the 95% level. Waste load variability must be recognized and incorporated in a WLA analysis in order to properly incorporate stream quality variability around given water quality standards.

2. Intermittent Loads

Loading for intermittent sources depends on a number of factors that may influence both the flow and the concentration. The flow from urban runoff is usually highly transient resulting from variable precipitation, so at times there is no load being discharged. For discharges from combined sewers, therefore, several input loads can be estimated:

1. Equivalent annual (or other interval) loading rate (comparable to continuous load)
2. Average load discharged per event of overflow
3. Distribution of load within an event of overflow.

Figure 7 shows the variability of intermittent rainfall events, volume of precipitation, resulting runoff and loading. Data are usually available on hourly rainfall or daily totals. Note that several quantities are of importance: the volume of precipitation, the duration of the event and the interval between events. The seasonal variation of rainfall should be recognized since the variation in rainfall intensity may vary by significant amounts throughout the year.

A statistical procedure has been developed (Di Toro, 1978) that allows one to make an estimate of the mean load and the expected high load events with a given probability. The procedure requires estimates of the following for each stream event as shown in Table 2.

TABLE 2. EVENTS FOR STATISTICAL LOAD ESTIMATION

Parameter	For each storm	Mean	Coef. of variation[a]
Intensity	i	I	ν_i
Duration	d	D	ν_D
Time Between Storms	δ	Δ	ν_s

[a] Coef. of variation = standard deviation/mean

These statistics can be computed for a given length of record such as across all months of the year or within an entire year. Now it can be shown (Di Toro, 1978) that the statistical distribution of the rainfall statistics have a gamma probability density function. Therefore, one can estimate the high load events if the coefficient of variation of precipitation is known. Finally, it is assumed that this coefficient of variation applies also to the runoff resulting from the events.

The simplest estimate of the runoff flow $Q_R[L^3/T]$ is from the so-called Rational formula:

$$Q_R = CIA$$

where I is the rainfall rate (L/T], A is the area over which the runoff will occur, $[L^2]$, and C is the runoff coefficient. The value of C depends on land uses, population density and degree of imperviousness, and ranges from 0.1-0.3 for population densities of about 1 person/acre (rural) to 0.7-0.9 for heavy industrial and commercial areas with densities greater than 50 persons/acre. Note that if I is in/hr, A in acres then Q is in acre-in/hr which is equal to about 1 cfs. Therefore Q(cfs) = CI(in/hr)A(acres)

The mean load per overflow event is given by (Di Toro, 1978):

$$W_R = \bar{c}\ Q_r$$

where c is the average concentration during the event and Q_r is the flow during the event; assuming that $\bar{c}$ and Q do not depend on each other.

Table 3 shows the multiples of W_R that are expected to occur with a given frequency for various values of the coefficient of variation of the rainfall.

TABLE 3. FREQUENCY OF OCCURRENCE OF LOAD FROM INTERMITTENT SOURCES

	Multiples of W_R		
Rainfall Intensity	% of Events with Load ≥ Than Value Shown		
Coef. of Variation	50	10	5
0.5	0.9	1.3	1.7
1.0	0.5	2.4	3.2
1.5	0.3	2.5	3.7
3.0	0.1	2.6	5.2

Using Table 3 then, if the coefficient of variation for a given location is 1.5, then 50% of the events would be expected to have a load equal to or less than

0.3 W_R, 10% of the events would have loads $\geq$ 2.5 W_R and 5% of events would yield loads of $\geq$ 3.7 W_R. In order to convert the % frequency (a relative probability) to number of events, the average number of storms is needed and can be estimated from

$$\bar{N} = T/\Delta$$

where $\bar{N}$ = average number of storms and T is the length of period being used. With $\bar{N}$, the % frequency can be converted to number of events. For example, suppose Δ = 72 hrs (i.e. 3 days between storms), then $\bar{N}$ = 120 events for T = 1 year. A 5% frequency then corresponds to about 18 events in a year where the load would be $\geq$ 3.7 times the mean load.

The long term average loading rate can be estimated from

$$W_A = \frac{W_R D}{\Delta}$$

where D is the average duration of storms [T] and Δ is the average time between storms [T]. One should have at least 5 years of rain gage data to estimate these parameters.

C. Water Quality Variability

A number of water quality standards include the specification of an allowable frequency of occurrence and are usually specified under a defined environmental condition, such as the minimum 7 day average flow once in 10 years. The scientific and engineering basis for these specifications should always be subject to re-evaluation under given situations of waste load allocations.

Examples of time variable water quality standards include

1) Fecal coliform bacteria levels not to exceed a geometric mean of 1000 MPN/100 ml and not greater than 2000 MPN/100 ml in more than 10% of samples
2) Dissolved oxygen levels to be above 5 mg/ℓ "at all times"
3) Dissolved oxygen levels to be above 5 mg/ℓ for at least 18 hours of the day

It is important to examine the variation of in-stream water quality variables to evaluate the expected ranges of that variable under specific environmental conditions. Emphasis will be placed on dissolved oxygen because of the greater availability of data for that variable.

Variability in water quality is of particular importance in the evaluation of the feasibility of criteria and associated standards. The basic mathematical modeling frameworks for waste load allocations usually do not include the many mechanisms that may give rise to water quality fluctuations at a given location and over a given period of time. In general water quality variations can be divided into three broad categories:

a) Variability resulting from direct variability in waste load input (see preceding discussion)

b) Variability caused by indirect effects from external inputs. For DO, as an example, this would include diurnal DO variations resulting from phytoplankton which in turn may have been stimulated by nutrient discharges.

c) "Background" variability representing all other random or quasi-random influences on water quality

Deterministic time variable models in water quality permit the estimation of at least some aspects of the first two categories and are discussed in the Water Quality Modeling section of these notes. Background variability however involves other phenomena and is discussed further here.

1. Background variability

Background variability is the random variation in water quality due to factors that are not included in a deterministic modeling framework. This variability is usually associated with random oscillations that are due to such phenomena as

1) local velocity and temperature variations

2) random variations in meteorological variables such as solar radiation from hour to hour and day to day

3) random variations in ecosystem behavior such as photosynthesis and respiration by aquatic plants

4) variation due to sampling techniques such as grab samples composite sampling, sampling of water parcels

Most water quality models do not include these phenomena directly. Time variable features usually include the more or less regular seasonal variations in water temperature and solar radiation and the more or less regular diurnal variations due to algal photosynthesis. Although it is possible to construct models that incorporate random variations similar to those des-

cribed, operationally such model frameworks are difficult to understand and implement. As a consequence, the notion of "background" variability is introduced in an attempt to incorporate some of the above mentioned random variations. Figures 8 and 9 illustrate these variations for the upper Delaware River (Hydroscience, 1975). The first figure is an interesting example of two stations having the same monthly mean DO of 7.7 mg/ℓ but with variability (as measured by the standard deviation) differing by a factor of 2. The increasing variability for the upstream station at Easton, Pa. to the downstream station is shown by the frequency histograms. Figure 9 shows a more detailed analysis of the July 1969 Trenton data and illustrates how one can interpret and utilize available data on water quality variability. As shown, when the average daily dissolved oxygen is high the diurnal amplitude is high, when at the lower end of the daily average distribution, diurnal amplitude is significantly decreased. This, again, probably reflects the fact that the daily average decreases as a result of changes in the daily weather and hydrological patterns, which in turn affects the diurnal amplitude.

In summary, the following estimates for Trenton (the more critical area for the data shown) were derived from the above analysis:

a) standard deviation of day-to-day average daily dissolved oxygen = 0.9 mg/l;

b) average diurnal amplitude during summer months = 1.5 mg/l

c) diurnal amplitude at 5% frequency level - 0.8 mg/l;

d) diurnal amplitude at 5% frequency level = 50% of the mean amplitude.

The procedure, then, for combining the statistical analysis with a time-variable water quality model to estimate future water quality conditions during summer months is:

1. time-variable model results give mean daily dissolved oxygen diurnal amplitude under future loading conditions and different temperature and flow conditions;

2. mean daily dissolved oxygen minus 2(0.9) equals the value of average daily dissolved oxygen at Trenton which will be exceeded 95% of the time (daily dissolved oxygen will be less 5% of the time).

3. if no change in dissolved oxygen diurnal amplitude is estimated, then the minimum dissolved oxygen value is estimated to be equal to or less than $[[\overline{DO} - 2(0.9)] - 0.8]$ mg/l for 5% of the time,

4. if a change in the average diurnal amplitude is estimated (as for example, if the aquatic plants increase in biomass) then the 5% value of the diurnal amplitude is taken at 50% of the estimated increased diurnal fluctuation,

For example:

Predicted average daily dissolved oxygen = 8.0 mg/l. Therefore, the daily average at Trenton is $\leq$ 8-2(0.9) $\leq$ 6.2 mg/l for 5% of the days in the month

For no predicted change in diurnal amplitude: The minimum daily value at Trenton is $\leq$ 6.2 - 0.8 $\leq$ 5.4 mg/l 5% of the time.

If the diurnal amplitude is estimated to increase to 3.0 mg/l, the minimum daily value at Trenton is $\leq$ 6.2 - 0.5(3) $\leq$ 4.7 mg/l, 5% of the time.

This example illustrates the general procedure for utilizing available time series data to estimate the percent of time that a particular water quality variable (e.g. DO) would be expected to be below a certain value.

REFERENCES

Federal Register. 1980. Construction grants program; intent to issue revised guidance concerning review of advanced treatment project; request for comments. Vol. 45, No. 121, July 20, pp. 41890-41894.

Hydroscience, Inc. 1975. Time variable water quality analyses and related studies of the Upper Delaware River - Port Lewis to Trenton. Prepared for Del. River Basin Comm., West Trenton, N.J., 164 pp. + Append.

Metcalf and Eddy. 1972. Wastewater engineering, collection, treatment, disposal. McGraw-Hill Book Co., N.Y., N.Y. 782 pp.

Mueller, J.A. and A. Anderson. Waste load inputs into marine waters. Draft prepared for NOAA.

Randtke, S.J. and P.L. McCarty. 1977. Variations in nitrogen and organics in wastewaters. Jour. Env. Eng. Div. ASCE, EE4:539-550.

Roper, R.E. Jr., R.D. Dickey, S. Marman, S.W. Kim, R.W. Yandt. 1979. Design effluent quality. Jour. Env. Eng. Div. ASCE, EE2:309-321.

Thomann, R.V. 1980. Principles of waste load allocation. Notes from First EPA Seminar Series, 1980-81. Manhattan College, Bronx, N.Y., 14 pp.

Thomann, R.V. 1972. Systems analysis and water quality management. McGraw-Hill Book Co., N.Y., N.Y., 22 pp.

Thomann, R.V. 1970. Variability of waste treatment plant performance. Jour. San. Engr. Div., ASCE, SA3:819-837.

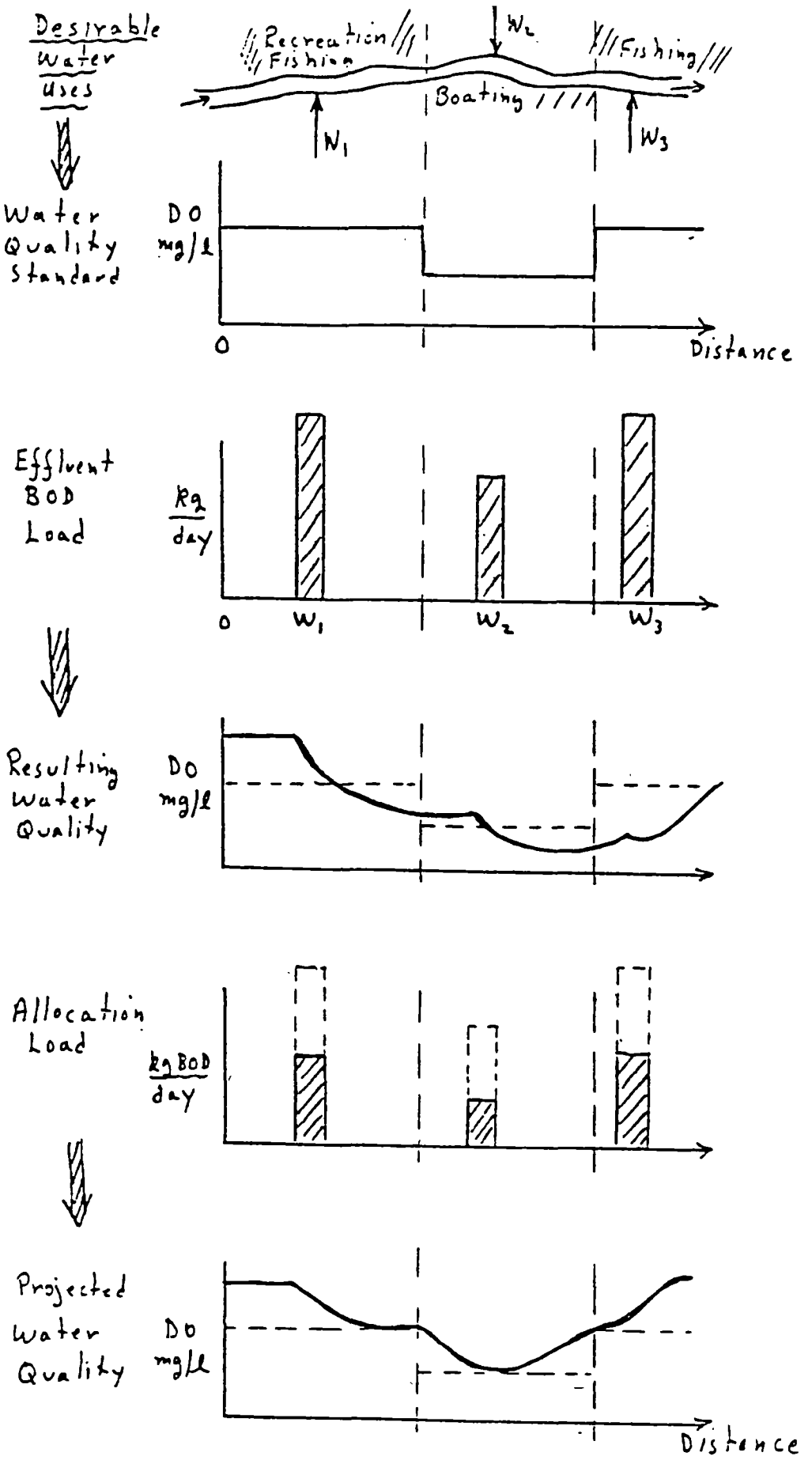

Figure 1. Representation of waste load allocation problem.

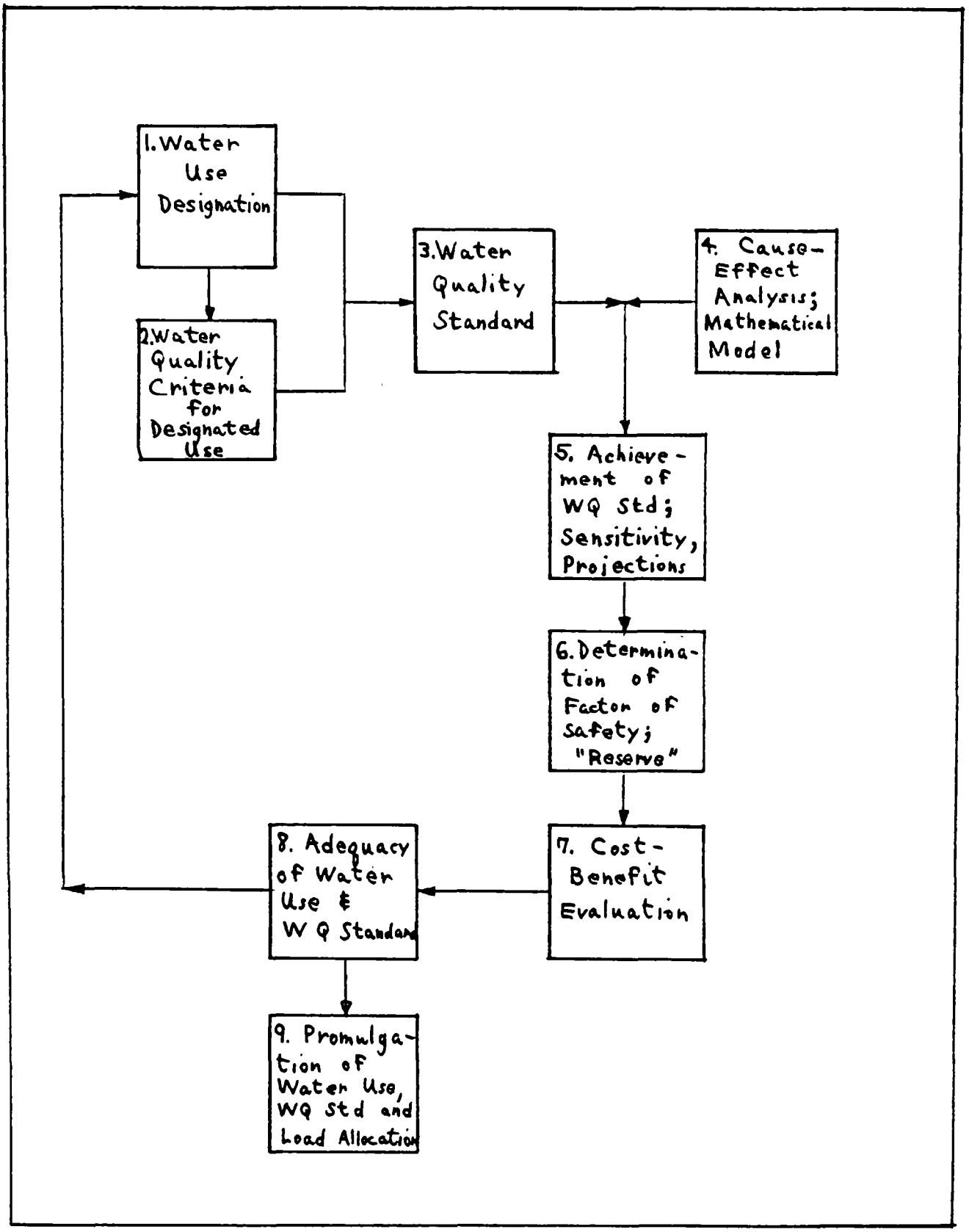

FIG. 2 Principal Steps in Waste Load Allocation Process

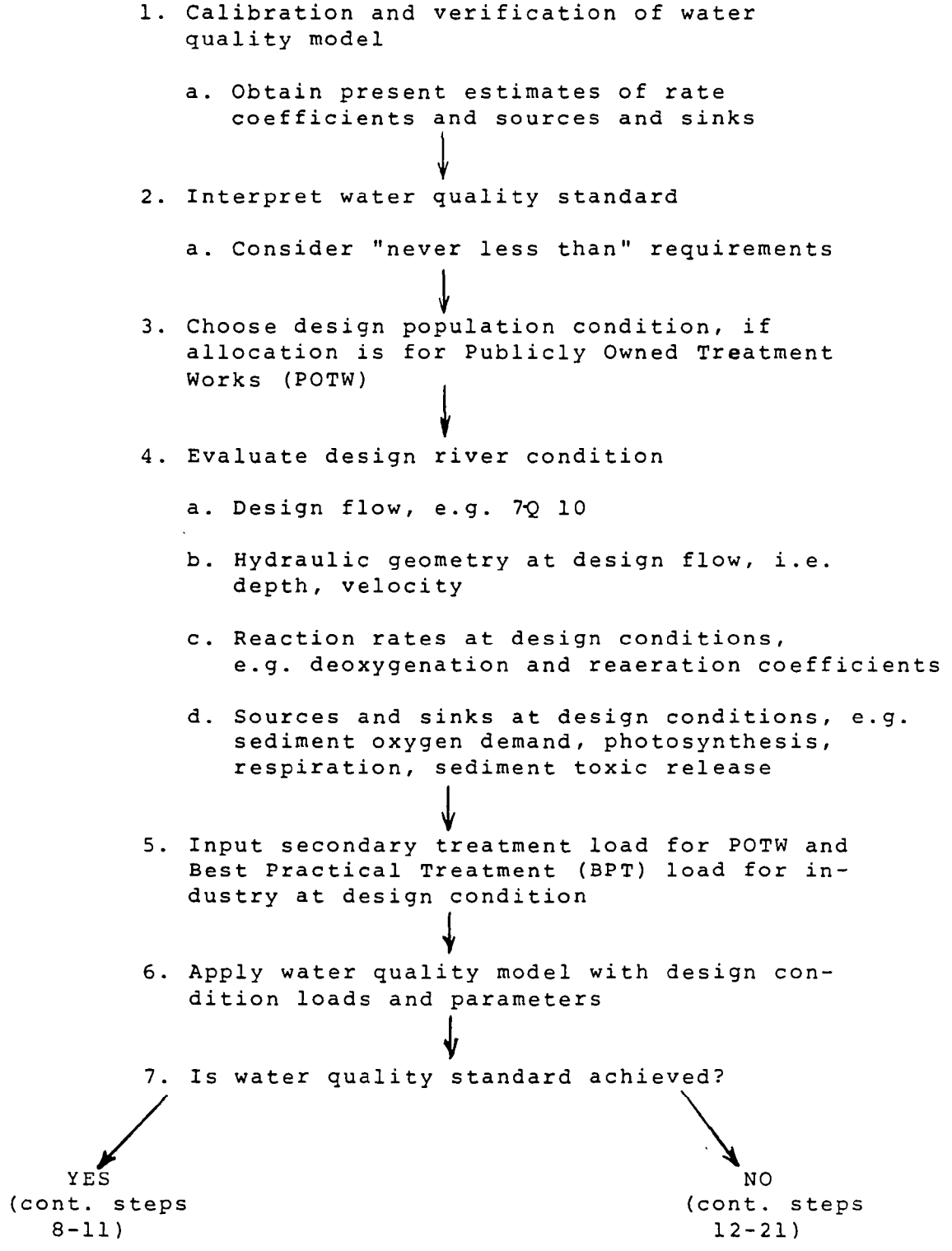

Figure 3. Steps in WLA Process

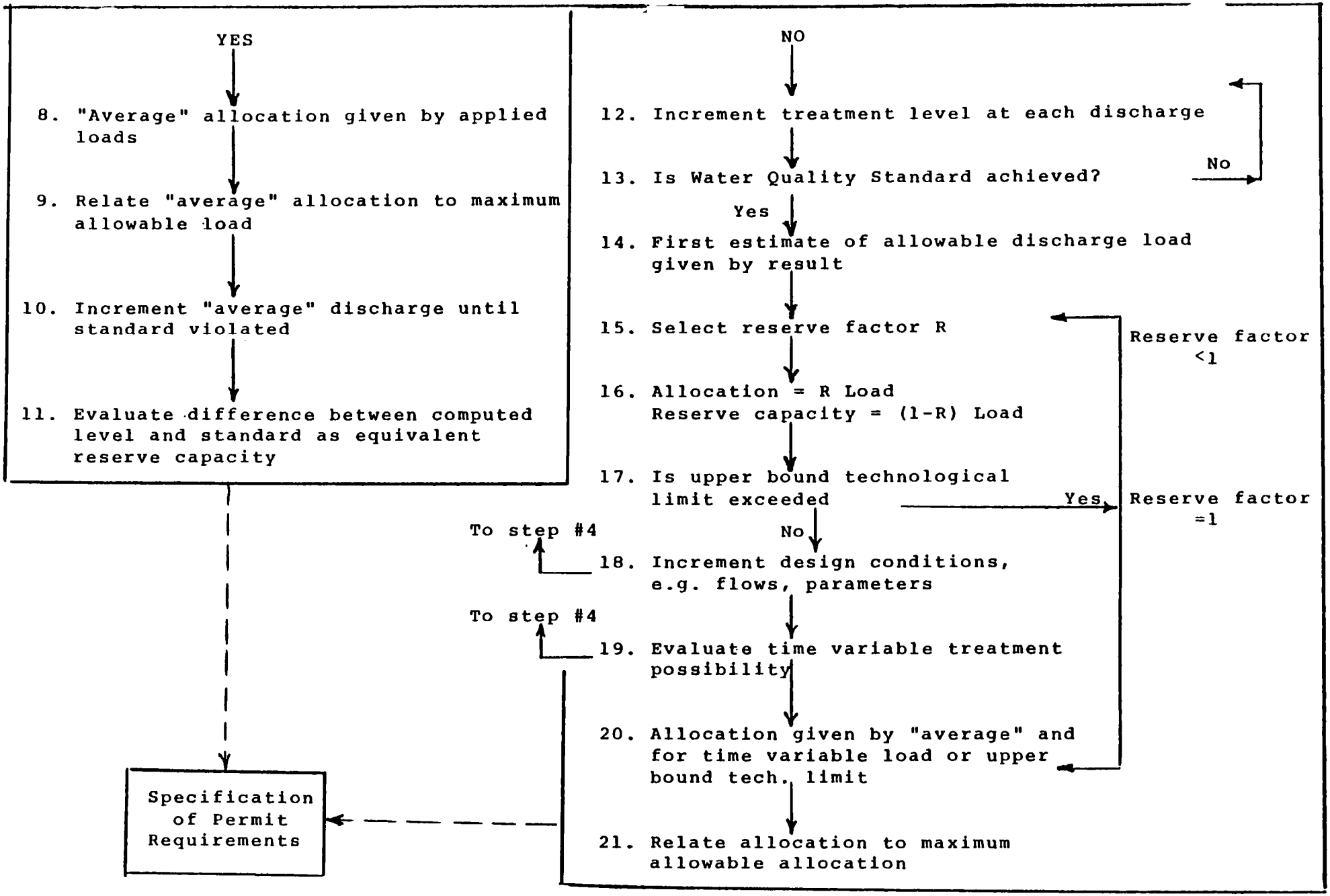

Figure 3. (continued) Steps in WLA Process

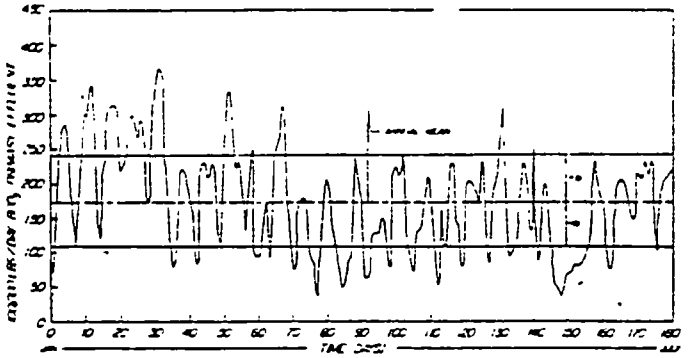

(c)

TIME SERIES PLOT, PLANT NO. 6, PRIMARY EFFLUENT

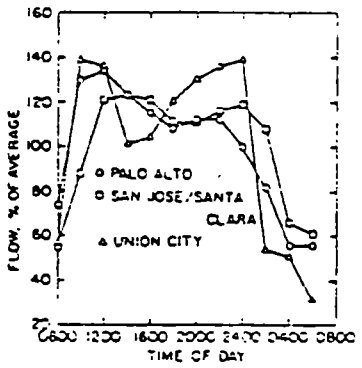

(a)

Normalized Diurnal Variation in Flow at Three Treatment Plants

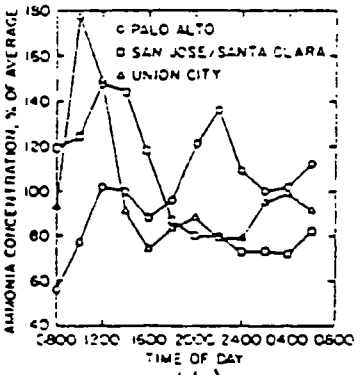

(b)

Normalized Diurnal Variation in Concentration of Ammonia in Primary Effluents

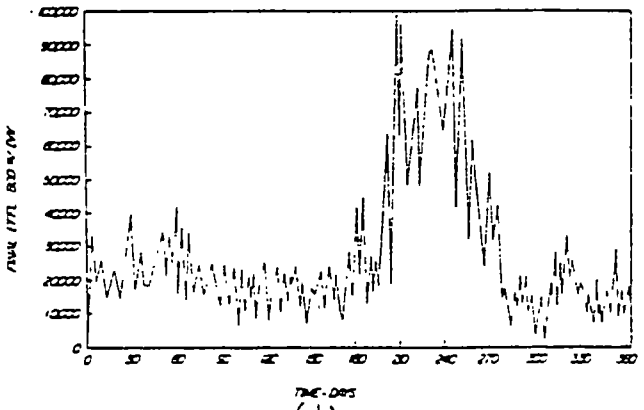

(d)

TIME SERIES PLOT, PLANT NO. 4, ACTIVATED SLUDGE EFFLUENT SEASONAL LOAD VARIATION

FIG. 4 Examples of Temporal Variation in Waste Load

a) & b) diurnal variation in Flow and Primary Effluent NH_3 (from Rundtha & McCarty, 1977)

c) & d) weekly & seasonal BOD Variations (from Thomann, 1970)

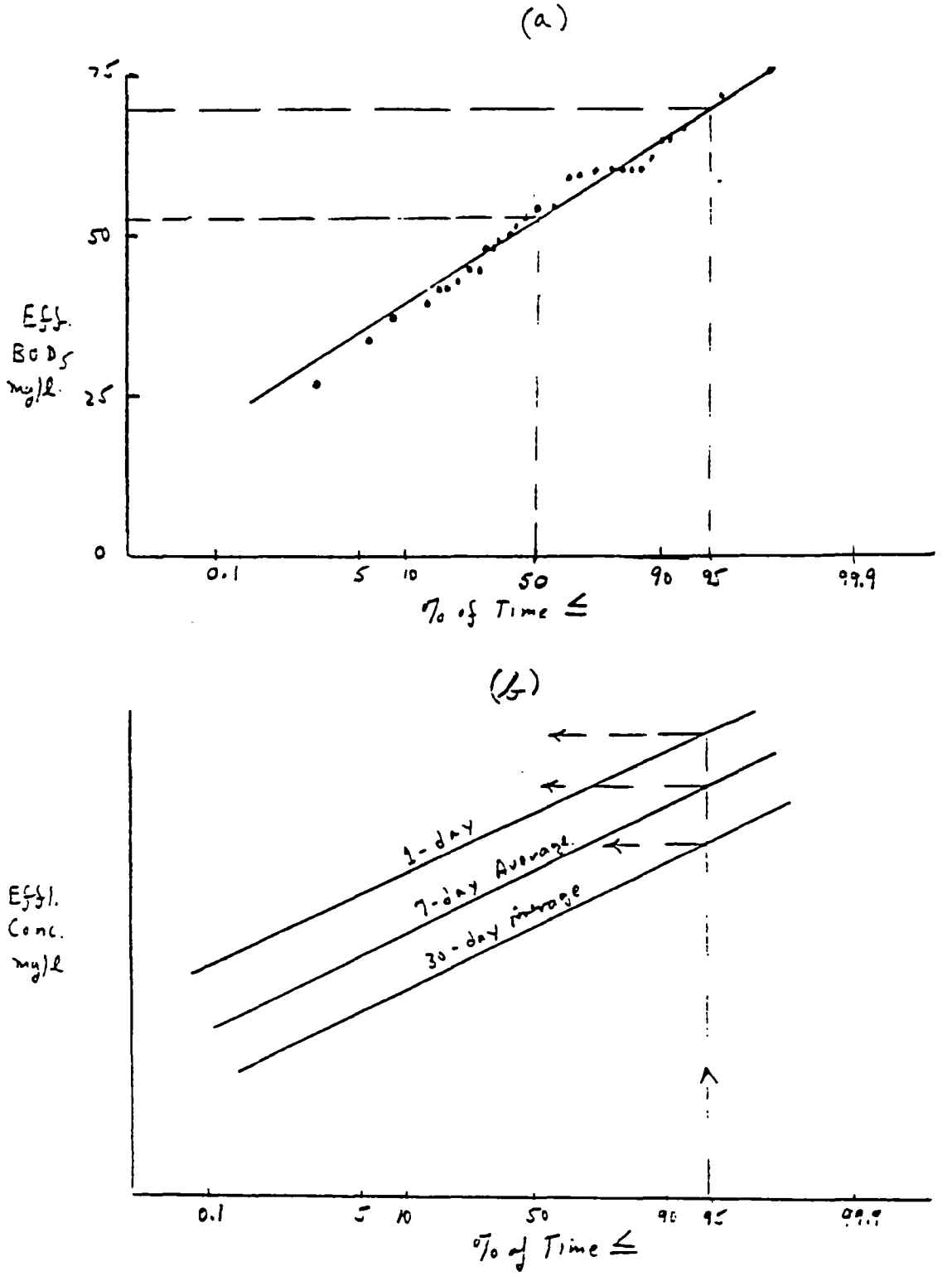

FIG. 5 a) Frequency Distribution of BOD_5 for Westernport, Md treatment plant
b) Illustration of Frequency Distribution of different Averaging of Effluent Concentrations

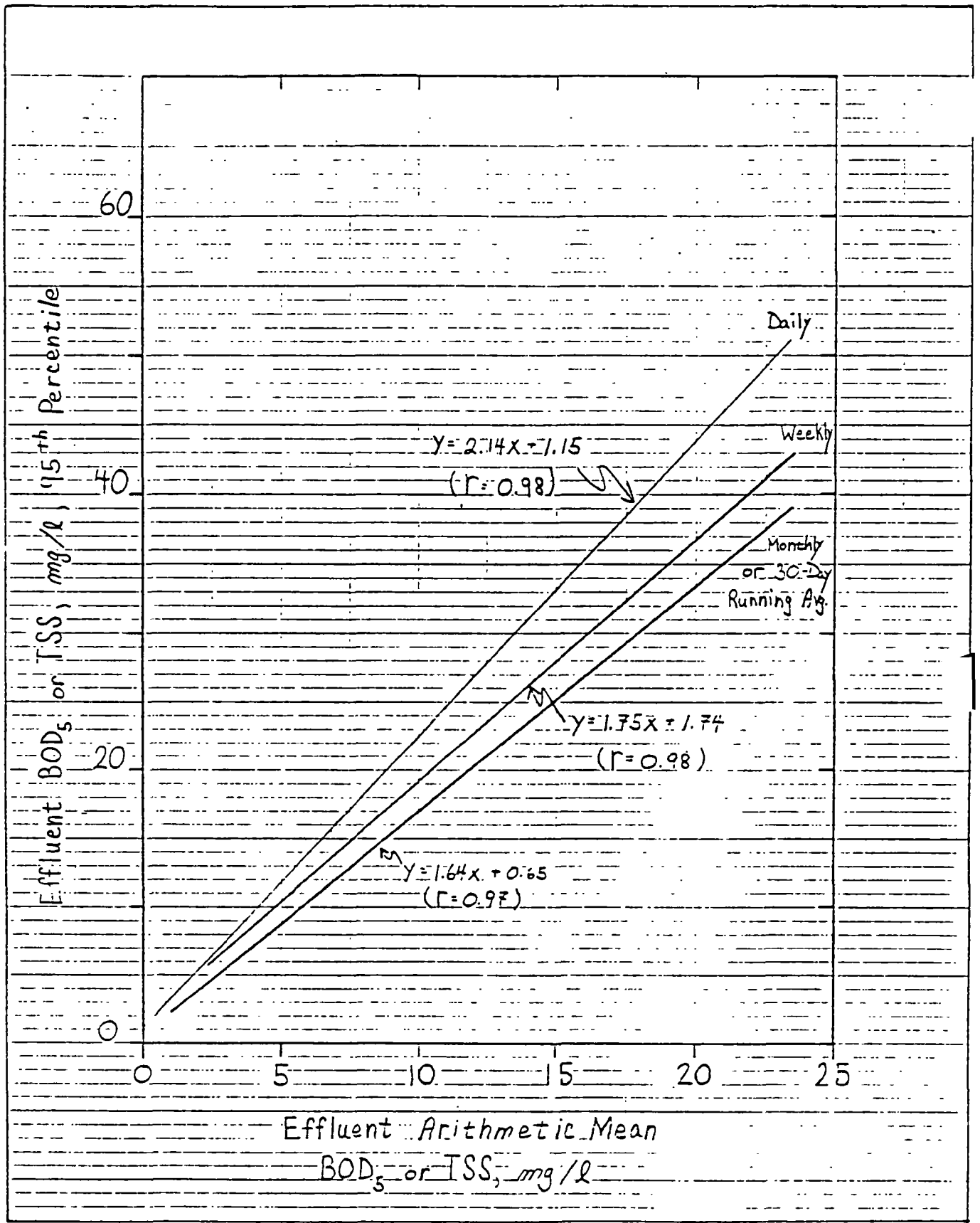

Fig 6 — Generalized 95th-percentile mean relations derived from secondary & AWT plant data (From Roper et al, 1979)

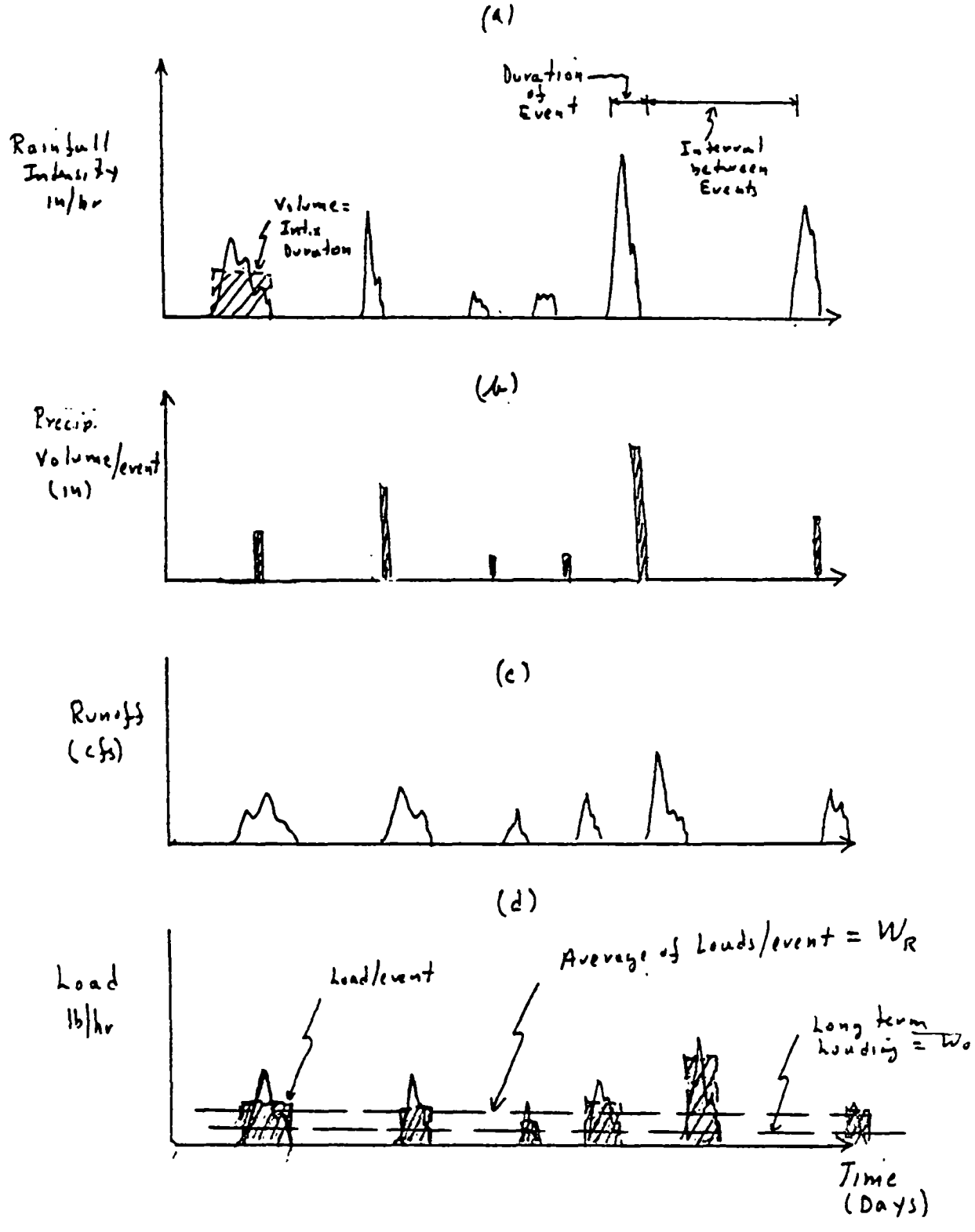

FIG. 7 a) Rainfall intensity events, b) Volume, c) Runoff and d) Load for intermittent-type discharges.

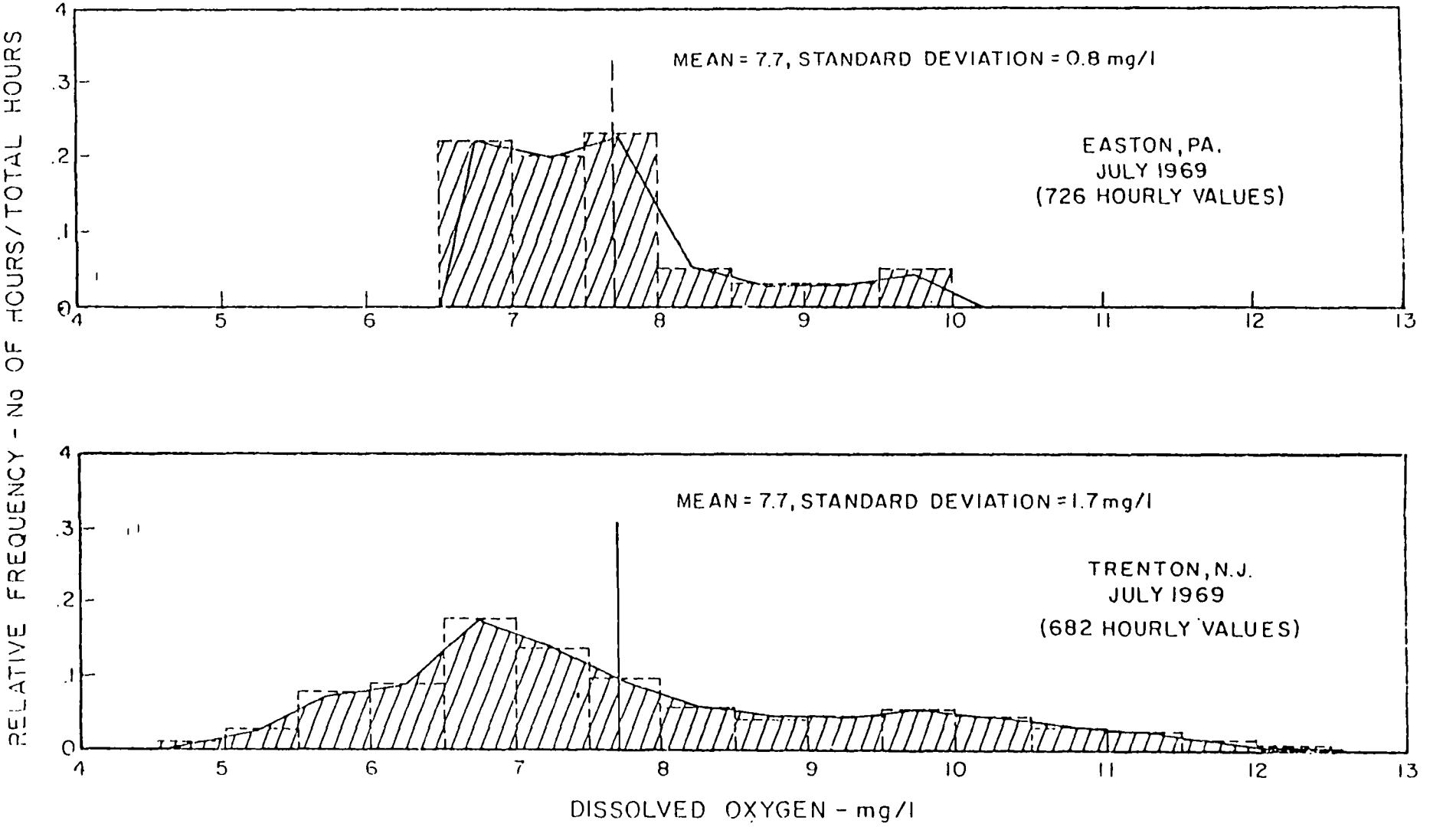

FIGURE 8

HISTOGRAM OF HOURLY DISSOLVED OXYGEN

EASTON, PENNSYLVANIA & TRENTON, NEW JERSEY

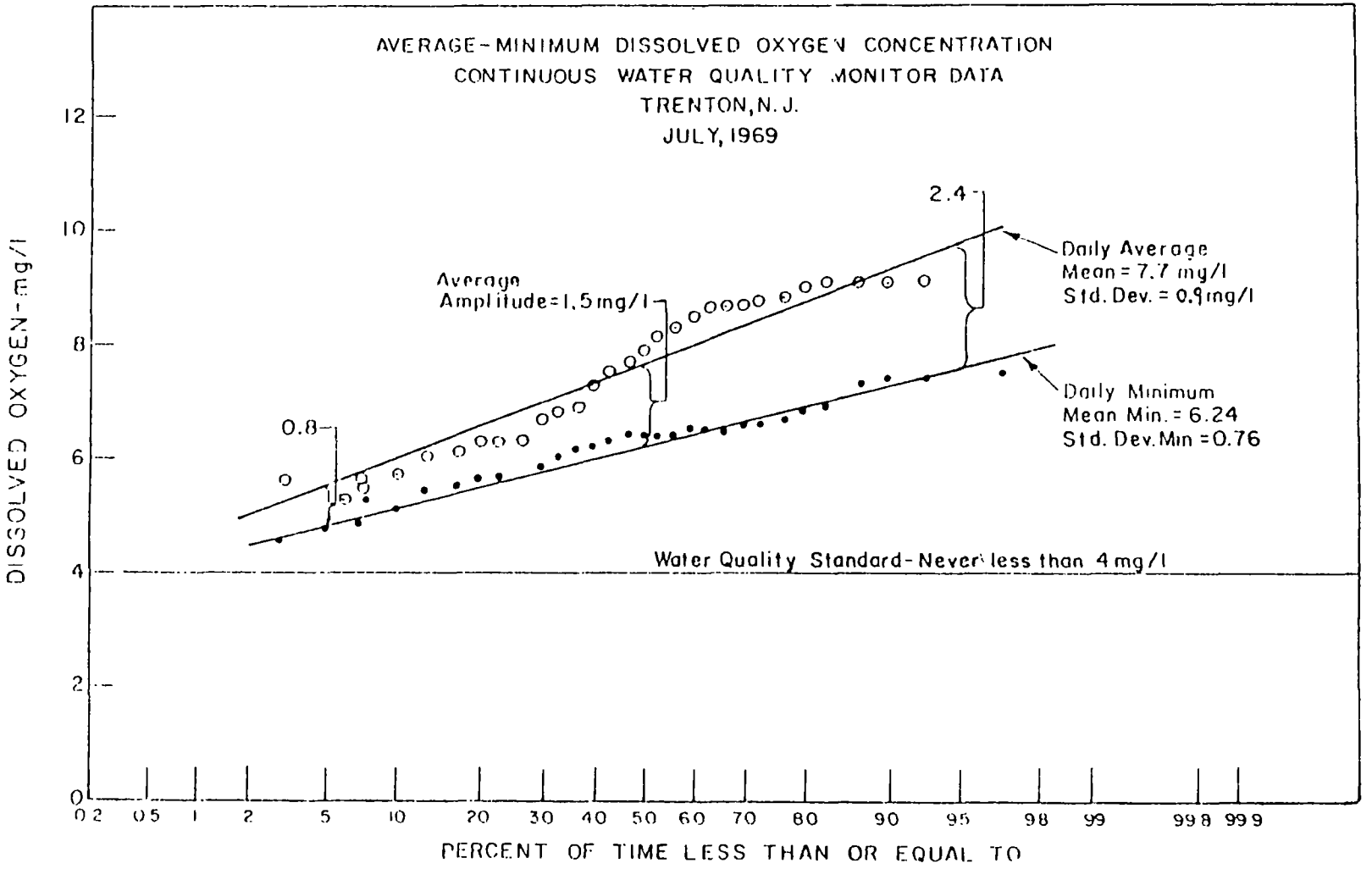

FIGURE 9

STATISTICAL DISTRIBUTION OF DISSOLVED OXYGEN CONCENTRATION
AT TRENTON, N.J.- JULY, 1969

MEASURES OF VERIFICATION*

Introduction

There are two basic reasons for constructing representations of natural water systems through mathematical modeling. First is the need to increase the level of understanding of the cause-effect relationships operative in water quality and secondly, to apply that increased understanding to aid the decision making process. Water quality models are largely syntheses of a number of phenomena; water transport, complicated reaction kinetics, and externally generated residuals inputs. The builder of water quality models acts as one part of a three part interaction which includes the specialist who generates process details (e.g., uptake of nutrients by phytoplankton) and the manager who is concerned with the problem specification and ultimately its resolution in some sense. Figure 1 shows this interaction.

For more than fifty years now, this relationship has continued in a great variety of increasingly complex water quality modeling situations. But one of the common threads throughout this period has been the constantly recurring question of the validity, credibility, and utility of the water quality models. Indeed even in the historical roots of water quality modeling, as embodied in the famous Ohio River dissolved oxygen studies of the 1920's, this question of model validity was present. Resurveys of the Ohio River between 1914 and 1930 were considered critical to a justification of the basic history theory of deoxygenation and reaeration (Crohurst, 1933). Indeed the works of Streeter and Phelps (1925) addressed the question of model validity quite directly by numerous qualitative comparisons to observed data and through quantitative comparisons by computing, for example the root mean square error between

*Robert V. Thomann in: "Workshop on Verification of Water Quality Models", US EPA ERL Athens, Georgia, EPA-600/9-80-016, April 1980.

dissolved oxygen theoretical calculations and observed values. One easily gains the impression from a reading of these early works that analysis of the relationships between observed and computed values, both qualitatively and statistically was a normally acceptable and expected procedure

As the issues of water quality become more complex, requiring the interaction of numerous variables in space and time, the questions of model credibility increase. The responses to these questions often tend to be somewhat qualitative; e.g., "The results appear reasonable" or "The major features of the observed behavior have been captured" or "The comparison between observed and computed values is marginal but sufficient for most purposes." Increasingly, most assessments of model validity do not seem to directly answer the basic questions of the manager, the specialist or the general public. Common questions are: "How good is the model?", "What is the level of confidence that we can place on your results?", "How do two models purporting to represent the same water quality phenomena compare to each other?"

In the light of the questions raised on model credibility, it is appropriate to address the issue of what measures of verification, if any, might be useful in today's water quality modeling setting. However, a brief review of the principal components of a water quality model is necessary to clarify and propose some language that might be applicable to this issue of model verification. Within the context of water quality problems, the basic issues discussed apply also to models of input generation and water transport.

Figure 2 shows the principal components of a mathematical modeling framework. The upper two steps enclosed with the dashed lines, namely "Theoretical Construct" and "Numerical Specification" constitute what is considered a mathematical model. This is to distinguish the simple writing of equations for a model from the equally difficult task of assigning a set of representative numbers to inputs and parameters. Following this initial model specification are the steps of a) model calibration, i.e., the first "tuning" of model output to observed data and b) the step of model verification i.e., the use of the calibrated model on a different set of water quality data. This verification data set should presumably represent a condition under a sufficiently perturbed condition (i.e., high flows, decreased temperature, changed waste input) to provide an adequate test for the model. Upon the completion of this verification or auditing step, the model would be considered verified.

Stages of Model Credibility

The following definitions are therefore offered:

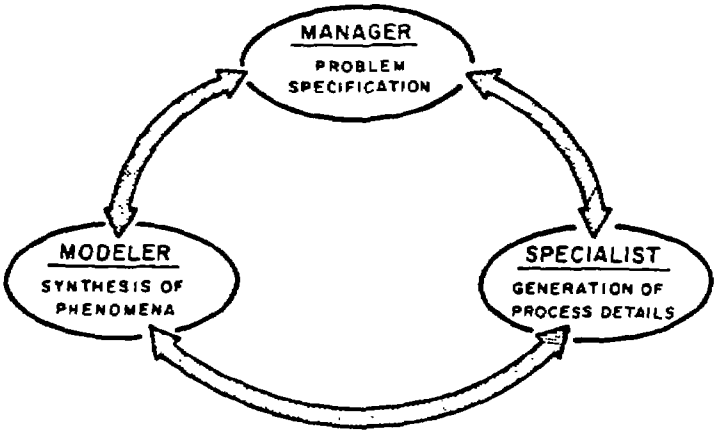

FIGURE 1. RELATIONSHIP BETWEEN MODELER, SPECIALIST AND MANAGER IN WATER QUALITY

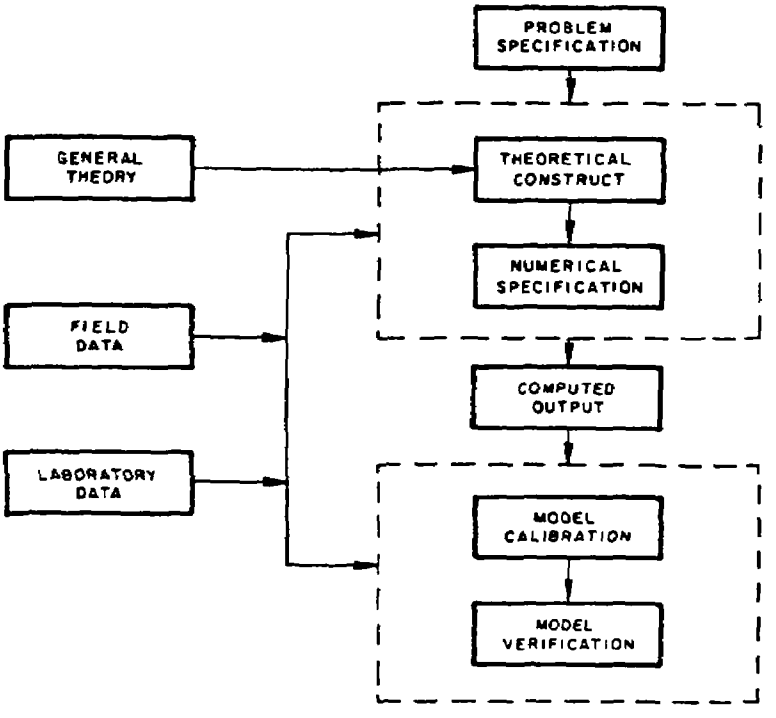

FIGURE 2. PRINCIPAL COMPONENTS OF MATHEMATICAL MODELING FRAMEWORK

1. Model: A theoretical construct, together with assignment of numerical values to model parameters, incorporating some prior observations drawn from field and laboratory data, and relating external inputs or forcing functions to system variable responses.

2. Model Calibration: The first stage testing or tuning of a model to a set of field data, preferably a set of field data not used in the original model construction; such tuning to include a consistent and rational set of theoretically defensible parameters and inputs.

3. Model Verification: Subsequent testing of a calibrated model to additional field data preferably under different external conditions to further examine model validity.

The calibrated model, it should be noted, is not simply a curve-fitting exercise, but should reflect wherever possible more fundamental theoretical constructs and parameters. Thus, models that have widely varying coefficients (i.e., deoxygenation coefficients) to merely "fit" the observed data are not considered calibrated models.

The verified model is then often used for forecasts of expected water quality under a variety of potential scenarios. However, it is apparently rare that following a forecast, and a subsequent implementation of an environmental control program, that an analysis is made of the actual ability of the model to predict water quality responses. This can be termed a "post-audit" of the model, as shown in Figure 3. Somehow it seems that once a facility has been constructed, the federal and state agencies, municipalities, and industries are somewhat reluctant to return to the scene of a water quality problem to monitor the response of the water body. A fourth step therefore in determining model credibility is suggested as follows:

4. Model Post-Audit: A subsequent examination and verification of model predictive performance following implementation of an environmental control program.

Need for Measures of Verification

Increase in Model Complexity. The most obvious need for some measures of model verification is the fact that water quality models have increased greatly in complexity. Figures 4-7 illustrate this progression. From relatively simple two linear system models of biochemical oxygen demand and dissolved oxygen for the first forty years of model development to the new complex non-linear interactive eutrophication and toxic substances models, the ability to describe model performance has become increasingly difficult. The number of state variables in some models has increased dramatically. It is not unusual today

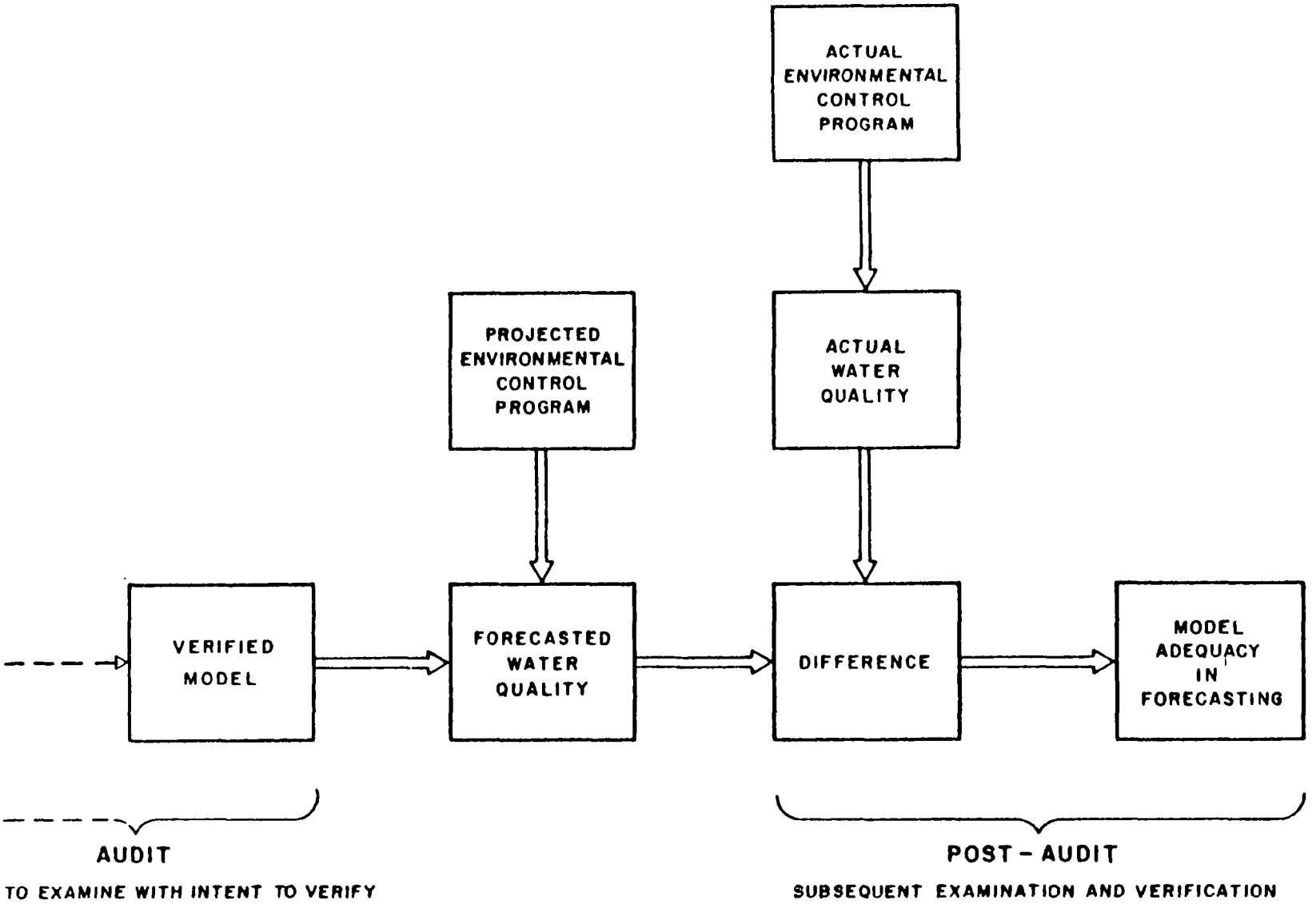

FIGURE 3. AUDITING AND POST AUDITING OF WATER QUALITY MODELS

to construct models with up to 20 or more state variables. Furthermore, as illustrated in Figures 4-7, the physical dimensionality now encompasses the range from the more traditional one-dimensional streams to fully three-dimensional estuaries, bays and lakes.

As the number of state variables and physical dimensionality has increased, the overall ability of the analyst to comprehend model output has decreased. This is simply due to the overall size of the model. For example; if a "compartment" is considered as a state variable, i = 1,...m, positioned at some spatial location j = 1...n, then the total number of compartments to be solved for a fully interactive model is m times n. Figure 8 shows the growth of the number of model compartments since the earliest work of the two state variable problems of BOD and DO. The almost explosive growth in the number of model compartments, coincidental with passage of major water quality legislation is evident.

Increase in Complexity of Questions. The second major reason for some quantitative measures of verification is the fact that the level of questions in water quality has increased in complexity. Many of the water quality issues today extend well beyond the traditional problem of raw or inadequately treated sewage. In that traditional framework, it generally was clear that some treatment of municipal sewage would probably improve water quality, specifically dissolved oxygen. However, some of the water quality questions today may involve such complex interactions that it is not clear that certain environmental controls will in fact produce the classical result. The Potomac estuary eutrophication problem is a case in point. It is not clear that nitrogen removal at the Washington, D.C. Blue Plains plant actually will result in any reduction in the phytoplankton population that could not be achieved solely by phosphorus control. Similarly, it is not entirely clear that extensive dredging of PCB deposits in the Upper Hudson will result in a reduction of the PCB body burden of the striped bass in the Lower Hudson estuary to levels below the FDA requirement.

The complexity of the problem then leads to the very real possibility that environmental control measures may be called for by model predictive analyses when in fact the implementation of such controls may produce little or no response in water quality. The economic, political, and social consequences of "wrong" answers therefore become more acute in today's problem setting. Some quantifiable measure of model performance in improving understanding or predictive performance would seem, therefore, to be of considerable importance.

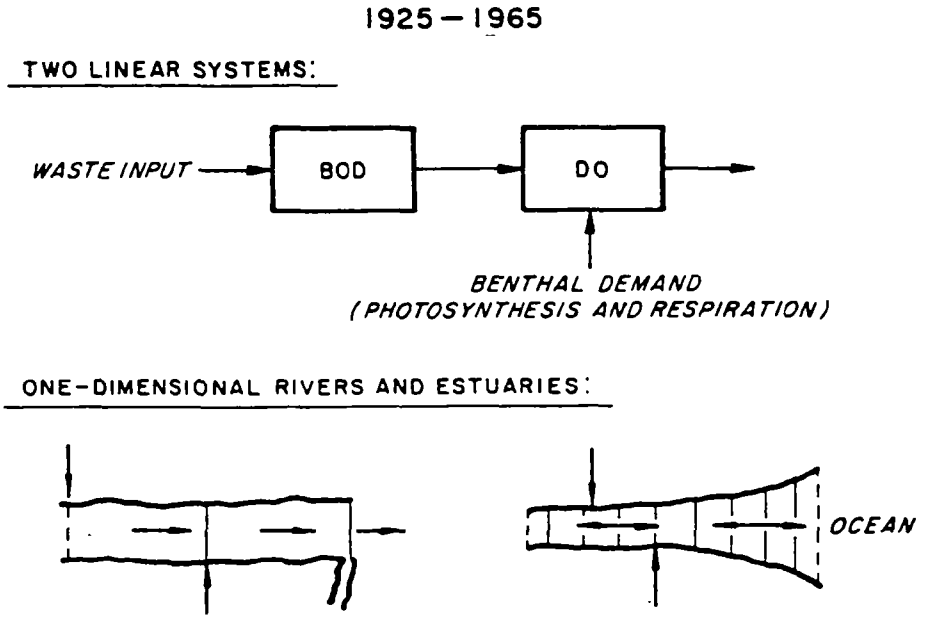

FIGURE 4. WATER QUALITY MODELS, 1925-1965

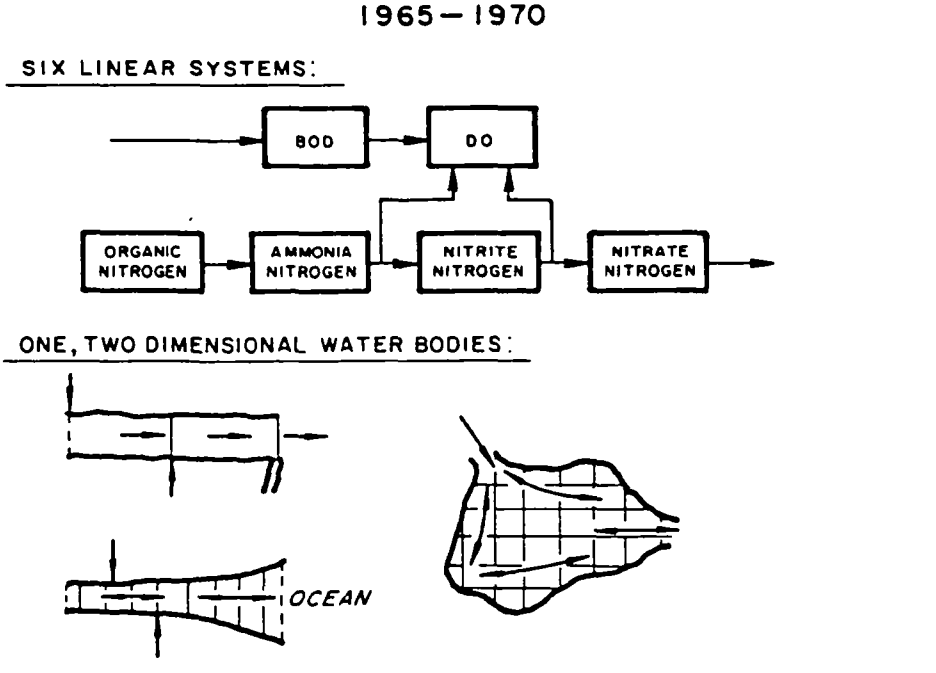

FIGURE 5. WATER QUALITY MODELS, 1965-1970

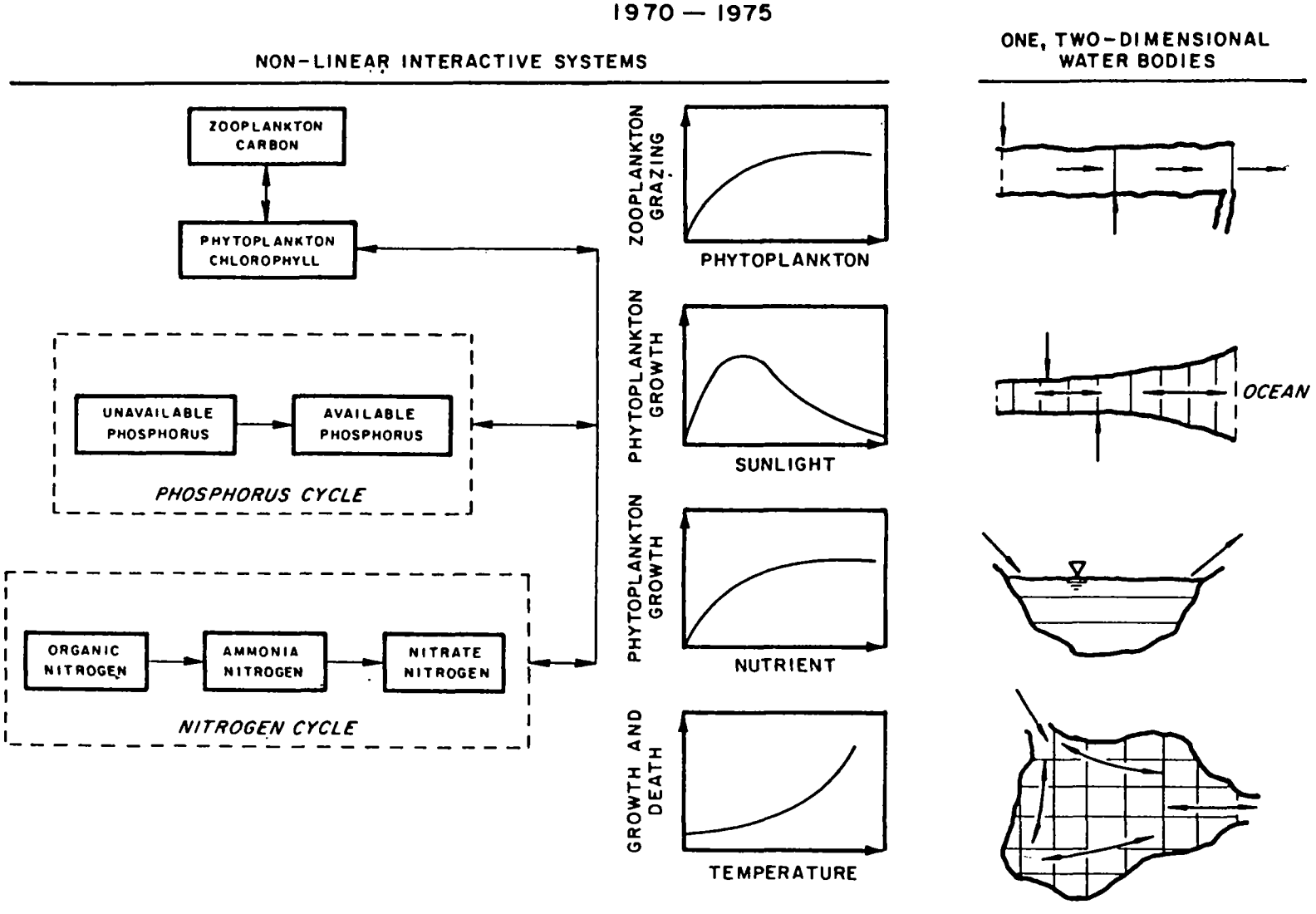

FIGURE 6. WATER QUALITY MODELS 1970-1975

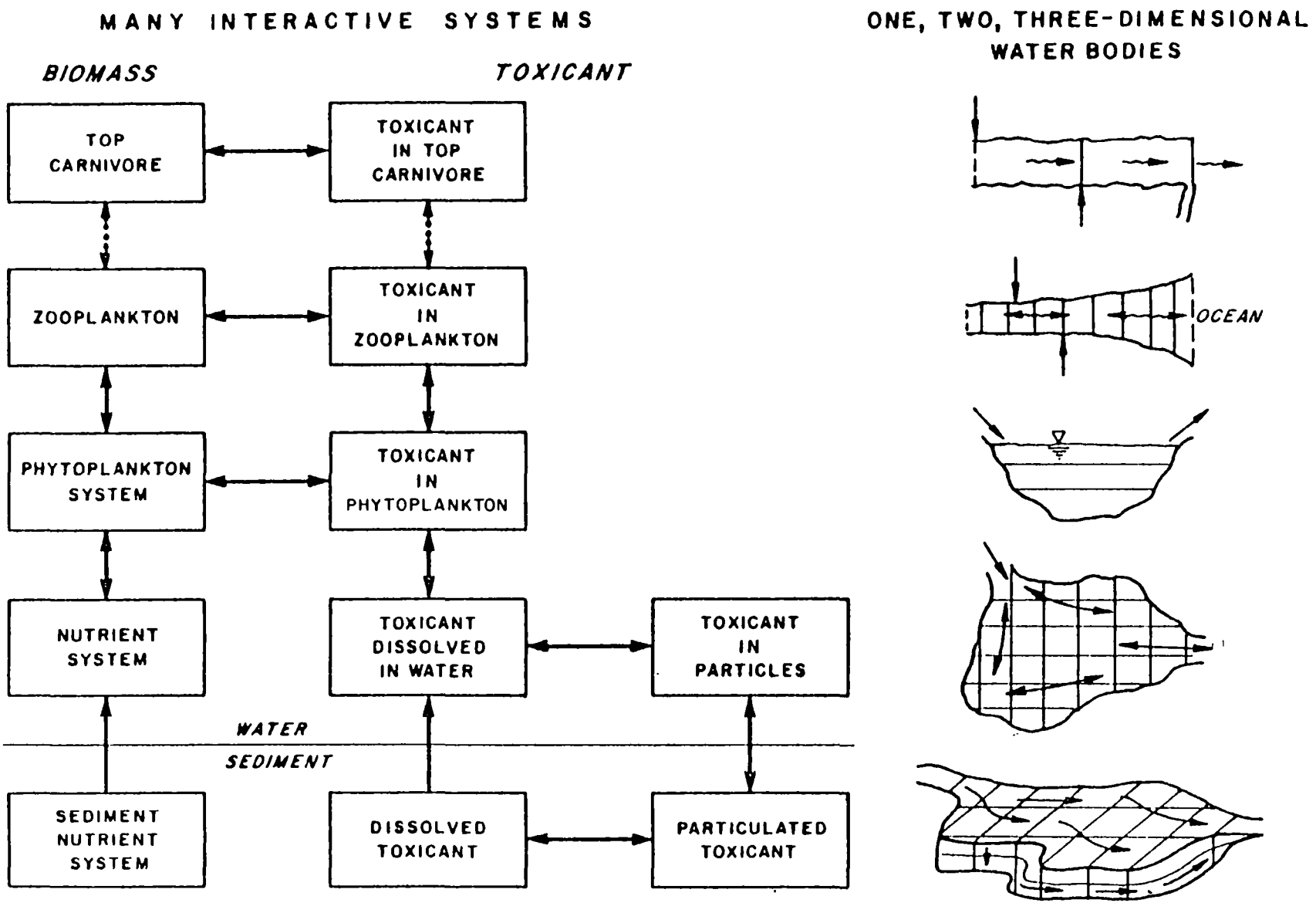

FIGURE 7. WATER QUALITY MODELS 1975-?

Some Verification Measures

Qualitative Measures

Probably the most direct and easily understood measure of model performance is to present qualitative comparisons of observed data and computed values. This is most often done in the form of overplotting data and theory or tabulating the comparison between the two and then drawing qualitative judgmental conclusions about the adequacy of the model and its suitability for projection purposes. A plot of data versus theory can be a most graphical measure of model credibility - easily understood and clearly visual. But for some problems, such a simple qualitative measure is not possible or simply not adequate. This is particularly so for time variable models of several state variables and multi-dimensional systems. For models of this type, as well as the simpler model framework, some statistical comparisons may provide further understanding of model credibility.

Statistical Comparisons

A variety of simple statistical comparisons may be appropriate to quantify model verification status. Such measures would be intended to supplement the qualitative comparisons. Examples of statistical analyses between observed and computed values are:

1) Regression analyses
2) Relative error
3) Comparison of means
4) Root mean square error

1) Regression Analyses

A perspective on the adequacy of a model can be obtained by regressing the calculated values with the observed values. Therefore, let the testing equation be

$$\bar{x} = \alpha + \beta\bar{c} + \varepsilon \qquad (1)$$

where α and β are the true intercept and slope respectively between the calculated values, $\bar{c}$, and the observed values, $\bar{x}$, and ε is the error of $\bar{x}$. The regression model equation (1) assumes, of course, that $\bar{c}$, the calculated value from the water quality model, is known with certainty which is not the actual case. With equation (1), standard linear regression statistics can be computed, including

a) The square of the correlation coefficient, r^2, (the % variance accounted for) between calculated and observed

b) Standard error of estimate, representing the residual error between model and data

c) Slope estimate, b, of β and intercept estimate, a, of α

d) Test of significance on the slope and intercept. The null hypothesis on the slope and intercept is given by $\beta = 1$ and $\alpha = 0$. Therefore, the test statistics

$$\frac{b-1}{s_b} \quad \text{and} \quad \alpha/s_a$$

are distributed as student's t and n-2 degrees of freedom. The variance of the slope and intercept, s_b^2 and s_a^2 are computed according to standard formulae. A two-tailed "t" test is conducted on b and a, separately, with a 5% probability in each tail, i.e. a critical value of t of about 2 provides the rejection limit of the null hypothesis.

Regressing the calculated and observed values can result in several situations. Figures 9(b) and (c) shows that very good correlation may be obtained but a constant fractional bias may exist ($b<1$, $b>1$); also Figure 9(a) indicates that poor correlation may be obtained with slope = 1 and intercept = 0. Finally, Figure 9(d) indicates the case of good correlation but for an $a > 0$ a constant bias may exist. Evaluation of r^2, b and a, together with the residual standard error of estimate, can provide an additional level of insight into the comparison between model and data.

2) Relative Error

Another simple statistical comparison is given by the relative error defined as

$$e = \frac{|\bar{x} - \bar{c}|}{\bar{x}} \qquad (2)$$

Various aggregations of this error across regions of the water body or over time can also be calculated and the cumulative frequency of error over space or time can be computed. Estimates can then be made of the median relative error as well as the 10% and 90% exeedance frequency of error. The difficulties with this statistic are its relatively poor behavior at low values of $\bar{x}$ and the fact that it does not recognize the variability in the data. In addition, the statistic is poor when $\bar{x} > \bar{c}$ since under that condition the maximum relative error is 100%. As a result, the distribution of this error statistic is most poorly behaved at the upper tail. Nevertheless, if the

median error is considered, this statistic is a readily understood comparison and provides a gross measure of model adequacy. It can also be especially useful in comparisons between models.

3) Comparison of Means

A third measure is to conduct a simple test of the differences between the observed mean and the computed mean. Letting $\bar{d} = \bar{x} - \bar{c}$, the test statistic distributed as a student's "t" probability density function is given by

$$t = \frac{\bar{d} - \delta}{s_{\bar{d}}} \tag{3}$$

where δ is the true difference between model and data and $s_{\bar{d}}$ is the standard deviation of the difference given by a pooled variance of observed and model variability. If these latter quantities are assumed equal then

$$s_{\bar{d}} = \sqrt{2}s_{\bar{x}} \tag{4}$$

where $s_{\bar{x}}$ is the standard error of estimate of the observed data and is given by

$$s_{\bar{x}}^2 = \frac{s_x^2}{N} \tag{5}$$

4) Root Mean Square Error

Finally, a measure of the error between the model and the observed data is also given by the root mean square (rms) error as

$$r = \sqrt{\frac{\Sigma(x_i - c_i)^2}{N}} \tag{6}$$

As before, the rms error can be computed across a spatial profile or over time at a single location. The rms error is statistically well-behaved and provides a direct measure of model error. If expressed as a ratio to mean value (across a profile or over time), it represents a second type of relative error. The disadvantage of the rms error is that it does not readily lend itself to pooling across variables to assess overall model credibility.

Each of the above measures displays model credibility from different statistical viewpoints. Some are apparently useful

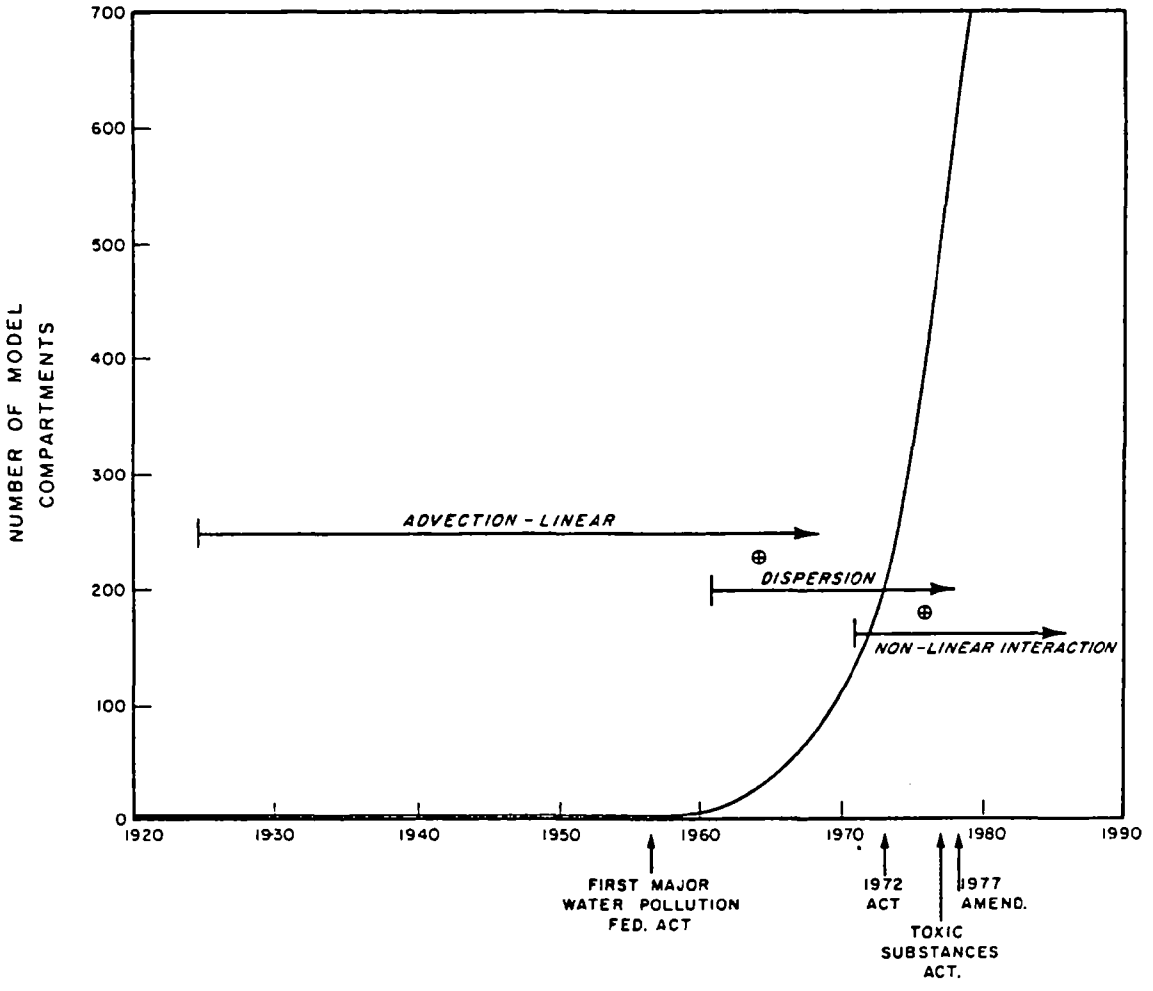

FIGURE 8. INCREASE OF NUMBERS OF MODEL COMPARTMENTS WITH TIME

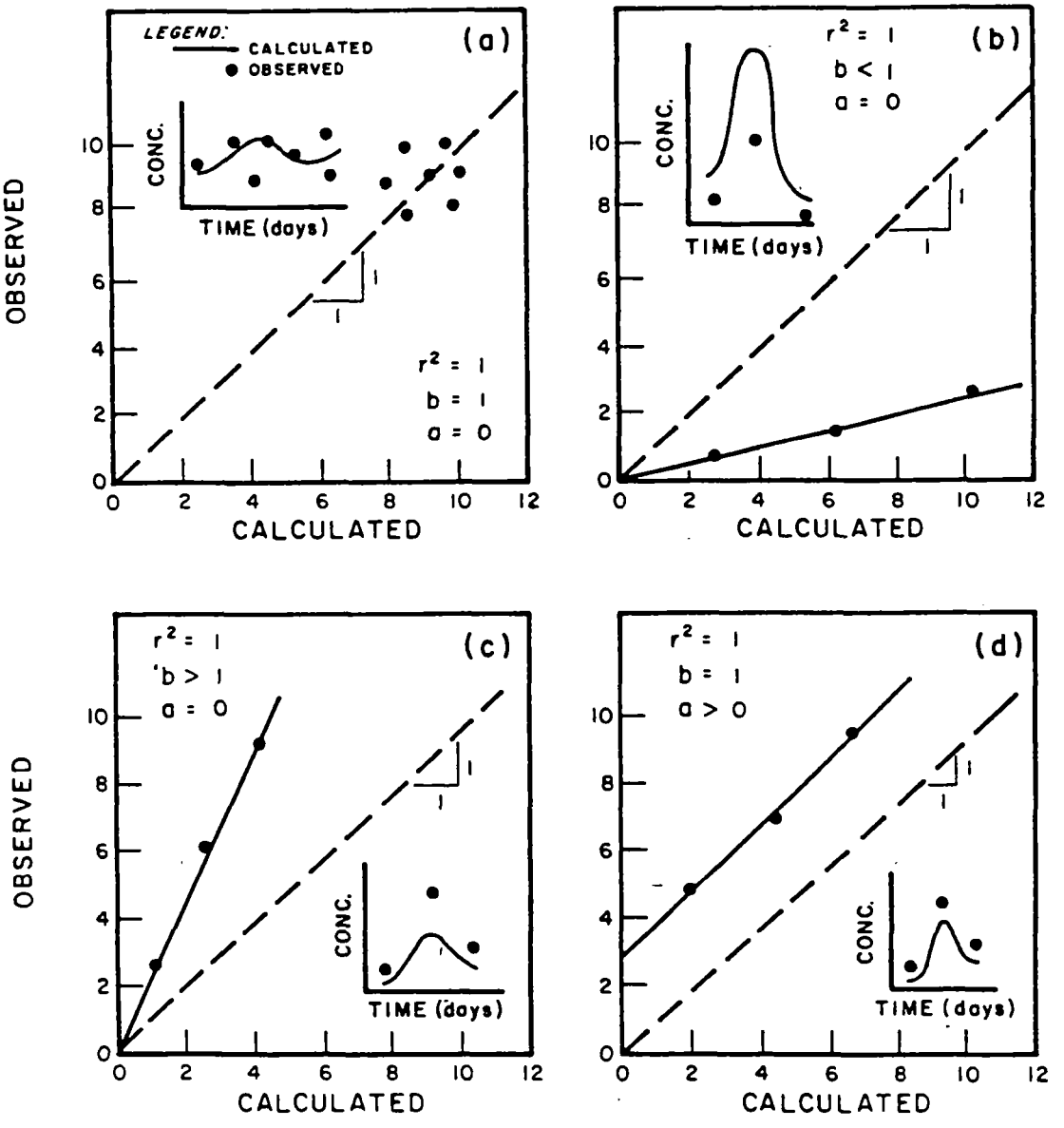

FIGURE 9. POSSIBLE CASES IN REGRESSION BETWEEN CALCULATED AND OBSERVED VALUES

for diagnostic purposes while others appear to be directly of value in succinctly describing model verification status.

Some Examples of Quantitative Verification Analyses

Dissolved Oxygen Models

In order to illustrate the present state of the art of model calibration/verification, a brief review was made of nineteen models of dissolved oxygen. This water quality variable was chosen since DO models have been the most extensively used and over the longest time period. The engineering reports for the fifteen water bodies were examined and relative errors, rms errors, and regression analyses were evaluated. All of the water bodies were analyzed by Hydroscience, Inc. It was assumed that the personnel engaged in the modeling analyses carried out the calibration/verification steps consistent with the definitions given above and not just to "curve fit" the model to the data.

The models included several small streams in New Jersey (less than 10 cfs), larger river systems such as the Ohio River and the Upper Mississippi River, bays and estuaries and a large model of the entire New York Harbor complex. A listing is shown in Table 1.

The distribution of the median relative error for these models is shown in Figure 10. For each water body, the error represents the median relative error where 50% of the stations (or times) had errors less than the values shown. Across all models, one-half of the models had median relative errors greater than 10% and one half of the models had median relative errors less than 10%.

As a crude measure, therefore, of the present state of the art of DO models calibration/verification, one might suggest an overall median relative error of 10%. It should, of course, be noted that this is not the error of actual prediction but merely the error representative of a present level of understanding of observed behavior of dissolved oxygen. The degree to which the results shown in Figure 10 is representative of all DO models is not known. More detailed analyses of a larger sample would be necessary.

Lake Ontario Eutrophication Models

A variety of models have been constructed of the eutrophication of Lake Ontario at several time and space scales and with different levels of kinetic detail (Thomann, et. al., 1979 and Thomann and Segna, 1979). Extensive application of the above quantitative measures of calibration/verification was made for a three-dimensional model of the Lake for one year and for a two segment vertical model over a ten year period.

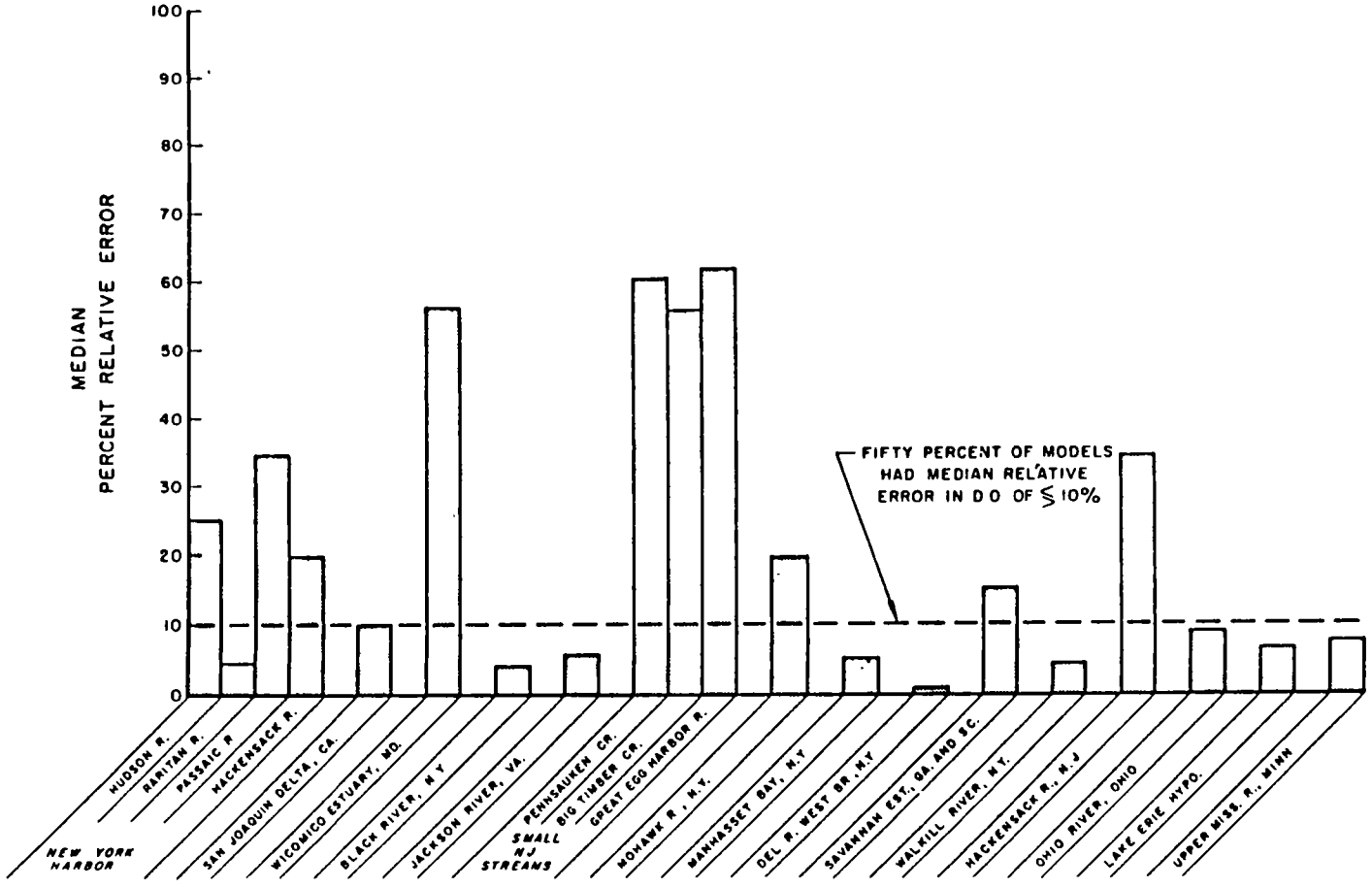

FIGURE 10. SOME RELATIVE ERRORS OF DISSOLVED OXYGEN MODELS

TABLE 1

WATER BODIES
EXAMINED FOR DISSOLVED
OXYGEN VERIFICATION STATISTICS

	Location	Remarks
1.	New York Harbor Hudson River Raritan River Passaic River Hackensack River	425 segment 3 Dimen. model
2.	San Joaquin Delta, Calif.	DO model part of eutrophication model
3.	Wicomico Estuary, Md.	A tidal tributary of Ches. Bay
4.	Black River, N.Y.	A tributary of Lake Ontario
5.	Jackson R., Va.	
6.	Small N.J. Streams 6a. Pennsauken Cr. 6b. Big Timber Cr. 6c. Grt. Egg Harbor R.	Tributaries of Delaware River and Bay
7.	Mohawk River, N.Y.	In vicinity of Utica, N.Y.
8.	Manhasset Bay, N.Y.	Bay of Long Island Sound
9.	Delaware R. West Br., N.Y.	
10.	Savannah Estuary, Ga., S.C.	
11.	Wallkill R., N.J.	
12.	Hackensack R., N.J.	
13.	Ohio R., Ohio	In vicinity of Cinn., Ohio
14.	Lake Erie Hypolimnion	DO model part of eutrophication model - time variable
15.	Upper Miss. R., Minn.	DO model part of eutrophication model - time variable

Figure 11 shows the median relative error across all variables at three levels of spatial aggregation - 67 segments, eight regions, and whole lake two layer scale. Five state variables were included in the pooled error (chlorophyll, total phosphorus, dissolved orthophosphorus, ammonia, and nitrate). The median relative error over the year was the highest at the smaller spatial scale (44%) and lowest at the whole lake scale (17%). This indicated that the model did not capture more local spatial phenomena as well as it reproduced overall lake behavior.

Figures 12-14 show the verification statistics from the analysis of 10 years of data on Lake Ontario using the two layer model. Two kinetic regimes are shown. Lake 1 kinetics are fairly standard and Lake 1-A kinetics included a more complex phytoplankton compartment (diatoms and non-diatoms), silica limitation and other kinetic changes in nutrient recycle. Figure 12 shows an example of the chlorophyll verification results for both regression analyses and relative error distribution. The regression results indicated some improvement in slope with the increased kinetic complexity but no improvement in the correlation or intercept. The median relative error for chlorophyll decreased from 42% to 30% with the inclusion of the more complex kinetics. Figure 13 shows the results of the student's t-test comparing observed and computed monthly means over the six state variables. For the indicated standard errors, the Lake 1-A kinetics gave a verification score of 70%, i.e., 70% of the variable-months where a comparison could be made showed no statistically significant difference between observed and computed means. If the standard errors are taken at one-half the values indicated, the score drops to 40%. Figure 14 shows the median relative errors for each variable and for all variables. The latter test indicated an overall relative error for the ten years of analysis and all variables of 22-32%.

A Suggestion

On the basis of the above concepts and illustrations together with the apparent growing need to be more definitive in assessing model credibility, it is suggested that quantitative measures of calibration and verification of models be an integral part of modeling whenever possible. This includes a pressing need to conduct post-auditing studies of model projections and resulting water quality.

The suggestion for quantitative measures of water quality model verification is aimed at responding to the many questions often raised at various stages in the decision making process. There are, however, advantages and disadvantages to quantitative measures of model verification. Some of the disadvantages are:

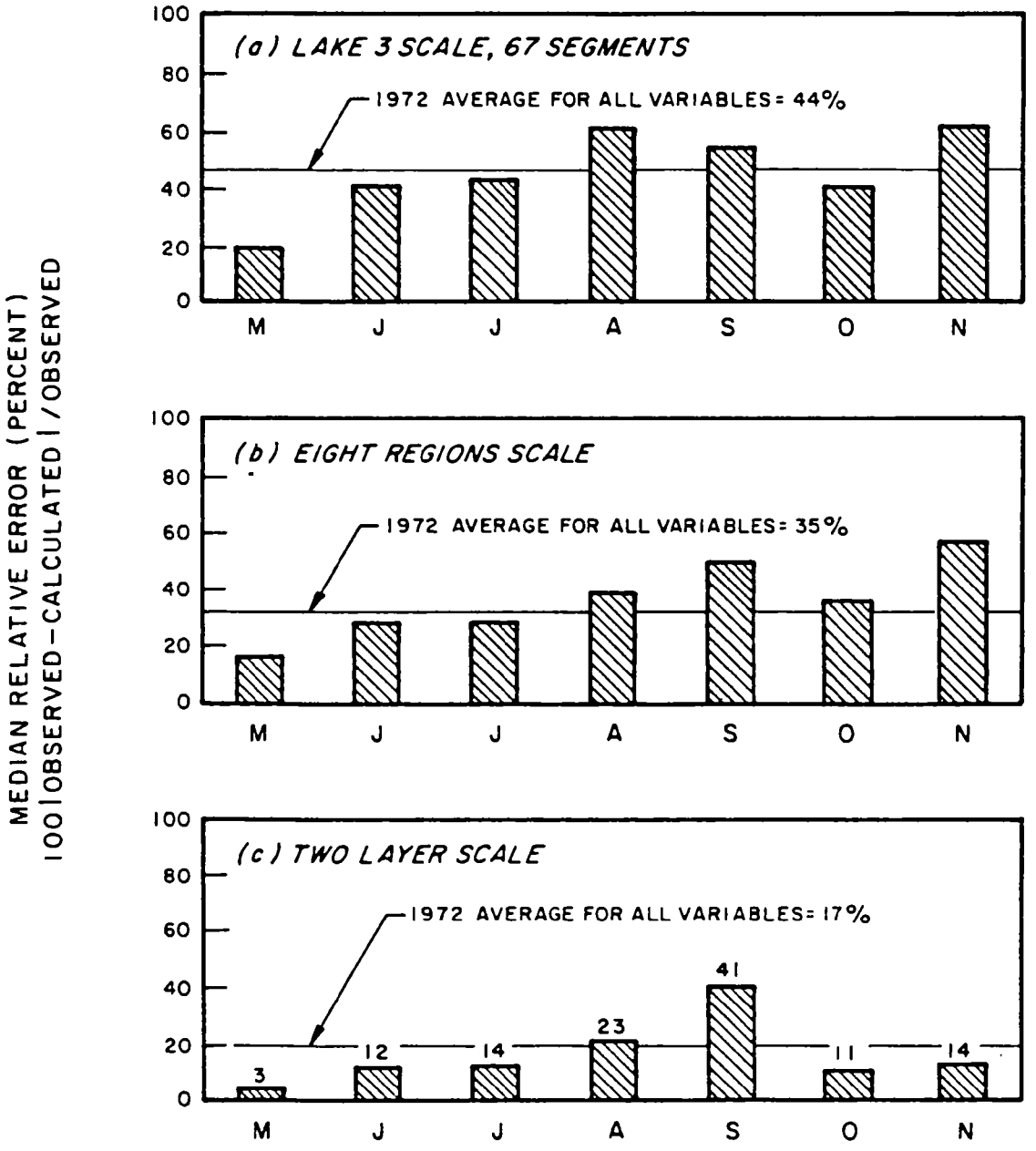

FIGURE 11. LAKE ONTARIO
MEDIAN RELATIVE ERROR AT THREE SPATIAL SCALES

THOMANN et al. 1979a

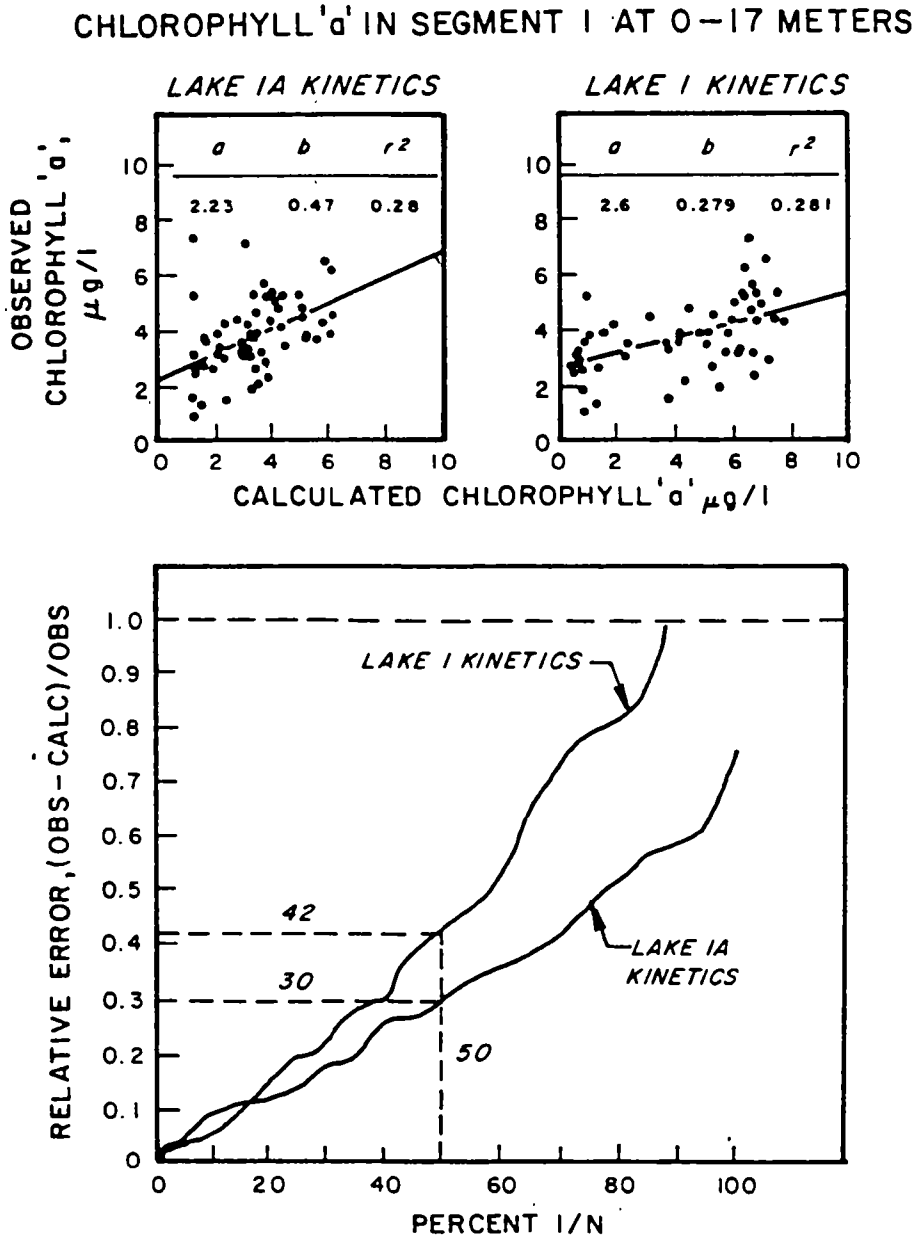

FIGURE 12. LAKE ONTARIO
CHLOROPHYLL VERIFICATION, TEN YEAR ANALYSIS

THOMANN AND SEGNA, 1979b

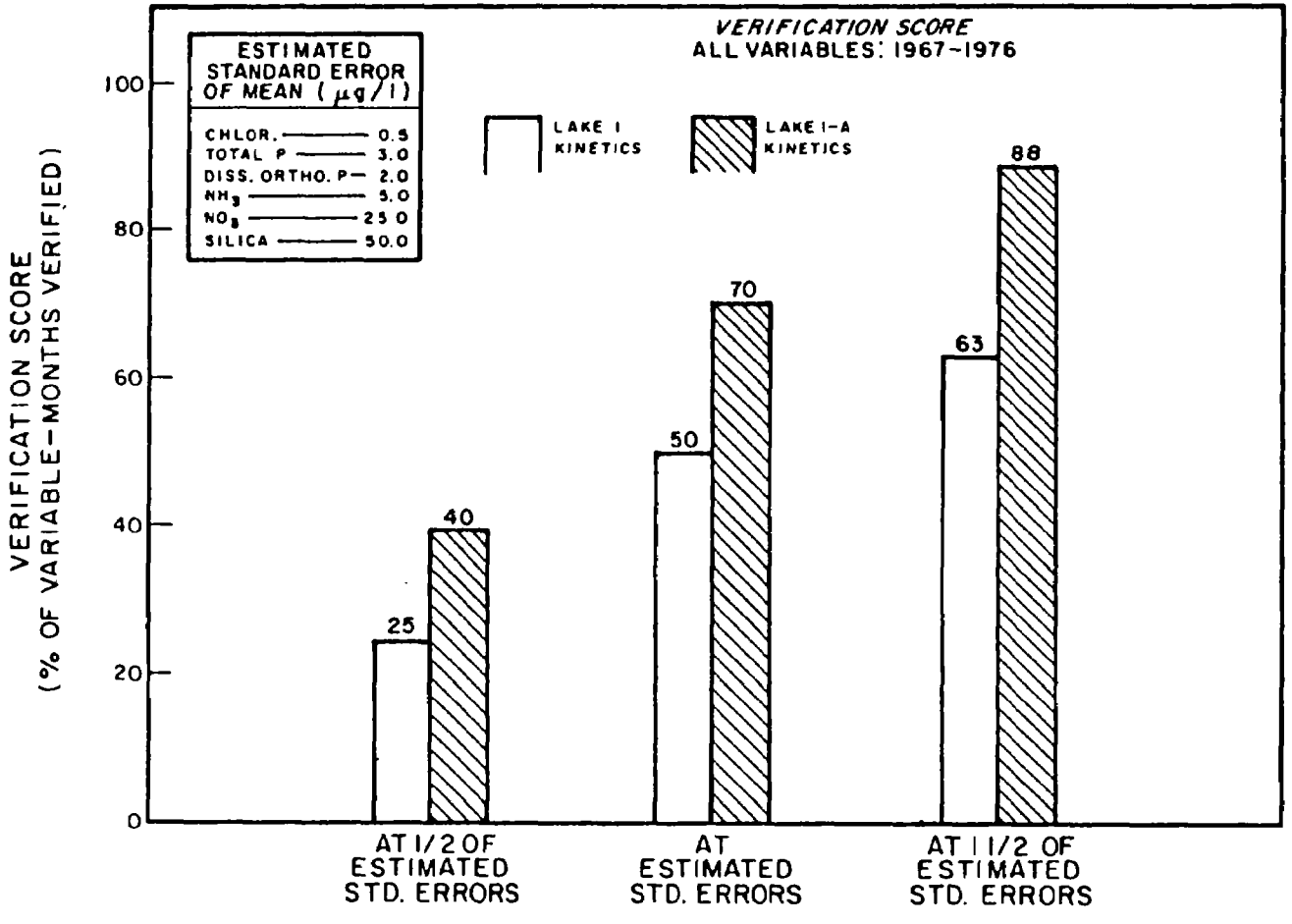

FIGURE 13. LAKE ONTARIO
VERIFICATION SCORES, ALL VARIABLES, TEN YEAR ANALYSIS.

THOMANN AND BEGNA 1978b

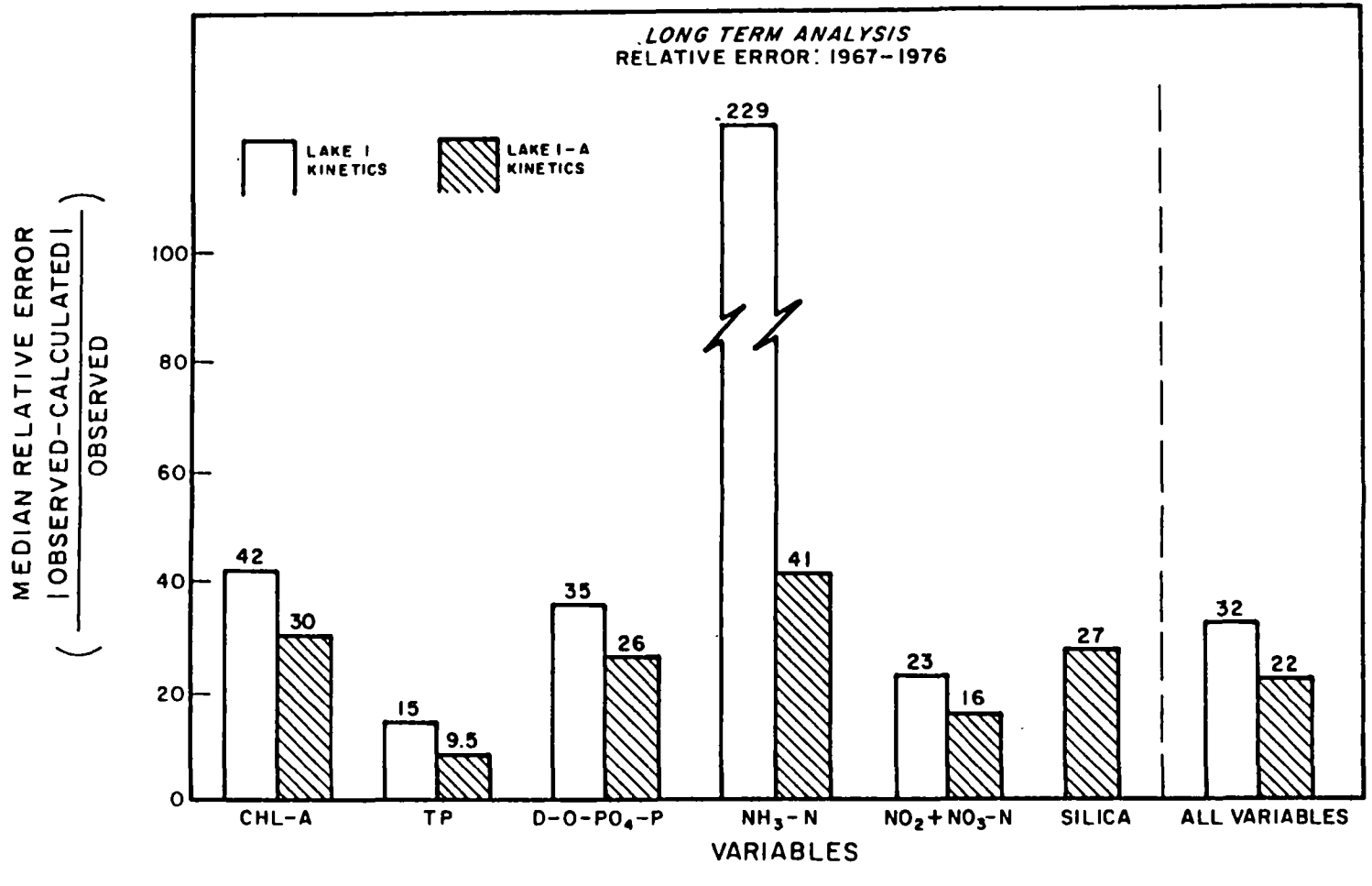

FIGURE 14. LAKE ONTARIO
MEDIAN RELATIVE ERROR, TEN YEAR ANALYSIS

THOMANN AND SEGNA 1979b

1) An urge would be created to "curve fit" model to data to improve verification statistics

2) Not all of the credibility of a model is subsumed in verification statistics

3) Good verification statistics do not necessarily imply the ability to accurately predict future water quality

4) Single measures of verification may be grasped at too readily and engineering judgment as a measure of model credibility may degenerate into "What's your median relative error?"

The advantages are:

1) Some measures, albeit imperfect ones, would be available for decision makers to assess model credibility and status

2) A basis would be provided for comparison of models

3) Some estimate could be made of changes in the state of the art of model performance

4) Modelers would be stimulated to question their model output with quantitative measures

5) A diagnostic tool would be available to determine relative improvement of a given model under more complex frameworks.

A quantitative measure of model performance, therefore, may be a mixed blessing. At the very least, the time appears appropriate to address the issue of the need and value of such measures to assess model status. It is through such discussions that perhaps some consensus can be reached on the advisability of such measures or on possible alternative means of describing the validity of water quality models.

Acknowledgments

Part of the work reported on herein was supported by a grant from the Environmental Protection Agency, Large Lakes Research Station, Grosse Ile, Michigan to Manhattan College. Additional support was also received by Hydroscience, Inc. through a consulting agreement. Grateful appreciation is expressed to both parties for this support. Special thanks are due also to Mary P. Thomann and Robert J. Thomann for their diligent computations of the DO error statistics.

REFERENCES

1. Crohurst, H.R., 1933. A study of the pollution and natural purification of the Ohio River, IV. A resurvey of the Ohio River between Cinn., Ohio and Louisville, Ky., including a discussion of the effects of canalization and changes in sanitary conditions since 1914-1916. U.S. Pub. Health Service, Pub. Health Bull. No. 204, 111 pp.

2. Hydroscience, Inc., 1968. Water quality analysis for the Markland Pool of the Ohio River. Malcolm Pirnie Engrs. White Plains, N.Y. 121 pp. and Figs.

3. Hydroscience, Inc., 1970. Water quality analysis of the Savannah River Estuary. American Cyanamid Co., Wayne, N.J., 75 pp. and Table and Figs.

4. Hydroscience, Inc., 1973. Water quality analysis of Manhasset Bay. W.F. Cosulich Assoc., Plainview, N.J., 53 pp. and Figs. and Append.

5. Hydroscience, Inc., 1973. Water quality analysis for the Wallkill River, Sussex County, New Jersey. Sussex Co. Mun. Utilities Auth., Newton, N.J. 81 pp. and Tables and Figs.

6. Hydroscience, Inc., 1974. Water quality analysis of the Hackensack River. Clinton Bogert Assoc., Fort Lee, N.J., 77 pp. and Figs. and Append.

7. Hydroscience, Inc., 1974. Water pollution investigations: Black River of New York. EPA-905/9-74-009 U.S. EPA, Regs. II and V, N.Y. and Chicago, 95 pp.

8. Hydroscience, Inc., 1974. Development and application of a steady-state eutrophication model of the Sacramento - San Joaquin Delta. Bay Valley Consultants, San Fran., Calif. 228 pp. and Append.

9. Hydroscience, Inc., 1975. Water quality analysis of the West Branch of the Delaware River, N.Y., DEC, Albany, N.Y., 102 pp. and Append.

10. Hydroscience, Inc., 1975. Water quality analysis of Pennsauken Creek, Cooper River, Big Timber Creek and Upper Great Egg Harbor River, N.J. DEP, Trenton, N.J., 163 pp. and Append.

11. Hydroscience, Inc., 1976. Water quality analysis of the Jackson River, Vol. I, Westvaco Corp., Covington, Va., 87 pp. and Append.

12. Hydroscience, Inc., 1978. NYC 208 Task Report, Seasonal steady-state modeling (PCP Task 314). Hazen and Sawyer Engrs. N.Y., N.Y., 667 pp.

13. Hydroscience, Inc., 1978. Upper Mississippi River, 208 Grant, water quality modeling study, preliminary report. Met. Waste Control Comm., St. Paul, Minn.

14. Streeter, H.W., and Phelps, E.B., 1925. A study of the pollution and natural purification of the Ohio River, III. Factors concerned in the phenomena of oxidation and reaeration. U.S. Pub. Health Serv., Pub. Health Bull. No. 146, 75 pp.

15. Thomann, R.V., R.W. Winfield and J.J. Segna, 1979 a. Verification analysis of the Ontario and Rochester embayment three dimensional Eutrophication Model. EPA Report in Final Manuscript.

16. Thomann, R.V., and J.J. Segna, 1979 b. Dynamic phytoplankton-phosphorus model of Lake Ontario. To be presented at Phosphorus Management Conf., Rochester, N.Y.

ONE-DIMENSIONAL TIME VARYING ANALYSIS OF STREAMS AND RIVERS*

This section presents various time variable mathematical models for describing water quality variations in streams. The modeling efforts have progressed to the point where a sufficient degree of reliability has been obtained to form the basis for making water quality predictions. These predictions have been applied almost exclusively to water quality problems resulting from the discharge of wastes from municipal and industrial sources. The classical mass balance partial differential equations appear to be reasonably satisfactory for a number of situations. The time variability of various water quality parameters covers a relatively wide spectrum, from the hour-to-hour types of fluctuations resulting from fine microscale phenomena to the day-to-day and season-to-season types of fluctuations reflecting broader scale climatological conditions.

Efficient computational schemes are available to describe the water quality responses in streams due to time variability of waste loads, water temperatures, and river flows. A variety of verifications of the stream models has been accomplished, primarily for dissolved oxygen. The dissolved oxygen verifications indicate that the models generally describe the major features of the time and space variability in both streams and estuaries.

* Donald J. O'Connor

A general mathematical description of natural systems of fresh water which exhibit significant variation of water quality variables in one-dimension are considered below. The variation is assumed to be along the longitudinal axis of flow, with uniformity assumed over the width and depth of channel. Water systems, which may be characterized in this fashion, include the majority of fresh water streams; many rivers, both tidal and non-tidal; and some estuaries. The primary purpose of this section is to develop the equations which are generally applicable to the analysis of water quality in fresh water streams. In most cases, the stream may be defined as a flowing system in which the advective component of the flux is the significant factor in the mass transport; however in some cases the dispersive component may be important in time-variable analysis.

BASIC EQUATIONS

The basic equation of an advective system is developed in the usual fashion by a mass balance over a differential volume. Consider a body of fresh water flowing within a specific, defined boundary. The direction of flow is along the longitudinal axis (x); there are no vertical (y) or lateral (z) gradients of concentration. Turbulent mixing is sufficient to produce uniformity of concentration over the cross-sectional area of flow, but insufficien to cause a significant spreading or distortion along the flow axis. A definition sketch is shown below:

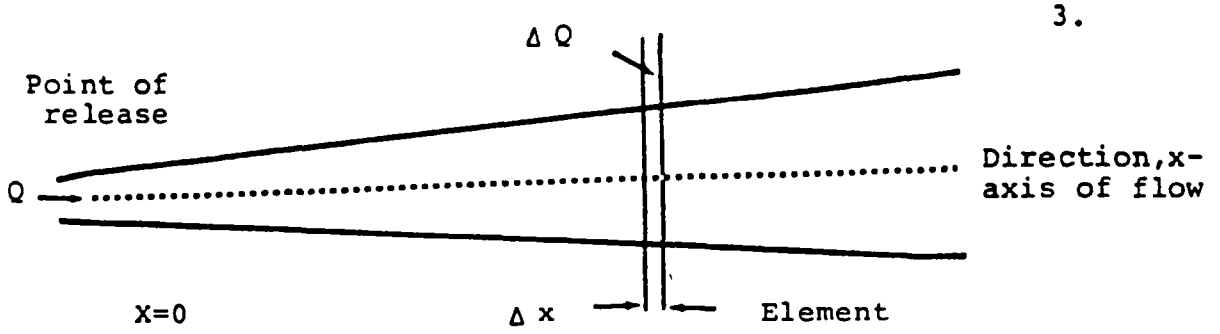

The origin, x = 0, is usually established at the location of the discharge of the wastewater to the stream. Uniformity of concentration over the cross-section is usually effected within a relatively short distance from the outfall. This condition is brought about by the lateral and vertical mixing of the stream or by an appropriate diffuser design. In any case, the assumption of the homogeneity over the cross is realizable from a practical viewpoint.

A mass balance around the elemental volume ($V = A \Delta x$) considers the increase in concentration from c to $c + \Delta c$ over the time interval Δt. At the upstream face the concentration associated with the flow entering the element is c and at the downstream face the concentration leaving is $c + (\partial c/\partial x) \Delta x$. In addition to the change in concentration, it is also appropriate to consider a change in flow ΔQ over the element Δx. This condition is characteristic of many natural streams, in which the increase in flow is due to ground water intrusion or a decrease due to evaporation. By definition, the transport into and from the element is negligible. The change in mass $V\Delta c$ is the net result of the inflow and sources on the one hand, and the outflow and sinks on the other. Furthermore,

allowances for other sources and sinks, including the common physical chemical biological reactions, are made by incorporating them in a single term, S:

$$V\Delta c = Qc\ \Delta t - (Q + \Delta Q)\ (c + \frac{\partial c}{\partial x}\ \Delta x)\ \Delta t \pm S\ \Delta t \qquad (1)$$

Expanding, simplifying and dividing by Δt, there results

$$V\ \frac{\Delta c}{\Delta t} = - Q\ \frac{\partial c}{\partial x}\ \Delta x - c\Delta Q \pm SV$$

Divising through by volum e, V, which equals $A\Delta x$, and simplifying, equation (1) becomes:

$$\frac{\partial c}{\partial t} = - \frac{1}{A}\ \frac{\partial}{\partial x}\ (Qc) \pm S \qquad (2)$$

Equation (2) is the fundamental equation of water quality models of an advective system, which is appropriate for the analysis of most natural streams, particularly those which are either shallow or rapid. The derivative on the right-hand side of eq. (2) is the rate of change of material with mass Qc with respect to distance This derivative can be expanded as follows:

$$- \frac{1}{A}\ \frac{\partial}{\partial x}\ (Qc) = - \frac{1}{A}\ \left[Q\ \frac{\partial c}{\partial x} + c\ \frac{\partial Q}{\partial x} \right] \qquad (3a)$$

If the flow rate is constant downstream, the second derivative is zero, and the coefficient of the concentration derivative becomes the velocity, U = Q/A. It is sometimes useful to ex-

press the advective flow in terms of the velocity, U, and the area, A, in place of their product, Q, the rate of flow:

$$-\frac{1}{A}\frac{\partial}{\partial x}(Qc) = -\frac{1}{A}\frac{\partial}{\partial x}(UAc) = -\left[U\frac{\partial c}{\partial x} + c\frac{\partial U}{\partial x} + \frac{cU}{A}\frac{\partial A}{\partial x}\right] \qquad (3b)$$

The expansion indicates the relative influence of the various parameters and their rates of change with distance and permits evaluation of the error introduced by the common assumption of constancy of the parameters U and A.

INSTANTANEOUS MASS RELEASE

A fundamental experiment which can be carried out in a natural body of water is an instantaneous release of a tracer material such as dye. The mass of material, M, is introduced into the water over a time interval, Δt, which is short relative to the time scale of the processes which govern mass transport in the water body. In the case of a stream, Δt should be in the order of minutes. In addition to being added over a short interval, the mass is usually distributed over the cross section with area A, of the stream. This uniformity over the cross-section is convenient for an analysis of the results of the experiment in terms of one spatial dimension, that along the direction of flow.

In the idealization of the mass transport in a stream, represented by equation (2), the only mass transport mechanism is the advective flow, Q, in the stream. Thus the mass of dye introduced at time $t = 0$ at location $x = 0$ over the time interval $0 \leq t \leq \Delta t$ will move down the stream with the water

velocity U = Q/A. The basic result of the assumption that only advection transports mass is that the mass of dye remains in the parcel of water into which it was introduced and does not spread into any other adjacent parts of the water. It is further assumed that both the area A and velocity U are constants. The length of this parcel of water, denoted by Δx, is $\Delta x = U\Delta t$, and the concentration within the parcel is the mass of dye introduced, M, divided by the volume of water into which it was introduced, and this volume is given by the length of the parcel times its cross sectional area A, i.e. $A\Delta x$. Therefore the concentration is $M/A\Delta x = M/AU\Delta t$. The location of the parcel at any time t is given by the simple relation that the distance travelled at a velocity U during a time t is Ut. Having obtained the concentration of the dye in the parcel and its location at any time t, it is now possible to write an equation for the dye concentration distribution in space and time resulting from the initial discharge of mass, M, over $0 \leq t \leq \Delta t$ at $x = 0$. The equation is

$$c(x,t) = \frac{M}{UA\Delta t} \qquad 0 \leq t - \frac{x}{U} \leq \Delta t \qquad (4)$$

$$c(x,t) = 0 \qquad \text{otherwise}$$

which states that the concentration of dye at location x is zero except over the time interval $\frac{x}{U} \leq t \leq \frac{x}{U} + \Delta t$ during which time the parcel of water at concentration $M/UA\Delta t$ passes by location x. This solution is illustrated in fig. (1a).

To demonstrate that this behavior is indeed predicted by eq. (4), let $c_i(x)$ represent the initial concentration distribution in the stream at t = 0 i.e. $c(x,0) = c_i(x)$. Then by the argument presented above, the concentration at location x at time t should be $c_i(x)$ displaced by the distance travelled during the time from release to time t, that is, Ut. Hence the solution is:

$$c(x,t) = c_i(x - Ut) \tag{5}$$

To see that this solution satisfies the differential equation

$$\frac{\partial c}{\partial t} + U \frac{\partial c}{\partial x} = 0 \tag{6}$$

it is necessary to substitute the solution into this equation. Performing the indicated differentiations:

$$\frac{\partial}{\partial t}\left[c_i(x - Ut)\right] = \frac{\partial c_i(z)}{\partial z}\frac{\partial z}{\partial t} = \frac{dc_i(z)}{dz}(-U) \tag{7}$$

$$\frac{\partial}{\partial x}\left[c_i(x - Ut)\right] = \frac{\partial c_i(z)}{\partial z}\frac{\partial z}{\partial x} \quad \frac{dc_i(z)}{dz}$$

where z = x -Ut and the chair rule is used for taking partial derivatives with respect to x and t. Substituting these results into eq. (2) yields

$$-U\frac{dc_i}{dx} + U\frac{dc_i}{dx} = 0 \tag{8}$$

which is an identity for any c_i so that the solution $c(x,t) = c_i(x-Ut)$ does indeed satisfy the conservation of

mass equation for a stream. The physical interpretation of this result is that the only effect of the stream on the concentration of conservative mass is to transport the mass downstream without any modification of its shape whatsoever. This behavior is illustrated in fig. (16). $c_i(x)$, due to some irregularity in introducing the dye into the stream, is also somewhat irregular. This shape is preserved exactly as the parcel of water moves downstream; no modification of its shape occurs. It is this idealization of the actual behavior of natural streams which is embodied in equation (6).

The idealization proposed in the previous sections for the model of a stream neglected the mechanisms in natural rivers and streams which cause mixing of adjacent parcels of water. These mechanisms include turbulent diffusion, vertical and lateral velocity gradients and the effect of small variations in the geometry of the river. To account for these effects an additional mass transport term, the eddy dispersion term, is included in the conservation of mass equation. The behavior of this equation is more complex than the purely advective equation since the eddy dispersion causes adjacent parcels of water to exchange mass thus producing a smoothing and spreading of the dye mass as it travels downstream.

It is the purpose of this section to illustrate the behavior of these solutions and investigate their relationship to the solutions of the purely advective model. It is assumed

that the parameters ε, A, and Q are constants in time and space and that S = 0. It is convenient to investigate the solution of the river equation to a truly instantaneous discharge of mass, M, at t = 0 and x = 0. In effect, a truly instantaneous discharge occurs when Δt, the interval over which mass is introduced, shrinks to zero. In mathematical terms, this corresponds to an initial concentration in the river given by the following limit:

$$c(x,0) = \lim_{\Delta t \to 0} \frac{M}{UA\Delta t} \qquad 0 \leqslant x \leqslant U\,t \qquad (9)$$

$$= 0 \qquad \text{elsewhere}$$

This equation is of course a mathematical idealization since it requires that an infinite concentration to exist over a zero length of river. In practice however, all that is required is that Δt be small. It should be remarked that the above equation is not a mathematically legitimate limit. It is meant to be only indicative of a function which will be made more precise subsequently, the delta function. In any case, it represents a very narrow spike of concentration at x = 0 due to a mass discharge at x = 0. The solution of the river conservation of mass equation for this initial concentration is:

$$c(x,t) = \frac{M}{2A\sqrt{\pi\varepsilon t}}\, e^{-(x-Ut)^2/4\varepsilon t} \qquad (10)$$

The concentration profile which results is illustrated in Figure (1c). The peak concentration moves with velocity U. However, in contrast to the stream model solution, the

shape of the concentration profile changes as it progresses downstream. The peak concentration decreases and the longitudinal extent of the concentration profile increases as time elapses. Thus the shape of the concentration profile is modified by the eddy dispersion. This occurs because adjacent parcels of water are mixing both upstream and downstream of its original location. In addition, the mass transport effect of the velocity is to transport the whole distribution downstream at a velocity U.

To further illustrate this smoothing effect, suppose the initial concentration at x = 0 and t = 0 is somewhat irregular as in the stream model example. The resulting concentration distribution is illustrated in Figure (1d). The initial irregularity is smoothed out by the action of dispersion and the concentration profile which results at a later time is more regular than the original distribution. It is the importance and degree of this smoothing and spreading that determines which model is used in a particular practical application.

In addition to the concentration distributions portrayed at specific times, it is also convenient to examine the distribution of mass which is observed at specific locations as time passes as represented by equation (10). These distributions are examined in figures (1e) and (1f). Whereas the mass distributions are symmetrical with respect to space as shown

in figure (1c), they are markedly skewed along the temporal axis. This is due to the basic mechanism of dispersion which produces more spreading as time increases. Thus at a fixed time the dispersion experienced both upstream and downstream of the center of the concentration profile is the same and so the distribution is symmetric in space at a fixed time. However at a fixed point in space the concentration profile which is observed experiences more dispersion as time passes so that the initial portion of the profile is more peaked relative to the later portion observed at a later time which is more dispersed and therefore more skewed and spread out. It is these profiles which are normally observed in actual dye dispersion experiments in the prototype.

TIME-VARYING MASS DISCHARGE

A more realistic problem, for which the solution is similar to that in the previous section, is the distribution due to a continuous release of mass, W(t), at x = 0. The initial dilution produces a concentration $c_b(t) = W(t)/UA$ at x = 0. By analogy to the previous section, it seems reasonable to try $c(x,t) = c_b(t - x/U)$ as the solution to equation (2). The boundary condition is obviously satisfied and it is easily shown by direct substitution that equation (2) is satisfied as well.

The general solution to the time variable stream equation (2) strictly speaking involves both an initial condition

$c_i(x)$ which describes the concentration distribution at $t = 0$ for $x \geq 0$ and a boundary condition $c_b(t)$ which describes the concentration at a point $x = 0$ for $t > 0$. By combining the two solutions obtained above, the general solution is:

$$c(x,t) = c_i\ (x - Ut) \qquad x > Ut \qquad (11a)$$

$$c(x,t) = c_b\ (t - x/U) \qquad x < Ut \qquad (11b)$$

The solutions for a non-conservative mass discharge are similar to these equations. The consideration of mass equation is:

$$\frac{\partial c}{\partial t} + U \frac{\partial c}{\partial x} = - Kc \qquad (12)$$

and for initial and boundary conditions $c_i(x)$ and $c_b(t)$, the solution is:

$$c(x,t) = c_i\ (x - Ut)\ e^{-Kt} \qquad x > Ut \qquad (13a)$$

$$c(x,t) = c_b\ (t - x/U)\ e^{-K\ x/U} \qquad x < Ut \qquad (13b)$$

For example, assuming a variable discharge rate from a waste treatment plant, which frequently has a typical diurnal pattern, and assuming a constant fresh water flow and cross-sectional area of the stream and a simple periodic function to describe the discharge, the concentration is:

$$c(x,t) = \left[L_o + a_o \sin \frac{[t - x/U]}{p}\ \pi\right] e^{-\frac{Kx}{U}} \qquad (14)$$

in which

$L_o = \frac{W}{Q}$ = mean concentration over the period, p, at x=0, the location of the waste discharge

a_o = amplitude at x = 0

p = period of the cycle.

The initial variaton, at x = 0, is transferred downstream at a velocity, U, and is attenuated by the characteristic reaction. At any location, x, the variation of the concentration lags the initial by a time interval equal to x/U.

An example of a time-varying waste water discharge, W, and its effect on the dissolved oxygen concentration in the Ohio River downstream from the City of Cincinnati is presented in Figure 2. The four spatial profiles of dissolved oxygen below the major source of wastewater from the Mill Creek Treatment plant were measured on four successive days following a weekend, during which period the mass rate of BOD discharge from the plant is less than the 5-day work week. The effect on the dissolved oxygen concentration of the reduced BOD discharge entering over the weekend is clearly evident as compared to that concentration resulting from the weekday discharge. The peak of the weekend concentration is propagated downstream at the velocity of stream. This case is discussed more fully in a subsequent section. The data is presented at this point to indicate at least qualitatively the nature of the phenomenon as observed in one river and its counterpart in the equations above.

PHOTOSYNTHESIS AND THE DIURNAL DISSOLVED OXYGEN VARIATION IN STREAMS*

The concentration of dissolved oxygen is a significant factor in the evaluation of water pollution and in the management of water quality. In relatively unpolluted waters the dissolved oxygen concentration may fluctuate about the saturation value, a state which results from the dynamic equilibrium among the biological, chemical and physical components of the environment. There is a great diversity of species with no one form predominating, sources and sinks of oxygen are in approximate balance, and the concentration remains close to saturation, with some diurnal variation due to the temperature and photosynthetic activity of green plants. By contrast, in a stream receiving untreated wastewaters, the natural balance is upset, bacteria predominant and, among many other effects, a marked depression of the dissolved oxygen results. In many streams, into which are discharged wastewaters from intermediate or secondary treatment processes, the dissolved oxygen condition reflects characteristics of both these extremes and it is quite common to observe both bacterial and algal effects. The classic sag in the dissolved oxygen distribution may be observed, superimposed on which is a diurnal fluctuation due to algae growths, stimulated by the nutrients from the waste source or from the end products of earlier reactions. On the one hand, the bacteria

---

*O'Connor, D.J., Di Toro, D.M., J. ASCE Vol. 96, SA2, April 1970.

produce a typical longitudinal distribution of dissolved oxygen deficit, the components of which are the carbonaceous and nitrogenous sources in the wastewater, the latter being more significant in secondary effluents. On the other, the algal effects cause a typical diurnal fluctuation, which generally increases in amplitude downstream from the source, reaching a peak and subsequently decreasing to levels characteristic of upstream stretches. It is the specific purpose of this section to present a mathematical formulation of the effect of these factors on the dissolved oxygen concentration in rivers, particularly with respect to the photosynthetic effect.

Theory

The most general form of equation which describes the longitudinal distribution of dissolved oxygen or any non-conservative or conservative substance is developed by a mass balance employing the continuity equation. The specific form of the equation for a given stream is determined by the hydraulic, hydrological and geomorphological characteristics of the drainage basin and river channel, on the one hand, and the various physical, chemical and biological characteristics of the aquatic environment and wastewater discharges on the other. For the rivers and conditions considered in this section, Equation (2) takes on the following form for the concentration of dissolved oxygen.

$$\frac{\partial c}{\partial t} = - \frac{Q}{A} \frac{\partial c}{\partial x} + K_a (c_s - c) - K_d L(x) - K_n N(x) + P(x,t) - R(x) - S(x) \qquad (15)$$

in which

c = concentration of dissolved oxygen

c_s = saturation value of dissolved oxygen

K_a = reaeration coefficient

K_d = coefficient of carbonaceous oxidation

$L(x) = L_o e^{-K_r \frac{x}{\bar{U}}}$ = distribution of carbonaceous BOD. $U=Q/A$

K_n = coefficient of nitrogenous oxidation

$N(x) = N_o e^{-K_n \frac{x}{\bar{U}}}$ = distribution of nitrogenous BOD. $U=Q/A$.

$P(x,t)$ = algal photosynthetic oxygen source

$R(x)$ = algal respiration sink

$S(x)$ = benthic bacterial respiration sink.

The common sources of dissolved oxygen are those due to atmospheric reaeration, the photosynthetic contribution of the algae and incoming flow, while the sinks are the respiratory functions of bacteria and algae in both planktonic and benthic environments. The bacterial respiration is composed of carbonaceous and nitrogenous components. The bacterial respiration of benthic community is assigned as a separate sink. The algae in both floating and stationary form are included as a single source. For the sake of mathematical simplicity the spatial distributions of both the photosynthetic source and the respiration sink are assumed to begin abruptly at $x = 0$ and remain constant for $x > 0$. The effect of any upstream algal activity, i.e. for $x < 0$, is taken into account in the boundary condition at $x = 0$. The temporal form of the respiration sink is assumed to be a constant R. This

is the traditional assumption and it appears to be justifiable to within the accuracies of the data so far available. The temporal variation of the photosynthetic oxygen source is a result of the solar radiation incident on the algae present. The variation of oxygen production with increasing solar radiation and the attenuation of solar radiation with increasing depth have been investigated.* With increasing solar radiation the rate of oxygen production increases to a saturation value and then decreases. For a bright day, at the top layer of water, the oxygen production may be less at midday than during the morning and afternoon. However, solar radiation decreases with depth so that in the middle of the euphotic zone the oxygen may be more or less proportional to the sunlight intensity. If the average over depth is taken then the shape of the cross-sectional average photosynthetic oxygen production rate resembles the shape of the incident solar radiation.** For the sake of simplicity the temporal form of the photosynthetic oxygen source is assumed to be representable by a half-cycle sine wave. If more complete information is available this assumption can be refined. Let P(t) represent the rate of photosynthetic oxygen production as a function of time, thus P(t) is given by

$$P(t) = P_m \sin\left[\frac{\pi}{p}(t-t_s)\right] \quad t_s \leq t \leq t_s + p$$
$$= 0 \qquad\qquad\qquad\qquad t_s + p \leq t \leq t_s + 1 \qquad (16)$$

---

* Ryther, John H., "Photosynthesis in the Ocean as a Function of Light Intensity" Limnology & Oceanography, Vol. I,1956 pp. 61-70.

** Westlake, D.J. "A Model for Quantitative Studies of Photosynthesis by Higher Plants in Streams" Air and Water Pollution Journal, Vol. 10, pp. 883-896.

where

P_m = the maximum rate of photosynthetic oxygen production (mg/l day)

t_s = the time at which the source begins (days)

p = the fraction of the day over which the source is active (days).

This function is assumed to repeat periodically every day. Equation (16) specifies P(t) for one day only; its periodic extension can be expressed as a Fourier series:

$$P(t) = P_M \left\{ \frac{2p}{\pi} + \sum_{n=1}^{\infty} b_n \cos \left[2\pi n \, (t - t_s - p/2) \right] \right\} \qquad (17a)$$

where

$$b_n = \cos (n\pi p) \; \frac{4\pi/p}{(\pi/p)^2 - (2\pi n)^2} \qquad (17b)$$

Using this expression for the photosynthetic oxygen source and expressing Equation (1) in terms of dissolved oxygen deficit, $D(x,t) = c_s - c(x,t)$, results in

$$\frac{\partial D}{\partial t} + \frac{Q}{A} \frac{\partial D}{\partial x} = - K_a D + K_d L(x) + K_N N(x) + S - P(t) + R \qquad (18)$$

in which S is assumed to be constant.

For an initial condition $D(x,0) = 0$, $x > 0$, and an arbitrary boundary condition $D_o(t)$, Equation (18) has as its solution:

$$D(x,t) = D_o\ (t - \tfrac{x}{U})\ e^{-K_A \frac{x}{U}} \tag{19a}$$

$$+ \frac{K_d\ L_o}{K_A - K_d}\left[e^{-K_r \frac{x}{U}} - e^{-K_A \frac{x}{U}}\right] \tag{19b}$$

$$+ \frac{K_N\ N_o}{K_A - K_N}\left[e^{-K_N \frac{x}{U}} - e^{-K_A \frac{x}{U}}\right] \tag{19c}$$

$$+ \frac{S}{K_A}\left[1 - e^{-K_A \frac{x}{U}}\right] \tag{19d}$$

$$+ R\left[1 - e^{-K_A \frac{x}{U}}\right] \tag{19e}$$

$$- P_m \left\{ \frac{2p}{\pi K_A}\ (1 - e^{-K_A \frac{x}{U}}) \right. \tag{19f}$$

$$+ \sum_{n=1}^{\infty} \frac{b_n}{\sqrt{K_A^2 + (2\pi n)^2}} \cos\left[2\pi n(t - t_s - p/2) - \tan^{-1}\left(\frac{2\pi n}{K_A}\right)\right] \tag{19g}$$

$$\left. - e^{-K_A \frac{x}{U}} \sum_{n=1}^{\infty} \frac{b_n}{\sqrt{K_A^2 + (2\pi n)^2}} \cos\left[2\pi n(t - t_s - p/2 - x/U) - \tan^{-1}\left(\frac{2\pi n}{K_A}\right)\right] \right\} \tag{19h}$$

It has been assumed in this solution that the periodic photosynthetic source has been active for a long time i.e. a periodic steady state has been achieved.

Equations 19b, 19c and 19d are the well known deficit solutions due to BOD and benthic sinks of DO. Equation 19a is the solution for a time-varying initial deficit of DO. The portion of the dissolved oxygen deficit solution due to the photosynthetic source and respiration sink is made up of three parts. The average daily photosynthetic oxygen production (equation 19f) and the respiration (Equation 19e) portion of the solution are constant in time and build up to their equilibrium values of P_{av}/K_a and R/K_a respectively as x/U increases. The term Equation 19g is independent of position and represents the solution after the effect of the initial abrupt beginning of the photosynthetic source at x = 0 has decayed to zero. The portion of the solution which is due to the abrupt beginning (Equation 19h) is multiplied by an exponential which goes to zero as x/U increases. For large K_a, as is the case in the streams to be analyzed herein, the diurnal fluctuation of the solution due to the photosynthetic source has zero amplitude at x = 0 and increases to the steady state amplitude given by Equation 19g.

The following effects have not been included in this solution: the time variation of the flow, the time variation of the temperature and wastewater discharges, and the effect of dispersion. In the streams to which this solution is applied it is assumed that the primary cause of the diurnal variation of the dissolved oxygen is the algal oxygen production.

EXAMPLES

Five rivers have been selected for analysis, the Grand River[1], the Clinton River[2] and the Flint River[3] in Michigan; the Truckee River[4] in Nevada, and the Ivel River[5] in Great Britain. The selection is based on the availability of historical data which is complete enough for the proposed analysis, the emphasis being on the diurnal behavior of dissolved oxygen and the effect of the nitrogenous BOD component. The data available for analysis was observed during periods when a reasonable approximation of a steady-state flow and temperature prevailed.

The average cross-sectional area for each river except the Flint and the Ivel is obtained from the reported time of passage studies and average river flows. For the Flint River, detailed cross-sectional information, Figure 9, is available, for the Ivel the average depths are reported in all cases except the Grand for which it has been subsequently obtained and the Ivel for which it has been back calculated from the reported exchange coefficient. Using these data, the reaeration coefficient is calculated from the formula:

$$K_a = (D_L U)^{1/2}/H^{3/2} \qquad (20)$$

The reported average temperatures are then used to correct this value to the stream condition during the survey and establish the saturation value of dissolved oxygen. The coefficient of 1.025 was used to make the temperature adjustment for the reaeration coefficient[6].

The procedure followed for the analysis of the carbonaceous and nitrogenous BOD data relies on the observed river values, although

known effluent concentrations and flows from treatment plant in the reaches analyzed are used to establish loads. The carbonaceous and nitrogenous reaction coefficients, K_d and K_n, are determined from a plot of the logarithm of the particular component of the BOD versus distance from the source. The slope of the line, multiplied by the velocity, yields the coefficient. The nitrogenous and carbonaceous components of the BOD data are obtained in a variety of ways: nitrification suppression using methylene blue for the Grand; estimated ultimate first stage BOD, organic nitrogen and ammonia measurements for the Truckee; 5-day BOD and some ammonia measurements for the Flint. There is no reported nitrogen data for the Clinton, and the Ivel is relatively unpolluted, having no significant concentration of BOD. The concentrations, L_o and N_o were taken from the direct measurements and checked whenever possible, by a mass balance upstream and downstream of the waste discharge.

The BOD analysis establishes the sinks of oxygen due to the carbonaceous and nitrogenous-BOD. There remains the algal source and sink of oxygen. The procedure adopted to obtain P_m and R is largely one of trial and error based primarily on the magnitude of the diurnal fluctuation at the various stations downstream and guided by whatever qualitative information is available about the algal populations. The two times t_s and p are established using the time of sunrise and sunset. It has been found that that best fits are obtained if t_s is slightly later than sunrise and if p is slightly less than the total time between sunrise and sunset. This is probably due to the fact that the assumed shape of the photosynthetic oxygen source rises and sets more quickly than

apparently is the case.

The procedure is as follows: the diurnal dissolved oxygen data at the first station establishes the boundary condition. This condition, the carbonaceous and nitrogenous BOD sinks, and assumed values of P_m and R are used for the first uniform segment of river. A uniform segment ends at either a load which alters the BOD concentrations and possibly the structure of the algal population, or a discontinuity in area or depth, or a discontinuity in P_m and R reflecting a change in algal productivity. At such a point the values of the parameters change and numerical calculations are initiated again. The boundary condition used is the diurnal distribution calculated for the end of the previous segment. In effect, this procedure makes possible the solution of more general stream configurations which are limited only to piecewise constant spatial parameters. Using this technique the values of P_m and R which best fit the data are chosen. The choice of P_m is guided by the fact that the magnitude of the diurnal fluctuation at a station is directly proportional to P_m so the change in P_m which is required to fit the data can be calculated after one trial. The appropriate value of R can be chosen by expressing the data as deficit of DO and trating the respiration source of deficit independently of the other sources and sinks. Since the respiration is assumed to be a constant in time, its effect is only to lower the average daily value of the DO. Hence the appropriate value can be obtained from a spatial plot of the time averaged data. Using this procedure, then, it is possible to chose P_m and R more-or less independently since the P_m is chosen using the magnitude of the diurnal fluctuations as a guide and the R is chosen using

average values. Therefore under the assumption that respiration is a constant in time it is possible to separate these two algal effects. It should be recognized, however, that the respiration is, in effect, all respiration not accounted for by other sinks of DO, and to that extent is not necessarily only algal respiration. For example, it may be benthic respiration which has not taken explicity into account. On the other hand, the final choice of R does reflect all that is known about the river oxygen balance, e.g. benthic respiration can be independently assigned, and, to that extent, it can be reliably estimated.

Tabulations of hydraulic characteristics, the parameters, and the boundary conditions employed in this analysis are presented as follows: Table 1 includes the location of beginning of the segments, their lengths (X), cross-sectional areas (A), depths (H), temperatures (T) and river discharge (Q), reaeration coefficient (K_a), and carbonaceous and nitrogenous reaction coefficients (K_d, K_n). The time variable initial conditions of dissolved oxygen are presented in Table 2. Table 3 lists the parameters defining the algae effects: the time (t_s) at which the photosynthetic oxygen source begins, the period (p) over which the source is non zero, the maximum rate (P_m) of photosynthetic oxygen production, the daily average rate of photosynthetic oxygen production $P_{av} = 2p\ P_{m/\pi}$, the rate of algal respiration (R) and the ratio of P_{av} to R.

Grand River

The Grand River is located in the southwestern part of Michigan, flows westerly to Lake Michigan and has a drainage area of 5,620 square miles. The City of Lansing is located approximately 150 miles upstream from the mouth of the river. The analysis of a survey conducted in August 1960 extends from the discharge of the waste treatment plant to a point about 25 miles downstream. The treatment plant is a biological process of the activated sludte type. The possibility of nitrification as an important factor in the oxygen balance was recognized at the time of the survey and nitrification suppressed BOD's by methylene blue were also obtained. No benthic respiration is assumed since the river velocities prior to the survey were large enough to scour the bottom. Insufficient information is available upstream of the Lansing waste discharge to include this region in the analysis. The analysis is begun at the Lansing treatment plant using river conditions extrapolated from downstream values as the initial conditions. No diurnal DO fluctuation is assumed for the boundary condition. The reach up to the Grand Ledge Dam, Stations 1, 8, 9, 10, is assumed to be spatially uniform. Downstream of the dam, Stations 11, 12, 13, 14, profuse attached aquatic plants alter the composition of the algal community and it becomes much more productive. Accordingly at the dam a new segment is begun with different P_m and R. A comparison of the calculated profiles and observed data are shown in Figures 3 and 4.

In particular it is clear that the nitrogenous BOD is an important factor in the oxygen balance in streams. For the second

segment analyzed two curves are shown corresponding to $P_m = 50$ and $P_m = 65$ mg/l-day. These two curves are intended to describe the data taken on the two successive days, August 29th and 30th. The solar radiation data available[7], Figure 3, indicates that the second day was indeed brighter than the first; hence a larger production of oxygen is expected. This effect is not clearly discernible in the data upstream of the dam. For the first segment the ratio of average daily photosynthetic production of oxygen to the average daily respiration $P_{av}/R = 0.35$, indicating that the planktonic community is a net liability to the dissolved oxygen resources of the stream. Downstream from the dam the ratio equals 1.1 and 1.4 respectively which implies the converse. In this stretch of the stream the algal community includes benthic algae and larger aquatic plants as well as any planktonic algae which may be present.

Clinton River

The Clinton River, located in the southeast cornner of Michigan in the Lower Peninsula, discharges into Lake St. Clair. The basin has a drainage area of approximately 740 sq. mi. The reach considered in this analysis of survey conducted during August 23-25, 1960 starts at mile point 44.87, Station 2, below the Pontiac Waste Treatment Plant effluent at mile point 46.39 and ends at mile point 34.98, Station 8. A boundary condition is established at Station 2 by fitting a two term Fourier series to be observed dissolved oxygen data. The reach including Stations 3, 4, 5 and 6 is assumed to be spatially uniform. The aquatic vegetation in this

stretch seems to be mainly attached bottom plants. Between Station 6 and Station 7 the algal population appears to increase in productivity and the survey report cites "numerous weed beds" in this reach. To account for this spatial change a new segment is established 0.5 miles below Station 6 and includes Stations 7 and 8. In this segment the productivity increases markedly while the respiration decreases slightly. The ratio of P_{av} to R changes from 0.43 to 0.84. This pattern is similar to that encountered in the analysis of the Grand River. The resulting theoretical curves are compared to the data in Figure 5.

Truckee River

The Truckee River is located near the western border of Nevada and flows in a northeasterly direction from Lake Tahoe to Pyramide Lake, Nevada, a distance of 106 miles. The reach considered in this analysis begins at mile point - 2.8 (river miles below the Reno U.S.G.S. gage) designated as Station 1 and ends at Station 7, mile point 21.0. The survey was conducted in the period from July 10 to 25, 1962. Within the reach there are three principle sources of wastewater: the Reno Waste Treatment Plant effluent at mile point 0.7, the effluent from the Sparks Waste Treatment Plant which enters at mile point 6.0 and Steamboat Creek entering at mile point 5.7 whose flow is partially irrigation return waters and agriculture drainage. The latter two sources will be treated as one combined source at mile point 5.9. For this analysis, therefore, the reach will be divided into three sections: Station 1 to the Reno Waste Treatment Plant, Reno to Sparks - Steamboat Creek, and Sparks - Steamboat Creek to Station 7.

The analysis of the carbonaceous BOD follows that given in the report of the survey. Five-day BOD's, corrected for the onset of nitrification, are used to obtain ultimate carbonaceous BOD. The available nitrogen data comprises measurements of organic nitrogen, ammonia nitrogen, nitrite nitrogen and nitrate nitrogen. No appreciable ammonia nitrogen is found in section 1. At the beginning of section 2 the abrupt increase of ammonia nitrogen can be attributed to the Reno effluent. There follows a substantial decrease of both ammonia nitrogen and total nitrogen in section 2. For section 3 ammonia is seen to decrease further while total nitrogen is approximately constant. The nitrate values increase correspondingly. The ammonia nitrogen values can be converted to their nitrogenous BOD equivalents using a stochiometric balance (NBOD = 4.6 x NH_3-N). In order to account for the decrease in total nitrogen in Section 2 it is hypothesized that the benthic algae in this section are metabolizing that fraction of the ammonia necessary to account for the decrease in total nitrogen. This is taken in to account by introducing a benthic sink of NBOD in section 2 only. The remaining NBOD is assumed to oxidize to nitrate following a first order reaction.

The algae population in the three sections are described in the survey report: Station 2 "...abnormally profuse growth of a filamentous alga (Cladophora)"; Station 3 "... lack of Cladophora ... in its place the tolerant blue-green oscillatoria and the green filamentous algae Stigeoclonium were quite evident"; Stations 5, 6, and 7, "The tolerant algal forms found at Station 3 were not observed at Stations 5, 6 and 7, however growths of Cladophora were present. Sparce growths of a rooted aquatic pondweed (Potamogeton) were present at

Stations 5 and 6, but not at Station 7." Photoplankton samples at three stations (1A, 3, 5) within the reach were analyzed; diatoms were the dominant form and the number per ml. were respectively 1310, 7680 and 6380. Hence the division of the reach into three sections also coincides with the changes in algal populations.

An interesting phenonomena is observed to occur between Station 4 upstream of the combined load at mile point 5.9 and Station 5 the next downstream at mile point 8.7. The diurnal fluctuation of DO at Station 4 is 7 mg/l while at Station 5 it is 2 mg/l. This decrease in diurnal fluctuation cannot be explained as a result of a decrease in P_m since the effects of the upstream fluctuations at Station 4 would still be quite significant at Station 5. The decrease in diurnal fluctuation is due to the low concentration of DO of the incoming wastewater which not only lowers the average value of DO but also decreases the amplitude of the diurnal fluctuation. The value of P_m in section 3 decreases as can be seen from the distribution of DO at Stations 6 and 7. The theoretical curves are compared to the data in Figures 4 and 5.

In O'Connell's[8] analysis of the reach between Stations 2 and 4, the values of maximum photosynthetic production (P_m) and average daily respiration (R), as shown in their Figure 5 are P_m = 50 mg/l-day and R = 17 mg/l-day for Station 2B, which are comparable to the values arrived at in the above analysis. However as shown in their Figure 6, they also obtain a spatially varying photosynthetic production and respiration. Unfortunately detailed dissolved oxygen data between Stations 2, 3 and 4 is not available in the survey reports so that further analysis is not possible. There are good

physical reasons to suppose that the algal photosynthetic source and sink do not change abruptly as has been assumed herein, however for the data currently available this simplification is warranted.

Ivel River

The Ivel River, located in Great Britain, is a shallow chalk stream. Diurnal dissolved oxygen data is available at two stations; each station was sampled every 15 minutes for 24 hours during May 1959. Following the same procedure as previously outlined, the upstream station diurnal dissolved oxygen data is approximated using a two-term Fourier series and the data at the downstream station is compared to the theoretical prediction. The result is shown in Figure 8; the parameters are listed in Tables 1 to 3. In order to fit the afternoon data, the period of sunlight is extended one hour more than is justifiable from the solar radiation data. Since the solar radiation measurements were taken 16 miles from the river site there is a possibility that this data is not representative. A comparison can be attempted between the photosynthetic production and respiration rates estimated by Edwards and Owens[5] and those indicated in Table 3. Unfortunately the average depth of the Ivel is only an estimate based on the reported exchange coefficient and formula for the reaeration coefficient. However using this value of H = 0.45 m, Edwards' and Owens' estimates in concentration units are: P_m = 58 mg/l-day and R = 17 mg/l-day which are comparable to the estimates arrived at by this analysis.

Flint River

The Flint River, located in the eastern-central portion of Michigan, has a drainage area of 1,350 sq.mi. The reach analyzed in this paper extends from Station 6, Stevenson St., Flint, to Station 15, Dodge Rd., of the July 28-29, 1959 Survey of the Michigan Water Resources Commission. River cross-sectionings at 500 ft. intervals are available and the cross-sectional area and depth are presented in Figure 9. The variation of the cross-sectional area and depth as a function of distance downstream necessitates the division of the reach under analysis into five uniform segments which approximately account for the observed variations. The two major point sources of BOD and DO deficit are the Flint and the Flushing Sewage Treatment Plants, both of which are trickling filters. The carbonaceous and nitrogenous BOD concentration of the effluent of the Flint STP is reported; the corresponding information for the Flushing STP is estimated from the available river BOD and nitrogen data. The existence of a benthal deposit is reported below the Flint STP and its effect on the oxygen balance is estimated from the river DO data. Although the carbonaceous BOD information is adequately representative, the nitrogenous BOD information is somewhat limited, comprising four ammonia concentrations taken a week before the actual survey.

At the beginning of section 1, the initial conditions are established from the reported river data (Table 2). A relatively high rate of nitrogenous BOD oxidation in this section is confirmed

by the available river ammonia data. The Flint load marks the beginning of section 2. As usual materials balance between the reported loads of CBOD, NBOD, and an assumed dissolved oxygen concentration of zero in the effluent with calculated distributions establishes the initial conditions. In this short segment, a benthic respiration load due to a reported sludge deposit is included. Since no independent measurement of the oxygen uptake rate of the sludge deposit is available it is difficult to distinguish its effect on the river dissolved oxygen from the algal respiration. Hence the assumed benthic and algal respirations are arbitrarily assigned although the magnitude of their sum is that required by the observed oxygen data. The diurnal distribution of dissolved oxygen at Station 10 is a result of both a decrease of algal productivity due to water quality conditions which are not conducive to algal growths and the deficit contributed by the Flint Treatment Plant. This phenomenon has also been observed in the Truckee.

The dissolved oxygen data in section 3 reflects the increased photosynthetic production of oxygen. The authors report that this section of the river is "nearly choked with submerged grass-like aquatic vegetation probably Vallisneria or Sagittaria". As a consequence the afternoon dissolved oxygen distribution reaches nearly a saturated level at the end of the section. However the morning distribution shows almost zero DO throughout the stretch. With these low DO concentrations prevailing during part of the day it is reasonable to assume that no appreciable nitrification is

occurring in this section. Although not explicitly confirmed by the river ammonia data, this assumption seems justifiable in light of the concentrations of both ammonia and dissolved oxygen in the section.

It is interesting to note that there are significant departures from the theoretical diurnal dissolved oxygen distribution and the observed distribution at Station 12 (see Figure 10). Here the DO is substantially zero during the late evening and early morning hours. This low dissolved oxygen appears to be affecting the bacterial and/or algal activity, as indicated by the shape of the diurnal dissolved oxygen curve.

The dissolved oxygen data at Stations 13 and 14 in section 4 after the Flushing STP show a recovery and also indicate that a phytoplankton activity is significant. The amount of rooted aquatic vegetation is reported as sparce; yet the diurnal dissolved oxygen data indicate that the average photosynthetic oxygen production is $P_{av} = 19$. In section 5, the average daily oxygen photosynthetic production increases to $P_{av} = 22$, in accordance with the observed increase in the amount of grass-like aquatic plants from sparce to moderate.

The spatial distribution of dissolved oxygen at the two times reflecting the extreme conditions are presented in Figure 9. The theoretical diurnal curves are compared to the data in Figure 10.

CONCLUSION

The computations based on the proposed formulation agree reasonably well with observations in various fresh water streams. Both carbonaceous and nitrogenous components of bacterial activity, atmospheric reaeration, benthal deposits and the photosynthetic and respiratory contribution of the algae and other aquatic plants have been considered. Although primarily directed to an analysis of the dissolved oxygen condition, the analysis may be used for productivity and respiration studies of aquatic communities. The photosynthetic effect can be the dominant factor in the diurnal variation of dissolved oxygen as shown by the rivers investigated in this paper. These effects are primarily due to algae, although larger rooted plants may be important in some cases. The growth of the aquatic vegetation is stimulated by nutrients discharged to the streams from the various sources within the drainage basin, particularly the effluent waters from treatment plants.

Correlations of computed profiles and observed data in both the spatial and temporal domains are favorable. Therefore, more confidence can be placed in the ability to predict the effects of wastewater discharges on receiving waters. Particularly important is the effect of the demand of the nitrogenous component on the oxygen resources. It is significant to date that all of the streams analyzed in this paper receive effluents from biological treatment plants. The importance of nitrification has been demonstrated indicating the need to take this factor into account with respect to secondary treatment. It can be generally expected that this pattern of increased algal activity and nitrification

will occur when secondary treatment facilities are installed. The method of analysis presented provides a further technique for water pollution analysis and should be useful in comprehensive planning of water pollution control facilities.

Further work should be directed to analysis of stream conditions before and after treatment facilities are constructed and of time variable phenomena such as rresh water flow, temperature and wastewater discharge.

Acknowledgment

This work was supported by a research grant from the Federal Water Pollution Control Administration - WP-01468.

APPENDIX IV.—NOTATION

The following symbols are used in this paper:

A = cross-sectional area;
b_n = nth Fourier coefficient of photosynthetic oxygen source;
c_s = saturation value of dissolved oxygen;
$c(x,t)$ = concentration of dissolved oxygen;
$D(x,t)$ = dissolved oxygen deficit concentration;
$D_o(t)$ = boundary condition of dissolved oxygen deficit;
D_L = diffusivity of dissolved oxygen;
H = river depth;
K_a = reaeration coefficient;
K_d = deoxygenation coefficient of carbonaceous BOD;
K_n = deoxygenation coefficient of nitrogenous BOD;
$L(x)$ = carbonaceous BOD concentration;
L_o = $L(o)$;
$N(x)$ = nitrogenous BOD concentration;
N_o = $N(o)$;
$P(t)$ = photosynthetic oxygen source;
P_m = maximum rate of photosynthetic oxygen production;
P_{av} = average daily photosynthetic oxygen production;
p = duration in time of photosynthetic oxygen source;
Q = volumetric flow rate;
R = algal respiration sink of dissolved oxygen;
$S(c,x,t)$ = total sources and sinks;
S = benthic respiration sink of dissolved oxygen;
s = LaPlace transform variable;
T = period of photosynthetic oxygen source = 1 day;
t = time;
t_s = time at which photosynthetic source begins;
U = Q/A = stream velocity;
W = loading rate, in pounds per day BOD;
x = distance downstream;
x/U = travel time from x = 0; and
ω_o = radian frequency of the photosynthetic oxygen source = $2\pi/T$.

References

1. Courchaine, Robert J., State of Michigan Report on Oxygen Relationships of Grand River, Lansing to Grand Ledge, 1960 Survey, Water Resources Commission, Mich., May 1962.

2. Gannon, John J., River BOD Abnormalities, Dept. of Environmental Health, School of Public Health, Univ. of Mich., Nov. 1963.

3. Courchaine, Robert J., State of Michigan Report on Oxyge.. Relationships of Flint River, Flint to Montrose, 1959 Survey, Water Resources Commission, April 1960.

4. O'Connell, R.L. et al. Report of Survey of the Truckee River, Field Operations Section, Technical Services Branch, Div. of Water Supply & Pollution Control, PHS, July 1962.

5. Edwards, R.W., and Owens, M., "The Effects of Plants on River Conditions IV. The Oxygen Balance of a Chalk Stream', J.Ecol. 50, pp 207-220, Feb. 1962.

6. Churchill, M.A., Elmore, H.L., Buckingham, R.A., Prediction of Stream Reaeration Rates, Proc. ASCE J. San.Engr.Div., SA 4 p. 1, July 1962.

7. Strommen, N.D., Personal Communication, Weather Bureau, East Lansing, Mich.

8. O'Connell, R.L., and Thomas, N.A., "Effects of Benthic Algae on Stream Dissolved Oxygen", J. San. Eng. Div., ASCE, Vol. 91, No. SA3, June 1965, Proc. paper #345.

APPENDIX

NUMERICAL CALCULATION METHODS*

For complex natural systems it is often necessary to solve the conservation of mass equations numerically. Consider the following general equation:

$$\frac{\partial c}{\partial t} + U(x,t)\ \frac{\partial c}{\partial x} = S\ (c,x,t) \qquad (1)$$

in which t = time; x = distance downstream; c(x,t) = concentration of the substance being considered; U(x,t) = velocity of the stream; and S(c,x,t) = distributed sources and sinks of the substance being considered.

For a boundary condition at x = 0

$$c(0,t) = c_b(t)\ \ t \geq 0 \qquad (2a)$$

and an initial condition at t = 0

$$c(x,0) = c_i(x)\ \ x \geq 0 \qquad (2b)$$

the solution of Eq. 1 specifies the concentration over the region $x \geq 0$, $t \geq 0$.

Two analytical techniques have been employed to obtain solutions for this equation: the method of characteristics (9,10), and the LaPlace transform (5,12).

The method of characteristics which was developed by J. Massau in graphical form, has been successfully applied to

---

*Di Toro, D.M., J. ASCE, Vol. 95, SA4, Aug. 1969

propagation problems (1) and particularly to problems of open channel flow (4). The LaPlace transform is a powerful technique for obtaining solutions to the preceding equations in certain simplified situations, i.e., when the equation is linear, and the parameters are functions of time only. However, for the general equation with the velocity as a function of both space and time and for the source term involving possibly a nonlinear expression in concentration (e.g. a second order reaction term) no known general solution for arbitrary initial and boundary conditions is available. It is of interest, therefore, to inquire into numerical techniques that are applicable to these more complex problems in stream analysis.

The basic technique for obtaining numerical procedures for the solution of differential equations involves the replacement of the derivatives in the equation with finite difference approximations. A summary has been given (2,3) of techniques applicable to Eq. 1 for which the x,t plane is divided into a rectangular grid and the derivatives with respect to x and t are expressed as differences. Both explicit and implicit techniques have been investigated. Implicit techniques become unwieldy when Eq. 1 is nonlinear since the resulting simultaneous equations which must be solved at each time increment are also nonlinear. Explicit techniques tend to become inaccurate for initial conditions and parameters which are not smooth. The resulting increase in computing time and computer memory necessary

to preserve accuracy can be significant since the spacing of the spatial grid, Δx, and the temporal grid, Δt, must satisfy a stability criterion: $U\Delta t/\Delta x \leq 1$. Also, there is no method available to estimate the resulting error for a specific choice of Δx and Δt so that the accuracy of the resulting calculations is in doubt.

A second class of numerical techniques which are applicable to the solution of Eq. 1 are based directly on the original idea of Massau, i.e., the equation is integrated along its characteristics. The analytical basis of the proposed numerical method is the observation that Eq. 1 can be reduced to a coupled pair of ordinary differential equations using the method of characteristics. These equations can then be integrated using standard numerical techniques for a set of ordinary differential equations. A direct application (8) of the method of characteristics to Eq. 1 transforms this equation into two ordinary differential equations.

$$\frac{dx(t)}{dt} = U\,[x(t),t] \tag{3a}$$

$$\frac{dc[x(t),t]}{dt} = S\{c[x(t),t],\ x(t),t\} \tag{3b}$$

The curves $x(t)$ obtained from the solution of Eq. 3a are called the characteristics of Eq. 1 and this family of curves specifies the direction along which the solution propagates.

The method is based on the well known idea of integrating quasi-linear partial differential equations along the characteristics of the Eq. 6. However for the case of Eq. 1 the important difference which makes this method superior to the methods based on a rectangular grid is that, in contrast to other equations, Eq. 1 has only one family of characteristics, all of which allow propagation only in the downstream direction. Hence the solution along each characteristic can be obtained independently of the solution along neighboring characteristics.

A physical argument can be given which expresses the content of the method of characteristics. The consequence of having assumed that dispersion is not of significance is that cross-sectional segments of water of differential thickness in the x direction retain their identity as they flow downstream. If the velocity is known then it is possible to calculate the position of any segment of water and to follow it downstream. It is as if a segment of water is tagged with dye, so that its position can be determined as a function of time (11). What occurs inside this segment of water is described by an ordinary differential equation in time Eq. 3b. The coefficients of this equation which are functions of time can be evaluated directly since time can be determined, e.g. by a clock; the coefficients which are functions of position or position and time can also be evaluated since the position of the segment of water being considered is known from the

solution of Eq. 3a. Hence, the behavior of each differential segment of water can be calculated once its initial concentration is established at some initial point in space and time. This initial point corresponds to the point at which an initial or boundary condition is established.

The initial conditions for Eqs. 3a and 3b are determined from the initial and boundary conditions of Eq. 1. Consider the segment of water which passes $x = 0$ at $t = t_o$ for some $t_o \geq 0$. The initial conditions that apply to Eqs. 3 are established as the segment passes into the region under consideration. Hence the initial conditions are given by the boundary condition (Eq. 2a) of Eq. 1, i.e. for $t = t_o$,

$$x(t_o) = 0 \tag{4a}$$

$$c(0,t_o) = c_b\ (t_o) \tag{4b}$$

For these initial conditions, each solution of the pair of differential equations, Eq. 3, specifies the behavior of $c(x,t)$ within the segment of water that passes $x = 0$ at $t = t_o$.

For those segments that are already in the region of interest, $x \geq 0$, at $t = 0$, the initial conditions for the pair of Eqs. 3 are specified by the initial condition, Eq. 2b, of Eq. 1. That is for the point $x = x_o$, $x_o \geq 0$ at $t = 0$, the initial conditions for Eq. 3 are

$$x(0) = x_o \tag{5a}$$

$$c(x_o,0) = c_i\ (x_o) \tag{5b}$$

For these initial conditions, each solution of the pair of differential equations (Eq. 3) specifies the behavior of $c(x,t)$ within the segment of water that is at x_o at $t = 0$.

By choosing initial positions, x_o, along $t = 0$ and using Eqs. 5 as initial conditions, and choosing initial times t_o along $x = 0$ and using Eqs. 4 as initial conditions, it is possible to obtain $c(x,t)$ over the region $x \geq 0$, $t \geq 0$. Hence the complete solution is calculated by repeatedly solving Eqs. 3 for the various initial conditions.

The accuracy of the resulting solution can be estimated in the following way. Since the transformation from the partial differential equation, Eq. 1, to the pair of ordinary differential equations, Eqs. 3a, b, is exact, no error has been introduced. The accuracy of the numerical solution of the ordinary differential equations can be controlled using the predictor-corrector methods (7) for the numerical solution of the ordinary differential equations. These techniques are quite efficient and can be programmed to adjust the time increment Δt to maintain a specified level of error. The error in the calculations is independent of the choice of the spacing of the initial points x_o and t_o along the boundaries. Hence a coarse grid can be specified for the calculation with a resulting saving in computation time without regard to a stability criterion.

APPENDIX - REFERENCES

1. Abbott, Michael B., Introduction to the Method of Characteristics, American Elsevier, New York, 1966.

2. Birkhoff, Garrett, Partial Difference Methods in Proc., IBM Scientific Computing Symposium Large-Scale Problems in Physics, IBM Corp., 1965, pp 20-21.

3. Birkhoff, G. and Kimes, T. F., "CHIC Programs for Thermal Transients," Report WAPD-TM 245, Bettis Atomic Poser Laboratory, Pittsburgh, Pa., 1962, Appendix B, pp. 12-16.

4. Chow, Ven Te, Open-Channel Hydraulics, McGraw Hill Book Co., 1959, Chapt. 20.

5. Di Toro, D.M. and O'Connor, D.J. "The Distribution of Dissolved Oxygen in a Stream with Time Varying Velocity," Water Resources Res. 4(3), June 1968, pp. 639-646.

6. Forsythe, G.E. and Wasow, N.R., Finite Difference Methods for Partial Differential Equations, John Wiley and Sons, N.Y. 1960, p. 64.

7. Hamming, R.W., Numerical Methods for Scientists and Engineers, McGraw Hill Book Co., New York, 1962, Chapt. 15.

8. Hildebrand, F.B., Advanced Calculus for Applications, Prentice-Hall Publishing Co., 1963, pp. 379-382.

9. Ippen, Arthur T. and Harleman, Donald R. F.,"One Dimensional Analysis of Salinity Intrusion in Estuaries," Tech. Bull. No.5 Committee on Tidal Hydraulics, Corps of Engineers, U.S. Army, Vicksburg, Miss., June 1961.

10. Li, Wen-Hsiung, "Unsteady Dissolved Oxygen Sag in a Stream," Journal of the Sanitary Engineering Division, ASCE, Vol. 88, SA 3, Proc. Paper 3129, May 1962, pp. 75-85.

11. O'Connell, R.L., et ~~al,~~ Report of Survey of the Truckee River, July 1962, Robert A. Taft Sanitary Engineering Center, PHS., Cincinnati, Ohio, 1962, pp. 32-33.

12. O'Connor, D.J. and Di Toro, D.M., "An Analysis of Dissolved Oxygen Varition in a Flowing Stream," Advances in Water Quality Improvement, E. F. Gloyna and W.W. Eckenfelder Jr., Eds., University of Texas Press, 1968, pp. 96-102.

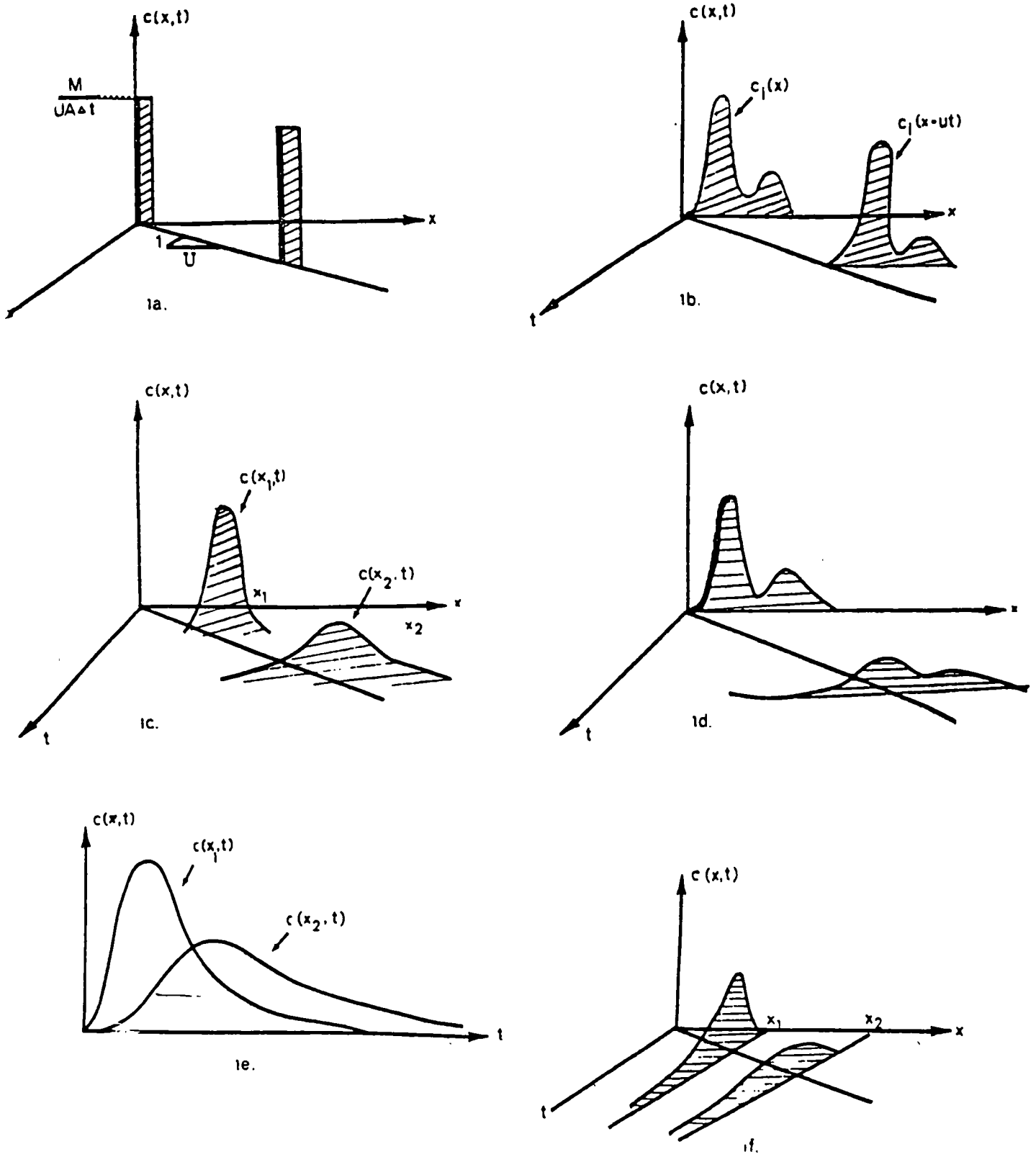

FIGURE 1
IMPULSE RESPONSE FOR STREAM

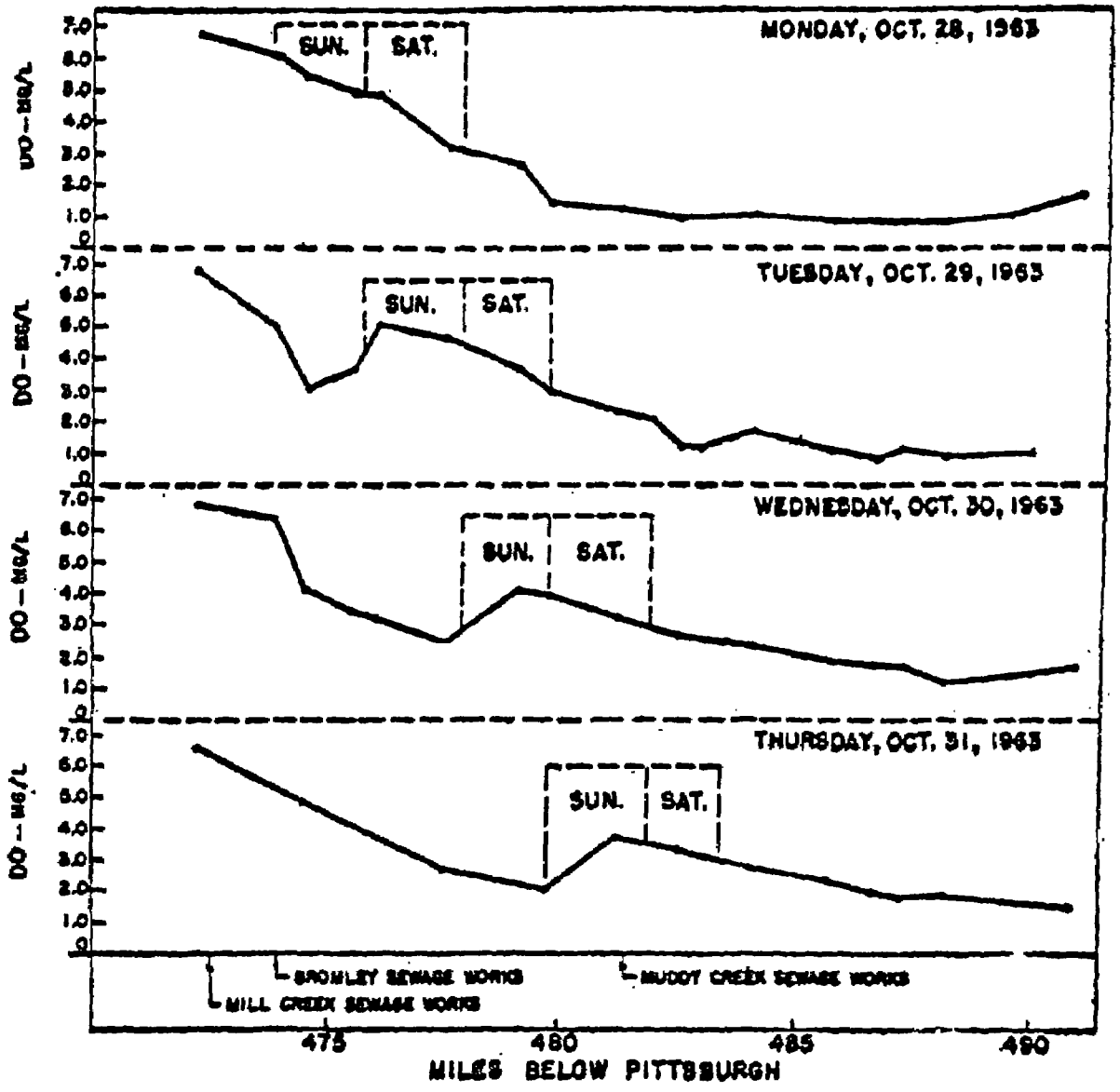

Fig. 2. Effect of weekday and weekend waste discharges on Ohio River dissolved oxygen.

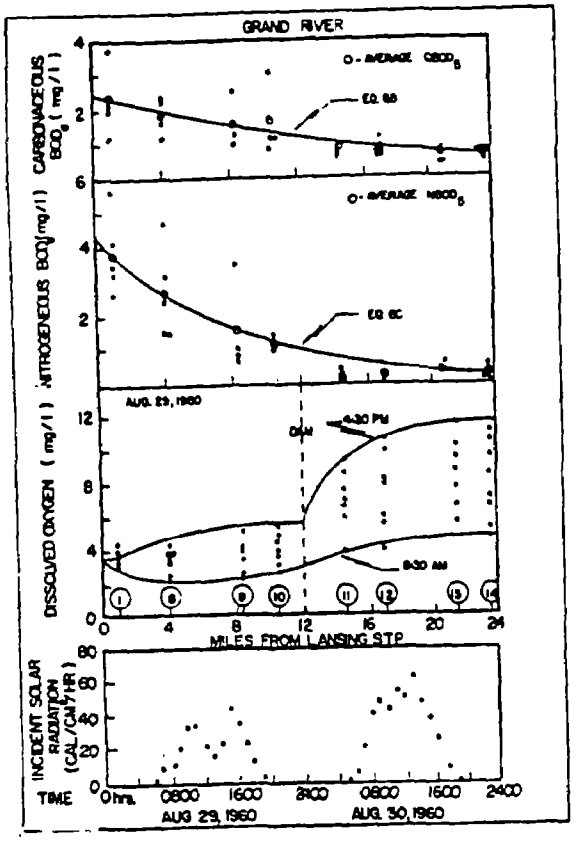

Fig. 3

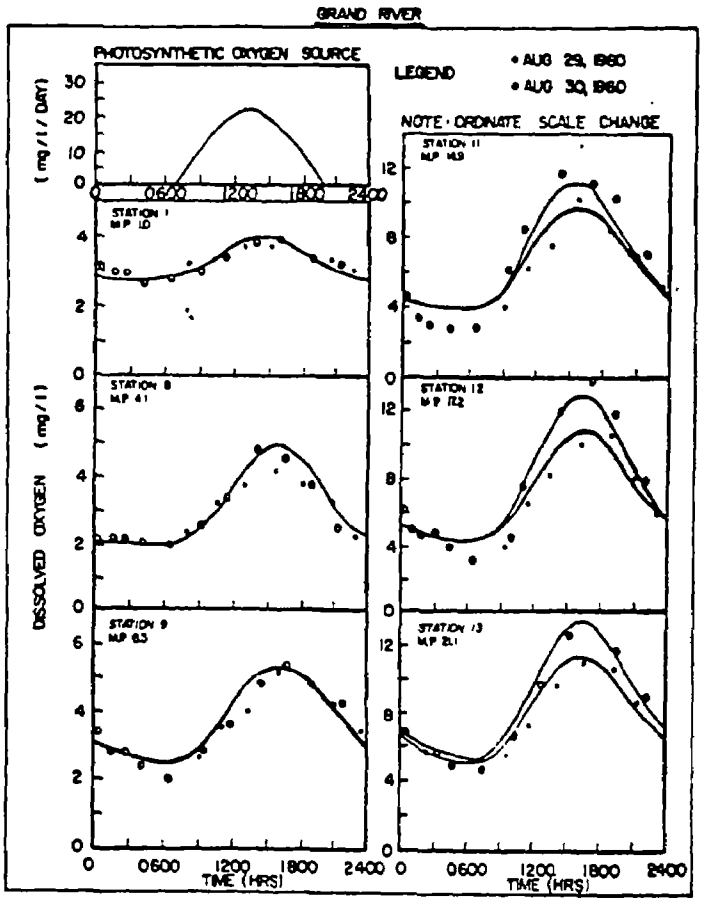

Fig. 4

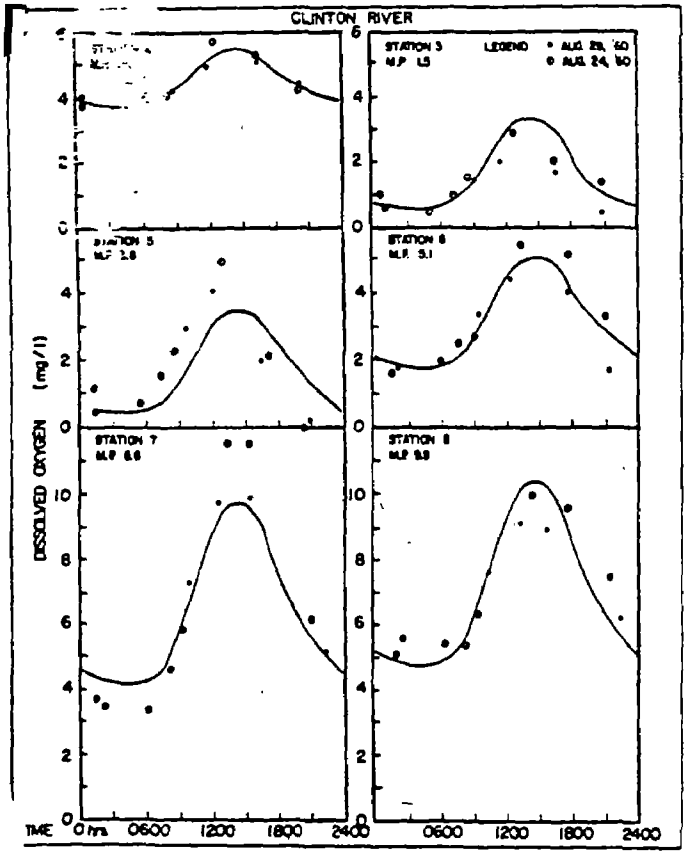

Fig. 5

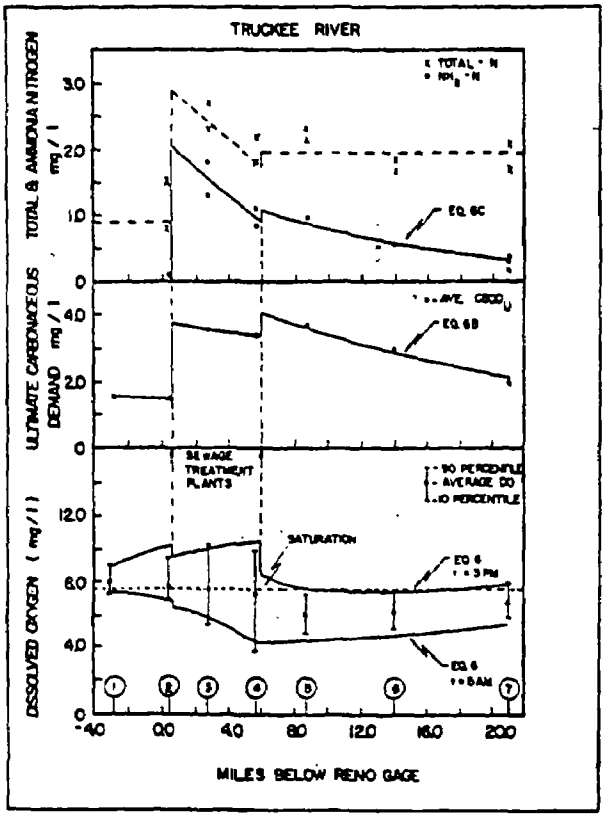

Fig. 6

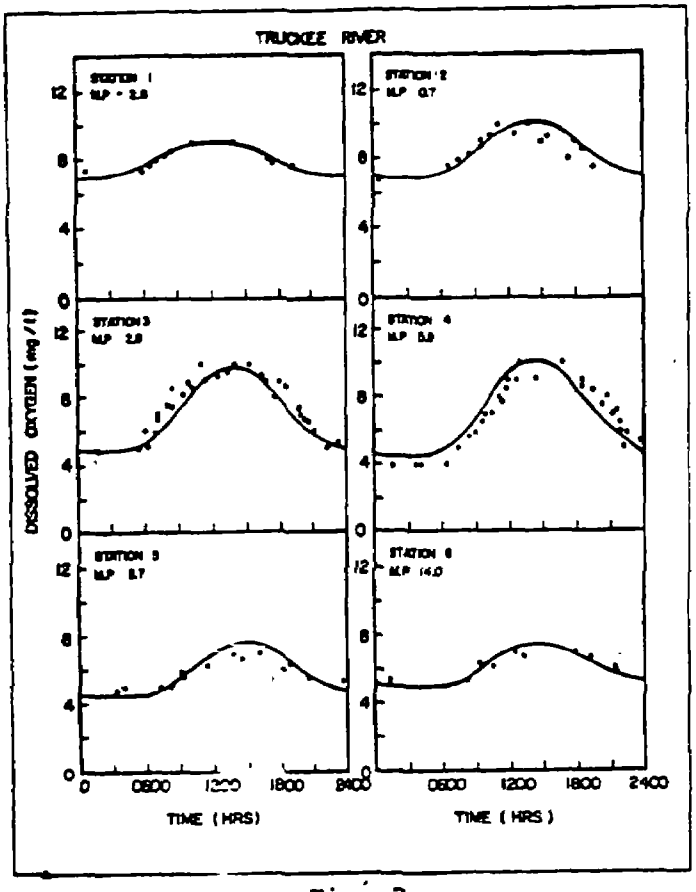

Fig. 7

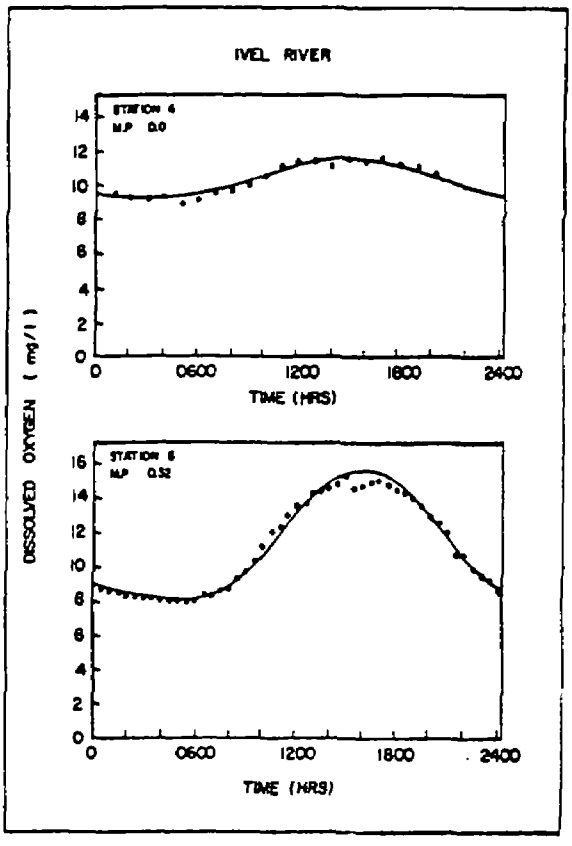

Fig. 8

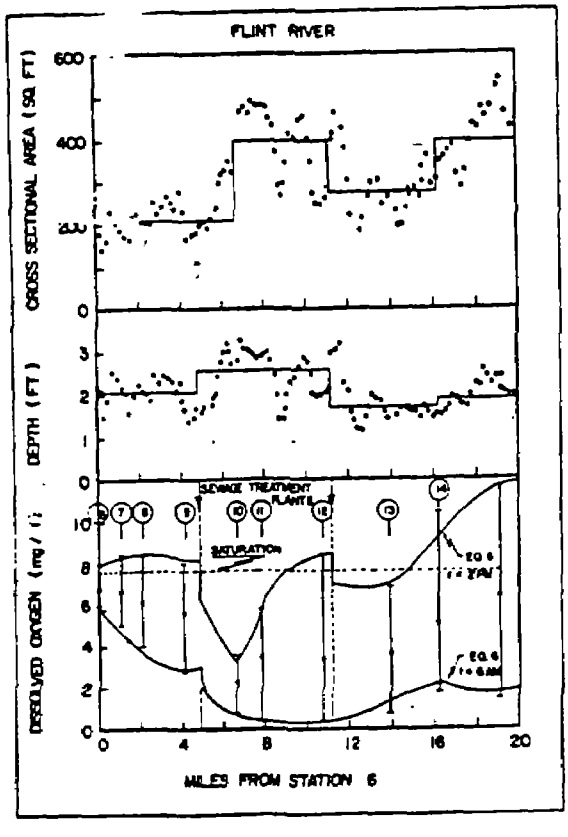

Fig. 9

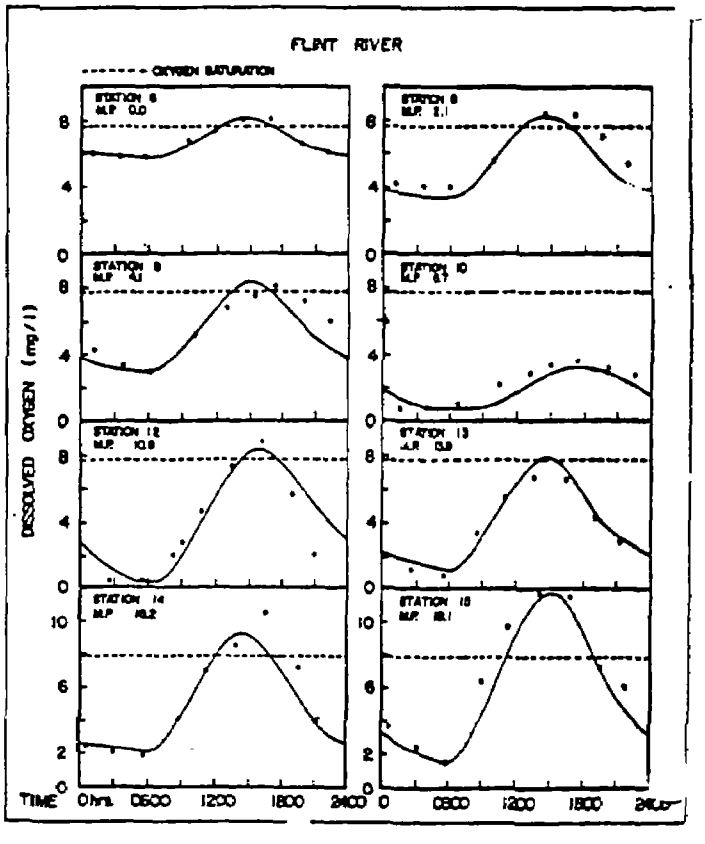

Fig. 10

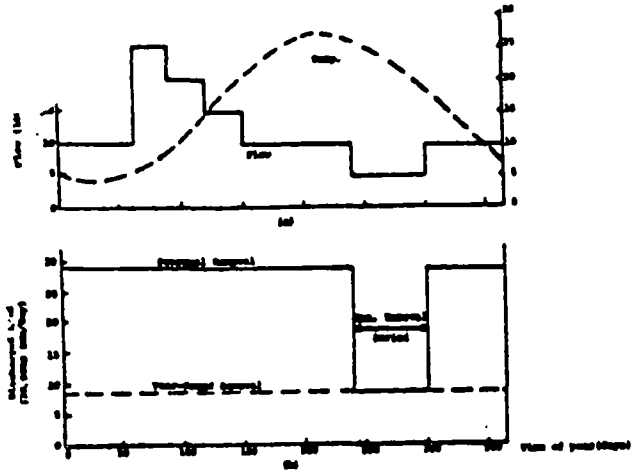

Fig. 11 Conditions for time variable treatment scheme.

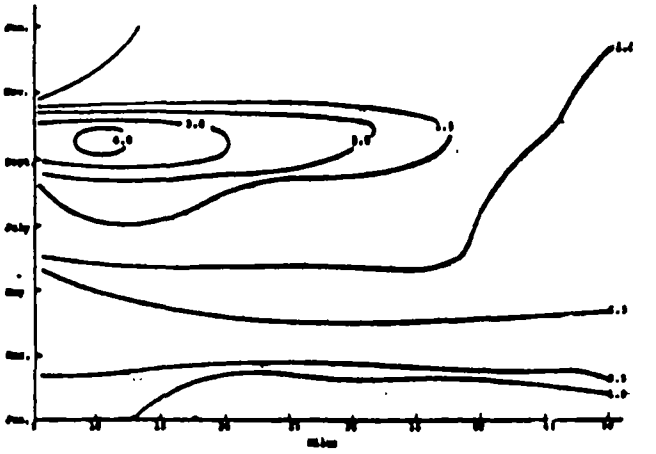

Fig. 12 Spatial and temporal variation of dissolved oxygen deficit (milligrams per liter) for constant treatment.

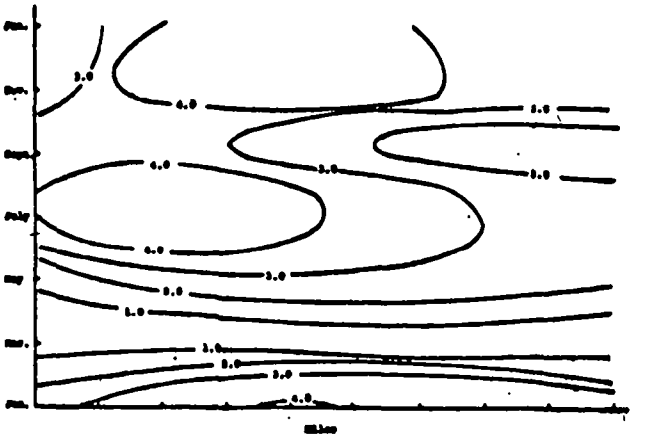

Fig. 13 Spatial and temporal variation of dissolved oxygen deficit (milligrams per liter) for seasonal treatment.

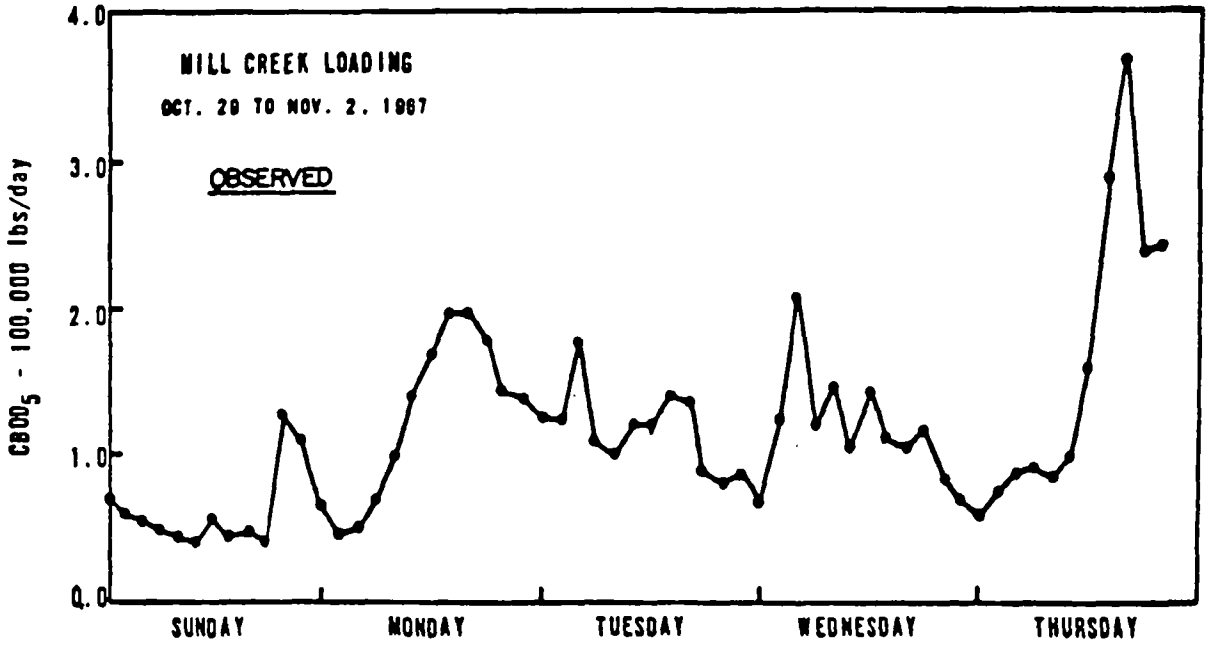

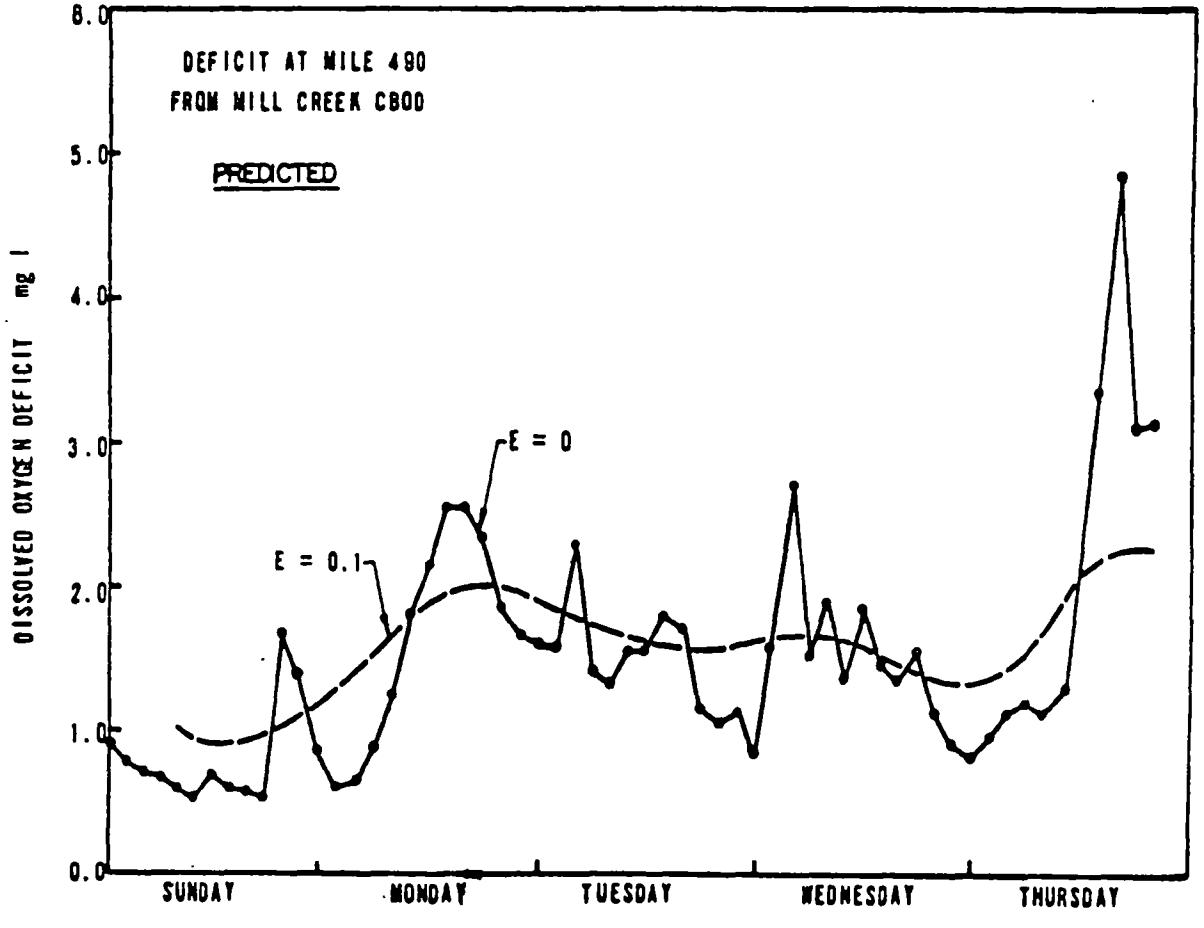

Figure 14

EFFECT OF DISPERSION ON DISSOLVED OXYGEN DEFICIT

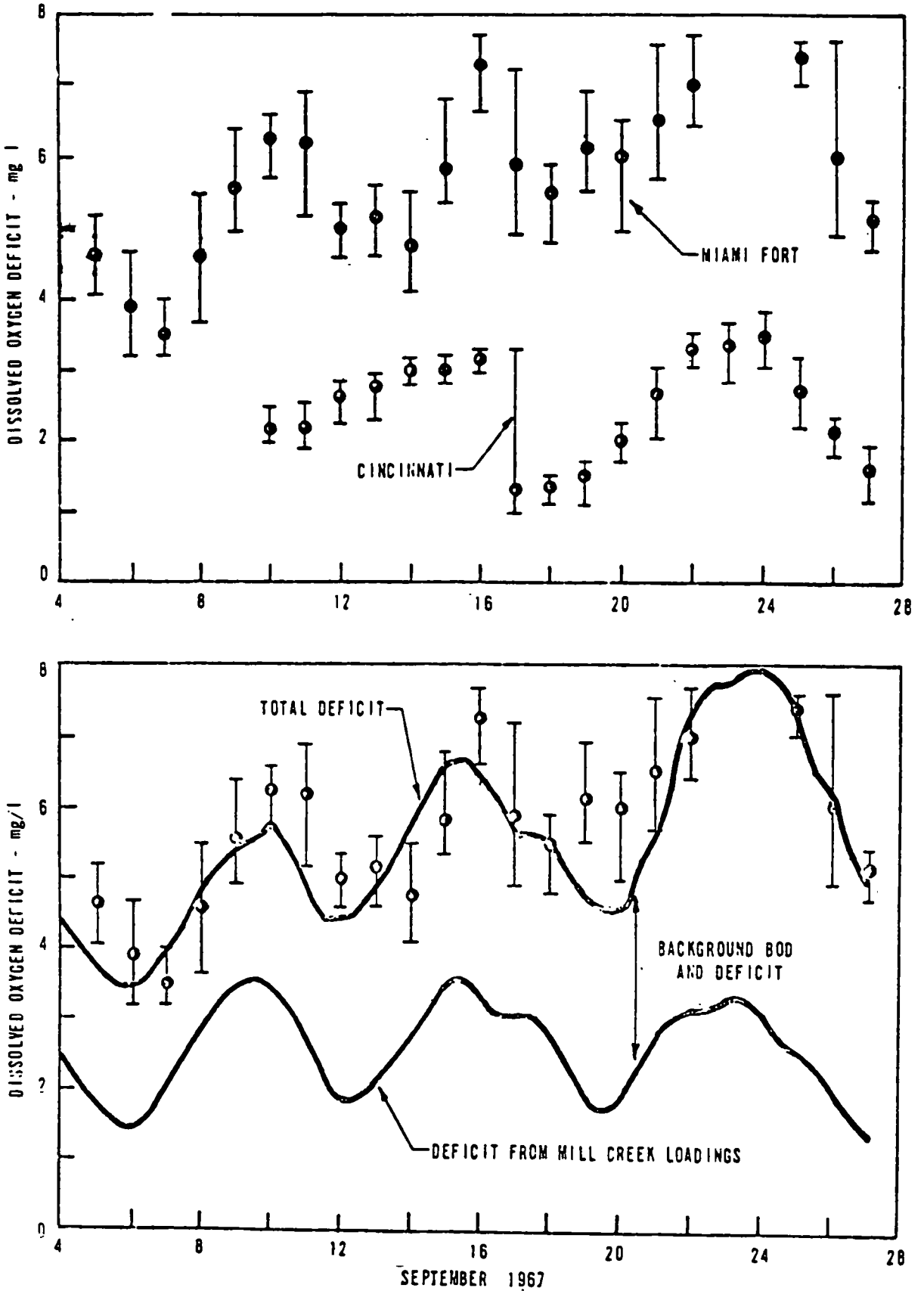

Figure 15
CALCULATED AND OBSERVED TIME VARIABLE DEFICIT

TABLE 1.—HYDRAULIC AND PHYSICAL CHARACTERISTICS

River	Segment number	Segment location, in miles	Segment length, in miles	Cross-sectional area, A, in square feet	Depth, H, in feet	Temperature, T, in degrees Celsius	Discharge, Q, in cubic feet per second	Reaeration, K_a, per day	CBOD Deoxygenation	NBOD Deoxygenation
									K_d, per day	K_n, per day
(1)	(2)	(3)	(4)	(5)	(6)	(7)	(8)	(9)	(10)	(11)
Grand	1[a,c]	0.0	12.0	320.0	1.90	28.0	295.0	5.5	0.80	1.90
	2	12.0	11.6	320.0	1.90	28.0	296.0	5.5	0.80	1.90
Clinton	1[a]	0.0	5.5	44.6	1.58	21.0	33.0	6.0	3.5	—
	2	5.5	4.4	44.6	1.58	21.0	33.0	6.0	3.5	—
Truckee	1[a,c]	2.5	9.5	150.0	1.67	27.8	150.0	6.8	0.49	2.4
	2[b,c,f]	0.7	5.2	150.0	1.67	27.8	196.0	6.8	0.49	2.4
	3[b,c]	5.9	15.1	150.0	1.67	27.8	271.0	8.0	1.3	2.4
Ivel	1	0.0	0.32	75.0	1.5	16.0	11.2	3.4	—	—
Flint	1[a,c]	0.0	4.9	210.0	2.1	28.0	134.0	4.2	0.78	2.0
	2[b,d]	4.9	1.8	210.0	2.6	28.0	174.0	3.5	0.95	0.1
	3[e]	6.7	4.5	400.0	2.6	28.0	174.0	2.5	0.95	0.1
	4[a,c]	11.2	5.0	280.0	1.7	28.0	204.0	6.1	0.95	2.50
	5	16.2	2.9	400.0	1.9	28.0	204.0	2.7	0.95	2.50

[a] Initial CBOD estimated from river data.
[b] Initial CBOD calculated using W/Q.
[c] Initial NBOD estimated from river data.
[d] Initial NBOD calculated using W/Q
[e] Benthal demand = 20 mg per l-day
[f] Sink of NH_3-N due to benthic algae = 4.6 mg per l-day.

TABLE 2.—FOURIER COEFFICIENT FOR INITIAL CONDITION OF DISSOLVED OXYGEN[a]

River (1)	A_0, in milligrams per liter (2)	A_1, in milligrams per liter (3)	θ_1, in days (4)	A_2, in milligrams per liter (5)	θ_2, in days (6)
Grand	3.5	—	—	—	—
Clinton	4.46	0.623	-0.110	0.235	-0.204
Truckee	7.97	1.04	-0.0810	—	—
Ivel	10.43	1.27	-0.0807	0.157	-0.205
Flint	6.66	1.12	-0.122	0.347	-0.232

[a] $C(t) = A_0 + \sum_{k=1}^{2} A_k \sin [2\pi k (t - t_s - \theta_k)]$.

TABLE 3.—ALGAL SOURCE PARAMETERS

River (1)	Segment number[a] (2)	P_m milligrams per liter-day (3)	P_{av} milligrams per liter-day (4)	R milligrams per liter-day (5)	P_{av}/R (6)	t_s Sunrise (7)	p, in period-hour (8)
Grand	1	22.0	7.6	22 0	0.35	0700	13
	2	50 0	17.3	16.0	1.1		
		65.0	22.5		1.4		
Clinton	1	27 0	8.6	20.0	0.43	0600	12
	2	47.0	15.0	18 0	0.84		
Truckee	1	30 0	11.2	7 0	1.6	0500	14
	2	50.0	18.8	9.5	2.0		
—	3	25.0	9.3	12.0	0.78		
Ivel	1	53.0	19.7	10.0	2.0	0700	14
Flint	1	35.0	11.1	15.0	0 74	0600	12
	2	5.0	1.6	5.0	0.32		—
	3	45.0	14.3	15.0	0.96		
	4	60.0	19.1	17 0	1.1		
	5	70.0	22.3	20.0	1.1		

[a] See Table 1 for hydraulic and physical data of segments.

TIME VARIABLE WATER QUALITY MODELS ESTUARIES, HARBORS, AND OFF-SHORE WATERS*

I. INTRODUCTION

For certain problem contexts, a need exists for describing the dynamic variation of water quality in brackish and marine waters. This is especially true for problems concerned with localized effects in the immediate vicinity of waste discharges or for problems concerned with the seasonal variation of water quality. A spectrum of time scales exists, the range of which extends from modeling hour-to-hour fluctuations in salinity or temperature to seasonal or year-to-year fluctuations in phytoplankton populations.

A major task in dynamic, time variable water quality modeling in the marine area is therefore a proper choice of its dominant time and space scale. Figure 1 shows two examples of different scales of phenomena. Such a choice requires a careful examination and articulation of the question posed in each specific problem context. A model that represents short term fluctuations may not be appropriate from

* Robert V. Thomann

a computational viewpoint for analyzing seasonal effects. Conversely, if the problem context demands information on the short term (hour-to-hour or day-to-day) oscillations, then the water quality model must incorporate the hydrodynamic and reaction kinetics on that time scale.

Several problem contexts that require time variable models are discussed below and range over the time spectrum mentioned previously. These problem contexts are:

a) In Boston Harbor, the movement of digested sewage solids throughout a tidal cycle when the solids are discharged only during the first three hours of ebb tide;

b) In off-shore areas, the settling and dispersion of waste material (over several hours) discharge after from a moving barge;

c) Seasonal variations in water quality for the Delaware and Potomac estuaries.

In each of these problem contexts, the underlying hydrodynamic regime is assumed to be known. If the circulation and/or transport patterns are not known, a separate hydrodynamic model must be employed.

II. THEORY

a) Basic Equations

In all cases, the appropriate starting point is a mass balance of the water quality variable, s_1, around an infinitely small fluid volume. The appropriate equation in three dimensions is given by:

$$\frac{\partial s_1}{\partial t} = \frac{\partial}{\partial s}(E_x \frac{\partial s_1}{\partial x}) + \frac{\partial}{\partial y}(E_y \frac{\partial s_1}{\partial y}) + \frac{\partial}{\partial z}(E_z \frac{\partial s_1}{\partial z})$$

$$- \frac{\partial}{\partial x}(U_x s_1) - \frac{\partial}{\partial y}(U_y s_1) - \frac{\partial}{\partial z}(U_z s_1) - K_{11}(x,y,z,t,s_1)s_1 \qquad (1)$$

$$+ W(x,y,z,t) \pm \sum(x,y,z,t)$$

where $E_{x,y,z}$ are the dispersion coefficients in each respective spatial direction, $U_{x,y,z}$ is the velocity in each direction, K_{11} is the decay coefficient, $W(x,y,z,t)$ represents the waste input of variable, s_1, and $\sum(x,y,z,t)$ represents all other sources and sinks of s_1. Note that the decay coefficient is written in a general form as a function of the variable, s_1. For first order decay, of course, the reaction coefficient is independent of s_1. In vector form, Equation (1) is:

$$\frac{\partial s_1}{\partial t} = (\nabla \cdot [E](\nabla s_1) - \nabla \cdot \vec{U} s_1) - K_{11} s_1 + W \pm \sum \qquad (2)$$

where [E] is a diagonal matrix of dispersion coefficients, (∇s_1) is a column vector, $\vec{U}$ is the velocity vector and:

$$\nabla \equiv \frac{\partial}{\partial s}\vec{i} + \frac{\partial}{\partial y}\vec{j} + \frac{\partial}{\partial z}\vec{k}$$

The first two terms in Equation (2) represent the dispersive and advective field given by the hydrodynamic circulation and degree of turbulence. As indicated above, the field of motion is assumed to be given. In time variable models, this field of motion may be quite important, as for example, in intra-tidal models for estuaries where the x-component of the U vector dominates.

If the variable, s_1, interacts with a second variable, call it s_2, then one can write the equation for the second variable as:

$$\frac{\partial s_2}{\partial t} = (\nabla \cdot [E](\nabla s_2) - \nabla \cdot \vec{U}s_2) - K_{22}s_2 + K_{12}s_1 + W_2 \pm \zeta_2 \qquad (3)$$

where K_{12} is the feed forward coupling of variable s_1 to variable s_2. In the most general case, one can examine the interaction between n variables, s_1, $s_2 \ldots s_n$ where feedback as well as feedforward loops occur. Therefore, a complete set of equations is given by:

$$\frac{\partial s_1}{\partial t} = (\nabla\cdot[E](\nabla s_1) - \nabla\cdot\vec{U}s_1) - K_{11}s_1 + K_{21}s_2 + \ldots K_{n1}s_n + W_1 \pm \sum_1$$

$$\frac{\partial s_2}{\partial t} = (\nabla\cdot[E](\nabla s_2) - \nabla\cdot\vec{U}s_2) + K_{12}s_1 - K_{22}s_2 + K_{32}N_3 + \ldots K_{n2}s_n + W_2 \pm \sum_2$$

$$\vdots \qquad (4)$$

$$\frac{\partial s_n}{\partial t} = (\nabla\cdot[E](\nabla s_n) - \nabla\cdot\vec{U}s_n) + K_{1n}s_1 + K_{2n}s_2 + \ldots K_{n-1,n}s_{n-1} - K_{nn}s_n + W_n \pm \sum_n$$

where K_{ij} are reaction coefficients (in general functions of space, time and the concentration variables, s_1, $s_2 \ldots s_n$); for $j > i$ the reactions are feedforward reactions, for $j < i$, the reactions are feedback reactions, and for $j = i$, K_{ii} is the total reaction for variable s_i where, in general, $K_{ii} \geq \sum_j K_{ij} (j \neq i)$. In state vector form, Equation (4) can be written as:

$$\frac{\partial(s)}{\partial t} = \underset{\substack{\downarrow \\ \text{hydrodynamic} \\ \text{field}}}{(\nabla \cdot F)} + \underset{\substack{\downarrow \\ \text{reaction} \\ \text{kinetics}}}{[K]^T(s)} + \underset{\substack{\downarrow \\ \text{source and} \\ \text{sink field}}}{(W) \pm (\sum)} \qquad (5)$$

where $(\nabla\cdot F)$ is an n x 1 vector representing the effect of the hydrodynamic field on water quality ($F \equiv [E]\nabla s - \vec{U}s$); $[K]^T$ is the transpose of the reaction kinetic matrix (n x n) given by:

$$[K] = \begin{vmatrix} -K_{11} & K_{12} & K_{13} & & \cdots & K_{1n} \\ K_{21} & -K_{22} & K_{23} & & \cdots & K_{2n} \\ K_{31} & K_{32} & -K_{33} & K_{34} & \cdots & K_{3n} \\ & & & & & \vdots \\ K_{n1} & K_{n2} & K_{n3} & & \cdots & K_{nn} \end{vmatrix}$$

(s) is an n x 1 state vector of water quality and (W) and ($\sum$) are n x 1 vectors of input sources and sinks. The major components of the general water quality problem are therefore made clear by Equation (5). The first term on the righthand side represents the dispersion and advection of the water quality state variable, the second term represents the kinetic interaction between each of the water quality variables, and the final term represents the discharge or input of a waste material and incorporates any other sources or sinks. As indicated in the Introduction, the essence of time variable modeling (indeed all water quality modeling) is the proper assessment of the role of each of these factors and within that determination, a proper assessment of the need for complete time and space detail. Once the determination of the relative importance of the flow field, reaction kinetics and input field has been made, two steps follow: (a) a representation fo the spatial derivatives in Equation (4) by finite difference approximation and (b) an exact specification of the reaction kinetics.

B) Spatial Approximation

In approximating the spatial derivatives of Equation (4), the region of interest is segmented into n finite volume

segments. Dispersion and advection phenomena now must incorporate the actual cross sectional area of the water body in the direction of the fluid flow. Consider first the finite difference approximation in the x-direction. Figure 2 shows the notation where V is the volume of the segment and Δx is the length of the segment. For simplicity, each segment is considered equal in length, although in general this need not be so.

A finite difference approximation to the first derivative of s is given by[1]:

$$\left(\frac{ds}{dx}\right)_k \approx \frac{s_{k,k+1} - s_{k-1,k}}{\Delta x} \tag{6}$$

where the subscript k on the derivative indicates an evaluation of the derivative in the center of segment k, $s_{k,k+1}$ is the concentration at the boundary between segment k and k+1 and $s_{k-1,k}$ is the concentration at the boundary between k-1 and k. In Equation (6) let the boundary concentrations be linearly related to the concentrations in the center of each adjoining segment, s_{k-1} and s_{k+1}. Thus, let:

$$s_{k,k+1} = \alpha_{k,k+;}s_k + \beta_{k,k+1}s_{k+1} \tag{7}$$

and:

$$s_{k-1,k} = \alpha_{k-1,k} s_{k-1} + \beta_{k-1,k} s_k$$

where α is a weighting fraction (to be specified later) and $\beta = 1-\alpha$. With Equation (7), Equation (6) can then be written as:

$$\left(\frac{ds}{dx}\right)_k \simeq \frac{\beta_{k,k+1} s_{k+1} + (\alpha_{k,k+1} - \beta_{k-1,k}) s_k - \alpha_{k-1,k} s_{k-1}}{\Delta x} \qquad (8)$$

Two cases are of interest. For all $\alpha = \frac{1}{2} = \beta$, one obtains:

$$\left(\frac{ds}{dx}\right)_k \simeq \frac{s_{k+1} - s_{k-1}}{2\Delta x} \qquad (9)$$

which is a central difference approximation to the derivative. For all $\alpha = 1$ ($\beta = 0$), one obtains:

$$\left(\frac{ds}{dx}\right)_k \simeq \frac{s_k - s_{k-1}}{\Delta x} \qquad (10)$$

which is a backward difference approximation to the derivative. For arbitrary α, the approximation Equation (8) weights either upstream or downstream concentrations more heavily. A stability criterion for choosing the weights (or equivalently, specifying the segment size) is given below.

Several points should be noted. For the backward difference scheme, Equation (10), a Taylor series expansion for s_{k-1} about s_k can be shown to give[2]:

$$\left(\frac{\partial s}{\partial x}\right)_k = \frac{s_k - s_{k-1}}{\Delta x} + \left\{ \frac{\Delta x}{2} \left(\frac{\partial^2 s}{\partial x^2}\right)_k - \frac{(\Delta x)^2}{6} \left(\frac{\partial^3 s}{\partial x^3}\right)_k + \cdots \right\}$$

In one dimension then, the solution of the difference equation is equivalent to solution of the equation given by[2]:

$$\frac{\partial s}{\partial t} + U\frac{\partial s}{\partial x} - E\left(1 + \frac{\Delta x|U|}{2}\right) \frac{\partial^2 s}{\partial x^2} = 0 \qquad (11)$$

where higher order errors have been neglected. It can be seen in Equation (11) that an additional amount of psuedo or "numerical" dispersion has been introduced into the equation. Only for $\Delta x|U| << E$ does the difference approximation approach the original differential equation. For larger $\Delta x|U|/2$, special care must be taken in interpreting the results of the calculation.

Returning to Equation (6), the second derivative approximation is given by the derivative of (6) evaluated at $x = K$ or:

$$\left(\frac{d^2 s}{dx^2}\right)_k \approx \frac{1}{\Delta x}\left[\left(\frac{ds}{dx}\right)_{k,k+1} - \left(\frac{ds}{dx}\right)_{k-1,k}\right] \approx \frac{1}{(\Delta x)^2}\left[s_{k+1} - s_k + s_{k-1}\right] \qquad (12)$$

The advective terms in Equation (1), i.e., terms of the form $\frac{\partial}{\partial x}(Us)$ can therefore be written [using Equation (8)] as:

$$-\frac{\partial}{\partial x}(Us) \approx \frac{1}{\Delta x}\left[\left(\alpha_{k-1,k} \frac{Q_{k-1,k}}{A_{k-1,k}} s_{k-1} + \beta_{k-1,k} \frac{Q_{k-1,k}}{A_{k-1,k}} s_k\right)\right.$$
$$\left. - \left(\alpha_{k,k+1} \frac{Q_{k,k+1}}{A_{k,k+1}} s_k + \beta_{k,k+1} \frac{Q_{k,k+1}}{A_{k,k+1}} s_{k+1}\right)\right] \qquad (13)$$

where Q is the mass flow rate, A is the cross sectional area, and $U = Q/A$.

The dispersive terms in Equation (1), i.e., terms of the form $\frac{\partial}{\partial x}E\frac{\partial s}{\partial x}$ can be written (using Equation (12)) as:

$$\frac{\partial}{\partial x}(E\frac{\partial s}{\partial x}) = \frac{1}{(\Delta x)^2}[E_{k,k+1}(s_{k+1} - s_k) + E_{k-1,k}(s_{k-1} - s_k)] \qquad (14)$$

In one dimension, therefore, and for a single variable, s_1, the differential equation can be written as:

$$\begin{aligned} V_k\frac{ds_{1,k}}{dt} &= [Q_{k-1,k}(\alpha_{k-1,k}s_{1,k-1} + \beta_{k-1,k}s_{1,k})] && (1)\\ &- [Q_{k,k+1}(\alpha_{k,k+1}s_{1,k} + \beta_{k,k+1}s_{1,k+1})] && (2)\\ &+ E'_{k-1,k}(s_{1,k-1} - s_{1,k}) + E'_{k,k+1}(s_{1,k+1} - s_{1,k}) && (3)\\ &- K_{11,k}(s_1,t)s_{1,k}V_k + W_{1,k} \pm \Sigma_{1,k} && (4) \end{aligned} \qquad (15)$$

where $E'_{kj} = \frac{E_{kj}A_{kj}}{x}$, $V_k = \bar{A}_k(\Delta x)$ and $\bar{A}_k$ is some suitable average cross sectional area for segment k. The terms designated on the righthand side of Equation (15) have the following meaning:

(1) - mass of s_1 advected into segment k
(2) - mass of s_1 advected out of segment k
(3) - tidal dispersion of substance s_1
(4) - reaction kinetics of s_1, sources and sinks of s_1.

Equation (15) can therefore be arrived at by considering a mass balance equation around a finite reach of the estuary. Complete details are given in (3,4).

For multi-dimensional systems, the mass transport and dispersion terms interact with additional segments so that the differential equation for a single variable, s_l, is:

$$V_k \frac{ds_{l,k}}{dt} = \sum_j (-Q_{kj}(\alpha_{kj} s_{l,k} + \beta_{kj} s_{l,k})) + E'_{kj}(s_{ij} - s_{ik}) - K_{ll,k}(s_{l,t})\, s_{l,k} V_k + W_k \pm \sum_k \quad (16)$$

where the summation extends over all j segments bordering on k.

Note that for both the one dimensional and multi-dimensional system, the advective and dispersive fields are assumed known.

C. - Numerical Dispersion Positivity and Stability

Since the Equations (15) and (16) represent spatial approximations to derivatives, some errors are introduced into the analysis. Primary among these is the numerical dispersion, which appears in certain forms of the differential equations due to the assumption of a completely mixed finite volume.

Equation (11) shows the nature of this dispersion. Other aspects of the differencing scheme must also be considered. All solutions to any water quality model should be everywhere positive in order to reflect the physical nature of the problem. Also, solutions to the finite difference forms of the mass balance equations should differ from analytical solutions to the assigned equations by a fixed, hopefully small, error, which remains bounded throughout the simulation. Stability of the solution is therefore mandatory.

Unfortunately, there are no set procedures that one can follow to optimally choose a spatial grid size and/or time step for numerical integration. The size of available computational facilities and the nature of the problem (i.e., the effects of numerical dispersion) are important considerations. However, certain guidelines can be given.

First, consider the requirement of positivity, i.e., that all solutions be positive and examine Equation (16). These equations can be written in matrix form as[3] where the subscript designating the variable has been dropped, therefore, s_1, $s_2 \ldots s_n$ represents the distribution of a single variable in the n finite segments of the water body.

$$
\begin{aligned}
a_{11}\left(\frac{d}{dt}\right)s_1 &+ a_{12}s_2 + a_{13}s_3 + \ldots + a_{1n}s_n = W_1 \pm \zeta_1 \\
a_{21}s_1 &+ a_{22}\left(\frac{d}{dt}\right)s_2 + a_{23}s_3 + \ldots a_{2n}s_n = W_2 \pm \zeta_2 \\
&\vdots \\
a_{n1}s_1 &+ a_{n2}s_2 + \ldots\ldots + a_{nn}\left(\frac{d}{dt}\right)s_n = W_n \pm \zeta_n
\end{aligned}
\qquad (17)
$$

Equation (17) become tridiagonal in form for one-dimensional estuaries. It can be shown that for a positive solution, the terms off the main diagonal must be negative. The terms below the diagonal are always negative. Those above the diagonal are of the form:

$$\beta_{ij}Q_{ij} = E'_{ij}$$

Thus, for these terms to be negative:

$$\alpha_{ij} \geq 1 - E'_{ij}/Q_{ij}$$

or:

$$\alpha_{ij} \geq 1 - E/\Delta x U \qquad (18)$$

Two courses of action are now possible: a grid size (Δx) can be chosen a priori depending on the size of the computational facilities available. If Equation (18) is satisfied by internal computation of α, then positivity will be guaranteed, and the spatial condition for stability will be satisfied.

On the other hand, one can solve Equation (18) for Δx as:

$$\Delta x < E/U(1 - \alpha) \tag{19}$$

so that if central differences are used ($\alpha = \frac{1}{2}$):

$$\Delta x < 2E/U \tag{20}$$

Note that if $\alpha = 1$, (a backward difference),

$$\Delta x < \infty$$

implying that positivity (and spatial stability) are always guaranteed regardless of mesh size for backward differences, and note also that if $E = 0$,

$$\Delta x < 0$$

implying that it is not possible to find a finite difference scheme which will have zero dispersion and will always generate positive solutions. As soon as a difference scheme is chosen, one must be willing to accept a certain level of numerical dispersion.

It can also be shown that in order to maintain stability for an explicit time differencing, the main diagonal term must be all positive. This leads to the following general stability criterion (for constant coefficients):

$$1 + U\frac{\Delta t}{\Delta x}(\beta - \alpha) - \frac{2E\Delta t}{\Delta x^2} - K\Delta t > 0 \qquad (21)$$

For central differences, ($\alpha = \beta = \frac{1}{2}$), this criterion becomes:

$$2E\frac{\Delta t}{\Delta x^2} + K\Delta t < 1 \qquad (22)$$

and for K = 0, a conservative substance,

$$\frac{\Delta t}{\Delta x^2} < \frac{1}{2E} \qquad (23)$$

This is the usual expression given for stability[5,6]. Note however, that the criterion given by Equation (23) assumes central differences and conservative substances. For a fixed spatial grid, the effect of introducing first order decay is to require a reduction in the time step necessary for stability.

Returning to Equation (21), for a completely advective system and backward difference ($\alpha = 1$), the criterion simply becomes:

$$1 - U\frac{\Delta t}{\Delta x} - K\Delta t > 0 \qquad (24)$$

and for K = 0,

$$U\Delta t < \Delta x \qquad (25)$$

As indicated previously, (Equation (11)), the numerical dispersion introduced by a backward difference is $U\Delta x/2$.

In addition, numerical dispersion is also introduced by the explicit time differencing.[7] Therefore, for a variable spatial differencing scheme and forward explicit time differencing, the dispersion introduced is given by

$$E_{num} = u\Delta x \left[(\alpha - 1/2) - \frac{u\Delta t}{2\Delta x}\right] \qquad (26)$$

Now the issue is clear (at least for explicit schemes). If central spatial differences are used ($\alpha = 1/2$), the numerical dispersion due to spatial truncation is eliminated and if enough additional dispersion is added to the original equation (i.e. equal to $u^2\Delta t/2\Delta x$) then the solution will not have any numerical dispersion. However, the space and time constraints of Equations (20) and (22) must still be met. This may result in small spatial grids and small time steps. In any event, each situation must be considered separately.

Choosing proper spatial and time grids for approximations to the partial differential equations is still very much an art. Considerations of computer size, nature of problems and degree of accuracy, and simplicity of the resulting finite difference equations, all influence the choice.

REFERENCES

[1] Shaw, F.S., Relaxation Methods, An Introduction to Approximational Methods for Differential Equations. Dover Pub., Inc., 1953, New York.

[2] Torrance, K.E., Comparison of Finite-Difference Computations of Natural Convection, Jour. of Res., Nat. Bur. of Stds., Vol.72B, No.4, October-December, 1968 pp.281-301

[3] Thomann, R.B., Systems Analysis and Water Quality Management, in press, to appear 1971, Env. Sci. Serv., Prit. Co., Wilton, Connecticut.

[4] Thomann, R.V., Mathematical Model for Dissolved Oxygen. ASCE, Jour. San. Engr. Div., Vol. 89, No. SA5, October 1963

[5] Kent, R., Diffusion in a Sectionally Homogeneous Estuary ASCE, Jour. San. Engr. Div., Vol. 86, No. SA2, March 1960, pp. 15-47

[6] Leendertse, J.J., Digital Techniques: Finite Differences Chapt. VI, Solution Techniques in Estuarine Modeling: An Assessment, Prep. for Nat. Coastal Res. Prog., WQO, EPA by Tracor, Inc., Austin, Texas, 1971, pp.277-302.

[7] Bella, D.A., Grennev, W.J. Finite - Difference Convection Errors. Jour. San. Engr. Div., Vol. 96, No. SA6, Dec. 1970, pp. 1361-1375.

III. APPLICATIONS OF TIME VARIABLE WATER QUALITY MODELS

A. Inter-Tidal Seasonal Models

Time variable water quality models have been used to determine the effect of waste load removal programs on the low frequency variations of water quality, especially seasonal oscillations. Specific applications have been made to the Delaware and Potomac estuaries, among others. The time scale of interest is therefore considered to incorporate one year with the smallest time inverval as a tidal cycle or daily average. The independent variable in Eq. (5) is therefore interpreted in this manner.

Seasonal variations are particularly important in large estuaries and bays since these bodies of water tend to "dampen" any input fluctuations of short term (hourly) frequency. Furthermore, large scale waste treatment programs will generally affect day to day variations in water quality. Local spatial and short term fluctuations are gradually controlled by other influences such as specific manner of disposal (see Boston Harbor application below) or details of the geomorphological structure.

An inter-tidal time variable model has been constructed for water quality (especially dissolved oxygen) for the Delaware Estuary. First order kinetics were used throughout and two basic partial differential equations were utilized. Thus Eq. (5) becomes:

$$\frac{\partial L}{\partial t} = \frac{1}{A}\frac{\partial uL}{\partial x} + \frac{1}{A}\frac{\partial}{\partial x}\left(EA\frac{\partial L}{\partial x}\right) - K_{11}L + W(x,t)$$

$$\frac{\partial c}{\partial t} = \frac{1}{A}\frac{\partial uc}{\partial x} + \frac{1}{A}\frac{\partial}{\partial x}\left(EA\frac{\partial c}{\partial x}\right) + K_{12}L + K_{22}(c_s - c) \pm \sum_c \qquad (27)$$

where L = oxygen demanding material (carbonaceous and nitrogenous)

c = dissolved oxygen

K_{22} = reaeration rate

c_s = saturation value of dissolved oxygen

The reaction coefficient matrix is therefore a simple interactive first order system given by

$$[K] = \begin{bmatrix} -K_1 & K_{12} \\ 0 & -K_{22} \end{bmatrix}$$

For the Delaware estuary, the reach from Trenton, N.J. to the entrance to Delaware Bay, a distance of about 86 miles, was divided into 30 sections as shown in Figure (3). Two spatial grid sizes were used; Δx was chosen as 10,000 feet in the area of greatest spatial gradients and 20,000 feet otherwise. A variable weight differencing scheme was used in the time variable simulations with L and ξ (Eq. 15) computed at each step in the program. This insured stability and positivity. The amount of numerical dispersion introduced by this scheme for the Delaware ranged from a high of about 1-5 mi^2/day during transient high runoff conditions, to a minimum of about 0-0.5 mi^2/day during most of the low flow months of the year, the critical times. It should be noted that the velocity in the above model is the net tidal velocity, usually a low number during critical months of the year. The numerical dispersion is therefore usually not critical in inter-tidal average models such as the Delaware. The previous values of the numerical dispersion

can be compared to actual values of dispersion used in the model of 4-7 mi^2/day.

In the Delaware computer program, a set of initial values is chosen and numerical integration is used to compute the solution at the next time step. After each step is completed, the new values of the dependent variables are downgraded to become the initial values for the next time step. Jeglic (7) controls truncation errors by a halving and doubling procedure which, while sacrificing some computational time does not require the user to specify an integration interval.

The computer runs that have been made indicate integration intervals of four to fifteen steps per prototype day. The average problem for the Delaware required about four IBM-7094 minutes per simulated month.

Verification analyses have been minimized at length by MacEwen& Tortoriello[8] and Thomann[3]. These analyses have indicated relatively good agreement between the model and the prototype observations. However, transient fluctuations (order of several days period) were not duplicated by the model implying the presence of other, probably higher order effects on water quality which are not incorporated in the model.

After verification, the model has been used for a variety of simulations. Fig. (4) shows a typical temporal distribution of dissolved oxygen in section 13. The "normal loads" plot is for 1964 base line conditions. The 95% removal plot considers

carbonaceous waste removal only. The time variable effects of variable waste discharge can therefore be assessed. Note the major effect of waste removal during summer months due to increased reaction rates.

Fig. 5 shows the complete time-space surface generated by the DO model for the Delaware. The regions of low DO appear as depressions and the objective of a water quality management program is to improve both the time and space variations of DO to a "desirable" level. Spatial profiles at specific times of the year and temporal variations at specific locations are obtained directly from the contour plot.

For the Potomac estuary, the river was divided into 28 sections with a Δx ranging from 1.3 to 8.6 miles. Details of the model and applications are given in Hetling[9] and Jaworski (10,11). Equations similar to (27) were finite differenced with a variable differencing scheme on the advective term. This is similar to the Delaware estuary applications. Fig. 6 shows a comparison between observed DO values and those computed by the time variable model. Recently, Jaworski[10] has reported on the use of an intra-tidal model that is run out to a dynamic steady-state for several water quality variables. Fig. 7 shows the results of this use of intra-tidal model that is run out to a dynamic steady-state for several water quality variables. Fig. 7 shows the results of this use of an intra-tidal time variable model. Fig. 8 shows a comparison between the chloride concentrations at Possum Point and a seasonal inter-tidal conservative

variable models For this case, Eq. (5) becomes simply:

$$\frac{\partial c}{\partial t} = -\frac{1}{A}\frac{\partial uc}{\partial x} + \frac{1}{A}\frac{\partial}{\partial x}\left(E\frac{\partial c}{\partial x}\right) + W(x,t) \qquad (28)$$

where c is now chloride concentrations and W(x,t) is simply the source of salt at the mouth of the estuary. The reaction matrix [K] is zero everywhere. Fig. 8 thus illustrates the application of a seasonal type time variable model to another water quality variable, the amount of sea salts that enter an estuary. This becomes particularly important during times of drought when the presence of salts may interfere with the use of the estuary for municipal water supply.

B. Intra Tidal Models

Several intra-tidal (hour to hour) models have been constructed primarily of conservative substances such as salt or simple first-order kinetic systems such as coliform bacteria. Leenderste[12] for example has constructed a detailed hydrodynamic and water quality model for Jamaica Bay. For that work, a grid size of 500 feet was used which resulted in 4,758 grid made points equivalent to about 2,000 segments. Relatively elaborate input and output hardware and software was used to prepare the problem for computation and to display results in a readily obtainable form. Graphic computer input and output devices greatly facilitated the representation of data. Details are found in (12).

Another example of the application of intra-tidal modeling is given by Boston Harbor where two problem contexts were examined[13]:

a) preliminary evaluation of time and space distribution of coliform bacteria due to transient storm water overflows.

b) preliminary evaluation of the fate of digested sludge solids discharged only in certain stages of the tidal cycle.

For the second application, conservation of mass equations were employed as before except that the segments are oriented both along the axis of flow in Boston Harbor (the x-direction) and vertically across the depth of the harbor (the z-direction). Bottom segments were added to act as repositories for the sludge solids that reached the bottom. The equations for the segments in the column into which the sludge solids are discharged are formed as follows for the top segment, call it k:

$$V_k \frac{dc_k}{dt} = E'_{k,k+1} (c_{k+1}-c_k) - uA_{k,k+1}c_k - \sum_j Q_{kj}(t)c_j \qquad (29)$$

where u is the settling velocity of the sludge. The terms on the righthand side of this equation represent, respectively, the vertical turbulence, the settling velocity mass transport, and the tidal flow.

For the middle segment, k+1, the conservation of mass equation is:

$$V_{k+1} \frac{dc_{k+1}}{dt} = E'_{k,k+1} (c_k-c_{k+1}) + E'_{k+1,k+2}(c_{k+2}-c_{k+1}) + uA_{k,k+1}c_k - uA_{k+1,k+2}c_{k+1} - \sum_j Q_{kj}(t)c_j + W(t) \qquad (30)$$

where W(t) is the source of solids due to the sludge discharge. The third segment equation is similar to the equation for segment k. The bottom segment equation is:

$$V_{k+3} \frac{dc_{k+3}}{dt} = uA_{k+2,k+3}c_{k+2} \qquad (31)$$

Thus, this equation accumulates the settling solids in each column, and the rate at which the solids build up is the deposition rate.

These equations are used for all columns in the model with the exception of the first column at the head of the Inner Harbor and the last column at the ocean boundary where no transfer is specified across the edges of the boundary. Thus, the only sink of sludge solids is deposition on the bottom.

The Δx for this model varies from about 0.2 mile in the immediate vicinity of the major discharge to about 1.5 miles at distances removed from the input. The Δz (vertical grid size) varied depending on the depth of water but generally averaged about 15 feet in each of three vertical segments. An additional bottom segment of arbitrary Δz = 1 foot was included as noted above.

A variable time step was used with smaller steps being employed during load discharge. Δt therefore varied from .01 hours to .05 hours. With this model, the behavior of the sludge as discharged at specific intervals could be tracked. The most important effect however was the build-up of sludge solids on the bottom. Fig. 9 shows the end result of the application of this model and does indicate that sludge solids may be deposited in the Inner Harbor area (mile 0.0 to mile 7.0).

Additional References

7. Jeglic, J.M. DECS III, Mathematical Simulation of the Estuarine Behavior. Prepared for FWPCA by General Electric Re-Entry Systems Dept., Philadelphia, Pa. Dec. 1966.

8. MacEwen, P.K. and Tortoriello, R.C. Forecasting of Water Quality Data in the Delaware River Estuary Proc. Nat. Symp. on Data & Instrumentation for Water Quality Management, J.E. Kerrigan Ed., Univ. of Wisc., Madison, Wisc. 1970 pp 99-123.

9. Hetling, L., A Mathematical Model for the Potomac River - What it Has Done and What it Can Do. Presented at 1966 Fall Meeting of Interstate Comm. on Potomac River Basin.

10. Jaworski, N.A. et al Nutrient Management in the Potomac Estuary. Tech. Rpt. 45, Ches. Tech.Supp. Lab., WQO, EPA, Annapolis, Md. Jan 1971, 61 pp.

11. Jaworski, N.A. et al A Technical Assessment of Current Water Quality Conditions and Factors Affecting Water Quality in the Upper Potomac Estuary. Tech. Rpt. No. 5, Ches.Tech.Sup. Lab. Mid-Atl. Reg., FWPCA, March 1969, V Chapt.

12. Leenderste, J.J. A Water Quality Simulation Model for Well-Mixed Estuaries and Coastal Seas. Vol. I, Principles of Computation. Memo. RM-6230-RC, The Rand Corp., Santa Monica, Calif.

13. Development of Water Quality Model of Boston Harbor Prep. by Hydroscience, Inc., Westwood, N.J. for Commonwealth of Mass., Water Res. Comm., Boston, Mass., March 1971.

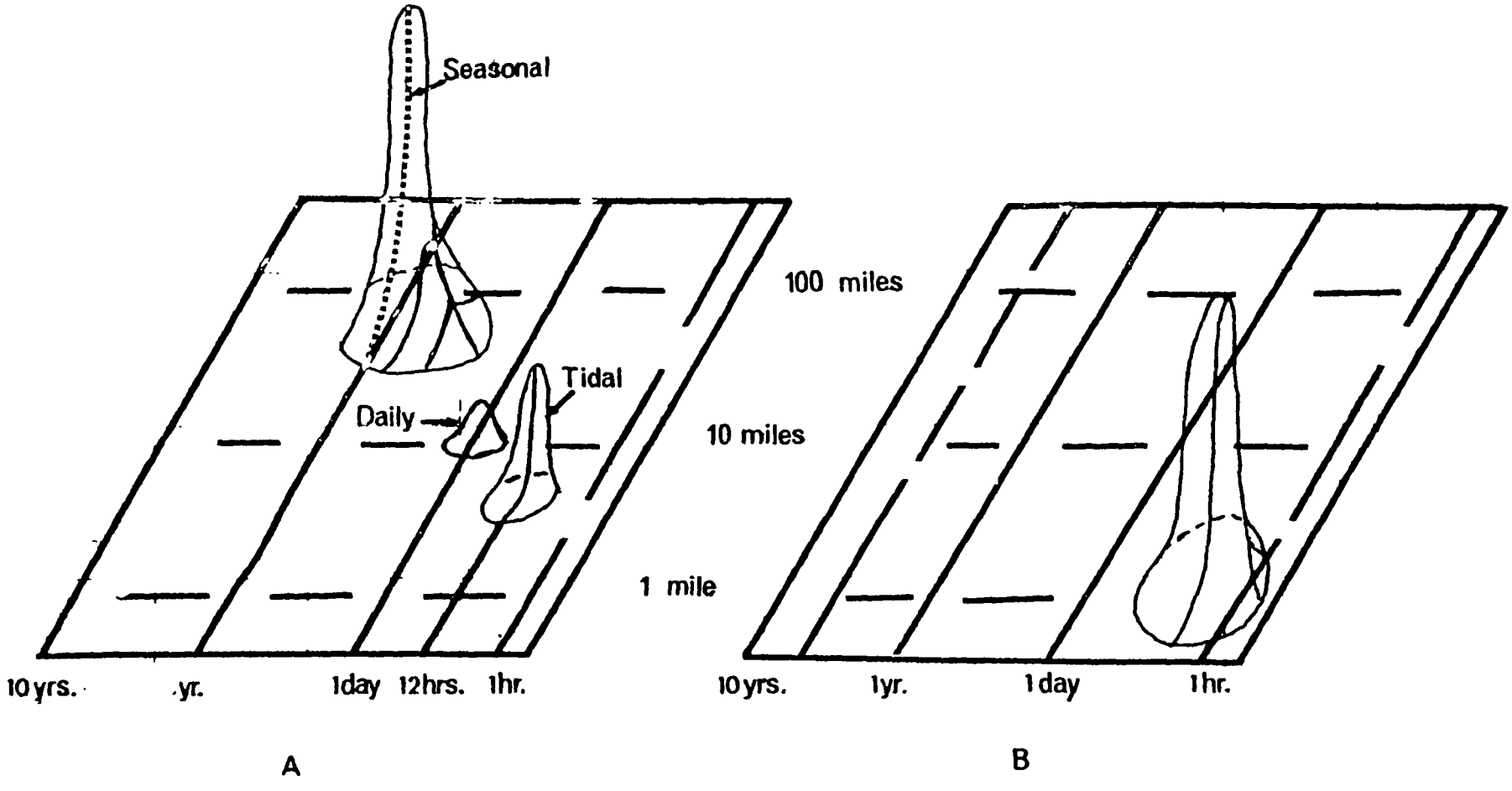

FIGURE 1

Two Examples of Significant Time and Space Variations in Water Quality
(A) Dissolved Oxygen in Delaware Estuary
(B) Iron in Off-Shore Water After Discharge from Moving Waste Barge
Spatial scale represents horizontal distances.

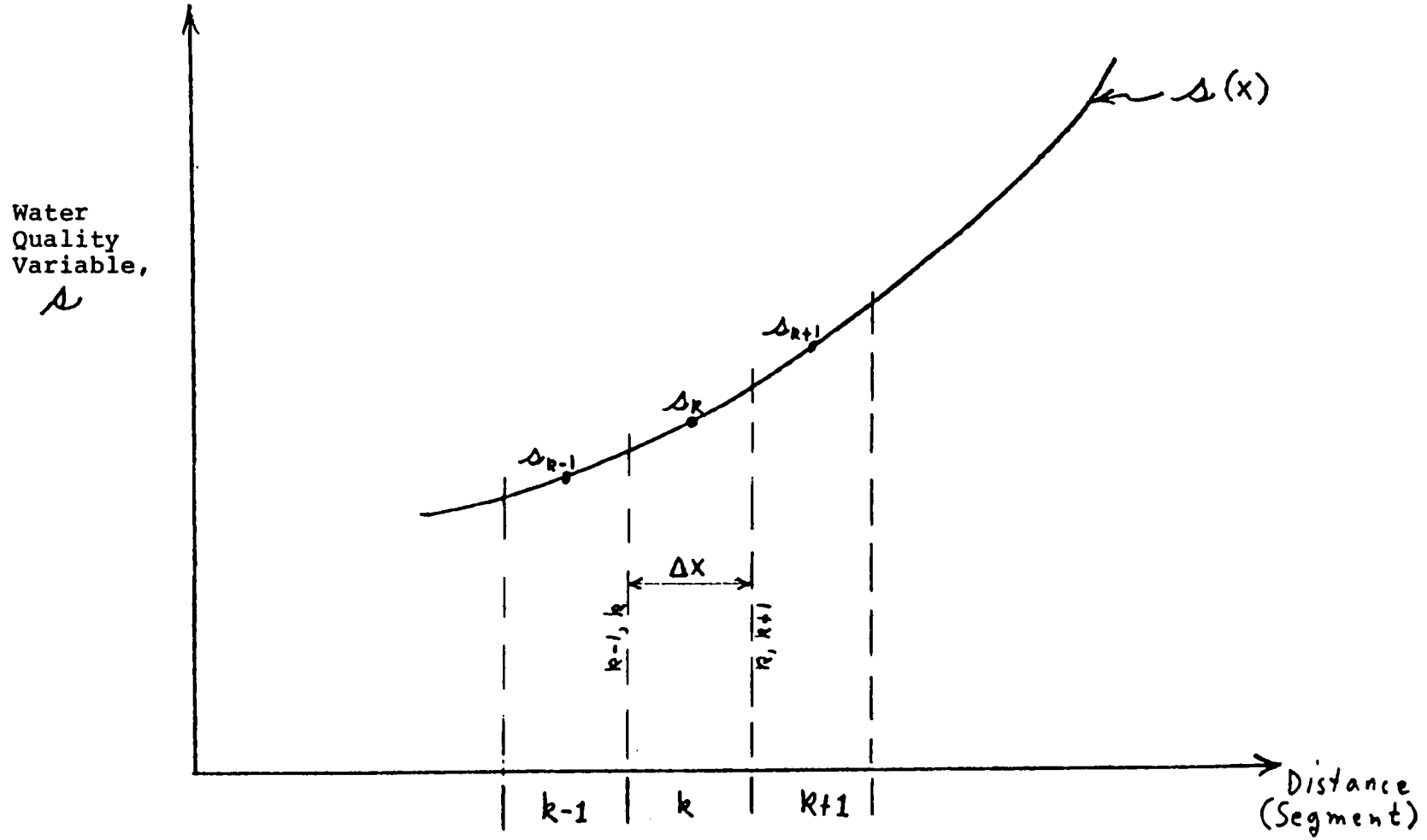

Fig. 2 Approximation in x-direction

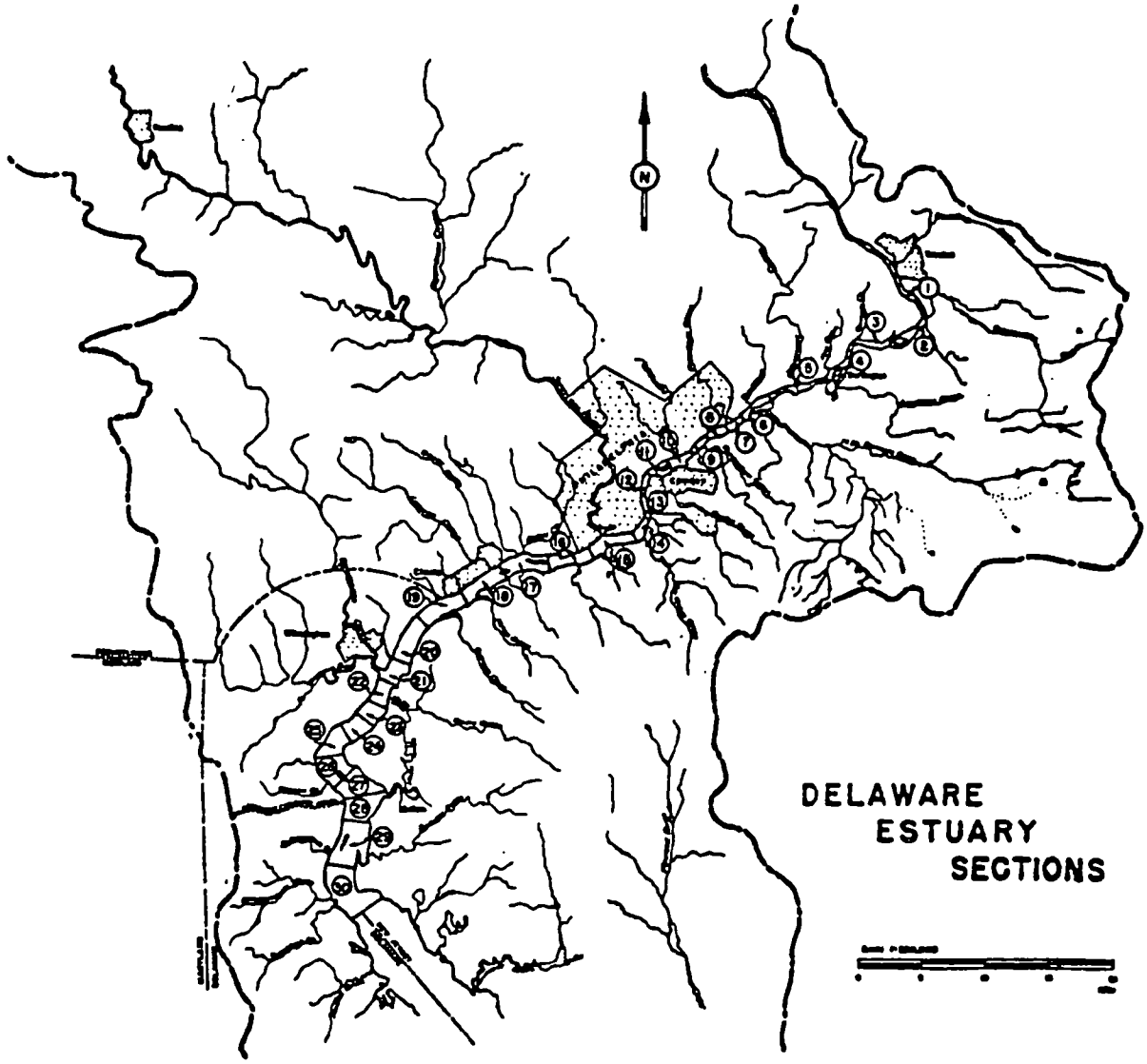

Figure 3

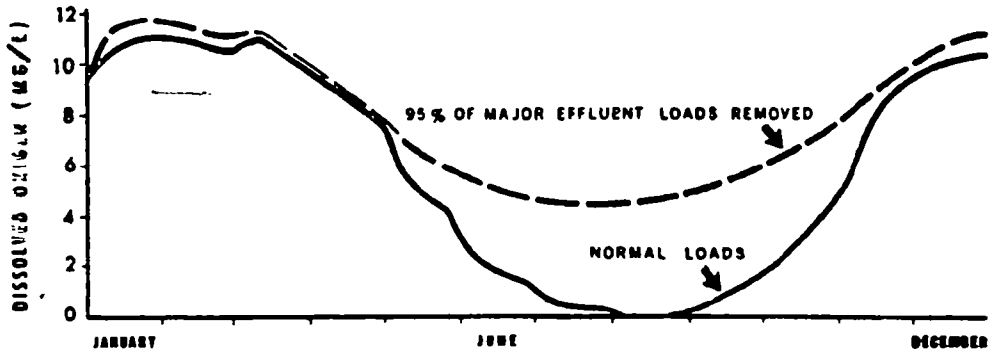

Figure 4 Temporal Distribution of Dissolved Oxygen

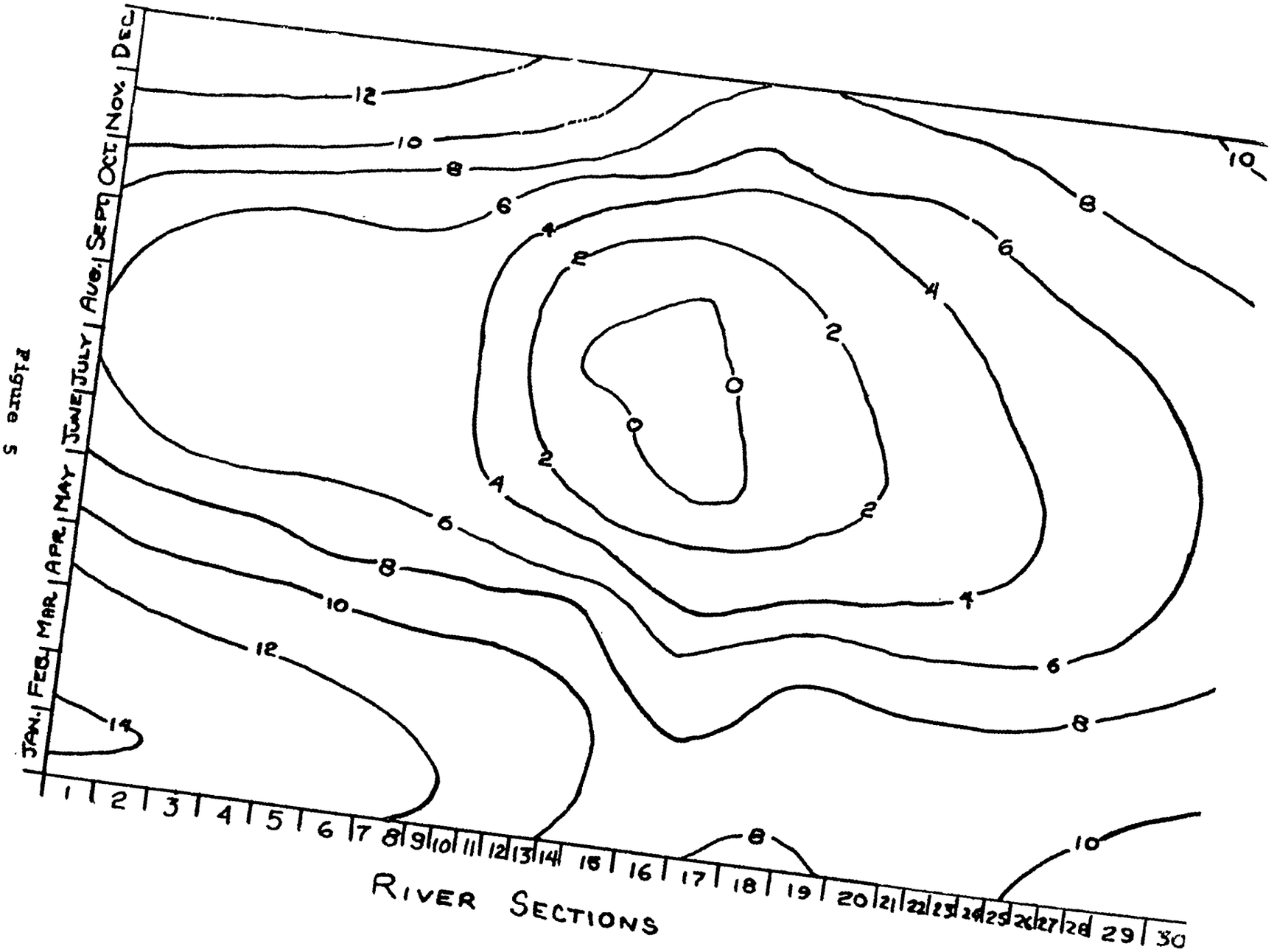
JAN.
FEB.
MAR.
APR.
MAY
JUNE
JULY
AUG.
SEPT.
OCT.
NOV.
DEC.
12
10
8
6
4
2
0
2
4
6
8
10
12
14
8
10
1 2 3 4 5 6 7 8 9 10 11 12 13 14 15 16 17 18 19 20 21 22 23 24 25 26 27 28 29 30
RIVER SECTIONS

FIGURE 5

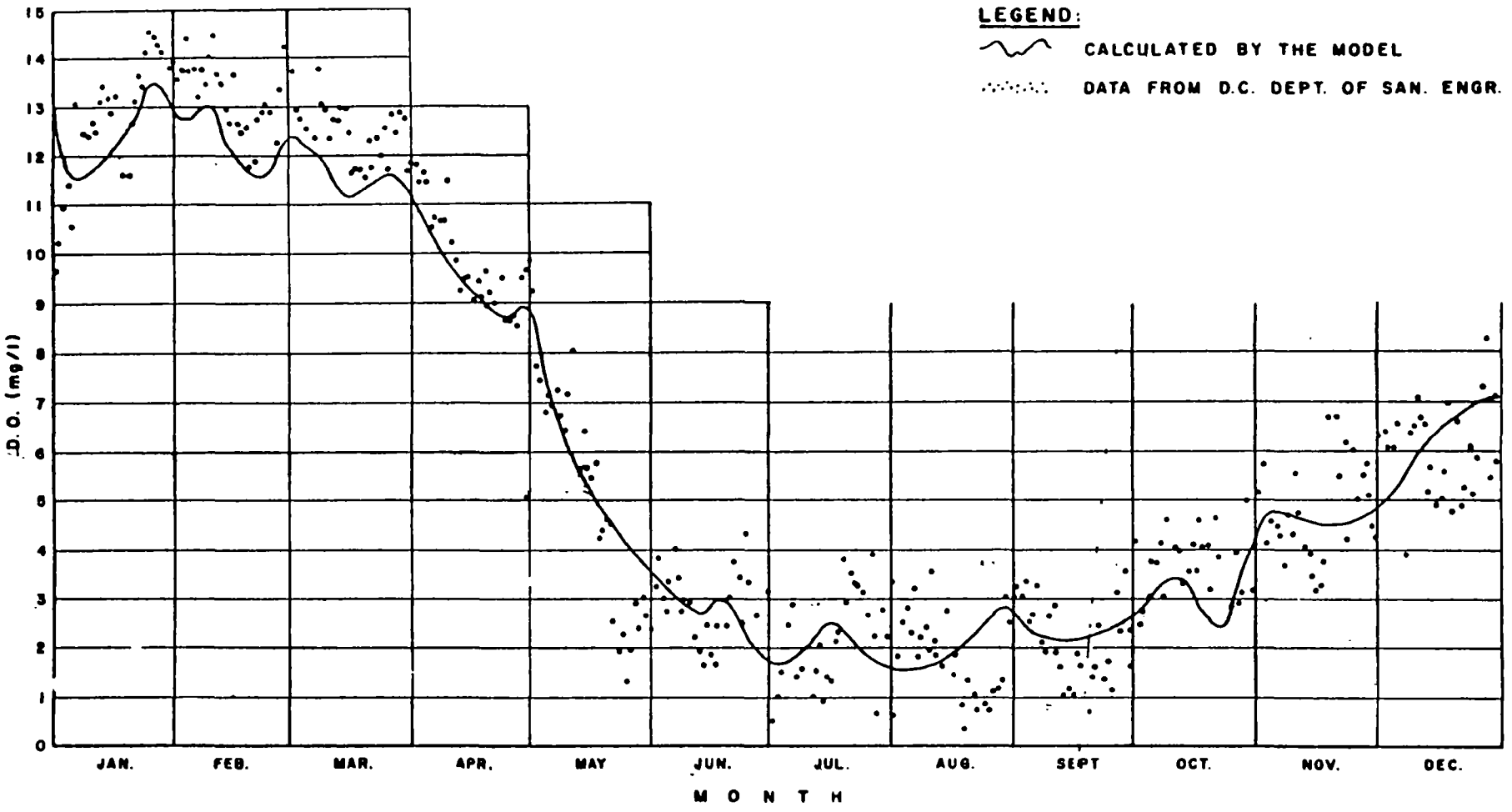

POTOMAC ESTUARY
DISSOLVED OXYGEN CONCENTRATION AT
WOODROW WILSON BRIDGE

Figure 6

DO CONCENTRATIONS

POTOMAC ESTUARY

SEPT. 22, 1968

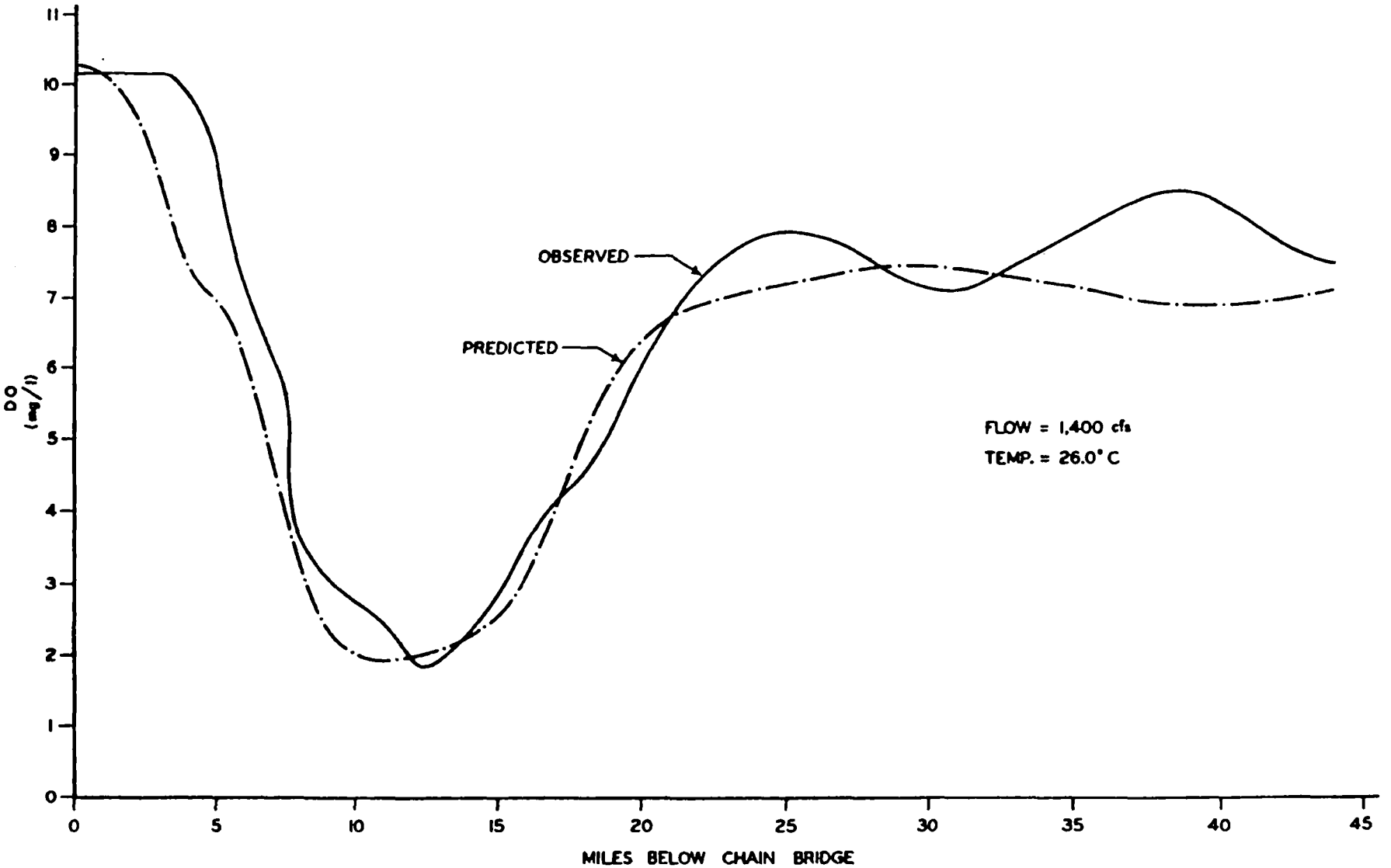

Figure 7

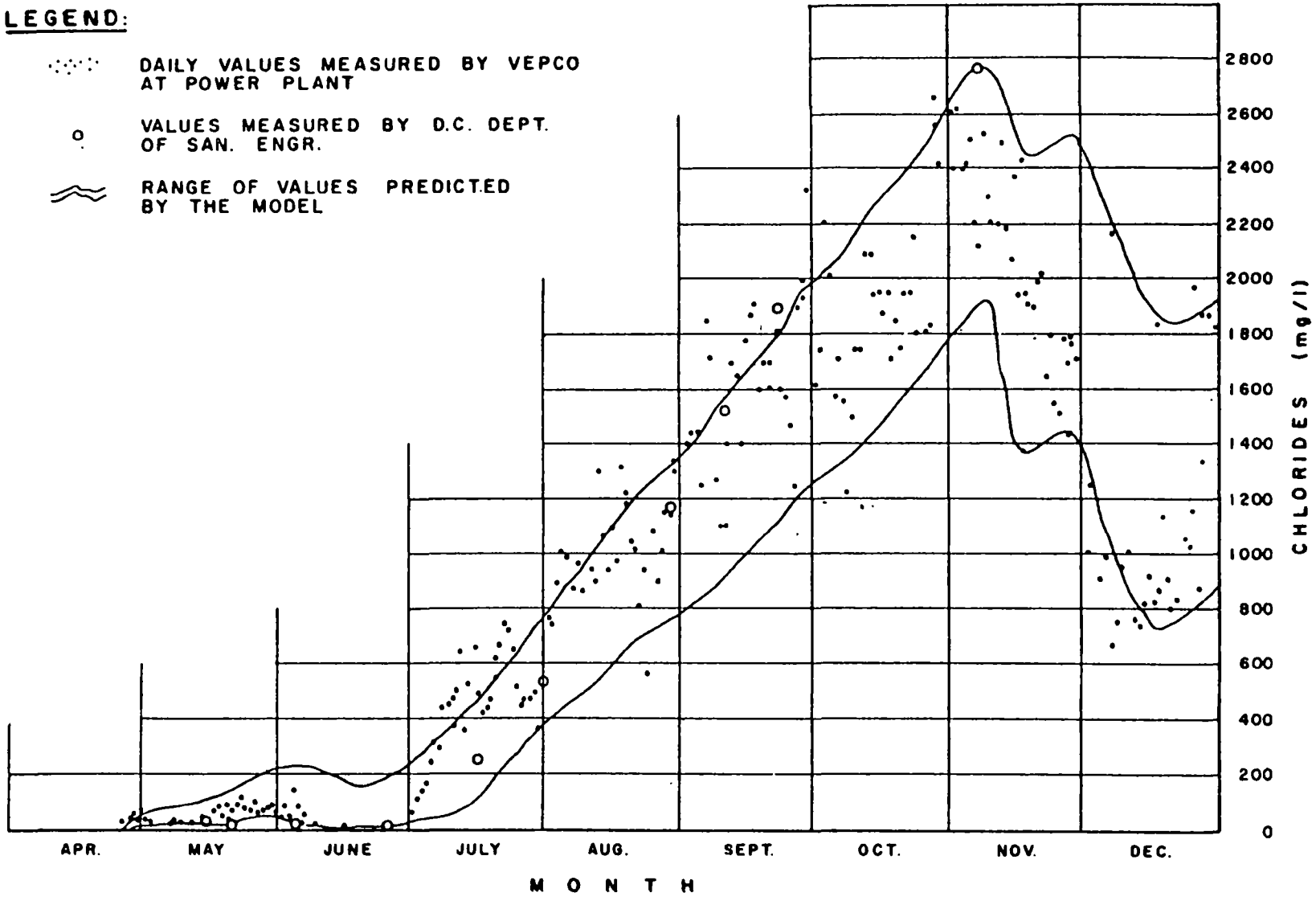

POTOMAC ESTUARY

1963 CHLORIDES AT POSSUM POINT

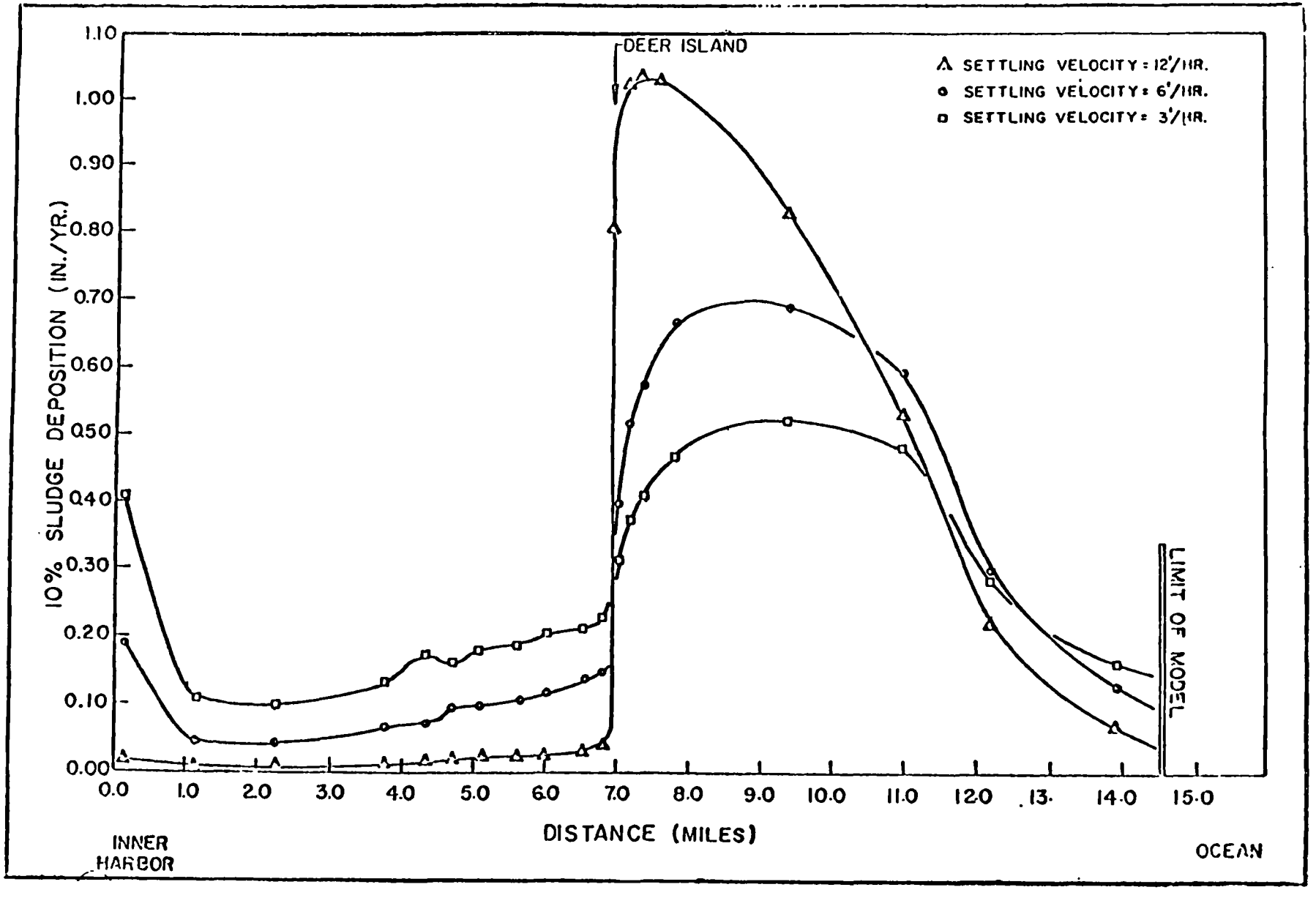
DEER ISLAND
SETTLING VELOCITY = 12'/HR.
SETTLING VELOCITY = 6'/HR.
SETTLING VELOCITY = 3'/HR.
10% SLUDGE DEPOSITION (IN./YR.)
1.10
1.00
0.90
0.80
0.70
0.60
0.50
0.40
0.30
0.20
0.10
0.00
0.0
1.0
2.0
3.0
4.0
5.0
6.0
7.0
8.0
9.0
10.0
11.0
12.0
13.
14.0
15.0
LIMIT OF MODEL
DISTANCE (MILES)
INNER HARBOR
OCEAN

Figure 9

Relationship Between Waste Load Variability and Water Quality Response[1/]

Theoretical Background

In a one-dimensional stream or estuary with a wasteload discharged at x = 0, the time rate of change of dissolved oxygen (DO) as a result of the discharge of waste material expressed as biochemical oxygen demand (BOD) is given by the following pair of partial differential equations:

$$\frac{\partial L}{\partial t} = -\frac{1}{A}\frac{\partial}{\partial x}(QL) + \frac{1}{A}\frac{\partial}{\partial x}\left(EA\frac{\partial L}{\partial x}\right) \pm \Sigma_L \qquad (1)$$

$$\frac{\partial c}{\partial t} = -\frac{1}{A}\frac{\partial}{\partial x}(Qc) + \frac{1}{A}\frac{\partial}{\partial x}\left(EA\frac{\partial c}{\partial x}\right) \pm \Sigma_c \qquad (2)$$

where

L = carbonaceous BOD and/or nitrogeneous BOD

c = dissolved oxygen

Q = net river flow

A = cross-section area

E = dispersion coefficient

$\Sigma_{L,c}$ = sources and sinks of DO and BOD, respectively

Various authors have utilized this pair of equations under a variety of assumptions and obtained either analytical solutions or solutions to difference forms of equations.

The equations as they stand are linear, and as such the principle of super position applies. From the point of view of systems analysis, the notion of a frequency transfer function is particularly relevant to describing the relationship between waste load variability and water quality response. This notion can be developed and derived by assuming a harmonic variation in the waste load, W and developing the periodic output response. The ratio of the harmonic input to the harmonic output is formally termed the "frequency transfer function." For the case of streams where E approaches zero and the stream parameters are constant, one can examine the response of the system by assuming the input to be varying with a specific frequency and

[1/] Robert V. Thomann

zero lag. Thus,

$$L_o(t) = \bar{L}_o + L_{oA}\sin\omega t \tag{3}$$

where $L_o(t)$ is the time variable initial stream BOD due to a waste load of W lbs/day, $\bar{L}_o$ is the mean BOD, L_{oA} is the amplitude, and ω is the input frequency equal to $2\pi/T$ where T is the period. If equation 3 is used as an input forcing function for the constant parameter stream case of equation 1 given by:

$$\frac{\partial L}{\partial t} = -\frac{Q}{A}\frac{\partial L}{\partial x} - K_r L \tag{4}$$

where K_r is the removal of BOD from the stream, the solution is given by:

$$L = [\bar{L}_o + L_{oA}\sin(\omega t - \frac{\omega x}{u})]e^{-K_r x/u} \tag{5}$$

where u = stream velocity. Equation 5 can be written as:

$$L = \bar{L}_o e^{-K_r x/u} + A_L L_{oA}\sin(\omega t - \theta_L) \tag{6}$$

where

$$A_L = e^{-K_r x/u} \tag{6a}$$

$$\theta_L = \frac{\omega x}{u} \tag{6b}$$

A and θ are known as the amplitude characteristic and phase characteristic of the system. In general, these quantities are both functions of ω; although as can be seen here, the amplitude characteristic for constant parameter stream case is independent of input frequency. In complex notation:

$$\phi(i\omega) = A(\omega)e^{i\theta(\omega)}$$

where $\phi(i\omega)$ is the frequency transfer function and $i = \sqrt{-1}$.

For the case of dissolved oxygen deficit, $D = c_s - c$, the constant parameter

stream model for zero initial conditions is

$$\frac{\partial D}{\partial t} = -u \frac{\partial D}{\partial x} - K_a D + K_d L(t) \tag{7}$$

where K_a is the atmospheric reaeration rate and L(t) is given by equation 6. Under these conditions, the amplitude and phase characteristics can be shown to be

$$A_D = \frac{K_d}{K_a - K_r}(e^{-K_r x/u} - e^{-K_a x/u}) \tag{8a}$$

$$\theta_D = \frac{\omega x}{u} \tag{8b}$$

and

$$D = \bar{D}(x) + A_D L_{oA} \sin(\omega t - \omega x/u) \tag{9}$$

where $\bar{D}(x)$ is the classical DO deficit profile given by

$$\bar{D} = \frac{K_d \bar{L}_o}{K_a - K_r}(e^{K_r x/u} - e^{-K_a x/u})$$

It is seen, then, that once the frequency transfer function in terms of its amplitude characteristic and phase characteristic is known, the harmonic response due to an input of varying frequency can be determined via equation 6. The frequency transfer function forms a very useful descriptor of how the system will behave to a wide variety of time variable waste load inputs. For example, the formal Fourier transform of the frequency transfer function yields the so-called "impulsive response" function. This impulsive response function represents the time-variable response due to a delta function input of waste load. A convolution operation can thus be carried out with the impulsive response function to yield the time variable response in BOD or dissolved oxygen due to any arbitrary waste load input (Thomann, 1972). Thus, knowledge of the frequency transfer function or the impulsive response function provides one with the ability to describe analytically the time variable response in dissolved oxygen due to a harmonically varying input, a delta function type input, or an arbitrary functional form.

An additional important class of waste load inputs is the stochastic case, i.e. the case where the input is randomly varying with a known variance. It is assumed therefore that the variance of the waste load input is known. If a linear system such as given by the dissolved oxygen equation for a stream is considered (equation 7) and the transfer function is known, it is appropriate to begin the analysis of the output response by inputting the variance of the input waste load to the system.

For the case of streams the amplitude characteristics are given by equations 6a and 8a, respectively. The BOD output variance as a function of x is given by

$$\sigma^2_L(x) = A^2_L \sigma^2_{Lo}$$

or

$$\sigma^2_L(x) = (e^{-2K_r x/u})\sigma^2_{Lo} \tag{10}$$

The DO deficit variance as a function of x is given by the following expression:

$$\sigma^2_D(x) = A^2_D \sigma^2_{Lo} \tag{11}$$

or

$$\sigma^2_D(x) = \left[\frac{K_D}{K_a - K_r}(e^{-K_r x/u})\right]^2 \sigma^2_{Lo}$$

It should be recalled that equations 10 and 11 are for constant stream parameters and no upstream BOD or deficit. If the upstream conditions include BOD or deficit, this can be taken into account usually under an independence assumption. Dispersion is also not included.

For the BOD equation 10 shows that the variance decays with distance at twice the rate that the mean decays. The variance in the DO generally has the same shape as the mean, with a maximum variance at the point of maximum deficit. When dispersion is included, the amplitude characteristic is frequency dependent due to the inclusion of the tidal dispersion term in equations 1 and 2 (Thomann, 1972).

Effect of Dispersion on Stream Water Quality Response

Thomann (1973) has derived some general rules for the effect of dispersion on the amplitude characteristic and hence on the degree to which waste load variability is transmitted downstream (see also Di Toro, 1969 and Li, 1972). In that work, the effect of dispersion was related to the following dimensionless quantities

$$P = KE/u^2$$
$$\omega^* = \omega/K$$
$$x^* = Kx/u$$

As a general guide [Hydroscience, Inc., 1971], P = <0.01 for upstream feeder streams, 0.01-0.5 for main drainage rivers, 0.5-1.0 for large rivers, 1.0-10.0 for tidal rivers, and >10 for estuaries. Primary interest therefore centers about the range of P from 0.01 to 1.0. That is, What is the effect of dispersion equivalent to these levels on the dynamic response of water quality? Since frequency and distance are given in dimensionless terms that depend on K and u, Table 1 provides the conversions necessary to interpret readily the range of these numbers.

As is shown in Table 1, for waste load inputs varying with a period of 7 days, ω^* ranges from 9.0 to 0.9; the higher value is associated with slowly reactive substances (K = 0.1/day) such as BOD.

Figure 1 shows the amplitude attenuation as computed from Eq. (1) compared with the zero dispersion case Eq. (5). This figure therefore represents the in-stream amplitude concentration change expected from a unit input amplitude varying with a period corresponding to ω^*. The substantial difference between the zero dispersion case and the case for P > 0 can be seen at increasing ω^*. Figure 2 is a plot of the amplitude characteristic over a wide range of P and for fixed ω^*.

TABLE 1. Period Equivalent to Dimensionless Frequency ω^*

Period of Input, days	K - 0.1/day	K - 0.5/day	K - 1.0/day
360	0.17	0.03	0.02
30	2.1	0.42	0.21
7	9.0	1.80	0.90
1	62.8	12.6	6.28

The use and interpretation of Figures 1-2 can best be seen by means of two examples.

Example 1, Biochemical oxygen demand. Assume that a waste discharge input is varying with a period of 7 days and discharging biochemical oxygen demand into a river where the organic matter decays at a first-order rate of 0.1/day. The river velocity is 0.2 ft/sec (3.2 mi/day). Dye dispersion studies in the river have indicated a longitudinal dispersion coefficient of about 1 mi^2/day. Then $P = KE/u^2 \simeq 0.01$, $\omega^* = 2\pi/TK = 9.0$ (Table 1), and K/u = 0.031/mile. Table 2, constructed from Figure 1(a) and the preceding information, shows the effect of longitudinal dispersion on the response of biochemical oxygen demand. Thus at 10 miles downstream the difference between responses is already 24%, and at

TABLE 2. Amplitude Characteristic for Example 1, Biochemical Oxygen Demand

x, miles	x^*	mg/l Water Quality Amplitude per mg/l Waste Input Amplitude, P = 0	P = 0.01	Difference, mg/l	Difference, %
0	0	1.0	0.98	0.02	2
10	0.3	0.74	0.56	0.18	24
30	0.9	0.41	0.20	0.21	51
60	1.8	0.16	0.05	0.11	69

$\omega^* = 9.0$, P = 0.01, K/u = 0.031/mile.

30 miles downstream the difference is 51%. Figure 3 shows this effect. If the system is highly reactive, the situation is different. The effect can be shown by reexamining example 1 for an order of magnitude increase in decay rate.

Example 2, coliform bacteria. In this example K = 1.0/day, T = 7 days, u = 0.2 ft/sec, E = 1 mi^2/day, $P = KE/u^3 \simeq 0.1$, $\omega^* = 0.9$, and K/u = 0.3/mile. Table 3, using Figure 4, shows the comparison. As is shown in this table, because of the high reaction rate the process is almost entirely complete when

TABLE 3. Amplitude Characteristic for Example 2 - Reactive Variable, K = 1/day

x, miles	x^*	mg/l Water Quality Amplitude per mg/l Waste Input Amplitude, P = 0	P = 0.01	Difference, mg/l	Difference, %
0	0	1.0	0.84	0.16	16
2	0.6	0.55	0.43	0.12	22
5	1.5	0.22	0.17	0.05	23
10	3.0	0.05	0.035	0.015	30

$x^* = 3.0$, at which point maximum differences are about 30% but are at very low concentrations. Intermediate differences are about 20%. For the same river situation therefore the effect of longitudinal dispersion is less pronounced for highly reactive substances than for more slowly reactive substances for input periodic fluctuations to about 30 days. For shorter-term input fluctuations (e.g. 7 days or less) the effect becomes progressively more important.

For variables such as dissolved oxygen, the amplitude attenuation is evaluated from Eq. (7). Figure 4 shows the amplitude attenuation of the maximum dissolved oxygen deficit relative to the waste load input amplitude expressed in mg/ℓ at the outfall, i.e. W/Q where Q is the total river flow noted. The effect of dispersion on a time variable waste input is generally less for upland rivers than for larger rivers, as is shown in Figure 4. In Figure 4a, with a reaeration ratio ($K_a/K_d = 5$), if the input is varying with a period of 7 days or less, the effect of assuming zero dispersion may become important. For $P = 0.1$ and $\alpha = 0.5$, characterizing some main drainage rivers, the effect of dispersion is most pronounced as shown in Figure 4b. The magnitude drops significantly where for an input of 7 days, the response for $P = 0.1$ is about 30% of the response for $P = 0$.

The effect of dispersion in the large rivers, which are generally more sluggish and have a lower reaeration, is even more pronounced, as is shown in Figure 4c. Indeed, input fluctuations varying with periods of about 7 days or less are completely attenuated under a condition of $P = 0.5$.

These results indicate in general that estimates of the time variable effect of waste discharges should recognize the potential importance of stream dispersion in attenuating effluent variability. This especially true for larger main stream rivers. However, for most small stream situations where K_a/K_d is large, and velocities greater than about 0.5 ft/sec, the effect of dispersion on the water quality response due to a time variable effluent is small and can generally be neglected.

REFERENCES

Thomann, R.V. 1972. Systems analysis and water quality management. McGraw-Hill Book Co., N.Y., 287 pp.

Thomann, R.V. 1973. Effect of longitudinal dispersion on dynamic water quality response of streams and rivers. Water Res. Res. 9(2):355-366.

Di Toro, D.M. 1969. Stream equations and methods of characteristics. J. Sanit. Eng. Div. Amer. Soc. Civil Eng., 95(SA4), 699-703.

Hydroscience, Inc. 1971. Simplified mathematical modeling of water quality. Westwood, N.J., pp. 36-46.

Li, W. 1972. Effects of dispersion on DO-sag in uniform flow. J. Sanit. Eng. Div. Amer. Soc. Civil Eng., 98(SA1), 169-182.

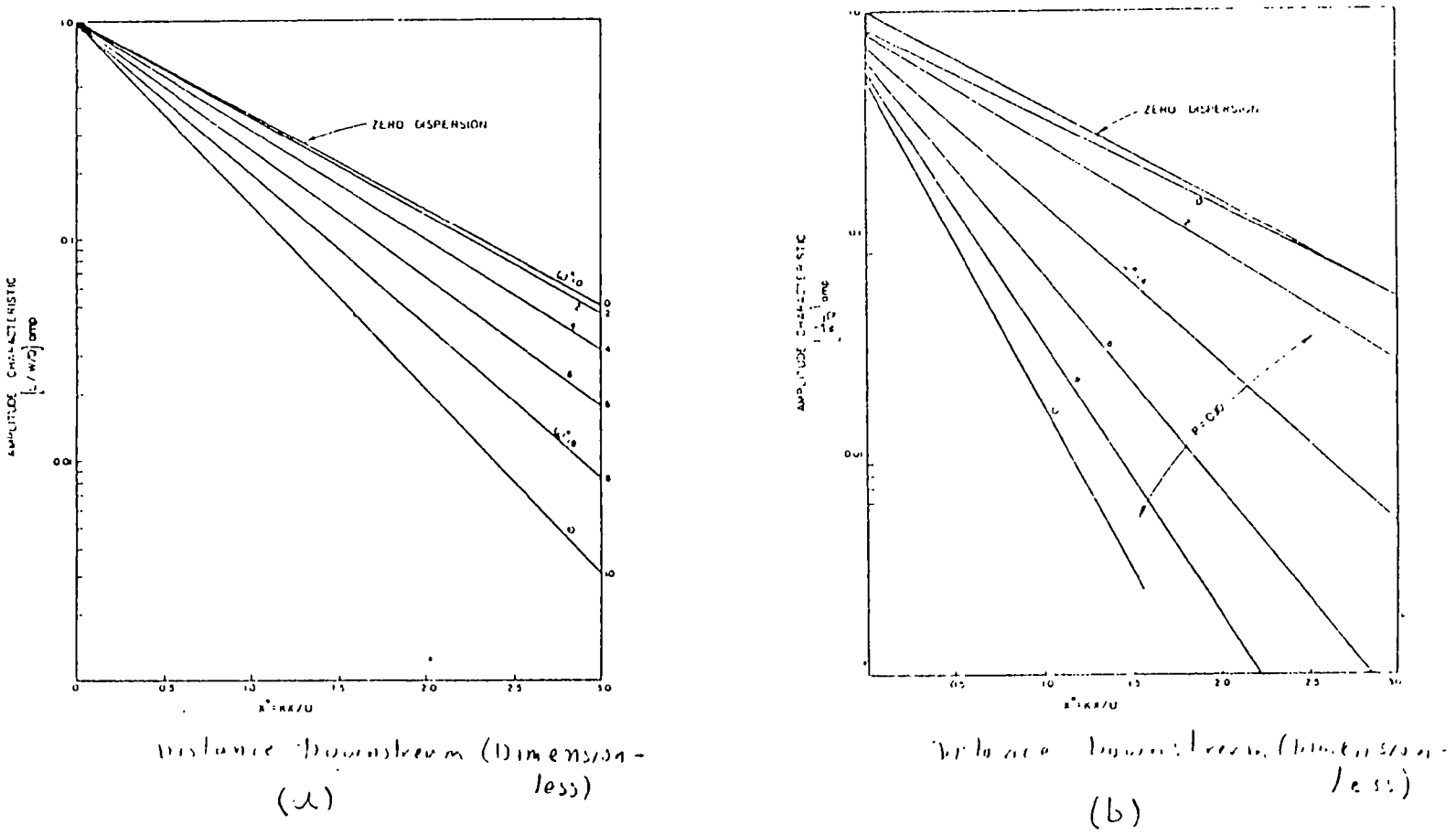

Figure 1. Amplitude characteristic of a single nonconsecutive variable, $\omega^* = 0\text{-}10$; (a) P = 0.01 and (b) P = 0.1; $P = KE/u^2$

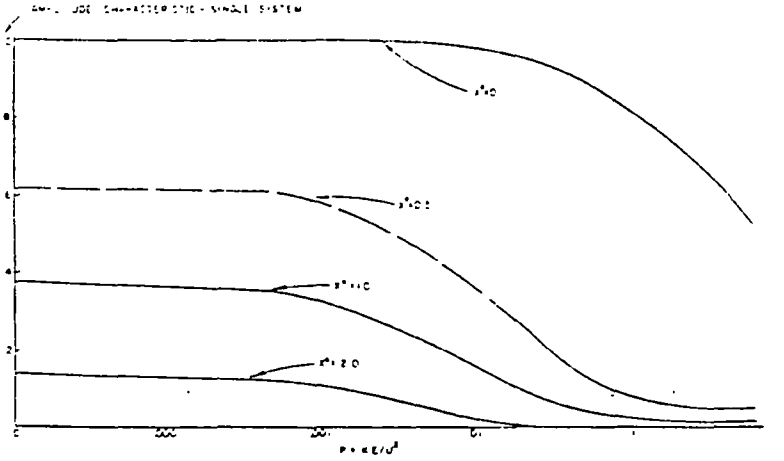

Figure 2. Amplitude characteristic for nonconservative variable for variable $P = KE/u^2$ and for $\omega^* = K/\omega = 10$

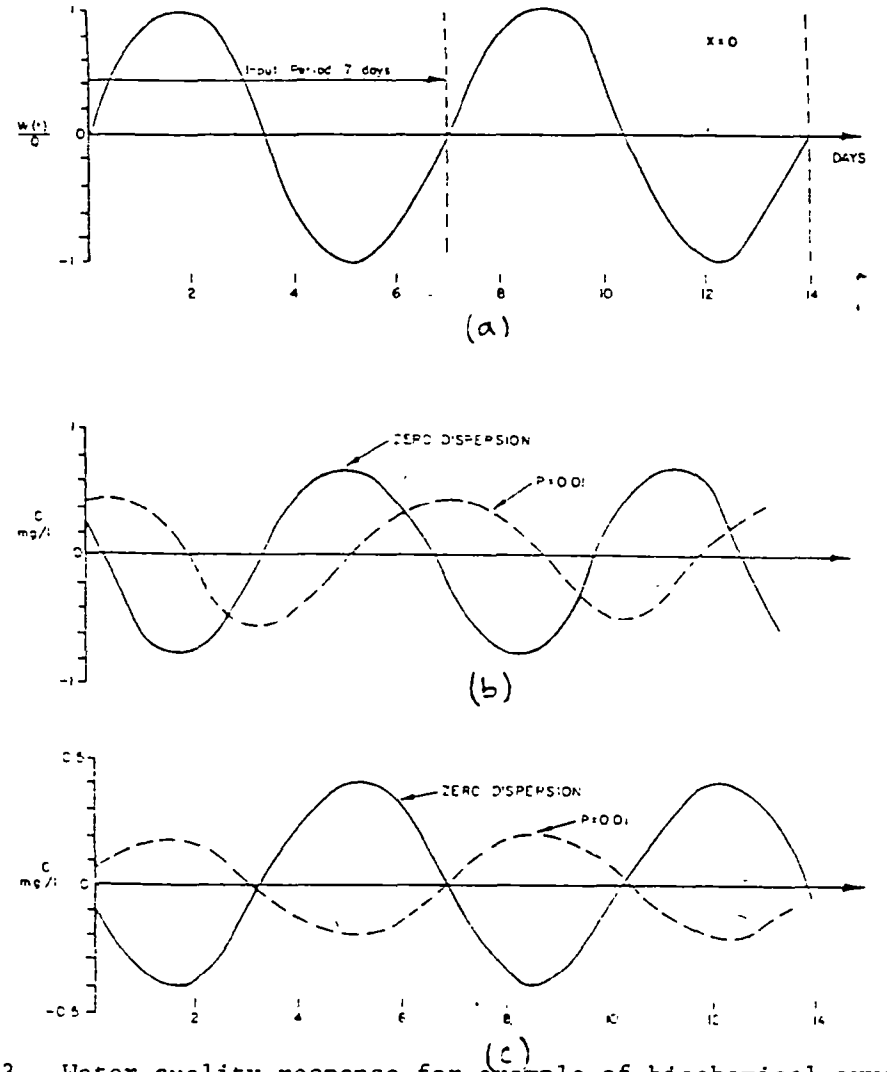

Figure 3. Water quality response for example of biochemical oxygen demand: a) waste load input; and BOD response at b) 10 miles and c) 30 mi.

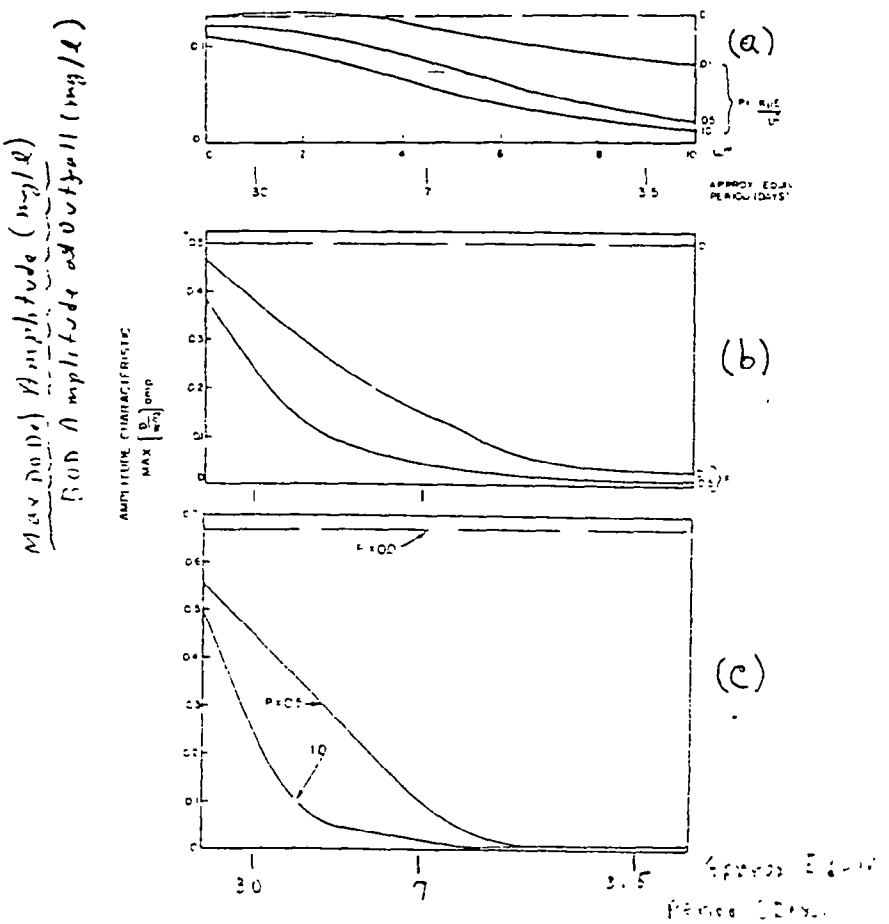

Figure 4. Amplitude characteristic for maximum DO deficit for three river systems: a) $K_a/K_d = 5$; b) $K_a/K_d = 0.5$; c) $K_a/K_d = 0.2$.

Example of Time Variable D.O. Modeling
Upper Delaware River[1/]

The purpose of this modeling analysis (Hydroscience, 1975) was to evaluate the effect of increased BOD loading on DO and the impact of a projected regional STP load for the Upper Delaware River (Figures 1 and 2). Flows in the Delaware average about 12000 cfs at Trenton and low flows of about 2500 cfs. Depths vary from 2-10 feet. The analysis was complicated by the presence of significant rooted aquatic macrophyte beds in the lower reaches of the study area (Figure 3). The impact of the weed bed on BOD was interesting and is shown in Figure 4. The upper panel indicates the particulate BOD upstream of the weed bed while Figure 4(b) shows the particulate BOD above and below the weed bed and indicates that about 30% of the particulate BOD is removed from the overlying water column as it passes through the weed bed. The flow during this period was about 4380 cfs, a rather high summer flow.

The model consisted of two reaches of 141 finite difference segments for Mile 218 to Mile 175 and 136 segments for Mile 175 to Mile 134. This is a total of 277 segments of about 0.3 miles in length. Figure 5 shows the depth distribution over the study reaches. The model was run in a backward difference mode so that the numerical dispersion introduced was:

$$E_{num} = \frac{U\Delta x}{2}$$

for Δx as the segment length. For a velocity of about 0.5-1 ft/sec. (8-16 mi/day) for Reach 2 and Δx = 0.3 miles, this results in numerical dispersion of about 1.2-2.4 mi^2/day.

A dye study conducted on the upper Delaware permitted an estimate of river dispersion. Typical results are shown in Figure 6 where the total dispersion ranged from 1.6 mi^2/day at Frenchtown to 4 mi^2/day at Trenton.

Examples of the time variable calibration to the DO data at Trenton are shown in Figures 7 and 8. The variations in waste treatment plant effluents were dampened rapidly in the calculation due to the river dispersion. Phytoplankton and weed mass DO production did however contribute markedly to variations in DO. Figure 7 shows the progressive increase in diurnal variation of DO as calibrated by the model and the accompanying

[1/] Robert V. Thomann

observed DO. The model did not completely calculate the diurnal range however especially in terms of calculating the minimum values. Figure 8(a) indicates that the model approximately duplicated the observed daily ranges but did not properly respond to a day to day transient weather effect of cloudy days from July 18-23. The rapid drop of daily mean values of almost 3 mg/ℓ was generally not captured by the model (DW is a weed respiration rate). Figure 8(b) shows that the diurnal amplitude was modeled correctly but the mean value did not respond as rapidly as the observed data. These results illustrate the random day to day fluctuations in DO which are difficult to model because of uncertainties in photosynthesis and respiration effects.

Based on the modeling analysis, Figure 9 shows the estimated number of days/month that the instantaneous daily DO will be less than a given level under different loading conditions. For example, the projections indicate under condition (B) that about 7 days per month would have minimum DO levels less than 5 mg/ℓ for the region below Eastern. Table 1 shows the number of days/month that the minimum DO will be less than 4, 5 and 6 mg/ℓ for different river discharges.

Table 1

River Discharge (cfs)	Recurrence Intervals (yrs)	No. of days < Minimum DO Objective (mg/ℓ) 4	5	6
4700	2	1	6	16
2700	20	1	4	15

REFERENCE

Hydroscience, Inc. 1975. Time variable water quality analyses and related studies of the Upper Delaware River - Port Jervis to Trenton. Prepared for Delaware River Basin Commission. West Trenton, N. J., 164 pp. and 5 Appendices.

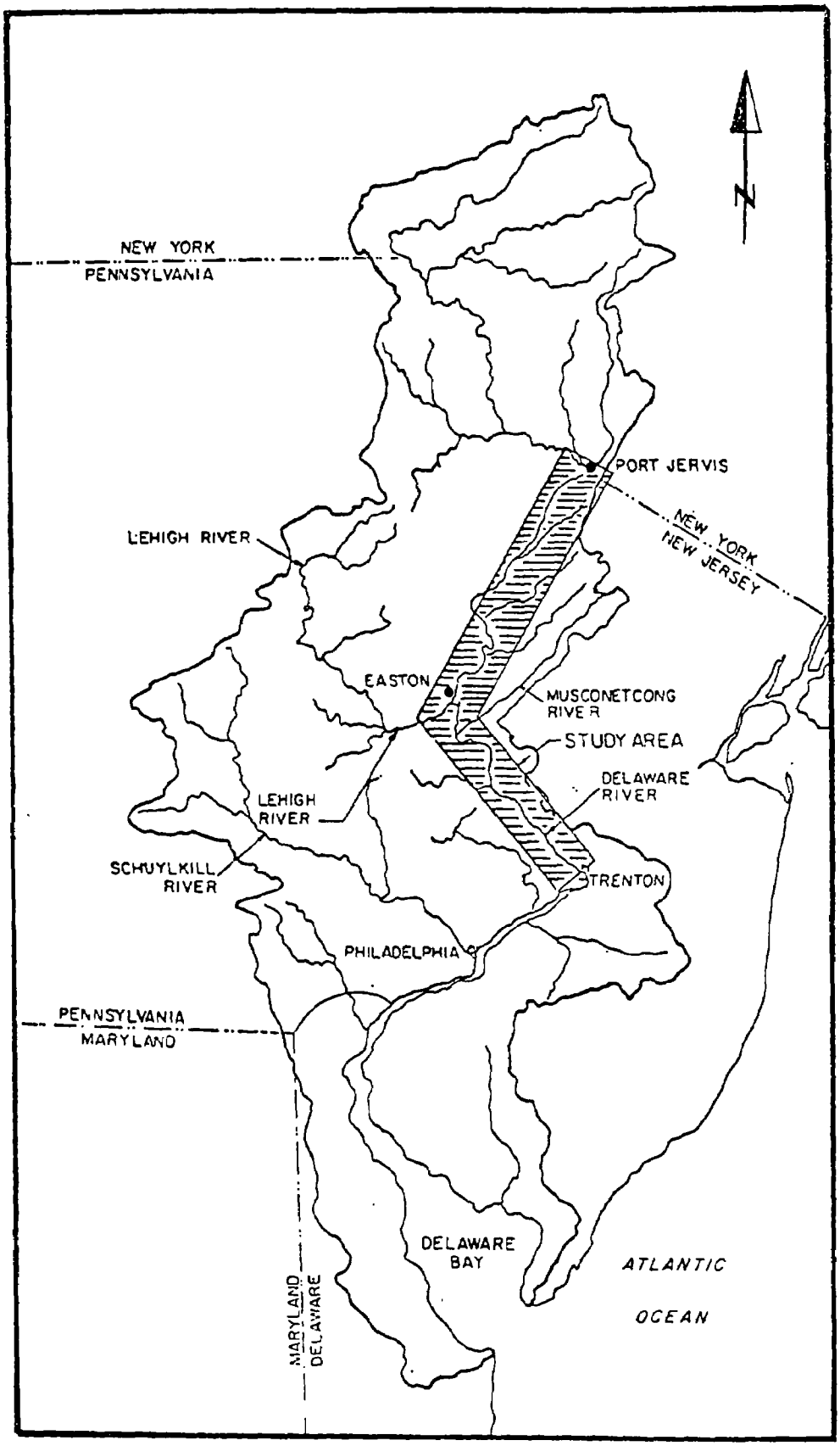

FIGURE 1

DRAINAGE AREA OF THE DELAWARE RIVER

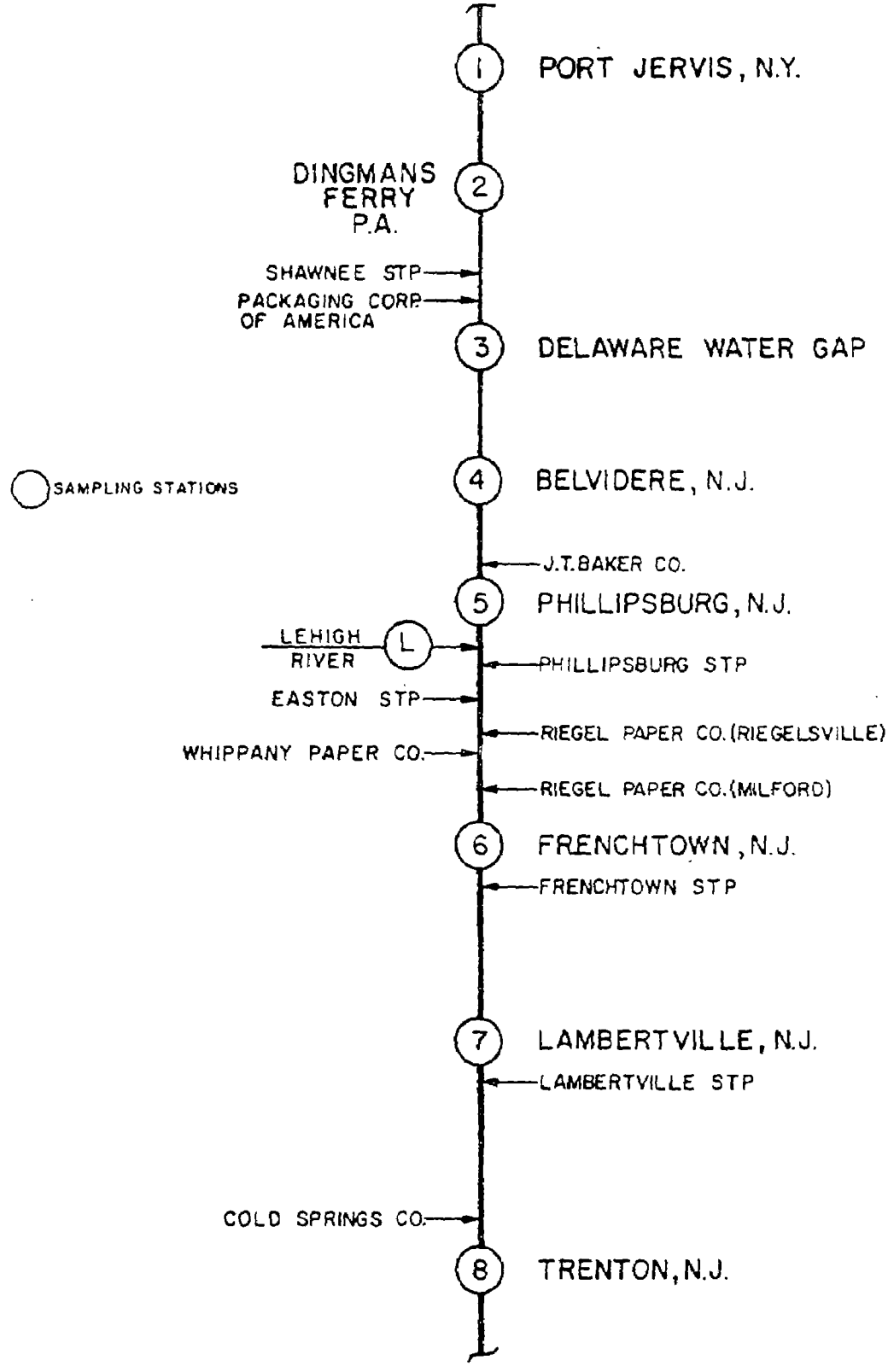

FIGURE 2

SCHEMATIC OF THE DELAWARE RIVER

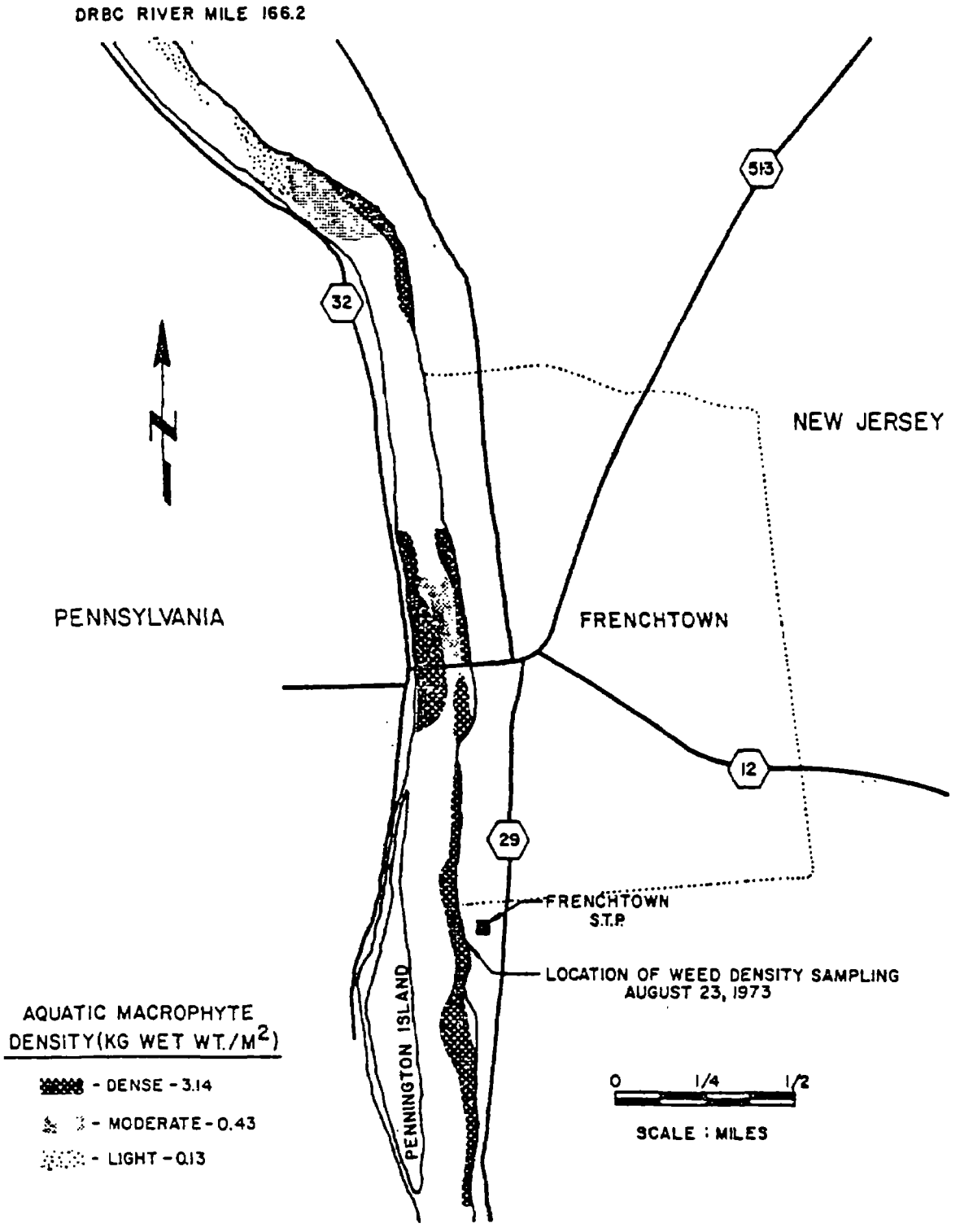

AFTER: MAZA AND CRAIGHEAD, 1968

FIGURE 3

DISTRIBUTION OF AQUATIC MACROPHYTES
VICINITY OF FRENCHTOWN, NEW JERSEY

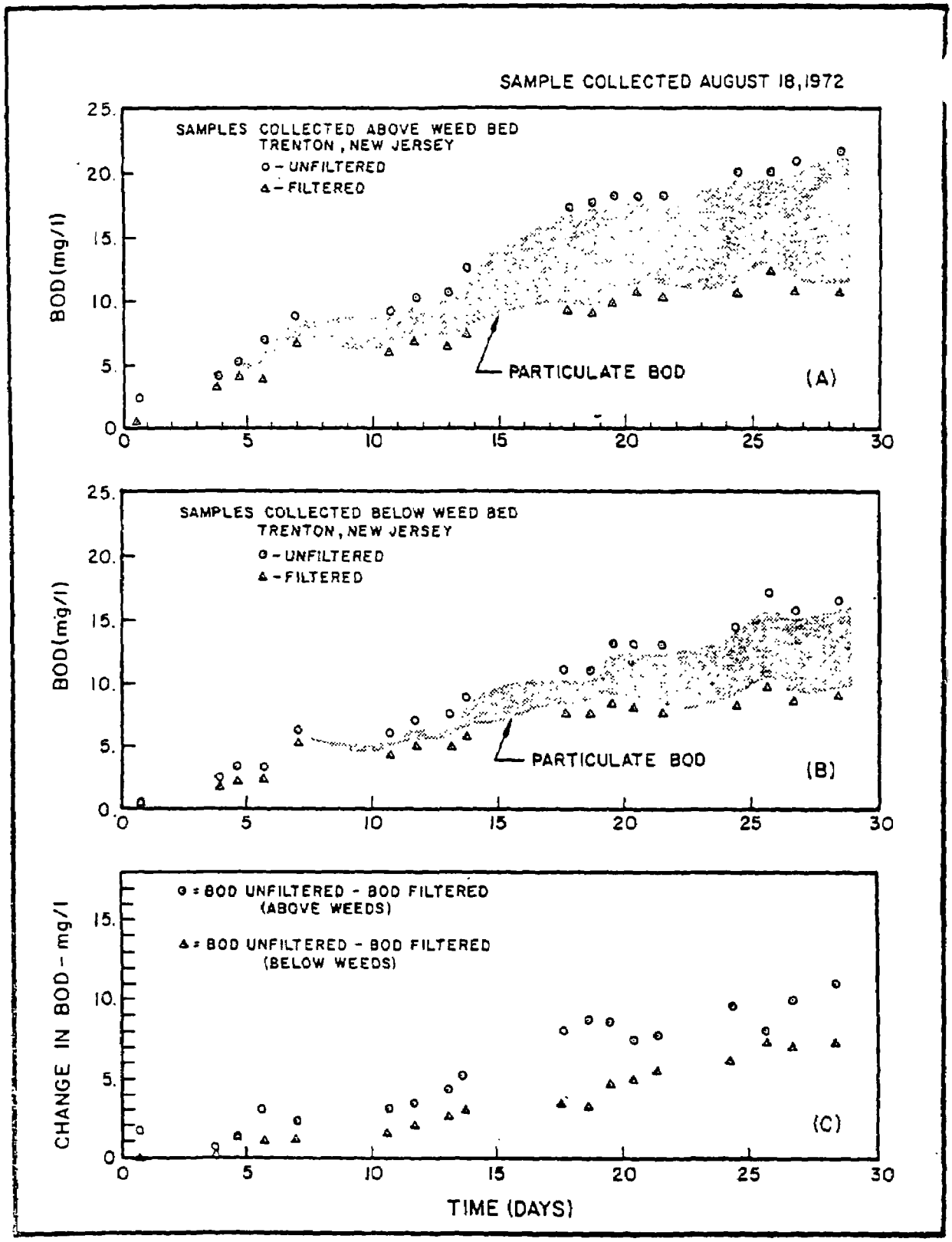

FIGURE 4

EFFECT OF WEED ON LONG TERM BOD

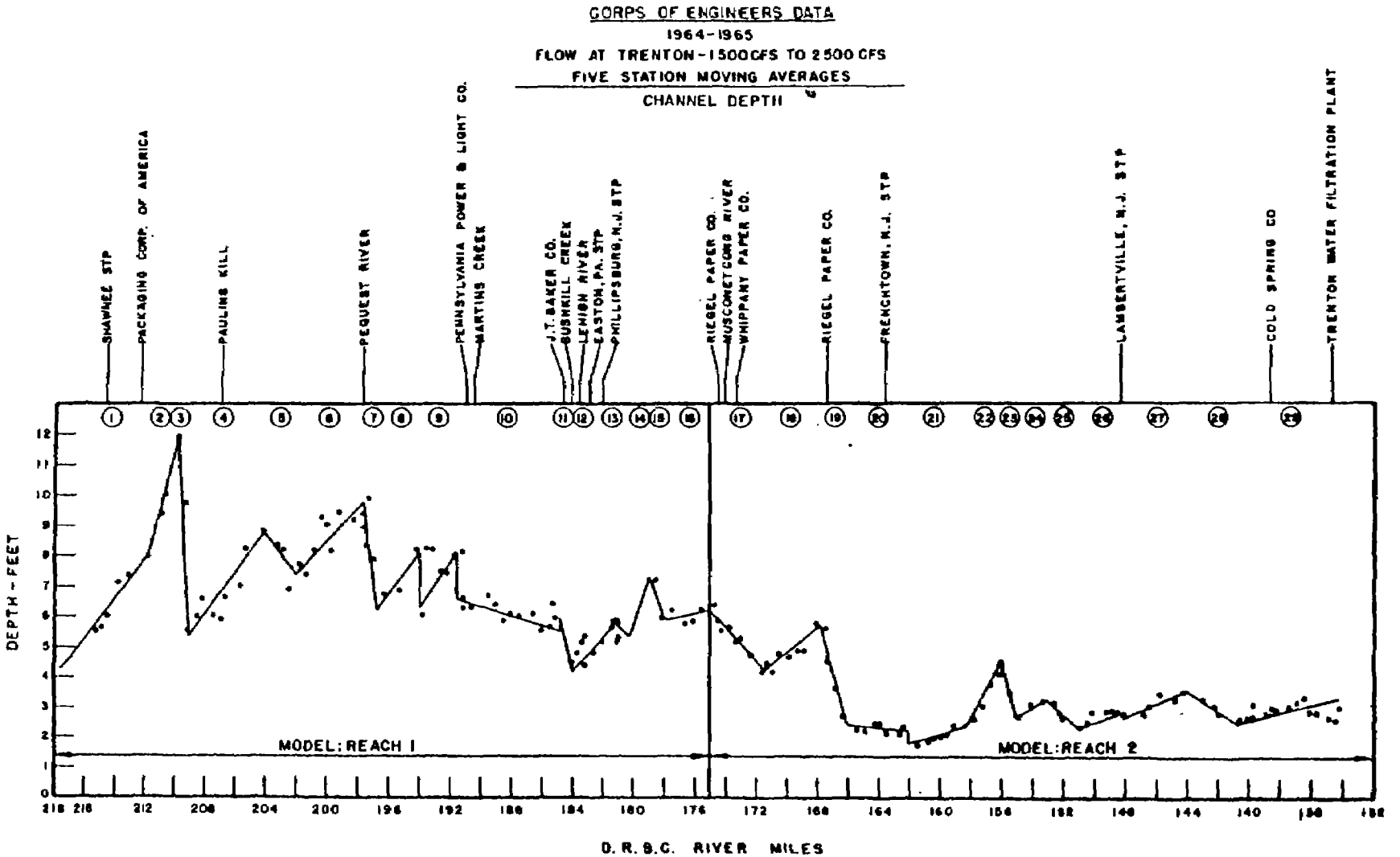

FIGURE 5

RIVER CHANNEL CHARACTERISTICS - DEPTH

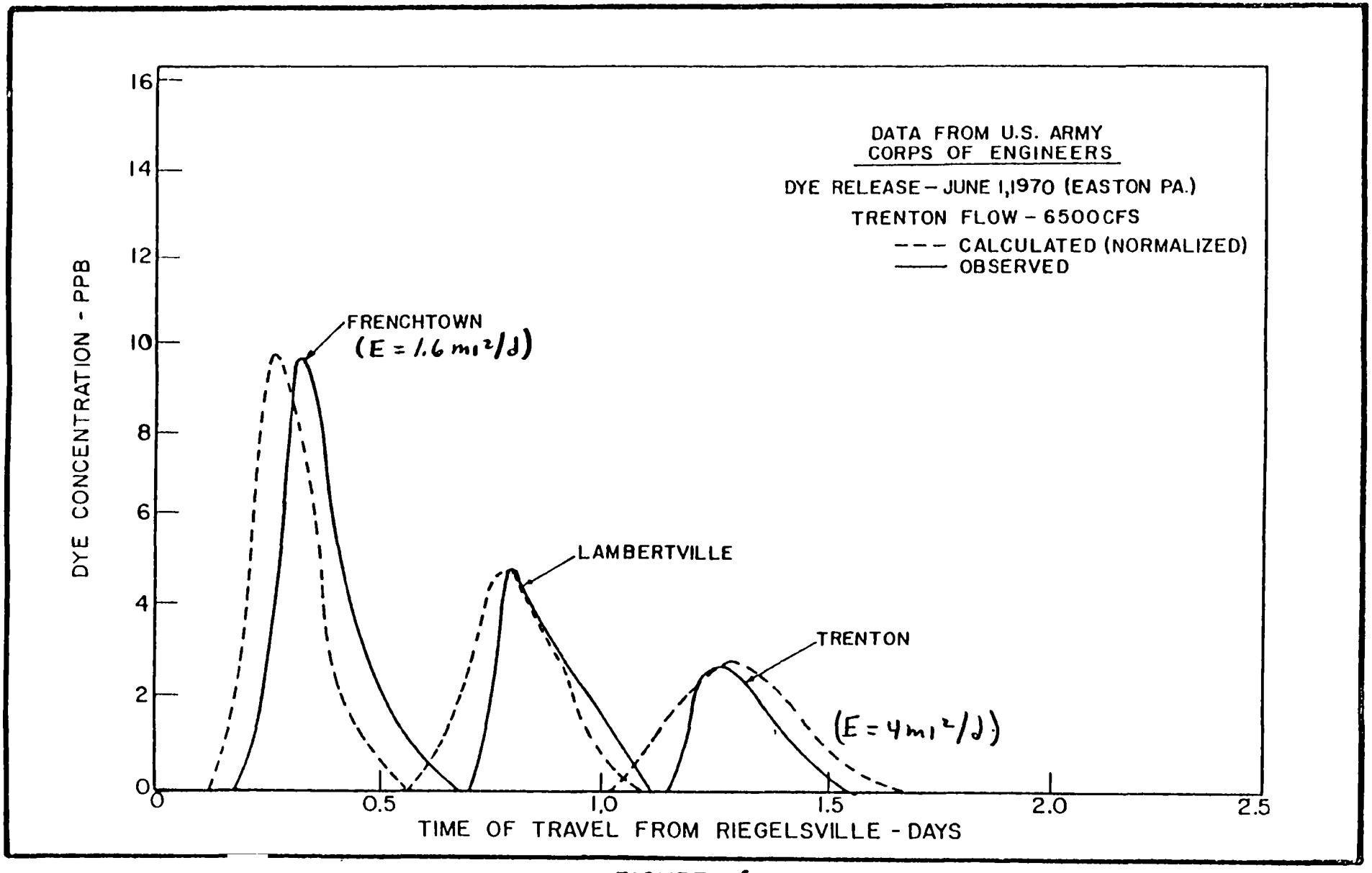

FIGURE 6

OBSERVED AND COMPUTED DYE CONCENTRATIONS

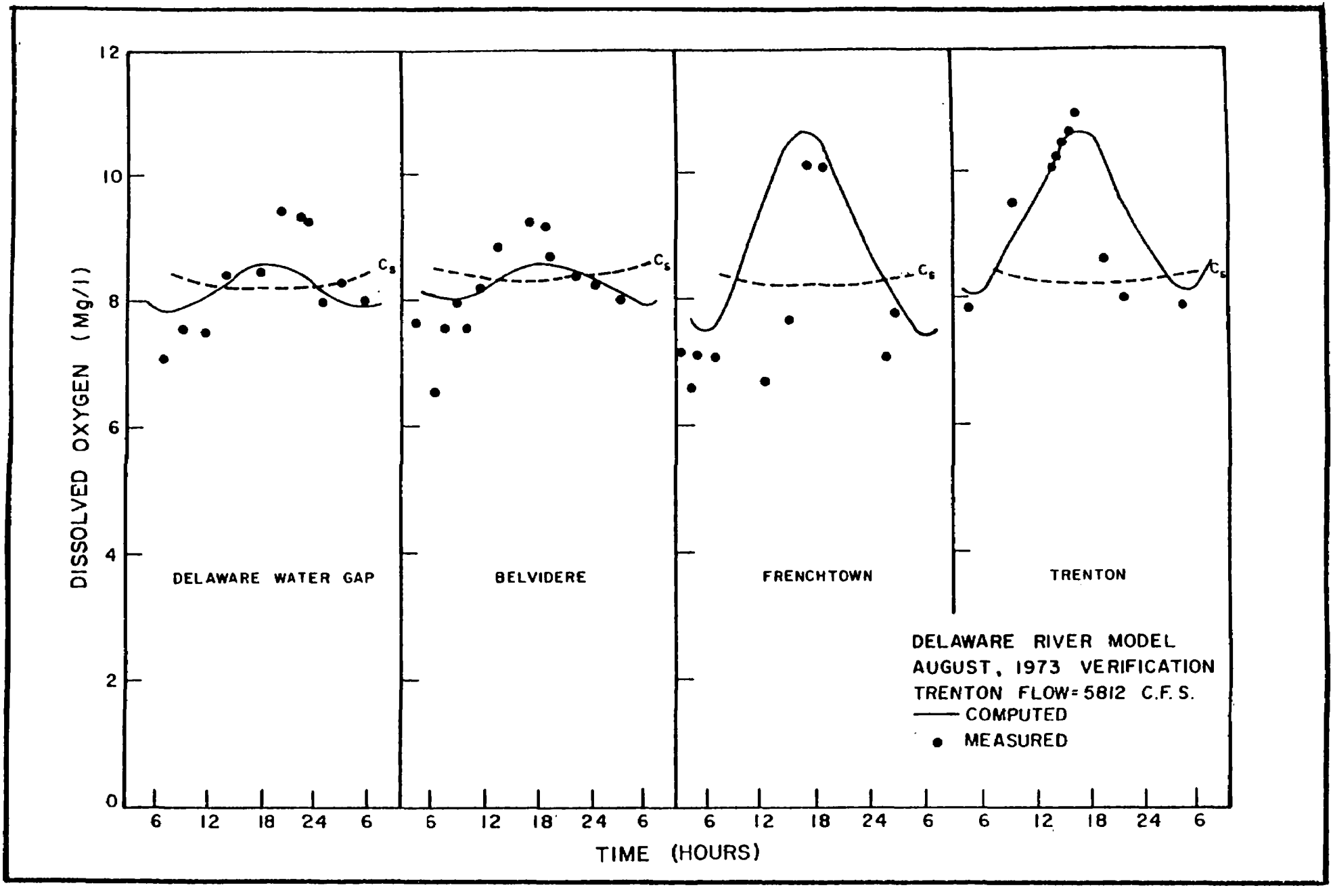

FIGURE. 7

DISSOLVED OXYGEN VERIFICATION - AUGUST, 1973

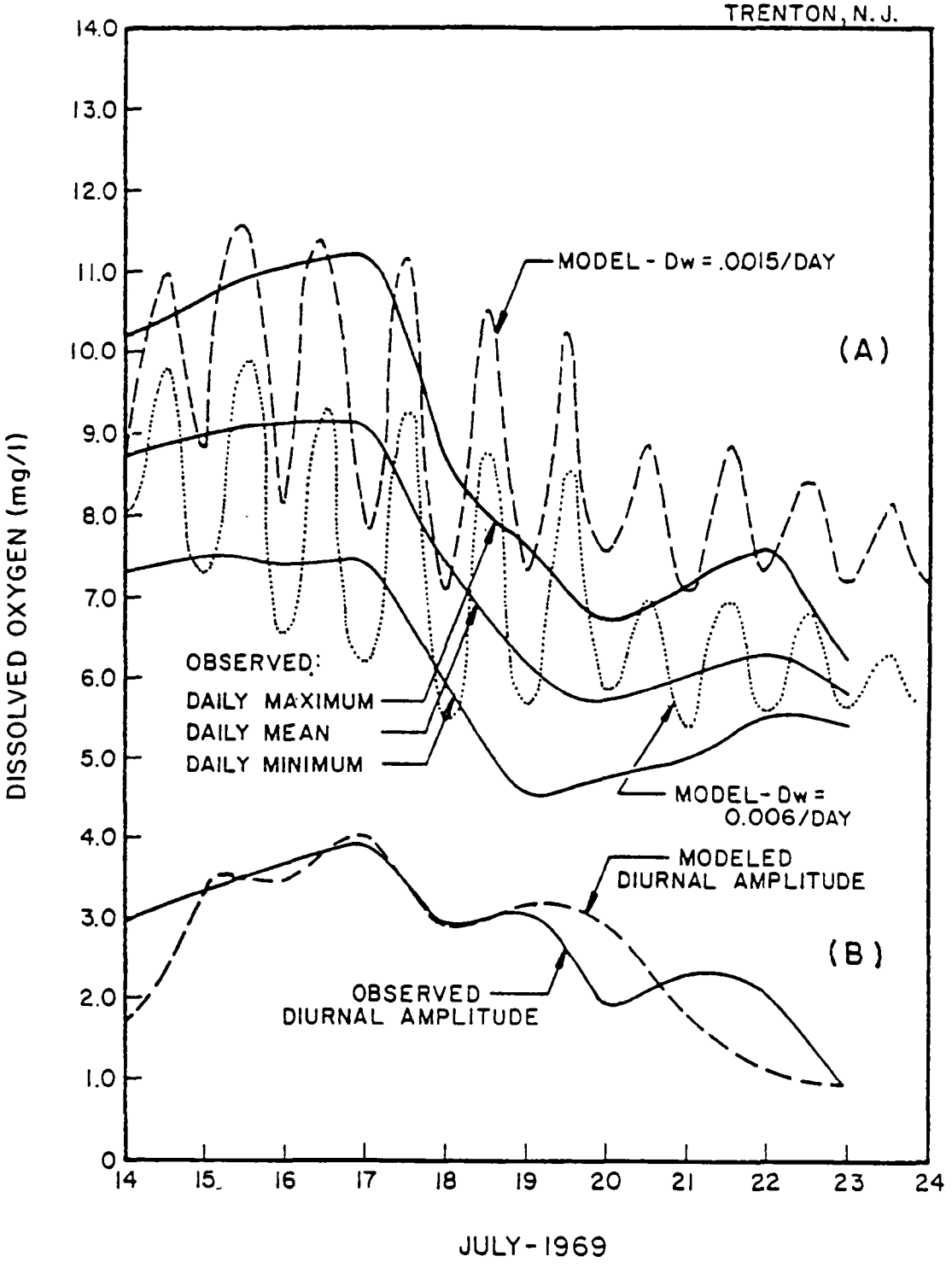

FIGURE 8

COMPARISON OF COMPUTED AND OBSERVED
DIURNAL DISSOLVED OXYGEN

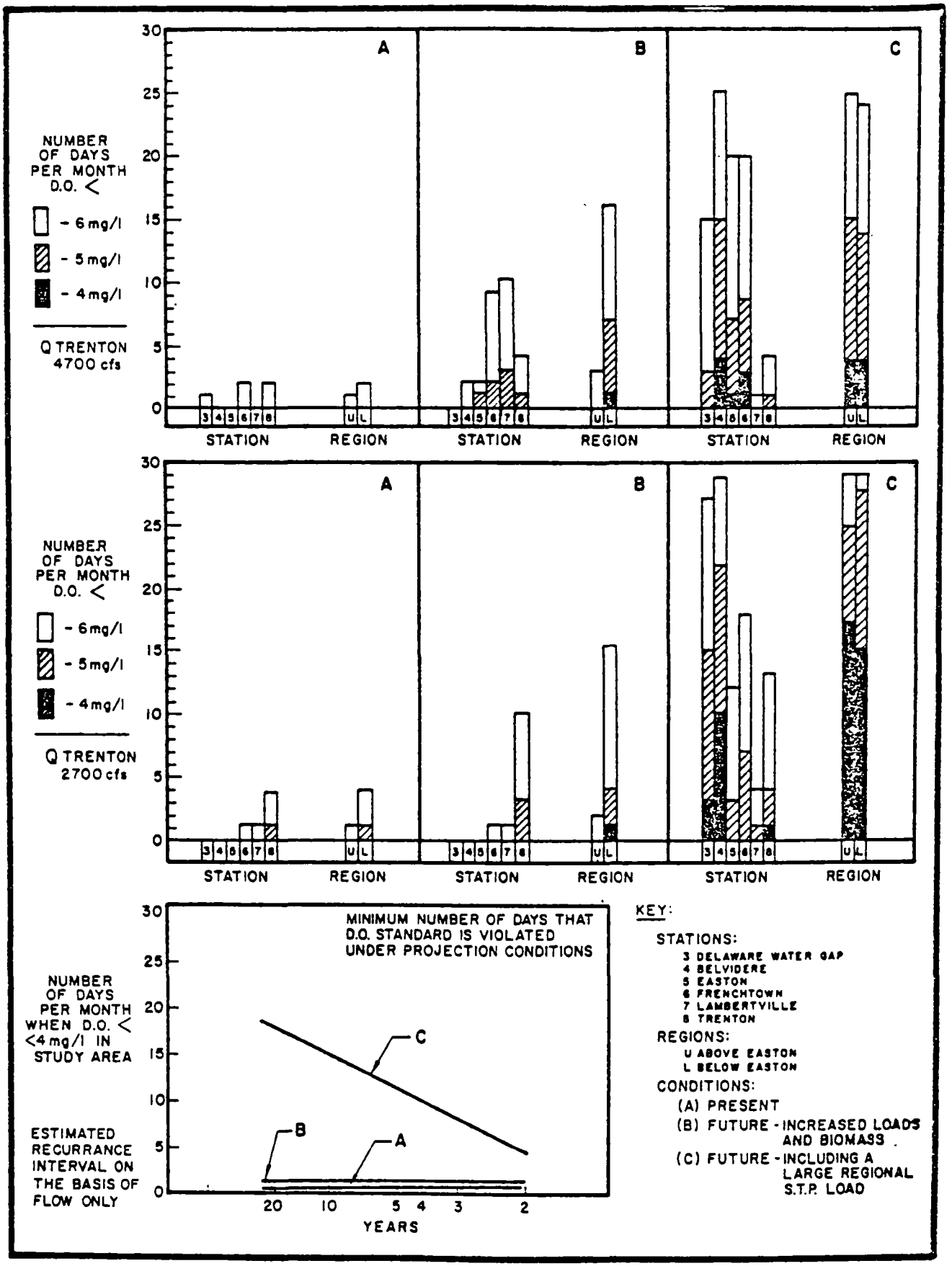

FIGURE 9

SUMMARY OF MODEL PROJECTIONS

The Eutrophication Problem*

Introduction

Even the most casual observer of water quality has probably had the dubious opportunity of walking along the shores of a lake that has turned into a sickly, green "pea soup." Or perhaps, one has walked the shores of a slow moving estuary or bay and had to step gingerly to avoid rows of rotting, matting, stringy aquatic plants. These problem areas have been grouped under a general term called eutrophication. The unraveling of the causes of eutrophication, the analyses of the impact of man's activities on the problem and the potential engineering controls that can be exercised to alleviate the condition have been a matter of interest for only the past several decades.

Eutrophication is the excessive growth of aquatic plants, both rooted and planktonic to levels that are considered to be in interference with desirable water uses. The growth of aquatic plants results from many causes which will be explored in this chapter. One of the principal stimulants, however, is the level of nutrients such as nitrogen and phosphorus. In recent years, this problem has been increasingly acute due to the discharge of such nutrients by municipal and industrial sources, as well as agricultural and urban runoff. Figure 8-1 shows the general problem framework. It has often been observed that there was an increasing tendency for some bodies of waters (e.g. lakes, reservoirs, estuaries) to exhibit great increases in the severity and frequency of phytoplankton blooms.

This increased phytoplankton production results in several consequences:

a) Aesthetic and recreational interferences - algal mats, decaying algal clumps, odors
b) Large diurnal variations in dissolved oxygen (DO) can result in zero DO at night; which, in turn, can result in death of fish
c) Phytoplankton biomass settles to bottom - creates benthal oxygen demand, which, in turn, results in low values of DO in hypolimnion of lakes and reservoirs.
d) Large diatoms and filamentous algae can clog water treatment plant filters and result in reduced time between backwashing.
e) Extensive growth of rooted aquatic macrophytes interfere with navigation, aeration and channel carrying capacity.
f) Toxic algae have sometimes been associated with eutrophication in coastal regions and have been implicated in the occurrence of "red tide," which may result in paralytic shellfish poisoning.

The eutrophication problem can then be defined as:

> The input of organic and inorganic nutrients into a body of water which stimulates the growth of phytoplankton or rooted aquatic plants resulting in the interference with

* Robert V Thomann

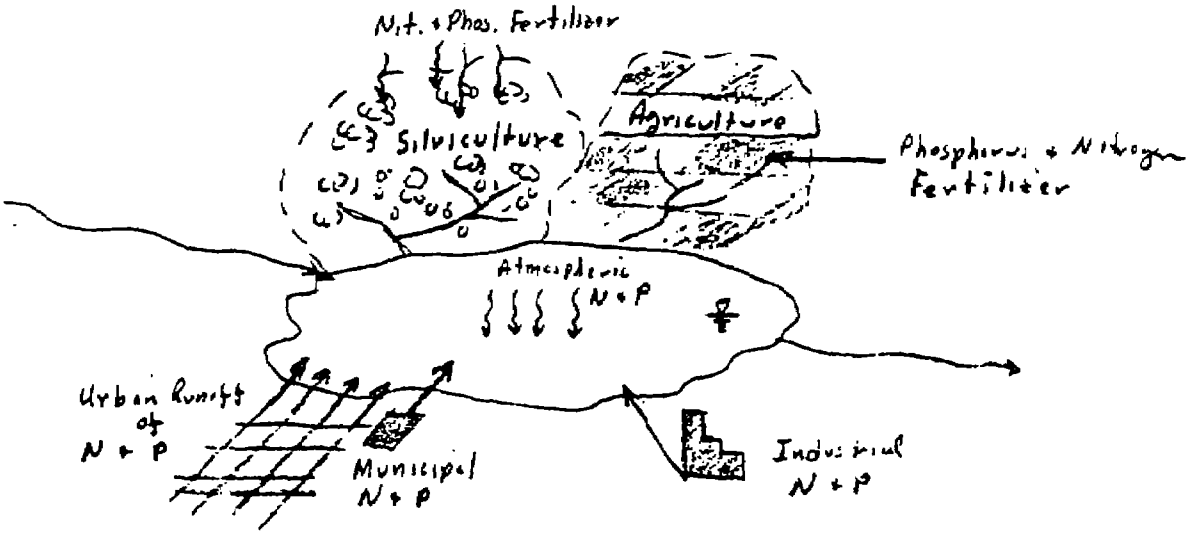

Figure 8-1 Sources of nutrients in eutrophication problem.

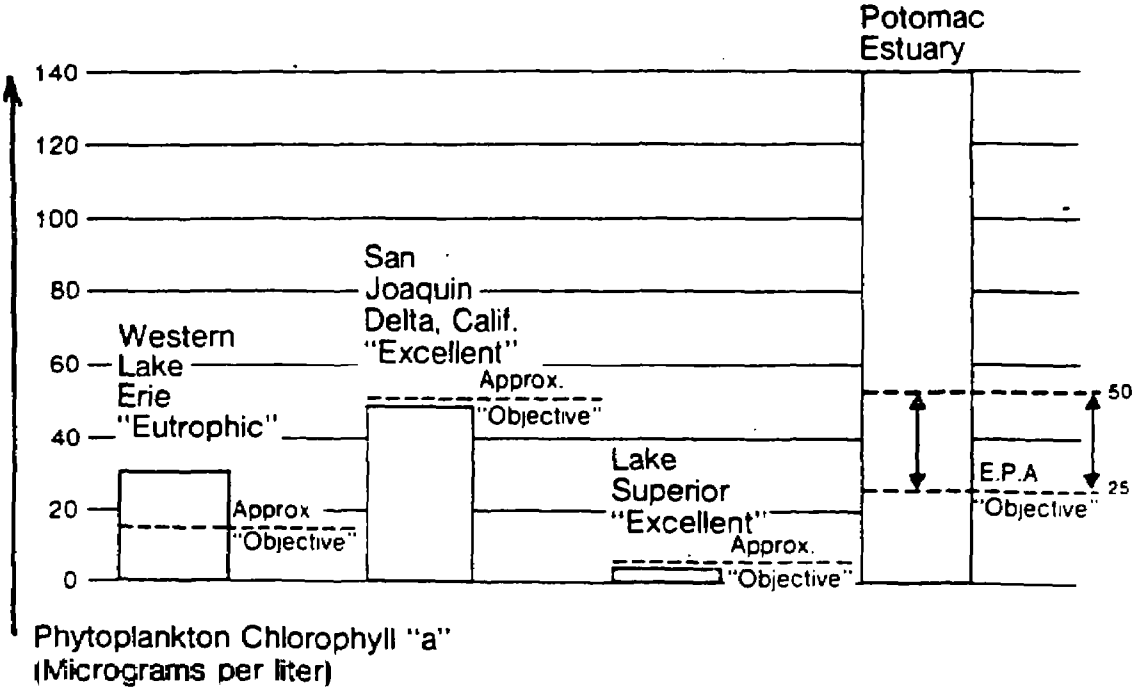

Figure 8-2. Range of chlorophyll "a" average concentrations and "objectives"

desirable water uses of aesthetics, recreation, fish maintenance and water supply.

The condition of a water body is then described in terms of its trophic state, i.e. its degree of eutrophication or lack thereof. For lakes, three designations have been used:

1) Oligotrophic - clear, low productivity lakes
2) Mesotrophic - intermediate productivity lakes
3) Eutrophic - high productivity lakes relative to a basic natural level.

The level of eutrophication due to excessive amounts of phytoplankton can be measured using several criteria:

a) Counts (Number/ml) of specific phytoplankton species, e.g. Asterionella formosa. This is the most direct count of species trends but requires a considerable effort by trained specialists in phytoplankton identification. Also, conversion to biomass measures is difficult because of variations in cell sizes for given species.

b) Cell volume ($\mu m^3/\mu \ell$) of species. An excellent measure permitting ready conversions to biomass as dry weight or carbon and grouping of data into different categories (e.g. "diatoms" and "others"). However, this measure requires an extensive analytical and data reduction effort.

c) Chlorophyll a concentrations ($\mu g/\ell$). A measure of the gross level of phytoplankton, easily obtained without extensive effort in laboratory. However, chlorophyll does not provide information on species levels nor does it permit grouping into classes of phytoplankton. Chlorophyll a is the most common measure used in eutrophication studies.

"Undesirable" levels of phytoplankton vary considerably depending on water body. For example, the following levels represent present levels which,in some way, are considered undesirable:

Open Lake Michigan - 2-5 µg chlorophyll/ℓ

Open Lake Ontario - 5-10 µg chlorophyll/ℓ

Western Lake Erie - 30 µg chlorophyll/ℓ

Sacramento, San Joaquin Delta - 50-100 µg chlorophyll/ℓ

Potomac Estuary - >100 µg chlorophyll/ℓ

Objectives for "Desirable" levels of chlorophyll vary widely depending on the type of problem and the nature of the water body. Figure 8-2 illustrates the range in present observed chlorophyll concentrations and that level considered desirable in some sense. In general, lakes and reservoirs tend to have lower desirable levels of phytoplankton. Chapra and Tarapchak (1976) have summarized several objectives for North Temperate lakes as follows:

Eutrophic - ≥ 6 to 10 µg chlor a/ℓ

Mesotrophic - 1 to 10 µg chlor a/ℓ

Oligotrophic- < 1 to 5 µg chlor a/ℓ

Some other levels that have been cited include the Potomac estuary at 25 µg chlor a/ℓ and the Sacramento-San Joaquin Delta at 25-50 µg/ℓ.

Basic Aspects of Eutrophication

Principal Mechanisms

The essence of the photosynthetic process centers about the chlorophyll-containing plants which can utilize radiant energy from the sun, convert water and carbon dioxide into glucose, and release oxygen as a by-product. The photosynthesis reaction can be written as

$$6\ CO_2 + 6\ H_2O \xrightarrow{\text{Photosynthesis}} C_6H_{12}O_6 + 6\ O_2$$

The production of oxygen is accomplished by the removal of hydrogen atoms from the water, forming a peroxide which is broken down to water and oxygen. The water body is now subjected to an "atmosphere" of pure oxygen as compared to the water surface where reaeration comes from an atmosphere containing only about 20% oxygen. Since all saturation values of DO are referred to the standard atmosphere, photosynthesis can result in supersaturated oxygen values. Values as high as 150-200% of the air saturation levels are not uncommon. Because the photosynthetic process is dependent on solar radiant energy, the production of oxygen proceeds only during daylight hours. Concurrently with this production, however, the algae require oxygen for respiration which proceeds continuously. A number of trace elements are required and are usually available in most natural systems. As indicated above, nutrients such as nitrogen and phosphorus are also necessary for phytoplankton growth.

The basic phenomena underlying the process of phytoplankton growth in the North Temperate regions are summarized in Figure 8-3. Increasing solar radiation provides the energy source for the photosynthesis reaction. Phytoplankton biomass then begins to increase as water temperature increases and as a result, nutrients in dissolved form are utilized by the plankton. This mechanism continues until nutrients reach levels that will no longer support growth at which the increase in phytoplankton biomass ceases. A decline is then observed, due often to zooplankton predation and often a late summer-early fall bloom may be observed again due to nutrient recycling. Biomass then declines as solar radiation and temperature decrease to the lower levels of late fall and early winter.

The principal variables of importance then in the analysis of eutrophication are:

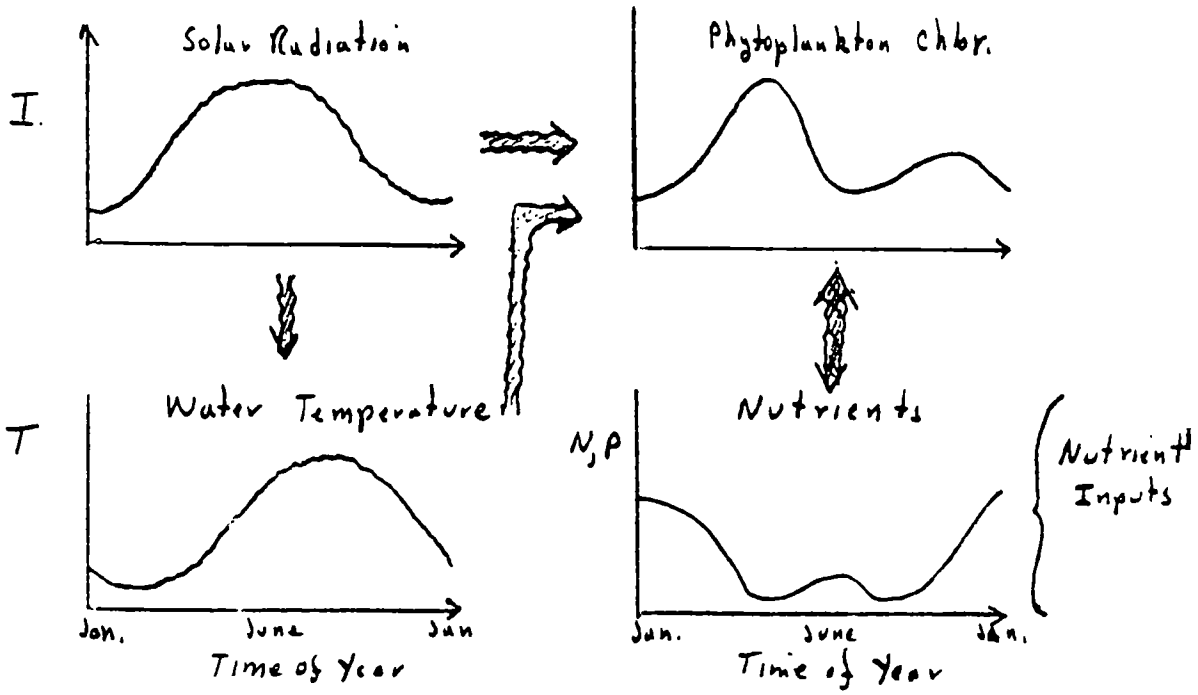

Figure 8-3 Basic process of phytoplankton-nutrient interaction.

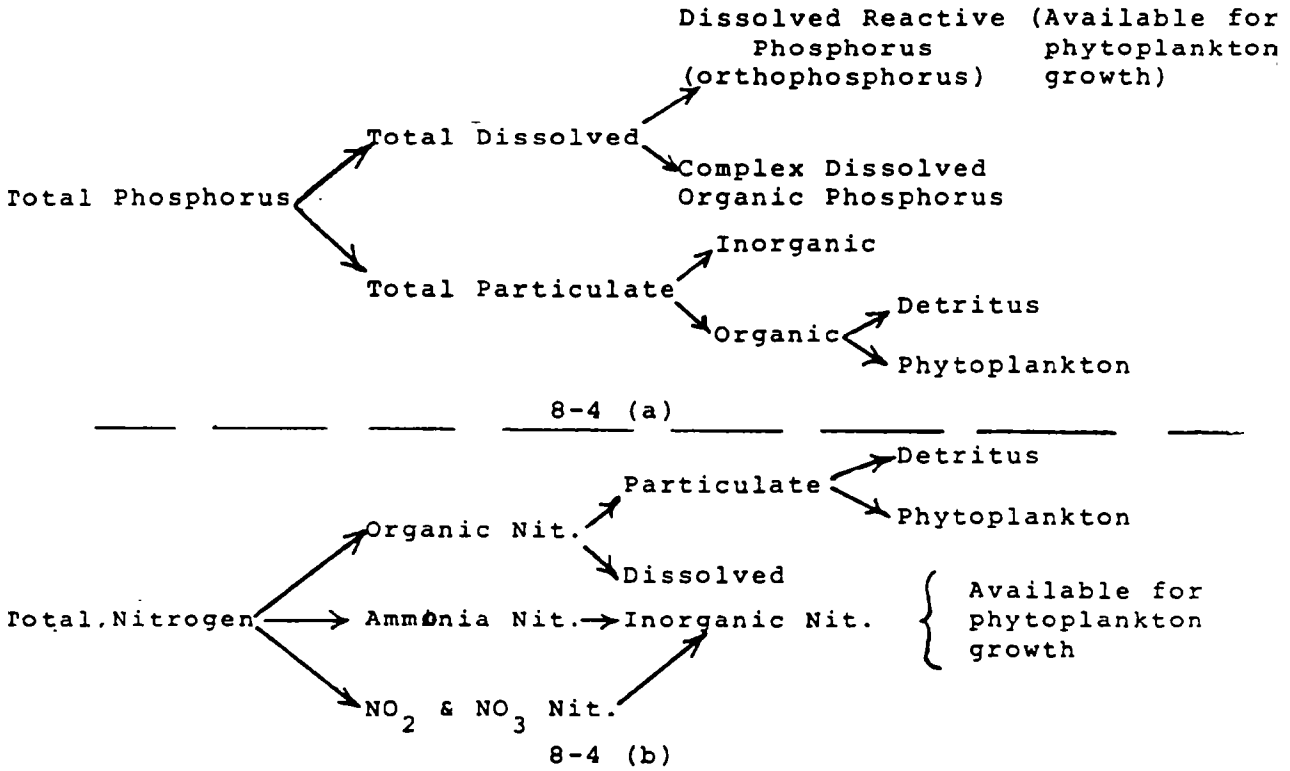

Figure 8-4 Principle components of nutrients: (a) Phosphorus (b) Nitrogen

a) Solar radiation at the surface and with depth
b) Geometry of water body; surface area, bottom area, depth, volume
c) Flow, velocity, dispersion
d) Water temperature
e) Nutrients
   i) Phosphorus
   ii) Nitrogen
   iii) Silica
f) Phytoplankton - Chlorophyll "a"/ℓ
g) Zooplankton - mg carbon/ℓ

It should be recognized that the nutrients above are present in several forms in a body of water, and not all forms are readily available for uptake by the phytoplankton. The more important categories are shown in Figure 8-4(a) and 8-4(b). Total phosphorus is composed of two principle components: the total dissolved form and the total particulate form. The dissolved form, in turn, is composed of several forms, one of which is the dissolved reactive phosphorus. This form of phosphorus is available for phytoplankton growth. The particulate phosphorus forms include inorganic soil runoff phosphorus particulates and the organic particulate phosphorus which include detritus and the phytoplankton phosphorus.

Total nitrogen is composed of four major components, the organic, ammonia and nitrite plus nitrate forms. The latter three forms make up the total inorganic nitrogen and is the form utilized by the phytoplankton for growth. The organic form of nitrogen represents both a dissolved and particulate component. The particulate form, in turn, is composed of organic detritus particles and the phytoplankton.

Figure 8-4 A shows the phytoplankton dynamic behavior for the epilimnion of Lake Ontario. The schematic of the lake shown in Figure 8-4A(a) shows the principal inputs and physical mechanisms that influence the phytoplankton growth. As shown in Figure 8-4A(b), the chlorophyll a level for the upper layer of Lake Ontario is low until the spring when solar radiation and water temperature increases. A peak value of about 5-10 µg chlor. a/ℓ is reached in the May-June period. Concurrently, available phosphorus levels (Fig. 8-4A(d)) were reduced to levels that caused a cessation of phytoplankton growth. Fig. 8-4A(c) shows the growth of zooplankton in the summer through predation of the phytoplankton. This interaction of the zooplankton on phytoplankton growth is discussed in more detail later.

Figure 8-4 B shows similar dynamic interactions between chlorophyll and phosphorus for Saginaw Bay and southern Lake Huron. The concentrations of chlorophyll in Saginaw Bay of between 20-40 µg chlor.a/ℓ are indicative of the eutrophic status of that body of water.

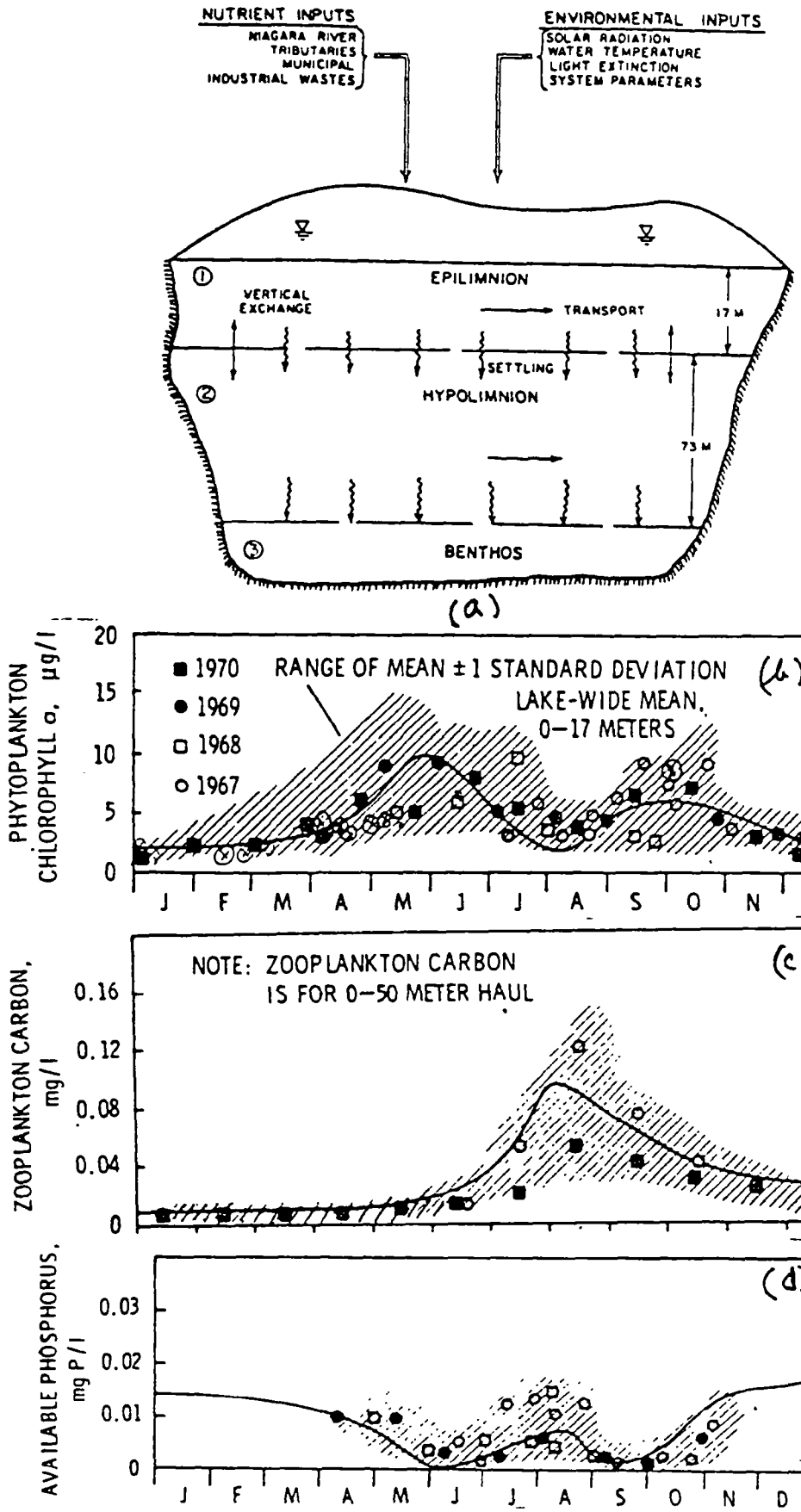

Fig 8-4A Phytoplankton dynamics in Lake Ontario. a) Schematic of vertical regimis b) phyto. chlor a, epilimnion c) zoop. Carbon, d) Avail. phosphorus. (After Thomann et al, 1974)

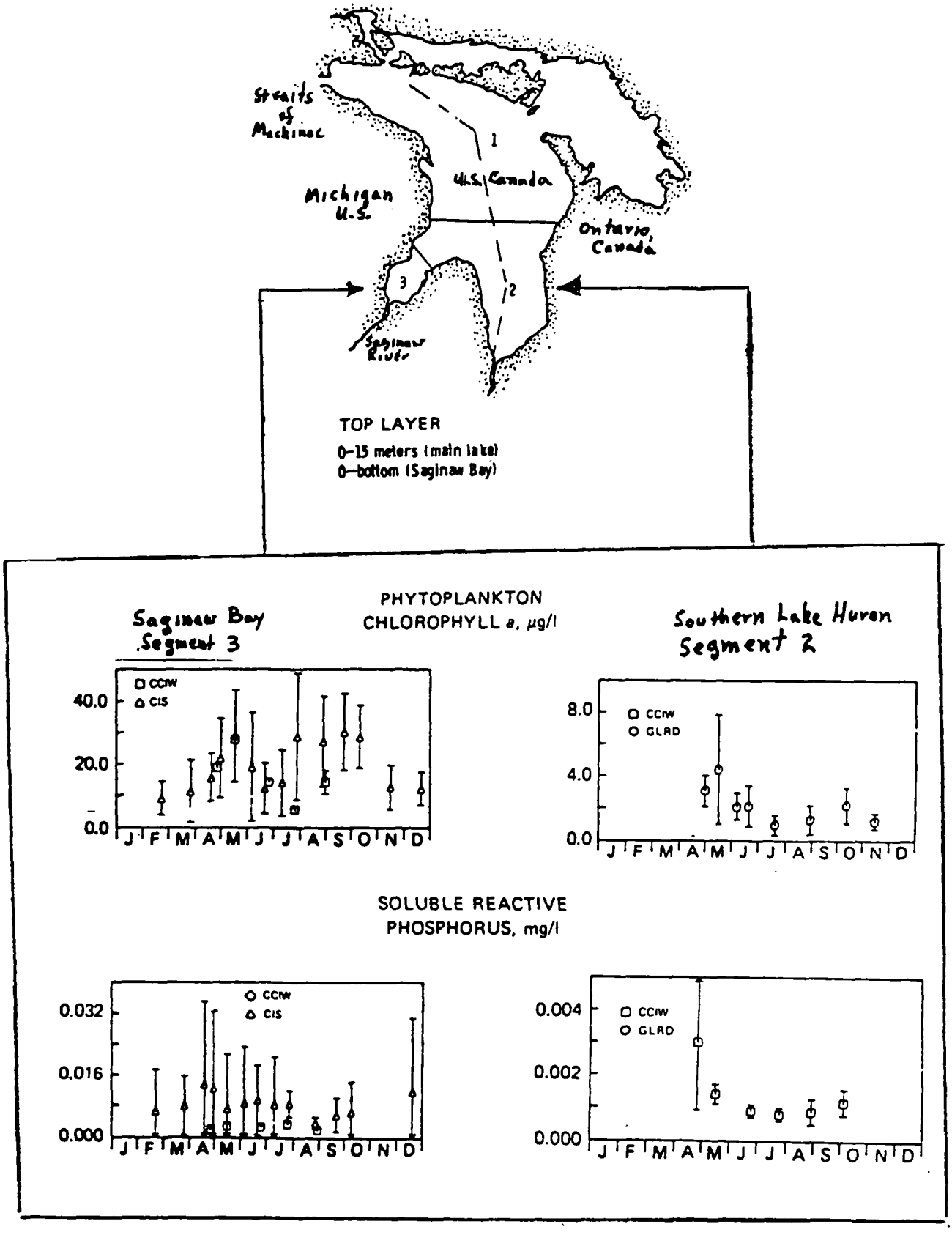

Fig 8-48 Phytoplankton dynamics, Saginaw Bay, Mich and Southern Lake Huron (After DiToro and Matystik, 1980)

External Sources of Nutrients

As shown in Figure 8-1, the principal external sources of nutrient inputs are:

a) Municipal wastes
b) Industrial wastes
c) Agricultural runoff
d) Forest (commercial) runoff
e) Urban and suburban runoff
f) Atmospheric fallout

Table 8-1 to 8-3 and Figure 8-5 summarize some of the data on these inputs from several sources (Eisenreich et al., 1977; Gakstatter et al., 1978; Hydroscience, 1977a, 1977b; Rast and Lee, 1978; Thomann, 1972; IJC, 1978).

TABLE 8-1

Mean Nutrient Inputs from Municipal Wastewaters

	Influent (mg/l)	Conventional Secondary Treatment Effluent (mg/l)	After Phosphorus Removal Processes (mg/l)
Phosphorus (as P)			
Total P-W/detergent	5-10	7.0	1-3
W/O detergent	2-5	4	
Ortho P-W/detergent	2-5	5	1-2
W/O detergent		3	
Nitrogen (as N)			
Total N	50	18	14
Inorganic N	30	8	7

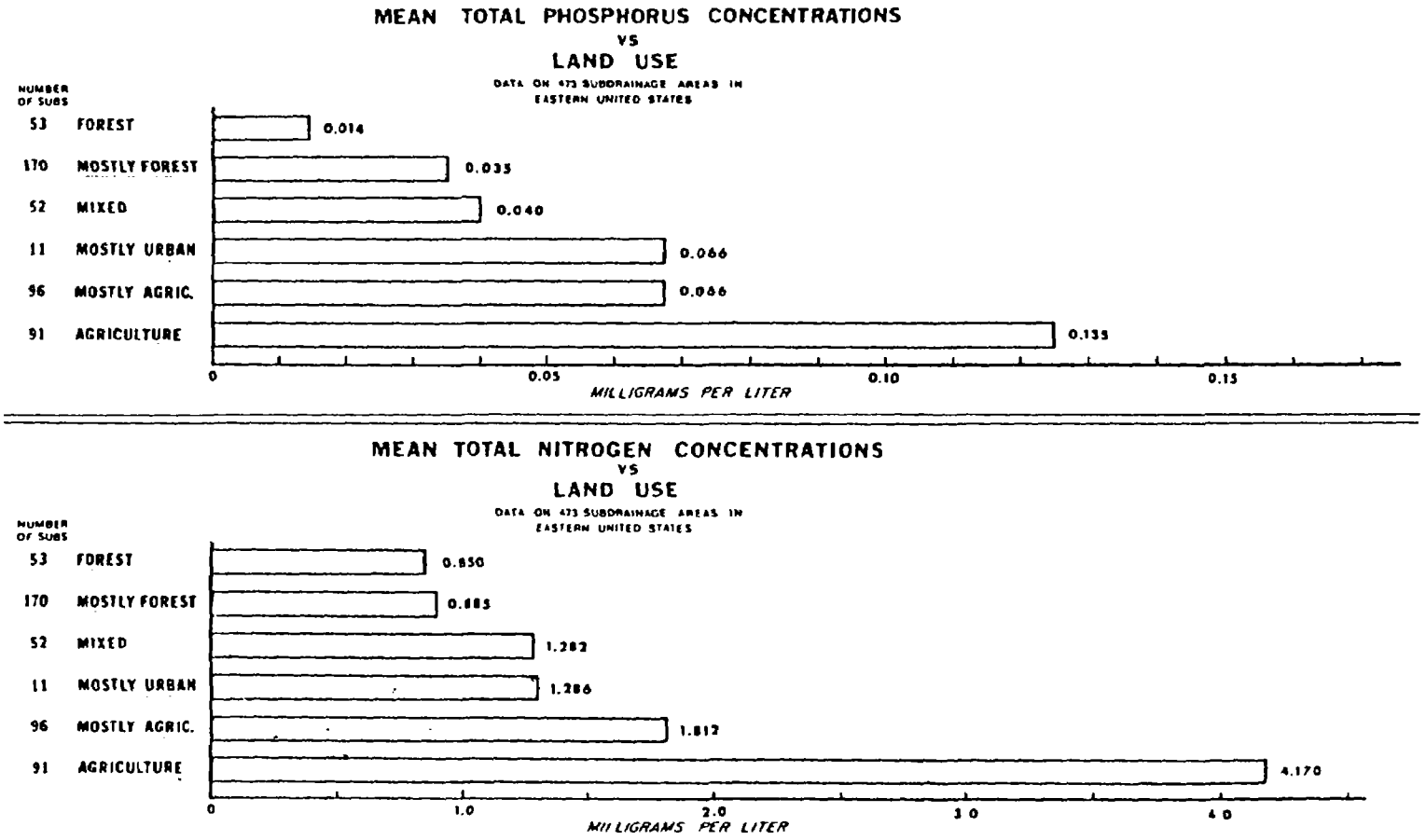

Figure 7. Mean total phosphorus and total nitrogen concentrations in streams draining different land use categories. (From Bartsch and Gakstatter, 1978).

TABLE 8-2

Great Lakes Basin - Rural Land
Phosphorus Loads Developed by
International Joint Commission

Land Use	kg Total p/ha-yr Type of Soil Sand	Coarse Loam	Fine Loam	Clay
Row Cropping (> 50% row crops)	0.25	0.65	1.05	1.25
Mixed Farming (25-50% row crops)	0.10	0.20	0.55	0.85
Forage (< 25% row crops)	0.05	0.05	0.40	0.60
Grassland	0.05	0.05	0.05	0.25

TABLE 8-3

Other Non-Point Source
Loadings

kg/ha-yr

Type	Total Phosphorus Mean	Range	Total Nitrogen Mean	Range
Forest-Natural	0.4	(.01-.9)	2.9	(1.3-10.2)
Atmospheric	0.2	(.08-1.0)		
Urban	2.5	(.1-10)	5.0	(1-20)
Agricultural-General	0.5	(0.1-5)	5.0	(.5-50)

Table 8-1 and Figure 8-5 show typical concentration values for nitrogen and phosphorus; the former from municipal point sources and the latter from non-point sources in the eastern United States. Tables 8-2 and 8-3 provide estimates of loading of phosphorus and nitrogen. The Great Lakes Basin loads shown in Table 8-2 represent the results of a wide spread sampling program of phosphorus loading from differing agricultural practices and soil types. As shown in Table 8-3, the range of loading from all non-point sources is rather wide and reflects various ranges in the flow or precipitation rates. The values given in Table 8-3, however, are useful as general guidelines.

Omernik (1977) has summarized nutrient data from non-point sources from a nationwide network of 928 watersheds under the National Eutrophication Study of 1972-1974. A simple regression model was used to relate runoff concentrations to the percent of land in agricultural use and the percent of land in urban use. Tables 8-4 and 8-5 show these results for total phosphorus and nitrogen concentrations for different regions and land use distribution.

Sediment Release Rates of Nutrients

In addition to the external sources of nutrients, the release of nutrients from the sediments may also be important. Of course, it should be recognized that the presence of excessive levels of nutrients in the sediments of water bodies is due to the external sources. However, for some situations, the problem can be separated and the effect of nutrient release on phytoplankton dealt with as a continuous source. The impact of sediment nutrient release can be significant and result in continuing eutrophication problems even after point sources have substantially reduced. Table 8-5 a shows some reported nutrient fluxes from the sediments under both aerobic and anaerobic conditions. The latter situation greatly increases the flux of nutrients.

Simplified Lake Phytoplankton Models

A considerable effort has been expended in the past 10 years to develop empirical and theoretical analyses of eutrophication that could be easily applied. All of the efforts to date have focused on lakes and incorporate several key assumptions in the analysis. The simplified phytoplankton models have proven to be of significant value in first estimates of the probable effects of reduction of nutrient inputs. Some of the key references are listed at the end of this section.

The basic approach underlying several of the models is the mass balance of the assumed limiting nutrient-phosphorus. Total phosphorus is used as the indicator variable of trophic status. Vollenweider (1968) in his first paper, of a largely empirical

TABLE 8-4 ESTIMATED MEAN TOTAL PHOSPHORUS CONCENTRATIONS (mg/l) FOR NATIONWIDE AND REGIONAL MODELS *

	Nationwide Model		Regional Models					
			East		Central		West	
% Ag + % Urb	Ave P Conc	67% Limits	Ave P Conc	67% Limits	Ave P Conc	67% Limits	Ave P Conc	67% Limits
0	0.020	(.010-.042)	0.015	(.008-.026)	0.018	(.008-.037)	0.028	(.013-.060)
25	0.033	(.016-.067)	0.026	(.014-.048)	0.032	(.015-.066)	0.048	(.022-.103)
50	0.052	(.025-.106)	0.045	(.024-.083)	0.058	(.028-.120)	0.083	(.038-.178)
75	0.083	(.041-.170)	0.078	(.042-.144)	0.103	(.049-.213)	0.141	(.065-.303)
100	0.133	(.065-.272)	0.136	(.073-.251)	0.185	(.089-.382)	0.240	(.111-.516)

* FROM OMERNIK (1977)

TABLE 8-5 ESTIMATED MEAN TOTAL NITROGEN CONCENTRATIONS (mg/l) FOR NATIONWIDE AND REGIONAL MODELS *

	Nationwide Model		Regional Models					
			East		Central		West	
% Ag + % Urb	Ave N Conc	67% Limits	Ave N Conc	67% Limits	Ave N Conc	67% Limits	Ave N Conc	67% Limits
0	0.57	(0.35-0.92)	0.51	(0.33-0.77)	0.57	(0.37-0.88)	0.63	(0.34-1.16)
25	0.90	(0.56-1.46)	0.87	(0.57-1.32)	0.83	(0.54-1.28)	0.95	(0.52-1.75)
50	1.45	(0.89-2.34)	1.49	(0.98-2.26)	1.22	(0.79-1.88)	1.42	(0.77-2.61)
75	2.31	(1.43-3.74)	2.55	(1.68-3.88)	1.78	(1.15-2.74)	2.13	(1.16-3.92)
100	3.69	(2.28-5.97)	4.37	(2.87-6.64)	2.61	(1.69-4.02)	3.19	(1.73-5.87)

* FROM OMERNIK (1977)

Location	Flux - Aerobic Conditions mg/m^2-day Tot.Diss P	NH_3-N	Si-Silicon	Flux - Anaerobic Conditions mg/m^2-day Tot.Diss P	NH_3-N	Si-Silicon	Reference
Muddy R., Boston MA	3.2			16(32 Max)			Fillos & Swanson (1975)
Lake Warner, Amherst, MA	0.4			13(8 Max)			
Lake Ontario	0.2						Bannerman,etal.(1975
Lake Erie-							
Western Basin	6.0	44					DiToro & Connolly (1980)
Central Basin	3.0	30					
Eastern Basin	2.0	22					
White Lake, Muskegon Co., Michigan				34 (23)[2]	44	297	Freedman & Canale (1977)
Cape Lookout Bight,No.Car.		40(winter) 325(summer)					Martens et al.(1980)
LaJolla Bight	2.4(-13 to 16)						Hartwig (1975)
Potomac Estuary	1-10						USGS Data

nature, related external nutrient loading in g/m^2 of lake surface area per year to depth and noticed that the population of lakes divided into two broad areas related to the state of eutrophication From that work, other investigators have continued to incorporate a more basic theoretical structure and have necessarily relaxed some of the earlier levels of judgement that were required in the analysis. These latter efforts have also attempted in semi-empirical ways to estimate not just the phosphorus level but the more relevant variable of phytoplankton chlorophyll. Chapra and Tarapchak (1976) have summarized the simplified scheme as the following series of steps:

a) Estimate loading of total phosphorus to the lake
b) Determine mean annual concentration of total phosphorus in the lake
c) Estimate the spring concentration of total phosphorus in the lake from mean annual concentration
d) Compute mean summer concentrations of chlorophyll a from spring concentrations of total phosphorus.

Basic Mass Balance - Nutrients

The assumptions used in the simple analysis are:

a) Completely mixed lake
b) Steady State
c) Single Nutrient Phosphorus limited - Max level of phosphorus specified
d) Total phosphorus used as measure of trophic status

The third assumption indicates that only one nutrient need be considered, i.e. that all other nutritional requirements for phytoplankton are met. For lakes, phosphorus is often but not always nutrient that limits growth and, therefore, is often the cause of increased phytoplankton resulting from phosphorus discharges.

The last assumption is particularly interesting. Instead of attempting to describe all of the complex interactions indicated previously (solar radiation, temperature, nutrient and phytoplankton), a surrogate variable is chosen to represent the state of the lake. The measure of trophic status,therefore, in the simple mass balance lake models is the total phosphorus. Empirical relationships are then used to relate the total phosphorus concentration to phytoplankton chlorophyll levels.

The basic mass balance equation is given by following the principles of Chapter 5 for a completely mixed lake. Figure 8-6 shows the schematic of the system. The equation is:

$$\frac{Vdp}{dt} = Q_{in}p_o - K_s pV - Qp \qquad (8\text{-}1)$$

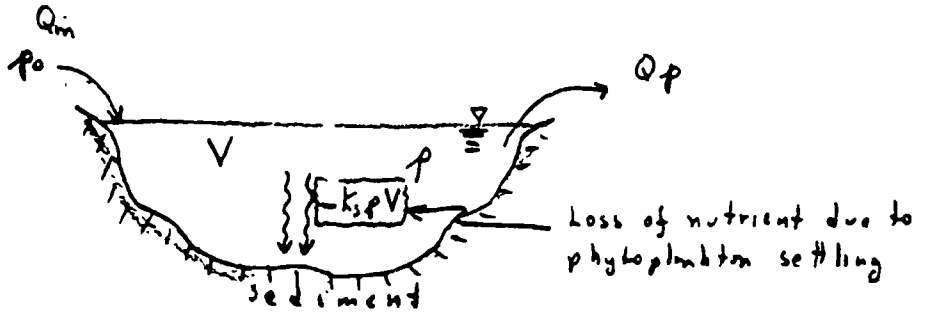

Fig 8-6 Schematic of phosphorus mass balance - completely mixed lake

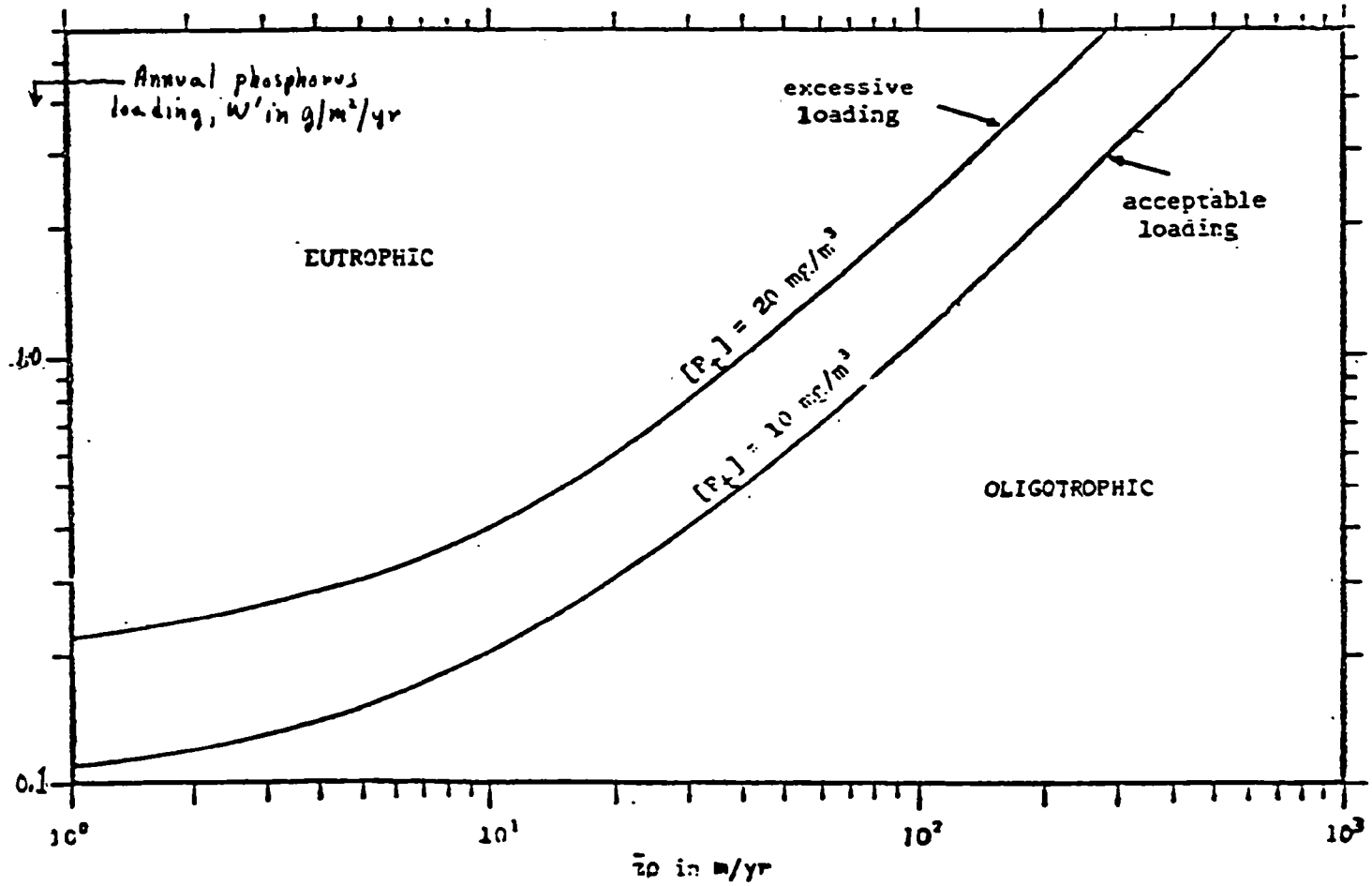

Fig. 8-7: Nutrient loading/lake trophic condition after Vollenweider (1975)

or $$\frac{Vdp}{dt} = W - K_s pV - Qp \qquad (8\text{-}1a$$

where:

V = volume of lake $[L^3]$

p = phosphorus (total) in lake, $[M/L^3]$; e.g. µg/ℓ

Q = outflow

Q_{in} = inflow $[L^3/T]$; e.g. m^3/S

p_o = influent phosphorus concentration, $[M/L^3]$; e.g. µg/ℓ

W = external sources of phosphorus, $[M/T]$; e.g. g/s

K_s = overall loss rate of total phosphorus due to settling of particulate forms, $[1/T]$; e.g. (1/day)

At steady state, Eq. (8-1) is given by

$$p(Q + K_s V) = Q_{in} p_o$$

or

$$p = \frac{Q_{in} p_o}{Q + K_s V} = \frac{Q_{in}}{V} \left(\frac{1}{\frac{Q}{V} + K_s}\right) p_o$$

and if it is assumed that $Q_{in} = Q$, then

$$p = \left(\frac{\rho}{\rho + K_s}\right) p_o \quad \text{for } \rho = \frac{Q}{V} = \frac{1}{t_d} \text{ where } t_d = \text{detention time of lake} \qquad (8\text{-}2)$$

A second form at steady state is given from Eq. (8-1a):

$$p = \left(\frac{W}{V}\right)\left(\frac{1}{\rho + K_s}\right)$$

$$= \frac{W}{A_s \bar{z}}\left(\frac{1}{\rho + K_s}\right) \text{ for } A_s = \text{lake surface area } [L^2]; \text{ and then}$$

$$p = \frac{W'}{\bar{z}(\rho + K_s)} \qquad (8\text{-}3)$$

where W' = areal phosphorus loading rate $= \frac{W}{A}\left[\frac{M}{T\text{-}L^2}\right]$; e.g. g/m^2-yr.

and $\bar{z}$ = average depth of the lake $[L]$; e.g. meters.

The difficulty of using Eqs. (8-2) or (8-3) is that K_s, the net loss rate, is not readily known nor can it be measured in a direct experimental way. However, if information is available on the input and output from the lake, an estimate can be made of K_s. Suppose, therefore, that a number of lakes are examined where p, W', $\bar{z}$ and p can be estimated, then Eq. (8-3) permits estimation of K_s. Vollenweider (1975) deduced that

$$K_s = \frac{10}{\bar{z}} \qquad (8\text{-}4)$$

for $\bar{z}$ in meters and K_s in yrs^{-1}.

Since $K_s = \frac{v_s}{\bar{z}}$ where v_s is the settling rate[L/T], then for v_s = 10 m/yr., Eq. (8-4) is equivalent to a net settling rate of .0274 m/day. Other estimates of 16 m/yr. and 12.4 m/yr are discussed by Chapra and Tarapchak (1976). Given the empirical relationship of Eq. (8-4), Eq. (8-3) can be written as

$$p = \frac{W'}{10+\bar{z}\rho} \qquad (8\text{-}5)$$

Note that $\bar{z}\rho = \frac{V}{A_s} \cdot \frac{Q}{V} = \frac{Q}{A_s} = q_s$. The quantity Q/A_s is the areal water loading or "overflow rate", and is designated as q_s [$L^3/T\text{-}L^2$]

Now the question of what level of p is "acceptable" and what level is "excessive" must be addressed so that estimates of allowable loading W' can be obtained. One objective set that has been suggested is:

Acceptable total phosphorus level = .010 mgP/ℓ (g/m^3) = 10 μgP/ℓ (mg/m^3)

Excessive total phosphorus level = .020 mgP/ℓ = 20 μgP/ℓ

Then the loading rates can be computed from Eq. 8-5 using these levels as

$$W'_{10} = .01(10 + \bar{z}\rho); \quad \left(\frac{g}{m^2 yr}\right) = \left(\frac{g}{m^3}\right)\left(\frac{m}{yr}\right) \qquad (8\text{-}6)$$

$$W'_{20} = .02(10 + \bar{z}\rho) \qquad (8\text{-}7)$$

Figure 8-7 shows these relationships from Vollenweider (1975). With the estimated $\bar{z}\rho$, and the annual loading rate, the trophic status of the lake can be estimated. If the level is eutrophic, the estimated load reduction can be read directly from the plot.

Other Semi-Empirical Approaches

Modifications of earlier work (Vollenweider, 1976) have also indicated that the following expression may be appropriate:

$$K_s \simeq \sqrt{\rho}$$

Then from Eq. (8-3),

$$p = \frac{W'}{\bar{z}(\rho + \sqrt{\rho})}$$

$$p = \frac{W'}{\bar{z}\rho(1 + \sqrt{1/\rho})} \qquad (8\text{-}8)$$

Attempts have also been made to extend the above analyses to include other measures of the state of eutrophication. Rast and Lee (1978) give the following expressions for North American lakes:

Chlorophyll "a": $\log [ch] = 0.76 \log [p] - .259$ (8-9)
for chlorophyll in µg/ℓ and phosphorus in mg/m^3.

Secchi depth: $\log (z_s) = - .359 [p] + .925$ (8-10)
for secchi depth in meters

Eq. 8-10 relates the total phosphorus to the secchi depth as a measure of clarity. Other relationships of total phosphorus to the dissolved oxygen problem are explored later.

Figure 8-8 shows the relationships between median total phosphorus and mean chlorophyll a concentration for a number of lakes and reservoirs in the northeastern U.S. (Gakateller, 1978). The empirical relationship shown in the figure compares reasonably well with Eq. 8-9 of Rast and Lee (1978). The notation of trophic status provides an approximate division between the three states of oligotrophy, mesotrophy and eutrophy.

These empirical relationships permit estimation of chlorophyll a, secchi depth if the total phosphorus in the lake can be estimated from data or from equations such as Eq. (8-3) or (8-8).

The approach of Chapra and Tarapchak (1976) follows the steps outlined in the introduction above and begins with Eq. (8-3) which relates external loading to total annual phosphorus in the lake. The spring concentration of total phosphorus is given empirically by

$$p = 0.9\ p_s \qquad (8\text{-}$$

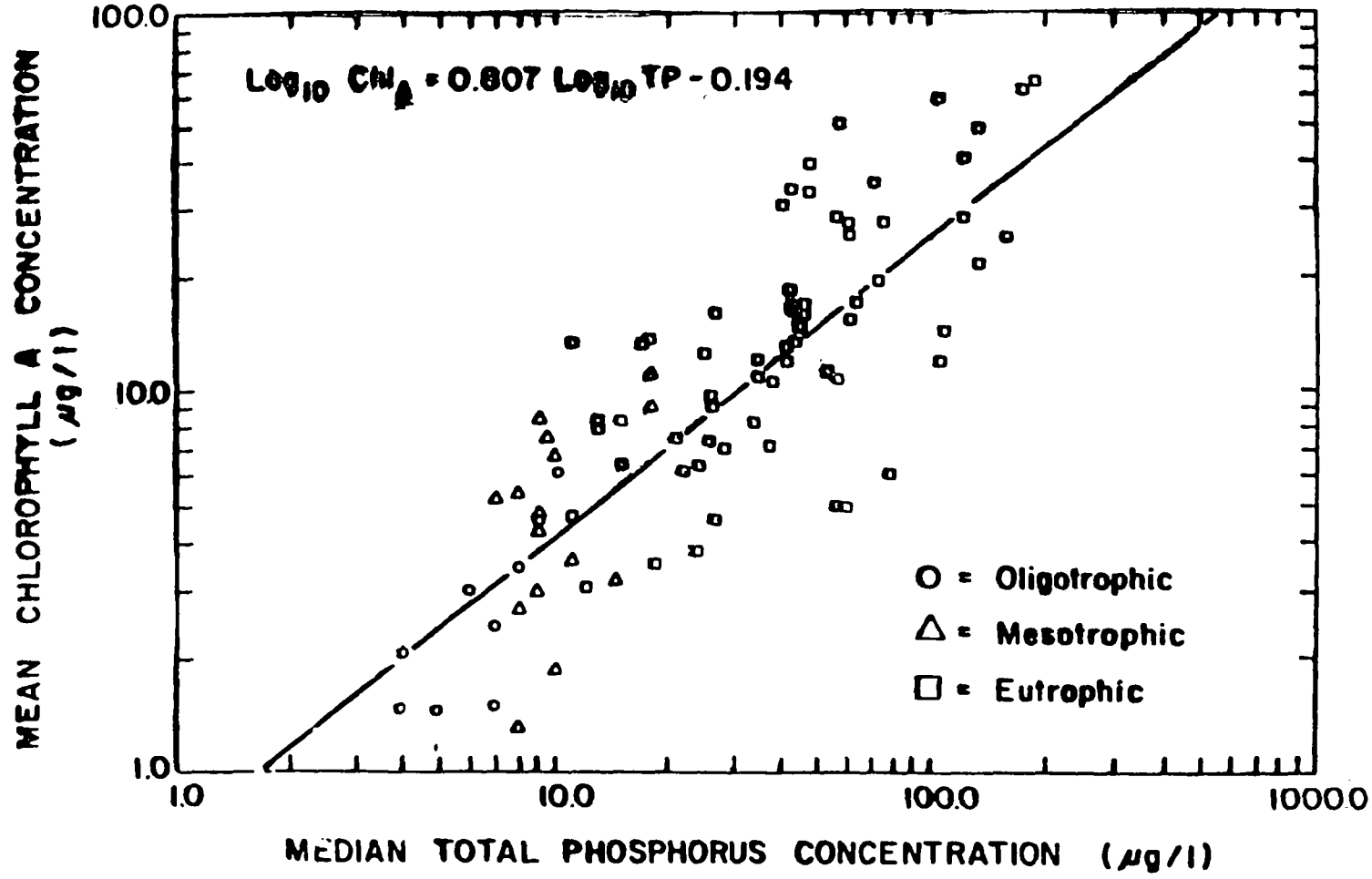

Figure 2-9 The relationship between chlorophyll A and total phosphorus concentrations in northeastern U.S. lakes and reservoirs included in the survey. (From Bartsch and Gakstatter, 1978).

where p_s is the spring total phosphorus. The final step of computing mean summer chlorophyll is given by Dillon and Rigler (1974) as

$$Ch\ell\ a = .731\ (p_s)^{1.449} \tag{8-12}$$

Eq.(8-12), and (8-13) were then combined to give

$$Ch\ell\ a = 1866\ [W'/(q_s + 12.4)]^{1.449} \tag{8-13}$$

where Chℓ a is in g/ , W' is in g/m^2-yr and q_s is in m/yr and a net sedimentation rate of 12.4 m/yr was used. This equation permits estimation of the mean summer chlorophyll directly from the external loading, a very desirable trait.

Eq. (8-14) can also be rearranged to evaluate the loading required for a given chlorophyll level. Thus,

$$W' = .0055\ (Ch\ell\ a)^{0.69}\ (q_s + 12.4) \tag{8-14}$$

Chapra and Tarapchak (1976) chose the following mean summer chlorophyll levels as objectives:

$$\text{Acceptable: } Ch\ell\ a = 2.7\ \mu g/\ell \tag{8-15}$$
$$\text{Excessive: } Ch\ell\ a = 9.0\ \mu g/\ell \tag{8-16}$$

These levels are equivalent to total annual phosphorus levels of 13.4 and 30.7 μgP/ℓ for the acceptable and excessive levels respectively. With the objectives of expressions (8-15) and (8-16),

$$W'_{acceptable} = 0.011\ (q_s + 12.4) \tag{8-17}$$
$$W'_{excessive} = 0.025\ (q_s + 12.4) \tag{8-18}$$

These expressions are essentially identical to Eqs. (8-6) and (8-7) lending support to the credibility of each. As such, the loading rates of Figure 8-7 separate a trophic status of lakes from about 3 μg chlor/ℓ at the acceptable level to about 9 μg chlor/ℓ at the excessive level. It should be stressed again that all these results apply as a general criterion for lakes only and as a rule, only for lakes in the North Temperate regions of the world.

Variability of Net Effective Settling Velocity

The completely mixed nutrient mass balance equation which forms the basis for the simplified Vollenweider analysis rests heavily on the assumption that the net effective settling velocity is 10 m/yr. When only external loads are considered, this parameter in the mass balance incorporates phenomena such as

1) fraction of incoming phosphorus in particulate form

2) concentration of suspended solids in the lake

3) resuspension of particulate phosphorus from bottom sediments

4) diffusive flux of dissolved phosphorus from the sediments.

The net effective settling velocity may, therefore, be expected to vary as a function of these mechanisms. There is no simple direct way to represent all these phenomena in a single parameter reflective of all lake and impoundment situations. The range in v_s is large as shown in Figure 8-8A. The data for this Figure are from U.S. lakes and impoundments and were compiled from Rast and Lee (1978), Bachmann and Canfield (1979), Schreiber and Rausch (1979), and Higgins and Kim (1981). Only positive values for v_s are plotted; for some reservoirs (e.g. see Higgins and Kim, 1981) the computed net settling velocity is negative which indicates that the mass output of the impoundment exceeds the input mass. This could result from net positive resuspension in the reservoir.

It is clear from Fig. 8-8A that the variability in v_s is great. The U.S. lakes, as distinct from impoundments, vary within about one order of magnitude (approximately 3-30 m/yr.). This is a sufficiently large range and could markedly influence the calculation of the allowable phosphorus load.

Impoundments, in general, vary about three orders of magnitude with no clear correlation to the hydraulic loading rate. The net settling rate for impoundments is, however, generally greater than that for lakes by a substantial amount. This probably reflects an increase in particulate phosphorus fractions and associated settling velocity.

Figure 8-8A shows the importance of not relying too heavily on the simplified Vollenweider plot of Figure 8-7. Each individual lake and impoundment will have an associated v_s that should be evaluated on a rite specific basis.

However, from the point of view of engineering control, the simple nutrient mass balance equation coupled with the empirical expressions indicated above provide an excellent starting point for assessing the efficacy of proposed nutrient reduction programs. For other situations where a) the assumptions used for the simple analyses are no longer sufficient, b) water bodies such as estuaries and bays must be analyzed, and c) additional quantitative understanding of the processes of eutrophication is desired, it is important to explore phytoplankton relationships with a simple dynamic modeling framework.

PHYTOPLANKTON GROWTH AND DEATH

A simple mass balance equation for the phytoplankton can be obtained by following the basic principles outlined previously, i.e. summing all sources and sinks of phytoplankton. Therefore, considering a completely mixed lake, the equation is:

$$V \frac{dp}{dt} = V(G_p - D_p)\, P - A\, v_s\, P + Q_{in} P_{in} - QP \qquad (8\text{-}19)$$

where P = phytoplankton chlorophyll [M/L^3]; e.g. µg/ℓ

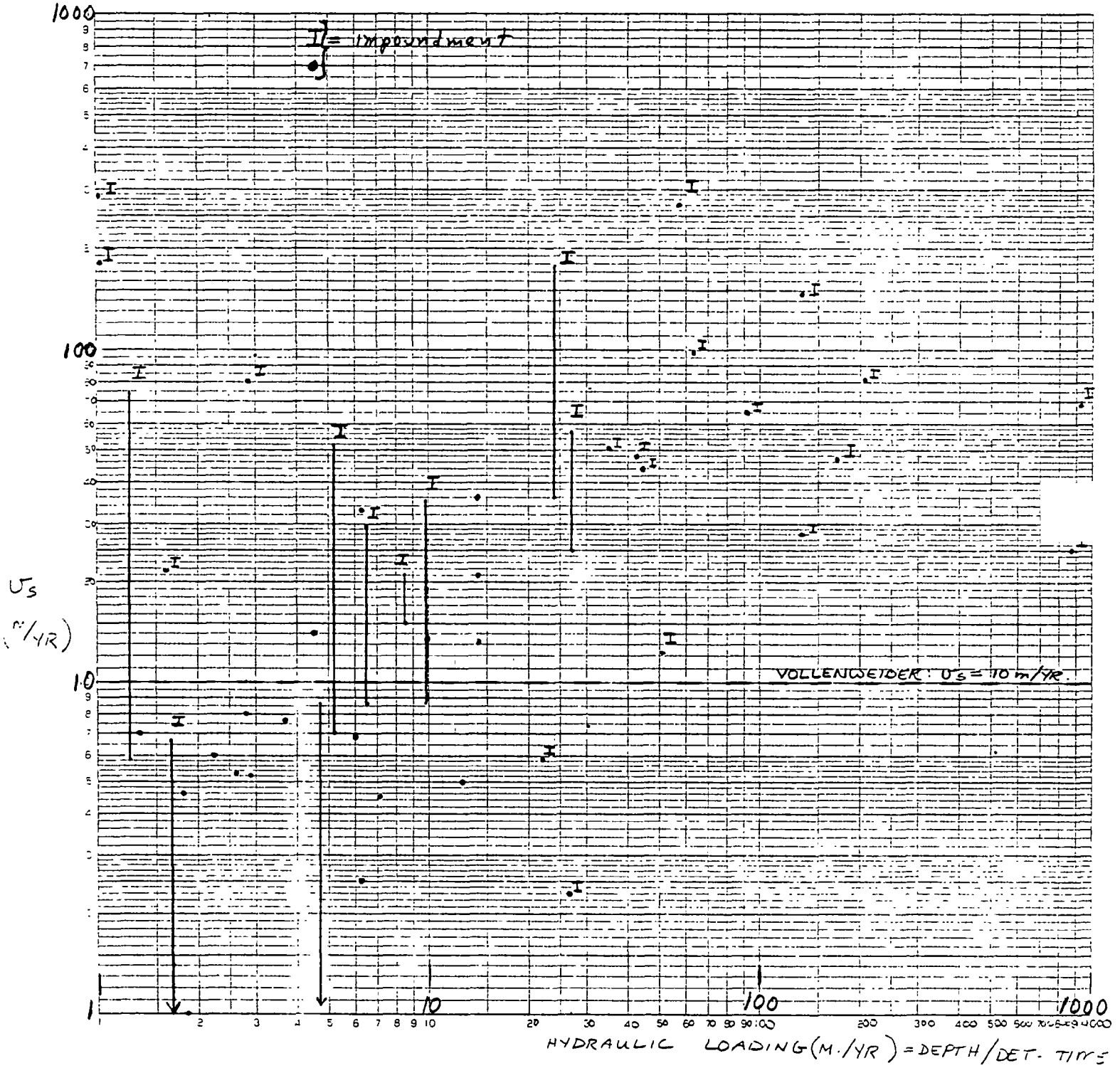

Fig 8-8A Range of net settling velocity as a function of hydraulic loading

Full Logarithmic, 3 × 3 Cycles

P_{in} = phytoplankton chlorophyll [M/L^3] in incoming flow (M/L^3)

G_p = growth rate of phytoplankton [T^{-1}], e.g. (1/day)

D_p = death rate of phytoplankton [T^{-1}]

v v_s = settling rate of phytoplankton [M/T], e.g. (m/day)

A = area through which settling is occurring [L^2]

The first term on the right hand side of Eq. 8-19 represents the net growth rate of the phytoplankton, i.e. growth minus death. This term is a new term in the mass balance equations for completely mixed systems considered thus far. The second term is the mass of phytoplankton lost to the sediment from settling. Note that:

$$A\, v_s = \frac{V v_s}{H} = V K_p$$

where H is the mean depth [L] and K_p [T^{-1}] is the net loss rate = v_s/H.

Estimates of v_s range from about 0.1-0.3 m/day and represent the net loss of phytoplankton through the bottom interface of the water body. This net settling depends on phytoplankton species, time of day and nutritional status of the plankton. In general, living phytoplankton have settling velocities that are considerably less than non-living particulate matter. Burns and Rosa (1980) carried out a series of experiments using special in situ settling experiments. Table 8-5B summarizes some of their results.

TABLE 8-5B
Some Results of In Situ Settling Experiments in Lake George
(From Burns and Rosa, 1980)

Particle Type	Settling velocity m/day
Particulate Organic Carbon	
1-10 m	0.2
10-64 m	1.5
>64 m	2.3
Phytoplankton	
sconedesmus acutiforms	0.10
selenastrum minutum	0.15
cryptomonas crosa	0.30

The third term is the mass of phytoplankton chlorophyll entering the lake with the inflow. The last term is the usual mass transport of phytoplankton out of the system due to lake outflow.

The growth and death of the phytoplankton represents an important term and will be explored more fully. Consider then the kinetic expression:

$$\frac{dP}{dt} = (G_p - D_p)P \qquad (8\text{-}20)$$

as representative of phytoplankton behavior in a batch type vessel. The solution to this equation for initial condition P_o is:

$$P = P_o \exp (G_p - D_p)\, t \qquad (8\text{-}21)$$

Several conditions are now possible, i.e.

$G_p > D_p$ (Net production of phytoplankton)

$G_p = D_p$ (Stationary growth)

$G_p < D_p$ (Net decline in phytoplankton)

Figure 8-9 shows the time behavior of these three conditions. The principal dynamics of phytoplankton growth are therefore contained in behavior of the growth and death of the phytoplankton over the seasons of the year. A more detailed evaluation of the behavior of these kinetic terms is of some importance in understanding the interaction of nutrients and phytoplankton chlorophyll.

Phytoplankton Growth - G_p

The growth rate of the phytoplankton, as noted earlier, depends on three principal components:

i) Temperature
ii) Light
iii) Nutrient

The classical approach is to assume that these effects are multiplicative, although there is no a priori rationale for this assumption. The use of a multiplicative effect of each of these components is, however, somewhat justified from data collected from laboratory experiments (DiToro, et al., 1975). The growth rate can then be written as:

$$G_p = [\text{Temp Effect}] \cdot [\text{Light Effect}] \cdot [\text{Nutrient Effect}]$$
$$= G(T) \cdot G(I) \cdot G(N) \qquad (8\text{-}22)$$

Temperature Effect

Now consider a situation where the available light for growth is at an optimum level and nutrients are plentiful. Then the growth of the phytoplankton will be dependent only on the temperature effect. This relationship of temperature and growth rate can be determined from work by Eppley (1972), among others and is approximated by

$$G(T) = G_{max} (1.066)^{T-20} \qquad (8\text{-}23)$$

where $G_{max} = 1.8/\text{day}$ (approximately)

This relationship between the growth rate and temperature is shown in Figure 8-10. Note that the relationship expresses the maximum growth rate as a function of water temperature assuming that no other effect (e.g. light or nutrients) is limiting growth.

The value suggested for G_{max} of 1.8/day is an average condition for a mixed phytoplankton population. Various species of phytoplankton, however, have different growth rates, and, in general, the range of G_{max} is about 1.5-2.5/day.

Light Effect

If now the temperature is held constant and the available

$$P = P_0 \exp(G_p - D_p)t$$

(a) $G_p > D_p$

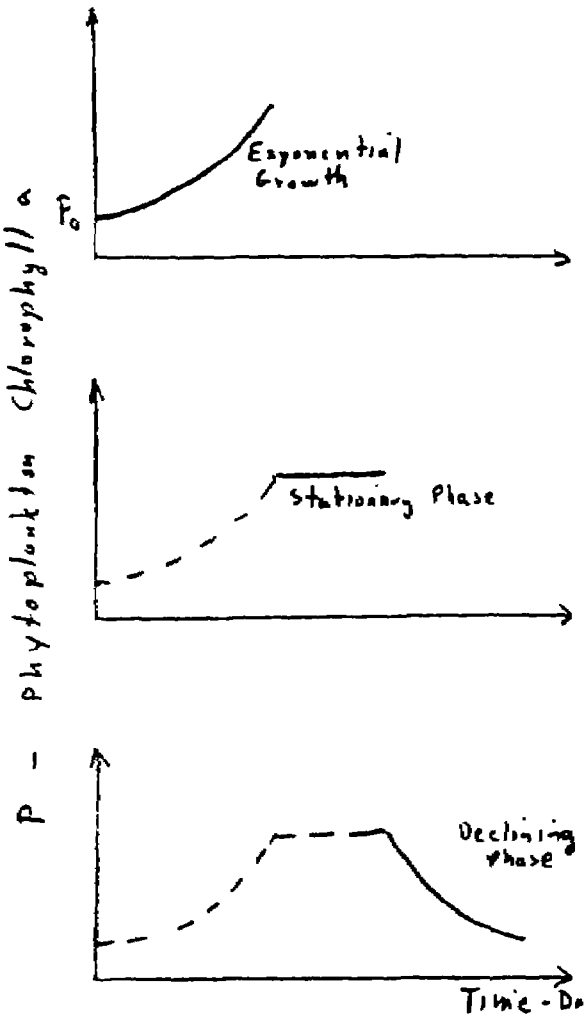

(b) $G_p = D_p$

(c) $G_p < D_p$

Fig. 8-9 Time variable behavior of phytoplankton for three conditions on net growth.

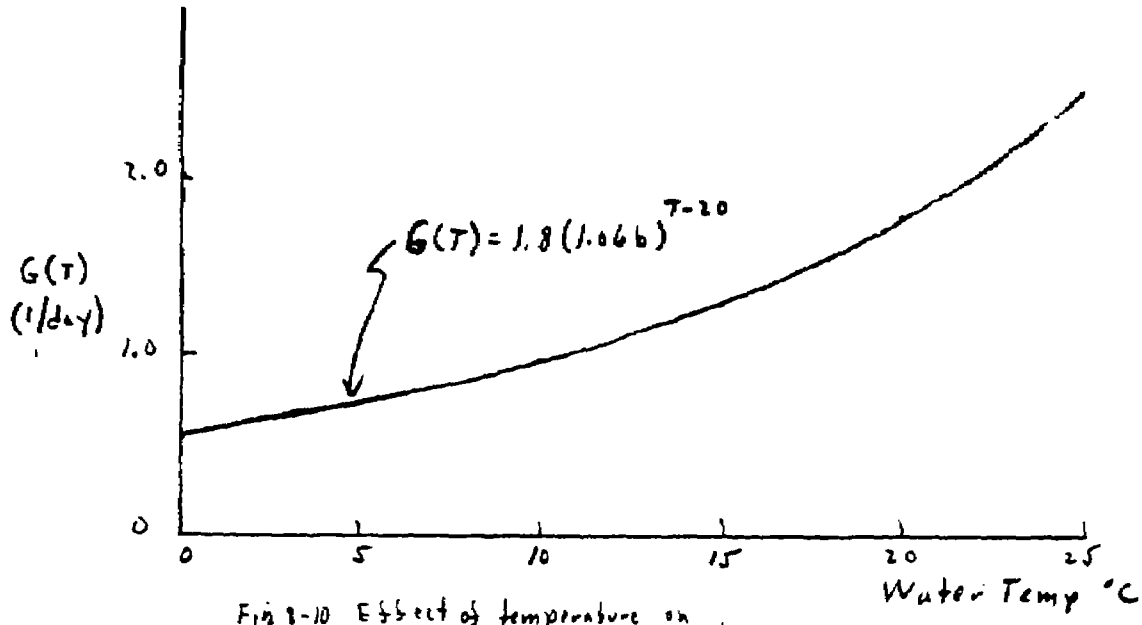

Fig 8-10 Effect of temperature on growth rate of phytoplankton

light is allowed to vary, it is observed that as the radiation increases, photosynthesis increases up to a maximum level. Further increases in light levels tend to result in photoinhibition and a subsequent decrease in photosynthesis. Figure 8-11 (from DiToro et al., 1971) shows this effect and also indicates that the optimum light intensity varies for the different phytoplankton groups.

An equation that represents Fig. 8-11 (a) is given by

$$F(I) = \frac{I}{I_s} \exp\left[-I/I_s + 1\right] \qquad (8\text{-}24)$$

where I_s = saturating light intensity (gm-cal/cm^2), i.e. the light intensity at which the relative photosynthesis is a maximum. Values of I_s for mixed populations of phytoplankton are approximately 100-400 ly/day with 300 ly/day as an approximate average. Note that when $I = I_s$, $F(I) = 1$. Eq. (8-24) represents the relative photosynthesis as a function of light intensity at any given point in space and time. Often, however, the modeling analysis is more tractable by calculating average conditions over a given depth of water and over a fixed interval of time (usually one day). Following DiToro et al. (1971), and referring to Chapter 2, Eq. 2-4, it is known that

$$I(Z) = I_o \exp\left(-K_e z\right)$$

Substituting this equation into Eq. 8-24 gives $F(I(Z))$. But, the incoming solar radiation, I_o, is of course a function of the time of day as shown in Fig. 8-12. If the simplifying assumption is made that

$$I_o = I_a \qquad 0<t<f \qquad (8\text{-}25)$$

$$= 0 \qquad f<t<1$$

as shown in Fig. 8-12, (where f is the photoperiod), then the average over depth, z and over one day is given by

$$G(I_a) = \int_t \int_z F(I(t,z))\, dtdz$$

$$= \frac{2.718f}{K_e z} \left(\exp(-\alpha_1) - \exp\left(-\alpha_0\right)\right) \qquad (8\text{-}26)$$

where

$$\alpha_1 = (I_a/I_s) \exp\left(-K_e z\right) \qquad (8\text{-}26\ a)$$

$$\alpha_0 = I_a/I_s \qquad (8\text{-}26\ b)$$

It should be recalled here that the extinction coefficient, K_e, depends on the inorganic solids, detrital particles as well as

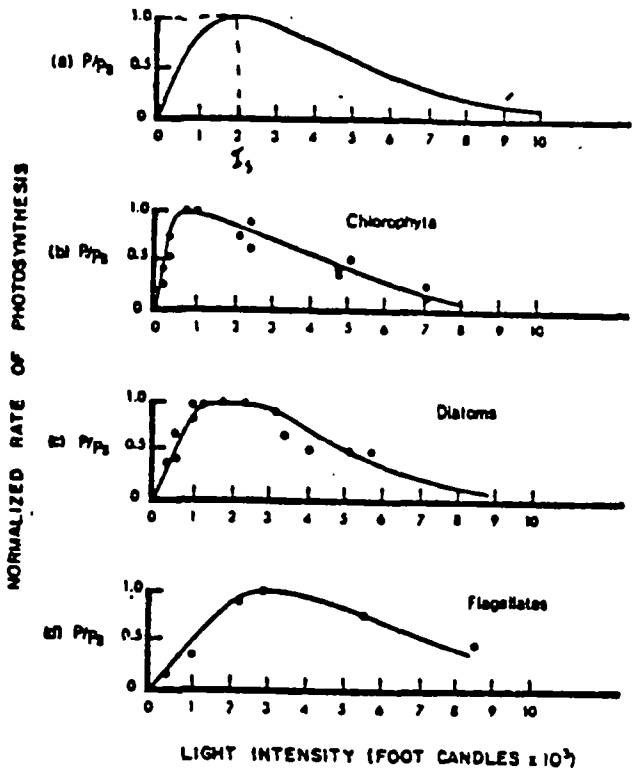

Fig. 8-11 Normalized rate of photosynthesis vs. incident light intensity. From DiToro et al, 1971 using data and theoretical curve[a] from Steele (1965); curves (b), (c) and (d), data from Ryther (1956)

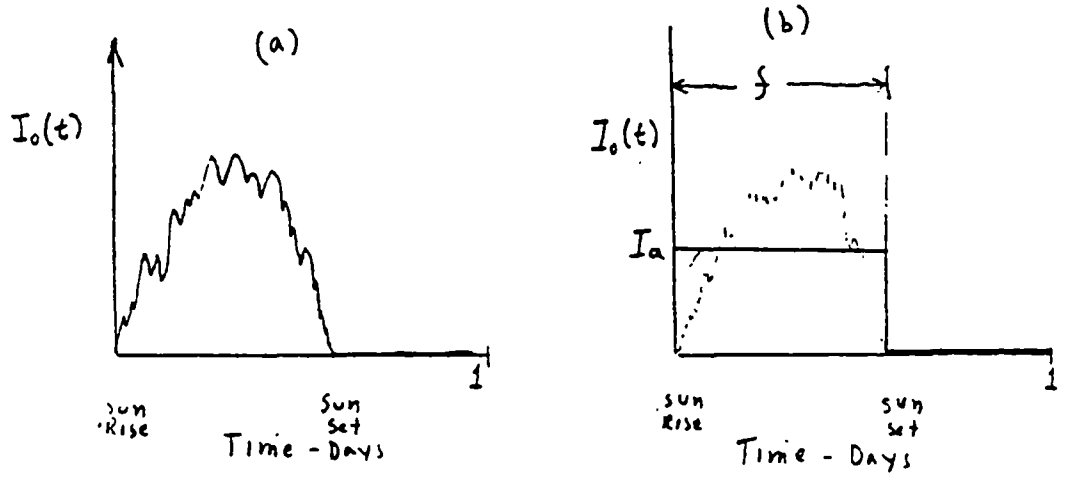

Fig 8-12 (a) Actual variation of solar radiation over 1 day for a clear day (b) Approximation for averaging.

the phytoplankton levels. Eqs. 2-7 and 2-8 indicate these relationships.

G(I), the light effect as given by Eq. 8-26 is dimensionless and is used as a multiplier in Eq. 8-22. The behavior of $G(I_a)$ is shown in Fig. 8-13(a). For a typical range of I_a of 250-500 ly/day, the value of $G(I_a)$ ranges from 0.10 to 0.50, i.e. the overall effect of non-optional light conditions due to light extinction with depth is to reduce the growth rate by about 50-90%.

Nutrient Effect

The final effect on the growth that must be evaluated is the effect of varying nutrient levels on the growth rate of the phytoplankton. Therefore, consider again all conditions on temperature and light to be constant and at optimum levels and consider the nutrient concentrations to be varying. The result of this effect is quite significant and is shown in Figure 8-13 (b). At a nutrient level of zero, there is, of course, no growth since, as noted previously, the phytoplankton requires at least some critical nutrients to begin or stimulate the growth of the population. As the nutrient level is increased, growth commences, i.e. $G(N)>0$. However, as nutrient levels continue to increase, the effect on the growth rate of the phytoplankton is reduced and asymptotically approaches unity. An expression for this effect on the growth of the phytoplankton is

$$G(N) = \frac{N}{K_{mN}+N} \qquad 8\text{-}27$$

where N is the concentration $[M/L^3]$ of the nutrient needed for phytoplankton growth (e.g. phosphorus or nitrogen) and K_{mN} is the concentration of the nutrient $[M/L^3]$ at which the nutrient effect, G(N), = 1/2. K_{mp} is called the "Michaelis" constant after the work of Michaelis-Menton on uptake kinetics of organisms on substrates. The implications of this effect are quite profound. Suppose a present nutrient input is such as to result in a concentration of the nutrient that is substantially greater than K_{mN}, i.e.

$$N_b >> K_{mN}$$

where N_b is the nutrient concentration before any nutrient reduction. If a nutrient control program is initiated, but the reduction in input load only reduces the nutrient concentration to a level of about two-three times the Michaelis constant, then there will be no effect on the phytoplankton growth. The treatment program may then be ineffective. The nutrient effect on phytoplankton, therefore, is a marked contrast to other types of water quality problems where reductions in input load (as in BOD reduction) can generally be considered as being advantageous.

Table 8-6 shows some typical values for the values of K_{mN} for different nutrients.

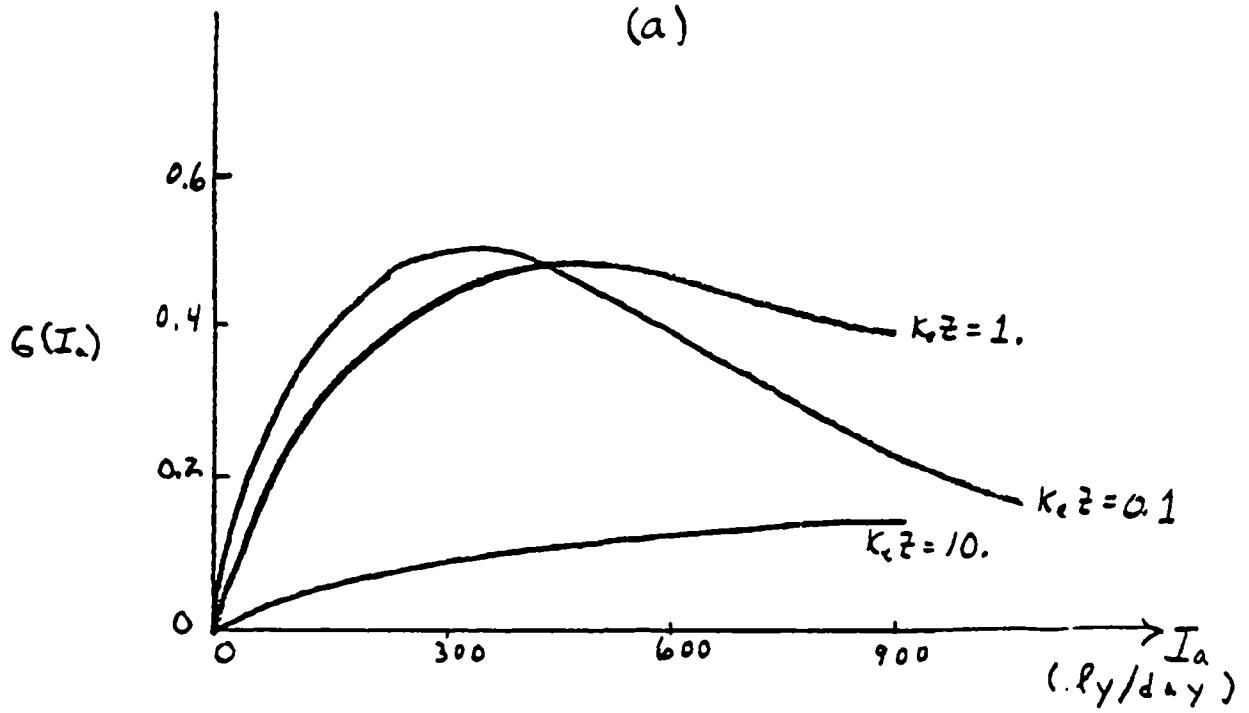

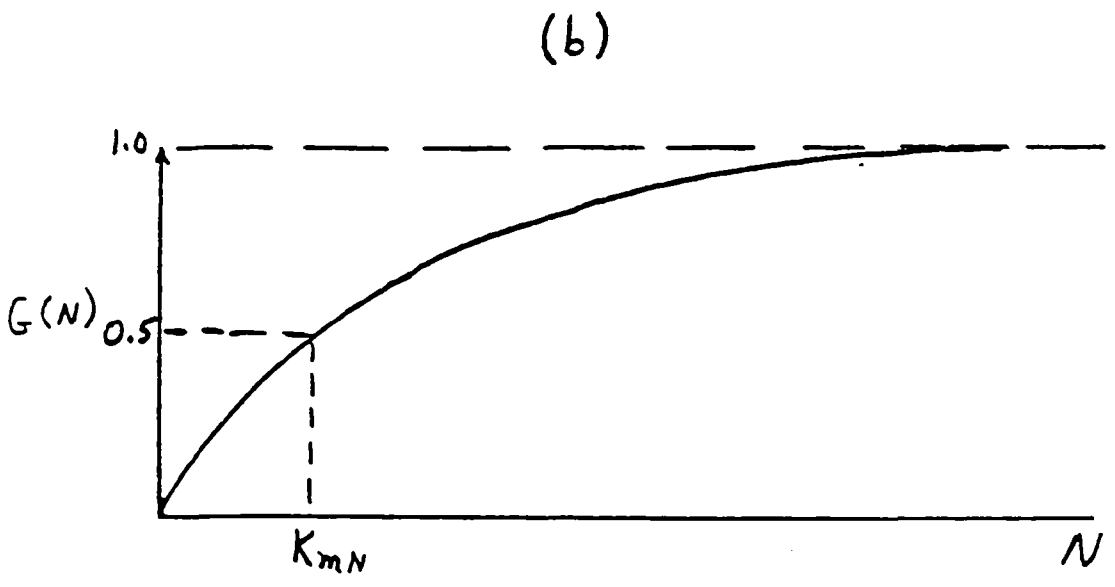

Fig. 8-13 a) Relationship of light effect for average depth and across one day; I_s = 300 ly/day, f = 0.5.
b) Relationship of nutrient effect

Table 8-6

Typical Values for K_{mN}
Half Saturation Constants for Phytoplankton Growth

Nutrient	K_{mN}
Nitrogen	10-20 µg N/ℓ
Phosphorus	1 - 5 µg P/ℓ
Silica (for diatoms only)	20-80 µg Si/ℓ

When more than one nutrient may be important in the problem context, then the nutrient effect is given by

$$G(N) = \text{Min}\left\{\frac{N_1}{K_{mN_1} + N_1} ; \frac{N_2}{K_{mN_2} + N_2} \ldots\right\} \qquad (8\text{-}28)$$

where the minimum of the expression in brackets is to be taken as the nutrient effect. That is, the individual nutrient limitation expressions are computed and the minimum value is chosen for G(N).

The full expression for the phytoplankton growth rate is therefore given from Eqs. (8-23), (8-26) and (8-28) as

$$G_p = G_{max}\,(1.066)^{T-20}\left[\frac{2.718f}{K_e z}\left(\exp(-\alpha_1) - \exp(-\alpha_0)\right)\right]$$
$$\left[\text{Min}\left(\frac{N_1}{K_{mN_1} + N_1} ; \frac{N_2}{K_{mN_2} + N_2}; \ldots\right)\right] \qquad (8\text{-}29)$$

Phytoplankton Death - D_P

The second component of phytoplankton kinetics is the overall death or mortality rate of the plankton. The basic components of D_p are:

i) Endogeneous respiration rate at which phytoplankton oxidize their organic carbon to CO_2 per unit weight of phyto-organic carbon, and

ii) zooplankton predation or grazing of the phytoplankton.

The death rate can, therefore, be written as the sum of these two components, i.e.

$$D_P = D_{P1}(T) + D_z \qquad (8\text{-}30)$$

where $D_{P1}(T)$ is the endogenous respiration rate as a function of temperature, T and D_z is the death rate due to zooplankton grazing.

The endogenous respiration rate is given by:

$$D_{Pl} = 0.1(1.08)^{T-20} \qquad (8\text{-}31)$$

for D_{Pl} in day^{-1} and T in ^{o}C, Fig. 8-14 shows this relationship.

The loss of phytoplankton due to grazing by herbivorous zooplankton is, proportional to the number or concentration of zooplankton that is present. The death rate due to grazing, D_z can, therefore, be written as

$$D_z = C_c z \qquad (8\text{-}32)$$

where C_g is the grazing (filtering) rate of zooplankton (liter/day-mg/zoopl. Carbon) and z is zooplankton concentration in equivalent carbon units (mg C/l). Much work has been done on measurements of the zooplankton grazing rate and Table 8-7 summarizes some of the data (DiToro, et al., 1971, Thomann, et al., 1975). The filtering rate of the zooplankton is, of course, a complicated function of the age, size, temperature and species.

Table 8-7

Range of Zooplankton Grazing Rates

Organism or Location	Grazing Rate liter/day-mg Zoop. Carb.
Rotifer (0.1 µg)	1.5-4
Copepod and Cladoceran (1-10 µg)	2 - 5
Georges Bank	2 - 3
Lake Ontario	1.5-3

Eq. 8-32 introduces the zooplankton as a new variable. The concentration of the zooplankton may be known or can be estimated. If so, the known concentration can be used in the equation either as an average value during grazing periods or as a time variable value. It is preferable to attempt to calculate the concentration and then compare such a calculated concentration to the observed zooplankton levels. One can, therefore, write an equation for the growth and death of the zooplankton in a manner similar to the phytoplankton (Eq. 8-20). Thus,

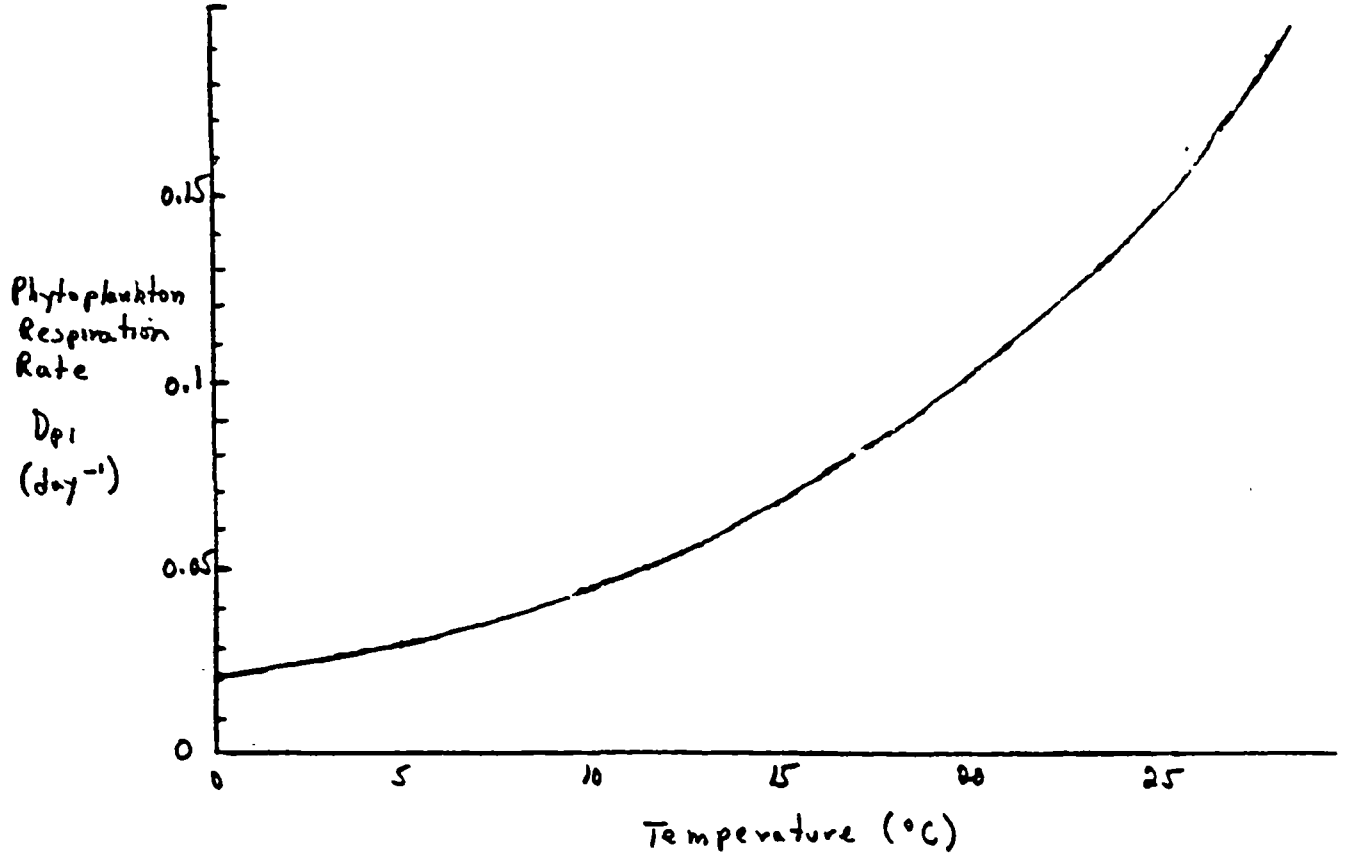

Figure 8-14 Phytoplankton respiration rate as a function of water temperature

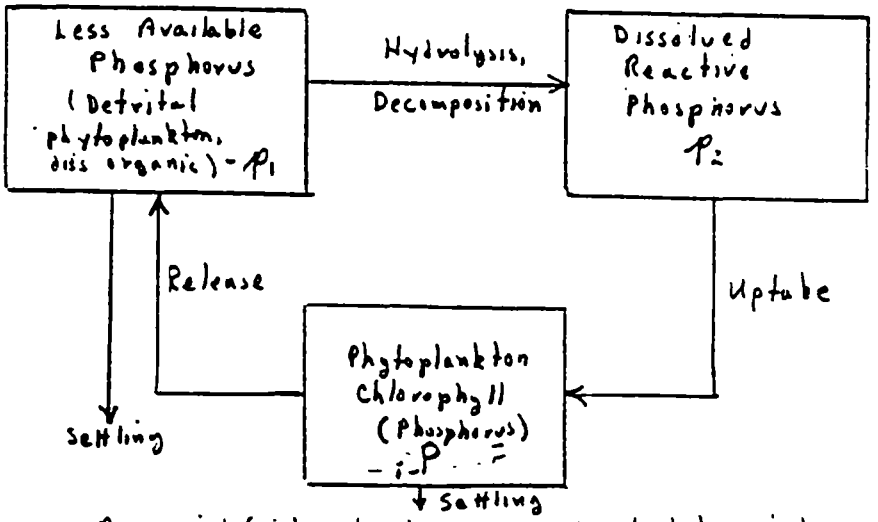

Fig 8-15 A simplified phosphorus - phytoplankton interaction

$$\frac{dZ}{dt} = (G_Z - D_Z)\ Z \qquad (8-$$

where G_Z and D_Z are the growth and death rates respectively of the zooplankton. The growth rate of the zooplankton depends on the rate at which the zooplankton feed on the phytoplankton (the grazing rate, C_g), the amount of phytoplankton available (the chlorophyll level, P) and the efficiency of assimilation or conversion of phytoplankton biomass to zooplankton biomass. The growth rate can then be written as

$$G_Z = a_1' C_g (a_{Zp} P) \qquad (8-34)$$

where a_1' is the efficiency of assimilation (mg Zoopl. Carb./my Phyto. Chlor.). A balance of the units is:

$$1/day = \frac{mg\ Z(cbn)}{mg\ P(Chl)} \cdot \frac{\ell}{day\text{-}mg\ Z(cbn)} \cdot \left(\frac{mg\ Z(cbn)}{mg\ P(chl)}\ \frac{mg\ P(chl)}{\ell}\right)$$

It is also known, however, that the efficiency of assimilation, a_1' is not a constant and depends on the phytoplankton concentration, i.e. at high dense concentrations of phytoplankton, the zooplankton simply cannot assimilate the phytoplankton. Therefore, let

$$a_1' = a_1 \frac{K_g}{K_g + P}$$

where K_g is the phytoplankton chlorophyll concentration at which zooplankton efficiency is limited by a factor of one-half. Substitution into the growth rate, Eq. (8-34) gives

$$G_Z = a_p a_1 \frac{K_g}{K_g + P} C_g P$$

or

$$G_z = a_p a_1 K_g C_g \left(\frac{P}{K_g + P}\right) \qquad (8-35)$$

This latter expression indicates that G_Z, the growth rate of the zooplankton reaches a saturation level at values of $P >> K_g$. Typical values for the coefficients are: a_{Zp}=50-100 and a_1=0.6. Thomann, et al. (1975) used K_g=10 µg chlor/ℓ for Lake Ontario and DiToro et al. (1977) used 60 µg chlor/ℓ for the Sacramento-San Joaquin Delta.

The death rate for the zooplankton biomass is simply the sum of the respiration, individual death rate and predation by the next level in the food chain. Thus,

$$D_Z = K_Z\ (T) + D_Z' \qquad (8-36)$$

where $K_Z(T)$ is the respiration of the zooplankton and is about .02/day at 20°C and D_Z' represents the other losses of zooplankton due to death and higher order predation. This latter coefficient is usually an empirical parameter to be adjusted unless high order forms are also modeled.

The growth and death of phytoplankton is, therefore, a function of several environmental variables: water temperature, sunlight, turbidity and zooplankton. From a water quality engineering viewpoint, the time and space dependence of phytoplankton also depends most significantly on the nutrients available for growth. Such dependence is quite non-linear as shown in Fig. 8-13 (b) and, as a result, reductions in ambient nutrient concentrations may not always result in reductions in phytoplankton biomass. It is important then to examine the relationship between phytoplankton and nutrients in some additional detail.

Nutrient-Phytoplankton Interactions

With the basic principles of phytoplankton growth and death in hand, the interactions of the nutrient and phytoplankton systems can be evaluated by first considering the nutrient mass balance equations with the direct and explicit inclusion of the phytoplankton. It is instructive to begin with a single nutrient that is limiting, say phosphorus and all other nutrients are in excess supply. For phosphorus then, assume that dissolved reactive phosphorus (see Fig. 8-4) is available for uptake by the phytoplankton as shown in Fig. 8-15. The phosphorus thus absorbed is incorporated into the phytoplankton cellular material. Upon respiration and cell lysis (cell disintegration), the cellular phosphorus of the phytoplankton is released in two principal forms: as particulate organic (detrital) phosphorus and as complexed dissolved organic phosphorus. Both of these forms are grouped under a general heading of "less available" phosphorus. Bacterial degradation and hydrolysis reactions then convert these less available organic forms to the inorganic phosphorus from which is again available for phytoplankton uptake, thus completing the cycle.

This simplified phosphorus-phytoplankton cycle can now be used to illustrate several important points. Consider this cycle to be operative in a completely mixed system such as shown in Fig. 8-6. The mass balance equation for each form is then given by the following equations:

$$V \frac{dp_1}{dt} = W_1 - Qp_1 - K_{22}Vp_1 + D_p Va_p P \qquad (8\text{-}37)$$

$$V \frac{dp_2}{dt} = W_2 - Qp_2 - K_{12}Vp_1 - G_p a_p P \qquad (8\text{-}38)$$

$$V \frac{dP}{dt} = W_3 - QP - v_{s3}AP + (G_p - D_p)P \qquad (8\text{-}39)$$

In the equations, p_1 and p_2 are the unavailable and available phosphorus forms respectively and P is the photoplankton chlorophyll in [M/L^3]. W_1 and W_2 are the inputs [M/T] of less available and available phosphorus respectively; W_3 is the input of phytoplankton chlorophyll; K_{12} is the rate [1/T] of conversion of unavailable to available phosphorus; and K_{22} is the loss rate of p_1 due to conversion to available phosphorus as well as any settling of particulate forms, i.e.

$$K_{22} = K_{12} + \frac{v_{s1}}{Z} \qquad (8\text{-}40)$$

for v_{s1} as the effective settling rate [L/T] of particulate forms of less available phosphorus. Similarly, in Eq. (8-39), v_{s3} is the settling rate [L/T] of the phytoplankton and finally, a_p is the phosphorus to chlorophyll ratio of the phytoplankton [M-P/M-Chl]. The first two of these equations require some additional discussion. The third equation has already been reviewed (see Eq. 8-19).

Eq. (8-37), the mass balance equation for the less available phosphorus form includes a source term, $D_p V a_p p$. This term represents the production of less available phosphorus forms due to the death rate of the phytoplankton, D_p.

Typical units are:

$$D_p \qquad V \qquad a_p \qquad\qquad P$$

$$\left[\frac{1}{\text{day}}\right] \quad [\ell] \quad \left[\frac{\mu g \text{ Phos.}}{\mu g \text{ Chl.}}\right] \quad \left[\frac{\mu g \text{ chl}}{\ell}\right] = \frac{\mu g \text{ Phos}}{\text{day}}$$

The second equation (8-38) includes the generation of available phosphorus due to degradation of less available forms in the term $K_{12} V p_1$. In addition, the uptake of available phosphorus is given by $G_p a_p P$. The rate of growth of the phytoplankton and conversion of the inorganic phosphorus to the phytoplankton biomass is accounted for stoichiometrically in the nutrient equation by this term. The production of phytoplankton chlorophyll is, therefore, accompanied by a reduction in the available phosphorus. For each µg/ℓ of chlorophyll produced, the available phosphorus is reduced stoichiometrically by a_p, the phosphorus to chlorophyll ratio. This can readily be seen by assuming for Eqs. (8-37) to (8-39) a batch reactor vessel that has no external inputs, no flow through the vessel, is kept stirred so the settling velocity is zero and the rate of conversion of less available to available phosphorus forms is fast. Only two variables then need be considered; the available phosphorus and the phytoplankton. Therefore,

$$\frac{dp_2}{dt} = -G_p a_p P + D_p a_p P = -(G_p - D_p) a_p P \qquad (8\text{-}41)$$

and

$$\frac{dP}{dt} = (G_p - D_p)\ P \qquad (8\text{-}42)$$

Now $a_p P$ represents the available phosphorus equivalent of the phytoplankton, thus

$$P_2 = a_p P$$

and Eq. (8-41) becomes

$$\frac{dp_2}{dt} = -(G_p - D_p)\ p_2 \qquad (8\text{-}43)$$

During the active growth phase of the phytoplankton then, where $G_p > D_p$, (see previous discussion on Eq. (8-21)), an equivalent P uptake of phosphorus occurs. At the end of the growth phase of the phytoplankton, where, for example, 100 µgChl/ℓ were produced, then the product of a_p and the 100 µgChl/ℓ is the amount of available phosphorus that had to be supplied.

Phytoplankton - DO Relationships

Introduction

The relationship between the growth and death of phytoplankton and the dissolved oxygen is a particularly important one. From the DO balance point of view, photosynthesis can result in significant variations in oxygen in a water body (See Chapter 6). Also, the production of phytoplankton biomass due to the discharge of nutrients can result in the deposition of phytoplankton cells to the sediment. The oxidation of this organic material then becomes part of the sediment oxygen demand and can significantly influence the DO. An example is shown in Figure 8-16 where the DO for the central basin of Lake Erie is shown. The rapid decline of the DO in the hypolimnion in the summer is clearly indicated and is due, in large measure, to the phytoplankton production in the epilimnion. The DO balance equation includes the effect of photosynthesis and respiration by aquatic plants. These terms are given as

$+ P_{av}$ (mg O_2/ℓ-day) - Photosynthesis

$- R'_{av}$ (mg O_2/ℓ-day) - respiration

and represent the direct input or utilization of oxygen through the phytoplankton dynamic of growth and death discussed above. The mass balance equation for dissolved oxygen discussed in Chapter 6 includes these effects as source and sink terms, i.e.

$$\frac{dc}{dt} = K_a (c_s - c) - K_d L + P - R$$

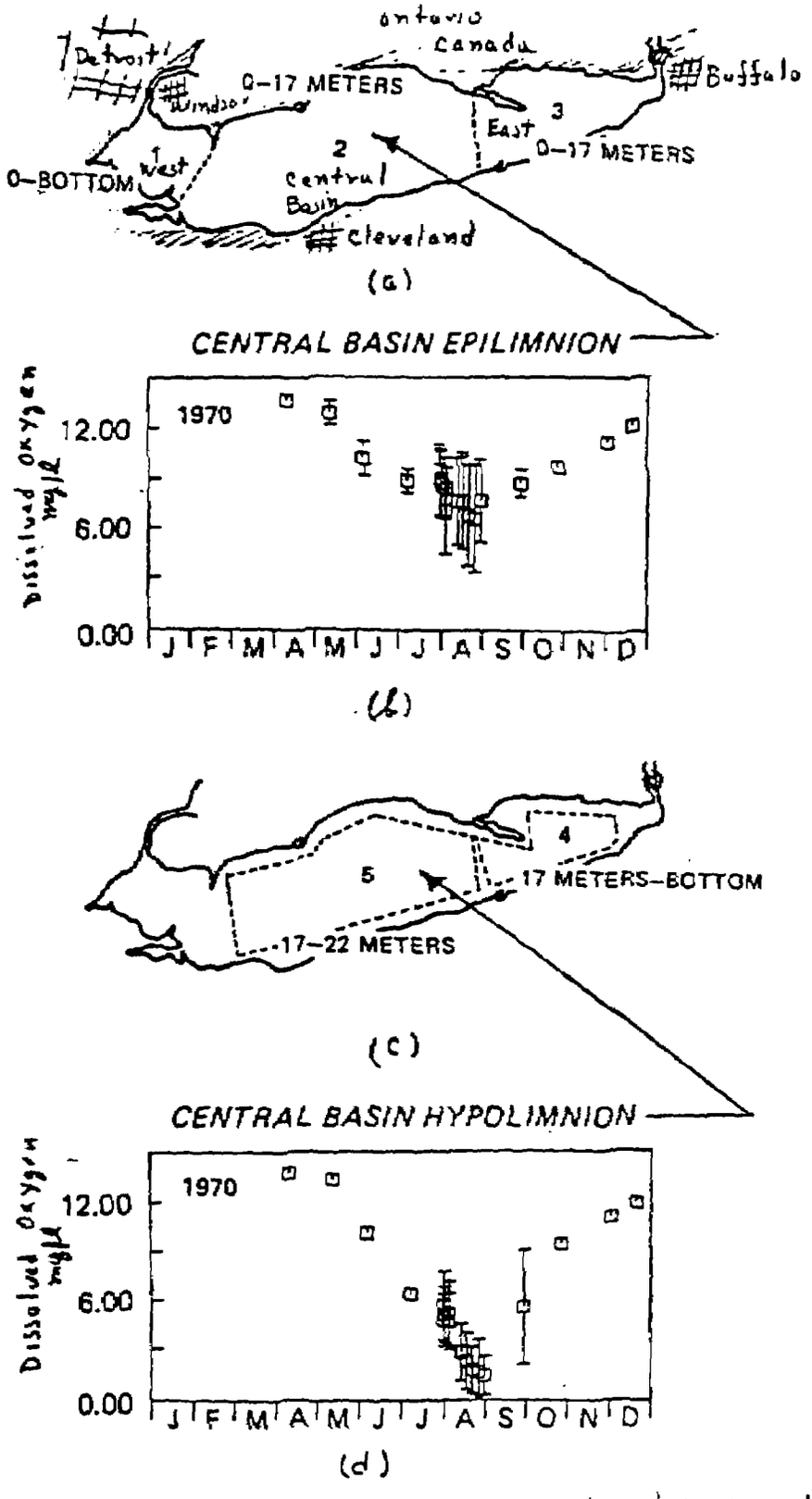

Fig. 8-16 Dissolved oxygen of Lake Erie (a) Location of epilimnion regions, (b) DO of central Basin epilimnion (c) Location of hypolimnion regions, (d) DO of central Basin hypolimnion (After DiToro, Connolly, 1980)

The connection between the phytoplankton equations given above and the P and R in the equation is of particular importance when the DO response due to changes in phytoplankton population must be computed.

It can be recognized from the preceding development that the quantity $G_p P$ is the µg chlorophyll produced/ℓ - day. Now every µg chlorophyll that is produced represents production of phytoplankton carbon to a ratio of about 50-100 µg carbon produced per µg chlorophyll. The stoichiometric oxygen equivalent of this carbon (see Chapter 6) is approximately 2.67 µg oxygen. Therefore, if a_{cp} is the carbon chlorophyll ratio,

$$a_{op} = 2.67\, a_{cp} \tag{8-44}$$

where a_{op} is the µgDO/µg chlorophyll produced. For a_{cp} of 50-100 µg C/µg Chlor, a_{op} is 133-266 µg DO/µg chlor. The average production of oxygen over a day and over depth is then given by

$$p'_{av} = a_{op}\, G_p\, P \tag{8-45}$$

which can be used as the source term for the DO balance where p'_{av} (mg^{O}/ℓ-day) is the average production.

Following the preceding development for the gross growth rate, G_p (Eq. 8-29):

$$p'_{av} = a_{op}\, [G_{max}(1.066)^{T-20}\, G(I)G(N)]P \tag{8-46}$$

The maximum oxygen production at saturated light interacting and excess nutrients is given by:

$$p'_s = a_{op} G_{max}(1.066)^{T-20} \tag{8-47}$$

If now G_{max} 1.88/day, T=20°C and a_{op}=.133 mg O_2/µg Chlor, then

$$p'_s = 0.25\ P \tag{8-48}$$

which is the same as the simple relationships given in Chapter 6 under photosynthesis (see Eq.). Eq. 8-46 is, however, the preferred equation for calculating the average DO photosynthetic production for use in DO balance equations. If G(N) ≈ 1, then the equation reduces to Eq. ( ) where the DO production was influenced by light only. Eq. 8-48 is used in the absence of any other data.

The uptake of oxygen due to the endogeneous respiration of the phytoplankton also follows the preceding development. Thus,

$$R'_{av} = a_{op}\, D_p P \tag{8-49}$$

where it can be recalled that $D_p P$ is the rate of endogenous respiration of the phytoplankton [μg Chlor/ℓ - day]. If $D_p \simeq 0.1$/day and $a_{op} \simeq .25$ mg O_2/μg Chlor, then

$$R'_{av} = .025\ P \tag{8-50}$$

which is the same as Eq. (6-). Note, however, that Eq. 8-49 is the operative equation and for a range of a_{op} and D_p that R'_{av} as a function of chlorophyll may vary considerably from the simple relationships of Eq. (8-50).

The net production of oxygen is then given by Eqs. 8-46 and 8-49 as

$$p'_{net} = p'_{av} - R'_{av}$$

Eutrophication Control Techniques

The control of the eutrophication of various water bodies can take a variety of forms. Perhaps such forms can best be seen by once again reviewing the mass balance equations for phytoplankton chlorophyll and a single nutrient, such as phosphorus. Thus, for a completely mixed system, Eq. (8-19) can be repeated here for the phytoplankton

$$V\frac{dP}{dt} = V(G_p - D_p)\ P - Av_s\ P + Q_{in}P_{in} - QP \tag{8-51}$$

and Eq. 8-41 with inputs and flow can be used for the nutrient, i.e.

$$V\frac{dp}{dt} = W + Q_{in}p_{in} + W_s - (G_p - D_p)P - v_{s1}A_p - Q_p \tag{8-52}$$

where p is a representative of the controlling nutrient and W_s is the nutrient input from the sediment. The engineering control techniques essentially aim at changing the components of these equations in the direction of decreasing plant biomass. As with engineering controls for the dissolved oxygen problem, principal interest first centers on control of the inputs, in this case, the nutrient inputs. It can be recalled, however, that there are really three principal control areas:

1) control of inputs
2) alteration of system kinetics
3) in-stream treatment and flow control

For the eutrophication problem then, the engineering techniques include:

1) Reduction of nutrient input (W)
2) Changing of internal cycling of nutrients (G_p and D_p)
3) Acceleration of nutrient transport through system (QP and Q_p)
4) Direct biological and chemical control of plants (dp/dt)

Each of these control techniques have relative advantages and disadvantages when applied to a specific problem context. The principal considerations of each will now be reviewed in turn.

Reduction of Nutrient Input

There are five means of reducing the direct input of nutrients:

1) Wastewater treatment of municipal and industrial point sources and CSO, including phosphorus removal by chemical treatment and nitrogen removal by chemical and biological treatment

2) Alteration of non-point nutrient inputs through land conservation practices and changes in agricultural use of nutrients. These practices would include reduction of erosion, testing of soil before fertilizer application, reduction in winter fertilizing, and use of buffer strips.

3) Diversion of nutrient input to a different water body where impact is less

4) Treatment and control of nutrient at inflow point including treatment of entire river inflow and building of detention basins or storage reservoirs.

5) Modification of preduct usage to reduce generation of nutrient at source (e.g. non-phosphate detergents.)

Changing of Internal Cycling of Nutrients

The control options under this approach include:

1) Dredging of nutrient rich sediments
2) Hypolimnetic aeration
3) Chemical precipitation of nutrients
4) Sealing of sediments to reduce nutrient exchange
5) Lake or reservoir drawdown

Acceleration of Nutrient Outflow

Techniques under this approach include:

1) Selective discharge from water body such as lakes
2) Increased flow through water body.

Direct Biological and Chemical Control

Direct impact on the plant biomass itself can be achieved by:

1) Harvesting of plants
2) Use of aquatic herbicides, e.g. copper sulfate
3) Use of organisms (e.g. grossy carp) that graze on nuisance aquatic plants

REFERENCES

Chapra, S.C. and S.J. Tarapchak, 1976. A chlorophyll a model and its relationship to phosphorus loading plots for lakes. Water Res. Res., Vol. 12, No. 6, pp. 1260-1264.

Dillon, P.J. and F.H. Rigler, 1974. The phosphorus-chlorophyll relationship in lakes. Limnol. Oceanogr., 19(4), pp. 767-773.

Dillon, P.J. and F.H. Rigler, 1975. A simple method for predicting the capacity of a lake for development based on lake trophic status. J. Fish. Res. Bd. Can., 31(9), pp. 1519-1531.

Rast, W. and G.F. Lee, 1978. Summary Analysis of the North American (US Portion) OECD Eutrophication Project: Nutrient Loading-Lake Response Relationships and Trophic State Indices. US EPA, EPA-600/3-78-008. Corvallis Environmental Research Laboratory, Corvallis, Oregon, 454 pp.

Thomann, R.V., 1977. Comparison of lake phytoplankton models and loading plots. Limnol. & Ocean., Vol. 22, No. 2, pp. 370-373.

Uttormark, P.D. and J.P. Wall, 1975. Lake classification - a trophic characterization of Wisconsin lakes. U.S. Environmental Protection Agency, Corvallis Environmental Research Laboratory. Report No. EPA-660/3-75-033. 165 pp.

Uttormark, P.D. and M.L. Hutchins, 1978. Input/output models as decision criteria for lake restoration. Tech. Rpt. WIS, WRC, 78-03, Water Res. Center, Univ. of Wisc., Madison, Wisc. 62 pp.

Vollenweider, R.A., 1968. Scientific fundamentals of the eutrophication of lakes and flowing waters, with particular reference to nitrogen and phosphorus as factors in eutrophication. Organ. Econ. Coop. Dev., Paris. Technical Report No. DAS/CSI/68.27. 159 pp.

Vollenweider, R.A. and P.J. Dillon, 1974. The application of phosphorus loading concept to eutrophication research. Tech. Rep. 13690, 42 pp. Nat. Res. Counc. of Can., Ottawa, Ont.

Vollenweider, R.A., 1975. Input-output models with special reference to the phosphorus loading concept in limnology. Schweiz. Z. Hydrol. 37:53-83.

Vollenweider, R.A., 1976. Advances in defining critical loading levels for phosphorus in lake eutrophication. Mem. Ist. Ital. Idrobiol. 33:53-83.

Hydroscience, 1977b National assessment of water quality. Prepared for National Commission on Water Quality. Washington, D.C.

Bartsch, A.F. and J.H. Gakstatter, 1978. Management decisions for lake systems on a survey of trophic status, limiting nutrients, and nutrient landings in American-Soviet Symposium on Use of Mathematical Models to Optimize Water Quality Management, 1975, EPA-600/9-78-024, ERL, ORD, USEPA Gulf Breeze, Florida 32561, pp. 372-394.

Eisenreich, S.J. et al., 1977. Atmospheric loading of phosphorus and other chemicals to Lake Michigan. J.Grt. Lakes Research, Inter. Assoc. Great Lakes Research, Vol. 3, No. 3-4, pp. 291-304.

Gakstatter, J.H. et al., 1978. A survey of phosphorus and nitrogen levels in treated municipal wastewater. JWPCF, Vol. 50, pp. 718-722.

Hydroscience, Inc., 1977 a. The effects of forest management on the water quality and aquatic biota of Apalachicola Bay, Florida. Prepared for the Buckeye Cellulose Corp., Perry, Florida, 6 Chap. + 4 Append.

International Joint Commission, 1978. Environmental management strategy for the Great Lakes system. Final Report of Int. Ref. Group on Great Lakes Pollution from Land Use Activities; Windsor, Ontario. 115 pp.

Thomann, R.V., 1972. Systems Analysis and Water Quality Manageme, McGraw-Hill Book Co., N.Y., N.Y. 286 pp.

Omernik, J.M., 1977. Non-point source-stream nutrient level relationships: a nationwide study. EPA-600/3-77-105, Corvallis ERL, ORD, USEPA, Corvallis, Oregon. 151 pp. + plates.

Steele, J.H. 1965. Notes on some theoretical problems in production ecology in primary production in aquatic environments, C.R. Goldman, Ed., Mem. Inst. Hydrobiology, University of California Press, Berkeley, California, p. 383-98.

Ryther, J.H., 1956. Photosynthesis in the ocean as a function of light intensity. Limnology and Oceanography, No. 1, pp. 61-70.

Welch, E.B. and M.A. Perkins, 1979. Oxygen deficit-phosphorus loading relation in lakes. Jour. WPCF. Vol. 51, No. 12, pp 2823-2828.

DiToro, D.M. et al., 1977. Estuarine phytoplankton biomass models-verification analyses and preliminary applications. In The Sea: Ideas and Observations on Progress in the Study of the Seas. Ed. E.D. Goldberg, J. Wiley and Sons, N.Y., N.Y., pp. 969-1020.

DiToro, D.M., D.J. O'Connor and R.V. Thomann, 1971. A dynamic model of the phytoplankton population in the Sacramento-San Juaquin Delta. Advances in Chemistry, No. 106. American Chemical Society, pp. 131-180.

Eppley, R.W. 1972. Temperature and phytoplankton growth in the sea. Fishery Bulletin. Vol. 70, No. 4, pp. 1063-1085.

Thomann, R.V., R.P. Winfield and D.M. DiToro, 1974. Modeling of phytoplankton in Lake Ontario (IFYGL) Inter. Assoc. Great Lakes Research, Proceedings 17th Conference, pp. 135-149.

Fillos, J. and W.R. Swanson, 1975. The release rate of nutrients from river and lake sediments. Jour. WPCR, Vol. 47, No. 5, pp. 1032-1042.

DiToro, D.M. and J.P. Connolly, 1980. Mathematical models of water quality in large lakes. Part 2: Lake Erie. In Press, U.S. EPA, Duluth, Minn., Grosse Ile Lab., Grosse Ile, Michigan.

Bannerman, et al., 1975. Phosphorus uptake and release by Lake Ontario sediments. EPA-660/3-75-006, NERC, ORD, U.S.EPA, Corvallis, Oregon, 51 pp.

Freedman, P.L. and R.P. Canale, 1977. Nutrient release from anaerobic sediments. Jour. Env. Eng. Div., ASCE, Vol. 103, No. EE2, pp. 233-244.

Martens, C.S. et al., 1980. Sediment-water chemical exchange in the coastal zone traced by in situ Random-222 flux measurements. Science, Vol. 208, pp. 285-288.

Hartwig, E.O. 1975. The impact of nitrogen and phosphorus release from a siliceous sediment on the overlying water. Third Int. Estuarine Conf., Galveston, Texas. Paper No. COO-3279-20, 33 p.

Rast, W. and G.F. L-e. 1977. Report on nutrient load-eutrophication response of Lake Wingia, Wisconsin. In North American project - a study of U.S. water bodies, L. Seyb and K. Randolph, U.S. EPA Env. Res. Lab., Corvallis, Oregon, pp. 337-372.

DiToro, D.M. and J.P. Connolly. 1980. Mathematical models of water quality in large lakes, Part 2: Lake Erie. EPA-600/3-80-065, ERL, ORD, U.S. EPA, Duluth, Minn. 231 pp.

DiToro, D.M. and W.F. Matystik, Jr. 1980. Mathematical models of water quality in large lakes, Part 1: Lake Huron and Saginaw Bay. EPA-600/3-80-056, ERL, ORD, U.S. EPA, Duluth, Minn., 166 p.

Burns, N.M. and F. Rosa, 1980. In situ measurement of the settling velocity of organic carbon particles and 10 species of phytoplankton. Limnology & Oceanography 25(5):855-864.

Rast, W. and G. Fred Lee, 1978. Summary analysis of the North American (U.S. portion) OECD eutrophication project: nutrient loading-lake response relationships and trophic state indices. U.S. EPA, EPA-600/3-78-008, ORD, Corvallis, Oregon, 455 pp.

Bachmann, R.W. and D.E. Canfield, Jr. 1979. Role of sedimentation in the phosphorus budget of natural and artificial Iowa lakes. Project A-063-IA, Iowa State University, Ames, Iowa, 95 pp.

Higgins, J.M. and B.R. Kim, 1981. Phosphorus retention models for Tennessee Valley Authority reservoirs. Water Res. Res.17(3): 571-576.

Water Research Vol. 14 pp 1651 to 1665
© Pergamon Press Ltd 1980 Printed in Great Britain

0043-1354/80/1101-1651$02.00/0

A Steady State Eutrophication Model for Lakes

JERALD L. SCHNOOR[1] and DONALD J. O'CONNOR[2]

[1]Civil and Environmental Engineering, The University of Iowa, Iowa City, IA 52242 and
[2]Environmental Engineering and Science, Manhattan College, Bronx, NY 10471, U.S.A.

(*Received May* 1980)

INTRODUCTION

The nutrient loading models of Vollenweider (1968, 1969) and Dillon & Rigler (1974) have been used with success to assess the trophic state of lakes. However, these models do not quantitatively relate nutrient concentrations to phytoplankton concentrations, a primary concern in water quality management. More extensive nutrient-phytoplankton models have been developed which are time and space variable, but also considerably more expensive to utilize (O'Connor, 1973; Thomann *et al.*, 1975; Di Toro & Connolly, 1979).

In this paper, an alternate approach to eutrophication modeling is developed via simplifying assumptions of the kinetic and transport equations. Both steady state and non-steady state cases are investigated for a short detention time reservoir in Central Texas, Lake Lyndon B. Johnson (LBJ) and a long detention time Great Lake, Lake Ontario. The steady state solution to 81 of the phosphorus limited lakes of the U.S. National Eutrophication Survey (NES) is also discussed. The steady state approach is useful as a management tool when detailed analyses are not feasible.

MODEL DEVELOPMENT

A schematic of phytoplankton kinetics is presented in Fig. 1. Inorganic nutrient is input by natural and man-made sources, W_1, and is formed by mineralization of organic nitrogen, K_o. It is diminished by washout, $1/\tau$, and by phytoplankton uptake, K_g, via Lotka-Volterra (1956) kinetics. The phytoplankton undergo washout and losses to form organic nutrient via K_1. Phytoplankton also sink out of the water column at a rate, K_s. Organic nutrient is present due to natural and man-made sources, W_2, as well as from phytoplankton decay. Particulate organic nutrient undergoes sedimentation, K_s, and total organic nutrient mineralizes with rate constant K_o. If inorganic nutrient is returned from the sediment, that input must be externally supplied by W_1.

Only one nutrient is considered limiting to growth, but it is straightforward to consider others as well. Zooplankton grazing is assumed to be included in the phytoplankton loss rate, K_1, which converts viable phytoplankton to organic nutrient.

A significant simplification is affected when the system is considered to be composed of two or more compartments (e.g. the epilimnion and the hypolimnion or the euphotic and non-euphotic zones) each of which is assumed to be completely mixed. In essence, the completely mixed model represents a spatially averaged concentration within each compartment. Completely mixed compartments are interrelated via bulk dispersion or an exchange coefficient as by Imboden (1974).

A further simplification is facilitated if the entire impoundment can be considered as a completely mixed system or if only the epilimnion is simulated with internal inputs from the hypolimnion. Impoundments of short detention time (large densimetric Froude number) can often be considered as completely mixed. Again the simplification represents a spatial averaging with depth, and the following equations result.

$$\frac{dN_I}{dt} = K_o N_o - K_g N_I P - \frac{N_I}{\tau} + \frac{W_I}{D} \tag{1}$$

$$\frac{dP}{dt} = K_g N_I P - K_1 P - \frac{P}{\tau} - K_s P \tag{2}$$

$$\frac{dN_o}{dt} = K_1 P - K_o N_o - K_s N_o - \frac{N_o}{\tau} + \frac{W_2}{V} \tag{3}$$

where

N_I = inorganic nutrient concentration, ML^{-3}
P = phytoplankton nutrient concentration, ML^{-3}
N_o = organic nutrient concentration, ML^{-3}
τ = mean hydraulic detention time, T
W_1 = input rate of inorganic nutrient, MT^{-1}
W_2 = input rate or organic nutrient, MT^{-1}
V = impoundment volume, L^3.

The addition of equations (1)–(3) yields:

$$\frac{dN_T}{dt} = -\frac{N_T}{\tau} - K_s N_o + \frac{W_T(t)}{V} - K_s P \tag{4}$$

where

$$N_T = N_I + P + N_o$$

$$\frac{dN_T}{dt} = \frac{dN_I}{dt} + \frac{dP}{dt} + \frac{dN_o}{dt}$$

$$W_T = W_1 + W_2$$

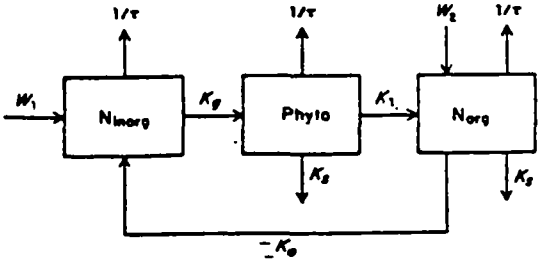

Fig. 1. Kinetics and transport of nutrient–phytoplankton system.

Note that the build up of total nutrient concentration in an impoundment is determined by only three factors: the addition of nutrients W_T/V, the washout of nutrients N_T/τ, and the net loss of nutrient to the sediment $K_s(N_0 + P)$. It is the kinetic coefficients which determine the partitioning of the nutrient among inorganic, organic, or planktonic mass.

Assuming steady state for equations (1)–(3), the three nonlinear, ordinary differential equations become a set of algebraic equations that are easily solvable:

$$N_i = \frac{K_1 + (1/\tau) + K_s}{K_g} \tag{5}$$

$$P = \frac{\alpha(N_g - N_i) + (N_r K_0/K_1)}{\tau(\alpha K_g N_i - K_0)} \tag{6}$$

$$N_0 = \frac{P + (N_r/\tau K_1)}{\alpha} \tag{7}$$

where

$$\alpha = \frac{K_0 + K_s + (1/\tau)}{K_1}$$

$N_r = \frac{W_2\tau}{V}$ = average inflow organic nutrient concentration

$N_g = \frac{W_1\tau}{V}$ = average inflow inorganic nutrient concentration

The resulting equations comprise an analytical model that is easily applied to impoundment situations. It is not developed empirically, and thus it is applicable to impoundments of varying geomorphology and locality. The principal disadvantage of the model is the need to estimate the various rate constants required.

It is interesting to note that equations (5)–(7) are consistent with the Dillon & Rigler (1974) model. Summing the equations and assuming steady state, one arrives at equation (8) after rearranging.

$$\frac{W_T\tau}{A}\left[1 - \frac{fK_s N_T AH}{W_T}\right] = HN_T \tag{8}$$

where

$W_T = W_1 + W_2$, the total nutrient input, MT^{-1}.
A = surface area, L^2.
$f = (N_0 + P)/N_T$, fraction of phytoplankton plus organic nutrient to total nutrient.
$N_T = P + N_0 + N_i$, total nutrient concentration, ML^{-3}.
H = mean depth, L.

Upon inspection, the term $fK_s N_T AH/W_T$ is the fraction of phosphorus retained in the sediment, R. Therefore, equation (8) is an analytical development of the Dillon and Rigler plot, $\log W_T\tau(1 - R)/A$ vs $\log H$. The model equations (1)–(3), from which equation (8) is derived, have the added advantage that they explicitly involve the phytoplankton as well as nutrient concentration.

ESTIMATION OF COEFFICIENTS

Field data such as those gathered in the U.S. National Eutrophication Survey may be used to establish average annual or seasonal concentrations of nutrients in lakes. For the instances where reasonable measurements of N_i, P, and N_0 are available, it is possible to estimate the kinetic coefficients. Equations (1)–(3) contain three state variables (N_i, P, N_0) and four coefficients (K_g, K_1, K_s, K_0), or three equations with four unknowns. Assuming that K_g can be calculated from productivity measurements or estimated from similar prototype systems, equations (1)–(3) were solved for K_1, K_s, K_0.

$$K_1 = K_g N_i - \frac{1}{\tau} - K_s \tag{9}$$

$$K_s = \left(\frac{W_T}{V} - \frac{N_T}{\tau}\right)\left(\frac{1}{N_0 + P}\right) \tag{10}$$

$$K_0 = \frac{1}{N_0}\left(K_g N_i P + \frac{N_i}{\tau} - \frac{W_i}{V}\right) \tag{11}$$

Equation (9) states that under steady state conditions, the gross growth rate minus the washout and sinking rate is equal to the total loss rate of phytoplankton, K_1. Equation (10) shows that the mass rate of sedimentation, $K_s(N_0 + P)$, is equal to the mass rate of total nutrient input minus outflow. The mass rate of nutrient recycled, $K_0 N_0$, increases with primary production ($K_g N_i P$) and decreases with the inorganic input minus the outflow of inorganic nutrient according to equation (11).

In addition to "back-calculating" the rate constants, it is possible to determine a range for these constants from field and laboratory studies. The autocatalytic growth rate constant, K_g, can be calculated from light and dark bottle C-14 primary production measurements. Primary production is equal to $K_g \times N_i \times P$ multiplied times a conversion factor for carbon to phosphorus ($\sim 40\,g\,C\,g^{-1}P$) and divided by the photoperiod in hours. For Lake LBJ, the predicted productivity was $3.0\,mg\,C\,m^{-3}$ which compared favorably with depth-integrated primary production field data of Davenport (1975).

CALIBRATION OF MODEL FOR LAKE LBJ, 1972

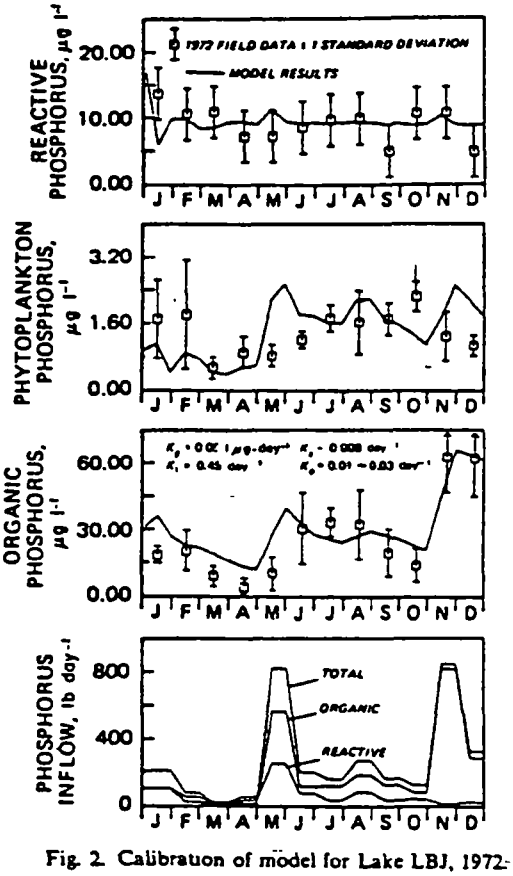

Fig. 2. Calibration of model for Lake LBJ, 1972.

The death rate constant, K_1, is actually the sum of the endogenous decay and predation rates on phytoplankton. Endogenous decay rates of phytoplankton in the dark were reported as 0.05–0.20 per day by Riley *et al.* (1949) and as high as 0.25 per day for *Chlorella* at 35°C by Sorokin (1959). Total loss rates of phytoplankton were measured in Castle Lake by Jassby & Goldman (1974) to be 0.2–0.8 per day, but this figure includes sinking rates.

Literature values for sinking rates, v_p, of freshwater phytoplankton by Smayda (1974) ranged from 0.26 to 0.76 m day^{-1}, while Titham & Kilham (1976) reported 0.08–1.87 m day^{-1}. Organic matter in the ocean sinks at 0.18–13 m day^{-1} according to McCave (1975). Organic and phytoplankton sinking velocities must be divided by the mean depth of the water body to yield the sedimentation coefficient, K_p. It should be noted that the organic sinking rate coefficient, K_p, is truly an "effective" or "apparent" sinking rate since only the particulate fraction would sink of the total (dissolved + particulate) organic nutrient present. Effective sinking rates or loss rates for total phosphorus in lakes have been reported by Chapra (1975) and others and average 0.1 m day^{-1} with a range of 0–0.4 m day^{-1}.

Perhaps the least is known about the hydrolysis or mineralization rate constant, K_0. Verhoff & Heffner (1979) measured K_0 to be less than 0.004 per day for three U.S. river waters, while calculations of data by Richey *et al.* (1978) indicate a range of 0.0005–0.11 per day for carbon in four freshwater lakes. The mathematical models of Thomann (personal correspondence, 1979) and Di Toro & Connolly (1979) are currently utilizing a K_0 for phosphorus of approx. 0.03 per day at 20°C in the Great Lakes.

RESULTS AND DISCUSSION

Lake Lyndon B. Johnson

Lake Lyndon B. Johnson (LBJ) is the third of a series of seven impoundments in the Highland Lakes chain of Central Texas. It is a mainstream impoundment of the Colorado River containing a volume of 1.71×10^8 m^3 and a mean depth of 6.7 m. With an annual average hydraulic detention time of approx. 80 days, it receives no significant wastewater loads but is classified as eutrophic according to most classification criteria. Summertime anaerobic conditions do occur in the hypolimnion of Lake LBJ (Schnoor & Fruh, 1979).

Equations (1)–(3) were utilized to simulate Lake LBJ for 1972 and 1973. The euphotic zone of Lake LBJ occupies greater than 50% of the total volume, and the model assumption of complete mixing is quite reasonable over much of the year. The sinking rate of phytoplankton was assumed to be negligible relative to the death rate. Results for the 1972 calibration of the model are given in Fig. 2. Molybdate reactive phosphorus (inorganic) and organic phosphorus field measurements are plotted as vertically averaged concentrations. Phytoplankton phosphorus was calculated from 1972 specie counts and biovolumes per specie determined by Davenport (1975) during 1973–1974. Phosphorus content of the cell was assumed to be 1% by dry weight and dry weight was assumed as 25% of wet weight as per Stumm & Morgan (1970) and Parsons & Takahashi (1973). Error bars plotted on the data points in Fig. 2 refer to ±1 SD due to spatial variations in measurement.

An interesting feature of the calibration in Fig. 2 is that three of the four model coefficients were held constant while only the hydrolysis (mineralization) rate was allowed to vary in a sinusoidal pattern with temperature. Better fits to the data could have been achieved with time variable coefficients, but the goal of this modeling effort was to simplify to as great a degree as possible. As it is, the general agreement between model results and measured data shown in Fig. 2 demonstrates that a simple model can begin to approximate complex lake dynamics.

A verification of the model was performed by holding all coefficients constant for another simulation, 1973, an independent data set. Results are presented in Fig. 3. The data of 1973 is a particularly stringent test for the model since hydraulic and nutrient inflows were considerably different than in 1972, especially following a 100 yr recurrence-interval storm which occurred in October, 1973. Again, the model results compare favorably to the measured data through September, but during October the growth rate was nearly extinguished by the effect of a tremendous amount of debris which carried into the lake: the secchi disc depth was approx. 2 in., and much of the surface was covered with floatables. It was necessary to decrease K_s to a fraction of its original value during and after the storm, 0.006 l μg^{-1}-day. Still organic P does not match the measured data very well during the last 3 months (Fig. 3). Probably the inflow of organic phosphorus to the lake was grossly underesti-

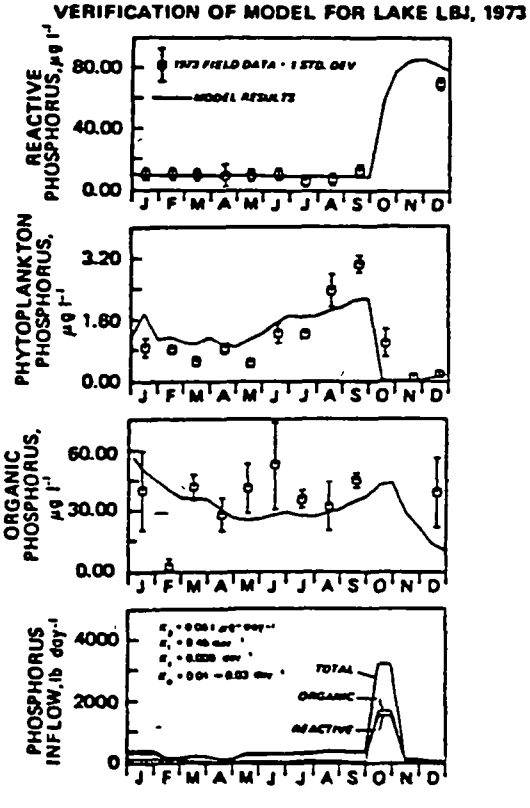

Fig. 3. Verification of model for Lake LBJ, 1973.

mated, since sampling was too infrequent to accurately gauge the amount of nutrient inflow during the storm. Secondly, internal scour of organic phosphorus from the sediment was not measured.

It is interesting to note that the predicted phytoplankton concentration approaches zero during the 1973 storm, day 300. A neighborhood stability analysis was performed on equations (1)–(3). It yields the required conditions necessary to keep the model numerically stable. The washout condition, $1/\tau < (N_q K_p - K_1)$, was violated in the model during the storm event which resulted in a near-zero phytoplankton standing crop. The measured phytoplankton standing crop also became near-zero, but nature has nonlinear mechanisms for keeping systems stable that are not always included in models (e.g. sheltering, migration, dispersal, predator–prey switching etc.).

Some advantages of this simplified eutrophication model for Lake LBJ as compared to the nutrient loading models of Vollenweider (1969) and Dillon & Rigler (1974) include: the capability of separating the effects of organic nutrient inputs from inorganic inputs (bioavailability), the calculation of nonsteady state blooms and periodicities, the direct determination of phytoplankton standing crop, and a better understanding of the nutrient flux rates via phyto growth and death, organic nutrient hydrolysis and sedimentation.

Equations (5)–(7) are the steady state approximations of equations (1)–(3). They may be thought of as time averages through the year. For Lake LBJ in 1972, the solution of equations (5)–(7) yields the yearly average phosphorus concentrations:

$$\text{inorganic P} = 9.22\ \mu g\, l^{-1}$$

$$\text{phytoplankton P} = 1.47\ \mu g\, l^{-1}$$

$$\text{organic P} = 27.7\ \mu g\, l^{-1}$$

As can be seen from Fig. 2, these values do indeed approximate time-averages of the dynamic solution.

The calculated steady state 1973 Lake LBJ concentrations (excluding the heavy storm period of October to December) are:

$$\text{inorganic P} = 9.23\ \mu g\, l^{-1}$$

$$\text{phytoplankton P} = 1.37\ \mu g\, l^{-1}$$

$$\text{organic P} = 29.8\ \mu g\, l^{-1}$$

Summer and winter steady-state averages were also approximated for Lake LBJ in 1972 and 1973. Since the original time variable model (equations 1–3) is nonlinear, the steady state solution utilizing time-averaged coefficients will not precisely equal the time average of the dynamic solution, but it does provide a reasonable approximation.

Lake Ontario

Equations (1)–(3) were also applied to Lake Ontario, a Laurentian Great Lake with a detention time of approximately eight years. In this case, both diatom and non-diatom populations were simulated since two distinct peaks in abundance have been noted, Glooschenko *et al.* (1974). Only the epilimnion (the top 17 m) was simulated because below that depth, the hypolimnion lacks a viable phytoplankton population. Nutrient flux from the hypolimnion to the epilimnion was externally specified as input data.

The results of the Lake Ontario simulation are given in Fig. 4. Data are from 1967 to 1973 monitoring cruises by the Canada Centre for Inland Waters. Chlorophyll *a* rather than phytoplankton biovolumes were measured on the cruises, so a conversion factor for phytoplankton phosphorus to chlorophyll of 1:1 was assumed. [A check was made with biovolumes from Munawar & Nauwerck (1971) which supported the assumption.]

Note the agreement between observed data and computed results. The time-averaged coefficients used in the simulation were: $\bar{K}_1 = 0.034\ \text{day}^{-1}$, $K_s = 0.0059\ \text{day}^{-1}$, $K_g = 0.00351\ \mu g^{-1}\text{-day}^{-1}$ and $\bar{K}_0 = 0.02\ \text{day}^{-1}$. The hydrolysis rate constant, K_0, was input as a sinusoidal function which approximately tracked temperature periodicity (see Fig. 5). Phosphorus inflows of 35,000 kg day^{-1} were taken

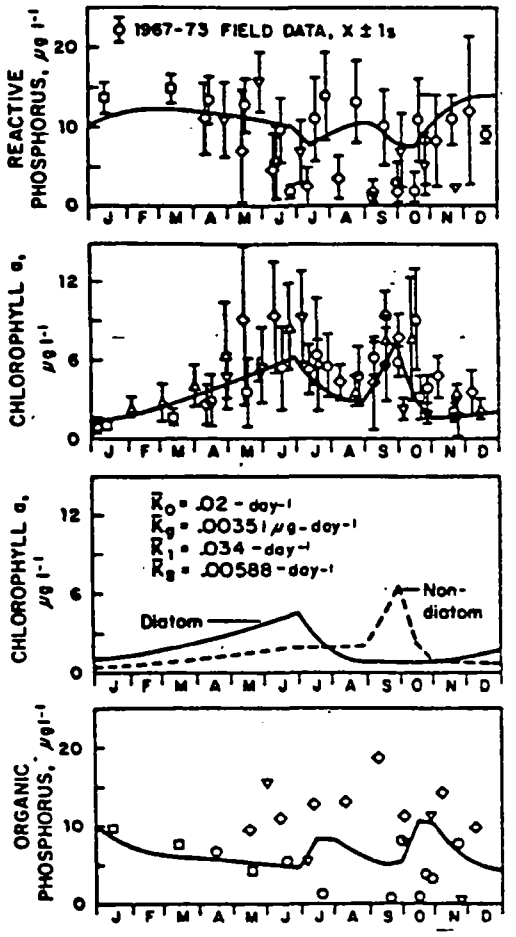

Fig. 4. Lake Ontario simulation with two phytoplankton taxa.

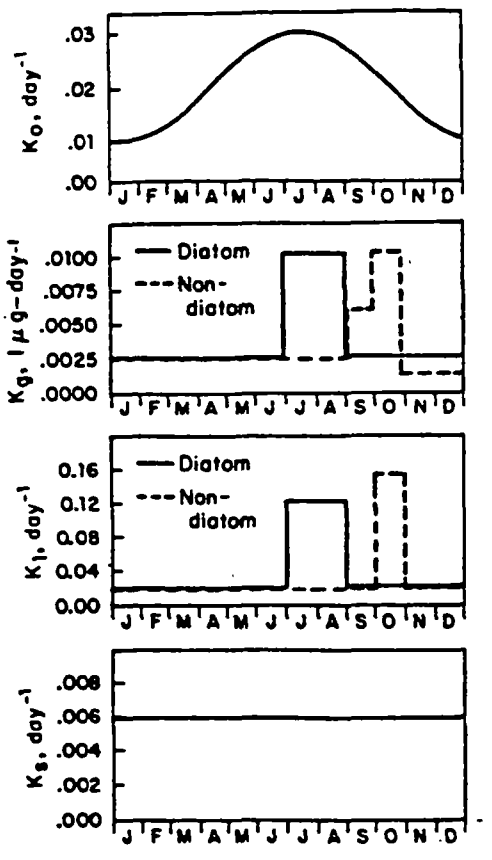

Fig. 5. Rate constants used in the Lake Ontario simulation.

from Thomann *et al.* (1975) including an internal nutrient flux of 105,000 kg day^{-1} from the hypolimnion to the epilimnion during the unstable months of September and October and a smaller flux of 35,000 kg day^{-1} during January through May. The September–October flux helps to support the second peak in phytoplankton chlorophyll, and is transported from the hypolimnion through the thermocline by turbulent diffusion. A two layer model, including the hypolimnion as well as the epilimnion, would have allowed calculation of this flux rather than accounting for it as a specified input. It should be added that the double phytoplankton peak consistently appears in chlorophyll measurements of Lake Ontario, but the community biovolume measurements of Munawar & Nauwerck (1971) did not indicate the first peak and die-off.

Peak diatom concentrations occurred on or about July 1 and declined due to an increasing death rate. The decrease in net production by diatoms may have been exacerbated by silica limitation at that time of year. The peak non-diatom population (blue-green algae, green algae, and phytoflagellates) occurred on October 1 and declined similarly. Inorganic phosphorus concentrations predicted by the model did not decline as low in the summertime as has been observed in field data, possibly due to an erroneously high hydrolysis rate constant or due to excessive phosphorus inputs specified from the hypolimnion. Organic phosphorus field data was sparse and difficult to use to draw conclusions. The steady state solution using time-averaged coefficients, Equations (5)–(7), yielded annual mean concentrations of 9.8 μg P l^{-1} for reactive phosphorus, 3.6 μg l^{-1} chlorophyll *a*, and 5.7 μg l^{-1} organic phosphorus. This steady state model could prove very useful as a management tool for predicting improvements in water quality as a function of mandate effluent control.

National eutrophication survey lakes

Shown in Table 1 is the phosphorus nutrient data from the USEPA National Eutrophication Survey (1975) of northeastern and north-central United States Lakes. Only those lakes which were phosphorus limited for at least one sampling period are listed. Phosphorus limitation is taken to be an inorganic nitrogen to dissolved phosphorus ratio of greater than 14:1 and/or a phosphorus limitation in an algal assay performed in connection with NES. The column marked PHYTO P is estimated from the ratio of phytoplankton phosphorus (that phosphorus associated with phytoplankton) to measured chlorophyll *a* of 0.4 to 1.0. This ratio has not been widely discussed in the literature. However percentages of phosphorus to algal biomass (dry weight) are normally 0.5–3.0 according to Parsons & Takahashi (1973), while chlorophyll *a* to algal dry weight biomass range from 0.3 to 3.0% in Lakes Onondaga (Murphy & Welter, 1976), LBJ, Erie (Munawar & Munawar, 1976) and Ontario (Glooschenko *et al.*, 1974). Epply *et al.* (1977) found that phytoplankton carbon to chlorophyll ratios fall between 10–100. These ratios are quite variable, both from lake to lake and seasonally, but an average of 1.0 μg l^{-1} chlorophyll *a* per μg l^{-1} phytoplankton phosphorus is typical. Organic phosphorus (excluding phytoplankton phosphorus) in Table 1 is calculated as the total minus the dissolved and phytoplankton phosphorus. Dissolved phosphorus is the molybdate-reactive phosphorus which passes a 0.45 micron Millipore filter.

If the sedimentation coefficient, K_p and the nutrient loading determine the total phosphorus in a lake or reservoir, then it is the kinetic coefficients K_p, K_1, and K_0 which determine the nutrient partitioning. Figure 6 illustrates the phosphorus partitioning in the NES P-limited lakes. The shaded area of Fig. 6 shows the region where oligotrophic lakes fall. Oligotrophic lakes have a small percentage of organic phosphorus (0–20%), moderate percentages of phosphorus tied up in phytoplankton (18–40%), and large dissolved phosphorus fractions (55–80%). Other lakes are described according to their region on the partition diagram of Fig. 6.

Table I

Nutrient Data from National Eutrophication Survey

	LAKE	TROPHIC STATUS	STATE	τ_w, days	M_i DISS P µg/ℓ	TOT P µg/ℓ	Chl *a* µg/ℓ	EST. P PHYTO P µg/ℓ	EST. M_o ORG P µg/ℓ	V VOL m^3	W_T TOT P LOAD kg/yr	H MEAN DEPTH m
1	LAKE ZOAR	E	CONN	5	29	43	18.3	11.9	2.1	2.96×10^7	154,771	7.5
2	LILLINONAH	E	CONN	17	48	54	11.1	5.6	0.4	9.15×10^7	223,569	11.9
3	HOUSATONIC	E	CONN	0.6	29	39	8.2	8.2	1.8	3.86×10^6	118,236	2.9
4	LONG	M	MAINE	438	6	8	3.2	1.6	0.4	2.05×10^8	2,757	10.4
5	MATTAWAMKEAG	M	MAINE	42	7	11	2.0	2.0	2.0	4.99×10^7	7,937	3.7
6	MOOSEHEAD	O	MAINE	1100	3	5	1.5	1.0	1.0	5×10^9	24,612	16.5
7	RANGELEY	O	MAINE	1020	5	7	2.4	1.6	0.4	3.47×10^8	2,168	14.3
8	SEBAGO	O	MAINE	1970	3	4	1.5	0.98	0.02	3.59×10^9	9,261	30.8
9	BAY OF NAPLES	O	MAINE	26	3	5	1.8	1.2	0.8	1.32×10^7	1,574	4.3
10	HAGER POND	HE	MASS	24	482	1525	198.5	198.5	845	1.5×10^5	13,098	1.5
11	HARRIS POND	E	MASS	6.2	23	52	12.9	12.9	16	8.64×10^5	3,859	2.4
12	LAKE ALLEGAN	E	MICH	7	61	135	20.3	20.3	54	2.18×10^7	201,510	3.4
13	BARTON	E	MICH	81	31	61	27.8	27.8	2.2	8.54×10^6	3,011	6.1
14	BELLEVILLE	E	MICH	25	60	122	28.3	28.3	34.0	3.14×10^7	80,925	6.1
15	CHARLEVOIX	O	MICH	1170	4	6	3.0	1.95	0.05	1.17×10^9	8,580	16.8
16	CHEMUNG	E	MICH	1530	13	32	13.0	13.0	6.0	1.06×10^7	272	8.5
17	FORD	E	MICH	15	63	111	15.0	15.0	33.0	1.87×10^7	68,685	4.4
18	JORDAN	E	MICH	304	138	171	20.5	20.5	13.0	1.27×10^7	1,991	7.3
19	MACATAWA	HE	MICH	77	68	159	25.6	25.6	65.0	2.66×10^7	45,705	3.7
20	ROSS RES.	E	MICH	2	20	35	10.4	10.4	5.0	1.79×10^6	20,249	1.5
21	THORNAPPLE	E	MICH	11	28	45	14.7	14.7	2.3	7.14×10^6	15,283	4.3
22	UNION	E	MICH	2	22	47	15.7	15.7	9.3	1.91×10^6	19,687	0.9
23	CRYSTAL	O	MICH	1200	7	9	2.9	1.89	0.11	1.23×10^7	204	4.2
24	HIGGINS	O	MICH	5690	4	6	1.0	0.65	1.35	5.79×10^8	1,029	14.9
25	HOUGHTON	E	MICH	475	8	16	9.2	6.0	2.0	1.87×10^8	4,816	2.3

26	THOMPSON	E	MICH	152	25	41	12.0	12.0	4.0	2.86×10^{6}	431	2.7
27	ZUMBRO	E	MINN	18	330	401	12.5	12.5	59.0	5.09×10^{8}	205,673	5.5
28	ST. CROIX	E	MINN	23	36	55	10.2	10.2	9.0	2.92×10^{8}	295,347	8.8
29	FOREST	E	MINN	2080	10	21	10.5	6.83	4.18	3.10×10^{7}	1,016	3.4
30	GREEN	M	MINN	1350	9	15	4.9	4.9	1.1	1.4×10^{8}	2,036	6.4
31	ANDROSIA	E	MINN	47	10	25	13.0	13.0	2.0	4.83×10^{7}	24,549	7.9
32	BADGER	E	MINN	108	13	22	2.1	2.1	7.0	1.72×10^{6}	907	1.2
33	BARTLETT	E	MINN	694	28	136	49.5	49.5	58.0	3.20×10^{6}	458	2.6
34	BLACKHOFF	E	MINN	257	24	43	12.8	12.8	6.0	3.26×10^{6}	902	4.4
35	CASS	E	MINN	313	9	20	8.7	8.7	3.0	4.8×10^{8}	22,227	7.6
36	EMBARRASS	E	MINN	22	13	25	4.9	4.9	7.0	5.33×10^{6}	3,501	2.6
37	LEECH	M	MINN	1900	9	15	6.2	4.0	2.0	2.13×10^{9}	17,964	4.7
38	MADISON	E	MINN	1200	20	50	30.8	20.0	10.0	1.8×10^{7}	1,601	4.0
39	MALMEDAL	E	MINN	475	30	125	41.0	41.0	54.0	1.42×10^{6}	218	1.8
40	MINNETONKA	E	MINN	5480	18	47	16.6	16.6	13.0	4.04×10^{8}	---	6.9
41	MINNEWASKA	E	MINN	4640	17	35	7.6	7.6	10.4	1.73×10^{8}	4,236	6.0
42	PELICAN	M	MINN	1200	11	32	11.4	11.4	9.6	1.06×10^{8}	2,517	2.4
43	SUPERIOR	E	MINN	8	44	79	6.2	6.2	29.0	5.58×10^{7}	353,052	3.8
44	SWAN	M	MINN	876	9	13	3.8	2.5	1.5	1.28×10^{8}	4,975	12.1
45	POWDERMILL POND	E	N.H.	6.5	16	33	6.2	6.2	11.0	3.78×10^{6}	4,685	2.5
46	WINNIPE SAUKEE	O	N.H.	1460	4	6	2.1	1.4	0.6	2.42×10^{8}	22,317	13.1
47	KELLY FALLS	E	N.H.	1.5	15	24	7.0	7.0	2.0	1.20×10^{6}	15,020	2.3
48	GLEN LAKE	E	N.H.	3	15	28	3.8	3.8	9.2	2.07×10^{6}	8,023	3.4
49	CANADICUA	O	N.Y.	5480	5	9	4.3	2.8	1.2	1.68×10^{9}	6,041	39.0
50	CANNONSVILLE RES.	E	N.Y.	210	22	46	30.0	19.5	4.5	3.73×10^{8}	82,780	19.2
51	CARRYFALLS RES.	M	N.Y.	38	6	10	3.1	3.1	1.0	1.41×10^{8}	18,639	5.4
52	CASSADAGA	E	N.Y.	180	11	26	9.7	9.7	5.3	4.67×10^{6}	680	18.3
53	CAYUGA	M	N.Y.	4090	8	14	3.2	3.2	2.8	9.39×10^{9}	84,086	54.6
54	CROSS	E	N.Y.	7	42	76	19.5	19.5	15.0	4.85×10^{7}	295,220	5.5

Table 1 (cont'd)

	LAKE	TROPHIC STATUS	STATE	τ_w, days	N_I DISS P µg/ℓ	TOT P µg/ℓ	Chl µg/ℓ	EST. P PHYTO P µg/ℓ	EST. N_O ORG P µg/ℓ	V VOL m^3	W_T TOT P LOAD kg/yr	H MEAN DEPTH m
55	KEUKA	O	N.Y.	2850	5	8	5.7	2.85	0.15	1.07×10^{9}	4,939	22.6
56	SARATOGA	E	N.Y.	150	16	25	11.8	7.7	1.3	1.29×10^{8}	26,086	7.9
57	SACANDAGA	M	N.Y.	166	6	9	4.8	2.4	0.6	9.27×10^{8}	21,873	7.6
58	SCHROON	O	N.Y.	153	3	4	2.1	0.9	0.1	2.39×10^{8}	6,540	14.3
59	SENECA	M	N.Y.	12300	6	10	6.1	3.05	0.95	1.56×10^{10}	6,700	88.7
60	SWINGING BRIDGE RES.	E	N.Y.	92	20	57	28.7	28.7	8.3	4.65×10^{7}	24,540	13.4
61	CONESUS	E	N.Y.	621	13	20	9.9	6.4	0.6	1.15×10^{8}	4,925	8.9
62	LOWER ST. REGIS	E	N.Y.	110	8	17	7.9	7.9	1.1	9.56×10^{6}	762	5.1
63	SLATTERSVILLE RES.	E	R.I.	5	11	32	8.1	8.1	13.0	2.02×10^{6}	4,698	2.4
64	CHAMPLAIN	M	VT	949	10	18	11.1	7.2	0.8	2.19×10^{10}	571,600	19.4
65	CLYDE POND	E	VT	3.6	6	21	7.5	7.5	7.5	1.94×10^{6}	4,712	3.4
66	HARRIMAN RES.	M	VT	78	7	9	1.8	1.8	0.2	9.19×10^{7}	7,791	10.4
67	LAMOILLE	E	VT	1	10	18	3.5	3.5	4.5	1.05×10^{6}	15,605	1.7
68	ARROWHEAD	E	VT	3.5	9	15	8.5	5.5	0.5	1.04×10^{7}	37,628	3.1
69	WATERBURY RES.	M	VT	83	4	7	5.2	2.6	0.4	4.57×10^{7}	4,825	12.7
70	TROUT	M	WI	--	5	9	2.7	2.7	1.3	1.8×10^{8}	---	11.5
71	EAU CLAIRE	E	WI	10	38	89	19.6	19.6	31.0	1.04×10^{7}	40,884	2.3
72	OCONOMOWOC	E	WI	209	7	12	3.1	3.1	1.9	3.05×10^{7}	---	9.6
73	SHAWANO	E	WI	548	8	20	11.9	7.7	4.3	7.97×10^{7}	1,810	3.2
74	TAINTER	E	WI	10	81	111	13.7	13.7	16.0	2.81×10^{7}	139,000	4.1
75	WAPOGASSET	E	WI	194	15	43	16.6	16.6	11.0	2.54×10^{7}	3,415	5.3
76	WAUSAU	E	WI	2	33	59	5.0	5.0	21.0	1.71×10^{7}	220,458	2.2
77	WISCONSIN	E	WI	4	37	58	51.4	20.6	0.4	6.48×10^{7}	547,868	1.8
78	GENEVA	M	WI	10600	6	15	5.8	5.8	4.2	3.96×10^{8}	---	18.6
79	COMO	E	WI	401	12	48	16.4	23.6	12.3	4.98×10^{6}	---	1.3
80	BIG EAUPLLINE RES.	E	WI	158	30	71	35.5	35.5	5.5	1.33×10^{8}	41,116	4.8
81	GRAND	E	WI	11	150	190	65.3	33.0	7.0	1.14×10^{6}	8,118	1.2

HE - hypereutrophic
E - eutrophic
M - mesotrophic
O - oligotrophic

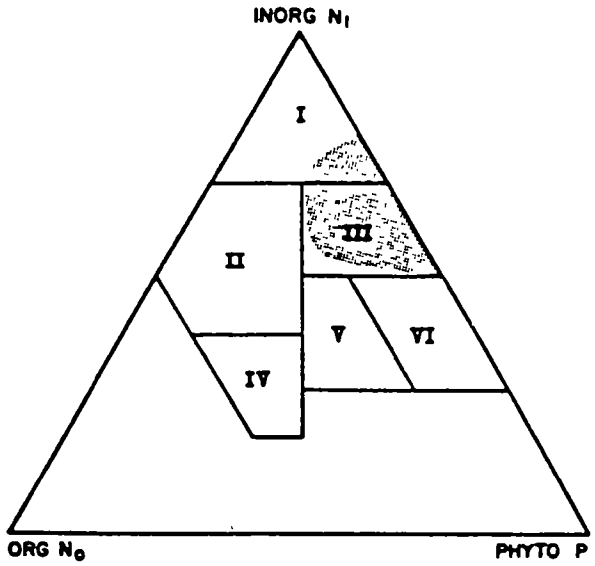

Fig. 6. Phosphorus partitioning diagram and groupings of lakes. Shaded area represents region of oligotrophic lakes. Roman numerals group lakes of similar kinetic coefficients.

Region
- I—highly eutrophic,
- II—eutrophic,
- III—mesotrophic, little eutrophic,
- IV—highly eutrophic,
- V—little eutrophic,
- VI—little eutrophic.

In general there is a rough pattern of increasing eutrophic tendency as the percentage of organic phosphorus increases. Each region on the diagram groups lakes of roughly similar kinetic coefficients.

Figure 7 gives a plotting of the actual NES phosphorus limited lakes for the northeast and north-Central United States. Considerable scatter exists among the 81 lakes, which includes lakes of differing geohydrologies, morphologies and nutrient loadings. Figure 8 gives the percentage of each nutrient component as a function of the total phosphorus for these same lakes. The dashed lines of Fig. 8 approx. ± 1 SD in percentage. There is a tendency for the organic fraction to increase as total phosphorus increases. The percentage of phytoplankton phosphorus first increases and then decreases while the dissolved fraction displays the opposite trend. On the average, phytoplankton account for 25–30% of the total phosphorus present. The wide scatter of data for lakes with greater than 100 $\mu g\,l^{-1}$ total phosphorus in Fig. 8 indicates that lakes may operate quite differently in the highly eutrophic state, either containing a large

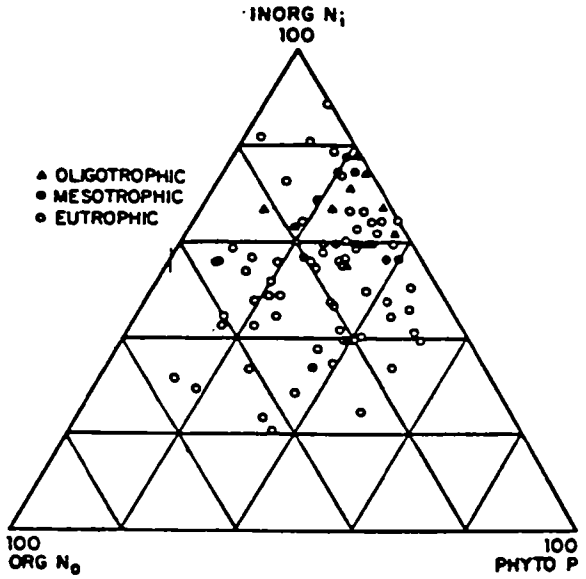

Fig. 7. Phosphorus partitioning diagram for the NES phosphorus limited lakes.

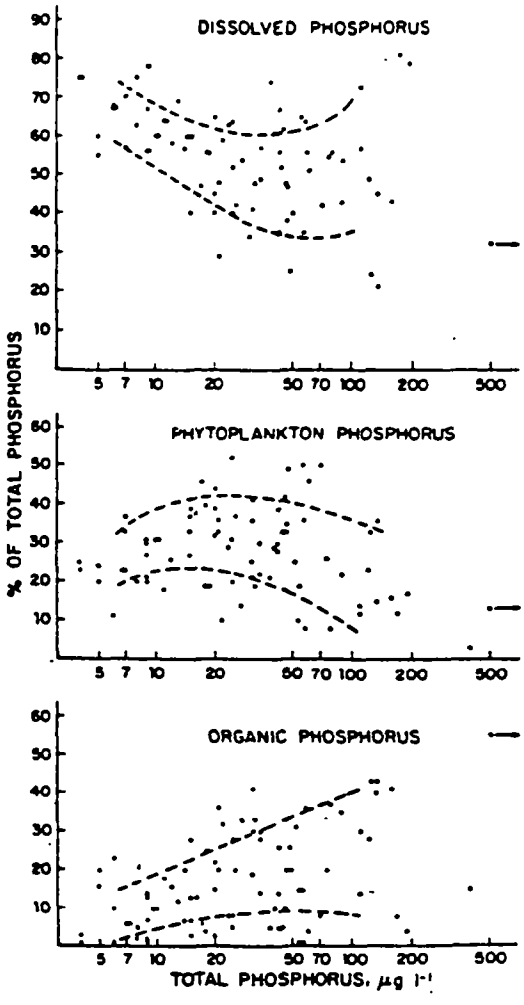

Fig. 8. Percentage of each phosphorus species vs total phosphorus.

concentration of organic or else dissolved inorganic phosphorus.

The method of Dillon & Rigler (1974) does not relate phosphorus loading to chlorophyll or standing crop. However, they suggest that their model could be combined with a total phosphorus to chlorophyll *a* correlation, yielding an estimate of standing crop directly. While the method is quite useful in predicting total phosphorus levels in lakes, there is some uncertainty (see Table 2). There is also uncertainty involved in total phosphorus to chlorophyll correlations (correlation coefficient = 0.78 for NES lakes, USEPA (1974). Combining the two multiples the uncertainty. Figure 9 shows the results of combining the two relationships for selected phosphorus limited lakes from the National Eutrophication Survey. The scatter of data is to be expected, but Fig. 9 illustrates the difficulty in utilizing this approach for the prediction of lake recovery in restoration projects. If the predicted chlorophyll *a* is significantly less than that measured, the calculation is in error and the project money spent will not bring about the desired water quality objective. A more detailed solution is warranted when public money is being investigated for lake restorations. The alternative approach suggested here requires more information and survey data than that of the nutrient loading models, but it also yields more information.

The U.S. National Eutrophication Survey Data was utilized to estimate the kinetic coefficients as given by equations (9)–(11) for each lake. Unfortunately, organic and dissolved phosphorus loadings were not separately measured, so it was necessary to divide the total phosphorus loading between inorganic and organic loadings in proportion to the respective lake concentrations. Phytoplankton growth coefficients, K_p, were initially assumed and the results of equations (9)–(11) ranged from 0.010 to 0.050 l μg^{-1}-day for K_p, 0.05–0.50 day^{-1} for K_1, 0.0–0.20 day^{-1} for K_p and 0.0–0.2 day^{-1} for K_0. Considerable scatter was evident in the data, but lakes within each region of Fig. 6 did display central tendencies.

CONCLUSIONS

The modeling approach developed herein has relative advantages over both the approaches of Vollenweider (1968, 1969) and Dillon & Rigler (1974) and the more complex, multi-variable efforts of Thomann *et al.* (1975). It has been shown that steady state simplification of equations (1)–(3) is consistent with the Dillon and Rigler method plus it yields estimates of standing crop directly. The time variable form of the equations was used successfully to simulate seasonal variations in Lake LBJ and Lake Ontario.

A relative disadvantage of this approach compared to the nutrient loading models is the need to estimate coefficients. However, there are only four coefficients (the sedimentation, hydrolysis, autocatalytic growth, and death rate constants), and equations (9)–(11) can aid in the initial estimation when coupled with gross productivity measurements and field survey data.

The sedimentation rate constant controls the amount of phosphorus lost to the deep sediment and therefore the total phosphorus concentration in the lake. It is the hydrolysis, growth and death rate constants which determine the partitioning of nutrients among the various organic, inorganic, and phytoplankton fractions. Among the lakes sampled in the northeast and north-central United States, it was determined that phytoplankton accounted for 10–40% of the total phosphorus present, while dissolved P was 35–75% and organic 0–40% of the total. In general, there was a pattern of increasing eutrophic tendency as the percentage of organic phosphorus increases. Ranges on the rate constants for the 81 phosphorus limited lakes of the U.S. National Eutrophication Survey were estimated.

Acknowledgements—We wish to thank the Modeling Group, Phosphorus Management Strategies Task Force of the Great Lakes Research Advisory Board, International Joint Commission for helpful discussions regarding eutrophication modeling, including: Drs Jim Falco, Walter Rast,

Table II

Dillon & Rigler, Phosphorus Model Combined with NES Chlorophyll Correlation

	LAKE	TROPHIC STATUS	STATE	τ_w, days	L g/m^2-yr	R	H m	$\frac{L(1-R)}{\bar{Y}}$ g/m^2	TOT P* PREDICTED µg/ℓ	TOT P MEASURED µg/ℓ	Chl a† PREDICTED µg/ℓ	Chl a MEASURED µg/ℓ
1	LAKE ZOAR	E	CONN	5	39.2	0.25	7.5	0.403	54	43	20	18.3
2	LILLINONAH	E	CONN	17	29.1	0.40	11.9	0.812	68	54	25	11.1
3	HOUSATONIC	E	CONN	0.6	88.9	0.16	2.9	0.123	42	39	14	8.2
4	LONG	M	MAINE	438	0.14	0.50	10.4	0.083	8	8	2	3.2
5	MATTAWAMKEAG	M	MAINE	42	0.59	0.29	3.7	0.048	13	11	3.6	2.0
6	MOOSEHEAD	O	MAINE	1100	0.08	0.46	16.5	0.132	8	5	2	1.5
7	RANGELEY	O	MAINE	1020	0.09	0.49	14.3	0.128	9	7	2.3	2.4
8	SEBAGO	O	MAINE	1970	0.08	0.57	30.8	0.015	0.5	4	0.07	1.5
9	BAY OF NAPLES	O	MAINE	26	0.51	0.19	4.3	0.029	7	5	1.7	1.8
10	HAGER POND	HE	MASS	24	131	0.73	1.5	2.325	1550	1525	1017	198.5
11	HARRIS POND	E	MASS	6.2	10.7	0.35	2.4	0.118	48	52	16.7	12.9
12	LAKE ALLEGAN	E	MICH	7	31.4	0.23	3.4	0.464	136	135	57	20.0
13	BARTON	E	MICH	81	2.15	0.01	6.1	0.473	78	61	30	28.0
14	BELLEVILLE	E	MICH	25	15.7	0.25	6.1	0.809	133	122	56	28.0
15	CHARLEVOIX	O	MICH	1170	0.12	0.63	16.8	0.145	8.6	6	2.2	3.0
16	CHEMUNG	E	MICH	1530	0.22	0.63	8.5	0.338	39.8	32	13.4	13.0
17	FORD	E	MICH	15	16.2	0.19	4.4	0.538	122	111	50.4	15.0
18	JORDAN	E	MICH	304	1.14	0.17	7.3	0.791	108	171	43.7	20.5
19	MACATAWA	HE	MICH	77	6.35	0.73	3.7	0.362	98	159	38.9	25.6
20	ROSS RESER.	E	MICH	2	17.0	0.14	1.5	0.080	53	35	18.8	10.4
21	THORNAPPLE	E	MICH	11	9.21	0.21	4.3	0.219	50.9	45	17.9	14.7
22	UNION	E	MICH	2	9.29	0.10	0.9	0.046	51.1	47	18	15.7
23	CRYSTAL	O	MICH	1200	0.07	0.73	4.2	0.062	14.8	9	4.2	2.9
24	HIGGINS	O	MICH	5690	0.03	0.70	14.9	0.124	8.3	6	2.1	1.0
25	HOUGHTON	E	MICH	475	0.06	0.52	2.3	0.037	16.1	16	4.6	9.2

Table II (cont'd)

	LAKE	TROPHIC STATUS	STATE	T_w days	L g/m²-yr	R	H m	L(1-R)/$\bar{z}$ g/m²	TOT P* PREDICTED µg/ℓ	TOT P MEASURED µg/ℓ	Chl a† PREDICTED µg/ℓ	Chl a MEASURED µg/ℓ
26	THOMPSON	E	MICH	152	0.41	<0.0	2.7	0.169	62.6	41	22.9	12.0
27	ZUMBRO	E	MINN	18	83.3	0.44	5.5	2.30	418	330	216	12.5
28	ST. CROIX	E	MINN	23	8.89	0.33	8.8	0.375	42.6	55	14.5	10.2
29	FOREST	E	MINN	2080	0.11	<0.0	3.4	0.635	187	21	83.5	10.5
30	GREEN	M	MINN	1350	0.09	0.67	6.4	0.114	17.8	15	5.2	4.9
31	ANDROSIA	E	MINN	47	4.02	0.37	7.9	0.326	41.3	25	14.0	13.0
32	BADGER	E	MINN	108	0.63	<0.0	1.2	0.186	155	22	67.0	2.1
33	BARTLETT	E	MINN	694	0.37	0.57	2.6	0.302	116	136	47.5	49.5
34	BLACKHOFF	E	MINN	257	1.22	0.84	4.4	0.137	31.1	43	10.0	12.8
35	CASS	E	MINN	313	0.35	0.63	7.8	0.111	14.6	20	4.1	8.7
36	EMBARRASS	E	MINN	22	1.71	<0.0	2.6	0.103	39.6	25	13.3	4.9
37	LEECH	M	MINN	1900	0.04	0.54	4.7	0.096	20.4	15	6.1	6.2
38	MADISON	E	MINN	1200	0.36	0.76	4.0	0.285	71.2	50	26.7	30.8
39	MALMEDAL	E	MINN	475	0.28	<0.0	1.8	0.364	202	125	91.5	41
41	MINNEWASKA	E	MINN	4640	0.15	0.90	6.0	0.191	31.8	35	10.3	16.6
42	PELICAN	M	MINN	1200	0.06	0.46	2.4	0.107	44.6	32	15.4	11.4
43	SUPERIOR	E	MINN	8	24.0	0.59	3.8	0.216	56.8	79	20.4	6.2
44	SWAN	M	MINN	876	0.47	0.79	12.1	0.237	19.6	13	5.8	3.8
45	POWDERMILL POND	E	N.H.	6.5	3.11	0.06	2.5	0.052	20.8	33	6.2	6.2
46	WINNIPE SAUKE	O	N.H.	1460	0.12	0.77	13.1	0.110	8.4	6	2.1	2.1
47	KELLY FALLS	E	N.H.	1.5	28.8	0.33	2.3	0.079	34.4	24	11.3	7.0
48	GLEN LAKE	E	N.H.	3	13.1	0.32	3.4	0.073	21.5	28	6.5	3.8
49	CANADIGUA	O	N.Y.	5480	0.14	0.65	39.0	0.735	18.9	9	5.6	4.3
50	CANNONSVILL RES.	E	N.Y.	210	4.26	0.71	19.2	0.711	37.0	46	12.3	30.0
51	CARRYFALLS RES.	M	N.Y.	38	0.71	0.28	5.4	0.053	9.8	10	2.6	3.1

53	CAYUGA	M	N.Y.	405	0.49	0.52	54.6	2.[illegible]	48.2	14	16.8	3.2
54	CROSS	E	N.Y.	7	33.5	0.23	5.5	[illegible]	90.0	76	35.2	19.5
55	KEUKA	O	N.Y.	[illegible]	0.10	0.53	22.6	0.367	16.2	8	4.6	5.7
56	SARATOGA	E	N.Y.	150	1.60	0.53	7.9	0.309	39.1	25	13.1	11.8
57	SACANDAGA	M	N.Y.	166	0.18	0.26	7.6	0.061	8.0	9	2.0	4.8
58	SCHROON	O	N.Y.	153	0.39	<0.0	14.3	0.163	11.4	4	3.1	2.1
59	SENECA	M	N.Y.	12300	0.38	0.80	88.7	2.56	28.9	10	9.2	6.1
60	SWINGING BRIDGE, RES.	E	N.Y.	92	7.07	0.59	13.4	0.731	54.6	57	19.5	28.7
61	CONESUS	E	N.Y.	621	0.38	0.57	8.9	0.278	31.2	20	10.1	9.9
62	LOWER ST. REGIS	E	N.Y.	110	0.41	0.11	5.1	0.110	21.6	17	6.5	7.9
63	SLATTERSVILLE RES.	E	R.I.	5	5.59	0.17	2.4	0.064	27	32	8.5	8.1
64	CHAMPLAIN	M	VT.	949	0.51	0.48	19.4	0.684	35	18	11.5	11.1
65	CLYDE POND	E	VT.	3.6	8.27	0.15	3.4	0.069	20.3	21	6.0	7.5
66	HARRIMAN RES.	M	VT.	78	0.88	0.17	10.4	0.156	15	9	4.2	1.8
67	LAMOILLE	E	VT.	1	25.2	0.20	1.7	0.055	32	18	10.4	3.5
68	ARROWHEAD	E	VT.	3.5	11.3	0.27	3.1	0.079	25	15	7.7	8.5
69	WATERBURY RES.	M	VT.	83	1.34	0.24	12.7	0.232	18	7	5.2	5.2
71	EAUCLAIRE	E	WI.	10	9.04	<0.0	2.3	0.248	108	89	43.7	19.6
73	SHAWANO	E	WI.	548	0.07	0.23	3.2	0.081	25.3	20	7.9	11.9
74	TAINTER	E	WI.	10	20.3	0.12	4.1	0.489	119	111	49	13.7
75	WAPOGASSET	E	WI.	194	0.71	0.43	5.3	0.215	40.6	43	13.7	16.6
76	WASAU	E	WI.	2	28.4	<0.0	2.2	0.156	70.9	59	26.5	5.0
77	WISCONSIN	E	WI.	4	15.2	0.05	1.8	0.158	87.8	58	34.2	51.4
80	BIG EAU PLEINE RES.	E	WI.	158	1.49	0.24	4.8	0.490	102	71	40.8	35.5
81	GRAND	E	WI.	11	8.57	0.16	1.2	0.217	181	190	80.4	65.3

*$\frac{L(1-R)}{\tau H}$ = tot P predicted

†$\log_{10} P_{total} = 0.846 \log_{10} \text{Chl } a - 2.356$

L = tot phosphorus loading
R = fraction of phosphorus retained
τ = mean annual hydraulic detention time
H = mean depth

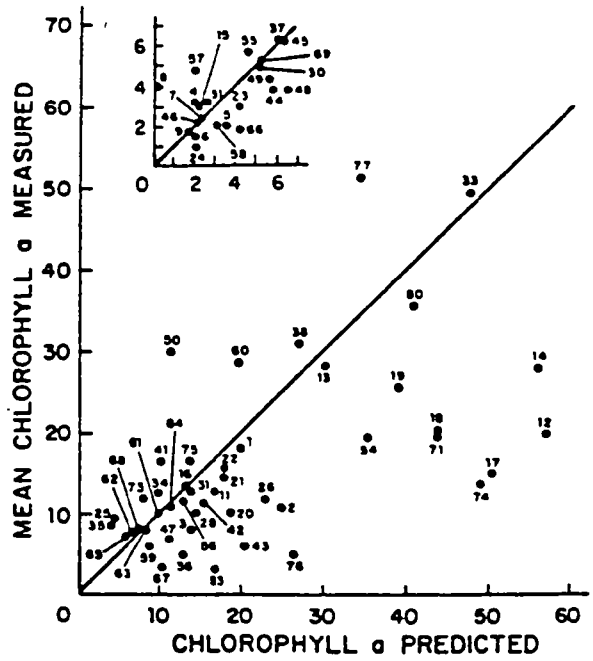

Fig. 9. Measured vs predicted chlorophyll for the Dillon & Rigler (1974) model combined with the NES total phosphorus to chlorophyll correlation, USEPA (1974).

Frank Verhoff and Mr John Mancini. The calculations of Table 2 were provided by Mr Frank Murphy, Environmental Engineering and Science Graduate Program, Manhattan College, Bronx, New York. The financial support of the National Science Foundation and an NSF Postdoctoral Fellowship to Dr Schnoor is gratefully acknowledged.

REFERENCES

Chapra S. C. (1977) Total phosphorus model for the Great Lakes. *J. environ. Engn. Div. Am. Soc. civ. Engrs* 103, 147–161.

Davenport J. B. (1975) Phytoplankton succession and the productivity of individual algae species in a central Texas reservoir. M.S. Thesis. University of Texas, Austin, TX.

Dillon P. J. & Rigler F. H. (1974) A test of a simple nutrient budget model predicting the phosphorus concentrations in lake water. *J. Fish. Res. Bd Can.* 31, 1771–78.

Di Toro D. M. & Connolly J. P. (1979) Mathematical models of water quality in large lakes, Part 2: Lake Erie. U.S. Environmental Protection Agency, in press, Washington, DC.

Eppley R. W., Harrison W. G., Chisholm S. W. & Stewart E. (1977) Particulate organic matter in surface waters off southern California and its relationship to phytoplankton. *J. mar. Res.* 35, 671–696.

Glooschenko W. A., Moore J. E., Munawar M. & Vollenweider R. A. (1974) Primary production in lakes Ontario and Erie: a comparative study. *J. Fish. Res. Bd Can.* 31, 253–263.

Imboden D. M. (1974) Phosphorus model of lake eutrophication. *Limnol. Oceanogr.* 297–304.

Jassby A. D. & Goldman C. R. (1974) Loss rates from a lake phytoplankton community. *Limnol. Oceanogr.* 19, 618–627.

Lotka A. J. (1956) *Elements of Mathematical Biology.* Dover, New York.

McCave I. N. (1975) Vertical flux of particles in the ocean. *Deep-Sea Res.* 22, 491–502.

Munawar M. & Nauwerck A. (1971) The composition and horizontal distribution of phytoplankton in Lake Ontario during the year 1970. *Proc. Conf. Great Lakes Res.* 14, 69–78.

Munawar M. & Munawar I. F. (1976) A lakewide study of phytoplankton biomass and its species composition in Lake Erie. *J. Fish. Res. Bd Can.* 33, 581–600.

Murphy C. B. Jr & Welter G. J. (1976) Indices of algal biomass and primary production in Onondaga Lake. National Conference of Environmental Engineering Research Development and Design, ASCE Env. Eng. Div., Seattle, WA.

O'Connor D. J. (1973) Dynamic water quality forecasting and management. U.S. Environmental Protection Agency, EPA-660/3-73-009, Washington, DC.

Parsons T. R. & Takahashi M. (1973) *Biological Oceanographic Processes.* Pergamon Press, New York.

Richey J. E., Wissmar R. C., DeVol A. H., Likens G. E., Eaton J. S., Wetzel R. G., Odum W. E., Johnson N. M., Loucks O. L., Prentki R. T. & Rich P. H. (1978) Carbon flow in four lake ecosystems. *Science* 202, 1183–1186.

Riley G. A., Stommel & Bumpus (1949) Ecology of plankton. *Bull. Bingham Ocean. Coll.* 12, 3.

Schnoor J. L. & Fruh E. G. (1979) Dissolved oxygen model of a short detention time reservoir with anaerobic hypolimnion. *Wat. Resour. Bull.* 15, 506–518.

Smayda T. J. (1974) Some experiments on the sinking characteristics of two freshwater diatoms. *Limnol. Oceanogr.* 19, 628–635.

Sorokin C. (1959) Tabular comparative data for the low and high temperature strains of chlorella. *Nature* 184, 643–644.

Stumm W. & Morgan J. J. (1970) *Aquatic Chemistry.* Wiley-Interscience, New York.

Thomann R. V., DiToro D. M., Winfield R. P. & O'Connor D. J. (1975) Mathematical modeling of phytoplankton in Lake Ontario. U.S. Environmental Protection Agency, EPA-660/3-75-005. Washington, DC.

A Dynamic Model of Phytoplankton Populations in Natural Waters*

Introduction

The quality of natural waters can be markedly influenced by the growth and distribution of phytoplankton. Utilizing radiant energy, these microscopic plants assimilate inorganic chemicals and convert them to cell material which, in turn, is consumed by the various animal species in the next tropic level. The phytoplankton, therefore, are the base of the food chain in natural waters, and their existence is essential to all aquatic life.

The quality of a body of water can be adversely affected if the population of phytoplankton becomes so large as to interfere with either water

---

*Dominic M. Di Toro, Donald J. O'Connor, Robert V. Thomann
Environmental Engineering and Science Program
Manhattan College

use or the higher forms of aquatic life. In particular, high concentrations of algal biomass cause large diurnal variations in dissolved oxygen which can be fatal to fish life. Also, the growths can be nuisances in themselves, especially when they decay and either settle to the bottom or accumulate in windrows on the shoreline. Phytoplankton can cause taste and odor problems in water supplies and, in addition, contribute to filter clogging in the water treatment plant.

The development of large populations of phytoplankton and, in some cases, larger aquatic plants can be accelerated by the addition of nutrients which result from man's activities or natural processes. The resulting fertilization provides more than ample inorganic nutrients, with the resulting development of excessive phytoplankton. This sequence of events is commonly referred to as eutrophication.

Generally, the management of water systems subjected to accelerated eutrophication because of waste discharges has been largely subjective. Extensive programs of nutrient removal have been called for, with little or no quantitative prediction of the effects of such treatment programs. A quantitative methodology is required to estimate the effect of proposed treatment programs that are planned to restore water quality or to predict the effects of expected future nutrient discharges. This methodology should include a model of the phytoplankton population which approximates the behavior of the phytoplankton in the water body of interest and, therefore, can be used to test the effects of the various control procedures available. In this way, rational planning and water quality management can be instituted with at least some degree of confidence that the planned results actually will be achieved.

This paper presents a phytoplankton population model in natural waters, constructed on the basis of the principle of conservation of mass. This is an elementary physical law which is satisfied by macroscopic natural systems. The use of this principle is dictated primarily by the lack of any more specific physical laws which can be applied to these biological systems. An alternate conservation law, that of conservation of energy, can also be used. However, the details of how mass is transferred from species to species are better understood than the corresponding energy transformations. The mass interactions are related, among other factors, to the kinetics of the populations and it is this that the bulk of the paper is devoted to exploring.

Conservation of mass has been successfully applied to the modeling of the dissolved oxygen distribution in natural waters as well as the distribution of salinity and other dissolved substances. The resulting models have proved useful in guiding engineering and management decisions concerned with the efficient utilization of water resources and the protection of their quality. It is felt that the phytoplankton model presented

herein can serve a similar purpose by providing a basis for predicting the effects of nutrient control programs on the eutrophication of natural waters.

Thus, the primary purpose of this paper is to introduce a quantitative model of phytoplankton population dynamics in natural waters. It is within this problem context that the simplifications, assumptions, and generally the structure of the model is formulated. An attempt is made to make the equations representative of the biological mechanisms while still retaining a sufficient simplicity so that the result is tractable and useful.

Review of Previous Models

The initial attempts to model the dynamics of a phytoplankton population were based on a version of the law of conservation of mass in which the hydrodynamic transport of mass is assumed to be insignificant. Let $P(t)$ be the concentration of phytoplankton mass at time t in a suitably chosen region of water. The principle of conservation of mass can be expressed as a differential equation

$$\frac{dP}{dt} = S$$

where S is the net source or sink of phytoplankton mass within the region. If hydrodynamic transport is not included, then the rate at which P increases or decreases depends only on the internal sources and sinks of phytoplankton in the region of interest.

The form of the internal sources and sinks of phytoplankton is dictated by the mechanisms which are assumed to govern the growth and death of phytoplankton. Fleming (1939), as described by Riley (*1*), postulated that spring diatom flowering in the English Channel is described by the equation

$$\frac{dP}{dt} = [a - (b + ct)]P$$

where P is the phytoplankton concentration, a is a constant growth rate, and $(b + ct)$ is a death rate resulting from the grazing of zooplankton. The zooplankton population, which is increasing owing to its grazing, results in an increasing death rate which is approximated by the linear increase of the death rate as a function of time.

A less empirical model has been proposed by Riley (1946) (*1*) based on the equation

$$\frac{dP}{dt} = [P_h - R - G]P$$

where P_h is the photosynthetic growth rate, R is the endogenous respiration rate of the phytoplankton, and G is the death rate owing to zooplankton grazing. A major improvement in Riley's equation is the attempt to relate the growth rate, the respiration rate, and the grazing to more fundamental environmental variables such as incident solar radiation, temperature, extinction coefficient, and observed nutrient and zooplankton concentration. As a consequence, the coefficients of the equations are time-variable since the environmental parameters vary throughout the year. This precludes an analytical solution to the equation, and numerical integration methods must be used. Three separate applications (*2, 3, 4*) of these equations to the near-shore ocean environment have been made, and the resulting agreement with observed data is quite encouraging.

A complex set of equations, proposed by Riley, Stommel, and Bumpus (1949) (*5*) first introduced the spatial variation of the phytoplankton with respect to depth into the conservation of mass equation. In addition, a conservation of mass equation for a nutrient (phosphate) was also introduced, as well as simplified equations for the herbivorous and carnivorous zooplankton concentrations. The phytoplankton and nutrient equations were applied to 20 volume elements which extended from the surface to well below the euphotic zone. In order to simplify the calculations, a temporal steady-state was assumed to exist in each volume element. Thus, the equations apply to those periods of the year during which the dependent variables are not changing significantly in time. Such conditions usually prevail during the summer months. The results of these calculations were compared with observed data, and again the results were encouraging.

Steele (1956) (*6*) found that the steady-state assumption did not apply to the seasonal variation of the phytoplankton population. Instead, he used two volume segments to represent the upper and lower water levels and kept the time derivatives in the equations. Thus, both temporal and spatial variations were considered. In addition, the differential equations for phytoplankton and zooplankton concentration were coupled so that the interactions of the populations could be studied, as well as the nutrient–phytoplankton dependence. The coefficients of the equations were not functions of time, however, so that the effects of time-varying solar radiation intensity and temperature were not included. The equations were numerically integrated and the results compared with the observed distribution. Steele applied similar equations to the vertical distribution of chlorophyll in the Gulf of Mexico (*7*).

The models proposed by Riley *et al.* and Steele are basically similar. Each consider the primary dependent variables to be the phytoplankton, zooplankton, and nutrient concentration. A conservation of mass equa-

tion is written for each species, and the spatial variation is incorporated by considering finite volume elements which interact because of vertical eddy diffusion and downward advective transport of the phytoplankton. Their equations differ in some details (for example, the growth coefficients that were used and the assumptions of steady state) but the principle is the same. In addition, these equations were applied by the authors to actual marine situations and their solutions compared with observed data. This is a crucial part of any investigation discussion wherein the assumptions that are made and the approximations that are used are difficult to justify *a priori*.

The models of both Riley and Steele have been reviewed in greater detail by Riley (*1*) in a discussion of their applicability and possible future development. The difficulties encountered in formulating simple

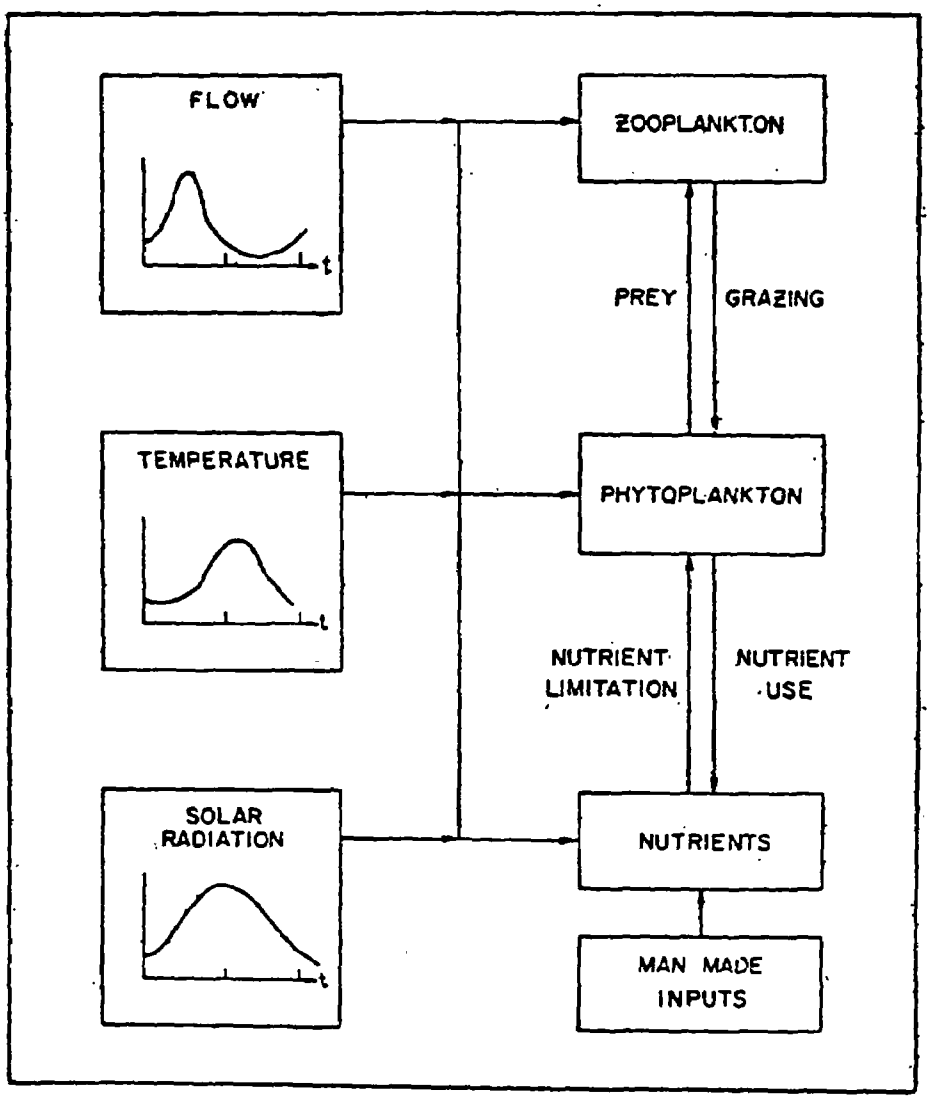

Figure 1. Interactions of environmental variables and the phytoplankton, zooplankton, and nutrient systems

theoretical models of phytoplankton–zooplankton population models were discussed by Steele (*8*).

Other models have been proposed which follow the outlines of the equations already discussed. Equations with parameters that vary as a function of temperature, sunlight, and nutrient concentration have been presented by Davidson and Clymer (*9*) and simulated by Cole (*10*). A set of equations which model the population of phytoplankton, zooplankton, and a species of fish in a large lake have been presented by Parker (*11*). The application of the techniques of phytoplankton modeling to the problem of eutrophication in rivers and estuaries has been proposed by Chen (*12*). The interrelations between the nitrogen cycle and the phytoplankton population in the Potomac Estuary has been investigated using a feed-forward–feed-back model of the dependent variables, which interact linearly following first order kinetics (*13*).

The formulations and equations presented in the subsequent sections are modifications and extensions of previously presented equations which incorporate some additional physiological information on the behavior of phytoplankton and zooplankton populations. In contrast to the majority of the applications of phytoplankton models which have been made previously, the equations presented in the subsequent sections are applied to a relatively shallow reach of the San Joaquin River and the estuary further downstream. The motivation for this application is an investigation of the possibility of excessive phytoplankton growths as environmental conditions and nutrient loadings are changed in this area. Thus, the primary thrust of this investigation is to produce an engineering tool which can be used in the solution of engineering problems to protect the water quality of the region of interest.

Phytoplankton System Interactions

The major obstacle to a rigorous quantitative theory of phytoplankton population dynamics is the enormous complexity of the biological and physical phenomena which influence the population. It is necessary, therefore, to idealize and simplify the conceptual model so that the result is a manageable set of dependent systems or variables and their interrelations. The model considered in the following sections is formulated on the basis of three primary dependent systems: the phytoplankton population, whose behavior is the object of concern; the herbivorous zooplankton population, which are the predators of the phytoplankton, utilizing the available phytoplankton as a food supply; and the nutrient system, which represents the nutrients, primarily inorganic substances, that are required by the phytoplankton during growth. These three systems are affected not only by their interactions, but also by external environmental variables.

The three principal variables considered in this analysis are temperature, which influences all biological and chemical reactions, dispersion and advective flow, which are the primary mass transport mechanisms in a natural body of water, and solar radiation, the energy source for the photosynthetic growth of the phytoplankton.

In addition to these external variables, the effect of man's activities on the system is felt predominately in the nutrient system. Sources of the necessary nutrients may be the result of, for example, inputs of wastewater from municipal and industrial discharges or agricultural runoff. The man-made waste loads are in most cases the primary control variables which are available to affect changes in the phytoplankton and zooplankton systems. A schematic representation of these systems and their interrelations is presented in Figure 1.

In addition to the conceptual model which isolates the major interacting systems, a further idealization is required which sets the lower and upper limits of the temporal and spatial scales being considered. Within the context of the problem of eutrophication and its control, the seasonal distribution of the phytoplankton is of major importance, so that the lower limit of the temporal scale is on the order of days. The spatial scale is set by the hydrodynamics of the water body being considered. For example, in a tidal estuary, the spatial scale is on the order of miles whereas in a small lake it is likely a good deal smaller. The upper limits for the temporal and spatial extent of the model are dictated primarily by practical considerations such as the length of time for which adequate information is available and the size of the computer being used for the calculations.

These simplifying assumptions are made primarily on the basis of an intuitive assessment of the important features of the systems being considered and the experience gained by previous attempts to address these and related problems in natural bodies of water. The basic principle to be applied to this conceptual model, which can then be translated into mathematical terms, is that of conservation of mass.

Conservation of Mass

The principle of conservation of mass is the basis upon which the mathematical development is structured. Alternate formulations, such as those based on the conservation of energy, have been proposed. However, conservation of mass has proved a useful starting point for many models of the natural environment.

The principle of conservation of mass simply states that the mass of the substances being considered within an arbitrarily selected volume must be accounted for by either mass transport into and out of the volume

or as mass produced or removed within the volume. The transport of mass in a natural water system arises primarily from two phenomena: dispersion, which is caused by tidal action, density differences; turbulent diffusion, wind action, etc.; and advection owing to a unidirectional flow —for example, the fresh water flow in a river or estuary or the prevailing currents in a bay or a near-shore environment. The distinction between the two phenomena is that, over the time scale of interest, dispersive mass transport mixes adjacent volumes of water so that a portion of the water in adjacent volume elements is interchanged, and the mass transport is proportional to the difference in concentrations of mass in adjacent volumes. Advective transport, however, is transport in the direction of the advective flow only. In addition to the mass transport phenomena, mass in the volume can increase resulting from sources within the volume. These sources represent the rate of addition or removal of mass per unit time per unit volume by chemical and biological processes.

A mathematical expression of conservation of mass which includes the terms to describe the mass transport phenomena and the source term is a partial differential equation of the following form

$$\frac{\partial P}{\partial t} = \nabla \cdot E \nabla P - \nabla \cdot QP + S_P \tag{1}$$

where $P(x, y, z, t)$ is the concentration of the substance of interest—*e.g.*, phytoplankton biomass—as a function of position and time; E is the diagonal matrix of dispersion coefficients; Q is the advective flow rate vector; S_P is the vector whose terms are the rate of mass addition by the sources and sinks; and ∇ is the gradient operator. This partial differential equation is too general to be solved analytically, and numerical techniques are used in its solution.

An effective approximation to Equation 1 is obtained by segmenting the water body of interest into n volume elements of volume V_j and representing the derivatives in Equation 1 by differences. Let V be the $n \times n$ diagonal matrix of volumes V_j; A, the $n \times n$ matrix of dispersive and advective transport terms; S_P, the n vector of source terms S_{Pj}, averaged over the volume V_j; and P, the n vector of concentrations P_j, which are the concentrations in the volumes. Then the finite difference equations can be expressed as a vector differential equation

$$V\dot{P} = AP + VS_P \tag{2}$$

where the dot denotes a time derivative. The details of the application of this version of the dispersion advection equation to natural bodies of water has been presented by Thomann (*14*) and reviewed by O'Connor *et al.* (*15*).

The main interest in this report is centered on the source terms S_{Pj} for the particular application of these equations to the phytoplankton population in natural water bodies. It is convenient to express the source term of phytoplankton, S_{Pj}, as a difference between the growth rate, G_{Pj}, of phytoplankton and their death rate, D_{Pj}, in the volume V_j. That is

$$S_{Pj} = (G_{Pj} - D_{Pj})P_j \tag{3}$$

where G_{Pj} and D_{Pj} have units [day^{-1}]. The subscript P identifies the quantities as referring to phytoplankton; the subscript j refers to the volume element being considered. The balance between the magnitude of the growth rate and death rate determines the rate at which phytoplankton mass is created or destroyed in the volume element V_j. Thus, the form of the growth and death rates as functions of environmental parameters and dependent variables is an important element in a successful phytoplankton population model.

Phytoplankton Growth Rate

The growth rate of a population of phytoplankton in a natural environment is a complicated function of the species of phytoplankton present and their differing reactions to solar radiation, temperature, and the balance between nutrient availability and phytoplankton requirements. The complex and often conflicting data pertinent to this problem have been reviewed recently by Hutchinson (1967) (*16*), Strickland (1965) (*17*), Lund (1965) (*18*), and Raymont (1963) (*19*). The available information is not sufficiently detailed to specify the growth kinetics for individual phytoplankton species in natural environments. Hence, in order to accomplish the task of constructing a growth rate function, a simplified approach is followed. The problem of different species and their associated nutrient and environmental requirements is not addressed. Instead, the population is characterized as a whole by a measurement of the biomass of phytoplankton present. Typical quantities used are the chlorophyll concentration of the population, the number of organisms per unit volume, or the dry weight of the phytoplankton per unit volume (*20*). With a choice of biomass units established, the growth rate expresses the rate of production of biomass as a function of the important environmental variables. The environmental variables to be considered below are light, temperature, and the various nutrients which are necessary for phytoplankton growth.

Light and Temperature. Consider a population of phytoplankton, either a natural association or a single species culture, and assume that the optimum or saturating light intensity for maximum growth rate of biomass is present and illuminates all the cells, and further that all the

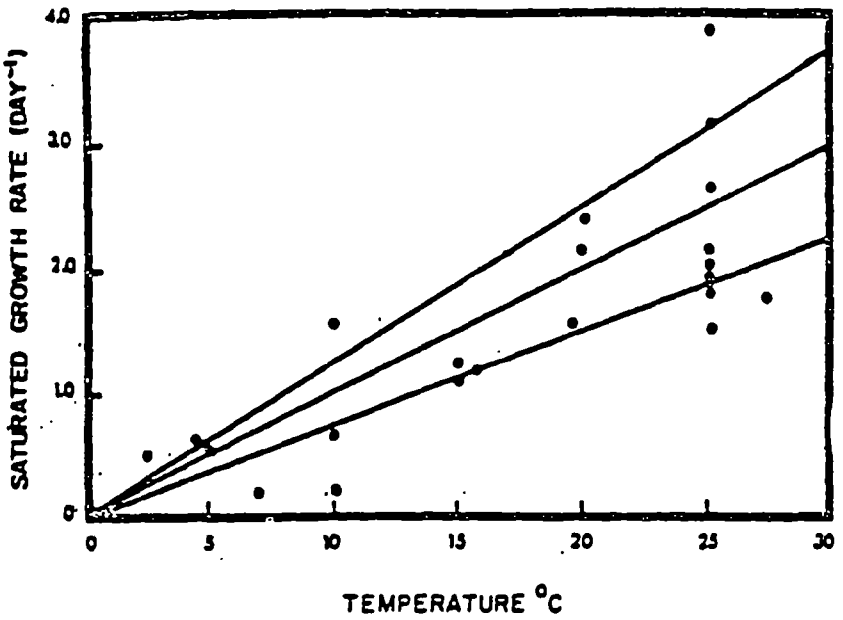

Figure 2. Phytoplankton saturated growth rate (base e) as a function of temperature

necessary nutrients are present in sufficient quantity so that no nutrient is in short supply. For this condition, the growth rate that is observed is called the maximum or saturated growth rate, K'. Measurements of K' (base e) as a function of temperature are shown in Figure 2 and listed in Table I. The experimental conditions under which these data were collected appear to meet the requirements of optimum light intensity and sufficient nutrient supply. The data presented are selected from larger groups of reported values, and they represent the maximum of these reported growth rates. The presumption is that these large values reflect the maximum growth rates achievable. From an ecological point of view, it is necessary to consider the species most able to compete, and, in terms of growth rate, it is the species with the largest growth rate which will predominate. A straight-line fit to this data appears to be a crude but reasonable approximation of the data relating saturated growth rate K' to temperature, T

$$K' = K_1 T \tag{4}$$

where K_1 has values in the range 0.10 ± 0.025 day^{-1} °C^{-1}. This coefficient indicates an approximate doubling of the saturated growth rate for a temperature change from 10° to 20°C, in accordance with the generally reported temperature-dependence of biological growth rates. The optimum temperature for algal growth appears to be in the range between 20° and 25°C, although thermophilic strains are known to exist (*27*). At higher temperatures, there is usually a suppression of the saturated growth rate, and the straight-line approximation is no longer valid. It should

also be noted that the scatter in the data in Figure 2 is sufficiently large so that the linear dependence on temperature and also the magnitude of K' can vary considerably in particular situations.

In the natural environment, the light intensity to which the phytoplankton are exposed is not uniformly at the optimum value but it varies as a function of depth because of the natural turbidity present and as a function of time over the day. Thus, the phytoplankton in the lower layers are exposed to intensities below the optimum and those at the surface may be exposed to intensities above the optimum so that their growth rate would be inhibited. Figure 3b,c,d from Ryther (*28*) are plots of the photosynthesis rate normalized by the photosynthesis rate at the optimum or saturating light intensity *vs.* the light intensity, I, incident on the populations. Figure 3a is a plot of function

$$F(I) = \frac{I}{I_s} \exp\left[-\frac{I}{I_s} + 1\right] \tag{5}$$

for $I_s = 2000$ ft-candles, proposed by Steele (*8*) to describe the light-dependence of the growth rate of phytoplankton.

The similarity between this function and data from Ryther is sufficient to warrant the use of this expression to express the influence of nonoptimum light intensity on the growth rate of phytoplankton. Other workers have suggested different forms for this relationship (*29*, *30*).

Table I. Maximum Growth Rates as a Function of Temperature

Ref.	*Organism*	*Temperature,*	*Saturated Growth Rate, $K'(Base_e, Day^{-1})$*
21	*Chlorella ellipsoidea*	25	3.14
	(green alga)	15	1.2
22	*Nannochloris atomus*	20	2.16
	(marine flagellate)	10	1.54
23	*Nitzschia closterium*	27	1.75
	(marine diatom)	19	1.55
		15.5	1.19
		10	0.67
5	Natural association	4	0.63
		2.6	0.51
24	*Chlorella pyrenoidosa*	25	1.96
24	*Scenedesmus quadricauda*	25	2.02
25	*Chlorella pyrenoidosa*	25	2.15
25	*Chlorella vulgaris*	25	1.8
25	*Scenedesmus obliquus*	25	1.52
25	*Chlamydomonas reinhardti*	25	2.64
26	*Chlorella pyrenoidosa*	10	0.2
	(synchronized culture)	15	1.1
	(high-temperature strain)	20	2.4
		25	3.9

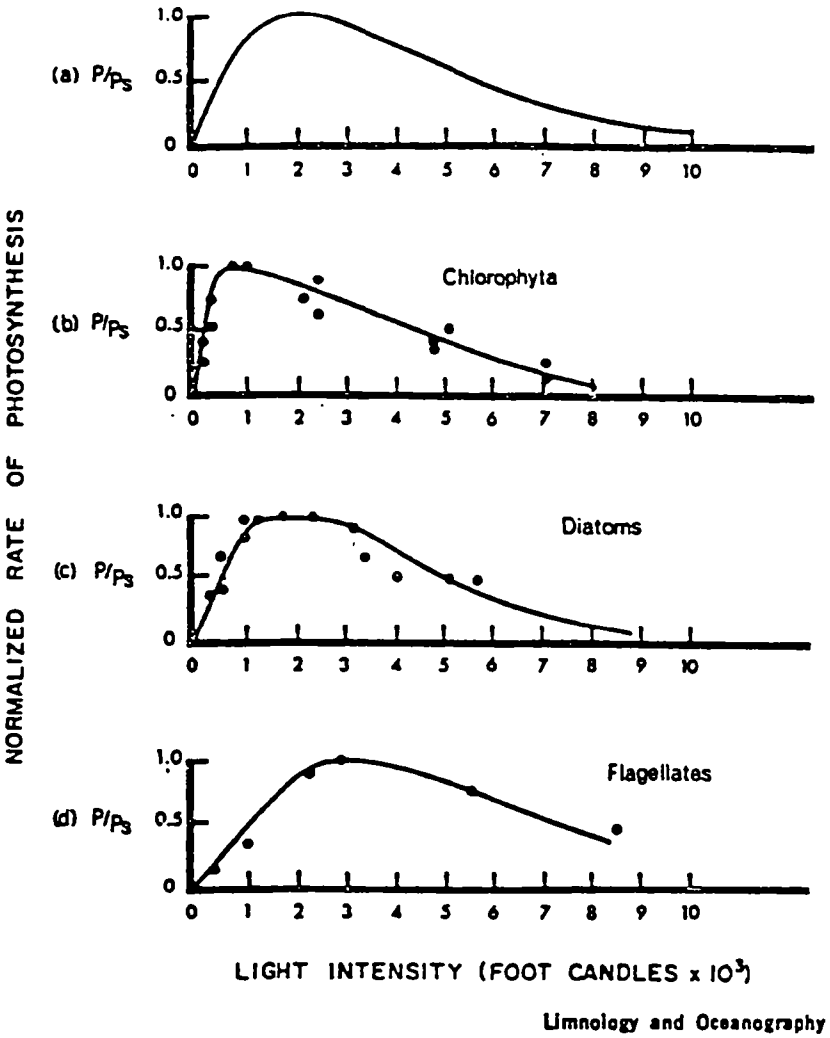

Figure 3. Normalized rate of photosynthesis vs. *incident light intensity: (a) Theoretical curve after Steele* (8); *(b,c,d) Data after Ryther* (28)

These variations approximately follow the shape of Equation 5 for low light intensities but differ for the region of high light intensities, usually by not decreasing after some optimum intensity is reached. In particular, Tamiya *et al.* (*21*) have investigated the growth rate of *Chlorella ellipsoidea* to various light and temperature regimes. The saturated growth rates as a function of temperature are included in Figure 2. The influence of varying light intensity fits the function —

$$F(I) = \frac{I}{I + K'/\alpha} \tag{6}$$

where K' is the saturated growth rate and α is a constant ($\alpha = 0.45$ day^{-1} kilolux^{-1}). However, since K' is a function of temperature, the saturating light intensity for Equation 6 is also a function of temperature. Similar data obtained by Sorokin *et al.* (*26*) using a high-temperature strain of *Chlorella pyrenoidosa* support the temperature-dependence of the satu-

rating light intensity for chlorella. Therefore, in using Equation 5, a temperature-dependent light saturation intensity may be warranted.

At this point in the analysis, the effect of the natural environment on the light available to the phytoplankton must be included. Equation 5 expresses the reduction in the growth rate caused by nonoptimum light intensity. This expression can therefore be used to calculate the reduction in growth rate to be expected at any intensity. However, this is too detailed a description for conservation of mass equations which deal with homogeneous volume elements, V_j, and the growth rate within these elements. What is required is averages of the growth rate over the volume elements.

In order to calculate the light intensity which is present in the volume V_j, the light penetration at the depth of water where V_j is located must be evaluated. The rate at which light is attenuated with respect to depth is given by the extinction coefficient, k_e. That is, at a depth z, the intensity at that depth, $I(z)$, is related to the surface intensity, I_0, by the formula

$$I(z) = I_0 \exp(-k_e z) \tag{7}$$

where $z = 0$ is the water surface and z is positive downward. Thus, the reduction of the saturated growth rate at any depth z resulting from the nonoptimum light intensity present is given by Equation 7, substituted into Equation 5.

$$F[I(z)] = \frac{I_0 e^{-k_e z}}{I_s} \exp\left[\frac{-I_0 e^{-k_e z}}{I_s} + 1\right] \tag{8}$$

To apply this equation to the finite volume elements, within which it is assumed that the phytoplankton concentration is uniform, it is necessary to average this reduction factor throughout the depth of the volume element V_j. Let H_{0j} and H_{1j} be the depths of the surface and bottom, respectively, of the volume element V_j. For example, if the volume element V_j extends from the water surface to the bottom of the water body, then $H_{0j} = 0$ and H_{1j} is the water depth at the location of V_j. For the sake of simplicity, it is assumed that this is the case. If $H_{0j} \neq 0$, a straightforward generalization of the following average is required.

In addition to an average over depth, it is also expedient to average the phytoplankton growth rate over a time interval. Since the time scale within which this analysis is addressed is the week-to-week change in the population over a year, a daily average is appropriate. For simplicity, it is assumed that the incident solar radiation as a function of time over a day is given by the function

$$\begin{aligned} I_o(t) &= I_o \qquad 0 < t < f \\ I_o(t) &= 0 \qquad f < t < 1 \end{aligned} \tag{9}$$

where f is the daylight fraction of the day (*i.e.*, the photo period) and I_a is the average incident solar radiation intensity during the photo period.

Let r_j be the reduction in growth rate attributed to nonoptimum light conditions in volume V_j, averaged over depth and time. Then r_j is given by

$$r_j = \frac{1}{H_j} \int_0^{H_j} \frac{1}{T} \int_0^{f} \frac{I_a e^{-k_{ej}z}}{I_s} \exp\left[\frac{-I_a e^{-k_{ej}z}}{I_s} + 1 \right] dt\, dz \qquad (10)$$

where $T = 1$ day, the time-averaging interval, $H_{1j} = H_j =$ the depth of segment V_j, and k_{ej} is the extinction coefficient in V_j. The result is

$$r_j = \frac{1}{k_{ej}H_j} e^{-\alpha_{1j}} - e^{-\alpha_{0j}} \qquad (11)$$

where

$$\alpha_{1j} = \frac{I_a}{I_s} e^{-k_{ej}H_j} \qquad (12)$$

$$\alpha_{0j} = \frac{I_a}{I_s}$$

The integral given by Equation 10 is a form of an integral used by Steeman Nielson (1952), Talling (1957), and Ryther and Yentsch (1957), as described by Vollenweider (1958) (*30*), and, in particular, Steele (*8*), for the purpose of relating an instantaneous rate (*e.g.*, growth, photosynthesis, etc.) to an average day rate and an average depth rate.

The reduction factor r_j is a function of the extinction coefficient k_{ej} of the volume V. However, the extinction coefficient is a function of the phytoplankton concentration present if their concentration is large. Thus, an important feedback mechanism exists which can have a marked effect on the growth rate of phytoplankton. As the concentration of phytoplankton in a volume element increases, the extinction coefficient, particularly at the green wavelengths, starts to increase. This mechanism is called self-shading. The most straightforward approach to including this effect into the growth rate expression is to specify the extinction coefficient as a function of the phytoplankton concentration

$$k_{ej} = k'_{ej} + h(P_j) \qquad (13)$$

where k'_{ej} is the extinction coefficient attributable to other causes and k_{ej} includes the phytoplankton's contribution. The function $h(P_j)$ has been investigated by Riley (*31*), who found that it can be approximated by

$$h(P_j) = 0.0088\ P_j + 0.054\ P_j^{2/3} \quad (14)$$

where P_j has the units μg/liter chlorophyll$_a$ concentration and h has units m^{-1}. A more recent investigation (*32*) shows that this relationship applies to coastal waters of Oregon for a range in chlorophyll$_a$ concentration of from 0 to 5.0 mg Chl_a/m^3.

A theoretical basis for this relationship is the Beer-Lambert law, which expresses the extinction coefficient in terms of the concentration of light-absorbing material. For dense algal cultures, this law has been experimentally verified (*33*). A similar relationship based on this law has been proposed by Chen (*12*) from the data of Azad and Borchardt (*34*)

$$h(P_j) = 0.17\ P_j \quad (15)$$

For h in m^{-1} and P_j, the phytoplankton concentration is mg/liter of dry weight. This expression gives values comparable with Equation 14 for a reasonable conversion factor for the units involved.

To summarize the analysis to this point, the saturated growth rate K' has been estimated from available data and its temperature dependence established. The reduction to be expected from nonoptimum light intensities has been quantified and used to calculate the reduction in growth rate, r_j, to be expected in each volume element V_j as a function of the extinction coefficient and the depth of the segment. The mechanism of self-shading has been included by specifying the chlorophyll dependence of the extinction coefficient. It remains to evaluate the effect of nutrients on the growth rate.

Nutrients. The effects of various nutrient concentrations on the growth of phytoplankton has been investigated and the results are quite complex. As a first approximation to the effect of nutrient concentration on the growth rate, it is assumed that the phytoplankton population in question follow Monod growth kinetics with respect to the important nutrients. That is, at an adequate level of substrate concentration, the growth rate proceeds at the saturated rate for the temperature and light conditions present. However, at low substrate concentration, the growth rate becomes linearly proportional to substrate concentration. Thus, for a nutrient with concentration N_j in the j^{th} segment, the factor by which the saturated growth rate is in the j^{th} segment reduced is: $N_j/(K_m + N_j)$. The constant, K_m, which is called the Michaelis or half saturation constant, is the nutrient concentration at which the growth rate is half the saturated growth rate. There exists an increasing body of experimental evidence to support the use of this functional form for the dependence of the growth rate on the concentration of either phosphate (*35*), nitrate, or ammonia (*36*) if only one of these nutrients is in short supply. An

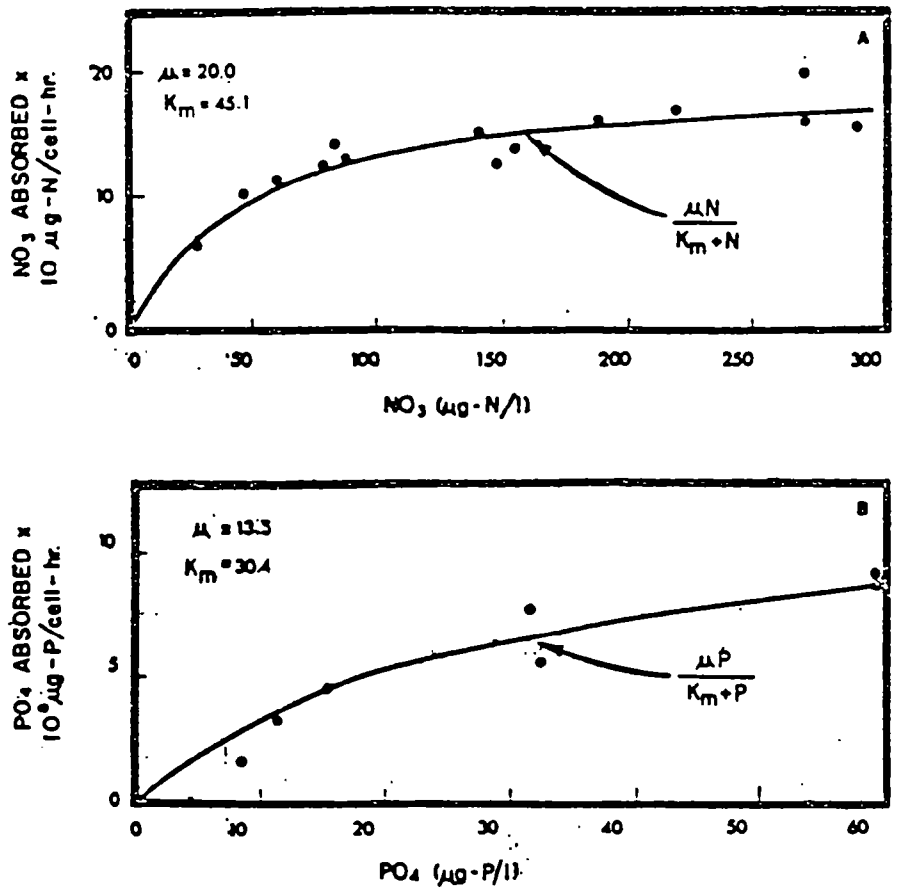

Figure 4. Nutrient absorption rate as a function of nutrient concentration: comparison of Michaelis Menton theoretical curve with data from Ketchum (37)

example of this behavior, using the data from Ketchum (37), is shown in Figure 4a for the nitrate uptake rate as a function of nitrate concentration and in Figure 4b for the phosphate uptake as a function of phosphate concentration. These results are from batch experiments. Similar results from chemostat experiments, which seem to be more suitable but more lengthy for this type of analysis, have also been obtained. Table II is a listing of measured and estimated Michaelis constants for ammonia, nitrate, and phosphate. The estimates are obtained by taking one-third the reported saturation concentration of the nutrients. These measurements and estimates indicate that the Michaelis constant for phosphorus is approximately 10 μg P/liter and for inorganic nitrogen forms in the range from 1.0 to 100 μg N/liter, depending on the species and its previous history.

The data on the effects of the concentration of other inorganic nutrients on the growth rate is less complete. Since algae use carbon dioxide as their carbon source during photosynthesis, this is clearly a nutrient which can reduce the growth rate at low concentrations (43). Reported saturation concentration for Chlorella is $< 0.1\%$ atm (24).

The silicate concentration is a factor in the growth rate of diatoms for which it is an essential requirement. The saturated growth rate concentration is in the range of 50–100 μg Si/liter (*17*).

There are a large number of trace inorganic elements which have been implicated in the growth processes of algae, among which are iron [for which a Michaelis constant of 5 μg/liter for reactive iron has been reported (39)], manganese, calcium, magnesium, and potassium (*18*). However, the significance of these elements in the growth of phytoplankton in natural waters is still unclear. Trace organic nutrients have also been shown to be necessary for most species of algae: 80% of the strains studied require vitamin B_{12}, 53% require thiamine, and 10% require biotin (*44*). Presumably, these nutrients are available in sufficient quantities in natural waters so that their concentration does not appreciably affect the growth rate.

In the preceeding discussion of nutrient influences on the growth rate, it is tacitly assumed that only one nutrient is in short supply and all the other nutrients are plentiful. This is sometimes the case in a natural body of water. However, it is also possible that more than one nutrient is in short supply. The most straightforward approach to formulating the growth rate reduction caused by a shortage of more than one nutrient is to multiply the saturated growth rate by the reduction factor for each nutrient. This approach has also been suggested by Chen (*12*).

Table II. Michaelis Constants for Nitrogen and Phosphorus

Ref.	*Organism*	*Nutrient*	*Michaelis Constant, μg/Liter as N or P*
38	*Chaetoceros gracilis* (marine diatom)	PO_4	25
39	*Scenedesmus gracile*	total N	150
		total P	10
40	Natural association	PO_4	6[a]
	Microcystis aeruginosa (blue-green)	PO_4	10[a]
41	*Phaeodactylum tricornutum*	PO_4	10
36	Oceanic species	NO_3	1.4–7.0
	Oceanic species	NH_3	1.4–5.6
36	Neritic diatoms	NO_3	6.3–28
	Neritic diatoms	NH_3	7.0–120
36	Neritic or littoral Flagellates	NO_3	8.4–130
		NH_3	7.0–77
42	Natural association Oligotrophic	NO_3	2.8
		NH_3	1.4–8.4
42	Natural association Eutrophic	NO_3	14
		NH_3	18

[a] Estimated.

As an example, the data from Ketchum (37) for the rate of phosphate absorption as a function of both phosphate and nitrate concentration can be satisfactorily fit with a product of two Michaelis–Menton expressions. The resulting fit, obtained by a multiple nonlinear regression analysis, is shown in Figure 5. The Michaelis constants that result are 28.4 μg NO_3–N/liter and 30.3 μg PO_4–P/liter, with a saturated absorption rate of 15.1×10^{-8} μg PO_4–P/cell-hr. This approximation to the growth rate behavior as a function of more than one nutrient must be regarded as only a first approximation, however, since the complex interaction reported between the nutrients is neglected.

The result of the above investigation is the following growth rate expression. For the case of one limiting nutrient, N, with Michaelis constant K_m, the growth expression for the rate in the j^{th} segment is

$$G_{Pj} = K_1 T_j \left(\frac{2.718 f}{k_{ej} H_j} \left(e^{-\alpha_{1j}} - e^{-\alpha_{0j}} \right) \right) \left(\frac{N_j}{K_m + N_j} \right) \qquad (16)$$

in which Equations 4 and 11 have been combined. This is the functional

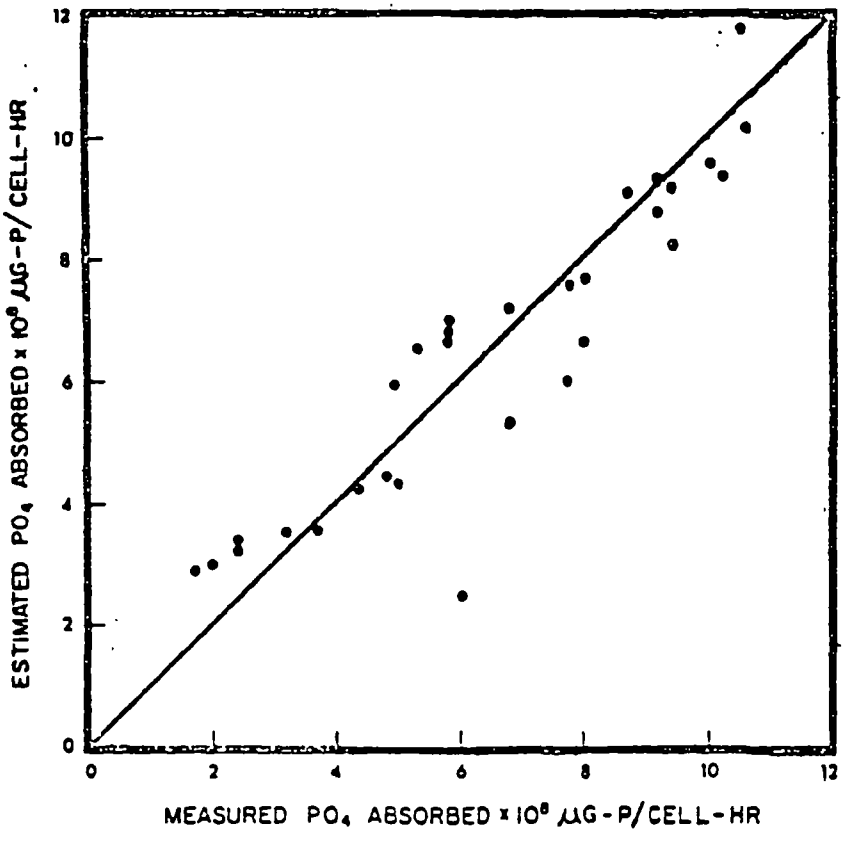

Figure 5. Measured phosphate absorption rate, after Ketchum (37), vs. phosphate absorption rate estimated using $\mu N_1 N_2 / (K_{m1} + N_1)(K_{m2} + N_2)$ *where* N_1 *and* N_2 *are the nitrate and phosphate concentrations, respectively*

form that is used subsequently in the applications of these equations to natural phytoplankton populations.

Comparisons with Other Growth Rate Expressions

The most extensive investigation of the relationship between the growth rate of natural phytoplankton populations and the significant environmental variables, within the context of phytoplankton models, is that of Riley *et al.* (1949) (5). The expression which results from their work is

$$\log\left[\frac{G_P}{K'I_0 - G_P}\right] = 22.884 + \log \nu_p - \log I_0 - \frac{6573.8}{T'} \tag{17}$$

where G_P is the growth rate (day^{-1}), $K' = 7.6$, I_0 = average daily incident solar radiation (ly/min), T' = temperature in °K, and ν_p is the nutrient reduction factor for phosphate concentration, N_P, defined as

$$\nu_p = 1.0 \qquad N_P > 0.55 \text{ mg-at}/m^3 \tag{18}$$

$$\nu_p = (0.55)^{-1}N_P \qquad N_P < 0.55 \text{ mg-at}/m^3$$

In order to compare this expression with that in the previous section, let the nutrient reduction factor be replaced by a Michaelis–Menton expression.

$$\nu_p = \frac{N_p}{K_{mp} + N_p} \tag{19}$$

where K_{mp} is the Michaelis constant for phosphate. To be comparable with Equation 16, K_{mp} should equal approximately 0.20 mg-at/m³ (6.2 mg P/m³). Using Equation 19 for ν_p, the growth rate expression becomes

$$G_P = K'I_0\left[\frac{\tau_l(T)}{\tau_l(T) + I_0}\right]\left[\frac{N_P}{K_m\left[\frac{I_0}{\tau_l(T) + I_0}\right] + N_p}\right] \tag{20}$$

where

$$\log_{10} \tau_l(T) = \frac{22.9\ (T) - 336.4}{T + 273} \tag{21}$$

and T is temperature in degrees centigrade. To compare this expression with that proposed in the previous section, consider first the nutrient saturated growth rate as a function of solar radiation intensity and temperature. The equations are compared in Figure 6a as a function of total daily solar radiation for three temperatures. The dotted line is Equation

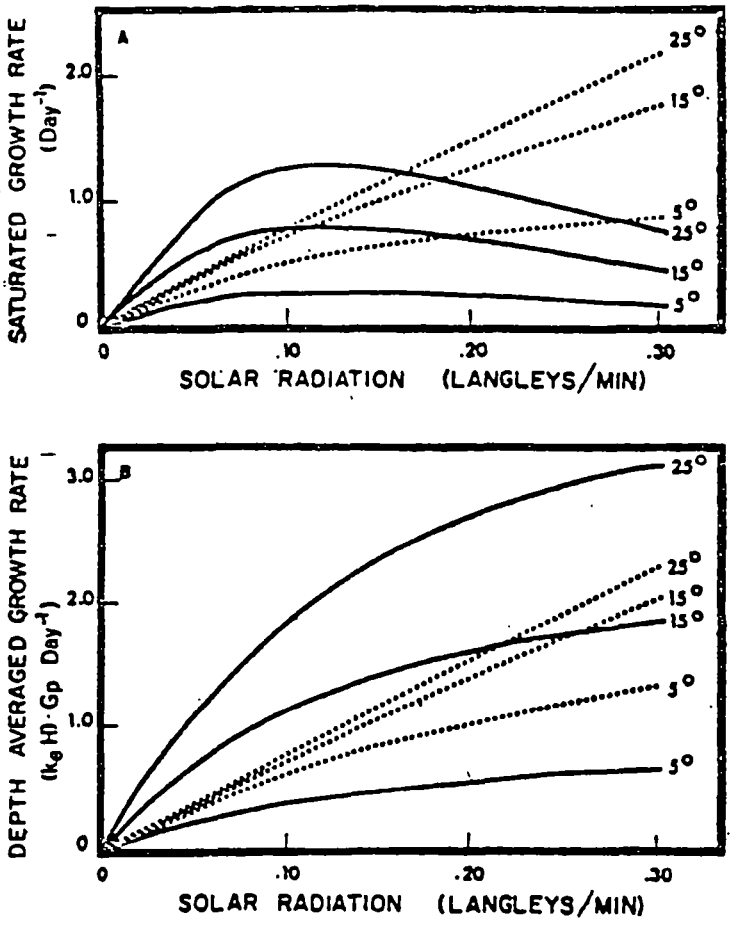

Figure 6. Comparison of phytoplankton growth rates as a function of incident solar radiation intensity and temperature

20, and the solid line is the product of Equations 4 and 5. The rate expressions are comparable, although two differences are apparent. In Riley's expression the effect of temperature is less pronounced in the 15° to 25°C range, and the effect of higher daily average solar radiation intensities is opposite (*i.e.*, tends to increase the rate) to that of Equation 5 based on Steele's expression. The growth rate equations averaged over depth are compared in Figure 6b. The depth average rate resulting from Riley's expression is

$$G_P = \frac{K'\tau_i(T)}{k_e H} \ln [1 + I_0/\tau_i(T)] \qquad (22)$$

which is compared with Equation 16. The differences are now more pronounced. In particular, the higher growth rates at lower light intensities given by Equation 16 are reflected in the increased depth average growth rate. This is not unexpected since the majority of the population is exposed to lower light levels at the lower depths. Also, the dependence

on temperature is quite different, being linear in the case of Equation 16 but practically suppressed in Equation 22.

An interesting feature of Riley's Equation 20 is the multiplication of the Michaelis constant by an expression which depends on temperature and light intensity. The effect is to lower the Michaelis constant at high temperatures and at high light intensity levels, which seems to be a reasonable behavior for a phytoplankton population.

More elementary growth rate formulations have been proposed which do not span the range of conditions attempted in Equations 16 and 20. In particular, a common proposal is to make the growth rate linearly proportional to the various environmental variables. For example, Davidson and Clymer (1966) (9) assumed that the growth rate is proportional to phosphate concentration and photo period and a temperature factor given by $\exp\,[-(T - 18)^2/18]$. This temperature factor is quite different from all others proposed and greatly magnifies the effect of temperature on the growth rate. For example, at $T = 18°C$, the factor equals 1.0, whereas at $T = 9°C$, the factor drops to 0.01, a 100-fold decrease, compared with approximately a 2-fold decrease predicted by Equations 16 and 20. This exaggerated effect seems to be unrealistic.

A complete investigation of the environmental influences on the growth rate is still to be made. In particular, it has been emphasized that there is an interaction between nitrogen and phosphorus limitations as well as other effects which influence the phytoplankton growth rate. Also, these effects are different for differing species. The species-dependent effects are important in the problem of the seasonal succession of phytoplankton species.

For any particular application, it is advisable to investigate the growth rate of the already-existing population, as the resulting expression may differ significantly from the general over-all behavior as described by Equations 16 and 20. Also, in dealing with natural associations of species of phytoplankton, the various constants which result from such an investigation can be considered to be averages over the population, and so they represent in some average way the population behavior as a whole.

Phytoplankton Death Rate

Numerous mechanisms have been proposed which contribute to the death rate of phytoplankton: endogenous respiration rate, grazing by herbivorous zooplankton, a sinking rate, and parasitization (27). The first three mechanisms have been included in previous models for phytoplankton dynamics, and they have been shown to be of general importance.

Endogenous Respiration. The endogenous respiration rate of phytoplankton is the rate at which the phytoplankton oxidize their organic carbon to carbon dioxide per unit weight of phytoplankton organic carbon. Respiration is the reverse of the photosynthesis process and as such contributes to the death rate of the phytoplankton population. If the respiration rate of the population as a whole is greater than the photosynthesis or growth rate, there is a net loss of phytoplankton carbon, and the population biomass is reduced in size. The respiration rate as a function of temperature has been investigated, and some measurements are presented in Figure 7 and Table III. A straight line seems to give an adequate fit of the data; that is, Respiration Rate $= K_2T$. For the respiration rate in days^{-1} and T in °C, the value of K_2 is in the range 0.005 ± 0.001. The lack of any more precise data precludes exploring the respiration rate's dependence on other environmental variables. However, an important interaction has been suggested by Lund (*18*). During nutrient-depleted conditions, "many algae pass into morphological or physiological resting stages under such unfavorable conditions. Resting stages are absent in *Asterionella formosa*, and this is why a mass death occurs in the nutrient-depleted epilimnion after the vernal maximum." In terms of the respiration rate, the resting stage corresponds to a lowering of the respiration rate as the nutrient concentrations decrease. Thus, a Michaelis–Menton expression for the respiration rate nutrient dependence may also be required, and this dependence should be investigated experimentally. This mechanism is quite significant from a water quality point of view since the deaths of algae after a bloom is of primary concern in protecting

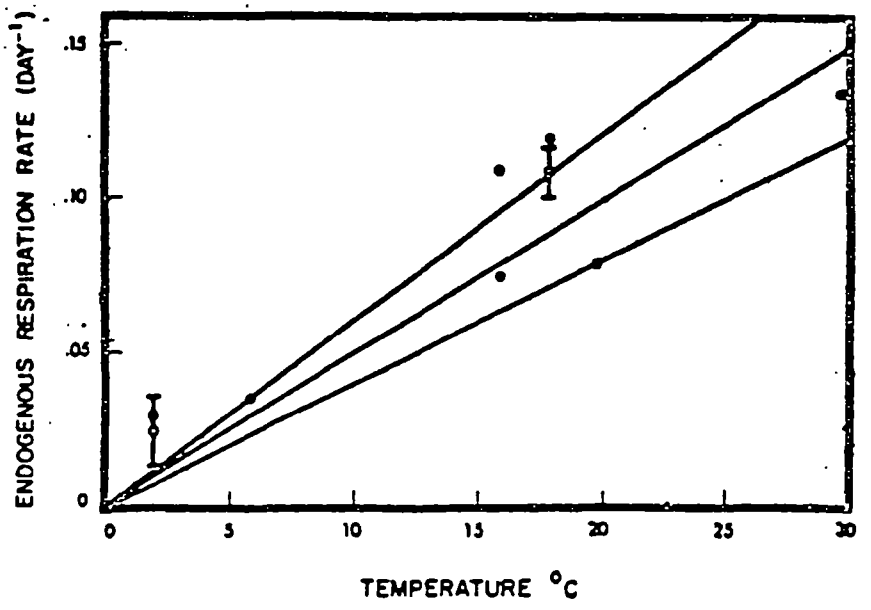

Figure 7. Endogenous respiration rate of phytoplankton vs. temperature; after Riley (5)

Table III. Endogenous Respiration Rates of Phytoplankton (5)

Organism	*Temperature, °C*	*Endogenous Respiration Rate, Day^{-1} (Base$_e$)*
Nitzschia closterium	6	0.035
	35	0.170
Nitzschia closterium	20	0.08
Coscinodiscus excentricus	16	0.075
	16	0.11
Natural association	2	0.03
	18	0.12
	2.0	0.024 ± 0.012
	17.9	0.110 ± 0.007

the quality of natural bodies of water. The resulting mass of dead algal cells becomes a sink of dissolved oxygen which can dangerously lower the available oxygen for fish and other aquatic animals.

Grazing by Zooplankton. The interaction between the phytoplankton population and the next trophic level, the herbivorous zooplankton, is a complex process for which only a first approximation can be given. A basic mechanism by which zooplankters feed is by filtering the surrounding water and clearing it of whatever phytoplankton and detritus is present. Thus, the presence of zooplankton contribute to the death rate of phytoplankton since many species of zooplankton prey on phytoplankton as a food source. The filtering or grazing rate of some species of zooplankton have been measured and are presented in Table IV. The grazing rate is sometimes reported as a volume of water filtered per unit time per individual. In order to be applicable to a natural zooplankton population consisting of differing species, these grazing rates are converted to a filtering rate per unit biomass of zooplankton and denoted by C_g. A convenient biomass unit for zooplankton concentration is their dry weight. As can be seen from Table IV, the resulting values of C_g vary considerably. This variation is not unexpected since the measurement of grazing rates of zooplankters is a difficult procedure and subject to large variations in the estimates.

Variations of the filtering rate with temperature change have been reported (*47*). Examples of this variation are presented in Figure 8 for four species of genus *Daphnia*, a small crustacea (*49*); two species of *Acartia* (*52*); and two species of *Centropages* (*47*), both copepods. The copepods show a marked grazing rate temperature-dependence while the grazing rates of the Daphnia do not vary as markedly. The filtering rate also varies as a function of the size of the phytoplankton cell being ingested (*53*), the concentration of phytoplankton (*51*), and the amount of particulate matter present (*54*). Selective grazing of certain phytoplankton species has also been reported (*49*). The complexity of this

aspect of phytoplankton mortality is such that the use of one grazing coefficient to represent the process must be viewed as a first approximation. However, since this mathematical expression does represent a physiological mechanism that has been investigated and for which reported values of C_g are available, this approximation is a realistic first step. Also, it is difficult to see, aside from refinements as to temperature and phytoplankton concentration dependence, what further improvements could be made in the formulation so long as the phytoplankton and zooplankton population are represented by a biomass measurement which ignores the species present and their individual characteristics. For simplicity in this investigation, the grazing rate is assumed to be a constant. The death rate of phytoplankton resulting from the grazing of zooplankton is given by the expression $C_g Z_j$, where Z_j is the concentration of herbivorous zooplankton biomass in the j^{th} volume element.

For models of the phytoplankton populations in coastal oceanic waters and in lakes, the sinking rate of phytoplankton cells is an important contribution to the mortality of the population. The cells have a net downward velocity, and they eventually sink out of the euphotic zone to the bottom of the water body. This mechanism has been investigated and included in phytoplankton population models (*5*, *12*). However, for the application of these equations to a relatively shallow vertically well mixed river or estuary, the degree of vertical turbulence is sufficient to eliminate the effect of sinking on the vertical distribution of phytoplankton.

Table IV. Grazing Rates of Zooplankton

Ref.	*Organism*	*Reported Grazing Rate*	*Grazing Rate, Liter/Mg Dry Wt.-Day*
	Rotifer		
16	*Brachionus calyciflorus*	0.05–0.12[a]	0.6–1.5
	Copepod		
5	*Calanus sp.*	67–208[b]	0.67–2.0
45	*Calanus finmarchicus*	27[a]	0.05
46	*Rhincalamus nasutus*	98–670[a]	0.3–2.2
47	*Centropages hamatus*		0.67–1.6
	Cladocera		
48	*Daphnia sp.*		1.06
49	*Daphnia sp.*		0.2–1.6
50	*Daphnia magna*	81[a]	0.74
51	*Daphnia magna*	57–82[a]	0.2–0.3
	National Association		
5	Georges Bank	80–110[b]	0.8–1.10

[a] Ml/ animal-day.
[b] Ml/mg wet wt-day.

Therefore, considering only the phytoplankton respiration and the predation by zooplankton, the death rate of phytoplankton is given by the equation

$$D_{Pj} = K_2 T + C_u Z_j \qquad (23)$$

and for a zooplankton biomass concentration Z_j, the mortality rate can be calculated from this equation.

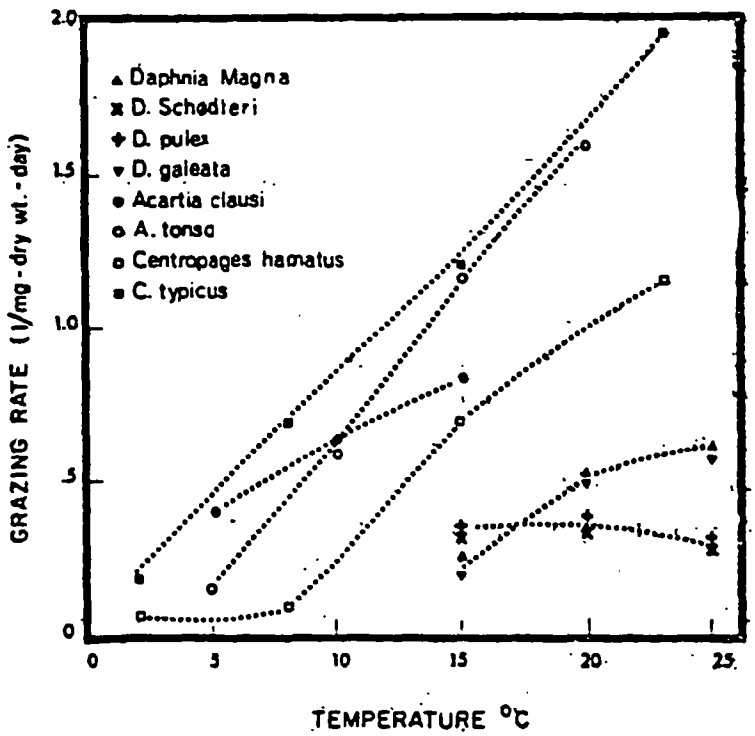

Figure 8. Grazing rates of zooplankton vs. temperature

This completes the specification of the growth and death rates of the phytoplankton population in terms of the physical variables: light and temperature, the nutrient concentrations, and the zooplankton present. With these variables known as a function of time, it is possible to calculate the phytoplankton population resulting throughout the year. However, the zooplankton population and the nutrient concentrations are not known *a priori* since they depend on the phytoplankton population which develops. That is, these systems are interdependent and cannot be analyzed separately. It is therefore necessary to characterize both the zooplankton population and the nutrients in mathematical terms in order to predict the phytoplankton population which would develop in a given set of circumstances.

The Zooplankton System

As indicated in the previous section, the zooplankton population exerts a considerable influence on the phytoplankton death rate by its feeding on the phytoplankton. In some instances, it has been suggested that this grazing is the primary factor in the reduction of the concentration of phytoplankton after the spring bloom. In the earlier attempts to model the phytoplankton system, the measured concentration of zooplankton biomass was used to evaluate the phytoplankton death rate resulting from grazing. However, it is clear that the same arguments used to develop the equation for the conservation of phytoplankton biomass can be applied directly to the zooplankton system. In particular, the source of zooplankton biomass S_{zj} within a volume element V_j can be given as the difference between a zooplankton growth rate G_{zj} and a zooplankton death rate D_{zj}. Thus, the equation for the source of zooplankton biomass, which is analogous to Equation 3, is

$$S_{zj} = (G_{zj} - D_{zj})Z_j \tag{24}$$

where G_{zj} and D_{zj} have units day^{-1} and Z_j is the concentration of zooplankton carbon in the volume element V_j. The magnitude of the growth rate in comparison with the death rate determines whether the net rate of zooplankton biomass production in V_j is positive, indicating net growth rate, or negative, indicating a net death rate.

As in the case of the phytoplankton population, the growth and death rates, and in fact the whole life cycle of individual zooplankters, are complicated affairs with many individual peculiarities. The surveys by Hutchinson (*16*) and Raymont (*19*) give detailed accounts of their complex biology. It is, however, beyond the scope of this paper to summarize all the differences and species-dependent attributes of the many zooplankton species. The point of view adopted is macroscopic, with the population characterized in units of biomass. The resulting growth and death rates can be thought of as averages over the many species present. These simplifications are made in the interest of providing a model which is simple enough to be manageable and yet representative of the over-all behavior of the populations.

Growth Rate. The grazing mechanism of the zooplankton provides the basis for the growth rate of the herbivorous zooplankton, G_{zj}. For a filtering rate C_p, the quantity of phytoplankton biomass ingested is C_pP_j, where P_j is the phytoplankton biomass concentration in V_j. To convert this rate to a zooplankton growth rate, a parameter which relates the phytoplankton biomass ingested to zooplankton biomass produced, a utilization efficiency, a_{zp}, is required. However, this utilization efficiency or yield coefficient is not a constant. At high phytoplankton concentra-

tions, the zooplankton do not metabolize all the phytoplankton that they graze, but rather they excrete a portion of the phytoplankton in undigested or semidigested form (55). Thus, utilization efficiency is a function of the phytoplankton concentration. A convenient choice for this functional relationship is $a_{ZP}K_{mP}/(K_{mP} + P_j)$ so that the growth rate for the zooplankton population is

$$G_{Z_j} = a_{ZP}C_g K_{mP}\left(\frac{P_j}{K_{mP} + P_j}\right) \tag{25}$$

The resulting growth rate has the same form as that postulated for the nutrient—phytoplankton relationship, namely, a Michaelis–Menton expression with respect to phytoplankton biomass. In fact, the argument which is used to justify its use in Equation 16 can be repeated in this context. The difference is that in this case the substrate or nutrient is phytoplankton biomass, and the microbes are the zooplankton. The Michaelis constant K_{mP} is the phytoplankton biomass concentration at which the growth rate G_{Zj} is one-half the maximum possible growth rate $a_{ZP}C_g K_{mP}$. The fact that at high phytoplankton concentrations the zooplankton growth rate saturates was incorporated by Riley (1947) (55) in the first model proposed for a zooplankton population.

The assimilation efficiency of the zooplankton at low phytoplankton concentrations, a_{ZP}, which is the ratio of phytoplankton organic carbon utilized to zooplankton organic carbon produced has been estimated by Conover (56) for a mixed zooplankton population. The results of 26 experiments gave an average of 63% and a standard deviation of 20%. Other reported values are within this range. Experimental values for K_{mP}, which in effect set the maximum growth rate of zooplankton, are not available and would probably be highly species-dependent. Perhaps a more effective way of estimating K_{mP} is first to estimate the maximum growth rate at saturating phytoplankton concentrations, $a_{ZP}C_g K_{mP}$, and then calculate K_{mP}. Growth rates for copepods through their life cycle average 0.18 day^{-1} (46). For the Georges Bank population, Riley used 0.08 day^{-1} (55) for the maximum zooplankton growth rate. For a value of the grazing coefficient C_g of 0.5 liter/mg-dry wt-day and an assimilation coefficient of 65%, the Michaelis constant for zooplankton assimilation, K_{mP}, ranges between 0.25 and 0.55 mg-dry wt/liter of phytoplankton biomass. However, these values should only be taken as an indication of the order of magnitude of K_{mP}. It is probable that its value can vary substantially in different situations.

The fact that the growth rate reaches a maximum or saturates is an important feature of the formulation of the zooplankton growth rate since

in some cases the phytoplankton concentration during part of the year exceeds that which the zooplankton can effectively metabolize. If the zooplankton growth rate is not limited in some way and, instead, is assumed simply to be proportional to the phytoplankton concentration, as proposed in simpler models, the resulting zooplankton growth rate during phytoplankton blooms can be very much larger than is physiologically possible for zooplankton, an unrealistic result. The saturating growth rate also has implications in the mathematical properties of the resulting equations. In particular, the behavior differs significantly from the classical Volterra Preditor–Prey equations (57). This is discussed further in a subsequent section.

The growth of the zooplankton population as a whole, of which the herbivorous zooplankton are a part, is complicated by the fact that some zooplankters are carnivorous or omnivorous. Thus, the nutrient for the total population should include not only phytoplankton but also organic detritus as a food source since this is also available to the grazing zooplankton. However, for cases where the phytoplankton are abundant and the growth rate saturates for the significant growing periods, the simplification introduced by ignoring the detritus is probably acceptable.

Death Rate. The death rate of herbivorous zooplankton is thought to be caused primarily by the same mechanisms that cause the death of the phytoplankton, namely, endogeneous respiration and predation by higher trophic levels. The endogeneous respiration rate of zooplankton populations has been measured and the results of some of these experiments are presented in Figure 9 and Table V.

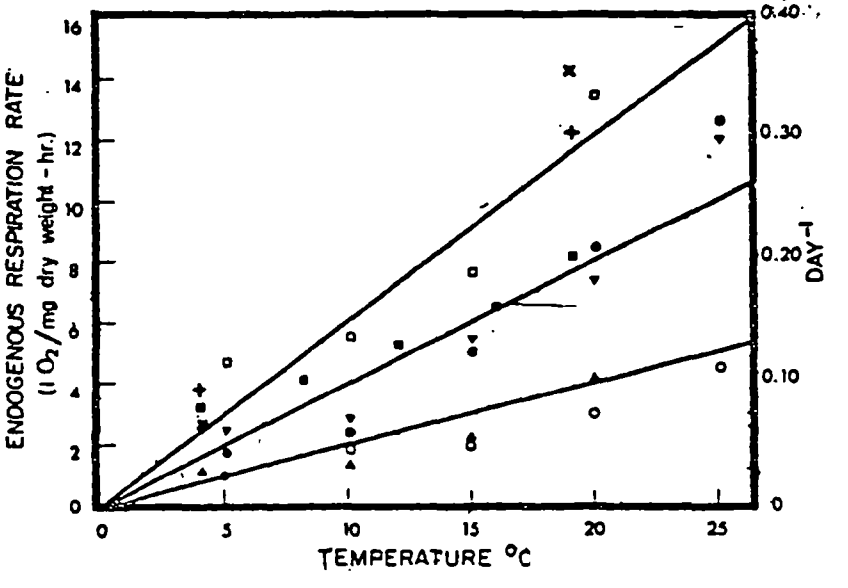

Figure 9. Endogenous respiration rate of zooplankton vs. temperature

Table V. Endogenous Respiration Rate of Zooplankton

Ref.	*Organism*	*Plotting Symbol*	*Temp., °C*	*Respiration Rate, Ml O_2/Mg Dry Wt-Day*
58	Cladocerans	×	18	14.2
			4	2.7
58	Copepods	+	18	12.2
			4	3.8
58	Copepods	■	18	8.2
			16	6.5
			12	5.2
			8	4.1
			4	3.4
1	*Calanus finmarchicus*	▲	20	4.2
			15	2.3
			10	1.4
			4	1.3
59	*Diaptomus leptopus*	▼	25	12.1
			20	7.4
			15	5.3
			10	2.8
			5	2.5
59	*D. clavipes*	●	25	12.5
			20	8.5
			15	5.1
			10	2.4
			5	1.8
59	*D. siciloides*	□	25	21
			20	13.5
			15	7.8
			10	5.5
			5	4.8
59	*Diaptomus sp.*	○	25	4.3
			20	3.0
			15	2.1
			10	1.7
			5	1.1

It is clear from these measurements that the respiration rate of zooplankters is temperature-dependent. It is also dependent on the weight of the zooplankter in question and its life cycle stage (59). As a first approximation, a straight line dependence is adequate, and the endogeneous respiration rate is given by the equation: respiration rate = K_3T where $K_3 = 0.2 \pm 0.1$ (day °C)$^{-1}$. The conversion from the reported units to a death rate is made by assuming that 50% of the zooplankton

dry weight represents the carbon weight and that carbohydrate (CH_2O) is being oxidized. The data are somewhat variable and serve only to establish a range of values within which the respiration rate of a natural zooplankton association might be expected.

The death rate attributed to predation by the higher trophic levels, specifically the carnivorous zooplankton, has been considered by previous models in a more or less empirical way. The complication resulting from another equation and the uncertainty as to the mechanisms involved are quite severe at this trophic level. In particular, it is probable that an equation for organic detritus is necessary to describe adequately the available food. Hence, it is expedient to break the causal chain at this point and assume that the herbivorous zooplankton death rate resulting from all other causes is given by a constant, the magnitude of which is to be determined empirically. The severity of this assumption can be tested by examining the sensitivity of the solutions of the phytoplankton and zooplankton equations to the magnitude of this constant. Hence, the resulting zooplankton death rate is given by

$$D_{Zj} = K_3 T + K_4 \tag{26}$$

where K_4 is empirically determined.

With the growth and death rates given by Equations 25 and 26, respectively, the source term for herbivorous zooplankton biomass is given by Equation 24. The conservation of mass equation which describes the behavior of Z_j is given by Equation 2, with Z_j as the dependent variables replacing P_j and S_{Zj} replacing S_{Pj} as the source terms.

This completes the formulation of the equations which describe the zooplankton system. The equations for the nutrient system remain to be formulated.

The Nutrient System

The conservation of mass principle is applied to the nutrients being considered in the same way as it has been previously applied to the phytoplankton and zooplankton biomass within a volume segment. The number of mass conservation equations required is equal to the number of nutrients that are explicitly included in the growth rate formulation for the phytoplankton. For the sake of simplicity, the formulation for only one nutrient is discussed below.

The source term S_{Nj} in the conservation of mass equation for the concentration of the nutrient N_j in the j^{th} volume segment V_j is the sum of all sources and sinks of the nutrient within V_j. The primary interaction between the nutrient system and the phytoplankton system is the reduction or sink of nutrient connected with phytoplankton growth. The rate

of increase of phytoplankton biomass is $G_{Pj}P_j$. To convert this assimilation rate to the rate of utilization of the nutrient, the ratio of biomass production to net nutrient assimilated is required. Over a long time interval, this ratio approximates the nutrient-to-biomass ratio of the phytoplankton population. For example, if the nutrient being considered is total inorganic nitrogen and the phytoplankton biomass is characterized in terms of dry weight, then this ratio is the nitrogen-to-dry-weight ratio of the population. For both nitrogen and phosphorus, these ratios have been studied for a number of phytoplankton species and natural associations. An example of this information is presented in Table VI, condensed from Strickland (*17*). If a_{NP} is the nutrient-to-phytoplankton biomass ratio of the population, then the sink of the nutrient owing to phytoplankton growth is $a_{NP}G_{Pj}P_j$.

A secondary interaction between the biological systems and the nutrient systems is the excretion of nutrients by the zooplankton and the release of nutrients in an organic form by the death of phytoplankton and zooplankton. The excretion mechanism has been considered by Riley

Table VI. Dry Weight Percentage[a] of Carbon, Nitrogen, and Phosphorus in Phytoplankton[b]

	% Carbon		% Nitrogen		% Phosphorus	
Phytoplankter	*Average*	*Range*	*Average*	*Range*	*Average*	*Range*
Myxophyceae	36	(28–45)	4.9	(4.5–5.8)	1.1	(0.8–1.4)
Chlorophyceae	43	(35–48)	7.8	(6.6–9.1)	2.9	(2.4–3.3)
Dinophyceae	43	(37–47)	4.4	(3.3–5.0)	1.0	(0.6–1.1)
Chrysophyceae	40	(35–45)	8.4	(7.8–9.0)	2.1	(1.2–3.0)
Bacillariophyceae	33	(19–50)	4.9	(2.7–5.9)	1.1	(0.4–2.0)

[a] The units are (mg of carbon, nitrogen, or phosphorus)/(mg dry weight of phytoplankton) × 100%.
[b] Condensed from Strickland (*17*).

(*40*) in a generalization of the equations of Steele. The rate of phosphorus excretion has also been measured experimentally (*60*). Using the formulation for zooplankton growth rate proposed herein, the rate of nutrient excretion is the rate grazed, $a_{NP}C_gP_jZ_j$, minus the rate metabolized, $a_{NP}G_{Zj}Z_j$; that is, the excretion rate is

$$a_{NP}C_gZ_jP_j\left(1 - \frac{a_{ZP}K_{mP}}{K_{mP} + P_j}\right) \tag{27}$$

At high phytoplankton concentrations, almost all the grazed phytoplankton is excreted since the bracketed term in Equation 27 approaches unity.

There is a difficulty, however, in using this term directly as a source of nutrient. To illustrate this difficulty, assume that the nutrient is inor-

ganic nitrogen. A part of the excreted nitrogen, however, is in organic form, and a bacterial decomposition into the inorganic forms must precede utilization by the phytoplankton. The same is true for the nutrient released by the death of phytoplankton, $a_{NP}K_2TP_j$, and that released by the death of zooplankton, $a_{NZ}K_3TZ_j$, where a_{NZ} is the nutrient-to-zooplankton biomass ratio. Therefore, strictly speaking, a conservation of mass equation for the organic form of the nutrient is required. The organic form is then converted to the inorganic form. For the case of nitrogen, the kinetics of this conversion have been investigated and applied to stream and estuarine situations (*13*). If the conversion rate is large by comparison with the other rates in the phytoplankton and zooplankton equations, then the direct inclusion of these sources is approximatey correct.

The sources of nutrients arising from man-made inputs, such as wastewater discharges and agricultural runoff, are included explicitly into the source term since these sources are usually the major control variables available to influence the biological systems. An extensive review of the magnitude and relative importance of these sources of nutrients, primarily nitrogen and phosphorus, has recently been made (*61*). A useful distinction is made between diffuse sources such as agricultural runoff loads and ground water infiltration, which are difficult to measure and control, and point sources such as wastewater discharges from municipal and industrial sources, for which more information is available. The nitrogen and phosphorus loads from agricultural runoff are quite variable and depend on many variables such as soil type, fertilizer application, rainfall, and irrigation practice. The nutrient sources from point loads can be estimated more directly. For example, the nutrient load from biologically treated municipal wastewater is in the order of 10 g/capita-day total nitrogen and 2 g/capita-day total phosphorus. The ratio of per capita phosphorus to physiologically-required phosphorus is approximately 2 to 3, the excess being primarily the result of detergent use. Industrial loads can also be important, especially effluents from food processing industries. If the required loading rates are available, their loads should be included in the nutrient mass balance equations. In particular, if the investigation of the phytoplankton population is directed at the probable effects of increasing or decreasing the nutrient load, these loads must be explicitly identified and their magnitude assessed.

Let W_{Nj} be the rate of addition of the nutrient to the j^{th} volume element. This source is then included as a component in the nutrient source term in the mass balance equation.

An important additional source of inorganic nutrients which may influence the availability of nutrients is the interaction of the overlying

water either with the underlying mineral strata if exposed or with whatever sediment is present. These interactions can complicate the source term but they should be included if they add significantly to the available nutrient.

The source term which results from the inclusion of the phytoplankton utilization sink, the zooplankton excretion and the mortality sources, and the man-made additions is

$$S_{Nj} = \frac{W_{Nj}}{V_j} - a_{NP}G_{Pj}P_j + a_{NP}C_0Z_jP_j\left(1 - \frac{a_{ZP}K_{mP}}{K_{mP} + P_j}\right) + a_{NP}K_2TP_j + a_{NZ}K_3TZ_j \tag{28}$$

Any additional sources and sinks that contribute can be added to the source term as needed. With the source term formulated, the conservation of nutrient mass equation is given by Equation 2 with N_j as the dependent variable replacing P_j and S_{Nj} replacing S_{Pj}.

The Equations of the Model

In the previous sections, the equations for phytoplankton and zooplankton biomass and nutrient concentration within one volume element have been formulated. The resulting equations are an attempt to describe the kinetics of the growth and death of the phytoplankton and zooplankton populations and their interaction with the nutrients available. The form of the equations for the volume V_j are as follows:

$$\dot{P}_j = [G_{Pj}(P_j, N_j, t) - D_{Pj}(Z_j, t)]P_j + S_{Pj}(P_j, Z_j, N_j, t) \tag{29}$$

$$\dot{Z}_j = [G_{Zj}(P_j, t) - D_{Zj}(t)]Z_j + S_{Zj}(P_j, Z_j, t) \tag{30}$$

$$\dot{N}_j = S_{Nj}(P_j, Z_j, t) \tag{31}$$

where G_{Pj} and D_{Pj} are given by Equations 16 and 23, G_{Zj} and D_{Zj} are given by Equations 25 and 26, and S_{Nj} by Equation 28. The dependence of the growth and death rates on the concentration of the three dependent variables and time is made explicit in this notation.

These equations describe only the kinetics of the populations in a single volume element V_j. However, in a natural water body there exists significant mass transport as well. The mass transport mechanisms can be conveniently represented by the matrix A with elements a_{ij}. If for particular segments i and j the matrix element a_{ij} is nonzero, then the volume segments V_i and V_j interact, and mass is transported between the two segments. Letting P, Z, and N be the vectors of elements P_j, Z_j, and N_j and letting S_P, S_N, S_Z be the vectors of elements S_{Pj}, S_{Zj},

and S_{Xj}, the conservation of mass equations for the three systems including the mass transport and kinetic interactions are

$$V\dot{P} = AP + VS_P \tag{32}$$

$$V\dot{Z} = AZ + VS_Z \tag{33}$$

$$V\dot{N} = AN + VS_N \tag{34}$$

where V is the diagonal matrix of the volumes of the segments. These are the equations which form the basis for the phytoplankton population model. The detailed formulation and evaluation of the mass transport matrix has been discussed elsewhere (*14, 15, 62*).

The form of Equations 32–34 makes explicit the linear and nonlinear portions of the equations. In the equation for P, the phytoplankton biomass, the concentration P_j, in the volume element V_j, is linearly coupled to the other P_k's through the matrix multiplication by A. However, there is no nonlinear interaction between P_j and any other P_k, $k \neq j$. The reason is that the transport processes are described by linear equations. It is usually the case, however, that the A matrix is a function of time, since at least the advective terms usually vary in time. The nonlinear terms in the vector S_P involve P_j itself and the corresponding Z_j and N_j. Hence, the P equation is coupled to the Z and N equations through this term. Note, however, that P_j is not coupled to the Z_k, $k \neq j$, in any other segment, so that the coupling takes place only within each volume segment.

Therefore, the nonlinearities provide the coupling between the phytoplankton, zooplankton, and nutrient systems. This coupling is accomplished within each volume and does not extend beyond the volume boundary. The coupling among the volumes is accomplished by the linear transport interaction represented by the matrix A. This matrix may be time-varying but its elements are not functions of the phytoplankton, zooplankton, or nutrient concentrations. Hence, in many ways these equations behave linearly. In particular, their spatial behavior is unaffected by the nonlinear source terms. However, the temporal behavior and the relationships between each P_j, Z_j, and N_j are distinctly nonlinear.

Comparison with Lotka-Volterra Equations

The classical theory of predator–prey interaction as formulated by Volterra involves two equations which express the growth rate of the prey and the predator (*57*). Within the context of phytoplankton and zooplankton population, the prey is the phytoplankton and the predator the zooplankton. In the notation of the previous sections, for a one-volume system, the Lotka–Volterra equations are:

$$\frac{dP}{dt} = (G_P - D_P')P - C_g PZ \tag{35}$$

$$\frac{dZ}{dt} = - D_Z Z + a_{ZP} C_g PZ \tag{36}$$

where all the coefficients, G_P, D'_P, C_g, D_Z, and a_{ZP} are assumed to be constants and $G_P > D'_P$. This is a highly simplified situation since, as indicated previously, the growth and death rates are functions of time and, in the case of the phytoplankton growth rate, of the phytoplankton and nutrient concentrations as well. However, for a situation with adequate nutrients and low initial phytoplankton concentration, the nonlinear interaction is small initially, and the time variation of G_P can be small during the summer months. In any case, the analysis of this simplified situation is quite instructive.

Although no analytical solution is available for these simplified equations, their properties are well understood (63). In particular, the equations have two sets of singular points corresponding to the solution of the righthand side of Equations 35 and 36 equated to zero: the trivial solutions $P^* = 0$, $Z^* = 0$, and

$$P^* = \frac{D_Z}{a_{ZP} C_g}, \qquad Z^* = \frac{G_P - D'_P}{C_g} \tag{37}$$

A perturbation analysis of Equations 35 and 36 about this singular point shows that the solutions whose initial conditions are close to P^*, Z^*, oscillate sinusoidally about this singular point. Hence, no constant solution is possible. The prey and predator populations continually oscillate and are out of phase with each other. When the predator predominates, the prey is reduced, which in turn causes the predator to die for lack of food, which allows the prey to proliferate for lack of predator, which then causes the predator to grow because of the prey available as a food supply, and so on. The interesting feature is that these oscillations continue indefinitely.

The classical Lotka–Volterra equations assume an isolated population with no mass transport into or out of the volume being considered. To simulate the effect of mass transport into the volume, assume that an additional source term of phytoplankton biomass exists and has constant magnitude P_0. For this situation, the equations become

$$\frac{dP}{dt} = (G_P - D'_P)P - C_g PZ + P_0 \tag{38}$$

$$\frac{dZ}{dt} = D_Z Z + a_{ZP} C_g PZ \tag{39}$$

The nontrival singular point for these equations is

$$P^* = \frac{D_Z}{a_{ZP}C_g}, \qquad Z^* = \frac{a_{ZP}P_0}{D_Z} + \frac{(G_P - D'_P)}{C_g} \tag{40}$$

A perturbation analysis about this singular point yields a second order linear ordinary differential equation whose characteristic equation has the roots λ_1 and λ_2 where

$$\lambda_{1,2} = -\frac{a_{ZP}P_0C_g}{2D_Z} \pm \sqrt{\left[\frac{a_{ZP}P_0C_g}{2D_Z}\right]^2 - a_{ZP}C_gP_0 - (G_P - D'_P)D_Z} \tag{41}$$

Since for $P_0 > 0$, these roots have negative real parts, this singular point is a stable focus, and the steady state values given by Equation 40 are approached either by a damped sinusoid or an exponential (63). Note that for $P_0 = 0$, the classical case, the roots are purely imaginary, and the oscillation persists indefinitely.

This analysis suggests that the effect of transport into the system stabilizes the behavior of the equations and in particular allows the solutions to achieve a constant solution. This is in marked contrast to the behavior of the classical Lotka–Volterra equations.

Another modification, which has been introduced into the zooplankton equations, changes the behavior of the proposed equations in contrast to the Lotka–Volterra equations. It has been argued that the zooplankton growth rate resulting from grazing must approach its maximum value when the phytoplankton population becomes large since the zooplankters cannot metabolize the continually increasing food that is available. Thus, the growth rate $a_{ZP}C_gPZ$ is replaced by $a_{ZP}C_gZP\,K_{mP}/(P + K_{mP})$ where K_{mP} is a Michaelis constant for the reaction. The equations then become

$$\frac{dP}{dt} = (G_P - D'_P)P - C_gPZ + P_0 \tag{42}$$

$$\frac{dZ}{dt} = -D_ZZ + \frac{a_{ZP}C_gZPK_{mP}}{P + K_{mP}} \tag{43}$$

The nonzero singular points are

$$P^* = \frac{D_ZK_{mP}}{a_{ZP}C_gK_{mP} - D_Z} \tag{44}$$

$$Z^* = \frac{P_0}{C_gP^*} + \frac{(G_P - D'_P)}{C_g} \tag{45}$$

This solution reduces to the previous situation, Equation 40, for large K_{mP}. This is expected since for K_{mP} large with respect to P, the expression $K_{mP}/(P + K_{mP})$ approaches one. However, an interesting modification from classical predator–prey behavior occurs if the following condition is met

$$a_{ZP}C_0K_{mP} = D_Z + \varepsilon \tag{46}$$

where ϵ is a small positive number. For this condition, P^* is large and positive. What happens in this case is that the zooplankton population, although it continues to grow exponentially, cannot grow quickly enough to terminate the phytoplankton growth by grazing, and the phytoplankton continue to grow exponentially until P^* is reached. Of course, in the actual situation, for which G_P is not a constant, other phenomena such as nutrient depletion and self-shading exert their effect, and the growth may be stopped sooner. However, if the growth rate of zooplankton at a phytoplankton concentration equal to the Michaelis constant K_{mP} is only slightly larger than their death rate D_Z, then the zooplankton alone do not rapidly terminate the bloom.

This condition is an important dividing line for the possible behavior of the phytoplankton–zooplankton equations set forth in the previous sections. In particular, it indicates what must be true for a system wherein the zooplankton are a significant feature in the resulting phytoplankton solution. However, if Equation 46 is satisfied, then the zooplankton are not the dominant control of the phytoplankton population.

Application-San Joaquin River

As an example of the application of the equations proposed herein, consider the phytoplankton and zooplankton population observed at Mossdale Bridge on the San Joaquin River in California during the two years 1966–1967. Mossdale is located approximately 40 miles from the confluence of the San Joaquin and the Sacramento Rivers. The data presented below have been supplied to the authors by the Department of Water Resources, State of California (64), as part of an ongoing project to assess the effects of proposed nutrient loads and flow diversions on the water quality of the San Francisco Bay Delta. A more complete report of this investigation is forthcoming (62).

In order to simplify the spatial segmentation and the calculations, a one-volume segment is chosen for the region of the San Joaquin for which Mossdale is representative. The volume of this segment is, of course, somewhat arbitrary, and a more representative spatial segmentation would remove this uncertainty. However, it is instructive to consider the behavior of the solution of this simplified model.

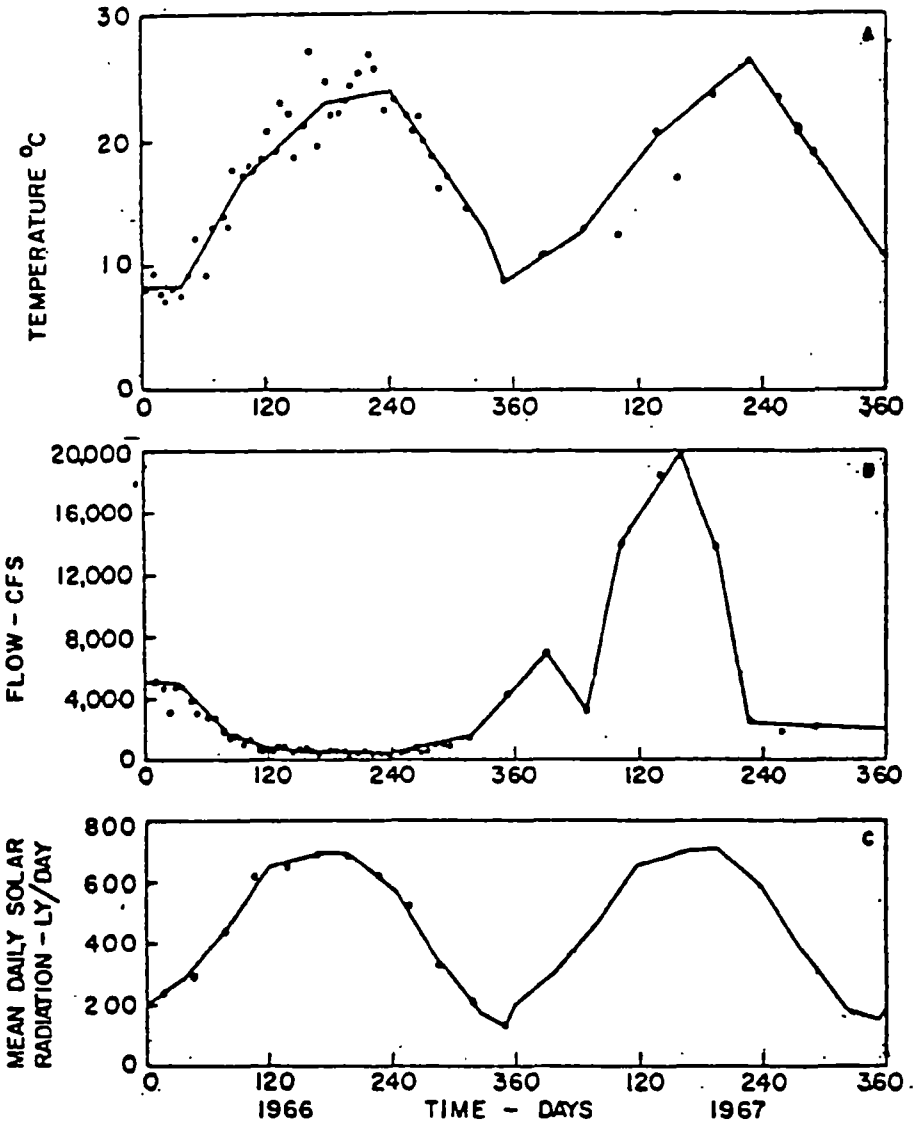

Figure 10. Temperature, flow, and mean daily solar radiation; San Joaquin River, Mossdale, 1966–1967

The nutrient data available indicate that phosphate, bicarbonate, silicate, calcium, and magnesium are available at concentrations well above the levels for which it has been suggested that these nutrients limit growth. Only the ammonia and nitrate concentrations are low, and they both decrease markedly during the 1966 spring bloom. Hence, these nutrients must be considered explicitly. To simplify the computations, the ammonia and nitrate nitrogen are combined, and the nutrient considered is total inorganic nitrogen.

There is some uncertainty concerning the magnitude and the temporal variation of the inorganic nitrogen load being discharged to the system during the time interval of interest. For lack of a better assumption, the inorganic nitrogen load W_N being discharged into the volume is assumed to be a constant, the magnitude of which is determined by

comparison with the observed inorganic nitrogen concentration data at Mossdale.

The variation of the environmental variables being considered—namely, temperature, solar radiation, and advective flow in the San Joaquin during the two-year period of interest—and the straight line approximations that are used directly in the numerical computation are shown in Figure 10. The influent advective flow, which is assumed to have constant concentrations of phytoplankton and zooplankton biomass and inorganic nitrogen, is routed through the volume. Since Mossdale is located above the saline portion of the San Joaquin, no significant dispersive mass transfer is assumed to exist by comparison with the advective mass transfer.

The equations which represent this one-segment model are

$$\dot{P} = (G_P - D_P)P + \frac{Q}{V}(P_0 - P) \tag{47}$$

$$\dot{Z} = (G_Z - D_Z)Z + \frac{Q}{V}(Z_0 - Z) \tag{48}$$

$$\dot{N} = -a_{NP}G_P P + \frac{W_N}{V} + \frac{Q}{V}(N_0 - N) \tag{49}$$

where $Q = Q(t)$ is the advective flow entering and leaving the volume; V is the volume of the segment; P_0, Z_0, and N_0 are the phytoplankton, zooplankton, and inorganic nitrogen concentration of the flow entering the volume. The remaining terms have been defined previously by Equations 16, 23, 25, and 26. In the nutrient equation, only the direct source of inorganic nitrogen, W_N, has been included; the organic feedback terms representing excreted nitrogen, etc., Equation 28, have been dropped. Since the magnitude of W_N is uncertain and is assigned by comparison with observed data and computed model output, these feedback terms can be thought of as being incorporated in the value obtained for W_N.

The solution of Equations 47, 48, and 49 requires numerical techniques. For such nonlinear equations, it is usually wise to employ a simple numerical integration scheme which is easily understood and pay the price of increased computational time for execution rather than using a complex, efficient, numerical integration scheme where unstable behavior is a distinct possibility. A variety of simple methods are available for integrating a set of ordinary first order differential equations. In particular, the method of Huen, described in Ref. 65, is effective and stable. It is self-starting and consists of a predictor and a corrector step. Let $y = f(t,y)$ be the vector differential equation and let h be the step size.

The predictor is that of Euler: with y_0 the initial condition vector at t_0, the predictor value of y at $t_0 + h = t_1$ is

$$y_1^* = y_0 + hf(t_0, y_0) \tag{50}$$

The corrector value is simply

$$y_1 = y_0 + \frac{h}{2}[f(t_0, y_0) + f(t_1, y_1^*)] \tag{51}$$

That is, the corrector uses the predictor value at t_1 to estimate the slope at t_1 which is averaged with the slope at t_0 to provide the slope of the straight line approximation. A variation of this method is discussed at some length by Hamming (*66*).

Another simple two-step method is that of Runge, described in Ref. *67*. The Euler predictor is used with a half-step integration.

$$y^* = y_0 + \frac{h}{2} f(t_0, y_0) \tag{52}$$

This value of y^* is used to estimate the slope at the midpoint of the interval, which is then used as the slope of the straight line approximation

$$y_1 = y_0 + hf(t_0 + \frac{h}{2}, y^*) \tag{53}$$

Both of these methods are second order methods, being accurate to terms of order Δt^2 in a comparison of Taylor series expansions of the exact and approximate values, and both methods require two derivative evaluations per step. The method of Runge has been used in the calculations presented below.

The equations themselves are programmed for solution using a continuous simulation language and a digital computer. The language, in this case CSMP/1130, is based on a block diagram, analog computer, representation of the differential equations. The flexibility of these languages which allow changes in the equation structure to be made easily is an asset in modeling complex systems.

The biomass variables used in the calculations are total cell counts for the phytoplankton and rotifer counts for the zooplankton. The rotifer population represented the large majority of the zooplankton present on a weight basis as well. In order to relate these variables to comparable units, a series of conversion factors have been used. The phytoplankton count–chlorophyll concentration ratio was measured. However, the carbon–chlorophyll or dry weight–chlorophyll conversions are unknown. Hence, the conversion to an organic carbon basis is made rather arbi-

Table VII. Parameter Values for the Mossdale Model

Notation	*Description*	*Parameter Value*
K_1	Saturated growth rate of phytoplankton	0.1 day^{-1} °C
I_s	Light saturation intensity for phytoplankton	300 ly/day
k'_e	Extinction coefficient	4.0 m^{-1}
H	Depth	1.2 m
K_m	Michaelis constant for total inorganic nitrogen	0.025 mg N/liter
f	Photoperiod	0.5 + sin [0.0172 (t − 165)] day
K_2	Endogenous respiration rate of phytoplankton	0.005 day^{-1} $°C^{-1}$
C_g	Zooplankton grazing rate	0.13 liter/mg - C - day
P_0	Influent phytoplankton chlorophyll concentration	5.0 μg Chl/liter
a_{ZP}	Zooplankton conversion efficiency	0.6 mg C/mg - C
K_{mP}	Phytoplankton Michaelis constant	60 μg Chl/liter
D_Z	Zooplankton death rate	0.075 day^{-1}
Z_0	Influent zooplankton carbon concentration	0.05 mg C/liter
a_{NP}	Phytoplankton nitrogen–carbon ratio	0.17 mg N/mg - C
C/Chl	Phytoplankton carbon to total chlorophyll ratio	50 mg C/mg - Chl
N_0	Influent total inorganic nitrogen concentration	0.1 mg N/liter
W_N	Direct discharge rate of nitrogen	12500 lbs/day
V	Segment volume	9.7 × 10^8 ft^3
	Phytoplankton total cell count/phytoplankton	100 cells/ml = 1.75 μg Chl/liter
	Zooplankton count/ zooplankton carbon ratio	10^4 No./liter = 1.30 mg C liter

trarily. However, the carbon-to-chlorophyll ratio which results (*see* Table VII) is within the range reported in the literature. The same problem exists with the rotifer counts to rotifer carbon conversion: the value used is given in Table VII.

The comparison of the model output and the observed data for the two-year period for which data are available is shown in Figure 11. The parameter values used in the equations are listed in Table VII.

It is clear from both the data and the model results that a classical predator–prey situation is observed in 1966: the spring bloom of phytoplankton resulting from favorable temperature and light intensity provides the food for zooplankton, which then reduce the population during

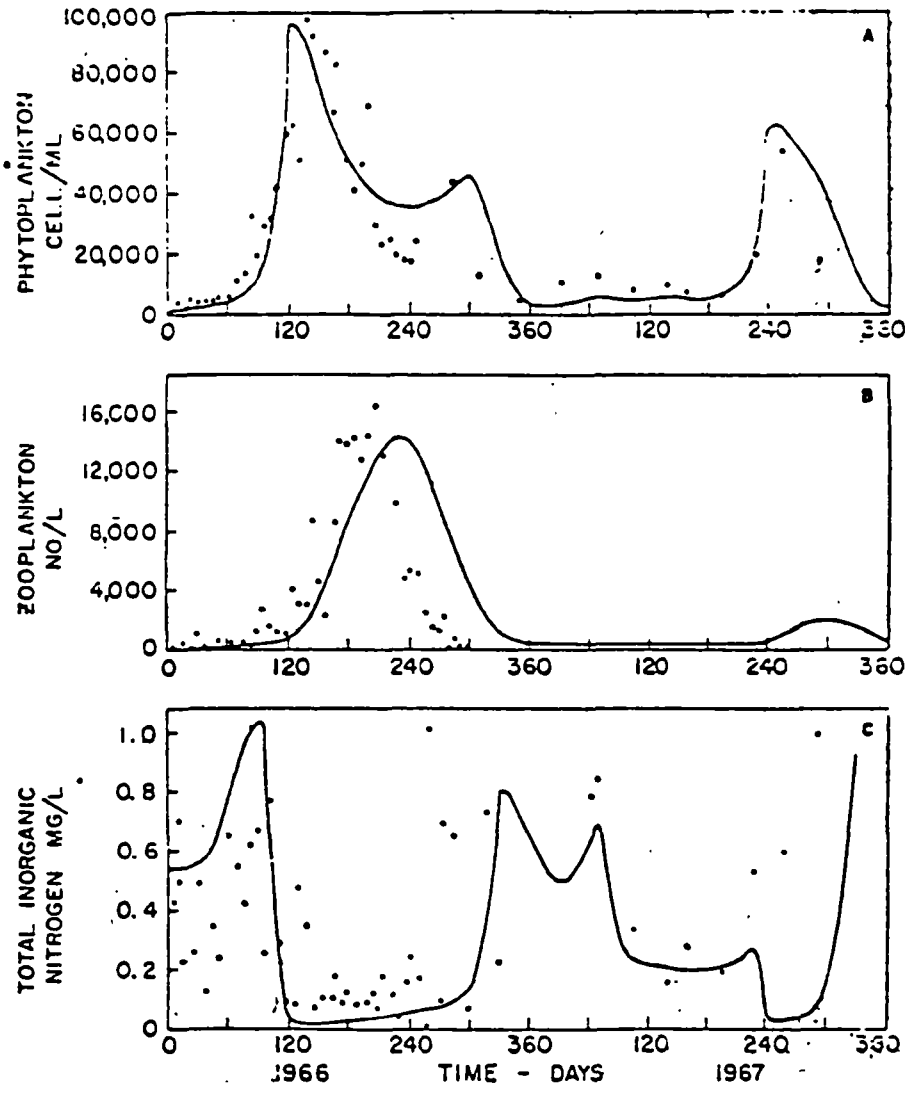

Figure 11. Phytoplankton, zooplankton, and total inorganic nitrogen; comparison of theoretical calculations and observed data; San Joaquin River, Mossdale, 1966–1967

the summer. The decrease of the zooplankton and the subsequent slight secondary bloom of phytoplankton complete the cycle for the year. It is not clear, however, from a casual inspection of the data, whether the zooplankton population terminated the phytoplankton growth, as in classical predator–prey situations, whether the nutrient concentration dropped to a limiting value that reduced the growth rate, or a combination of the two. This point is elaborated in the next section.

The situation in 1967 is quite different. No significant phytoplankton growth is observed until late in the year. The controlling variable in this case is the large advective flow during the spring and summer of 1967 (*see* Figure 10) which effectively washes out the population in the region. Only when the flow has sufficiently decreased so that a population can

develop do the phytoplankton show a slight increase. However, the dropping temperature and light intensity level terminate the growth for the year.

Growth Rate-Death Rate Interactions

The behavior of the equations which represent the phytoplankton, zooplankton, and nutrient systems in one volume can be interpreted in terms of the growth and death rates of the phytoplankton and zooplankton. The equations are as before

$$\frac{dP}{dt} = (G_P - D_P)P + \frac{Q}{V}(P_0 - P) \tag{54}$$

$$\frac{dZ}{dt} = (G_Z - D_Z)Z + \frac{Q}{V}(Z_0 - Z) \tag{55}$$

where P_0 and Z_0 are the concentrations of phytoplankton and zooplankton carbon in the influent flow, Q. A more useful form for these equations is

$$\frac{dP}{dt} = [G_P - (D_P + \frac{Q}{V})]P + \frac{Q}{V}P_0 \tag{56}$$

$$\frac{dZ}{dt} = [G_Z - (D_Z + \frac{Q}{V})]Z + \frac{Q}{V}Z_0 \tag{57}$$

A complete analysis of the properties of these equations is quite difficult since the coefficients of P and Z are time variables and also functions of P and Z. However, the behavior of the solution becomes more accessible if the variation of these coefficients is studied as a function of time. The expressions $G_P - (D_P + Q/V)$ and $G_Z - (D_Z + Q/V)$ can be considered the net growth rates for phytoplankton and zooplankton. The advective or flushing rate, Q/V, is included in these expressions since it acts as a death rate in one segment system.

The sign and magnitude of the net growth rate controls the behavior of the solution. For a linear equation, for which the net growth rate is not a function of the dependent variable (*i.e.*, P or Z), the type of solution obtained depends on the sign and magnitude of the net growth rate. That is, for the equation

$$\frac{dP}{dt} = \alpha P + \frac{Q}{V}P_0 \tag{58}$$

where α, Q, and V are constant, the solution is

$$P(t) = P(o)\, e^{\alpha t} + P_0 \frac{Q}{\alpha V} (e^{\alpha t} - 1) \tag{59}$$

For α negative, that is, for a negative net growth rate, the solution tends to the steady state value $P_0\, Q/|\alpha|V$. However, for α positive, the solution grows exponentially without limit. Thus, for α negative but $|\alpha|$ small, or for α positive, the solution becomes large; whereas for α negative but $|\alpha|$ large, the solution stays small. Hence, the behavior of the solution can be inferred from the plots of the net growth rates. Figure 12a is a plot of the following terms from the 1966 Mossdale calculation: G_P without the Michaelis–Menton multiplicative factor included—*i.e.*, the growth rate at nutrient saturation denoted by $G_P\ (I,T)$; G_P itself denoted by $G_P\ (N,I,T)$—*i.e.*, the growth rate considering the nutrient effects. The net growth rate $G_P - (D_P + Q/V)$ is also plotted. Similarly, in Figure 12b, the growth rate of zooplankton G_Z, the mortality rate D_Z, the flushing rate $Q(t)/V$, and the net growth rate $G_Z - (D_Z + Q/V)$ are plotted.

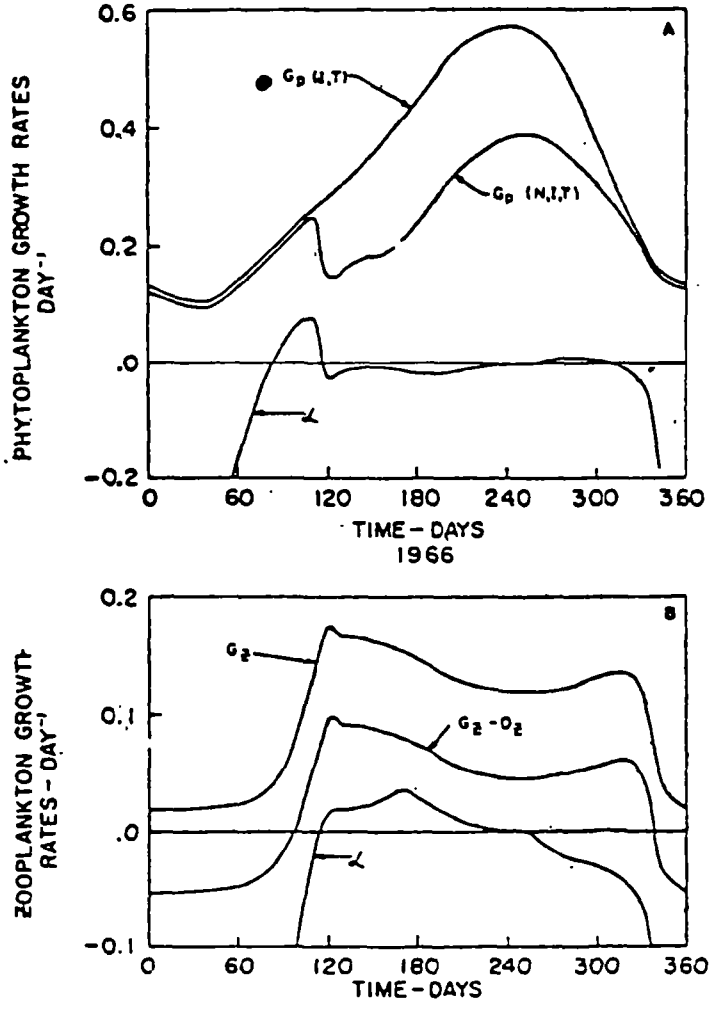

Figure 12. Theoretical growth rates for phytoplankton and zooplankton populations

The analysis of the 1966 model calculations can now be made by inspecting these figures. The net growth rate for the phytoplankton $G_P - (D_P + Q/V)$ becomes positive at $t = 85$ days owing to an increase in G_P, the result of rising temperature and light intensity, and a decrease in Q/V as the advective flow decreases. The positive net growth rate of the population causes their numbers to increase exponentially fast until the nutrient begins to be in short supply. This is evidenced by the departure of the G_P curve from the G_P at nutrient saturation curve. At the same time, the D_P curve is showing a marked increase because of the increased zooplankton population and their grazing. The result is that the net growth rate becomes zero and then negative as the zooplankton reduce the phytoplankton population by grazing. The growth of the zooplankton can be analyzed in a similar fashion using Figure 12b. The net growth rate becomes positive when the phytoplankton population is large enough to sustain the zooplankters. Then the zooplankton grow until they have reduced the phytoplankton population to a level where they are no longer numerous enough to sustain the zooplankton. The net zooplankton growth rate then becomes negative and the population diminishes in size. This small zooplankton population no longer exerts a significant effect on the death rate of the phytoplankton, D_P, and its value decreases, causing the net phytoplankton growth rate to become positive again, and the smaller autumn bloom results. The decreasing temperature and light intensity and the increasing advective flow then effectively terminate the bloom as the year ends.

Summary and Conclusions

A model of the dynamics of phytoplankton populations based on the principle of conservation of mass has been presented. The growth and death kinetic formulations of the phytoplankton and zooplankton have been empirically determined by an analysis of existing experimental data. Mathematical expressions which are approximations to the biological mechanisms controlling the population are added to the mass transport terms of the conservation equation for phytoplankton, zooplankton, and nutrient mass in order to obtain the equations for the phytoplankton model. The resulting equations are compared with two years' data from the tidal portion of the San Joaquin River, California. Similar comparisons have been made for the lower portion of Delta and are reported elsewhere (62).

It is recognized that certain parameters in the model have been estimated from the data which are then used to demonstrate the veracity of the model. The parameters used in the verification were either obtained from prototype measurements or estimated from the range of

values reported in the literature. The refinement of the later set of parameters was made by comparing the observed 1966 data and calculated results. The model was further verified by applying the parameters obtained in the 1966 analysis to the data of the following year. The parameter values finally used were all within the ranges of reported literature values. The agreement achieved between the available data and the model calculations is sufficiently encouraging to prompt further effort in this direction.

The primary aim of this investigation, presenting a useful model as a component in solution of the eutrophication problems, in our opinion, has been achieved. The resulting equations are admittedly complex and require numerical methods for solution. It is anticipated as with all modeling activities that the structure presented herein will be expanded and modified in the future to incorporate additional features of the eutrophication phenomena. In particular, the model as it is presently structured does not address the species changes that might result as the environment is changed. This is a problem of some consequence, and refinements and expansion of the number of species considered is an area for future work (*12*). However, the initial application of these equations to an actual problem area with specific eutrophication problems has been sufficiently successful to support its engineering use as a preliminary step in the assessment of a potential or actual eutrophication problem.

Acknowledgment

The authors are pleased to acknowledge the participation of John L. Mancini of Hydroscience Inc. in the research reported herein, as well as the assistance of Gerald Cox and Jack Hodges of the Department of Water Resources and Harold Chadwick of the Department of Fish and Game, State of California.

The research was sponsored in part by a research grant to Manhattan College from the Federal Water Quality Administration and in part from research funds made available by Hydroscience, Inc.

The application of the phytoplankton model to the San Joaquin River was sponsored by the California Water Resources Commission and carried out by Hydroscience Inc.

Literature Cited

(1) Riley, G. A., *Theory of Food-Chain Relations in the Ocean*, "The Sea," p. 438–63, M. N. Hill, Ed., Interscience, New York, 1963.
(2) Riley, G. A., "Factors Controlling Phytoplankton Populations on Georges Bank," *J. Marine Res.* (1946) 6 (1), 54–73.
(3) Riley, G. A., "Seasonal Fluctuations of the Phytoplankton Populations in New England Coastal Waters," *J. Marine Res.* (1947) 6 (2), 114–25.

(4) Riley, G. A., Von Arx, R., "Theoretical Analysis of Seasonal Changes in the Phytoplankton of Husan Harbor, Korea," *J. Marine Res.* (1949) 8 (1), 60–72.

(5) Riley, G. A., Stommel, H., Bumpus, D. F., "Quantitative Ecology of the Plankton of the Western North Atlantic," *Bull. Bingham Oceanog. Coll.* (1949) 12 (3), 1–169.

(6) Steele, J. H., "Plant Production on Fladen Ground," *J. Marine Biol. Assoc. U.K.* (1956) 35, 1-33.

(7) Steele, J. H., "A Study of Production in the Gulf of Mexico," *J. Marine Res.* (1964) 22, 211–22.

(8) Steele, J. H., *Notes on Some Theoretical Problems in Production Ecology*, "Primary Production in Aquatic Environments," C. R. Goldman, Ed., *Mem. Inst. Idrobiol.*, p. 383–98, 18 Suppl., University of California Press, Berkeley, 1965.

(9) Davidson, R. S., Clymer, A. B., "The Desirability and Applicability of Simulating Ecosystems," *Ann. N. Y. Acad. Sci.* (1966) 128 (3), 790–4.

(10) Cole, G. R., "A Look at Simulation through a Study on Plankton Population Dynamics," Report BNWL-485, p. 1–19, Battelle Northwest Laboratory, Richland, Washington, 1967.

(11) Parker, R. A., "Simulation of an Aquatic Ecosystem," *Biometrics* (1968) 24 (4), 803–22.

(12) Chen, C. W., "Concepts and Utilities of Ecologic Model," *J. Sanit. Eng. Div., Am. Soc. Civil Eng.* (Oct. 1970) 96, 1085–97.

(13) Thomann, R. V., O'Connor, D. J., DiToro, D. M., "Modeling of the Nitrogen and Algal Cycles in Estuaries," *5th Intern. Water Pollution Res. Conf., San Francisco, Calif., July 1970.*

(14) Thomann, R. V., "Mathematical Model for Dissolved Oxygen," *J. Sanit. Eng. Div., Proc. Am. Soc. Civil Eng.* (October 1963) 83, SA5, 1–30.

(15) O'Connor, D. J., Thomann, R. V., "Stream Modeling for Pollution Control," *Proc. IBM Sci. Computing Symp. Environ. Sci., November 14–16, 1966*, p. 269.

(16) Hutchinson, G. E., "A Treatise on Limnology Vol. II. Introduction to Lake Biology and the Limnoplankton," p. 306–54, Wiley, New York, 1967.

(17) Strickland, J. D. H., *Production of Organic Matter in the Primary Stages of the Marine Food Chain*, "Chemical Oceanography," Vol. 1, p. 503, J. P. Riley and G. Skivow, Eds., Academic, New York, 1965.

(18) Lund, J. W. G., "The Ecology of the Freshwater Phytoplankton," *Biol. Rev.* (1965) 40, 231–93.

(19) Raymont, J. E. G., "Plankton and Productivity in the Oceans," p. 93–486, Pergamon, New York, 1963.

(20) Vollenweider, R. A., Ed., "Manual on Methods for Measuring Primary Production in Aquatic Environments," Ch. 2, p. 4–24, Blackwell Scientific Publications, Oxford, England, 1969.

(21) Tamiya, H., Hase, E., Shibata, K., Mituya, A., Iwamura, T., Nihei, T., Sasa, T., *Kinetics of Growth of Chlorella with Special Reference to Its Dependence on Quantity of Available Light and on Temperature*, "Algal Culture From Laboratory to Pilot Plant," p. 204–34, J. S. Burlew, Ed., Publ. 600, Carnegie Institute of Washington, D. C., 1964.

(22) Yentsch, C. S., Lew, R. W., "A Study of Photosynthetic Light Reactions," *J. Marine Res.* (1966) 24 (3).

(23) Spencer, C. P., "Studies on the Culture of a Marine Diatom," *J. Marine Biol. Assoc. U.K.* (1954) 28; *quoted by* Harvey, H. W., "The Chemistry and Fertility of Sea Waters," p. 94, Cambridge University Press, 1966.

(24) Myers, J., *Growth Characteristics of Algae in Relation to the Problem of Moss Culture*, "Algal Culture From Laboratory to Pilot Plant," p. 37–54, Publ. 600, J. S. Burlew, Ed., Carnegie Institute of Washington, D. C., 1964.
(25) Sorokin, C., Krauss, R. W., "The Effects of Light Intensity on the Growth Rates of Green Algae," *Plant Physiol.* (1958) 33, 109–13.
(26) Sorokin, C., Krauss, R. W., "Effects of Temperatures and Illuminance on Chlorella Growth Uncoupled from Cell Division," *Plant Physiol.* (1962) 37, 37–42.
(27) Fogg, G. E., "Algal Cultures and Phytoplankton Ecology," p. 20, University of Wisconsin Press, Madison, Wis., 1965.
(28) Ryther, J. H., "Photosynthesis in the Ocean as a Function of Light Intensity," *Limnol. Oceanog.* (1956) 1, 61–70.
(29) Shelef, G., Oswald, W. J., McGauhey, P. H., "Algal Reactor for Life Support Systems," *J. Sanit. Eng. Div., Proc. Am. Soc. Civil Eng.* (February 1970) 96, SA1.
(30) Vollenweider, R. A., *Calculation Models of Photosynthesis—Depth Curves and Some Implications Regarding Day Rate Estimates in Primary Production Measurements*, "Primary Production in Aquatic Environments," C. R. Goldman, Ed., *Mem. Inst. Idrobiol.*, p. 425–57, 18 Suppl., University of California Press, Berkeley, 1965.
(31) Riley, G. A., "Oceanography of Long Island Sound 1952–1954. II. Physical Oceanography," *Bull. Bingham Oceanog. Coll.* (1956) 15, 15–46.
(32) Small, L. F., Curl, H., Jr., "The Relative Contribution of Particulate Chlorophyll and to the Extinction of Light off the Coast of Oregon," *Limnol. Oceanog.* (1968) 13 (1), 84.
(33) Oswald, W. J., Gotaas, H. B., Ludwig, H. F., Lynch, V., "Photosynthetic Oxygenation," *Sewage Ind. Wastes* (1953) 25 (6), 692.
(34) Azad, H. S., Borchardt, J. A., "A Method for Predicting the Effects of Light Intensity on Algal Growth and Phosphorus Assimilation," *J. Water Pollution Control Federation* (1969) 41 (11), part 2.
(35) Dugdale, R. C., "Nutrient Limitation in the Sea: Dynamics, Identification, and Significance," *Limnol. Oceanog.* (1967) 12 (4), 685–95.
(36) Eppley, R. W., Rogers, J. N., McCarthy, J. J., "Half Saturation Constants for Uptake of Nitrate and Ammonium by Marine Phytoplankton," *Limnol. Oceanog.* (1969) 14 (6), 912–20.
(37) Ketchum, B. H., "The Absorption of Phosphate and Nitrate by Illuminated Cultures of Nitzschia Closterium," *Am. J. Botany* (June 1939) 26.
(38) Thomas, W. H., Dodson, A. N., "Effects of Phosphate Concentration on Cell Division Rates and Yield of a Tropical Oceanic Diatom," *Biol. Bull.* (1968) 134 (1), 199–208.
(39) Lake Tahoe Area Council, South Lake Tahoe, Calif., "Eutrophication of Surface Waters—Lake Tahoe, May 1969," p. 33, 95705, Report for Federal Water Pollution Control Adm., Dept. of Interior, WPD 48-02.
(40) Riley, G. A., "Mathematical Model of Regional Variations in Plankton," *Limnol. Oceanog.* (1965) 10 (Suppl.), R202–R215.
(41) Gerloff, Skoog, "Nitrogen as a Limiting Factor for the Growth of Microcystis Aerugmosa in Southern Wisconsin Lakes," *Ecology* (1957) 38, 556–61.
(42) MacIsaac, J. J., Dugsdale, R. C., "The Kinetics of Nitrate and Ammonia Uptake by Natural Populations of Marine Phytoplankton," *Deep Sea Res.* (1969) 16, 415–22.
(43) Kuentzel, L. E., "Bacteria, Carbon Dioxide, and Algal Blooms," *J. Water Pollution Control Federation* (October 1969) 41 (10).
(44) Droop, M. R., *Organic Micronutrients*, "Physiology and Biochemistry of Algae," p. 141–60, R. A. Lewin, Ed., Academic, New York, 1962.

(45) Adams, J. A., Steele, J. H., *Shipboard Experiments on the Feeding of Calanus Finmarchicus*, "Some Contemporary Studies in Marine Science," p. 19–35, H. Barnes, Ed., G. Allen and Unwin Ltd., London, 1966.

(46) Mullin, M. M., Brooks, E. R., "Laboratory Culture, Growth Rate, and Feeding Behavior of a Planktonic Marine Copepod," *Limnol. Oceanog.* (1967) 12 (4), 657–66.

(47) Anraku, M., Omori, M., "Preliminary Survey of the Relationship Between the Feeding Habits and the Structure of the Mouth Parts of Marine Copepods," *Limnol. Oceanog.* (1963) 8 (1), 116–26.

(48) Wright, J. C., "The Limnology of Canyon Ferry Reservoir, I. Phytoplankton–Zooplankton Relationships," *Limnol. Oceanog.* (1958) 3 (2), 150–9.

(49) Burns, C. W., "Relation between Filtering Rate Temperature and Body Size in Four Species of Daphnia," *Limnol. Oceanog.* (1969) 14 (5), 693–700.

(50) Ryther, J. H., "Inhibitory Effects of Phytoplankton upon the Feeding of Daphnia Magna with Reference to Growth, Reproduction and Survival," *Ecology* (1954) 35, 522–33.

(51) McMahon, J. W., Rigler, F. H., "Feeding Rate of Daphnia Magna Straus in Different Foods Labeled with Radioactive Phosphorus," *Limnol. Oceanog.* (1965) 10 (1), 105–13.

(52) Conover, R. J., "Oceanography of Long Island Sound, 1952–1954. VI. Biology of *Acartia Clausi* and *A. tonsa*," *Bull. Bingham Oceanog. Coll.* (1956) 15, 156–233.

(53) Mullin, M. M., "Some Factors Affecting the Feeding of Marine Copepods of the Genus Calanus," *Limnol. Oceanog.* (1963) 8 (2), 239–50.

(54) Burns, C. W., Rigler, F. H., "Comparison of Filtering Rates of Daphnia in Lake Water and in Suspensions of Yeast," *Limnol. Oceanog.* (1967) 12 (3), 492–402.

(55) Riley, G. A., "A Theoretical Analysis of the Zooplankton Population of Georges Bank," *J. Marine Res.* (1947) 6 (2), 104–13.

(56) Conover, A. J., "Assimilation of Organic Matter by Zooplankton," *Limnol. Oceanog.* (1966) 11, 338–45.

(57) Lotka, A. J., "Elements of Mathematical Biology," p. 88–94, Dover, New York, 1956.

(58) Bishop, J. W., "Respiration Rates of Migrating Zooplankton in the Natural Habitat," *Limnol. Oceanog.* (1968) 13 (1), 58–62.

(59) Comita, G. W., "Oxygen Consumption in Diaptomus," *Limnol. Oceanog.* (1968) 13 (1), 51–7.

(60) Martin, J. H., "Phytoplankton Zooplankton Relationships in Narragansett Bay III," *Limnol. Oceanog.* (1968) 13 (1).

(61) Vollenweider, R. A., "Scientific Fundamentals of the Eutrophication of Lakes and Flowing Waters, with Particular Reference to Nitrogen and Phosphorus as Factors in Eutrophication," p. 117, Organization for Economic Cooperation and Development Directorate for Scientific Affairs, Paris, France, 1968.

(62) O'Connor, D. J., DiToro, D. M., Thomann, R. V., Mancini, J. L., "Phytoplankton Population Model of the Sacramento–San Joaquin Delta Bay," Technical Report to Department of Water Resources, State of California, by Hydroscience, Inc., Westwood, N. J., 1971.

(63) Davis, H. T., "Introduction to Nonlinear Differential and Integral Equations," p. 99–109, Dover, New York, 1962.

(64) Department of Water Resources, State of California, private communication, 1966.

(65) Stiefel, E. L., "An Introduction to Numerical Mathematics," p. 163, Academic, New York, 1966.
(66) Hamming, R. W., "Numerical Methods for Scientists and Engineers," p. 194–210, McGraw-Hill, New York, 1962.
(67) Levy, H., Baggott, E. A., "Numerical Solutions of Differential Equations," p. 91–110, Dover, New York, 1950.

RECEIVED May 27, 1970.

SIMPLIFIED PHYTOPLANKTON MODELING FOR STREAMS[1]

Introduction

It is becoming increasingly apparent that as more advanced degrees of waste treatment are installed, the water quality of streams may shift into more difficult problem contexts. For example, when primary or poorly treated secondary effluent was discharged to a stream, the principal water quality effects were sludge deposits, low or anaerobic dissolved oxygen conditions, high turbidity and an aquatic ecosystem dominated by pollution tolerant organisms. As the treatment level increases, light penetration is enhanced, there is a shift to an aquatic ecosystem that may be dominated by the primary producers - the phytoplankton and the periphyton as well as rooted aquatic macrophytes. The nutrient balance then becomes more important since the biomass may be stimulated by excess nutrient discharges. High concentrations of phytoplankton or periphyton can result in marked diurnal variations in dissolved oxygen. Therefore, as the mean value of D.O. is improved, the diurnal range may increase due to the stimulated presence of the primary producers. It is important then to analyze the potential impacts of nutrient discharges on resulting plant biomass. In these notes, phytoplankton are considered as the principal plant form resulting from the discharge of nutrients.

The Principle of the N/p Ratio

Considerable progress has been made in recent years in describing the basic mechanisms of phytoplankton dynamics in lakes and estuaries. The models that have been developed usually involve complicated interactions between nutrients and phytoplankton growth and hence do not generally lend themselves to simplified computations. Other simplified models for total phosphorus in lakes have also been developed but the applicability to streams is not direct. In order to provide a first and very simplified approach to a nutrient balance in a stream, the ratio of the nitrogen to phosphorus concentration is useful.

[1] Robert V. Thomann and John Mueller

The N/p ratio can be examined especially where there is a tradeoff to be made between nitrogen removal or phosphorus removal. One can see this tradeoff by examining the total nitrogen (TN) or inorganic nitrogen (IN) to total phosphorus (Tp) or inorganic phosphorus (Ip) ratios under different levels of treatment. When TN/Tp or IN/Ip are less than about 7-10, nitrogen will often be the limiting nutrient, while if the ratio is greater than about 7-10, phosphorus is considered as the limiting nutrient. The use of these bounds on the ratio can be easily seen by the following calculation.

Consider that a certain percentage of the inorganic nutrient forms (the forms available for plant uptake) will be ultimately converted to plant biomass. A good estimate is about 50-75%. With the cell stoichiometry of 1 μg P/μg chlorophyll and 7 μg N/μg chlorophyll, the maximum amount of biomass that would result can be estimated.

Figure 1 shows the basic principle. For an effluent concentration of 22 mg Inorganic N/ℓ and 5 inorganic p/ℓ, (representative of high rate activated sludge (HRAS), without any phosphorus removal), the following maximum chlorophyll concentrations can be computed using a 75% conversion:

$$\text{IN:}\quad 22\ \frac{\text{mgN}}{\ell}(.75)\cdot\frac{1\ \mu\text{g chlor}}{7\ \mu\text{gN}}\cdot 1000\ \frac{\mu\text{g}}{\text{mg}} = 2357\ \frac{\mu\text{g chlor}}{\ell}$$

$$\text{Ip:}\quad 5\ \frac{\text{mgP}}{\ell}(.75)\cdot 1\ \frac{\mu\text{g chlor}}{\mu\text{gP}}\cdot 1000\ \frac{\mu\text{g}}{\text{g}} = 3750\ \frac{\mu\text{g chlor}}{\ell}$$

Applying the notion of a limiting nutrient, the total amount of phosphorus would not be converted to the 3750 μg chlor/ℓ because the nitrogen then would be totally exhausted. Therefore, nitrogen would run out first, would limit growth and the maximum biomass would be 2357 μg chlor/ℓ. Of course, there may be many reasons (e.g. length of river) that would prevent this maximum level from being reached. The reasoning underlying the boundary of TN/Tp of 7-10, is therefore founded on the cell stoichiometry of the phytoplankton and a conversion of available nutrient forms. At high (> 7-10) TN/Tp, the phosphorus concentration would run out before nitrogen and hence would limit growth.

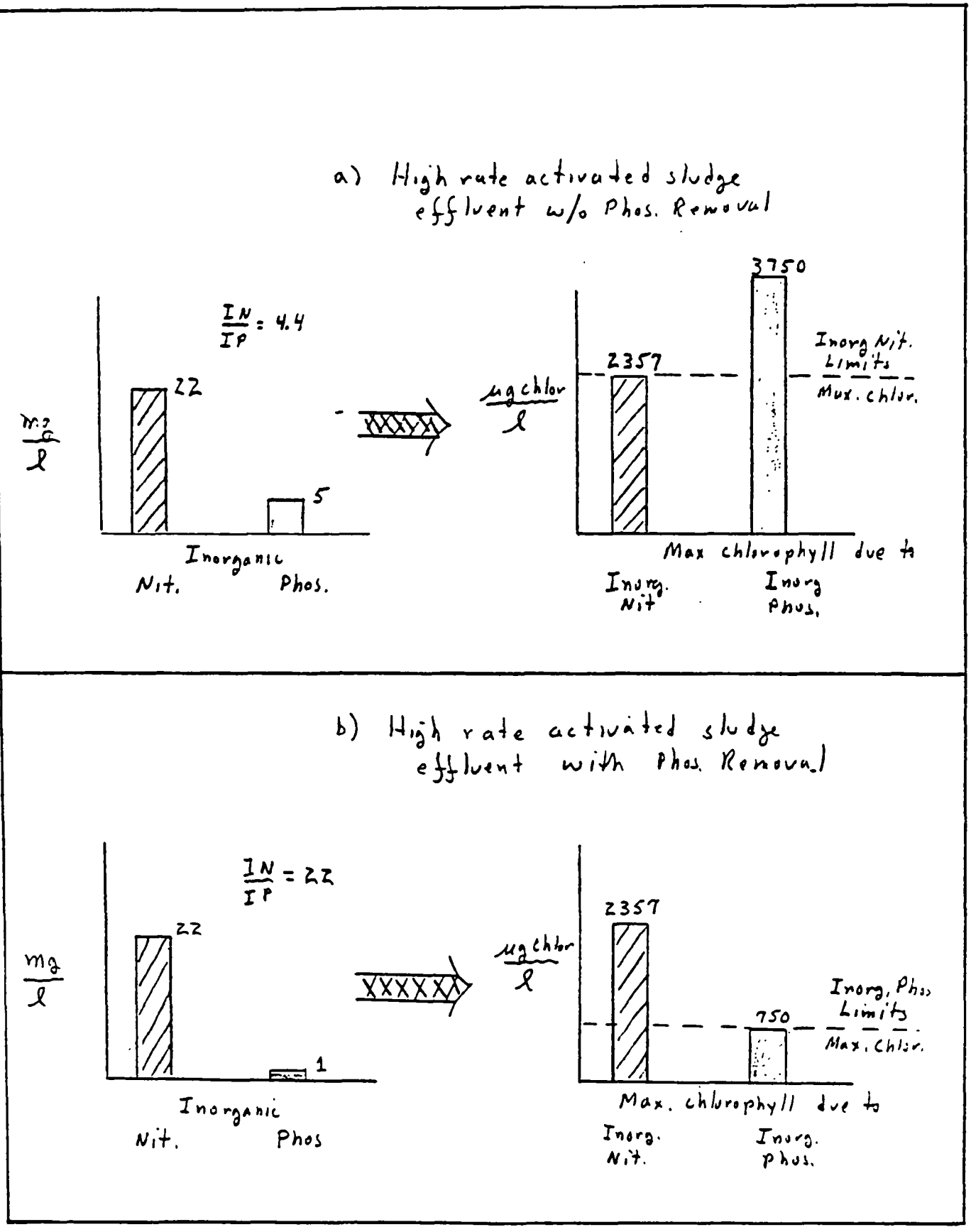

Figure 1. Illustration of principle of nitrogen - phosphorus ratios in controlling phytoplankton biomass

Figure 1(b) shows the situation where HRAS with phosphorus removed is applied. Now the IN/Ip ratio is 22, the maximum biomass possible (at 75% inorganic phosphorus conversion) is 750 µg/ℓ chlor and phosphorus limits the maximum production.

At different levels of treatment, the ratio of TN/Tp in the stream at the point of discharge will vary depending on the ratio of river flow to effluent flow. Table 1 summarizes this ratio for streams that are dominated by the plant effluent (i.e., approximately 50% or greater of the river flow is effluent flow). Note that under higher rate activated sludge and HRAS plus nitrification, nitrogen would be limiting. But if a biomass problem exists and some nutrient control is necessary, then HRAS and phsophorus removal will shift the system from nitrogen to phosphorus removal. Again, under certain conditions of effluent flow to river flow, phosphorus may be the limiting nutrient under different levels of treatment.

Figure 2 shows the relationship between the ratio of TN/TP for different ratios of the plant effluent flow to the total river flow. The upstream flow is assumed to have the following nutrient characteristics:

TN = 1.45 mg N/ℓ

Tp = .052 mg P/ℓ

TN/Tp = 28

Note that in general, runoff from non-point sources will tend to have high TN/Tp ratios indicating that phosphorus is the limiting nutrient for non-point source situations. Figure 2 shows that when the effluent flow is less than about 2% of the total river flow, phosphorus would tend to be the limiting nutrient (TN/Tp > 10). For effluent/river flow ratios greater than about 2%, the limiting nutrient depends on the treatment process. For all ratios, HRAS and P removal results in phosphorus a limiting situation.

Table 2 shows some N/P ratios for various sources. It can be seen that non-point source runoff tends to have high N/p ratios while marine waters tend to have low N/p ratios.

TABLE 1

N/p and Limiting Nutrient for Different Treatment Levels

Treatment Level[1]	Eff. Conc. mg/ℓ[2] TN	IN	Tp	Ip	TN/Tp	IN/Ip	Max. chlor.[3] µg/ℓ	Limiting Nutrient
Raw	40	25	10	7	4	3.6	2678	N
HRAS	27	22	8	5	3.4	4.4	2357	N
HRAS + Nitrif.	26	22	7	5	3.7	4.4	2357	N
HRAS + P removal	27	22	1	1	27.0	22.0	750	P
HRAS + N removal	3	2	8	5	0.4	0.4	214	N
HRAS + P rem. + N rem.	3	2	1	1	3.0	2.0	214	N

[1] HRAS - High rate activated sludge

[2] TN, IN - total and inorganic nitrogen respectively; Tp, Ip - total and inorganic phosphorus, respectively

[3] Calculated from .75 conversion of inorganic nutrient, 1 µg chlor/µg P and 1 µg chlor/7 µg N; i.e. min $\{.75\ (Ip) \cdot 1000;\ .75\ (IN) \cdot \frac{1000}{7}\}$

TABLE 2

N/p Ratios for Point Source, Non-Point Source and Marine Waters[1/]

Source	TN/Tp	IN/Ip	Limiting Nutrient	Reference
Point - HRAS w/o P removal	3	4	N	
HRAS w P removal	27	22	P	
Non-Point - 50% Agric. & Urb.	28	25[2/]	P	Omernik (1977)
Marine Waters		2[3/]	N	Goldman et al.(1973)

[1/] TN/Tp - Total nitrogen/Total phosphorus; IN/Ip - Inorganic nitrogen/inorganic phosphorus, both on mg/ℓ/mg/ℓ basis

[2/] For IN = 0.53 mg N/ℓ and Ip = .021 mg P/ℓ in non-point surface runoff

[3/] For IN = 33 µg N/ℓ and Ip = 15 µg P/ℓ

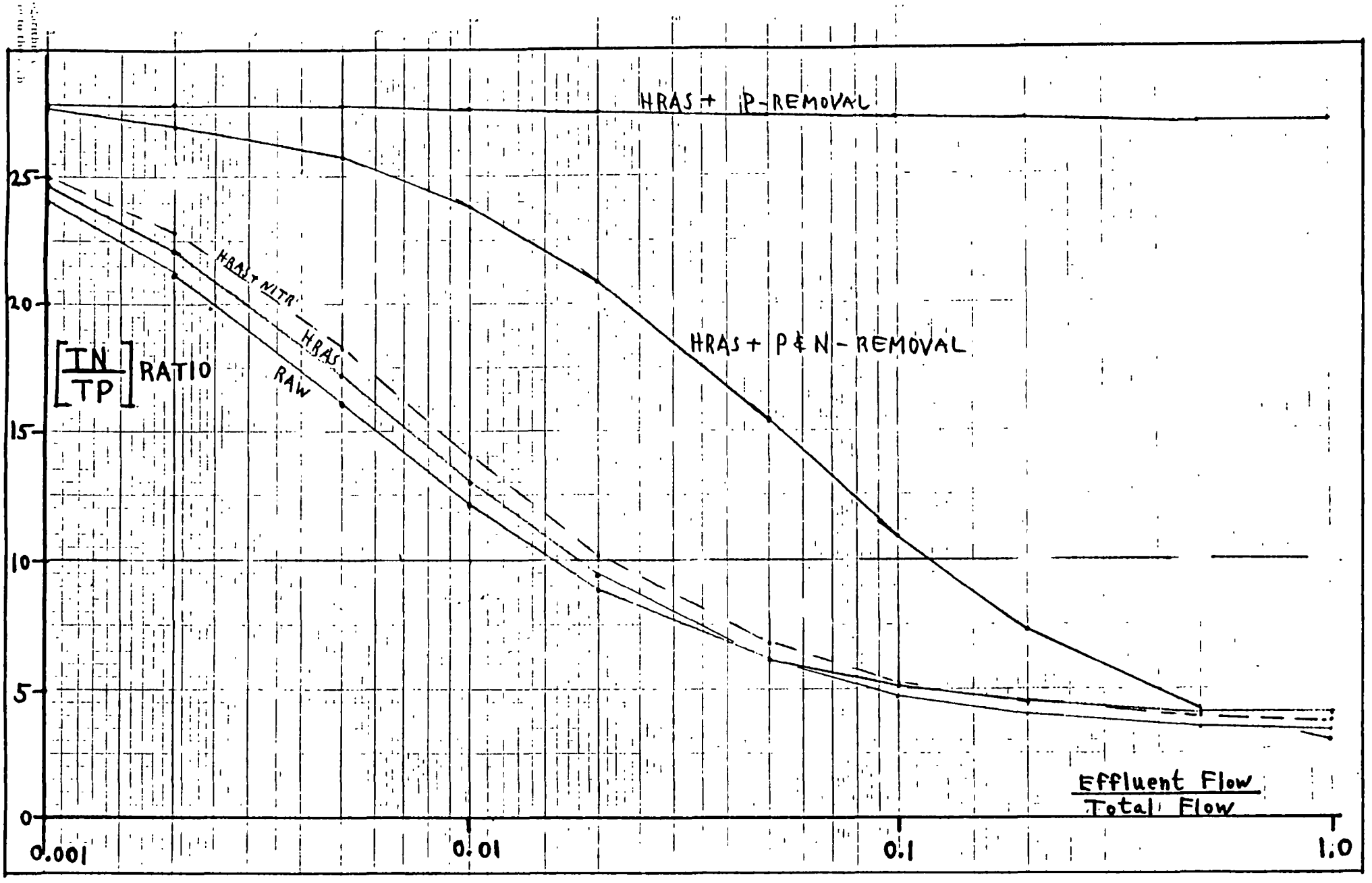

Figure 2. TN/TP as a function of plant effluent flow/total river flow for different levels of treatment. Treatment effluent concentrations from Table 1, river concentrations: TN = 1.45 mg N/ℓ; TP = .052 mg P/ℓ.

The N/p ratio is therefore a useful first approximation to determining the significance of each nutrient in controlling phytoplankton biomass. One should not however necessarily conclude that because nitrogen is the limiting nutrient in a given situation that nitrogen is the nutrient to be controlled. As the point source example indicated if a system were controlled by nitrogen, the installation of HRAS + P removal would shift the system to phosphorus limitation.

A Simple Stream Model Using the Principle of N/p Ratio

For streams there are several aspects of the above discussion that should be recognized.

1) The distance and hence the time of travel for stream nutrient problem contexts generally tend to be short, perhaps on the order of less than 10 days. This would be equivalent to distances of less than about 100 miles for streams moving at 1 ft/sec. Most stream stretches of interest would be shorter than this so that the travel time would be less than the 10 day period. As a result, the chlorophyll biomass may not have enough time to grow to the maximum level calculated from the N/p ratio approach discussed above. The rate of growth of the phytoplankton and the travel time of the stream length are therefore of specific importance.

2) Phytoplankton growth dynamics indicate that the concentrations of nitrogen and phosphorus that limit growth are relatively small compared to normal ambient levels of nutrients in streams subject to point source discharges. This can be seen by considering Eq. 8-22 of these notes, i.e.

$$G_p = G(T) \cdot G(I) \cdot G(N) \tag{1}$$

where G_p is the growth rate of the phytoplankton (day^{-1}), G(T), G(I) and G(N) are the effects of temperature, light and nutrients respectively on the growth rate. From Eq. 8-28, the nutrient effect is given by:

$$G(N) = \text{Min}\left\{\frac{IN}{K_{MN}+IN} ; \frac{Ip}{K_{Mp}+Ip}\right\} \tag{2}$$

At concentrations of the nutrient greater than about 5 times the half saturation concentration, the effect of the nutrient on the growth rate G(N) is less than 10%. That is, at IN and Ip at five times K_{MN} and K_{Mp}, G(N) = 0.83

and therefore has a relatively small effect on the overall growth rate of phytoplankton as seen from Eq. (1) above. Table 8-6 of these notes shows that the Michaelis concentration (the concentration at which growth rate is reduced by 1/2) for nitrogen is about 10 - 20 μg N/ℓ and for phosphorus is about 1 - 5 μg P/ℓ. Therefore, for IN and Ip greater than about 0.1 mg N/ℓ and .025 mg P/ℓ, respectively, these nutrients will not have any effect on the growth rate. Considering Tables 1 and 2, it is seen that, depending on stream dilution, the concentrations of IN and Ip will generally be significantly above these levels. Figure 3 shows this fact for upstream IN and Ip of 0.53 mg N/ℓ and 0.21 mg P/ℓ respectively (Omernik, 1977). As indicated, for nitrogen, the concentration at the outfall never reaches limiting levels simply because the upstream IN concentrations alone is above the maximum limiting concentration of about 0.1 mg N/ℓ. For phosphorus, when the effluent flows are greater than about 5 - 10% of the total river flow, then the Ip at the outfall will be above maximum limiting phosphorus concentration. It should be stressed however that these considerations are meant as a guide only since limiting nutrient concentrations may be reached at some downstream location from the outfall. As a general rule however, Figure 3 indicates that for ratios of effluent flow to total river flow of greater than about 10%, both phosphorus and nitrogen will tend to be present in excess concentrations. For "small" streams where effluent flow is equal to greater than upstream flow especially at drought conditions, then it is almost certainly true that the nutrients will be in excess and will not limit phytoplankton growth for a given stretch of river.

A simple model can now be constructed using the above considerations and the principle of the N/p ratio. Assume that a steady-state condition prevails. The analysis is therefore representative of a given flow and temperature regime that has held steady long enough for conditions to have reached an equilibrium state. Consider the phytoplankton equation at steady-state as:

$$u \frac{dP}{dx} = \frac{dP}{dt}^{*} = (G_p - D_p - v_s/H)P = G_n P \qquad (3)$$

where P is phytoplankton chlorophyll (μ chlor/ℓ) G_p is given by Eq. (1). D_p is respiration rate [day^{-1}], v_s is net settling from water column (m/day)

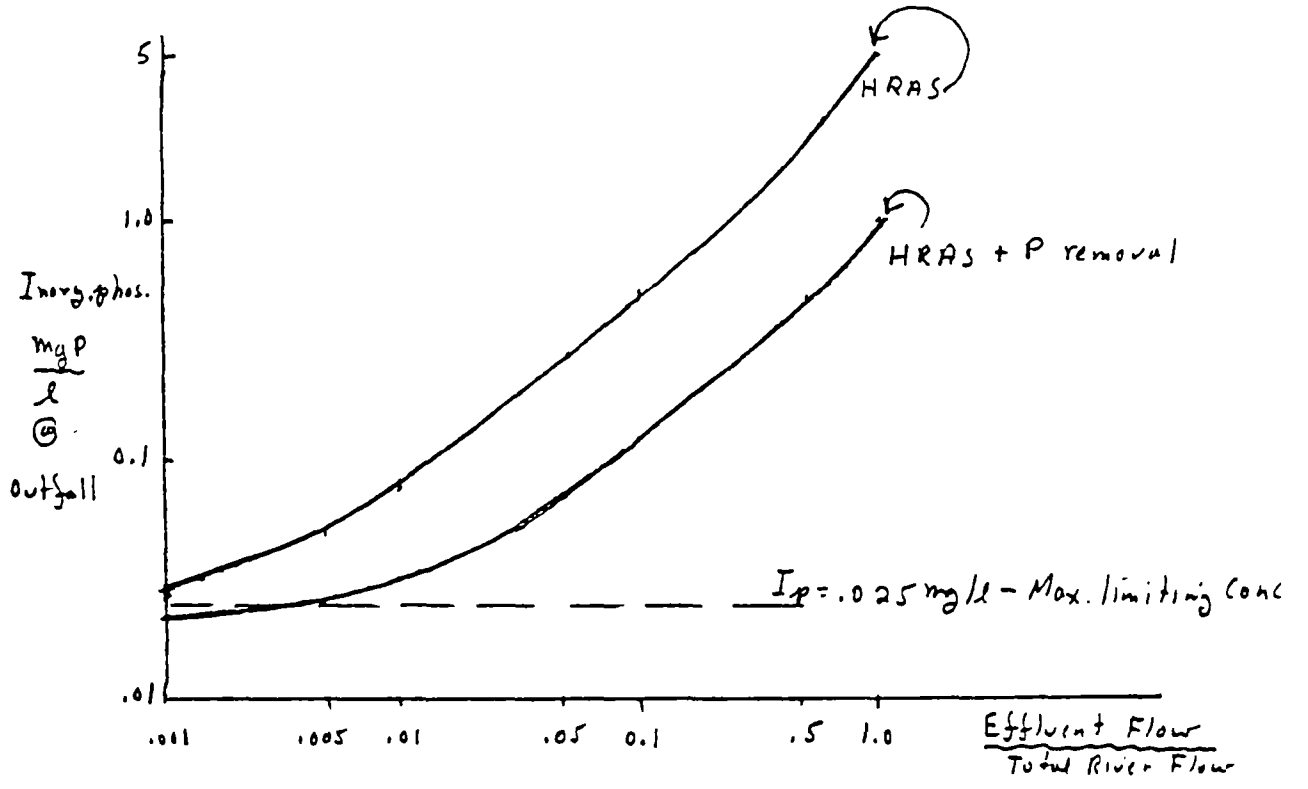

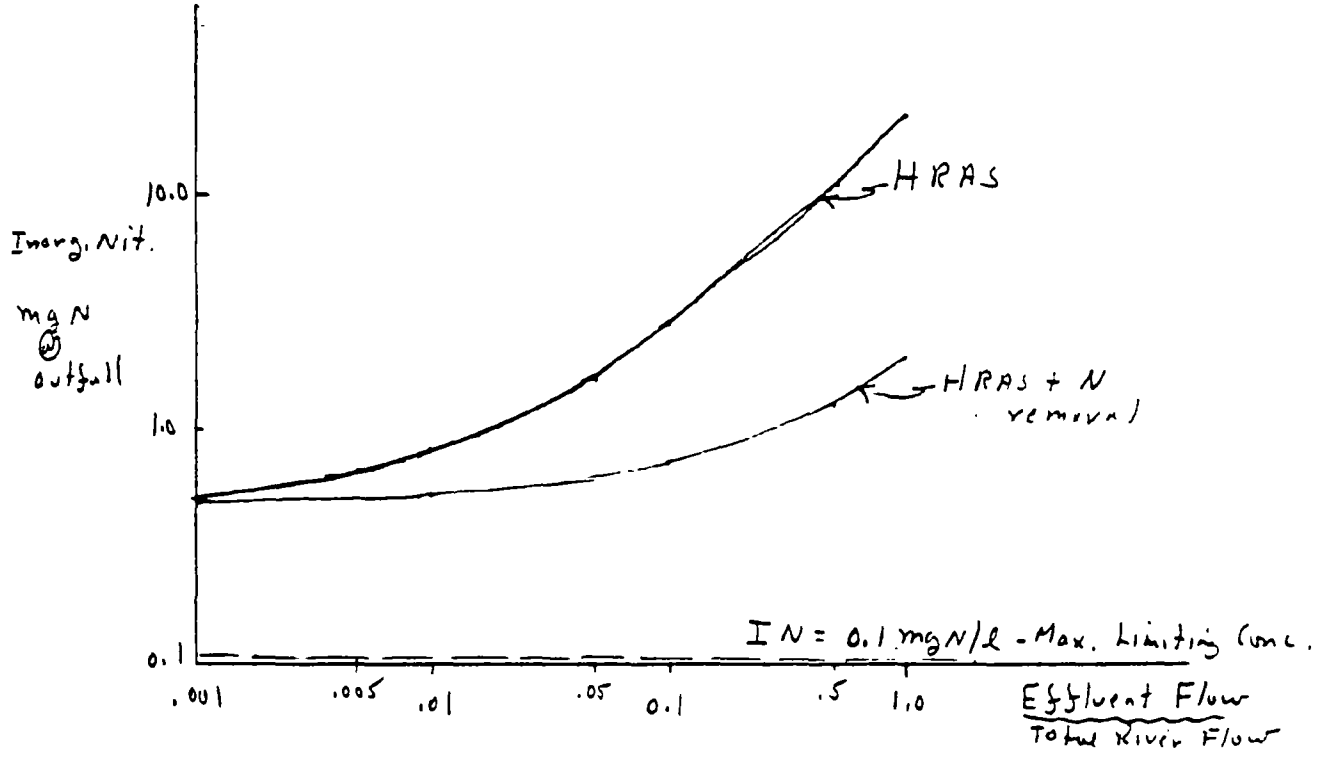

Figure 3. Inorganic phosphorus and nitrogen at outfall for different ratios of effluent flow to total river flow.

H is stream depth, u is stream velocity, x is distance and t^* is travel time (day) and:

$$G_n = G_p - D_p - v_s/H \tag{4}$$

If $G_p \neq f(IN,Ip)$ then G_n is a function only of temperature, light, extinction coefficient and net settling velocity. Figure 4 shows the behavior of G_n as a function of several environmental variables representative of conditions in smaller shallow streams. Thus the assumption of excess nutrients permits solution of Eq. (3) as:

$$P = P_o \exp (G_n)t^* \tag{5}$$

where P_o is the phytoplankton chlorophyll at the outfall.

Figure 5 shows the possible forms of Eq. (5). Because of light limitations and settling effects, G_n may be less than zero in which case there will be an exponential decrease of phytoplankton with travel time. G_n may also be zero where growth is just balanced by respiration and settling. The biomass then remains constant with distance. Finally, G_n may be positive resulting in exponential growth of the phytoplankton. The ultimate biomass then results from conversion of the IN or Ip at the outfall as discussed previously.

The inorganic nutrient equation can now be examined in the light of the preceding N/p discussion. Assume that a given fraction of IN or Ip will constitute the nutrient pool from which the growth of the phytoplankton will draw nutrients. Let the inorganic pool nitrogen = N_i and the inorganic pool phosphorus = p_i. A fraction of 0.75 used earlier is a good approximation, i.e. 75% of the total inorganic nutrient is available for conversion to phytoplankton. The residual 25% of the nutrient recycles into the detrital pool and less available forms and is also lost by settling.

Therefore, the nutrient equation is for phosphorus:

$$\frac{dp_i}{dt^*} = -a_p G_p P \tag{6}$$

and for nitrogen:

$$\frac{dN_i}{dt^*} = -a_N G_p P \tag{7}$$

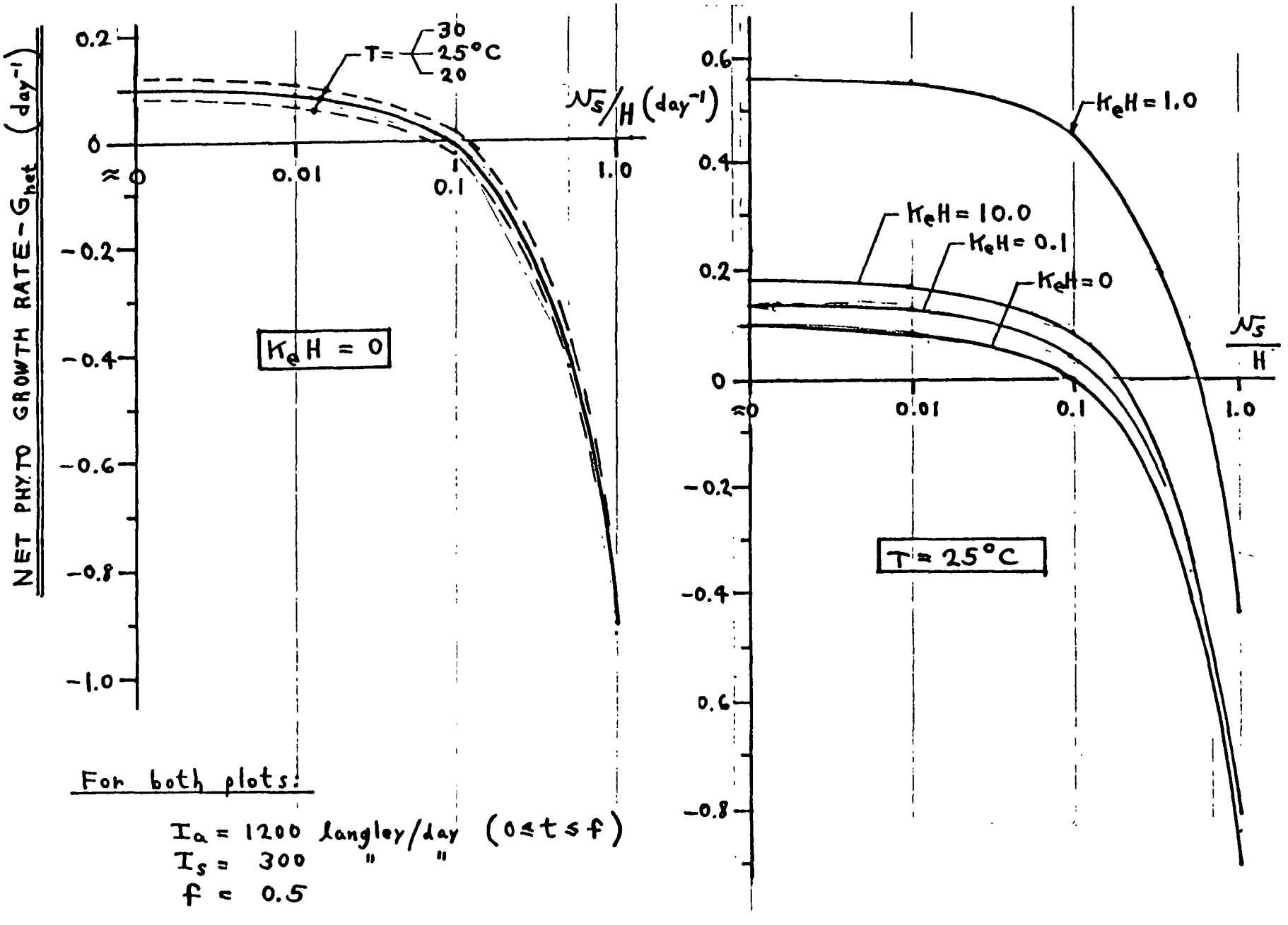

F 1. VARIATION of NET PHYTO. GROWTH RATE with TEMP, LIGHT, SETTLING

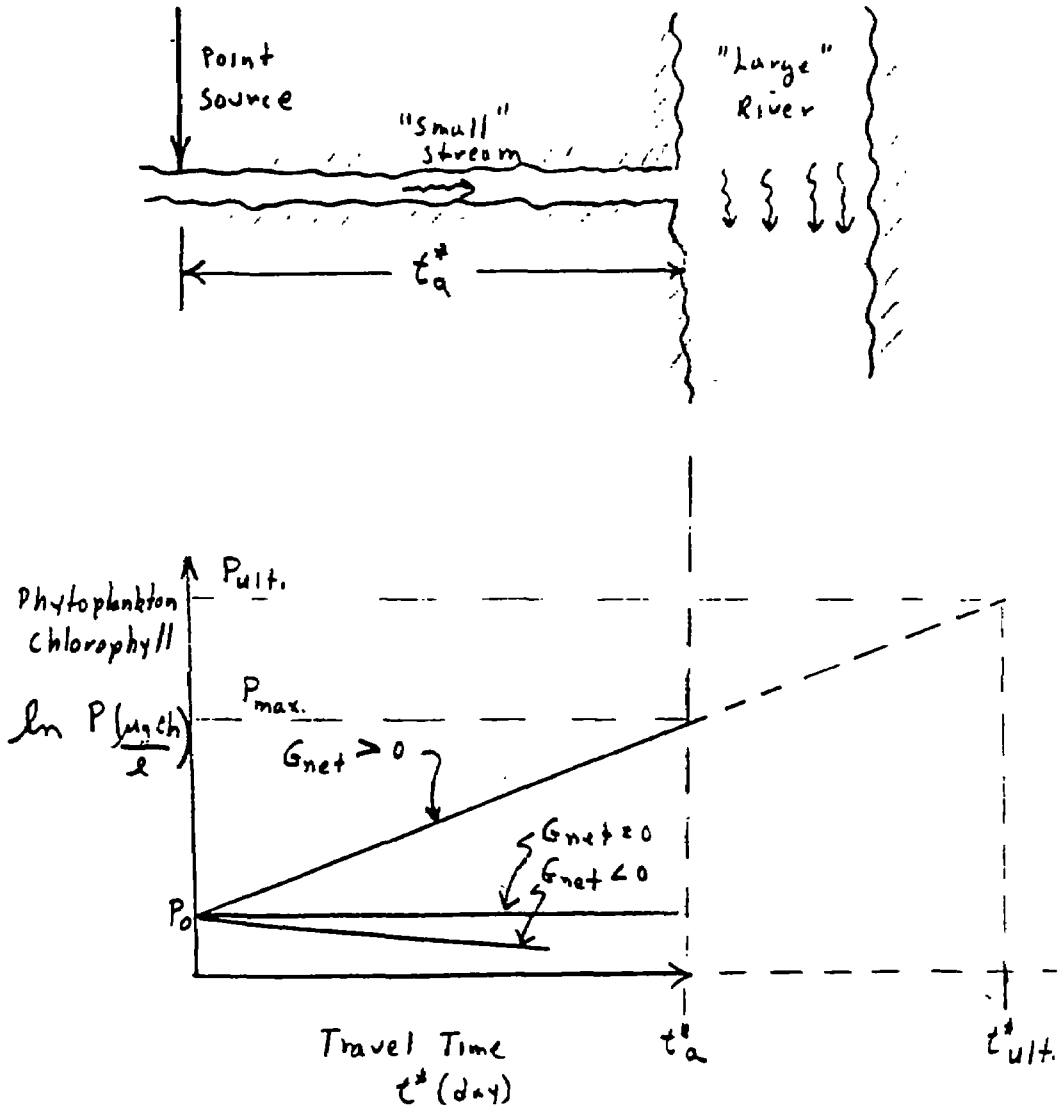

Figure 5. Schematic of relationship between phytoplankton chlorophyll, net growth and travel time.

where a_p = 1 µg phos/µ chlor and a_N = 7 µg N/µg chlor. The chlorophyll is given by Eq. (5) and substituting into Eqs. (6) and (7) and solving gives:

$$p_i = \frac{a_p G_p P_o}{G_n} (1 - e^{G_n t^*}) + p_{io} \qquad (8)$$

$$\text{for } p_i > 25 \text{ µg P/ℓ}$$

and

$$N_i = \frac{a_N G_p P_o}{G_n} (1 - e^{G_n t^*}) + N_{io} \qquad (9)$$

$$\text{for } N_i > 100 \text{ µg N/ℓ}$$

where p_{io} and N_{io} are phosphorus and nitrogen at the outfall in the river and note that the equations are only applicable for the inorganic nutrients above the maximum limiting concentration of p_i = 25 µg/ℓ and N_i of 100 µg/ℓ.

If estimates of G_p and G_n are obtained from previous expressions and P_o and initial conditions at outfall are available, then the travel time to reach the maximum nutrient concentration can be computed. This will then fix the maximum biomass to be expected over that reach. Solving Fig. (8) for t^*_{25} at p_i = 25 µg P/ℓ gives:

$$t^*_{25} = \frac{1}{G_n} \ln \frac{P'_o + p_{oi} - 25}{P'_o} \qquad (10)$$

where

$$P'_o = \frac{a_p G_p P_o}{G_n} \qquad (10a)$$

Figure 6 shows t^*_{25} for various conditions on the parameters. Using G_p = 1/day and G_n = 0.1/day, and for p_{oi}, the initial available phosphorus concentration of greater than 1000 µg P/ℓ, (see Figure 3), which covers small effluent dominated streams with HRAS and w/o P removal, Figure 5 indicates that t^*_{25} is generally greater than 5 - 10 days. Therefore, for small effluent dominated streams, if the study length is less than about 5 - 10 days, the phosphorus will still be above 25 µg P/ℓ and therefore in excess. At average velocities of 0.5 - 1 ft/sec, this is equivalent to about 40 - 160 miles, well within the study reaches usually under investigation. Note however from Figure 6 that the phytoplankton concentration at the outfall is an important parameter to be specified. At high initial chlorophyll levels at the outfall the time of travel to reach the ultimate con-

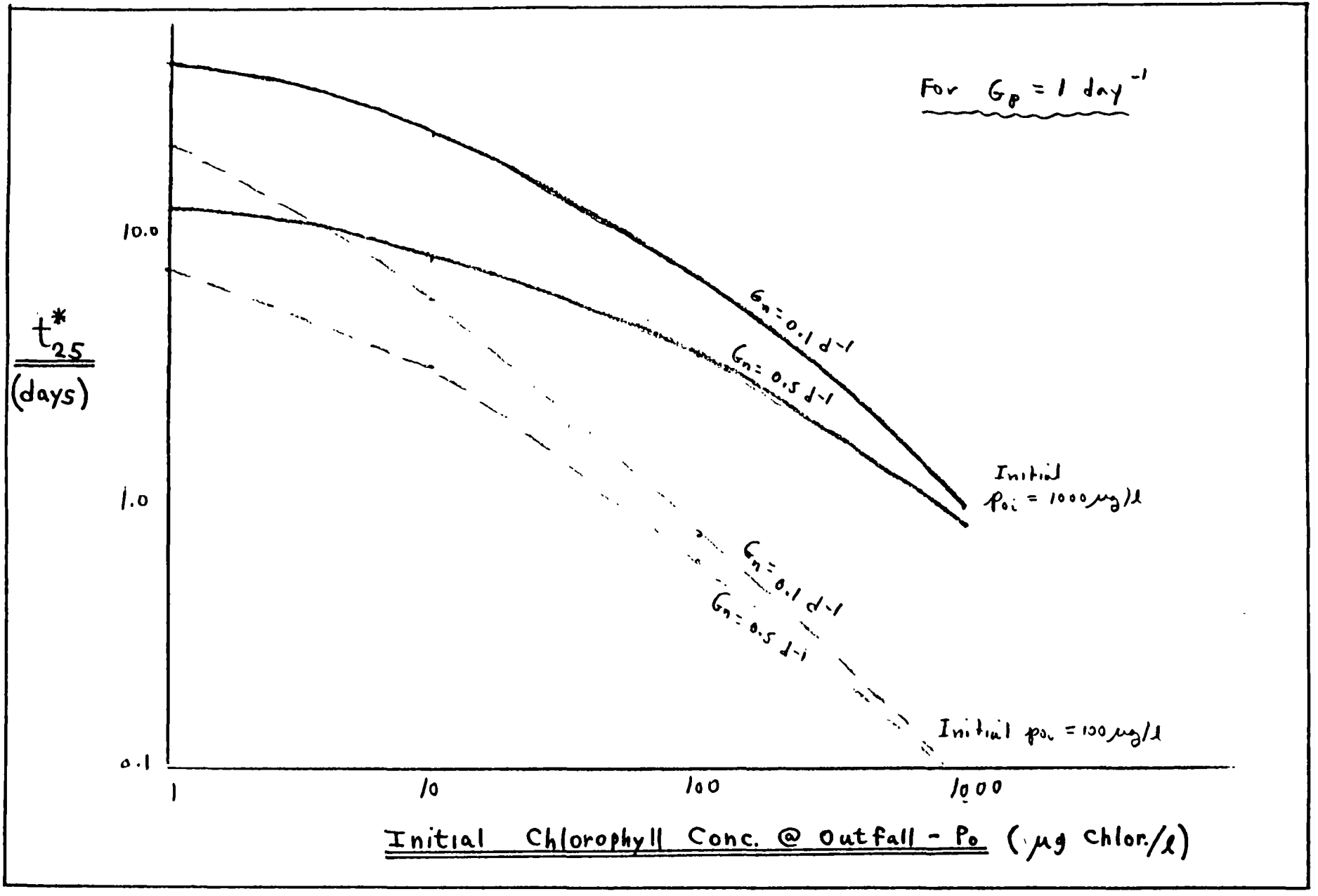

Figure 6. Relationship between t^*_{25}, the travel time to p_i of 25 µg/l and nutrient and phytoplankton parameters.

centration of phytoplankton is of course markedly reduced since a sufficient "seed" biomass already exists at the outfall. For small streams however one would not normally expect upstream concentrations to be greater than 100 µg chlor/ℓ.

In this simple model then, the only way in which the maximum phytoplankton biomass will decrease as a function of nutrient removal at a point source is to reduce the time to reach the maximum limiting nutrient concentration. Figure 7 shows this effect. If t^*_{25} remains greater than t^*_a, the actual stream length after phosphorus removal then there will be no reduction in biomass. This is because the stream is simply not long enough for a given net growth rate to result in a nutrient limitation.

To summarize this simple model then, the following procedure is suggested.

1) Compute G_n from Eq. (4) and Eqs. 8-29 and 8-30, or estimate G_n from available phytoplankton data on the stream using Eq. (5).
2) For a given inorganic phosphorus concentration at the outfall estimate percent available for phytoplankton growth, say 75%.
3) Calculate t^*_{25} from Eq. (10) and compare actual stream length t^*_a to t^*_{25}. If t^*_a is less than t^*_{25}, then $P_{max} = P_o \exp G_n t^*_a$. If t^*_a is greater than t^*_{25} then the biomass is at least $P_{max} = P_o \exp G_n t^*_{25}$ and is probably slightly greater than this amount.
4) Estimate the new p_{oi} under a phosphorus removal program.
5) Calculate the new t^*_{25} under the removal program.
6) Compare $(t^*_{25})_{new}$ to t^*_a. If $(t^*_{25})_{new} < t^*_a$ then a biomass reduction will occur and the maximum biomass is given approximately by $P = P_o \exp G_n (t^*_{25})_{new}$. If $(t^*_{25})_{new} \geq t^*_a$ then no reduction in biomass will occur as a result of the treatment program.

The case where $G_n = 0$ is an interesting one. For this case, $P = P_o$, a constant. Therefore,

$$\frac{dp_i}{dt^*} = -a_p G_p P_o \qquad (11)$$

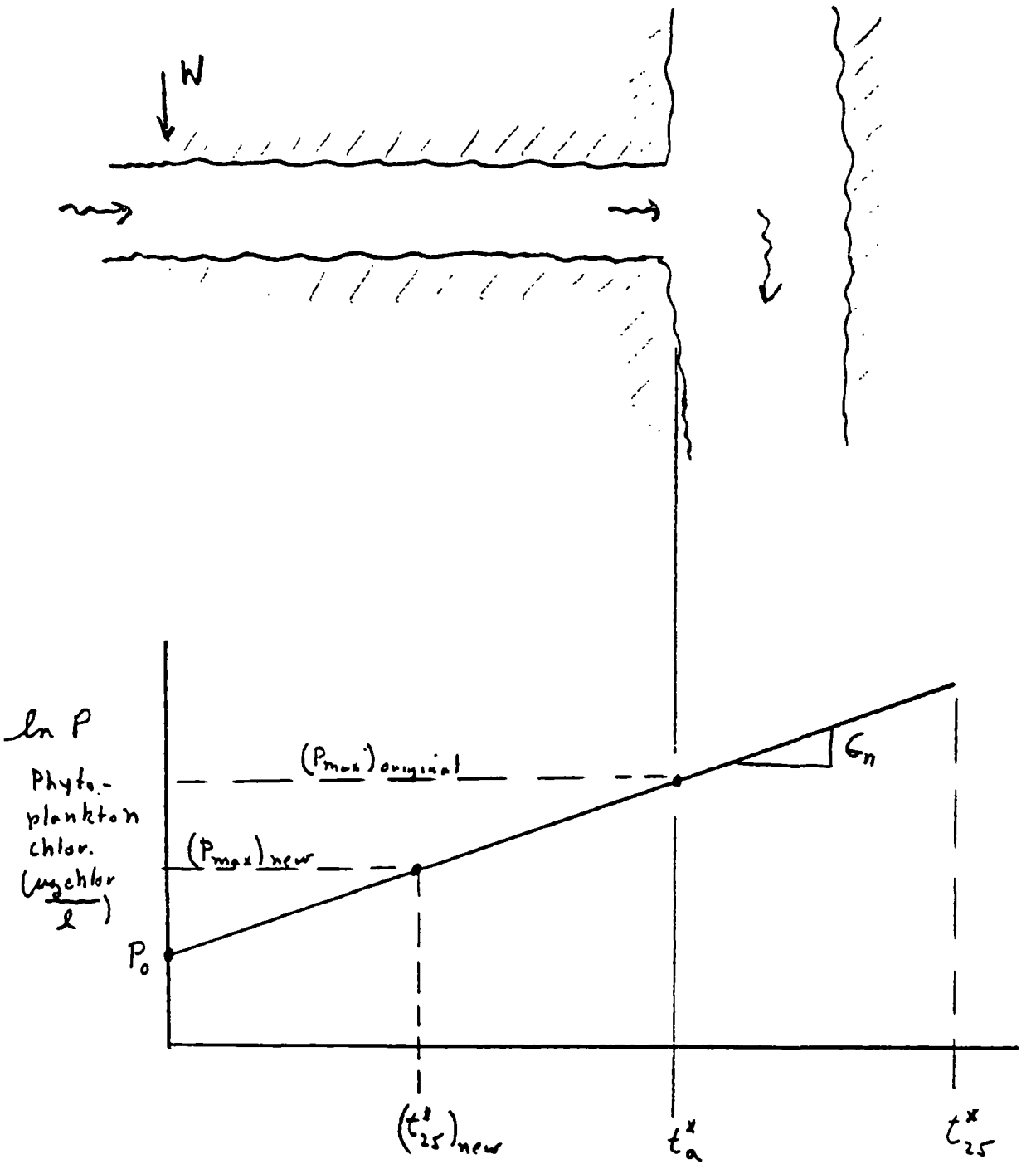

Figure 7. Relationship between phytoplankton chlorophyll and travel time showing reduction in biomass due to reduction in time of travel to limiting nutrient.

which is also a constant. The inorganic phosphorus would therefore decline linearly with travel time as:

$$p_i = -a_p G_p P_o t^* + p_{io} \tag{12}$$

The distance to t^*_{25} is therefore:

$$t^*_{25} = \frac{p_{io} - 25}{a_p G_p P_o} \tag{13}$$

However, it can be noted that for this case, reduction of nutrients at the source will not alter the biomass. Again this only applies for the excess nutrient region. If p_{io} is reduced such that $t^*_a > (t^*_{25})_{new}$ then it can be presumed that a reduction in biomass will occur but the actual reduction cannot be computed since it will represent the limiting nutrient region.

Extension of Simple Stream Model

One of the more sensitive assumptions made in the preceding simple model is the specification of the amount of inorganic nutrient available for conversion. Since this can result in a 25-50% reduction of outfall nutrient available for phytoplankton growth, it is an assumption that can be further examined. Consider again the reach of the stream where the nutrients are considered to be in excess and examine two nutrient forms: p_o as the organic or less available form of phosphorus and p_i as the inorganic phosphorus form available for uptake by the phytoplankton. In this context, p_o is operationally defined as total phosphorus biomass the sum of phytoplankton phosphorus and dissolved inorganic phosphorus. The three equations then that describe this interaction are:

$$\frac{dp_o}{dt^*} = DP - K_{oi} p_o - \frac{v_{so}}{H} p_o \tag{14}$$

$$\frac{dp_i}{dt^*} = K_{oi} p_o - a_p G_p P \tag{15}$$

$$\frac{dP}{dt^*} = G_n P \tag{16}$$

where K_{oi} is the hydrolysis or biodegradation of organic forms to inorganic phosphorus and v_{so} is the net loss rate of the organic phosphorus. Since nutrients are in excess, Eq. (16) is decoupled from Eqs. (15) and (14) and the solution is given by Eq. (5). Substitution of this equation into Eq. (14) gives the following:

$$\frac{dp_o}{dt^*} + K_o p_o = DP_o \exp G_n t^* \tag{17}$$

where $K_o \quad K_{oi} + v_{so}/H$. The solution is:

$$p_o = \frac{DP_o}{K_o + G_n}(e^{G_n t^*} - e^{-K_o t^*}) + p_{oo} e^{-K_o t^*} \tag{18}$$

where p_{oo} is the organic phosphorus at the outfall.

Substitution of this equation and Eq. (5) into Eq. (15) permits solution of the inorganic nutrient form as:

$$p_i = p_{i1}(e^{G_n t^*} - 1) + p_{i2}(1 - e^{-K_o t^*}) + p_{io} \tag{19}$$

where

$$p_{i1} = \frac{1}{G_n}\left[\frac{K_{oi} DP_o}{K_o + G_n} - a_p G_p P_o\right] \tag{19a}$$

and

$$p_{i2} = \frac{1}{K_o}\left[p_{oo} - \frac{K_{oi} DP_o}{K_o + G_n}\right] \tag{19b}$$

and p_{io} is the initial inorganic phosphorus at the outfall. In principle all the coefficients in these equations can be estimated either from field data or from the literature. These equations can be used again only for the excess nutrient region of the streams and only if data are available on the separate phosphorus forms.

Relationships to D.O.

For some stream situations, the phytoplankton concentration itself may not be a matter of great concern in terms of any nuisance condition created

by high chlorophyll concentrations. However, the relationship between the resulting phytoplankton biomass and the dissolved oxygen resources may be of significant concern. This is especially true for the diurnal variations in D.O. occasioned by the phytoplankton. The basic D.O. equation including only sources and sinks due to phytoplankton is:

$$u \frac{dc_p}{dx} = K_a(c_s - c_p) + P'_{av} - R'_{av} \tag{20}$$

where c_p is the D.O. variation due to photosynthetic effect K_a is the reaeration coefficient and P'_{av} and R'_{av} are the average daily phytoplankton D.O. production and respiration respectively. Now:

$$P'_{av} = a_{op} G_p P \tag{21}$$

$$R'_{av} = a_{op} DP \tag{22}$$

where a_{op} = 0.133 - 0.266 mg DO/µg chlor. If now D_p is designated as the deficit resulting from photosynthesis, i.e.

$$D_p = c_s - c_p,$$

then

$$\frac{dD_p}{dt^*} = -a_{op}(G_p - D)\, P\,(t^*) - K_a D_p \tag{23}$$

Several possibilities now can be examined on $P(t^*)$. These would be cases where data were available on $P(t^*)$ and inferences can be drawn of the effect of $P(t^*)$ on the average D.O. regime.

Case I: $P(t^*) = \text{constant} = P_o$

For this case, $\frac{dP}{dt^*} = 0$ and $(G_p - D) = (v_s/H)$. Thus if $v_s/H \neq 0$, then $G_p > D$ and there is a positive production of D.O. given by:

$$D_p = -\frac{a_{op}(G_p - D)P_o}{K_a}\left(1 - e^{-K_a t^*}\right) \tag{24}$$

If however it is determined that $v_s = o$, then growth just balances respiration (to maintain P_o) and $G_p - D = o$. Therefore, there is no net production of D.O. If then from the data, the phytoplankton is a constant with distance, then either there is a net production of oxygen for $v_s/H \neq o$, or the production is zero for $v_s = o$.

Case II: $P = p_o \exp G_n t^*$; $G_n > o$

For this case growth exceeds respiration and settling and there is a net production of oxygen. Substitution into Eq. (23) gives:

$$\frac{dD_p}{dt^*} = -a_{op}(G_p - D)P_o e^{G_n t^*} - K_a D_p \tag{25}$$

The solution then is:

$$D_p = -\frac{a_{op}(G_p - D)P_o}{K_a + G_n}\left(e^{G_n t^*} - e^{-K_a t^*}\right) \tag{26}$$

which is approximately exponential. It should be recalled that this case can only apply to the "excess nutrient" region which is less than t^*_{25} (for phosphorus) as discussed earlier.

Case III: $P = p_o \exp G_n t^*$; $G_n < D$.

With net growth less than zero, these data would show phytoplankton declining with distance downstream. In such a case, respiration and net settling exceed growth and there may or may not be a net utilization of oxygen. If $v_s = o$, then $D > G$, and a net utilization occurs. For $v_s \neq o$ however, G_p may still exceed D and a net production could occur. This can only be determined by a specific analysis of the actual stream. Substitution into Eq. (23) gives:

$$\frac{dD_p}{dt} = -a_{op}(G_p - D)P_o e^{-G_n t^*} - K_a D_p \tag{27}$$

and the solution is:

$$D_p = - \frac{a_{op}(G_p - D)}{K_a - G_n}(e^{-G_n t^*} - e^{-K_a t^*}) \qquad (28)$$

These D.O. equations coupled to the simplified phosphorus-phytoplankton model discussed earlier permit the model analyst to analyze the response due to nutrient reduction on both the phytoplankton as well as the D.O.

An example of the impact of phosphorus reduction on ambient chlorophyll a concentrations follows.

REFERENCES

Goldman, J.C., D.R. Tenore, H.I. Stanley. 1973. Inorganic nitrogen removal from wastewater: effect on phytoplankton growth in coastal marine waters. Science, Vol. 180:955-956.

Omernik, J.M. 1977. Non-point source-stream nutrient level relationships: a nationwide study. EPA-600/3-77-105, Corvallis, ERL, USEPA, Corvallis, Oreg., 151 pp. + plots.

EXAMPLE - SIMPLIFIED PHOSPHORUS ANALYSIS IN STREAMS*

DATA

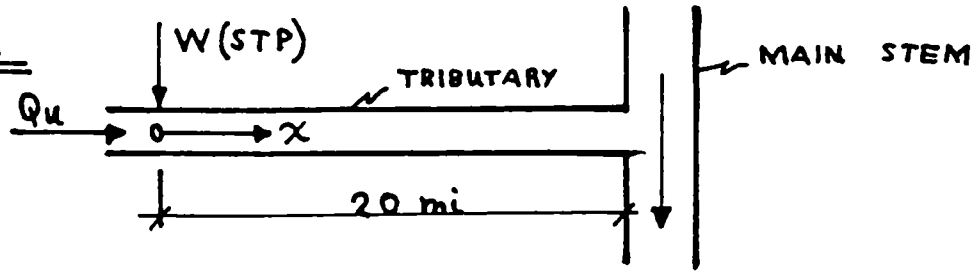

Item		Condition: Present	Condition: Design
FLow - upstream	cfs	20	12
- STP	MGD	0.25	0.30
Stream - Depth (H)	ft	3.0	2.2
- Velocity (u)	fps	0.5	0.4
- Water Temperature (T)	°C	23	25
Sunlight - Daily Solar Radiation	langley/day	600	600
- Photoperiod (f)		0.5	0.5
- Stream Light Extinction Coefficient (Ke)	ft^{-1}	0.33	0.33
Inorganic Phosphorus Concentration	mg/l		
- Upstream		0.02	0.02
- STP effluent		5	1
Chlorophyll a Concentration	µg/l		
- Upstream ($x \leq 0$)		25	25
- Downstream ($x = 20$ mi)		65	

PROBLEM Estimate the maximum chlorophyll a concentration in the twenty mile reach of the tributary under "Design" conditions.

SOLUTION

A. PRESENT CONDITIONS

. Determine Net Phytoplankton Growth Rate (G_n)

Assume an exponential increase of phytoplankton between $x = 0$ & 20 miles (confirmed by data).

* JOHN A MUELLER

$$t^*_{20} = 20 \text{ mi} / \left(0.5 \text{ fps} \times 16.4 \frac{\text{mpd}}{\text{fps}} \right) = 2.44 \text{ days}$$

$$P_{20} = P_0 e^{G_m t^*_{20}}, \quad 65 = 25\, e^{G_m \times 2.44},$$

$$G_m = \left[\ln (65/25) \right] / 2.44 = \underline{\underline{0.391/\text{day}}}$$

3/4

2. Estimate Net Phyto Settling Rate (N_S)

$$G_m = G_p - D_p - N_S/H \quad , \quad N_S = H(G_p - D_p - G_m)$$

G_p

$$G_p = G(T) \cdot G(I)$$

$$G(T) = 1.8 \times 1.066^{(23-20)} = 2.18/\text{day}$$

$$G(I) = \frac{e\, f}{k_e H} \left[\exp(-\alpha_1) - \exp(-\alpha_0) \right]$$

$$\alpha_0 = I_a / I_s = \left(600 \text{ ly/day} / 0.5 \right) / 300 \text{ ly/day} = 4.00$$

$$\alpha_1 = \alpha_0 \exp(-k_e H) = 4.00 \exp(-0.33 \times 3.0) = 1.47$$

$$G(I) = \frac{2.718 \times 0.5}{0.33 \times 3.0} \left[\exp(-1.47) - \exp(-4.00) \right] = 0.287$$

$$G_p = G(T) \cdot G(I) = 2.18/\text{day} \times 0.287 = 0.626/\text{day}$$

$$D_p = 0.1 \times 1.08^{(23-20)} = 0.126/\text{day}$$

$$\therefore N_S = 3.0 \text{ ft} \left(0.626 - 0.126 - 0.391 \right) \text{day}^{-1} = \underline{\underline{0.327 \text{ ft/day}}}$$

3. Check for Nutrient Limitation

$$P_0' = \frac{a_p G_p P_0}{G_m} = \frac{1 \mu\text{g IP}}{\mu\text{g Chl a}} \times \frac{0.626}{\text{day}} \times \frac{25 \mu\text{g Chl a}}{l} \Big/ 0.391/\text{day} = 40 \frac{\mu\text{g IP}}{l}$$

$$f_{i0} = \frac{\Sigma W}{\Sigma Q} = \frac{20 \text{ cfs} \times 0.02 \text{ mg/l} + 0.25 \text{ MGD} \times 1.55 \text{ cfs/MGD} \times 5 \text{ mg/l}}{(20 + 0.25 \times 1.55) \text{ cfs}}$$

$$f_{i0} = 0.115 \text{ mg/l} = 115 \mu\text{g/l}$$

$$t^*_{25} = \frac{1}{G_m} \ln \left(\frac{P_0' + f_{i0} - 25}{P_0'} \right) = \frac{1}{0.391/\text{day}} \ln \left(\frac{40 + 115 - 25}{40} \right) = 3.01 \text{ days}$$

Since actual travel time to $x = 20$ mi, $t^*_a = 2.44$ days, is less than $t^*_{25} (= 3.01)$, no inorganic phosphorus nutrient limitation occurs for $0 \le x \le 20$ and preceding analysis is accurate.

B. DESIGN CONDITIONS

1. Estimate Net Phyto Growth Rate (G_n)

Assume that net settling rate of phyto is same as present condition ($\therefore \nu_s = 0.327/day$) and that light extinction coefficient will be same as present ($\therefore K_e = 0.33/ft$).

$\alpha_0 = 4.00$ as previously, $\alpha_1 = 4.00 \exp(-0.33 \times 2.2) = 1.935$

$$G(I) = \frac{2.718 \times 0.5}{0.33 \times 2.2}\left[\exp(-1.935) - \exp(-4.00)\right] = 0.236$$

$$G_p = 1.8 \times 1.066^{(25-20)} \times 0.236 = 0.585/day$$

$$D_p = 0.1 \times 1.08^{(25-20)} = 0.147/day$$

$$G_n = 0.585 - 0.147 - (0.327/2.2) = \underline{0.289/day}$$

2. Calculate Maximum Possible Phyto Conc. in Tributary (@ x=20 mi)

$t_a^* = 20/(0.4 \times 16.4) = 3.05$ days

Assuming upstream chlorophyll a (P_0) remains same as @ present,

$$P_{x=20} = P_0 e^{G_n t_a^*} = 25 \times \exp(0.289 \times 3.05) = \underline{60 \mu g\ Chl\ a/l}$$

3. Check for Nutrient Limitation

$P_0' = (1 \times 0.585 \times 25)/0.289 = 50.6\ \mu g\ IP/l$

$P_{i0} = 10^3(12 \times 0.02 + 0.3 \times 1.55 \times 1)/(12 + 0.3 \times 1.55) = 56.6\ \mu g\ IP/l$

$$t_{25}^* = \frac{1}{0.289} \ln\left(\frac{50.6 + 56.6 - 25}{50.6}\right) = 1.68 \text{ days}$$

Since t_a^* (= 3.05 days) is greater than t_{25}^* (= 1.68 days), the phyto. growth rate will be affected by the inorganic phosphorus nutrient limitation beyond $x = 11$ miles ($= 1.68 \times 0.4 \times 16.4$).

At $t_{25}^* = 1.68$ days,

$$P = 25\, e^{0.289 \times 1.68} = 41 \mu g\ Chl\ a/l$$

Therefore, the maximum phytoplankton concentration in the twenty mile reach would be in the range of

$$\underline{41 \mu g/l < Chl\ a(max) < 60 \mu g/l}$$

B. DESIGN CONDITIONS (cont'd)

4. t^*_{25} for Original Loading

$$P_o' = 50.6\ \mu g/l$$

$$\phi_{io} = 10^3 (12 \times 0.02 + 0.3 \times 1.55 \times 5) / (12 + 0.3 \times 1.55) = 205.8\ \mu g/l$$

$$t^*_{25} = \frac{1}{0.289} \ln \left(\frac{50.6 + 205.8 - 25}{50.6} \right) = 5.26 \text{ days}$$

Note that the load reduction has decreased the value of t^*_{25} from 5.26 days to 1.68 days.

5. t^*_{25} for Effluent Concentration of 0.2 mg/l

$$P_o' = 50.6\ \mu g/l$$

$$\phi_{io} = 10^3 (12 \times 0.02 + 0.3 \times 1.55 \times 0.2) / (12 + 0.3 \times 1.55) = 26.7\ \mu g/l$$

$$t^*_{25} = \frac{1}{0.289} \ln \left(\frac{50.6 + 26.7 - 25}{50.6} \right) = 0.114 \text{ days}$$

For this low effluent concentration, instream phytoplankton would be at a minimum of:

$$P = 25\, e^{0.289 \times 0.114} = 26\ \mu g/l \text{ Chl a}.$$

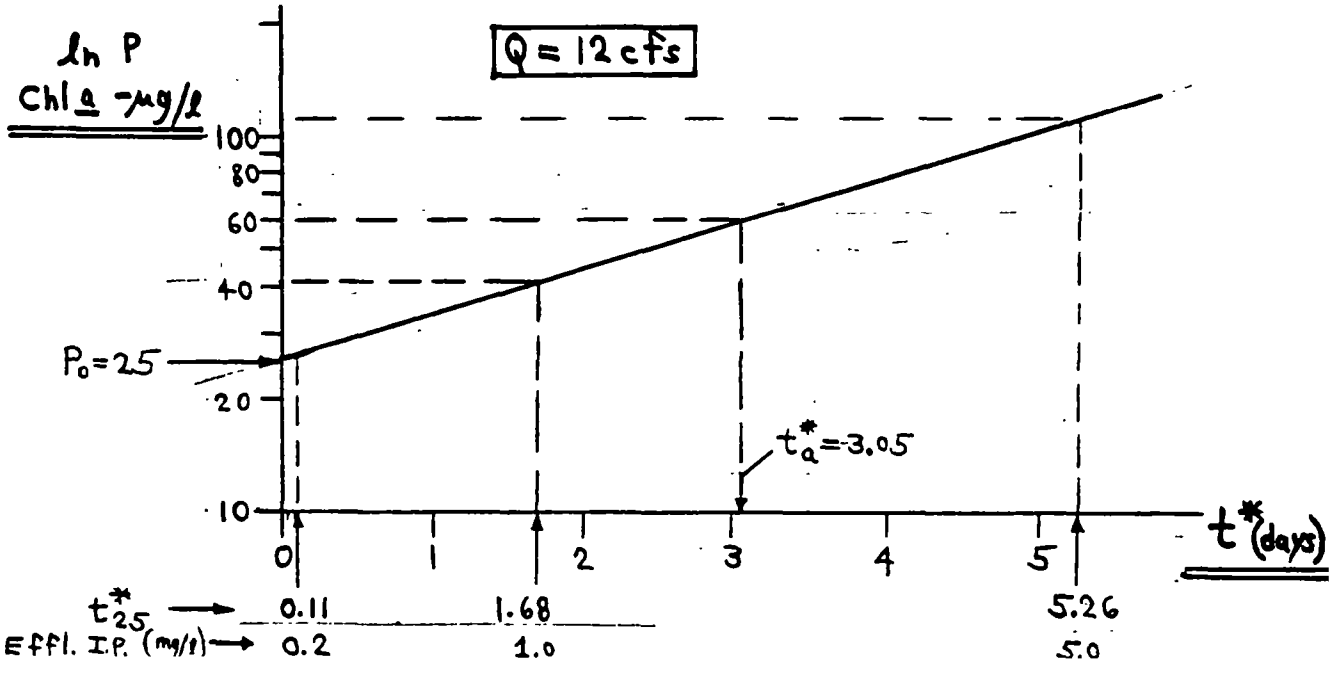

EFFECT OF SINUSOIDAL LOAD VARIATION ON STREAM DISSOLVED OXYGEN CONCENTRATIONS *

DATA

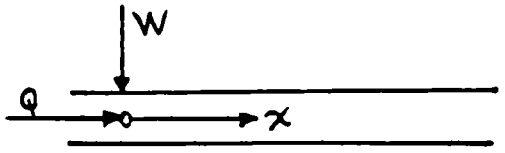

$Q = 100$ cfs $\quad K_r = 0.25$/day
$u = 4$ mi/day $\quad K_d = 0.25$/day
$C_s = 8.0$ mg/l $\quad K_a = 0.75$/day

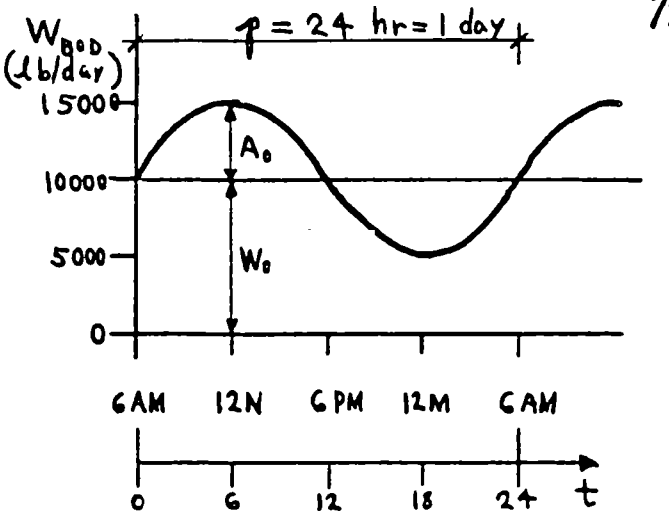

PROB

Calculate diurnal dissolved oxygen concentrations at $x = 6$, x_c, and 11 miles downstream of load.

SOLN

$$l(x,t) = L_o(t)\, e^{-K_r x/u}$$

where l = BOD concentration

$$L_o(t) = L_o + a_o \sin\left[(2\pi/T)(t - x/u)\right]$$

$$L_o = W_o/Q = 10000\ \text{lb/day}/(100\ \text{cfs} \times 5.4) = 18.55\ \text{mg/l}$$

$$a_o = A_o/Q = 5000/(100 \times 5.391) = 9.28\ \text{mg/l}$$

$$D(x,t) = \frac{K_d}{K_a - K_r} L_o(t) \left(e^{-K_r x/u} - e^{-K_a x/u}\right)$$

where D = dissolved oxygen deficit

$$C(x,t) = C_s - D(x,t)$$

where $C(x,t)$ = dissolved oxygen concentration

* JOHN A MUELLER

With $x_c = \dfrac{u \ln(K_a/K_r)}{K_a - K_r}$,

$$x_c = \frac{4 \text{ mi/day} \ \ln(0.75/0.25)}{(0.75-0.25)} = 8.79 \text{ miles},$$

& $t_c = x_c/u = 8.79/4 = 2.20$ days

$$L_o(t) = 18.55 + 9.28 \sin\left[\left(\frac{2\pi}{1 \text{ day}}\right)\left(t(\text{days}) - \frac{x}{4 \text{ mi/day}}\right)\right]$$

$$D(x,t) = \frac{0.25}{0.75-0.25} L_o(t)\left(e^{-0.25x/4} - e^{-0.75x/4}\right)$$

$$C(x,t) = 8.0 - D(x,t)$$

For $x = x_c = 8.79$ mi,

$$L_o(t) = 18.55 + 9.28 \sin\left[2\pi\left(t - \frac{8.79}{4}\right) = 2\pi(t-2.20)\right]$$

$$D(x_c,t) = 0.5\left(18.55 + 9.28 \sin[2\pi(t-2.20)]\right)\left(e^{-0.25 \times \frac{8.79}{4}} - e^{-0.75 \times 8.79/4}\right)$$

$$= 3.57 + 1.79 \sin[2\pi(t-2.20)]$$

$$C(x_c,t) = 8.0 - \left\{3.57 + 1.79 \sin\left[2\pi(t-2.20)\right]\right\}$$

$$= 4.43 - 1.79 \sin\left[2\pi(t-2.20)\right] \longleftarrow$$

Similarly for $x = 6$ and 11 miles,

$$C(6,t) = 4.74 - 1.68 \sin\left[2\pi(t-1.5)\right] \longleftarrow$$

$$C(11,t) = 4.52 - 1.74 \sin\left[2\pi(t-2.75)\right] \longleftarrow$$

Plots of the diurnal D.O. variation at the three locations are on the next sheet. Note the periodic nature of the D.O. Also note the time lag of 0.2 days (4.8 hr) from 12 NOON, the maximum load, to the maximum daily deficit at x_c.

Spatial plots of D.O. at 6AM & 12 NOON are shown to graphically display expected results. Spatial sampling of the stream would not yield typical sag.

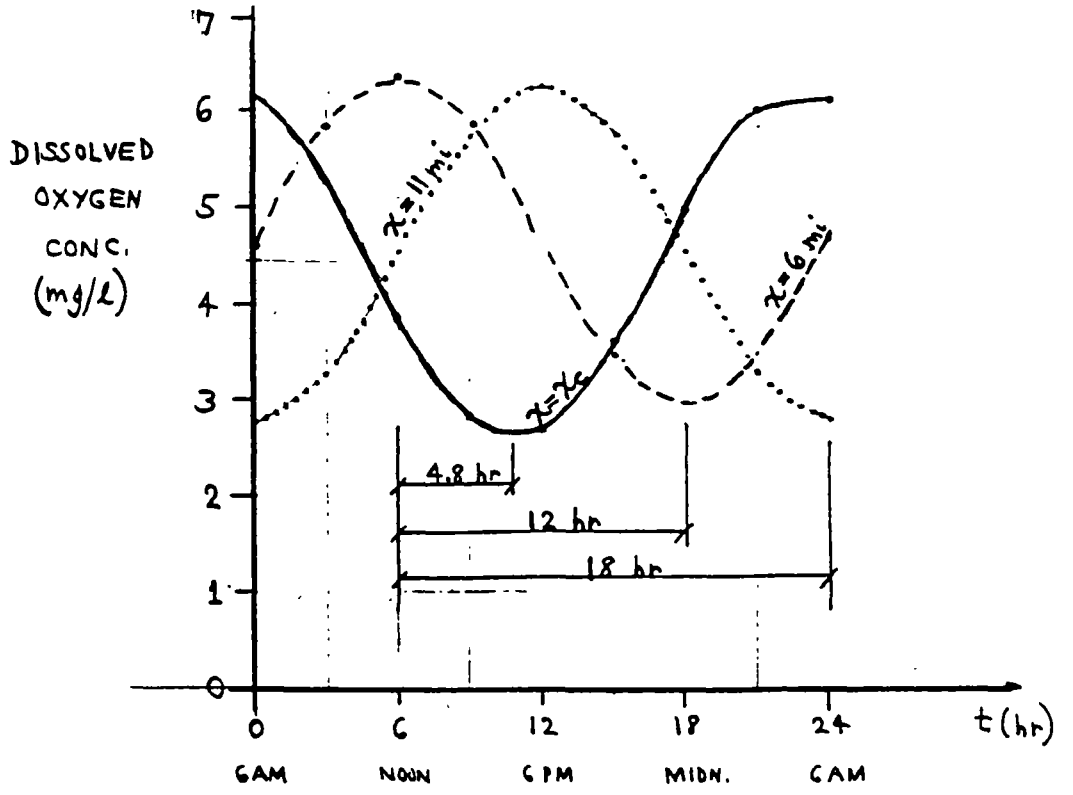
DISSOLVED OXYGEN CONC. (mg/L)
7
6
5
4
3
2
1
0
x=11 mi
x=6 mi
x=0
4.8 hr
12 hr
18 hr
0
6
12
18
24
t (hr)
6AM
NOON
6PM
MIDN.
6AM

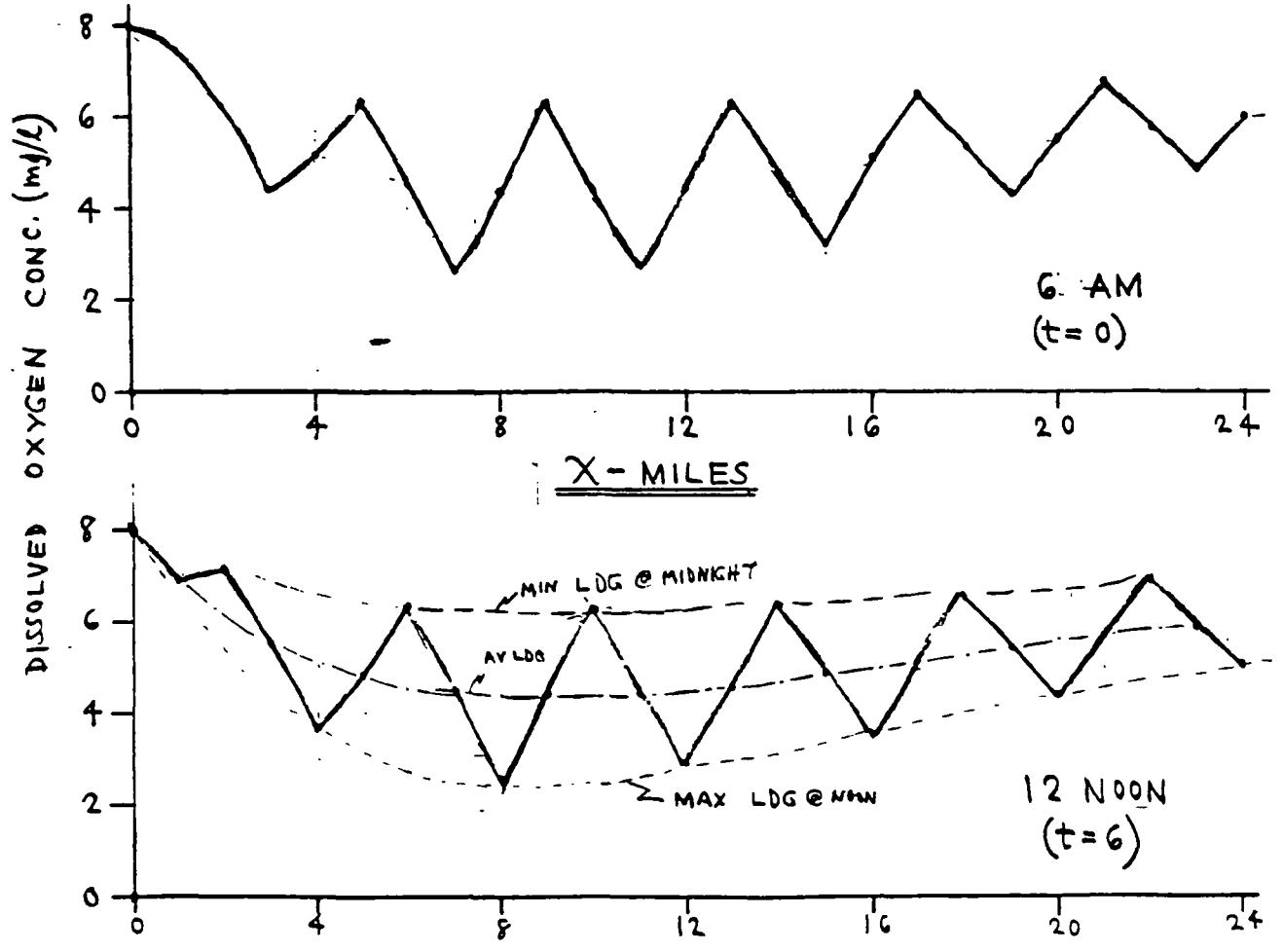
DISSOLVED OXYGEN CONC. (mg/L)
8
6
4
2
0
6 AM
(t=0)
0
4
8
12
16
20
24
X - MILES
MIN LDG @ MIDNIGHT
AV LDG
MAX LDG @ NOON
12 NOON
(t=6)

THE WICOMICO RIVER ESTUARY
AN ESTUARINE EUTROPHICATION EXAMPLE[1/]

Background

The purpose of modeling the Wicomico River, a tributary to Chesapeake Bay, was to illustrate the general methodology of applying mathematical models to determine waste load allocations for a eutrophied estuary. Eutrophied conditions, upstream of Chesapeake Bay in the vicinity of major outfalls, as observed in the Wicomico River, are typical of many Maryland rivers. The Wicomico River analysis also incorporates most of the complexities encountered in a modeling study.

The Wicomico River study area is shown in Figure W-1, and extends from the dam on Johnson's Pond in Salisbury, Maryland to the mouth of Ellis Bay, a distance of approximately 22 miles. The river is tidal to the dam with a mean daily tidal range at Salisbury of 3.0 feet. The salinity generally varies from about 10 ppt at the mouth to less than 1 ppt throughout the upper 1/3 to 1/2 of the estuary length depending on tidal stage, season and weather factors. The maximum salinity observed in the vicinity of Salisbury is reported (Webb and Heidel, 1970) to be about 0.1 ppt at U.S. Highway 50 (MP 21). As such, the river is essentially fresh water throughout its upper reaches.

At mean low tide, the average depths in the tidal portion of the Wicomico River vary from 6 feet at the mouth, increasing to 20 feet midway up river, and decreasing to 8 feet at Salisbury. A center channel provides for some water-borne commerce and is used principally by oil tankers and barges.

The total drainage area of the Wicomico River basin is 239 square miles. Approximately 90 percent of the Wicomico River watershed is rural - about equally divided between farm, forest and marsh. The population of this area is about 50,000 of which about 70 percent is concentrated in the vicinity of Salisbury. The raising of chickens, related feed and processing industries,

[1/] Abstracted from Salas and Thomann, (1975).

and the production and processing of other farm products are an important part of the economy. Several industries which specialize in manufactured products are located at Salisbury.

The major waste source in the tidal portion of the Wicomico River is the Salisbury Sewage Treatment Plant (STP) (refer to Figure W-1) which receives both domestic (40 percent of volume) and industrial (60 percent of the volume) waste (Pheiffer and Donnelly, 1972). This secondary treatment plant discharged an average of about 4 million gallons per day with a BOD_5 of approximately 3,000 lb/day.

Hydrology

The United States Geological Survey (USGS) maintains one gaging station on a continuous basis in the Wicomico River watershed. This station is located on Beaverdam Creek (drainage area = 19.5 square miles) (Figure W-1) which is a tributary to the tidal Wicomico River near Salisbury. Average stream flow in the creek for the 38 years of record is 23.9 cfs with maximum and minimum recorded discharges of 1,480 cfs and 0.4 cfs, respectively. The 7 day-10 year low flow is 1.4 cfs (Walker, 1971). Low flows, however, are affected by regulation at the dam in Beaverdam Creek.

The North Prong of the Wicomico River above the dam (which separates the tidal and non-tidal portions of the Wicomico River) at Salisbury crosses the Naylor Mill Paleo channel (an ancient filled river channel). This paleo channel has been reported (Boggess and Heidel, 1968) to highly influence the low flow conditions in the upper Wicomico River resulting in high yields. This may be contrasted to probably lower yields in the lower Wicomico River where groundwater infiltration is not as pronounced. As such, the freshwater flow is disproportionate to the drainage area under low flow conditions with the majority of the freshwater flow emanating from within the upper reaches of the watershed.

Correlations were developed with measured discharge data to estimate the freshwater flow in the Wicomico River for the periods of analyses.

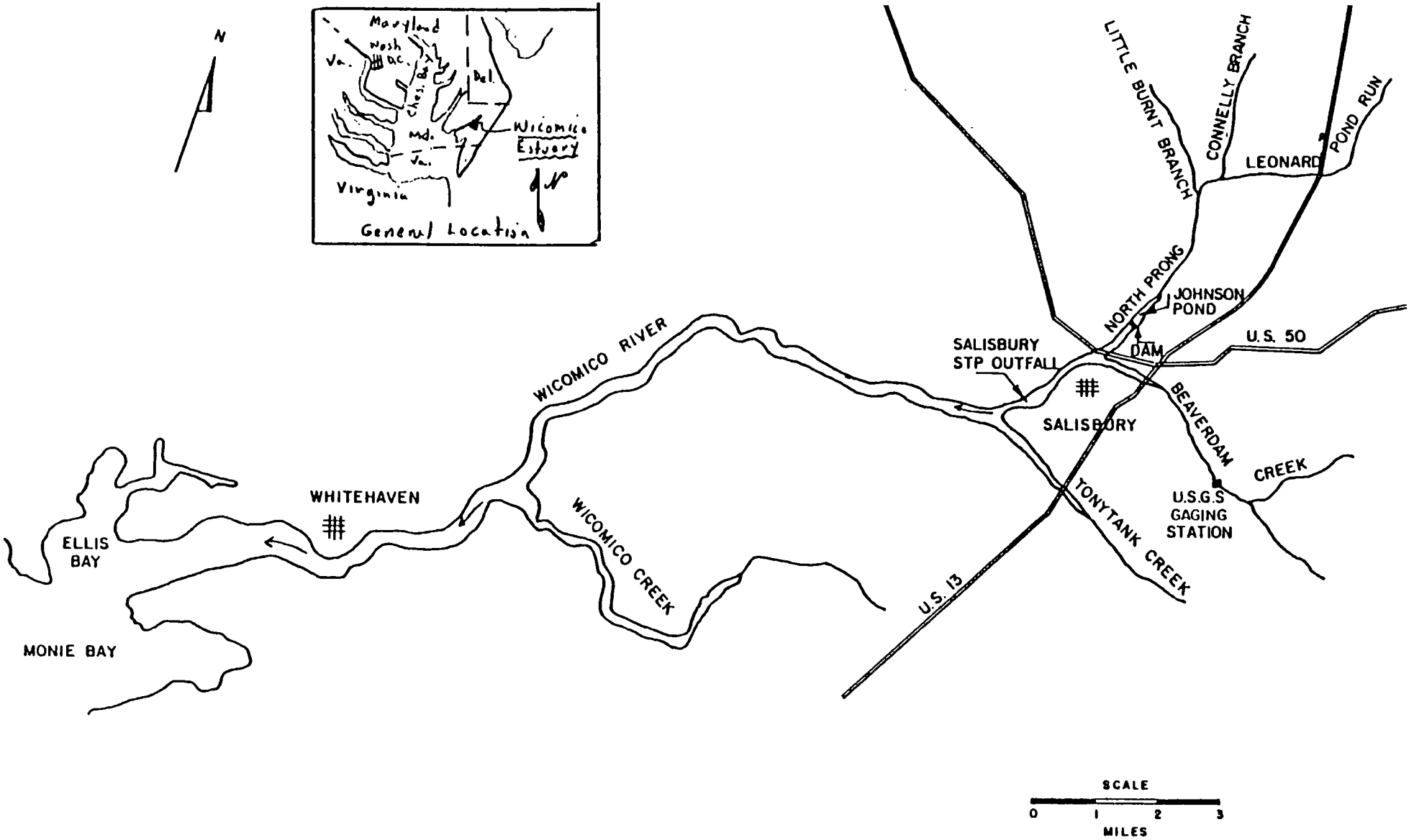

FIGURE W1

LOCATION MAP — WICOMICO RIVER

General Description and Analysis of Available Data

Major water quality sampling efforts in the Wicomico River were conducted by the Federal Water Pollution Control Administration (FWPCA) during the summer of 1967 under relatively high flow periods. Spatial coverage extended from above the Johnson Pond Dam at Salisbury to the mouth of the Wicomico River as shown in Figure W-2. Tributaries to the Wicomico River were also monitored. Measurements were taken at high and low water slack during August. Parameters that were most frequently measured were temperature, secchi disk, total and fecal coliform, chlorides, dissolved oxygen, BOD, and suspended and volatile solids. Dissolved oxygen and BOD were measured at both the surface and mid-depth at many stations. Nutrient and chlorophyll 'a' measurements were limited to three stations. The highest chlorophyll 'a' levels were observed at Quantico Wharf (Station 5). The average was about 92 µg/l with values often greater than 100 µg/l. Review of subsequent data indicated that this was insufficient spatial coverage and that peak concentrations for these parameters were probably missed.

Daily precipitation records in the area for the month of August 1967 indicate that substantial rainfall of greater than 6.2 inches fell during the three days just prior to the August 7 survey and about 5.5 inches fell during the second survey as measured at Salisbury. The impact on dissolved oxygen levels was significant. Figure W-3 presents the spatial profiles of dissolved oxygen for high and low water slack during August 7 to 11. As can be seen, the dissolved oxygen in the upper reaches in the vicinity of Salisbury progressed from at or near saturation ($\simeq$ 8 mg/l) on August 7 to dissolved oxygen levels of less than 5 mg/l from MP 20 to 8 during August 10 and 11. Precipitation with consequent cloud cover was observed during these latter two days.

For the survey periods, low and high water slack generally occurred during mid-morning and late afternoon, respectively. As such, the dissolved oxygen data taken during the slack water runs serve to partially indicate the extent of diurnal variation in dissolved oxygen concentrations. As can be seen in Figure W-3, during the latter two days, dissolved oxygen throughout the day was generally the same in the upper Wicomico River. This indicates a suppression of photosynthetic activity probably due to the reduction of available sunlight by cloud cover.

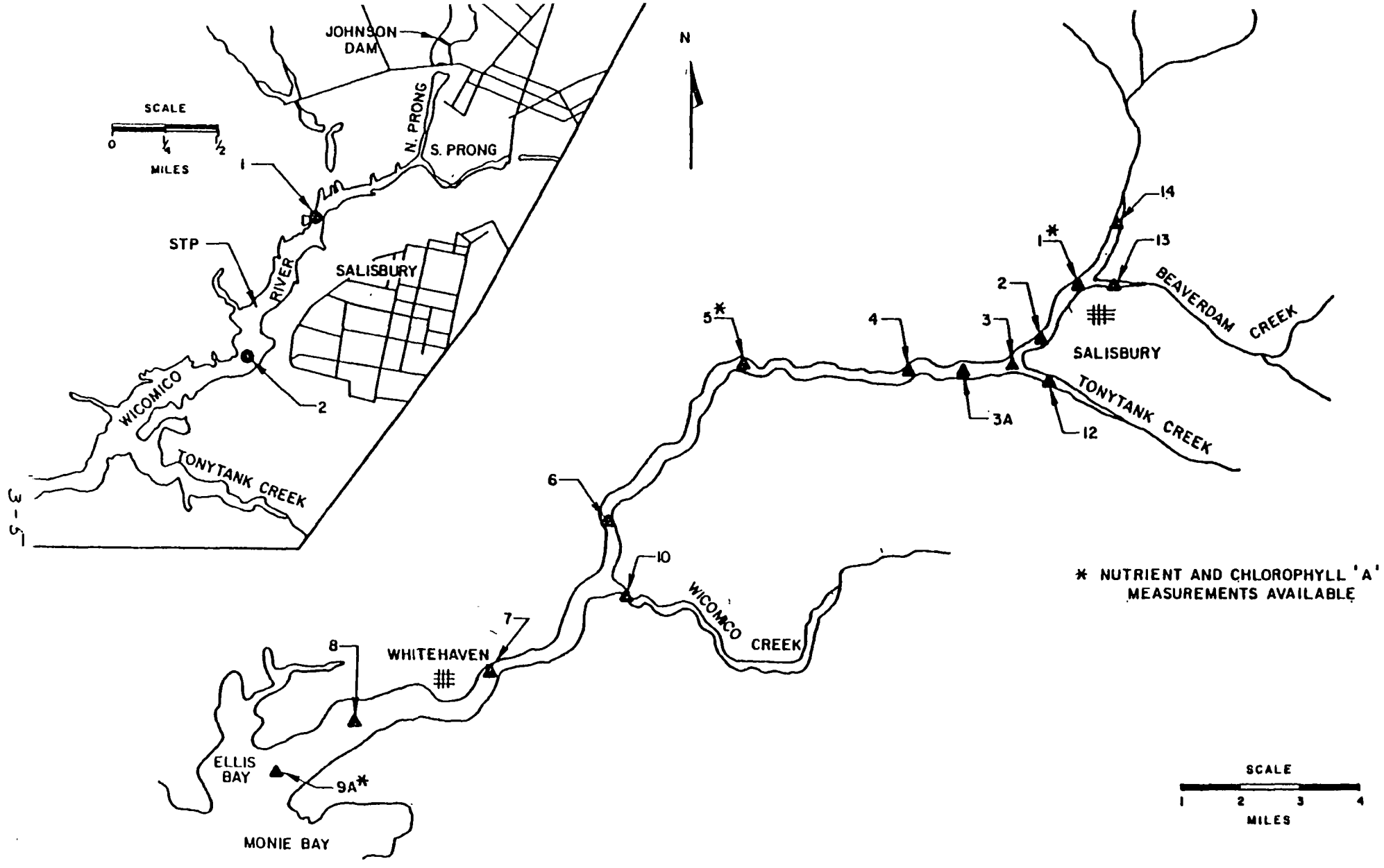

FIGURE W2

WICOMICO RIVER

SAMPLING STATION LOCATIONS – FWPCA SURVEYS SUMMER 1967

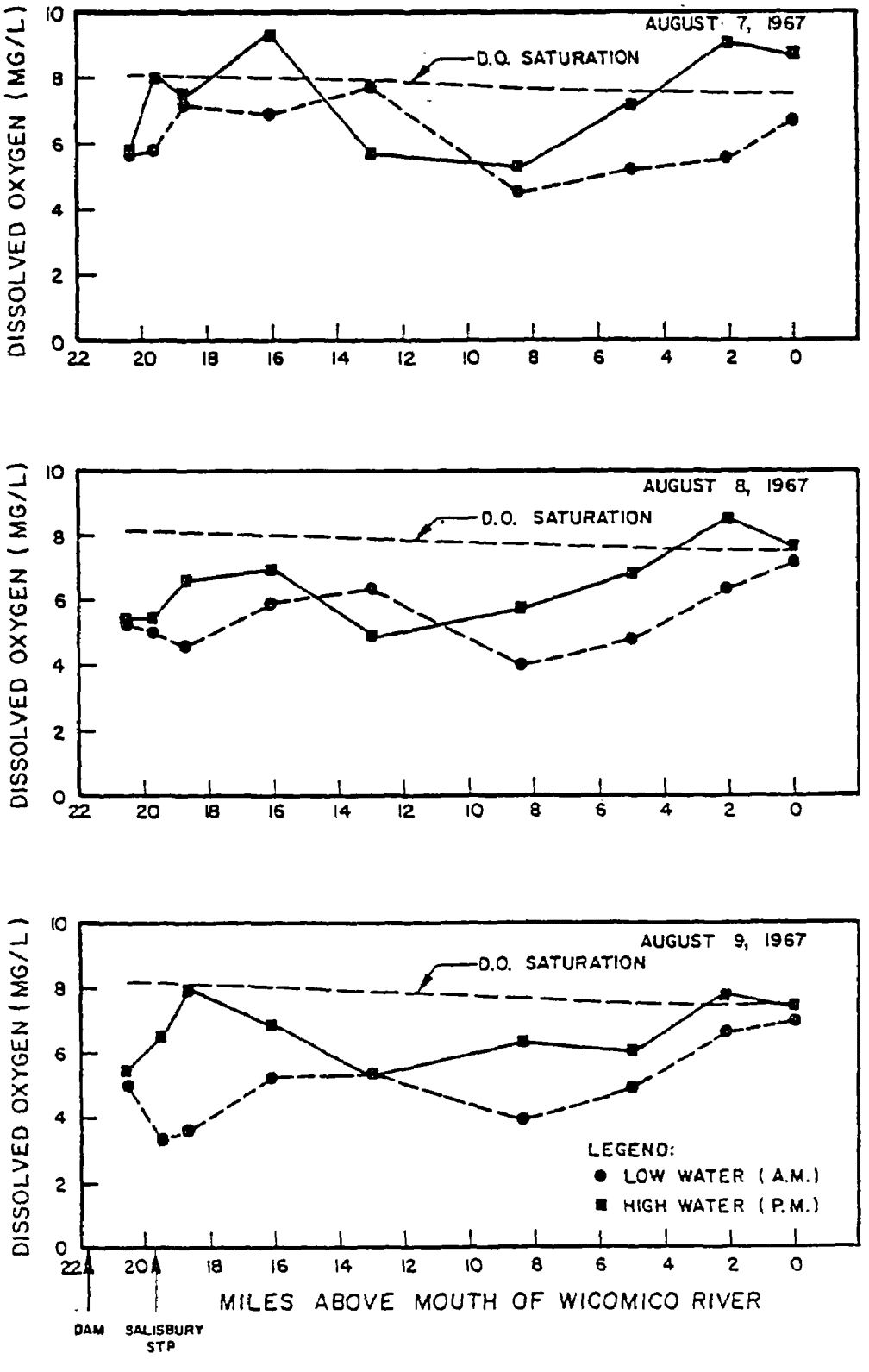

FIGURE W3

DISSOLVED OXYGEN-WICOMICO RIVER

AUGUST 7 TO 11, 1967

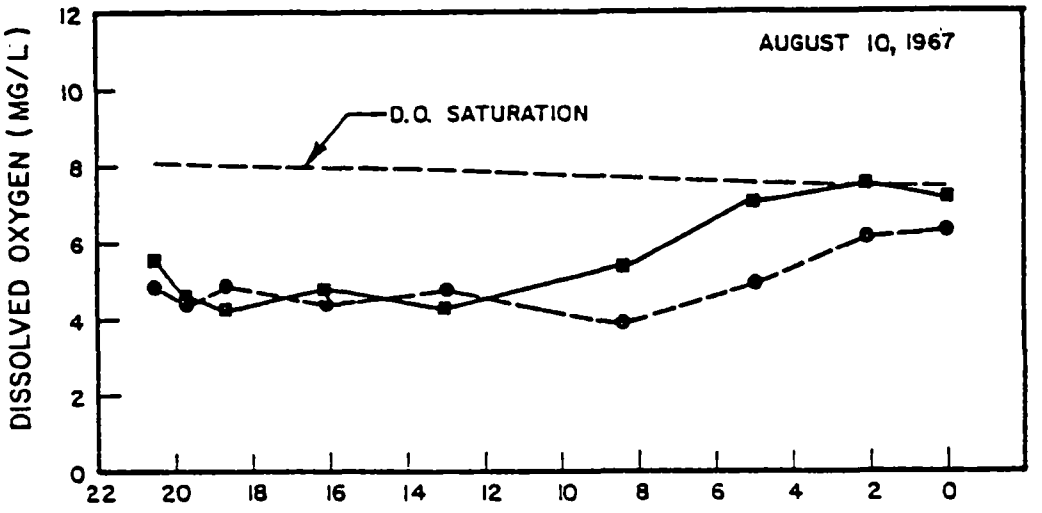

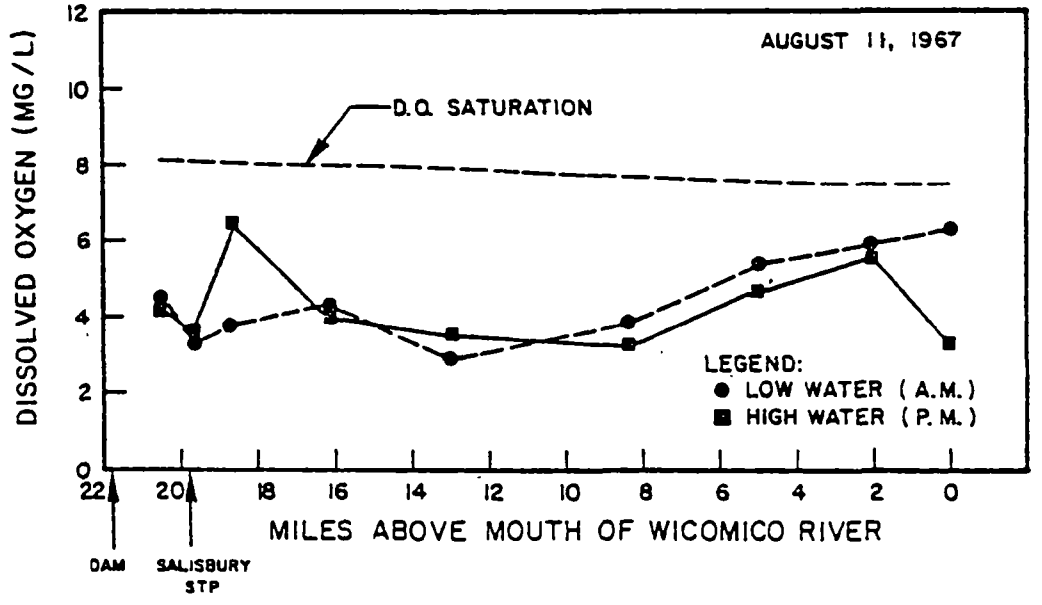

FIGURE W3 (Cont'd)
DISSOLVED OXYGEN WICOMICO RIVER
AUGUST 7 TO 11, 1967

The State of Maryland also conducted extensive monitoring of water quality in the Wicomico River in July and August 1971. The stations sampled by the State are, in most cases, essentially identical to those used by the FWPCA in 1967 as presented in Figure W-2. Parameters measured included secchi disk, temperature, total and inorganic phosphorus, TKN, ammonia, nitrite-nitrate, chlorophyll 'a', total and fecal coliform, dissolved oxygen, total organic carbon, conductivity, and salinity. BOD was a notable exception. Sampling during these surveys was conducted once a day generally during the morning hours. During the July survey sampling was initiated after predicted low water slack, whereas during the August survey sampling was completed prior to predicted low water slack. Both surveys were conducted under relatively dry weather conditions when compared to the 1967 surveys. A steady state modeling framework was utilized in the analysis of the Wicomico River which implies a constant flow regime. Therefore, the critical summer period of July 1971 was chosen for calibration of the model. The data taken during August 1971 were utilized for verification of the model. Due to the transient conditions caused by the heavy rainfall during the surveys conducted in 1967, these periods could not be analyzed in a steady state modeling framework.

The dissolved oxygen data observed during the two surveys conducted in the summer of 1971 are presented in Figure W-4. Dissolved oxygen levels were generally high with the standard of 5 mg/l generally met throughout the estuary.

Supersaturation is encountered at times over a large portion of the upper river, especially in the vicinity of the Salisbury STP discharge. The dissolved oxygen was progressively measured later in the day during each of the days in the July survey. Therefore, the difference in dissolved oxygen at stations during the July survey period partially indicate the extent of the diurnal variation in dissolved oxygen due to photosynthetic activity. In August, measurements were generally taken during the same period.

Figure W-5 presents the spatial distribution of total and inorganic nitrogen, total and inorganic phosphorus and algal biomass as measured by chlorophyll 'a' during the July and August 1971 survey period. Peak chlorophyll 'a' levels of greater than 250 µg/l occur near Salisbury and decline to about 25 µg/l near the mouth. Inorganic nitrogen concentrations (summation of ammonia,

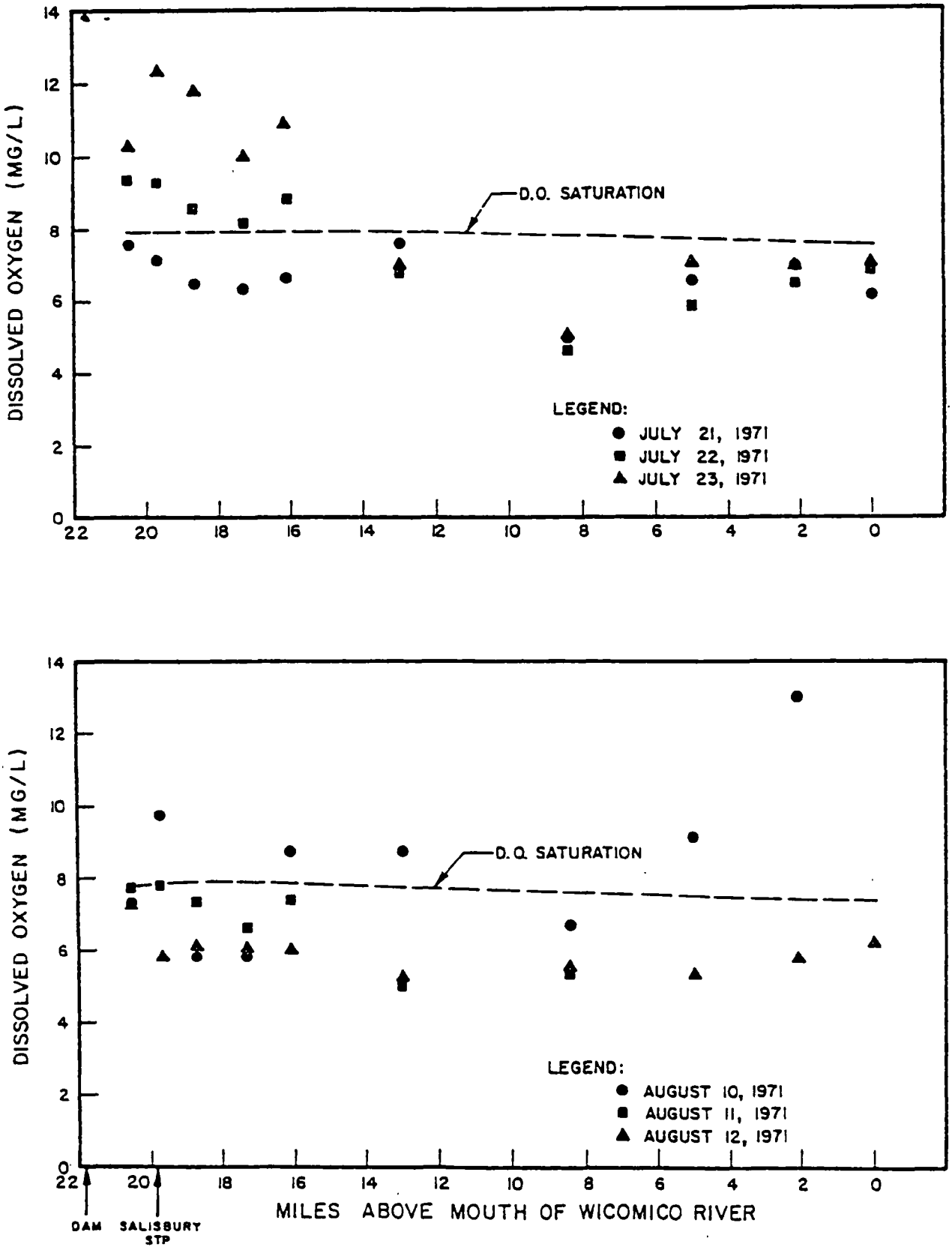

FIGURE W4

DISSOLVED OXYGEN – WICOMICO RIVER

SUMMER 1971

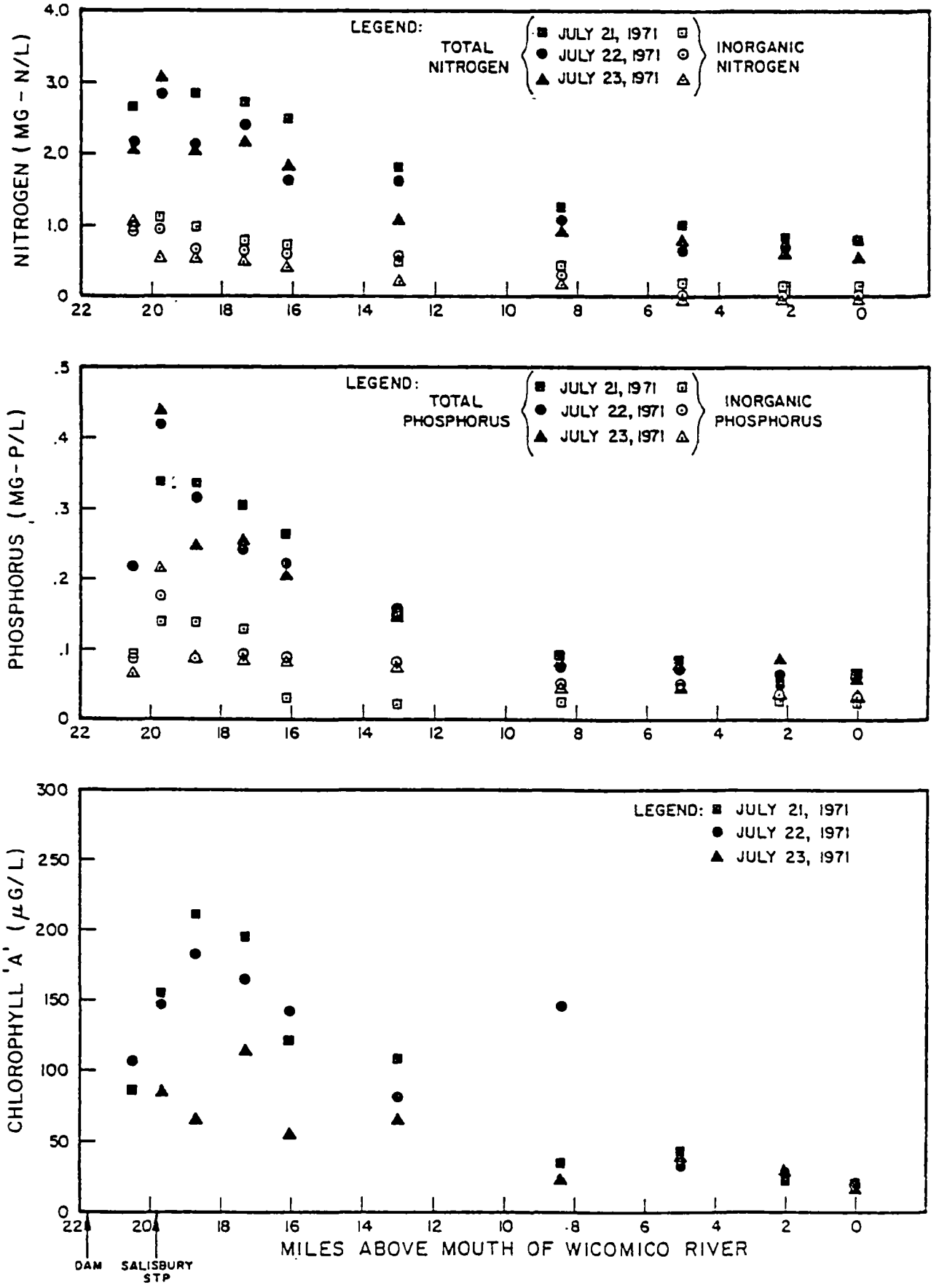

FIGURE W5

WATER QUALITY DATA – WICOMICO RIVER

JULY 21 TO 23, 1971

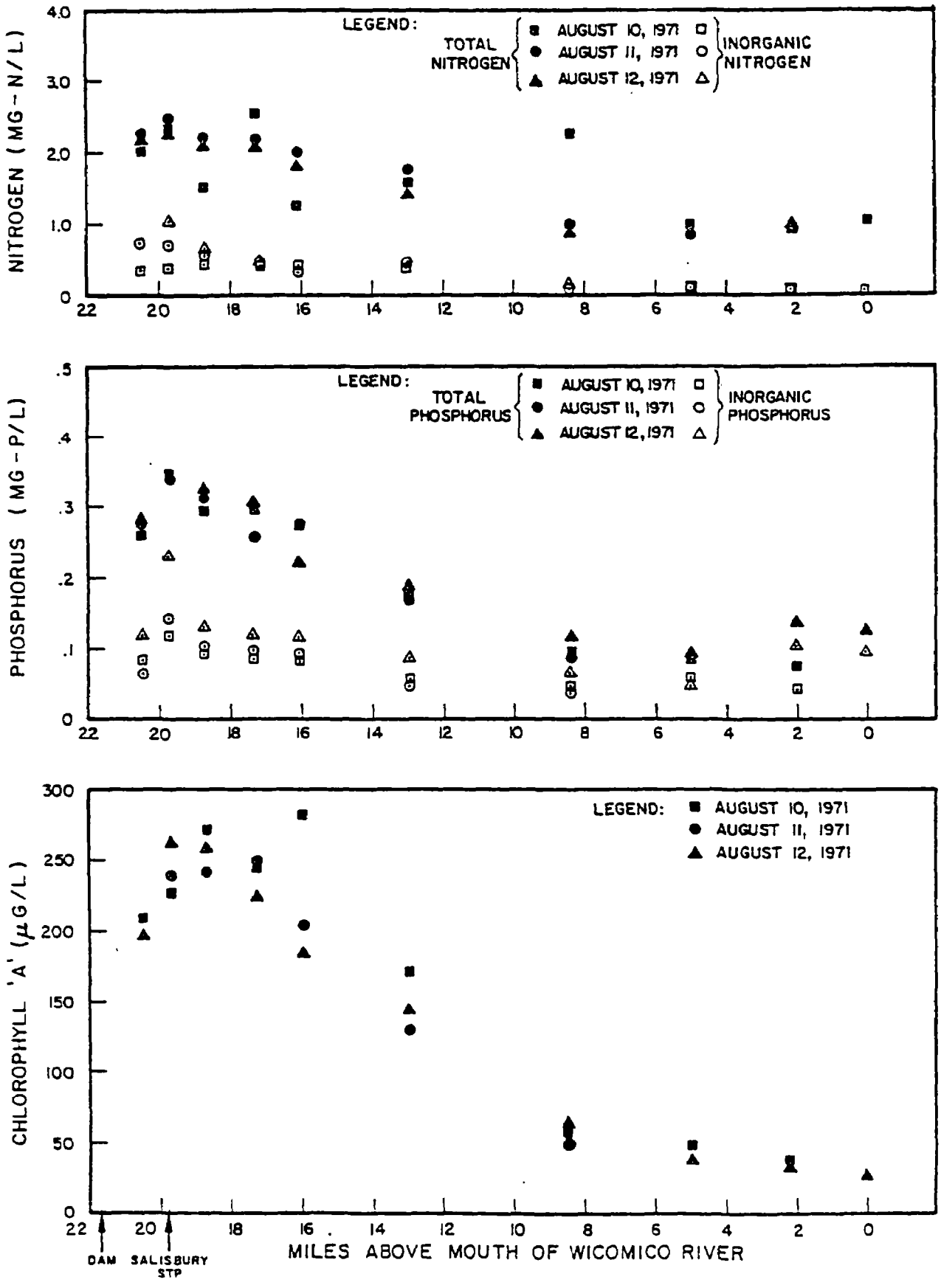

FIGURE W5 (cont'd)

WATER QUALITY DATA - WICOMICO RIVER

AUGUST 10 TO 12, 1971

nitrite and nitrate nitrogen) of about .5 to 1.0 mg-N/l occur near Salisbury with a decline downstream to less than 0.1 mg-N/l. Inorganic phosphorus concentrations of about 0.1 to 0.2 mg-P/l occur near Salisbury with a decline downstream to less than .05 mg-P/l. Comparison of these data to the Michaelis-Menton half saturated growth constants of .005 mg-P/l and .025 mg-N/l for inorganic phosphorus and inorganic nitrogen, respectively, indicates that neither nitrogen nor phosphorus appeared to be significantly limiting phytoplankton growth in the upper Wicomico River. The lower 5-8 miles of the estuary however appear to be limited by nitrogen. This limitation does not appear to be influencing the upper phytoplankton flows since the growth of that bloom has ceased about 10 miles further upstream. Total nitrogen and total phosphorus both peak in the vicinity of the Salisbury STP discharge. A rapid decline in total nutrients is observed downstream and cannot be simply accounted for by freshwater dilution. The principle water quality problem therefore is relatively high chlorophyll levels, coupled with occasional low D.O. values.

Waste Loads

The major waste source in the tidal portion of the Wicomico River is the Salisbury Sewage Treatment Plant (STP). Operational data for the plant indicated an average BOD_5 load of 3,000 lbs/day which was utilized in the calibration and verification analyses.

No nutrient data were available for the above periods. Based on a single sample taken by the Environmental Protection Agency (EPA) on April 6, 1972 a total phosphorus effluent load of 179 lbs-P/day (7.2 mg-P/l) and a total kjeldahl nitrogen (TKN) load of 593 lbs-N/day (23.6 mg-N/l) were calculated and applied in the verification analysis.

During July, 1974, the WRA analyzed composite samples of the effluent from the Salisbury STP. The resulting loads are presented in the following table:

TABLE 1

SALISBURY SEWAGE TREATMENT PLANT EFFLUENT LOADS-JULY, 1974

Parameter	Flow = 6.7 cfs Concentration (mg/l)	Load (lbs/day)	UOD Load (lbs/day)
BOD_5	31.8	1,157	1,701
TKN	16.3	600	2,743
Total Nitrogen as N	16.8	628	-
Total Phosphorus as P	3.8	123	-

The TKN and total phosphorus loads are consistent with the loads calculated from the EPA data. As will be discussed subsequently, the loads in Table 1 were utilized in the projection analyses.

Mathematical Model Development

Based on time and budgetary constraints, a steady state finite segment model (Thomann, 1972) was chosen for the analysis of water quality in the Wicomico River. Primary emphasis was placed on the evaluation of dissolved oxygen and total phosphorus and total nitrogen to estimate the eutrophication potential of the estuary under different loading alternatives.

The segmentation used in the analysis of the Wicomico River is presented in Figure W-6. Twenty-four segments, usually one mile in length, were utilized. The data for determining the geometry of each section were obtained from the U.S. Coast and Geodetic Survey. The mean low water depths from these charts were increased to mean tide levels. Figure W-7 presents the spatial distribution of mean tide depths, cross-sectional areas and cumulative volume of the system.

The USGS gaging station records at Beaverdam Creek (drainage area - 19.5 sq. mi.) were the only freshwater flow data available for the periods of analyses in the summer of 1971. Estimations of freshwater flow in the mainstream of the Wicomico River were determined from correlations developed from limited data taken by the USGS during other periods. These data were plotted on a log-log scale and the line of best fit was utilized to estimate the freshwater flow at Naylor Mill Road as a function of measured flow at Beaverdam Creek. The

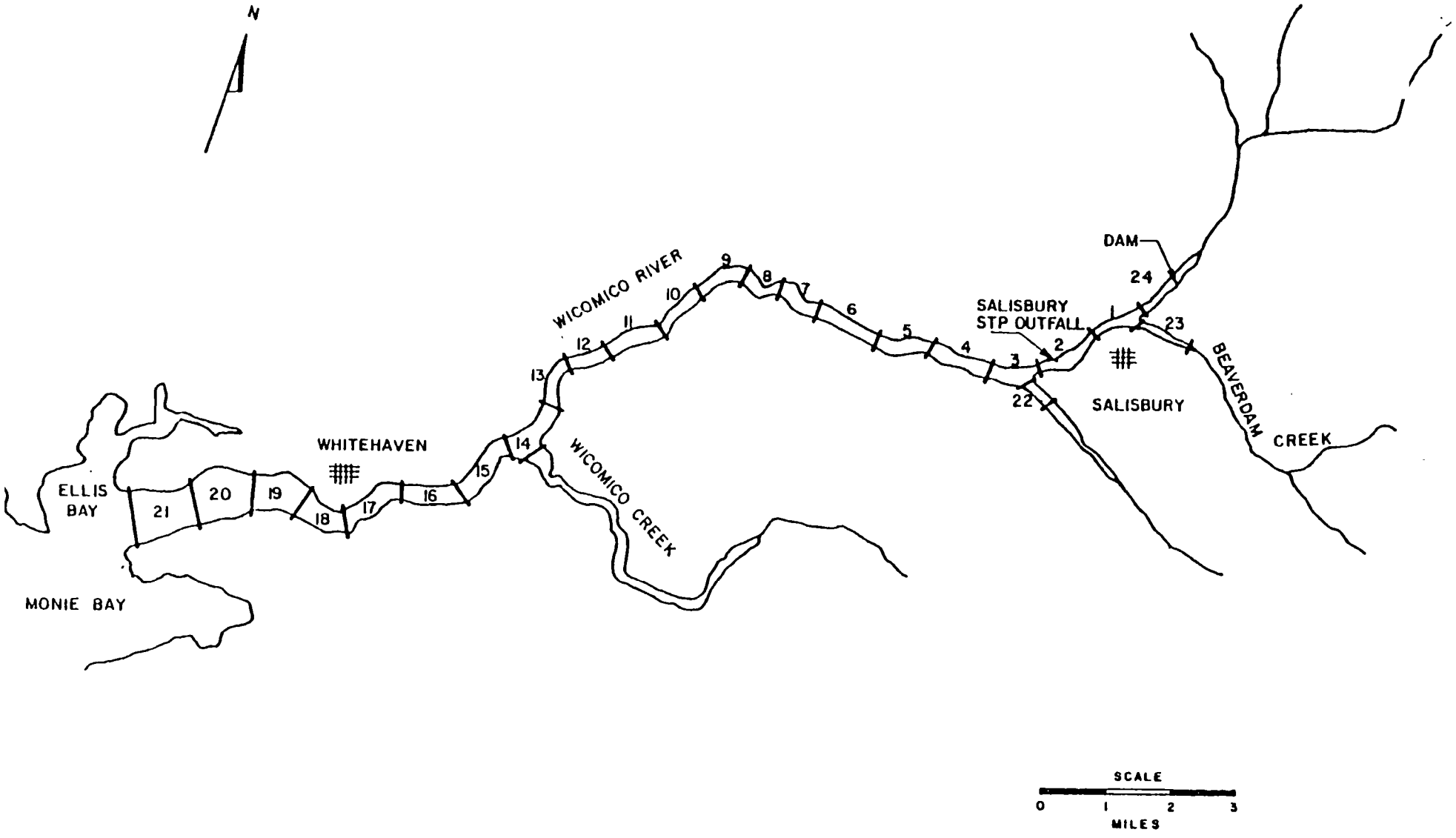

FIGURE W6

MODEL SEGMENTATI - WICOMICO RIVER

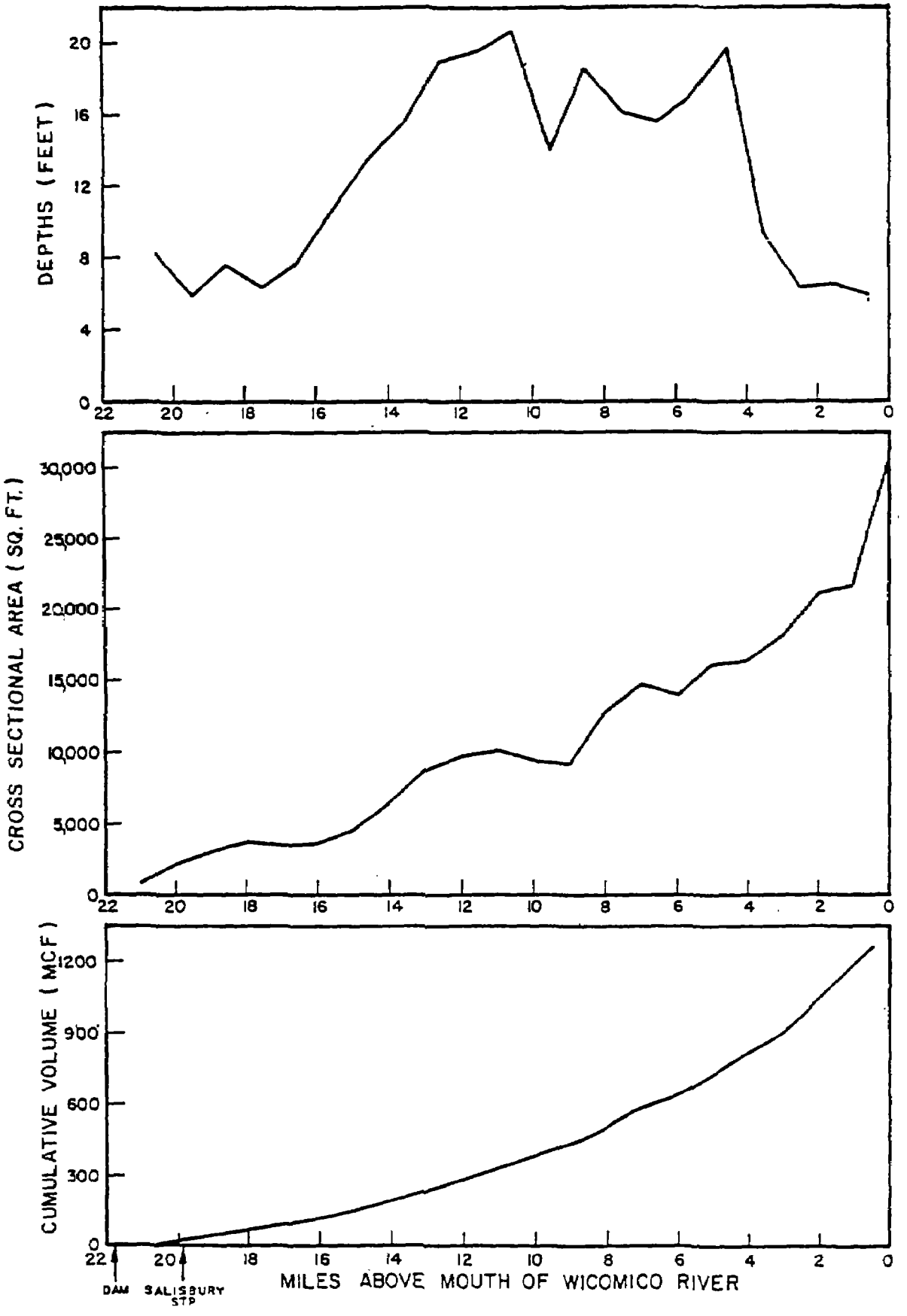

FIGURE W7

GEOMETRY OF WICOMICO RIVER

drainage area of the Wicomico River at Naylor Mill Road is 24.8 sq. mi.

Two other correlations were developed from information presented in Boggess and Heidel (1968). With these correlations, freshwater flow could be obtained at key locations in the upper Wicomico River. The modeling analyses were performed with flow assumed constant below Tonytank Creek. Subsequent sensitivity runs, in which flow was incremented at a rate of 0.1 cfs/sq. mi., did not significantly affect the water quality parameters evaluated in this study.

The time necessary for a system to attain equilibrium is critical in any type of steady state evaluation. A generally constant flow was recorded at Beaverdam Creek for the summer of 1971. For the analysis of salinity measured during the two surveys in 1971, two month flow averages were applied and are considered consistent with the time to equilibrium for a conservative substance in the Wicomico River under the final advective-dispersive regime utilized. Substances with kinetic interactions come to equilibrium more quickly than conservative substances. For these substances, two-week flow averages were deemed appropriate. Table 2 summarizes the flow regime inputted to the model for the two periods analyzed and the 7 day - 10 year low condition used in the projection analysis.

TABLE 2

FRESHWATER FLOW AT KEY LOCATIONS IN WICOMICO RIVER

	7 day-10 yr. Low Flow	July 1971		August 1971	
		2 Months	2 Weeks	2 Months	2 Weeks
Beaverdam Creek	1.4	18.0	14.8	16.0	21.0
North Prong at Isabella	23.0	55.0	49.0	50.0	61.0
Tonytank	2.4	6.5	6.0	6.0	7.5
Total Below Tonytank Creek	26.8	79.5	69.8	72.0	89.5

Transport Verification

Salinity was utilized as a conservative tracer substance to determine the dispersional characteristics of the system and comparisons were made between computed and observed salinities for the July 1971 survey. Adjustments were made to the dispersion coefficients until such time that acceptable correlations between the observed data and model results were achieved. Observed salinity concentrations at the boundaries of the model were the only salinity inputs to the model. The adjusted dispersion coefficients were subsequently checked by applying the same dispersive regime to the August 1971 survey. The resulting model verifications are presented in Figure W-8, in which comparisons between computed and observed data for the two periods of analysis are presented. Longitudinal dispersion coefficients, as noted, ranged from 0.3 to 0.8 miles^2/day. Vertical homogeneity is assumed in the model. This assumption is consistent with observed conditions for most parameters in the Wicomico River especially in the critical upper reaches.

As can be seen in Figure W-8, salinity was generally at or near background levels above MP 16. The dispersion coefficient of 0.3 miles^2/day used in this region was merely an extrapolation of downstream dispersion coefficients which served to set an upper limit. In order to evaluate the dispersional characteristics of this upper reach, a dye tracer study was performed by the State of Maryland. The proper determination of the dispersional characteristics in this region is critical since the Salisbury STP discharges within this reach.

An instantaneous release of 40 lbs. of dye was dumped at high slack tide, 6:20 p.m. on July 22, 1974, in the vicinity of the Salisbury STP discharge. Longitudinal spatial distributions of the dye were measured at subsequent high and low water slack periods. The observed dye distributions are shown in Figure W-9. These dye data were used to obtain an estimate of dispersion coefficients using simplified analytical solutions for instantaneous discharges (see Thomann, 1972).

The dispersion coefficients calculated from the dye data varied from 0.04 to 0.26 miles^2/day and are of the same order as those used in the model (0.3 miles^2/day) for this portion of the river. Sensitivity analyses were performed using a dispersion value of 0.1 miles^2/day for this region and indicated no

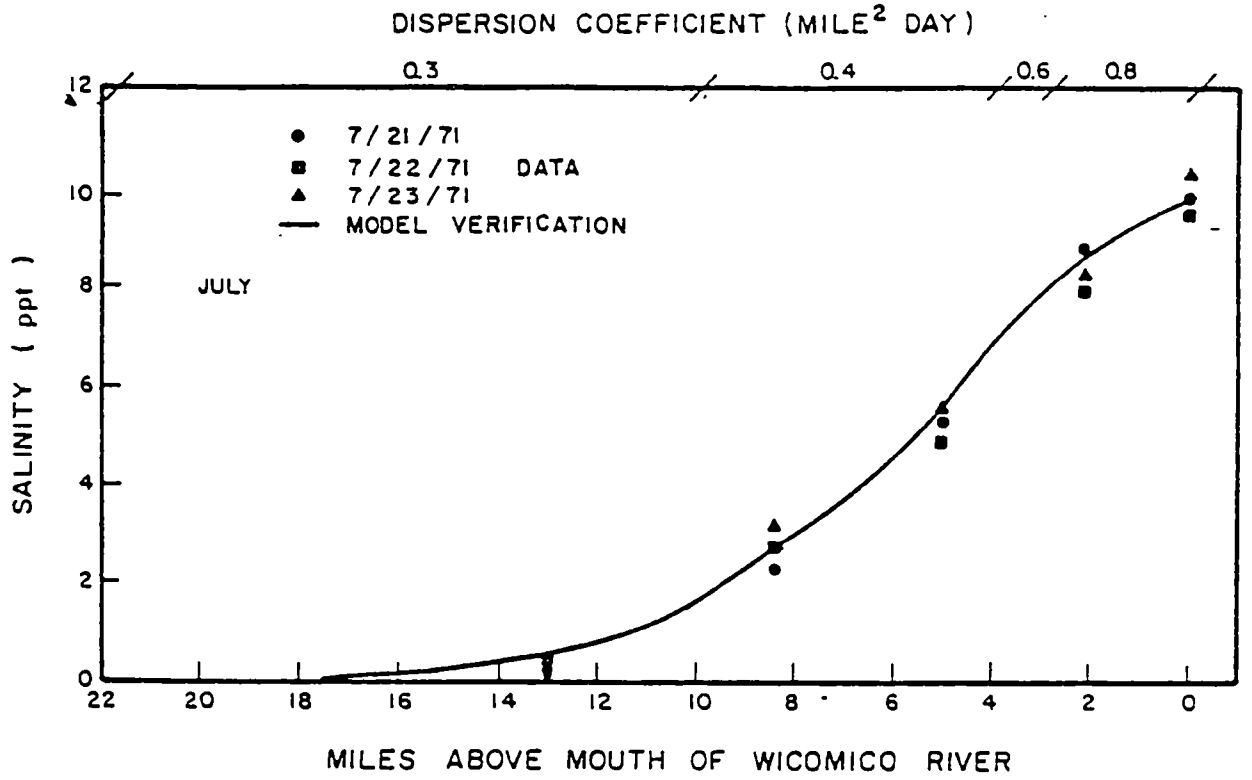

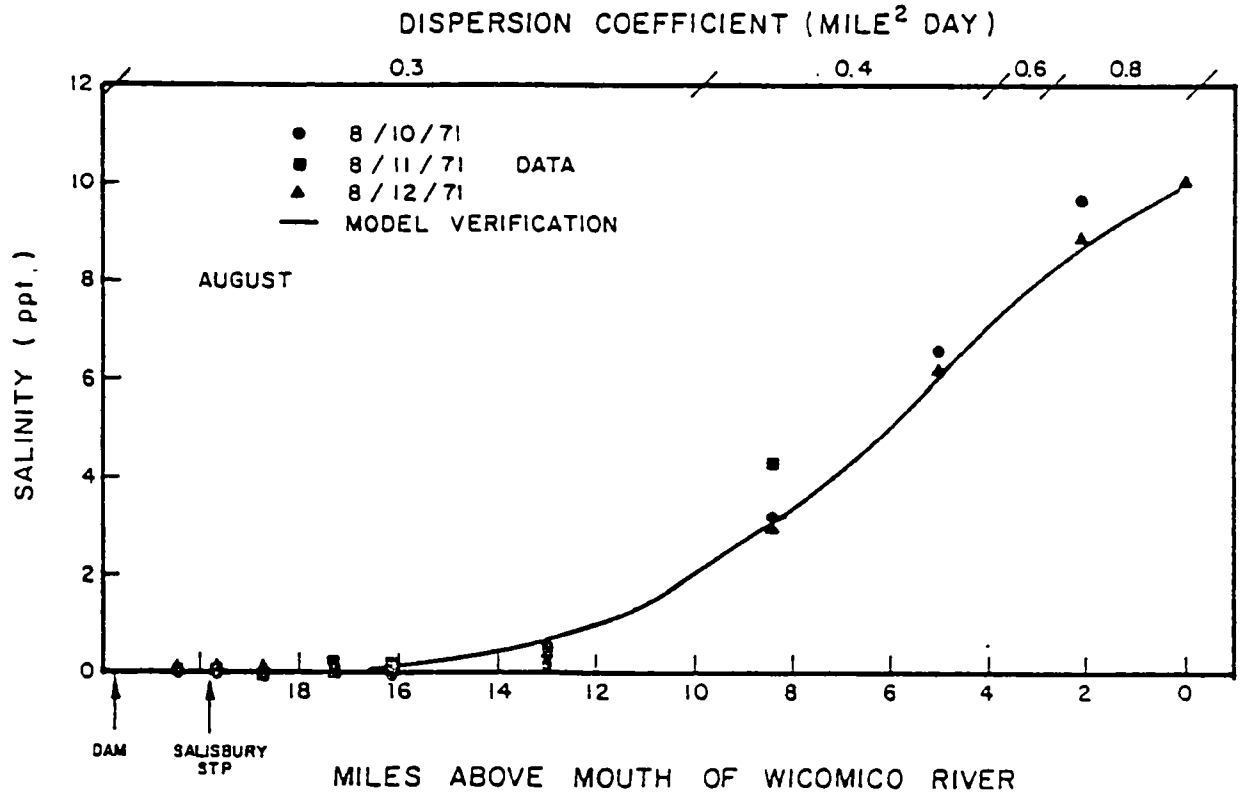

FIGURE W 8
SALINITY VERIFICATION — WICOMICO RIVER
SUMMER 1971

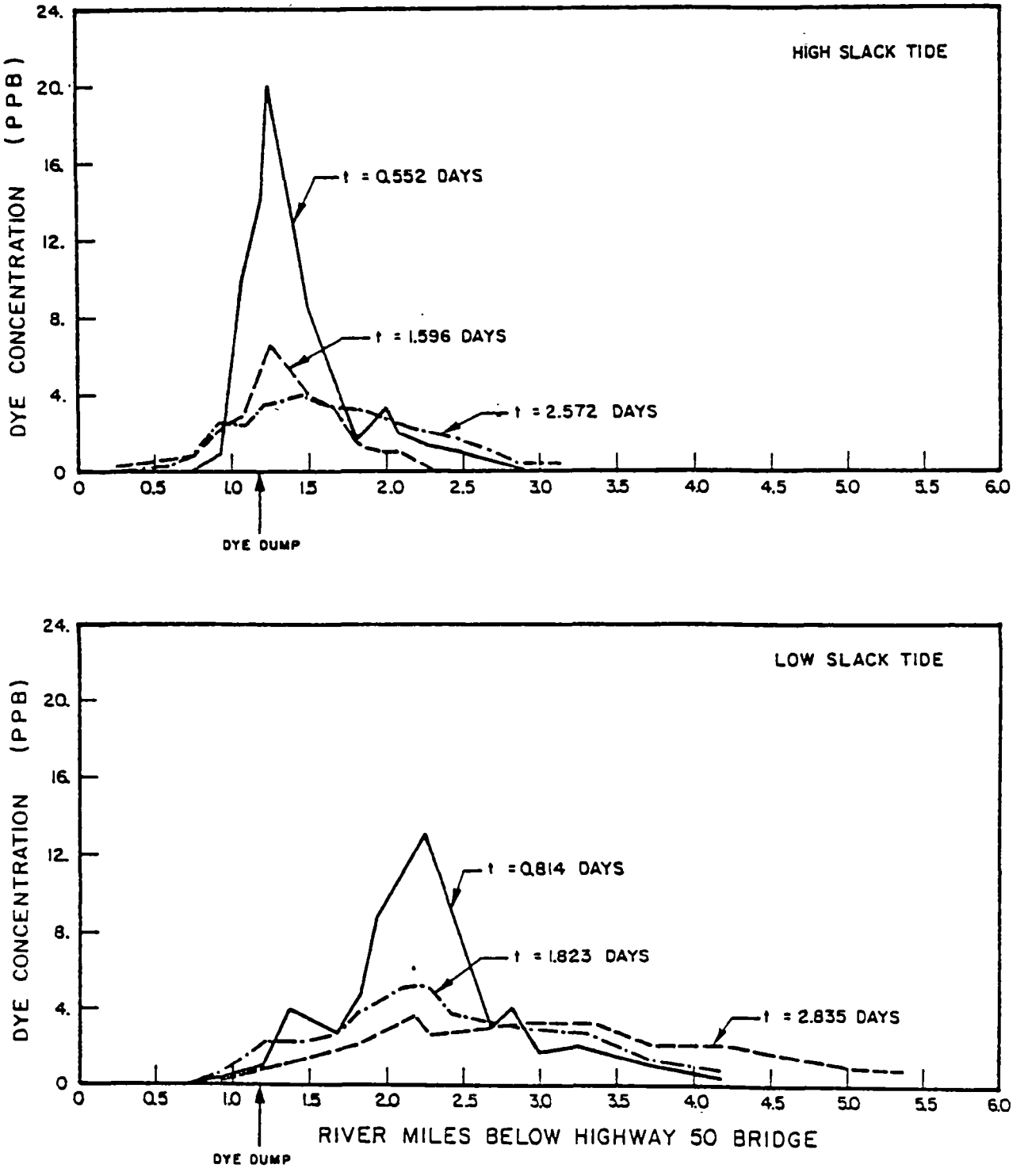

FIGURE W9

DYE DISTRIBUTION — WICOMICO RIVER

JULY 22 TO 24, 1974

significant effect on the calculated distributions. The higher dispersion coefficient of 0.3 miles^2/day initially developed, was used in all model analyses.

Model Verification-Dissolved Oxygen

Upon completion of the verification of the transport regime, the analysis proceeded to the evaluation of reactive substances.

The Salisbury carbonaceous BOD_5 load used in the modeling analysis was 3,000 lb/day based on available operating records. This load was corrected to ultimate carbonaceous oxygen demand utilizing a ratio of 1.43. A TKN nitrogen discharge of 590 lb/day was estimated from limited data and was converted to ultimate nitrogenous oxygen demand by multiplying by 4.57.

Dissolved oxygen deficit boundary conditions for the Wicomico River at the dam at Salisbury, Beaverdam Creek, Tonytank Creek and Ellis Bay were determined directly from observed data.

The reaeration coefficients, K_a, for each segment were computed using the O'Connor-Dobbins formulation where average tidal velocities were taken from the tidal current tables. Reaeration coefficients for the Wicomico River varied from 0.1 to 1.2/day after temperature correction.

A deoxygenation rate of 0.3/day at 20°C for both carbonaceous (K_d) and nitrogenous (K_n) oxygen demanding materials was used in the modeling evaluations. Coefficients were corrected for temperature by using a $\theta = 1.047$ for carbonaceous and 1.08 for nitrogenous. No information on the dissolved oxygen uptake of the bottom sediments in the Wicomico River was available. Based on the literature a 1 to 2 gm-O_2/m^2-day sediment oxygen demand (SOD) is typical of estuarine muds. An SOD rate of 1 gm-O_2/m^2-day was used in all segments of the Wicomico River except segments 2, 3, and 4 which are located in the vicinity of the Salisbury STP outfall. A higher rate of 2 gm-O_2/m^2-day was used in these segments on the basis of a higher rate of deposition of solids and phytoplankton at that location.

A review of the observed dissolved oxygen data indicates that algal photosynthesis and respiration appear to have a significant effect on dissolved oxygen levels in the Wicomico River, especially in the vicinity of the Salisbury STP. Chlorophyll 'a' levels in this vicinity frequently exceed 150 µg/l. The

photosynthetic production of oxygen was estimated using general procedures as follows. Based on numerous analyses conducted in other areas the saturated photosynthetic oxygen production rate (P_s) under optimum conditions was estimated by the following:

$$P_s \text{ (mg/l-day)} = 0.25 \text{ Chlorophyll 'a' } (\mu g/l) \quad (1)$$

This saturated rate was corrected for non-optimal light and depth and time averaged in accordance with Equations 8-26. Average incident solar radiation and photoperiod were obtained. The light extinction coefficient (K_e) was estimated from available secchi disk measurements in accordance with the following:

$$K_e = 1.7/\text{secchi disk} \quad (2)$$

This relationship has been verified with extensive data. Algal respiration was estimated to equal 10% of P_s and was applied over the depth of the water column.

With the determination and assignment of the foregoing input parameters, the model was applied to the July and August surveys of 1971.

Favorable comparisons between the calculated and observed dissolved oxygen profiles in the region between the mouth of the Wicomico River and approximately MP 12, were achieved with the direct application of the parameters described above. However in the regions where abundant algae were present, some changes in the theoretically computed rates for photosynthesis had to be made in the model. Figure W-10 shows a comparison of the theoretical rates and the final values used in the verification. The differences can be explained by the limited information on some of the parameters used in the analytical method and by the complexity and uncertainties of the phenomenon. Final verifications for the two survey periods are presented in Figure W-11. The agreement between the observed and computed values is reasonably good. A maximum oxygen deficit of 3.5 mg/l at MP 10.5 was computed for the period of July 1971. A maximum oxygen deficit of 2.5 mg/l at MP 8.5 was computed for the period of August 1971. Dissolved oxygen at or near saturation was calculated in the vicinity of the Salisbury STP discharge.

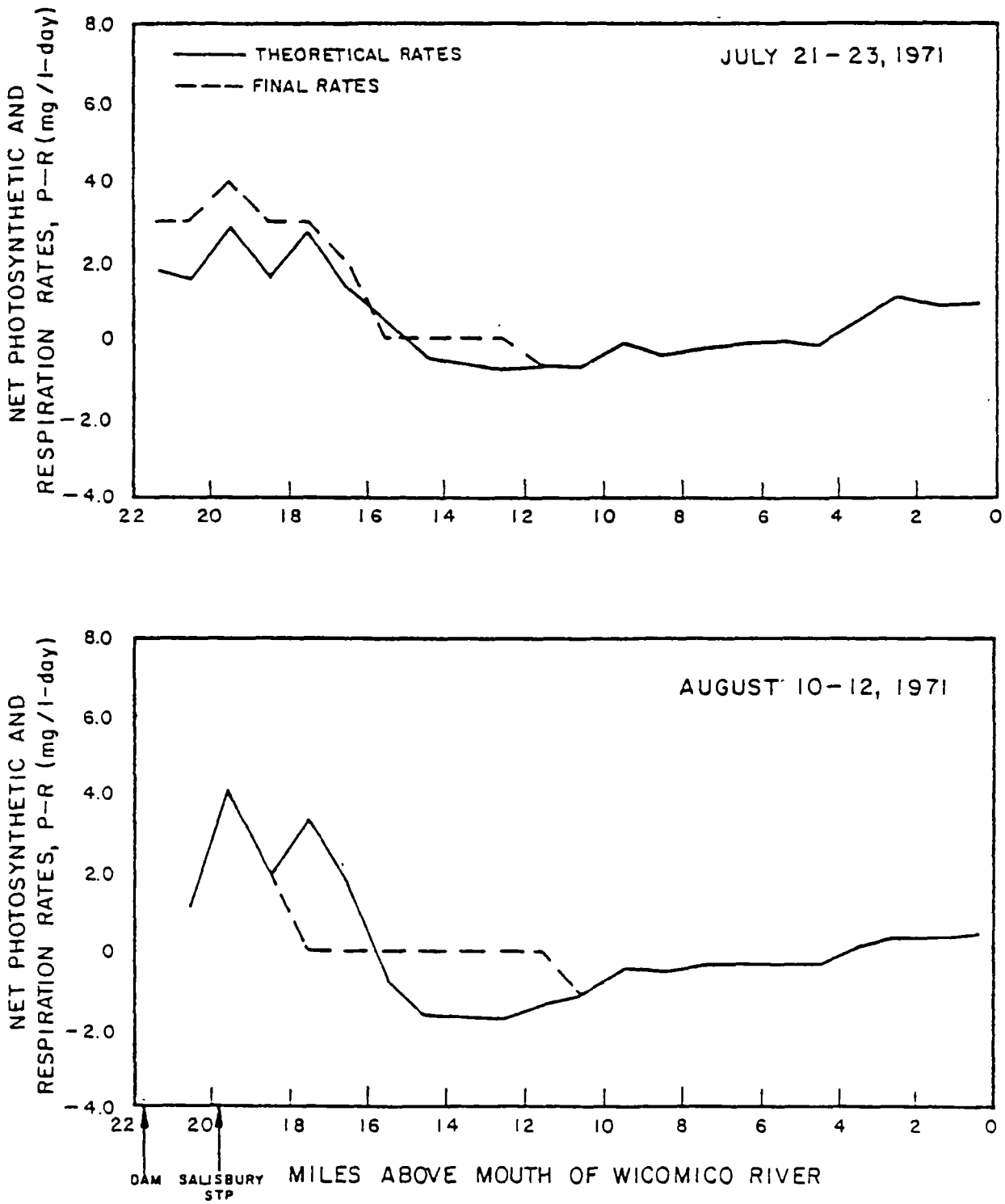

FIGURE W 10

COMPARISON OF THEORETICAL AND FINAL NET PHOTOSYNTHETIC RATES

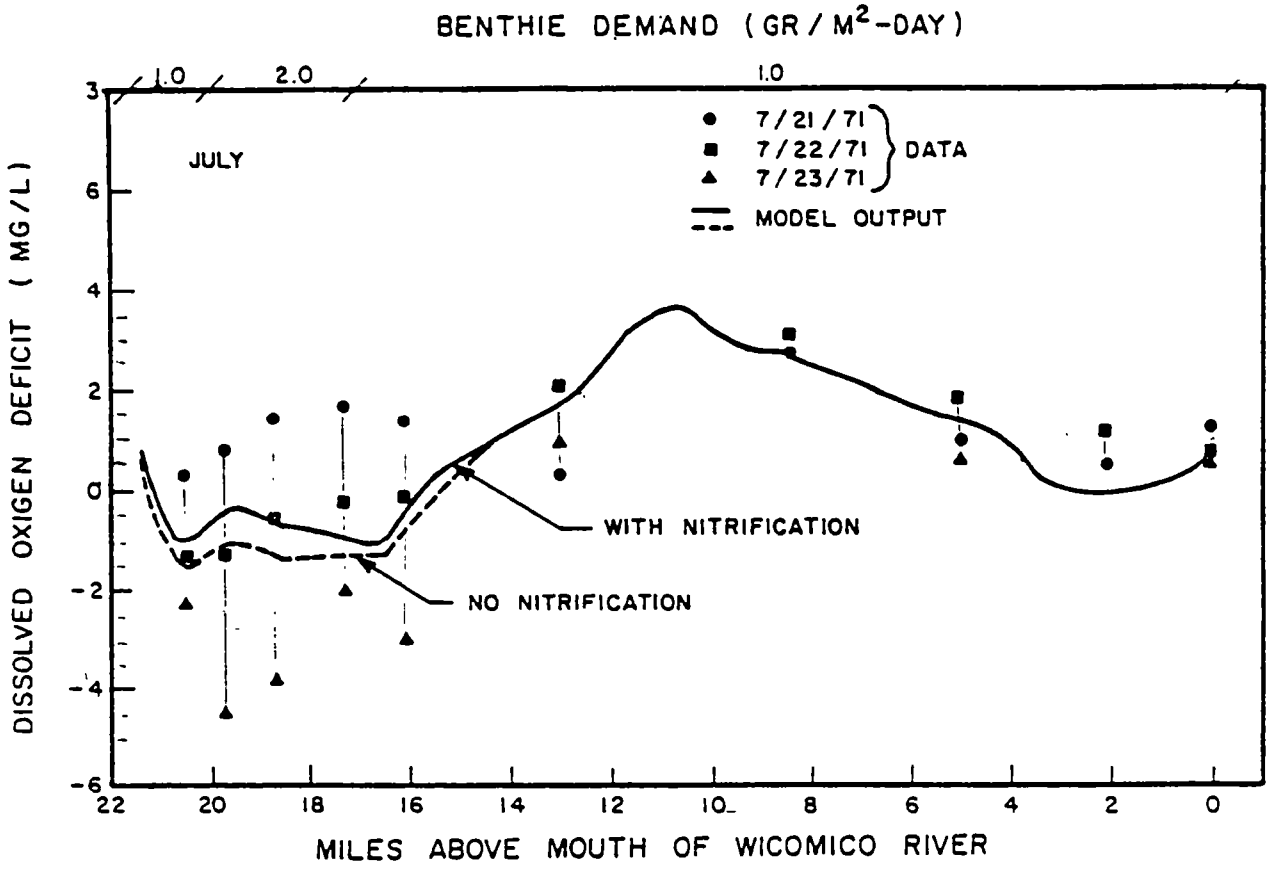

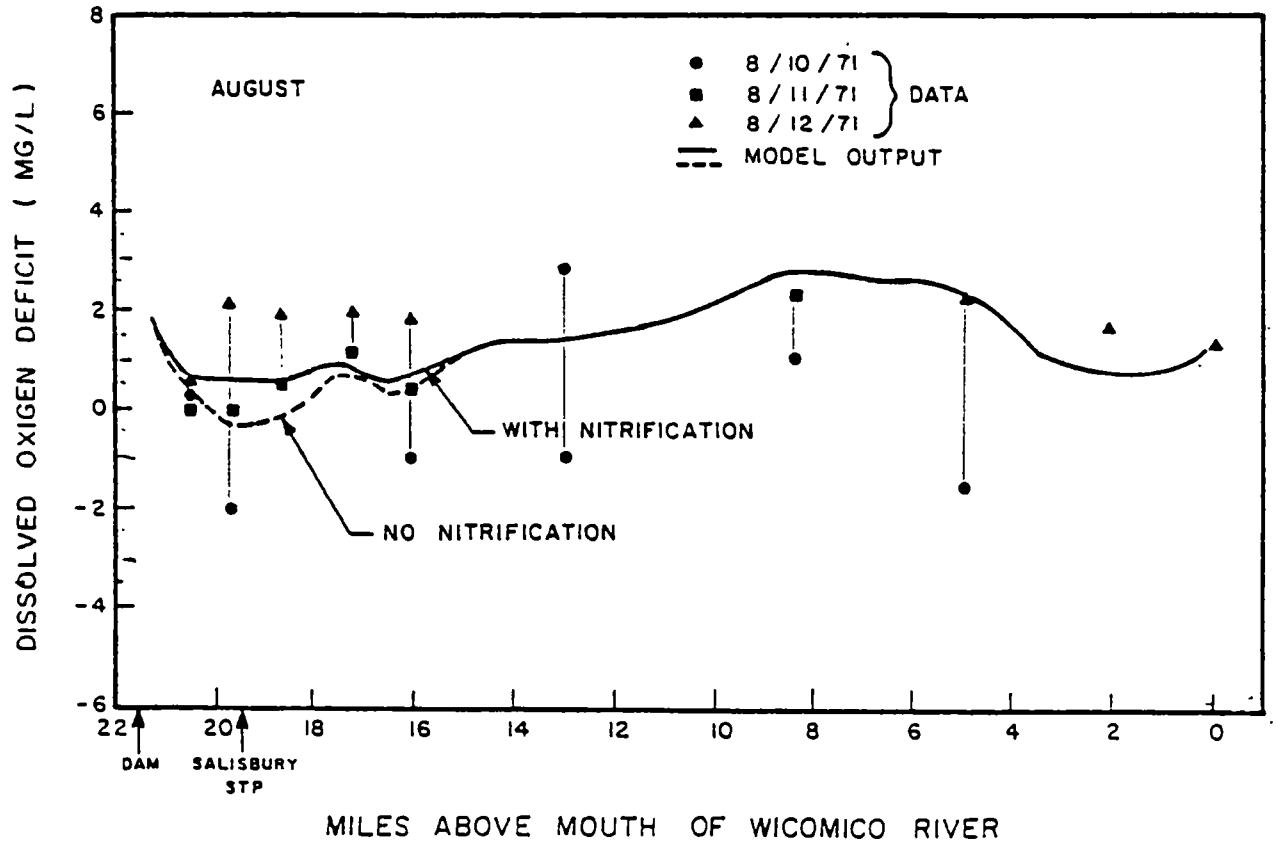

FIGURE W.11

DISSOLVED OXYGEN VERIFICATION - SUMMER 1971

WICOMICO RIVER

Phytoplankton can utilize both ammonia and nitrate-nitrate as nitrogen sources. Whether the ammonia is first oxidized by the autotrophic bacteria to nitrate and then utilized by the phytoplankton cannot be ascertained from the observed data in this study. In Figure W-11, the computed profiles are presented with and without the inclusion of the nitrification phenomena. As can be seen, the response of the system is such that the model may be considered verified with or without the inclusion of the nitrification phenomena.

The major components of the deficit profile for the July 1971 survey are presented in Figure W-12. The impact on dissolved oxygen of the Salisbury STP carbonaceous BOD load is limited to the upper six miles of the River with a peak deficit of about 1.0 mg/l. The inclusion of the nitrification phenomena adds an additional 0.8 mg/l to the peak deficit response. This may be contrasted to the more significant impact on dissolved oxygen levels due to the benthal demand and algal photosynthesis less respiration. Phytosynthesis less respiration is calculated to contribute as much as 4 mg/l of dissolved oxygen in the critical upper reaches of the River. Further downstream, where the River is deeper, photosynthesis less respiration consumes as much as 2 mg/l. The relatively minor impact of the Salisbury STP input indicates that the severe depressions in dissolved oxygen observed in 1967 were probably not due solely to the direct discharge of carbonaceous and nitrogenous oxygen demanding substances from the Salisbury STP.

Nutrient Analyses

Total nitrogen and total phosphorus were modeled in the Wicomico River. Budgetary and time constraints did not allow for the specific modeling of phytoplankton biomass. The impact of nutrient removal policies on phytoplankton biomass can, therefore, only be implied from these analyses and the application of the principles of nitrogen/phosphorus ratios.

Utilizing the observed nutrient loadings and boundary conditions, total nitrogen and total phosphorus were initially analyzed as conservative materials, i.e., no decay. Comparisons between calculated and observed profiles indicate a loss of nutrients from the water column is due to the settling of detritus and phytoplankton cells. For total phosphorus, favorable comparisons between calculated results and observed data for both surveys were

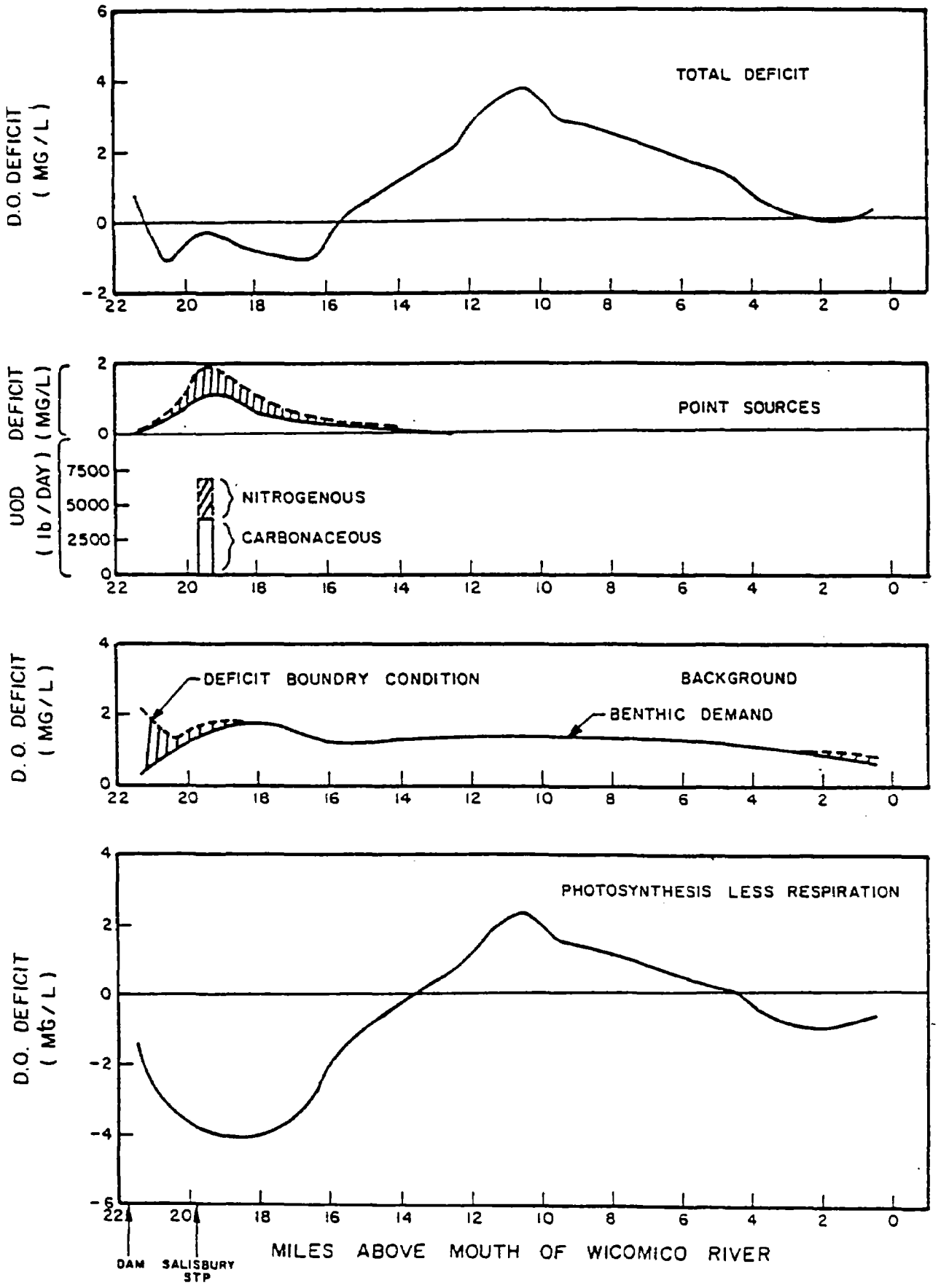

FIGURE W 12

COMPONENT DEFICITS FOR JULY 1971

DISSOLVED OXYGEN VERIFICATION

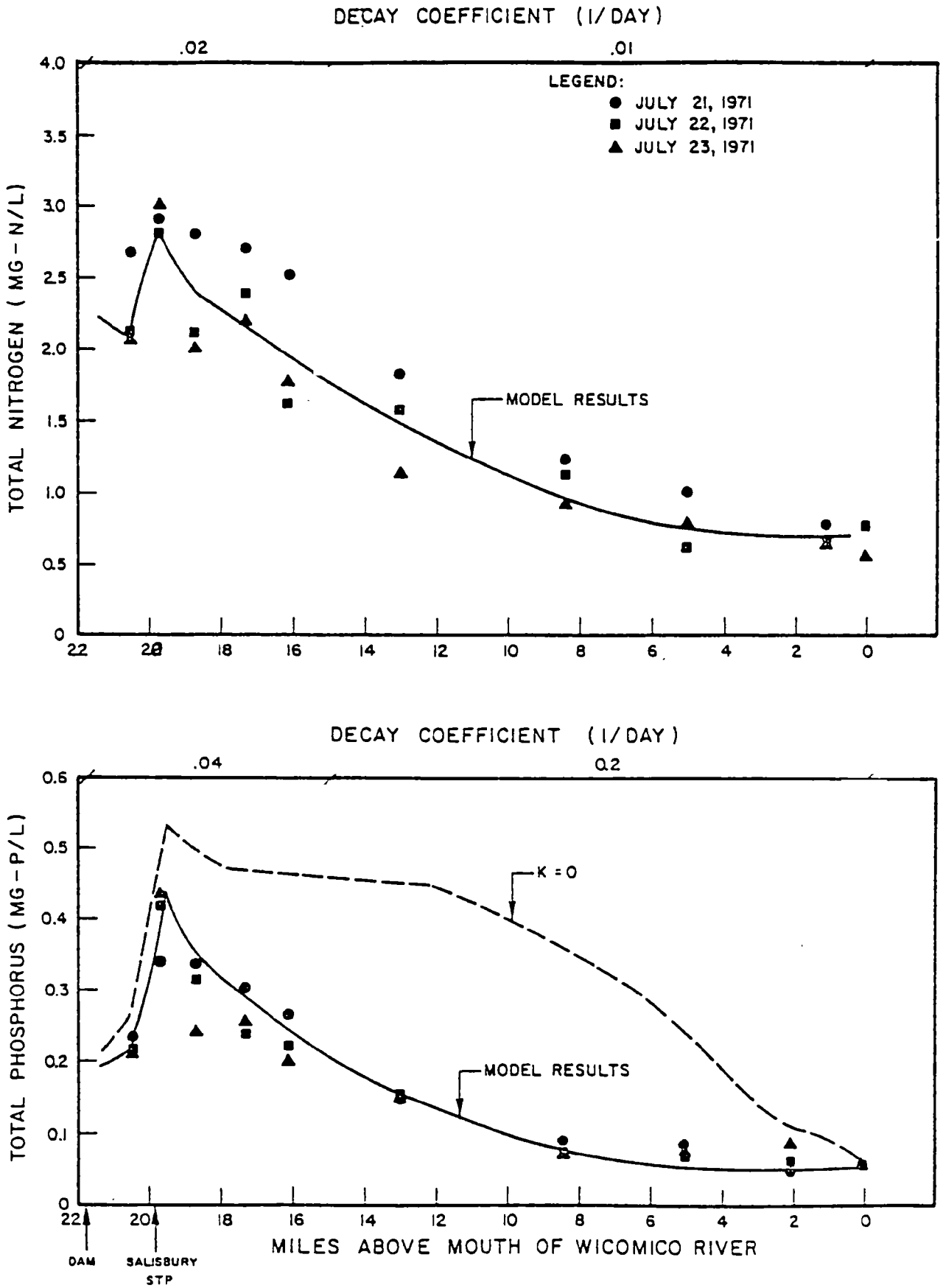

FIGURE W 13
NUTRIENT VERIFICATION – WICOMICO RIVER
JULY 1971

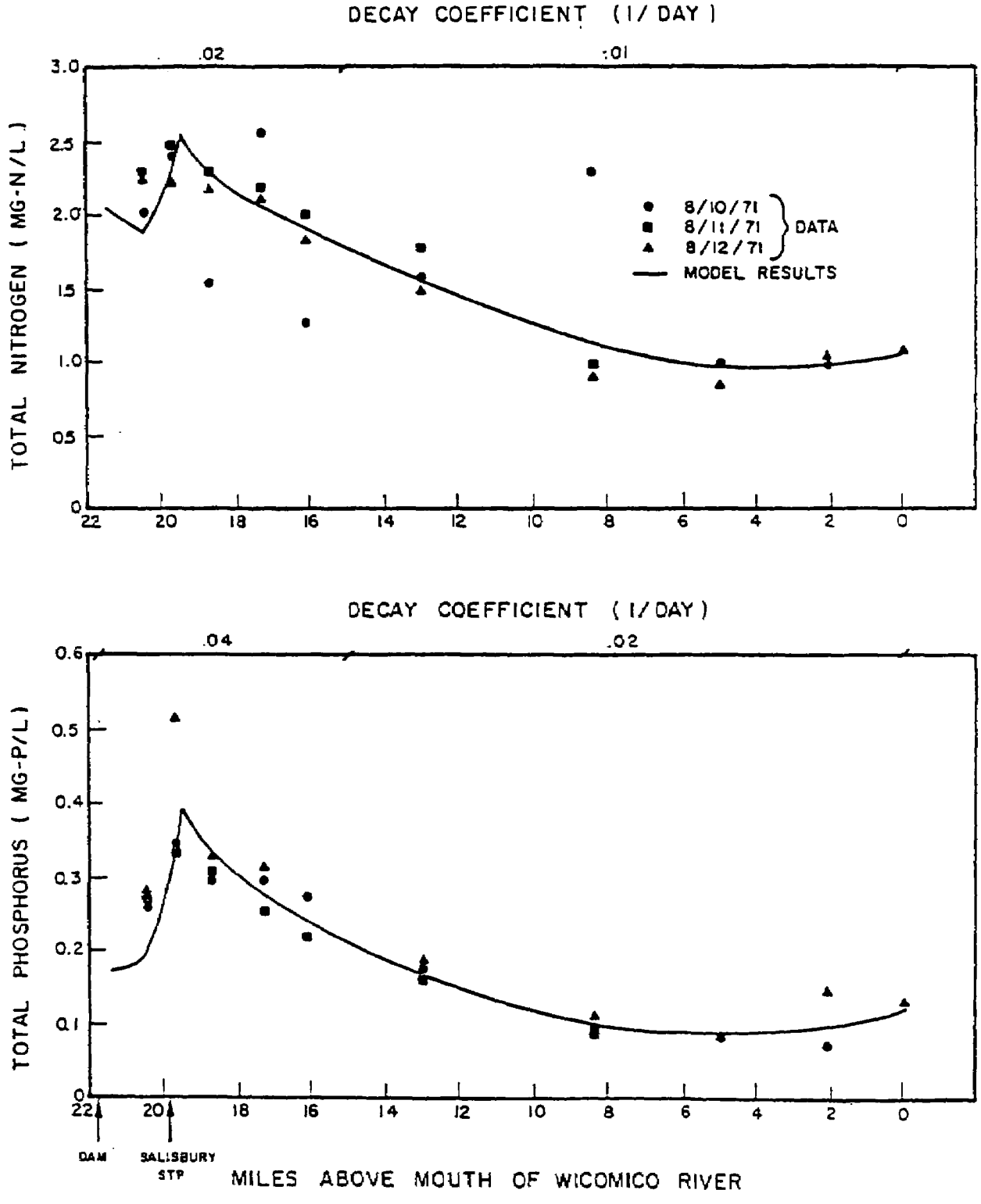

FIGURE W 14
NUTRIENT VERIFICATION – WICOMICO RIVER
AUGUST 1971

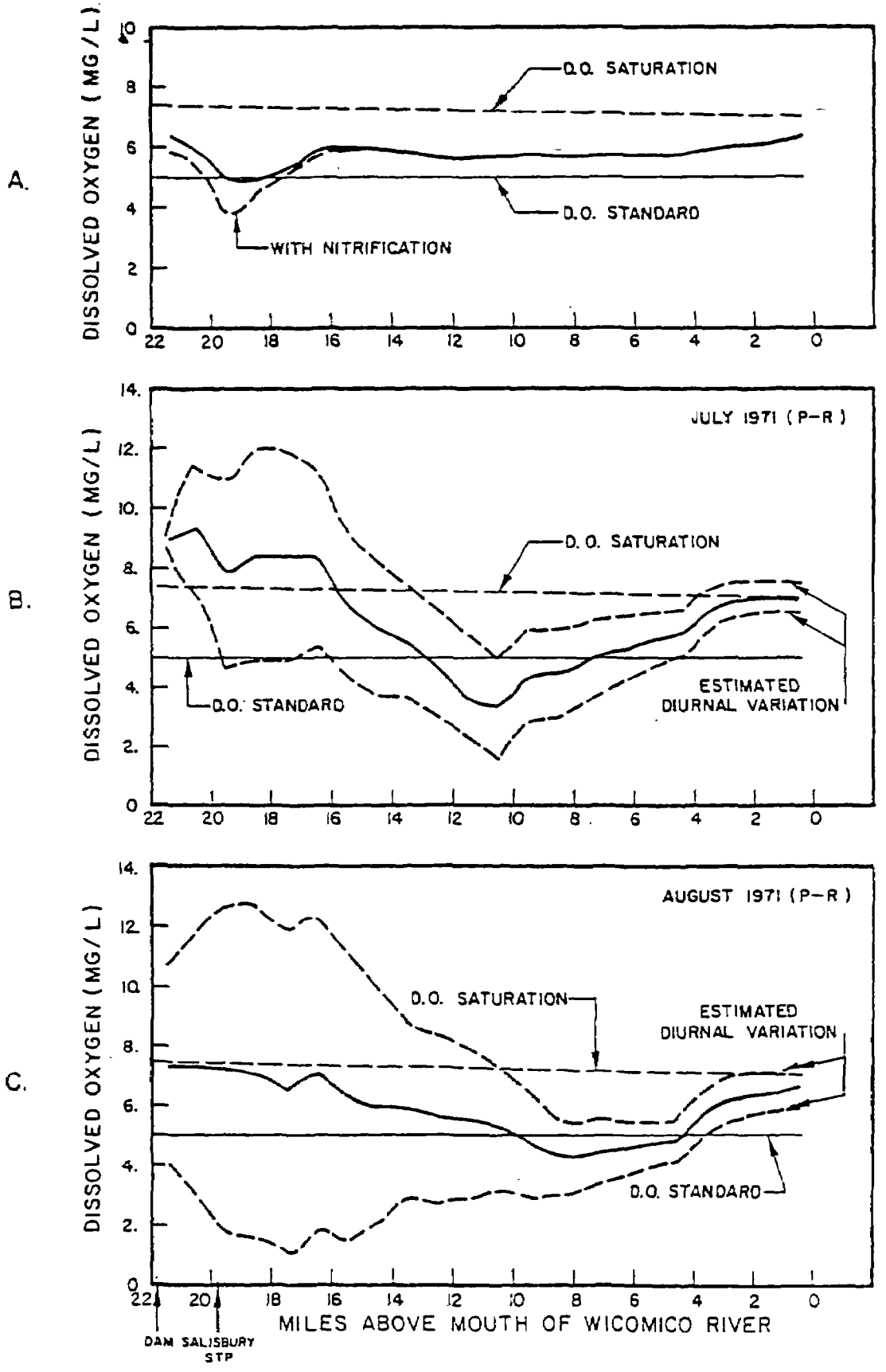

FIGURE W1.5

DISSOLVED OXYGEN PROJECTIONS

DAY - 10 YEAR LOW FLOW

achieved using decay rates of 0.04 and 0.02/day for different portions of the river as shown in Figures W-13 and W-14. This is equivalent to a net effective phosphorus settling rate of about 0.4 ft/day. The calculated profile for total phosphorus, as a conservative substance, is also shown in Figure W-13 for the July 1971 condition. For total nitrogen, as shown in Figures W-13 and W-14, favorable comparisons were achieved for both surveys using a similar distribution of decay rates but halved in magnitude. It can be noted that the ratio of N/p at the outfall is about 7 indicating that either nitrogen or phosphorus may be controlling growth of the phytoplankton downstream.

Waste Discharge Analysis

The two factors chosen for establishing critical periods for the allocation analysis in the Wicomico River were low advective flow and high temperature. The 7 day-10 year low flow (refer Table 2), was employed at a critical water temperature of 30°C. Dissolved oxygen saturation values were computed based on the temperature and salinity distribution projected under the low flow condition utilizing a salinity boundary of 10 ppt at Ellis Bay. The loads used in the projection analysis, as shown in Table 1, were based on data taken during July 1974. All kinetic constants developed in the calibration and verification analyses were applied.

Projected dissolved oxygen profiles under three conditions are presented in Figure W-15. Dissolved oxygen deficit boundary conditions were disregarded on the basis that they did not significantly affect dissolved oxygen in the areas of critical deficit. In Figure W-15A, the combined effect on dissolved oxygen in the Wicomico River due to the carbonaceous BOD load from the Salisbury STP and due to the benthal demand distribution is presented. As indicated, the dissolved oxygen standard is marginally met under these conditions. The inclusion of the nitrification phenomena results in violation of the standard by about 1 mg/l as shown in Figure W-15A. In Figure W-15B and W-15C, the combined effect on dissolved oxygen due to the carbonaceous and nitrogenous oxygen demand from the Salisbury STP, benthal demand and algal photosynthesis, and respiration are presented.

The algal photosynthetic and respiratory rate distributions used to develop these figures were the same as those used for the July and August 1971 model simulations (refer to Figure W-10), respectively. In the vicinity of the Salisbury STP where minimum dissolved oxygen levels are predicted as can be seen in Figure W-14A, average dissolved oxygen concentrations are at and above saturation in Figures W-14B and C. However, violations of the 5 mg/l average dissolved oxygen standard are projected to occur further downstream.

Calculated diurnal fluctuations in dissolved oxygen are also presented in Figure W-15B and C. Based on data from other areas, the diurnal ranges were estimated from the following:

$$D.O. = 0.18\ P_s$$

where P_s is calculated from Equation (1). A check of the above relationship was made using dissolved oxygen data taken on July 22, 1974 when a continuous recorder was installed at Harbor Point (MP 19.5). The maximum observed dissolved oxygen was 12.0 mg/l and the minimum was 6.0 mg/l in a 24 hour period. The observed chlorophyll 'a' level was 158 µg/l. Using the above relationship, the computed diurnal fluctuation in dissolved oxygen is 7.1 mg/l which is in approximate concurrence with the observed range of 6.0 mg/l. Note in Figures W-14B and C that the calculated diurnal range in dissolved oxygen decreases as one proceeds downstream. This is due to decreased levels of chlorophyll 'a'. Violations of the 4 mg/l instantaneous dissolved oxygen standard are projected at various locations, especially in Figure W-14C.

In conclusion, the direct impact on dissolved oxygen of the oxidizable loads emanating from the Salisbury STP are overshadowed by algal activity. As such, effluent limitations for the Salisbury STP should be directed to the control of phytoplankton through nutrient limitations.

Projections of total nitrogen and total phosphorus under the 7 day-10 year low flow conditions are presented in Figure W-16. Total nutrient loads from the Salisbury STP used in the projections are presented in Table 1.

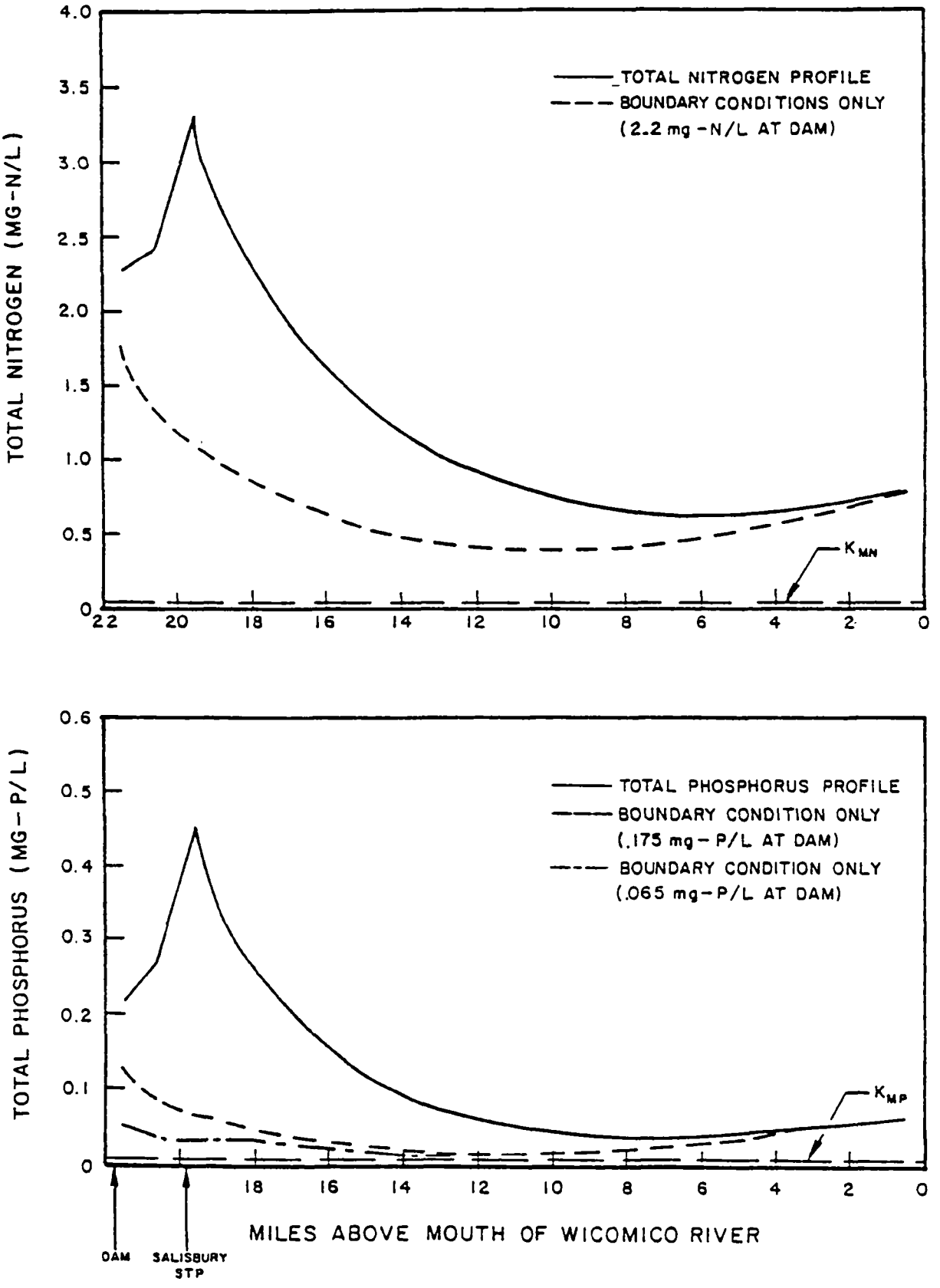

FIGURE W16

NUTRIENT PROJECTIONS

7 DAY - 10 YEAR LOW FLOW

The settling rates developed in the verification analysis were applied. The profiles in Figure W-16 present the calculated distributions resulting from 1) the combined input of the Salisbury STP and the boundary conditions, and 2) the boundary conditions alone. The boundary conditions used were the average values of the nutrients observed during the July and August 1971 surveys. Above the dam at Salisbury, total nitrogen and total phosphorus boundary concentrations were 2.2 mg-N/l and 0.175 mg-P/l, respectively for this period. Average profiles developed from other intensive data showed total nitrogen to be consistently about 2.0 mg-N/l, of which half was in the nitrate form, above the dam at Salisbury. However, a similar review of phosphorus data indicated a wide variability in phosphorus concentrations. The average from the other data indicated a total phosphorus boundary concentration of .065 mg-P/l above the dam. Figure W-16 presents projections for both total phosphorus boundary conditions.

As can be seen in this Figure, peak total nitrogen concentrations of greater than 3 mg-N/l are projected in the vicinity of the Salisbury STP outfall. Approximately 2/3 of this peak is attributed to the Salisbury STP load. With complete elimination of the Salisbury STP nitrogen load, residual concentrations of greater than 1 mg-N/l are projected due to the upstream boundary condition alone. Assuming complete conversion of the total nitrogen of 1 mg-N/l to phytoplankton biomass with a stoichiometric conversion factor of 10 mg-N/mg Chl 'a', there is a potential for chlorophyll 'a' levels of greater than 100 µg/l. Complete conversion, of course, would never be realized so the above chlorophyll 'a' level is meant only for comparative purposes.

An examination of projected total phosphorus concentrations shows peak concentrations in the vicinity of the Salisbury STP outfall of greater than 0.4 mg-P/l of which more than 3/4 is attributed to the Salisbury STP load. Total phosphorus concentrations due to the high and low boundary conditions alone are about .070 and .030, mg-P/l respectively, at the Salisbury STP outfall. Using a stoichiometric conversion factor of 1 mg-P/mg Chl 'a', potential chlorophyll 'a' levels are 70 and 30 µg/l for the high and low boundary conditions, respectively. Based on the above analyses, the removal of phosphorus relative to nitrogen will have a potentially greater impact in

the reduction of chlorophyll 'a' level under the lower phosphorus upstream boundary condition. With the higher phosphorus boundary condition the difference is marginal. Therefore, further evaluations to establish the total phosphorus levels above the dam and to eliminate the apparent discrepancies in the available data are imperative. In terms of total N/total P ratios, the boundary condition at the dam varies from 12-33 indicating that the potential exists for forcing the Wicomico to be phosphorus limited. Also, treatment to remove phosphorus at Salisbury would further force the system to phosphorus limitation and reduce existing phytoplankton biomass.

Conclusions

1. Chlorophyll 'a' levels in the Wicomico River in the vicinity of Salisbury have been observed to exceed 200 µg/l during the summer. Dissolved oxygen levels in this area vary from supersaturation during the day under dry weather conditions to less than 3 mg/l under wet weather-high runoff conditions.
2. Model analyses indicate that the effect of carbonaceous and nitrogenous oxygen demanding material discharged from the Salisbury Sewage Treatment Plant is limited to the upper six miles of the Wicomico River and is relatively small when compared to the net effect of algal activity on dissolved oxygen.
3. Neither nitrogen nor phosphorus appear to be significantly limiting phytoplankton growth in the upper Wicomico River although nitrogen may be limiting growth in the lower River.
4. The most significant sources of nutrients in the tidal portion of the Wicomico River are the Salisbury Metropolitan Area and the watershed upstream of the dam at Salisbury. The former source accounts for a significant proportion of total nutrients under low flow conditions. Upstream nutrient inputs, however, are still substantial under low flow conditions.
5. The modeling analysis of dissolved oxygen indicates that the reduction of the discharge of nitrogenous oxygen demanding materials from the Salisbury Sewage Treatment Plant will have a relatively insignificant effect on overall dissolved oxygen levels in the Wicomico River when compared to the fluctuations in dissolved oxygen due to algal activity.

Therefore, good secondary treatment is considered adequate at present.

6. The modeling analysis of total nitrogen and total phosphorus indicates that the reduction in the discharge of phosphorus relative to nitrogen from the Salisbury Sewage Treatment Plant will have a greater impact on phytoplankton biomass in the tidal portion of the Wicomico River with potential reductions in chlorophyll 'a' to less than 100 µg/l. Further reduction in chlorophyll 'a' will necessitate upstream controls of phosphorus.
7. Therefore, it is concluded that the first step in nutrient reductions to decrease chlorophyll 'a' levels in the tidal portion of the Wicomico River should be directed toward phosphorus.

Recommendations

1. Additional evaluations should be performed to more adequately define nutrient conditions, especially phosphorus, in the Wicomico River above the dam at Salisbury. Analyses should also be initiated to determine the impact of nutrient controls in the Wicomico watershed above the dam at Salisbury.
2. For the values of the parameters that were assumed in this study because of lack of data, such as the dissolved oxygen benthal demand, field or laboratory measurements should be made. Should nutrient controls be implemented, intensive monitoring before and after should be conducted to evaluate the impact on water quality.
3. The modeling framework should be expanded to include phytoplankton biomass. The model should also be continually refined in light of new data especially after the implementation of nutrient controls, if any.
4. Because of the loss of nutrients to the sediments, an investigation should be conducted on the sediment-water interactions towards determining the potential for the re-release of these nutrients under future conditions.
5. An evaluation of the effect of high runoff - low incident light conditions on dissolved oxygen in the Wicomico River should be conducted since such conditions appear to be critical.

REFERENCES

Boggess, D.H., and Heidel, S.G., "Water Resources of the Salisbury Area, Maryland", Report of Investigation No. 3, Maryland Geological Survey, U.S.G.S., 1968.

Pheiffer, T.H., Donnelly, D.K., Posschl, D.A., "Water Quality Conditions in the Chesapeake Bay System", Technical Report 55, Annapolis Field Office, Region III, Environmental Protection Agency, August 1972.

Salas, H.S. and R.V. Thomann, 1975. The Chesapeake Bay Waste Load Allocation Study. Prepared by Hydroscience, Inc. for the Maryland Dept. of Nat. Res., Water Res. Admin., Annapolis, Md., 287 pp.

Thomann, R.V., 1972. Systems Analysis and Water Quality Management. McGraw-Hill Book Co., New York, 287 pp.

Walker, P.N., "Flow Characteristics of Maryland Streams", Report of Investigation No. 16, Maryland Geological Survey, U.S.G.S. 1971.

Webb, W.E., and Heidel, S.G., "Extent of Brachish Water in the Tidal Rivers of Maryland", Report of Investigation No. 13, U.S. Geological Survey, 1970.

Examples of Sensitivity Analyses*

Water Body	Sensitivity	Remarks
Black R., N. Y.	K_d	CBOD problem; dam reaeration
New York Harbor, N. Y.	Q, K_d, K_n, K_a	Point and distributed sources of CBOD
North Canadian River, OK	K_a, K_d, K_n	Treatment decision

*John A. Mueller

Sensitivity Analysis

BLACK RIVER

New York

Ref: "Water Pollution Investigation: Black River of New York", Hydroscience, Inc. for USEPA, Region II and V; EPA-905/9-74-009

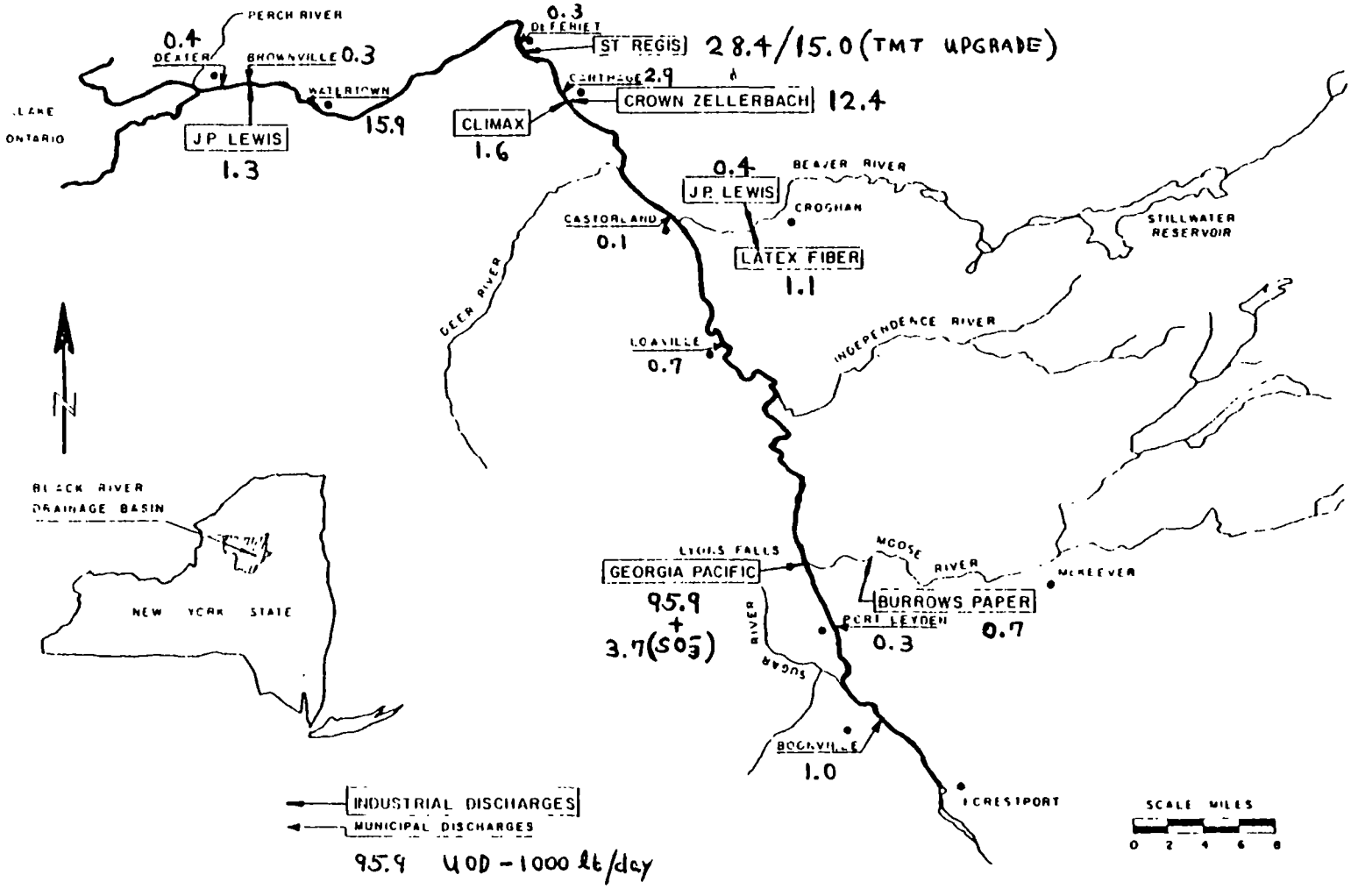

FIG. 1 BLACK R. with INDUSTRIAL AND MUNICIPAL WASTEWATER DISCHARGES

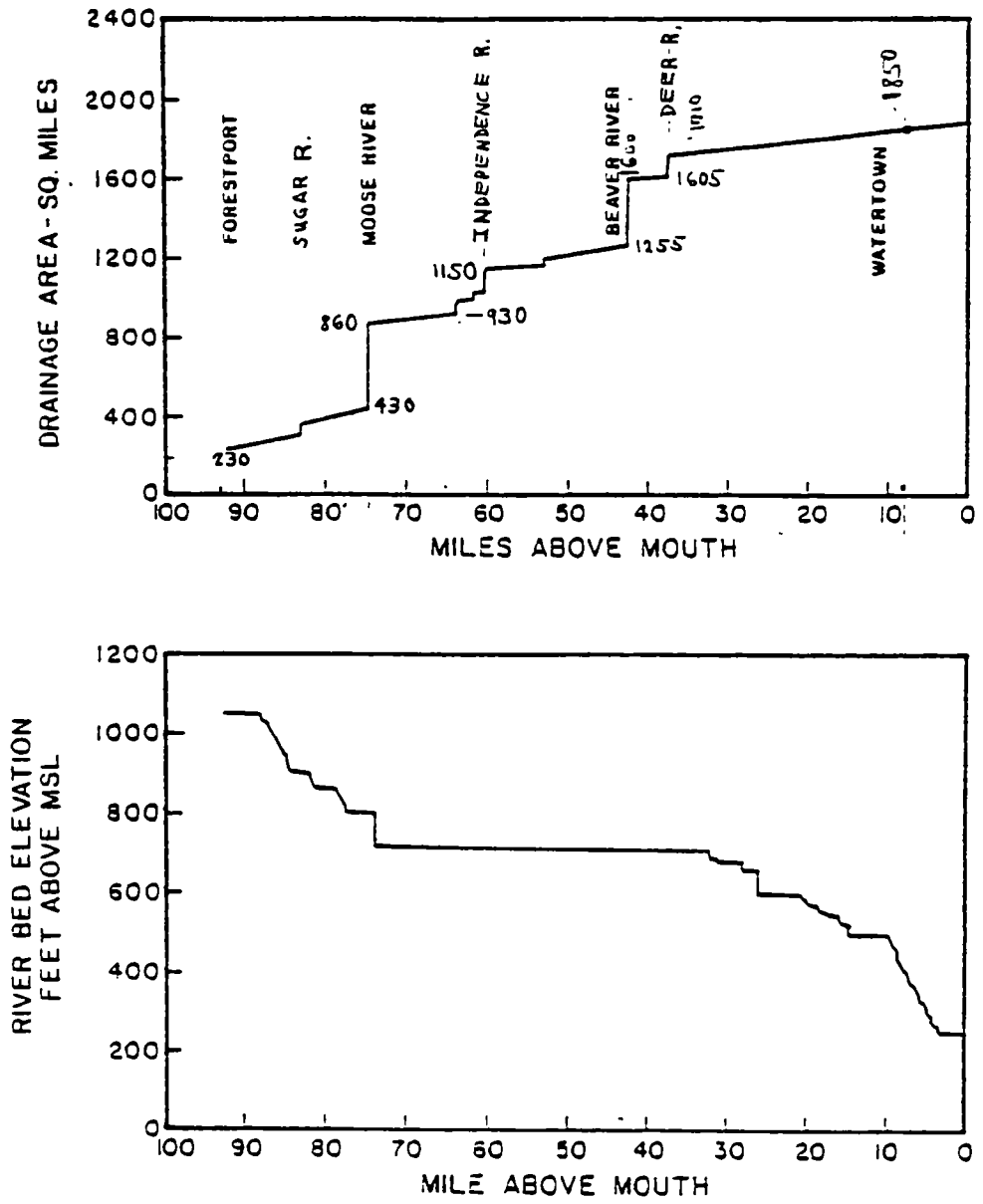

FIG.2 DRAINAGE AREA AND RIVER BED ELEVATION FOR BLACK RIVER (FORESTPORT TO MOUTH)

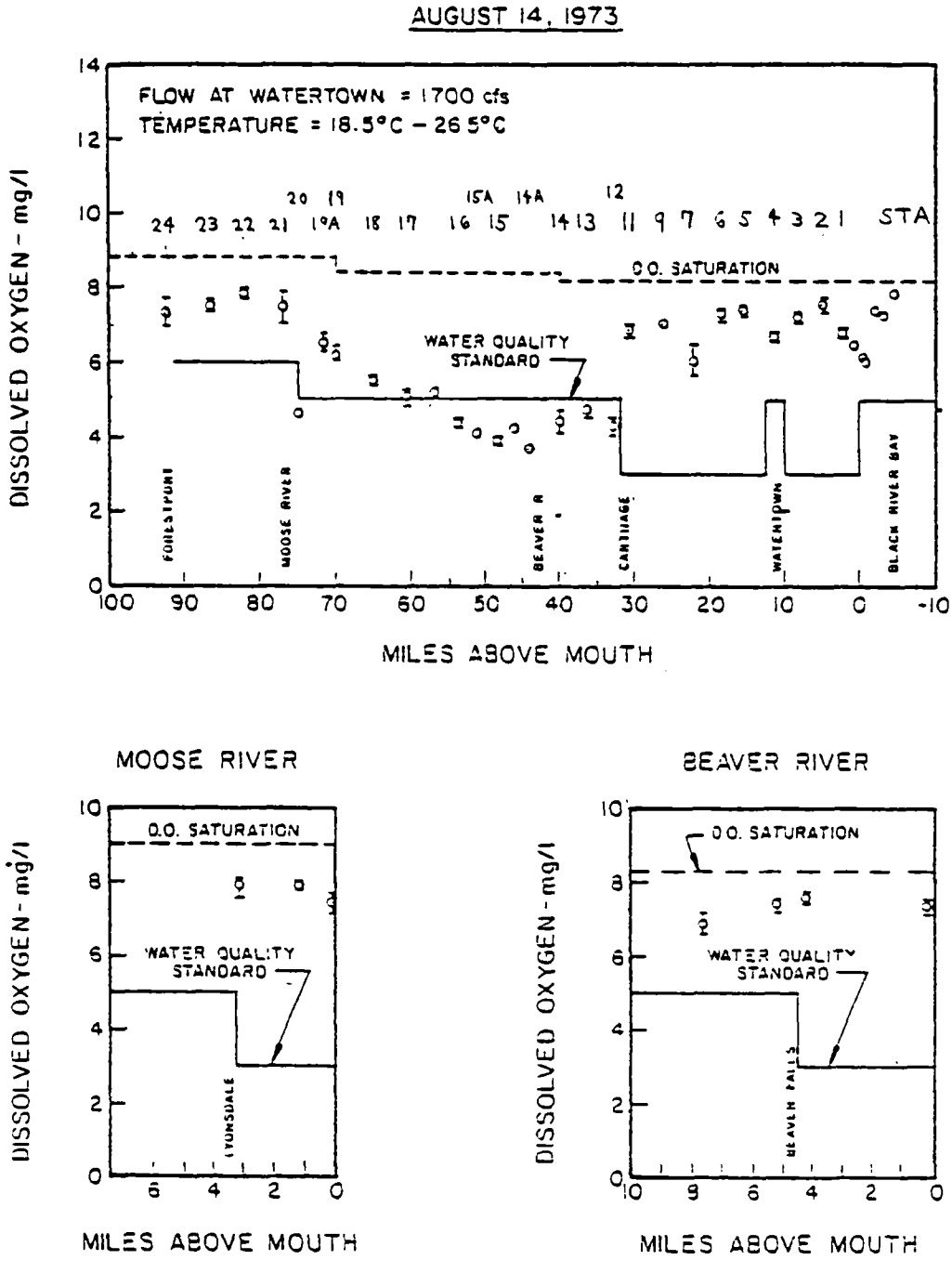

FIG. 3 RIVER DISSOLVED OXYGEN DATA (AUGUST 14, 1973)

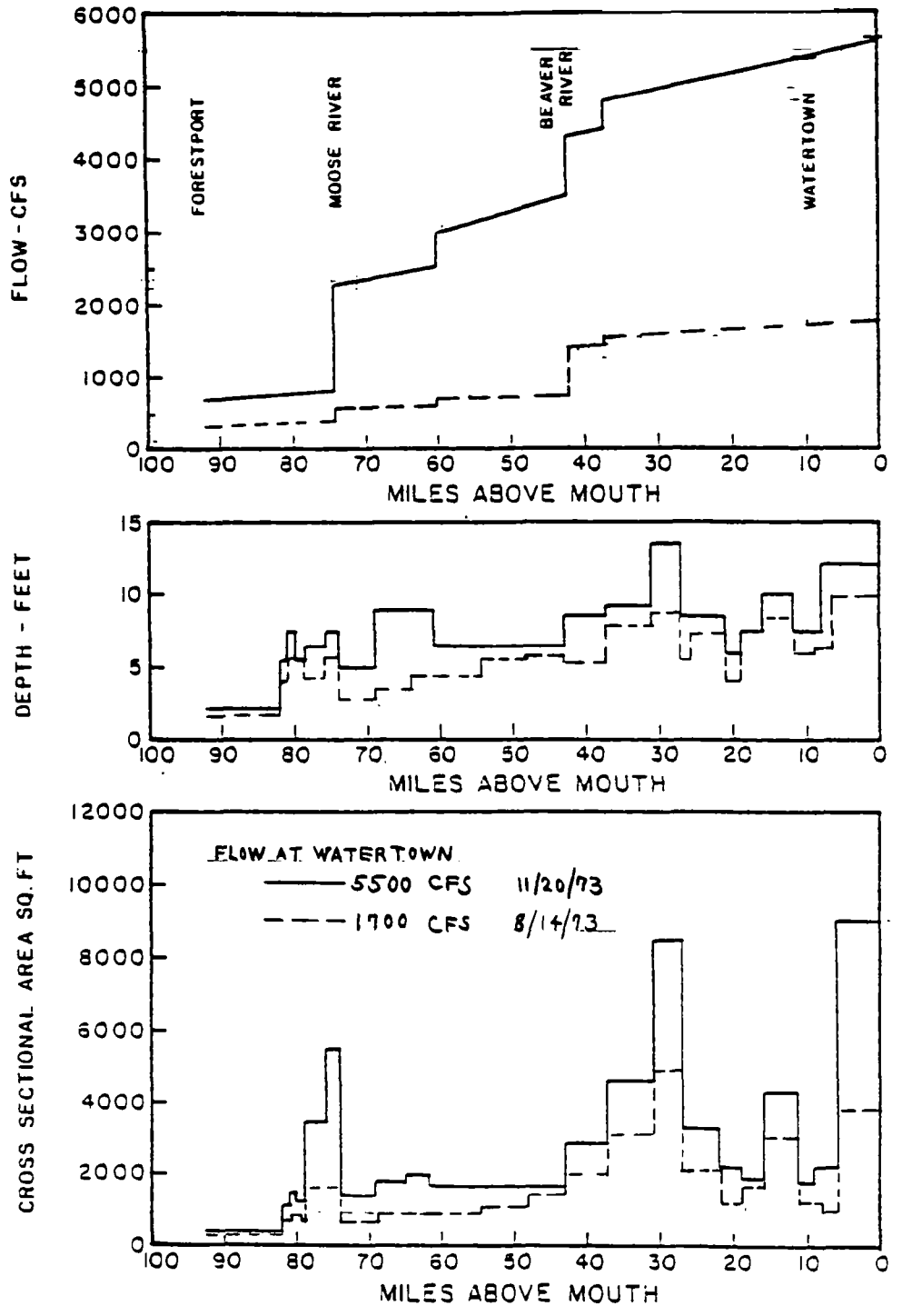

FIG. 4 FLOW, DEPTH, AND CROSS SECTIONAL AREA DISTRIBUTIONS

calculations by
John A Mueller

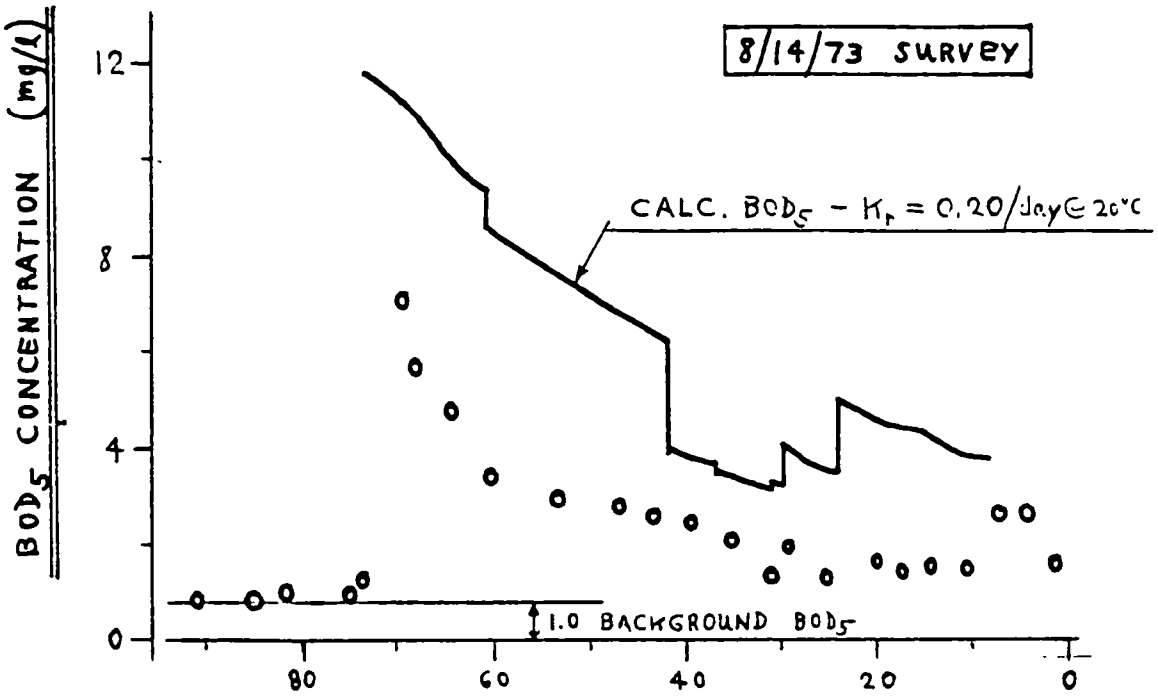

DATA: ○ BOD_5
□ BOD_u

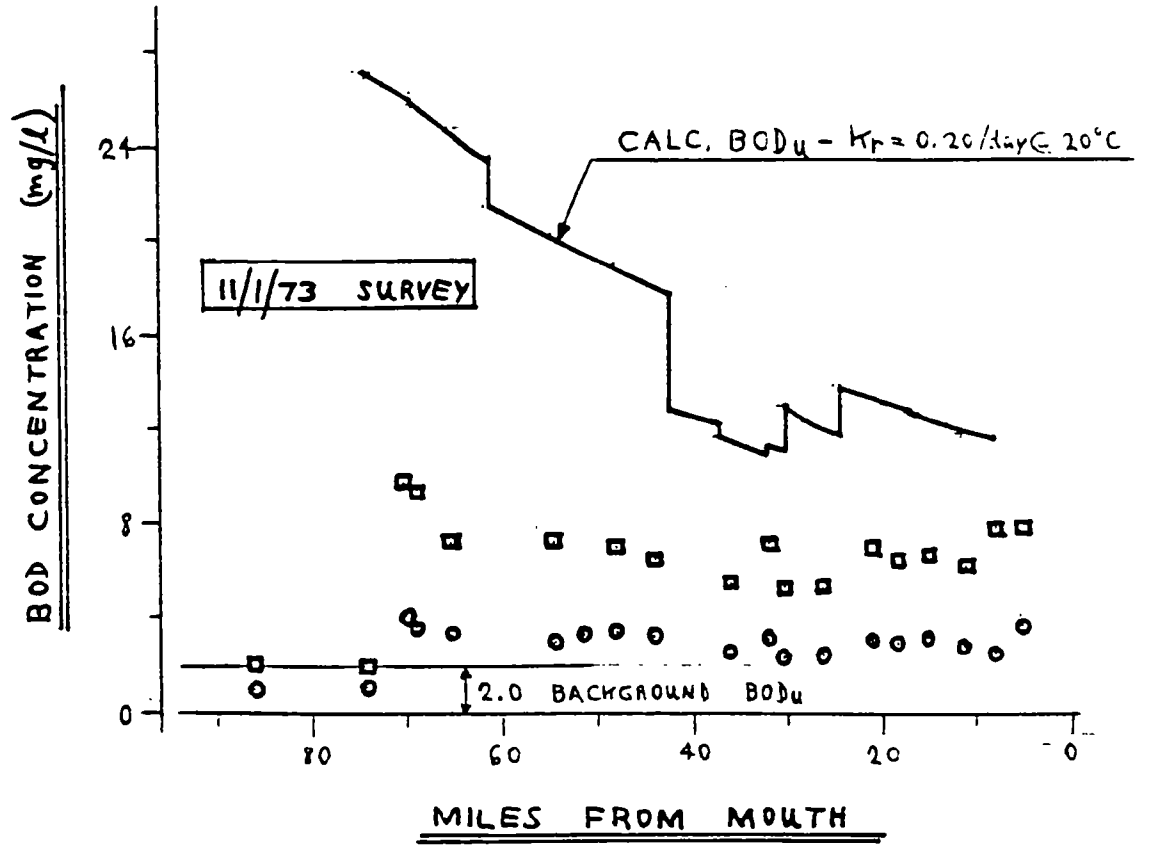

FIG. 5 CALCULATED VS MEASURED BOD - BLACK R, N.Y.

Compl. 11/24/79 JAM

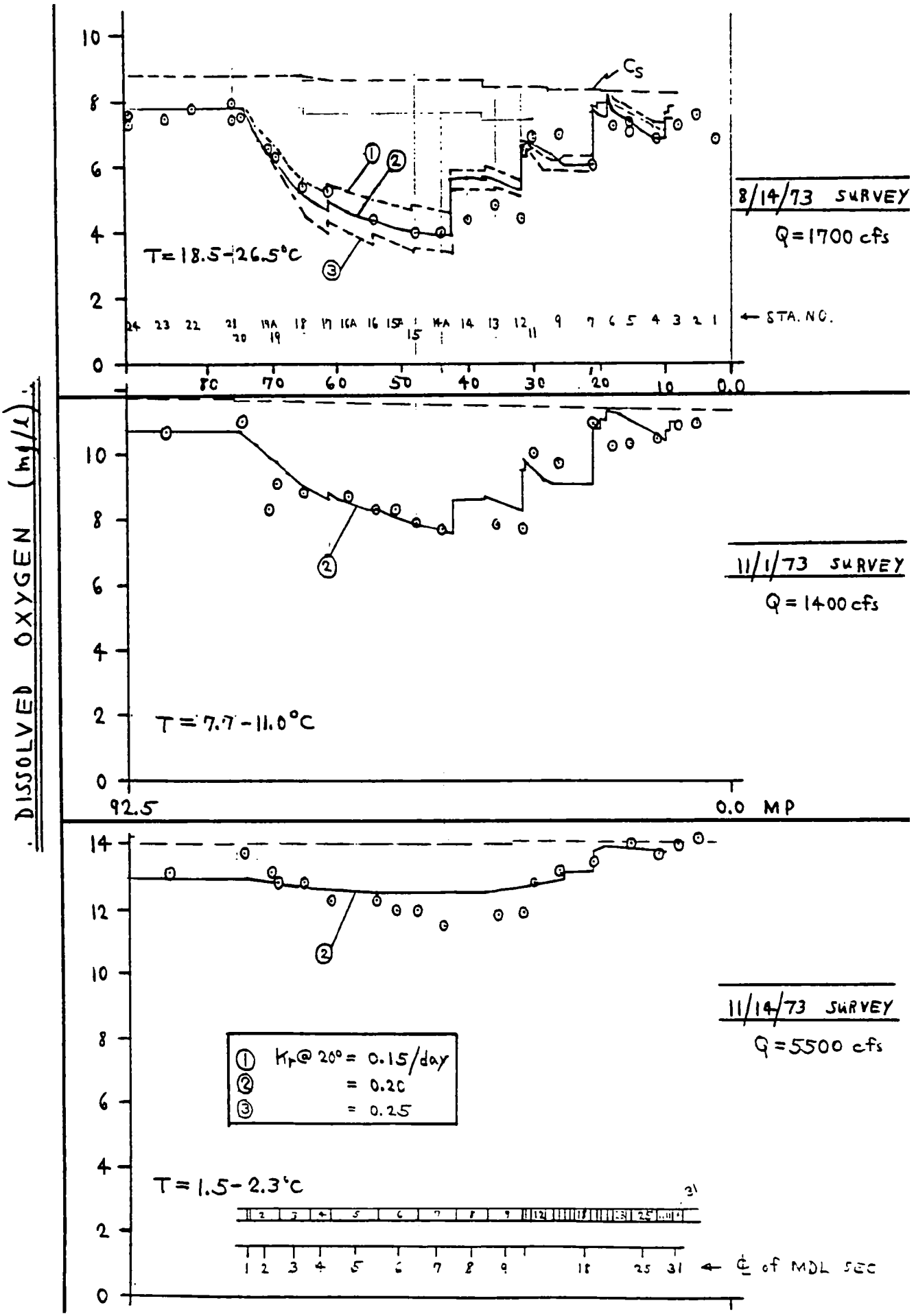

FIG.6 Black River Dissolved Oxygen Verifications

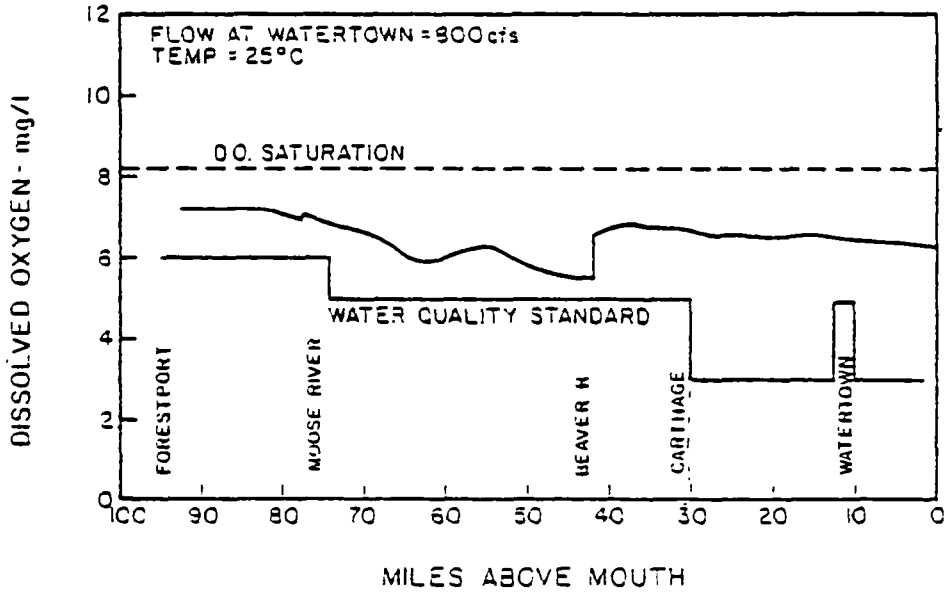

WASTEWATER LOADS

INDUSTRIAL - BEST PRACTICABLE CONTROL TECHNOLOGY CURRENTLY AVAILABLE

MUNICIPAL - SECONDARY TREATMENT

FIG. 7 DISSOLVED OXYGEN PROJECTION FOR LOW FLOW CONDITIONS

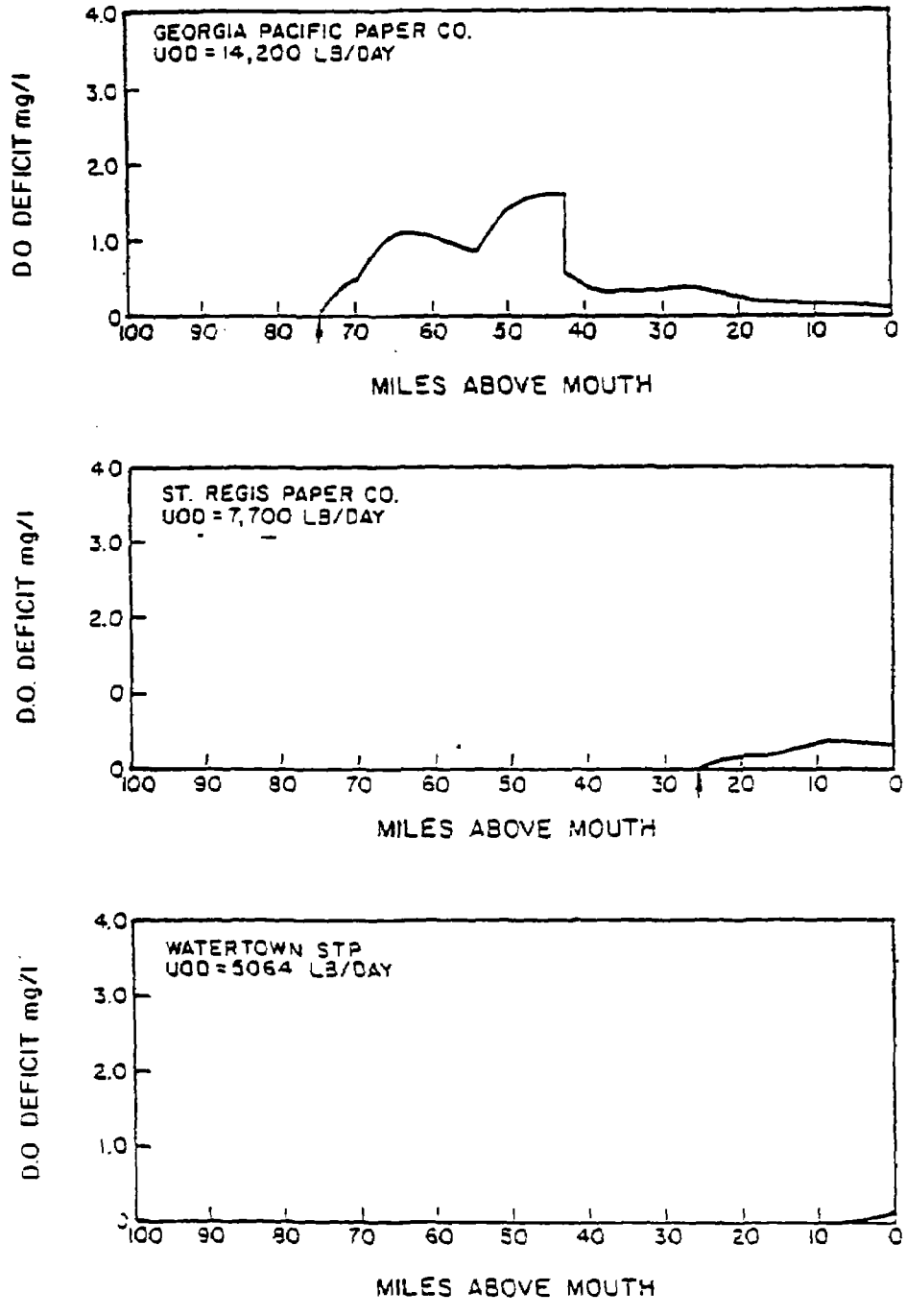

FIG. 8 DISSOLVED OXYGEN DEFICIT PRODUCED BY INDIVIDUAL WASTEWATER DISCHARGES

Sensitivity Analysis

HUDSON RIVER

&

NEW YORK HARBOR

New York

Ref: "Seasonal Steady State Modeling", Hydroscience, Inc., Task Report 314, NYC 208, prepared for Hagen & Sawyer, Engr. & NYC Dept. of Water Resources, Mar. 1978

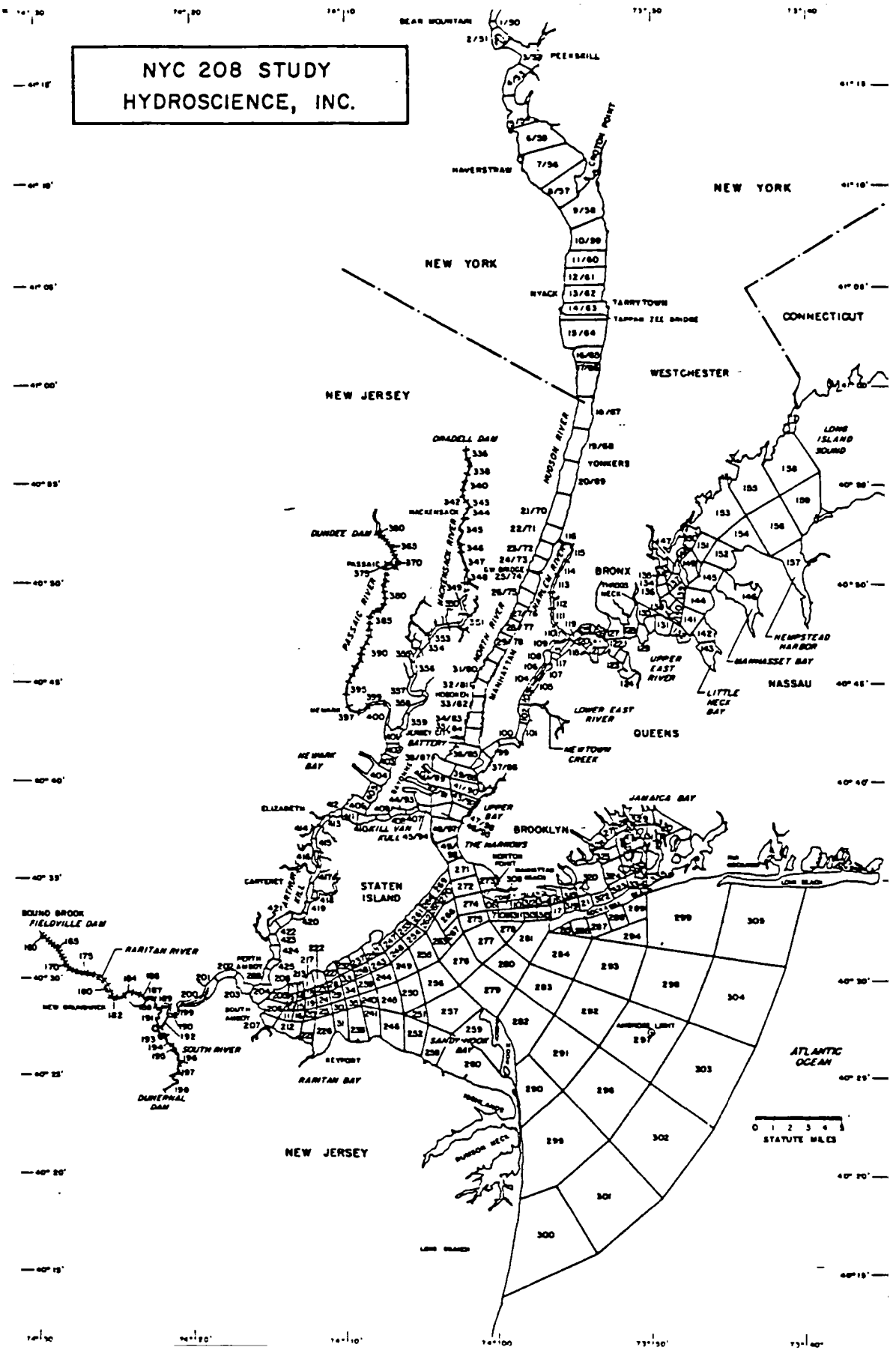

FIGURE 1

SCHEMATIC OF NYC 208 MODEL SEGMENTATION

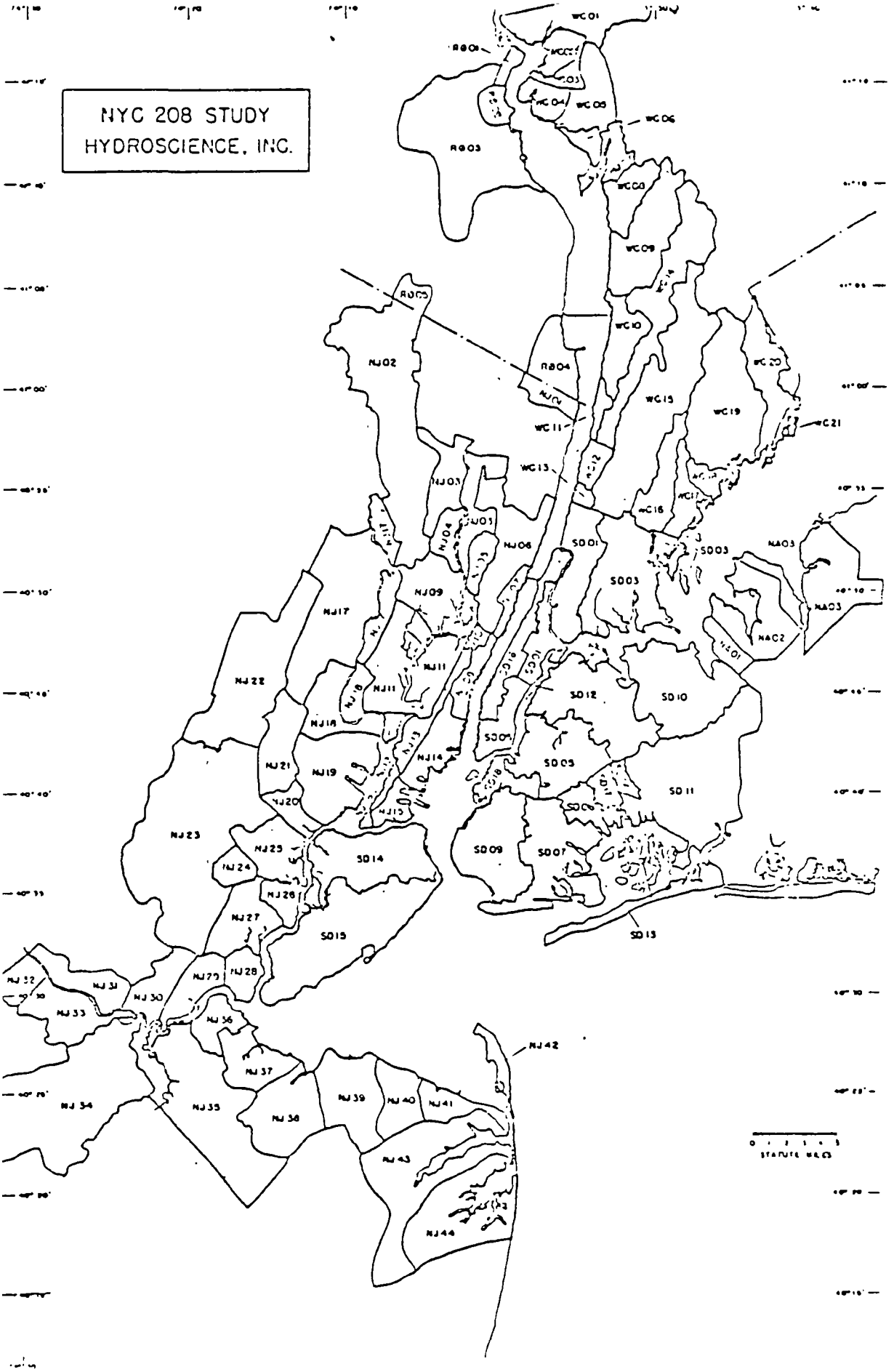

FIGURE 2
MAJOR FEATURES OF RAINFALL RUNOFF SIMULATOR

TABLE 1

SUMMARY OF TOTAL BOD_5 LOADS BY SOURCE AND YEAR

Period Verification	Total BOD_5 Loads (lbs/day)							
	New York	New Jersey	Bypass	Raw	Leakage	Misc	Runoff	Total Load
Sept. 1975	448014	1030610	129343	440021	107135	262760	435800	2.85×10^6
Nov.-Dec. 1976	527065	1219130	274150	281227	107135	262760	177600	2.85×10^6
July 1977	490687	949789	137506	281227	107135	262760	192000	2.42×10^6

SUMMARY OF TOTAL COLIFORM[1] LOADS BY SOURCE AND YEAR

Period Verification	Total Total Coliform Loads (MPN/100 ml x MGD x 8.34)[2]							
	New York	New Jersey	Bypass	Raw	Leakage	Misc	Runoff	Total Load
Sept. 1975	5340	23599	33313	47073	15604	219	19070	144219
Nov.-Dec. 1976	111435	402	40001	36529	15604	219	7775	211965
July 1977	13486	14554	25483	36529	15604	219	8374	114249

[1] All numbers x 10^6

[2] (MGD x MPN/100 ml x 8.34) x (4.54×10^6) = No/day of coliforms

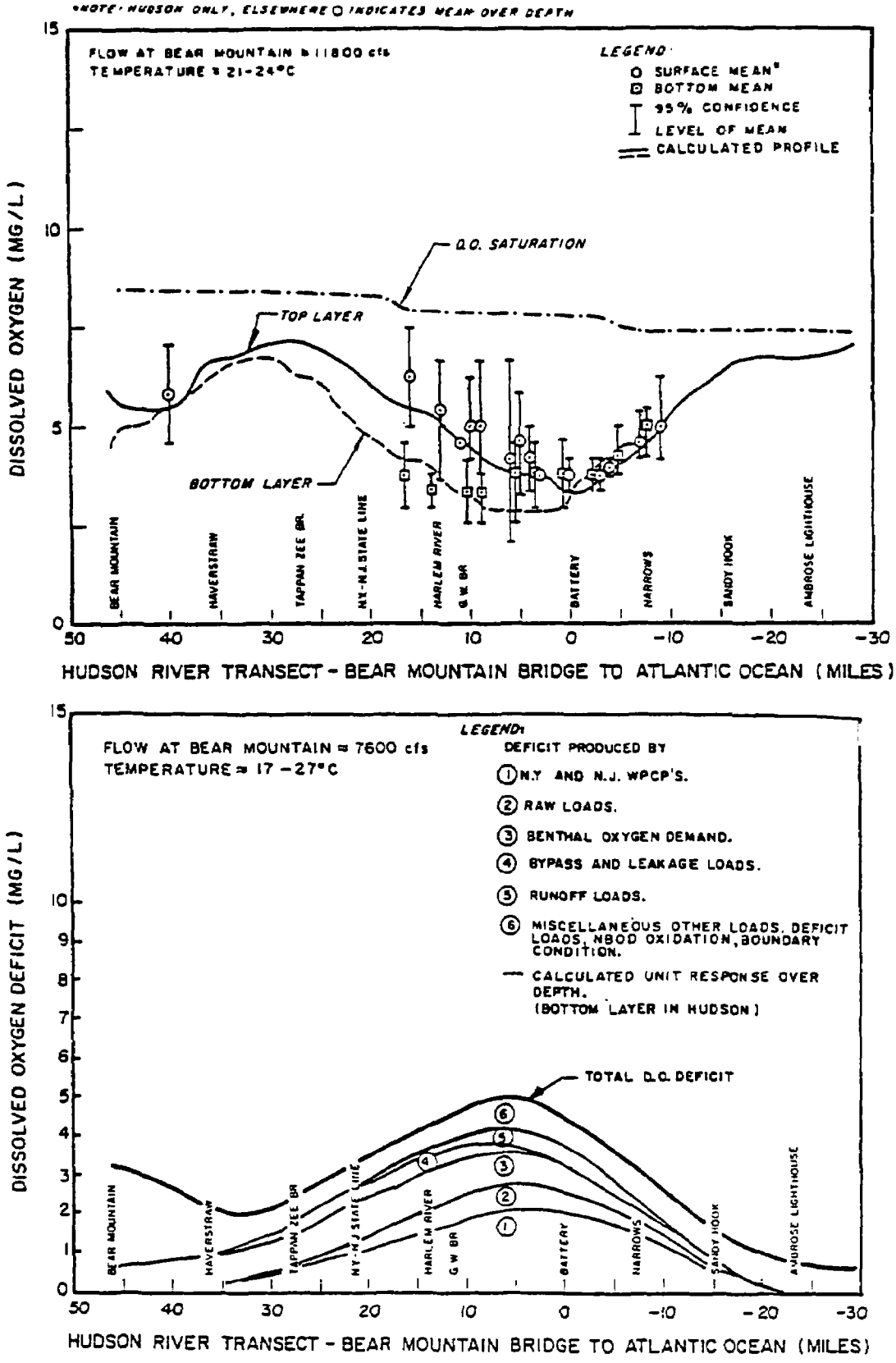

FIG. 3 DISSOLVED OXYGEN VERIFICATION + UNIT RESPONSES

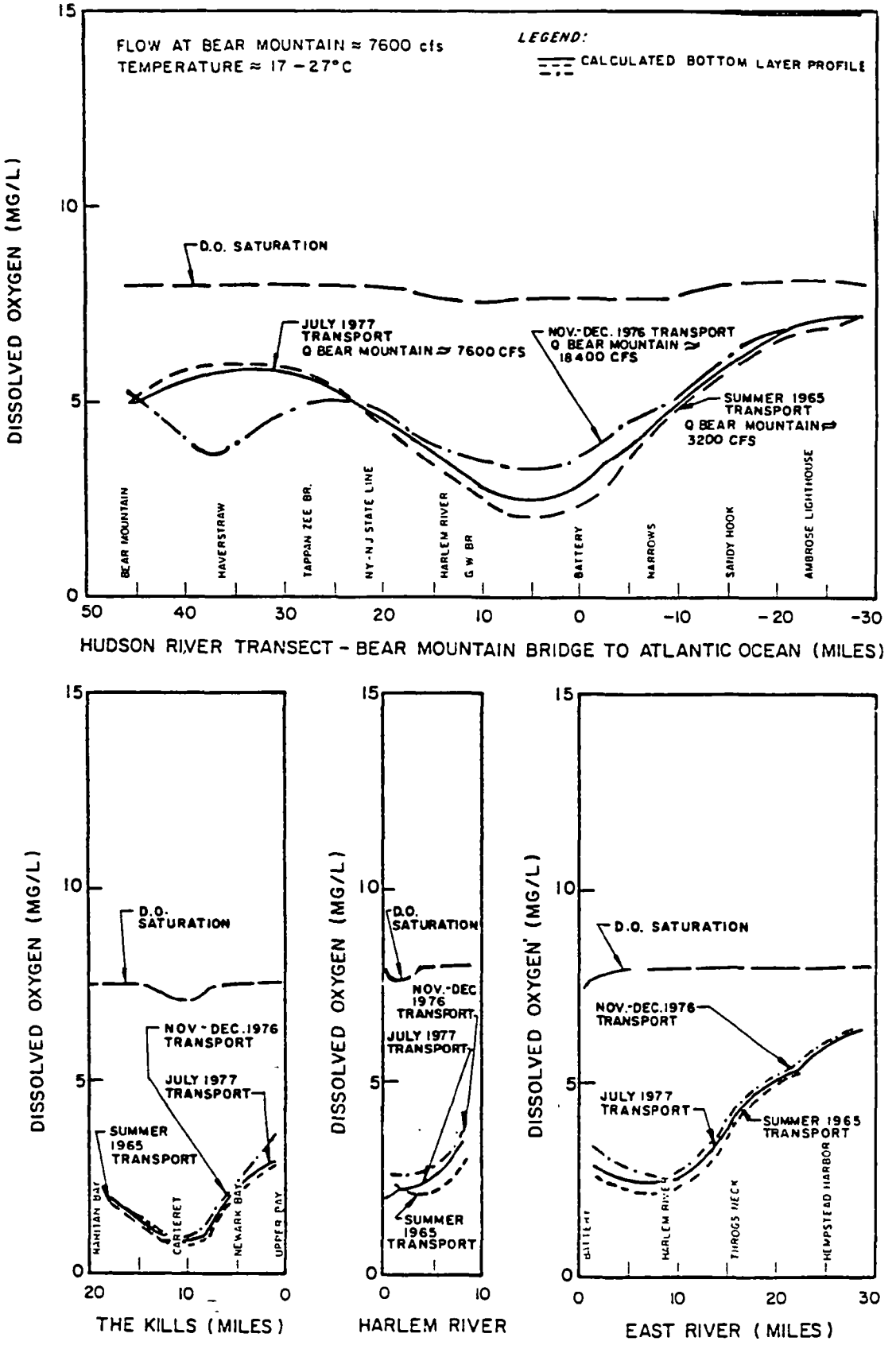

FIGURE 4
DISSOLVED OXYGEN SENSITIVY TO CHANGES IN SYSTEM TRANSPORT
(JULY 5-29 1977)

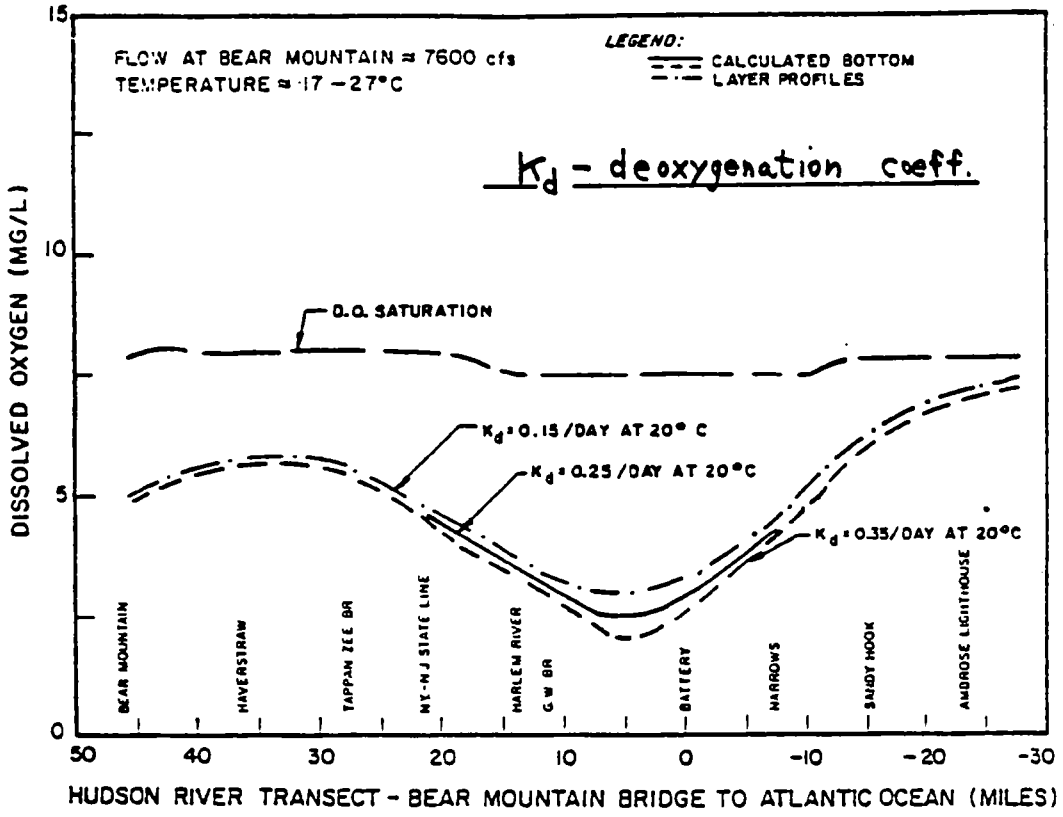

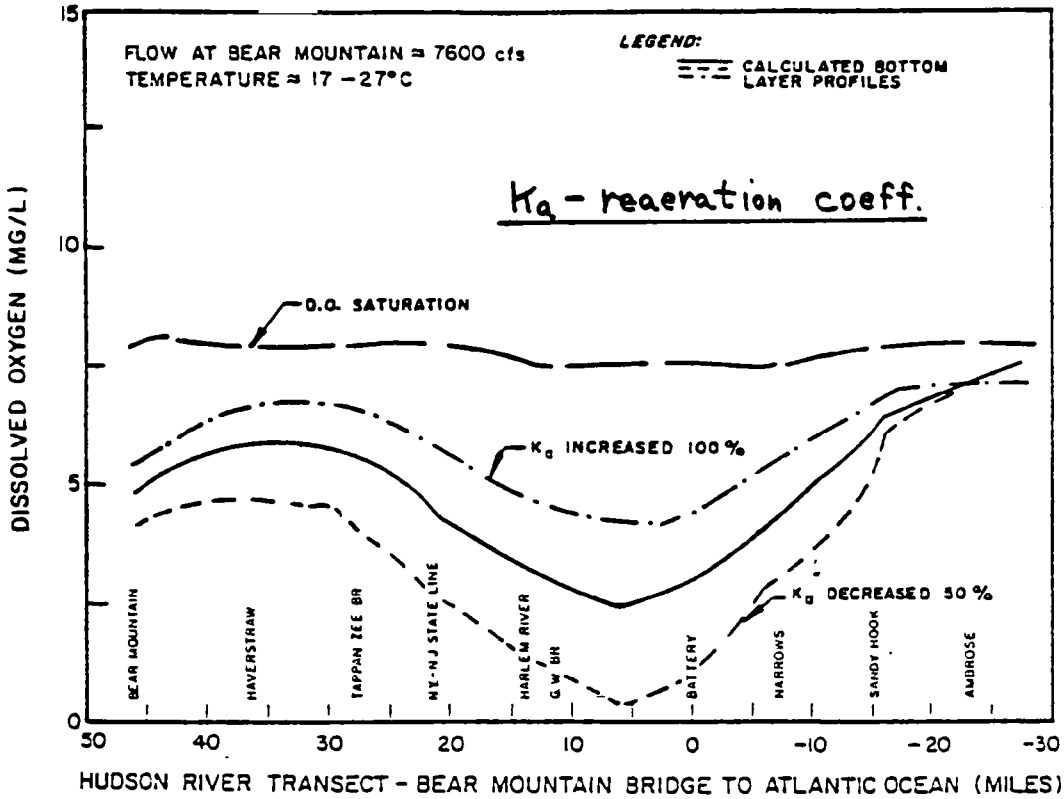

FIGURE 5
DISSOLVED OXYGEN SENSITIVITY TO K_d AND K_a
(JULY 5-29, 1977)

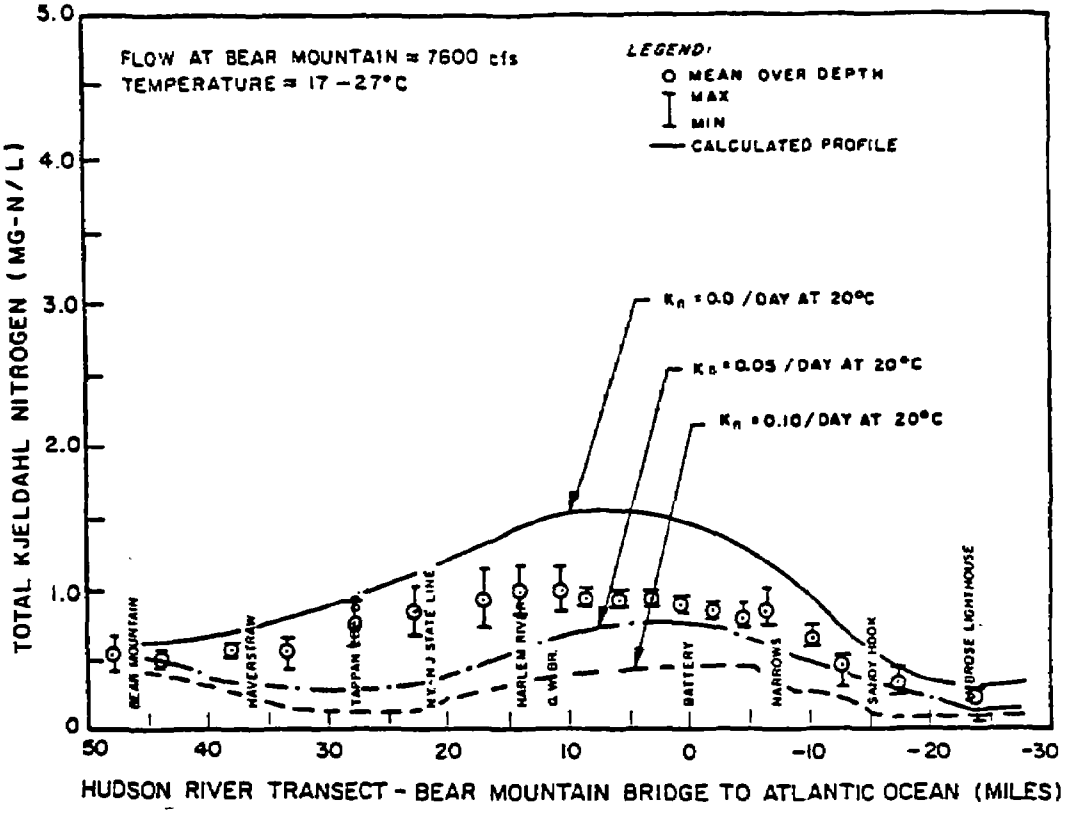

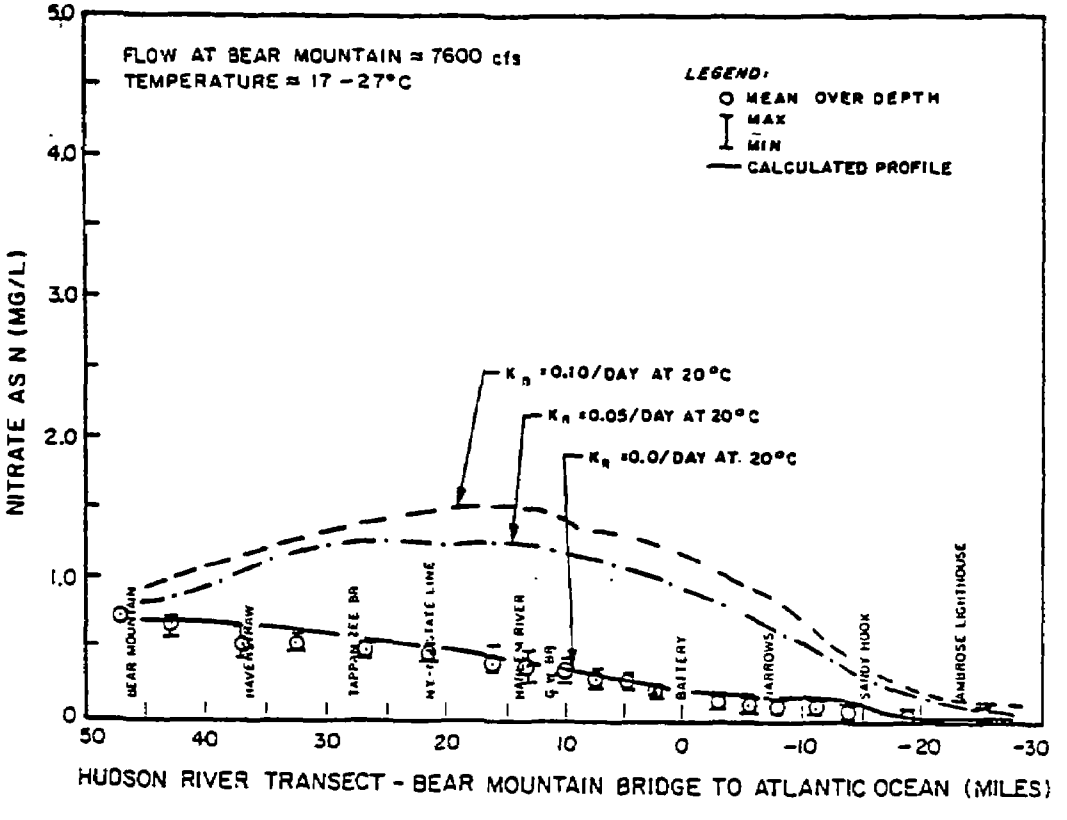

FIGURE 6
TKN SENSITIVITY TO NITRIFICATION RATE (K_n)
(JULY 5-29, 1977)

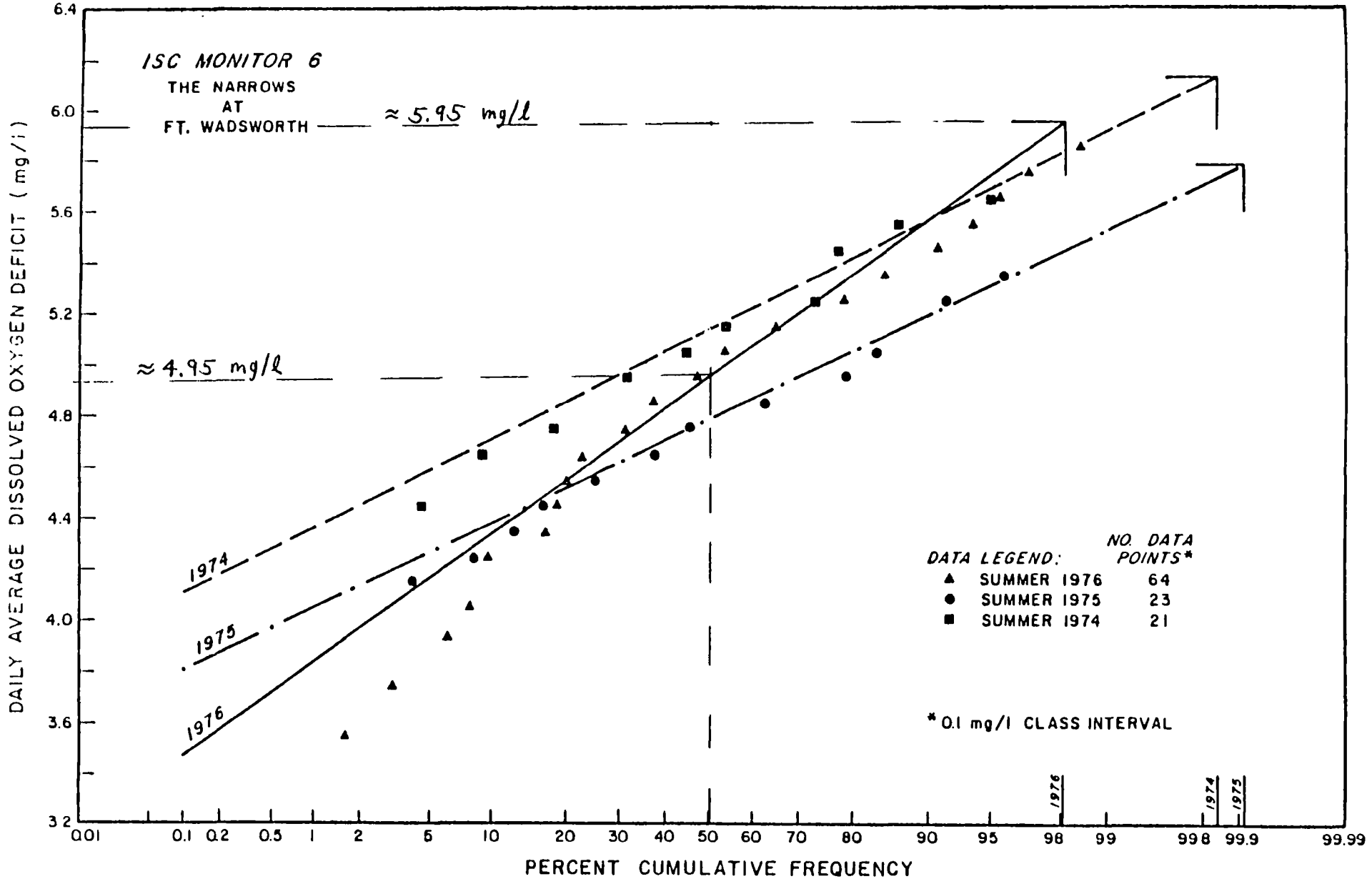

FIGURE 1

PROBABILITY PLOT OF SUMMER DAILY AVERAGE DISSOLVED OXYGEN DEFICIT-ISC MONITOR 6

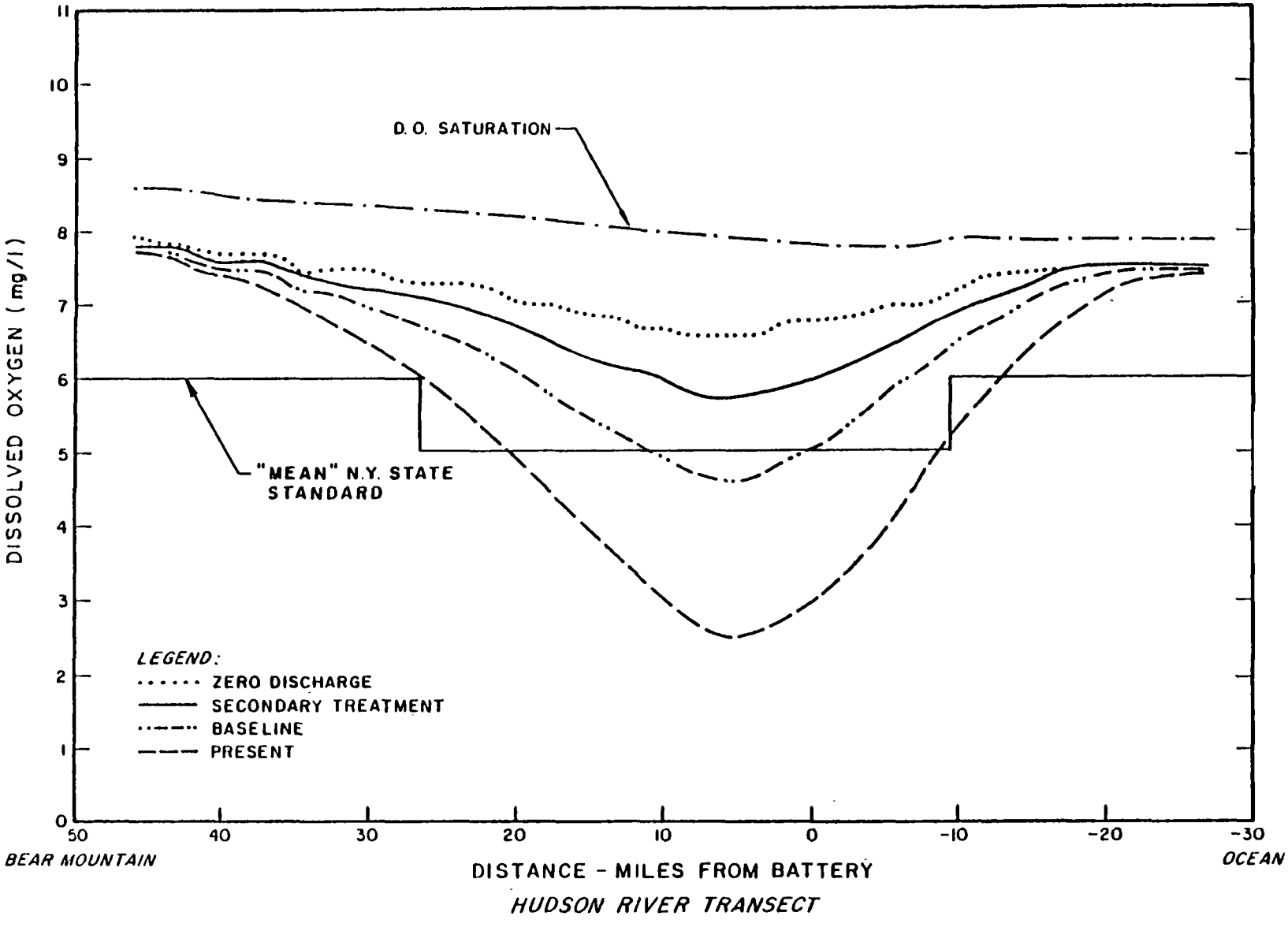

FIG. 8 PREDICTED DISSOLVED OXYGEN CONCENTRATIONS for ALTERNATIVES

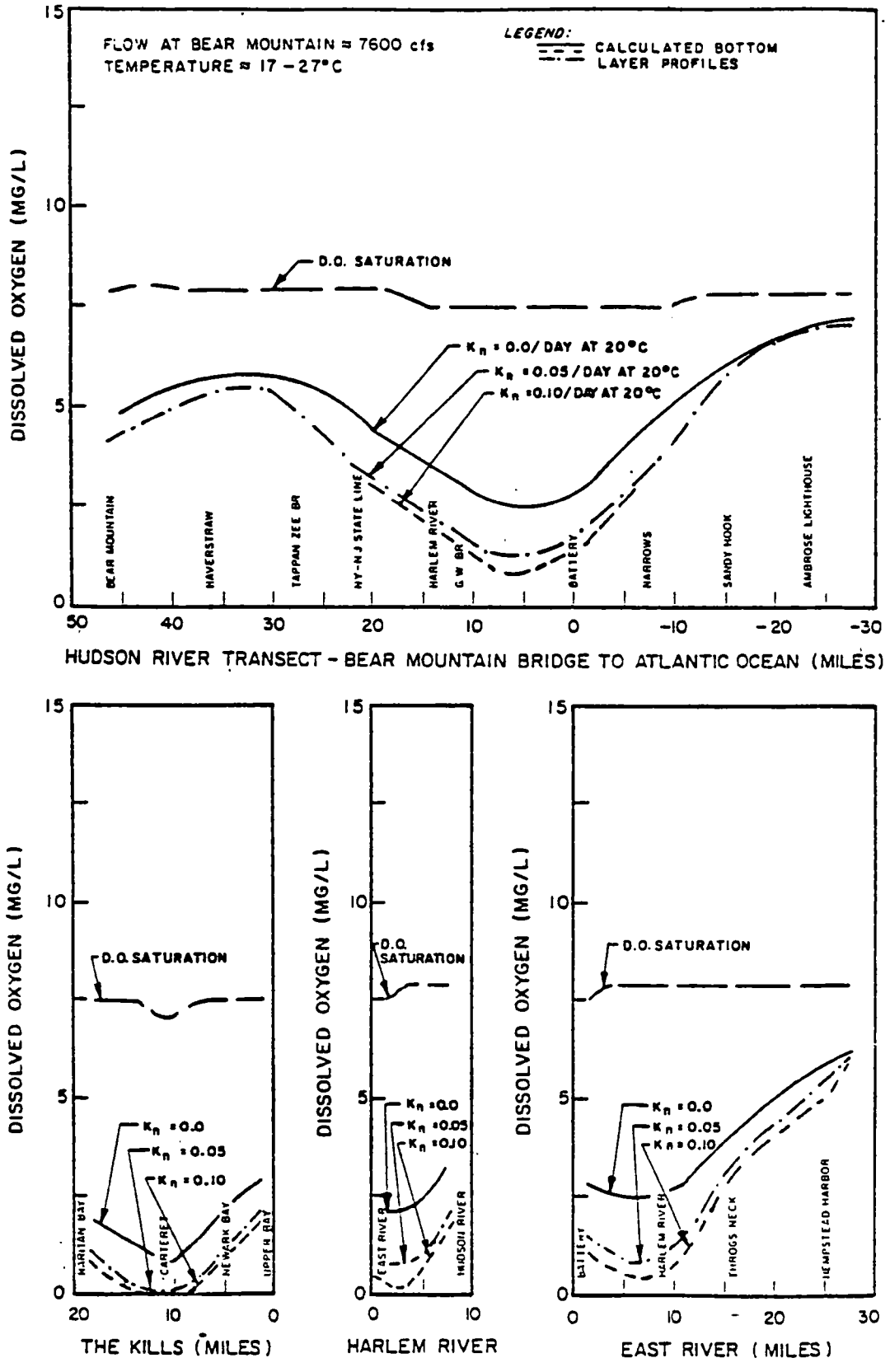

FIGURE 7
DISSOLVED OXYGEN SENSITIVITY TO NITRIFICATION RATE (K_n)
(JULY 5-29,1977)

Sensitivity Analysis

NORTH CANADIAN RIVER

OKLAHOMA

Ref: "Review of North Canadian River Water Quality Analysis", Gallagher, T.W. and Thomann, R.V., prepared by Hydro Qual, Inc., for USEPA Washington, June, 1981

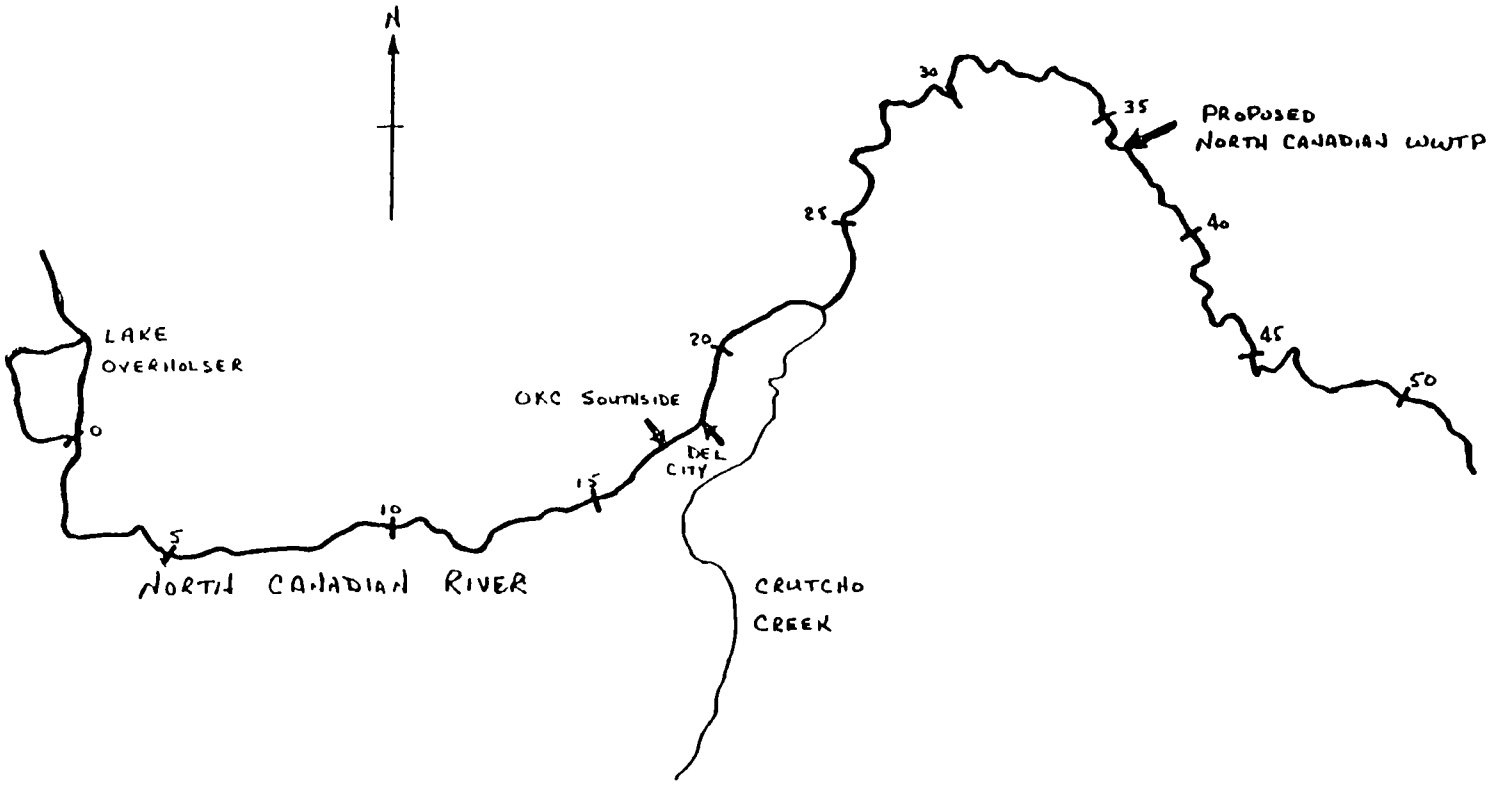

x[5] APPROXIMATE MILEPOINT

FIG. 1 MAP of STUDY AREA of NORTH CANADIAN CREEK, OKLAHOMA

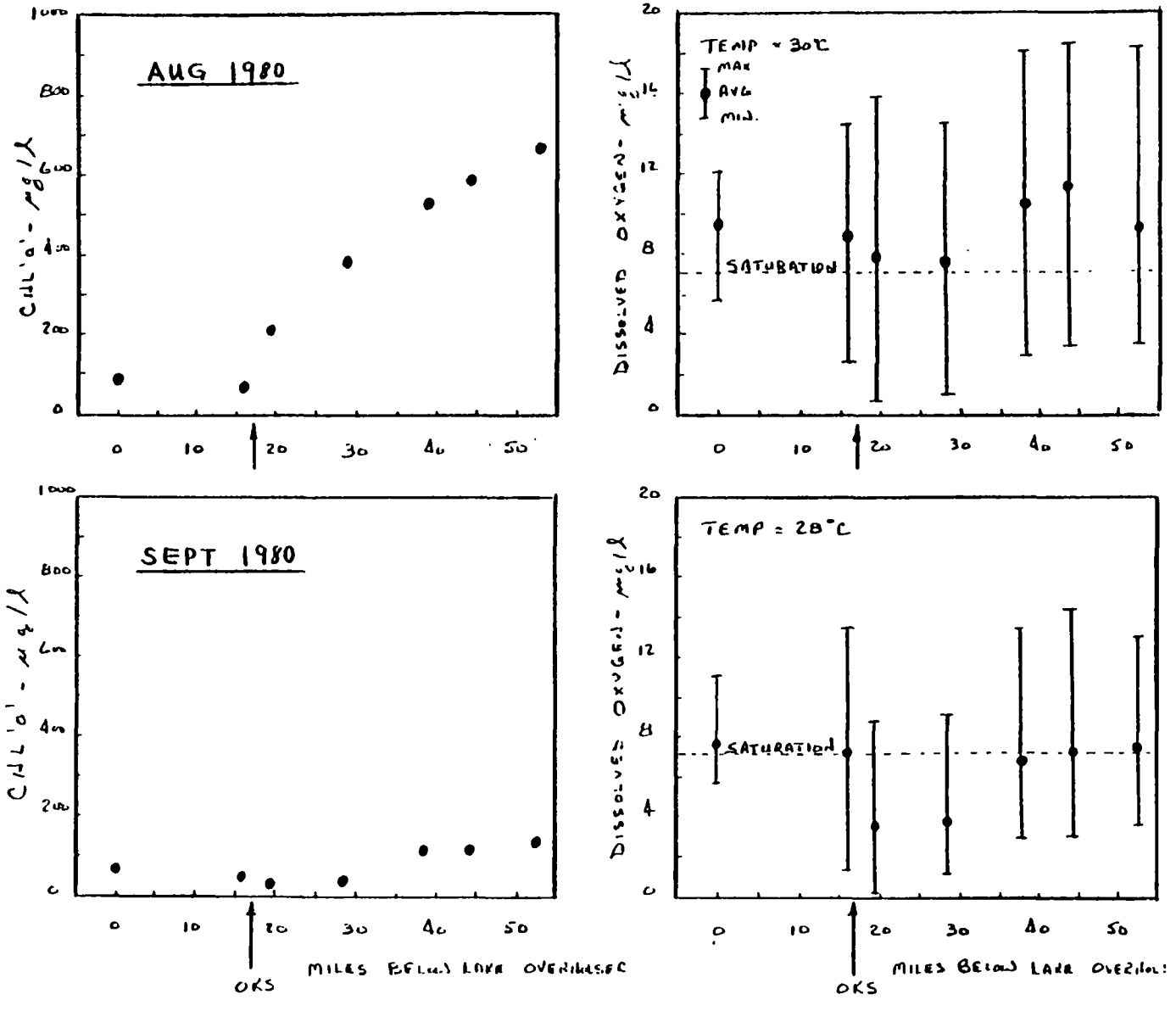

FIG. 2 RIVER CHLOPHYLL A & DISSOLVED OXYGEN DATA

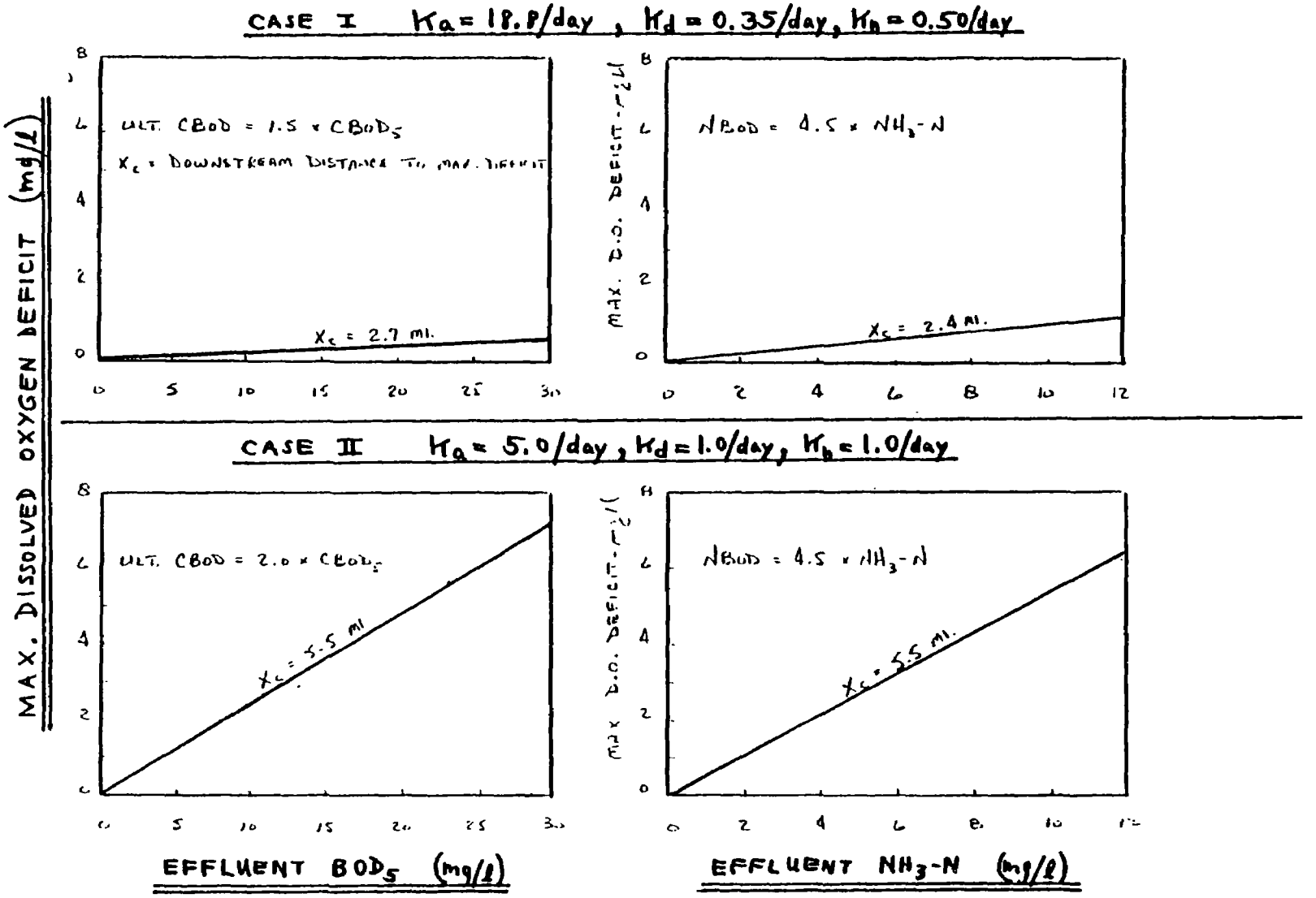

FIG. 3 SENSITIVITY of D.O. DEFICIT (MAX) TO KINETIC COEFFICIENTS

STATE OF OHIO
ENVIRONMENTAL PROTECTION AGENCY
BOX 1049
361 E. BROAD STREET
COLUMBUS, OHIO 43216

ROCKY FORK WASTELOAD ALLOCATION

Prepared by

Office of Wastewater Pollution Control
Division of Water Quality Planning and Assessment

June, 1981

Draft and Subject to Revision

DRAFT

Summary and Conclusions:

1. Wasteload allocations were conducted for Mansfield WWTP and, due to interaction, Heatherwood Subdivision, Lucas WWTP and eight (8) industries on the Rocky Fork of the Mohican River were included in the allocation process.

2. Mansfield WWTP, at present, is not meeting the effluent limits specified in its existing NPDES permit. Most of the industries are also discharging concentrations much higher than specified in their existing permits.

3. Wasteload allocations were conducted by employing the decay rates measured during the field survey. The results were compared with those obtained by employing text book decay rate values. In both cases, dissolved oxygen sag was not located in the Rocky Fork of the Mohican River. Preliminary studies indicate the D.O. sag to be located below the confluence with Black Fork.

4. High concentrations of heavy metals discharged by the industries, upstream of Mansfield, have a significant adverse impact on the performance of Mansfield WWTP.

5. Model calibration and verification was not considered due to presence of excessive amounts of conservative parameters and interaction between conservative and non-conservative parameters.

6. The field survey results and wasteload allocations clearly show the need to reduce the oxygen demanding pollutants ~~to~~ at least the recommended levels, in order to improve the water quality in Rocky Fork of the Mohican River.

7. Once mansfield WWTP and the industries meet their recommended effluent limits, another field survey should be conducted. The results will be used to calibrate and verify the model, and the wasteload allocations will be revised accordingly.

INTRODUCTION

A study was initially performed to determine effluent limitations and to complete AST Justification for the Mansfield WWTP on the Rocky Fork of the Mohican River. Conventional pollutants and metals are addressed in this report. Conventional pollutants are allocated to Mansfield WWTP and, due to interaction, Richland County Heatherwood Subdivision and Lucas WWTP's are included in the allocation process. Metals are an acknowledged problem (see "Biological Assessment") and have a major impact on the water quality of the Rocky Fork. Therefore, metals are allocated to eight (8) industries and Mansfield WWTP.

While water quality problems due to conventional pollutants can be attributed predominantly to the Mansfield WWTP, the metals problem is due to dischargers upstream of the Mansfield WWTP.

Design flow of 20.0 MGD exceeding the "Simplified Method" limit of 10.0 MGD and interaction with other dischargers necessitates using QUAL-II model to allocate loads to Mansfield WWTP. Biological and economic assessments are presented (see "Biological Assessment" and "Economic Assessment").

DISCHARGER

The Mansfield WWTP, located in the southeast portion of the City of Mansfield on Illinois Avenue, discharges to Rocky Fork at river mile 11.18 (see Figure 2). The planning area includes the entire incorporated area of the City of Mansfield and adjacent areas to the northwest, east, southwest and south, that are in the Rocky Fork drainage basin. In addition to domestic waste, the plant accepts waste from a number of industries, including food processing, metal surface preparation and plating, and tire and automobile manufacturing. The metals from these industries not only cause water quality standards violations once the effluent enters the stream, but can also inhibit plant performance.

Currently, the plant is an activated sludge type facility with separate sludge digestion and sludge filtering, with a design capacity of fifteen mgd and a maximum hydraulic capacity of twenty-five mgd. The treatment train consists of bar screens and grinders, two aerated grit tanks, twin primary settling tanks, six secondary aeration tanks, and two final clarifiers.

With industrial and population growth in the Mansfield area, the treatment plant must expand to 20.0 mgd from the current 15.0 mgd. Effluent limits were prepared for the Mansfield WWTP based on this design flow employing the QUAL-II SEMCOG version.

Figure 3: Water Quality Sampling Sites on Rocky Fork

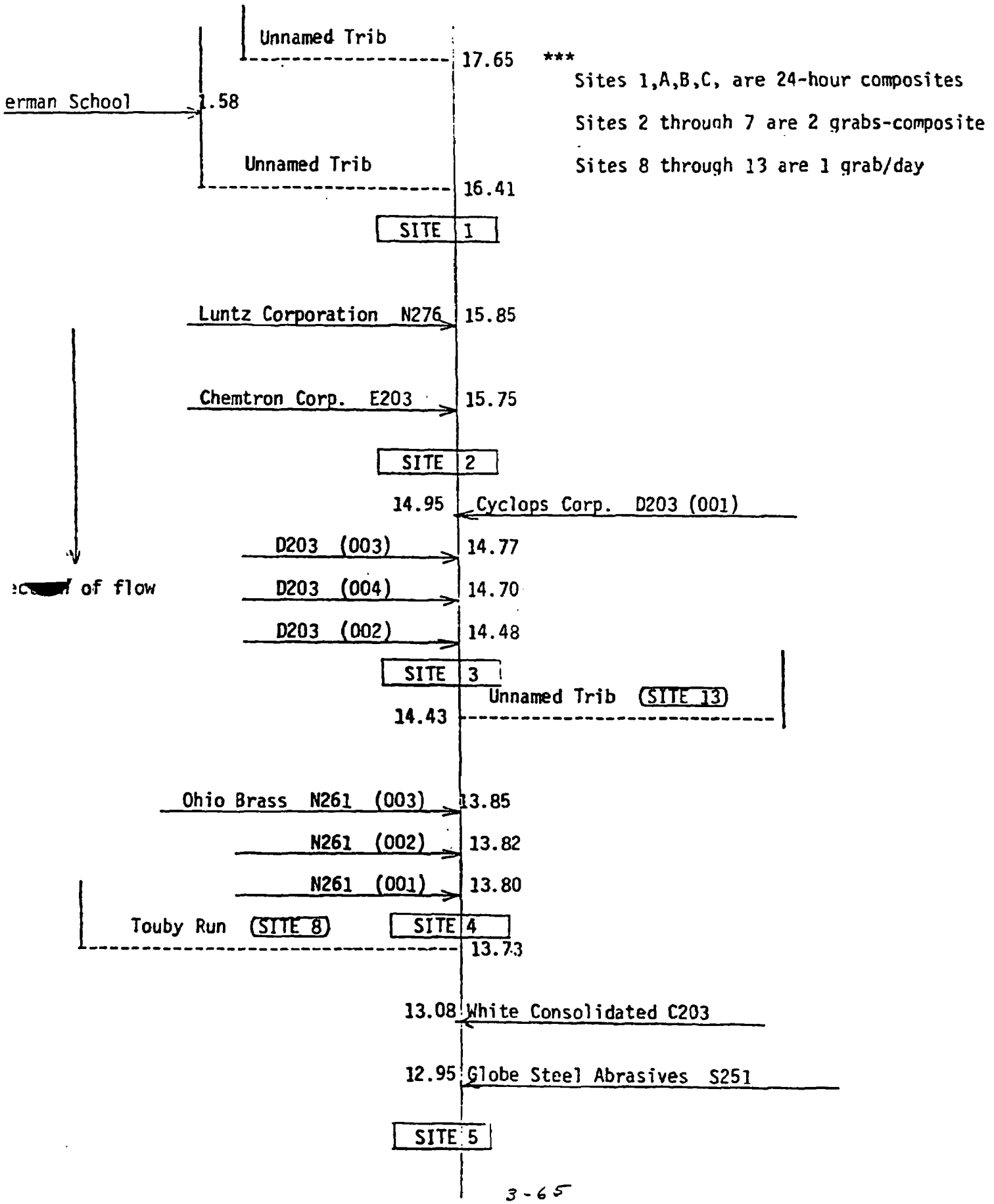

Figure 3: (Continued)

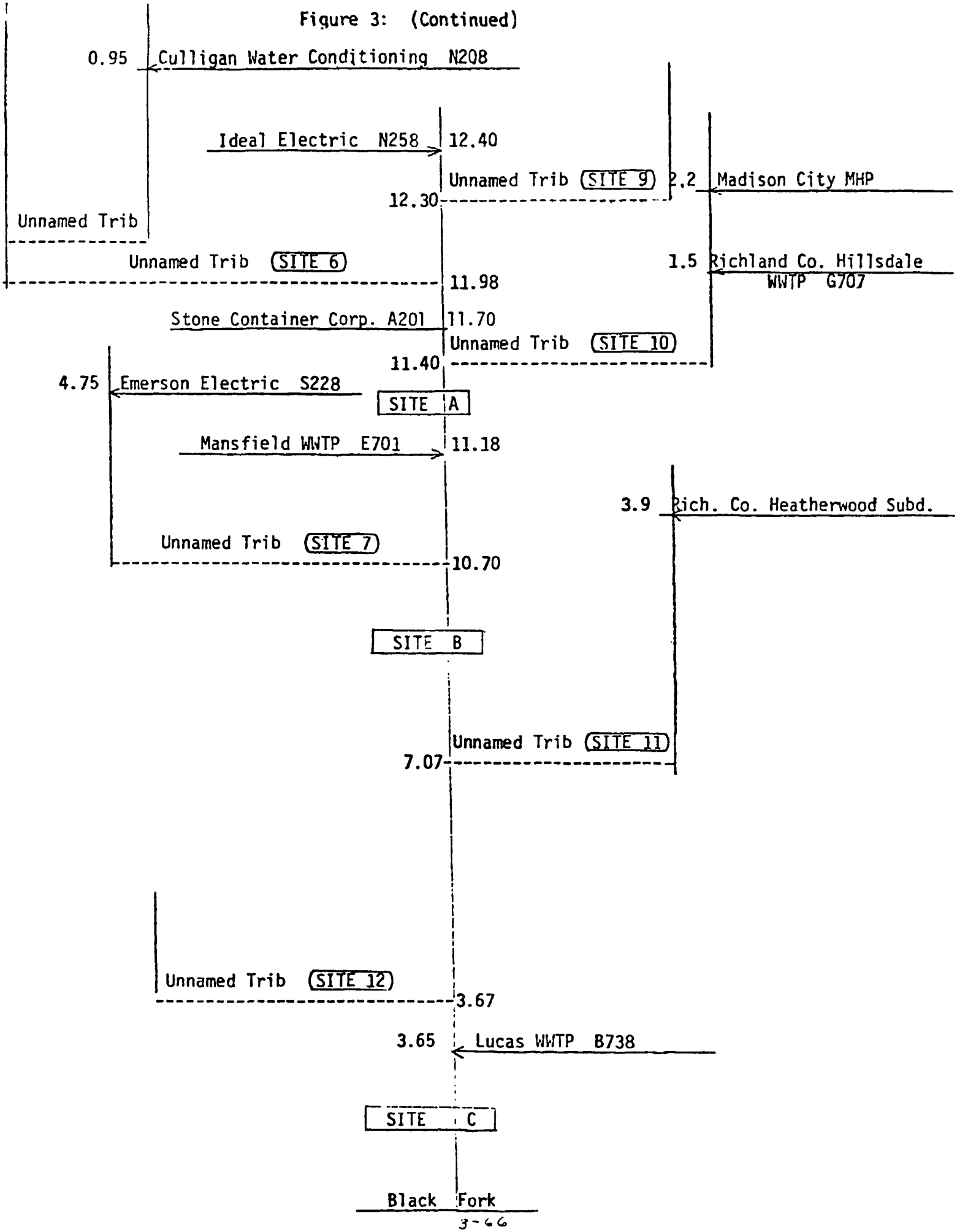

RESULTS

Wasteload allocation:

The proposed Mansfield WWTP was modeled under summer $Q_{7,10}$ conditions. The dissolved oxygen sag was not located in the Rocky Fork (see Graphs I and II). The treatment level of 10.0 mg/l BOD_5, 2.0 mg/l NH_3-N and 6.0 mg/l D.O. resulted in a dissolved oxygen concentration of 5.31 mg/l at the mouth of Rocky Fork without reaching the sag point. However, this treatment level can be considered as an interim summer limitation. The dissolved oxygen sag was determined, by preliminary analysis, to be located in the Black Fork, approximately 2.0 miles below the confluence of Rocky Fork. This finding is supported by the Biological Assessment of the Rocky Fork where, it was documented that violation of WQS for non-conservative parameters resulted from the effluent of Mansfield WWTP and the dissolved oxygen recovery was not apparent immediately below the confluence of Rocky Fork with Black Fork (see Biological Assessment).

Under winter design flow conditions, the background flow increases and temperature decreases. This changes the stream geometry and reaction rates. Winter temperature and pH also affect the NH_3-N standard. These changes result in winter allocations being less stringent than the summer limitations. The results of winter wasteload allocation appear in Table 3.

Due to interaction with Mansfield WWTP's effluent, the Heatherwood Subdivision and Lucas WWTP's were included in the wasteload allocation process. Heatherwood Subdivision is located on an unnamed trib and the treatment level of 10.0 mg/l BOD_5, 2.0 mg/l NH_3-N and 6.0 mg/l D.O. is adequate to maintain summer water quality standards. The discharge flow of Lucas WWTP is negligible compared to the upstream flow. Therefore, wasteload allocation for Lucas WWTP was conducted by neglecting the effect of Mansfield's discharge. Lucas WWTP can discharge 30.0 mg/l BOD_5, 15.0 mg/l NH_3-N and 5.0 mg/l D.O. and maintain Water Quality Standards in the stream. The results of winter wasteload allocation appear in Tables 4a and 4b.

Since the measured decay rates were considerably lower than the text values, a steady state simulation was conducted using 0.6 and 0.3 day^{-1} for K_{CBOD} and K_{NBOD}, respectively. Lower measured decay rates may be attributed to high concentrations of conservative parameters discharged by the industries. Results of the two simulations using the treatment level of 10.0 mg/l BOD_5, 2.0 mg/l NH_3-N and 6.0 mg/l D.O. were compared. The lowest D.O. concentration, under the measured decay rates, was 5.31 mg/l at the mouth of Rocky Fork. The simulation with the text values resulted in a D.O. concentration of 2.7 mg/l at the mouth (see Graphs III-V).

Alternative Treatment Levels:

Federal guidelines (5) require that alternative treatment levels be evaluated. They vary from secondary treatment to advanced secondary treatment with filtration and nitrification. The exact effluent BOD_5 and NH_3-N evaluated are listed in graphs I and II.

Sensitivity Analysis

In order to assess the impact of errors in measurement of the input variables utilized in the wasteload allocation process, the sensitivity of the allocated BOD_5 was calculated for Temp, pH, upstream BOD_5, K_1, K_2 and K_3.

BOD_5 was most significantly influenced by the reaeration rate (K_2). Using Owens option resulted in D.O. sag being located at RM 11.0, 0.4 miles below Mansfield WWTP, with a treatment level of 20.0 mg/l BOD_5, 3.0 mg/l NH_3-N and 5.0 mg/l D.O. However, the reaeration rate with Owens option varied between 94.49 and 30.92 day^{-1}.

Ohio EPA limits K_2 values to 20.0 day^{-1} and ammonia toxicity in the stream is 2.6 mg/l. Therefore, it is recommended that Tsivoglou option rather than Owens option be used.

Pre-treatment:

The industrial survey on the Rocky Fork has been completed.

The consultants are in the process of sampling the influent and effluent of the Mansfield WWTP as well as the industries considered to be the major contributors to the Mansfield WWTP.

The final report can be expected at the end of 1981.

RECOMMENDATIONS

ed on WLA results, it is recommended that the following be done to insure maintenance of stream use designations and WQS in the Rocky Fork of the Mohican River:

1) Once the Mansfield WWTP is upgraded to the recommended level, Ohio EPA, during the low flow season, should locate the D.O. sag.

2) Chemical data should be collected, on monthly basis, at the mouth of Rocky Fork and on Black Fork below the confluence of Rocky Fork.

3) Once Mansfield WWTP is upgraded and all other discharges contributing heavy metals comply with their permit limitations, Mansfield should install continuous monitors at the mouth of Rocky Fork and at the location of D.O. sag (composite and grab samples) for the following parameters:

D.O.
BOD
NH_3-N
TKN

CONCLUSION

The proposed 20.0 mgd WWTP at Mansfield can discharge an effluent of 10.0 mg/l BOD, 2.0 mg/l NH_3-N and 6.0 mg/l D.O. in the summer, and 25.0 mg/l BOD_5, 15.0 mg/l NH_3-N and 5.0 mg/l D.O. in the winter. These limits should be considered as interim limitations as the D.O. sag was not located under summer or winter conditions and the severely degraded biological condition of the stream below the Mansfield WWTP persisted downstream to the confluence with the Black Fork, with little improvement being shown (see Biological Assessment).

The Heatherwood Subdivision can discharge an effluent of 10.0 mg/l BOD_5, 2.0 NH_3-N, and 6.0 mg/l D.O. under summer and winter conditions. The summer and winter limitations are adequate to maintain water quality standards in the stream.

The Lucas WWTP can discharge an effluent of 30.0 mg/l BOD_5, 15.0 mg/l NH_3-N and 5.0 mg/l D.O. under summer and winter conditions and maintain water quality standards.

Ohio EPA requires extensive justificaton detailing the need and economic benefit of waste treatment greater than 10.0 mg/l BOD_5 and 2.0 mg/l NH_3-N. This justification must include comprehensive physical, chemical and biological studies. It is recommended that in the interim, the Mansfield WWTP NPDES summer and winter limitations be set at the recommended levels (as shown in Table 4).

Heavy metals affect the chemical and biochemical reaction of the non-conservative parameters. However, the complete affect of metals, in some cases, is not fully understood. Therefore, reduction of conservative and non-conservative parameters is essential to maintain stream use designations and water quality standards in the Rocky Fork of the Mohican River.

Once the plants are upgraded to meet the proposed permit limitations (as specified in Tables 4 through 5), it is recommended that Rocky Fork be evaluated by using the results of continuous monitoring data and another intensive survey from RM 11.2 of the Rocky Fork to the point of D.O. sag. The results of these surveys would be used for:

1) Calibration and verification of the model and establishment of constant rates.

2) conducting an additional stream assimilation study.

3) Evaluation of the stream use designation/attainability.

TABLE 3

Mansfield Wasteload Allocation Results
for Design Conditions

	Summer	Winter
BOD_5	N/A mg/l*	25.0 mg/l
TSS	N/A mg/l*	25.0 mg/l
NH_3-N	N/A mg/l*	15.0 mg/l
D.O.	N/A mg/l*	5.0 mg/l
Cn	4.24 lb/day	
Cd	2.14 lb/day	
Cr	16.68 lb/day	
Cu	10.01 lb/day	
Pb	5.381 lb/day	
Zn	33.55 lb/day	
Hg	0.033 lb/day	
O&G	834.4 lb/day	

*See results "Wasteload Allocation," page 18.

TABLE 4
Recommended Effluent Limits For Mansfield

	Summer	Winter
BOD_5	10.0 mg/l	25.0 mg/l
TSS	12.0 mg/l	25.0 mg/l
NH_3-N	2.0 mg/l	15.0 mg/l
D.O.	6.0 mg/l	5.0 mg/l
Cn	4.24 lb/day	4.24 lb/day
Cd	2.14 lb/day	2.14 lb/day
Cr	16.68 lb/day	16.68 lb/day
Cu	10.01 lb/day	10.01 lb/day
Pb	5.381 lb/day	5.381 lb/day
Zn	33.55 lb/day	33.55 lb/day
Hg	0.033 lb/day	0.033 lb/day
O&G	834.4 lb/day	834.4 lb/day

Table 4a
Recommended Effluent Limits for
Heatherwood Subdivision

	Summer	Winter
BOD_5	10.0 mg/l	10.0 mg/l
TSS	12.0 mg/l	12.0 mg/l
NH_3-N	2.0 mg/l	2.0 mg/l
D.O.	6.0 mg/l	6.0 mg/l

TABLE 4b
Recommended Effluent Limits For Lucas WWTP

	Summer	Winter
BOD_5	30.0 mg/l	30.0 mg/l
TSS	30.0 mg/l	30.0 mg/l
NH_3-N	15.0 mg/l	15.0 mg/l
D.O.	5.0 mg/l	5.0 mg/l

Table 5

Heavy Metals Allocation Results for Industries

ENTITY	FLOW (MGD)	PARAMETER	ALLOCATION (lb/day)
Luntz Corp	0.045	O&G	32.11
Cyclops Corp.	2.75	Fe	23.72
		O&G	84.46
Ohio Brass	0.359	Cu	1.51
		Zn	5.06
		O&G	7.41
White Consolidated	1.11	Cu	0.415
		Cr	3.21
		Cn	0.80
		Ni	14.61
		O&G	34.58
Globe Steel Abrasives	0.147	Fe	9.39
		Zn	1.59
Emerson Electric	0.064	O&G	2.67
Borg Warner Corp.	0.137	O&G	11.43
Stone Container Corp.	0.078	Cd	0.398
		Cr	0.906
		Cu	0.128
		Fe	2.14
		Pb	0.998
		Ni	4.12
		Zn	0.232
		O&G	14.27

Figure 2: Rocky Fork Schematic

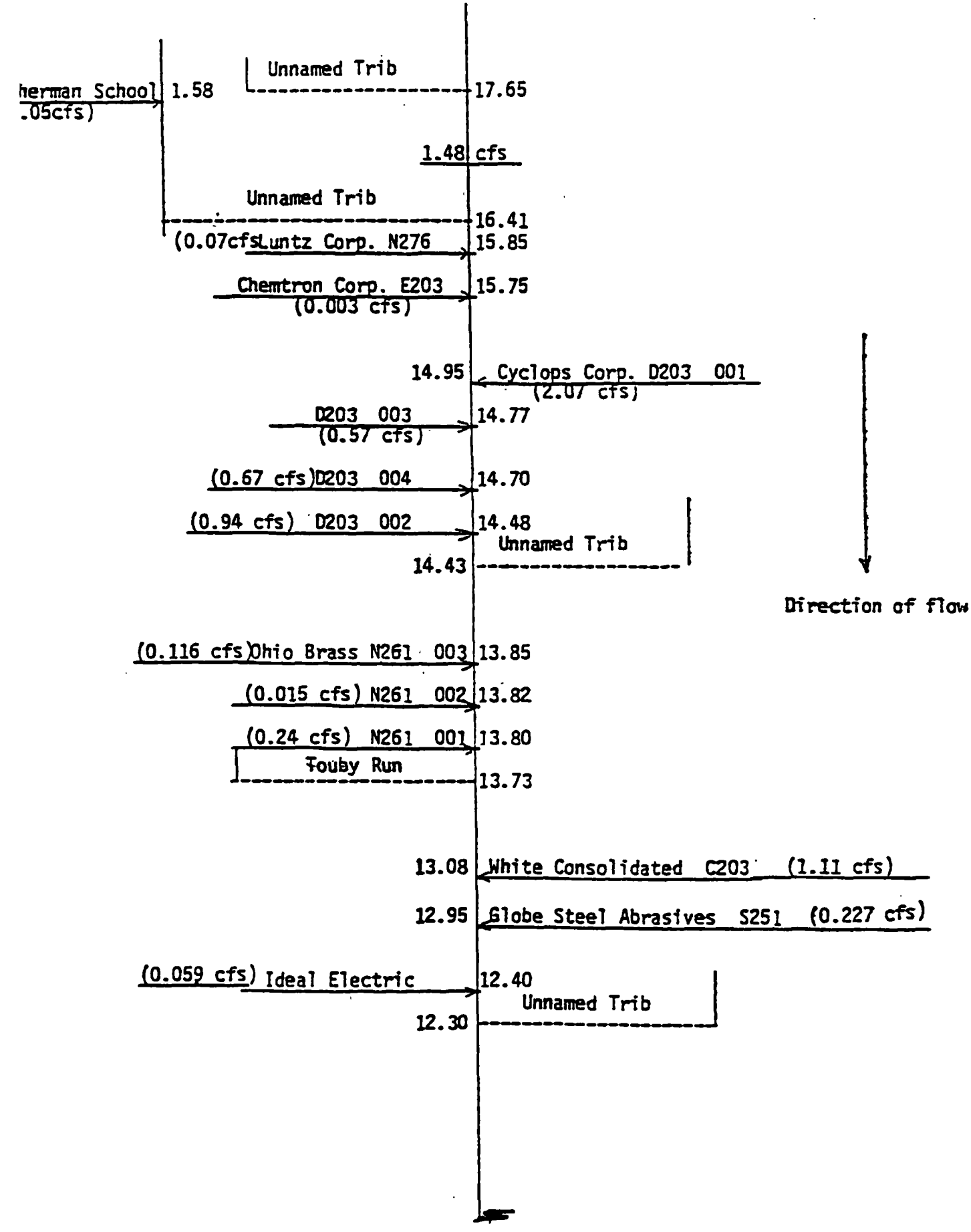

Figure 2 (Continued)

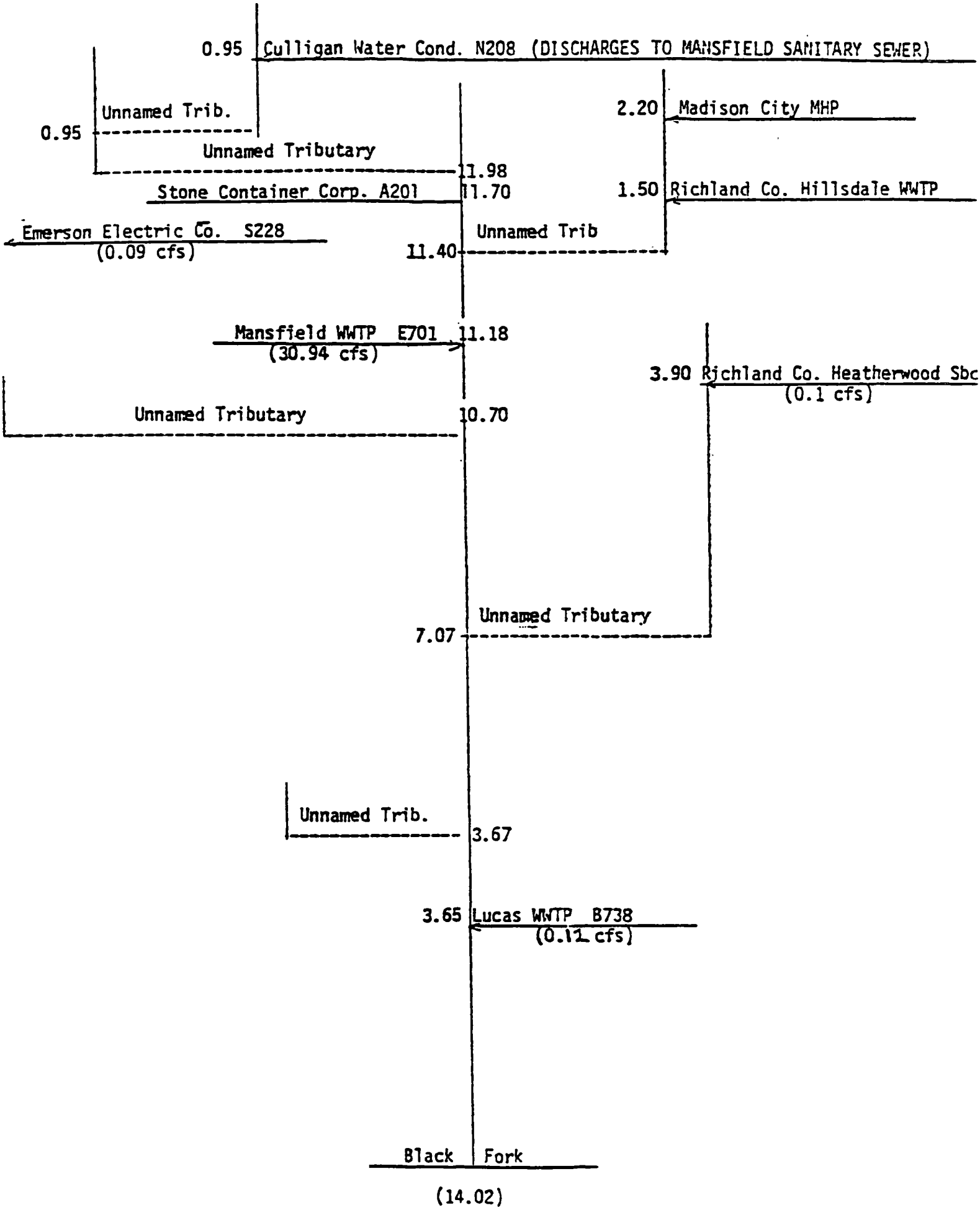

Graph I: NH_3-N vs River Mile

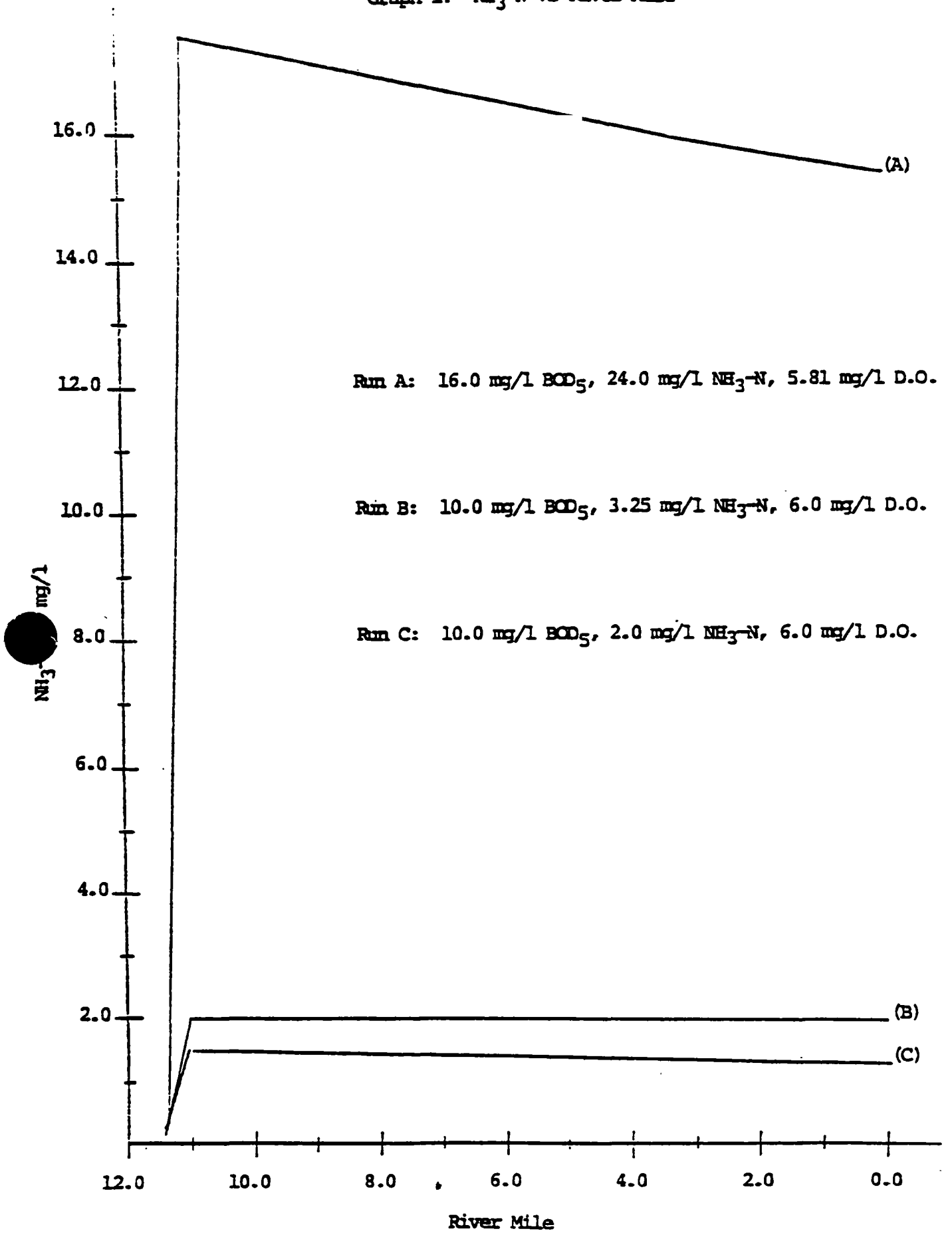

Graph II: D.O. vs River Mile

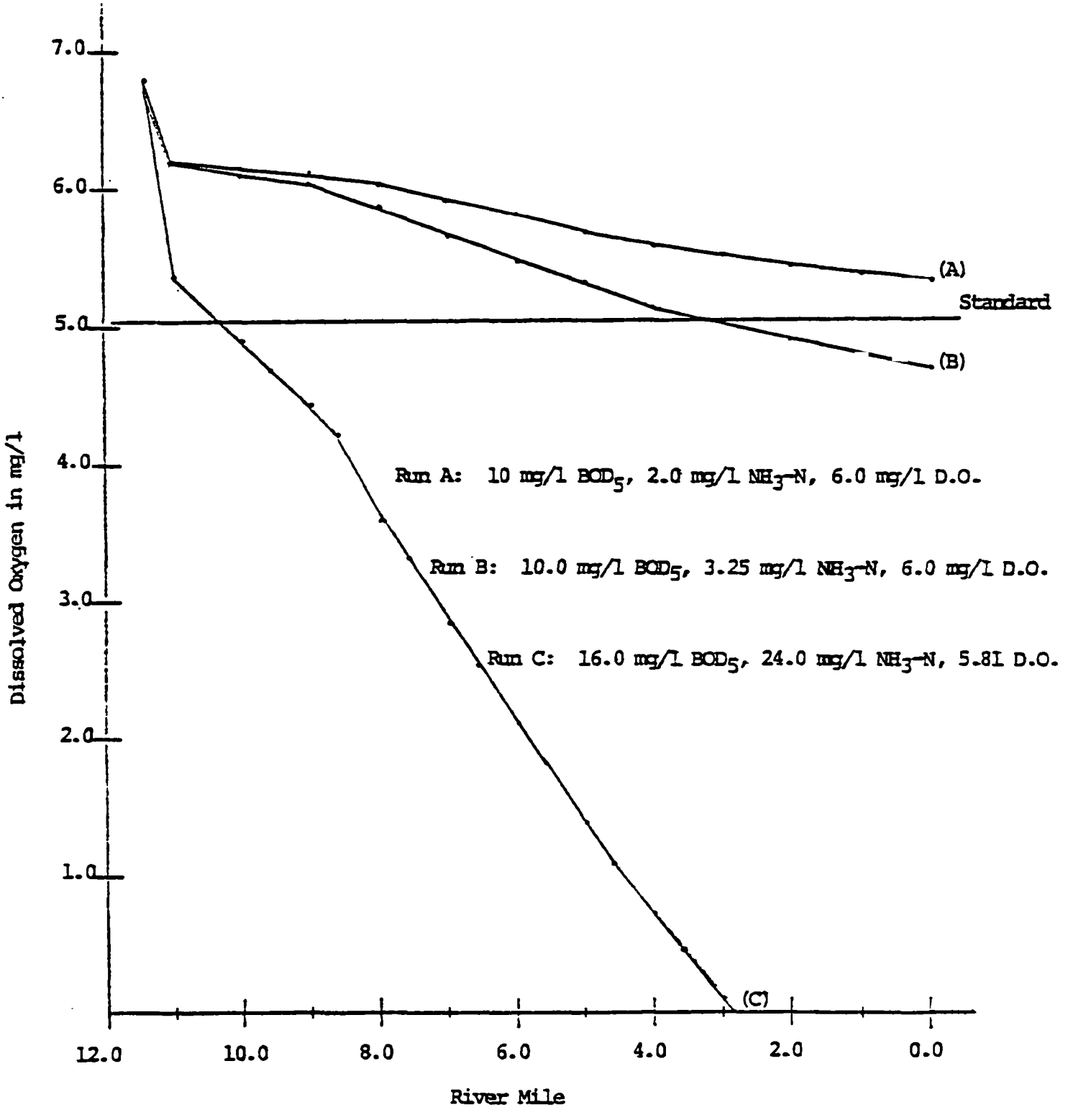

Graph III: BOD_5 vs River Mile

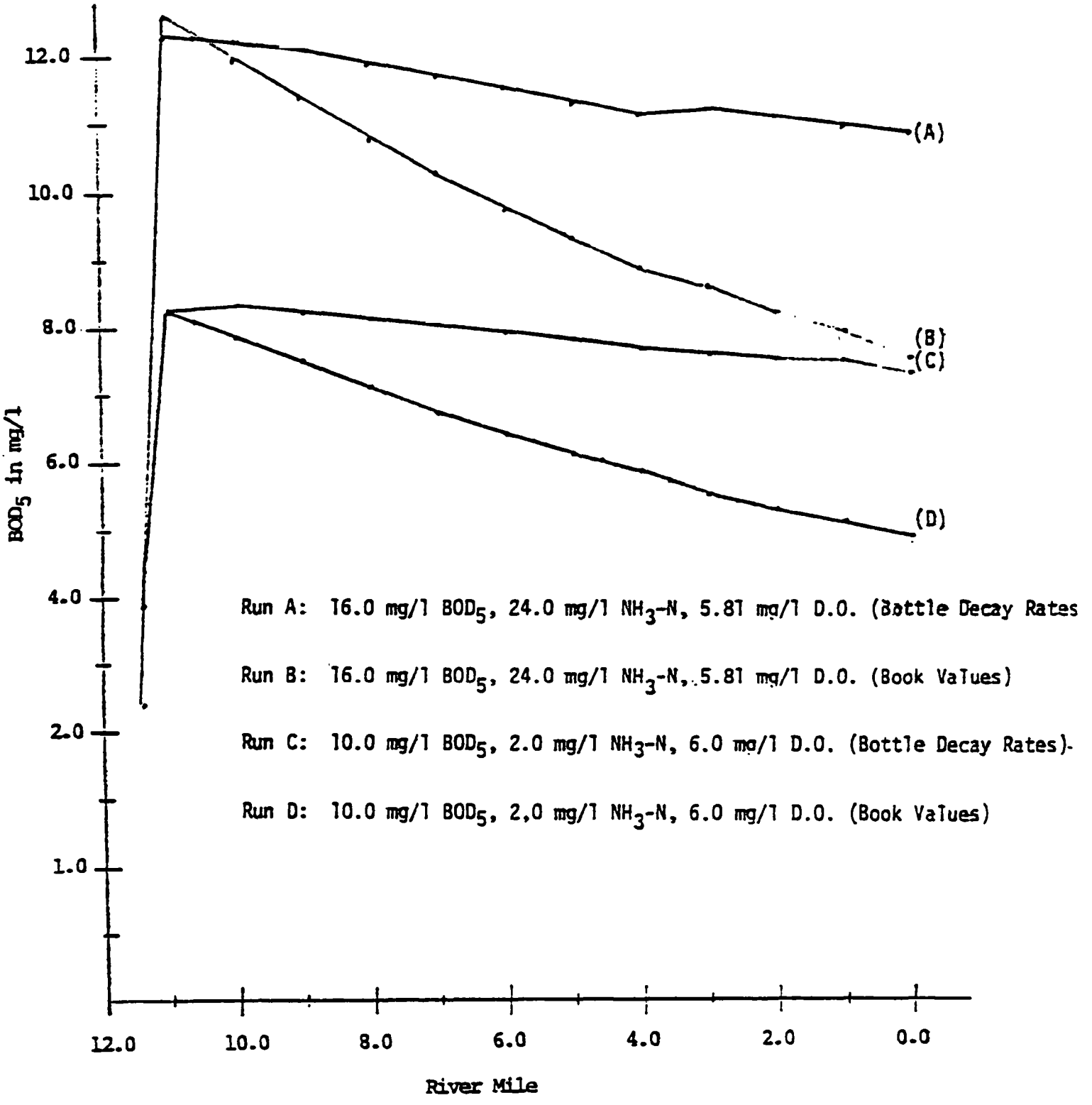

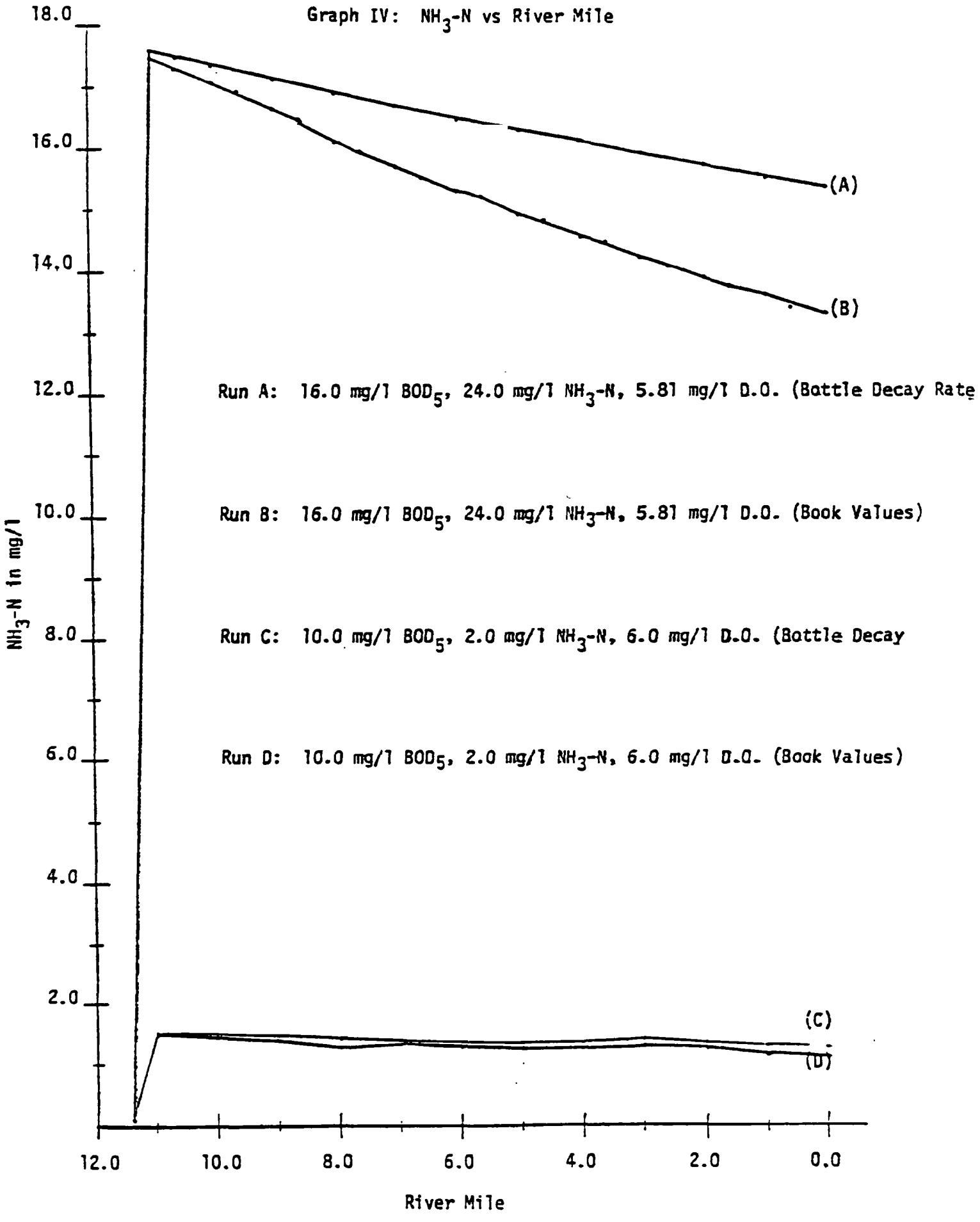
Graph IV: NH_3-N vs River Mile
18.0
16.0
14.0
12.0
10.0
8.0
6.0
4.0
2.0
NH_3-N in mg/l
(A)
(B)
(C)
(D)
Run A: 16.0 mg/l BOD_5, 24.0 mg/l NH_3-N, 5.81 mg/l D.O. (Bottle Decay Rate
Run B: 16.0 mg/l BOD_5, 24.0 mg/l NH_3-N, 5.81 mg/l D.O. (Book Values)
Run C: 10.0 mg/l BOD_5, 2.0 mg/l NH_3-N, 6.0 mg/l D.O. (Bottle Decay
Run D: 10.0 mg/l BOD_5, 2.0 mg/l NH_3-N, 6.0 mg/l D.O. (Book Values)
12.0
10.0
8.0
6.0
4.0
2.0
0.0
River Mile

Graph V: D.O. vs River Mile

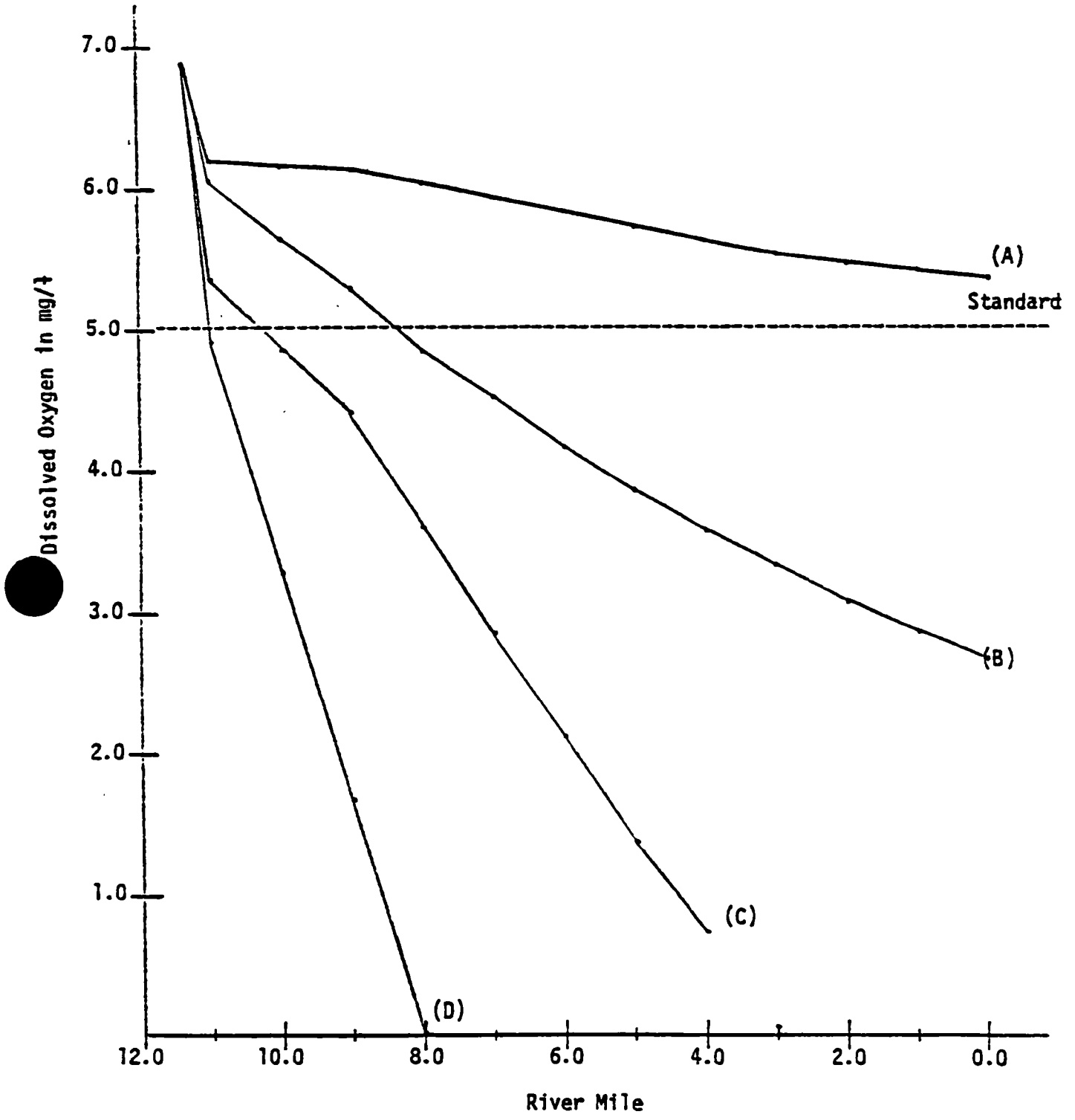

Run A: 10.0 mg/l BOD_5, 2.00 mg/l NH_3-N, 6.00 mg/l D.O. (Bottle Decay Rates)

Run B: 10.0 mg/l BOD_5, 2.00 mg/l NH_3-N, 6.00 mg/l D.O. (Book Values)

Run C: 16.0 mg/l BOD_5, 24.0 mg/l NH_3-N, 5.81 mg/l D.O. (Bottle Decay Rates)

Run D: 16.0 mg/l BOD_5, 24.0 mg/l NH_3-N, 5.81 mg/l D.O. (Book Values)

INTRODUCTION AND BASIC CONCEPTS*

The presence of toxic substances, such as organic chemicals and heavy metals, has become a major environmental problem in recent years. The substances are present in varying degrees in all phases of the environment - air, water and land. They are transferred between and among these media, undergo transformation within each and accumulate in viable and nonviable constituents. The magnitude and significance of the problem has become increasingly evident, particularly in the accumulation of toxic substances in both the terrestrial and aquatic food chains and in the release of these substances from land and water disposal areas. In this regard, the impact on the health and activities of man is more direct and significant than in the case of pollutants which the field has classically addressed. This concern led to the formulation of the Toxic Substances Control Act, enacted by Congress in 1976, and, in turn, to the subsequent promulgation of priority pollutants by the Environmental Protection Agency. The latter is under continuous review and periodic updating both by EPA and interested scientific groups in industry, research laboratory and environmental organizations.

A total ban on all organic chemicals is neither desirable nor practical. The benefits derived from the use of these substances are evident in many facets of our society - particularly with respect to the increased food production. The demand for these materials, more specifically the benefits derived from their use, continuously increases. A balance must therefore be sought between the extreme positions - complete ban and no control. Such a balance leads to the use of certain chemicals, which may be safely assimilated in the environment to such levels as to yield the benefits without deleterious effects. This goal necessitates the development of assessment methods which permit an evaluation and ultimately a prediction of environmental concentrations. The approaches developed herein are, therefore, directed to two broad areas: an evaluation of the present extent and distribution of these substances, with particular regard to their diminution and removal and secondly, a methodology to assess the potential impact of proposed chemicals, which may be introduced into the environment.

*D. J. O'CONNOR

Field surveys undoubtedly provide much insight into the nature of the first question, but this approach is evidently limited and not applicable to the analysis of the second, and potentially more important, question. In addition, the costliness and time factor of field surveys impose further disadvantages. Theoretical analysis, in conjunction with controlled laboratory experiments, is the preferred approach. The emphasis in the following sections is therefore directed to a review of the basic knowledge of the various phenomena and of the application of laboratory data to the analysis of the problem. This approach, which is less costly and time-consuming, lends itself to greater understanding of the problem and broader application to a variety of similar problems. Ultimately, however, the equations developed in this fashion may only be fully validated and tested by prototype data. Case histories and data on presently affected water systems should be fully documented and utilized for this purpose.

In the following sections of these notes, the various phenomena, which affect the transport, transformation and accumulation of organic chemicals and heavy metals in the various phases of the aquatic environment, are addressed. Taken into account is the exchange of these materials between the water and the other phases of the environment, air and land. However, the primary emphasis is directed to aquatic systems - specifically to the spatial and temporal distribution of these materials in the various types of natural water bodies - rivers, lakes, estuaries and the coastal zone. The approach taken is similar to that defining the distribution of substances which are natural components of biochemical and ecological cycles - oxygen, nutrients, minerals, dissolved and suspended solids and the basic elements of the food chain - bacteria and phytoplankton. While these constituents influence water quality and man's use of water, they do not have the potentially profound effect of toxic substances, which may impact directly the health and well-being of man. The basis of the determination of the hazardous assessment lies in our ability to define the distribution of these substances in the aquatic environment. While recognizing distinction between the effects and fate, it is important to appreciate their interrelationship in that any reliable hazard assessment is based fundamentally on a realistic and valid definition of the fate of toxic substances. The purpose of this course and these notes is to describe the various pheno-

mena which affect the fate and to develop the equations, incorporating these phenomena, which define the spatial and temporal distribution of toxic substances. The notes are accordingly divided into two general sections: the first which describes the various kinetic and transfer phenomena which affect organic chemicals and heavy metals and the second which presents various mathematical models of natural water systems, incorporating these kinetic terms with the transport characteristic of each type of natural system: streams, estuaries, lakes and the coastal zone.

In order to achieve some perspective of the overall approach, it is first appropriate to indicate the basic concepts which are employed in the development of the various analyses: the principle of mass balance, the dynamic equilibrium between the dissolved and particulate concentrations, and the kinetic interaction between these components.

A. BASIC PRINCIPLE - MASS BALANCE

Organic chemicals may exist in all phases of the aquatic environment - in solution, in suspension, in the bed and air boundaries, and in the various levels of the food chain. The interrelationships between and among these phases, which are shown diagrammatically in Figure A-1, relate to the transport, reactions and transfer of the substance. The approach taken is identical, in principle, to that used to define the distribution of water quality constituents, which are naturally part of biochemical and ecological cycles. The equations describing the spatial and temporal distribution of organic chemicals are developed using the principle of mass conservation, including the inputs with the transport, transfer and reactions components. The general expression for the mass balance equation about a specified volume, V, is:

$$V \frac{dc_i}{dt} = J_i + \Sigma R_i + \Sigma T_i + \Sigma W \qquad (1)$$

in which

c_i = concentration of the chemical in compartment, i.

J = transport through the system

R = reactions within the system

T = transfer from one phase to another

W = inputs

Equation (1) describes the mass rate of change of the substance due to the net effect of the various fluxes and transformations. The purpose of expressing the transfer rate (T), distinct from the transport (J) and reaction (R), is to provide a basis for the development of the equations, which describe more fully the relevant phenomena.

The general term "compartment" refers to each phase of the physiochemical regime - the dissolved and particulate in the water, atmosphere and bed - as well as to each element of the food chain - the phytoplankton, zooplankton, fish and detrital material. The transport, reaction and transfer terms may be positive or negative depending on the direction of kinetic routes between the chemical in compartment i and its concentration in other compartments with which it reacts or exchanges. The pathways are determined by the hydrodynamic and geophysical features of the natural water systems and by the physical, chemical and biological characteristics of both the system and the chemical. The hydrodynamic components transport material from one spatial location to another by dispersion and advective mechanisms. The physical factors transfer from one phase to another, such as exchange with the atmosphere, adsorption to and desorption from the suspended and bed solids and the settling and scour of these solids. The chemical factors transform the substance by processes such as photo-oxidation, hydrolysis and oxidation reduction reactions. The biological phenomena effect both transference and transformation: the latter primarily by microorganisms which may metabolize the chemical and the former by assimilation and excretion by the various aquatic organisms. Accumulation in the food chain is brought about by both ingestion of the chemical from the water and by predation on contaminated prey.

Consider the concentration, c, to be the dissolved component of the chemical in the water. It interacts with the particulate concentration, p. The interaction may be an adsorption-desorption process with the solids or an assimilation-depuration process with the aquatic organisms. In either case the particulate concentration is defined as:

$$p_i = r_i m_i \qquad (2)$$

p = particulate concentration in i compartment (M/L^3)

r_i = mass of chemical/unit of interacting mass (M/M)

m_i = concentration of the interacting species (M/L^3)

The mass balance equation for the particulate component, similar to equation (1), is then:

$$\frac{dp_i}{dt} = r_i \frac{dm_i}{dt} + m_i \frac{dr_i}{dt} = J + \Sigma R + \Sigma T + \Sigma W \qquad (3)$$

It is apparent from equation (3) that an equivalent expression must be written for the concentration of the interacting compartment, m_i. In principle, the analysis of the problem requires the simultaneous solution of the three equations: the concentration of the chemical dissolved in the water, c, the mass concentration of the chemical per unit mass of interacting species, r, and the concentration of the species itself, m. Since this compartment may be further subdivided (inorganic and organic solids, multiple species of fish), equation (2) is more generally expressed as a summation of the individual components of the interacting substances:

$$p_i = \sum_1^n r_i m_i \qquad (4)$$

The specific conditions for which the analysis is performed frequently permit simplifying assumptions to be made. In laboratory batch reactors and in certain prototype situations, the rate of change of the interacting species may be zero - i.e. a constant concentration of suspended solids or biomass. Thus $\frac{dm}{dt} = o$, from which an equilibrium concentration of solids or biomass follows, resulting in two simultaneous equations to be solved, instead of three.

B. DYNAMIC EQUILIBRIUM

As may be evident from the above discussion, one of the essential properties of the analysis of this water quality problem is the interaction between the dissolved and particulate states of the constituent, which, in time, leads to a dynamic equilibrium between the two components. Consider the most simplified conditions of a batch reactor in which the

mixing is of sufficient magnitude to maintain a uniform concentration throughout the volume of fluid. Assume the concentration of absorbing solids, m (M/L^3) is constant. Let c and p be the concentrations (M/L^3) of the dissolved and particulate components. If there is neither transfer nor decay of the chemical, the total concentration, c_T, remains constant in time and is equal to the sum of the dissolved and particulate:

$$c_T = c + p \tag{5}$$

The latter is related to the concentration of suspended solids, m, as shown by equation (2):

$$p = rm$$

The equilibrium between the dissolved concentration in the water and the mass concentration of the solids is usually expressed in terms of a partition coefficient:

$$\P = \frac{r}{c} = \frac{p}{mc} \tag{6}$$

or $$\Pm = \frac{p}{c}$$

Equation (6) is the linear portion of the Langmuir isotherm. Although not always representative of actual conditions, it is a reasonable approximation when the solid phase concentration, r, is much less than the ultimate absorbing capacity of the solids. Combining equations (5) and (6), the total concentration may be expressed as:

$$c_T = c + \Pmc = \frac{p}{\Pm} + p \tag{7}$$

The product, $\Pm$, is a convenient dimensionless parameter, characteristic of a particular system under equilibrium conditions. For a specified value of $\Pm$, the equilibrium distribution between the dissolved and particulate concentrations is established by equation (7), as shown in Figure A-2.

The distribution between the dissolved concentration and the particulate concentration in the various levels of the food chain may be expressed in an identical fashion. Accounting for the distribution for various types

of adsorbing solids and various levels of the food chain, each with its characteristic partition coefficient, equation (7) may be more generally expressed:

$$c_T = c[1 + \Sigma \P_i m_i] \tag{8}$$

The distribution may thus be categorized in accordance with the adsorbing solids (organics, clays, silts and sands) or the accumulating biomass (phytoplankton, zooplankton, fish and macrophytes). Since the total biomass mass in most natural water systems is usually an order of magnitude less than that of the non-viable solids, the equations defining each category may be decoupled and the former may be solved independently. Under those conditions in which it may be significant, it may be readily incorporated as shown in the above equation.

C. KINETIC INTERACTION

The equilibrium, described above, is a result of the kinetic interaction between the dissolved and particulate. This property which distinguishes the analysis from that of purely dissolved substances, leads to equations of a more complex form. In order to gain an insight into the nature of these interactions and an understanding of a practical simplification, consider the kinetics in a batch reactor, as described above, in which interaction is taking place between the dissolved and particulate components and the former is being transferred by volatilization or transformed by chemical or biological degradation:

$$p \underset{K_2}{\overset{K_1}{\rightleftharpoons}} c \xrightarrow{K_3} \tag{9}$$

The reversible reaction ($K_1 \rightleftharpoons K_2$) may represent the adsorption-desorption between the dissolved component and the particulate in inorganic phase (suspended or bed solids) or the assimilation-depuration in the organic phase (aquatic organisms). These kinetic coefficients may be functions of the solids concentrations, as discussed subsequently. In any case, their ratio is a measure of the distribution or partition coefficient. The non-reversible reaction (K_3) describes the decay or volatilization. The kinetic equations are:

$$\frac{dc}{dt} = -(K_2 + K_3)c + K_1 p \tag{10}$$

$$\frac{dp}{dt} = -K_1 p + K_2 c \tag{11}$$

By differentiating (10) and substituting (10) and (11) into the second-order differential equation, there results:

$$\frac{d^2c}{dt^2} + [K_1 + K_2 + K_3]\frac{dc}{dt} + K_1 K_3 c = o \tag{12}$$

An identical expression results for p. Assuming the initial concentration, c_o, is totally in the dissolved form, the initial condition is

$$c = c_o \text{ at } t = o$$

Applying the second condition:

$$\frac{dc}{dt} = -K_2 c_o \text{ at } t = o$$

the solution of the differential equation (8) subject to these initial conditions is:

$$c = c_o[\beta e^{gt} + (1-\beta)e^{ht}] \tag{13}$$

in which g,h are the positive and negative roots of the quadratic

$$g,h = -\frac{K}{2}[1 \pm m]$$

in which $K = K_1 + K_2 + K_3$

$$m = \sqrt{1 - \frac{4K_1K_3}{K^2}}$$

It may be readily shown that g and h are always real and negative.

In the case of adsorption-desorption, the assumption of instantaneous equilibrium is frequently made - i.e. the coefficients K_1 and K_2 are of sufficiently large magnitude so that the exchange between particulate and

dissolved occurs very rapidly. Furthermore, for organic chemicals, the decay coefficient is usually of a much smaller magnitude than the adsorption-desorption. Thus equation (12) simplifies to

$$[K_1 + K_2] \frac{dc}{dt} + K_1 K_3 c = o$$

or

$$\frac{dc}{dt} = \frac{- K_3}{1 + K_2/K_1} c \qquad (14)$$

in which

$\frac{K_2}{K_1}$ = distribution or equilibrium coefficient

An additional insight is gained by developing equation (14) in an alternate manner by adding equations (10) and (11) which yields

$$\frac{dc_T}{dt} = - K_3 c \qquad (15)$$

Assume the interaction between c and p is an adsorption-desorption process. The dissolved concentration, c, may therefore be expressed in terms of the total, c_T, by equation (7) substitution of which in (15) yields

$$\frac{dc_T}{dt} = - \frac{K_3}{1 + \P m} c_T \qquad (16)$$

The total concentration decays in accordance with the dissolved coefficient modified by the parameter $\P m$. As a physically realizable example, consider the transfer represents a volatilization process, in which K_3 is the gas transfer coefficient. The total concentration c_T decreases at a slower rate than would be the case if there were no partitioning to the particulate form, with the total in dissolved form ($\P m = o$). In defining the rate of change of the total, the decay or transfer coefficient is simply modified as shown by equation (16). Conversely, if the decay is associated

with the particulate component, the coefficient would be reduced by the fraction $\P m/[1 + \P m]$, in accordance with equation (7).

If both the particulate and dissolved components are subject to decay, by more than one mechanism, equation (16) becomes

$$\frac{dc_T}{dt} = - \left[\frac{\Sigma K_{ci}}{1 + \P m} + \frac{\P m \Sigma K_{pi}}{1 + \P m}\right] c_T \qquad (17)$$

in which the subscripts, c and p, refer respectively to the dissolved and particulate decay coefficients.

The assumption of "instantaneous" equilibrium as expressed by equation (14) through (17) is a valid representation, or model, of kinetic reactions provided the time to equilibrium, determined by K_1 and K_2 is rapid relative to the other phenomena which affect the substance K_c & K_p. This condition is generally applicable to the adsorption-desorption process, since its equilibrium time is usually much shorter (min-hours) than that of other kinetic effects, which may be in the order of days, months or years.

In summary, the models for the analyses of organic chemicals and heavy metals are similar to those developed for constituents which are natural components of ecological cycles. The terms relating to the particulate form and its interaction with the dissolved component are the additional components to be incorporated. These, with the other transform and reactive terms, cover the various pathways of distribution. Accordingly, each of these routes and the associated mechanisms are described in the subsequent sections which comprise the first half of these notes.

The second half is devoted to the development of models, which incorporate these reaction mechanisms with transport and inputs, to define the temporal and spatial distribution of toxic substances in natural systems. By virtue of their interactions with the solids in these systems, it is also necessary to analyze the distribution of the various types of solids. Furthermore, the exchange between the suspended and the bed constituents is taken into account. The models, which are developed in the second part of the notes describe both the physical-chemical effects in the inorganic realm, in conjunction with the solids, as well as accumulation and transfer through the various elements of the aquatic food chain. Application of these models to various natural systems are also presented.

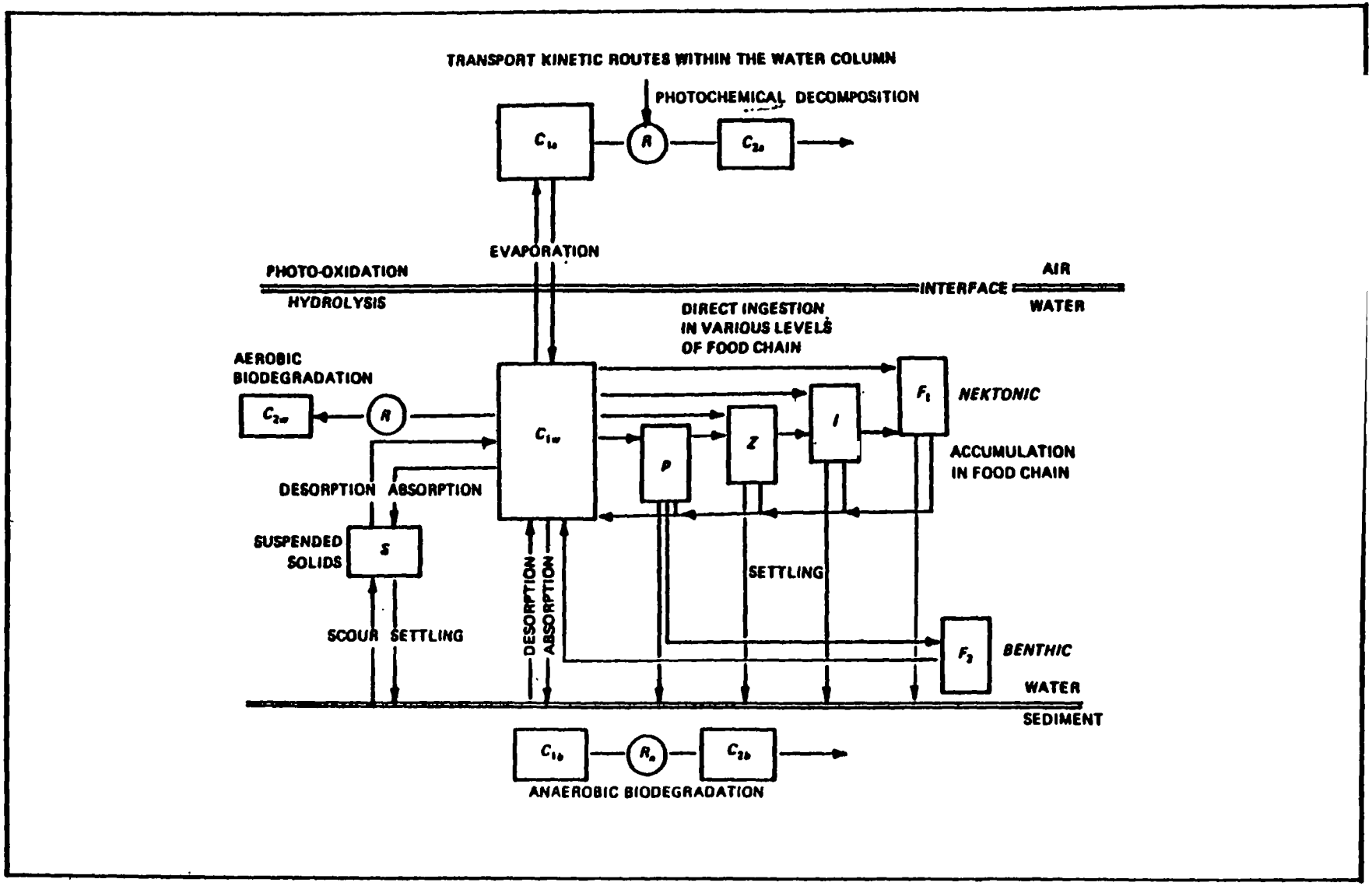

FIGURE A1

TRANSPORT - KINETIC ROUTES WITHIN THE WATER COLUMN

Note: Figure is for constant value of Π

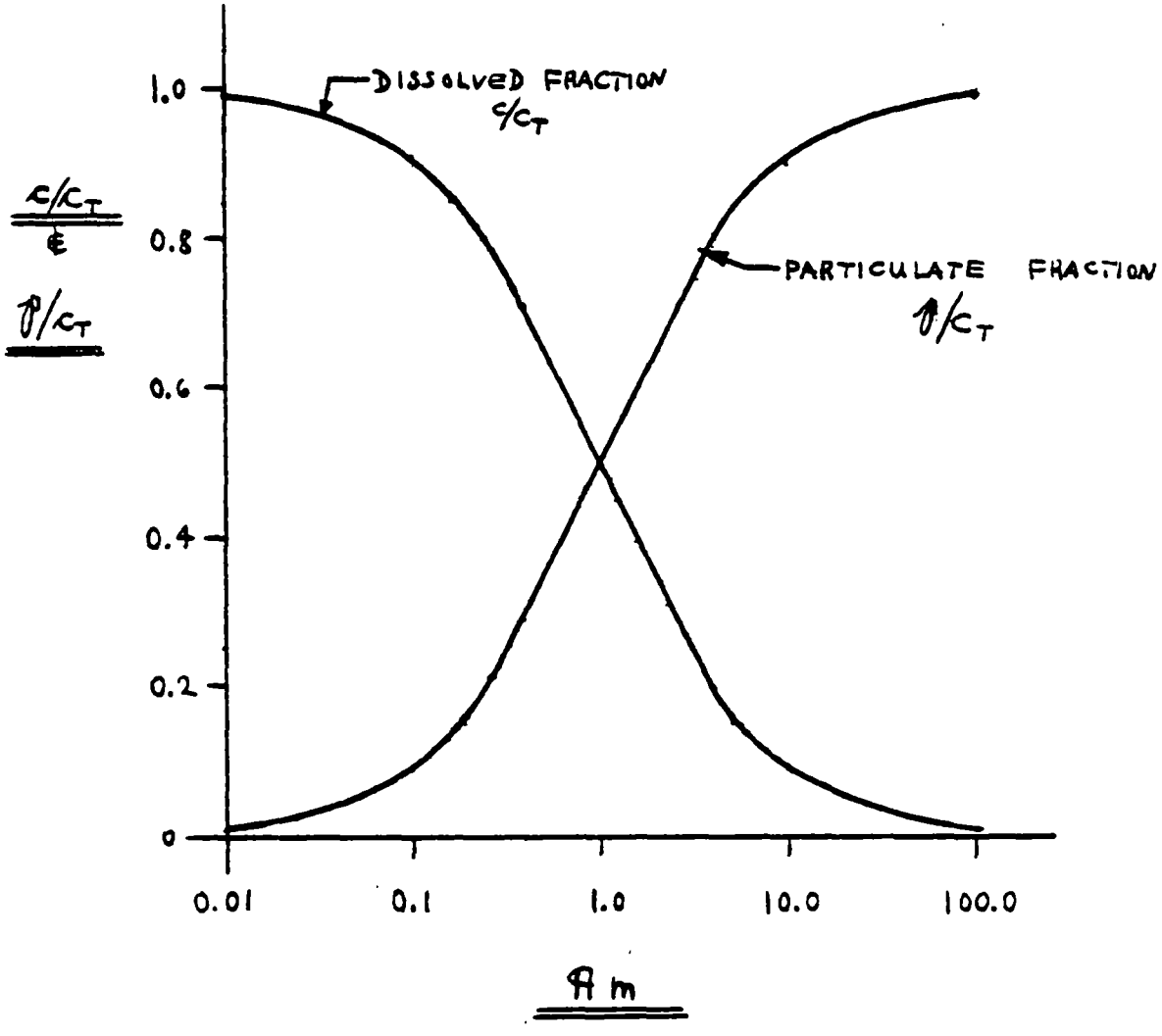

FIGURE A2 Equilibrium Concentrations of Dissolved and Particulate Toxicant as a Function of Πm

ADSORPTION-DESORPTION*

Adsorption is an important transfer mechanism within natural water systems, because of the significance of the substances which are usually involved in this process. The majority of radionuclides, heavy metal and organic chemicals are readily susceptible to adsorption. Bacteria and algae also have a similar tendency. The surfaces to which these constituents adhere are provided by the solids, either in suspension or in the bed. The clay, silica and organic content of the solids are the effective adsorbents by contrast to the sand and silt components.

The substance, in the complexed form may be then affected by additional processes such as flocculation and settling. If the flux due to the latter force is greater than that of the vertical mixing, the complex species deposit on the bed. In streams or rivers, they may then be subjected to resuspension during periods of high flow or intense winds and be transported to a reservoir or estuary. Since the hydrodynamic regime of each of these systems is more conducive to sedimentation than is that of a flowing stream, the ultimate repository of the complexed species frequently is in the bed of the reservoir or estuary. Furthermore, the physiochemical characteristics of the estuary tend to promote desorption and the constituent may be released to be recirculated with the estuarine system or transported to the ocean. Therefore, in analyzing the distribution of substances which are subject to adsorption, it may be necessary to take into account a sequence of events both with respect to the hydrologic and hydrodynamic transport through various systems, as well as the kinetic aspects of the transfer processes of adsorption-desorption and settling-scour within these systems.

The following sections describe the various factors which affect the adsorption-desorption processes and, based on these,

*Donald J. O'Connor
Kevin Farley

present the development of the relevant equilibrium relations and transfer equations.

1. Equilibrium

Adsorption is a process in which a soluble constituent in the water phase is transferred to and accumulates at the surface of the solids. The adsorptive capacity of a two-phase system depends on the degree of solubility of the constituent and the affinity of the constituent to the surface of the solid. The greater the degree of solubility the less is the tendency to be adsorbed. A number of organic compounds have both hydrophylic as well as hydrophobic groups - resulting in the orientation of the molecule at the interface. The hydrophylic component tends to remain in solution while the hydrophobic part adheres to the surface.

The molecular characteristics of a compound - its size and weight - are related to adsorption capacity, in a fashion consistent with solubility. For a given homologous series, the solubility is inversely proportional to molecular weight and it has been observed that the adsorption capacity increases with increasing molecular weight.

The affinity of the solute for the solid may be due to an attraction or interaction of an ionic, physical (van der Walls forces) or chemical nature. Most adsorption phenomena consist of combinations of the three forms and it is generally difficult to distinguish between them. The more general term "sorption" is used to describe the overall process.

In any case, one notable characteristic of the phenomenon is the dynamic equilibrium which is achieved between the concentration of solute remaining in solution and that on the surface of the adsorbent solid. At equilibrium, the rate of adsorption equals the rate of desorption. The equilibrium relationship between the concentration of solute and the amount adsorbed per unit mass of adsorbent is known as an

adsorption isotherm. The amount adsorbed per unit mass increases with increasing concentration of solute and usually approaches a limit as the capacity of the solid to accumulate is reached.

Equilibrium exists when the rates of adsorption and desorption are equal. The rate of adsorption depends on the concentration of the solute and the available sites on the adsorbing solid. The latter is proportional to the adsorptive capacity of the solid minus the amount of solute adsorbed. The rate of desorption is proportional to the amount of solute adsorbed:

$$\frac{dc}{dt} = K_1 c[c_{pc}-c_p] - K_2 c_p \qquad (14)$$

in which

c = dissolved concentration of solute (M/L)

c_p = particulate concentration (M/L)

c_{pc} = capacity of the adsorbent solids (M/L)

K_1 = adsorption coefficient $(\frac{1}{TM/L})$

K_2 = desorption coefficient $(\frac{1}{T})$

The overall reaction is second order with respect to adsorption and first-order with respect to desorption. The particulate concentration is a product of the concentration of adsorbing solids in the water, m, and the mass of the solute per unit mass of the adsorbent, r. Equation (14) may be expressed

$$\frac{dc}{dt} = K_1 c\, m[r_c-r] - K_2 rm \qquad (15)$$

At equilibrium, the rate of change of concentration is zero and equation (15) becomes after rearranging:

$$r = \frac{cr_c}{\frac{1}{b} + c} \tag{16}$$

in which $b = \frac{K_1}{K_2}$

Equation (16) is known as the Langmuir isotherm in which the parameter, b, is related to the energy of adsorption. At $r = r_c/2$, the concentration equals 1/b. Lacking direct experimental data on r_c, its value and that of 1/b may be evaluated graphically by a linear plot of $\frac{1}{c}$ versus $\frac{1}{r}$. The intercept equals $1/r_c$ and the slope $1/br_c$.

The capacity r_c depends on the nature, size and characteristics of the adsorbing solids, as shown in Figure 6. The various types of clays have greater capacities than silts and sands. The adsorption capacity is, thus, inversely proportional to the size of the particle, specifically to the ratio of its surface area to volume. Furthermore, the capacity is directly proportional to the organic content of the solids. In general solids, composed primarily of organic material, have greater capacities than the inorganic components. These materials include detrital matter, and various forms of viable organic substances, such as bacteria, plankton and macrophytes in natural systems and biological solids in treatment systems.

The Langmuir isotherm is based on the assumption that maximum absorption occurs when the surface of the adsorbent is saturated with a single layer of solute molecules. If one assumes that a number of adsorbate layers may form, the equilibrium condition, as depicted in Figure B-5, may have various points of inflection. Essentially an additional degree of freedom is introduced which reflects a greater degree of realism. The resulting relationships fit certain experimental data better than the Langmuir, particularly at the higher con-

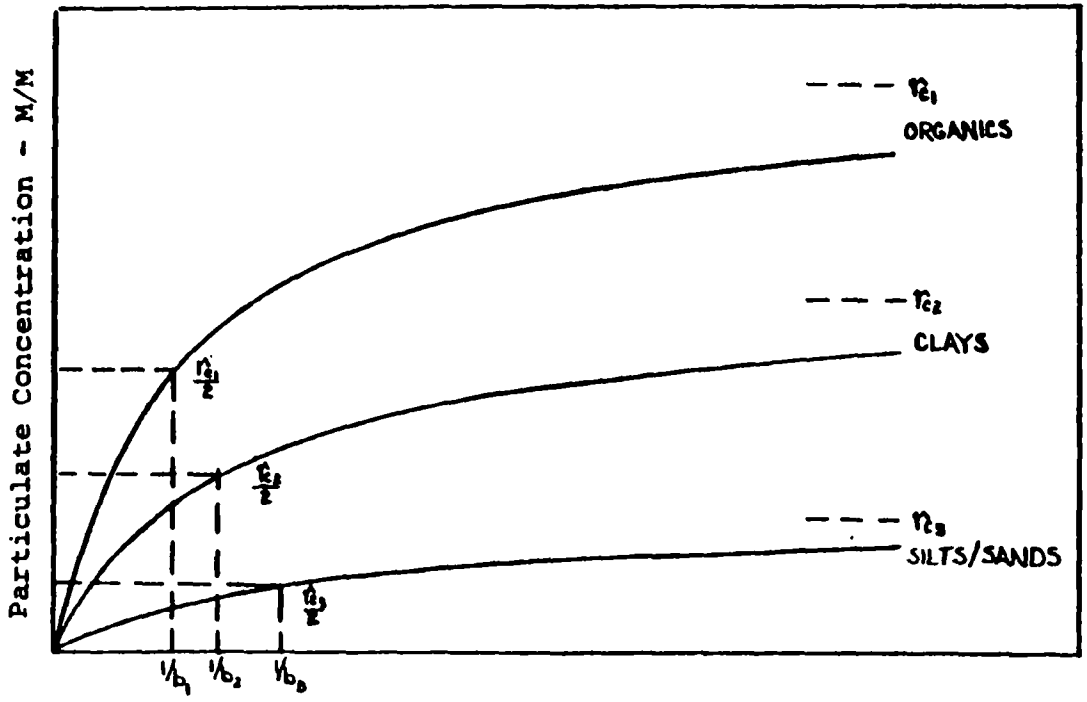

Figure B-5

Langmuir Adsorption Isotherms

centrations of solute. At lower concentrations the two isotherms may be approximately equivalent. In addition to the monolayer assumption, there are other conditions for which the Langmuir isotherm may not be appropriate. A semi-empirical relationship, known as the Fruendlich isotherm, which has been found to be more satisfactory in certain cases, is as follows

$$r = Kc^{1/n} \tag{17}$$

The value of the exponent n is usually less than unity. This isotherm has been widely used in the correlation of experimental data, particularly with respect to the adsorption by activated carbon in water and wastewater treatment processes.

It is generally accepted that the rates of adsorption and desorption occur very rapidly. Consequently equilibrium between the dissolved and particulate species, expressed by equations 16 or 17 is assumed to be established instantaneously.

The above isotherms appear to be particularly appropriate for the analysis of a singular adsorbate or those cases where one is predominant, such as PCB in the Hudson and kepone in the James River. When there are a number of compounds present, preferential adsorption and displacement may occur. Present research efforts are directed to the analysis of this problem. A competitive Langmuir isotherm and ideal solution theory are being applied in these cases.

2. Partition Coefficient

The partition coefficient is the ratio of the mass of substance adsorbed per unit mass of absorbent solids and the dissolved concentration of solute in the linear range of the Langmuir and Fruendlich isotherms. For very low concentrations of solute, $c << 1/b$, the Langmuir isotherm is linear:

$$r = \pi c \tag{18}$$

$$\text{in which} \quad \pi = \frac{K_1 r_c}{K_2}$$

The parameter, π, is a partition coefficient. At high concentrations of solute $c >> 1/b$, the adsorbent is saturated at its capacity r_c. These characteristics are more dramatically borne out when logarithmetic coordinates are used for various values of the partition coefficient.

The constant K in the Fruendlich isotherm is comparable to the partition coefficient. As the exponent n approaches unity, the isotherms are identical. Since the concentrations of organic chemicals in natural systems are generally low and, thus, well below the capacity of solids in these systems, the linear assumption is a reasonable approximation in many cases.

The partition coefficient incorporates the capacity parameter, r_c. Therefore, the same factors which influence its magnitude has a comparable effect on the partition coefficient. Large values are characteristic of organic material and clays, by contrast to silts and sands. Examples are shown in Figure B-6.

3. Dissolved - Particulate Distribution

Under equilibrium conditions, the distribution between the dissolved and particulate fraction is established not only by the partition coefficient as described above, but also by the concentration of the adsorbing solids. The solids may be suspended in the flowing water or relatively fixed in the bed of the system. Under extremely high flow in rivers or winds in lakes, the bed may be scoured and the solids are introduced into the overlying water for a brief period of time, after which they settle to the bed. In any case, assuming sufficient time has elapsed to establish adsorption equilibrium, the total concentration of organic chemical or metal,

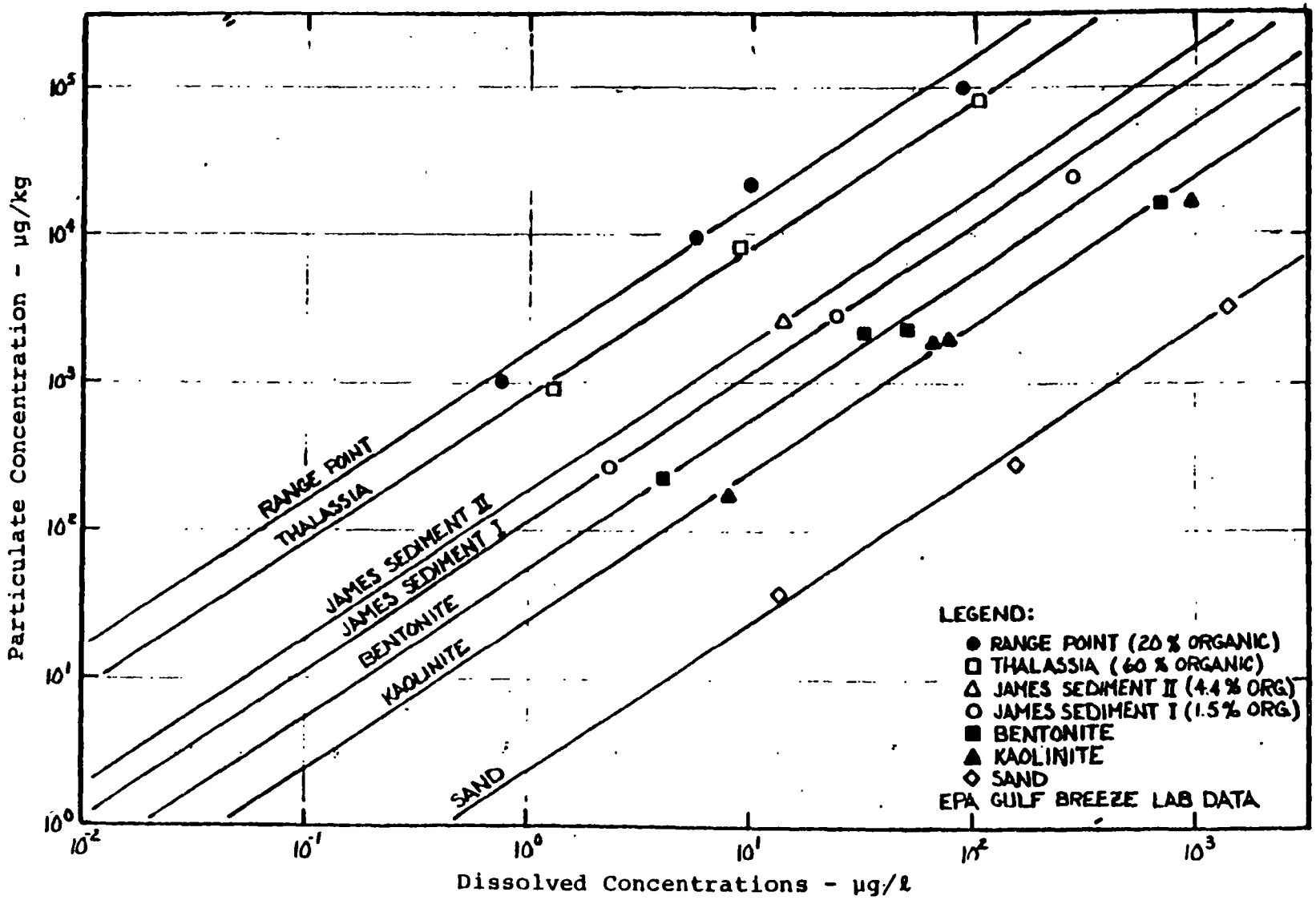

Figure B-6

Equilibrium Concentrations of Kepone

c_T, is the sum of the dissolved and particulate:

$$c_T = c + c_p \tag{19}$$

The dissolved component may be expressed in terms of the particulate fraction, r, and the partition coefficient, while the particulate concentration as a product of the concentration of adsorbing solids, m, and the particulate fraction:

$$c_T = \frac{r}{\pi} + rm \tag{20}$$

The particulate fraction as a function of solids concentration for various values of the partition coefficient is shown in Figure B-7.

Given a chemical or metal, with a large partition coefficient, whose major source is the bed solids, which is of uniform and constant concentration, this equation provides an approximate means of correlation. A linear plot of total concentration of chemical versus suspended solids concentration yields a straight line whose slope is r and intercept is r/π. An example is shown in Figure B-8 for mercury in the Mississippi and Mobile Rivers.

4. Transfer Rates

The discussion above concerned equilibrium conditions. The time required to achieve this condition involves the transfer and kinetic mechanisms between adsorbate and adsorbent. The sequence of processes, which characterize the transfer of a substance from solution to a material which has an adsorptive capacity, may be grouped in the following three steps: The first is the transfer of adsorbate through a liquid film to the surface of the adsorbent; the second is the diffusion of the adsorbate within the pores of the adsorbent; and the third is the fixation of the adsorbate on the interior pore or capillary surfaces of the adsorbent. The last step is usually assumed to be very rapid and equilibrium exists at this location. In some cases, the transfer of solute through the surface film or boundary layer is the rate-limiting step. If

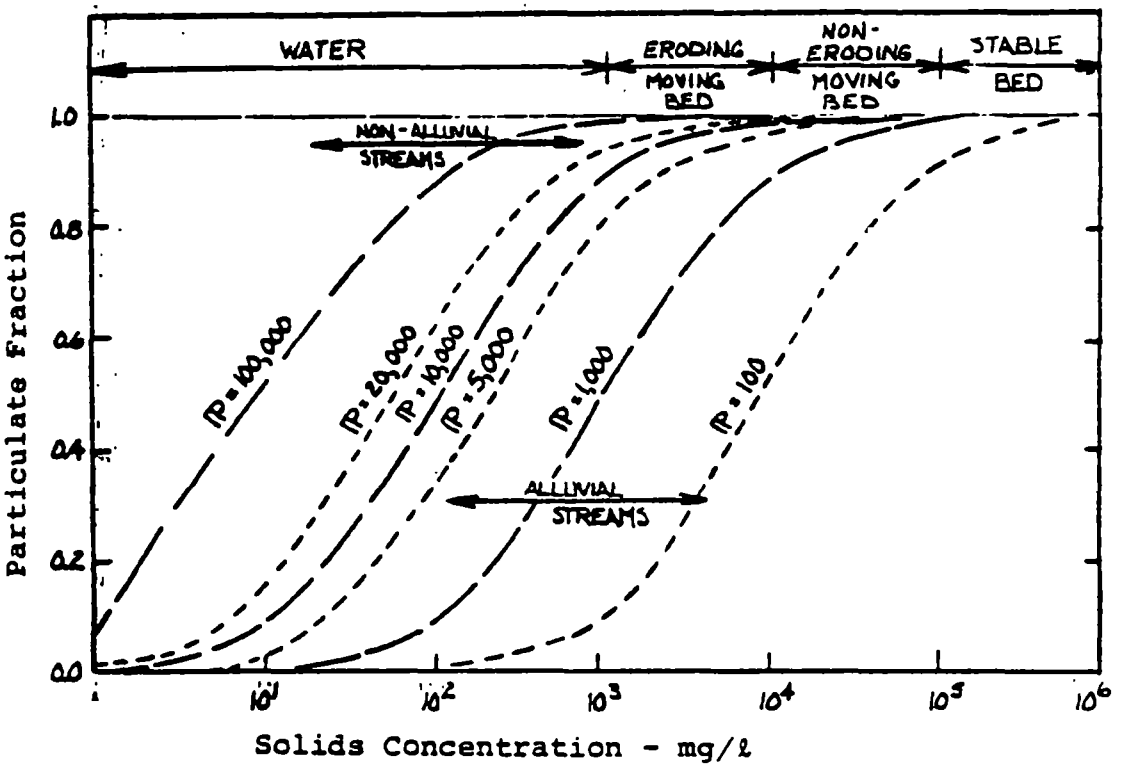

Figure B-7

Relationship - Particulate Fraction - Solids Concentration

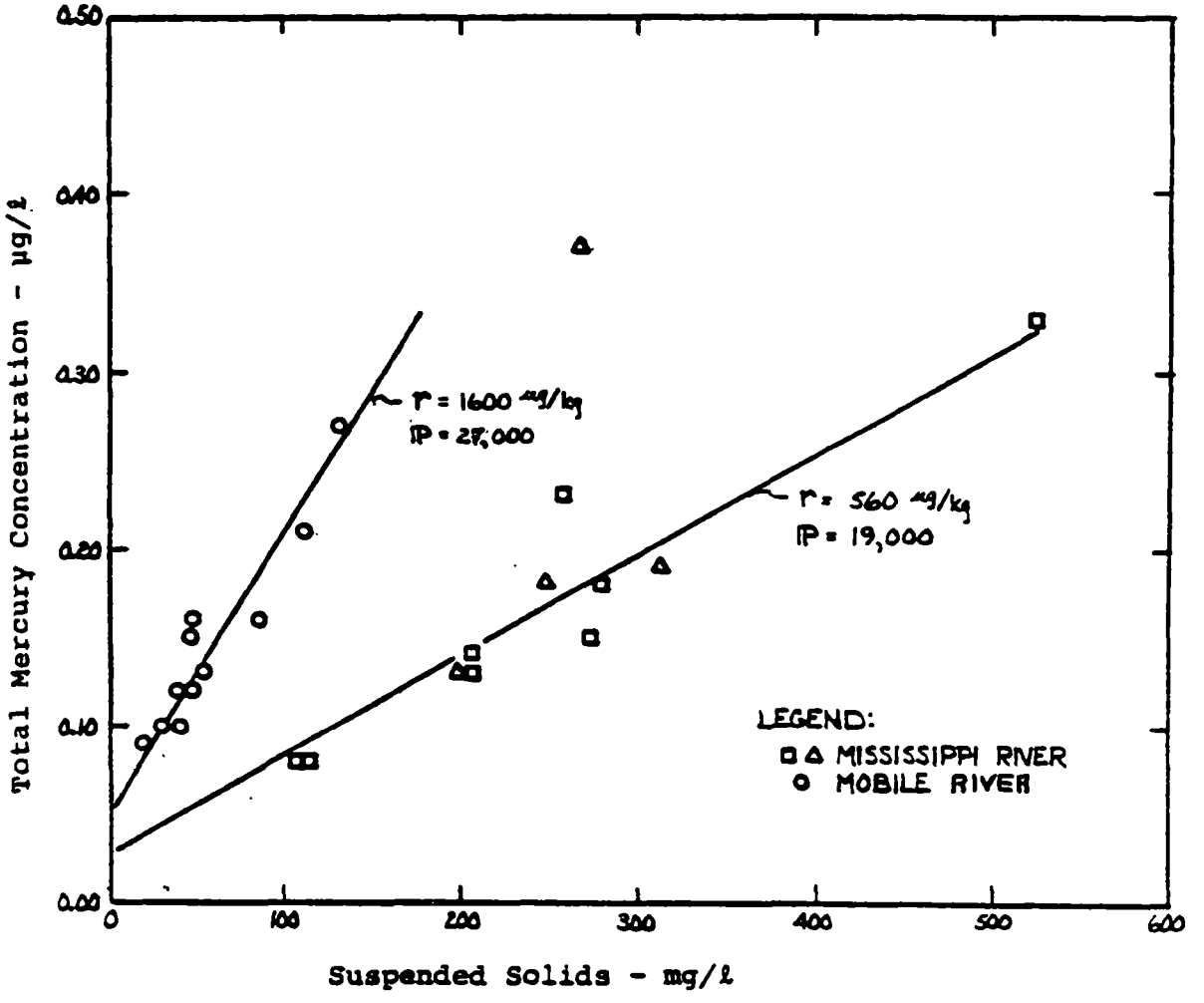

Figure B-8
Total Mercury - Suspended Solids Correlation

there is sufficient mixing due to the turbulence of the flowing water, the second step, that of diffusion within the porous material controls the rate.

In very dilute solution of both species, the frequency with which the solute comes in contact with the absorbent may determine the rate-limiting step. In some cases, adsorption may be occurring on contact of the solute with the bed material and the control may then localize in transfer through surface film on the exterior surface of the bed solids. The situation is comparable to the biological oxidation of organic matter, which takes place in the flowing water by the planktonic bacteria and in the channel bed by the benthic organisms. Both reactions occur simultaneously in natural systems, but in many cases, one or the other controls depending on the depth of the flow, the nature of bed and materials contained in each.

Given the steps described above, the reaction sequence may proceed in accordance with steps 1-2-3 or steps 1-3-2 depending on the nature of diffusion within the solid. In the latter case the diffusion is referred to as solid-phase internal diffusion. In the former sequence, it is fluid-phase pool diffusion. Various models have been constructed, incorporating these concepts and additional refinements. Most approaches include the three mechanisms: film transfer, diffusion in the particle and an interfacial equilibrium between liquid and solid phase concentrations.

The equilibrium coefficient, as previously discussed, may be readily determined in the laboratory for the various types of solids which may be encountered in natural systems.

The fluid phase film transfer coefficient appears to conform to general mass transfer correlations developed in the field of chemical engineering. In a simplified form the transfer coefficient is approximately:

$$K_L \propto \left[\frac{D_L U}{d}\right]^{\frac{1}{2}} \qquad (21)$$

in which D_L = diffusivity in liquid

U = flow velocity

d = effective particle diameter

The diffusivity in the above expression is that in liquid. The diffusivity within the pores is reduced by virtue of the size, porosity and tortuosity of the pore structure. A common correlation is of the form

$$D_p = \frac{D_L \epsilon}{2} \tag{22}$$

in which ϵ = internal porosity of the solid particle

The model is structured with transfer in two phases: liquid and pore. A flux balance is applied at the interface and the concentration equilibrium applied at the appropriate interface. A typical analysis is shown in Figure B-9.

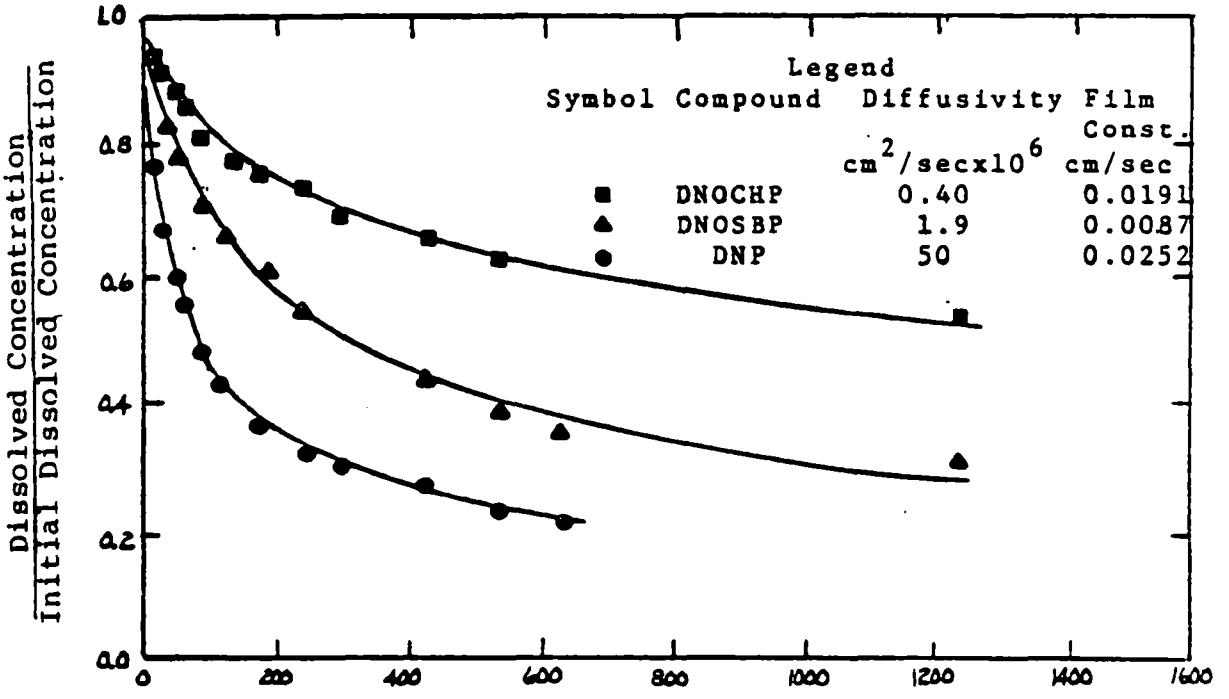

DNOCNP 2,4 - DINITRO - o - CYCLOHEXYLPHENOL

DNOSP 2,4 - DINITRO - o - SEC - BUTYLPHENOL

DNP 2,4 - DINITROPHENOL

Figure B-9

Example - Adsorption Kinetics

ADSORPTION-DESORPTION REFERENCES

DiGiano, F.A. and W.J. Weber, Jr. December, 1972. "Sorption Kinetics in Finite-Bath Systems." Journal of The Sanitary Engineering Division, ASCE, Vol. 98, No. SA6, Proc. Paper 9430, pp. 1021-1036.

Keinath, T.M. et al. April, 1976. "Mathematical Modeling of Heterogeneous Sorption in Continuous Contactors for Wastewater Decontamination." Final Report, U.S. Army Medical Res. Command.

Keinath, T.M. 1975. "Modeling and Simulation of the Performance of Adsorption Contactors," in Mathematical Modeling for Water Pollution Control Processes, ed. Thomas M. Keinath and Martin P. Wanielista, Ann Arbor, Mich. Ann Arbor Science Publ.

Matthews, A.P. and W.J. Weber, Jr. November 1975. "Effects of External Mass Transfer and Intraparticle Diffusion on Adsorption Rates in Slurry Reactors." Presented at the 68th Annual Meeting, American Institute of Chemical Engineering, Los Angeles, Calif.

Mattson, J.A. et al. July 1974. "Surface Chemistry of Active Carbon: Specific Adsorption of Phenols." Journal of Colloid and Interface Science, Vol. 48, No. 1.

Vermeulen, T. 1958. "Separation by Adsorption Methods," in Advances in Chemical Engineering. T.B. Dren and J.W. Hoopes, Jr., ed., Vol. 2, p. 147, Academic Press, New York.

Weber, T.W. and R.K. Chakravorti. March 1974. "Pore and Solid Diffusion Models for Fixed-Bed Adsorbers." AIChE Jour., Vol. 20, No. 2.

Weber, W.J. Jr. 1972. Physiochemical Processes for Water Quality Control. Wiley-Interscience, New York.

Weber, W.J. Jr. and J.C. Morris. April 1964. "Adsorption in Heterogeneous Aqueous Systems." Journal Amer. Water Works Assoc., Vol. 56, No. 4, pp. 447-456.

Weber, W.J. Jr. and R.R. Rumer Jr. Third Quarter 1965. "Intraparticle Transport of Sulfonated Alkylbenzenes in a Porous Solid: Diffusion With Nonlinear Adsorption." Water Resources Research, Vol. 1, No. 3.

Proceedings of The Kepone Seminar II. U.S. EPA Region III, Philadelphia, Pa., Sept. 1977.

SUMMARY OF REACTION RATE COEFFICIENTS

	pH, Temp	Chemical Hydrolysis day^{-1}	Direct Photolysis day^{-1}	Biolysis day^{-1}
Carbaryl	5	4.6×10^{-4}	0.11	2.3×10^{-5}
	6	5.3×10^{-3}		
	7	0.046	0.11	
	8	0.53		
	9	4.6		
Propham	7	6.9×10^{-5}	2.7×10^{-3}	0.22
Chloropropham	7	6.9×10^{-5}	5.7×10^{-3}	0.24
Malathion	6	slow		
	8,0°C	0.058		
	8,27°	0.46	slow	6.1
	8,40°	17.3		
Parathion	7,20°	2.8×10^{-3}	0.017	
Diazinon	7,20°	0.023	0.022	
2,4-D Butoxy	6,28°	0.63	0.049	
ethyl ester	9,28°	27.7		
Captan	8,28	1.39	slow	
Methocychlor	7,27°	1.9×10^{-3}	0.053	
			0.1-0.3*	
Toxaphene	7	slow	slow	
DDT	7,27	2.4×10^{-4}	1.3×10^{-4}	
Atrazine	3	0.011	0.017	
	11	8.6×10^{-3}		

* sensitized photolysis in natural waters

MODELING FRAMEWORK*

This section of the notes presents the development and application of various mathematical models which define the spatial and temporal distribution of toxic substances in natural water systems. The previous sections discussed the various transfer and kinetic factors which affect the concentration of such substances. These factors are now combined with the transport regimes characteristic of the different types of natural water systems, both freshwater and marine. The former include reservoirs/lakes and streams/tidal rivers, and the latter estuaries/embayments and the coastal zone.

The purposes of the modeling framework are twofold: the first relates to the general hazard assessment of proposed or existing chemicals which, in turn, may lead to waste-load allocation procedures. Such analyses may usually be accomplished by means of the spatial steady-state distributions. The second general purpose relates to the time-variable aspects of the problem. Such analyses apply to the effects of a short-term release of a toxic, such as an accidental spill or a storm overflow discharge. An equally important application in this regard is directed to the time required to build up to the steady and perhaps more significant the time required to cleanse a system from existing contamination.

As discussed in the previous sections, one of the most distinguishing characteristics of toxic substances is the partitioning between the dissolved and particulate components. Thus equations are developed for each of these components and in addition for those solids which provide sites for the adsorption of the substance. The analysis involves therefore, the solution of at least three simultaneous equations, describing the concentration of the various components in the water column. Furthermore, for those water systems which interact with the bed, additional sets of equations are developed to account for distribution in the benthal layer and its effect on water column concentrations. Given these concentrations, the dissolved and the particulate in the water column and in the bed, the distribution through the food chain is then considered.

* Donald J. O'Connor

In order to provide a perspective of the overall approach, the basic concepts which are employed in the analysis are first presented, followed by the development of the equations defining the dissolved, particulate and solids components. Certain sections which are contained in the first part of the notes are therefore repeated in the following in order to provide continuity of development.

A. BASIC PRINCIPLES

1. Mass Balance

Organic chemicals may exist in all phases of the aquatic environment - in solution, in suspension, in the bed and air boundaries, and in the various levels of the food chain. The interrelationships between and among these phases, which are shown diagrammatically in Figure 1, relate to the transport, reactions and transfer of the substance. The approach taken is identical, in principle, to that used to define the distribution of water quality consitutents, which are naturally part of biochemical and ecological cycles. The equations describing the spatial and temporal distribution of organic chemicals are developed using the principle of mass conservation including the inputs with the transport, transfer and reactions components. The general expression for the mass balance equation about a specified volume, V, is:

$$V \frac{dc_i}{dt} = J_i + \Sigma R_i + \Sigma T_i + \Sigma W \qquad (1)$$

in which

c_i = concentration of the chemical in compartment, i.

J = transport through the system

R = reactions within the system

T = transfer from one phase to another

W = inputs

Equation (1) describes the mass rate of change of the substance due to the net effect of the various fluxes and transformations. The purpose of expressing the transfer rate (T), distinct from the transport (J) and reactio

(R), is to provide a basis for the development of the equations, which describe more fully the relevant phenomena.

The general term "compartment" refers to each phase of the physiochemical regime - the dissolved and particulate in the water, atmosphere and bed - as well as to each element of the food chain - the phytoplankton, zooplankton, fish and detrital material. The transport, reaction and transfer terms may be positive or negative depending on the direction of kinetic routes between the chemical in compartment i and its concentration in other compartments with which it reacts or exchanges. The pathways are determined by the hydrodynamic and geophysical features of the natural water systems and by the physical, chemical and biological characteristics of both the system and the chemical. The hydrodynamic components transport material from one spatial location to another by dispersion and advective mechanisms. The physical factors transfer from one phase to another, such as exchange with the atmosphere, adsorption to and desorption from the suspended and bed solids and the settling and scour of these solids. The chemical factors transform the substance by processes such as photo-oxidation, hydrolysis and oxidation reduction reactions. The biological phenomena effect both transference and transformation: the latter primarily by microorganisms which may metabolize the chemical and the former by assimilation and excretion by the various aquatic organisms. Accumulation in the food chain is brought about by both ingestion of the chemical from the water and by predation on contaminated prey.

2. General Equations for Various Components

Consider the concentration, c, to be the dissolved component of the chemical in the water. It interacts with the particulate concentration, p. The interaction may be an adsorption-desorption process with the solids or an assimilation-depuration process with the aquatic organisms. In either case the particulate concentration is defined as:

$$p_i = r_i m_i \tag{2}$$

p = particulate concentration in i compartment M/L^3

r_i = mass of chemical/unit of interacting mass M/M

m_i = concentration of the interacting species M/L^3

The mass balance equation for the particulate component, similar to equation (1), is then:

$$\frac{dp_i}{dt} = r_i \frac{dm_i}{dt} + m_i \frac{dr_i}{dt} = J + \Sigma R + \Sigma T + \Sigma W \qquad (3)$$

It is apparent from equation (3) that an equivalent expression must be written for the concentration of the interacting compartment, m_i. In principle, the analysis of the problem requires the simultaneous solution of the three equations: the concentration of the chemical dissolved in the water, c, the mass concentration of the chemical per unit mass of interacting species, r, and the concentration of the species itself, m. Since this compartment may be further subdivided (inorganic and organic solids, multiple species of fish), equation (2) is more generally expressed as a summation of the individual components of the interacting substances:

$$p_i = \sum_1^n r_i m_i \qquad (4)$$

The specific conditions for which the analysis is performed frequently permit simplifying assumptions to be made. In laboratory batch reactors and in certain prototype situations, the rate of change of the interacting species may be zero - i.e. a constant concentration of suspended solids or biomass. Thus $\frac{dm}{dt} = o$, from which an equilibrium concentration of solids or biomass follows, resulting in two simultaneous equations to be solved, instead of three.

3. Dynamic Equilibrium

As may be evident from the above discussion, one of the essential properties of the analysis of this water quality problem is the interaction between the dissolved and particulate states of the constituent, which, in time, leads to a dynamic equilibrium between the two components. Consider the most simplified conditions of a batch reactor in which the mixing is of sufficient magnitude to maintain a uniform concentration throughout the volume of fluid. Assume the concentration of absorbing solids, m (M/L^3) is constant. Let c and p be the concentrations (M/L^3) of

the dissolved and particulate components. If there is neither transfer nor decay of the chemical, the total concentration, c_T, remains constant in time and is equal to the sum of the dissolved and particulate:

$$c_T = c + p \tag{5}$$

The latter is related to the concentration of suspended solids, m, as shown by equation (2):

$$p = rm$$

The equilibrium between the dissolved concentration in the water and the mass concentration of the solids is usually expressed in terms of a partition coefficient:

$$\P = \frac{r}{c} = \frac{p}{mc} \tag{6}$$

or $$\P m = \frac{p}{c}$$

Equation (6) is the linear portion of the Langmuir isotherm. Although not always representative of actual conditions, it is a reasonable approximation when the solid phase concentration, r, is much less than the ultimate absorbing capacity of the solids. Combining equations (5) and (6), the total concentration may be expressed as:

$$c_T = c + \P mc = \frac{p}{\P m} + p \tag{7}$$

The product, $\P m$, is a convenient dimensionless parameter, characteristic of a particular system under equilibrium conditions. For a specified value of $\P m$, the equilibrium distribution between the dissolved and particulate concentrations is established by equation (7), as shown in Figure A-2, Chap. I.

The distribution between the dissolved concentration and the particulate concentration in the various levels of the food chain may be expressed in an identical fashion. Accounting for the distribution for various types of adsorbing solids and various levels of the food chain, each with its characteristic partition coefficient, equation (7) may be more generally expressed:

$$c_T = c[1 + \Sigma \P_i m_i] \tag{8}$$

The distribution may thus be categorized in accordance with the adsorbing solids (organics, clays, silts and sands) or the accumulating biomass (phytoplankton, zooplankton, fish and macrophytes). Since the total biomass mass in most natural water systems is usually an order of magnitude less than that of the non-viable solids, the equations defining each category may be decoupled and the former may be solved independently. Under those conditions in which it may be significant, it may be readily incorporated as shown in the above equation.

4. Kinetic Interaction

The equilibrium, described above, is a result of the kinetic interaction between the dissolved and particulate. This property which distinguishes the analysis from that of purely dissolved substances, leads to equations of a more complex form. In order to gain an insight into the nature of these interactions and an understanding of a practical simplification, consider the kinetics in a batch reactor, as described above, in which interaction is taking place between the dissolved and particulate components and the former is being transferred by volatilization or transformed by chemical or biological degradation:

$$p \underset{K_2}{\overset{K_1}{\rightleftharpoons}} c \xrightarrow{K_3} \tag{9}$$

The reversible reaction ($K_1 \rightleftharpoons K_2$) may represent the adsorption-desorption between the dissolved component and the particulate in inorganic phase (suspended or bed solids) or the assimilation-depuration in the organic phase (aquatic organisms). These kinetic coefficients may be functions of the solids concentrations, as discussed subsequently. In any case, their ratio is a measure of the distribution or partition coefficient. The non-reversible reaction (K_3) describes the decay or volatilization. The kinetic equations are:

$$\frac{dc}{dt} = -(K_2 + K_3)c + K_1 p \tag{10}$$

$$\frac{dp}{dt} = - K_1 p + K_2 c \tag{11}$$

Addition of equations 10 and 11 yield

$$\frac{dC_T}{dt} = - K_3 c \tag{12}$$

If equilibrium is rapidly achieved by contrast to the other time constants, specifically identified as K_s in this example, the dissolved component, c, may be expressed in terms of the total concentration, c_T, by equation (7), substitution of which in (12) yields

$$c = c_o[\beta e^{gt} + (1-\beta)e^{ht}] \tag{13}$$

in which g,h are the positive and negative roots of the quadratic

$$g,h = - \frac{K}{2} [1 \pm m]$$

in which $K = K_1 + K_2 + K_3$

$$m = \sqrt{1 - \frac{4K_1K_3}{K^2}}$$

It may be readily shown that g and h are always real and negative.

In the case of adsorption-desorption, the assumption of instantaneous equilibrium is frequently made - i.e. the coefficients K_1 and K_2 are of sufficiently large magnitude so that the exchange between particulate and dissolved occurs very rapidly. Furthermore, for organic chemicals, the decay coefficient is usually of a much smaller magnitude than the adsorption-desorption. Thus

$$[K_1 + K_2] \frac{dc}{dt} + K_1K_3c = o$$

or

$$\frac{dc}{dt} = \frac{- K_3}{1 + K_2/K_1} c \tag{14}$$

in which

$$\frac{K_2}{K_1} = \text{distribution or equilibrium coefficient}$$

An additional insight is gained by developing equation (14) in an alternate manner by adding equations (10) and (11) which yields

$$\frac{dc_T}{dt} = - K_3 c \tag{15}$$

Assume the interaction between c and p is an adsorption-desorption process. The dissolved concentration, c, may therefore be expressed in terms of the total, c_T, by equation (7) substitution of which in (15) yields

$$\frac{dc_T}{dt} = - \frac{K_3}{1 + \P m} c_T \tag{16}$$

The total concentration decays in accordance with the dissolved coefficient modified by the parameter $\P m$. As a physically realizable example, consider the transfer represents a volatilization process, in which K_3 is the gas transfer coefficient. The total concentration c_T decreases at a slower rate than would be the case if there were no partitioning to the particulate form, with the total in dissolved form ($\P m = o$). In defining the rate of change of the total, the decay or transfer coefficient is simply modified as shown by equation (16). Conversely, if the decay is associated with the particulate component, the coefficient would be reduced by the fraction $\P m/[1 + \P m]$, in accordance with equation (7).

If both the particulate and dissolved components are subject to decay, by more than one mechanism, equation (16) becomes

$$\frac{dc_T}{dt} = - \left[\frac{\Sigma K_{ci}}{1 + \P m} + \frac{\P m \Sigma K_{pi}}{1 + \P m}\right] c_T \tag{17}$$

in which the subscripts, c and p, refer respectively to the dissolved and particulate decay coefficients.

The assumption of "instantaneous" equilibrium as expressed by equation (14) through (17) is a valid representation, or model, of kinetic reactions provided the time to equilibrium, determined by K_1 and K_2 is rapid relative to the other phenomena which affect the substance, K_c & K_p. This condition is generally applicable to the adsorption-desorption process, since its equilibrium time is usually much shorter (min-hours) than that of other kinetic effects, which may be in the order of days, months or years.

In summary, the models for the analyses of organic chemicals and heavy metals are similar to those developed for constituents which are natural components of ecological cycles. The terms relating to the particulate form and its interaction with the dissolved component are the additional components to be incorporated. These, with the other transfer and reactive terms, cover the various pathways of distribution. Accordingly, each of these routes and the associated mechanisms are described in the subsequent sections which comprise the first half of these notes.

The second half is devoted to the development of models, which incorporate these reaction mechanisms with transport and inputs, to define the temporal and spatial distribution of toxic substances in natural systems. By virtue of their interactions with the solids in these systems, it is also necessary to analyze the distribution of the various types of solids. Furthermore, the exchange between the suspended and the bed constituents is taken into account. The models, which are developed in the second part of the notes describe both the physical-chemical effects in the inorganic realm, in conjunction with the solids, as well as accumulation and transfer through the various elements of the aquatic food chain. Application of these models to various natural systems are also presented.

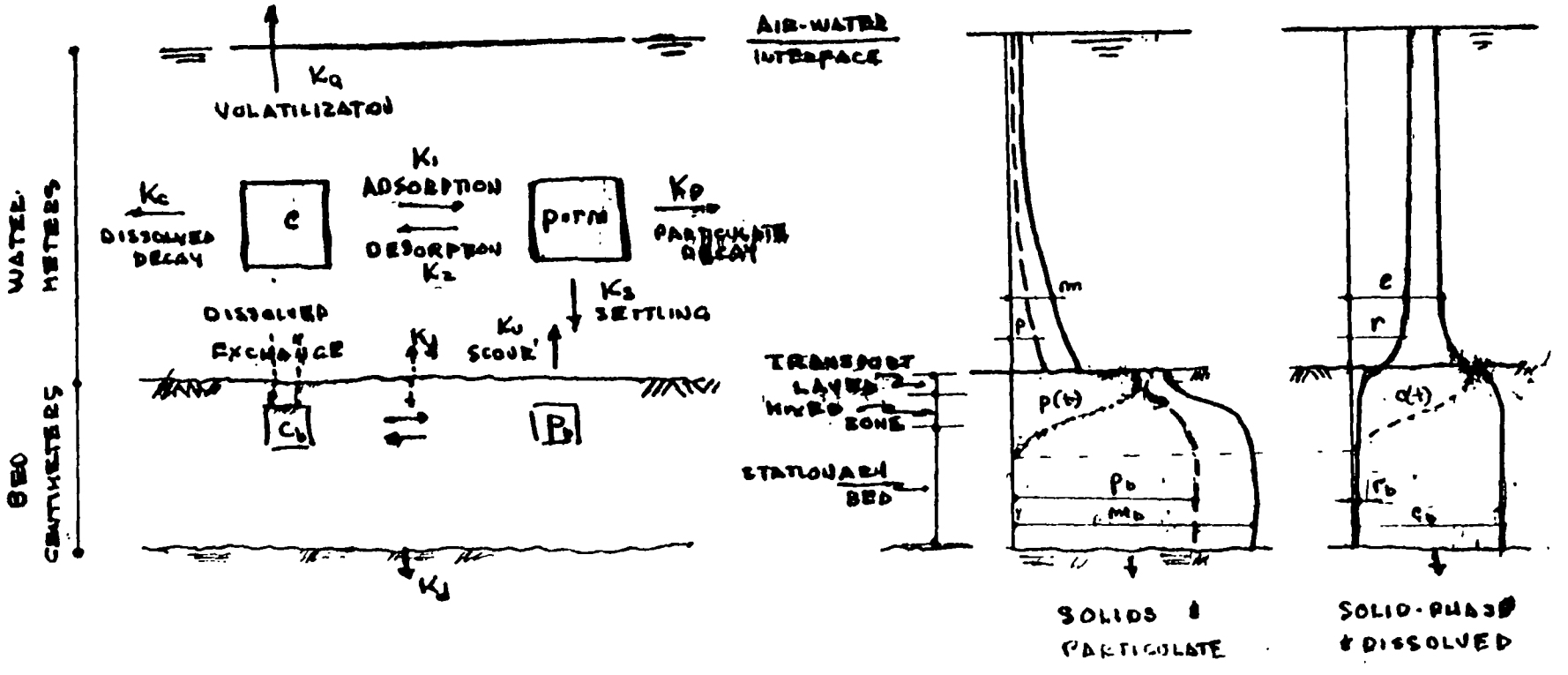

KINETIC & TRANSFER FACTORS

DISTRIBUTION OF SOLIDS & TOXIC

FIGURE 1

B. CLASSIFICATION OF ANALYSIS AND MODELS*

Equation (1) is the most general expression to define the distribution of a toxic substance in a natural water body. Given the characteristics of the drainage area and water system and the nature of the substance, it takes on a more definitive form. As described previously, the distribution between the dissolved and particulate components of the toxic material and the kinetic interactions are the essential factors, which are common to all types of models. What distinguishes the various models, discussed in the subsequent sections of the notes, are the transport components of a specific water system and the characteristics of the bed, with which it interacts. Thus, the basis of the classification lies, to some degree, in the transport regimes of the general types of water systems - lakes, streams and estuaries, but more significantly rests on the transport characteristics of the bed itself, and the magnitude of the water-bed interaction. The kinetic and transfer routes are common to all types. Each of these factors are discussed in this section, concluding with the proposed classification.

1. Kinetic and Transfer Routes

The components and their interactions are shown diagrammatically in Figure 1. The concentrations of the toxic substances are presented in both the water column and the bed. The distribution between the dissolved, c, and particulate, p, components is determined by the magnitude of the adsorption and desorption coefficients, K_1 and K_2, and the concentration of the adsorbing solids, m. Each of these components may be susceptible to decay and exchange, as shown. For conservative, non-volatile toxics these transform routes are negligible but the settling-resuspension transfers are potentially important for any substance, regardless of its other characteristics. These are the characteristics of the system and the substance which essentially determine the complexity of the analysis.

2. Transport Regimes

Each of the general types of natural water systems may be classified in accordance with characteristic fluid transport regime and the interaction of the water with the bed. The components of the transport field are the advective (U) and dispersive (E) elements which, in general, are expressed in three-dimensional space. Each of the systems to be considered - streams, estuaries, lakes and coastal waters - are usually characterized by a predomi-

* Donald J. O'Connor

nating component, in one of more dimensions. The transport in streams may be frequently approximated by a one-dimensional longitudinal analysis (A), in lakes by one or two dimensions (B), in which the vertical is the major component and in estuaries by a two-dimensional scheme (C) (longitudinal and vertical, as shown in Figure 2A. A spatially uniform condition (completely mixed) is type D whose transport coefficient is the detention time, t_o.

3. Bed Conditions

The bed conditions, which are relevant to the analysis are shown in Figure 2B. They may be classified as inactive, or stationary, and active; or mixed. The latter may be further subdivided: without and with horizontal transport. A further characteristic of bed conditions relates to the phenomenon of sedimentation. All natural water bodies accumulate, in varying degrees, materials which settle from the water column above. In freshwater systems, reservoirs and lakes are repositories of much of the suspended solids which are discharged by the tributary streams and direct drainage. In marine systems, estuaries and embayments accumulate solids in similar fashion and the coastal zones to a lesser degree. In flowing freshwater streams and tidal rivers, suspended solids may settle or scour depending on the magnitude of the velocity and shear associated with the flow. Bed conditions in these systems are therefore subject to seasonal and daily variations, while the beds of estuaries and lakes which are also subject to such variations, tend to accumulate material over long time scales. The increase in bed depth and concentration is expressed in terms of a sedimentation velocity, measured in terms of months or years, by contrast to the settling velocity of the various solids in suspension, measured in terms of hours or days.

4. Classification of Models

The classification, suggested in these notes, is essentially based on the types of bed conditions shown in Figure 2B, in conjunction with one of the three types of fluid transport shown in Figure 2A. The three general types are enumerated in a progressive fashion from the simpler to the more complex, as presented in Table 1 and described below. The final form of the equations is based essentially on one of the three types, in conjunction with the kinetic interactions shown in Figure 1.

TYPE I - STATIONARY BED

A stationary bed is basically characterized by zero to negilgible horizontal motion. This condition is most commonly encountered in lakes and reservoirs of relatively great depth, with minimal winds. It also occurs in freshwater streams under low flow conditions and in marine systems with little tidal mixing. It may therefore be associated with any one of the three transport systems shown in Figure 2A.

The essential characteristic of this type of system is relatively low degree of vertical mixing in the fluid. The hydrodynamic environment is one which permits the gravitational force to predominate and suspended particles of density greater than that of water settle. The accumulation of this material in the bed causes an increase in the thickness of the benthal layer, the rate of increase being referred to as a sedimentation velocity. The bed is also characterized by minimal or zero mixing in the layer in contact with the water.

TYPE II - MIXED LAYER

This condition, which is probably more common, is characterized by some degree of mixing in the contact layer of the bed. The mixing may be due to either physical or biological factors - increased levels of shear, associated with horizontal or vertical velocities and gradients or bioturbation, attributable to the movement of benthal organisms. It exists, therefore, in lakes where the wind effects extend to the bottom and in streams and rivers under moderate flow conditions.

In each of these cases, the shear exerted on the bed is sufficient to bring about mixing in interfacial layer, but not sufficient to cause significant erosion and bed motion. The net flux of material to the bed is the difference between the settling flux and that returned by the exchange due to the mixing. Thus, the bed thickness may increase or decrease and the sedimentation velocity may be positive or negative. The mixed layer interacts with a stationary bed beneath, as shown. This type of bed condition may also be associated with any of the three fluid transport types, but is more usually associated with type B and in the littoral zone of lakes, where the water depths are sufficiently shallow to permit wind effects to be transmitted to the bed.

TYPE III - BED TRANSPORT

This bed condition possesses both mixing and advective characteristics. The shearing stress exerted by the fluid is of sufficient intensity to cause erosion and resuspension of the bed and the fluid velocity of sufficient magnitude to induce horizontal motion of either or both the resuspended material and the interfacial bed layer. This phenomenon involves the complex field of sediment transport, which has been greatly developed in streams, but much less in estuaries and lakes. The bed system may now be envisioned as three distinct segments: a moving interfacial layer, a mixed zone and a stationary bed beneath. There is vertical exchange between the moving and mixed layers and the vertical transport in the bed is characterized by the sedimentation velocity.

This type of bed regime is associated only with types B and C fluid transport system. The direction of horizontal motion of the bed in accordance with velocity vector of the fluid in contact with the bed surface. In fresh water streams and rivers, the bed transport is downstream in the direction of flow. While in estuaries, the net bed transport is upstream in the saline zone due to the tidally averaged motion as shown in Figure 2B.

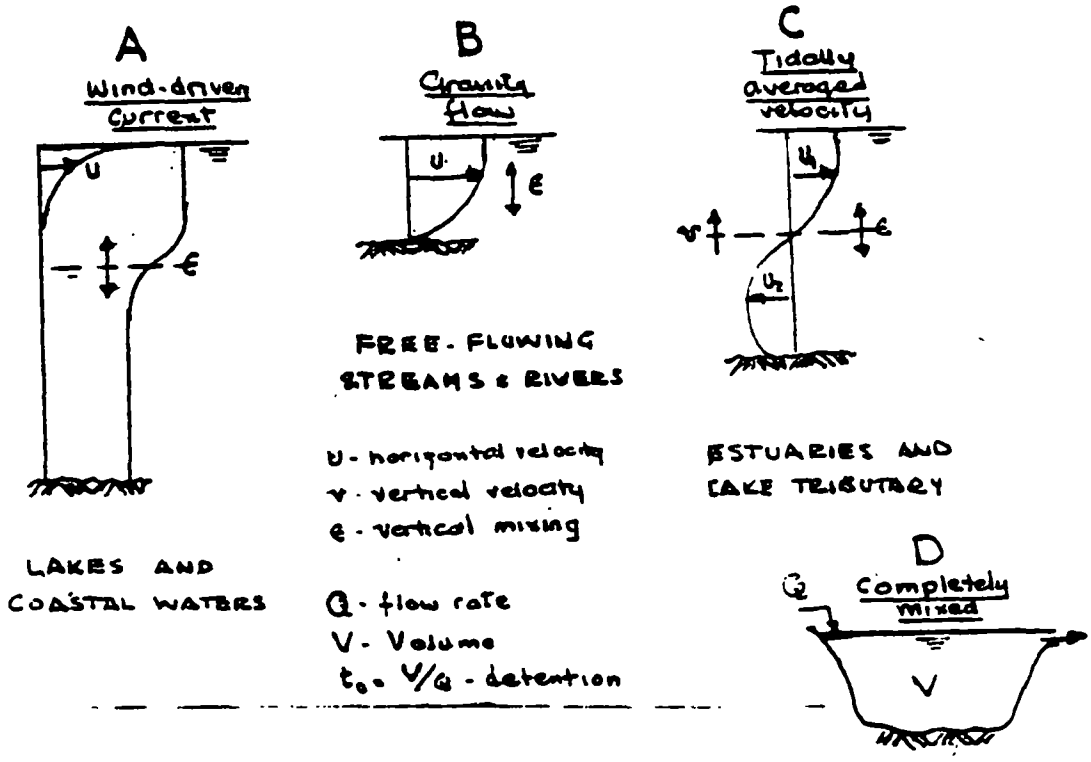

FIGURE 2A - TRANSPORT REGIMES

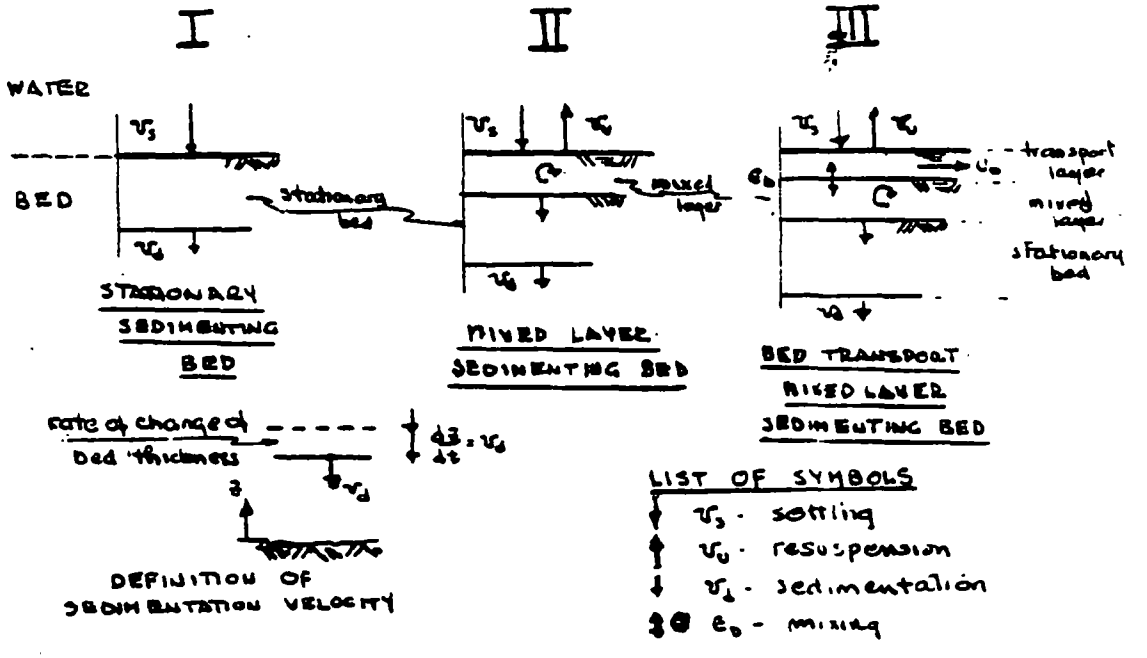

FIGURE 2B - BED CONDITIONS

TABLE 1

FLUID TRANSPORT REGIME	BED CONDITION I STATIONARY BED	BED CONDITION II MIXED LAYER WITH BED	BED CONDITION III SEDIMENT TRANSPORT WITH LAYER & BED
	U_b = 0, ε_b > 0	U_b = 0, ε_b > 0	U_b > 0, ε_b > 0
A LAKES RESERVOIRS COASTAL ZONE	DEEP, MINIMAL WINDS	MODERATE DEPTH, WINDS	LITTORAL ZONES
B STREAMS & RIVERS	LOW FLOW	MODERATE FLOW	HIGH FLOW
C ESTUARIES EMBAYMENTS	ENCLOSED BAYS MINIMAL TIDES	LITTORAL ZONES MAIN CHANNEL LOW FLOW	MAIN CHANNEL MODERATE FLOWS
D COMPLETELY MIXED	APPLICABLE TO ALL TYPES, PARTICULARLY TO LAKES RESERVOIRS & EMBAYMENTS		

LAKES AND RESERVOIRS

A. INTRODUCTION*

The analyses of water quality in lakes and reservoirs are considered in this section. Because of certain similarities which exist between lakes and oceans, many of the models described in this chapter are appropriate for problems in the coastal and off-shore regions of the oceans. The spectrum of time-space scales which characterize the analysis in these water bodies is much broader than that encountered in streams and estuaries. This difference is attributable not only to the geomorphology and dimensionality of the respective systems but also to the driving forces and components of the transport terms. Thus, many water quality analyses in rivers, tidal and non-tidal, are one-dimensional within the relatively defined boundary of channel cross section. Furthermore, this uni-dimensionality, which applies both to flow and quality frequently exists under steady-state conditions.

By contrast to the one-dimensional steady-state analysis, many water quality problems in lakes and oceans are time variable in two or three dimensions. The deep, relatively slow moving, hydraulic regime, over wide horizontal scales, is an important factor in this regard. Because of the greater depths, thermal differences and density structures are seasonally encountered. The vertical distribution of many constituents associated with these regimes is a significant water quality problem, which has a counterpart in the toxic problem.

A large scale analysis may frequently be used on the assumption of a spatially uniformity of concentration over the time unit of analysis. Since large scale problems (10-100 miles) are usually associated with equivalently long time scales, the incremental time step of the analysis may be of sufficient duration to justify the assumption of spatially uniformity. For example, if the concern is the long term build-up of conservative toxic substances which may occur over years or decades, an appropriate time step of such an analysis is the year. Over this period many lakes and reservoirs, with their characteristic spring and fall overturn

* Donald J. O'Connor

and mixing due to winds and seiches, reflect a spatially uniform condition. More specifically, the variations which occur over the year are small by contrast to the increase in concentration anticipated in future years. At this relatively large time-space scale, the typical time variable problem is the long term build-up of a toxic constituent. The steady-state relates to the equilibrium concentration, resulting from a constant input, and the time required to establish equilibrium, if indeed one is possible.

The following sections of this chapter describe the toxic distributions in completely mixed systems of lakes and reservoirs and secondly, address the analysis of the vertical distribution of toxic substances in these water bodies. The completely mixed analysis is coupled with Type I and II bed conditions with various applications. It is unlikely that a Type II condition would be encountered in lakes under this scale assumption. The vertical analysis is presented with a Type I bed condition with a specific example of quarry with lindane and DDE inputs. A final application is discussed with respect to Toxic Substances in the Great Lakes. In each case, the distribution of suspended solids is first developed, followed by the analysis of toxic substances, which receives input from the solids analysis.

B. ANALYSIS OF COMPLETELY MIXED SYSTEMS*

1. Type I Analysis - Stationary Bed - No Resuspension - Sedimentation

a) Suspended Solids

The concentration of suspended solids in a reservoir or lake depends on the physical characteristics of the incoming sediment and the hydraulic features of the system and inflow. The important characteristics of the solids are the grain size and settling velocity distributions and the behavior of the finer fractions with respect to aggregation and coagulation. The detention time and the depth of the water body are the significant hydraulic and geomorphological features. The following analysis assumes steady-state conditions in a completely mixed system, in which the concentration of solids is spatially uniform.

These assumptions are obviously crude, but of sufficient practicality to admit at least an order of magnitude analysis of the problem. They are precisely the assumption, implicit in the analysis of the "Trap Efficiency" of reservoirs in which the efficiency of removal of solids has been correlated to the ratio of the reservoir capacity to the tributary drainage area(1).

Consider a body of water whose concentration is spatially uniform throughout its volume, V, receiving an inflow, Q, as shown in Figure B-1. Under steady state conditions, hydraulic inflow and outflow are equal. The mass balance of the solids takes into account the mass inputted by the inflow, that discharged in the outflow and that removed by settling. The mass rate of change of solids in the reservoirs is the net of these fluxes:

$$V \frac{dm_1}{dt} = Qm_i - Qm_1 - v_s A_s m_1 \qquad (1)$$

in which

m_i = concentration of solids in inflow

m_1 = concentration of solids in water body

v_s = settling velocity of the solids

A_s = horizontal area thru which settling occurs

The flux Qm_i, equals the rate of mass input, W. Dividing through by the volume, V, the above equation becomes

$$\frac{dm_1}{dt} = \frac{W}{V} - m_1\left[\frac{1}{t_o} + K_s\right] \qquad (2)$$

* Donald J. O'Connor

in which

t_o = detention time = $\frac{V}{Q}$ (T)

K_s = settling coefficient $\frac{v_s}{H}$ $(\frac{L}{T})$

H = mean depth = $\frac{V}{A_s}$ (L)

Under the steady state condition, equation (2) may be expressed as,

$$m_1 = \frac{W/Q}{1 + K_s t_o} \tag{3a}$$

Division by W/Q yields

$$\frac{m_1}{W/Q} = \frac{1}{1 + K_s t_o} \tag{3b}$$

which is the fraction of the incoming solids remaining in suspension and, with the assumption of complete mixing, is also the concentration in the outflow. The fraction removed is simply

$$f = 1 - \frac{1}{1 + K_s t_o} \tag{4}$$

The dimensionless parameter, $K_s t_o$, represents the combined effects of the settling characteristics of the solids and the average detention time of the system. The coefficient, K_s, may be replaced by its equivalent, v_s/H, and the dimensionless parameter is v_s/v_o, in which $v_o = \frac{H}{t_o} = \frac{Q}{A}$, the overflow rate of the system.

It is apparent from the above development that conditions in the bed have no effect on the concentration in the water body, because there is no resuspension of the bed material. The benthal concentration, on the other hand, is due directly to the influx of the settling solids. The rate of change of mass of solids in the bed is therefore

$$\frac{dM_2}{dt} = + A_1 v_s m_1$$

The mass, M_2, equals the product of the bed volume V_2, and bed concentration, m_2. Thus

$$\frac{dM_2}{dt} = \frac{d(V_2 m_2)}{dt} = m_2 \frac{dV_2}{dt} + V_2 \frac{dm_2}{dt} = + A_s v_s m_1 \tag{5a}$$

Dividing through the A_s, and expressing the resulting $\frac{dz_2}{dt}$ as V_d, the final result is

$$\frac{dm_2}{dt} = \frac{v_s}{z} m_1 - \frac{v_d}{z} m_2 \qquad (5b)$$

at steady-state - i.e. when the mass settling rate equals the accumulation rate:

$$m_2 = m_1 \frac{v_s}{v_u} \qquad (5c)$$

b) Toxic Substances

The distribution of toxic substances, such as organic chemicals and heavy metals in reservoirs and lakes is established by application of the principle of continuity or mass balance, in a manner similar to that employed in the case of the suspended solids. Each phase, the dissolved and particulate, is analyzed separately, taking into account the adsorptive-desorptive interaction with the other. For the dissolved component, the mass balance includes decay and transfer terms[2][3] in addition to the inflow and outflow. The basic differential equation

$$\frac{dc_1}{dt} = \frac{W_c}{V} - \frac{c_1}{t_o} - K_c c_1 - K_o m_1 c_1 + K_2 p_1 \qquad (6)$$

in which

V = reservoir volume (L^3)
W_c = rate of mass input of the dissolved component (M/T)
c_1 = dissolved concentration in water body (M/L^3)
K_c = overall first order rate coefficients (T^{-1}) which may include biological degradation, hydrolysis, direct photolysis & volatilization.
K_o = the adsorption coefficient (L^3/M-T)
m = suspended solids concentration (M/L^3)
K_2 = the desorption coefficient (T^{-1})
p_1 = particulate chemical concentration (M/L^3)

For the particulate concentration:

$$\frac{dp_1}{dt} = \frac{W_p}{V} - \frac{p_1}{t_o} - K_{s_1} p_1 - K_2 p_1 + K_o m\, c_1 \qquad (7)$$

in which

W_p = rate of mass input of the particulate adsorbed chemical (M/T)

K_s = settling coefficient (T^{-1})

Adding equations (6) and (7) cancels the adsorption and desorption terms and yields the rate of change of the total concentration c_T in terms of the dissolved and particulate:

$$\frac{dc_{T_1}}{dt} = \frac{W}{V} - \frac{c_{T_1}}{t_o} - K_c c_1 - K_{s_1} p_1 \tag{8}$$

The sorption coefficients, K_o and K_2 are usually orders of magnitude greater than the decay and transfer coefficients of the dissolved and particulate. The rate at which equilibrium is achieved between the two phases is very rapid by contrast to the rates of transfer and decay. Thus liquid-solid phase equilibrium is assumed to occur instantaneously. The dissolved and particulate concentrations, c and p, may therefore be expressed in terms of c_T by equation 4, substitution of which in equation (8) yields:

$$\frac{dc_{T_1}}{dt} = \frac{W}{V_1} - \frac{c_{T_1}}{t_o} - \frac{K_{c_1}}{1 + \P m_1} c_{T_1} - \frac{K_{s_1} \P m_1}{1+\P m_1} c_{T_1}$$

Under steady-state conditions, the above may be expressed, after multiplying through by t_o:

$$c_{T_1} = \frac{W/Q}{1 + \frac{t_o}{1+\P m_1}[K_{c_1} + \P m_1 K_{s_1}]} \tag{9}$$

For those substances, whose dissolved components are not susceptible to transfer/decay, such as heavy metals, equation (9) reduces to

$$c_{T_1} = \frac{W/Q}{1 + K_{s_1} t_o [\frac{\P m_1}{1+\P m_1}]} \tag{10}$$

Note that equation (10) is identical to equation (3a) with the exception that the dimensionless settling parameter $K_s t_o$ is multiplied by the fraction $\frac{\P m_1}{1+\P m_1}$.

The latter term expresses the fraction of the total concentration which is in the particulate form. For values of $\P m >> 1$, it is apparent that equation (10) is identical to (3a). With reference to equations (9) and (10), the fraction removed is

$$f = 1 - \frac{C_T}{W/Q} \tag{11}$$

Inspection of equation (4) indicates that the removal efficiency of suspended solids is dependent on the detention time and settling coefficient, which is the ratio of the settling velocity of the solids and the average depth of the reservoir or lake. For heavy metals and conservative chemicals, the additional parameter required is the partition coefficient (equation 10). In the case of organic chemicals, which are susceptible to biodegradation, evaporative transfer, hydrolytic or photochemical reaction, knowledge of the relevant reaction coefficients is necessary (equation 9).

The detention time and average depth, which are readily determined, are based on the average seasonal or annual conditions, given the time and space scales of the analysis. The settling velocity and settling coefficient may be measured directly or implied from inflow-outflow concentrations in accordance with equations (3) and (4). The partition coefficient may also be evaluated directly, which, with the solids concentration, yields the dimensionless parameter $\P m$. Alternately given measurements of the total and dissolved concentrations of the heavy metal/organic chemical, the term $\P m$ may be calculated. With such information, the removal efficiency is readily computed for those metals and chemicals which are non-reactive.

As indicated above, certain chemicals may be subjected to additional transfer or transformation. The fundamental properties of the constituent are indicative of the potential magnitude of these routes - e.g. the vapor pressure and solubility are properties which permit assessment of the evaporative transfer (4)(5). Laboratory experiments may be necessary to determent the chemical and biological routes - e.g. the biodegradability of the substance (6)-(9). In any particular case, an assessment, either analytical or experimental, should be made to establish the degree to which transformation or transfer may be significant. Solutions of the above are shown in Figure B-2.

The bed concentration may be described by constructing its mass balance. Influx is due to the toxic substance associated with the settling solids and the volumetric accumulation is accounted for by the sedimentation velocity, as in the bed solids analysis (equation 5)

$$\frac{dc_{T_2}}{dt} = f_{p_1} K_{s_2} c_{T_1} - f_{p_2} K_{d_2} c_{T_2} \tag{12}$$

at steady state

$$c_{T_2} = \frac{f_{p_1} v_s}{f_{p_2} v_d} c_{T_1} \tag{13}$$

in which

f_{pn} = the fractions dissolved and particulate

v_s = settling velocity

v_d = sedimentation velocity

Since the bed solids concentration $m_2 >>> m_1$ and $\P m_2$ is usually $>>> 1$, as a reasonable approximation

$$f_{p_2} \sim 1 \text{ and } f_{d_2} \sim 0$$

$$c_{T_2} = p_2 = f_{p_1} \frac{v_s}{v_d} c_{T_1} = \frac{v_s}{v_d} p_1 \tag{14}$$

substituting for $p = rm$

$$r_2 m_2 = \frac{v_s}{v_d} r_1 m_1$$

since $v_d m_2 = v_s m_1$ under steady state, then

$$p_2 = r_1 \tag{15}$$

The above analysis does not take into account the possibility of the exchange of the dissolved component between the bed and the water. This is discussed in the following section, which considers solids resuspension - a condition more likely to enhance exchange of the dissolved component.

2. Type II Analysis - Mixed Bed - Resuspension

The type of analysis described in this section is identical to that of the previous, with the addition of a resuspension term in both the solids and toxic equations. The physical structure of the system is shown diagrammatically in Figure B-1, from which it is apparent that a mass balance equation must be developed for both the water column and the bed, since they are interactive.

a) Suspended Solids

The mass rate of change of solids in the water column is:

$$V_1 \frac{dm_1}{dt} = Qm_i - Qm_1 - V_s A_s m_1 + v_u A_s m_2 \qquad (16)$$

in which

v_u = resuspension velocity - L/T

m_2 = concentration of solids in the bed - M/L^3

and the remaining terms are as previously defined by equation (2) of the previous section.

Expressing the input flux of solids Qm_1 as W and dividing through by the volume V_i, yields

$$\frac{dm_1}{dt} = \frac{W}{V} - \frac{m_1}{to} - \frac{V_s}{H_1} m_1 + \frac{V_u}{H_1} m_z \qquad (17)$$

in which

H_1 = average depth of the water column

A mass balance of the bed solids includes the influx of the settling solids from the water and mass outflow from the bed due to the resuspension and sedimentation:

$$\frac{dm_2}{dt} = \frac{V_s m_1}{H_2} - \frac{V_u m_2}{H_2} - \frac{V_d m_2}{H_2} \qquad (18)$$

in which

H_2 = average depth of the bed

At steady-state conditions, $\frac{dm}{dt} = 0$, the concentration in the bed may be expressed in terms of the concentration in the water from (18):

$$m_2 = \alpha m_1 \tag{19}$$

in which

$$\alpha = \frac{v_s}{v_u + v_d}$$

Substitution of which in equation (17) under steady state yields

$$0 = \frac{W}{V} - m_1 \left[\frac{1}{t_o} + \frac{v_s}{H_1}\right] + \frac{v_u}{H_1} \cdot \frac{v_d}{v_u + v_d} m_1$$

Expressing $\frac{v_s}{H} = K_s$ and solving for m_1, after simplification, gives:

$$m_1 = \frac{W/Q}{1 + \beta K_{s_1} t_o} \tag{20}$$

in which

$$\beta = \frac{v_d}{v_u + v_d}$$

The value of α falls between zero and unity. The latter represents the case of no resuspension $v_u = 0$ and $\beta = 1$, reducing (20) to (3) and the former of no sedimentation $v_d = 0$, reducing (20) to

$$m_1 = W/Q \tag{21}$$

In this case the settling flux is exactly balanced by the resuspension flux, resulting in zero net change and the concentration of solids is simply that of a conservative substance, as indicated by (21).

The bed concentration follows from substitution of (20) in (19):

$$m_2 = \frac{\alpha\, W/Q}{1 + \beta K_s t_o} \tag{22}$$

Algebraic simplification yields

$$m_2 = \frac{W/Q}{\frac{1}{\beta} + \frac{v_d}{H_1} t_o} \tag{23}$$

For lakes or reservoirs of shallow or moderate depth ($H \sim 10M$), moderate high settling velocities ($v_s \sim 3M/DAY$) and low resuspension velocities

(v_u < 1CM/YR), the β term is more than an order less than the sedimentation term and (22) reduces to

$$m_2 = \frac{W}{K_{d_1} V} \tag{24}$$

in which

$$K_{d_1} = \frac{v_d}{H_1}$$

b) Toxic Substances

The equations for the toxic substance are developed in an identical fashion as in the Type I Analysis. Each phase in the water column, the dissolved, c, and the particulate, p, is analyzed separately with adsorption and desorption kinetics in addition to the input, outflow and settling terms. Furthermore, allowance is made for the exchange of the dissolved component between the water and the bed, expressed in terms of the difference in the dissolved concentrations. Addition of the two equations cancels the adsorption-desorption terms and yields:

$$\frac{dc_{T_1}}{dt} = \frac{W_{ct}}{V_1} - \frac{c_{T_1}}{t_o} - K_{s_1} p_1 + K_{u_1} p_2 + K_{b_1} (c_2 - c_1) \tag{25}$$

in which

the subscript 1 refers to the water column and 2 to the bed

c_{T_1} = total concentration of toxic in the water column

$K_{s_1} = \frac{v_s}{H_1}$ = selling coefficient (1/T)

$K_{u_1} = \frac{v_u}{H_1}$ = resuspension coefficient (1/T)

$K_{b_1} = \frac{K_m}{H_1}$ = dissolved exchange coefficient (1/T)

K_m = transfer coefficient of the dissolved between water and bed ($\frac{L}{T}$)

Expressing p and c as fractions of the total concentration (equation 4 of the previous chapter) and combining similar terms yields:

$$\frac{dc_{T_1}}{dt} = \frac{W_{cT}}{V} - [\frac{1}{t} + f_{p_1} K_{s_1} + f_{d_1} K_{b_1}] c_{T_1} + [f_{p_2} K_{u_1} + f_{d_2} K_{b_1}] c_{T_2} \tag{26}$$

the bed equation is developed in a similar fashion

$$\frac{dc_{T_2}}{dt} = [f_{p_1} K_{s_2} + f_{d_1} K_{b_2}] c_{T_1} - [f_{p_2}(K_{u_2} + K_{d_2}) + f_{d_2} K_{b_2}] c_{T_2} \qquad (27)$$

in which

$f_{p_{1,2}}$ = particulate fraction in each segment, 1 and 2

$f_{d_{1,2}}$ = dissolved fraction in each segment, 1 and 2

The working equations for the steady-state condition are developed in a manner similar to that of the solids. Under steady state conditions, the total concentration in the bed is expressed in terms of the total concentration in the water with equation (27). Substitution of (27) in (26) yields the water concentration as a function of the input load, W, and the parameters of the system. Since $m_2 >>> m_1$ and $\P m_2 >> 1$, $f_{p_2} \sim 1$ and $f_{d_2} \sim 0$. For this simplification, which is realistic for $\P > 1000$, the water and bed concentrations are respectively

$$c_{T_1} = \frac{W/Q}{1 + \beta f_d [\P m_1 K_{s_1} + K_{b_1}] t_o} \qquad (28)$$

$$c_{T_2} = \frac{f_p K_{s_2} + f_d K_{b_2}}{K_{u_2} K_{d_2}} c_{T_1} \qquad (29)$$

in which

$$\beta = \frac{v_u}{v_u + v_d}$$

$$f_d = \frac{1}{1+\P m_1}$$

$$f_p = \frac{\P m_1}{1+\P m_1}$$

$$K_s = \frac{v_s}{H}$$

$$K_b = \frac{K_m}{H}$$

$$K_u = \frac{v_o}{H}$$

$$K_d = \frac{v_d}{H}$$

For the condition of negligible exchange of the dissolved between water and bed ($K_b \sim 0$), the above equations reduce to

$$c_{T_1} = \frac{W/Q}{1+\beta f_{p_1} K_{s_1} t_o} \tag{30}$$

$$c_{T_2} = \alpha\, c_{T_1} \tag{31}$$

in which, in accordance with equation 14

$$\alpha = \frac{v_s}{v_u + v_d}$$

For toxics of high partition coefficient and systems of high solids ($\P m_1 \gtrsim 5$), the above respectively reduce to equations (21) and (19), the equivalent solids equations.

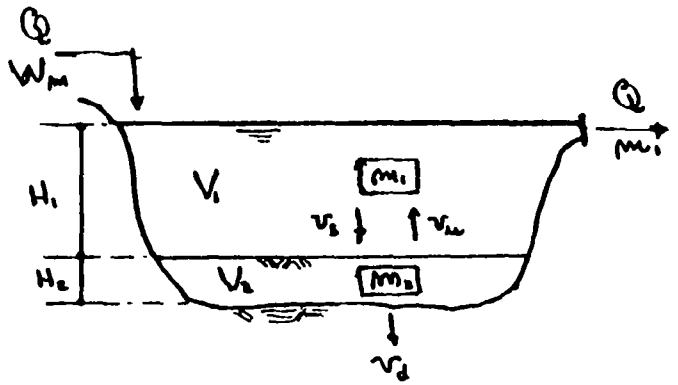

SOLIDS

SUBSCRIPTS

1 WATER

2 BED

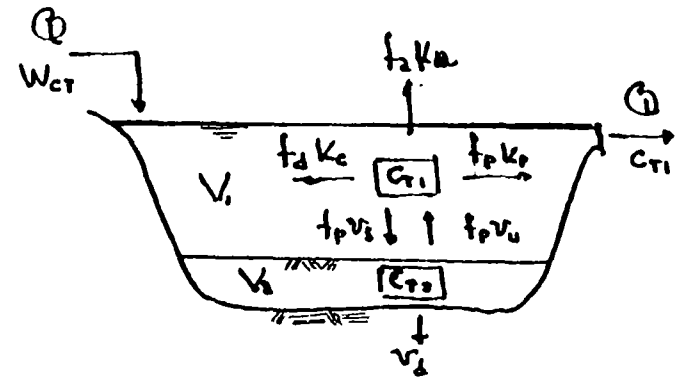

TOXIC

ANALYSIS TYPE	RESUSPENSION
I	$v_u = 0$
II	$v_u > 0$
Bed Transport	Zero

LEGEND		UNITS
W	MASS INFLUX	M/T
Q	FLOW	L^3/T
V	VOLUME	L^3
H	DEPTH	L
M	SOLIDS	M/L^3
C_T	TOXIC - TOTAL	M/L^3
f_d	DISSOLVED FRACTION	-
f_p	PARTICULATE FRACTION	-
v_s	SETTLING VELOCITY	L/T
v_u	RESUSPENSION VELOCITY	"
v_d	SEDIMENTATION VELOCITY	"
K_e	EVAPORATION COEFFICIENT	1/T
K_c	DISSOLVED DECAY	"
K_s	SETTLING COEFFICIENT	"
K_p	PARTICULATE DECAY	"

FIG. B-1 Schematic of Type I & Type II Solids Parameters

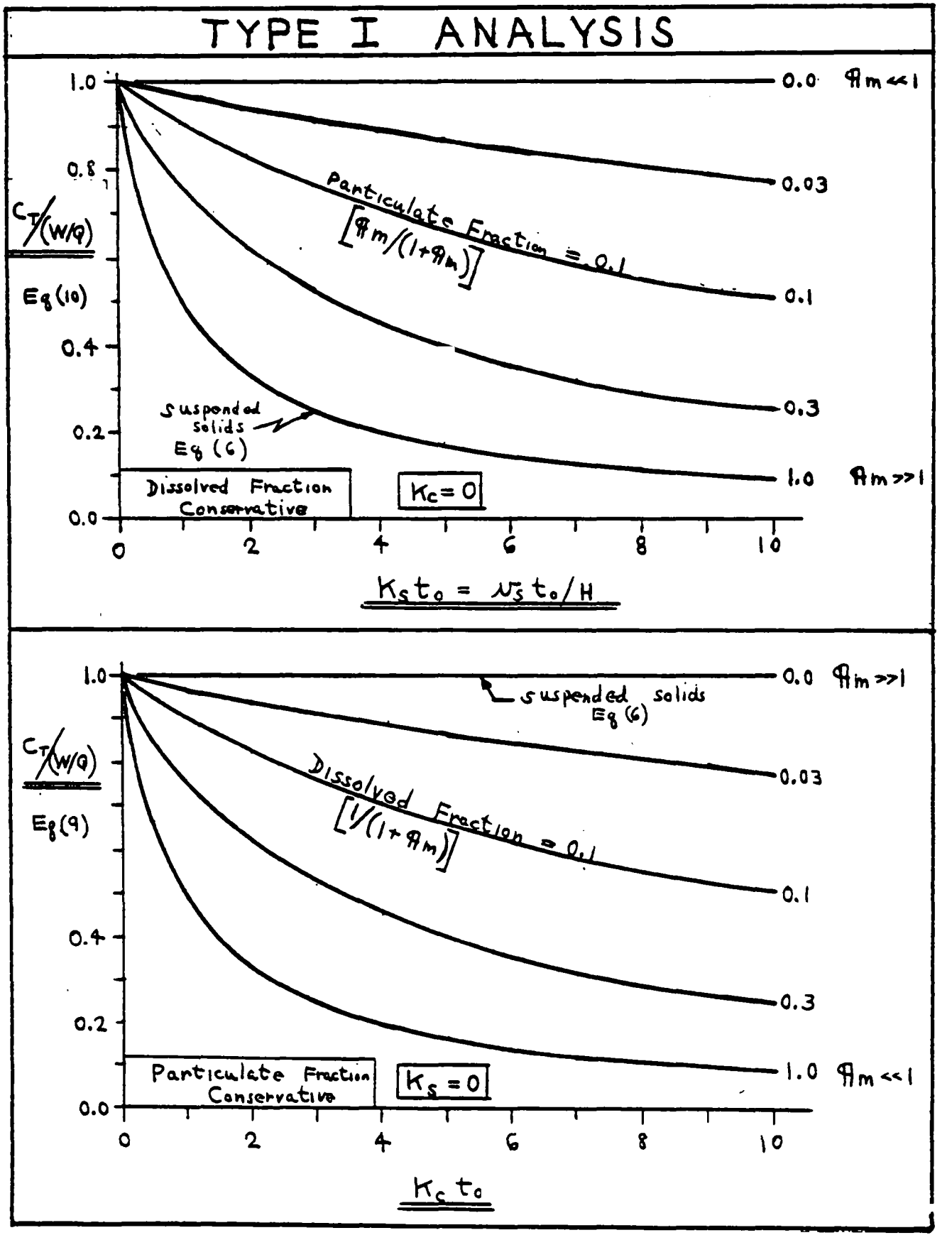

FIG. B-2 Fraction Remaining for Various Detention Times and Kinetic Parameters

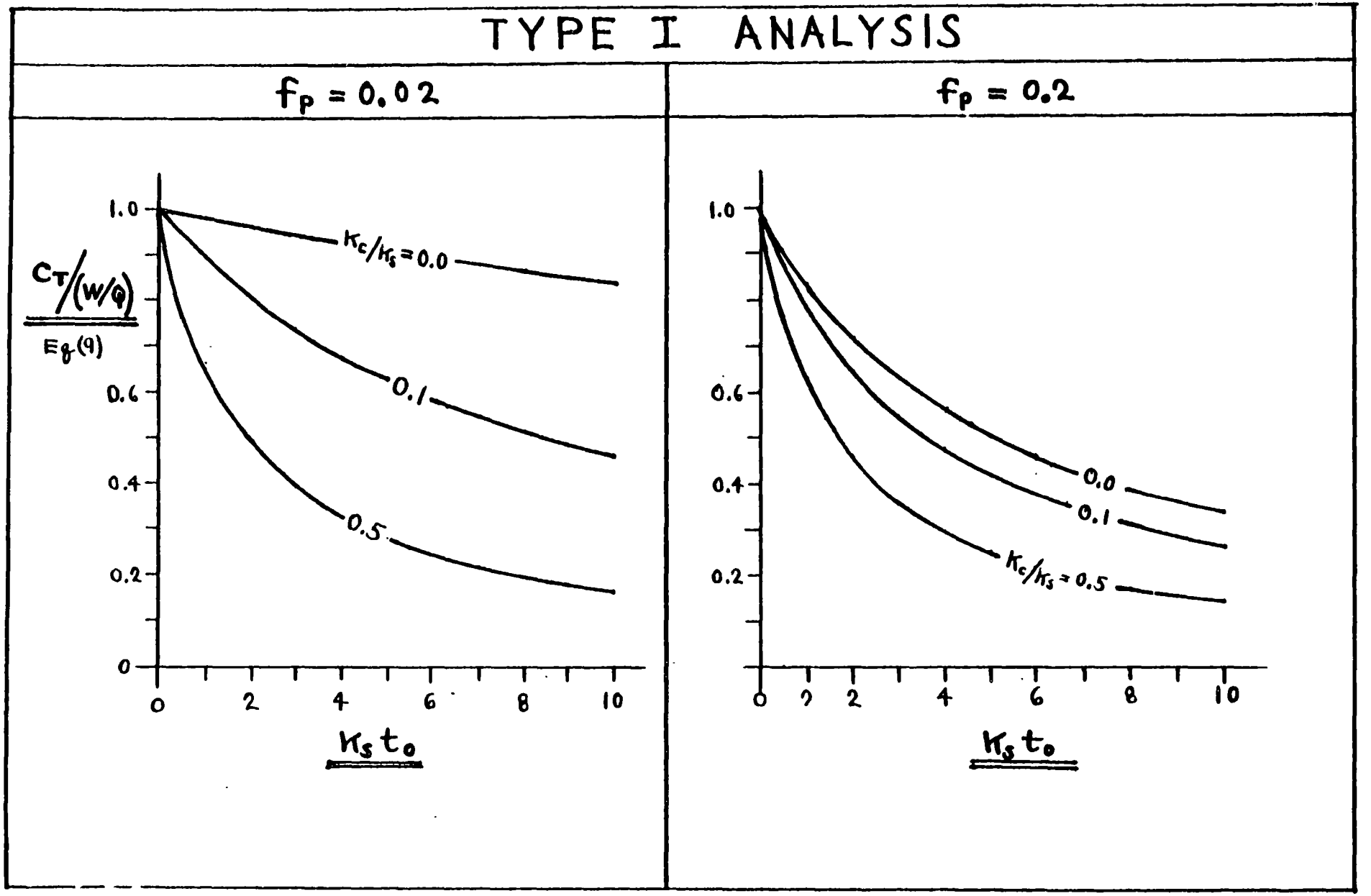

FIG. B-2 (cont'd) Fraction Remaining for Various Detention Times and Kinetic Parameters

Saginaw Bay - Solids and PCB Model*

Steady State Toxicant Model - Theory

In order to understand the interactions between sediments, water column solids and a given toxicant, several time variable models have been employed. These models attempt to incorporate the mechanisms of solids settling, sediment resuspension, net sedimentation and transfer to the deep sediments, interstitial diffusion of dissolved toxicant and other decay and transfer mechanisms. The difficulty with the more complex interactive time variable toxicant models is that the specification of the various parameters (e.g. resuspension velocity and surface sediment solids concentration) is not unique and various combinations of the parameters, within reported ranges, yield a similar calibration.

Consequently, it is desirable that a procedure be developed that utilizes available field data for calibration and that minimizes the number of parameters that must be specified. A simplified steady state approach provides a direction. Since the analysis framework is steady state, questions related to the time it would take to reach a new equilibrium state cannot be answered. Furthermore, the time for the entire system of water column and sediment to reach steady state may be long. On the other hand, as noted above, complex time variable models sometimes tend to obscure the principle mechanisms of net settling and water column-sediment exchanges. A steady state framework, therefore, is a simplified

---

* Robert V. Thomann and John A. Mueller

first approximation to chemical fate that does not address issues related to temporal questions but does provide a useful model for estimating chemical concentrations in a simpler way.

Suspended Solids Model

Consider first the steady state model for suspended solids in a multi-dimensional system. It is assumed that the bed sediment that is coupled to the water column is stationary. Figure 10 shows a definition sketch. The mass balance equation for the solids in segments #1, and 1s, using backward finite differences is

$$0 = W_1 - Q_{12}M_1 + E'_{12}(M_2-M_1) - v_{s1}AM_1 + v_{u1}AM_{1s} \quad (10)$$

$$0 = v_{s1}AM_1 - v_{u1}AM_{1s} - v_{sd1}AM_{1s} \quad (11)$$

where M_1 and M_2 = solids concentration in water column segment 1,2 [M_s/L^3_{w+s}; L_{w+s} = volume of water plus solids]

M_{1s} = solids concentration in sediment segment, 1s [M_s/L^3_{w+s}]

W_1 = input solids loading [M_s/T; M_s=mass of solids]

Q_{12} = flow from segment 1 to 2 [L^3_w/T]; A=sediment area [L^2]

E'_{12} = bulk dispersion between 1 and 2 [L^3_w/T]

v_{s1} = settling velocity [L/T]

v_{u1} = resuspension velocity [L/T]

v_{sd1} = sedimentation velocity [L/T]

A similar set of equations can be written for segments 2 and 2s.

Equation (11) can be solved for the sediment concentration as:

$$M_{1s} = \left[\frac{v_{s1}}{v_{u1}+v_{sd1}}\right]M_1 = \alpha_1 M_1 \quad (12)$$

where $\alpha_1 = \dfrac{v_{s1}}{v_{u1}+v_{sd1}}$

Substituting eq. (12) into eq. (10) and simplifying gives:

$$0 = W_1 - Q_{12}M_1 + E'_{12}(M_2-M_1) - w_{s1}AM_1 \quad (13)$$

where w_{s1} is the net loss of solids from water column segment #1 and is given by

$$w_{s1} = \frac{v_{s1}v_{sd1}}{v_{u1}+v_{sd1}} \quad (14)$$

Note that eq. (13) essentially states that for a multi-dimensional system such as Saginaw Bay, the sediment interaction can be substituted out of the equation set and incorporated in the net loss parameter, w_{s1}. A mass balance around the sediment segment then yields

$$v_{sd1}AM_{1s} = w_{s1}AM_1 \quad (15)$$

which simply states that the solids flux into the sediment layer from the water column is balanced by the solids flux leaving the sediment segment due to net sedimentation. In principle, the net sedimentation velocity can be measured so that the solids concentration in the sediment can be calculated from eq. (15). In practice, however, the spatial variability in the sedimentation velocity and the uncertainty in the sediment solids concentration that interact with the water column make it difficult to separate the two quantities. This is a reflection of the occurrence of nepholoid layers or "fluff" layers that are at the boundary between the water column and the bed sediment. As a consequence, in the absence of detailed data on v_{sd1} or M_{1s}, only the net flux to the sediment from the water column can be estimated. This assumes, of course, that all terms in the water column equation (13) are known with more certainty than the sedimentation velocity or the sediment solids.

If now suspended solids data are available for the water column then the equation set represented by eq. (13) can be used to obtain spatially varying estimates of w_{si} for any segment i. Note that the sediment segments are not included directly in the model but are incorporated in the net loss term.

Preliminary estimates of w_{si} may be obtained from eq. (15) or from solving eq. (13) directly for w_{si} with given water column solids concentrations. These estimates, however, may be subject to wide variations, including inconsistency in net sedimentation as a result of small changes in water column concentrations. The procedure finally adopted in this research was to obtain estimates of w_{si} from trial and error calculations of the water column model to calibrate to the observed suspended solids concentrations. A single set of net loss rates is then obtained that balances mass in the water column and sediment but does not require specification of the settling or resuspension velocities.

For the case of net gain from sediment, that is a steady state erosion zone, the water column equation is:

$$0 = W_1 - Q_{12}M_1 + E'_{12}\ (M_2-M_1) + v_{uB}AM_{1sB} \tag{16}$$

where v_{uB} is scour velocity and M_{1sB} is sediment solids concentration available for scour.

$$\text{Let } W_1 - Q_{12}M_1 + E'_{12}\ (M_2-M_1) = m \tag{17}$$

where m[M/T] is the net production (loss) of solids.

A useful procedure for this case is then:

1) Compute m, the net mass production or loss of solids for each segment

2) If m positive, then

$$m = w_{s1}AM_1 \text{ and}$$

$$w_{s1} = \frac{m}{AM_1}$$

3) If m negative, then

$$m = v_{uB}{}^{AM}{}_{lsB}$$

and if desired, v_{uB} the net scour velocity can be calculated.

Toxicant Model

The basic objective of the steady state toxicant model is to obtain a modeling framework that utilizes available field data for calibration, and eliminates the need for directly specifying sediment-water interactions. The approach then is not from first principles of detailed mechanisms of settling, resuspension and interstitial diffusion, but rather from an analysis of field data. It is assumed that laboratory data are available for the following:

1) water column rates of degradation, photolysis, vaporization, hydrolysis
2) sediment microbial degradation rates
3) partition coefficients at water column and sediment solids concentrations.

The available field data are combined with these laboratory data in such a way that overall loss and transfer coefficients are obtained.

The analysis begins from the point where the dissolved and particulate fractions of the chemical have been assumed in local equilibrium, and the total toxicant mass balance equation for a given segment has been obtained. The equation for segment 1 is then:

$$0 = W_{T1} - Q_{12}\, c_{T1} + E'_{12}(c_{T2}-c_{T1}) - v_{s1}{}^{Af}{}_{p1}c_{T1}$$

$$+ v_{u1}\, {}^{Af}{}_{p1s}c_{T1s} + E'_{1s}F_{D1s}c_{T1s} - E'_{1s}f_{D1}c_{T1}$$

$$- K_{11,1}f_{D1}\, V_1 c_{T1} \qquad (13)$$

The equation for the sediment segment, #1s is

$$0 = v_{s1} A\, f_{p1} c_{T1} - v_{u1} A\, f_{p1s} c_{T1s} + E'_{1s} f_{D1} c_{T1}$$

$$-E'_{1s} f_{D1s} c_{T1s} - v_{sd1} f_{p1s} A\, c_{T1s} - K_{11,s} f_{D1s} V_{1s} c_{T1s} \qquad (19)$$

where W_{T1} = input toxicant loading $[M_T/T]$

c_{T1}, c_{T2}, c_{T1s} = total toxicant concentration in segments 1, 2 and 1s respectively $[M_T/L^3_{w+s}]$

$K_{11,1}$ = overall loss rate of dissolved form (e.g. vaporization, decay) $[1/T]$

$K_{11,s}$ = decay of dissolved toxicant in sediment $[1/T]$

V_1, V_{1s} = volumes of segments 1 and 1s respectively $[L^3_{w+s}]$

E'_{1s} = interstitial water sediment - water column diffusion coefficient $[L^3_w/T]$

The fraction of toxicant in the particulate form is given by

$$f_{p1} = \frac{\pi_1 M_1}{1 + \pi_1 M_1} \qquad (20)$$

and the fraction dissolved is

$$f_{D1} = \frac{1}{1 + \pi_1 M_1} \qquad (21)$$

where π_1 is the partition coefficient $[M_T/M_s \div M_T/L^3_{w+s}]$ at ambient water column solids concentrations.

Similar expressions are used for f_{p1s} and f_{D1s}, the fraction particulate and dissolved respectively in the sediment segment, 1s, that is,

$$f_{p1s} = \frac{\pi_{1s} M_{1s}}{1+\pi_{1s} M_{1s}} \qquad (22)$$

and $$f_{D1s} = 1/1 + \pi_{1s} M_{1s} \qquad (23)$$

where π_{1s} is the partition coefficient at ambient sediment solids concentrations.

If now equations (9) and (10) are added, one obtains an interesting result:

$$0 = W_{T1} - Q_{12} c_{T1} + E'_{12} (c_{T2}-c_{T1}) - K_{11} f_{D1} V_1 c_{T1}$$

$$- v_{sd1} f_{p1s} Ac_{T1s} - K_{11s} f_{D1s} V_{1s} c_{T1s} \quad (24)$$

It can be noted that all of the sediment interaction terms are eliminated through the addition of the equations. This is a result of taking the mass balance around the water column and sediment so that the only loss terms are those that are net from the entire system. These net loss terms are fluxes out due to transport and dispersion, decay in water column and sediment and net sedimentation of mass out of the sediment segment. Of course, equation (24) still includes the sediment total toxicant concentration.

Therefore, let

$$\alpha_{T1} = \frac{c_{T1s}}{c_{T1}} = \Pi \frac{M_{1s}}{f_{p1s}} \quad (25)$$

where $$\Pi = \frac{r_{1s}}{c_{T1}} \frac{[M_T/M_s] \text{ sed.}}{[M_T + L^3_{w+s}] \text{ water}} \quad (26)$$

where r_{1s} is the toxicant concentration on a solids basis in the sediment.

The variable Π represents an overall partitioning between the solids toxicant concentration in the sediment and the total toxicant concentration in the water column. Note also from the solids balance discussed previously

$$\alpha_{T1} = \left(\frac{w_{s1}}{v_{sd1}}\right) \left(\frac{f_{p1}}{f_{p1s}}\right) \left(\frac{r_{1s}}{r_1}\right) \quad (27)$$

where r_1 is the water column toxicant concentration on a solids basis $[M_T/M_s]$. Substituting eq. (25) into (24) and simplifying gives:

$$0 = W_{T1} - Q_{12} c_{T1} + E'_{12} (c_{T2}-c_{T1}) - w_{T1} Ac_{T1} \quad (28)$$

where w_{T1} [L/T] is the net loss of toxicant and is given by

$$w_{T1} = K_{11} f_{D1} H_1 + \alpha_{T1} [v_{sd1} f_{p1s} + K_{11s} f_{D1s} H_{1s}] \quad (29)$$

where H_1 and H_{1s} are the depths of the water column and sediment respectively.

Equation (28) is a mass balance on the water column toxicant only and all sediment interactions are embedded in the net loss of toxicant w_{T1}. The estimate of this net loss rate can be obtained from the water column field data and a finite segment water quality model without sediment segments. The procedure then is

1) From c_{T1}, estimate w_{T1} for each segment using a water column model

2) From w_{T1} and laboratory data on decay rates in water column and sediment, and partition coefficients, and estimates of net sedimentation from field data and the solids balance model, compute α_{T1} from eq. (29) as

$$\alpha_{T1} = \frac{w_{T1} - K_{11} f_{D1} H_1}{\beta_1} \quad (30)$$

where $\beta_1 = v_{sd1} f_{p1s} + K_{11s} f_{D1s} H_{1s}$

3) Calculate the sediment toxicant concentration from eq. (27) as

$$r_{1s} = [\alpha_{T1} \left(\frac{f_{p1s}}{f_{p1}}\right) \left(\frac{v_{sd1}}{w_{s1}}\right)] r_1 \quad (31)$$

The latter calculation can be used as an additional calibration for the model if data on r_{1s}, the sediment toxicant concentration are available. Such is the usual case.

A very useful special case is obtained for those toxicants that are highly sorbed to solids and for which sediment decay and diffusion processes are negligible. PCBs are an example. If then it is assumed that K_{11s} and E'_{1s} are zero, then it can be shown that

$$w_{T1} = K_{11} f_{D1} H_1 + f_{p1} w_{s1} \quad (32)$$

and $r_{ls} = r_l$ (33

This result indicates that for PCB, if the net solids loss to the sediment, w_{sl} can be obtained and information is available on the partition coefficient, then the entire steady state PCB problem can be approached through the simple equations (32) and (33). For the case of no net sedimentation, then $w_{sl} = 0$ and

$$w_{Tl} = K_{ll} f_{Dl} H_l$$

and $r_{ls} = r_l$.

These special case models for $K_{ll}=0$ were applied to the PCB distribution in Saginaw Bay.

Application: Saginaw Bay Solids & PCB Model

After a considerable amount of time variable modeling on Saginaw Bay, including long-term calculations for the Great Lakes of Cesium-137, it was determined that the initial thrust on Saginaw Bay could best be accomplished via the steady-state model previously discussed that incorporates horizontal transport, net solids settling and resuspension and sedimentation, and the interaction of the solids with PCBs. Accordingly, the 5 segment Saginaw Bay model was prepared for a steady-state computation.

Segmentation & Transport Coefficients

The segmentation was obtained from the Grosse Ile Laboratory of the EPA under this cooperative agreement, including segment volumes, areas and depths. The dispersive exchange coefficients and the flows between each of the segments and Lake Huron were also obtained from hydrodynamic modeling conducted by the Grosse Ile Laboratory. That work, however, concentrated on the time variable aspects of 1977 and 1979 and, as a result, the coefficients of turbulent exchange and flow have to be modified tc represent a long-term steady-state condition. The temporally averaged flows and exchange coefficients that were used in the

steady-state computation for the five segments in the water column are as shown in figure 11 together with the segmentation.

A chloride calibration was then performed using these flows and bulk dispersion values. Chloride data were obtained from STORET for the years 1974 through 1977 and all data found in a segment were averaged for each annual period for that segment. Loadings consisted of the Saginaw River discharge and atmospheric sources (6670 kg/day), the latter values obtained from data in IJC (1977). Saginaw River chloride loadings for 1974 were estimated to be from 1.04 to 1.15 million kg/day according to Grosse Ile and Canale, and the 1977 discharge was 0.8 million kg/day as per Grosse Ile. For the simulation, the 1977 value was used. Boundary conditions were selected to be 6.3 mg/l for both segment 4 and 5 on the basis of available STORET data nearest the open lake boundary of the model. The comparison of calculated concentrations of chlorides with the 1974-1977 data in figure 12 indicates good agreement and, therefore, confirms the transport and dispersion regime as representative of steady state conditions.

Suspended Solids Calibration

The Saginaw River and smaller tributaries to the Bay, shoreline erosion, atmospheric fallout and phytoplankton biomass are the components of solids loads used to calibrate the solids in Saginaw Bay. Grosse Ile provided a long-term estimate of the Saginaw River load, whereas the contributions of other tributary drainage areas were estimated from average flows and a long-term average suspended solids concentration estimated for the Saginaw River. Bank erosion values were derived from county by county erosion volumes in Monteith and Sonzogni (1976) and proportioned to Saginaw Bay on the basis of shoreline length. Volumes of eroded material were converted to mass loadings by assuming a porosity of approximately 60% and a specific gravity of 2.65. To account for immediate settling of heavier fractions, a 50% reduction was used to obtain the final estimates. Atmospheric sources were obtained from the IJC report cited previously. Phytoplankton biomass was obtained from a algal model simulation performed

by the Grosse Ile Laboratory. A summary of all segment loads by class is contained in Table 2. The predominance of the Saginaw River and phytoplankton loadings is apparent.

Boundary conditions, consistent with limited available data, were selected primarily on the basis of trial and error. Preliminary computations indicated that initial estimates of approximately 2 mg/l solids at the open lake boundary were too low since calculated solids concentrations in segments 4 and 5 were well below observed values and mass balances of these segments indicated that the boundary fluxes dominated these segments. Final values of 4.3 mg/l for segment 4 and 5.5 mg/l for segment 5 were selected. The former value is thought to be more associated with advective flow entering the Bay from Lake Huron and the latter value more representative of observed segment 5 concentrations leaving the Bay with the net advective flow (see net circulation, figure 11).

Net removal rates of the suspended solids were then assigned to segments 2,4, and 5 where solids deposition zones are either documented to occur (segment 2) or estimated to occur (segments 4 and 5). No net removal rates were assigned to segments 1 and 3 since sedimentation appeared to be minimal there on the basis of sediment solids and PCB data in sediment cores. Initial values of the net removal rates were made from mass balances of each segment using observed water column solids concentrations. There were then input to the 5 segment Saginaw Bay model, using the transport coefficients previously calibrated, and adjusted until the calculated and observed suspended solids concentrations were in agreement. As seen in figure 13, the calculated values in the water column are in good agreement with the observed data of 1976 through 1979, when values of the net removal rate of 12.7, 13.8 and 9.7 meters/year are used for segments 2,4 and 5 respectively. Sensitivity analyses indicate that the differences in the net loss rates in segments 2,4 and 5 are not significant. Equally acceptable calibrations are obtained for values between 10 and 20 m/yr. for segments 2,4 and 5.

With the estimated net removal rate of solids w_s from the water column, the flux of solids into the bed is calculated as $w_{si}AM_l$ [M_s/T]. This is equal to the sedimentation flux which is calculated as $v_{sdl}AM_{ls}$. Since both v_{sdl} and M_{ls} vary with sediment depth, no single value can be specified. However, from eq. (15) the relationship between v_{sdl} and M_{ls} is unique. If v_{sdl} is selected, then M_{ls} is a predetermined value. Log-log plots of the relationships between the sedimentation rate and the bed solids concentration are included in the bottom of figure 13.

A considerable amount of effort was expended in determining the sediment concentrations of solids drawing on the work of Robbins (1980). From sediment cores located primarily in segment 2 of the Saginaw Bay model, a selected number of cores were examined for the sediment solids concentration at the midpoints of a 10 cm well-mixed layer and at the midpoints of two deeper 5 cm layers. The results are summarized in Table 3. For the well-mixed surface sediment layer, sediment concentrations average approximately 390,000 mg/l for nine cores with a range of approximately 230,000 to 900,000 mg/l. This range is shown in figure 13 for segment 2. If the lower value of the range is used, the corresponding sedimentation rate for the 10 cm well-mixed layer would be approximately 0.8 mm/yr., somewhat less than a previously reported value of 3 mm/yr. (Robbins, 1980).

These results indicate the utility of the simple steady state solids balance. The water column data are known with some accuracy and do not exhibit marked spatial gradients. Note that the maximum spatial differences in the average water column suspended solids is about a factor of four. In contrast, the spatial heterogenerity of the sediment is quite marked with regions of deposition, scour and no apparent net deposition. Suspended solids may then vary markedly in a given segment horizontally , but, most importantly, vertically. Boundary layer sediment solids "fluff" layers may be available for interaction with the surface water column at concentrations less than sediment data from cores. Conversely, estimated net

sedimentation velocities are often cited only for those regions of deposition and not over an area equivalent to a model segment of Saginaw Bay. The calculation discussed above provides a good estimate of the net flux to the sediment over the segment area. The trade off between net sedimentation over the segment area and sediment solids concentrations is shown in the lower figures of figure 13. If, as noted above, the solids data from the sediment cores are used, then the net sedimentation velocity varies from 0.25 to 0.8 mm/yr. or almost one order of magnitude less than the 3mm/yr. previously cited. If on the other hand, an average net sedimentation over the entire area of segment 2 is fixed at say 3 mm/yr., then the sediment solids concentration that is consistent with that sedimentation velocity is about 45,000 mg/l or one order of magnitude less than the average sediment solids in the top 5 cm of the cores. The results indicate, therefore, that with only the net flux of solids to the sediment as known with some confidence, then it is not possible to uniquely specify the net sedimentation or boundary layer sediment solids. Additional tracers (of which the radionuclides or PCBs are examples) would provide additional information that could aid in specifying the net sedimentation and sediment solids concentrations.

A mass balance of suspended solids for the entire model is presented in figure 14 for three flux categories: the external and internal loads, the net flux removed from the water column and the boundary transport. In the lower right panel, it is seen that 2,970,000 lb/day of solids enter the model, 40% (1,190,00 lb/day) is incorporated into the sediments, and the remaining 60% (1,780,000 lb/day) leaves the Bay and enters Lake Huron.

PCB Calibration

With the horizontal transport and net loss rate of suspended solids calibrated, analysis of the PCB concentrations can proceed. Total PCB loadings were obtained from the Grosse Ile Laboratory for 1979, the first year for which total PCB field data were available. As noted in Table 4, the Saginaw River load is approximately 75% of the total load and atmospheric

sources contribute an additional 25%. Although open lake concentrations are reported to be in the 1 ng/l range, the boundary condition was selected as 10 ng/l - the value needed to calibrate observed data in segments 4 and 5.

Partition coefficients were selected on the basis of observed dissolved and particulate fractions and values of 10,000, 50,000 and 100,000 µg/kg per µg/l were selected for segments 1, 2 and 3, and 4 and 5, respectively. These are in accord with values calculated from field measurements, as seen in Table 5. With the partition coefficients selected, the removal rates of total PCB are then calculated as the particulate fraction of the suspended solids net settling rate (see eq. (32) for $K_{11}=0$). For segment 2, for example, the net removal rate w_{T2} is:

$$w_{T2} = w_{s2} \times f_{p2}$$

where $$f_{p2} = \frac{2^{M}_{2}}{1+ {}_{2}M_{2}} = \frac{(.05)(11.2)}{1+(.05)(11.7)} = 0.37$$

and then $w_{T2} = (12.7)(.37) = 4.7$ m/yr.

Similarly, the net total PCB removal rates for segments 4 and 5 are 4.8 and 3.5 m/yr., respectively.

With the loads, boundary conditions and net removal rates described above, together with the horizontal transport, the steady state model is used to calculate total PCB concentrations in the water column. The top panel of figure 15 shows the agreement between calculated values and data observed in 1979. Dissolved and particulate fractions also agree well with observed data, as noted in the next two panels of the figure. The bottom panel displays the particulate PCB per unit weight of solids and, again, agreement between observed means and calculated values is good for the water column.

In the previous theoretical section of this report, it was shown that, for depositional areas, and areas where settling and resuspension were equal, the PCB per unit weight of solids in the water column (r_1) - a reproduction of the

bottom panel of figure 15. Directly below, is a plot of the PCB in the sediment (r_{1s}), where the solid line is the calculated value of r_{1s} assuming $r_{1s}=r_1$. The data are segment averaged sediment concentrations for 1979, provided by the Grosse Ile Laboratory. Agreement between calculated and observed means is good for segments 1 and 2. It is hypothesized that segment 3 may be a net erosion zone (see suspended solids calibration, figure 12) in which case the assumption that $r_{1s} = r_1$ is not appropriate.

A mass balance of total PCB is shown in figure 17 for the Saginaw River and atmospheric loads, net settling fluxes and boundary fluxes. As noted in the lower right panel, approximately 30% of the total PCB entering Saginaw Bay from external loads is incorporated into the sediments of the Bay and approximately 70% is exchanged with Lake Huron.

The separate effects of the external PCB loads (Saginaw River and atmospheric) and the boundary conditions are illustrated in figure 18. The total PCB due to both external loads and boundary conditions is compared with observed data in the top panel of the figure, where the peak concentration in segment 1 is seen to be approximately 24 ng/l. Of the 24 ng/l, approximately 6 ng/l is due to the boundary condition (center panel) and the remaining 18 ng/l is the effect of the loads. Thus, complete removal of the Saginaw River loads and maintenance of the boundary at 10 ng/l would result in at least a 75% reduction in the segment 1 PCB concentration under this new steady-state condition. Additional reduction would occur since some significant fraction of the boundary concentration is probably caused by the loads. Therefore, reducing the boundary concentration to lower open Lake Huron levels would reduce the concentration in segment 1. If, for example, the boundary decreased to a value of 5 ng/l, the concentration in segment 1, under the no-load situation, would be approximately 3 ng/l.

A mass balance of PCB for the external loads alone (figure 19) shows that approximately 10% of the load entering the Bay is incorporated in the sediment and 90% enters Lake

Huron - the bulk of it from segment 5. A similar balance for the boundary condition reveals a net source from Lake Huron into segment 4, and a net sink into the Bay sediments before the remaining mass returns to Lake Huron from segment 5 (figure 20).

Conclusion

A simplified procedure for estimating the concentrations of PCB in the water column and sediment of a water body due to external sources of PCB has been applied to Saginaw Bay. Due to its simplicity, many insights can be gained with respect to the factors governing the distribution of toxicant in a natural water system, including the net pathways of the material.

Further work is proceeding on testing the sensitivity of the results to the net removal rates and the impact of the PCB boundary conditions. The PCB simulation will be redone using 1979 flow and dispersion coefficients in order that transport and loading information would be synchronous.

TABLE 2

ESTIMATED LONG-TERM AVERAGE SUSPENDED SOLIDS INPUTS

Model Segment	Tributary Loads (lb/day)	Bank Erosion (lb/day)	Atmospheric Loads (lb/day)	Phytoplankton Mass (lb/day)	Total Loading (lb/day)
1	1,232,000*	28,200	10,100	132,200	1,402,500
2	123,900	92,600	31,400	341,600	589,500
3	34,900	63,900	15,100	143,300	257,200
4	21,900	124,100	23,700	176,300	346,000
5	43,700	50,700	24,700	251,300	370,400
Total	1,456,400	359,500	105,000	1,044,700	2,965,600

*Saginaw River 1,208,000

TABLE 3

SEDIMENT SOLIDS CONCENTRATIONS[1]

Station[2]	Core Solids Concentrations (mg/l (Bulk)) at Following Depths 5 cm	12.5cm	17.5 cm
1A	510,000	1,350,000	1,130,000
6A	250,000	700,000	730,000
11A	230,000	560,000	620,000
24-1	280,000	390,000	507,000
37-1	900,000	1,040,000	730,000
43-1	340,000	420,000	450,000
46-1	280,000	450,000	850,000
50-A	250,000	340,000	420,000
28-A	450,000	790,000	1,070,000
Mean	390,000	670,000	720,000
Std.Dev.	200,000	320,000	240,000

[1] Data from Robbins (1980)

[2] Stations all in Saginaw Bay model segment 2.

TABLE 4

ESTIMATED TOTAL PCB LOADING FOR 1979[1]

Segment	Tributary Loads (lb/day)	Atmospheric Loads (lb/day)	Total Loading (lb/day)
1	1.61[2]	0.05	1.66
2	-	0.16	0.16
3	-	0.07	0.07
4	-	0.12	0.12
5	-	0.12	0.12
Totals	1.61	0.52	2.13

[1] Source: USEPA ERL Grosse Ile

[2] Saginaw River

TABLE 5

Total PCB PARTITION COEFFICIENTS[1]

Segment	Partition Coefficient (π) from Observed Concentrations		π Used in Model
	Mean	Approx. Range	
1	10,000	700- 30,000	10,000
2	80,000	7,000-190,000	50,000
3	60,000	20,000-160,000	50,000
4	90,000	10,000-250,000	100,000
5	280,000	10,000-920,000	100,000

(1) All values in µg/kg per µg/l

Data from Grosse Ile Laboratory (1979)

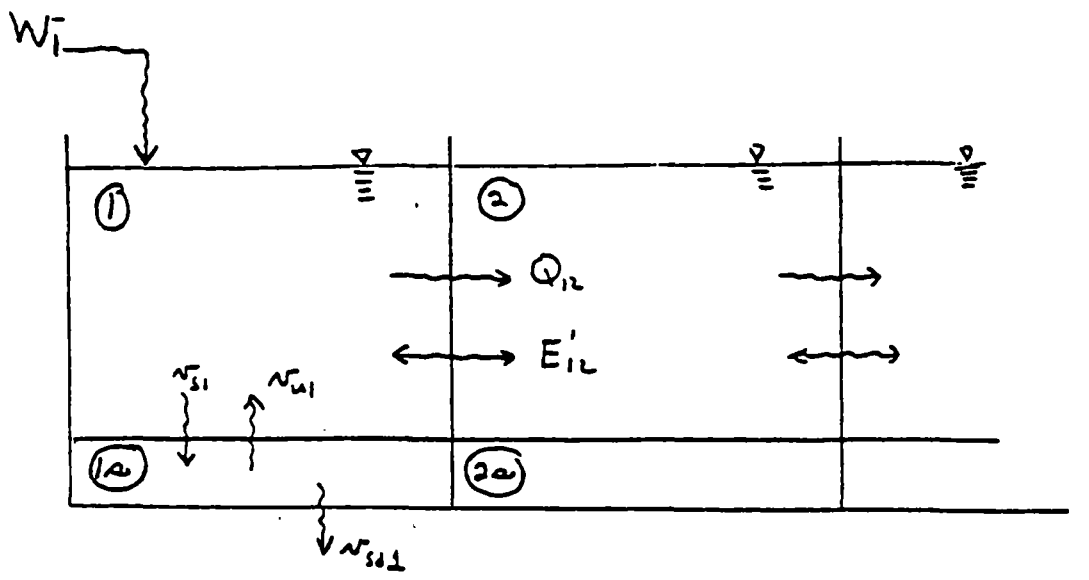

Fig. 10 · Definition sketch for steady state model.

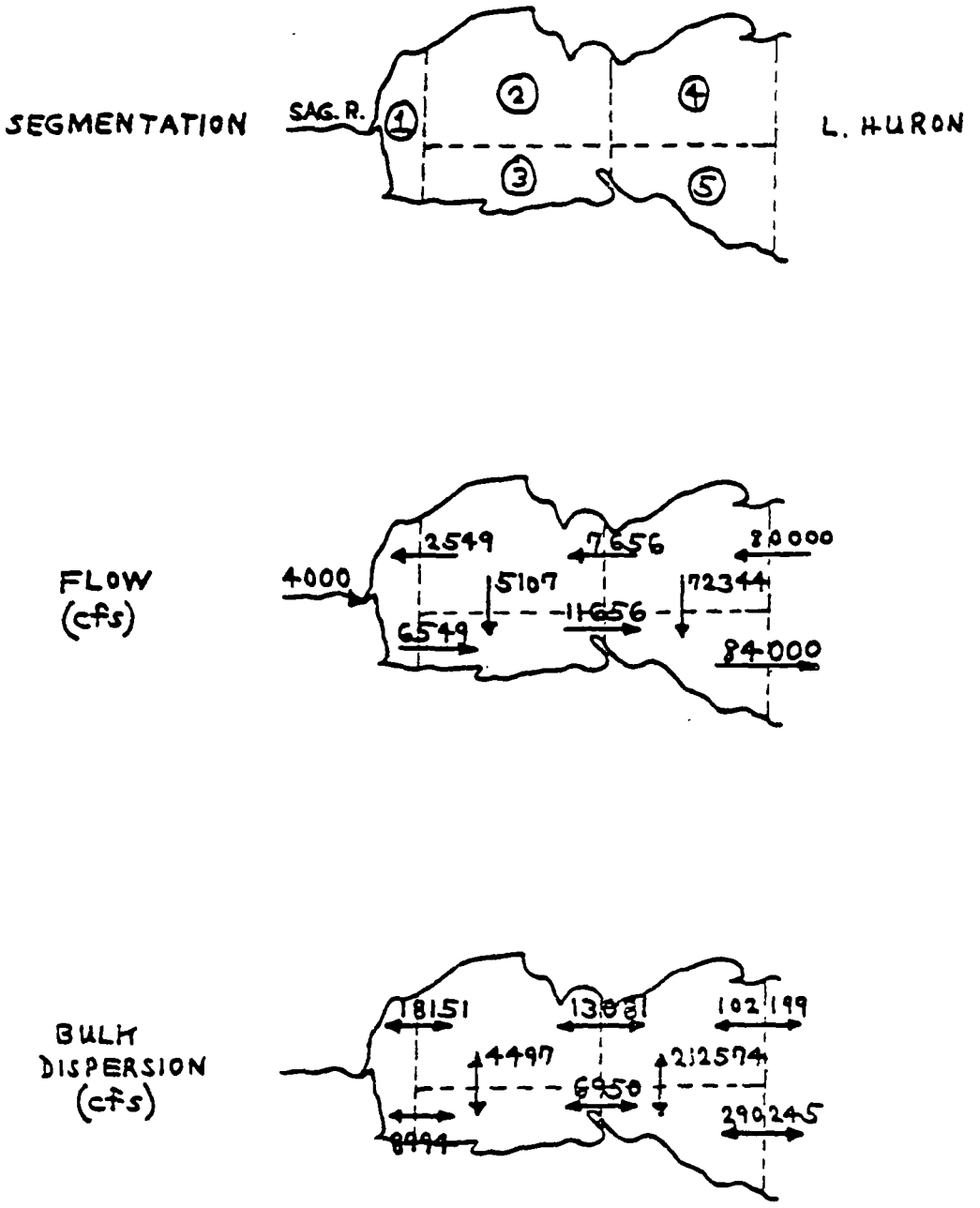

FIGURE 11 SEGMENTATION & ESTIMATED LONG-TERM AVERAGE TRANSPORT COEFFICIENTS IN SAGINAW BAY

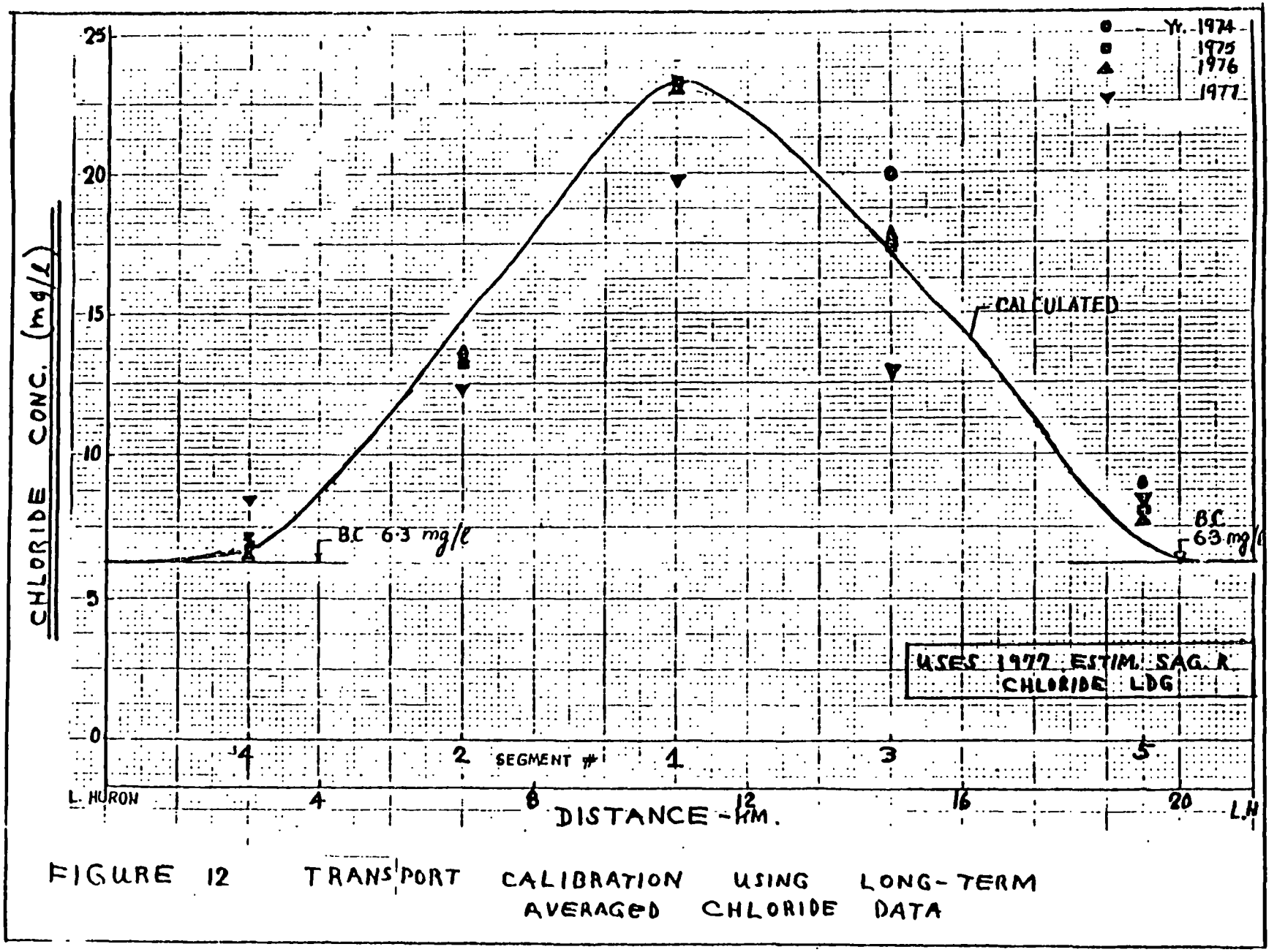

FIGURE 12 TRANSPORT CALIBRATION USING LONG-TERM AVERAGED CHLORIDE DATA

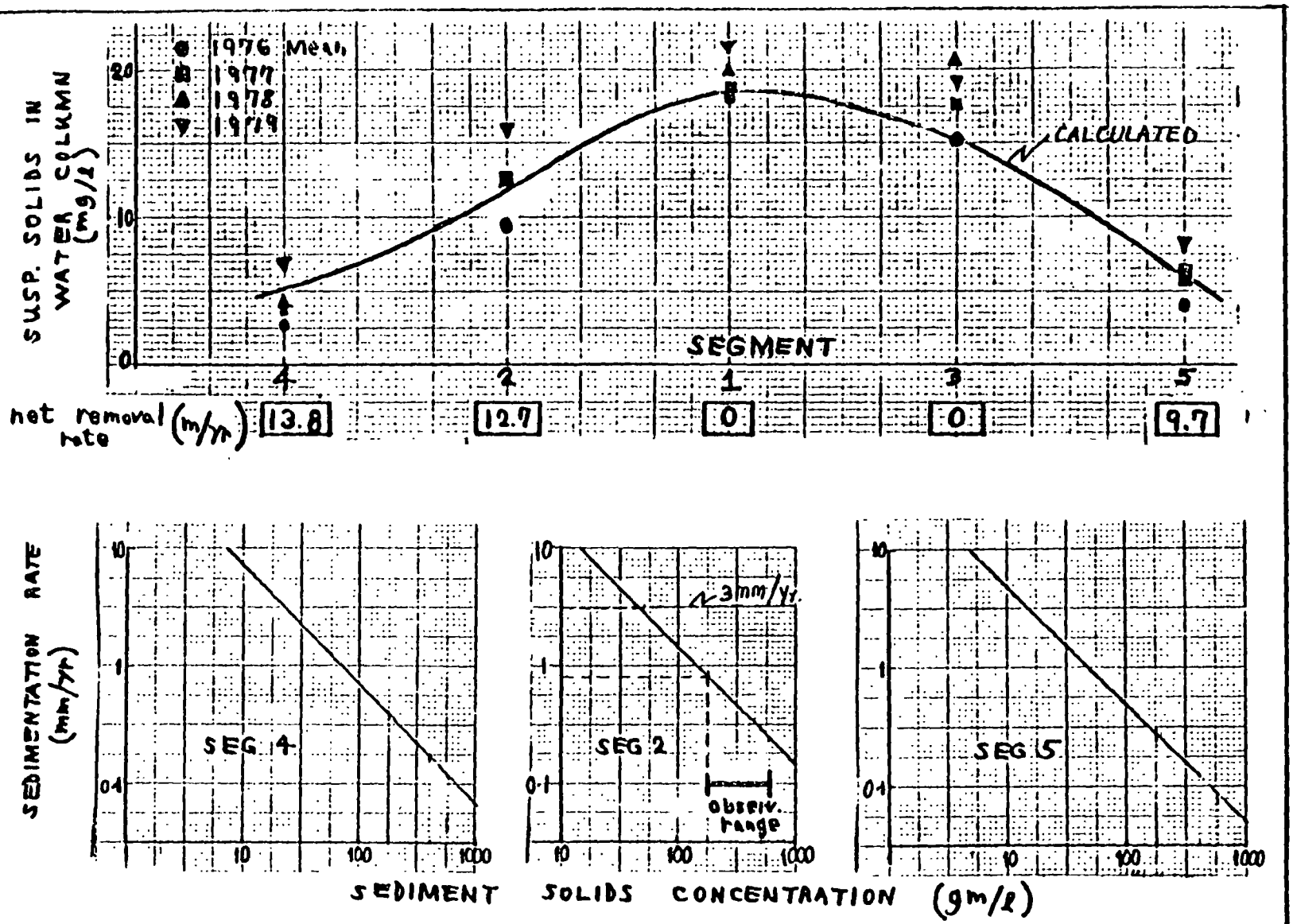

FIGURE 13 SOLIDS CALIBRATION USING LONG-TERM SOLIDS DATA

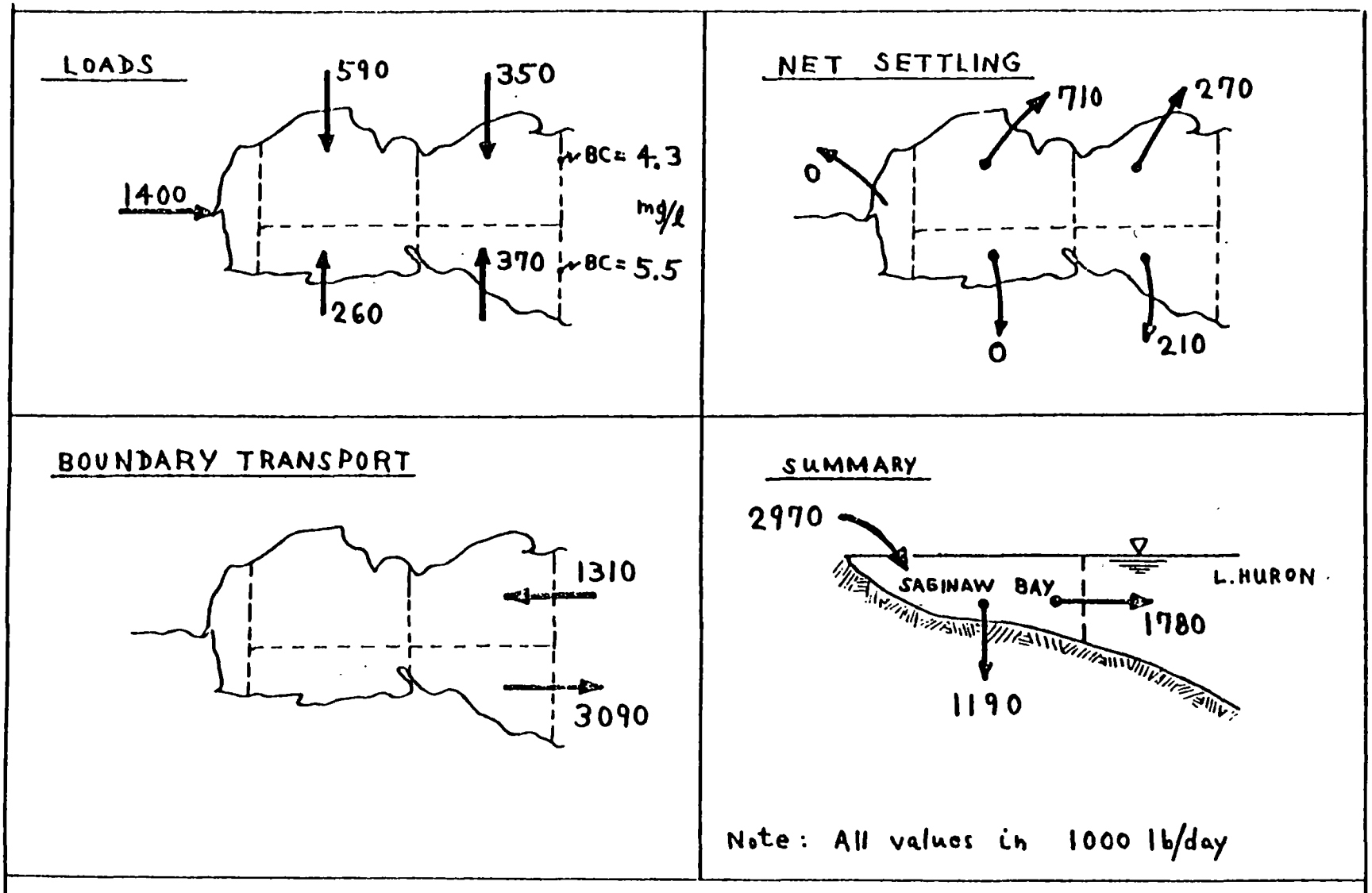

FIGURE 14 MASS BALANCE of TOTAL SUSPENDED SOLIDS UNDER LONG-TERM AVERAGE CONDITIONS

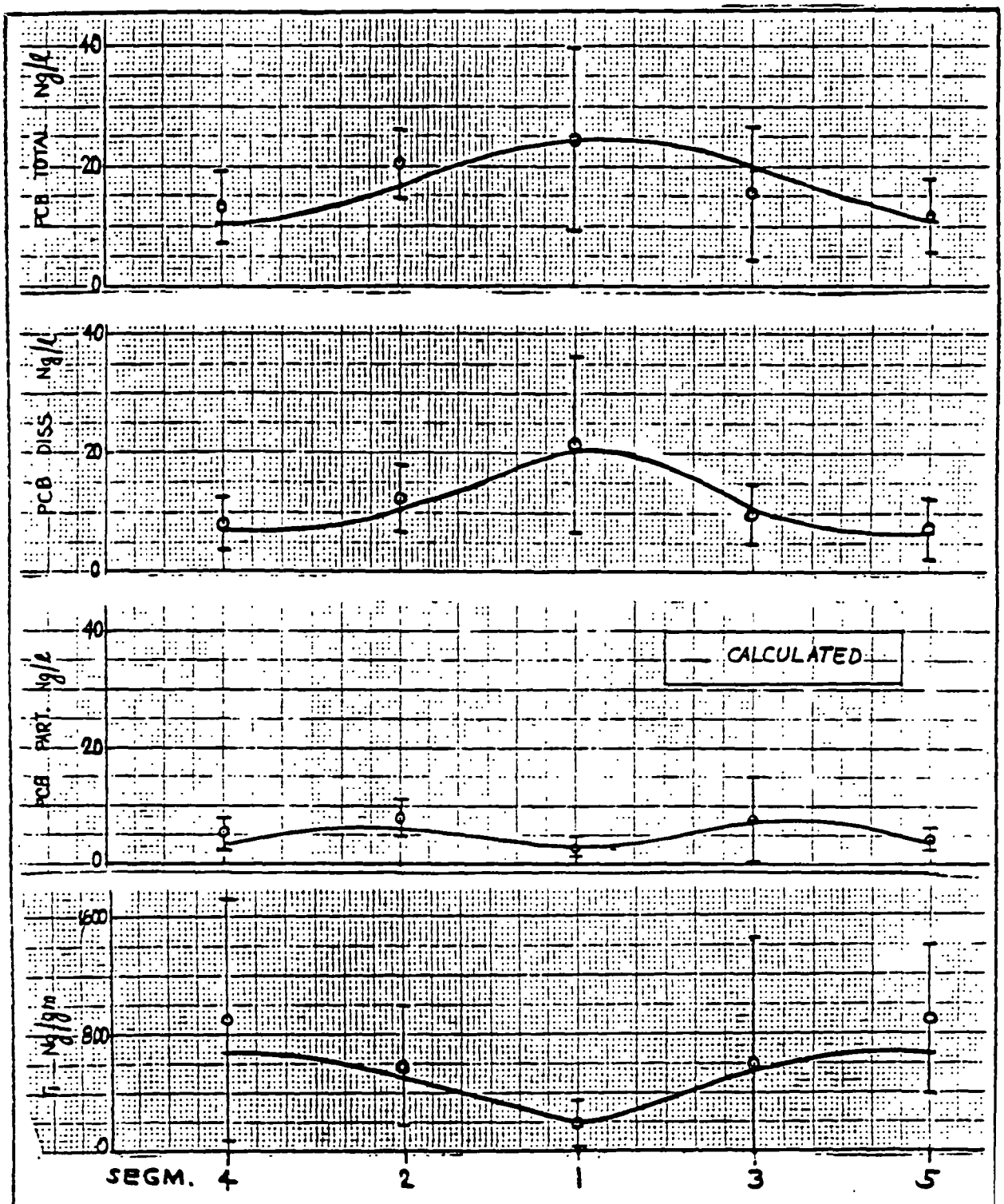

FIGURE 15 COMPONENTS OF PCB IN WATER COLUMN - 1979

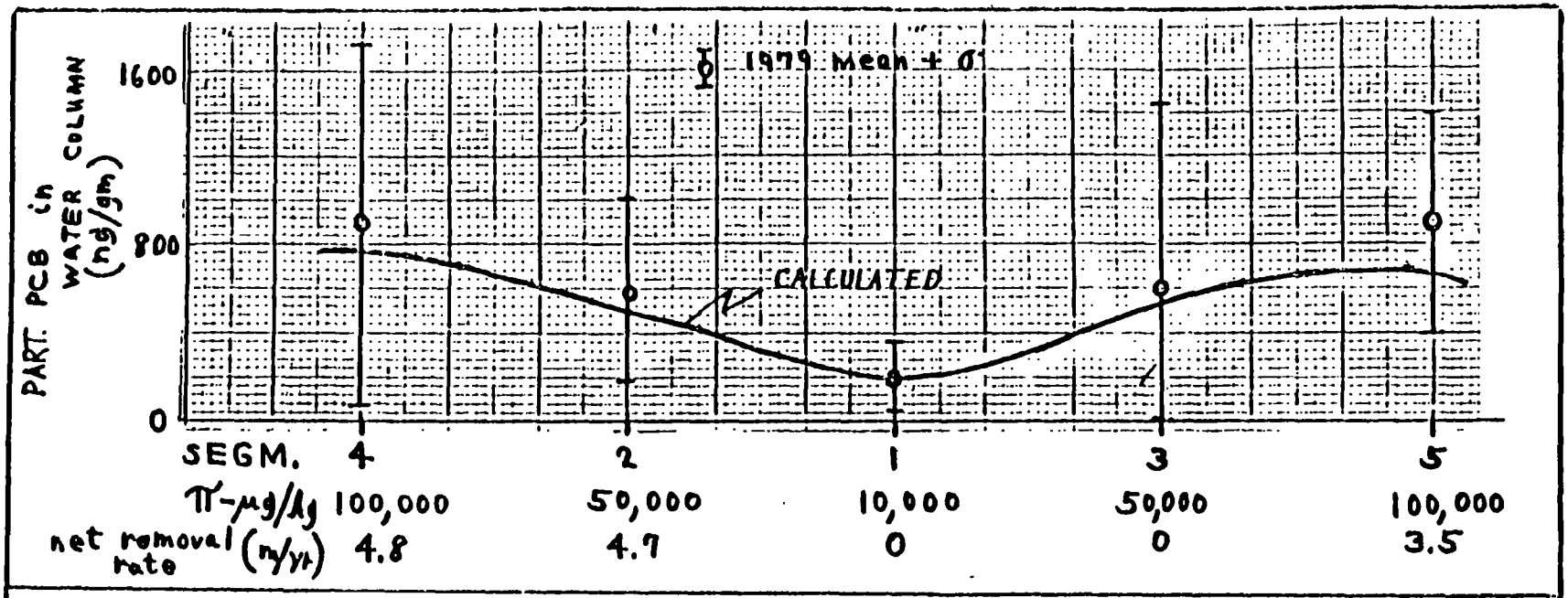

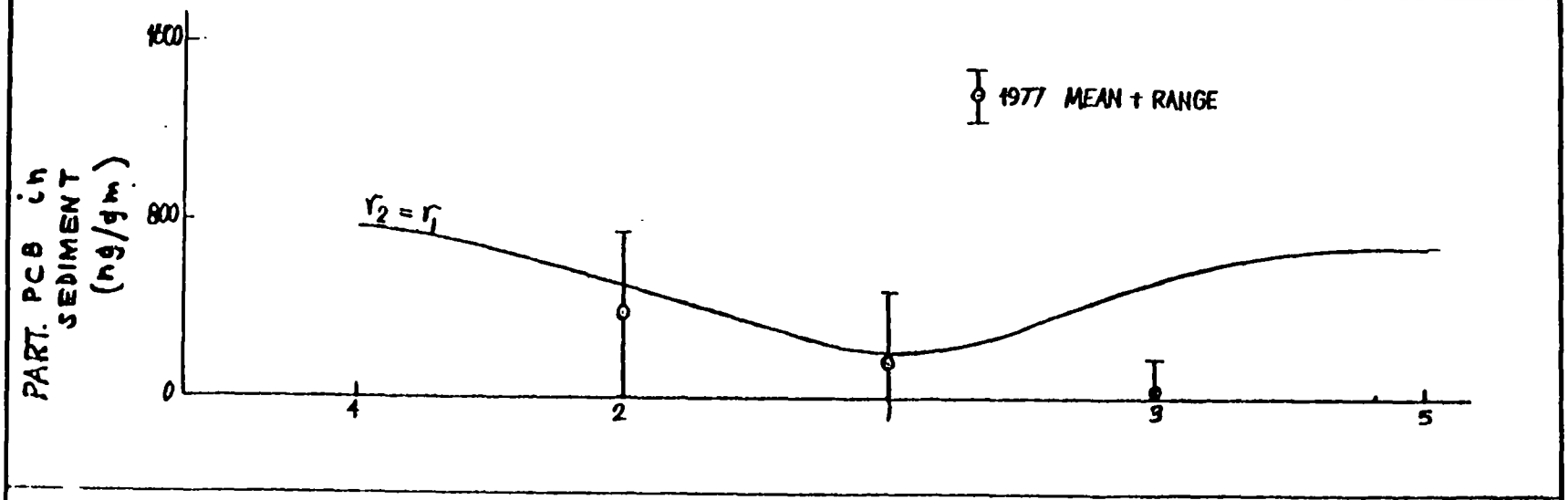

FIGURE 16 PART. PCB CALIBRATION USING 1979 LOADS + DATA

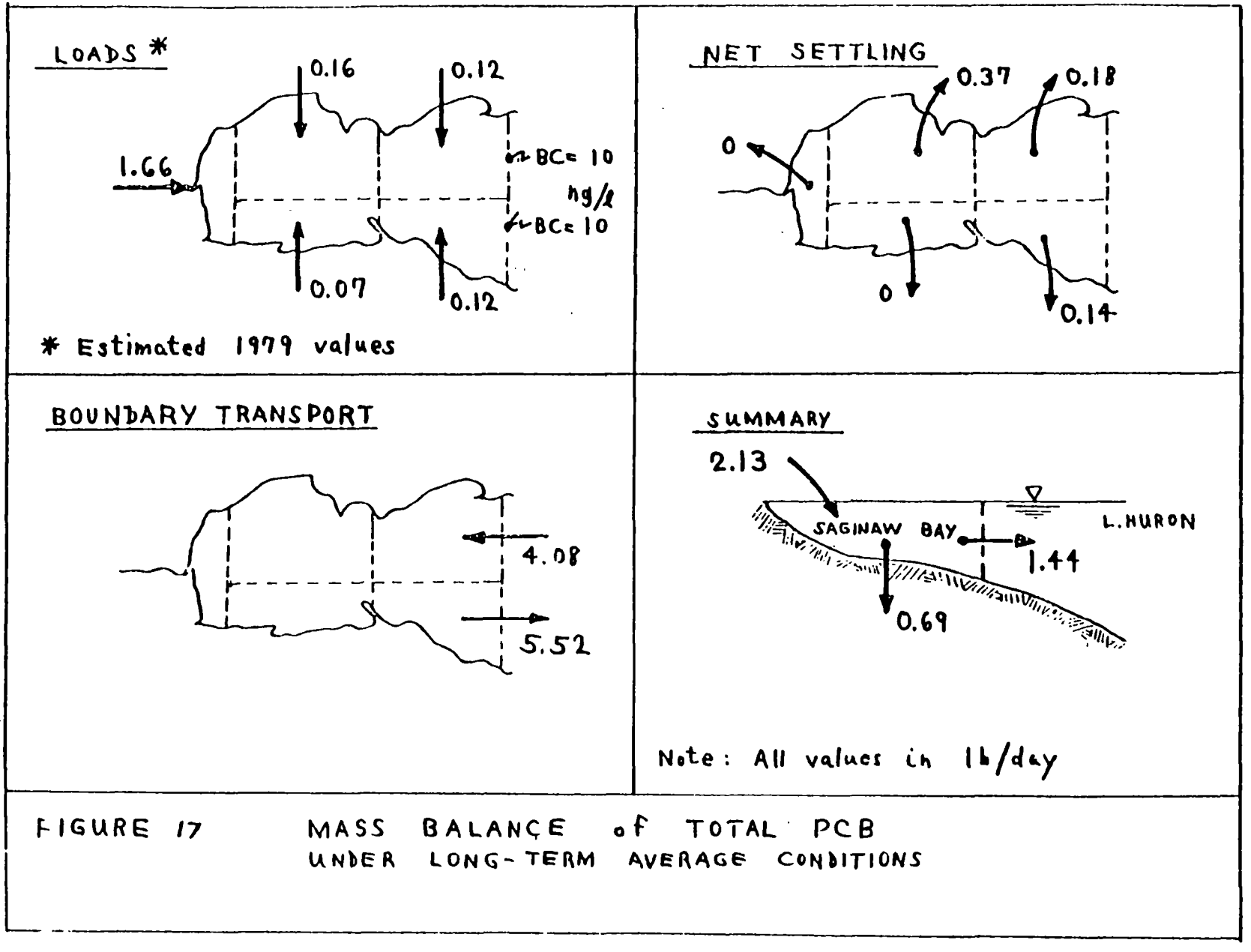

FIGURE 17 MASS BALANCE of TOTAL PCB UNDER LONG-TERM AVERAGE CONDITIONS

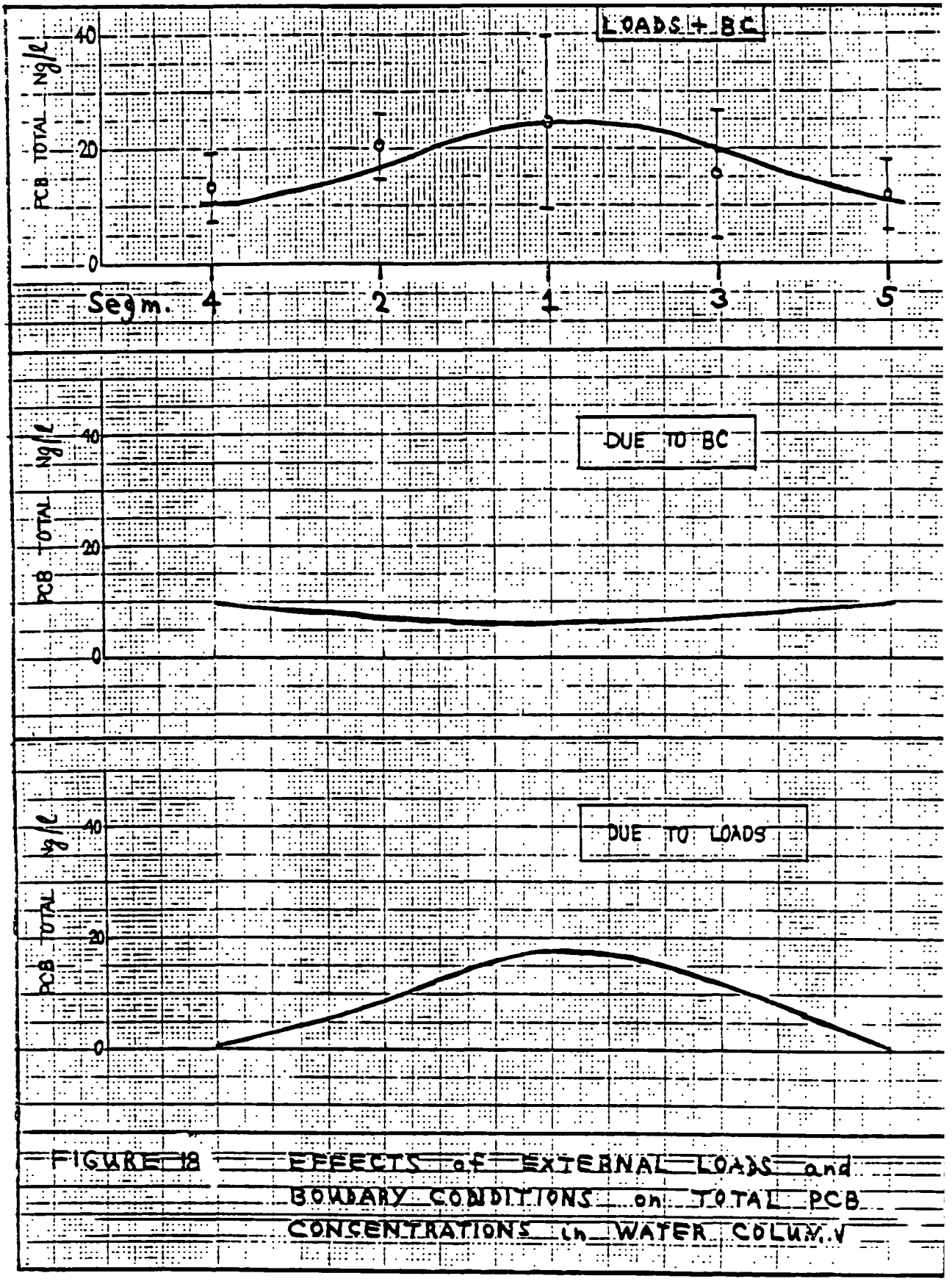

FIGURE 18 EFFECTS of EXTERNAL LOADS and BOUNDARY CONDITIONS on TOTAL PCB CONCENTRATIONS in WATER COLUMN

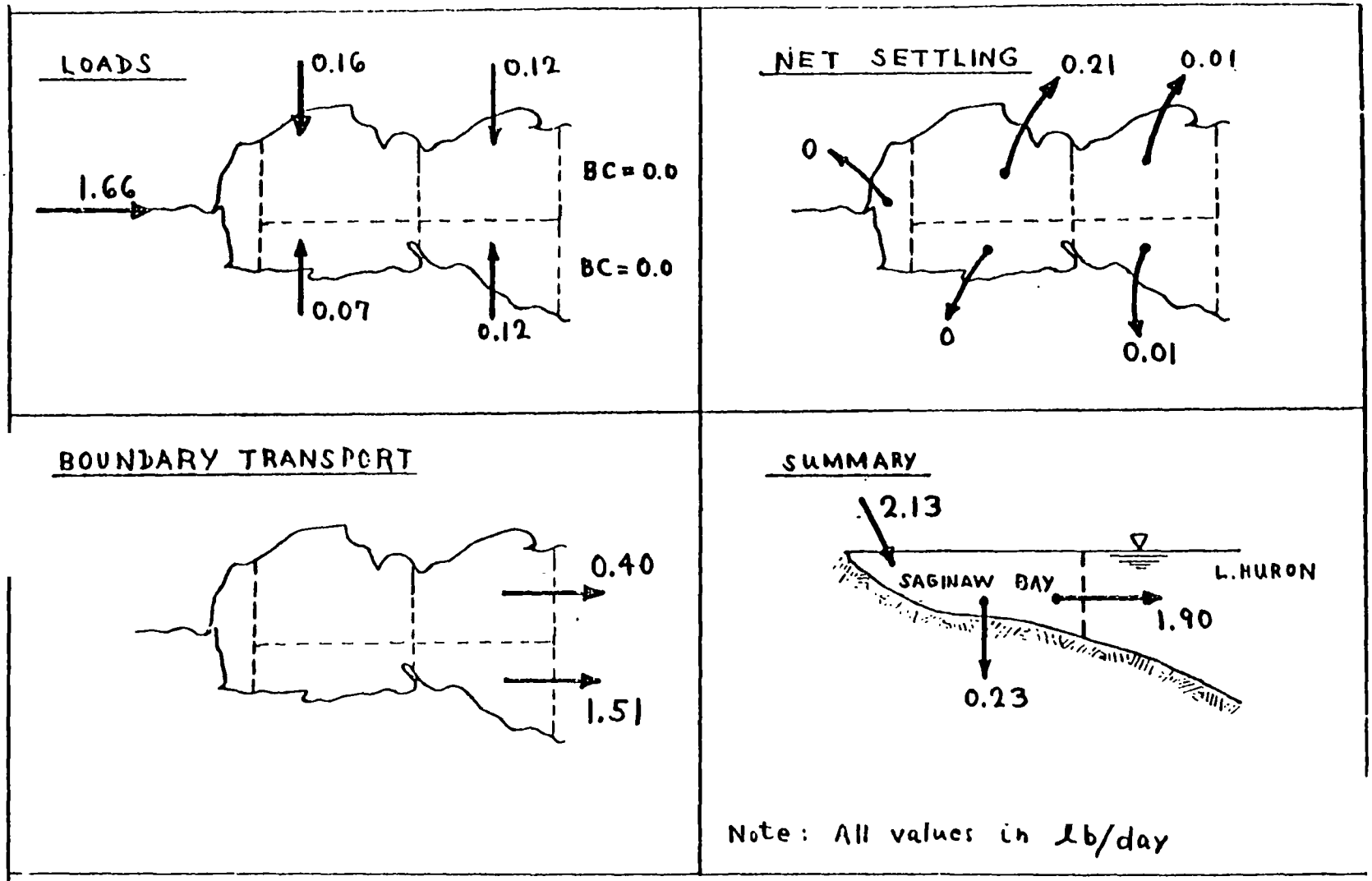

FIGURE 19 MASS BALANCE OF TOTAL PCB – EXTERNAL LOADS ONLY

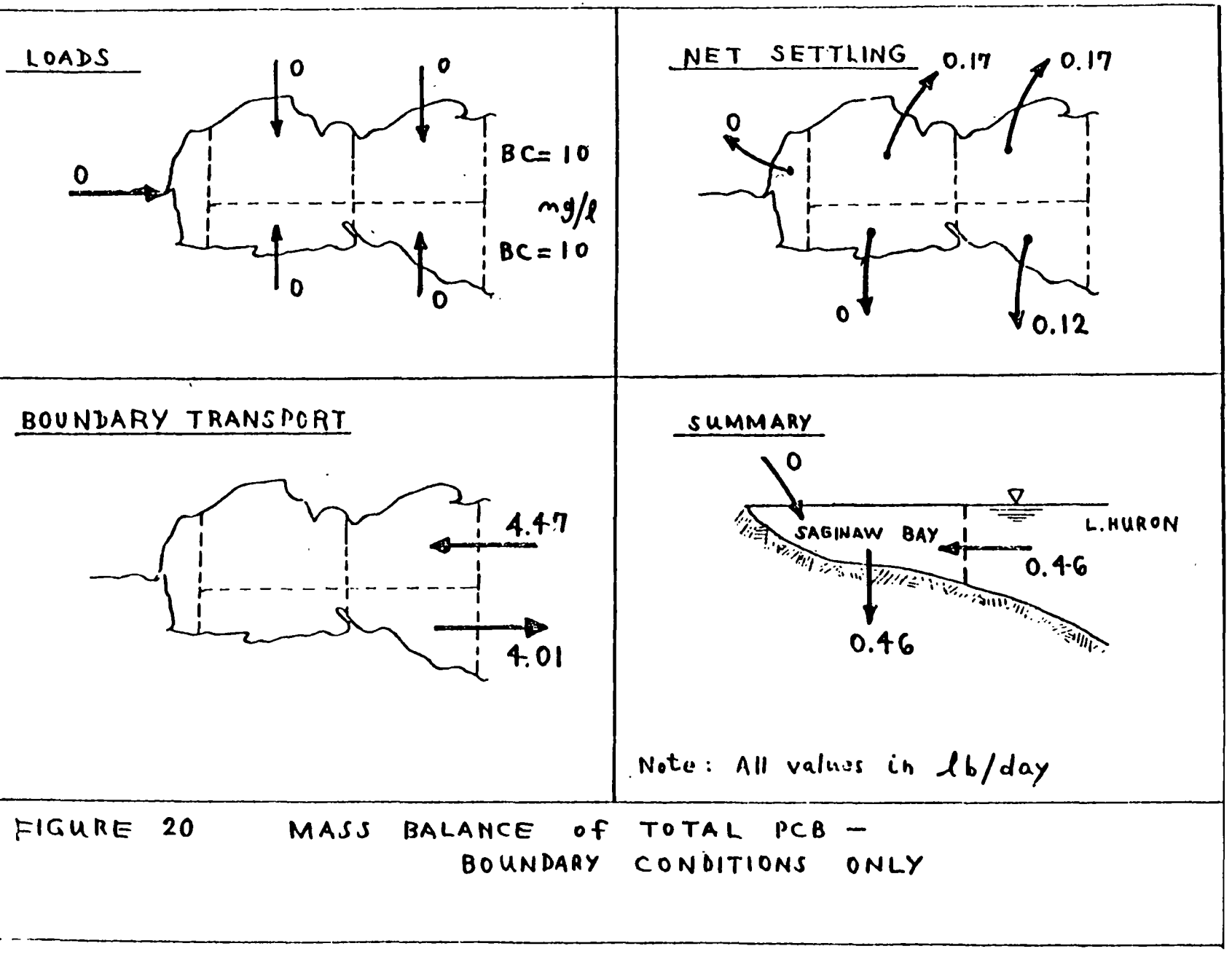

FIGURE 20 MASS BALANCE of TOTAL PCB — BOUNDARY CONDITIONS ONLY

STREAM & RIVER MODELS

A. INTRODUCTION*

This chapter of the notes describes the distribution of toxic substances in fresh water streams & rivers. The characteristic feature of these water bodies is the longitudinal advective motion induced by gravity due to the slope of the natural channel or by a head differential due to a backwater effect of a dam. In either case, the transport is due primarily to the advective component, rather than the dispersive component. In a steady-state analysis of the systems, the latter can frequently be neglected without introducing significant error. For those cases in which the dispersive component may be significant, reference is made to the following chapter of these notes. This section deals exclusively with streams and rivers, in which the advective translation is the significant transport mechanism of the water column.

The water flow and the various substances contained therein interact in varying degrees with the bed, which are classified in accordance with the three general types of bed conditions, as described previously. Type I is a stationary non-interacting bed receiving settling solids, with no resuspension. Type II treats a mixed bed with a net zero horizontal motion, but which is interacting with the water column. The shear produced by the flowing water causes mixing and resuspension of the interfacial bed layer, but is insufficient to induce bed motion. Type III covers the case in which the shear is of sufficient magnitude to induce both scour and bed transport. The following sections of this chapter cover Types I & II and Type III is dealt with in the estuary chapter.

*Donald J. O'Connor

B. LONGITUDINAL ANALYSIS*

The advective transport component, which is simply the flow velocity in fresh water streams and rivers, is common to the various types of analysis described above. Consequently, the discussion is first focused on this aspect, which is best considered in light of the concentration of a dissolved tracer, such as total dissolved solids or chlorides. The source of ions, such as these, is invariably the ground water inflow and possibly the waste-water input, itself, which in addition to containing the toxic substance also may have an appreciable concentration of dissolved solids.

1. TRANSPORT

Consider the case of an upstream tributary, in which the ground water inflow is an appreciable fraction of the river flow. An inflow of this nature produces a spatially increasing flow in the downstream direction. Consider further a variable cross sectional area, which in general also increases in the downstream direction. The mass balance takes into account inflow, ground water input and outflow. Assuming lateral homogeneity of concentration, the balance is taken about an elemental volume of cross sectional area A(x) and length Δx. The basic differential equation for the dissolved solids is

$$A \frac{\partial s}{\partial t} = \frac{\partial}{\partial x}(Qs) + s_g \frac{\partial Q_g}{dx} + s_s \frac{\partial Q_s}{dx} \qquad (1)$$

in which

s = concentration of a dissolved tracer

Q = flow

and the subscripts g and s refer to the ground water and surface runoff components, respectively.

Under steady state low flow conditions, the surface runoff is zero and the above equation, after expanding the first term on the right-hand side, reduces to:

$$\frac{ds}{dx} = \frac{s}{Q}\frac{dQ}{dx} + \frac{s_g}{Q}\frac{dQ}{\partial x} = q\,[s_g - s] \qquad (2)$$

in which

$$q = \frac{1}{Q}\frac{dQ}{dx} = \text{exponential flow increment}$$

The subscript is dropped from the flow since the only source of flow is the ground water. The solution is

*Donald J. O'Connor

$$s = s_g[1 - e^{-qx}] + s_o e^{-qx} \qquad (3)$$

in which

$$s_o = \frac{W}{Q_o}$$

W = mass input of dissolved solids at $x = o$

Q_o = flow at $x = o$

Depending on the relative magnitudes of the ground water concentration and the concentration due to the waste input, the spatial distribution of dissolved solids increases or decreases to an equilibrium value, s_g.

2. TYPE I ANALYSIS - STATIONARY NON-INTERACTIVE BED

The condition of a stationary, non-interactive bed occurs under low flow conditions in streams and rivers. The vertical mixing of the flowing water is sufficiently low to permit the settling of the suspended solids and to preclude motion and scour of the bed material. It is recognized that some fraction of the solids is probably maintained in suspension - e.g. the smaller clay sizes and/or the flocculent organic particles of low specific gravity. However the majority of the solids are susceptible to settling and accumulation in the bed.

a. Suspended Solids

As in the case of the dissolved solids, discussed above, consider an upstream tributary in which the ground water inflow is the source of water for the stream flow. However, in this instance, the concentration of suspended solids in the ground water is negligible. The basic differential equation, allowing for settling is therefore,

$$\frac{\partial m}{\partial t} = \frac{1}{A}\frac{\partial}{\partial x}(Qm) - K_s m \qquad (4)$$

in which

m = concentration of suspended solids

K_s = settling coefficient = $\frac{v_s}{H}$

v_s = settling velocity

H = average depth of the stream

Expanding the first term on the right hand side of the above equation and simplifying, the steady state form is

$$\frac{dm}{dx} = -\left(\frac{K_s}{U} + q\right) m \qquad (5)$$

in which

U = velocity = $\frac{Q}{A}$

q = exponential flow increment = $\frac{1}{Q}\frac{dQ}{dx}$

the solution is

$$m = m_o\, e^{-\left(\frac{K_s}{U} + q\right)x}$$

in which

m_o = boundary concentration at x = o.

It is assumed that the incremental flow is balanced by the increasing area resulting in a constant velocity, U. The boundary concentration may be due to the input of suspended solids from a point source - e.g. a treatment plant or tributary - or to an input from the upstream river segment of different hydraulic characteristics. The concentration approaches zero for large x.

In the subsequent development the effect of incremental flow due to ground water is not included. It may be readily introduced in the final working equations as an additional exponent as shown in the above equation. An example of this effect is discussed subsequently.

b. Toxic Substances

The equation for toxic substance are developed in a similiar fashion, using the mass balance principle. The dissolved component includes the transport with adsorption - desorption interaction with the particulate and allowance is made for a reaction or transfer effect. In this case, assume the transfer term is an evaporation loss:

$$0 = - U \frac{dc}{dx} - K_o m c + K_2 p - K_a c \qquad (7)$$

in which

K_a = evaporation coefficient

The particulate form is described in a similiar fashion with a settling term

$$0 = - U \frac{dp}{dx} + K_o m c - K_2 p - K_s p \qquad (8)$$

Addition of these equations yields

$$0 = - U \frac{dc_T}{dx} - K_a c - K_s p \qquad (9)$$

Substitution of the dissolved and particulate fractions for c and p gives

$$0 = -U \frac{dc_T}{dx} - c_T \left[f_d K_a + f_p K_s \right] \qquad (10)$$

in which

$$f_d = \frac{1}{1+¶m}$$

$$f_p = \frac{¶m}{1+¶m}$$

Assuming the river stretch is segmented such that each element may be approximated by a constant concentration of suspended solids; the solution

of the above is straightforward.

$$C_T = C_{To} e^{-[f_d K_a + f_p K_s]\frac{x}{u}} \tag{11}$$

in which

$C_T = \frac{W_T}{Q}$

W_T = mass discharge of total toxic $(\frac{M}{T})$

Q = river flow $(\frac{L^3}{T})$

Knowing the total concentration, the dissolved and particulate may be readily determined from the f_d and f_p equations.

If the effect of incremental flow is significant, the above equation is written in the following form:

$$C_T = C_{To} e^{-[(f_d K_a + f_p K_s)U^{-1} + q]x} \tag{12}$$

3. Type II Analysis - Mixed-Interactive Bed

This case describes a bed which is receiving solids due to the settling flux from the water column and returning solids by resuspension. The toxic substance in particulate form is transported by similar routes. The water column concentration is designated by subscript 1 and the bed by subscript 2. The analysis of each is discussed separately.

a) Suspended Solids

The basic equation for the solids is similar to that previously developed and in addition, includes a source term due to resuspension. The steady-state equation is:

$$0 = - U \frac{dm_1}{dx} - K_{s1} m_1 + K_{u1} m_2 \tag{13}$$

in which

K_{u1} = resuspension coefficient = $\frac{v_u}{H_1}$

m_2 = concentration of solids in the bed

v_u = resuspension velocity

The solution of this equation is:

$$m_1 = \frac{K_{u1} m_2}{K_{s1}} \left[1 - e^{-K_{s1} \frac{x}{u}}\right] + m_o e^{-K_{s1} \frac{x}{u}} \tag{14}$$

If the ground water flow is significant, the above is expressed as

$$m_1 = \frac{K_{u1} m_2}{K_{s1} + qU} \left[1 - e^{-(\frac{K_{s1}}{U} + q)x}\right] + m_o e^{-(\frac{K_{s1}}{U} + q)x} \tag{15}$$

The first term describes the build-up to spatial equilibrium of solids and the second term the decay by settling of the boundary solids. The spatial equilibrium concentration is

$$m_{e1} = \frac{Ku_1 m_2}{K_{s1}} = \frac{v_u m_2}{v_s}$$

The spatial distribution of solids will either build-up or decrease to the equilibrium values depending on the relative magnitudes of m_e and m_o.

The equation for the concentration of the solids in the bed includes a sedimentation term. Under steady-state:

$$0 = K_{s2} m_1 - K_{u2} m_2 \pm K_{d2} m_2 \tag{16}$$

in which

K_{d2} = sedimentation coefficient = $\frac{v_d}{H_2}$

H_2 = depth of the bed.

It is apparent that the sedimentation term, which reflects the thickness of the bed, may be either positive or negative, depending on the magnitudes of the settling and resuspension terms. Thus, the bed increases or decreases along the length of the river in accordance with the decrease or increase in the spatial distribution of suspended solids. At spatial equilibrium the bed thickness is constant and the equilibrium concentrations in water and bed are maintained in accordance with the above equation defining m_{1e}.

b) Toxic Substances

The basic equation for the toxic substance follows from the above considerations. The dissolved component is identical to that for the Type I analysis:

$$0 = - U\frac{dc_1}{dx} - K_o m_1 c_1 + K_2 p - K_a c_1 \qquad (17)$$

in which, as in the previous case, allowance is made for a decay or transfer. A volatilization transfer is assumed in the above.

The particulate component has an additional term due to the resuspension effect:

$$0 = - U\frac{dp_1}{dx} + K_{a1} c_1 - K_2 p_1 - K_{s1} p_1 + K_{u1} p_2 \qquad (18)$$

Addition of the dissolved and particulate components yields the equation for the total concentration.

$$0 = - U\frac{dc_T}{dx} - K_{a1} c_T - K_{s1} p_1 + K_{u1} p_2 \qquad (19)$$

Substitution of the dissolved and particulate fractions for c and p are replacing $p_2 = r_2 m_2$.

$$0 = - U\frac{dc_T}{dx} - \alpha c_T + K_{u1} r_2 m_2 \qquad (20)$$

in which $\alpha = f_d K_a + f_p K_s$

For the condition of spatial equilibrium of solids for which $m_1 = m_{e1}$ and

$K_{u1}m_2 = K_{s1}m_{e1}$, the solution is:

$$c_T = \frac{K_{s1}r_2m_{e1}}{\alpha}\left[1 - e^{-\alpha\frac{x}{u}}\right] + c_{To}e^{-\alpha\frac{x}{u}} \qquad (21)$$

Simplification of the first term yields

$$\frac{K_{s1}r_2m_{e1}}{\alpha} = \frac{r_2m_{e1}}{f_p + f_d\frac{K_L}{v_s}} \qquad (22)$$

in which K_L = evaporation transfer coefficient = K_aH_1 (L/T)

v_s = settling velocity of solids = $K_{s1}H_1$ (L/T)

For the case of spatially varying solids, the above equation may be used as an approximation by segmenting the system into a number of elements, such that the solids are approximately uniform in each, but varying from one to the other in accordance with the solids equation.

If the ground water flow is significant, the appropriate equation is

$$c_T = \frac{K_{s1}r_2m_{e1}}{\alpha}\left[1 - e^{-(\frac{\alpha}{u} + q)\,x}\right] + c_{To}e^{-(\frac{\alpha}{u} + q)x} \qquad (23)$$

It is to be noted that a direct simple analytical solution results for the condition of spatial equilibrium of the solids. For the case of spatially varying solids, however, the differential equation is

$$0 = -U\frac{dc_T}{dx} - \left[\frac{K_{a1} + K_{s1}\,\phi\,(x)}{1 + \phi\,(x)}\right]c_T + K_{s1}r_2m_{e1} \qquad (24)$$

in which $\phi\,(x) = \P m_{e1}(1 - e^{\frac{-K_{s1}x}{u}})$

Finite difference forms of the equation may be used to calculate the distribution of toxic chemical, in which the necessary solids concentrations both in the bed and water column are inputs to each segment of the system. The solids equations are solved for the appropriate concentrations, which are introduced into the toxic distribution.

Application to PCBs in the Hudson River *

INTRODUCTION AND GENERAL PROBLEM FRAMEWORK

The focus of this review is the description of the distribution and fate of polychlorinated biphenyls (PCBs) in the Hudson River and Estuary using a simplified model of the physical-chemical system. (An analysis of the fate of PCBs in the food chain is given in Chapter 10 of the Notes). A settlement between the New York State Department of Environmental Conservation (NYSDEC) and the General Electric Company (GE) concerning the contamination of the Hudson River by PCBs discharged by GE's facilities at Fort Edward, New York, called for an overall study of the Hudson. A more complete treatment of the model discussed here is given in (1). This model treats the entire river estuarine and harbor regions of the Hudson system in a simplified manner and does not address the details of estuarine sediment transport and exchange. The model is intended to provide some guidance on the order of magnitude response that may be anticipated under different environmental controls. Considerable research in this area is continuing and the results of that research may influence the conclusions drawn herein.

Figure 1 is a schematic of the Hudson River which indicates the mile points (MP) of key locations and also shows the divisions of the Hudson into reaches for the physical transport analysis and reaches for the biological analysis. From the Federal Dam at Troy to the Ocean, the Lower Hudson is tidal and depending on the average freshwater flow, the end of the salt water intrusion oscillates approximately between the Tappan Zee Bridge (MP 25) and Poughkeepsie (MP 75) and under severe drought conditions, it may reach as far north as MP 80. The long term monthly average discharge and the 1976 monthly average discharge from the Upper Hudson to the Lower Hudson are 13,270 cfs and 22,100 cfs respectively.

ANALYSIS OF WATER COLUMN AND SEDIMENT PCB DATA

The principle of the conservation of mass permits a first approximation to describing the spatial distribution of the various components of PCBs. The following assumptions are made: a) the mass of PCB in the food chain

* Robert V. Thomann

is small relative to that in the water column; b) a local equilibrium prevails between the particulate and dissolved phases of the PCBs; c) the adsorption phenomena is linear; d) the river system is in temporal steady state (although longer term trends may be present); and e) losses from the water column are principally through sedimentation, although some evaluations of losses due to evaporation and biodegradation has been made.(1) The general equation for the total PCB concentration, c_T(µg/l) in a dimensional system can be written as:

$$\frac{u\,dc_T}{dX} - E\,\frac{d^2c_T}{dX^2} + \left[\frac{¶m}{1+¶m}\,K_s + \frac{K_a+K_n+K_d}{1+¶m}\right] c_T = [W_{TB}+W_{TA}+W_{TE}] \qquad (1)$$

where x is distance downstream, u is the river or estuary velocity (cm/sec), E is the tidal dispersion (m^2/day), m is the mass of suspended solids (mg/l), "a" is a partition coefficient between the particulate and dissolved phases (µg/g ÷ µg/l), K_s, K_a, K_n, K_d are coefficients [day^{-1}] representing sedimentation, evaporation, photooxidation, and biodegradation, respectively; and W_{TB}, W_{TA} and W_{TE} are total input loads (kg/l-day) of PCB from bottom sediment interactions, atmospheric sources and other external sources, respectively. For the Upper Hudson area, W_{TA} can be assumed close to zero and W_{TB} can be given from the resuspended bed sediment load as $W_{TB} \approx r_b\,W_{ss}$ where r_b is the concentration of PCBs in the resuspended sediment (µg PCB/g sediment, a measurable quantity) and W_{ss} is the sediment input ($\frac{\text{kg sediment}}{\text{liter-day}}$). A mass balance on the suspended solids is therefore also required and is given by

$$\frac{udm}{dX} - E\,\frac{d^2m}{dX^2} + K_s m = W_{ss} \qquad (2)$$

With m from (2) and estimates of the coefficients for (1), c_T can be calculated. Since the total concentration is the sum of the particulate and dissolved, the dissolved concentration, c_D, can be calculated from:

$$c = c_T/(1+¶m) \qquad (3)$$

The concentration then provides an estimate of the dissolved form of PCB which may be available for uptake and bioconcentration by the aquatic food chain. The approach to analyzing the PCB column data was to first fit the suspended solids data using Equation (2) which provides an estimate of K_s and W_{ss} (but not uniquely). Then using field data of r_B and the determined distribution of m and K_s, the PCB data are calibrated using Equation (1). In using this latter equation, a knowledge of the partition coefficient ¶ is needed. The limited available data for the Upper Hudson River show a large variation from 20-500 µg/g per µg/l. Dexter[2] in his work examined the partitioning of PCB in the two phases and reported values from 13-75 µg/g per µg/l. A value of 100 µg/g per µg/l was chosen for this work. The reaches for the physical analysis of PCBs are shown in Figure 1.

For the Upper Hudson (north of Federal Dam), the model was applied to PCB surveys of March 18 and March 29-31, 1976. The resulting profiles and the survey data are shown in Figure 2 and as shown, the agreement between the observed data and the calculation is good. However, background and tributary PCBs had to be assigned based on rather meager data.

Figure 3 shows the calculation profile for the entire length of the Hudson to the Battery. In the lower Hudson, data on total PCBs were available only for the reach for MP 65 - MP 90. In the top graph of Figure 3 are shown two profiles resulting from different assumptions on bottom PCB concentration as shown in the bottom graph. The dashed line therefore in the water column PCB calculation corresponds to an assumption of 1 µg PCB/g sediment for the lower Hudson. It is estimated based on Figure 3 that the total PCB concentration from MP 0 to MP 110 ranges from 0.1 - 0.5 µg/l. The average dissolved PCB concentration (not measured) is estimated at about 0.1 µg/l (100 ng/l).

ANALYSIS OF DREDGING OF UPSTREAM SEDIMENTS

Various schemes have been suggested for reducing the effect of the upstream PCB sediments, including the removal of the contaminated sediment by dredging. Therefore, two dredging alternatives were considered and their impacts on the water column PCB were calculated.

Under the first alternative, only the Thompson Island pool at Fort

Edward is dredged to a bottom sediment PCB concentration of 1 µg/g. Under the second dredging alternative all pools of the Upper Hudson are dredged to a bottom sediment PCB concentration of 1 µg/g.

Figure 4A shows the results of the calculation under the two dredging alternatives and assuming that the bed sediment PCB concentration remains the same as at present. The average PCB concentration for the Upper Hudson is calculated to be appreciably reduced from approximate present levels of 0.5 µg/l to 0.28 µg/l and 0.14 µg/l under the two alternatives. This represents an approximate 20% and 70% reduction of level from the Upper Hudson to the Lower Hudson. These results assume no change in the estuary PCB sediment concentration. However, at the mean annual flow, the estuarine sediment PCBs are the primary source of estuarine water column PCBs. Therefore, if the contaminated sediment of the Upper Hudson were not partially or totally removed or inactivated, such sediment would continue to add to the contamination of estuarine sediments via the naturally occurring sediment discharged over the Troy Dam.

Recognizing this indirect effect and an approximate range of 20-70% reduction in load at Troy depending on the degree of dredging, it has been assumed that the bed sediment-bed load input may drop by 50%. The results of the calculation under this assumption are shown in Figure 4B. In this case the calculated total PCB concentration is almost halved and in the biologically active region, the average dissolved PCB concentration is estimated at 0.05 µg/l.

THE NO-ACTION ALTERNATIVE - UPPER HUDSON

If no action were taken, some notion of the time span required for the reduction of the PCB load to the estuary from the Upper Hudson may be gained by means of a mass balance. The mass balance is considered around the water column of the Upper Hudson for the March 18, 1976 survey, as shown in Fig. 5A. From the inputs to the calculated profile the load to the Upper Hudson due to the upstream conditions is 5 lb/day, due to the tributaries 2 lb/day, and at the flow of 12,700 cfs the load to the Estuary is 17 lb/day. This causes a net loss of 10 lb PCB/day from the bottom sediment. From a similar

mass balance at 48,700 cfs from the calculated profiles, for the March 29-31, 1976 profile, there is a net loss of 225 lb PCB/day from the bottom sediment. Using these net losses at the given flows (Fig. 6) and the long term monthly hydrograph, an approximate average daily net bottom PCB loss can be computed for the typical year. Following this procedure the approximate daily net bottom PCB loss is 15 lb/day on a yearly average. Then, for the estimated 450,000 lb of PCB in the entire volume of sediments of the upper Hudson, it would take at least several decades for these sediments to be "flushed out". This assumes the entire sediment volume would be flushed out. If only a fraction of the mass were "available" for scouring, then the response time would be reduced accordingly. In addition, other effects such as evaporative losses and biodegradation may reduce this time.

Evaporative losses can be computed by assuming that (1) the soluble component only will be depleted by means of gas transfer process and (2) that the PCB in the air is negligible when compared to the soluble component. Assuming that this gas transfer is liquid film controlled, the evaporative loss will be:

$$N = K_L A c$$

where

N = evaporative loss in (M/T)

K_L = liquid film coefficient in (L/T)

c = The dissolved PCB concentration in (M/L^3)

A = The surface area through which the transfer occurs (L^2)

the liquid-film coefficient was taken as 0.07 m/h, and the dissolved component for the March 18, 1976 survey is 0.2 µg/l averaged over the entire Upper Hudson. With this parameter, the evaporative loss is estimated at 15 lb/day.

If biodegradation is included at an assumed rate of $K_d = .25\ (day)^{-1}$, then there is an additional loss of 5 lb/day. It is also assumed in these calculations that the biodegradation process depletes only the dissolved component, but this is not known. A biodegradation process depleting the particulate component could also be postulated with, perhaps, different

rate. Thus if these processes for the dissolved component are included in the mass balance, the total net bottom loss is increased to 30 lb/day (Fig. 5B). Since these additional losses are depleting the dissolved component, it is of interest to consider the dissolved input. Assuming that the interstitial water is saturated with PCB, then the soluble input can balance approximately 40% of the PCB loss due to evaporation and biodegradation, Fig. 5C. The response time to "flush out" the Upper Hudson sediments is therefore reduced by a factor of about 2 when evaporative and biodegradation losses are included. Sediment burial and subsequent interstitial diffusion rates may also markedly reduce the time to flush out the Upper Hudson. Such a calculation would require a detailed model of the bed sediment PCB and interactors with the overlying water.

ACKNOWLEDGEMENT

Special thanks are due to Messrs. John St. John, Thomas Gallagher and Michael Kontaxis of Hydro Qual, Inc. (formerly Hydroscience, Inc.) for their valuable assistance and input into the work described herein. This project was part of a contract between Hydroscience, Inc. and the New York State Department of Environmental Conservation.

REFERENCES

1. HYDROSCIENCE, INC. 1978. Estimation of PCB reduction by remedial action on the Hudson River ecosystem. Prepared for New York State Department of Environ. Conservation by Hydroscience, Inc., Westwood, N.J.: 107.

2. DEXTER, R.N. 1976. An application of equilibrium adsorption theory to the chemical dynamics of organic compounds in marine ecosystems, Ph.D. Diss. Univ. of Wash. Seattle, Washington: 181.

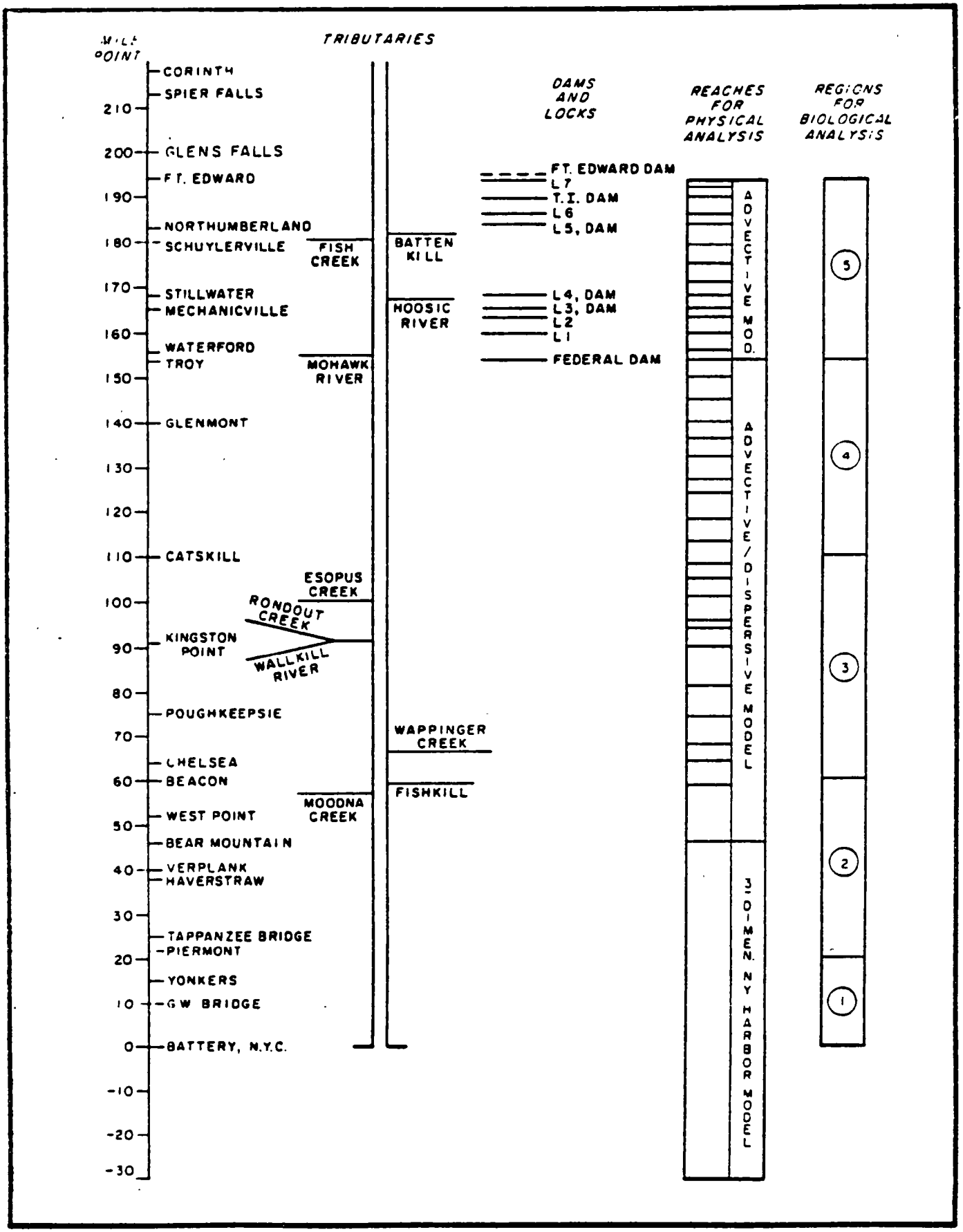

FIGURE 1

SCHEMATIC OF THE HUDSON RIVER AND SEGMENTATION USED IN PCB ANALYSIS (BIOLOGICAL AND PHYSICAL)

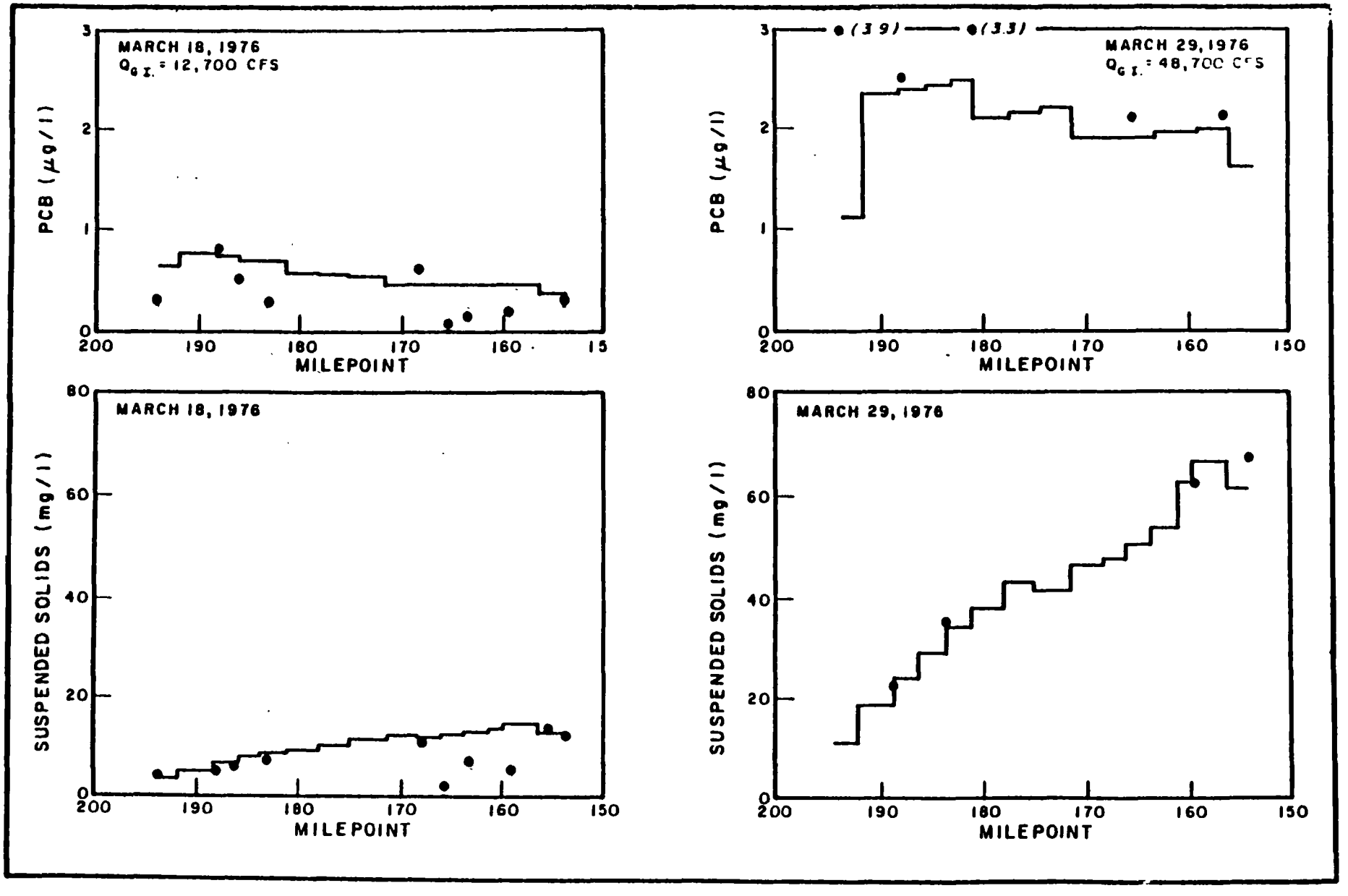

FIGURE 2

TOTAL PCB AND SUSPENDED SOLIDS CALCULATED PROFILES
(UPPER HUDSON RIVER)

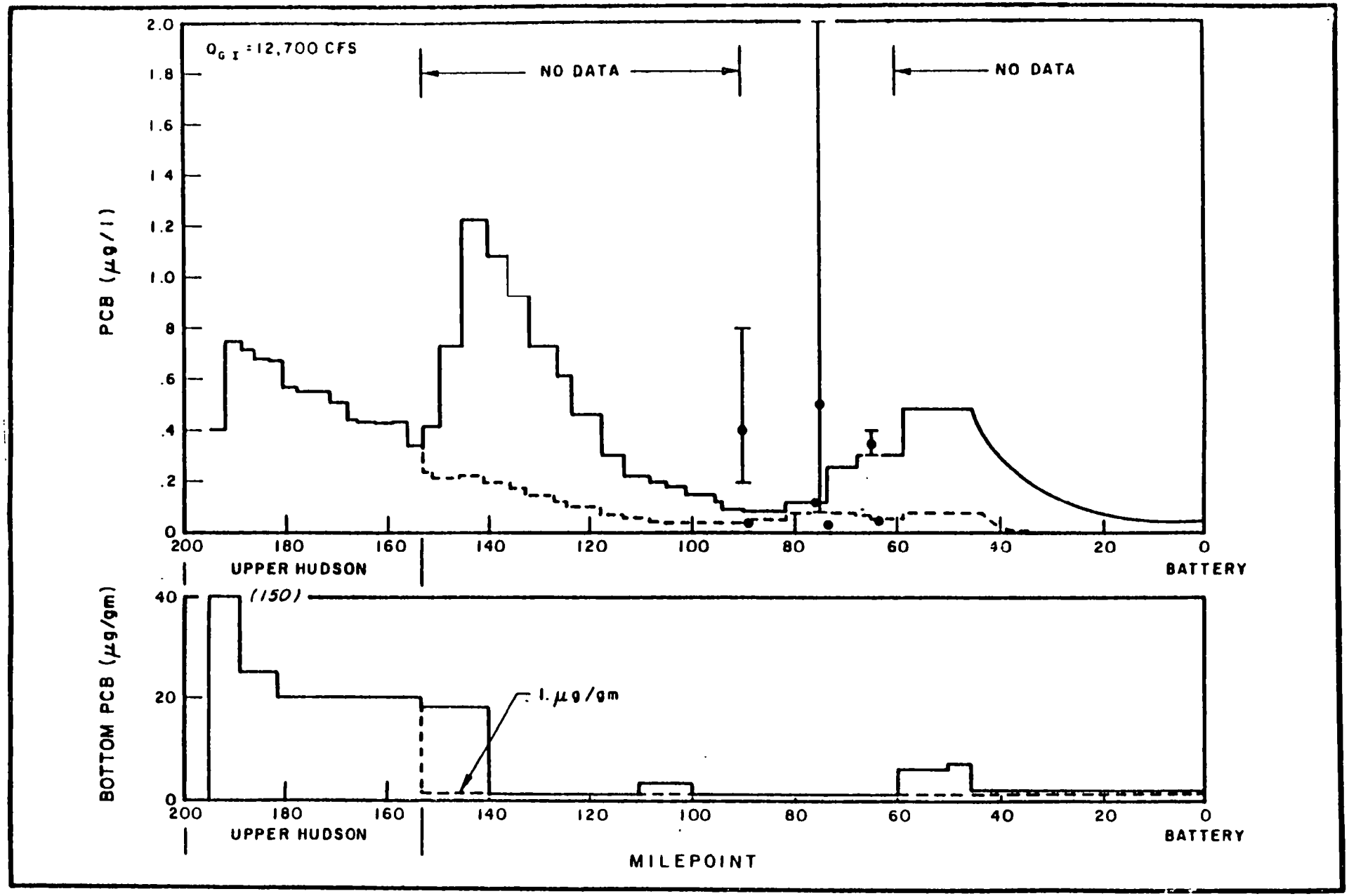

FIGURE 3

TOTAL PCB CALCULATED PROFILE AND BOTTOM PCB DISTRIBUTION

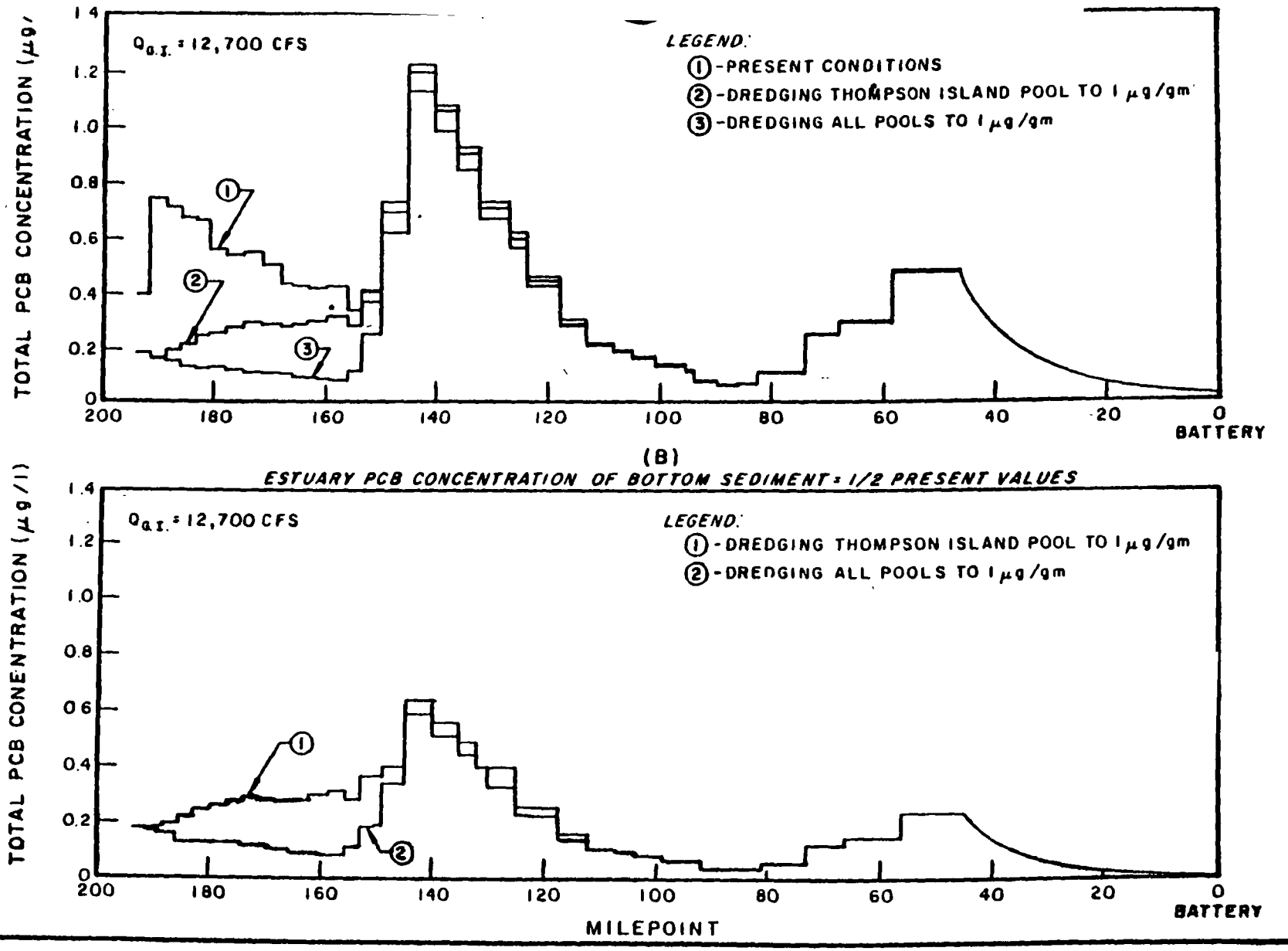

FIGURE 4
EFFECT OF REMEDIAL ACTION
ON PRESENT AND POSSIBLE FUTURE ESTUARINE CONDITIONS

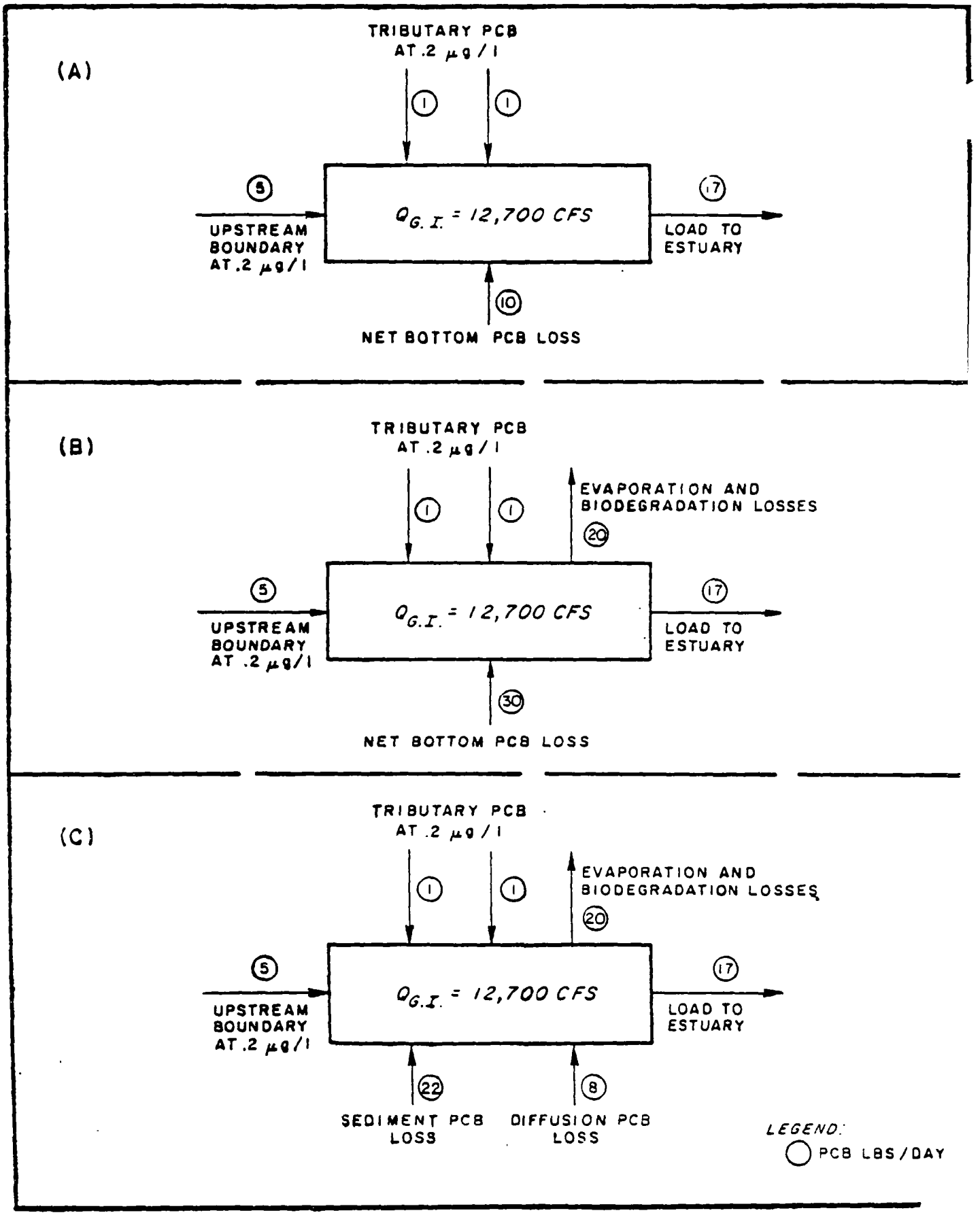

FIGURE 5

PCB MASS BALANCE
(UPPER HUDSON RIVER)

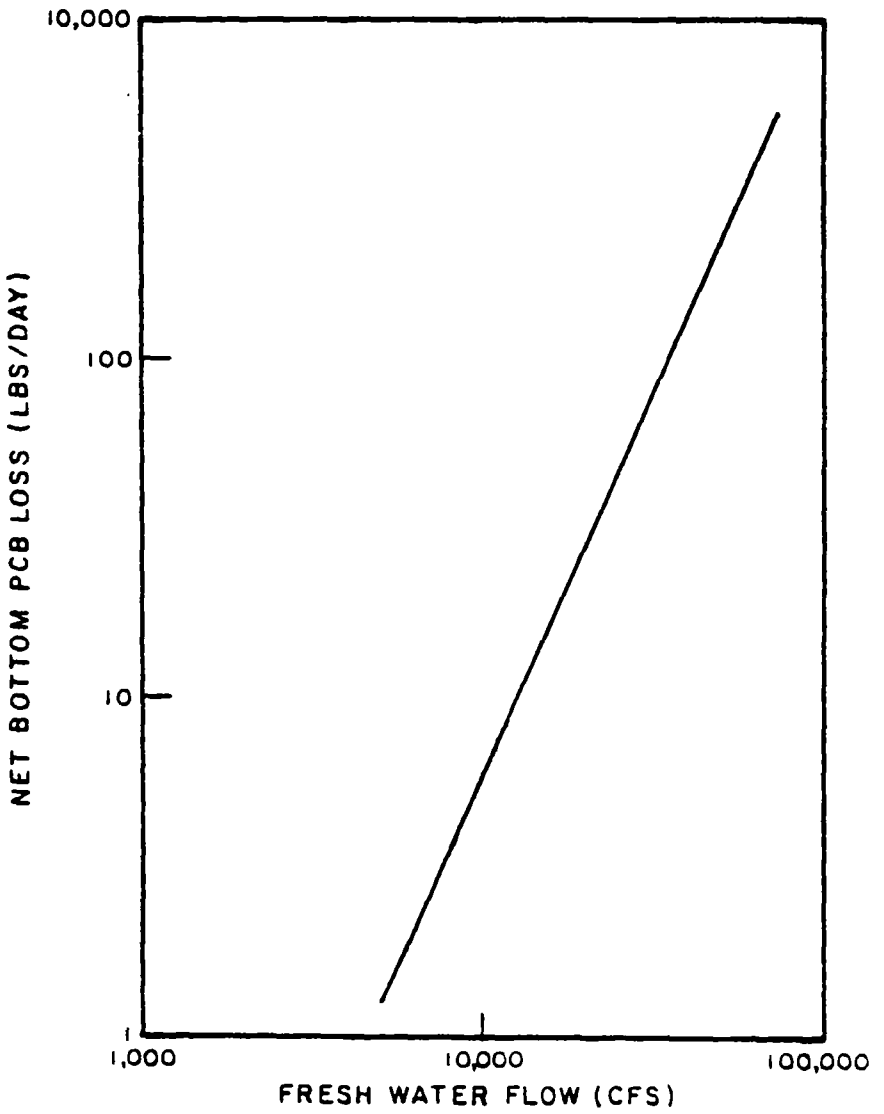

FIGURE 6

NET PCB LOSS FROM BOTTOM SEDIMENTS
(UPPER HUDSON RIVER)

APPLICATIONS* *TOXIC SUBSTANCES IN STREAMS*

The following applications relate to the distribution of Polychlorinated Biphenyls in the Hudson and heavy metals in a fresh water stream - zinc, nickel and copper. Type I and Type II analyses are employed as discussed in the respective examples.

1. Heavy Metals in a River

A map of the study area is presented in Figure 1-1. The major waste water discharges are from three municipal treatment plants, all of which are of activated sludge type. Industrial waste-waters are pretreated before entering the municipal plants. The major source of heavy metals is from the most upstream plant located at milepoint 47.

The drainage area is 760 square miles. The average annual flow is about 0.6 CFS/sq. mi., with a typical high flow in spring and low flow in late summer - early fall. A large percent of the flow in the river at the upstream site is due to the waste treatment plant, which discharges about 40 CFS. Pertinent hydrologic data are shown in Figure 1-2. As evident from the upper figure, the river flows through two different topographic terrains - average slope in the upstream reach is 13 feet per mile and in the downstream 3 feet per mile. In spite of the differences however, the velocities in each stretch are comparable, as shown in Figure 1-3, on which is also presented the depth-flow correlation.

Two surveys were conducted in 1978 - during May and July. Fifteen (15) stations were sampled as well as waste water inputs and tributaries. Water column and bed measurements were made on solids - dissolved and suspended and metals - soluble and particulate. Figure 1-4 presents the suspended solids and dissolved solids spatial distributions. The solid lines are calculated assuming steady-state conditions. The dissolved solids substantiate the flow distribution and the suspended solids were fit by assuming resuspension fluxes in accordance with equation (13) (Type II Analysis).

Laboratory experiments were conducted to determine the adsorption - desorption rates and the equilibrium concentrations, from which the partition coefficient was determined. A representative example of these data is shown in Figure 1-5. The time to equilibrium is relatively rapid - i.e. in the order of 1 or 2 hours - indicating the validity of the instantaneous equilibrium condition. It is more appropriate to employ the kinetic equations in the mile or so immediately downstream from the treatment plant, since an

*Donald J. O'Connor

hour is the order of the travel time in this stretch. However the instantaneous equilibrium condition is a reasonable first approximation.

The heavy metal distributions for zinc, nickel and copper are shown in Figure 1-6. The solid lines are calculated in accordance with equation 20, using numerical procedures. The finite-difference form of this and the related solids equations are straightforward. Since the constituents of concern are heavy metals, evaporative transfer is inoperative (Ka=0). The partition coefficients assigned for the three metals were 70,000, 20,000 and 50,000. Due to the increasing flow in river, due to ground water inflow, allowance for this dilution effect is made in accordance with equations (3) and (5).

Figures 1-7 and 1-8 present the observed values and the calculated profiles for the subsequent survey in July. The identical computational procedure was followed, with the important exception that a Type I analysis applied in this case. Equations (5) and (6) are used for the calculation of the suspended solids and equations (10) and (11) for the total concentration of heavy metals. The particulate and soluble fractions are readily determined knowing the partition coefficient and the concentration of suspended solids. Additional surveys were conducted in 1979. The July and August data and calculated profiles are presented in Figs. 1-9 through 1-12. A Type II analysis was the basis of calculation for both survey sets.

Additional insight is gained by an examination of Figs. 1-13 & 1-14, which display the bed concentrations of metals for the May and July survey of 1978. In the latter survey, a delineation between the fine and coarse - bed material was made. - A size of 75 μm was selected to distinguish the two general classes - sands vs. salts and clays. The solid phase concentration of finer solids is about an order of magnitude greater than that of the coarse. It is also interesting to note that the solid phase concentration in suspension tracks and exceeds that of the fines in the bed - probably due to the fact that the former contains smaller size particles, which generally have a greater adsorption capacity, than the fines in the bed. This information is presented to indicate the importance of the water-bed interaction with respect to the various size classes and the resulting effect in the water column. Subsequent modeling is being conducted to address these distinctions and bed transport. -

ACKNOWLEDGEMENT

The work reported above was performed by Hydroscience, Inc. The contributions of Thomas W. Gallagher, Dominic Di Toro and Michael Kontaxis are recognized.

2. Polychlorinated Biphenyls - Hudson River

The analysis reported in this section was part of a larger study which was directed to an evaluation of the need of remedial action with respect to PCBs in the Hudson River. Although the most contaminated areas are in the vicinity of the upstream source, above the Troy dam, the entire length of the river through the tidal regions has been affected to some degree. The primary emphasis of the study was placed on the accumulation of the chemical in the food chain - particularly the migratory fish. In the course of the project, a preliminary analysis was made of the physiochemical factors which determine the distribution of PCBs in the water and in the bed. A review of that analysis is presented in this example. A more detailed description of the project with emphasis on the food chain, is presented in a subsequent section.

It is specifically the purpose of this section to demonstrate the utility of the analytical solutions of the basic differential equations in order to make a preliminary assessment of the problem. Appreciating that such solutions usually represent idealized conditions - e.g. constant area, steady-state - nevertheless, they may be accepted as a first step providing a basis for a more detailed analysis. The major advantage of using these solutions lies in the fact that an evaluation of various factors is readily available - e.g. the selective effects on volatilization versus degradation. A secondary purpose of this example is to present the procedural approach and method of analyzing data. The latter was regarded as inadequate or, at least incomplete. This situation is not uncommon in water quality analysis - making the most of meager and perhaps inadequate data.

This application presented here deals exclusively with the fresh water portion of the River from the Federal Lock at Troy, milepoint 156 upstream to Fort Edward, milepoint 194. The upstream location is in the vicinity of the General Electric Plant, which was the original source of the PCBs. Although the discharge was discontinued, there are significant residual concentrations in the bed which affect the concentration in the water column in both upstream and downstream stretches.

A map of the area is shown in Figure 2-1. The river segment of interest in this example extends approximately from Troy to Glen Falls. The drainage area and flow variation from Glen Falls to the mouth are shown in Figure 2-2, the latter is based on the average annual flow of 13,000 CFS at

Green Island. This figure also indicates the types of transport in each segment - flowing stream, tidal river and saline estuary. The following analysis is related to the upper stream stretch.

Data was collected in 1976 and 1977 during high flow periods and the 1977 flows were extremely heavy floods, in the order of 1 in 50 - 100 years. The analysis of the 1976 data is presented in Figure 2-3, which indicates the concentration of suspended solids and PCB for the various flow periods. The solids distributions are calculated in accordance with equation (11) and the PCB with equation (23). Type II Analysis (water-bed interaction) is appropriate as is evident from the comparison of the observed data and computed profiles. The model portrays the general trend of both solids and PCB data, providing a reasonable fit for each set.

By contrast, the 1977 data were anomalous as shown in Figure 2-4. The March 29, 1976 data set and model results are presented for comparison. The suspended solids distributions are fairly well reproduced. The exceptionally high flow of 160,000 CFS resulted in large concentrations of solids to values of greater than 1,000 mg/liter. The PCB data, however, are erratic for this condition. High concentrations are expected, but the measurements indicated less than 1 µg per liter. Furthermore, these levels are completely at variance with the high flow of the previous year when measured values were in the order 10 µg/liter and greater.

There are many possible causes for the apparent inconsistency. The 1977 flood may have affected the tributaries to greater extent than the main branch thus introducing large concentrations of uncontaminated solids. This increased mass of solids acts as a dilutant for the presently contaminated solids, which desorb and re-absorb to the fresh solids. An alternate hypothesis may be presented: the excessively high flood may have resuspended large segments of the bed material, particularly the greater size and more dense solids, which have a slower solid phase concentration. In any case, the importance of tributary drainage and bed characteristics is further emphasized by this example, information on which was inadequate to analyze these high flow conditions.

ACKNOWLEDGEMENT

The application reported in this section was supported by Hydro-Science, Inc., Westwood, N. J.-

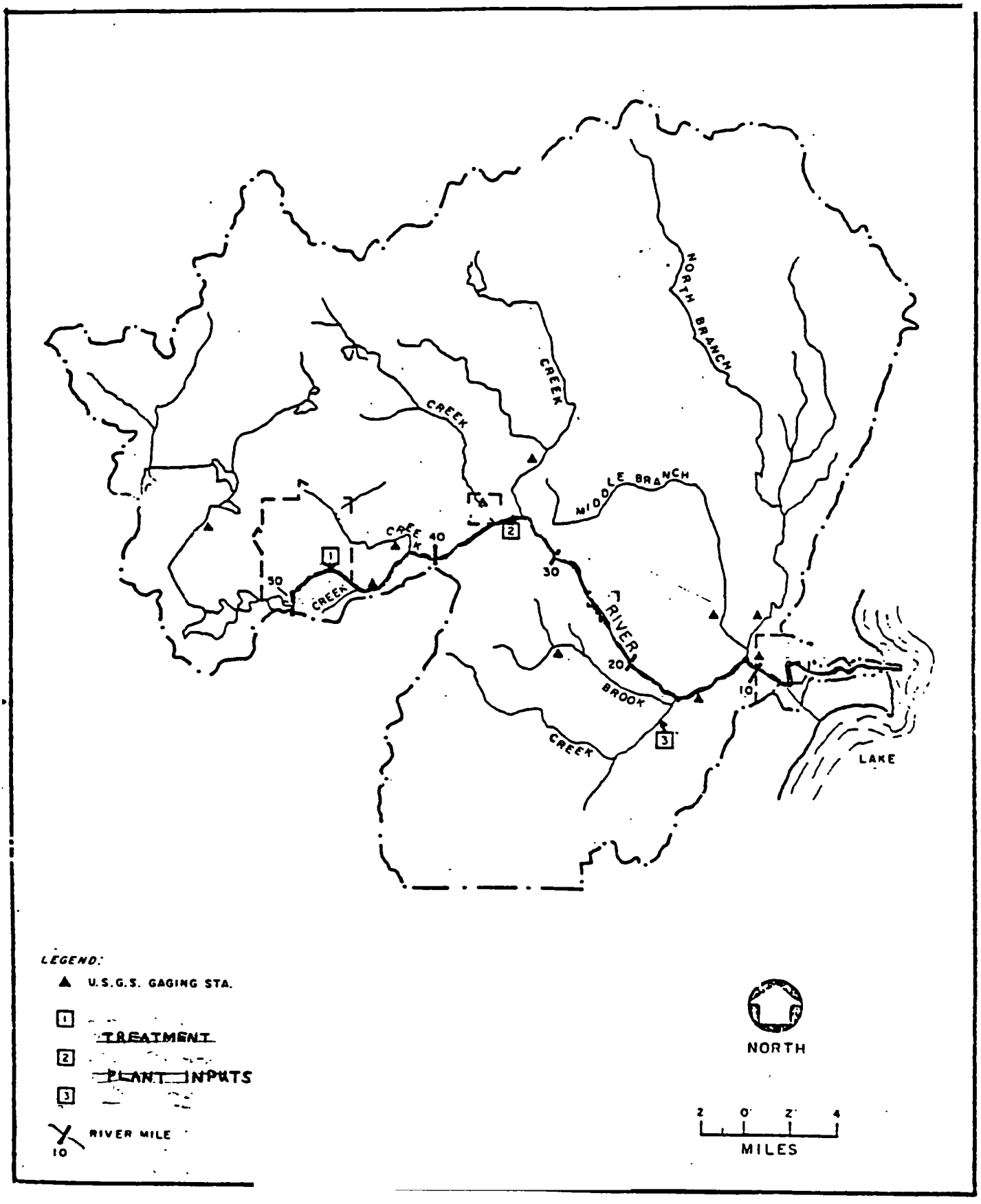

FIGURE 1. MAP OF STUDY AREA

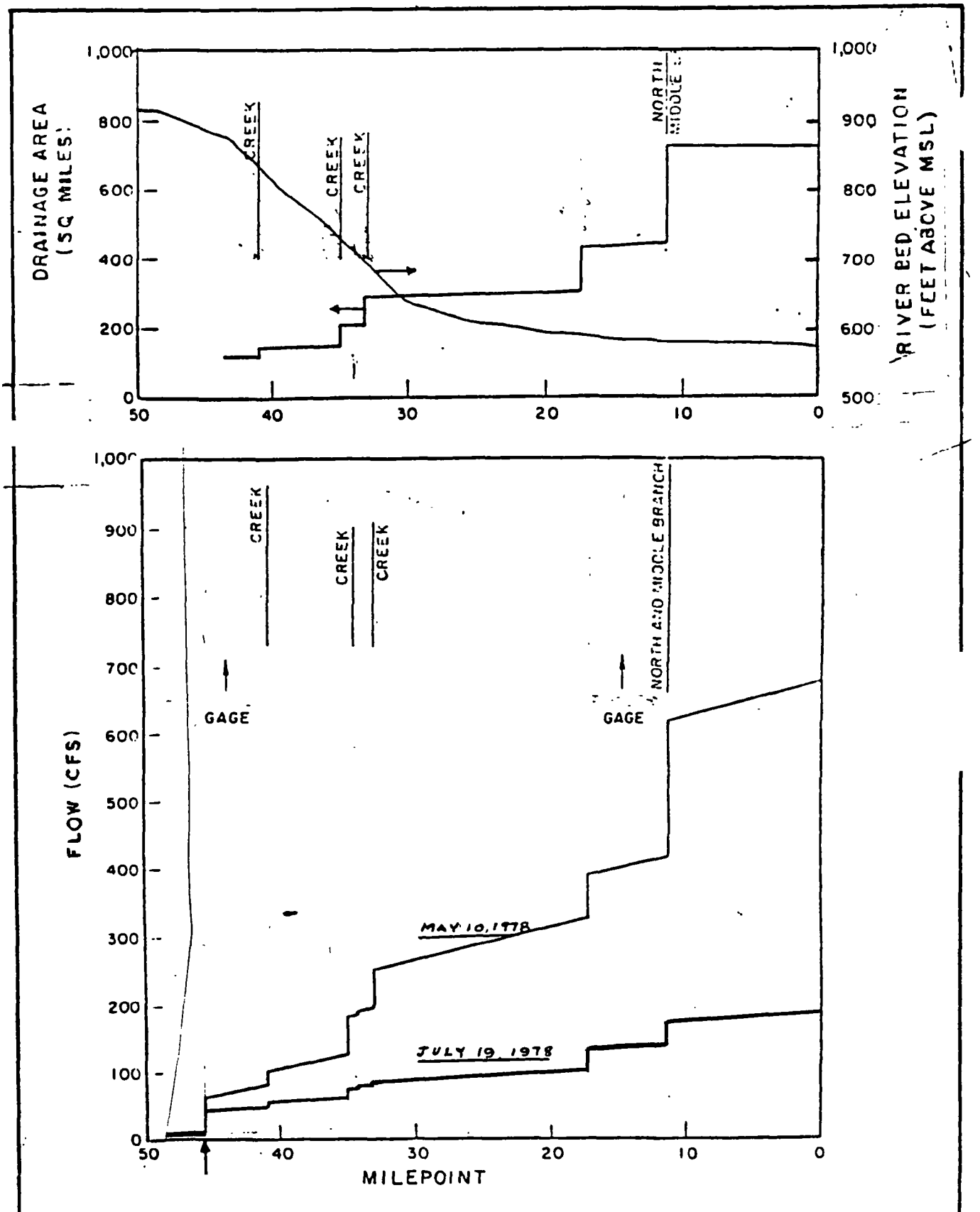

FIGURE 2. SLOPE, DRAINAGE AREA AND FLOW

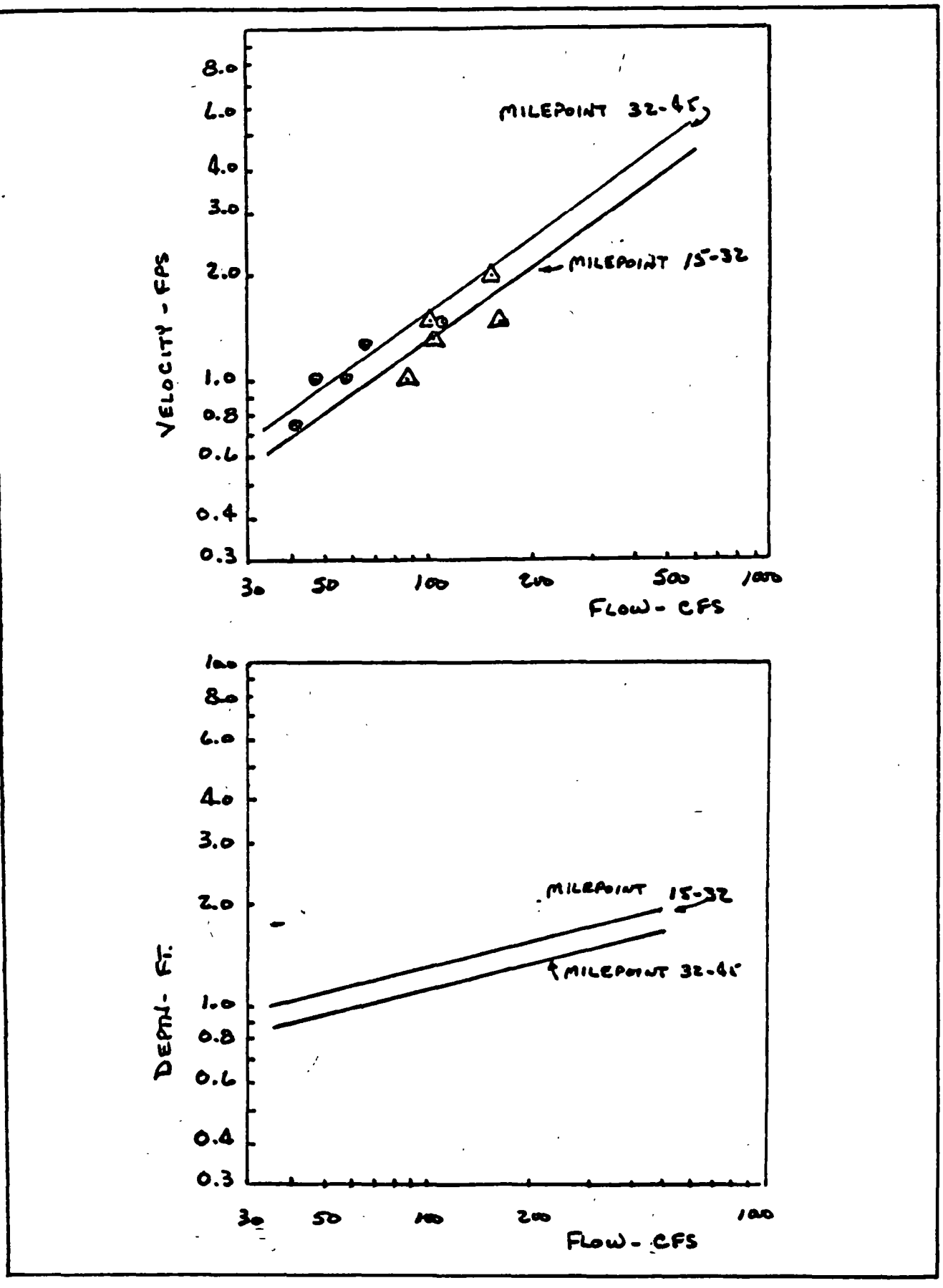

FIGURE 3. VELOCITY-DEPTH FLOW RELATIONS

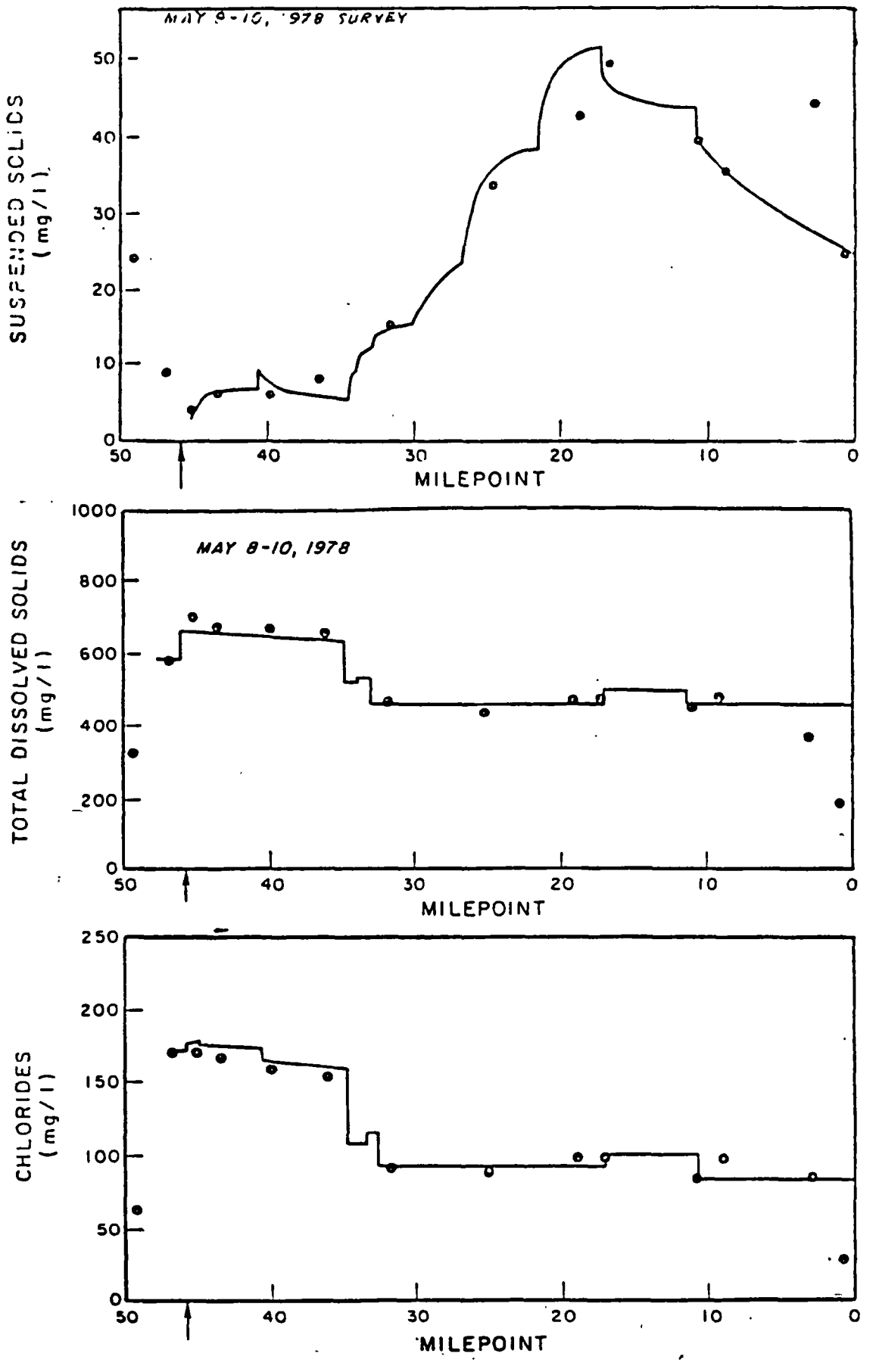

FIGURE 4. SUSPENDED & DISSOLVED SOLIDS - MAY 78

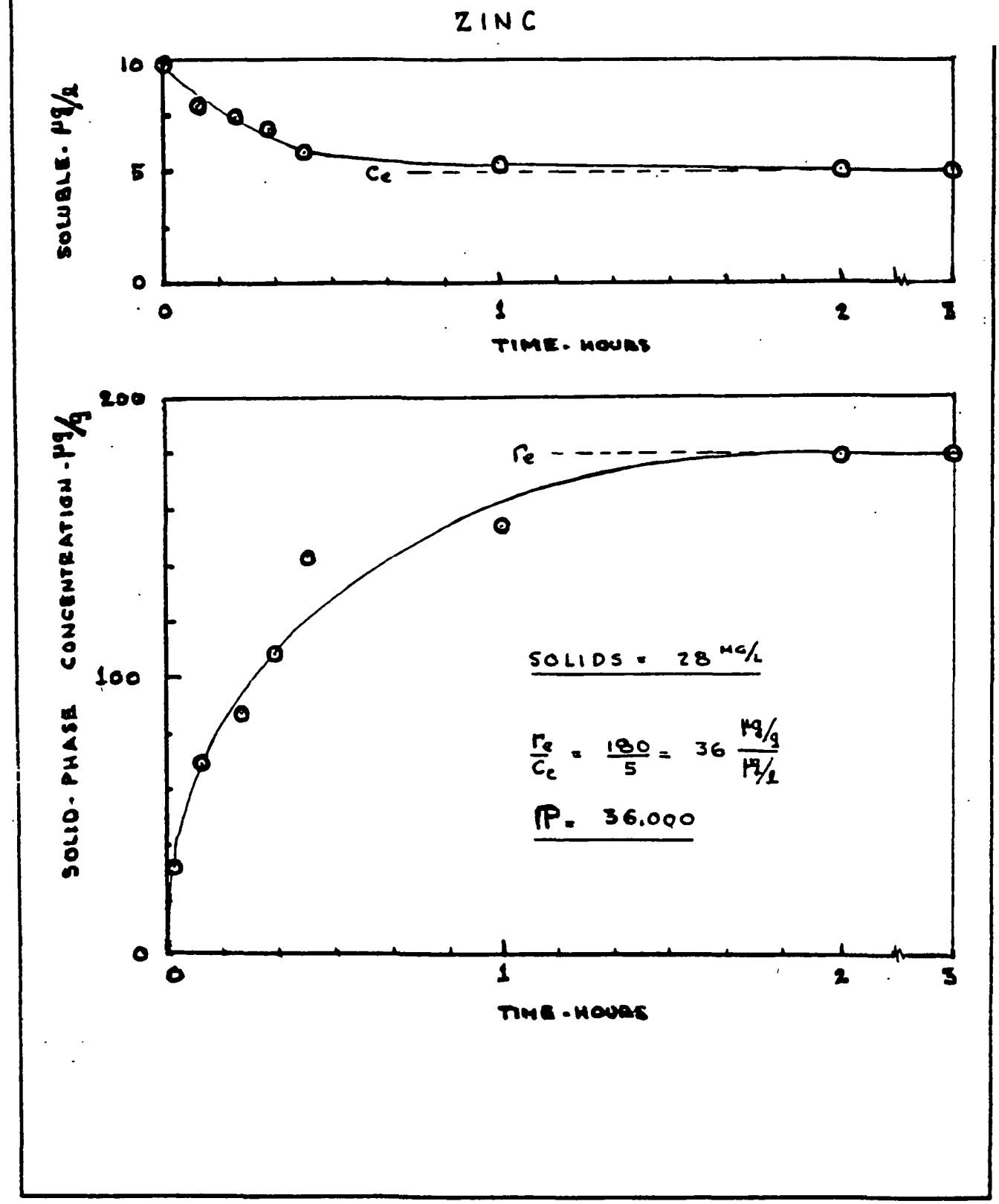

FIGURE 5. LABORATORY DATA ON ADSORPTION-DESORPTION

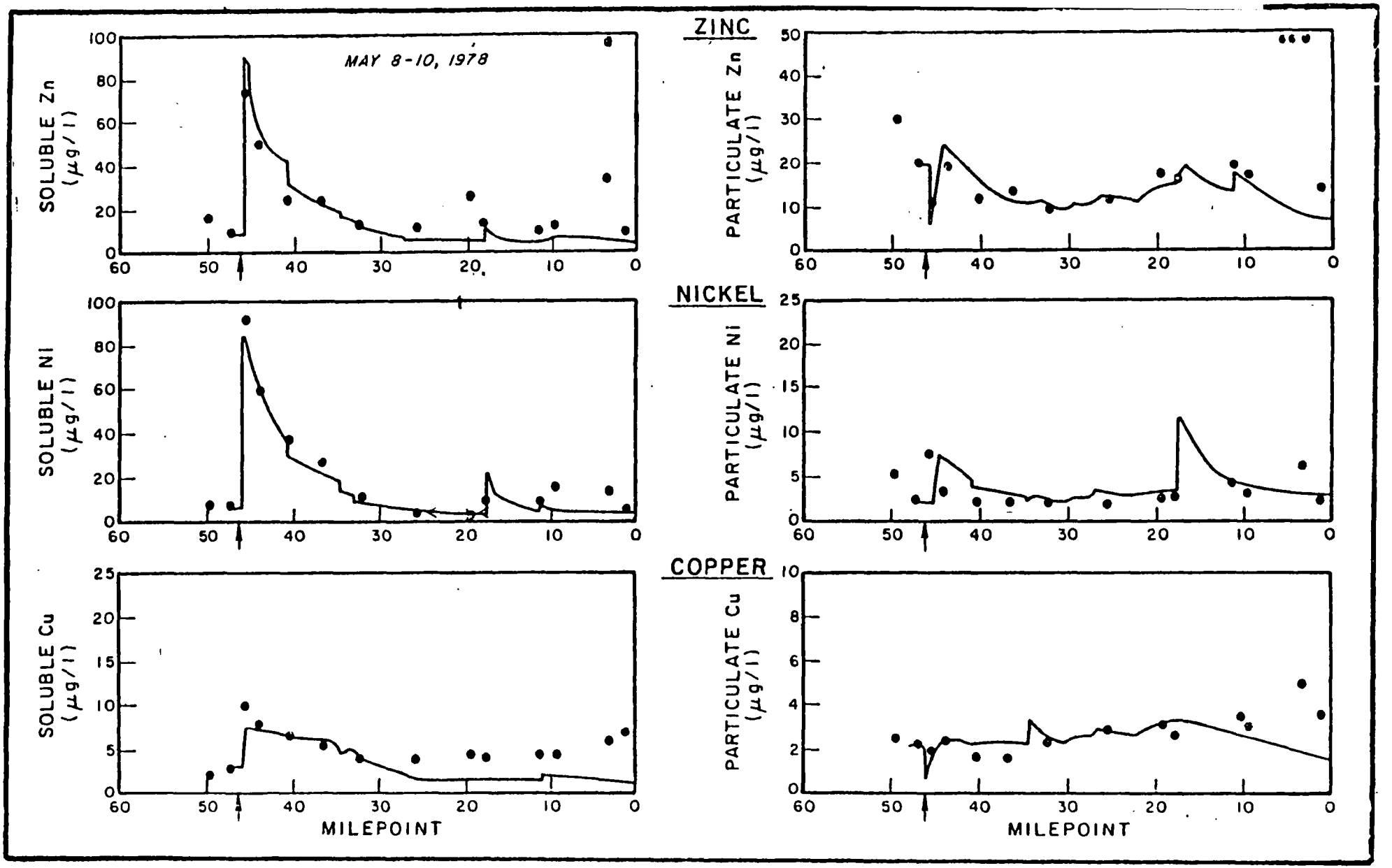

FIGURE 6. HEAVY METAL CONCENTRATIONS - MAY 78

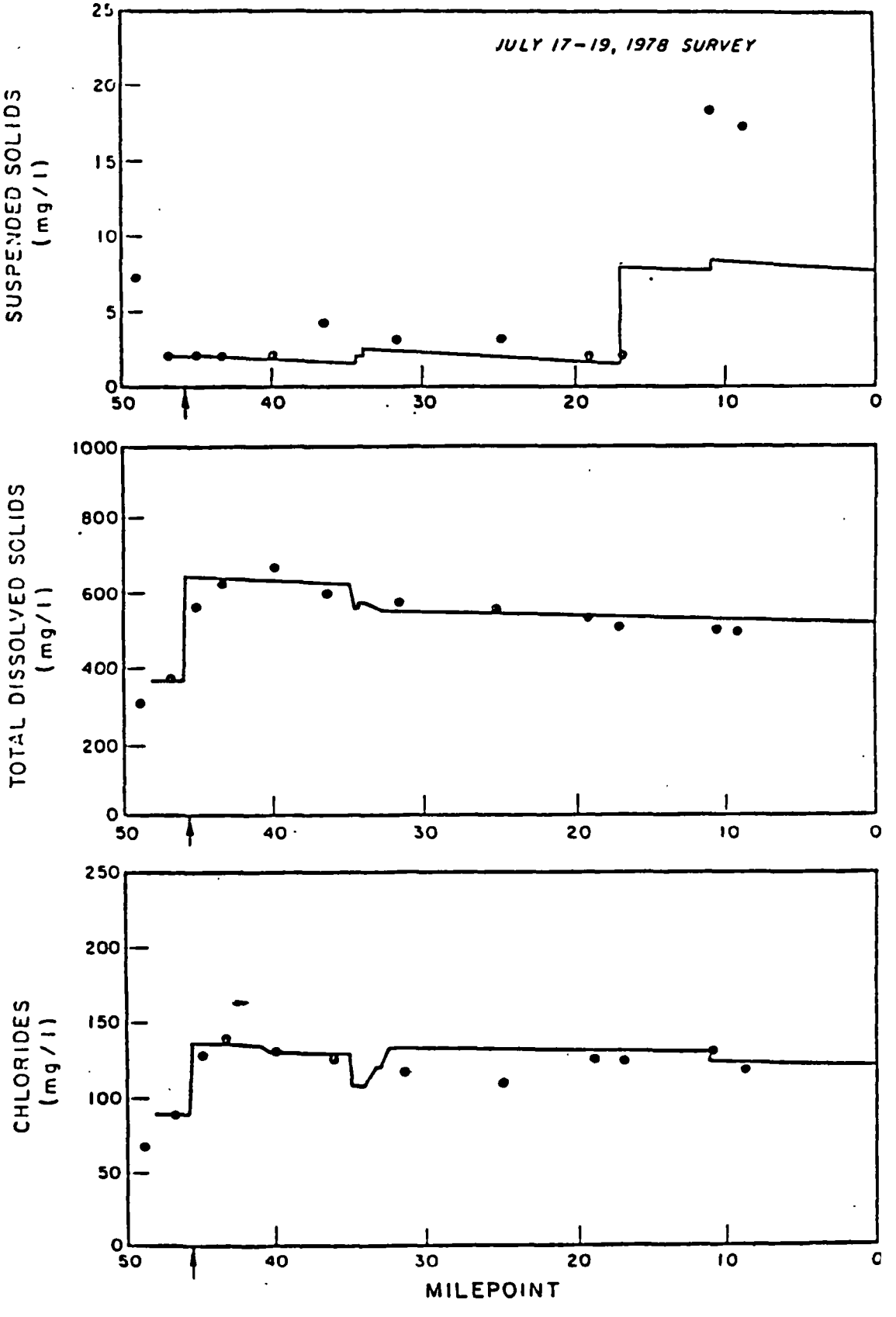

FIGURE 7. SUSPENDED & DISSOLVED SOLIDS - JULY 78

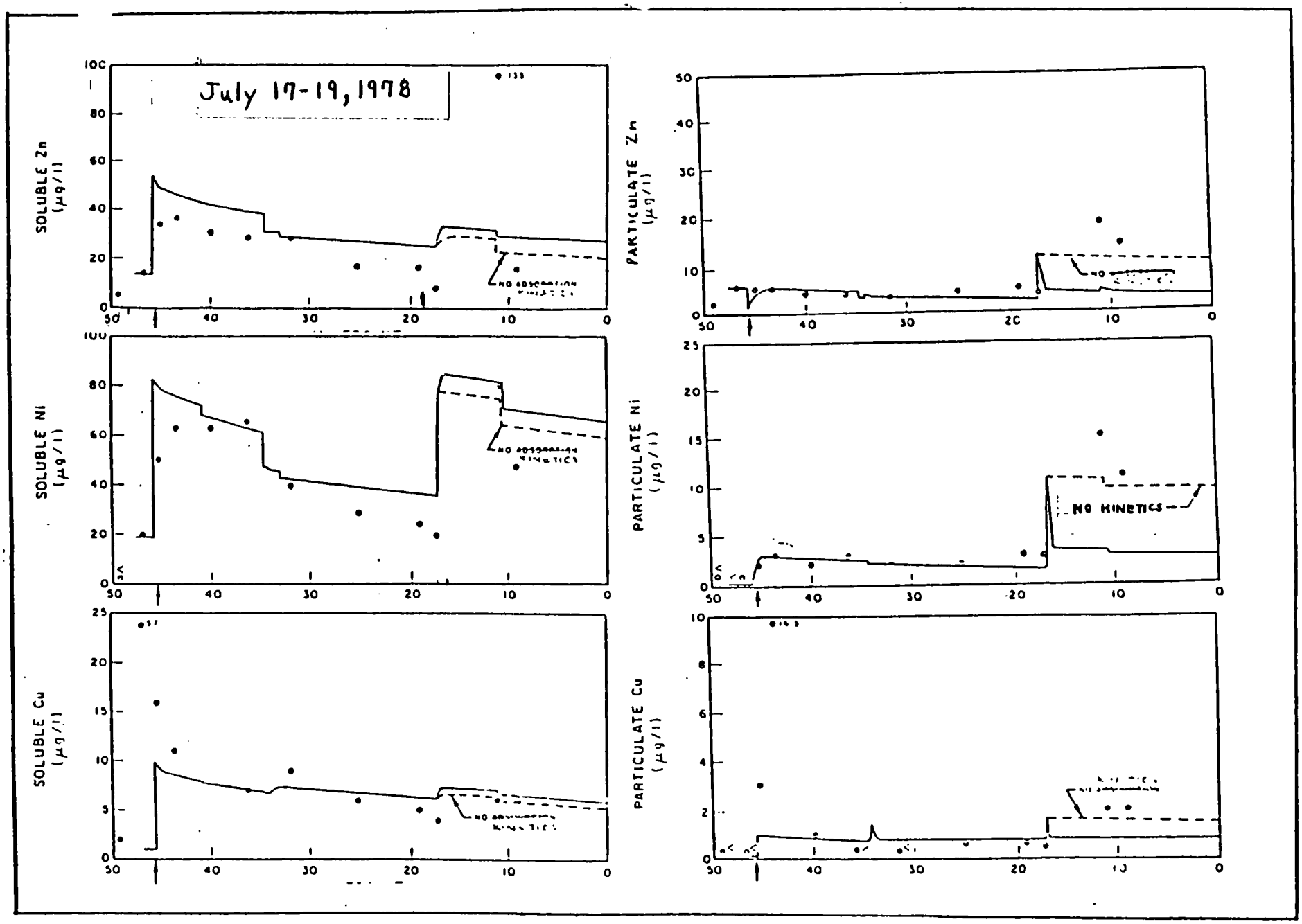

FIGURE 8. HEAVY M[illegible] CONCENTRATIONS - JULY 78

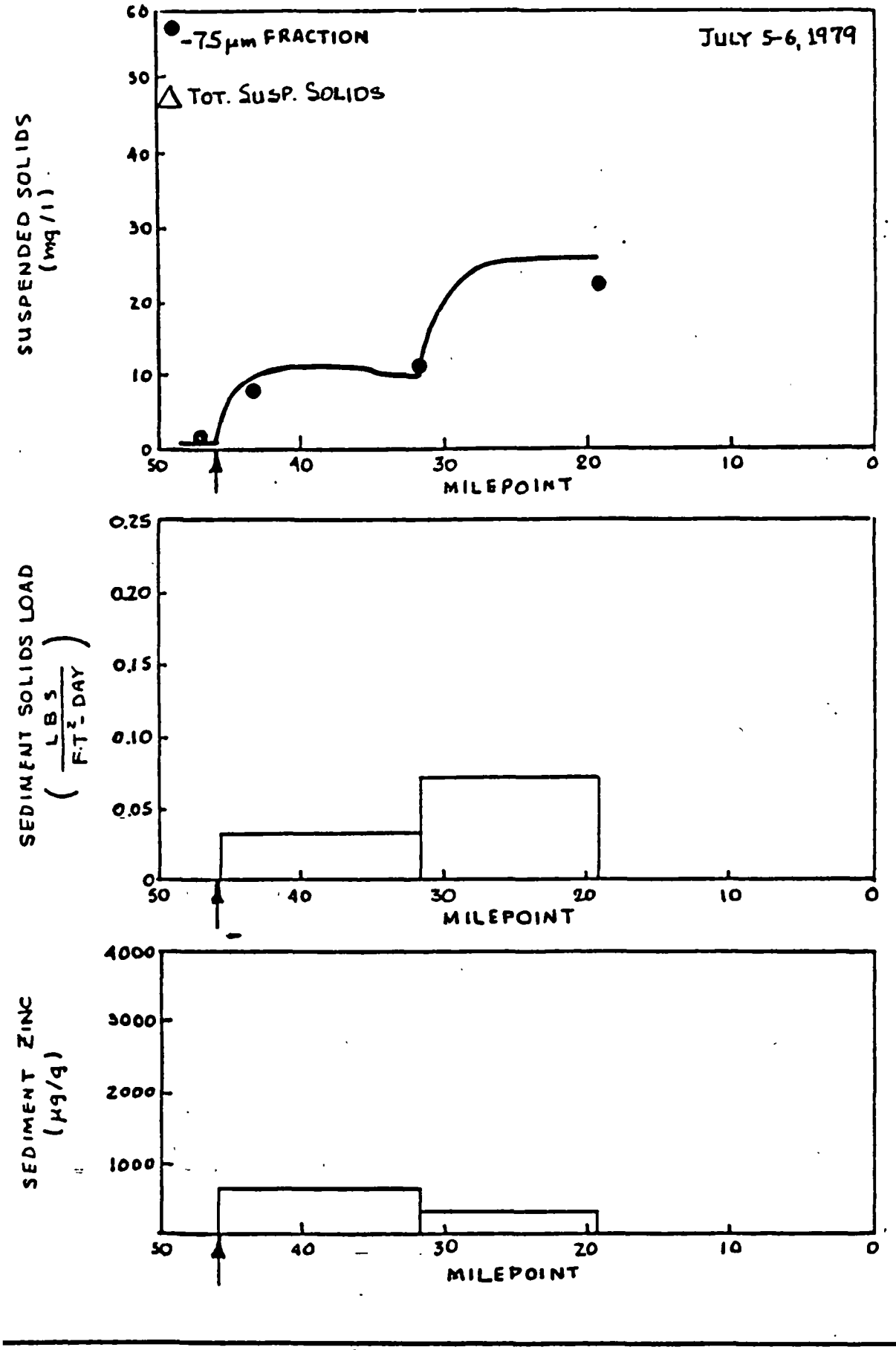

FIGURE 9. SUSPENDED SOLIDS - JULY 79

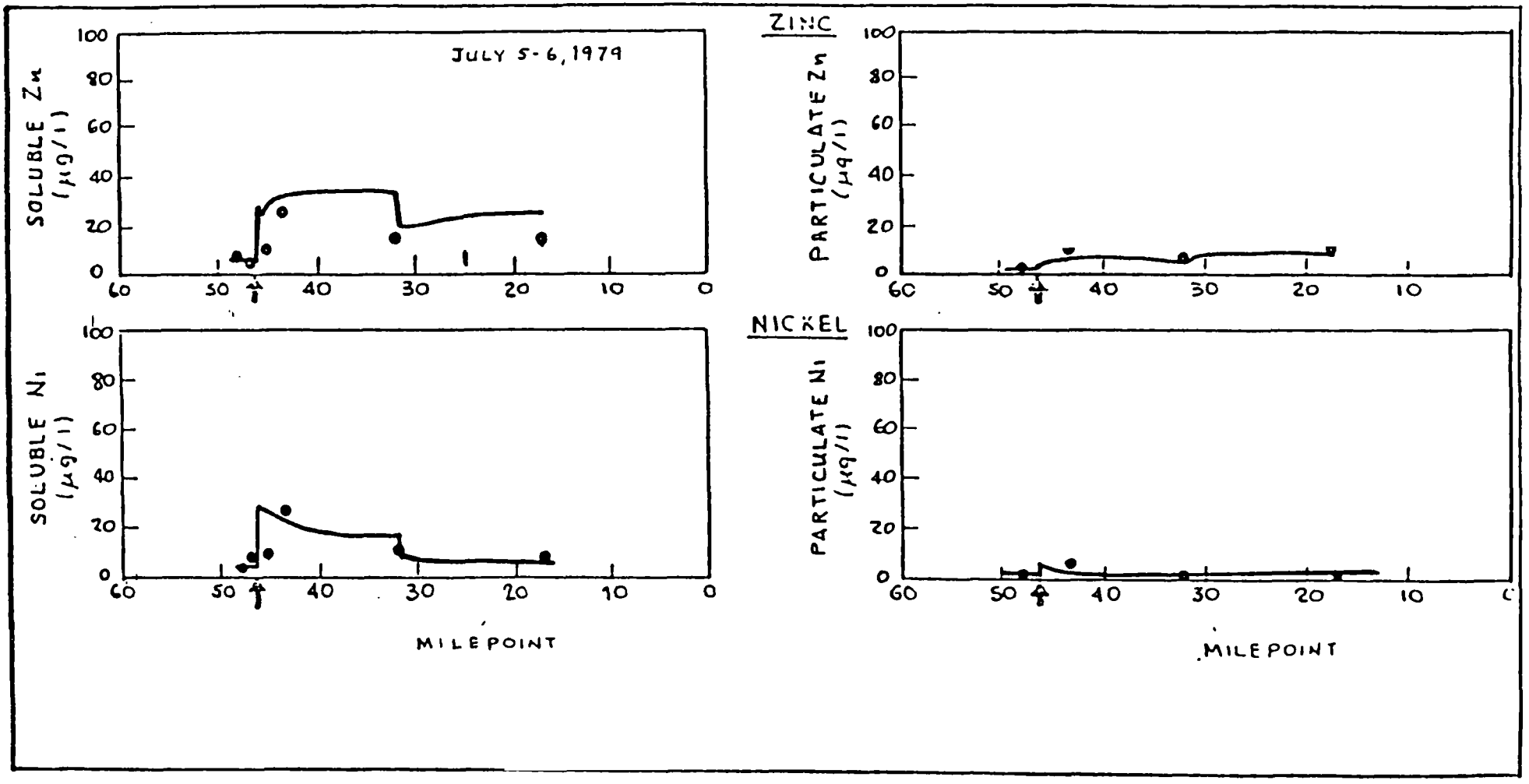

FIGURE 10. HEAVY METAL CONCENTRATIONS - JULY 79

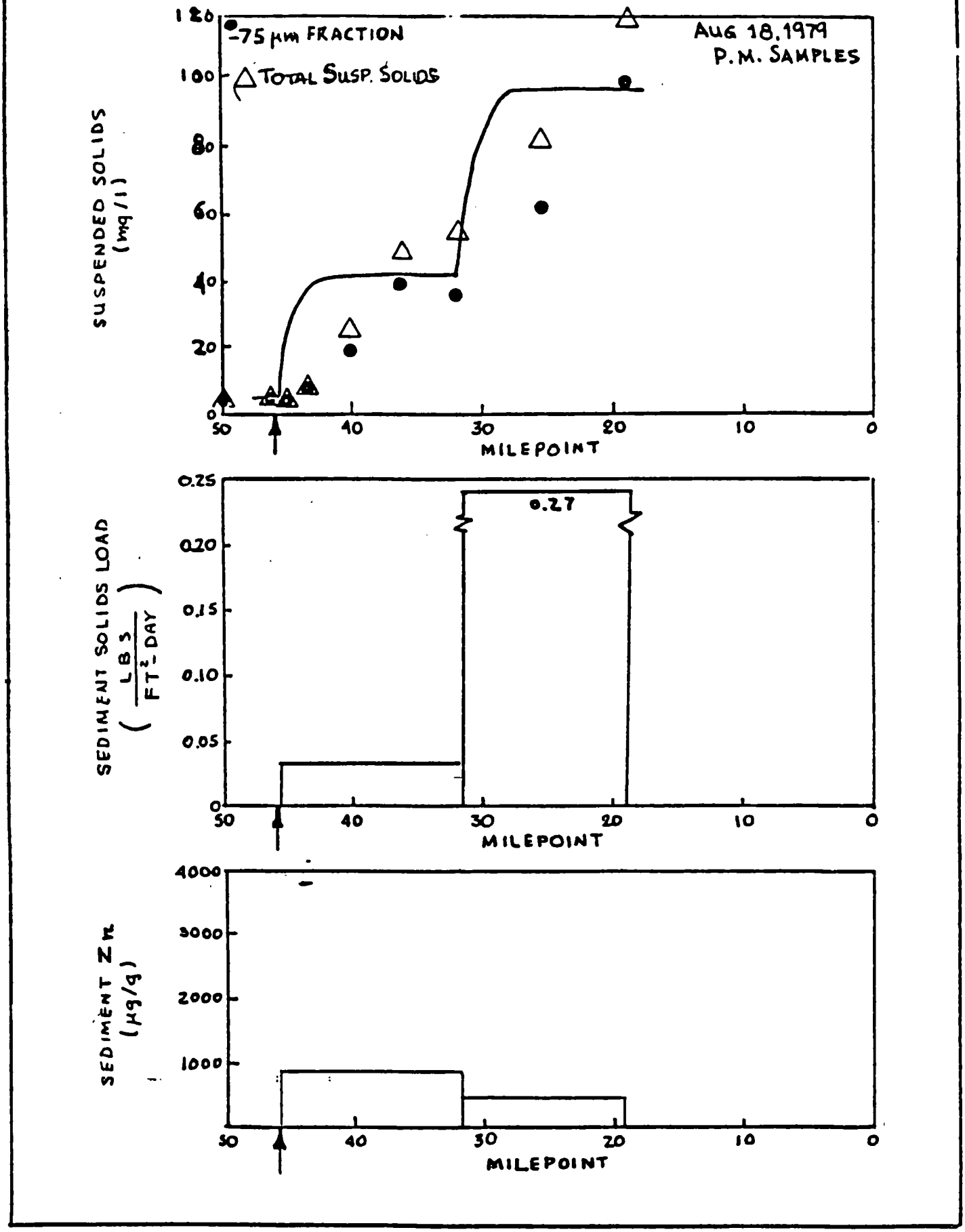

FIGURE 11. SUSPENDED SOLIDS - AUGUST 79

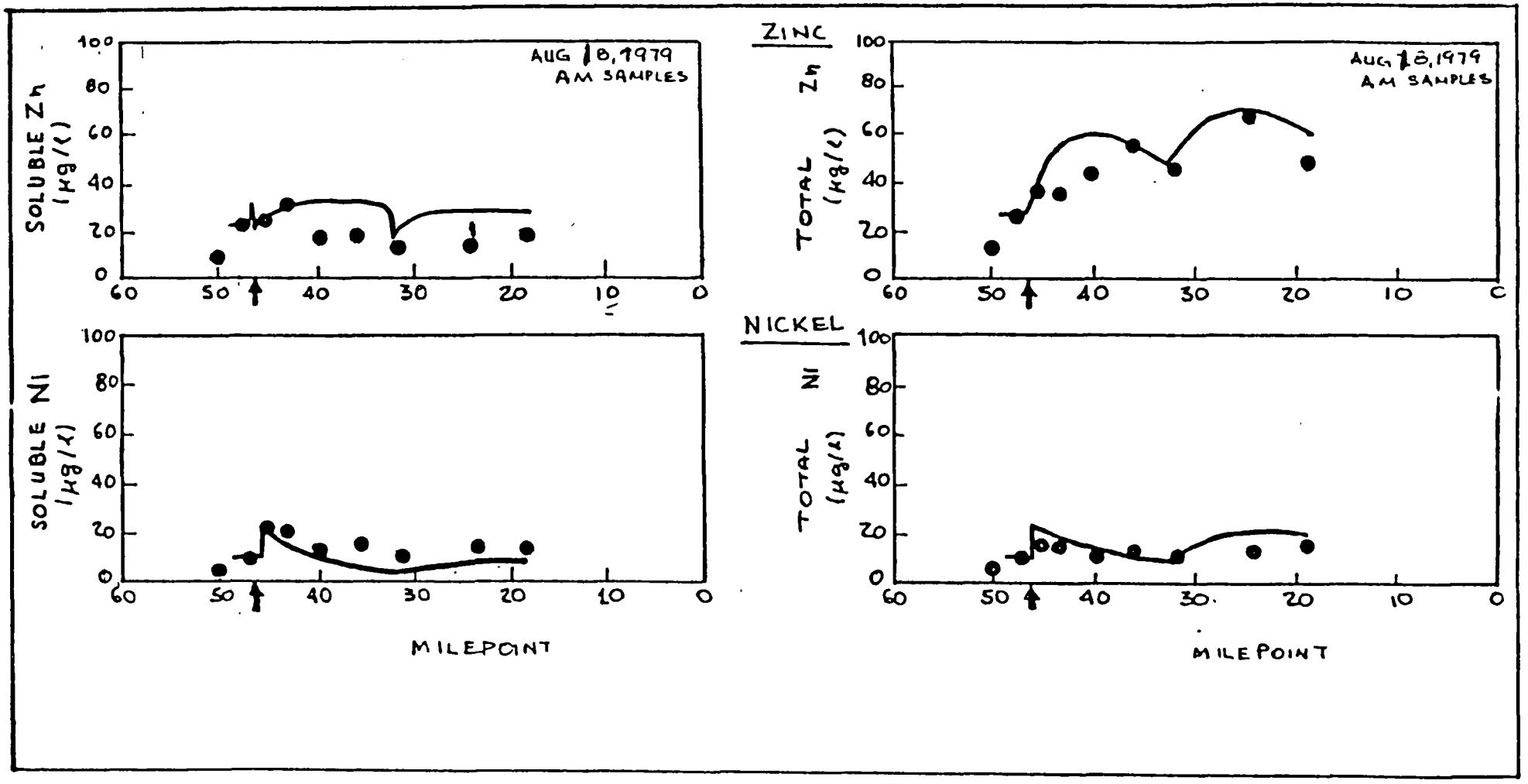

FIGURE 12. HEAVY METAL CONCENTRATIONS - AUGUST 79

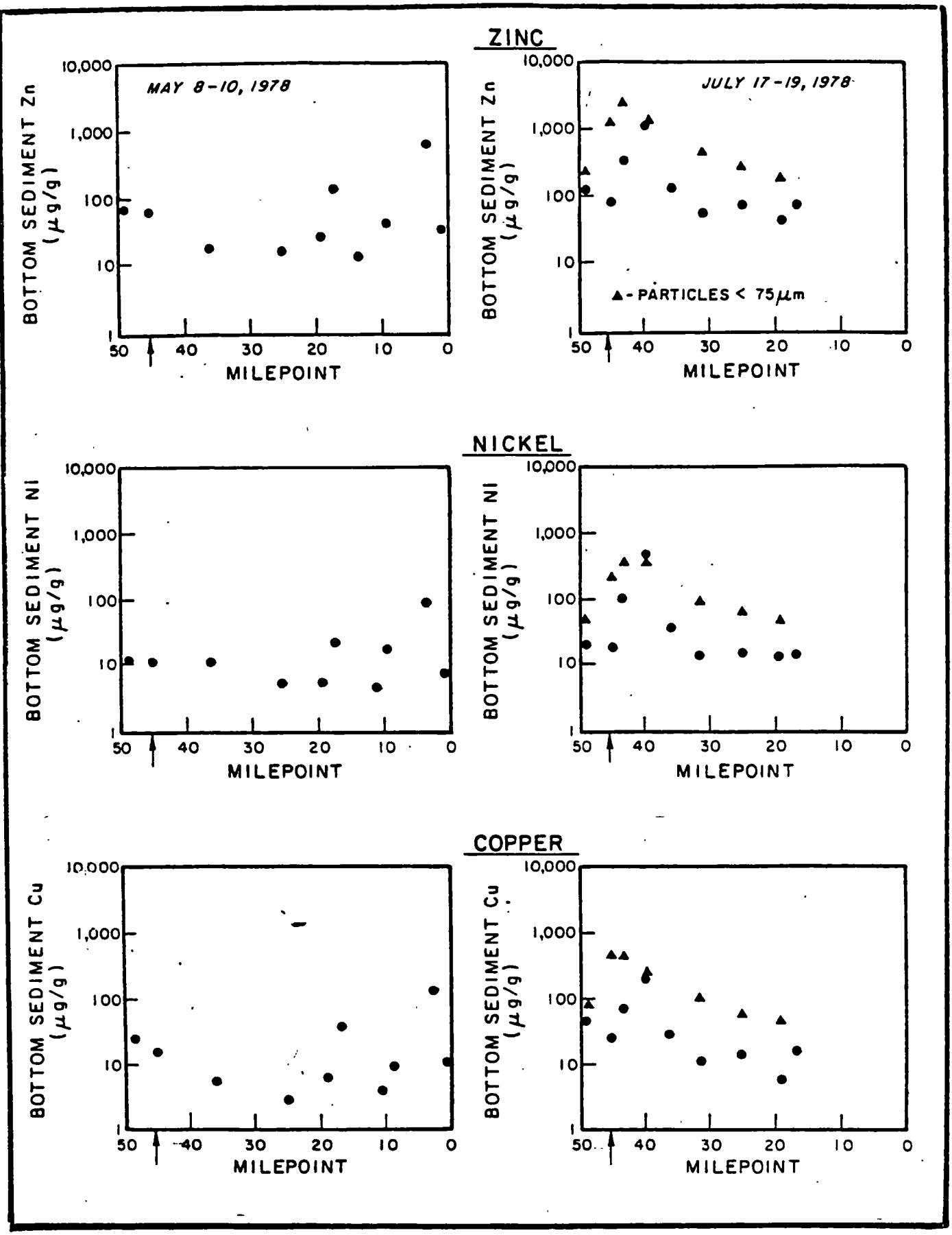

FIGURE 13. HEAVY METALS BED SEDIMENT

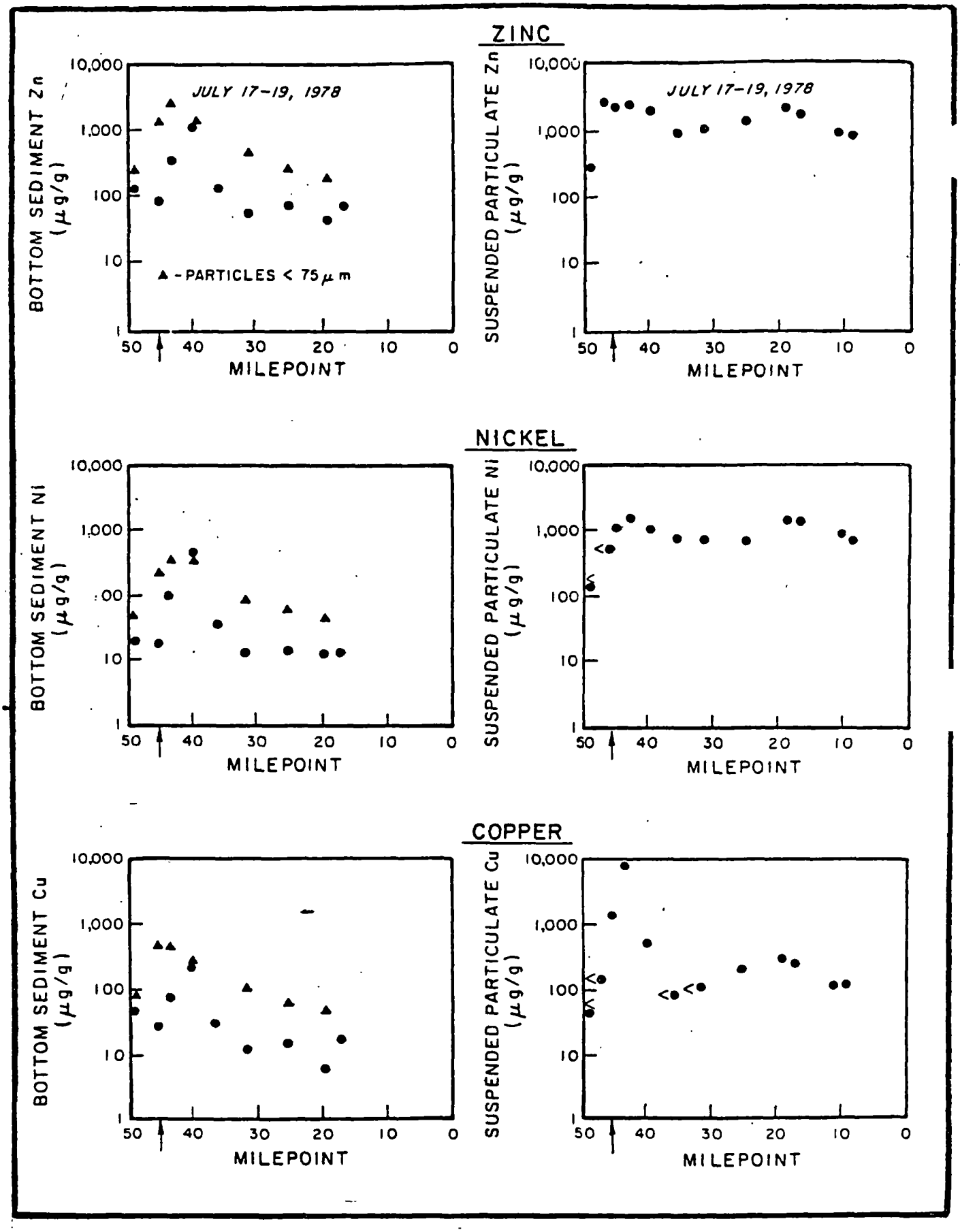

FIGURE 14. HEAVY METALS BED SEDIMENT & SUSPENDED SOLIDS

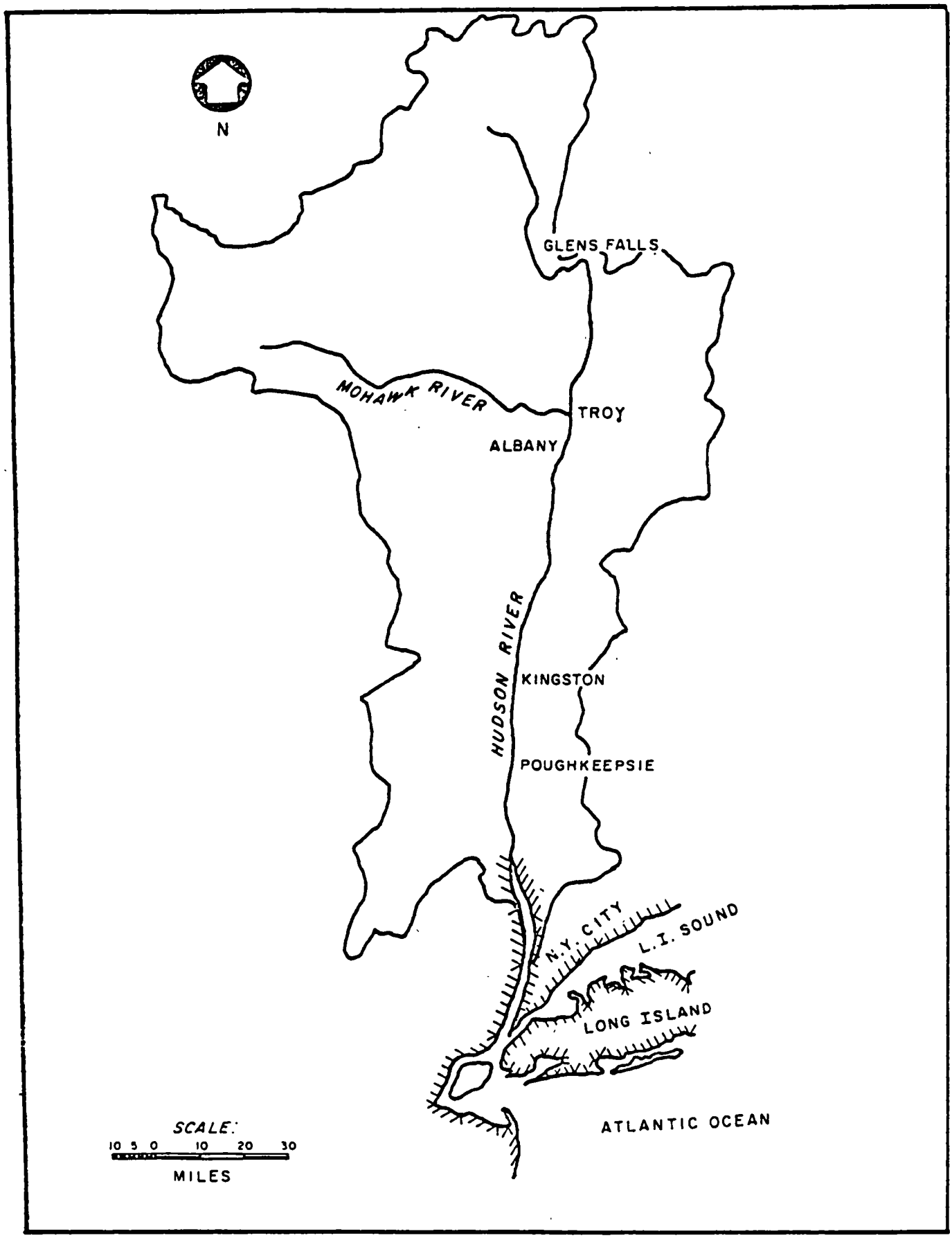

FIGURE 2-1

HUDSON RIVER BASIN

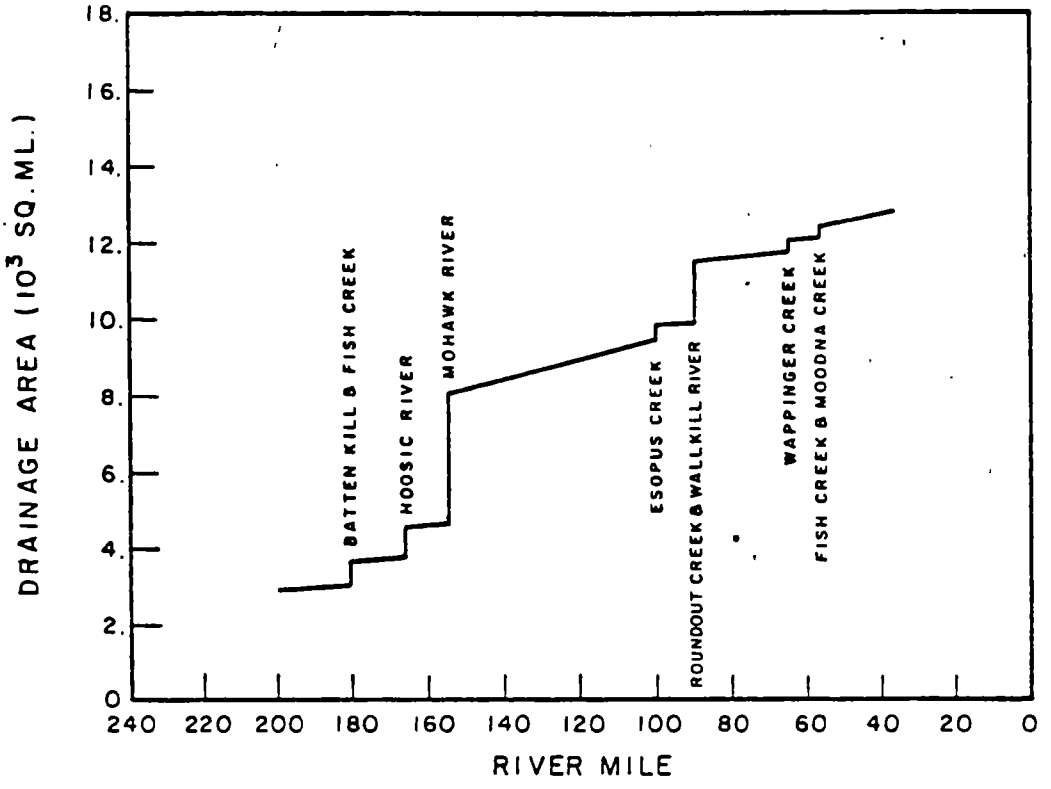

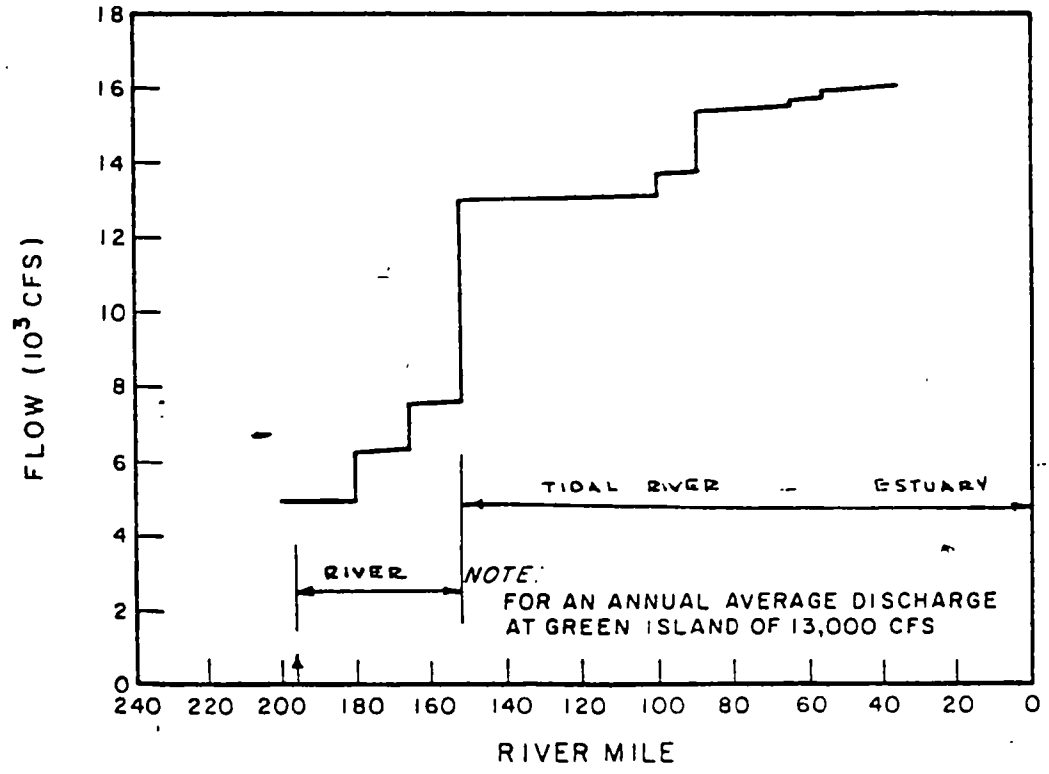

FIGURE 2-2

DRAINAGE AREA AND FLOW DISTRIBUTION

(GLENS FALLS TO STONY POINT)

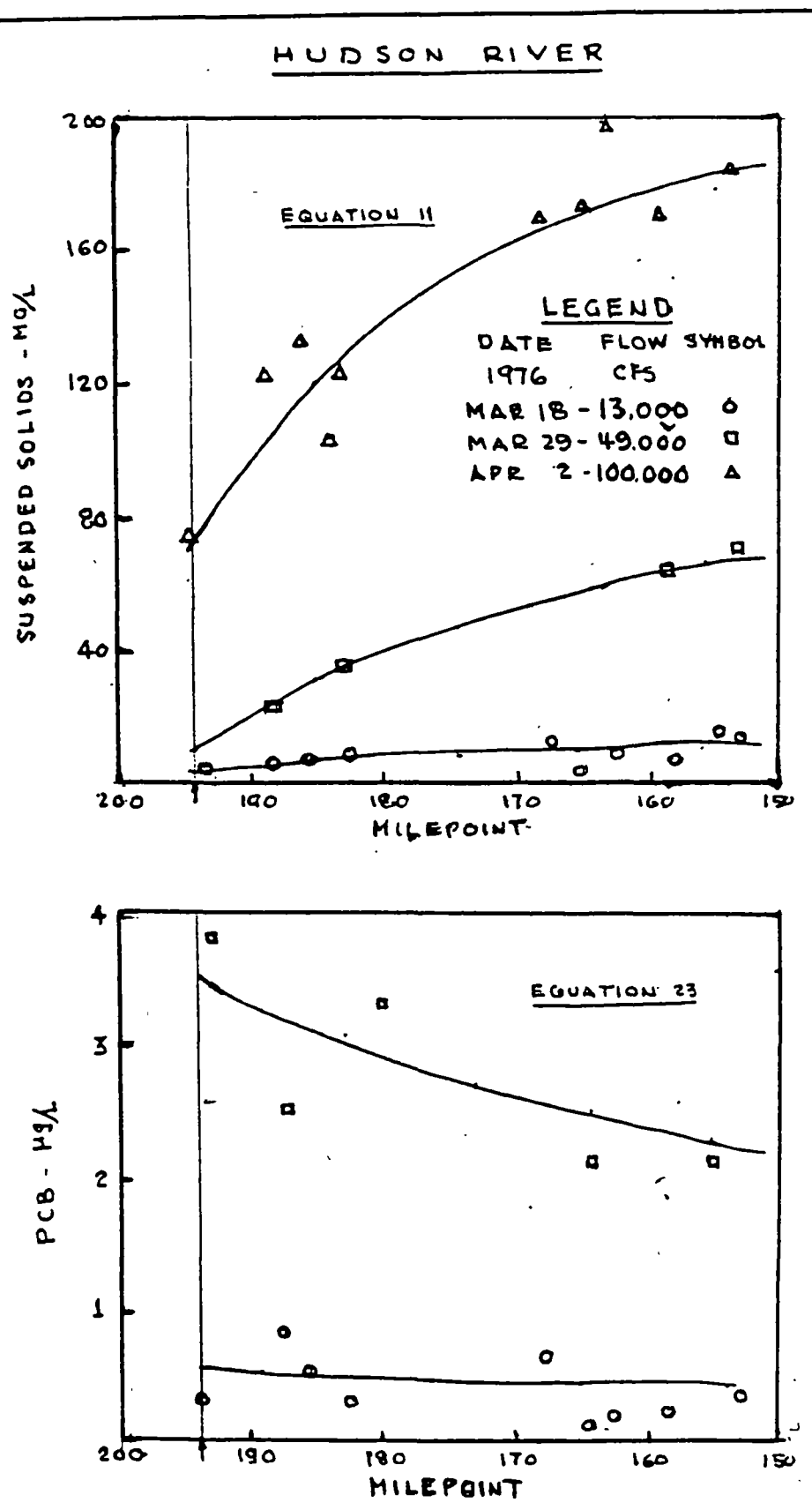

FIGURE 2-3. SOLIDS & PCB DISTRIBUTIONS - 1976

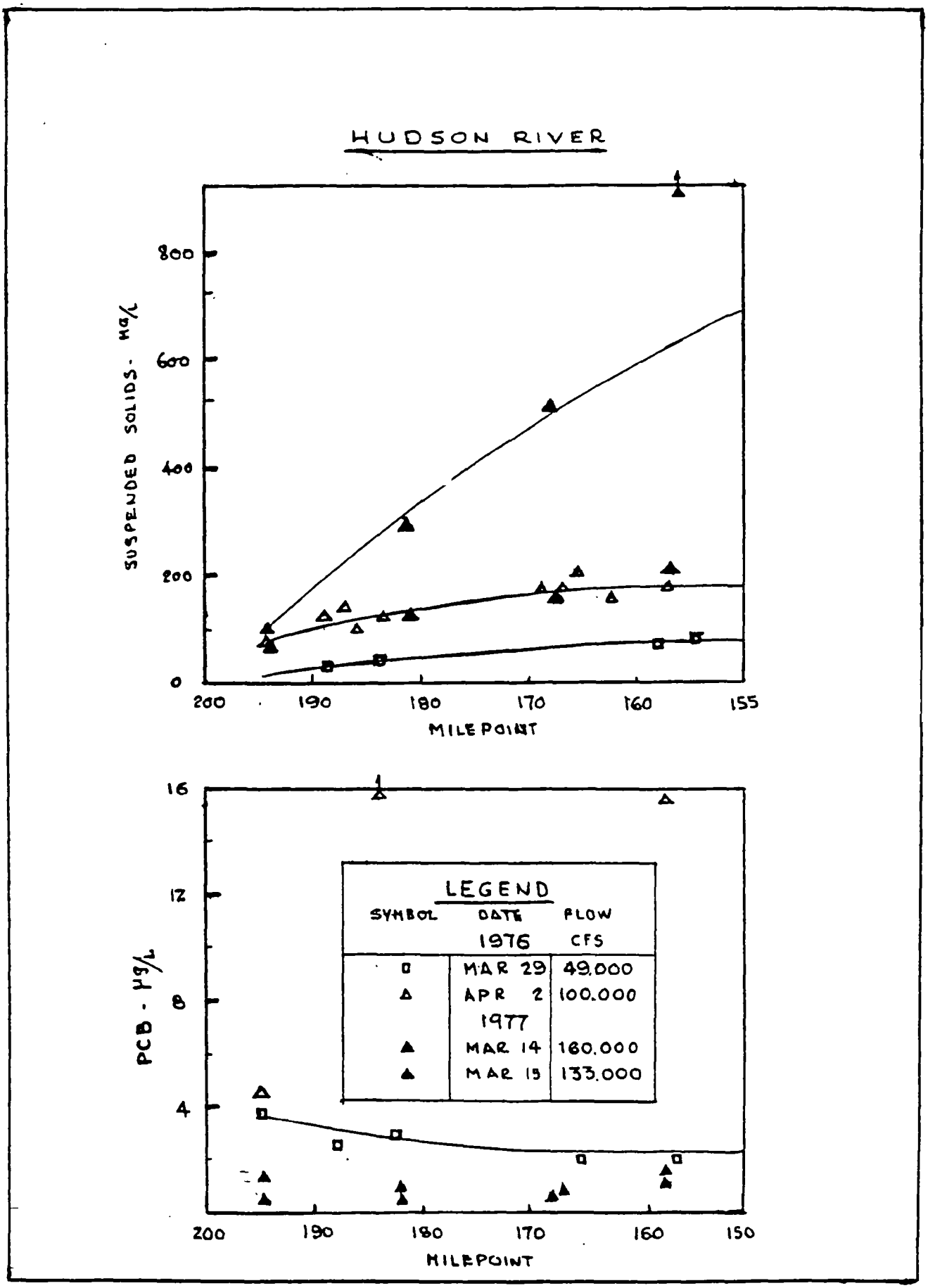

FIGURE 2-4. COMPARISON OF 1976-1977 DATA AND ANALYSIS

ANALYSIS OF COMPLETELY MIXED SYSTEMS* _ TOXIC SUBSTANCES

1. Type I Analysis - Stationary Bed - No Resuspension - Sedimentation

a) Suspended Solids

The concentration of suspended solids in a reservoir or lake depends on the physical characteristics of the incoming sediment and the hydraulic features of the system and inflow. The important characteristics of the solids are the grain size and settling velocity distributions and the behavior of the finer fractions with respect to aggregation and coagulation. The detention time and the depth of the water body are the significant hydraulic and geomorphological features. The following analysis assumes steady-state conditions in a completely mixed system, in which the concentration of solids is spatially uniform.

These assumptions are obviously crude, but of sufficient practicality to admit at least an order of magnitude analysis of the problem. They are precisely the assumption, implicit in the analysis of the "Trap Efficiency" of reservoirs in which the efficiency of removal of solids has been correlated to the ratio of the reservoir capacity to the tributary drainage area(1).

Consider a body of water whose concentration is spatially uniform throughout its volume, V, receiving an inflow, Q, as shown in Figure B-1. Under steady state conditions, hydraulic inflow and outflow are equal. The mass balance of the solids takes into account the mass inputted by the inflow, that discharged in the outflow and that removed by settling. The mass rate of change of solids in the reservoirs is the net of these fluxes:

$$V \frac{dm_1}{dt} = Qm_i - Qm_1 - v_s A_s m_1 \qquad (1)$$

in which

m_i = concentration of solids in inflow

m_1 = concentration of solids in water body

v_s = settling velocity of the solids

A_s = horizontal area thru which settling occurs

The flux Qm_i, equals the rate of mass input, W. Dividing through by the volume, V, the above equation becomes

$$\frac{dm_1}{dt} = \frac{W}{V} - m_1\left[\frac{1}{t_o} + K_s\right] \qquad (2)$$

* Donald J. O'Connor

in which

t_o = detention time = $\frac{V}{Q}$ (T)

K_s = settling coefficient $\frac{v_s}{H}$ $(\frac{L}{T})$

H = mean depth = $\frac{V}{A_s}$ (L)

Under the steady state condition, equation (2) may be expressed as,

$$m_1 = \frac{W/Q}{1 + K_s t_o} \tag{3a}$$

Division by W/Q yields

$$\frac{m_1}{W/Q} = \frac{1}{1 + K_s t_o} \tag{3b}$$

which is the fraction of the incoming solids remaining in suspension and, with the assumption of complete mixing, is also the concentration in the outflow. The fraction removed is simply

$$f = 1 - \frac{1}{1 + K_s t_o} \tag{4}$$

The dimensionless parameter, $K_s t_o$, represents the combined effects of the settling characteristics of the solids and the average detention time of the system. The coefficient, K_s, may be replaced by its equivalent, v_s/H, and the dimensionless parameter is v_s/v_o, in which $v_o = \frac{H}{t_o} = \frac{Q}{A}$, the overflow rate of the system.

It is apparent from the above development that conditions in the bed have no effect on the concentration in the water body, because there is no resuspension of the bed material. The benthal concentration, on the other hand, is due directly to the influx of the settling solids. The rate of change of mass of solids in the bed is therefore

$$\frac{dM_2}{dt} = + A_1 v_s m_1$$

The mass, M_2, equals the product of the bed volume V_2, and bed concentration, m_2. Thus

$$\frac{dM_2}{dt} = \frac{d(V_2 m_2)}{dt} = m_2 \frac{dV_2}{dt} + V_2 \frac{dm_2}{dt} = + A_s v_s m_1 \tag{5a}$$

Dividing through the A_s, and expressing the resulting $\frac{dz_2}{dt}$ as V_d, the final result is

$$\frac{dm_2}{dt} = \frac{v_s}{z} m_1 - \frac{v_d}{z} m_2 \qquad (5b)$$

at steady-state - i.e. when the mass settling rate equals the accumulation rate:

$$m_2 = m_1 \frac{v_s}{v_u} \qquad (5c)$$

b) Toxic Substances

The distribution of toxic substances, such as organic chemicals and heavy metals in reservoirs and lakes is established by application of the principle of continuity or mass balance, in a manner similar to that employed in the case of the suspended solids. Each phase, the dissolved and particulate, is analyzed separately, taking into account the adsorptive-desorptive interaction with the other. For the dissolved component, the mass balance includes decay and transfer terms[2][3] in addition to the inflow and outflow. The basic differential equation

$$\frac{dc_1}{dt} = \frac{W_c}{V} - \frac{c_1}{t_o} - K_c c_1 - K_o m_1 c_1 + K_2 p_1 \qquad (6)$$

in which

V = reservoir volume (L^3)

W_c = rate of mass input of the dissolved component (M/T)

c_1 = dissolved concentration in water body (M/L^3)

K_c = overall first order rate coefficients (T^{-1}) which may include biological degradation, hydrolysis, direct photolysis & volatilization.

K_o = the adsorption coefficient (L^3/M-T)

m = suspended solids concentration (M/L^3)

K_2 = the desorption coefficient (T^{-1})

p_1 = particulate chemical concentration (M/L^3)

For the particulate concentration:

$$\frac{dp_1}{dt} = \frac{W_p}{V} - \frac{p_1}{t_o} - K_{s_1} p_1 - K_2 p_1 + K_o m c_1 \qquad (7)$$

in which

W_p = rate of mass input of the particulate adsorbed chemical (M/T)

K_s = settling coefficient (T^{-1})

Adding equations (6) and (7) cancels the adsorption and desorption terms and yields the rate of change of the total concentration c_T in terms of the dissolved and particulate:

$$\frac{dc_{T_1}}{dt} = \frac{W}{V} - \frac{c_{T_1}}{t_o} - K_c c_1 - K_{s_1} p_1 \tag{8}$$

The sorption coefficients, K_o and K_2 are usually orders of magnitude greater than the decay and transfer coefficients of the dissolved and particulate. The rate at which equilibrium is achieved between the two phases is very rapid by contrast to the rates of transfer and decay. Thus liquid-solid phase equilibrium is assumed to occur instantaneously. The dissolved and particulate concentrations, c and p, may therefore be expressed in terms of c_T by equation 4, substitution of which in equation (8) yields:

$$\frac{dc_{T_1}}{dt} = \frac{W}{V_1} - \frac{c_{T_1}}{t_o} - \frac{K_{c_1}}{1 + \P m_1} c_{T_1} - \frac{K_{s_1} \P m_1}{1+\P m_1} c_{T_1}$$

Under steady-state conditions, the above may be expressed, after multiplying through by t_o:

$$\bar{c}_{T_1} = \frac{W/Q}{1 + \frac{t_o}{1+\P m_1}[K_{c_1} + \P m_1 K_{s_1}]} \tag{9}$$

For those substances, whose dissolved components are not susceptible to transfer/decay, such as heavy metals, equation (9) reduces to

$$c_{T_1} = \frac{W/Q}{1 + K_{s_1} t_o [\frac{\P m_1}{1+\P m_1}]} \tag{10}$$

Note that equation (10) is identical to equation (3a) with the exception that the dimensionless settling parameter $K_s t_o$ is multiplied by the fraction $\frac{\P m_1}{1+\P m_1}$

The latter term expresses the fraction of the total concentration which is in the particulate form. For values of ¶m >> 1, it is apparent that equation (10) is identical to (3a). With reference to equations (9) and (10), the fraction removed is

$$f = 1 - \frac{C_T}{W/Q} \tag{11}$$

Inspection of equation (4) indicates that the removal efficiency of suspended solids is dependent on the detention time and settling coefficient, which is the ratio of the settling velocity of the solids and the average depth of the reservoir or lake. For heavy metals and conservative chemicals, the additional parameter required is the partition coefficient (equation 10). In the case of organic chemicals, which are susceptible to biodegradation, evaporative transfer, hydrolytic or photochemical reaction, knowledge of the relevant reaction coefficients is necessary (equation 9).

The detention time and average depth, which are readily determined, are based on the average seasonal or annual conditions, given the time and space scales of the analysis. The settling velocity and settling coefficient may be measured directly or implied from inflow-outflow concentrations in accordance with equations (3) and (4). The partition coefficient may also be evaluated directly, which, with the solids concentration, yields the dimensionless parameter ¶m. Alternately given measurements of the total and dissolved concentrations of the heavy metal/organic chemical, the term ¶m may be calculated. With such information, the removal efficiency is readily computed for those metals and chemicals which are non-reactive.

As indicated above, certain chemicals may be subjected to additional transfer or transformation. The fundamental properties of the constituent are indicative of the potential magnitude of these routes - e.g. the vapor pressure and solubility are properties which permit assessment of the evaporative transfer (4)(5). Laboratory experiments may be necessary to determent the chemical and biological routes - e.g. the biodegradability of the substance (6)-(9). In any particular case, an assessment, either analytical or experimental, should be made to establish the degree to which transformation or transfer may be significant. Solutions of the above are shown in Figure B-2.

The bed concentration may be described by constructing its mass balance. Influx is due to the toxic substance associated with the settling solids and the volumetric accumulation is accounted for by the sedimentation velocity, as in the bed solids analysis (equation 5)

$$\frac{dc_{T_2}}{dt} = f_{p_1} K_{s_2} c_{T_1} - f_{p_2} K_{d_2} c_{T_2} \tag{12}$$

at steady state

$$c_{T_2} = \frac{f_{p_1} v_s}{f_{p_2} v_d} c_{T_1} \tag{13}$$

in which

f_{pn} = the fractions dissolved and particulate

v_s = settling velocity

v_d = sedimentation velocity

Since the bed solids concentration $m_2 >>> m_1$ and $\P m_2$ is usually $>>> 1$, as a reasonable approximation

$$f_{p_2} \sim 1 \text{ and } f_{d_2} \sim 0$$

$$c_{T_2} = p_2 = f_{p_1} \frac{v_s}{v_d} c_{T_1} = \frac{v_s}{v_d} p_1 \tag{14}$$

substituting for $p = rm$

$$r_2 m_2 = \frac{v_s}{v_d} r_1 m_1$$

since $v_d m_2 = v_s m_1$ under steady state, then

$$p_2 = r_1 \tag{15}$$

The above analysis does not take into account the possibility of the exchange of the dissolved component between the bed and the water. This is discussed in the following section, which considers solids resuspension - a condition more likely to enhance exchange of the dissolved component.

2. Type II Analysis - Mixed Bed - Resuspension

The type of analysis described in this section is identical to that of the previous, with the addition of a resuspension term in both the solids and toxic equations. The physical structure of the system is shown diagrammatically in Figure B-1, from which it is apparent that a mass balance equation must be developed for both the water column and the bed, since they are interactive.

a) Suspended Solids

The mass rate of change of solids in the water column is:

$$V_1 \frac{dm_1}{dt} = Qm_i - Qm_1 - V_s A_s m_1 + v_u A_s m_2 \qquad (16)$$

in which

v_u = resuspension velocity - L/T

m_2 = concentration of solids in the bed - M/L^3

and the remaining terms are as previously defined by equation (2) of the previous section.

Expressing the input flux of solids Qm_1 as W and dividing through by the volume V_i, yields

$$\frac{dm_1}{dt} = \frac{W}{V} - \frac{m_1}{to} - \frac{V_s}{H_1} m_1 + \frac{V_u}{H_1} m_z \qquad (17)$$

in which

H_1 = average depth of the water column

A mass balance of the bed solids includes the influx of the settling solids from the water and mass outflow from the bed due to the resuspension and sedimentation:

$$\frac{dm_2}{dt} = \frac{V_s m_1}{H_2} - \frac{V_u m_2}{H_2} - \frac{V_d m_2}{H_2} \qquad (18)$$

in which

H_2 = average depth of the bed

At steady-state conditions, $\frac{dm}{dt} = 0$, the concentration in the bed may be expressed in terms of the concentration in the water from (18):

$$m_2 = \alpha m_1 \tag{19}$$

in which

$$\alpha = \frac{v_s}{v_u + v_d}$$

Substitution of which in equation (17) under steady state yields

$$0 = \frac{W}{V} - m_1 \left[\frac{1}{t_o} + \frac{v_s}{H_1}\right] + \frac{v_u}{H_1} \cdot \frac{v_d}{v_u + v_d} m_1$$

Expressing $\frac{v_s}{H} = K_s$ and solving for m_1, after simplification, gives:

$$m_1 = \frac{W/Q}{1 + \beta K_{s_1} t_o} \tag{20}$$

in which

$$\beta = \frac{v_d}{v_u + v_d}$$

The value of α falls between zero and unity. The latter represents the case of no resuspension $v_u = 0$ and $\beta = 1$, reducing (20) to (3) and the former of no sedimentation $v_d = 0$, reducing (20) to

$$m_1 = W/Q \tag{21}$$

In this case the settling flux is exactly balanced by the resuspension flux, resulting in zero net change and the concentration of solids is simply that of a conservative substance, as indicated by (21).

The bed concentration follows from substitution of (20) in (19):

$$m_2 = \frac{\alpha\, W/Q}{1 + \beta K_s t_o} \tag{22}$$

Algebraic simplification yields

$$m_2 = \frac{W/Q}{\frac{1}{\beta} + \frac{v_d}{H_1} t_o} \tag{23}$$

For lakes or reservoirs of shallow or moderate depth ($H \sim 10M$), moderate high settling velocities ($v_s \sim 3M/DAY$) and low resuspension velocities

(v_u < 1CM/YR), the β term is more than an order less than the sedimentation term and (22) reduces to

$$m_2 = \frac{W}{K_{d_1} V} \tag{24}$$

in which

$$K_{d_1} = \frac{v_d}{H_1}$$

b) Toxic Substances

The equations for the toxic substance are developed in an identical fashion as in the Type I Analysis. Each phase in the water column, the dissolved, c, and the particulate, p, is analyzed separately with adsorption and desorption kinetics in addition to the input, outflow and settling terms. Furthermore, allowance is made for the exchange of the dissolved component between the water and the bed, expressed in terms of the difference in the dissolved concentrations. Addition of the two equations cancels the adsorption-desorption terms and yields:

$$\frac{dc_{T_1}}{dt} = \frac{W_{ct}}{V_1} - \frac{c_{T_1}}{t_o} - K_{s_1} p_1 + K_{u_1} p_2 + K_{b_1} (c_2 - c_1) \tag{25}$$

in which

the subscript 1 refers to the water column and 2 to the bed

c_{T_1} = total concentration of toxic in the water column

$K_{s_1} = \frac{v_s}{H_1}$ = selling coefficient (1/T)

$K_{u_1} = \frac{v_u}{H_1}$ = resuspension coefficient (1/T)

$K_{b_1} = \frac{K_m}{H_1}$ = dissolved exchange coefficient (1/T)

K_m = transfer coefficient of the dissolved between water and bed $(\frac{L}{T})$

Expressing p and c as fractions of the total concentration (equation 4 of the previous chapter) and combining similar terms yields:

$$\frac{dc_{T_1}}{dt} = \frac{W_{cT}}{V} - [\frac{1}{t} + f_{p_1} K_{s_1} + f_{d_1} K_{b_1}] c_{T_1} + [f_{p_2} K_{u_1} + f_{d_2} K_{b_1}] c_{T_2} \tag{26}$$

the bed equation is developed in a similar fashion

$$\frac{dc_{T_2}}{dt} = [f_{p_1} K_{s_2} + f_{d_1} K_{b_2}] c_{T_1} - [f_{p_2}(K_{u_2} + K_{d_2}) + f_{d_2} K_{b_2}] c_{T_2} \qquad (27)$$

in which

$f_{p_{1,2}}$ = particulate fraction in each segment, 1 and 2

$f_{d_{1,2}}$ = dissolved fraction in each segment, 1 and 2

The working equations for the steady-state condition are developed in a manner similar to that of the solids. Under steady state conditions, the total concentration in the bed is expressed in terms of the total concentration in the water with equation (27). Substitution of (27) in (26) yields the water concentration as a function of the input load, W, and the parameters of the system. Since $m_2 >>> m_1$ and $\P m_2 >> 1$, $f_{p_2} \sim 1$ and $f_{d_2} \sim 0$. For this simplification, which is realistic for $\P > 1000$, the water and bed concentrations are respectively

$$c_{T_1} = \frac{W/Q}{1 + \beta f_d [\P m_1 K_{s_1} + K_{b_1}] t_o} \qquad (28)$$

$$c_{T_2} = \frac{f_p K_{s_2} + f_d K_{b_2}}{K_{u_2} K_{d_2}} c_{T_1} \qquad (29)$$

in which

$$\beta = \frac{v_u}{v_u + v_d}$$

$$f_d = \frac{1}{1+\P m_1}$$

$$f_p = \frac{\P m_1}{1+\P m_1}$$

$$K_s = \frac{v_s}{H}$$

$$K_b = \frac{K_m}{H}$$

$$K_u = \frac{v_o}{H}$$

$$K_d = \frac{v_d}{H}$$

For the condition of negligible exchange of the dissolved between water and bed ($K_b \sim 0$), the above equations reduce to

$$c_{T_1} = \frac{W/Q}{1+\beta f_{p_1} K_{s_1} t_o} \tag{30}$$

$$c_{T_2} = \alpha\, c_{T_1} \tag{31}$$

in which, in accordance with equation 14

$$\alpha = \frac{v_s}{v_u + v_d}$$

For toxics of high partition coefficient and systems of high solids ($\P m_1 \gtrsim 5$), the above respectively reduce to equations (21) and (19), the equivalent solids equations.

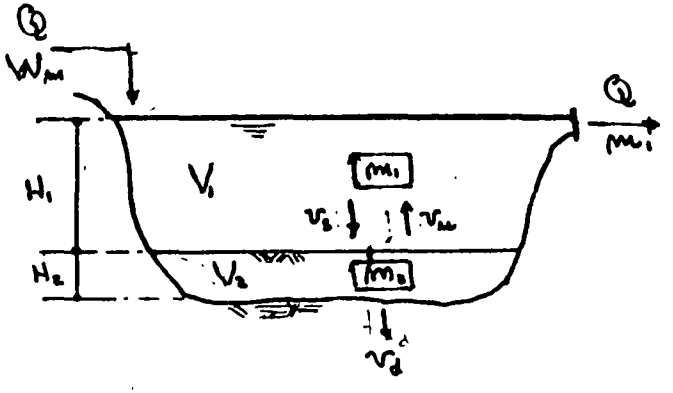

SOLIDS

SUBSCRIPTS

1 WATER

2 BED

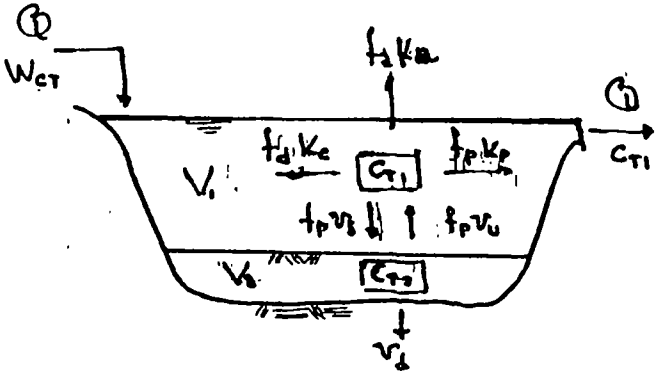

TOXIC

ANALYSIS TYPE — RESUSPENSION

I	$v_u = 0$
II	$v_u > 0$

Bed Transport Zero

LEGEND		UNITS
N	MASS INFLUX	M/T
Q	FLOW	L^3/T
V	VOLUME	L^3
H	DEPTH	L
m	SOLIDS	M/L^3
C_T	TOXIC - TOTAL	M/L^3
f_d	DISSOLVED FRACTION	-
f_p	PARTICULATE FRACTION	-
v_s	SETTLING VELOCITY	L/T
v_u	RESUSPENSION VELOCITY	"
v_d	SEDIMENTATION VELOCITY	"
K_{EA}	EVAPORATION COEFFICIENT	1/T
K_c	DISSOLVED DECAY	"
K_s	SETTLING COEFFICIENT	"
K_p	PARTICULATE DECAY	"

FIG. B-1 Schematic of Type I & Type II Solids Parameters

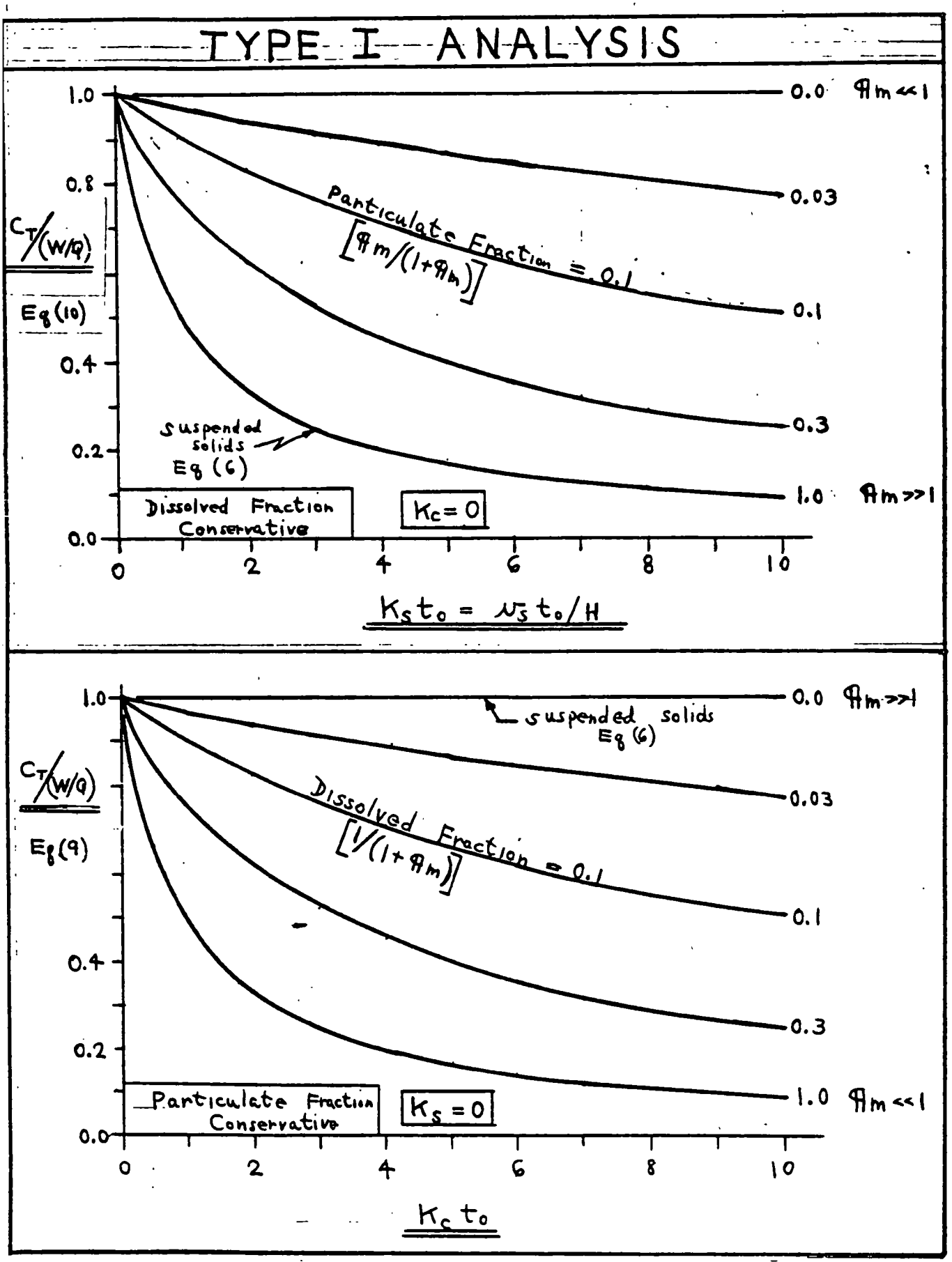

FIG. B-2 Fraction Remaining for Various Detention Times and Kinetic Parameters

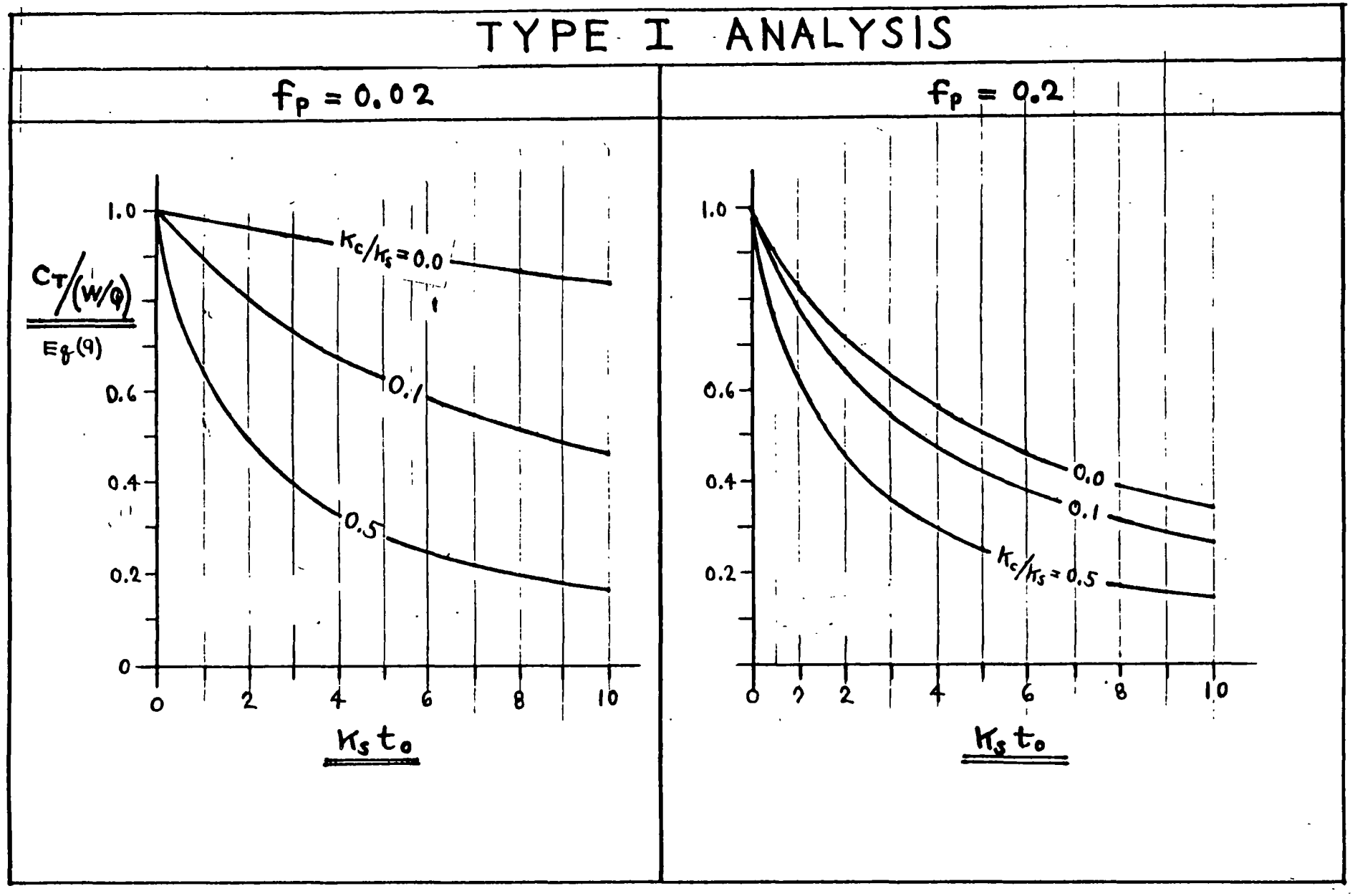

FIG. B-2 (cont'd) Fraction Remaining for Various Detention Times and Kinetic Parameters

3. Applications

The following analysis relates to the distributions of both organic chemicals and heavy metals in reservoirs. It is based primarily on the Type I Analysis, with reference to the Type II as appropriate.

a) Suspended Solids

A plot of equation (4) is presented in Figure B-3 for a range of settling coefficients, K_s. Common values of the settling velocity of solids in reservoirs are in the range of a few feet per day and average depths are 10-100 feet, yielding values of K_s' in the order of 0.1 per day with approximate limits of 0.025 to 0.5 as shown. The majority of the data is abstracted from reference (1) and supplemented by more recent measurements (10-13) from reservoirs for which concentrations of heavy metals and organic chemicals are also available. Data from the earlier reference are characterized by $K_s \geq 0.1$ per day. The latter data with $K_s \leq 0.1$ per day are representative of settling velocities between 0.25 and 2.5 feet per day, as shown in Figure 2. This figure presents the correlation in a more fundamental manner. It is evident from equation (4) that replacement of K_s with V_s/H yields the correlating term, t_o/H, with V_s as a parameter as shown in Figure B-4. Settling velocities, in the order of 0.5 to 5.0 feet per day, which is representative of clays and fine silts, encompass the majority of the data. These types of solids are most relevant to the problem, since they have a greater capacity to absorb organic chemicals and heavy metals than sands.

b) Heavy Metals and Organic Chemicals

A water quality survey of heavy metals and organic chemicals was conducted during the latter part of 1976 and the first few months of 1977 on the Trinity River through Lake Livingstone.(10). At a number of stations, measurements of the total and dissolved concentrations in the water columns and in the bed were made. Pesticides were measured in grab samples for Coralville Reservoir at inflow, outflow and in-lake stations during 1969 and 1976, while bi-weekly suspended solids measurements have been made since 1965 (11,12). Data for Lake Rathburn were collected bi-weekly from May through August, 1978.(13).

From these data, a value of the removal efficiency of each reservoir was determined and presented in Figure B-5. The range of suspended solids

removal (K_s = 0.02s, ¶m > 10) in accordance with equation (4) is shown for comparison. The purpose of this figure is simply to demonstrate the relative removal of the various constituents. For many of the heavy metals, it is to be noted that the removal is equivalent to that of the suspended solids, implying that the particulate fraction is predominant. For some of the organic chemicals the removal fraction is much less, indicative of a larger fraction in the dissolved state or a source from the bed. Constituents which have removal fractions greater than that of the suspended solids may be subject to additional mechanisms, such as biodegradation, evaporation, chemical hydrolysis and oxidation, and direct or sensitized photolysis.

Since both the dissolved and total concentrations were measured in the Livingston survey, it is possible to calculate the ¶m values for each substance.. Using these data a more fundamental relationship is presented in Figure B-6 for Lake Livingston in which the particulate fraction, as determined by the observations, is correlated to the fraction removed. The removal fraction is calculated in accordance with equation (11) for a range of values, representative of conditions in this reservoir. The sequence for pesticides shown in Figures B-5 and B-6 - Lindane, dieldrin, heptachlor and endrin - is in accord with increasing tendency to the particulate state. The data on metals indicate greater variation and are not as consistent, particularly with respect to copper.

Removal fractions for non-conservative substances (i.e. those which are removed by mechanisms in addition to settling) should exceed the expected removals caused by sedimentation of sorbed material. Heptachlor may be susceptible to evaporation and endrin to biological decay. Evaporation and biodegration may also affect dieldrin but to a lesser extent. Such factors may account for the fact that these substances indicate higher removals.

Mean removal fractions for Lasso, atrazine, and dieldrin in Rathbun Reservoir, are presented in Figure B-7. The representation in Figure B-7 is similar to that of Figure B-6 except that $K_s t_o$ is equal to 4.0 and isopleths of $K_c t_o$ are indicated for these reactive substances. It is estimated that the highly soluble herbicicides Lasso and atrazine undergo rather rapid biodegradation in natural waters with $K_c t_o$ = 10 and 4 respectively, and overall first order rate constants (K_c) of 0.06 and 0.02 per day. Grab samples and partition coefficients from other rivers and reservoirs in

Iowa indicate that a small fraction of Lasso and atrazine are in the particulate phase. Dieldrin removal rates were quite variable, but it appears that the removal is due primarily to sedimentation of sorbed material, and the estimated first order reaction rate constant (K_c) was nearly zero.

Equation (9) represents the most generalized correlation and is shown in Figure B-8. The dimensionless parameter is the product of the particulate fraction ($\P m/1 + \P m$) the reaction factor ($1 + K_c/K_s \P m$) and the settling term ($K_s t_o$). The vertical lines in the figure indicate the values of the latter term for the three reservoirs and are representative of purely particulate substances ($\frac{\P m}{1+\P m} = 1$) and conservative substances ($K_c = 0$). Data falling to the right of the respective verticals suggest that in addition to settling, transfer and/or decay may be operative. The most marked deviations are for copper and zinc with lower removals than calculated, which may be due to release from the bed (Type II Analysis). On the other hand, the fact that dieldrin is in reasonable agreement for the three reservoirs is encouraging. The remaining values are in general accord assuming Endrin and Lasso are nonconservative ($K_c = 0.05$/day). Atrazine and heptachlor are being removed by sedimentation of adsorbed chemical as well as by gas transfer and/or decay reactions.

Recognizing the simplicity of the analysis and appreciating the limited number of observations, it is apparent that comparisons such as presented in these figures are not necessarily validations of the model. It is encouraging to note that the observations are not inconsistent with the theoretical analysis and in order of magnitude indicate reasonable agreement.

Given the nature of the assumptions on which the model was formulated, it may be used to estimate long-term concentrations for average values of flow and loadings. Furthermore, the time to reach equilibrium or steady-state conditions may also be approximated. Additional field data are required to test and validate the model. Such field programs should be conducted in conjunction with laboratory measurements of sediment-water partitioning, volatilization and degradation reactions, the results of which may be incorporated directly in the model.

ACKNOWLEDGEMENTS

The support by EPA research funds in developing the above is gratefully acknowledged: Grant No. R804563-03, EPA Gulf Breeze Laboratory, Gulf Breeze, Florida, 1976-1979. Application of the Type I Analysis was used in an environmental assessment study by the U.S. Corps of Engineers of a proposed reservoir on the Trinity River, in which the data on the Livingstone Reservoir was collected. A report was submitted in 1978 to the Corps, whose support is acknowledged. Jerald Schnoor, University of Iowa, kindly provided the data on the Iowa reservoirs. This research is supported by Grant No. R806059-01, EPA Athens Laboratory, Georgia, 1979. Both are collaborating in reporting this work in a paper which has been submitted to "Environmental Science & Technology."

REFERENCES

1. Brune, G.M. Trans. Am. Geophys. Union. 1953, 34, 407-18.

2. Smith, J.H.; Mabey, W.R.; Bohonos, N; Holt, B.R.; Lee, S.S.; Chow, T.W.; Bomberger, D.C.; and Mill, T. "Environmental Pathways of Selected Chemicals in Freshwater Systems, Part I: Background and Experimental Procedures." 1977, U.S. Environmental Protection Agency; EPA-600/7-77-113.

3. Smith, J.H.; Mabey, W.R.; Bohonos, N.; Holt, B.R.; Lee, S.S.; Chow, T.W.; Bomberger, D.C.; and Mill, T. "Environmental Pathways of Selected Chemicals in Freshwater Systems, Part II: Laboratory Studies." 1978, U.S. Environmental Protection Agency; EPA-600/7-78-074.

4. Mackay, D.; Leinonen, P.J. Environ. Sci. Technol. 1975, 9, 1178-80.

5. Mackay, D.; Wolkoff, A.W. Environ. Sci. Technol. 1973, 7, 611-4.

6. Hushon, J.M.; Clerman, R.J.; Wagner, B.O. Environ. Sci. Technol. 1979, 13, 1202-7.

7. Karickhoff, S.W.; Brown, D.A.; Scott, T.A. Water Res. 1979, 13, 421-8.

8. Zepp, R.G.; Cline, D.M. Environ. Sci. Technol. 1977, 11, 359-66.

9. Paris, D.F.; Steen, W.C.; Baughman, G.L. Chemosphere. 1978, 4, 319.

10. "Trinity River Bottom Sediment Reconnaissance Study", Fort Worth District Corps of Engineers, Texas. June 1977.

11. Mehta, S.C. M.S. Thesis, The University of Iowa, Iowa City, Iowa. 1969.

12. McDonald, D.B. "Coralville Reservoir Water Quality Study, Water Years 1965-1978", Reports to U.S. Army Corps of Engineers, Rock Island, Illinois. 1979.

13. Kennedy, J.O. "Lake Rathbun Pesticide Study", University of Iowa Hygienic Laboratory, Iowa City, Iowa. 1978.

14. Sanders, W.M. III. "Exposure Assessment, A Key Issue in Aquatic Toxicology", in Aquatic Toxicology, ASTM, STP 667. 1979, pp. 271-283.

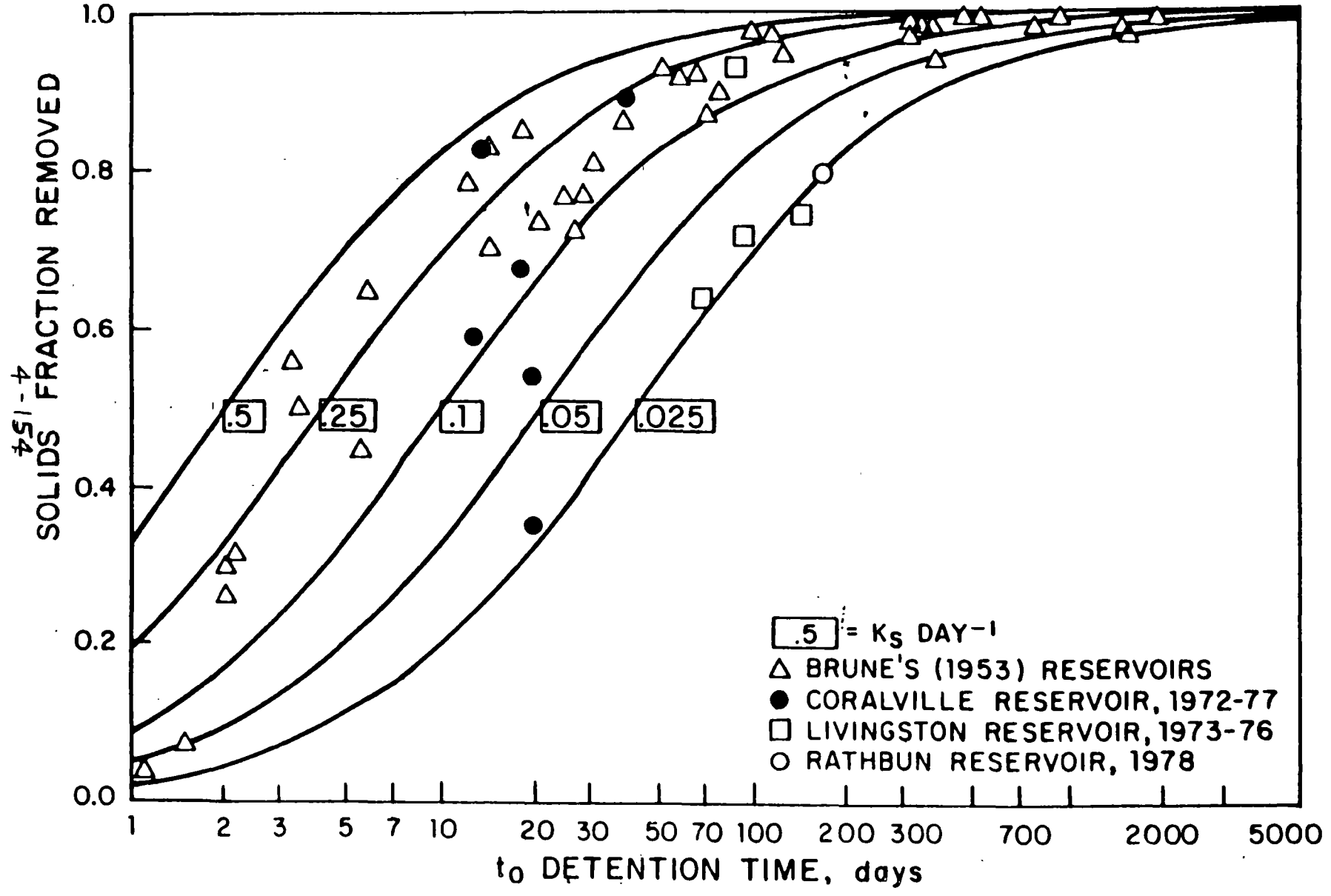

Figure B-3. Suspended Solids Re ! Detention Time Relationship

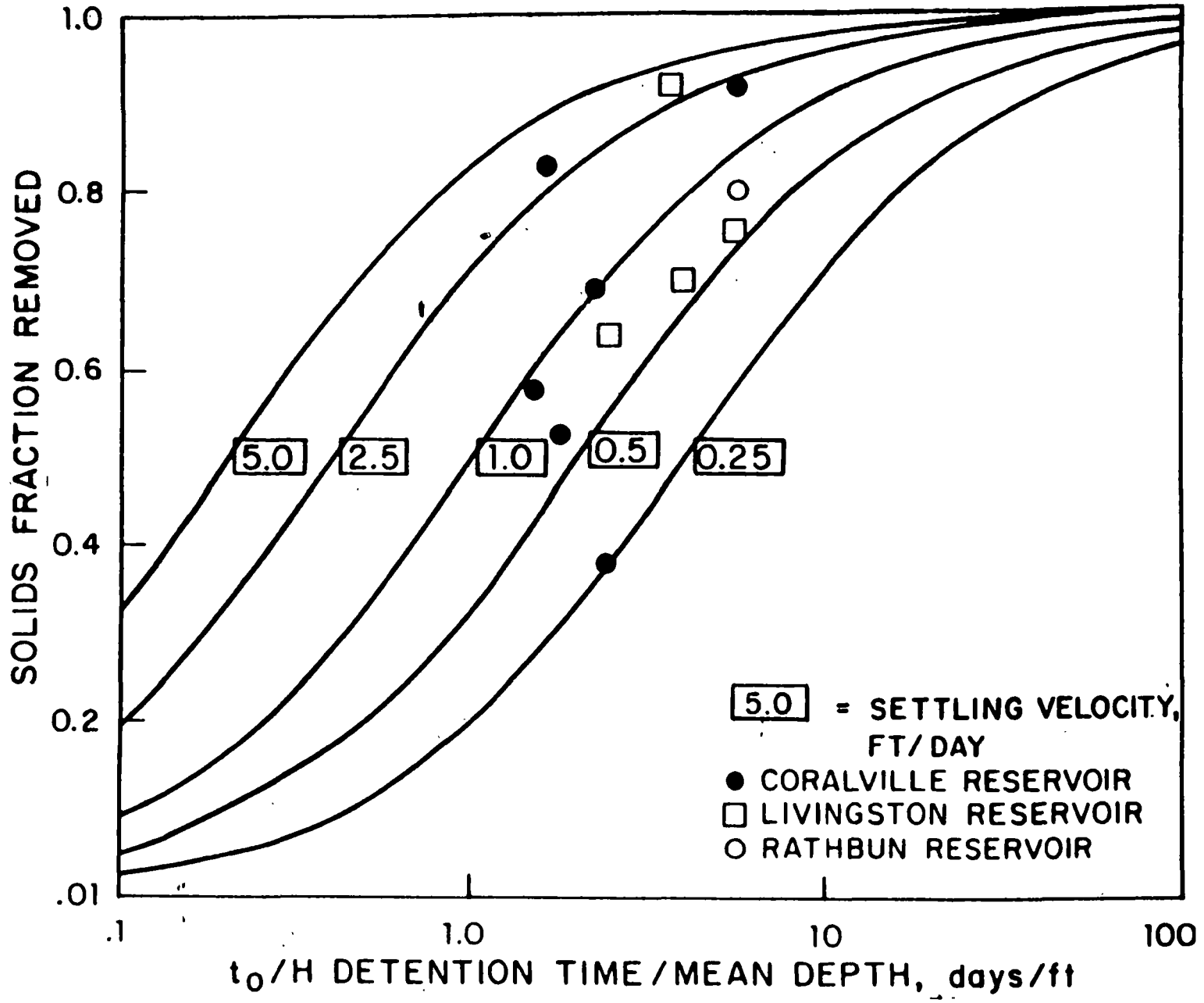

Figure B-4. Solids Removal versus Detention Time/Depth

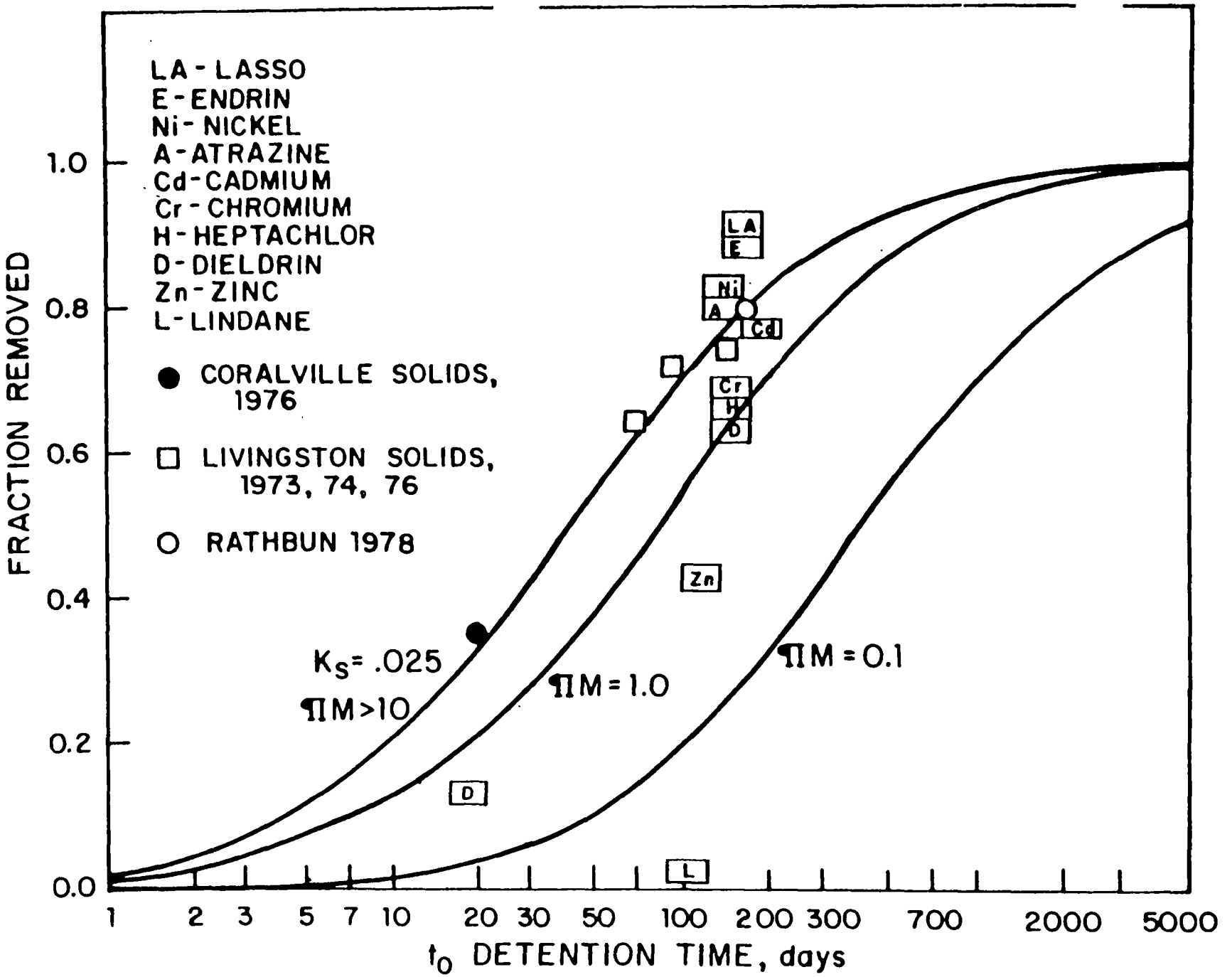

Figure B-5. Removal Fraction vs. Detention Time

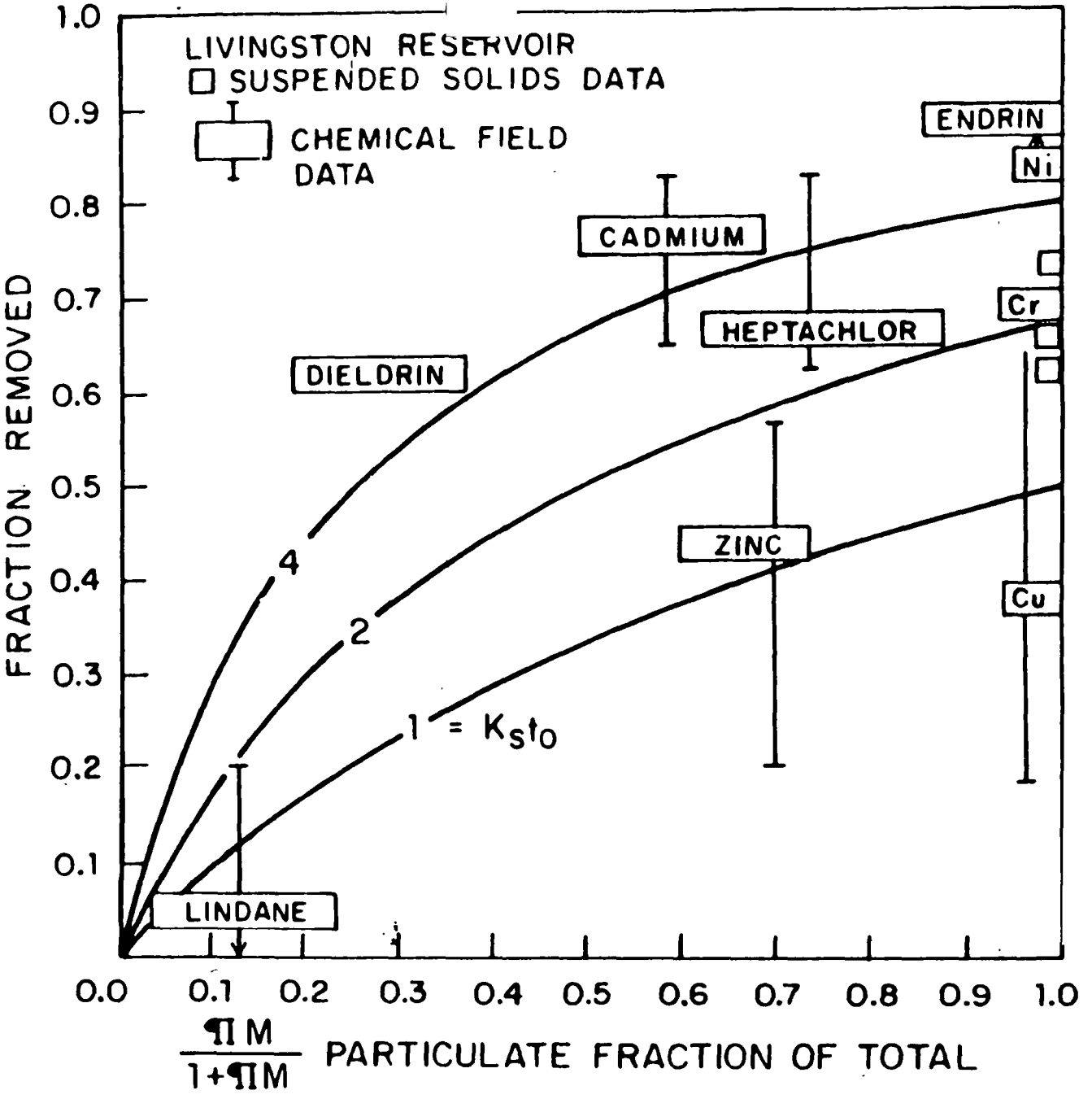

Figure B-6. Removal Fraction vs. Particulate Fraction

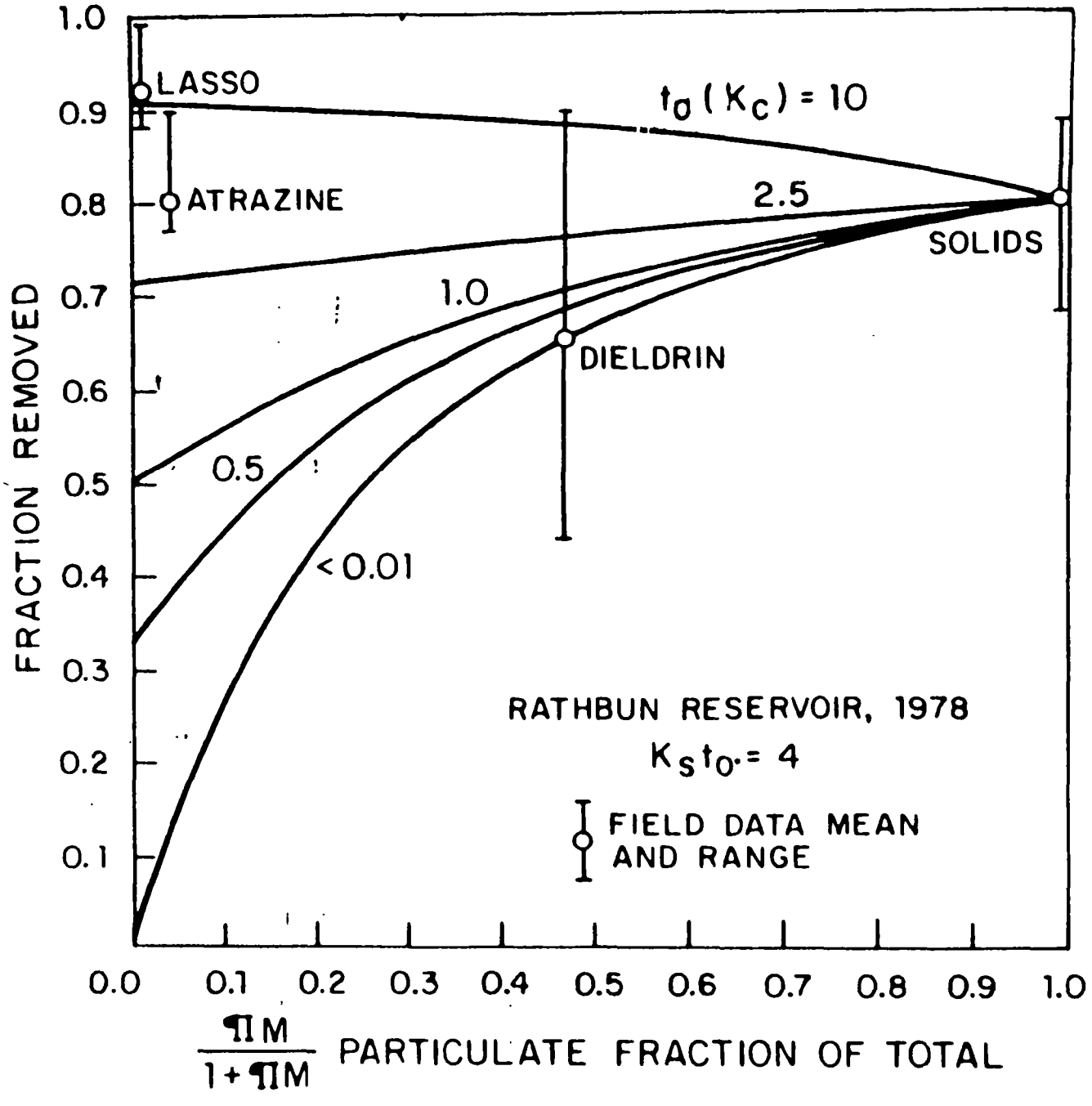

Figure B-7. Removal Fraction vs. Particulate Fraction with Reaction

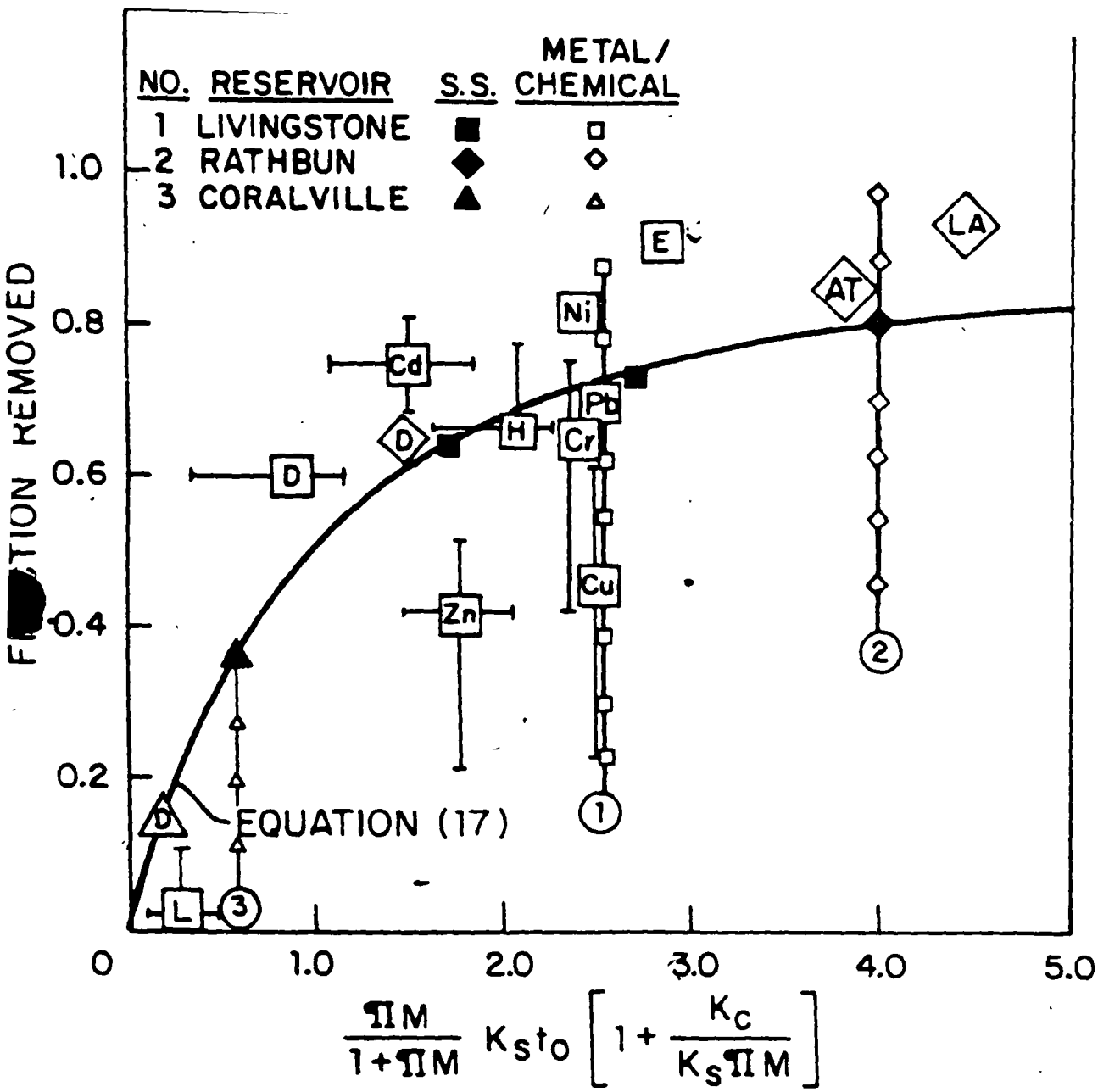

Figure B-8. Generalized Removal Function

AMMONIA TOXICITY[1/]

Background

The discharge of ammonia to streams, influences water quality in several ways: 1) ammonia may be oxidized by nitrifying bacteria resulting in a loss of dissolved oxygen, 2) ammonia may be utilized as a nutrient by floating and/or rooted aquatic plants and 3) high levels of ammonia may be directly toxic to fish. It is this latter effect that has been a matter of increasing concern in recent years although ammonia toxicity has been investigated for almost 50 years. (See McKee and Wolf, 1963).

Ammonia gas is very soluble in water (to about 100,000 mg/ℓ @ 20°C) and dissociates in water into ammonium and hydroxyl ions. The reaction is:

$$NH_3 + H_2O \rightleftarrows NH_4 + OH \rightleftarrows NH_4^+ + OH^- \qquad (1)$$

The ratio of the free unionized ammonia to the ammonium ion is a function of pH and temperature. The test for ammonia nitrogen in "Standard Methods" measures all forms of ammonia. Ruffier et al (1981) used the following relationship to calculate the % of NH_3:

$$\%\frac{NH_3}{NH_4^+} = 100/(1 + 10^{pK_a - pH}) \qquad (2)$$

where the pK_a values are temperature dependent and are given by Emerson (1975). pK_a varies from 9.4 @ 20°C to 9.2 @ 25°C. (Recall that $p(x) = -\log x = \log 1/x$ or $pK_a = \log 1/K_a$ where K_a is the ionization constant.) Figure 1 shows the relationship of the % NH_3 of total ammonia ($NH_3 + NH_4^+$) for various pH and temperature levels. The effect of pH may be especially significant in water quality studies since the range in pH may vary from 7-9 under conditions of high photosynthesis.

Fish Toxicity Levels

High levels of unionized ammonia interfere with the ability of the hemoglobin to combine with oxygen and the fish suffocates. Other effects include kidney failure and neurological and cytological failure. There is a strong interaction between low levels of oxygen and ammonia toxicity.

[1/] Robert V. Thomann

The criterion most often cited is the US EPA level of 0.02 mg/ℓ of NH_3. This level was based on a lethal concentration of 0.165 mg/ℓ to rainbow trout fry. As pointed out by Ruffier et al (1981) this latter concentration has been more accurately computed at 0.27 mg/ℓ. The EPA criterion therefore incorporates a factor of safety of 13.5. This factor of safety should be recognized in water quality analyses and waste load allocation studies. Indeed as summarized by McKee and Wolf (1963), NAS/NAE (1972), EPA (1976) and Ruffier et al (1981), the actual range of 96 hr-LC_{50} and threshold (infinite exposure) LC_{50} concentrations is very large. For example, 96 hr. and threshold levels which are appropriate for steady state water quality modeling ranges by about one order of magnitude from 0.32 mg/ℓ to 3.10 mg/ℓ for 96 hr. tests and from 0.16 to 1.5 mg/ℓ for the threshold levels. The median threshold LC_{50} level is about 0.33 mg/ℓ.

Water Quality Modeling Considerations

Since the percent unionized NH_3 is a function of pH and temperature, an assessment of the significance of these parameters must be made. Thus let $N_u = NH_3$, $N = NH_4^+$ and $N_T = N_u + N$. Also let

$$\delta = N_u/N_T = \frac{1}{2 + 10^{pK_a - pH}} \tag{3}$$

or

$$N_T = \frac{1}{\delta} N_u = \beta N_u \tag{3a}$$

For steady state stream modeling the relevant equation for the total NH_3, N_T, is

$$u \frac{dN_T}{dx} = -K_T N_T = -(K_N + K_p) N_T \tag{4}$$

where K_T is the loss rate of total ammonia. Note that this rate is a function of nitrifying bacteria present to oxidize the ammonia (i.e. K_N) and/or uptake of ammonia by plants (i.e. K_p). For some problems, one can obtain an estimate of the former oxidation rate from nitrification studies and an analysis of the formation of nitrate nitrogen. Substituting Eq. (3a) into Eq. (4), expanding and simplifying gives for N_u, the unionized form,

$$U\frac{dNu}{dx} = -[\frac{1}{\beta}\frac{ud\beta}{dx} - K_T]N_u \qquad (5)$$

where the term involving β is the influence of longitudinally varying pH and temperature on the percent of N_u. Note that it affects the reaction rate of the unionized form. This simply means that critical conditions (i.e., maximum N_u) may not necessarily be at the outfall but may be downstream depending on the change in pH and temperature. (In addition to the effect of pH and temperature, the loss of NH_3, a dissolved gas, due to evaporative exchange with the atmosphere should be considered if the fraction of NH_3 becomes large.) A very simple illustration is shown in Figure 2 where the pH is assumed to jump in discrete steps from 7-9. Maximum concentration of NH_3 occurs at $t^* = 10$ where pH = 9. Care should therefore be taken in properly accounting for spatial (and temporal) variations in pH (or temperature) in the computation of the unionized form of NH_3.

REFERENCES

Emerson, et al., 1975. Aqueous ammonia equilibrium calculations: effects of pH and temperature. Jour. Fish. Res. Bd. Can. 32:2379.

McKee, J.E. and H.W. Wolf. 1963. Water quality criteria. California State Water Quality Control Board, Pub. No. 3-A, 548 pp.

NAS/NAE. 1972. Water quality criteria, 1972. Comm. on Water Quality Criteria, Env. Studies Board Nat. Acad. of Sci., Nat. Acad. of Eng. Wash., D.C., 594 pp.

Ruffier, P.J., W.C. Boyle and J. Kleinschmidt. 1981. Short-term acute bioassays to evaluate ammonia toxicity and effluent standards. Jour. WPCF, 53(3):367-377.

US Env. Prot. Agency. 1976. Quality criteria for water. Wash., D.C.

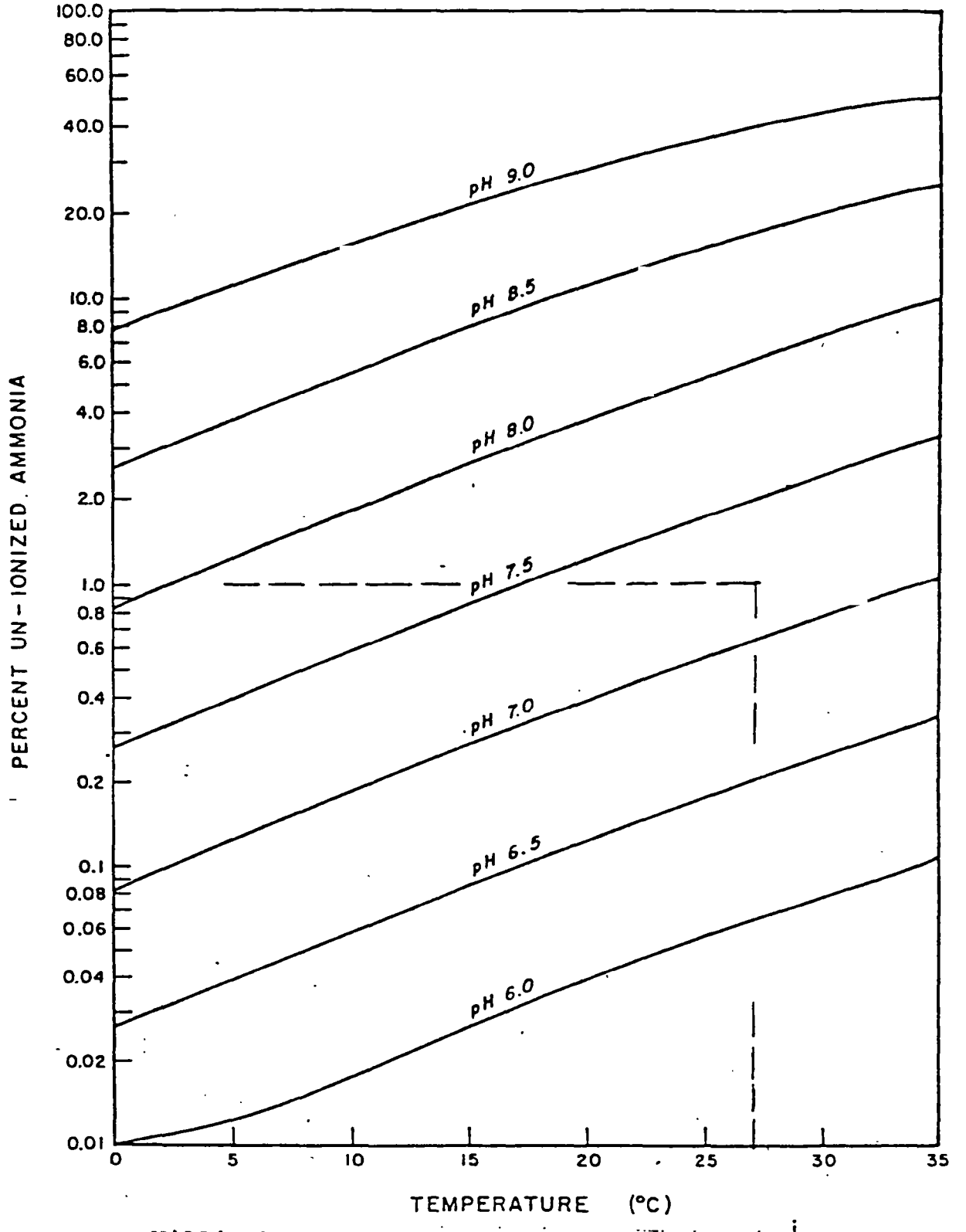

NOTE: REDRAWN FROM Willingham, William T., 1976, Ammonia Toxcity, U.S. Environmental Protection Agency, EPA-908/3-76-001, February, 1976.

FIG. 1 PERCENTAGE OF UN-IONIZED AMMONIA IN AMMONIA-WATER SOLUTION AT VARIOUS PH AND TEMPERATURE VALUES

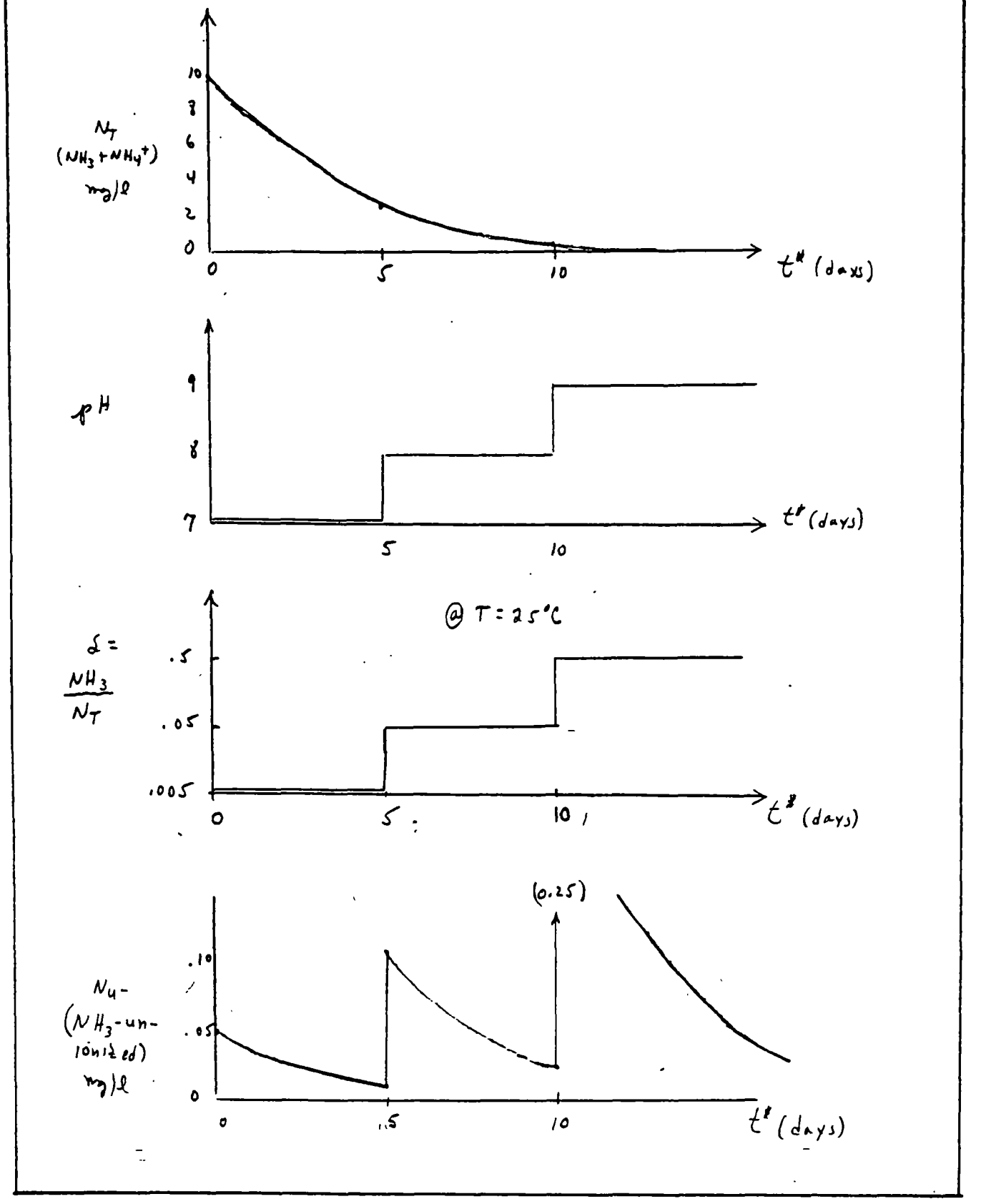

FIG. 2 VARIATION IN UNIONIZED NH_3 for VARIATION in pH

Toxics Concentrations in Streams*

For the case of an interactive bed, where the stream bed and water column have reached equilibrium concentrations of a chemical discharged by a point source/tributary, and where the suspended solids concentrations in the reach of interest are spatially constant in the water column and active bed, the following relation applies:

$$C_{T1} = \frac{W_{T1}}{Q} e^{-K_T x/u} \tag{1}$$

where

C_{T1} = concentration of total toxicant in water column

W_{T1} = original mass rate of chemical discharged into the water column

Q = longer-term average stream flow immediately downstream of the discharge/tributary input

u = stream velocity

x = distance downstream of the discharge.

The term K_T is the apparent removal rate of the total toxicant in the stream, where:

$$K_T = K_1 + \beta \frac{r_2}{r_1}(K_2 + f_{P2} w_d / H_2) \tag{2}$$

and

$$\beta = \frac{m_2 H_2 f_{P1}}{m_1 H_1 f_{P2}} \tag{3}$$

$$\frac{r_2}{r_1} = \frac{(w_u + w_d) f_{P2} + K_L (\pi_1/\pi_2) f_{d2}}{(w_u + w_d) f_{P2} + K_L f_{d2} + K_2 H_2}$$

Definitions of all symbols used are contained in Table 1.

Under the further assumptions that the stream reach is not sedimenting ($w_d = 0$), diffusion of the dissolved fraction of the chemical between the water and bed is negligible ($K_L = 0$) and there are no degradation mechanisms of the chemical in the active bed ($K_2 = 0$), Equations 2 and 3 simplify to:

$$K_T = K_1 \tag{4}$$

$$r_2 = r_1 \tag{5}$$

* John A. Mueller

Thus, the distribution of the total toxicant in the water column (C_{T1}) decays exponentially at a rate equal to the sum of the removal rates of the dissolved fraction ($K_T = K_1$).

It may be noted that settling and resuspension of the particulate fraction do not contribute to the decay of the total toxicant. Since there is no sedimentation and no degradation in the stream bed, net settling of the particulate toxicant in the water column is equal to the resuspension of the particulate fraction in the bed. Thus, there is no net flux of toxicant into, or out of, the bed and the distribution of the chemical in the water column is not affected by the particulate fraction with the associated suspended solids characteristics.

Wasteload Allocation Considerations

In the event of a reduction in an external load-together with a reduction in the streamflow-the water column and bed will eventually reach new equilibrium concentrations which are lower than those previously established. In the interim, the bed concentrations will be more reflective of the previous loading and long term average streamflow. Thus, an interim analysis would consist of calculating the water column concentrations as if the stream were subjected to the new external loading and a flux of chemical from the bed. The latter value is calculated as the product of the resuspension velocity and the previous steady state bed concentration. For the previous condition of no sedimentation, no degradation in the bed and no dissolved chemical diffusion between water column and bed, the interim value of the water column concentration is:

$$C_{T1} = \frac{W_{T2}}{Q_c} e^{-v_1 x/u_c} + \frac{v_2}{v_1 - K_T(u_c/u)} C_{T2}(0)\left(e^{-K_T x/u} - e^{-v_1 x/u_c}\right) \qquad (6)$$

where

W_{T2} = new loading

Q_c, U_c = critical flow and velocity

$v_1 = K_1 + f_{P1} w_s / H_1$

$v_2 = f_{P2} w_u / H_1$

u = original longer term stream velocity

$C_{T2}(o)$ = original bed toxicant concentration at $x = o$

The original bed concentration at the discharge location is:

$$C_{T2}(o) = \left(\frac{m_2}{m_1} \frac{f_{P1}}{f_{P2}}\right) \frac{W_{T1}}{Q} \tag{7}$$

where W_{T1} = original toxicant discharge rate

Q = longer term average streamflow

An example of the application of the preceding equations follows.

Reference

Di Toro, D.M., O'Connor, D.J., Thomann, R.V. and St. John, J.P., "Analysis of Fate of Chemicals in Receiving Waters", HydroQual, Inc., May 1981.

TABLE 1. Symbols Used in Stream Equations for Toxics

Symbol	Description	Unit
K_T	apparent removal rate of total toxicant in water column	1/T
K_1	decay rate of chemical in water column, including hydrolysis, photolysis, oxidation, biodegradation, volatilization	1/T
K_2	decay rate of total toxicant in the bed	1/T
K_L	diffusion rate of dissolved chemical between water and bed	L/T
C_{T1}, C_{T2}	total toxicant concentration	M/L^3
m_1, m_2	solids concentrations	M/L^3
r_1, r_2	particulate toxicant concentration, $r = f_P C_T/m$	M(tox)/M(sol)
H_1, H_2	depth of water, thickness of active bed	L
w_s, w_u, w_d	settling, resuspension, sedimentation velocities	L/T
π_1, π_2	partition coefficients	L^3/M
f_{d1}, f_{d2}	dissolved fraction, $f_d = (1 + \pi m)^{-1}$	-
f_{P1}, f_{P2}	particulate fraction, $f_P = \pi m/(1 + \pi m)$	-

Note: Subscripts 1 = water column, 2 - active bed

STREAM TOXICANT DISTRIBUTIONS IN WATER & BED

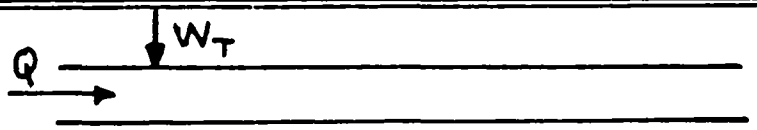

DATA

stream – depth	H_1	1.0 m
– bed thickness	H_2	0.01 m
– flow – average	Q	100 cfs
– design	Q_c	10 cfs
– velocity – average	U	1.64 mi/day
– design	U_c	0.164 mi/day
suspended solids		
concentration – water column	m_1	10 mg/l
– bed	m_2	10000 mg/l
settling velocity	w_s	0.83 m/day
sedimentation velocity	w_d	0.0 mm/yr
chemical		
mass discharge rate – present	W_{T1}	1000 lb/day
– design	W_{T2}	100 lb/day
decay rate – water column	K_1	0.1 /day
– bed	K_2	0.0 /day
partition coeff. – water	Π_1	10000 (μg/kg)/(mg/l)
– bed	Π_2	10000 "

PROBLEM Determine bed and water column concentrations of total chemical under present & design conditions.

SOLUTION

For all cases, the following parameters are constant.

$$w_u = w_s \times m_1/m_2 = 0.83 \text{ m/day} \times (10 \text{ mg/l} / 10000 \text{ mg/l}) = 8.3 \times 10^{-4} \text{ m/day}$$

$$f_{p1} = \Pi_1 m_1/(1+\Pi_1 m_1) = (10000 \times 10 \times 10^{-6})/(1+10000 \times 10 \times 10^{-6}) = 0.1/1.1 = 0.0909$$

$$f_{p2} = \Pi_2 m_2/(1+\Pi_2 m_2) = (10000 \times 10000 \times 10^{-6})/(1+10000 \times 10000 \times 10^{-6}) = 100/101 = 0.990$$

$$K_T = K_1 = 0.1/\text{day} \quad ; \quad v_2 = f_{p2}\, w_u/H_1 = 0.990 \times 8.3 \times 10^{-4}/1.0 = 8.22 \times 10^{-4}/\text{day}$$

$$v_1 = K_1 + f_{p1}\, w_s/H_1 = 0.1 + 0.0909 \times 0.83/1.0 = 0.1754/\text{day}$$

A. PRESENT LOADING

For Average Flow of 100 cfs

$$C_{T1} = C_{T1}(0)\ e^{-K_T x/u} = \frac{1000\ lb/day}{100\ cfs \times 5.4}\ e^{-0.1x/1.64} = \underline{1.85\ e^{-0.06097x}}$$

$$C_{T2} = C_{T2}(0)\ e^{-K_T x/u}$$

$$C_{T2}(0) = \frac{m_2}{m_1}\frac{f_{p1}}{f_{p2}}\ C_{T1}(0) = \frac{10000}{10} \times \frac{0.0909}{0.990} \times 1.85 = 170\ mg/l$$

$\underline{C_{T2} = 170\ e^{-0.06097x}}$ See Figs 1b and 1c for plots.

Effect of Resuspension on C_{T1}

$$C_{T1(BED)} = \frac{\nu_2}{\nu_1 - K_T(u/u)}\ C_{T2}(0)\left(e^{-K_T x/u} - e^{-\nu_1 x/u}\right)$$

$$= \frac{8.22 \times 10^{-4}}{0.1754 - 0.1(1)} \times 170 \times \left(e^{-0.1x/1.64} - e^{-0.1754x/1.64}\right)$$

$$= 1.85\left(e^{-0.06097x} - e^{-0.1070x}\right)$$ See Fig 1c.

MAX. EFFECT is at x_m, where

$$x_m = \frac{u}{\nu_1 - K_T(u_c/u)}\ \ln\left(\frac{\nu_1}{K_T(u_c/u)}\right)$$

$$= \frac{1.64}{0.1754 - 0.1(1)}\ \ln\left(\frac{0.1754}{0.1 \times 1}\right) = 12.22\ \text{miles}$$

$$\therefore\ C_{T1(BED)}\Big|_{max} = 1.85\left(e^{-0.06097 \times 12.22} - e^{-0.1070 \times 12.22}\right) = 0.378\ mg/l$$

For Design Flow of 10 cfs

Under the present load, and a short duration drought flow of 10 cfs, the water column will increase in concentrat. due to the reduced dilution of the present external load and the bed resuspension.

$$C_{T1} = C_{T1}(w.c.) + C_{T1}(BED)$$

$$= \frac{W_{T1}}{Q_c}\ e^{-\nu_1 x/u_c} + \frac{\nu_2}{\nu_1 - K_T(u_c/u)}\ C_{T2}(0)\left(e^{-K_T x/u} - e^{-\nu_1 x/u_c}\right) \quad (Eq.6)$$

$$= \frac{1000}{10 \times 5.4}\ e^{-0.1754x/0.164} + \frac{8.22 \times 10^{-4}}{0.1754 - 0.1 \times \left(\frac{0.164}{1.64}\right)} \times 170\left(e^{-0.1x/1.64} - e^{-0.1754x/0.164}\right) =$$

$$C_{T1} = 18.5\, e^{-1.070x} + 0.8447\left(e^{-0.06097x} - e^{-1.070x}\right)$$

As seen in Fig. 1d, after milepoint 5, the bed resuspension is the sole source of the water column concentrations. At milepoint 2.84 the bed effect is at a maximum, contributing 0.670 mg/l to the water column.

B. REDUCED LOADING - INITIAL BED CONC.

Until a new (lower) bed equilibrium concentration is established, bed concentrations will be decreasing from their initial values. For the transition period, a conservative estimate of water column concentrations will be given by Eq. 6.

In Fig. 2a, the original bed concentrations are shown.

Flow of 100 cfs

Under the reduced load & initial bed concentrations,

$$C_{T1} = \frac{W_{T2}}{Q} e^{-N_1 x/u} + \frac{N_2}{N_1 - K_T(u/u)} C_{T2}(0)\left(e^{-K_T x/u} - e^{-N_1 x/u}\right)$$

$$= \frac{.100}{100\times 5.4} e^{-0.1764x/1.64} + \frac{8.22\times 10^{-4}}{0.1754 - 0.1\times(1)}(170)\left(e^{-0.1x/1.64} - e^{-0.1754x/1.64}\right)$$

$$C_{T1} = \underbrace{0.185\, e^{-0.1070x}}_{C_{T1}(W.C.)} + \underbrace{1.85\left(e^{-0.06097x} - e^{-0.1070x}\right)}_{C_{T1}(BED)}$$

As seen in Fig 2b, the concentration in the water column at the outfall is now 0.185 mg/l, an order of magnitude lower than previously (Fig 1c). However, the concentrations beyond milepoint 12 are greater than 50% of the original values due to the bed.

Flow of 10 cfs

$$C_{T1} = \frac{W_{T2}}{Q_c} e^{-N_1 x/u_c} + \frac{N_2}{N_1 - K_T(u_c/u)} C_{T2}(0)\left(e^{-K_T x/u} - e^{-N_1 x/u_c}\right)$$

$$= \frac{100}{10\times 5.4} e^{-0.1764x/0.164} + \frac{8.22\times 10^{-4}}{0.1754 - 0.1\left(\frac{0.164}{1.64}\right)}(170)\left(e^{-0.1x/1.64} - e^{-0.1754x/0.164}\right)$$

$$= 1.85\, e^{-1.070x} + 0.845\left(e^{-0.06097x} - e^{-1.070x}\right)$$

From Fig 2c, maximum water column concentration is at $x=0$, and the sediment effect predominates for $x \geq 3$ miles.

C. REDUCED LOAD - FINAL BED CONC.

After a sufficient time has elapsed to allow bed concentrations to come to the lower equilibrium value, the following applies.

Average Flow of 100 cfs

$$C_{T1}(0) = 100/(100 \times 5.4) = 0.185 \text{ mg/l}$$

$$C_{T1} = 0.185\, e^{-0.1x/1.64} = 0.185\, e^{-0.06097x} \quad \text{(See Fig 3b.)}$$

$$C_{T2}(0)\Big|_{NEW} = \frac{m_2}{m_1}\frac{f_{p1}}{f_{p2}} C_{T1}(0) = \frac{10000}{10} \times \frac{0.0909}{0.990} \times 0.185 = 17 \text{ mg/l}$$

$$C_{T2} = 17\, e^{-0.06097x}, \text{ as shown in Fig 3a.}$$

Design Flow of 10 cfs

$$C_{T2} = 17\, e^{-0.06097x}, \text{ as above.}$$

$$C_{T1} = \frac{W_{T2}}{Q_c} e^{-v_1 x/u_c} + \frac{v_2}{v_1 - k_T(u_c/u)} C_{T2}(0)\Big|_{NEW} \left(e^{-k_T x/u} - e^{-v_1 x/u_c}\right)$$

$$= \frac{100}{10 \times 5.4} e^{-0.1754x/0.164} + \frac{8.22 \times 10^{-4}}{0.1754 \times 0.1\left(\frac{0.164}{1.64}\right)} (17)\left(e^{-0.1x/1.64} - e^{-0.1754x/0.164}\right)$$

$$= 1.85\, e^{-1.070x} + 0.0845\left(e^{-0.06097x} - e^{-1.070x}\right)$$

As seen in Fig 3c, the maximum water column concentration is 1.85 mg/l at the discharge location. It decreases rapidly to the new sediment-induced concentration - which has a peak value of 0.067 mg/l at milepoint 2.84.

D. SUMMARY FOR $Q_c = 10$ cfs

CONDITION	LOADING (lb/day)	MAXIMUM CONCENTRATION (mg/l)		
		ACTIVE BED	WATER COLUMN	
			LOAD-INDUCED	BED-INDUCED
PRESENT	1000	170	18.5	0.67
INTERIM	100	170	1.85	0.67
FINAL	100	17	1.85	0.067

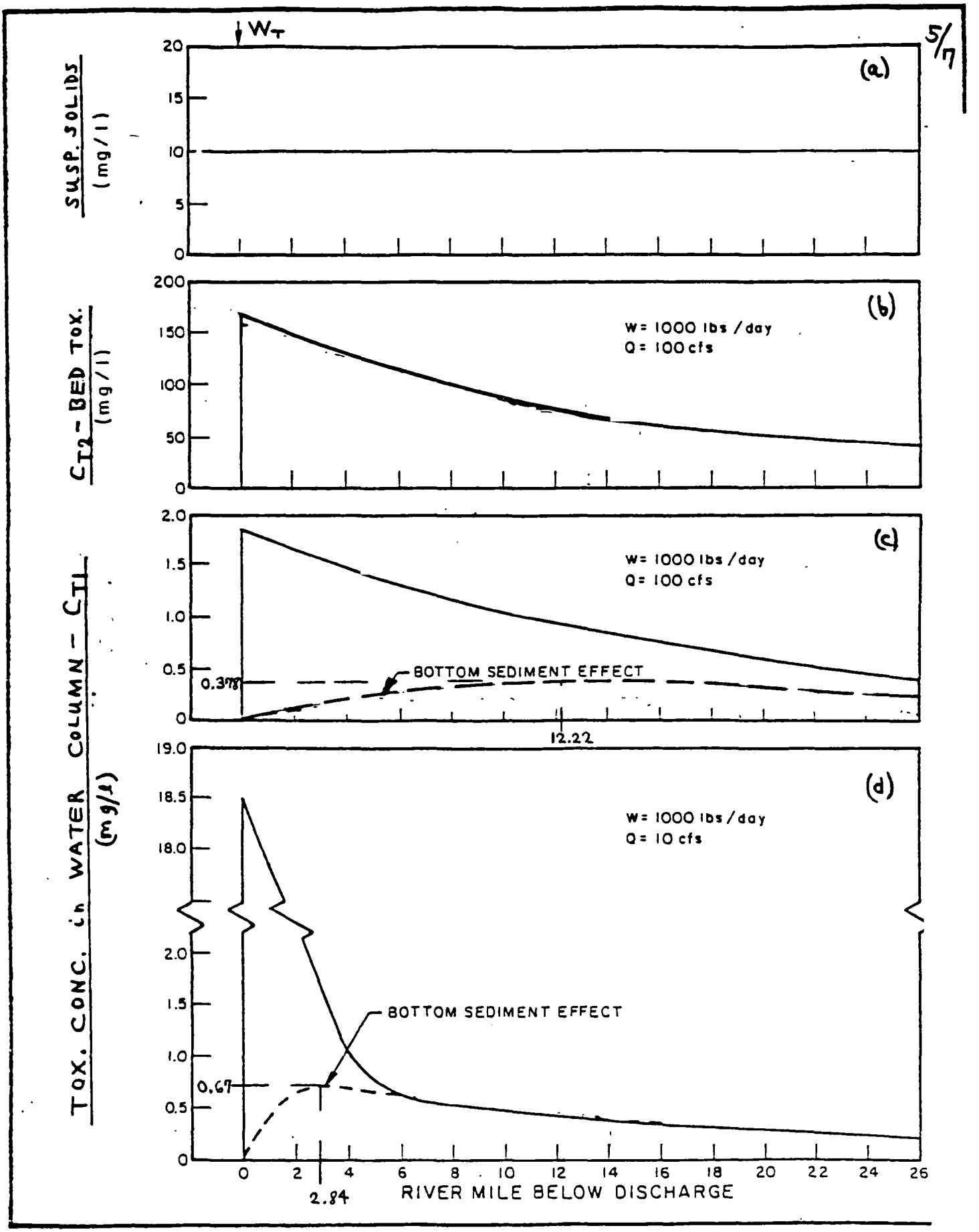

FIGURE 1

EXAMPLE RIVER SEDIMENT AND WATER COLUMN CONCENTRATION PROFILES FOR ORIGINAL LOAD

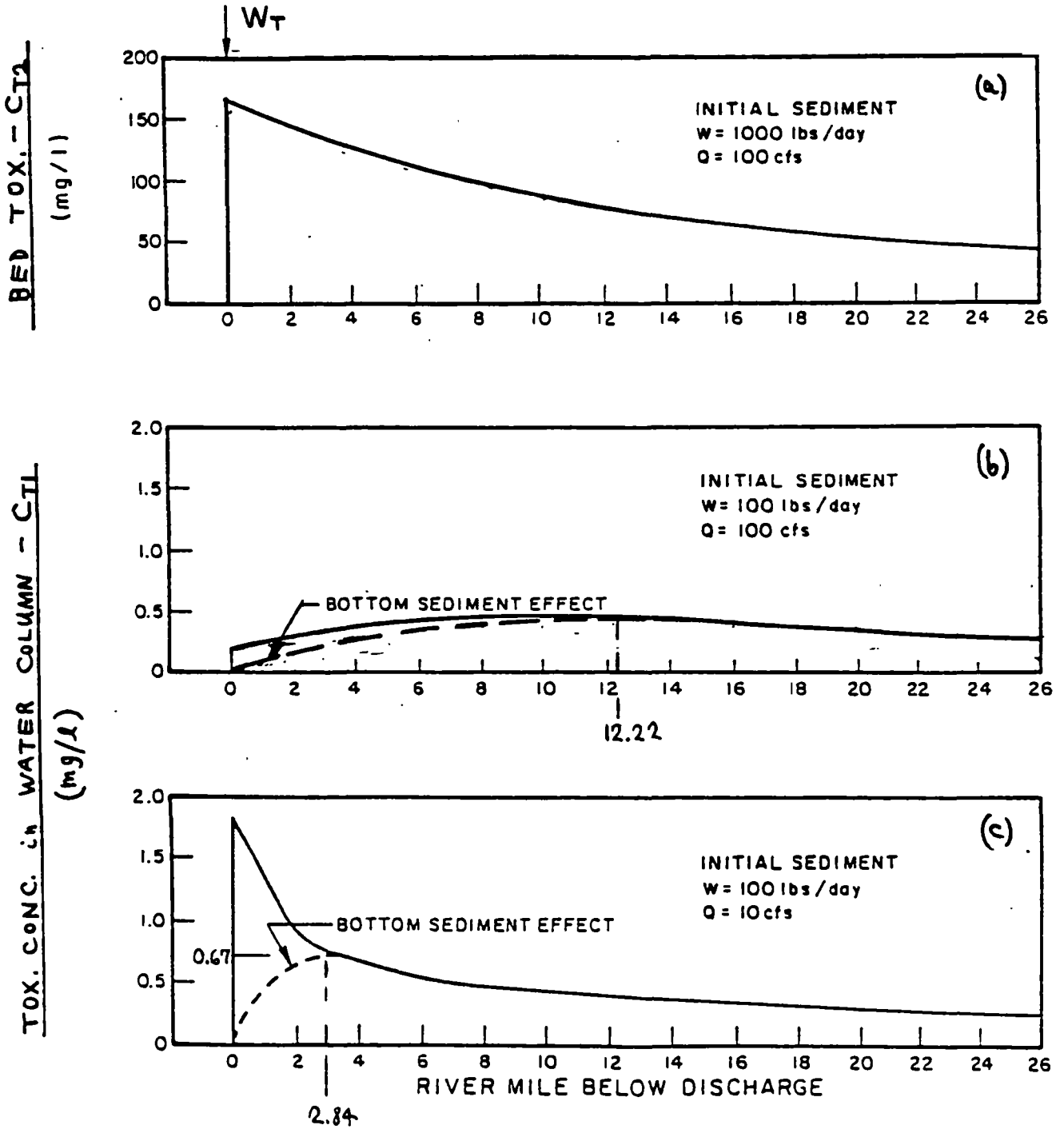

FIGURE 2

INTERIM RIVER SEDIMENT AND WATER COLUMN CONCENTRATION PROFILES FOR REDUCED LOAD

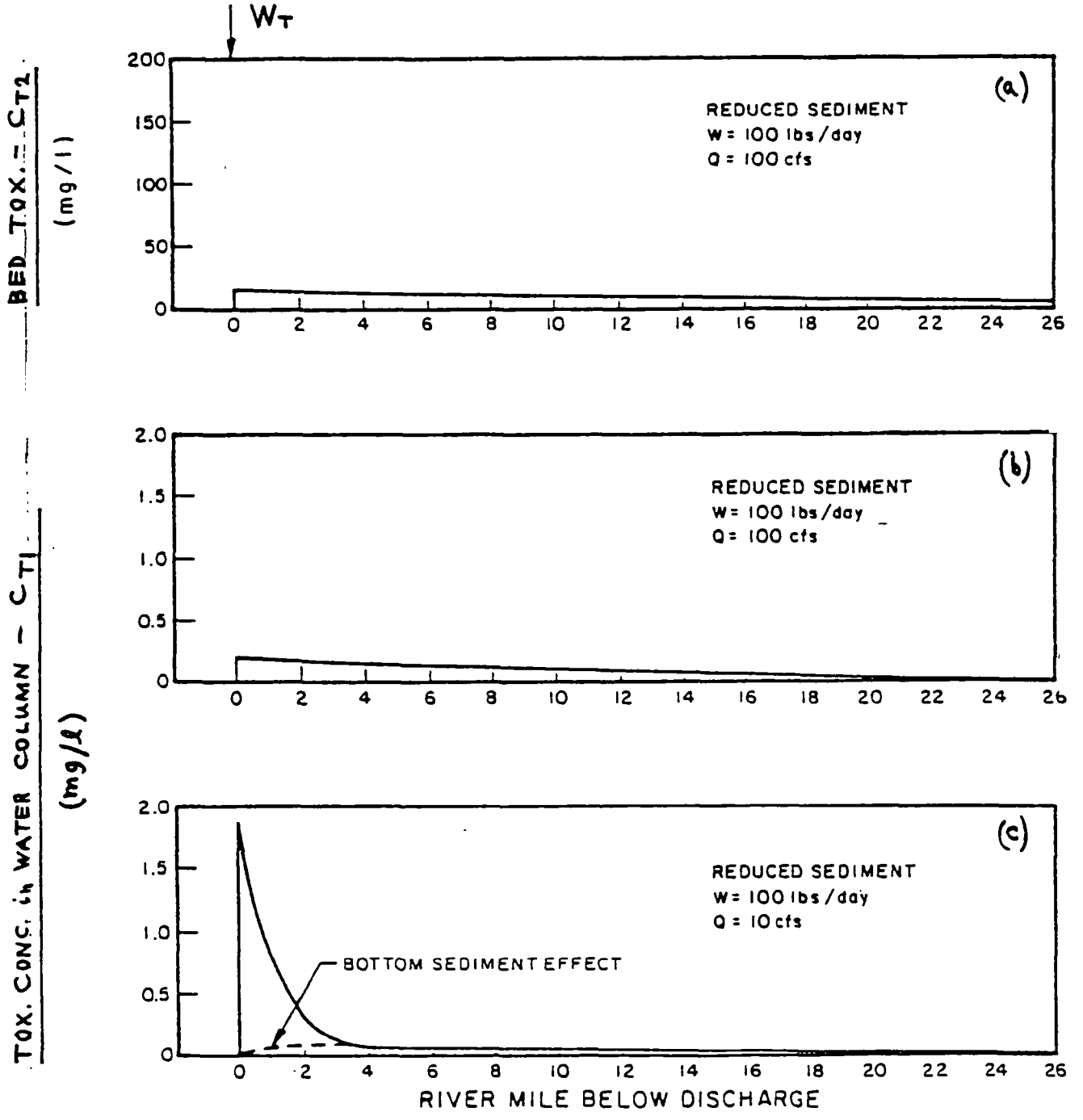

FIGURE 3

FINAL RIVER SEDIMENT AND WATER COLUMN CONCENTRATION PROFILES FOR REDUCED LOAD

TOXICS CONCENTRATIONS IN LAKES *

DATA

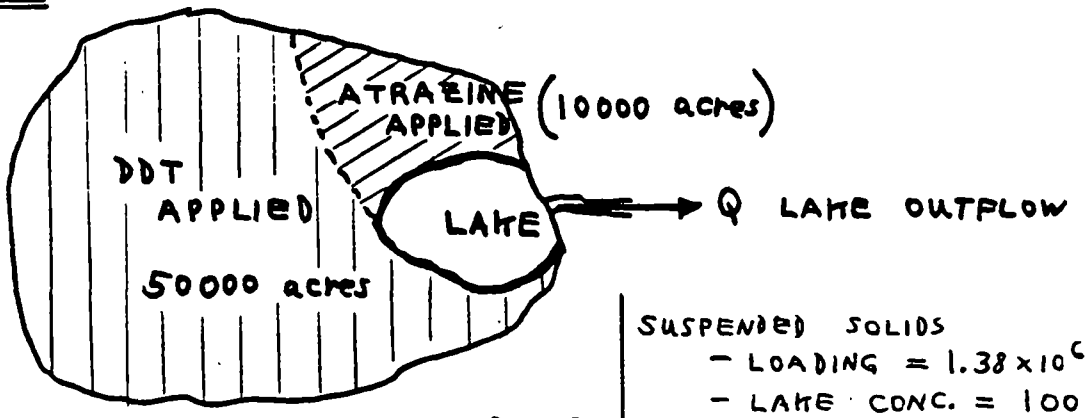

LAKE - VOLUME = 4.32×10^8 ft^3
- DEPTH = 4 ft

AVERAGE RUNOFF = 0.533 cfs/mi^2

SUSPENDED SOLIDS
- LOADING = 1.38×10^6 LB/DAY
- LAKE CONC. = 100 mg/l

CONC. OF TOXIC. IN RUNOFF
- ATRAZINE = 630 µg/l
- DDT = 14 µg/l

Pesticide	Hydrolysis	Photolysis	Volatilization/ Biodegradation	Φ $\frac{mg/kg}{mg/l}$
Atrazine	0.1/day	0.02/day	Assume Negligible	50
DDT	2.5×10^{-4}/day	1.5×10^{-4}/day		50 000

PROBLEM Assuming a steady state condition, estimate the concentrations of atrazine and DDT in the lake.

SOLUTION

Lake Detention Time

Runoff from atrazine drainage = $Q_A = \frac{10000 \text{ acres}}{640 \text{ acres/mi}^2} \times 0.533 \frac{\text{cfs}}{\text{mi}^2} = 8.3$ cfs

Runoff from DDT drainage = $Q_D = (50000/640) \times 0.533 = 41.7$ cfs

Lake Outflow $Q = Q_A + Q_D = 8.3 + 41.7 = 50.0$ cfs

Hydraulic Detention Time $t_o = \frac{V}{Q} = \frac{4.32 \times 10^8 \text{ ft}^3}{50 \text{ ft}^3/\text{s} \times 86400 \text{ s/day}} = \underline{100 \text{ days}}$

*JOHN A MUELLER

Estimate Suspended Solids Net Settling Rate (v_s)

$$m = \frac{W/Q}{1 + K_s t_o}$$

$$100\ mg/\ell = \frac{(1.38 \times 10^6\ lb/day)/(50.0\ cfs \times 5.4)}{1 + K_s\ (100\ days)}$$

$$K_s = v_s/H = 0.501/day$$

$$v_s = K_s H = 0.501/day \times 4\ ft = \underline{2.0\ ft/day}$$

Estimate Atrazine Conc. in Lake

$$W_{ATR} = 8.3\ cfs \times 0.630\ mg/\ell \times 5.4 = 28.2\ lb/day$$

$$C_T = \frac{W_{ATR}/Q}{1 + \frac{t_o}{1+fm}\left(K_c + fm\, K_s\right)}$$

$$fm = 50\ \frac{\mu g/kg}{\mu g/\ell} \times 100\ \frac{mg}{\ell} \times \frac{1\ kg}{10^6\ mg} = 0.005$$

$K_s = 0.50/day$; $K_c = \Sigma K_{DISS} = 0.1 + 0.02 = 0.12/day$

$$C_T = \frac{28.2/(50.0 \times 5.4)}{1 + \frac{100}{1+0.005}\left(0.12 + 0.005 \times 0.50\right)} = 0.0079\ mg/\ell = \underline{7.9\ \mu g/\ell}$$

Note: $C_{DISS} = C_T/(1+fm) = 7.9/(1+0.005) = 7.86\ \mu g/\ell$ | 99.5% DISS.

$C_{PART} = C_T(fm/(1+fm)) = 7.9 \times 0.005/1.005 = 0.04\ \mu g/\ell$ | 0.5% PART

Estimate DDT Lake Concentration

$$W_{DDT} = 41.7 \times 0.014 \times 5.4 = 3.15\ lb/day$$

$fm = 50000 \times 100/10^6 = 5$; $K_s = 0.50/day$

$K_c = 2.5 \times 10^{-4} + 1.5 \times 10^{-4} = 4.0 \times 10^{-4} = 0.0004/day$

$$C_T = \frac{3.15/(50.0 \times 5.4)}{1 + \frac{100}{1+5}\left(0.0004 + 5 \times 0.50\right)} = 0.00027\ mg/\ell = \underline{0.27\ \mu g/\ell}$$

Note: $C_{DISS} = 0.27/(1+5) = 0.045\ \mu g/\ell$ | 16.7 % DISSOLVED

$C_{part.} = 0.27 \times 5/(1+5) = 0.225\ \mu g/\ell$ | 83.3 % PARTICULATE

EXAMPLE WASTE LOAD ALLOCATION ANALYSIS *

The following waste load allocation analysis is designed to provide an example which is reasonably realistic but not so complex that it detracts from the example's principal intent, which is to:

- demonstrate the major steps in a waste load allocation analysis,
- show how the mathematical equations are applied, and
- present the relationship between water quality impacts and the overall task of performing a waste load allocation.

Because the purpose of this example is to present an overview of the steps required for a waste load allocation, emphasis is not placed on providing details on data requirements and calibration-validation procedures. These technical aspects are discussed more thoroughly in other sections of the manual.

Problem Setting. In this example, a city of approximately 60,000 people discharges its wastewater into a relatively small river with an average annual flow of about 250 cfs. The city's wastewater is presently treated by a trickling filter plant which provides about 85% BOD removal and has reached its design capacity of 7.5 MGD. The population is projected to increase by more than 50% to 92,000 people (with a range of 75,000 to 120,000 people) by the year 2000. Expansion of the treatment plant to a capacity of 11.5 MGD and provision of an activated sludge system for more efficient secondary treatment are proposed.

The river, for thirty miles downstream of the treatment plant discharge, is classified as B1 which has a designated water use for fish and wildlife

* Extracted from (with modification):
"Technical Guidance Manual for Performing Waste Load Allocations"; E.D. Driscoll, J.L. Mancini and P.A. Mangarella; for US EPA, Office of Water Regulations & Standards, Monitoring Branch, J.R. Pawlow, Proj. Off., Jan. 1981.

propagation. The pertinent water quality standards for this example are a minimum dissolved oxygen level of 5.0 mg/l and a maximum un-ionized ammonia concentration of 0.02 mg/l. The river is used locally for fishing and is bordered by several campgrounds and a state park. No water quality problems are documented, and the limited water quality data do not show any standards violations. A summary of the problem setting and treatment plant data is presented in Figures 2-11 and 2-12.

River Characteristics. The river flow is gauged by the USGS immediately upstream of the treatment plant discharge. The average monthly flows for a thirty-year period are summarized in Figure 2-13. The average annual flow is about 250 cfs with a minimum monthly average low flow of 100 cfs which occurs in the summer. However, minimum dissolved oxygen standards must be met for a minimum seven-consecutive-day flow with a return period of once every 10 years ($_7Q_{10}$). From a statistical analysis of the flow records, the $_7Q_{10}$ is determined to be 30 cfs.

Critical conditions of dissolved oxygen and un-ionized ammonia concentration in the river occur during the summer when the flow is low and the river temperature is high. From eleven years of river temperature data collected as part of a limited river monitoring program by treatment plant personnel, the maximum average monthly river temperature is 27°C and occurs in August. Therefore, design critical river conditions for water quality impact analyses are a river flow of 30 cfs and a river temperature of 27°C.

For this example, assume that three surveys have been conducted which measured stream cross-sectional area under different flow regimes. Cross-sections were measured at 20 locations within the 30-mile study area.

From cross-sectional area measurements, it is concluded that the river is relatively uniform in the study area and, therefore, one average cross-sectional area and length can characterize the study area for each flow condition. If the river cross-sectional area varied significantly with distance, the river would have been divided into smaller reaches, each of which would have approximately uniform geometry for each prevailing flow condition. Dye study techniques provide an alternative means of accurately determining average velocity for a given river section.

The average river velocity during each of the cross-sectional area survey periods was computed by applicaton of the continuity equation VELOCITY = FLOW/AREA. The average flow for each survey period was obtained from USGS records.

River cross-sectional area, depth and velocity generally form linear correlations with flow when the data are plotted on log-log scales. Figure 2-13 presents these log-log plots for the example problem. Interpolations and extrapolations of river geometry and velocity at specific flows can be made directly from the log-log plots or computed from the equation of the line of best fit. The equation for the line of best fit has the form: $Y = IQ^S$, where I is the intercept at Q = 1 cfs and s is the slope scaled directly from the plot (inches/inch). As shown in Figure 2-13, these log-log relationships are summarized as follows:

$$\text{AREA } (ft^2) = 19.5\ Q\ (cfs)^{0.6} \qquad (2\text{-}21)$$

$$\text{DEPTH } (ft) = 0.312\ Q\ (cfs)^{0.5} \qquad (2\text{-}22)$$

$$\text{VELOCITY } (fps) = 0.0513\ Q\ (cfs)^{0.4} \qquad (2\text{-}23)$$

Using the above equations, river area, depth and velocity can be computed for any river flow. If river geometry data are available at only one flow

regime, the relationship presented in the ADDENDUM (equations 2-3, 2-4, and 2-5) would be used to calculate river depth, area, and velocity at other flows.

Review of River Water Quality Data. Historical river water quality data within the study area are limited. As part of the state environmental department's overall monitoring program for this river basin, water samples are periodically collected at stations located at river milepoints 11 and 25. These data represent approximately one grab sample per month during the summer over a five-year period. A review of these data does not reveal any water quality problems with regard to dissolved oxygen and un-ionized ammonia. Because there is no evidence of a water quality problem, only secondary treatment at the expanded plant has been proposed. No additional funds for Advanced Secondary Treatment (AST) or Advanced Wastewater Treatment (AWT) have been proposed.

Considering the relatively good water quality, an appropriate level of effort for a waste load allocation (WLA) study initially can be limited to the analysis of a single river water quality data set collected during summer low flow conditions. Accordingly, a survey was conducted during two days in August when the river flow averaged 100 cfs and the river water temperature was 25°C. The results of this survey are presented in Figures 2-14 and 2-15.

The dissolved oxygen data in Figure 2-14, both August 1979 data and historical data, show river dissolved oxygen levels above the standard of 5.0 mg/l. The increase in river BOD_5 and ammonia concentrations at milepoint 1.0 show the impact of the treatment plant discharge. The gradually decreasing ammonia profile and increasing nitrite plus nitrate profile suggest that nitrification is occurring in the river.

Un-ionized ammonia, which is toxic to biological life, is dependent on the total river ammonia concentration, river pH, and river temperature. The higher the river pH and temperature, the higher the percentage of total ammonia that is in the un-ionized form. Figure 2-15 presents the measured total river ammonia concentration. The un-ionized ammonia concentration is determined from the relationship summarized in Figure 2-16, which relates un-ionized ammonia to pH and temperature. For a river temperature of 25°C and a pH of 7.2 (point A), un-ionized ammonia is 0.9 percent of the total ammonia concentration. During the August 1979 survey, the river un-ionized ammonia concentration was less than the standard of 0.02 mg/l.

Model Calibration Analysis. For this analysis, model calibration is the determination of the coefficients (reaction rates) of the equations that describe the spatial distribution of BOD, ammonia, nitrite plus nitrate, and dissolved oxygen. The equations for each of these constituents are summarized as follows:

BOD_5

$$L_5 = (L_5)_o \, e^{\frac{-K_r}{U} x} \qquad (2\text{-}24)$$

Ammonia (as N)

$$NH_3 = (NH_3)_o \, e^{\frac{-K_n}{U} x} \qquad (2\text{-}25)$$

Nitrite plus Nitrate (as N) (2-26)

$$(NO_2 + NO_3) = (NO_2 + NO_3)_o + \left[(NH_3)_o \left(1 - e^{\frac{-K_n}{U} x}\right)\right]$$

Dissolved Oxygen Deficit

$$D = \frac{K_d L_o}{K_a - K_r}\left[e^{\frac{-K_r}{U}x} - e^{\frac{-K_a}{U}x}\right] + \frac{K_n N_o}{K_a - K_n}\left[e^{\frac{-K_n}{U}x} - e^{\frac{-K_a}{U}x}\right] + D_o\, e^{\frac{-K_a}{U}x} \qquad (2\text{-}27)$$

In all these equations, the variables with the zero subscript are the concentrations at x = 0 (after integrating the upstream concentration and the treatment plant load). U is river velocity and K_r, K_d, K_n, and K_a are the BOD removal rate coefficient, BOD oxidation rate, nitrification rate, and atmospheric reaeration rate coefficients, respectively. L_o and N_o represent (respectively) the ultimate carbonaceous BOD and nitrogenous BOD at x = 0, and D_o is the initial oxygen deficit at x = 0.

Note that the oxidation of ammonia (as expressed by equation 2-25) is analogous to the oxidation of BOD. Whereas the oxidation of carbonaceous BOD produces carbon dioxide as the end product, the end product of ammonia oxidation is nitrite plus nitrate. Thus, the equation for nitrite plus nitrate states that the nitrite plus nitrate in the river is equal to the concentration at x = 0 plus the amount gained from ammonia oxidation. When all forms of nitrogen are expressed as N, the terms in equation 2-26 are directly additive.

The coefficients in equations 2-24 through 2-27 are determined by the following steps. The river velocity is calculated for the August 23-24, 1979 river flow using equation 2-23. The initial conditions (x = 0) are determined from a mass balance with the upstream concentration and the plant load. The BOD removal coefficient (K_r) is the value of K_r that provides the

best fit of the August 1979 BOD data with equation 2-24; for secondary effluents $K_d = K_r$ (no settling). The nitrification rate (K_n) is the value of K_n that simultaneously yields the best fit of both the ammonia and nitrite plus nitrate data with equations 2-25 and 2-26 respectively. The atmospheric reaeration rate is determined in accordance with Figure 2-6 . In addition, long-term BOD tests have been performed and indicate the ratio of ultimate to 5-day BOD to be 2.0. A summary of these calculations is shown in Table 2-2, and the calibration results are presented in Figure 2-17.

In this example, the calculation of the dissolved oxygen profile agrees with the measured data quite favorably and without any adjustments. Often the calculated dissolved oxygen profile does not initially agree with the data due to other sources and sinks of oxygen, such as nonpoint source loads, algal photosynthesis and respiration, and benthal oxygen demands. For the sake of simplicity, these complications have been omitted.

Model Projections. Having calibrated a model for BOD, DO, and nitrogen, i.e., defining site-specific coefficients and accepting that some reservations on reliability exist because the model was not tested against an independent data set, the model may be used to project water quality impacts that might be expected under conditions of interest. Two specific cases of interest are the water quality impacts of existing wastewater loads and for future design wastewater loads for the minimum river flow ($_7Q_{10}$) of 30 cfs. Dissolved oxygen, ammonia, and un-ionized ammonia profiles are presented for both cases in Figures 2-18 and 2-19. The model calculations for the design load condition are shown in Table 2-3.

The calculated profiles in Figure 2-18 show that present wastewater loads would result in dissolved oxygen and un-ionized ammonia water quality standards violations over approximately ten miles of river, if design drought flow conditions were to occur ($_7Q_{10}$ flow and a river temperature of 27°C). The lowest daily average dissolved oxygen concentration is about 3.0 mg/l, and the highest daily average un-ionized ammonia is twice the standard of 0.02 mg/l. At 27°C and with a pH of 7.2, un-ionized ammonia is 1 percent of the total ammonia concentration (point B - Figure 2-16).

Note that for the example, both the critical low flow ($_7Q_{10}$) and the maximum average monthly temperature have been used in the projection, even though historical records (summarized in Figure 2-13) show minimum average monthly flow and temperature to occur in different months. This tacitly assumes that although the minimum average monthly flow occurs in September, the critical $_7Q_{10}$ could occur in August, the month of maximum average temperatures. In areas where it can be shown that the $_7Q_{10}$ will occur in a month with lower temperature, then the appropriate combination should be used rather than each of the extreme values. For example, critical low flows frequently occur during October in the northeast. An appropriate approach in such cases would be to define the $_7Q_{10}$ and temperature condition for each of the critical months (say June-October), determine which month is most critical, and use that month in WLA calculations.

Calculated dissolved oxygen and un-ionized ammonia profiles for $_7Q_{10}$ flow conditions and the design wastewater load are presented in Figure 2-19. For the design load, the carbonaceous BOD is only slightly greater than the present load, but the ammonia and nitrogenous BOD loads are about 50% greater than present loads (see Figure 2-12). The minimum dissolved oxygen is about 2.6 mg/l, and the maximum un-ionized ammonia about 0.06 mg/l.

The projected dissolved oxygen and un-ionized ammonia profiles in Figures 2-18 and 2-19 indicate that whether or not the treatment plant expands from 7.5 MGD to 11.5 MGD, some reduction of wastewater BOD (carbonaceous and/or nitrogenous) and ammonia is required to meet water quality standards during critical low flow conditions. One method of computing the required reduction in wastewater BOD and ammonia is to calculate a series of dissolved oxygen and un-ionized ammonia profiles and, through trial and error, arrive at the proper combination of wastewater load reductions that meets water quality standards. An alternative to the trial and error method for dissolved oxygen is to separately calculate the dissolved oxygen deficit due to each BOD source (upstream BOD, plant carbonaceous BOD, plant nitrogenous BOD). This has been done for the design wastewater load case and is shown in Figure 2-20.

The top profile is the calculated dissolved oxygen distribution in which the lowest daily average dissolved oxygen concentration of 2.9 mg/l (maximum deficit of 5.1 mg/l) occurs at milepoint 4. The next three profiles are the components of the total dissolved oxygen deficit produced individually by the oxidation of upstream BOD, treatment plant carbonaceous BOD, and treatment plant nitrogenous BOD, respectively. On each deficit profile, the deficit produced at the critical point in the river, milepoint 4, is indicated. Note that the deficits of the component parts at milepoint 4 add up to the total deficit of 5.1 mg/l. Inspection of equation 2-27 shows that the carbonaceous and nitrogenous deficits are additive. The upstream BOD may be considered as a fraction of the total carbonaceous BOD in the river and thus separable from the plant carbonaceous BOD.

Knowing the relative contribution of each BOD source to the total deficit, it is an easy task to select combinations of wastewater BOD reductions

that will achieve water quality standards. At 27°C, dissolved oxygen saturation is 8.0 mg/l; therefore, for a dissolved oxygen standard of 5.0 mg/l, the allowable maximum deficit is 3.0 mg/l. Assuming that the upstream BOD deficit of 0.2 mg/l is uncontrollable, 2.8 mg/l of deficit would be available for the total of carbonaceous and nitrogenous plant BOD oxidation. Considering the un-ionized ammonia standard and the economics of nitrification versus advanced carbonaceous BOD removal suggests that providing nitrification facilities for the expanded treatment plant is a cost-effective step towards achieving water quality standards. Assuming that nitrifictation removes 90% of the ammonia (i.e., nitrogenous BOD) the un-ionized ammonia standard would be met and the nitrogenous BOD deficit would be reduced to 0.2 mg/l, yielding a total deficit of 3.1 mg/l (DO of 4.9 mg/l) at milepoint 4.

Although calculations show that nitrification and standard secondary treatment for the design plant flow of 11.5 MGD will not meet dissolved oxygen standards, the waste load allocation analysis should not be carried any further with currently available information. Before the model is used to calculate the additional carbonaceous BOD removal beyond secondary treatment that may be required, some additional steps should be taken. First, the model should be calibrated and validated against one or two more data sets to check the model coefficients under different flow regimes, especially lower flows than the first survey, if possible. A sensitivity analysis should be performed to relate the cost of required wastewater treatment to changes in population estimates. For example, if the population in the year 2000 is 75,000 people (projected minimum), will additional carbonaceous BOD treatment be required? A sensitivity analysis of the effect of different reserve policies on required treatment should also be performed. For example, what is the increase in wastewater treatment costs if the dissolved oxygen

reserved for future development is set at 0.5 mg/l versus 0.25 mg/l? It is clear from these questions that a final waste load allocation should be the result of more than a model projection. Such a decision takes many factors into consideration, one of which is the impact of a design wastewater load on water quality.

TABLE 2-2. CALIBRATION ANALYSIS

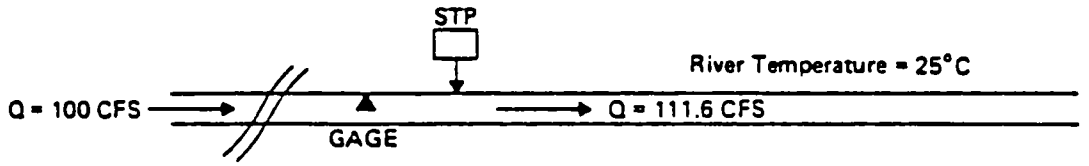

UPSTREAM CONDITIONS

- BOD_5 = 1.0 mg/ℓ
- NH_3(N) = 0.2 mg/ℓ
- DO = 8.2 mg/ℓ (SAT.)

PLANT EFFLUENT

- Q = 7.5 MGD (11.6 CFS)
- BOD_5 = 40 mg/ℓ (2502 lb/day)
- NH_3(N) = 15 mg/ℓ (938 lb/day)
- DO = 8.2 mg/ℓ (SAT.)

A. DETERMINATION OF RIVER DEPTH AND VELOCITY
(from equations in Figure 2-13)

$$\text{Depth} = 0.312\ Q^{0.5} = 0.312\ (111.6)^{0.5} = 3.3 \text{ ft.}$$
$$\text{Velocity} = 0.0513\ Q^{0.4} = 0.0513\ (111.6)^{0.4} = 0.34 \text{ ft./sec. (5.6 mi./day)}$$

B. DETERMINATION OF REACTION RATES

1. Reaeration (from Figure 2-6 or $K_a = 13\ U^{1/2}/H^{3/2}$)

$$K_a = 13\ (0.34)^{1/2}/(3.3)^{3/2} = 1.26/\text{day at } 20^\circ C$$
$$K_a \text{ at } 25^\circ C = 1.26 \times 1.024^5 = 1.42/\text{day}$$

2. BOD Removal and Oxidation Rates (from fit of river BOD data)*

$$K_r = K_d = 0.30/\text{day at } 20^\circ C$$
$$K_r \text{ and } K_d \text{ at } 25^\circ C = 0.30 \times 1.047^5 = 0.38/\text{day}$$

3. Nitrification Rate (from fit of river ammonia and nitrate data)*

$$K_n = 0.15/\text{day at } 20^\circ C$$
$$K_n \text{ at } 25^\circ C = 0.15 \times 1.08^5 = 0.22/\text{day}$$

* Note: Since data were collected at river temperature of 25°C, K_d and K_n determined from data fit would be 0.38 and 0.22 respectively. It is assumed here that analyst has converted to rates at 20°C for convenience (a) in comparing with published data, and (b) in subsequent calculations which may be at temperatures other than 20°C and 25°C.

C. INITAL CONDITIONS (at x = 0)

Concentration$_0$ = [Upstream load + Plant load (lb/day)]/Flow(CFS) x 5.4

BOD_5 (x = 0) = $(L_5)_0$ = $[1.0 \times 100 \times 5.4 + 2502]/(111.6 \times 5.4) = 5.05$ mg/ℓ

Ultimate CBOD (Lo) = 2 x BOD_5 = 2 x 5.05 = 10.1 mg/ℓ

NH_3-N (x = 0) = $[0.2 \times 100 \times 5.4 + 938]/(111.6 \times 5.4) = 1.74$ mg/ℓ

NBOD (x = 0) = 4.5 x NH_3-N = 4.5 x 1.74 = 7.8 mg/ℓ

TABLE 2-3. PROJECTION ANALYSIS (design load)

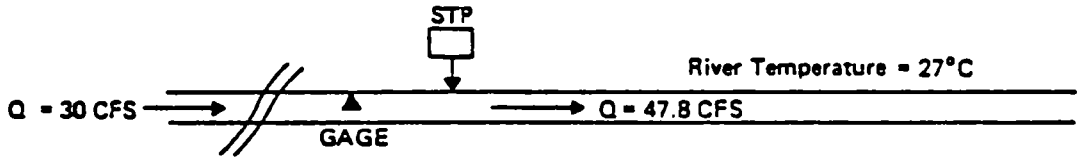

UPSTREAM CONDITIONS

BOD_5 = 1.0 mg/ℓ
NH_3(N) = 0.2 mg/ℓ
DO = 8.0 mg/ℓ (SAT.)

PLANT EFFLUENT

Q = 11.5 MGD (17.8 CFS)
BOD_5 = 30 mg/ℓ (2877 lb/day)
NH_3(N) = 15 mg/ℓ (1439 lb/day)
DO = 8.0 mg/ℓ (SAT.)

A. DETERMINATION OF RIVER DEPTH AND VELOCITY
(from equations in Figure 2-13)

Depth = $0.312\ Q^{0.5} = 0.312\ (47.8)^{0.5}$ = 2.2 ft.
Velocity = $0.0513\ Q^{0.4} = 0.0513\ (47.8)^{0.4}$ = 0.24 ft./sec. (3.9 mi./day)

B. DETERMINATION OF REACTION RATES

1. Reaeration (from Figure 2-6 or $K_a = 13\ U^{1/2}/H^{3/2}$)

$K_a = 13\ (0.24)^{1/2}/(2.2)^{3/2}$ = 1.95/day at 20°C
K_a at 27°C = 1.95×1.024^7 = 2.30/day

2. BOD Removal and Oxidation Rates (from Calibration Analysis)

$K_r = K_d$ = 0.30/day at 20°C
K_r and K_d at 27°C = 0.30×1.047^7 = 0.41/day

3. Nitrification Rate (from Calibration Analysis)

K_n = 0.15/day at 20°C
K_n at 27°C = 0.15×1.08^7 = 0.26/day

C. INITAL CONDITIONS (at x = 0)

Concentration$_0$ = [Upstream Load + Plant Load (lb/day)]/Flow (CFS) x 5.4
BOD_5 (x = 0) = $[1.0 \times 30 \times 5.4 + 2877]/(47.8 \times 5.4) = 11.8$ mg/ℓ
Ultimate CBOD (Lo) = 2 x BOD_5 = 2 x 11.8 = 23.6 mg/ℓ
NH_3-N (x = 0) = $[0.2 \times 30 \times 5.4 + 1439]/(47.8 \times 5.4) = 5.70$ mg/ℓ
NBOD (x = 0) = 4.5 x NH_3-N = 4.5 x 5.70 = 25.7 mg/ℓ

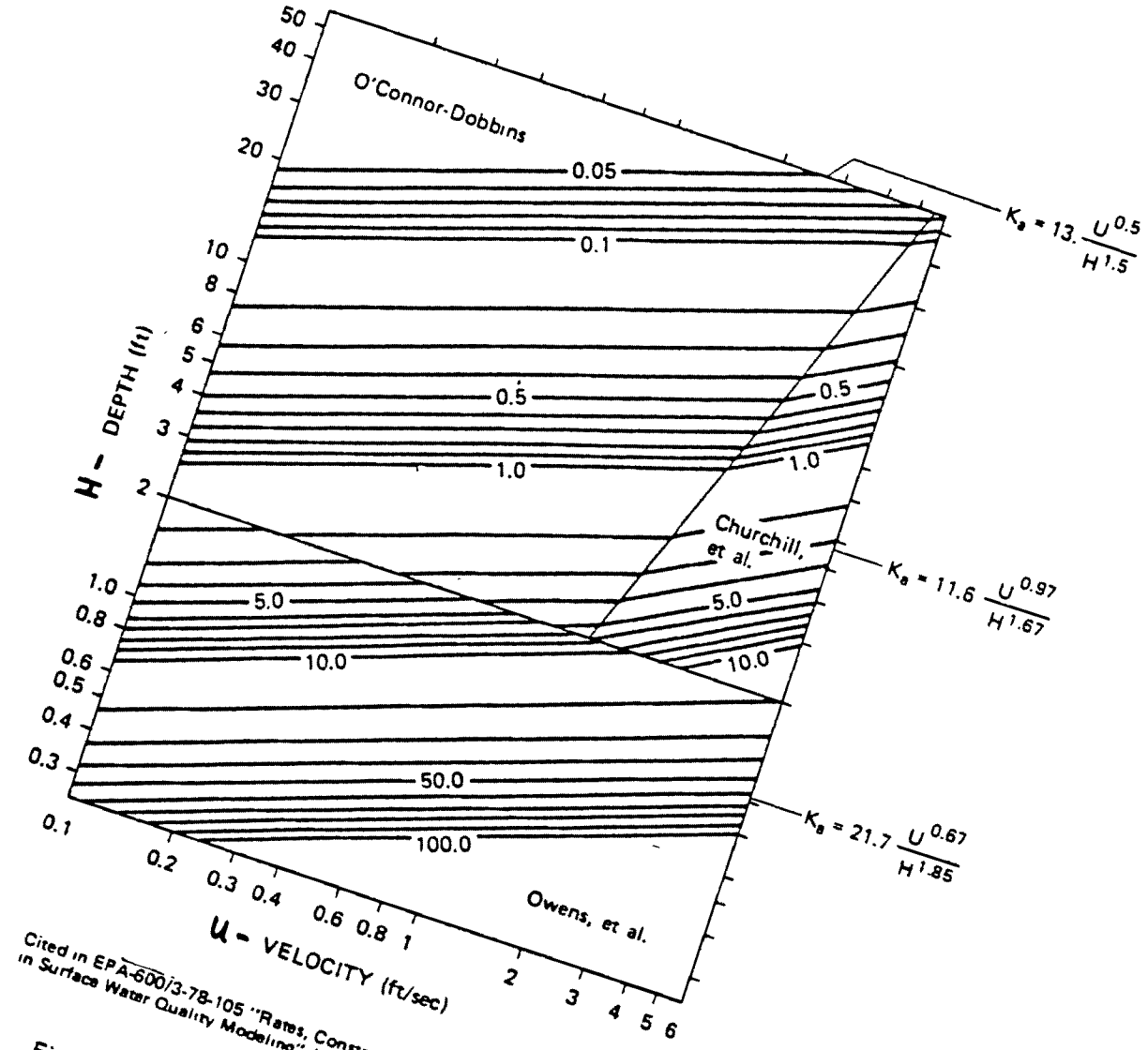

Cited in EPA-600/3-78-105 "Rates, Constants, and Kinetic Formulations in Surface Water Quality Modeling" (2) in modified form.

Figure 2-6. Reaeration rate coefficient (K_a) related to depth and velocity.

A. STUDY AREA

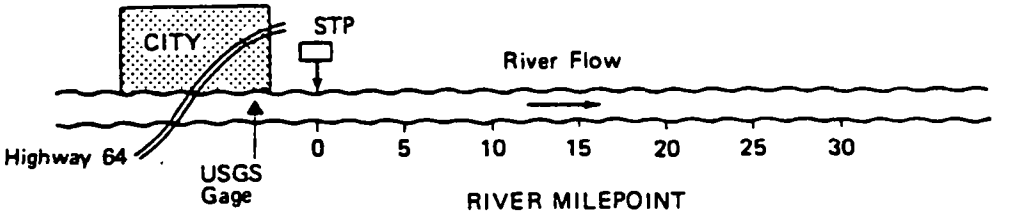

B. POPULATION PROJECTIONS

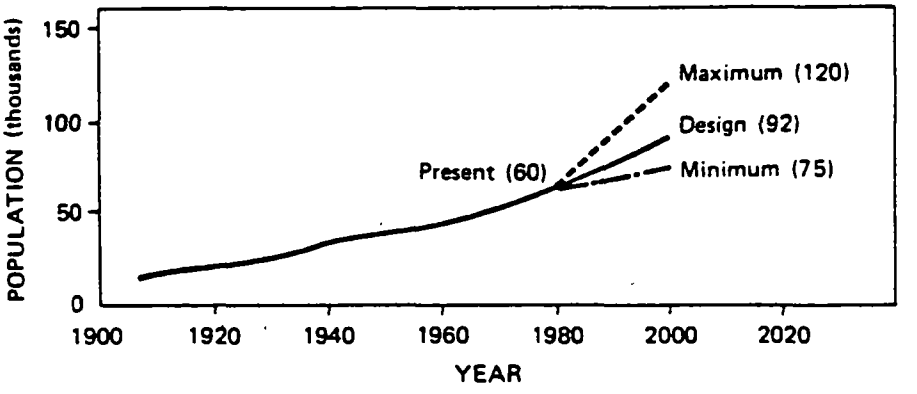

C. RIVER CLASSIFICATION AND USE

1. State Classification–B1
2. Designated Use–Fish and Wildlife Propogation
3. Water Quality Standards (partial)
   a. DO Concentration–Greater than 5.0 mg/ℓ
   b. Un-ionized Ammonia–Less than 0.02 mg/ℓ
4. Activities and Use
   a. Active and Locally Popular Fishery
   b. Several Campgrounds and State Park Have River as an Attraction
5. Problems
   No Documented Problems; Limited Water Quality Data Do Not Show Violations

Figure 2-11. Problem setting.

A. TREATMENT FACILITIES

Present: Trickling Filter Plant Constructed in 1958
Plant Now at Design Capacity of 7.5 MGD
Effluent Does Not Meet NPDES Permit for Secondary Treatment

Proposed: Activated Sludge System to Provide Efficient Secondary Treatment

B. EFFLUENT CHARACTERISTICS

		Present	Design①
Flow	MGD	7.5	11.5
BOD_5	mg/ℓ lb/day	40 2502	30 2877
$CBOD_u$②	mg/ℓ lb/day	80 5004	60 5754
NH_3-N	mg/ℓ lb/day	15 938	15 1439
NBOD③	mg/ℓ lb/day	68 4221	68 6475

① Preliminary Basis–Standard Secondary Treatment

② Long-term BOD Tests Indicate Ratio of $CBOD_u/BOD_5 = 2.0$

③ NBOD = Stoichiometric Oxygen Requirements for Oxidation of Reduced Nitrogen Forms = 4.57 x NH_3-N (effluent oxidizable organic nitrogen is negligible)

Figure 2-12. Treatment facilities and effluent characteristics.

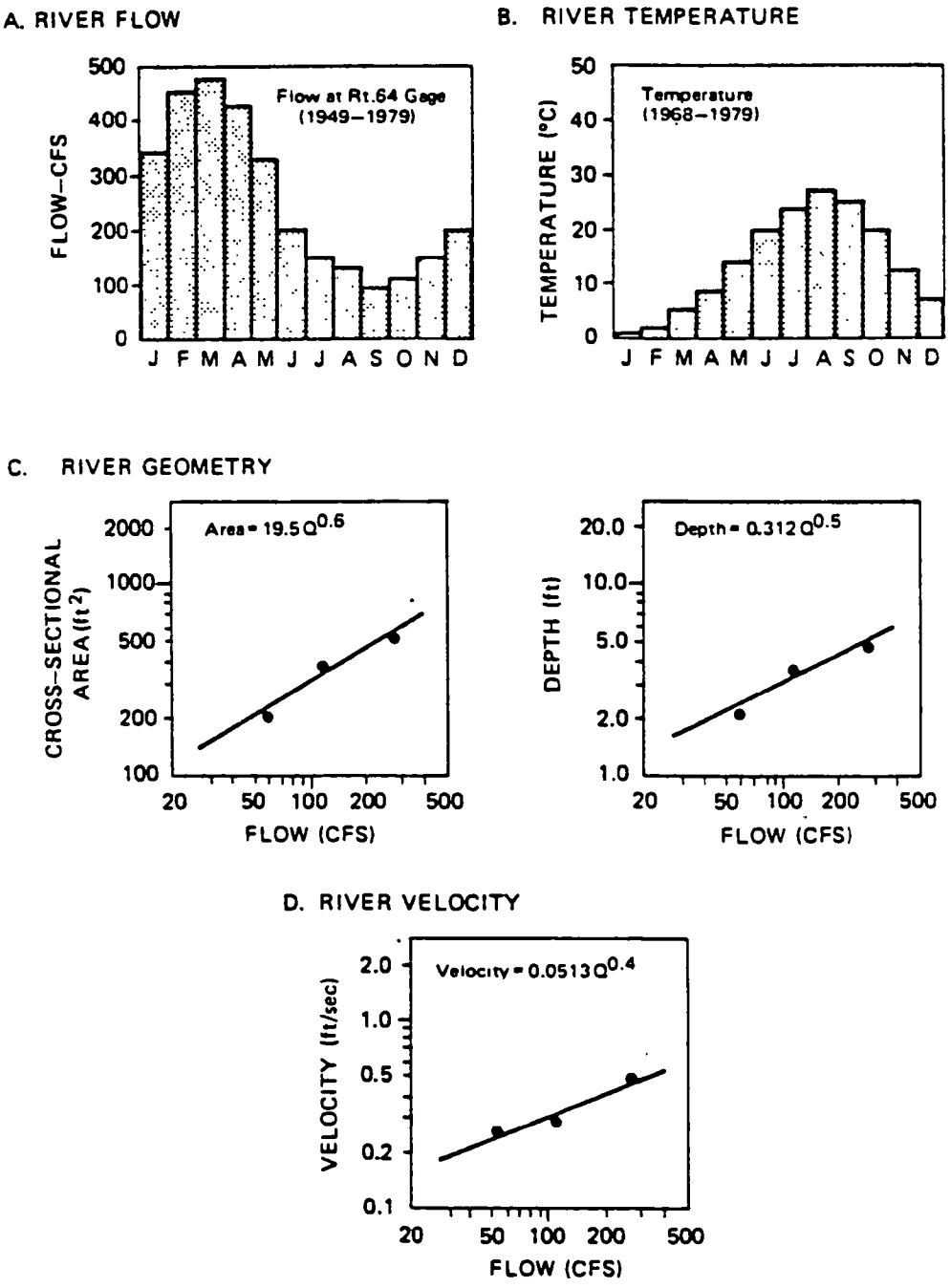

Figure 2-13. River flow, temperature, geometry, and velocity.

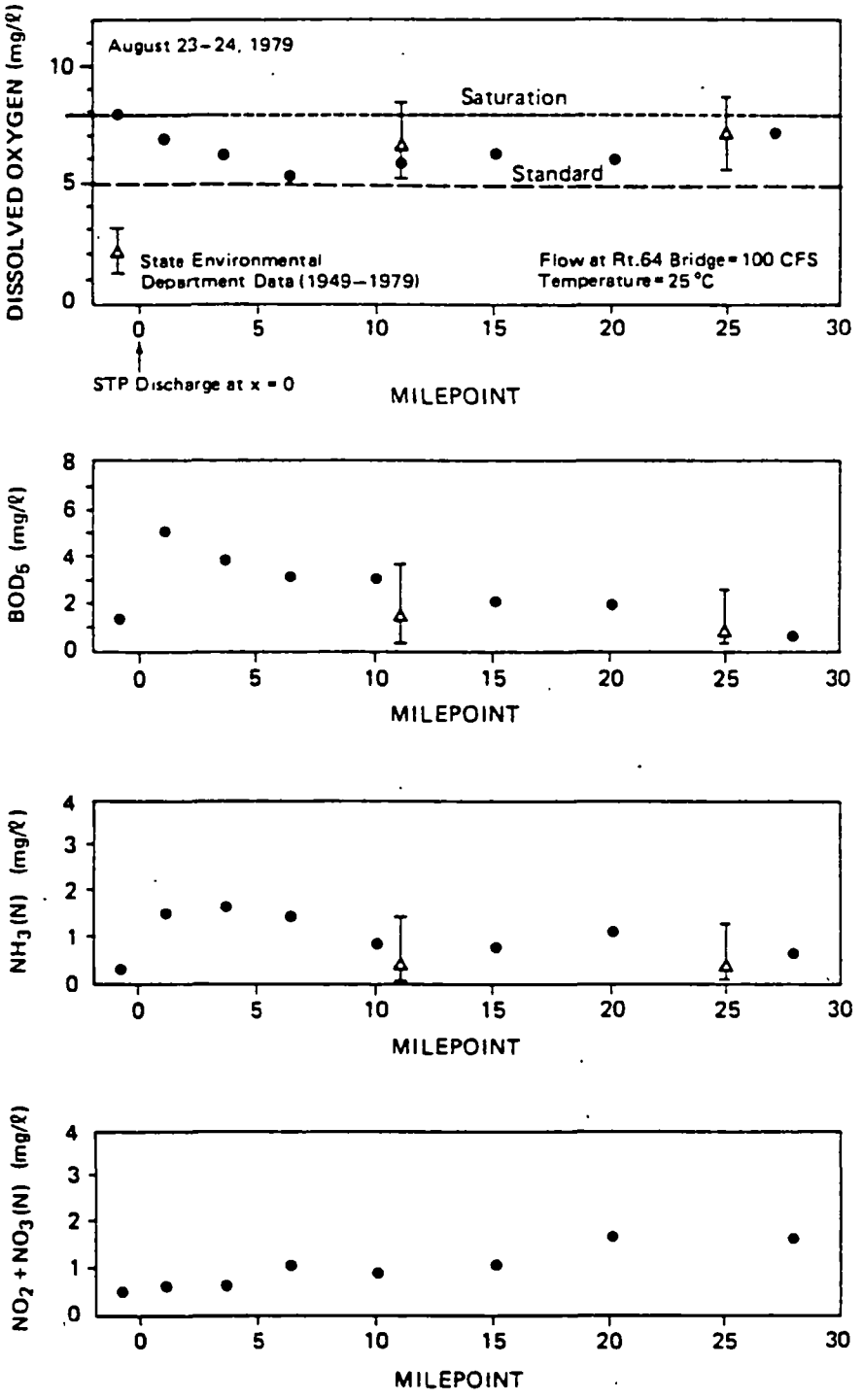

Figure 2-14. Dissolved oxygen, BOD, and nitrogen data (August 23-24, 1979).

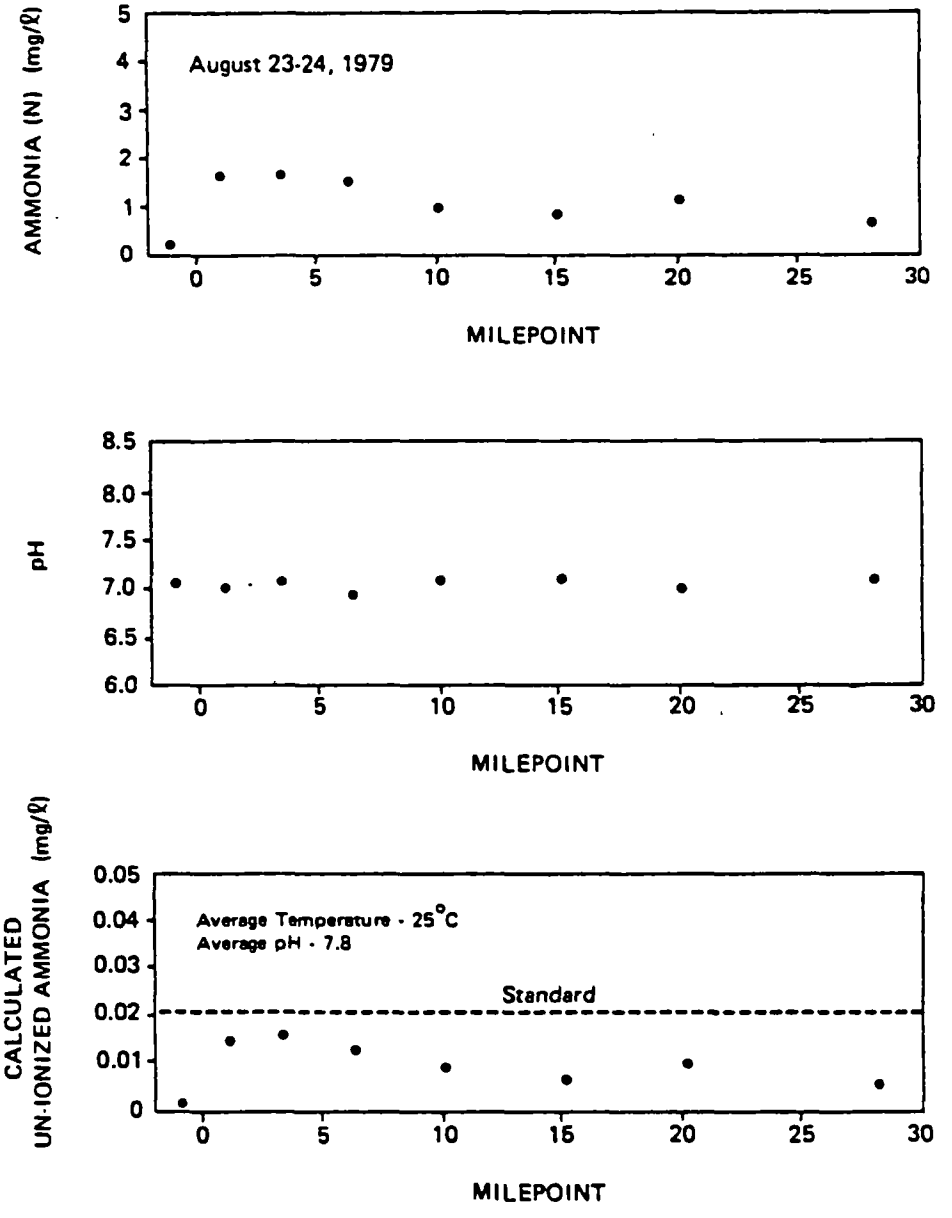

Figure 2-15. Ammonia, pH, and un-ionized ammonia data.

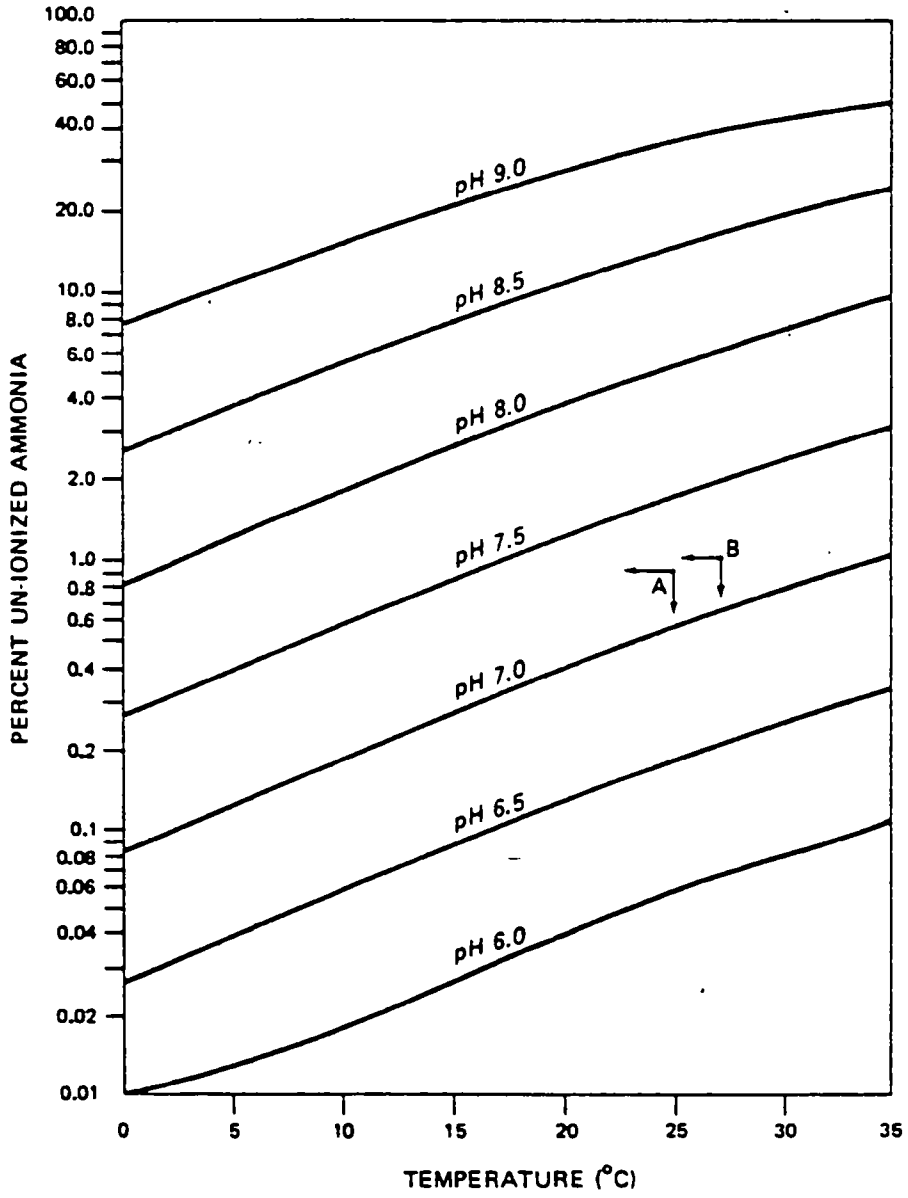

Note: Redrawn from
William T. Willingham
Ammonia Toxicity
USEPA 908/3-76-001
Feb. 1976 (4)

Figure 2-16. Percentage of unionized ammonia in ammonia-water solution at various pH and temperature values.

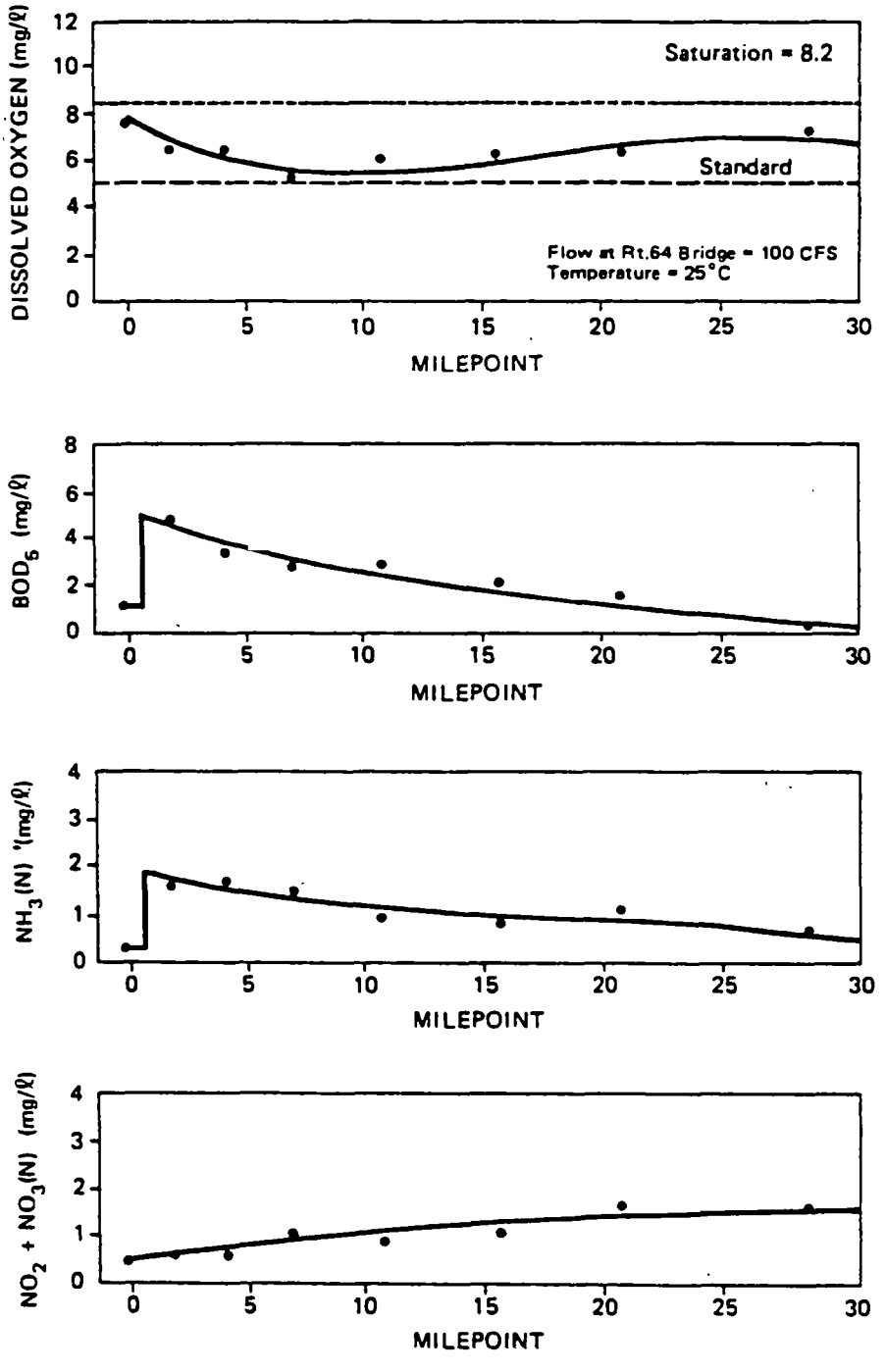

Figure 2-17. Model calibration analysis.

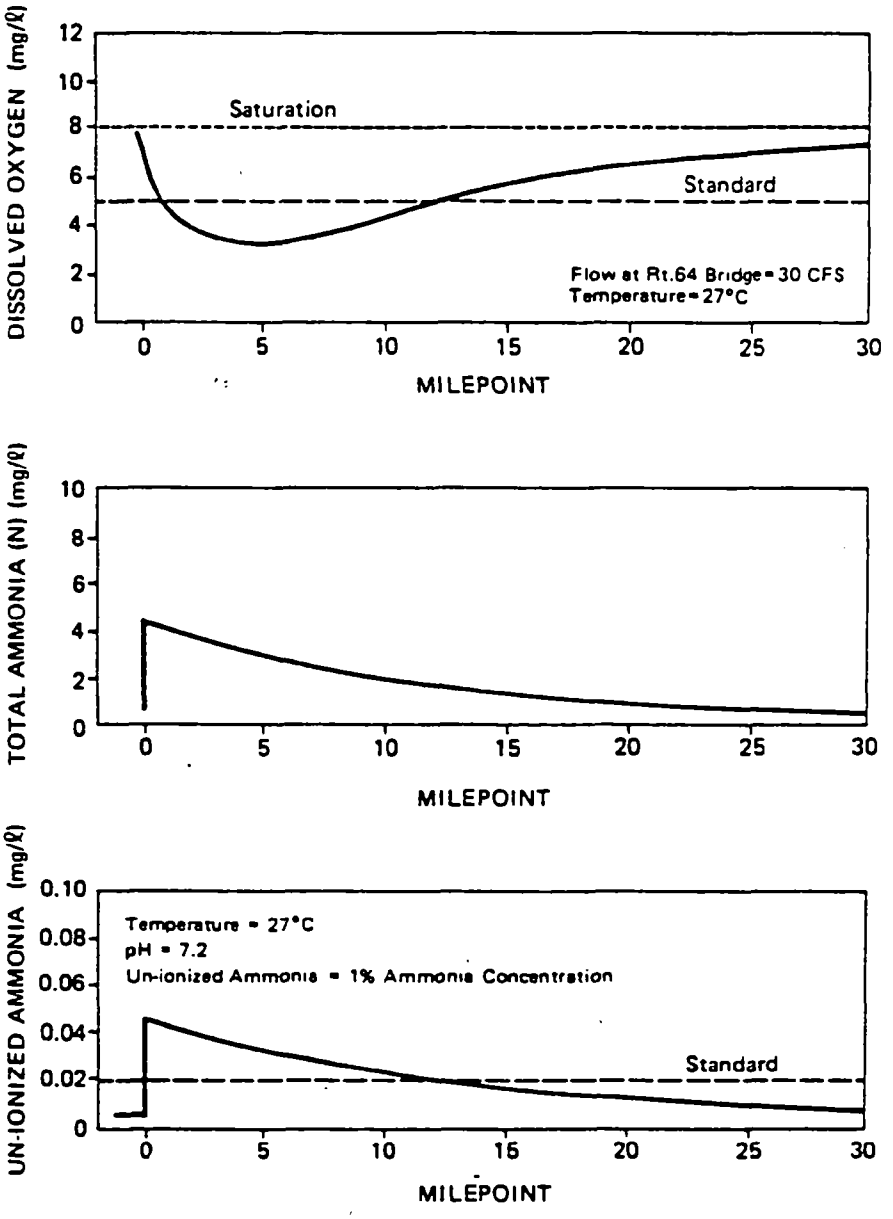

Figure 2-18. Projected dissolved oxygen, ammonia, and un-ionized ammonia (present wastewater load).

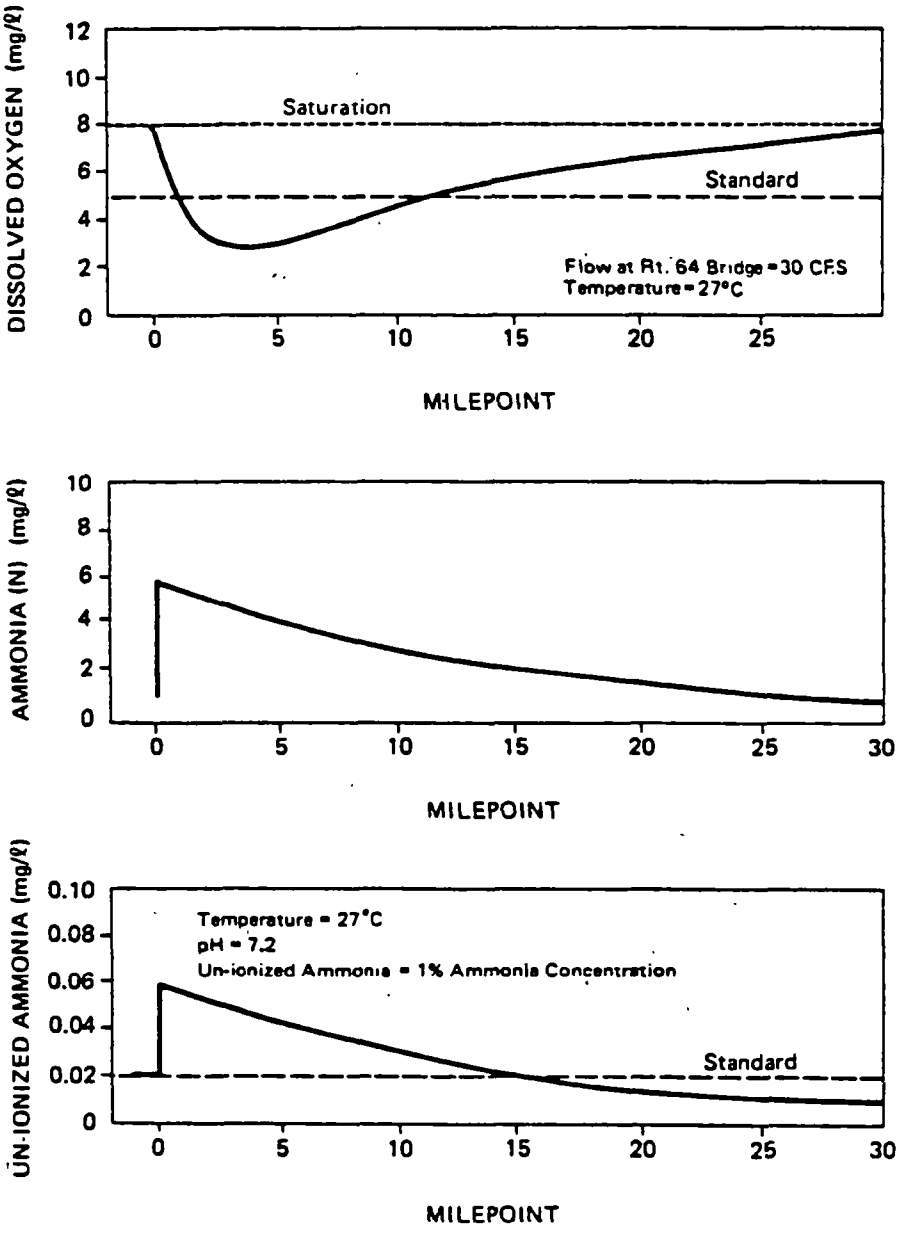

Figure 2-19. Projected dissolved oxygen, ammonia, and un-ionized ammonia (design wastewater load).

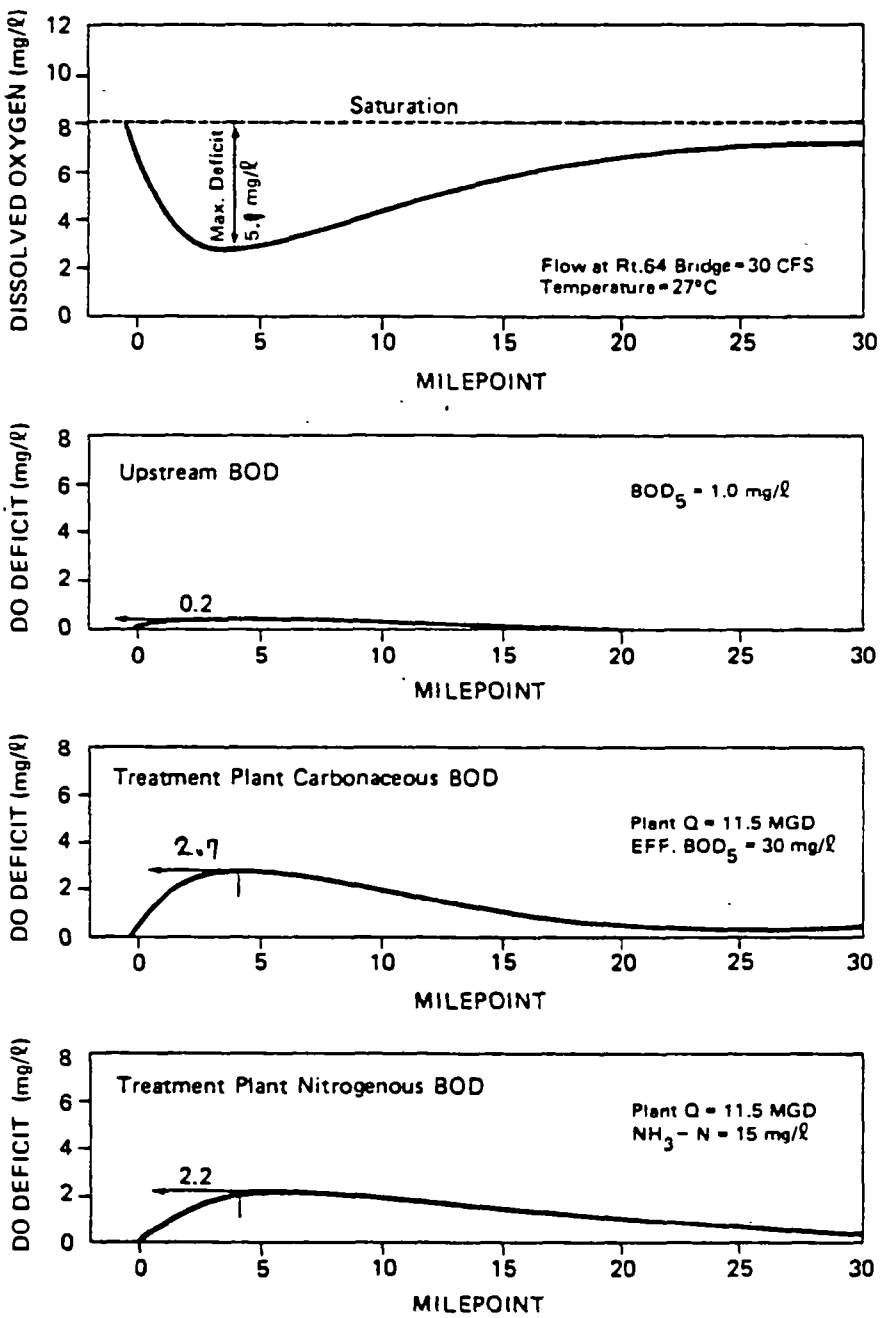

Figure 2-20. Dissolved oxygen component unit responses.

ADDENDUM

Variations in River Velocity, Depth, Area with Flow

Projections of water quality impacts for some future critical low-flow condition are normally required in waste load allocation studies. The predominant impact of reduced stream flow is usually to reduce dilution provided for the waste load. Thus initial concentrations of BOD (L_o) become significantly higher. However, reduced stream flows also result in changes in stream velocity and depth--factors which both strongly affect the reaeration rate coefficient. Therefore, the effect of stream flow changes on depth and velocity must be determined.

In some cases stream cross-sectional measurements and time of passage (travel time) information will be available from studies performed by USGS or state environmental agencies. In addition, data may be available from the Corps of Engineers in locations where projects have been designed. Time of passage data can be used to compute averages of velocity (U) and depth (H). Each set of data will be related to a specific stream flow regime, and different values can be expected for other flow regimes. In seeking information on depth/velocity relationships in a stream reach, it is important to distinguish between time of travel study data and information which might be derived from USGS flow gaging stations. Gaging stations are usually located

at places where the geometry favors the accurate determination of flow rate, and as a result, depth and velocity at such locations are not typical of general stream conditions.

Leopold and Maddox have suggested the following empirical relationship between the pertinent physical stream factors and stream flow.

$$U = aQ^n \quad (2\text{-}3)$$

$$H = bQ^m \quad (2\text{-}4)$$

$$W = cQ^f \quad (2\text{-}5)$$

where:

a, b, c are constants for the stream in question

m, n, f are exponents defining the basic relationships

Recognizing that stream flow is the product of cross-sectional area and velocity ($Q = A \times U$), and that cross-sectional area is the product of width and depth ($A = W \times H$), it can be shown that the sum of the exponents ($m + n + f$) is 1. Using this and experience from a variety of streams, the value of the exponents can be approximated as follows:

n = range (0.4 - 0.6); typical 0.5

m = range (0.3 - 0.5); typical 0.4

f = range (0 - 0.2); typical 0.1

Where the analyst has more than one set of data, a log-log plot of area (A), depth (H) and velocity (U) against stream flow (Q) will permit extrapolation to other flows of interest. The slope of such plots provides the local value of the exponents. When data at only a single flow regime is available,

estimates for other flows of interest can be developed by the following ratios, derived from the foregoing relationships:

velocity	: U_2/U_1	=	$(Q_2/Q_1)^{0.5}$	(2-6)
depth	: H_2/H_1	=	$(Q_2/Q_1)^{0.4}$	(2-7)
cross-sect. area	: A_2/A_1	=	$(Q_2/Q_1)^{0.5}$	(2-8)
travel time	: T_2/T_1	=	$(Q_2/Q_1)^{-0.5}$	(2-9)

It should be recognized that these relationships exist only in free-flowing streams, and that the exponents may vary by 50% for any river. Impounded reaches in rivers have exponents m and f=0, and n=1. Thus, acquiring data to develop site-specific relationships of this type is normally appropriate.

Because of the nature of the relationships, reduced stream flows tend to result in increased reaeration rates, principally due to the beneficial effect of shallower depths. For example, a 50% reduction in stream flow may increase K_a by about 30%. However, the net effect on stream DO impacts is negative because the improved reaeration is outweighted by increases in initial BOD concentations (L_o), which would double for a 50% reduction in stream flow.

Wasteload Allocation Analysis - Initial Deficit, Benthal Demand, P-R*

In the preceding example, the effects of point source and upstream sources of carbonaceous and nitrogenous BOD on the dissolved oxygen resources of a stream were examined. Three other sources which may significantly affect the dissolved oxygen in a stream include an initial deficit, benthal demand and algae - as expressed in photosynthesis and respiration (P-R). These three sources will be added to the CBOD and NBOD loads in the preceding example and their impacts examined under the design low flow condition.

Carbonaceous and Nitrogenous STP Loads

Under the STP design conditions, 11.5 MGD (17.8 cfs) will discharge 5754 lb/day of ultimate CBOD and 6475 lb/day of NBOD at mile zero. Dissolved oxygen deficits are calculated in accordance with equations 1 and 2 of Table 3 for the CBOD and NBOD. With the stream velocity of 3.9 m/day, the carbonaceous and nitrogenous decay rates of 0.41 and 0.26 per day and reaeration coefficient of 2.30 per day - all at the design stream temperature of 27°C, maximum dissolved oxygen deficits due to these sources amount to 2.73 mg/ℓ at milepoint 3.5 and 2.15 mg/ℓ at milepoint 4 for the CBOD and NBOD respectively (Table 1). Note that the maximum deficit due to the NBOD occurs downstream of that due to CBOD due to the slower reaction rate of the NBOD.

Upstream Boundary

Values of the five-day BOD of 1.0 mg/ℓ and ammonia nitrogen of 0.2 mg/ℓ, measured during the 100 cfs survey (see preceding example), are assumed to be the same for the 7 Q 10 flow of 30 cfs. It may be noted that this assumption is reasonably valid as long as the masses of these constituents which enter upstream of the STP are flow-dependent. If the primary source of these constituents is another upstream point source, the assumption would not be appropriate.

The in-stream decay rates of the upstream CBOD and NBOD are assumed to be the same as those of the STP. In some cases, the upstream constituents may be more refractory than the STP loads and lower reaction rates for the upstream sources should be assigned.

Dissolved oxygen deficits due to these sources are calculated as fractions of the corresponding STP deficits (equations 3 and 4, Table 3), since

* John A. Mueller

the reaction rates are the same. The combined maximum deficit due to both sources amounts to 0.20 mg/ℓ as seen in Table 1.

Initial Deficit

As in the previous example, the upstream waters are assumed saturated, containing 8.0 mg/ℓ of dissolved oxygen. The STP effluent is assumed to contain 2 mg/ℓ of dissolved oxygen. A mass balance of the upstream and STP dissolved oxygen results in a calculated D.O. immediately downstream of the STP of 5.77 mg/ℓ (Table 3). Since the saturation concentration of D.O. in the stream at 27°C is 8.0 mg/ℓ, an initial deficit of 2.23 mg/ℓ is introduced at x = 0. This initial deficit reaerates away according to equation 5, Table 3, becoming zero ten miles below the STP (Table 1).

Benthal Demand

Present benthal deposits are calculated to exert an oxygen demand of 2 g/m^2-day over the two mile reach downstream of the STP. Thereafter, a lower value of 0.8 g/m^2-day exists. Since the mass of BOD_5 discharged by the STP under future design conditions is approximately the same as that being discharged presently (2877 lb/day vs. 2502 lb/day, preceding example), the amount of suspended solids will be assumed to remain the same. Thus, the present level of benthal demand - primarily caused by settling of the STP solids - will be used for the STP design conditions.

The higher benthal demand over the first two miles of stream bed causes a maximum D.O. deficit of 0.90 mg/ℓ at milepoint 2 (Table 3, equation 6a). Downstream of this point the deficit is composed of a decreasing deficit due to reaeration of the initial 0.90 mg/ℓ deficit together with an increasing deficit due to the benthal demand of 0.8 g/m^2-day (Table 3, eq. 6b). As seen in Table 1, the peak deficit due to benthal deposits is 0.90 mg/ℓ at milepoint 2. At milepoint 10, the effect of the first two-mile deposit is insignificant and an equilibrium value of 0.52 mg/ℓ of deficit - due to the subsequent benthal deposits - is reached and this persists downstream.

Photosynthesis-Respiration

From light-dark bottles suspended in the stream during the 100 cfs survey, it is determined that the average daily photosynthetic oxygen production

rate (P) is 5 mg/ℓ-day and the respiration rate (R) is 3 mg/ℓ-day. Thus the net P-R of 2 mg/ℓ-day is a source of oxygen to the stream. These rates exist for many miles downstream of the STP and are caused primarily by algae resulting from nutrient discharges in the STP effluent. Since nutrient discharges will be increased under design conditions (ammonia nitrogen of 938 lb/day present vs. 1439 lb/day design) it is probable that the algal biomass will increase over present conditions and result in a higher P-R. Since P-R is a source of oxygen, the present value of 2 mg/ℓ-day will be assumed as a conservative estimate with respect to its effect on the average daily D.O. concentration.

Dissolved oxygen deficits, calculated according to equation 7, Table 3, are seen to range from zero at the STP location to an equilibrium level of -0.87 mg/ℓ at milepoint 10 (Table 1). The negative sign indicates a "sink" of deficit or a source of dissolved oxygen.

Total Deficit - Design Conditions

The total dissolved oxygen deficit due to the individual sources, i.e. STP CBOD and NBOD, upstream CBOD and NBOD, initial deficit, benthal demand and P-R, is a linear summation of the deficits caused by the individual sources. Values of the total deficit begin at 2.23 mg/ℓ at milepoint zero, increase to a maximum of 5.42 mg/ℓ at milepoint 2 and decrease thereafter to 0.31 mg/ℓ at milepoint 30 (Table 1). Note that the additional deficit due to the benthal deposits has been largely offset by the negative deficit due to net photosynthesis and respiration.

As indicated in Fig. 1, under design conditions of secondary treatment, the daily average dissolved oxygen violates the standard of 5 mg/ℓ over the first ten miles of stream. The critical deficit of 5.42 mg/ℓ occurs at milepoint 2, resulting in a minimum dissolved oxygen concentration of 2.58 mg/ℓ well below the water quality standard of 5 mg/ℓ.

Alternatives

As discussed in the previous example, secondary treatment with nitrification would probably be the most cost efficient method of reducing the dissolved oxygen deficit in the stream. Thus, secondary with nitrification is analyzed as the first alternative. Assuming a 90% reduction in the effluent

NBOD, and no incremental reduction in CBOD below 30 mg/ℓ, the total deficit under alternative one equals the total deficit under design conditions minus 90% of the deficit due to the STP NBOD. Referring to Table 1, the total deficit at milepoint 2 under alternative 1 would be 5.42 - 0.90 x 1.82 = 3.78 mg/ℓ. A summary of the deficits for all locations is contained in Table 2. As shown in Fig. 1, the dissolved oxygen concentrations have now improved considerably - when compared to the design case - but violation of the standard by a maximum of 0.8 mg/ℓ still occur from milepoint 0.5 to milepoint 4.5.

Examining the deficits by source in Table 1, the major remaining contributors are the STP CBOD and the initial deficit due to the low dissolved oxygen in the STP effluent. Assuming that further reduction in the CBOD (to an effluent BOD_5 concentration of approximately 20 mg/ℓ) is less economical than post aeration, alternative two consists of the addition of post aeration to alternative one. Thus, resulting dissolved oxygen deficits are calculated by subtracting the deficits due to the initial deficit (Table 1) from those of alternative 1 (Table 2). Within a tenth of a milligram per liter, the mean daily dissolved oxygen concentration now meets the required standard.

Minimum Daily Dissolved Oxygen

The presence of algae in the stream causes variations in the dissolved oxygen throughout the day. Minimum D.O. concentrations occur in the early morning and maximum values in the early afternoon. As indicated in the first series of seminars, the difference between the maximum and minimum daily dissolved oxygen concentrations, Δ, is approximately related to the average daily photosynthetic oxygen production rate, P, as follows:

$$\Delta = \frac{P}{2}$$

where Δ = D.O. max - D.O. min, mg/ℓ

P = Av. daily photosynthetic O_2 rate, mg/ℓ-day.

This approximation applies for streams having reaeration coefficients K_a < 2/day, for photoperiods of one-half day and for regions of the stream a sufficiently far distance downstream of the beginning of the algal presence

($\ell > 4\ U/K_a$). In the region of the maximum deficit for alternative 2, these conditions are reasonably fulfilled and one might expect

$$\Delta = \frac{5(mg/\ell\text{-day})}{2} = 2.5\ mg/\ell$$

Assuming the maximum and minimum daily D.O. concentrations are one-half Δ above and below the average daily D.O. - a reasonable approximation for reaeration coefficients less than approximately 2/day, the minimum daily dissolved oxygen would be 1.25 mg/ℓ below the daily average profile, as shown in Figure 1.

If the dissolved oxygen standard of 5 mg/ℓ is a "never-less-than" standard, requiring conformance at all times of the day, alternative two would not meet the standard. Additional reductions in the deficits due to the STP CBOD or benthal demands would be one way of achieving conformance. Another alternative would be to reduce nutrients, and thus reduce the algal population with its attendant diurnal dissolved oxygen swings.

TABLE 1. DISSOLVED OXYGEN DEFICITS BY SOURCE FOR STP DESIGN CONDITIONS

x (mi)	STP CBOD	STP NBOD	UPSTREAM CBOD	UPSTREAM NBOD	INIT. DEF.	BENTHAL	P-R	TOTAL
0	0.00	0.00	0.00	0.00	2.23	0.00	0.00	2.23
1	1.67	1.22	0.09	0.03	1.24	0.58	-0.39	4.44
2	2.43	1.82	0.14	0.04	0.69	0.90	-0.60	5.42
3	2.70	2.07	0.15	0.05	0.38	0.73	-0.72	5.36
3.5	2.73	2.13	0.15	0.05	0.28	0.67	-0.76	5.25
4	2.72	2.15	0.15	0.05	0.21	0.64	-0.79	5.13
5	2.61	2.12	0.15	0.05	0.12	0.58	-0.82	4.81
6	2.43	2.05	0.14	0.05	0.06	0.56	-0.84	4.45
8	2.04	1.85	0.11	0.04	0.02	0.53	-0.86	3.73
10	1.68	1.63	0.09	0.04	0.00	0.52	-0.87	3.09
15	1.00	1.18	0.06	0.03	0.00	0.52	-0.87	1.92
20	0.59	0.84	0.03	0.02	0.00	0.52	-0.87	1.13
25	0.35	0.60	0.02	0.01	0.00	0.52	-0.87	0.63
30	0.21	0.43	0.01	0.01	0.00	0.52	-0.87	0.31
Equation Used*	1	2	3	4	5	6a 6b	7	

*See Table 3

TABLE 2. DISSOLVED OXYGEN DEFICITS FOR ALTERNATIVES

x (mi)	TOTAL D.O. DEFICIT (mg/ℓ) Design	Altern. 1	Altern. 2
0	2.23	2.23	0.00
1	4.44	3.34	2.10
2	5.42	3.78	3.09
3	5.36	3.50	3.12
3.5	5.25	3.33	3.05
4	5.13	3.20	2.99
5	4.81	2.90	2.78
6	4.45	2.61	2.55
8	3.73	2.07	2.05
10	3.09	1.62	1.62
15	1.92	0.86	0.86
20	1.13	0.37	0.37
25	0.63	0.09	0.09
30	0.31	-0.08	-0.08

NOTES: Design = 11.5 MGD, 30 mg/ℓ BOD_5, 15 mg/ℓ NH_3-N

Altern 1 = Add Nitrification (BOD_5 = 30 mg/ℓ, NH_3-N = 1.5 mg/ℓ)

Altern 2 = Altern 1 + Post Aerate to D.O. = 8.0 mg/ℓ

TABLE 3. DISSOLVED OXYGEN DEFICIT EQUATIONS

STP

CBODU: $$D_1 = \frac{0.41 \times L_o}{2.30 - 0.41}(e^{-0.1051x} - e^{-0.5897x}) \quad (1)$$

$L_o = 5754/(47.8 \times 5.4) = 22.3$ mg/ℓ

$K_r/U = 0.41/3.9 = 0.1051/mi$

$K_a/U = 2.30/3.9 = 0.5897/mi$

NBOD: $$D_2 = \frac{0.26 \times N_o}{2.30 - 0.26}(e^{-0.0666x} - e^{-0.5897x}) \quad (2)$$

$N_o = 6475/(47.8 \times 5.4) = 25.1$ mg/ℓ

$K_n/U = 0.26/3.9 = 0.0666/mi$

UPSTREAM

CBODU: $$D_3 = 0.0563\ D_1 \quad (3)$$

$D_3 = D_1 \times L_o(UPSTR)/L_o(STP)$

$L_o(UPSTR) = 2.0 \times 1.0 \times 30/47.8 = 1.255$ mg/ℓ

$L_o(STP) = 22.3$ mg/ℓ

NBOD: $$D_4 = 0.0225\ D_2 \quad (4)$$

$D_4 = D_2 \times N_o(UPSTR)/N_o(STP)$

$N_o(UPSTR) = 4.5 \times 0.20 \times 30/47.8 = 0.565$ mg/ℓ

$N_o(STP) = 25.1$ mg/ℓ

NOTE: Reaction rates in the stream for upstream sources and STP assumed the same in this analysis.

INITIAL DEFICIT

D.O.(STP) = 2 mg/ℓ

D.O.(UPSTR) = 8.0 mg/ℓ (saturated = C_s)

$$D.O.\Big|_{x=o} = \frac{30 \text{ cfs} \times 8.0 \text{ mg/ℓ} + 17.8 \text{ cfs} \times 2 \text{ mg/ℓ}}{47.8 \text{ cfs}} = 5.77 \text{ mg/ℓ}$$

$$\therefore D_o = C_s - D.O.\Big|_{x=o} = 8.0 - 5.77 = 2.23 \text{ mg/ℓ}$$

$$D_5 = D_o e^{-K_a x/u}$$

$$D_5 = 2.23\ e^{-0.5897x} \quad (5)$$

TABLE 3. DISSOLVED OXYGEN DEFICIT EUATIONS (cont'd)

BENTHAL DEMAND

$0 \leq x \leq 2$ mi

$$D_6 = \frac{B}{K_a H}(1 - e^{-K_a x/u})$$

$B = 2$ g/m^2-day

H = depth in meters - 2.2/3.281 = 0.671m

$$D_6 = 1.30(1 - e^{-0.5897x}) \qquad (6a)$$

$$D_6\big|_{x=2} = 0.90 \text{ mg/}\ell$$

$x \geq 2$ mi $\quad B = 0.8$ g/m^2-day

$$D_6 = 0.90\, e^{-0.5897(x-2)} + 0.519(1 - e^{-0.5897(x-2)}) \qquad (6b)$$

P - R

$$D_7 = -\frac{P-R}{K_a}(1 - e^{-K_a x/u})$$

$P = 5$ mg/ℓ-day, $R = 3$ mg/ℓ-day

$$D_7 = -0.870(1 - e^{-0.5897x}) \qquad (7)$$

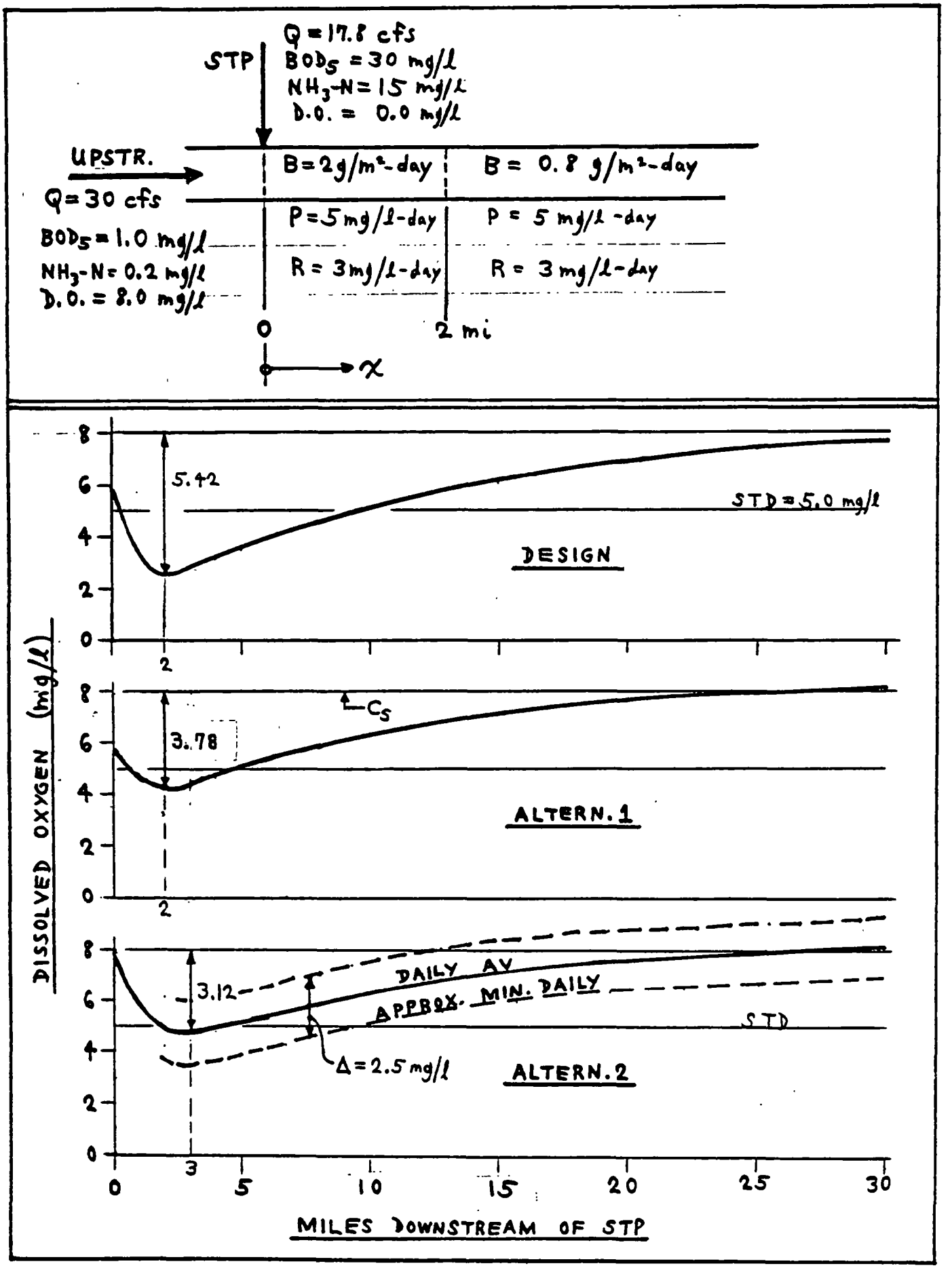

FIG. 1 DISSOLVED OXYGEN PROFILES - DESIGN + ALTERNATIVES

A Methodology for Estimating Future Benthal Demands in Streams*

Deposits of organic material on the bed of a stream may be caused by background sources and point sources. For the typical case of a single STP on a stream, a natural level of benthal demand would exist upstream of the plant, a higher value immediately downstream and an intermediate value above the natural level further downstream. Since the mass rate of total suspended solids discharged by the treatment plant into the stream is directly related to the magnitude of the benthal demand above the natural background level, an estimate of projected benthal demands can be made. Thus, the benthal demand downstream of the point source is the sum of the naturally occurring value , B(BACK), plus the increment due to the STP, B(STP). This latter increment is calculated as:

$$B(STP)\Big|_{present} = B(MEAS) - B(BACK)$$

where B(MEAS) are from field measurements.

For future conditions, the benthal demand due to the STP may be estimated from:

$$B(STP)\Big|_{future} = B(STP)\Big|_{present} \times \frac{\text{Mass TSS future}}{\text{Mass TSS present}}$$

Note that the time required to establish the new equilibrium value of the benthal demand is in the order of one to several years - a function of the annual hydrology of the stream and its flushing (scouring) characteristics. It is assumed that a sufficient period would elapse after STP upgrading to allow the benthal deposits to reach the new equilibrium.

Example

The STP of the previous examples discharges 7.5 MGD at present and 11.5 MGD under future design conditions. For the original treatment train of primary and trickling filters, the effluent TSS concentration is 60 mg/ℓ. The design treatment train of primary, activated sludge and nitrification results in an effluent TSS of 20 mg/ℓ.

* John A. Mueller and Robert V. Thomann

As shown in Figure 1, benthal demands are calculated to be 0.4, 2 and 0.8 g/m^2-day, for locations upstream, in the vicinity of and downstream of the STP, based on field measurements. Assuming the upstream benthal demand is caused by background sources similar to those downstream, the naturally occurring benthal demand would be 0.4 g/m^2-day for the entire stream. The calculated benthal demand due to the STP under present conditions immediately downstream is 1.6 g/m^2-day which is reduced to 0.8 g/m^2-day in the future (Fig. 1) since TSS loads will be reduced 50%.

Estimated future benthal demands are then 0.4, 1.2 and 0.6 g/m^2-day, as seen in Fig. 1. These lower values cause the peak dissolved oxygen deficit to decrease from 0.90 to 0.54 mg/ℓ at milepoint 2.

STP | 11.5 MGD (FUTURE) ; 7.5 MGD (PRESENT)

30 cfs → | B=0.4 g/m²-day | B=2 g/m²-day | B = 0.8 g/m²-day | (PRESENT)

0 2mi

STREAM

H = 2.2' = 0.671 m
U = 3.9 mi/day
Ka = 2.30/day @ 27°C

STP EFFLUENT TSS

PRESENT 60 mg/l
FUTURE 20 mg/l

BENTHAL DEMANDS DUE TO STP

PRESENT

$0 \le x \le 2$ mi $B(STP) = 2 - 0.4 = 1.6$ g/m²-day

$x \ge 2$ $B(STP) = 0.8 - 0.4 = 0.4$ g/m²-day

where $B(BACK) = 0.4$ g/m²-day (UPSTR of STP)

FUTURE

$0 \le x \le 2$ $B(STP) = 1.6 \times \left(\frac{11.5 \times 20}{7.5 \times 60} = 0.5\right) = 0.8$ g/m²-day

$x \ge 2$ $B(STP) = 0.4 \times (0.5) = 0.2$ g/m²-day

B= 0.4 g/m²-day | B= 1.2 | B= 0.6 (FUTURE)

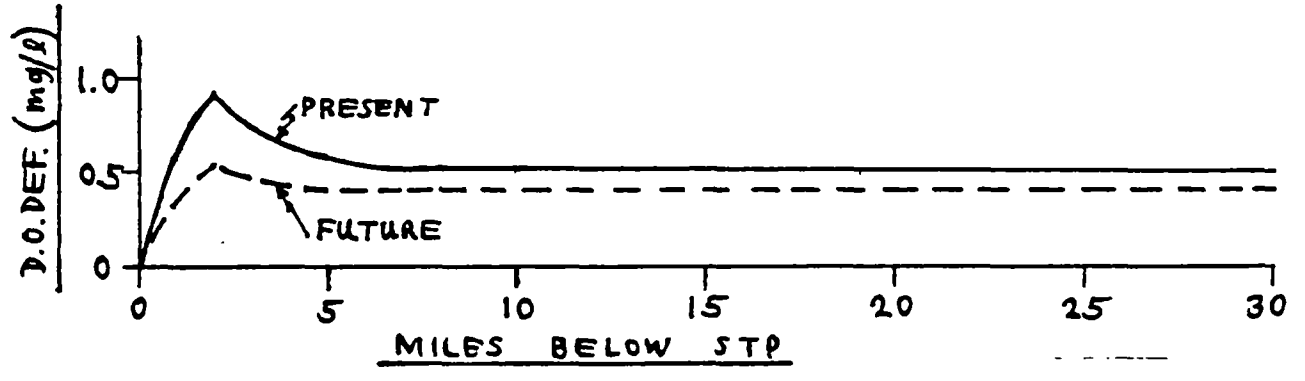

FIGURE 1 ESTIMATION OF FUTURE BENTHAL DEMANDS

CHAPTER 6

WASTE LOAD ALLOCATIONS

TREATMENT PROCESSES

WASTE LOAD ALLOCATIONS

TREATMENT PROCESSES

	Page Number
I. PRINCIPALS OF BIOLOGICAL TREATMENT	
BIOLOGICAL TREATMENT	6-1
II. SPECIFIC PROCESSES - BOD REMOVAL	
SECONDARY TREATMENT PROCESSES	6-9
A. ACTIVATED SLUDGE PROCESSES	6-9
B. PURE OXYGEN TREATMENT	6-15
C. ROTATING BIOLOGICAL CONTACTORS	6-19
D. CARROUSEL LOOP AERATION SYSTEM	6-19
E. DEEP SHAFT SYSTEM	6-26
F. COMBINED BIOFILM/SUSPENDED GROWTH PROCESSES	6-28
G. AEROBIC LAGOONS	6-28
H. PACT PROCESS	6-28
TYPICAL EFFLUENT CONCENTRATIONS	6-32
OPERATIONAL PROBLEMS	6-37
III. VARIABILITY/RELIABILITY	6-38
IV. NUTRIENT REMOVAL	6-50
I. MAJOR NITROGEN REMOVAL PROCESSES	6-50
INDUSTRIAL WASTES	6-61
II. DENITRIFICATION	6-69
III. PHOSPHORUS REMOVAL	6-70
V. BIOLOGICAL NUTRIENT REMOVAL	6-71
BARDENPHO PROCESS	6-71
PHOSTRIP	6-71
VI. COST OF TREATMENT	6-75
VII. PRIORITY POLLUTANTS/TOXICS	6-106

BIOLOGICAL TREATMENT

Biological waste treatment essentially consists of controlling environmental factors to enable a mixed culture of microorganisms to employ the organic matter in the waste as a food source for reproduction (synthesis) and energy (assimilation). In aerobic treatment systems, organisms are suspended in a liquid medium with the waste to be treated. Dissolved oxygen is required by the culture and sufficient time is allowed for the organisms to utilize the organics as a food source. The suspended and colloidal organic matter measured as BOD undergoes an initial reduction by adsorption to the organisms. Thereafter the rate of BOD removal is generally related to the BOD present and viable microorganisms in the system.

In the design of waste treatment facilities, the rate at which these reactions occur, the amount of oxygen and nutrients required, and the quantity of biological sludge produced in the reaction must be determined.

The reaction constant in the BOD removal equation is temperature dependent. It is possible to relate the effect of temperature on BOD removal by the following relationship:

$$K_t = K_{20}\theta^{(T-20)}$$

where

K_t = BOD removal coefficient at temperature T (°C)

K_{20} = BOD removal coefficient at 20°C

T = temperature in treatment system (°C)

θ = temperature coefficient (1.030 - 1.080)

In general, the system will approach some minimum BOD value, rather than zero concentration, due to an equilibrium between the bacteria and their liquor. The magnitude of the initial removal is a function primarily of sludge concentration, acclimatization, and waste composition. The rate of reaction is a function of temperature, nutrient level, concentration of waste, and sludge composition.

Table 6-1 summarizes the reactions and information that must be developed for the design of aerobic biological processes.

TABLE 6-1

BIOLOGICAL TREATMENT REACTIONS

$$\text{ORGANICS} + NH_3 + O_2 \xrightarrow{\text{cells}} C_5H_7NO_2 + CO_2 + H_2O$$

$$C_5H_7NO_2 + O_2 \xrightarrow{\text{cells}} CO_2 + H_2O + NH_3 + \text{cells}$$

KINETICS

$$\frac{dS}{dt} = \frac{k\,SX}{k_5 + S}$$

$$\frac{dS}{dt} = kX \qquad S >> k_5 \qquad \text{zero order}$$

$$= k' X S \qquad S << k_5 \qquad \text{1st order}$$

OXYGEN

$$O_2 \text{ Required} = a' BOD_R + b' X$$

$$O \text{ Transfer} = \frac{r}{K_{LA}(C_5 - C_L)} \qquad \text{Steady State}$$

BIO SLUDGE PRODUCTION

$$SSp = aBOD_r - b X$$

PROCESS DESIGN & CONTROL

Loading Rate

$$F/M = \frac{BOD_5 \text{ (lbs/day) Applied}}{MLVSS \text{ (lbs)}}$$

Sludge Age

$$\theta = \frac{V\ X}{a\ BOD_r Z - bXV}$$

or

$$\theta = \frac{VX}{wX_r + (Q-W)Xe}$$

NUTRIENTS

$$BOD_5 : N : P$$

$$100 : 4.5 : 0.8$$

Figure 6-1 presents a schematic representation of the removal of BOD by biological treatment as a function of the microorganisms in contact with the wastewater (MLVSS), X and the time of contact, t. At low Xt values which would represent high Food to Microorganism, F/M, ratios and low sludge age the BOD remaining changes sharply with small incremental increases in Xt. Under these conditions the system is unstable and it would be difficult to design a plant to provide consistent performance in this region. As Xt increases beyond this region effluent BOD remain relatively constant and stable operation is obtained.

Figures 6-2 and 6-3 shows effluent characteristics to the system loading rate.

Figure 6-4 summarizes from a number of studies performed by HydroQual the relationship between effluent soluble BOD_5 and system loading rates for a variety of industrial wastes.

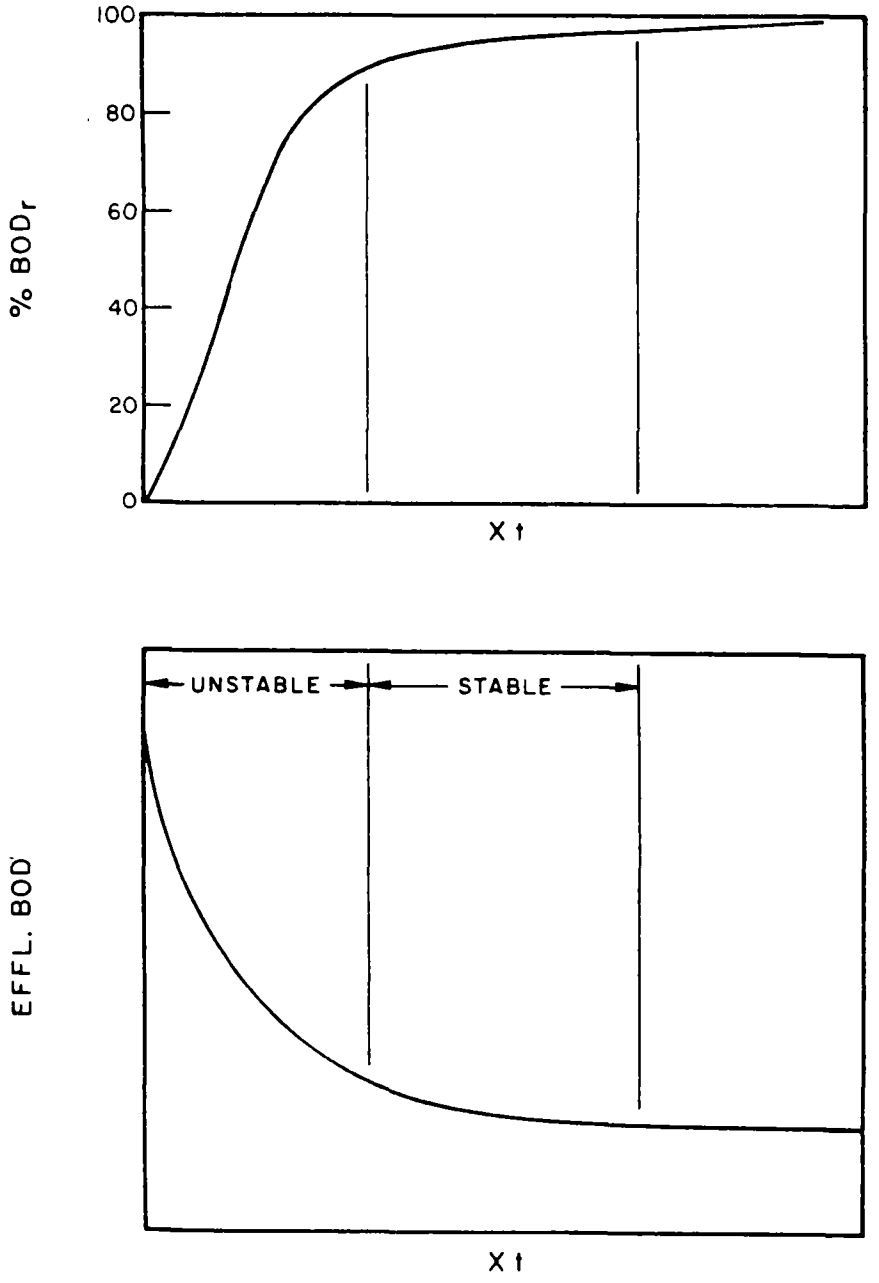

FIGURE 6-1

BOD REMOVAL

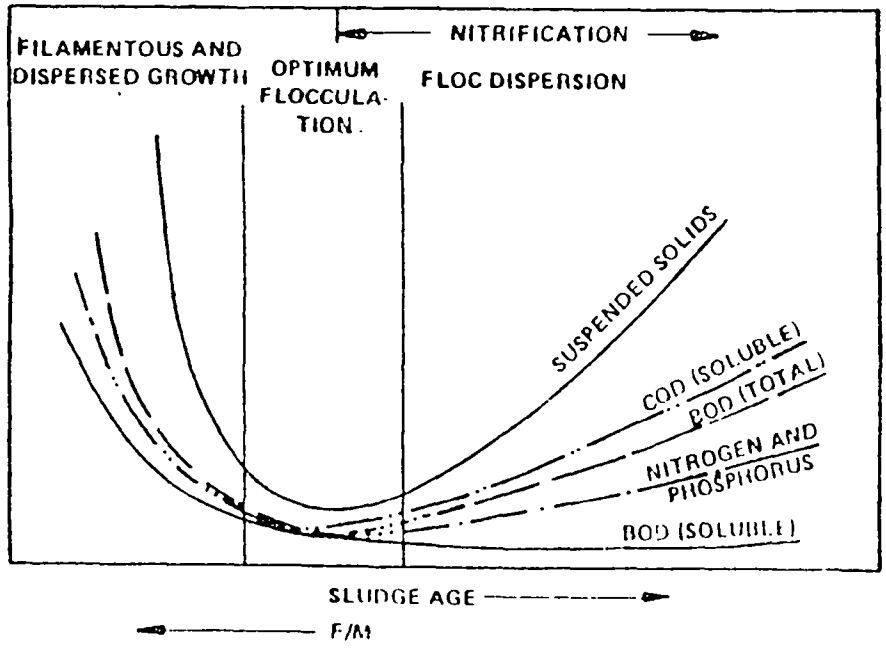

FIGURE 6-2

EFFLUENT CHARACTERISTICS AS RELATED TO SLUDGE AGE AND F/M

FIGURE 6-3

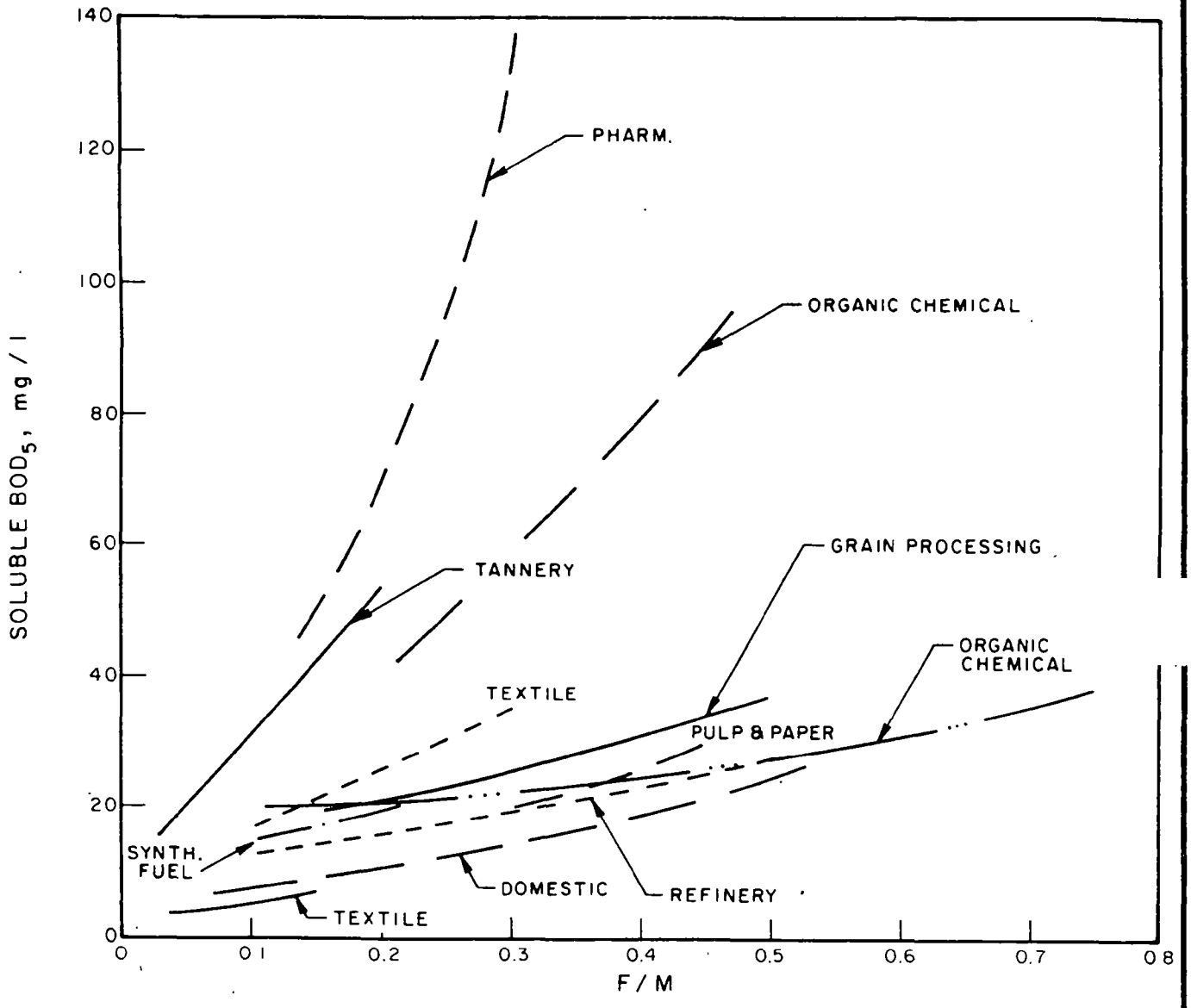

FIGURE 6-4

INDUSTRIAL WASTEWATER TREATABILITY

SECONDARY TREATMENT PROCESSES

A. ACTIVATED SLUDGE

The activated sludge process is a continuous system in which aerobic biological growths are mixed and aerated with wastewater and separated in a gravity clarifier. A portion of the concentrated sludge is recycled and mixed with additional wastewater. The process should provide an effluent with a soluble BOD of 10-30 mg/l, although the organic concentration of the effluent in terms of COD may be as high as 500 mg/l, depending on the concentration of bioresistant compounds originally in the wastewater. There are many impurities in industrial wastewaters such as oil and grease, which must be removed or altered by preliminary treatment before subsequent activated sludge treatment can be considered.

Many modifications of this process have been developed over the decades, the principal ones being shown in Figure 6-5. The conventional process employs long rectangular aeration tanks, which approximate plug-flow with some longitudinal mixing. This process is primarily employed for the treatment of domestic wastewater. Returned sludge is mixed with the wastewater in a mixing box or chamber at the head end of the aeration tank. The mixed liquor then flows through the aeration tanks, during which progressive removal of organics occurs. The oxygen utilization rate is high at the beginning of the aeration tanks and decreases with aeration time. Where complete treatment is achieved, the oxygen utilization rate will approach the endogenous level toward the end of the aeration tanks. The principal disadvantages of this system for the treatment of industrial wastewaters are (1) the oxygen utilization rate varies with tank length and requires irregular spacing of the aeration equipment or a modulated air supply; (2) load variation may have a deleterious effect on the activated sludge when it is mixed at the head end of the aeration tanks; (3) the sludge is susceptible to slugs or spills of acidity, causticity or toxic materials.

In the completely mixed system the aeration tank serves as an equalization basin to smooth-out load variations and as a diluent for slugs and toxic materials. Since all portions of the tank are mixed, the oxygen utilization rate will not vary with time and the aeration equipment can be equally spaced.

Step aeration is a variant between the conventional process and the completely mixed process and has been successfully employed for the treatment of domestic wastewaters. Table 6-2 and Figure 6-6 compare the impact of operational modes (conventional vs step aeration) on removal and oxygen requirement

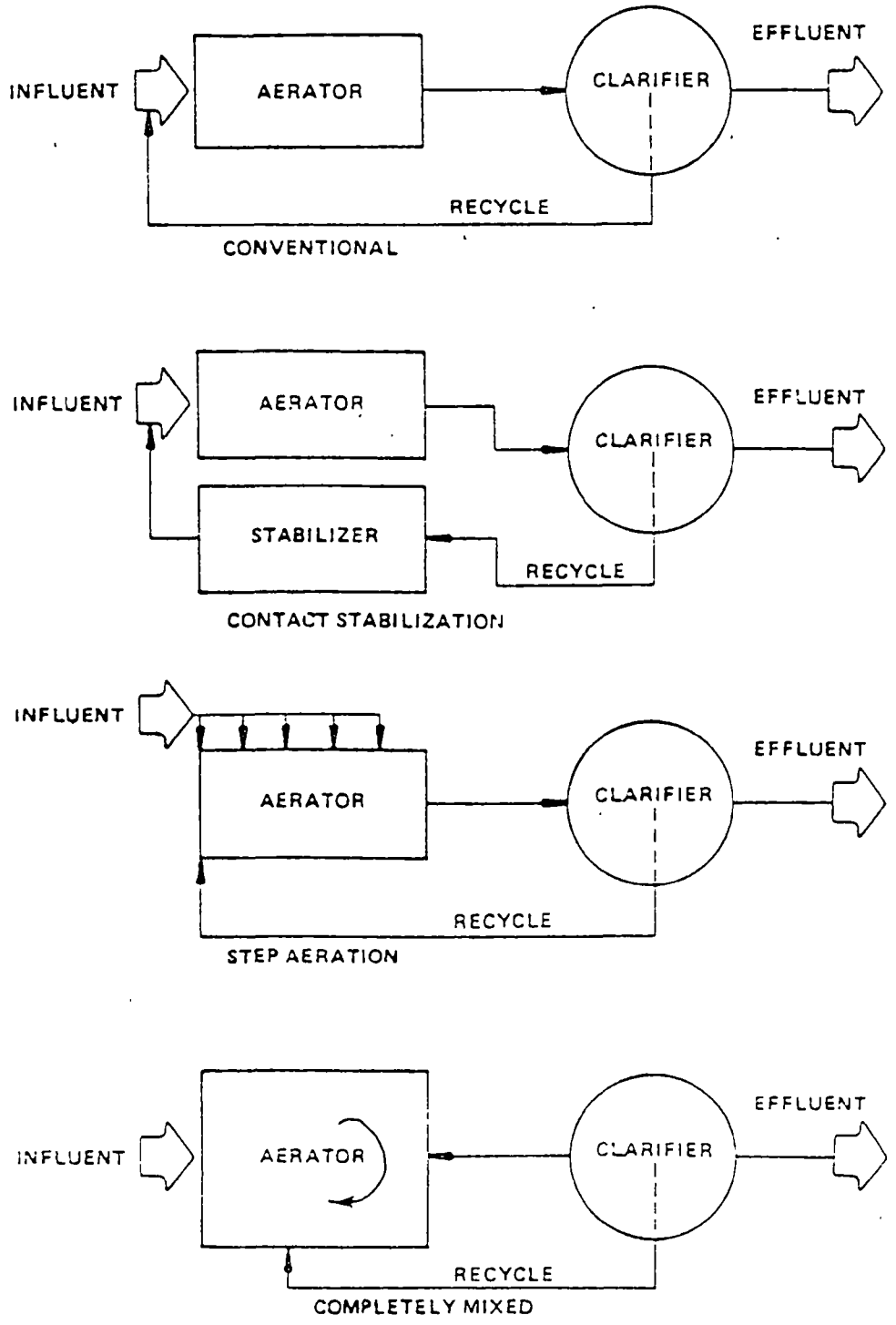

FIGURE 6-5
ACTIVATED SLUDGE SYSTEMS

TABLE 6-2

COMPARISON OF OPERATIONAL MODES
AT ULTIMATE PEAK LOADS

Parameter	Conventional Mode	Step Aeration Modes							
		Case I				Case II			
		Pass 1	Pass 2	Pass 3	Pass 4	Pass 1	Pass 2	Pass 3	Pass 4
Flow, mgd	74.6	37.3	37.3	0	0	24.8	24.9	24.9	0
BOD, 1,000 lbs/day	160	80	80	0	0	53.3	53.3	53.3	0
Recycle mgd	24.6	24.6	0	0	0	24.6	0	0	0
mg/l	12,000	12,000	--	--	--	12,000	--	--	--
F/M, lbs BOD/lb MLSS-day	.52	Average .46				Average .39			
X_a, gm/l	3.0	4.8	3.0	3.0	3.0	6.0	4.0	3.0	3.0
t, hrs. Q	3.9	3.9 Total				3.9 Total			
Temp (^oC)	30	30	30	30	30	30	30	30	30
Soluble BOD, mg/l	14	15	22	16	14	10	14	22	14
Oxygen Required 1,000 lbs/day	137.6 Total	142 Total				150 Total			
Distribution	103.9 14.4 9.9 9.9	65.3	55.7	11.6	9.4	52.7	45.9	40.2	11.2
Average DO, mg/l	0.5 2.5 2.4 2.4	1.0	1.0	3.0	3.0	1.5	1.5	2.5	2.5
Air Required 1,000 scfm	79.3 Total	84.9 Total				96.9 Total			
Distribution	55.2 10.3 7.1 6.7	37	31.6	9.0	7.3	32.1	28.0	28.8	8.0

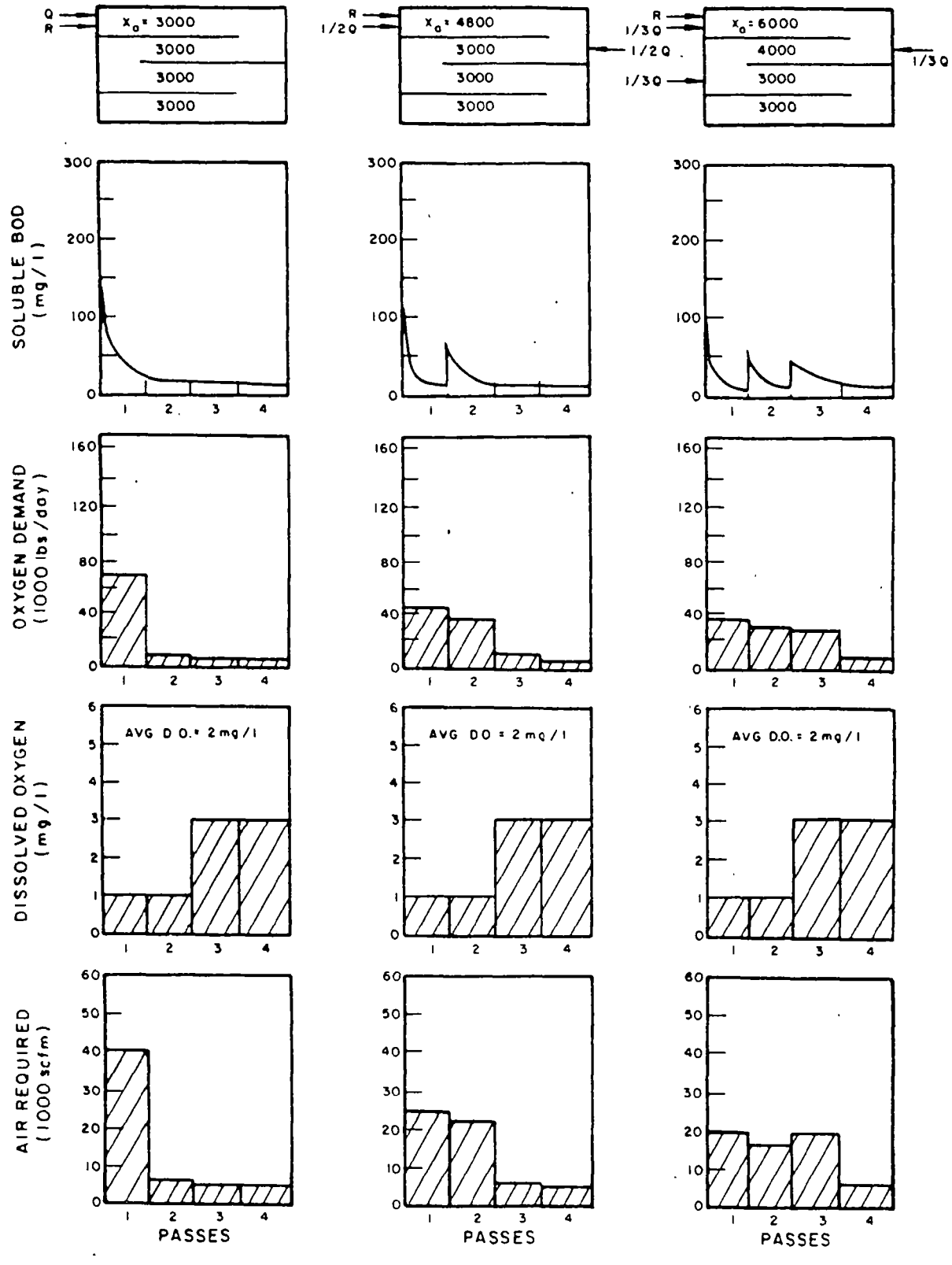

FIGURE 6-6

OXYGEN DEMAND AND AIR DISTRIBUTION ULTIMATE AVERAGE LOAD

at a 75 MGD combined domestic and industrial wastewater treatment plant.

In the extended aeration process, sufficient aeration time is provided to oxidize a large percentage of the biodegradable sludge synthesized from the BOD present in the wastewater.

The contact stabilization process is applicable to wastewaters containing a high proportion of the BOD in suspended or colloidal form. Since bio-adsorption and flocculation of colloids and agglomeration of suspended solids occur very rapidly, only short retention periods (15 - 30 minutes) are required to effect clarification as shown in Figure 6-7. After the contact period the activated sludge is separated in a clarifier. A sludge reaeration or stabilization period is required to stabilize the organics removed in the contact tank. The retention period in the stabilization tank is dependent on the time required to assimilate the soluble and colloidal material removed from the wastewater in the contact tank.

Effective removal in the contact period requires sufficient activated sludge to remove the colloidal and suspended matter and a portion of the soluble organics. The retention time in the stabilization tank must be sufficient to stabilize these organics. If it is insufficient, unoxidized organics will be carried back to the contact tank and the removal efficiency will be decreased. If the stabilization period is too long, the sludge will undergo excessive auto-oxidation and will lose some of its initial high removal capacity. Increasing retention period in the contact tanks will increase the amount of soluble organics removed and decrease required stabilization time. A large increase in contact time will negate the requirement for sludge stabilization. In this case, the process becomes the same as the conventional activated sludge process.

Increasing the biological solids level also decreases the stabilization time requirements since the organic loading for unit solids becomes less. The total oxygen requirements in the process are those required for synthesis of the organics removed and for endogenous respiration. The split of this oxygen between the contact tank and the stabilization tank depends on the solids level carried in both units and on the retention period in each tank. Increasing the contact tank solids level or retention period will increase the percentage of total oxygen to that unit.

DOMESTIC SEWAGE

A distinction must be made when considering the activated sludge process for the treatment of domestic sewage as compared to soluble industrial wastewaters, based upon the physical

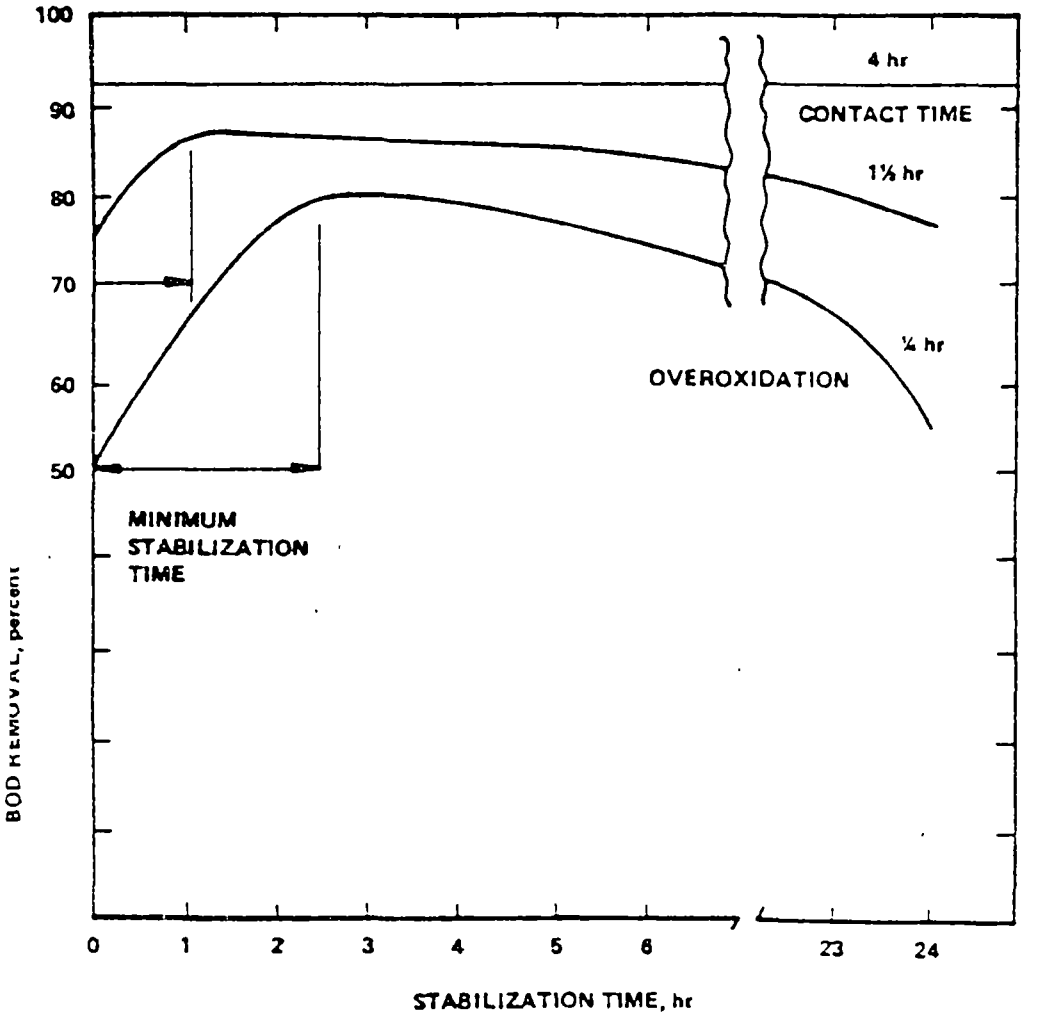

FIGURE 6-7a

SCHEMATIC REPRESENTATION OF
THE CONTACT-STABILIZATION PROCESS

composition of the wastewaters and the resulting mechanisms of removal. The organic content of domestic sewage consists of three components, suspended organics resulting from ground garbage, paper, rubber, etc., colloidal matter, and soluble organics consisting mainly of carbohydrates and some nitrogenous material. Most of the organics are in the form of particulates. Investigators have shown 35%, 40% and 25% of the total COD was present as suspended, colloidal, and soluble material, respectively in American sewage.

Typical design criteria for the unit processes that are contained in most activated sludge plants are shown on Table 6-3. Processes are selected and designed to be cost effective for the treatment of specific wastewater characteristics and situations. The design of a total treatment system integrates the various processes to produce the desired effluent quality. The "safety factor" incorporated into a design is a matter of good engineering judgment which should consider the specific needs, type process, reliability, waste variability, and cost.

B. PURE OXYGEN TREATMENT

I. General Design Considerations

F/M - 0.5 - 0.9 $\frac{\text{lbs/day BOD}_5}{\text{lb MLVSS}}$

MLVSS - 4,000 - 8,000 mg/l

Stages - 3 to 4

Oxygen Utilization - Avg. Load 90^+%

II. Special Design Considerations (Industrial)

1. O_2 Transfer
2. Alkalinity/pH
3. Temperature
4. Oxygen Utilization
5. Solids Clarification

III. Schematic - Figure 6-7b

IV. Performance - Figure 6-8

TABLE 6-5

ACTIVATED SLUDGE

DOMESTIC WASTEWATER

		BOD	SS
PRIMARY CLARIFIERS	800-1200 GPD/SF 2-3 HOURS	20-40% REMOVAL	40-70% REMOVAL
ACTIVATED SLUDGE			
AERATION BASIN	0.2-0.4 F/M		
TIME	4-8 HOURS		
FINAL CLARIFIERS	OR = 600-1200 GPD/SF FLUX = 20-30 LBS/FT^2/DAY	30 MG/L	30 MG/L
AIR FLOTATION			
WAS	2-4 LBS/HR/SF		
FLOAT SOLIDS	3-6%		
GRAVITY THICKEN			
PRIMARY	8-12%		

DEWATERING EQUIPMENT

	CHEM. CONDIT.	FEED SOLIDS	CAPACITY	CAKE SOLIDS
DCG	POLYMER	1-2%	200-400 LBS/HR	5-10%
MRP	POLYMER	5-10%	200-400 LBS/HR	12-14%
BELT FILTER PRESS	POLYMER	1-2%	300-400 LBS/HR	12-14%
VACUUM FILTRATION	CHEMICAL	2-5%	2-6 LBS/HR/SF	14-20%

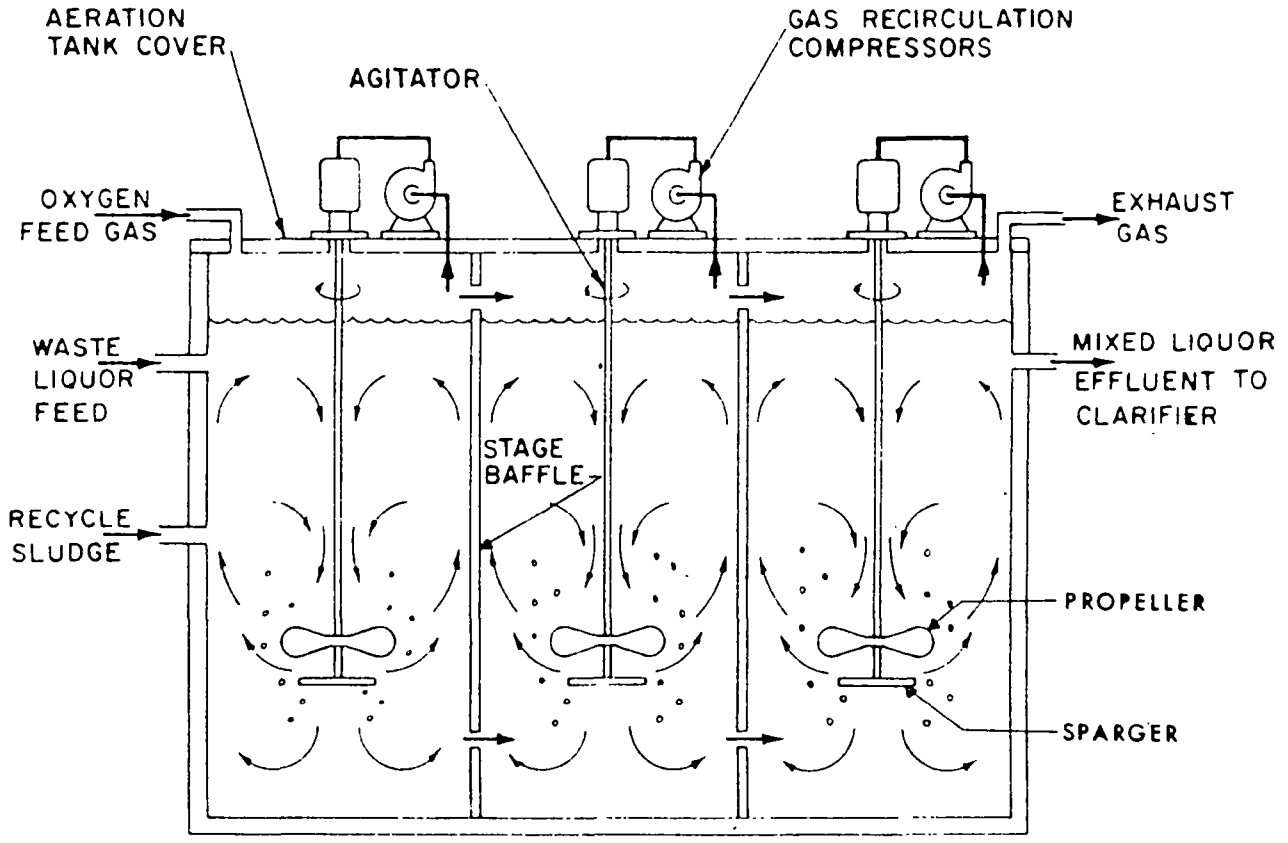

FIGURE 6-7b

SCHEMATIC DIAGRAM OF MULTI-STAGE
OXYGEN AERATION SYSTEM

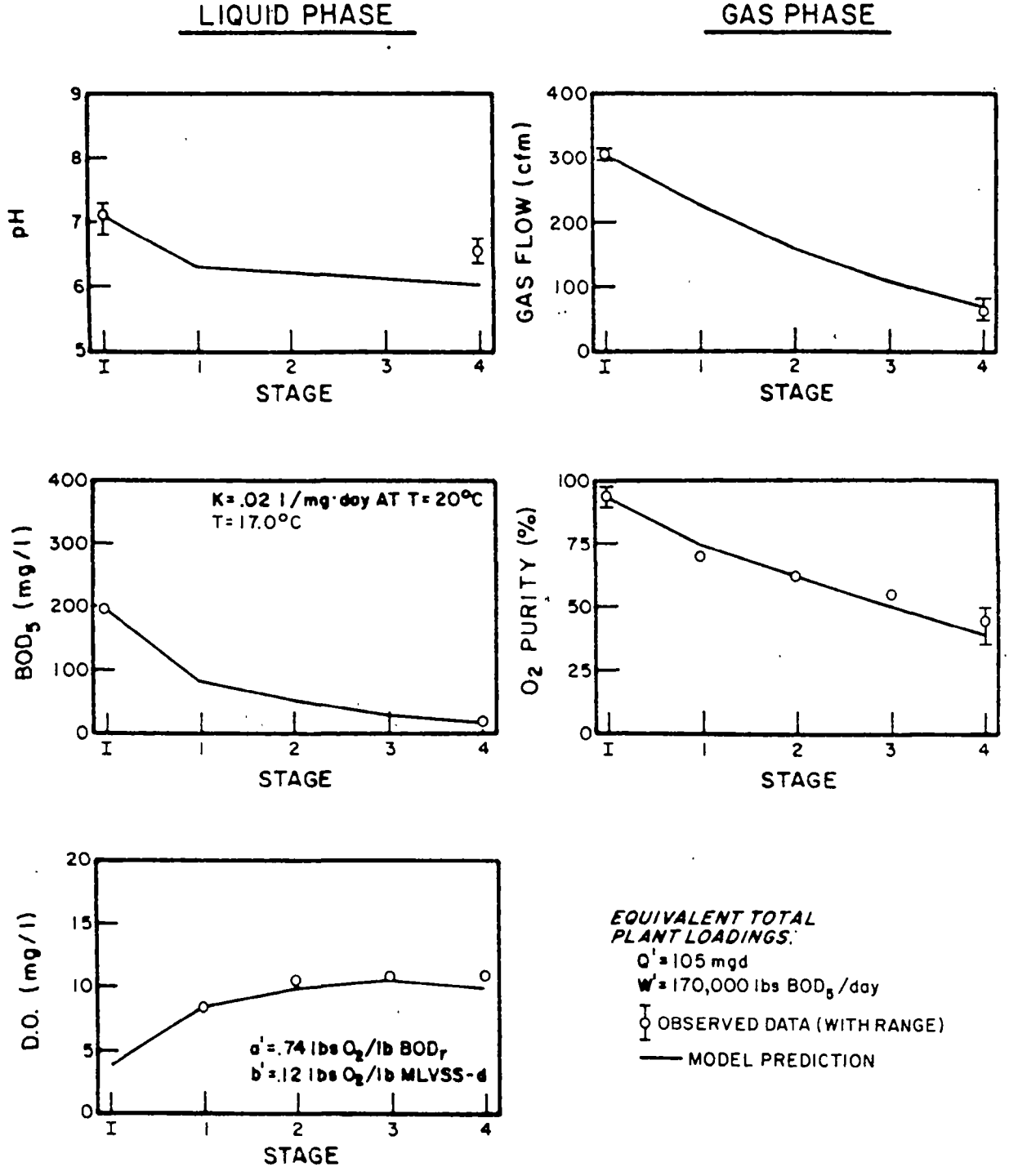
LIQUID PHASE
GAS PHASE
pH
GAS FLOW (cfm)
STAGE
K = .02 l/mg·day AT T = 20°C
T = 17.0°C
BOD5 (mg/l)
O2 PURITY (%)
D.O. (mg/l)
a' = .74 lbs O2/lb BODr
b' = .12 lbs O2/lb MLVSS-d
EQUIVALENT TOTAL PLANT LOADINGS:
Q' = 105 mgd
W' = 170,000 lbs BOD5/day
OBSERVED DATA (WITH RANGE)
MODEL PREDICTION

FIGURE 6-8

C. ROTATING BIOLOGICAL CONTACTORS

1. Domestic Wastewaters

Organic Loading Rates - 1-3 lbs/day BOD_5/1,000 sf

Hydraulic Rates - 0.75-1.5 gpd/ft^2

2. Variability

Fixed Film Process w/o Recycle

Subject to variability
Generally effl. variability ~ infl. variability

3. Temperature Effects

May not be significant on overall removal.

a. kinetic rate decreases $\theta = 1.10$

b. Active film layer increases due to increased oxygen saturation

4. Schematic - Figure 6-9

Design Relationship Domestic Wastewater - Figure 6-10

Sensitivity - Figures 6-11 to 6-13

D. CARROUSEL LOOP AERATION SYSTEM

The Carrousel system, originally developed in Netherlands is basically a low rate activated sludge (extended aeration) process that incorporates a mechanically aerated continuous channel. Oxygenation and circulation of mixed liquor is provided by conventional surface aeration equipment normally located at influent end and at the turn point of the loop, depending upon basin configuration. The system can be visualized to consist of two sections: the aeration zone, which is essentially completely mised, and the channel section, with a plug flow regime.

Due to the long sludge ages and the variable dissolved oxygen that exists in the basin the Carrousel process can be utilized for combined nitrification/denitrification. (See Figure 6-14).

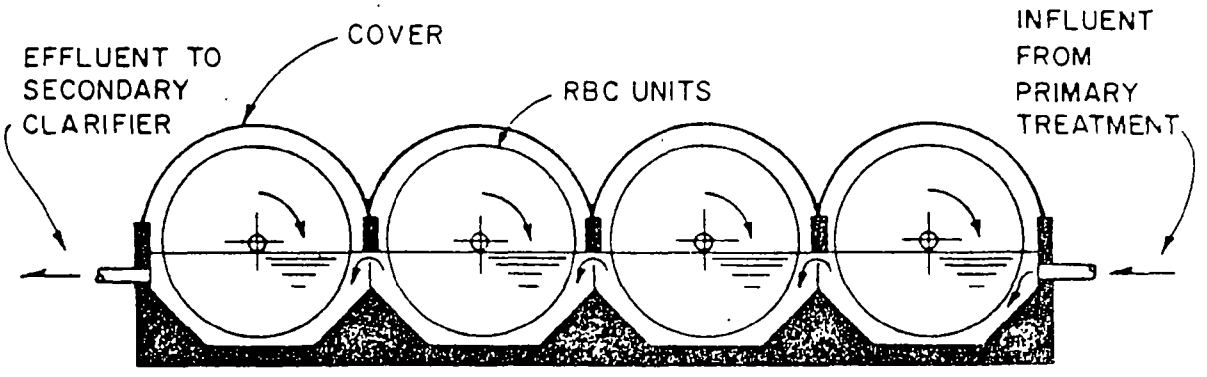

CONTOURED TANK FOR MULTIPLE RBC SHAFTS

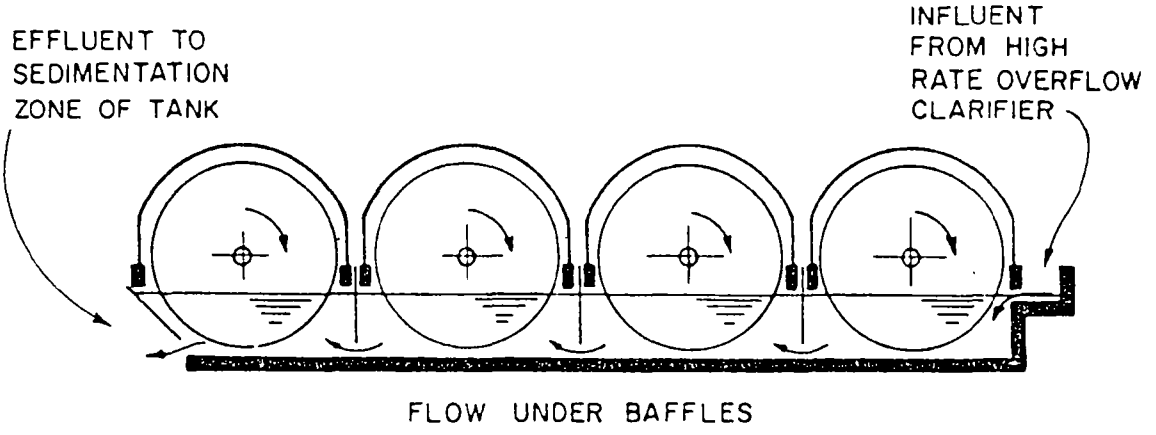

FLAT BOTTOM RBC TESTING TANK

FIGURE 6-9

RBC BOTTOM CONFIGURATIONS

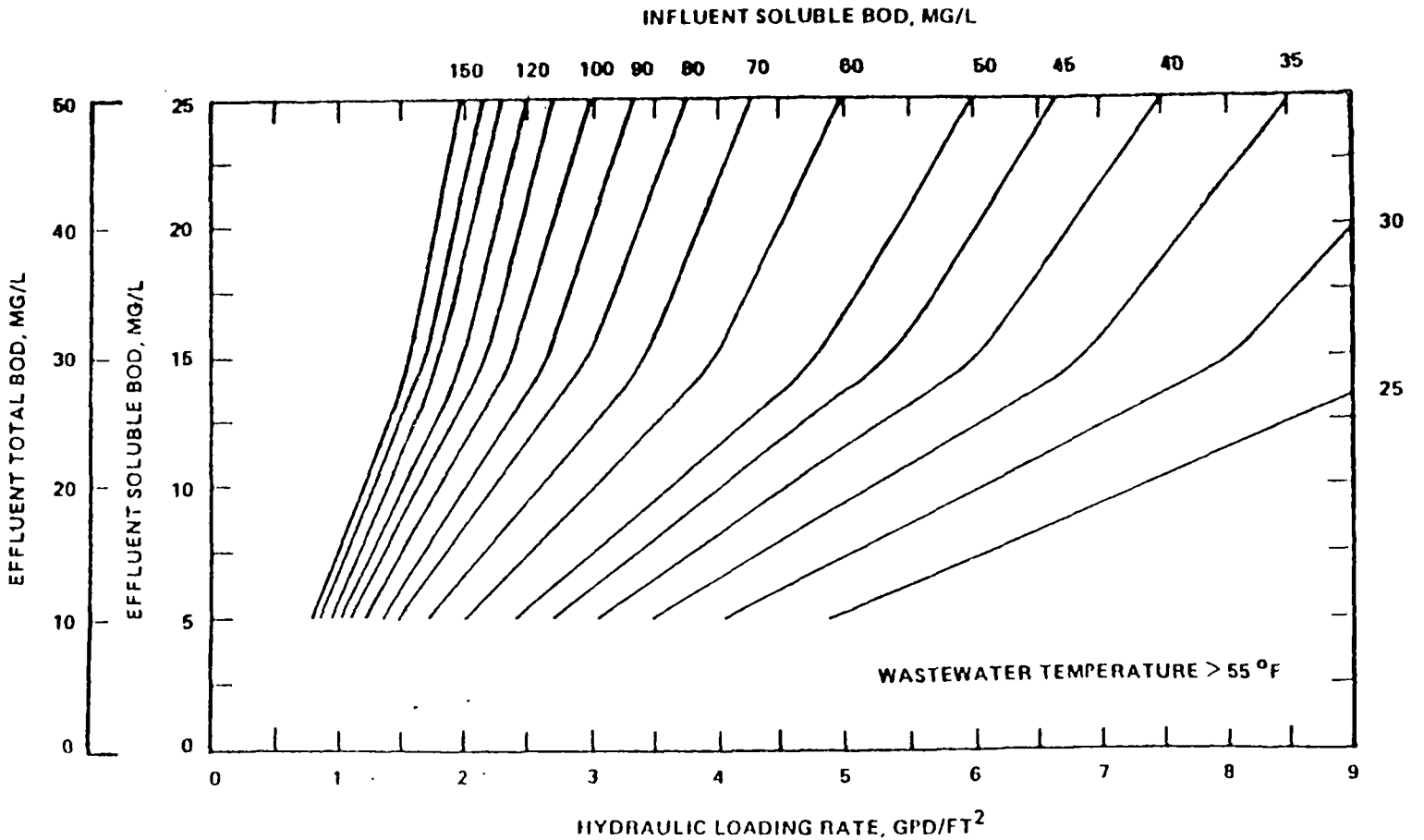

FIGURE 6-10

DESIGN RELATIONSHIP FOR BOD REMOVAL FROM DOMESTIC WASTEWATER

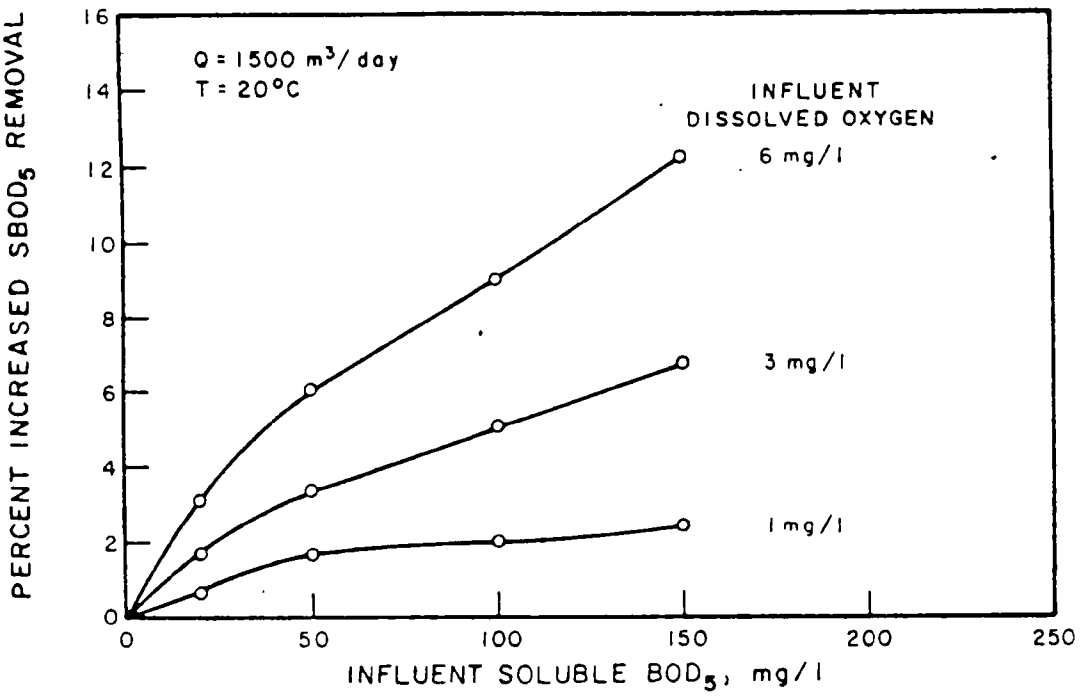

FIGURE 6-11

SINGLE STAGE PROCESS DESIGN CURVES RELATING THE EFFECT OF DISSOLVED OXYGEN ON $SBOD_5$ REMOVALS

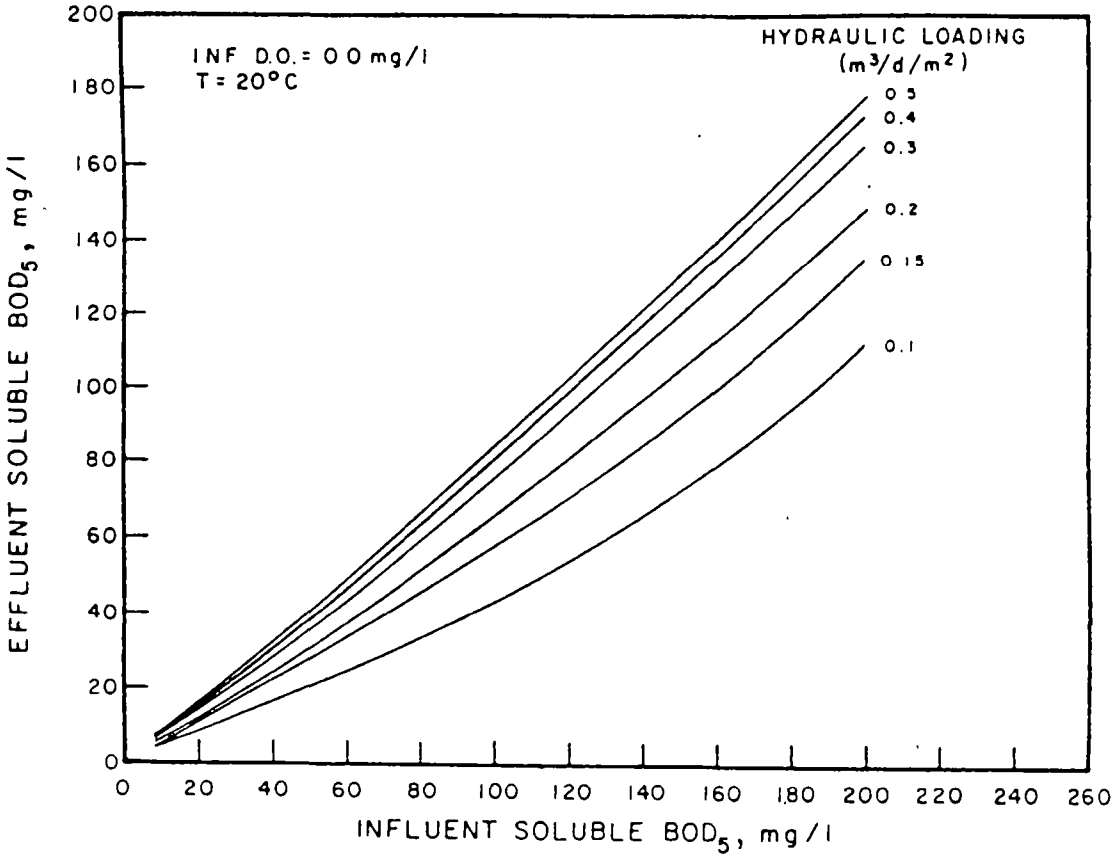

FIGURE 6-12

SINGLE STAGE PROCESS DESIGN SOLUTIONS RELATING EFFLUENT $SBOD_5$ TO INFLUENT $SBOD_5$ AND HYDRAULIC LOADING

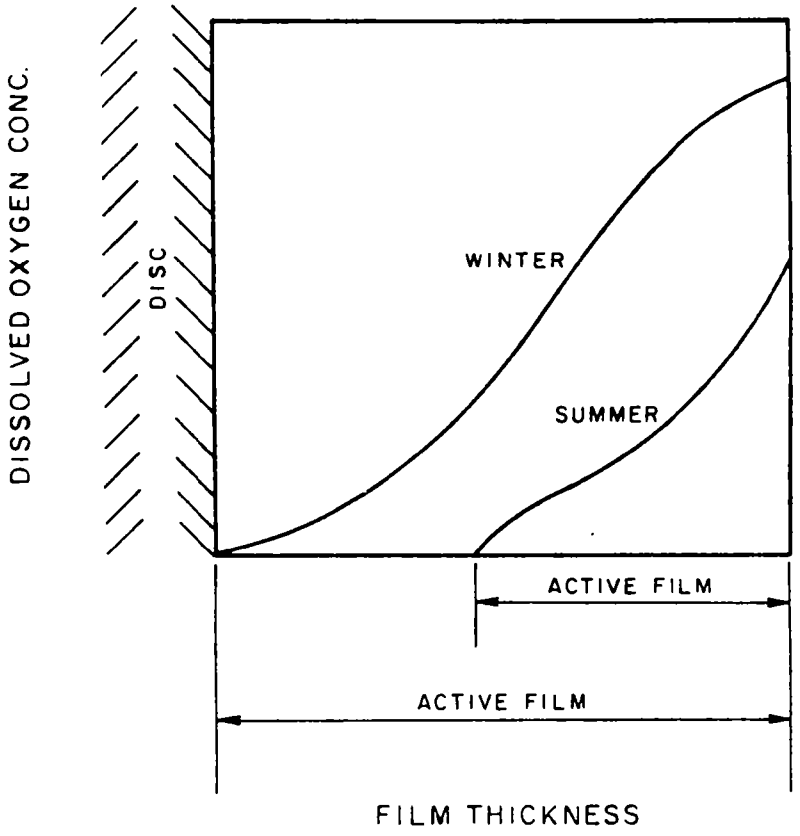
DISSOLVED OXYGEN CONC.
DISC
WINTER
SUMMER
ACTIVE FILM
ACTIVE FILM
FILM THICKNESS

FIGURE 6-13

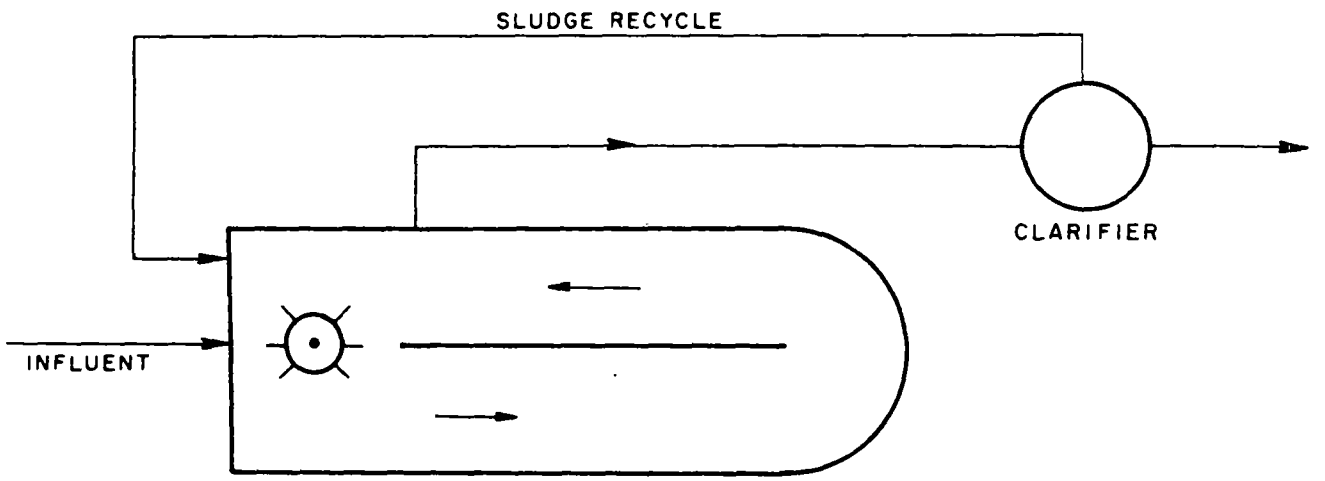

FIGURE 6-14

CARROUSEL PROCESS

E. DEEP SHAFT EFFLUENT TREATMENT SYSTEM

The Deep Shaft Effluent Treatment System, originally developed by Imperial Chemical Industries in Great Britain is basically a high rate activated sludge process, employing compressed air for oxygenation and circulation of wastewater. The heart of the process is the Deep Shaft bioreactor where aeration and substrate removal take place. A typical bioreactor consists of a totally cased and grouted vertical shaft 300-800 feet in depth, which is divided into a downcomer and riser section by a partition or a concentric tube arrangement. Air injection points are provided in both sections. The wastewater is circulated around the shaft using the air lift principle. During normal operation, the compressed air is injected in the downcomer section, while the injection point in the riser is used only for startup (Figure 6-15).

Solids-liquid separation is normally achieved by flotation in the Deep Shaft system which makes use of the air entrained in the biological flocs as they emerge to the top of the riser.

Average loading rates for the Deep Shaft process are in the range of 2 to 4 lbs BOD/lb MLVSS/day. Since the system is a very high rate process relatively large amounts of sludge are produced in treatment.

TYPICAL OPERATING PARAMETERS

- MLSS - 8,000-10,000 mg/l
- Residence Time per pass - 2-6 min.
- Retention Time - 1-4 hours
- F/M - 2-4 lbs BOD/lb MLVSS

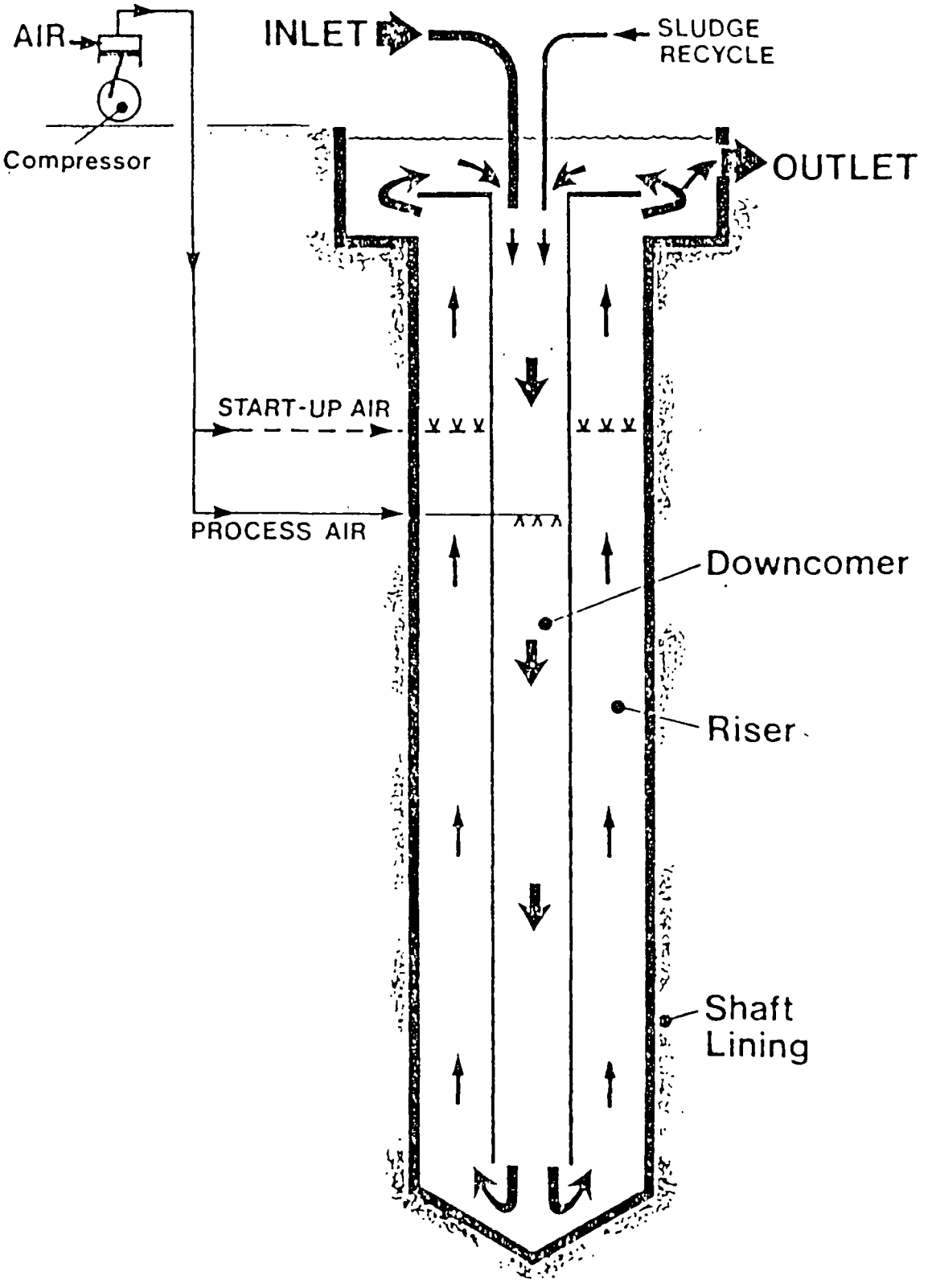

FIGURE 6-15

DEEP SHAFT

F. COMBINED BIOFILM/SUSPENDED GROWTH PROCESSES (ABF)

Combined biofilm/suspended growth processes employ a biofilm reactor upstream of a conventional activated sludge reactor. The first-stage biofilter is used as a roughing filter to remove most of the organics and buffer loadings to the aeration basin. Typically, about half to two-thirds of the system stabilization occurs in the biofilter, and the balance in the aeration basin. Thus, most stabilization occurs in the relatively energy-efficient biofilter and furthermore, net oxygenation efficiency is improved in the aeration basin since load fluctuations are reduced. Figure 6-25 is a schematic diagram of the activated biofilter process (ABF) which employs this concept. In this case, mixed liquor settled in the secondary clarifier is recycled and distributed over a horizontal-media biofilter. Thus, suspended growth microorganisms are combined with high-strength wastes in the highly aerobic environment of the biocell. Accordingly, the biocell is analogous to the contact basin in a contact-stabilization activated sludge process. However, the biocell plays a dual role in the ABF, since a biofilm growth develops also contributing to organic stabilization.

Aerobic conditions are maintained in the biocell through relatively high surface wetting rates, 1.5-4 gpm/sq. ft., and the horizontal media design. Performance of the ABF process is comparable to activated sludge. It is particularly applicable to high-strength wastes and wastes with widely-fluctuating loadings, since the contribution of the biofilter is accentuated in these situations.

G. AEROBIC LAGOONS

Aerobic lagoons are simple, mixed reactors without recycle. SRT is equivalent to the HRT in this configuration, thus relatively long HRTs are required to achieve reasonable stabilization efficiencies. Typical detention times range from 1 to 10 days. Clarification is required to provide good effluent quality. Aerobic lagoons are used where simplicity is necessary and land is abundant. Several industries use lagoon treatment systems.

H. PACT PROCESS

The "PACT" process (Dupont patent) is an activated sludge process employing powdered activated carbon (PAC) addition to the aeration tanks. Figure 6-16 presents a flow diagram of the process. Both virgin and regenerated PAC are added to the primary effluent based on attaining a certain PC concentration in the aeration tank. Cationic polymer is typically added to the aeration tank effluent to insure adequate clarification in the

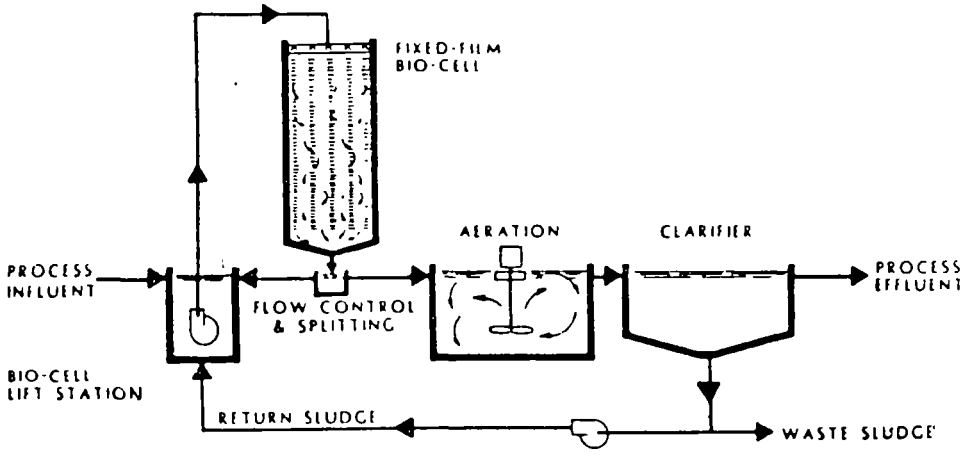

FIGURE 6-25

ABF PROCESS FLOW SCHEMATIC

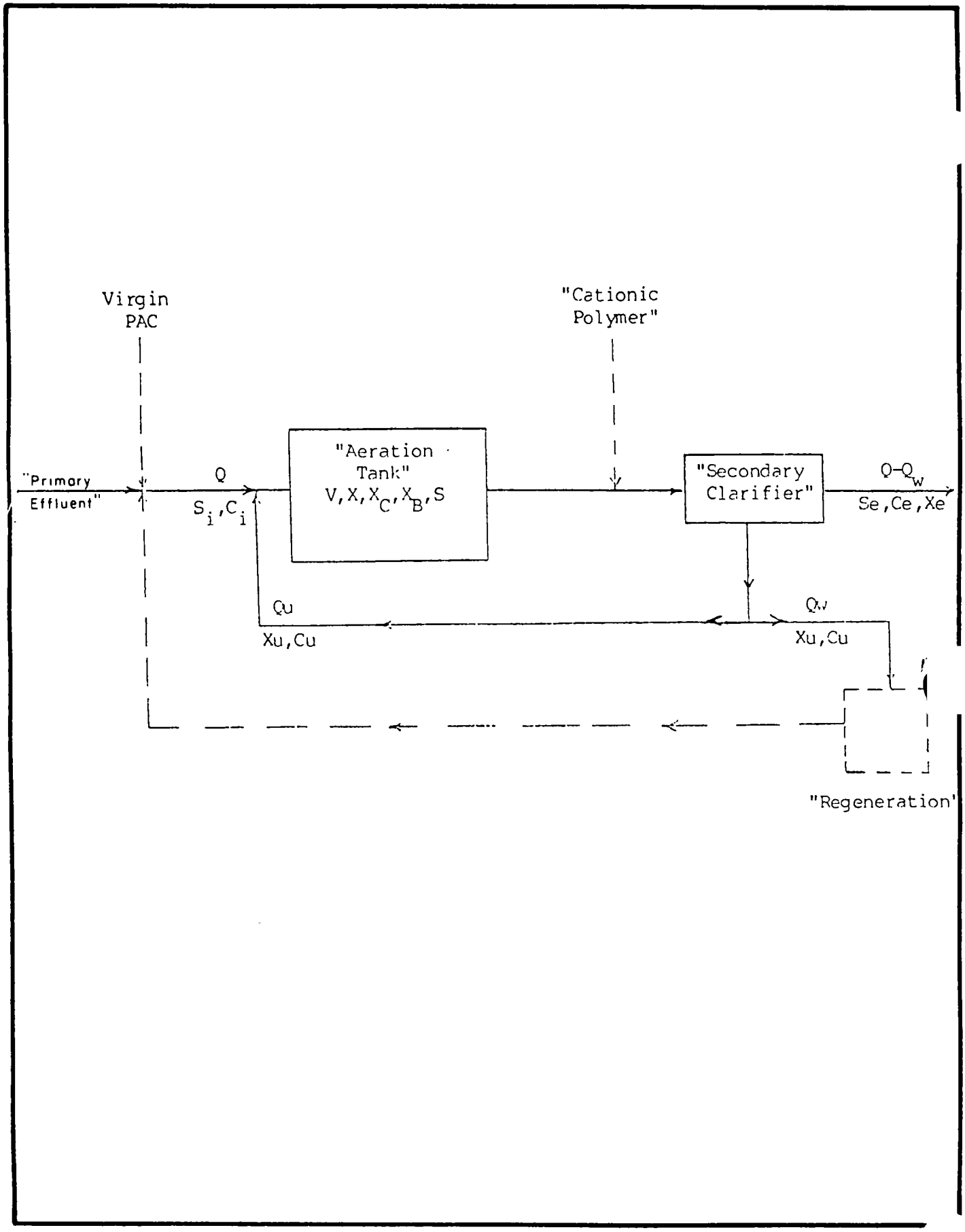

FIGURE 6-16

FLOW DIAGRAM OF "PACT" PROCESS

secondary clarifier. When economically feasible, thermal regeneration is utilized which also provides destruction ofo the waste activated sludge. Depending on the thermal regeneration process, thickening and dewatering may be utilized prior to regeneration. Acid washing of the regenerated PAC is also practiced at the Dupont Chambers Works Plant to reduce ash contents.

Process development was based on the ability to generate better effluent qualities than activated sludge alone, meeting more stringent effluent standards without separate granular activated carbon systems.

Use of high sludge ages will significantly reduce the carbon dosage required. Carbon dosages typically from 5 to 200 mg/l have been utilized. The full scale Chamber Works plant uses ~130 mg/l PAC with a portion regenerated by multiple hearth incineration. A 6 mgd municipal plant at Vernon, Connecticut, produces an effluent BOD of less than 5 mg/l and SS less than 10 mg/l after sand filtration. Virgin carbon feed is approximately 10 mg/l with an additional 300 mg/l of carbon recycled from wet air oxidation regeneration.

CONCLUSIONS

1. The PACT process will supply benefits over activated sludge by increased priority pollutant removals, especially base neutral and acid extractables. The PACT process also provides some protection against upsets and quicker recovery compared to activated sludge.

2. Increased removals are due to influent PAC dose. The degree of bioregeneration occurring in "PACT" units is relatively insignificant.

3. Wet air oxidation appears to be the best process for PAC regeneration, allowing ~95% recovery of the PAC.

4. Cationic polymer addition (1-5 mg/l) is required prior to secondary settling to remove PAC particles from the effluent. The PAC provides a weighting agent for the sludge allowing higher mass loadings on secondary clarifiers than conventional.

5. The PACT process is more costly than activated sludge but less costly compared to GAC. Above a certain size plant depending upon the method and cost of sludge disposal PACT process has been reported less costly than activated sludge. Carbon regeneration is not economical below carbon usage of 5,000 to 10,000 lbs/day.

TYPICAL EFFLUENT CONCENTRATIONS

Table 6-4 puts typical effluent BOD results from various treatment processes in properly operated and maintained treatment works as reported by the EPA in the Process Design Manual for Upgrading Existing Wastewater Treatment Plants, October, 1974.

A study conducted for the EPA resulted in a report on "Estimate of Effluent Limitations to be Expected from Properly Operated and Maintained Treatment Works. This is a 3 part manual illustrating development of data base from various types of treatment plants, primary, conventional, contact stabilization and extended aeration. Flow was normalized by dividing actual flow by design flow. Based on data, the study generally shows that up to design flow secondary treatment normally produces an effluent of 30 mg/l or less, and estimates the effluent which may be expected at normalized thus up to double the plant capacity. A typical curves showing data and estimated effluents for BOD and SS for conventional plants are shown in Figures 6-17 and 6-18.

As can be observed, typically plants produce effluent BOD and SS less than 30 mg/l up to design flow, however, for various reasons attributed to poor operation, this level is exceeded.

TABLE 6-4

LONG TERM AVERAGE PERFORMANCE OF WELL OPERATED PLANTS

	EFFLUENT BOD MG/L		# OF PLANTS
ACTIVATED SLUDGE	RANGE	AVERAGE	SURVEYED
CONVENTIONAL	6 TO 56	15	16
STEP AERATION	5 TO 18	12	15
CONTACT STABILIZATION (W/O PRIMARY TREATMENT < 10 MGD)	17 TO 50	21	8
COMPLETE MIX	6 TO 37	19	21
MODIFIED AERATION	58 TO 66	55	10
2 STAGE (FOR AMMONIA OXIDATION)	4 TO 21	12	11
OXYGEN ACTIVATED SLUDGE PLANTS	9 TO 25	15	19
TRICKLING FILTER PLANTS			
LOW RATE	14 TO 68	54	5
HIGH RATE	20 TO 66	39	6

REFERENCE: ESTIMATE OF EFFLUENT LIMITATIONS TO BE EXPECTED AT PROPERLY OPERATED AND MAINTAINED TREATMENT WORKS, EPA-CI NO. 68-01-4529

TABLE 6-4
(CONTINUED)

LONG TERM AVERAGE PERFORMANCE OF WELL OPERATED PLANTS[1]

ADVANCED TREATMENT METHODS

AEROBIC POLISHING LAGOONS

% BOD REMOVAL TF/AS EFFLUENTS: RANGE: 8-69%

AVERAGE: 45%

MICROSCREENS

SOLIDS REMOVAL AND BOD ASSOCIATED WITH

SOLIDS ON TF/AS EFFLUENTS: RANGE: 50-85% REMOVAL

INF. SS 6 TO 54 MG/L

EFF. SS 2 TO 15 MG/L

	FILTER INFLUENT BOD MG/L	FILTER EFFLUENT BOD MG/L
MEDIA FILTERS		
SAND		
1. ACTIVATED SLUDGE EFFLUENT	12 - 20	2 - 10
2. TRICKLING FILTER EFFLUENT	20 - 45	5 - 25
MULTI MEDIA		
ACTIVATED SLUDGE EFFLUENT		2 - 18

ACTIVATED CARBON COLUMNS

EFFLUENT BOD - 2-5 MG/L ON ACTIVATED SLUDGE EFFLUENT

(1) PROCESS DESIGN MANUAL FOR UPGRADING EXISTING WASTEWATER TREATMENT PLANTS, EPA TECHNOLOGY, TRANSFER OCT. 1974.

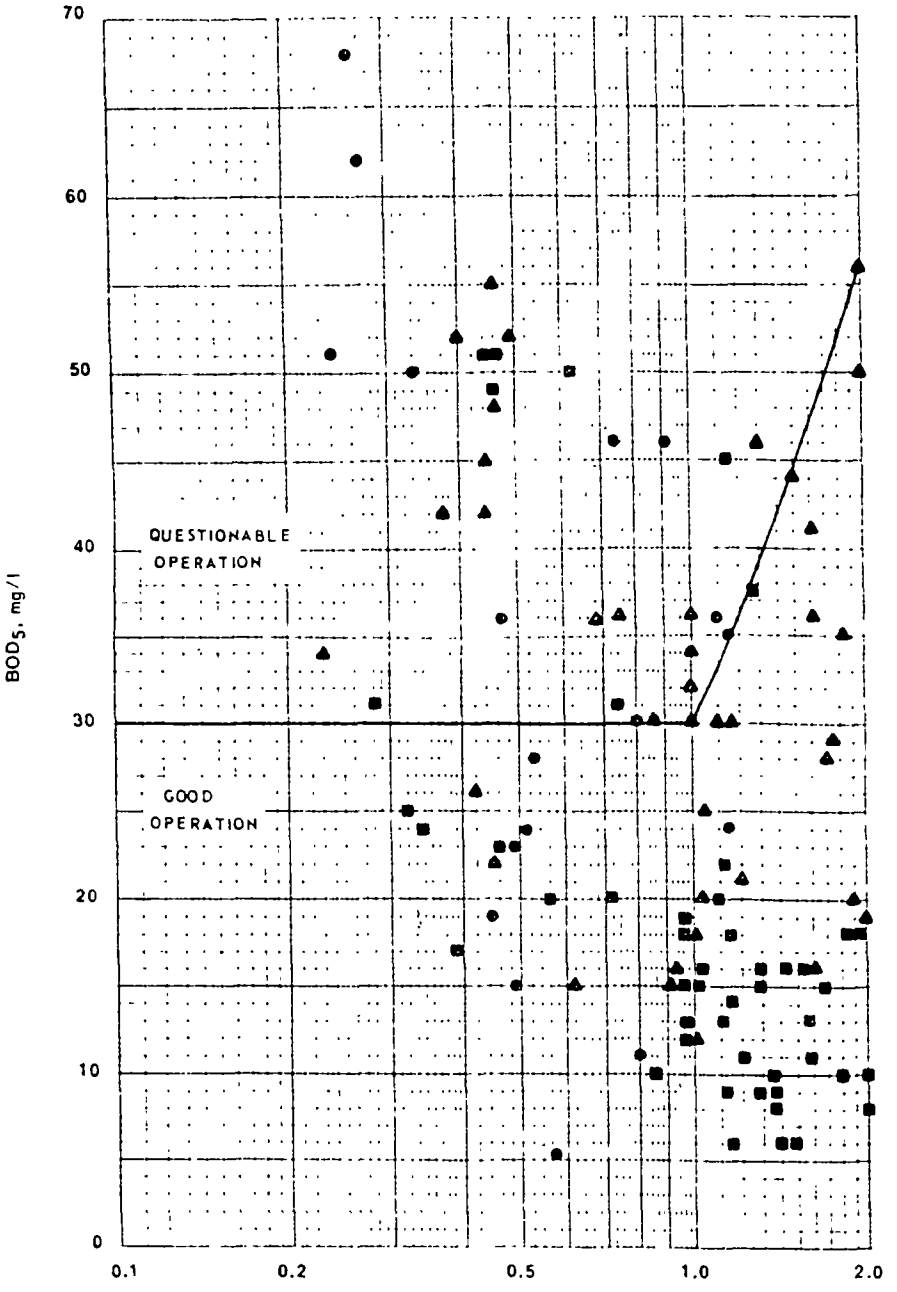

Figure 4. Conventional Activated Sludge, BOD_5

	NORMALIZED FLOW				
	<1.0				>1.0
	Total	Summer	Winter	Annual Ave.	
<60 mg/l BOD_5	98%	83%	99%		
< 50 mg/l	91%	83%	83%	99%	–
< 40 mg/l	78%	67%	67%	75%	–
< 30 mg/l	64%	50%	50%	75%	–

FIGURE 6-17

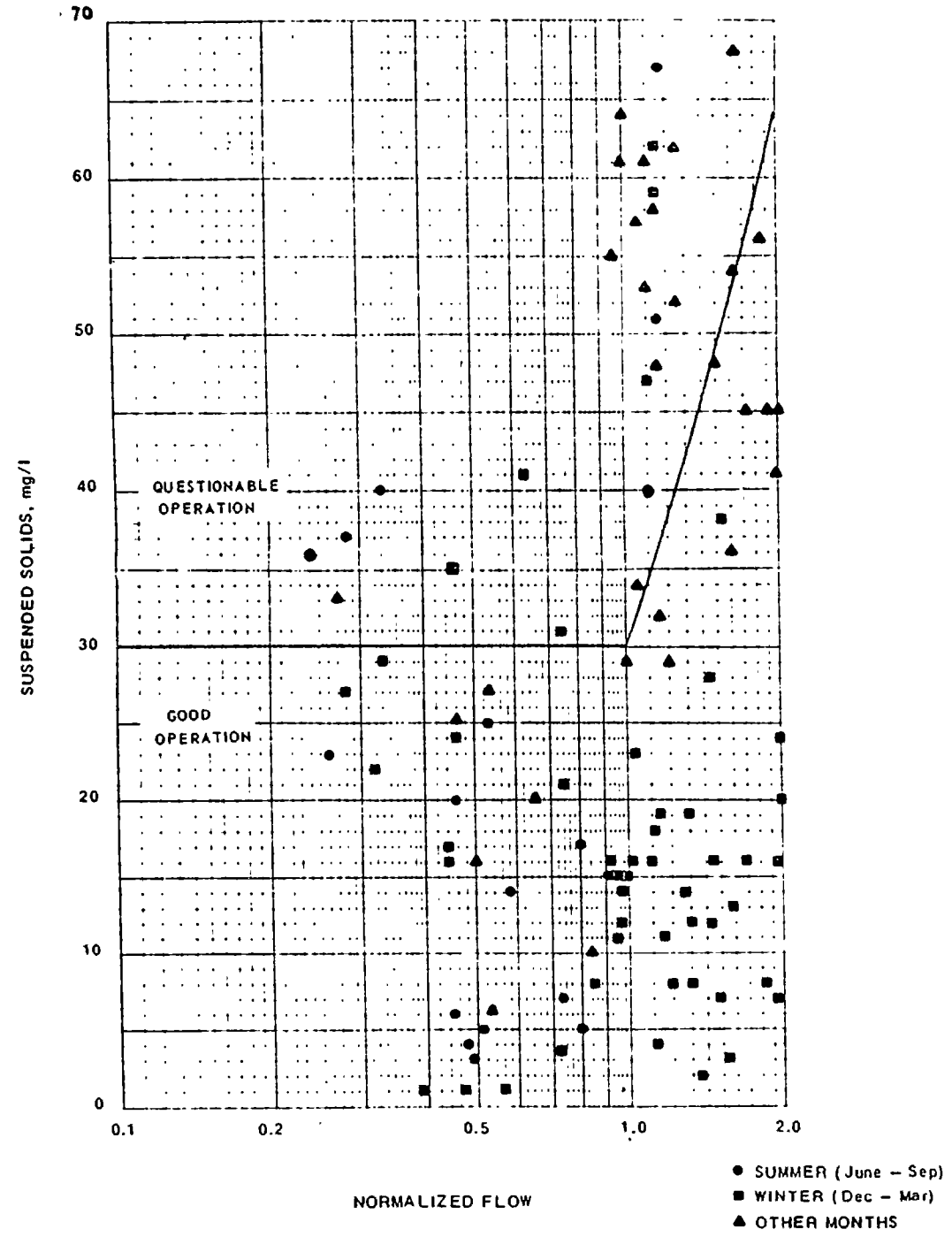

Figure 5. Conventional Activated Sludge, Suspended Solids

	NORMALIZED FLOW				
	<1.0				>1.0
	Total	Summer	Winter	Annual Ave.	
<60 mg/l BOD_5	99%				60%
<55 mg/l				99%	
<50 mg/l	97%		99%		20%
<40 mg/l	94%	99%	93%	91%	
<30 mg/l	79%	75%	79%	82%	

FIGURE 6-18

OPERATIONAL PROBLEMS

Operational problems at wastewater treatment plants can be caused by a wide variety of conditions including poor operation, deficiencies in the plant, waste characteristics and environmental conditions such as temperature. The most common operational problems experienced at wastewater treatment plants are generally related to the following:

(a) Inadequate Sludge Wasting

- high inventory of solids in clarifiers
- hign MLSS
- low F/M

(b) Inadequate Dissolved Oxygen

Other common process causes that contribute to poor performance of plants include

Hydraulic or Organic Overload
Shock Loadings
Inadequate Nutrients
Toxicity
Recycle Loads from Sludge Treatment

VARIABILITY/RELIABILITY

The ability of a treatment plant incorporating various treatment processes to reliably produce an effluent which does not exceed a maximum limit is determined by numerous factors some of which are listed in Table 6-5. Surveys and analysis of actual performance of treatment facilities have been done which clearly indicate that to meet a maximum week or maximum month discharge standard, the plant process must be designed to produce average concentrations significantly less than the standard. The selection of this value should be based on the risk and associated costs involved. As environmental limits are lowered and risk due to exceeding these limits increases, greater reliability is required which must be considered in the design bases, and ultimately both capital and operating costs. High expectation in effluent quality results in a need for additional or more sophisticated aparatus, special control systems, and in some cases increased treatment facilities including tertiary treatment units.

Niku, et. al. (1) studied thirty seven activated sludge plants and statistically analyzed one year's data. Table 6-6 illustrates the range in effluent BOD and solids concentrations found. For the plants studies, and the variability in effluent, to meet a given effluent limitation about 90% of the time, the long term mean effluent value (design) would have to be about 50% of the effluent limitation for SS and BOD.

Analyses of operating plant data by Hovey, et. al. for secondary treatment plants indicated that a plant would have to be designed for a long term average BOD of 17 mg/l in order to meet the secondary treatment standards of 30 mg/l as a MA30CD (maximum average 30 consecutive day) and 45 mg/l as a maximum 7 day average. Figure 6-19 graphically presents this analysis.

Figure 6-20 summarizes operational data at a meat processing plant (chicken) wen raw wastewater concentrations averaged about 1,200 mg/l. The extended aeration treatment plant with primary air flotation reduces BOD by more than 93%, however, roughly 30 percent of the time based on 30 day averages the plant exceeds permit limits. Generally the higher effluent concentrations exist during the cold temperature periods. Consideration of seasonal treatment is suggested when developing permit limits.

Figure 6-21 summarizes the performance of a lagoon treatment system for a pulp and paper wastewater located in the South. Treatment consists of a series of lagoons which provides greater than 40 days detention.

TABLE 6-5

FACTORS AFFECTING PLANT PERFORMANCE

1. Related to Waste Characteristics

   - Variability
     - diurnal
     - long term
     - seasonal
   - Industrial Contribution
     - slugs
     - toxicity
     - difficult to treat organics
   - Infiltration/Inflow
   - Temperature

2. Related to Design

   - Specific Treatment Processes
   - Design Parameters - margin for overloading
   - Spare/Emergency Capacity

3. Related to Plant Size - O&M

   - Accidents
   - Level of Expertise of Operators
   - Downtime for Repairs, Availability of Spare Parts
   - Response to Upsets/Problems
   - Financing

TABLE VII Percentile values of effluent BOD concentration.

Plant	Effluent BOD Percentiles						Normalized Percentiles					
	50%	80%	90%	95%	99%	100%	50%	80%	90%	95%	99%	100%
Port Huron	8	15	19	24	30	65	−0.24	0.72	1.27	1.82	2.28	7.57
Hyperion	8	12	14	17	21	25	−0.30	0.81	1.27	1.95	2.85	3.76
Central Sacramento	8	14	18	25	39	43	−0.30	0.41	1.11	2.19	4.06	4.95
Madison	15	24	32	42	57	76	−0.29	0.50	1.20	2.08	3.59	5.06
Calumet, Batt1	15	22	30	34	46	63	−0.35	0.62	1.19	1.92	3.21	5.05
Calumet, Batt2	13	23	30	35	41	60	−0.27	0.80	1.45	1.99	2.61	4.68
Calumet, Batt3	18	26	32	40	72	92	−0.28	0.41	0.91	1.63	4.41	6.15
Piscataway	12	21	29	39	56	202	−0.27	0.29	0.77	1.41	2.46	11.53
Johnson City	20	36	52	65	93	174	−0.21	0.59	1.21	1.79	3.09	6.65
Champion Papers	29	47	58	52	65	93	−0.12	0.57	1.26	1.86	2.98	5.22
Hastings	14	22	30	46	97	110	−0.27	0.21	0.70	1.66	4.73	5.51
Lower Potomac	15	20	25	30	42	52	−0.22	0.19	1.20	1.91	3.61	5.03
Tuscaloosa	13	25	34	36	62	92	−0.38	0.61	1.25	2.09	3.22	5.19
Hanover Park, A	16	37	44	63	93	212	−0.42	0.42	0.92	1.70	3.21	10.03
Hanover Park, B	16	32	58	70	105	170	−0.47	0.67	1.15	1.89	3.42	6.26
Pomona	5	6	8	10	14	16	0.01	0.44	1.23	2.03	3.63	4.42
Valencia	1	3	3	5	7	7	−0.68	0.76	1.45	2.20	3.61	3.61
San Jose Creek	2	3	3	4	4	4	−0.35	0.94	0.94	2.22	2.22	2.22
Long Beach	5	6	7	9	10	11	0.09	0.59	1.05	2.07	2.57	3.06
WSW Chicago A	7	11	13	15	18	20	−0.19	0.87	1.40	1.93	2.73	3.26
WSW Chicago B	4	6	7	8	14	18	−0.10	0.74	1.56	3.56	4.38	5.76
WSW Chicago C	4	6	7	8	11	11	−0.13	0.86	1.35	1.84	3.32	3.79
WSW Chicago D	4	4	5	7	9	10	−0.02	0.60	1.19	2.35	3.53	4.11
Delta Township 74	15	31	60	90	112	130	−0.35	0.52	1.52	2.43	3.25	4.26
Delta Township 75	10	16	24	30	47	61	−0.42	0.57	1.25	1.90	3.75	5.33
Delta Township 75	9	12	15	18	25	28	−0.01	0.67	1.35	2.01	3.03	3.31
Delta Township 76	12	17	21	25	32	35	−0.09	0.68	1.30	1.77	3.00	3.95
Delta Township 77	15	19	23	25	29	35	−0.12	0.79	1.35	1.71	2.21	3.20
East Lansing, N	2	7	10	13	16	24	−0.60	0.72	1.50	1.77	3.05	5.19
East Lansing, S	4	9	14	19	24	26	−0.35	0.53	1.31	2.29	3.57	3.52
Rocky Hill	9	13	17	29	45	50	−0.22	0.26	0.73	2.15	4.55	4.62
San Jose, Santa Clara	24	33	37	42	46	50	−0.40	0.91	1.32	1.65	2.23	2.65
Sidney	14	25	38	51	60	95	−0.31	0.62	1.21	2.01	2.59	4.94
Reno	8	13	16	19	23	40	−0.35	0.81	1.38	1.95	2.90	5.96
Topeka	25	44	60	70	155	248	−0.21	0.46	1.03	1.41	4.55	7.97
Renton	5	11	14	17	20	21	−0.37	0.91	1.56	2.20	2.84	3.05
San Bernardino	20	30	37	44	55	120	−0.08	0.70	0.25	1.60	2.66	7.75
					Average		−0.23	0.63	1.22	1.93	3.25	5.25

TABLE VIII. Percentile values of effluent SS concentration

Plant	Effluent SS Percentiles						Normalized Percentiles					
	50%	80%	90%	95%	99%	100%	50%	80%	90%	95%	99%	100%
Port Huron	7	16	21	26	62	120	−0.31	0.39	0.78	1.33	3.98	10.84
Hyperion	6	8	9	11	14	30	−0.13	0.65	1.02	1.76	2.88	8.82
Central Sacramento	11	16	20	23	26	28	−0.12	0.75	1.19	1.81	2.49	2.93
Madison	19	36	50	61	113	158	−0.32	0.45	1.09	1.73	3.97	6.01
Calumet, Batt1	17	26	36	46	86	115	−0.27	0.51	0.95	1.58	4.13	7.90
Calumet, Batt2	18	28	34	45	95	139	−0.24	0.38	0.75	1.43	4.72	7.26
Calumet, Batt3	11	21	32	38	110	213	−0.26	0.20	0.72	1.10	4.10	9.24
Piscataway	15	25	36	65	123	224	−0.23	0.15	0.57	1.66	3.81	7.65
Johnson City	23	56	101	130	220	422	−0.32	0.65	1.22	1.96	3.61	5.70
Champion Papers	56	71	80	93	114	150	−0.15	0.65	1.13	1.84	2.95	4.87
Hastings	6	11	17	36	76	186	−0.25	0.01	0.38	1.16	3.66	10.01
Lower Potomac	12	20	26	31	53	136	−0.23	0.16	0.98	1.31	3.10	10.50
Tuscaloosa	10	21	35	46	75	115	−0.25	0.37	1.21	1.86	3.60	7.67
Hanover Park, A	20	45	63	119	211	535	−0.35	0.23	0.61	1.76	3.69	10.46
Hanover Park, B	15	35	71	96	160	244	−0.38	0.29	1.35	1.29	3.87	6.31
Pomona	5	7	9	11	13	23	0.12	0.56	1.25	1.93	2.61	6.02
Valencia	1	3	7	9	13	22	−0.35	1.27	1.51	2.25	3.63	6.75
San Jose Creek	4	6	8	8	11	12	−0.23	0.71	1.65	1.65	3.06	3.52
Long Beach	8	11	13	16	19	24	−0.05	0.71	1.22	1.98	2.75	4.02
WSW Chicago, A	6	8	10	13	23	56	−0.22	0.22	0.77	1.34	3.58	19.96
WSW Chicago B	6	8	10	12	18	30	−0.07	0.24	1.0	1.54	3.15	9.17
WSW Chicago C	5	7	9	11	17	27	−0.25	1.39	1.91	1.69	3.63	6.87
WSW Chicago D	3	5	6	7	11	15	−0.50	0.69	1.25	1.67	3.15	5.62
Delta Township 74	10	28	45	63	95	220	−0.33	36	1.01	1.76	3.03	8.01
Delta Township 75	10	16	20	26	51	151	−0.15	0.32	0.61	1.11	3.31	10.95
Delta Township 75	8	11	17	22	28	55	−0.26	0.65	1.15	1.93	2.87	6.95
Delta Township 76	8	12	17	20	26	30	−0.16	0.56	1.17	2.01	3.10	3.84
Delta Township 77	7	13	16	21	35	62	−0.27	0.56	0.95	1.67	4.03	7.36
East Lansing, N	9	14	17	20	29	37	−0.17	0.69	1.21	1.73	3.26	3.66
East Lansing, S	8	15	19	23	30	35	−0.29	0.70	1.26	1.83	2.84	6.33
Rocky Hill	10	14	16	19	23	38	−0.19	0.65	1.06	1.69	2.73	7.74
San Jose, Santa Clara	22	30	36	43	52	62	−0.23	0.63	1.50	2.01	3.01	4.09
Sidney	18	30	38	48	75	111	−0.23	0.50	0.93	1.60	3.43	5.64
Reno	14	20	24	27	35	73	−0.10	0.65	1.20	1.60	3.01	7.57
Topeka	21	56	86	115	177	261	−0.38	0.51	1.33	2.15	3.73	6.63
Renton	6	10	12	14	22	27	−0.33	0.70	1.22	1.74	3.80	5.10
San Bernardino	14	35	43	47	56	61	−0.34	1.08	1.49	1.93	2.66	2.87
					Average		−0.25	0.52	1.05	1.72	3.40	6.93

percentiles Z_{1-p} of the standard normal distribution that is the number of standard deviations by which X differs from the mean.

Values of the *COK* for effluent concentrations for different coefficients of variation at different levels of reliability are given in Table V.

The results shown in Table V have a significant potential application in design. Values of *COK* given in Table V may be used in design of a treatment plant expected to perform a certain reliability. The coefficient of variation for effluent concentration should be estimated. Selection of the appropriate design value of the coefficient of variation C_X must be based on reasonable expectation of performance that is experienced just as are other design parameters now in use (for example, hydraulic residence time and overflow rate). This may be done from past experience or using the results from other similar treatment plants. Values of coefficient of variation for effluent BOD and SS for some treatment plants are given in Table II. Implications derived from Table V are best described by an example.

> To have 95% reliability that effluent BOD concentration is equal to or less than a certain standard X_s when C_X for the plant is estimated to be 0.70, the plant should be designed for the mean value equal to or less than 0.43 X_s. (If X_s = 30 mg/l, then average BOD = 0.43 × 30 = 12.9 mg/l or less. Similarly, for a less stringent standard of X_s = 40 mg/l, average BOD = 0.43 × 40 = 17.2 mg/l or less.)

As would be expected, the mean value of required effluent concentration varies inversely with reliability level and with the coefficient of variation in effluent concentration.

The relationships in Table V can be viewed in a slightly different context by reading Table VI. Here the fractional reliability for effluent concentration is presented as a function of C_X and the mean to standard concentration ratio (note that this ratio is equal to *COK* values). Results from Table VI may be used to estimate the reliability of a treatment plant under operation if the mean and standard deviation for the plant is known. For example, there is 87% reliability in a plant operating with a mean value of 0.6 X_s and a C_X = 0.70. In other words, in a long run operation, about 13% of the observed effluent variables would exceed 30 mg/l in a plant operating with mean value of 18 mg/l and standard deviation of 12.6 (C_X = 0.70). Table VI has been constructed based on percentiles Z_{1-p}.

$$Z_{1-p} = -\frac{\ln\left[\frac{m_X}{X_s}\left(1+C_X^2\right)^{-1}\right]}{\left[\ln\left(1+C_X^2\right)\right]^{0.5}} \qquad (18)$$

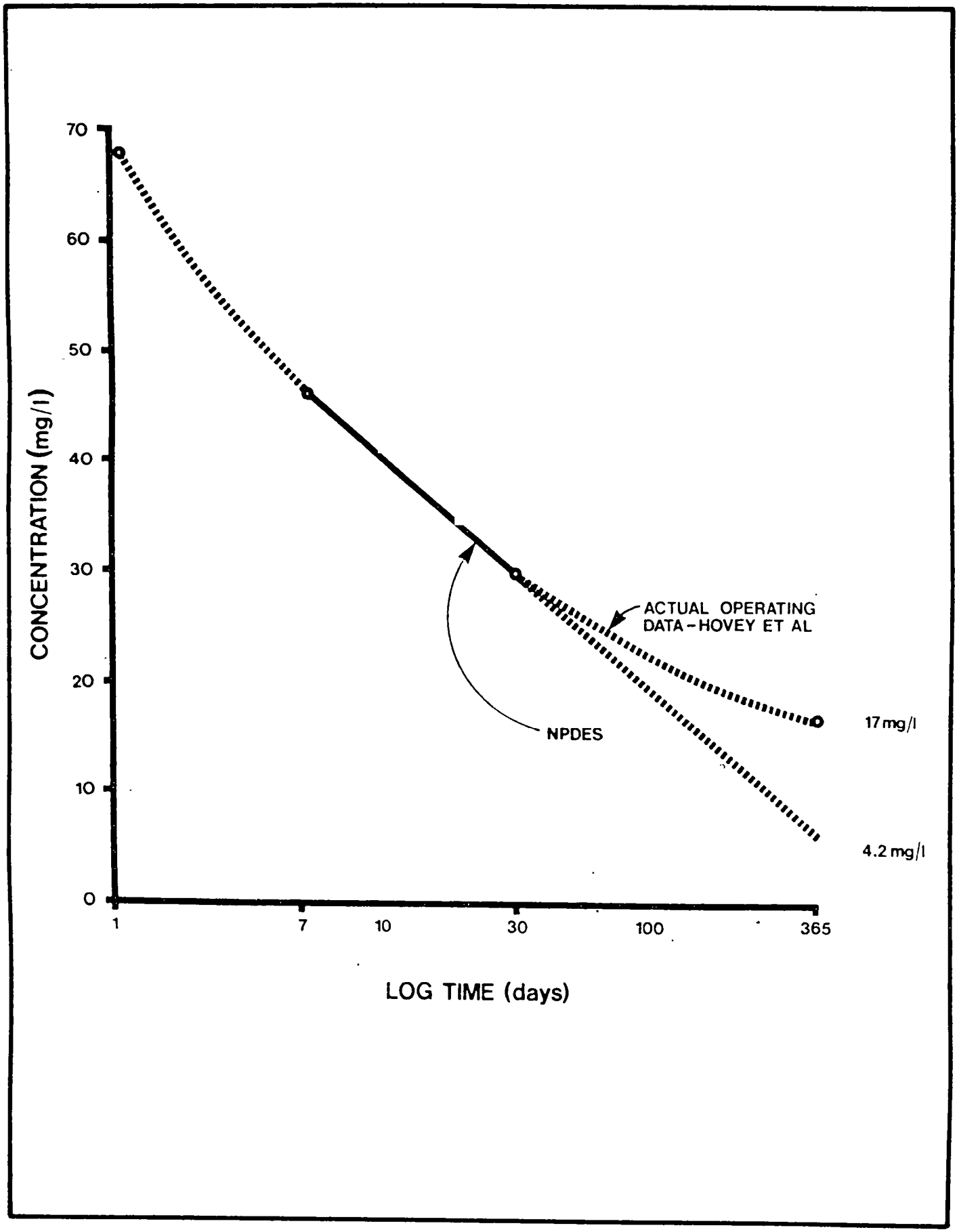
70
60
50
40
30
20
10
0
CONCENTRATION (mg/l)
1
7
10
30
100
365
LOG TIME (days)
ACTUAL OPERATING DATA - HOVEY ET AL
NPDES
17 mg/l
4.2 mg/l

FIGURE 6-19

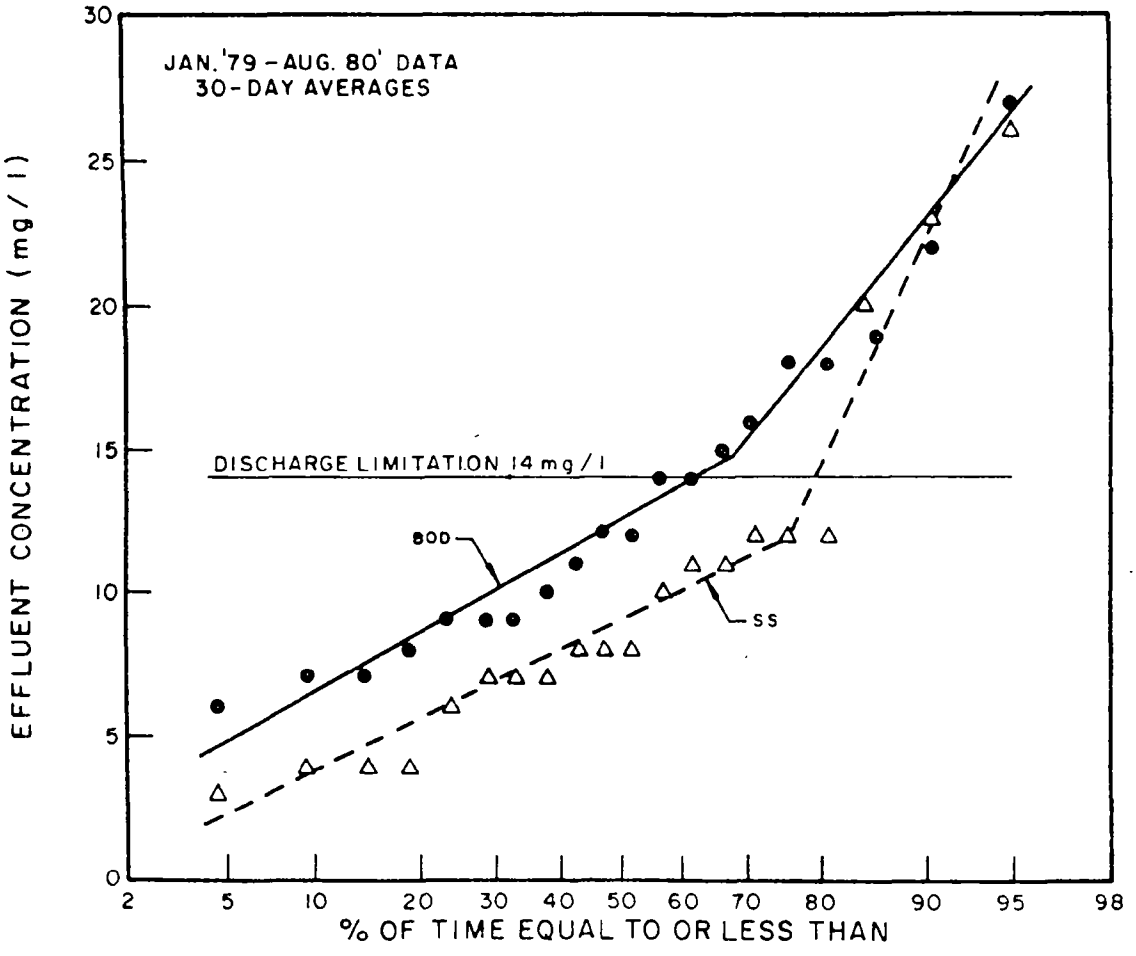

FIGURE 6-20

VARIABILITY IN EFFLUENT BOD AND SS

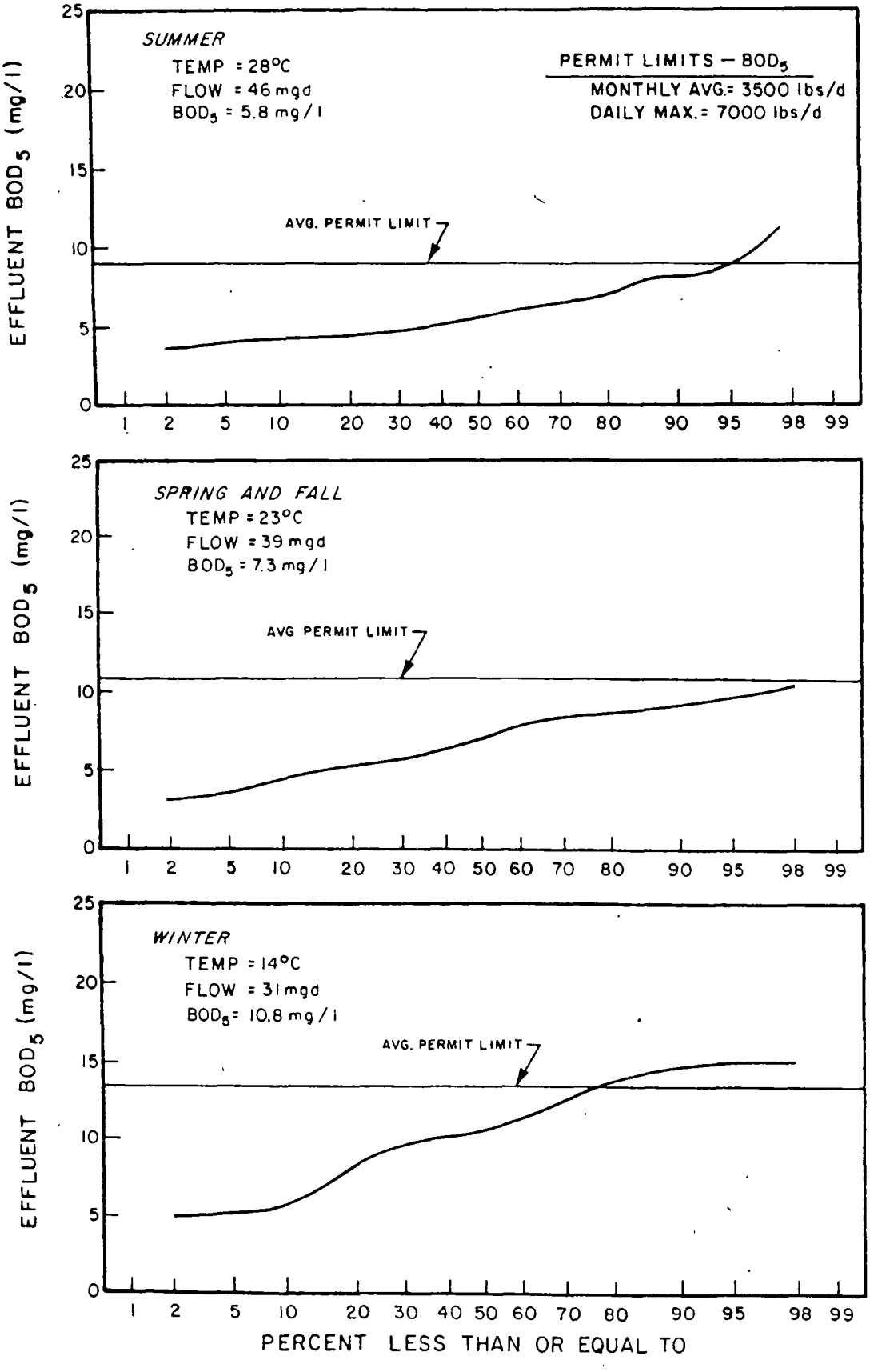

FIGURE 6-21

EFFLUENT BOD_5 BY SEASON

JUNE 1, 1979 — MAY 31, 1980

A Statistical Documentation of the Performance of Activated Sludge and Activated Stabilization Basin Systems Operating in the Paper Industry by the National Council of Air and Stream Impact 29th Purdue Industrial Wastes Conference 1974 was conducted. This study looked at 53 treatment systems in 7 manufacturing processes classifications. Figures 6-22 and 6-23 summarize the ratio between long term average effluent and 30 day average and maximum day for which permit standards are typically set.

The recently requested GAO survey of 242 randomly selected municipal plants found that 87% of the plants violated their NPDES permit for at least one month in the year, and 31% were in serious violation (exceeded permit limit in at least one category BOD TSS or fecal coliform for more than 4 consecutive months). Non-compliance was attributed to various factors including deficiencies in design (inadequate capacity) operation and maintenance, and equipment, and overloading by infiltration/inflow or industrial wastes. Non compliance was not related to potentially unrealistically low permit limitations. While the serious violations undoubtedly should be rectifiable, more consideration might be given to the problem of the occasional violation, and its significance with respect to effect on a receiving stream and the cost to increase reliability to the point that such violations are rare. This would be part of realistic overall allocation of loads based on water quality requirements, treatment capability, cost factors and various other tangible and intangible factors effecting treatment performance.

A study conducted for the EPA, "Evaluation of Operation and Maintenance Factors Limiting Biological Wastewater Treatment Plant Performance" (EPA 4002-79-078) reviewed thirty plants to determine causitive factors of limited performance. Table 6-7 presents actual performance data for the plants studied. Numerous problems in areas of design capacity, operation and maintenance were identified. Major problems were improper operator application of concepts and testing to process control, infiltration and inflow and industrial loading. It was estimated that compliance with NPDES permit limitations could be significantly increased as a result of implementing improvements in operational practices. Figure 6-24 from this report related O/M unit cost to size of plant.

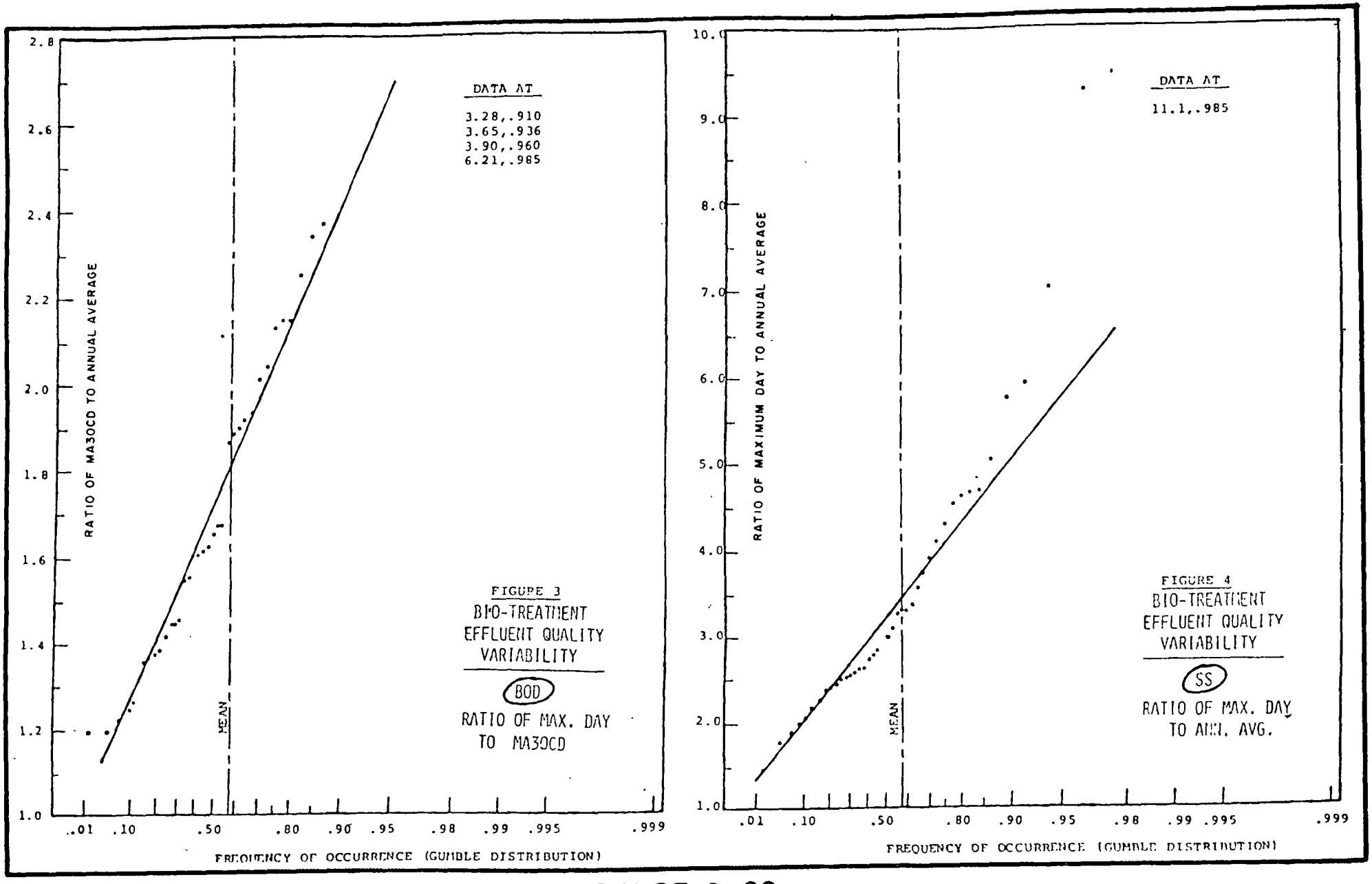
RATIO OF MA30CD TO ANNUAL AVERAGE
DATA AT
3.28,.910
3.65,.936
3.90,.960
6.21,.985
MEAN
FIGURE 3
BIO-TREATMENT
EFFLUENT QUALITY
VARIABILITY
BOD
RATIO OF MAX. DAY
TO MA30CD
FREQUENCY OF OCCURRENCE (GUMBLE DISTRIBUTION)
RATIO OF MAXIMUM DAY TO ANNUAL AVERAGE
DATA AT
11.1,.985
MEAN
FIGURE 4
BIO-TREATMENT
EFFLUENT QUALITY
VARIABILITY
SS
RATIO OF MAX. DAY
TO ANN. AVG.
FREQUENCY OF OCCURRENCE (GUMBLE DISTRIBUTION)

FIGURE 6-22

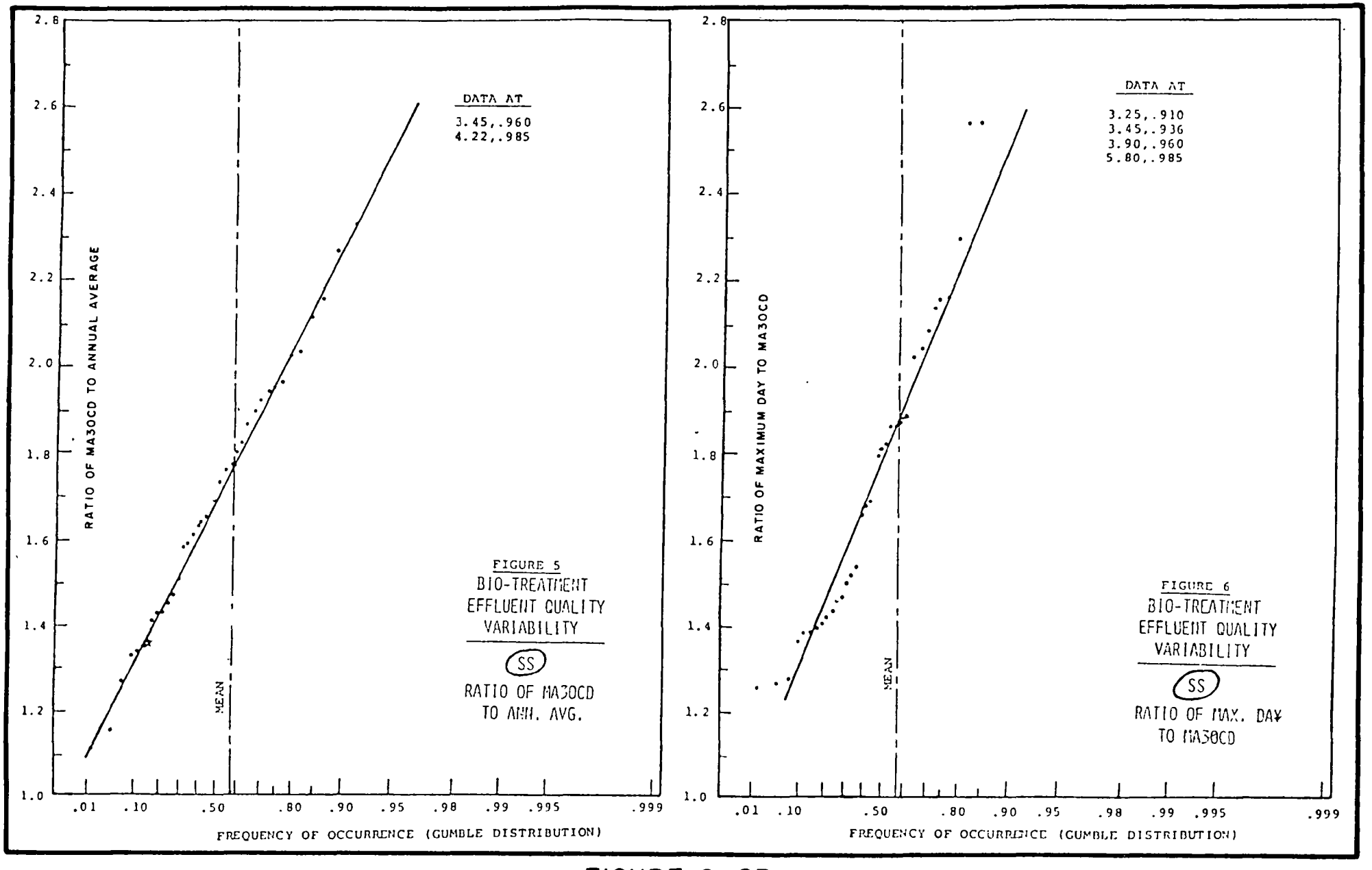
RATIO OF MA30CD TO ANNUAL AVERAGE
2.8
2.6
2.4
2.2
2.0
1.8
1.6
1.4
1.2
1.0
DATA AT
3.45,.960
4.22,.985
MEAN
.01 .10 .50 .80 .90 .95 .98 .99 .995 .999
FREQUENCY OF OCCURRENCE (GUMBLE DISTRIBUTION)
FIGURE 5
BIO-TREATMENT
EFFLUENT QUALITY
VARIABILITY
SS
RATIO OF MA30CD
TO ANN. AVG.
RATIO OF MAXIMUM DAY TO MA30CD
DATA AT
3.25,.910
3.45,.936
3.90,.960
5.80,.985
FIGURE 6
BIO-TREATMENT
EFFLUENT QUALITY
VARIABILITY
SS
RATIO OF MAX. DAY
TO MA30CD

FIGURE 6-23

TABLE 6-7

TABLE 15. CURRENT ANNUAL EFFLUENT CHARACTERISTICS OF PRELIMINARY EVALUATION PLANTS

Plant No.	Average Flow (m^3/d)	Average Flow (mgd)	Average BOD_5 Conc. (mg/l)	Average BOD_5 Load. (Kg/day)	Average BOD_5 Load. (lb./day)	Average S. S. Conc. (mg/l)	Average S. S. Load (Kg/day)	Average S. S Load (lb./day)	NPDES Permit Compliance BOD	NPDES Permit Compliance S.S
042	1,320	0.35	28	36	80	52	68	150	Yes	No
037	1,930	0.51	16	32	70	48	93	205	Yes	No
102	(N/A)	(N/A)	(N/A)	(N/A)	(N/A)	(N/A)	(N/A)	(N/A)	-	-
005	570	0.15	14	9	20	33	18	40	Yes	No
086	1,480	0.39	30	45	100	33	48	105	Yes	No
052	11,360	3.0	12	136	300	21	238	525	No	No
059	34,820	9.2	32	1,113	2,455	35	1,218	2,685	No	No
024	4,920	1.3	17	84	185	49	243	535	Yes	No
038	17,030	4.5	95	1,617	3,565	37	630	1,390	Yes	Yes
093	22,330	5.9	22	490	1,080	41	914	2,015	Yes	No
082	4,240	1.12	16	68	150	26	127	280	Yes	Yes
006	2,080	0.55	22	45	100	21	43	95	Yes	Yes
048	15,330	4.05	35	535	1,180	59	905	1,995	No	No
089	1,400	0.37	15	20	45	47	66	145	Yes	No
095	1,140	0.30	36	41	90	24	27	60	No	Yes
120	10,500	2.72	5	52	115	10	105	231	Yes	Yes
034	1,210	0.32	22	27	60	30	36	80	Yes	Yes
068	1,850	0.49	8	16	35	21	39	86	Yes	Yes
071	4,350	1.15	107	465	1,025	30	132	290	No	Yes
077	4,540	1.2	29	132	290	19	86	190	Yes	Yes
021	3,330	0.88	6	20	45	7	23	50	Yes	Yes
026	24,980	6.6	37	925	2,035	62	1,549	3,415	Yes	No
046	910	0.24	30	27	60	19	17	38	Yes	Yes
114	40,500	10.7	7	284	625	10	404	890	Yes	Yes
106	11,810	3.12	25	295	650	44	519	1,145	Yes	No
053	8,330	2.2	22	184	405	25	209	460	Yes	Yes
074	2,460	0.65	38	93	205	23	56	124	No	Yes
083	33,420	8.83	12	401	885	25	836	1,842	Yes	No
066	1,250	0.33	15	18	40	21	25	55	Yes	Yes
078	3,330	0.88	25	84	185	15	50	110	Yes	Yes
	272,520	72.0	26.8	7,294	16,080	32.0	8,725	19,235		

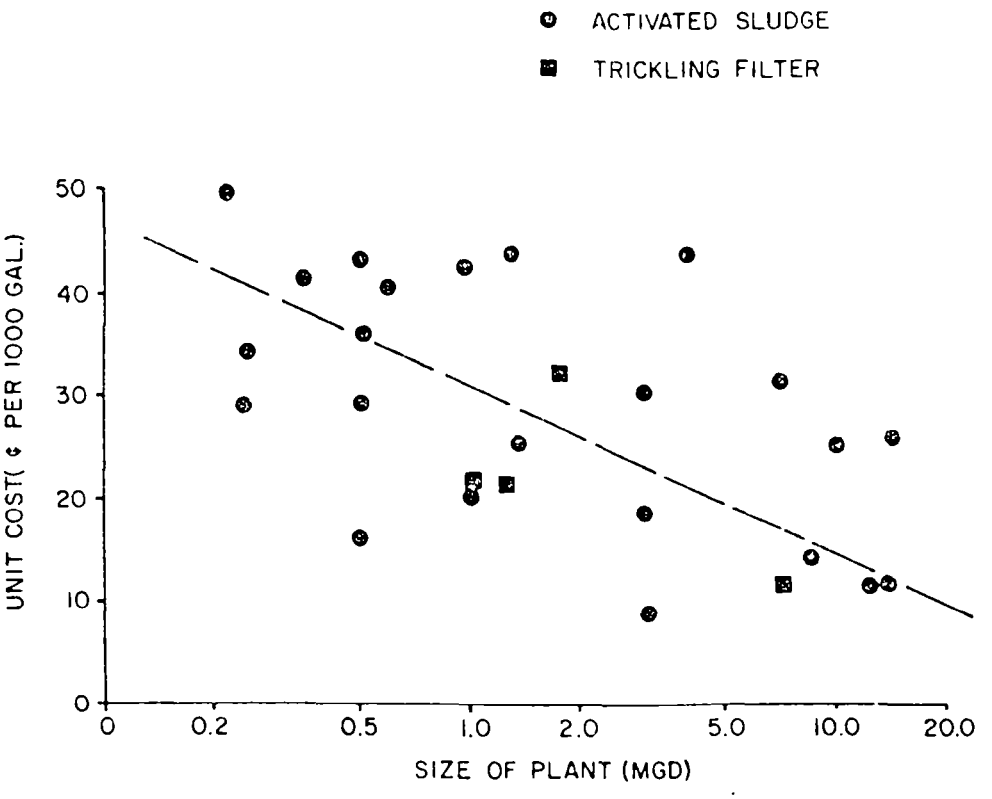

FIGURE 6-24

RELATIONSHIP BETWEEN OPERATION AND MAINTENANCE EXPENDITURES AND DESIGN PLANT FLOW

References:

(1) Performance of Activated Sludge Process and Reliability Based Design, JWPCF, Dec. 1979.

JWPCF Monitor-GAO Survey Finds Extensive Treatment Plant Non-compliance, p. 137, February 1981.

I. MAJOR NITROGEN REMOVAL PROCESSES

The major processes considered in this manual are nitrification-denitrification, breakpoint chlorination (or superchlorination), selective ion exchange for ammonium removal, and air stripping for ammonia removal (ammonia stripping). These are the processes which are technically and economically most viable at the present time.

Biological Nitrification-Denitrification

Biological nitrification does not increase the removal of nitrogen from the waste stream over that achieved by conventional biological treatment. The principal effect of the nitrification treatment process is to transform ammonia-nitrogen to nitrate. The nitrified effluent can then be denitrified biologically. Nitrification is also used without subsequent biological denitrification when treatment requirements call for oxidation of ammonia-nitrogen in the secondary stage or is removed by another process. Nitrification can be carried out in conjunction with secondary treatment or in a tertiary stage; in both cases, either suspended growth reactors (activated sludge) or attached growth reactors (such as trickling filters) can be used.

Biological denitrification can also be carried out in either suspended growth or attached growth reactors. As previously noted, an anoxic environment is required for the reactions to proceed. Overall removal efficiency in a nitrification-denitrification plant can range from 70 to 95 percent.

Breakpoint Chlorination

Breakpoint chlorination (or superchlorination) is accomplished by the addition of chlorine to the waste stream in an amount sufficient to oxidize ammonia-nitrogen to nitrogen gas. After sufficient chlorine is added to oxidize the organic matter and other readily oxidizable substances present, a stepwise reaction of chlorine with ammonium takes place. The overall theoretical reaction is as follows:

$$3Cl_2 + 2NH_4^+ \longrightarrow N_2 + 6HCl + 2H^+$$

In practice, approximately 10 mg/l of chlorine is required for every 1 mg/l of ammonia-nitrogen. In addition, acidity produced by the reaction must be neutralized by the addition of caustic soda or lime. These chemicals add greatly to the total

dissolved solids and result in a substantial operating expense. Often dechlorination is utilized following breakpoint chlorination in order to reduce the toxicity of the chlorine residual in the effluent.

An important advantage of this method is that ammonia-nitrogen concentrations can be reduced to near zero in the effluent. The effect of breakpoint chlorination on organic nitrogen is uncertain, with contradictory results presented in the literature. Nitrite and nitrate are not removed by this method.

Selective Ion Exchange for Ammonium Removal

Selective ion exchange for removal of ammonium from wastewater can be accomplished by passing the wastewater through a column of clinoptilolite, a naturally occurring zeolite which has a high selectivity for ammonium ion. The first extensive study was undertaken in 1969 by Battelle Northwest in a federally sponsored demonstration project. Regeneration of the clinoptilolite is undertaken when all the exchange sites are utilized and breakthrough occurs.

Filtration prior to ion exchange is usually required to prevent fouling of the zeolite. Ammonium removals of 90-97 percent can be expected. Nitrite, nitrate, and organic nitrogen are not affected by this process.

Air Stripping for Ammonia Removal

Ammonia in the molecular form is a gas which dissolves in water to an extent controlled by the partial pressure of the ammonia in the air adjacent to the water. Reducing the partial pressure causes ammonia to leave the water phase and enter the air. Ammonia removal from wastewater can be effected by bringing small drops of water in contact with a large amount of ammonia-free air. This physical process is termed desorption, but the common name is "ammonia stripping."

In order to strip ammonia from wastewater, it must be in the molecular form (NH_3) rather than the ammonium ion (NH_4^+) form. This is accomplished by raising the pH of the wastewater to 10 or 11, usually by the addition of lime. Because lime addition is often used for phosphate removal, it can serve a dual role. Again, nitrite, nitrate, and organic nitrogen are not affected.

The principal problems associated with ammonia stripping are its inefficiency in cold weather, required shutdown during freezing conditions, and formation of calcium carbonate scale in the air stripping tower.

The effect of cold weather has been well documented at the South Lake Tahoe Public Utility District where ammonia stripping is used for a 3.75 mgd tertiary facility. The stripping tower is designed to remove 90 percent of the incoming ammonium during warm weather. During freezing conditions, the tower is shut down. One mechanism of scale formation is attributed t the carbon dioxide in the air reacting with the alkaline wastewater and precipitating as calcium carbonate. In some instances, removal with a water jet has been possible; in other applications the scale has been extremely difficult to remove. Some factors which may affect the nature of the scale are: orientation of air flow, recirculation of sludge, pH of the wastewater, and chemical makeup of the wastewater.

Other Nitrogen Removal Processes

In addition to the processes listed above, there are other methods for nitrogen removal which might usefully be discussed. Most are in the experimental stage of development or occur coincidentally with another process.

Use of anionic exchange resins for removal of nitrate was developed principally for treatment of irrigation return waters. Two major unsolved problems are the lack of resins which have a high selectivity for nitrate over chloride and disposal of nitrogen-laden regenerants.

Oxidation ponds can remove nitrogen through microbial denitrification in the anaerobic bottom layer or by ammonia emission to the atmosphere. The latter effect is essentially ammonia stripping but is relatively inefficient due to a low surface-volume ratio and low pH. In a study of raw wastewater lagoons in California, removals of 35-85 percent were reported for well-operated lagoons.

Nitrogen in oxidation ponds is assimilated by algal cultures. If the algal cells are removed from the pond effluent stream, nitrogen removal is thereby effected. Methods for removal of algae are summarized in the EPA Technology Transfer Publication, Upgrading Lagoons.

It was noted previously that in secondary biological treatment and in nitrification, some nitrogen is incorporated in bacterial cells and is removed from the waste stream with the sludge. If an organic carbon source such as ethanol or glucose is added to the wastewater, the solids production will be increased and a greater nitrogen removal will be effected. Disadvantages are that large quantities of sludge are produced and that difficulties occur in regulating the addition of the

carbon source, with high effluent BOD_5 values or high nitrogen levels resulting.

Summary

Table 6-8 summarizes the effect of various treatment processes on nitrogen removal. Shown is the effect that the process has on each of the three major forms: organic nitrogen, ammonium, and nitrate. In the last column is shown normal removal percentages which can be expected from that process. Overall removal for a particular treatment plant will depend on the types of unit processes and their relation to each other. For example, while many processes developed for nitrogen removal are ineffective in removing organic nitrogen, incorporation of chemical coagulation or multimedia filtration into the overall flowsheet can result in a low concentration of organic nitrogen in the plant effluent. Thus, the interrelationship between processes must be carefully anlyzed in designing for nitrogen removal.

TABLE 6-8

EFFECT OF VARIOUS TREATMENT PROCESSES ON NITROGEN COMPOUNDS

Treatment process	Effect on constituent			Removal of total nitrogen entering process, percent[a]
	Organic N	NH_3/NH_4^+	NO_3^-	
Conventional treatment processes				
Primary	10-20% removed	no effect	no effect	5-10
Secondary	15-25% removed[b] urea → NH_3/NH_4^+	10% removed	nil	10-20
Advanced wastewater treatment processes				
Filtration[c]	30-95% removed	nil	nil	20-40
Carbon sorption	30-50% removed	nil	nil	10-20
Electrodialysis	100% of suspend organic N removed	40% removed	40% removed	35-45
Reverse osmosis	100% of suspend organic N removed	85% removed	85% removed	80-90
Chemical coagulation[c]	50-70% removed	nil	nil	20-30
Land application				
Irrigation	→ NH_3/NH_4^+	→ NO_3^- → plant N	→ plant N	40-90
Infiltration/percolation	→ NH_3/NH_4^+	→ NO_3^-	→ N_2	0-50
Major nitrogen removal processes				
Nitrification	limited effect	→ NO_3^-	no effect	5-10
Denitrification	no effect	no effect	80-98% removed	70-95
Breakpoint chlorination	uncertain	90-100% removed	no effect	80-95
Selective ion exchange for ammonium	some removal, uncertain	90-97% removed	no effect	80-95
Ammonia stripping	no effect	60-95% removed	no effect	50-90
Other nitrogen removal processes				
Selective ion exchange for nitrate	nil	nil	75-90% removed	70-90
Oxidation ponds	partial transformation to NH_3/NH_4^+	partial removal by stripping	partial removal by nitrification-denitrification	20-90
Algae stripping	partial transformation to NH_3/NH_4^+	→ cells	→ cells	50-80
Bacterial assimilation	no effect	40-70% removed	limited effect	30-70

[a] Will depend on the fraction of influent nitrogen for which the process is effective, which may depend on other processes in the treatment plant.

[b] Soluble organic nitrogen, in the form of urea and amino acids, is substantially reduced by secondary treatment.

[c] May be used to remove particulate organic carbon in plants where ammonia or nitrate are removed by other processes

2.6 References

1. Sawyer, C.N., and P.L. McCarty, *Chemistry for Sanitary Engineers.* New York, McGraw-Hill Book Co., 1967.

2. Christensen, M.H., and P. Harremoes, *Biological Denitrification in Wastewater Treatment.* Report 2-72, Department of Sanitary Engineering, Technical University of Denmark, 1972.

3. Delwiche, C.C., *The Nitrogen Cycle* Scientific American, 223, No. 3, pp 137-146 (1970).

4. Martin, D.M., and D.R. Goff, *The Role of Nitrogen in the Aquatic Environment.* Report No. 2, Department of Limnology, Academy of Natural Sciences of Philadelphia, 1972.

5. Sepp, E., *Nitrogen Cycle in Groundwater.* Bureau of Sanitary Engineering, State of California Department of Public Health, 1970.

6. McCarty, P.L., *et al., Sources of Nitrogen and Phosphorus in Water Supplies.* JAWWA, 59, pp 344 (1967).

7. Sylvester, R.O., *Nutrient Content of Drainage Water for Forested, Urban, and Agricultural Areas.* Algae and Metropolitan Wastes, Robert A. Taft Sanitary Engineering Center, Tech. Rep. W61-3, 1963.

8. Reeves, T.G., *Nitrogen Removal: A Literature Review.* JWPCF, 44, No. 10, pp 1896-1908 (1972).

9. *Nitrogenous Compounds in the Environment.* Hazardous Materials Advisory Committee (to the EPA), EPA-ASB-73-001, December, 1973.

10. Kaufman, W.J., *Chemical Pollution of Ground Waters.* JAWWA, 66, No. 3, pp 152-159 (1974).

11. Weibel, S.R., Anderson, R.J., and R.L. Woodward, *Urban-Land Runoff as a Factor in Stream Pollution.* JWPCF, 43, p 2033 (1971).

12. American Public Works Association, *Water Pollution Aspects of Urban Runoff.* FWPCA Report No. WP-20-15, January, 1969.

13. Burn, R.J., Krawczyk, D.F., and G.T. Harlow, *Chemical and Physical Comparison of Combined and Separated Sewer Discharges.* JWPCF, 40, pp 112 (1968).

14. Avco Economic Systems Corporation, *Storm Water Pollution From Urban Land Activity.* EPA Report No. 11034 FKL 07/70, July, 1970.

15. Weibel, S.R., *et al., Pesticides and Other Contaminants in Rainfall and Runoff.* JAWWA, 58, pp 1075 (1966).

16. Dept. of Biological and Agricultural Engineering, North Carolina State University at Raleigh, *Role of Animal Wastes in Agricultural Land Runoff.* EPA Report No. 13020 DGX 08/71, August 1971.

17. California Department of Water Resources, *Nutrients From Tile Drainage Systems.* EPA Report No. 13030 ELY 5/71-3, May 1971.

Biological Nitrification

$$NH_4^+ + O_2 + HCO_3^- \text{---> } C_5H_7NO_2 + H_2O + NO_3^- + H_2CO_3$$

1. Oxygen Required $\tilde{-}$ 4.5 lbs O_2/NO_3-N produced

2. Sludge Yield

   Nitrosomonas $\quad$ 0.04 - 0.13 lbs VSS/lb NH_3 oxid.

   Nitrobacter $\quad$ .02 - 0.07 lbs VSS/lb NO_2 oxid.

3. Alkalinity Destroyed

   7.14 mg Alk. per mg NH_4^+-N oxidized

4. pH ---> 6.5 to 8.5

5. Temperature

   $k_T = k_{20}\theta^{T-20}$

   θ = 1.1 t0 1.3 Activated Sludge

6. Sludge Age - (Figure 6-26)

   6 - 10 Days @ 20°C

Nitrification of municipal wastewaters can readily be accomplished in single or 2 stage activated sludge plants and in low rate trickling filters. Figures 6-27 and 6-28 show the treatment of 32 mgd in a single stage activated sludge plant and of 4 mgd in a low rate trickling filter plant at Flint, Michigan. Nitrogen balances developed during a 30 day evaluation period is shown on Table 6-9.

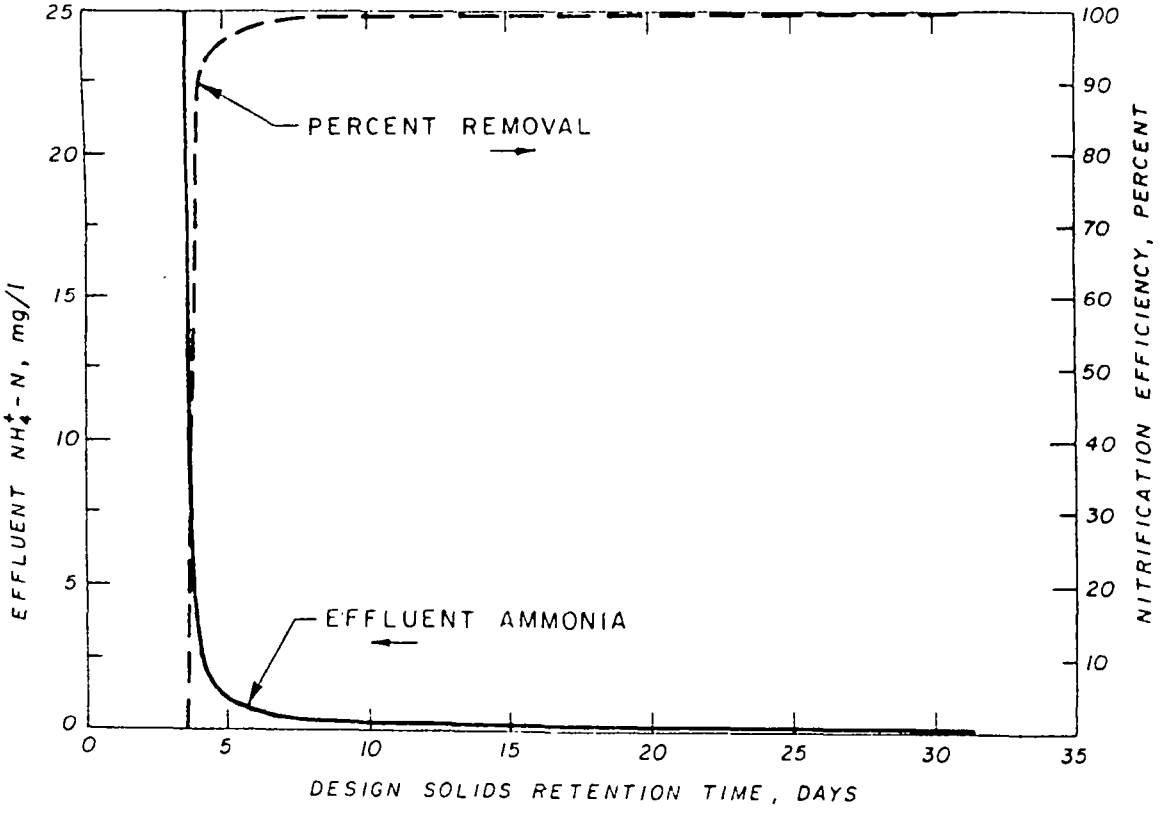

FIGURE 6-26

EFFECT OF SOLIDS RETENTION TIME ON EFFLUENT AMMONIA CONCENTRATION AND NITRIFICATION EFFICIENCY

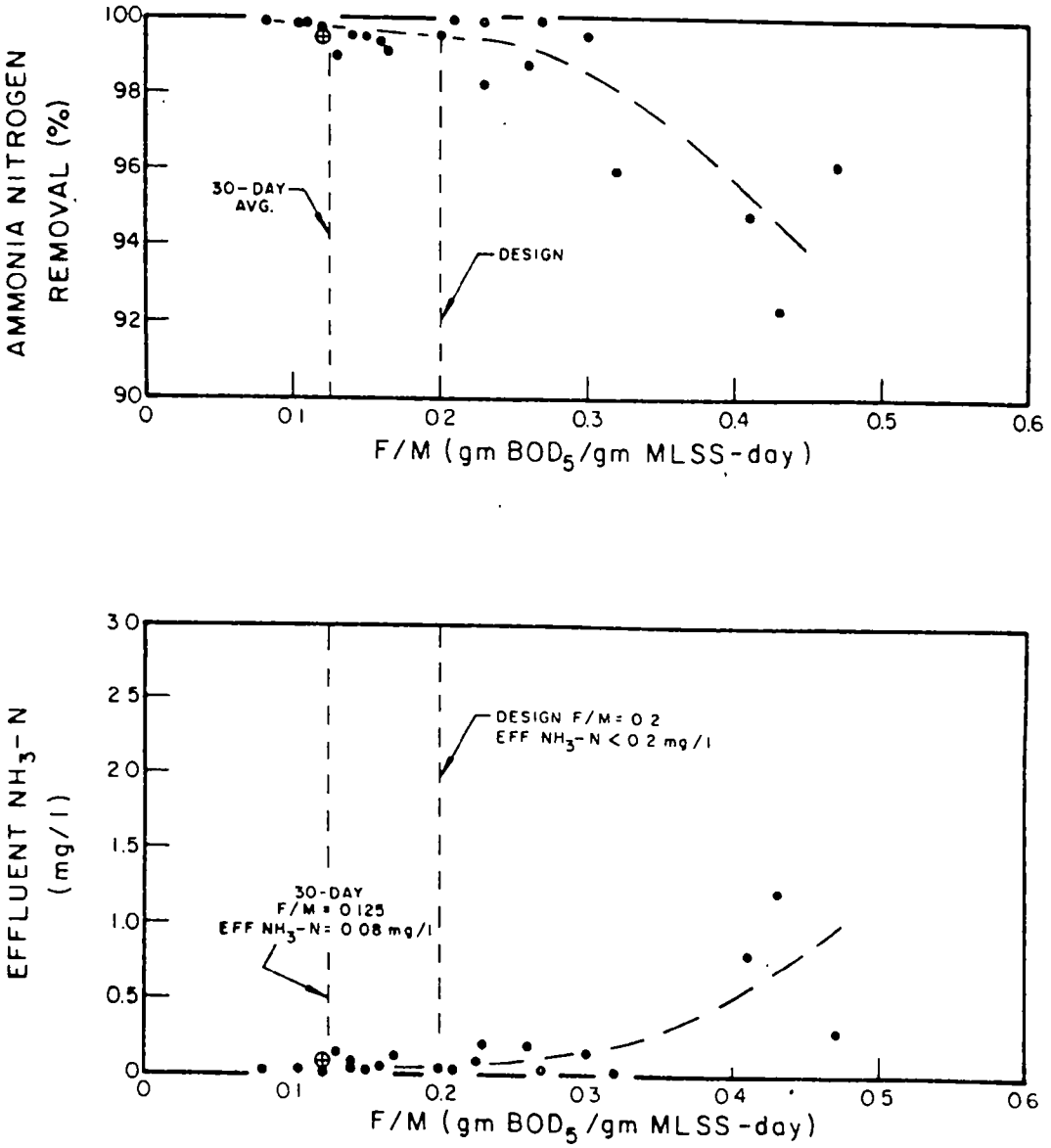

FIGURE 6-27

AMMONIA REMOVAL CHARACTERISTICS
ACTIVATED SLUDGE

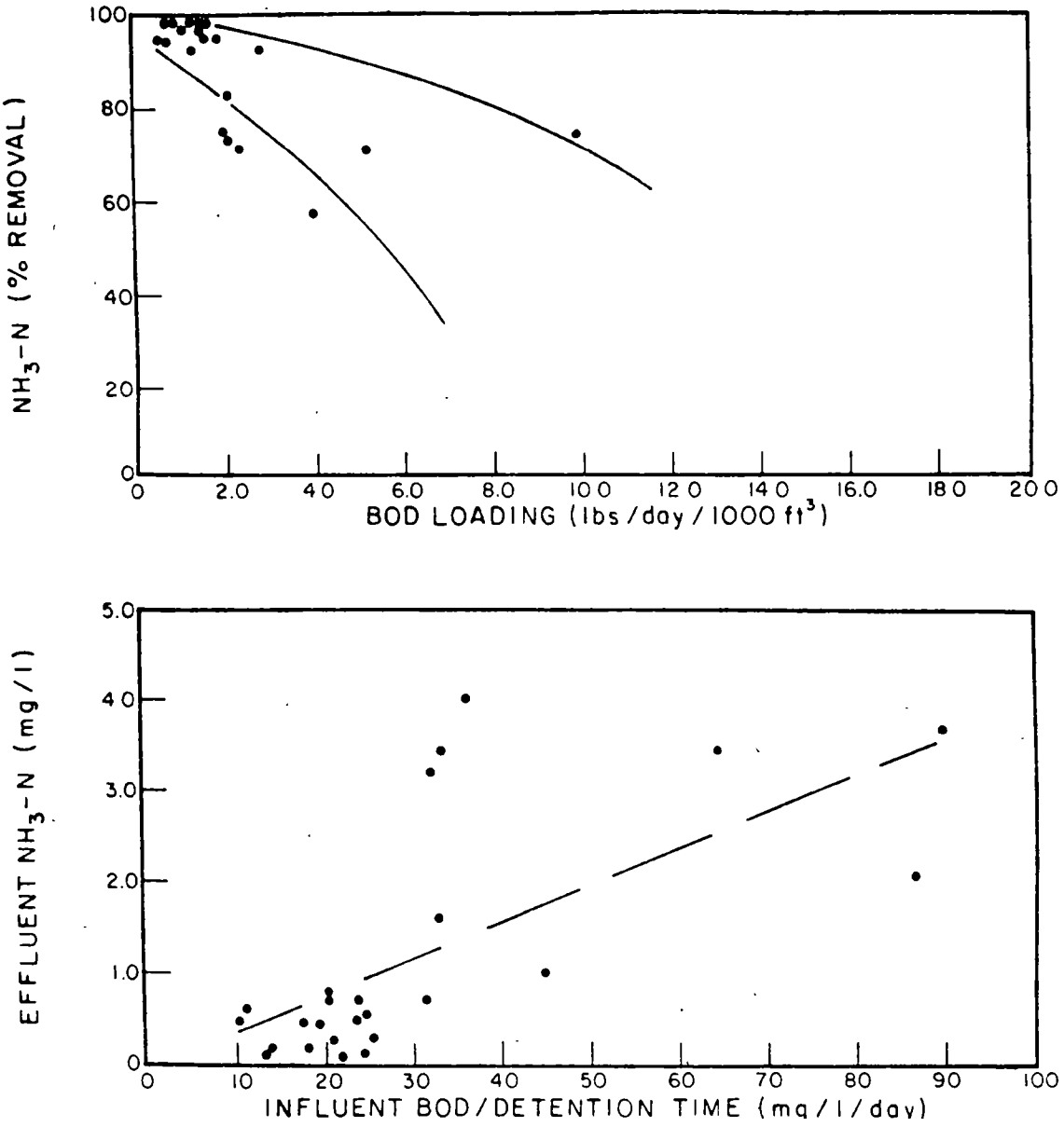

FIGURE 6-28

AMMONIA REMOVAL CHARACTERISTICS
TRICKLING FILTERS

TABLE 6-9

NITROGEN BALANCE
(30-Day Average)

Nitrogen[1]		Raw[3]	Primary Effluent	Trickling Filter Effluent	Activated Sludge Effluent
Organic[2]	(mg/l)	9.5	13.1	1.8	1.8
Ammonia	(mg/l)	12.0	13.5	1.1	0.08
Nitrite	(mg/l)	0.0	0.04	0.05	0.02
Nitrate	(mg/l)	0.0	0.07	13.6	14.4
Total N	(mg/l)	21.5	26.7	16.6	16.3[4]
Total N	(lbs/d)	6,560	9,085	550	4,430

1. Nitrogen species; concentrations expressed as nitrogen.

2. Computed as the difference between TKN and NH_3-N.

3. Sludge return streams not included in Raw.

4. Concentration in microstrainer washwater and soluble component of sludge waste streams. At a flow of 4.2 mgd, this is equivalent to 570 lbs N/day.

Nitrifying autotrophic organisms are more sensitive to environmental conditions and toxic inputs than are the heterotrophics. However, many industrial wastewaters can be nitrified. Table 6-10 summarizes information developed from studies performed by HydroQual on a variety of wastes. All were designed as single stage activated sludge systems except Case F and I where 2 stage systems were required due to toxicity effects of raw waste. Toxic materials were removed in the first stage system. Figure 6-29 presents the removal rate of TKN and ammonia for the latter case.

Figure 6-30 shows the hydrolysis of organic nitrogen to ammonia and the oxidation to nitrate developed from a batch laboratory experiment on an industrial wastewater.

Ammonia is oxidized to nitrite and then to nitrate. The rate limiting step is generally the oxidation to nitrite, hence the effluent from a nitrification process is predominantly nitrate with little nitrite. In some cases with industrial wastes containing high concentrations of unoxidized nitrogen oxidation proceeds only to the nitrite form. This appears to be due to inhibition caused by un-ionized ammonia concentration. Limited information is available and further investigation is necessary to confirm these observations (Figure 6-31).

Rotating Biological Contactors (RBC)

Nitrification in RBC systems can be shown from an analysis of the Gladstone, Michigan treatment plant. The plant was operated as a six stage unit in series. The physical dimensions of the plant are as follows:

1. Bio-surf Media Diameter, D = 3.6 meters
2. # layers/stage = 95.2
3. Wetted surface area/stage (SURF) = 43,000 ft^2
4. Rotational speed, ω = 1.65 rpm

Figure 6-32 presents the observed BOD_5, oxygen and nitrogen profiles through the plant. Figures 6-33 and 6-34 are calculated profiles of the biological distributions and mechanisms of nitrogen removal through the plant.

TABLE 6-10

EXAMPLES OF BIOLOGICAL NITRIFICATION

WASTE SOURCE AND STRENGTH	INFLUENT BOD (MG/L)	INFLUENT ORGANIC N (MG/L)	INFLUENT NH_3-N (MG/L)	LOADING RATE #/DAY BOD #MLSS	SLUDGE AGE (DAYS)	NITRATE AND NITRITE PRODUCTION #N/DAY # MLSS	AVERAGE EFFLUENT NH_3-N (MG/L)	AVERAGE EFFLUENT NO_3-N + NO_2-N (MG/L)
I. DOMESTIC WASTES	150-220	12-18	15-20	0.1-0.3	6-18	0.02-0.05	0-1	12-20
II. INDUSTRIAL WASTES								
A. ORGANIC ACIDS	500	3-8	25	0.12	11-28	0.01	LOW	30
B. PHARAMCEUTICAL AND ORGANIC CHEMICALS	250	80	25	0.05-0.1	>20	0.01	2	34
C. SYNTHETIC FIBERS AND POLYMERS	1,000	80	LOW	0.15	>20	0.005	5	18
D. SYNTHETIC FIBERS	5,000	700	50	0.17	30+	0.017	2	500+
E. NYLON	2,850	200	50	0.15-0.2	>10	0.012	2	250
F. PHARMACEUTICAL AND ORGANIC CHEMICALS[1]	200	75	625	0.02	>20	0.05	50-100	300-400[2]
G. INORGANIC WASTES	10	0	500-1000	0	>30	0.2	<1	50-1000
H. SLAUGHTER HOUSE - BEEF	400	30	50	.05	>30		<1	60
- CHICKEN	300	20	30	.1	>30		<1	40
I. ORGANIC CHEMICAL/PESTICIDE MFR.[1]	500		100	<0.1			<5	80

1-SECOND STAGE OF TWO-STAGE SYSTEM

2-PREDOMINANTLY NO_2-N

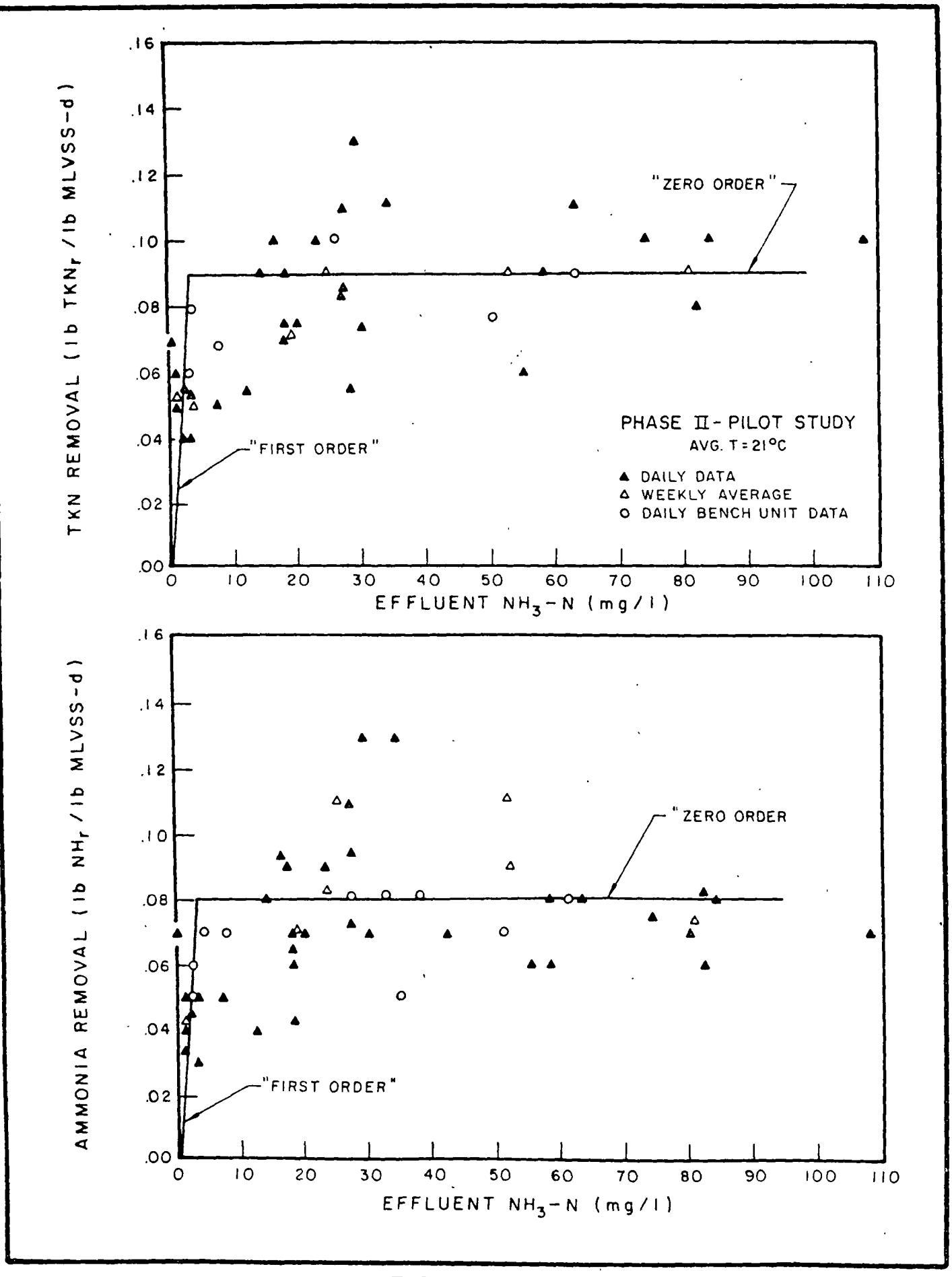

FIGURE 6-29
TKN AND AMMONIA REMOVAL

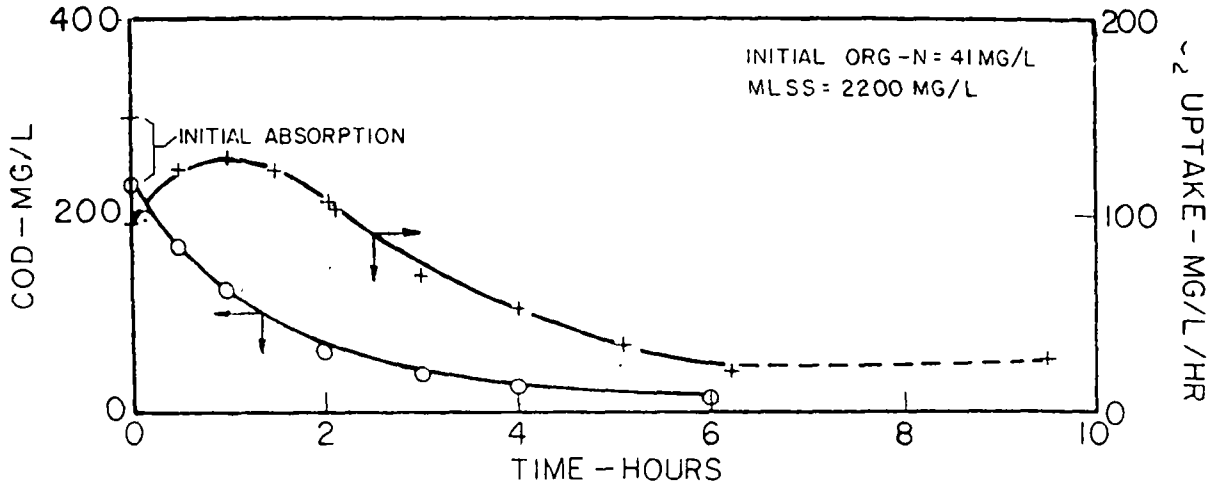

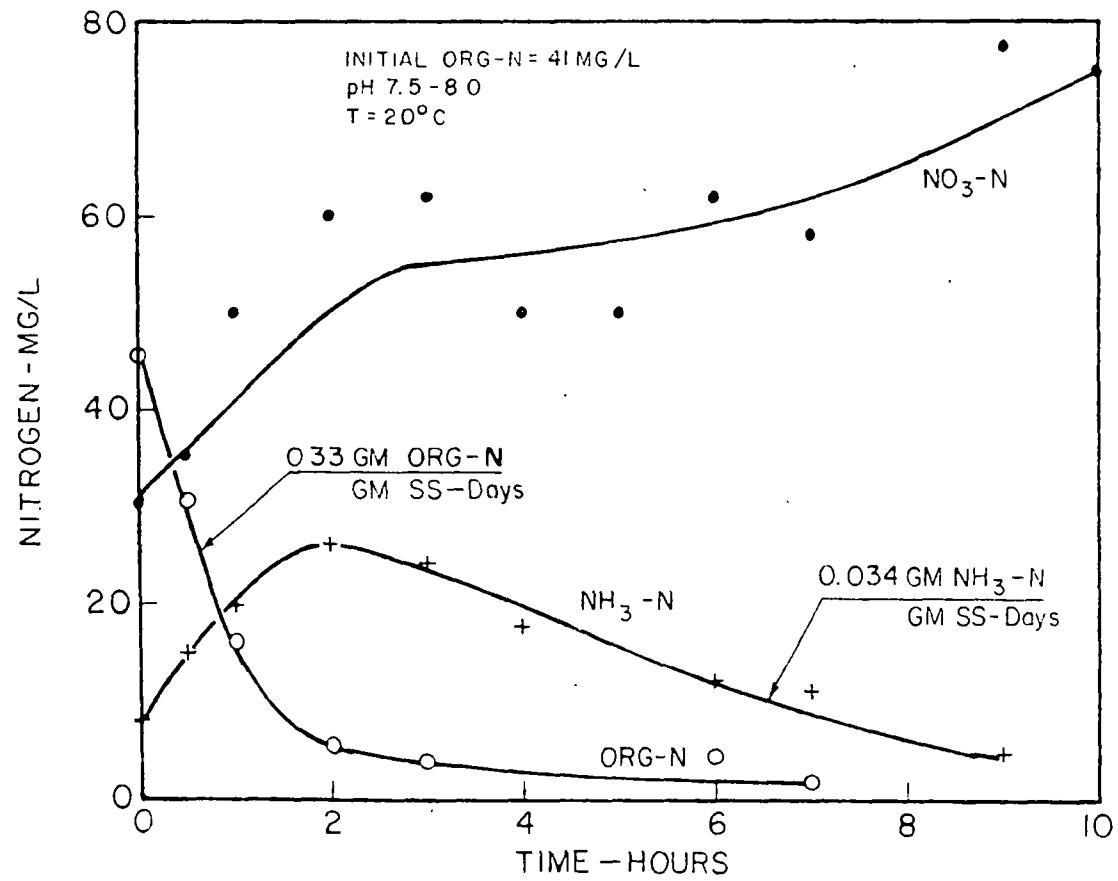

FIGURE 6-30

BATCH EXPERIMENT

SYSTEM No. I

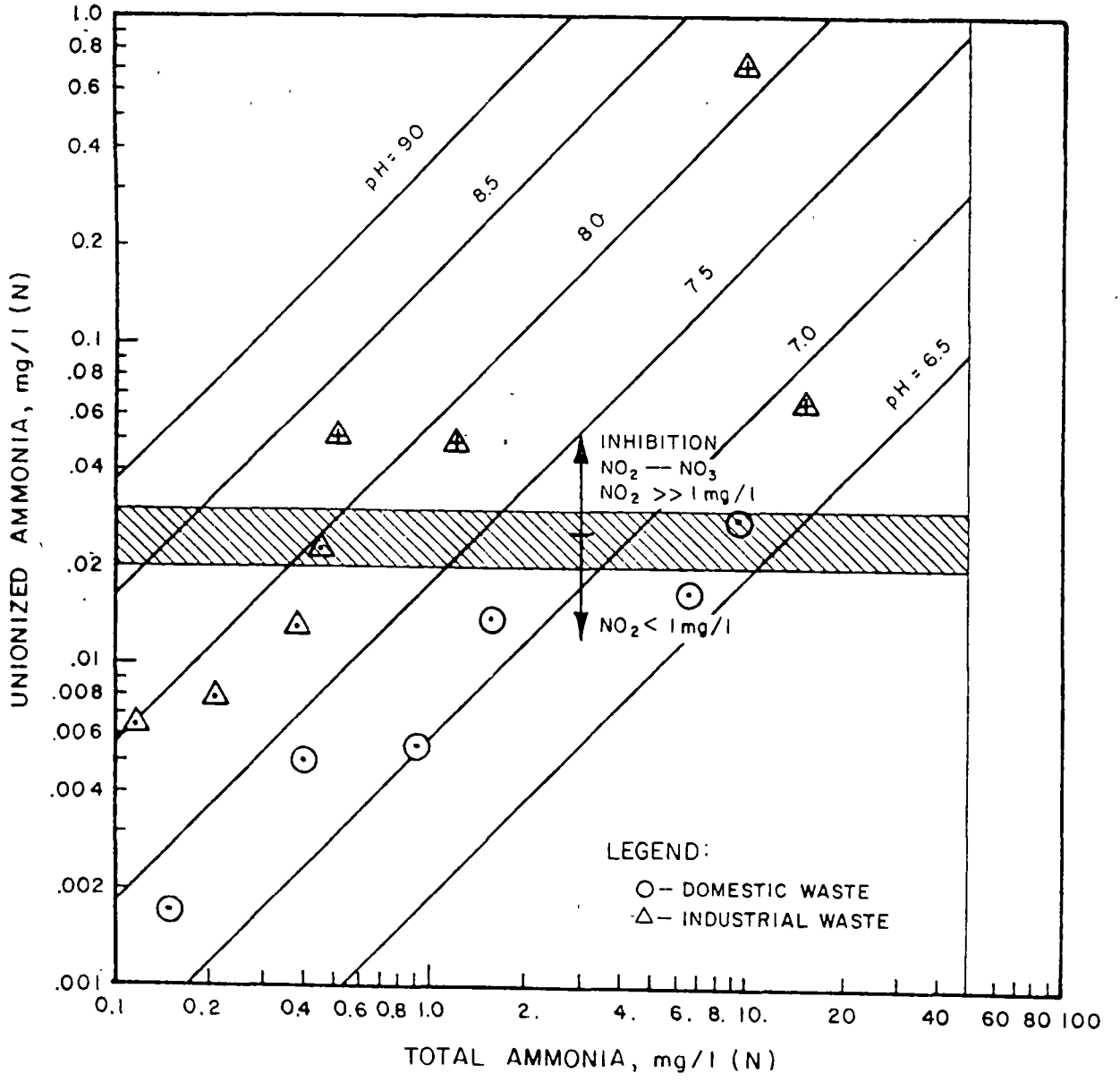

FIGURE 6-31

UNIONIZED AMMONIA – NITRITE EFFECTS

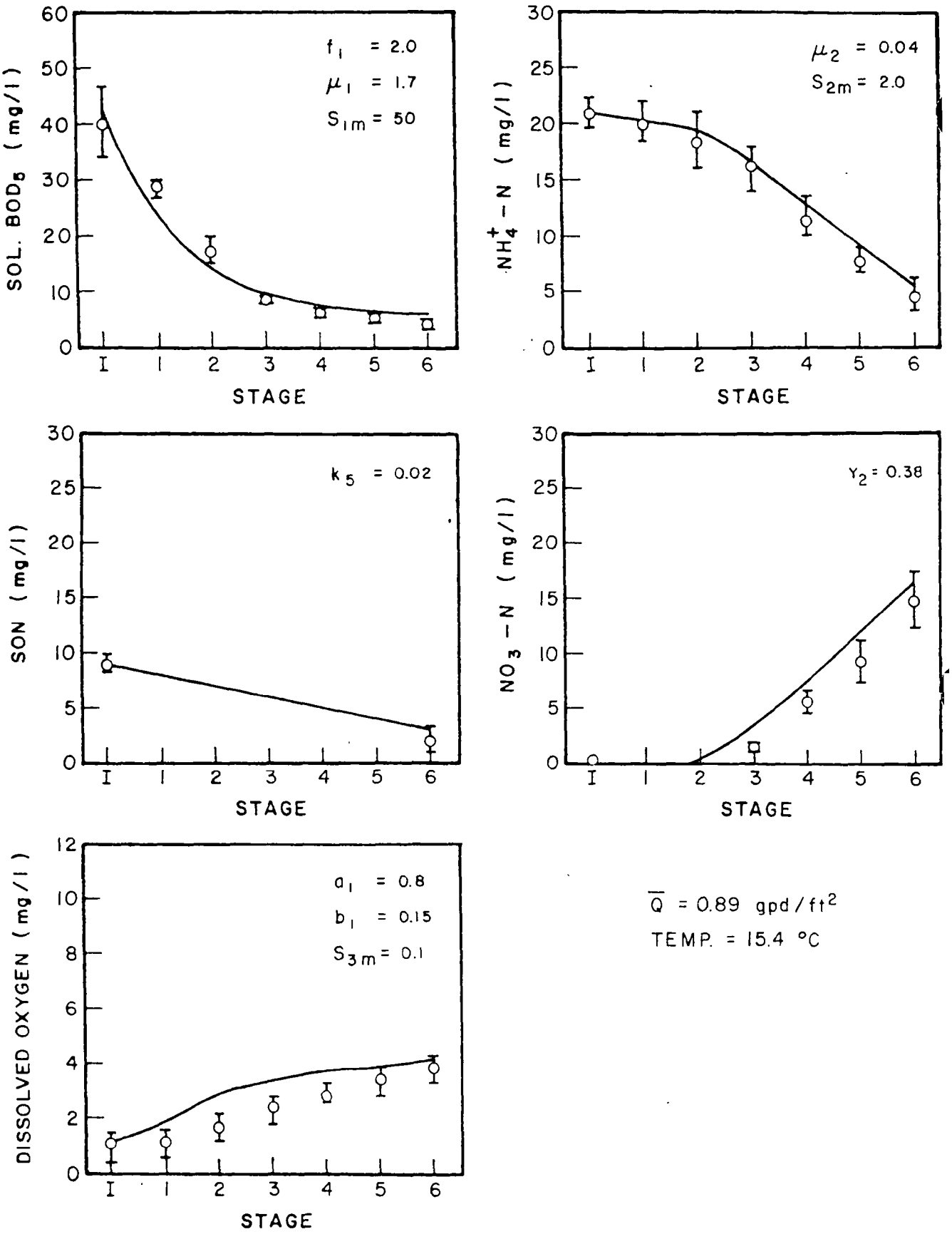

FIGURE 6-32
PRELIMINARY CALIBRATION – DATA SET 2

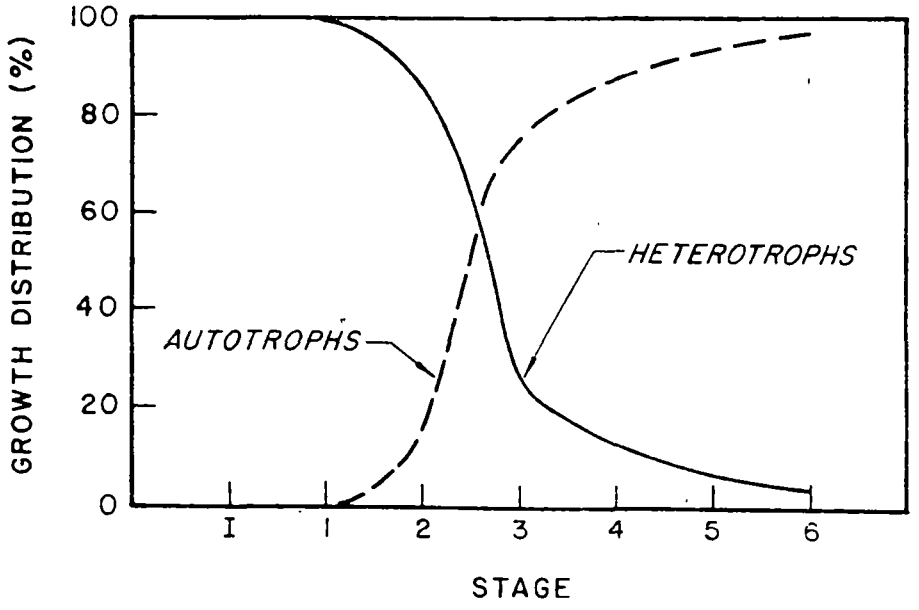

Q = 0.23 MGD

Q = 0.89 gpd / ft

T = 15.4 °C

FIGURE 6-33
GROWTH DISTRIBUTION FOR DATA SET 2

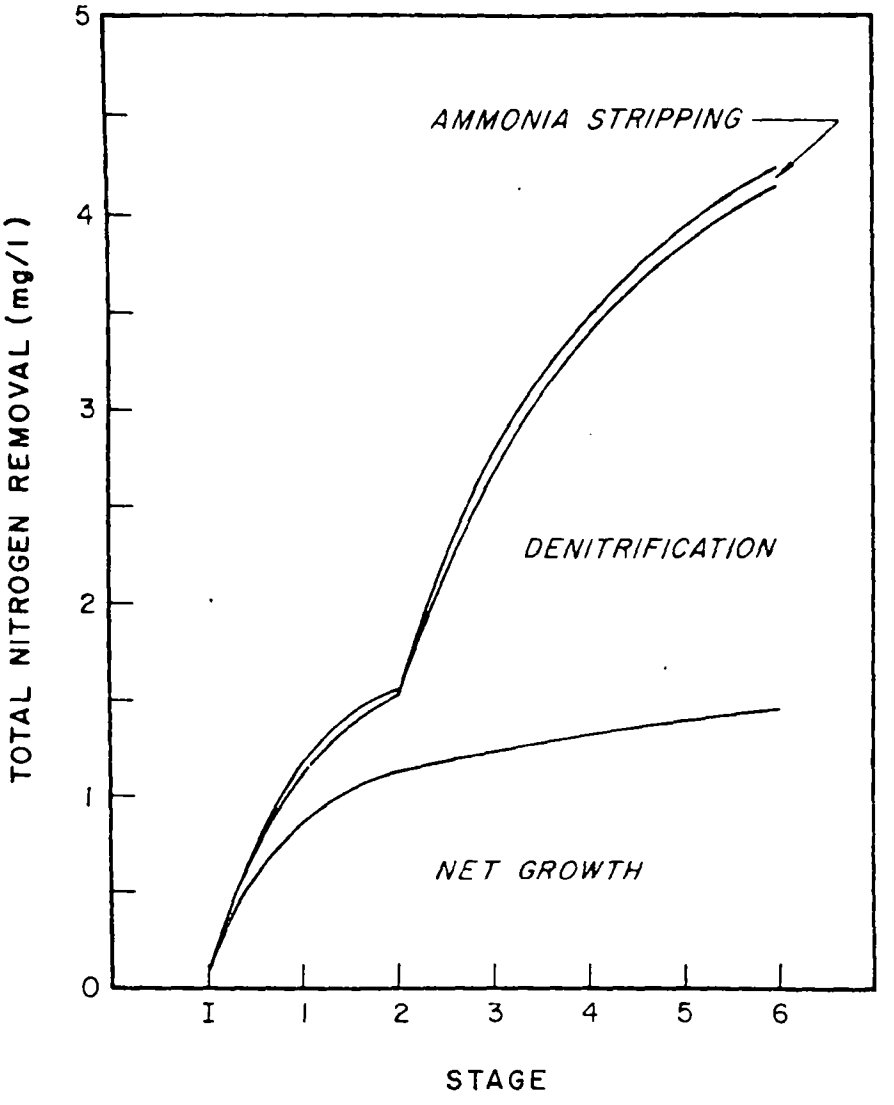

FIGURE 6-34
DISTRIBUTION OF TOTAL SOLUBLE NITROGEN REMOVAL
FOR DATA SET I

II. DENITRIFICATION

The biological process of denitrification involves the conversion of nitrate nitrogen to a gaseous nitrogen species. The gaseous product is primarily nitrogen gas but also may be nitrous oxide or nitric oxide. Gaseous nitrogen is relatively unavailable for biological growth, thus denitrification converts nitrogen which may be in an objectionable form to one which has no significant effect on environmental quality.

Denitrification is a two-step process in which the first step is a conversion of nitrate to nitrite. The second step carries nitrite through two intermediates to nitrogen gas.

An organic carbon source is required as an energy source in the reaction. BOD in the wastewaters or an external source such as methanol can be utilized.

III. PHOSPHORUS REMOVAL

The Chemical Removal of phosphates from wastewaters essentially involves two steps: (1) insolubilization or precipitation of the phosphate species by the addition of a metal salt, and (2) separation of the resulting chemical sludge. Whereas the choice of coagulant and point of application are mainly dictated by economic factors, the conditions of proper coagulant dosage, and pH range are governed by the relevant ionic equilibria.

The degree of insolubilization of phosphates is controlled by the concentration or applied dosage of metal ion (Law of Mass Action). In other words, the greater the quantity of metal coagulant added, the more phosphate will be removed from solution until some minimum (non-zero) concentration is attained.

The second factor which control the extent of phosphate precipitation is the pH or hydrogen ion concentration. The pH is an extremely important consideration in the chemical precipitation of phosphorus since hydrogen and/or hydroxyl ions may enter into either the primary (in the case of Ca^{++}) insolubilization reaction or other competitive precipitation or complexation reactions. As a result the coagulant may be partially or completely consumed by these competitive reactions and the phosphorus removal efficiency accordingly reduced. Implicit in the foregoing considerations is the fact that the selection of coagulant, proper dosage, and optimum pH is strongly influenced by the ionic composition of a given wastewater. As a consequence, these factors must be independently determined in each case.

TABLE 6-11

TYPICAL CHEMICAL COAGULANTS
FOR
PHOSPHORUS REMOVAL

	Typical Dose[1]	Optimum pH	Sludge Prod.[2]
Ca^{++}	1-3	11	variable
Fe^{+++}	1-3	5.3	2-3
Al^{+++}	2-3	6.0	3-5
Fe^{++}	1-3		2-3

(1) Moles of Metal/Mole of P

(2) mg Sludge/mg Metal

BARDENPHO PROCESS

Bardenpho Process was developed by James L. Barnard and its initial use occurred in South Africa. Several installations have been built in this country. The process basically provides biological removal of BOD, nitrification, denitrification and phosphorus without the additions of chemicals. The process is schematically shown on Figure 6-35. Basic principals to highlight are:

1. Anaerobic zone required to obtain subsequent P uptake by biological solids.

2. Anoxic zone which receives high recycle of nitrified waste. BOD of raw waste waters provide organic carbon for denitrification.

3. Nitrification F/M ~ Ø.1.

4. Further denitrification if low NO_3 is required in effluent.

Table 6-12 presents a cost comparison prepared by Bendick and Dallane on the Bardenpho process and several advanced waste treatment processes for a 1.4 mgd plant.

PHOSTRIP

Description

"Phostrip" is a combined biological-chemical precipitation process, Figure 6-36, based on the use of activated sludge microorganisms to transfer phosphorus from incoming wastewater to a small concentrated substream for precipitation. The activated sludge is subjected to anaerobic conditions to induce phosphorus release into the sub-stream and to provide phosphorus uptake capacity when the sludge is returned to the aeration basin. Settled wastewater is mixed with return activated sludge in the aeration tank. Under aeration, sludge microorganisms can be induced to take up dissolved phosphorus in excess of the amount required for growth. The mixed liquor then flows to the secondary clarifier where liquid effluent, now largely free of phosphorus, is separated from the sludge and discharged. A portion of the phosphorus-rich sludge is transferred from the bottom of the clarifier to a thickener-type holding tank: the phosphate stripper. The settling sludge quickly becomes anaerobic and, thereupon, the organisms surrender phosphorus, which is mixed into the supernatant. The phosphorus-rich supernatant, a low volume, high concentration substream, is removed from the stripper and treated with lime for phosphorus precipitation. The thickened sludge, now depleted in phosphorus, is returned to the aeration tank for a new cycle.

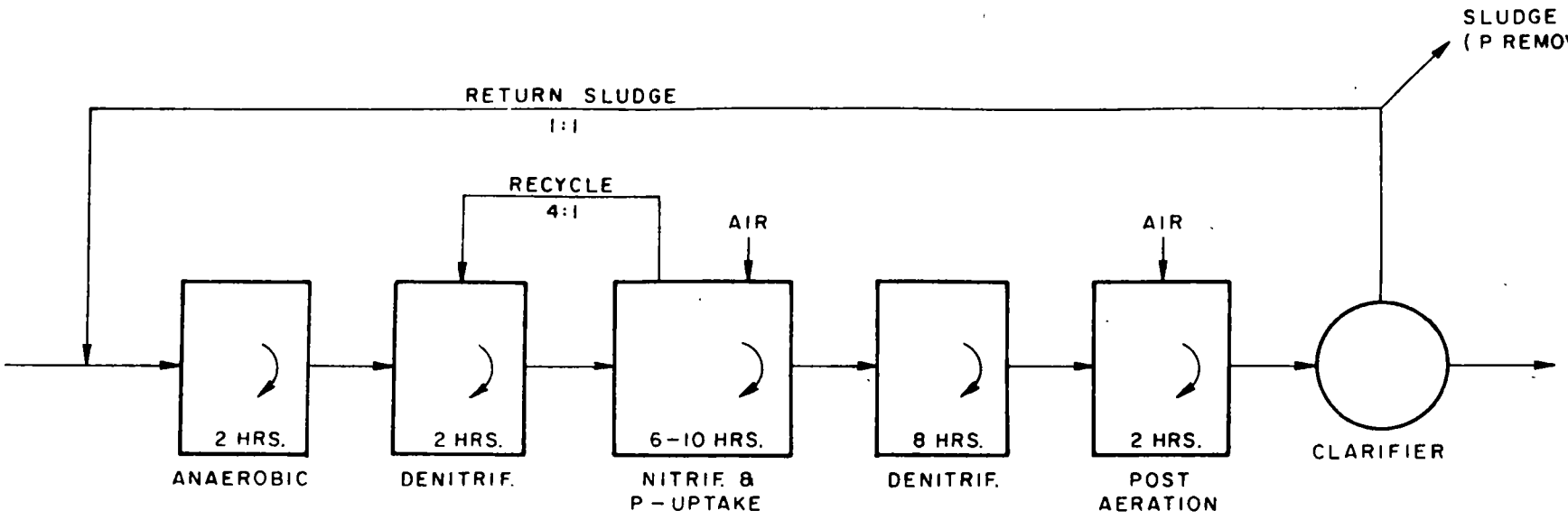

FIGURE 6-35

BARDENPHO PROCESS

TABLE 6-12

BARDENPHO PROCESS
COST COMPARISON

BASIS:

Flow = 1.4 mgd

Effluent Criteria -

BOD = 5 mg/l

SS = 5

Nitrogen = 3 mg/l

P = 1 mg/l

Process	Capital Cost ¢/1000 gal	O&M ¢/1000 gal	Total Annual Cost ¢/1000 gal
1. Conventional AWT 2 Sludge + Chem.	41.7	33.3	75
2. RBC + Filtration	27.9	35.5	63.4
3. Bardenpho + Sand Filter	30.0	26.5	56.5

Ref: Burdicke & Dallaire, Florida Sewage Treatment Plant First to Remove Nutrients with BACTERIA ALONE, Civil Engineering, Oct. 1978.

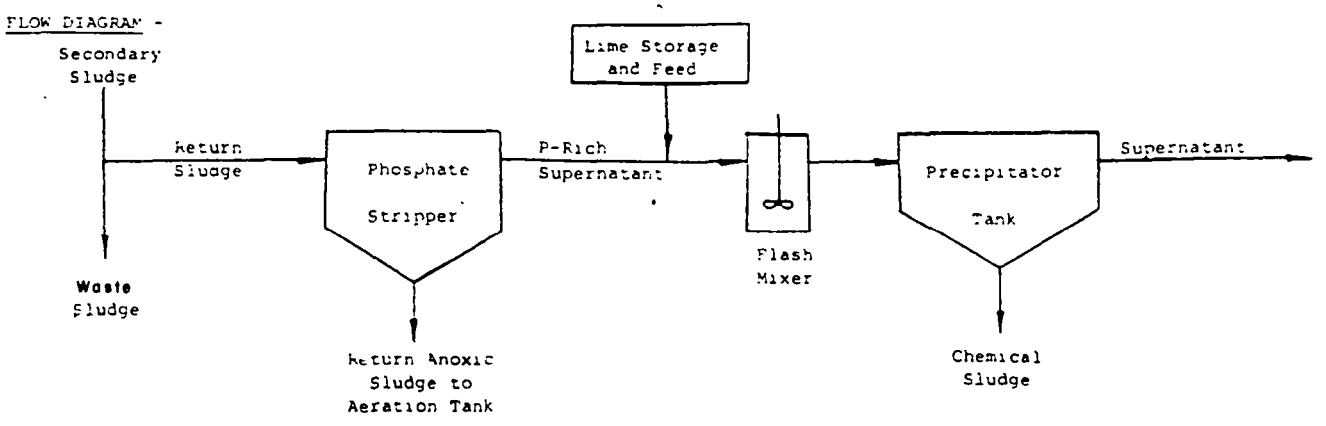
FLOW DIAGRAM -
Secondary Sludge
Lime Storage and Feed
Return Sludge
Phosphate Stripper
P-Rich Supernatant
Flash Mixer
Precipitator Tank
Supernatant
Waste Sludge
Return Anoxic Sludge to Aeration Tank
Chemical Sludge

FIGURE 6-36

Figures 6-37 and 6-38 show total construction cost and operation and maintenance costs for secondary treatment plants. Costs in January 1978 were obtained from the EPA document Construction Costs for Municipal Wastewater Treatment Plants: 1973-1977.

Figure 6-39 shows comparative capital costs of alternate secondary treatment processes (1978 Basis).

Table 6-13 presents a summary of cost estimates prepared by HydroQual for an 8 mgd industrial treatment facility where activated sludge, pure oxygen and RBC systems were considered.

The following analysis considered the cost of treatment of municipal wastewaters to produce various effluent qualities. The significant increase in costs (capital and O&M) with advanced treatment can be seen particularly as activated carbon is added.

Degree of Treatment vs Cost

The liquid process trains chosen for analysis are enumerated in Table 6-14. These cover a range of treatment efficiencies from conventional primary treatment to advanced schemes with carbon adsorption. Raw influent pumping is included as a common baseline that would usually be necessary for discharge of wastewater even with no further treatment.

Literature data are adjusted to 1977 values using the following price index levels: EPA Sewage Treatment Plant Construction Index (STP) = 275, Engineering News-Record Construction Cost (ENR) = 2,666, Wholesale Price Index (WPI) = 194, Consumer Price Index (CPI) = 182. All liquid treatment schemes include raw pumping, preliminary treatment (for screens, comminutors, grit removal, and flow metering), prethickening of sludge, and disinfection by chlorination. Processes with lime addition include dewatering and recalcination of lime sludge. Capital expenses are amortized over 20 years @ 6-5/8% interest. Costs for land acquisition are not included.

Figure 6-40 presents total annual costs for liquid treatment processes (excludes sludge treatment costs) of the various process trains in relation to the percent of SS they may be expected to remove. Processes utilizing chemical coagulants demonstrate higher costs for similar removals than do those without chemical addition. The breakdown into capital and operation and maintenance costs in Figure 6-41 shows the difference between the total cost curves is due principally to differences in operating costs with smaller differences evident in capital costs.

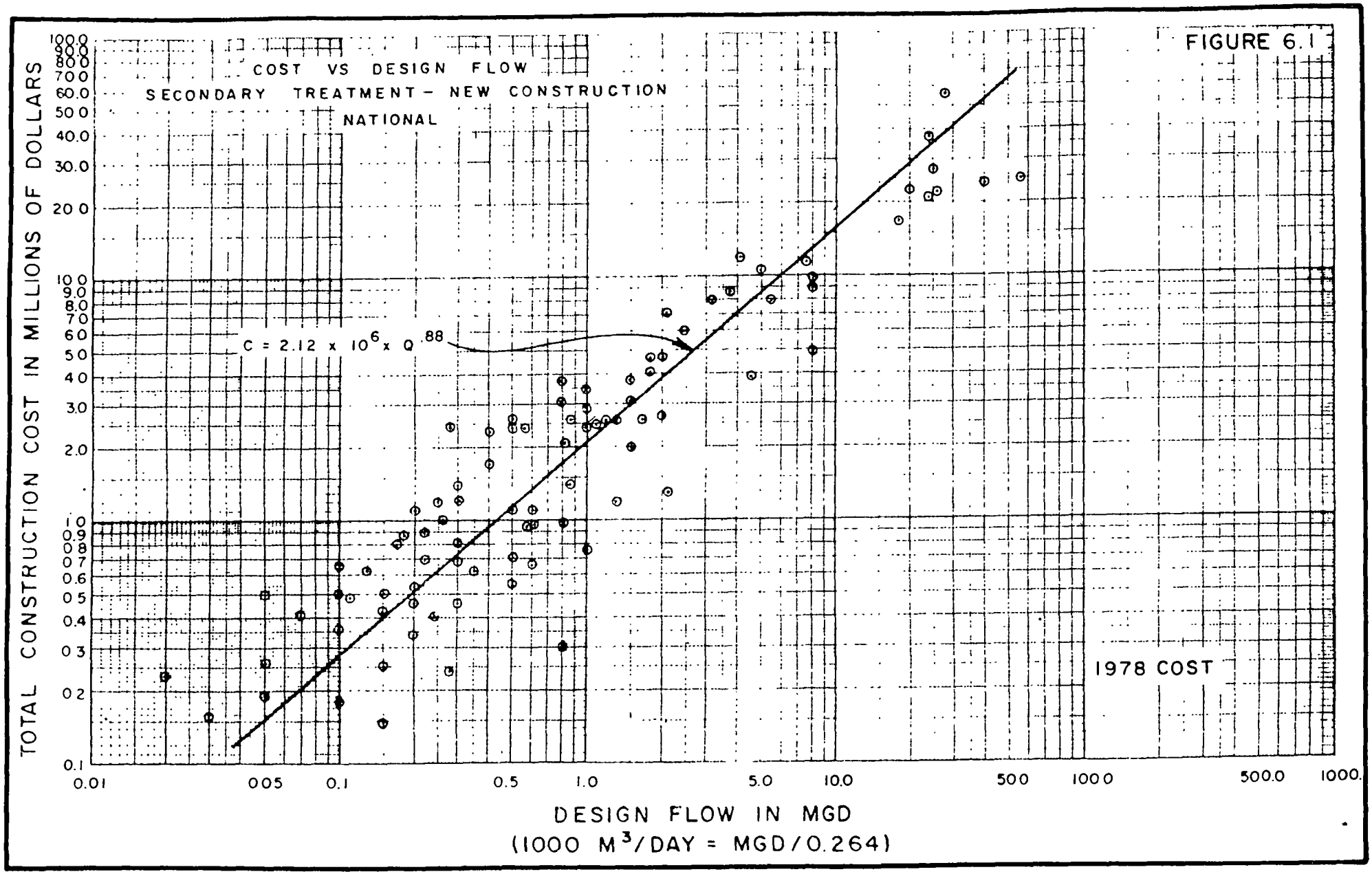
FIGURE 6.1
COST VS DESIGN FLOW
SECONDARY TREATMENT - NEW CONSTRUCTION
NATIONAL
C = 2.12 x 10^6 x Q^.88
1978 COST
TOTAL CONSTRUCTION COST IN MILLIONS OF DOLLARS
DESIGN FLOW IN MGD
(1000 M^3/DAY = MGD/0.264)
100.0
90.0
80.0
70.0
60.0
50.0
40.0
30.0
20.0
10.0
9.0
8.0
7.0
6.0
5.0
4.0
3.0
2.0
1.0
0.9
0.8
0.7
0.6
0.5
0.4
0.3
0.2
0.1
0.01
0.05
0.1
0.5
1.0
5.0
10.0
50.0
100.0
500.0
1000.

FIGURE 6-37

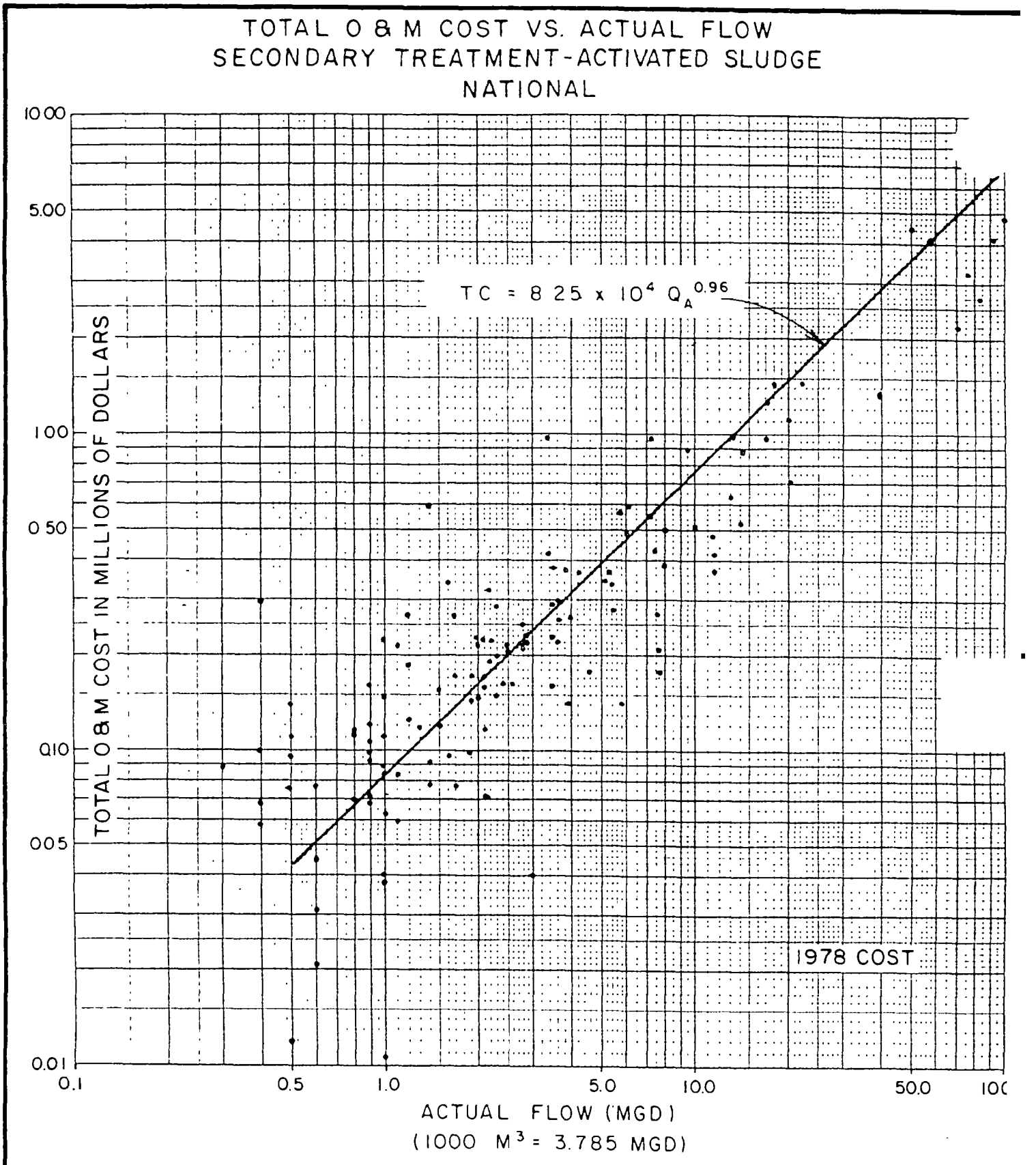
TOTAL O & M COST VS. ACTUAL FLOW
SECONDARY TREATMENT-ACTIVATED SLUDGE
NATIONAL
10.00
5.00
1.00
0.50
0.10
0.05
0.01
TOTAL O&M COST IN MILLIONS OF DOLLARS
TC = 8.25 x 10⁴ Q_A^0.96
1978 COST
0.1
0.5
1.0
5.0
10.0
50.0
ACTUAL FLOW (MGD)
(1000 M³ = 3.785 MGD)

FIGURE 6-38

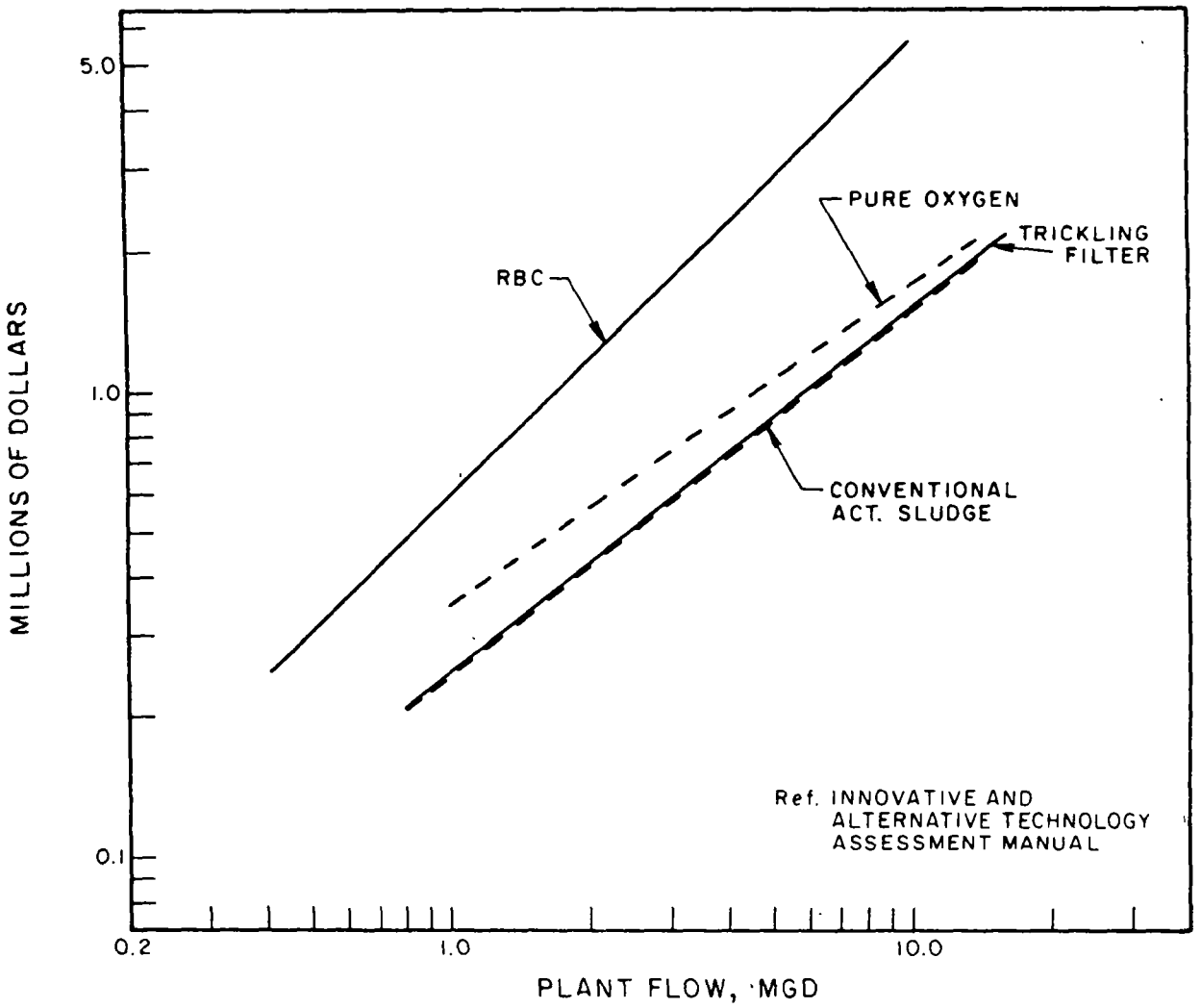

FIGURE 6-39

CAPITAL COST
BIOLOGICAL PROCESSES

TABLE 6-13

COST COMPARISON - INDUSTRIAL WASTEWATER

BASIS

	Average	Maximum
Raw Waste		
Flow	8.3 mgd	10.5 mgd
BOD_5	88,000 lbs/day	114,500 lbs/day
SS	20,800	35,000
Permit - Effl.		
BOD_5	90% Removal	80%
SS	100 mg/l	200 mg/l

Primary plant exists

	COST TREATMENT PROCESS		
	Act. Sludge	Pure Oxygen	RBC
Capital Cost[1]	$7,000,000	$7,000,000	$15,000,000
O&M Cost[1]	$870,000	$986,000	$540,000

1 - Sludge Dewatering and Disposal (Thickening, Dewatering & Landfill) not incl. These costs were an additional

Capital Cost = $4.7 million
O&M = $0.9 million

TABLE 6-14

ALTERNATIVE TREATMENT STRATEGIES EVALUATED IN STUDY

Process #	Name	Unit Processes		
		Physical-Chemical	Biological	Advanced
P	Raw Pumping Only	-	-	-
1	Conventional Primary	S	-	-
2	Polymer Primary	PS+FS	-	-
3	Alum Primary	ALS	-	-
4	2 Stage Lime Primary	TLS	-	-
5	High Rate Activated Sludge	S	HRAS	-
6	Conventional Activated Sludge	S	CAS	-
7	Two Sludge Nitrification	S	HRAS+NO_3	-
8	Three Sludge System	S	HRAS+NO_3+N_2	-
9	Advanced Lime, Ammonia Stripping	S	CAS	TLS+NH_3
10	Conventional Activated Sludge with Filtration	S	CAS	FM
11	Conventional Activated Sludge and Advanced	S	CAS	FM+CAD
12	Chemical Primary, Biological and Advanced	LS	NO_3+N_2	FM+CAD
13	Physical-Chemical	TLS	-	FM+CAD

ALS = alum addition + sedimentation
CAS = conventional activated sludge
CAD = carbon adsorption
FM = multimedium filtration
FS = fine screens
HRAS = high rate activated sludge
LS = lime addition + sedimentation
N_2 = biological denitrification
NH_3 = ammonia stripping
NO_3 = biological nitrification
PS = polymer addition + sedimentation
S = primary sedimentation
TLS = two stage lime addition + sedimentation

Note: All Processes include raw pumping, preliminary treatment and prethickening. Processes with lime addition (4, 9, 12, 13) include recalcination.

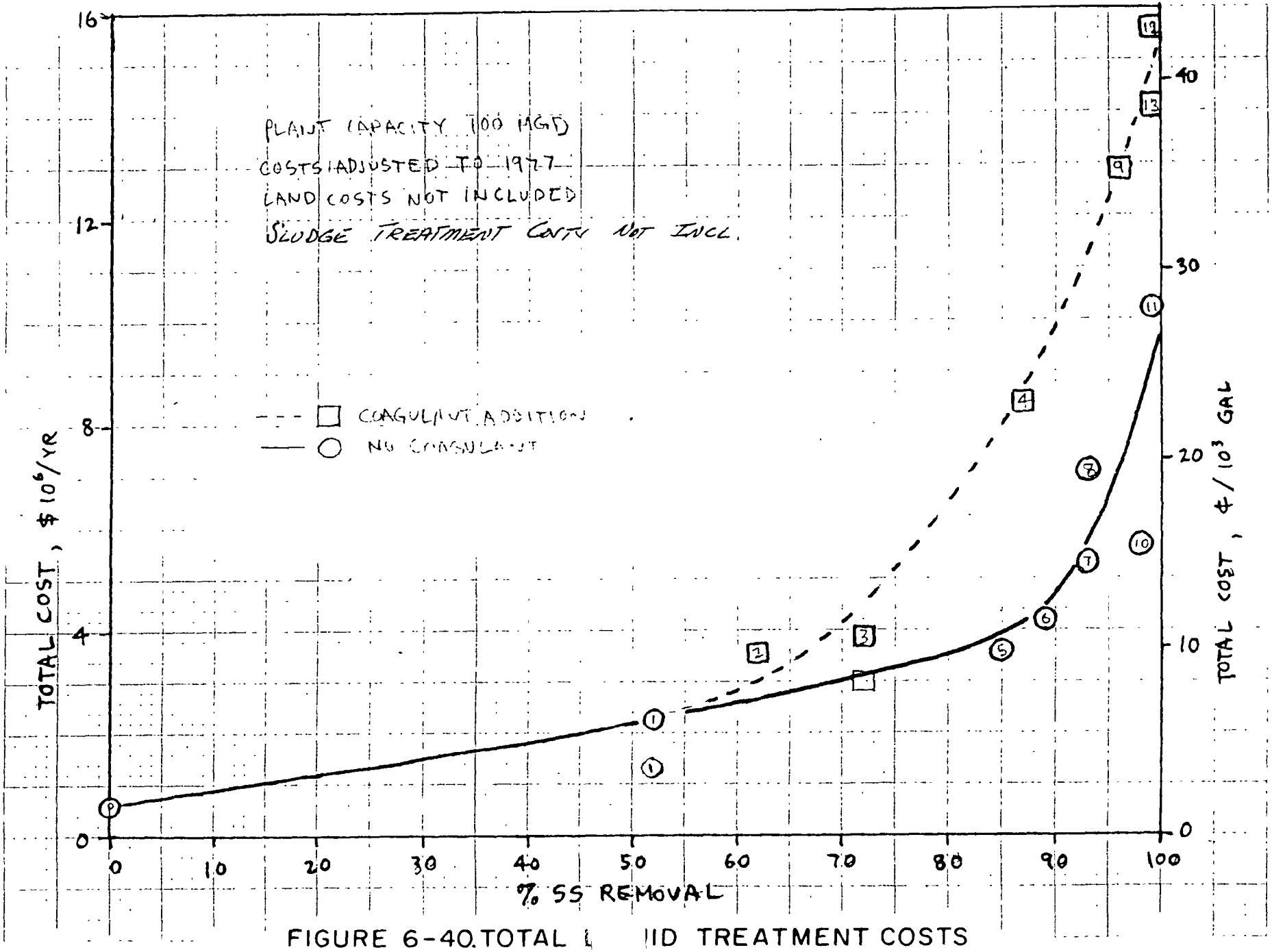

FIGURE 6-40. TOTAL [illegible] TREATMENT COSTS

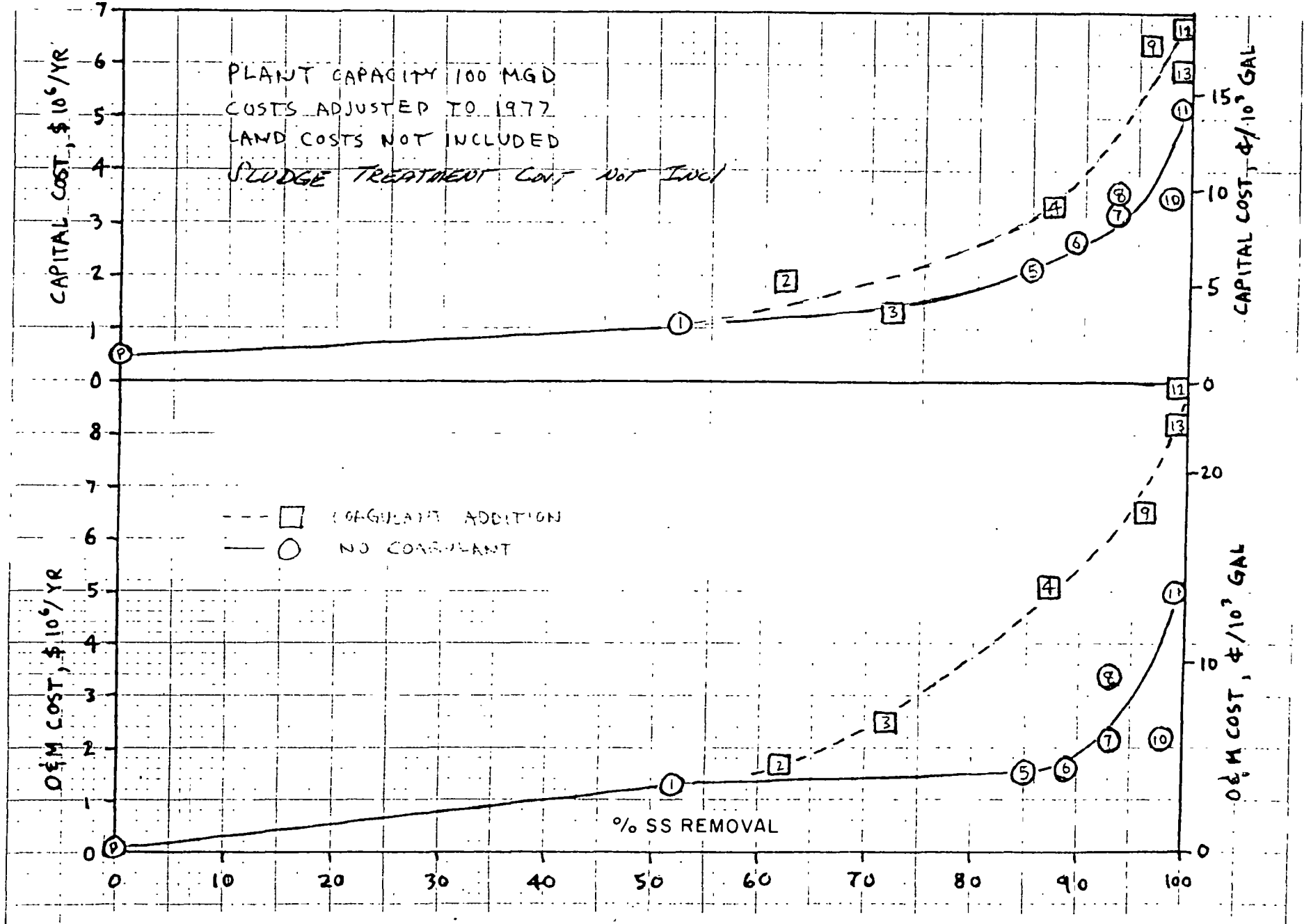

FIGURE 6-41. CAPITAL AND O&M COSTS FOR LIQUID TREATMENT PROCESSE

Sludge is the highly concentrated by-product of wastewater treatment. It can be composed of material removed directly from the waste; as in primary settling, or the biomass generated during secondary treatment, or a combination of a chemical additive and the contaminants it has removed. The nature and quantity of the sludge depends on the contaminants present in the influent and the processes used to remove them. The sludge treatment options selected for study are incineration, ocean disposal, land application, and landfill. Total annual costs are shown on Figure 6-42.

Schuckrow and Culp (19) have evaluated the comparative economics of a number of treatment systems including activated sludge, GAC, PAC and PACT. Table 6-15 indicates that the PACT system at plants >5 mgd is somewhat more expensive than conventional activated sludge or single stage nitrification. Physical-chemical systems with both granular and powdered carbon are significantly more expensive. The effluent qualities from the various processes is given in Table 6-16. The PACT process quality is anticipated to be somewhat greater than the activated sludge but lower than single stage nitrification. For the PACT process, 120 mg/l PAC dose was used with wet air oxidation requiring 17 mg/l makeup carbon. Multiple hearth incineration would have been significantly more expensive.

In comparing the cost of the activated sludge to the single stage nitrification, capital costs are greater due to the greater costs for secondary clarifiers (400 gpd/ft^2 compared to 600). Also, WAO and chemical feed system costs for the "PACT" process are greater than the reduction in vacuum filtration and incineration costs (primary only versus primary and secondary). The "PACT" plant in Vernon, Connecticut, @ 600 gpd/ft^2 provides an average effluent SS of 24 mg/l prior to filtration, thus the cost differential in secondary clarifiers should be negligible reducing the capital costs differential by ~30%. A cheaper sludge disposal alternative other than incineration would make the activated sludge costs significantly cheaper than the PACT costs.

The economic evaluation by Dupont (31) comparing GAC ($34 million) to the "PACT" process ($25 million) showed the costs for the carbon columns, initial carbon inventory and incinerator for the sludge to be the major cost differential. The PACT clarifier was designed at 950 gpd/ft^2 compared to 640 for the activated sludge providing another significant cost savings. From the full scale results, the median SS effluent concentration was somewhat greater than 30 mg/l but values as high as 900 mg/l at times occurred providing a mean of 87 mg/l.

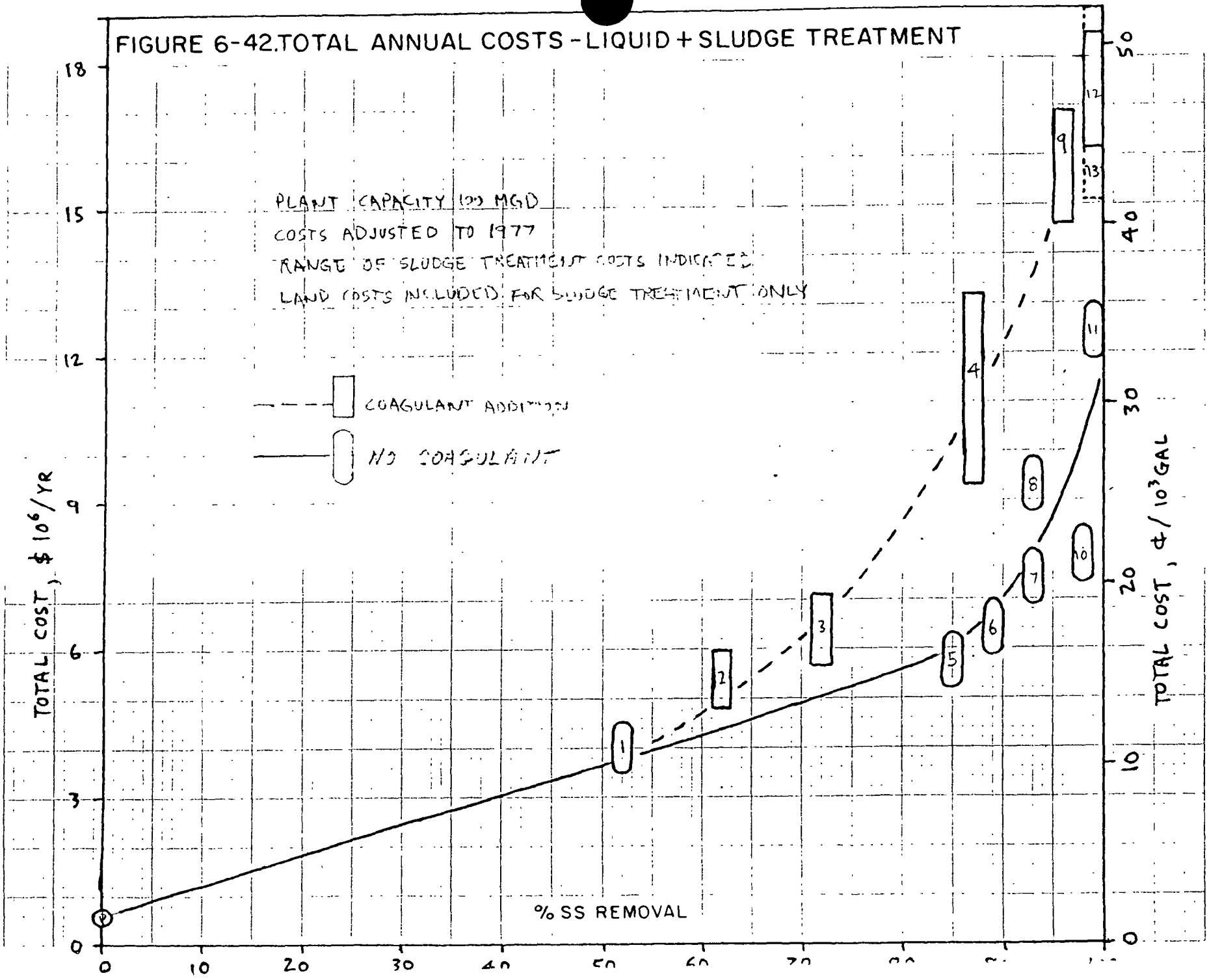
FIGURE 6-42. TOTAL ANNUAL COSTS - LIQUID + SLUDGE TREATMENT
PLANT CAPACITY 100 MGD
COSTS ADJUSTED TO 1977
RANGE OF SLUDGE TREATMENT COSTS INDICATED
LAND COSTS INCLUDED FOR SLUDGE TREATMENT ONLY
COAGULANT ADDITION
NO COAGULANT
TOTAL COST, $ 10^6/YR
TOTAL COST, ¢/10^3 GAL
% SS REMOVAL
0
3
6
9
12
15
18
10
20
30
40
50
1
2
3
4
5
6
7
8
9
10
11
12
13

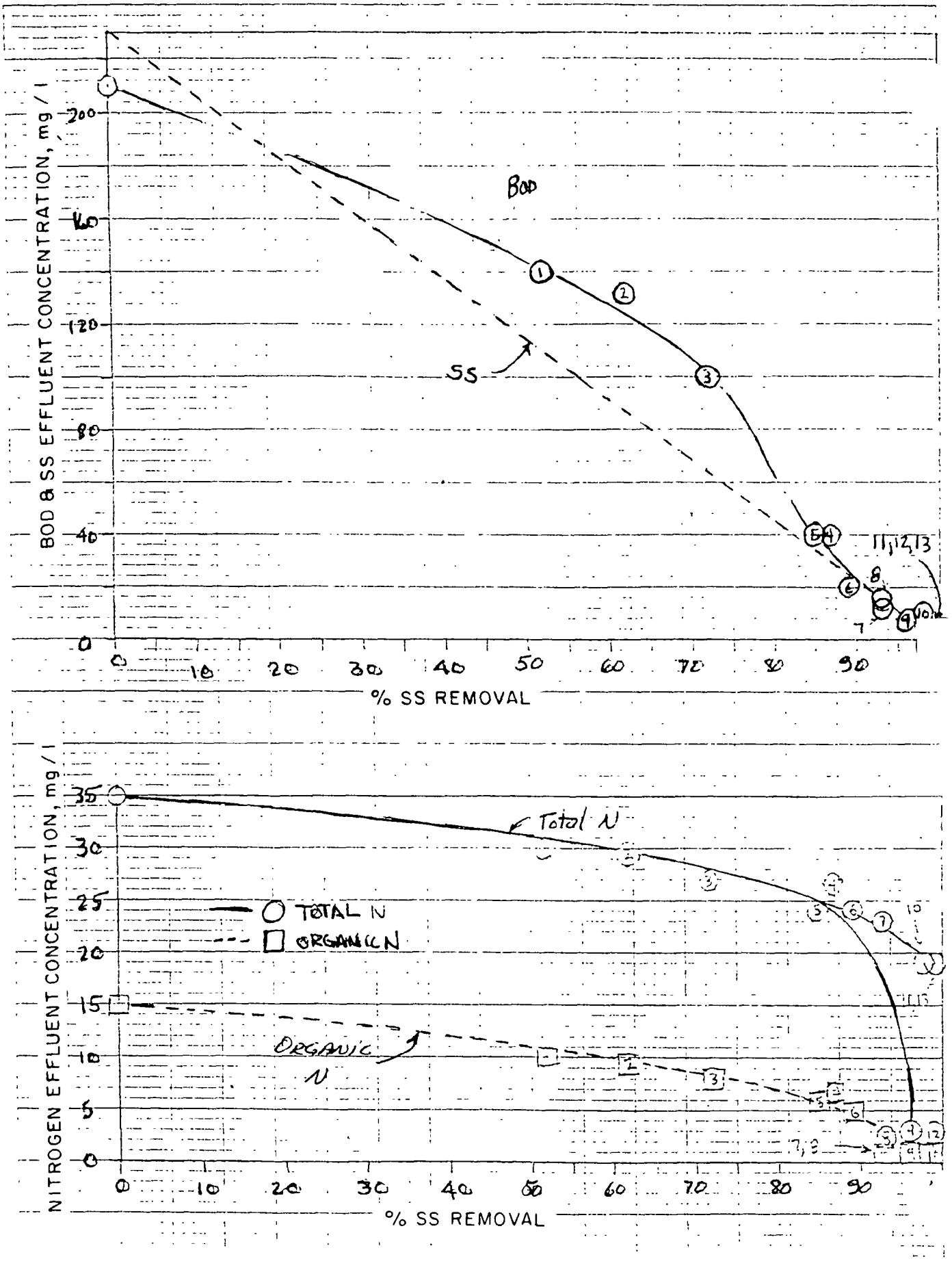

FIGURE 6-43. BOD AND NITROGEN EFFLUENT QUALITIES

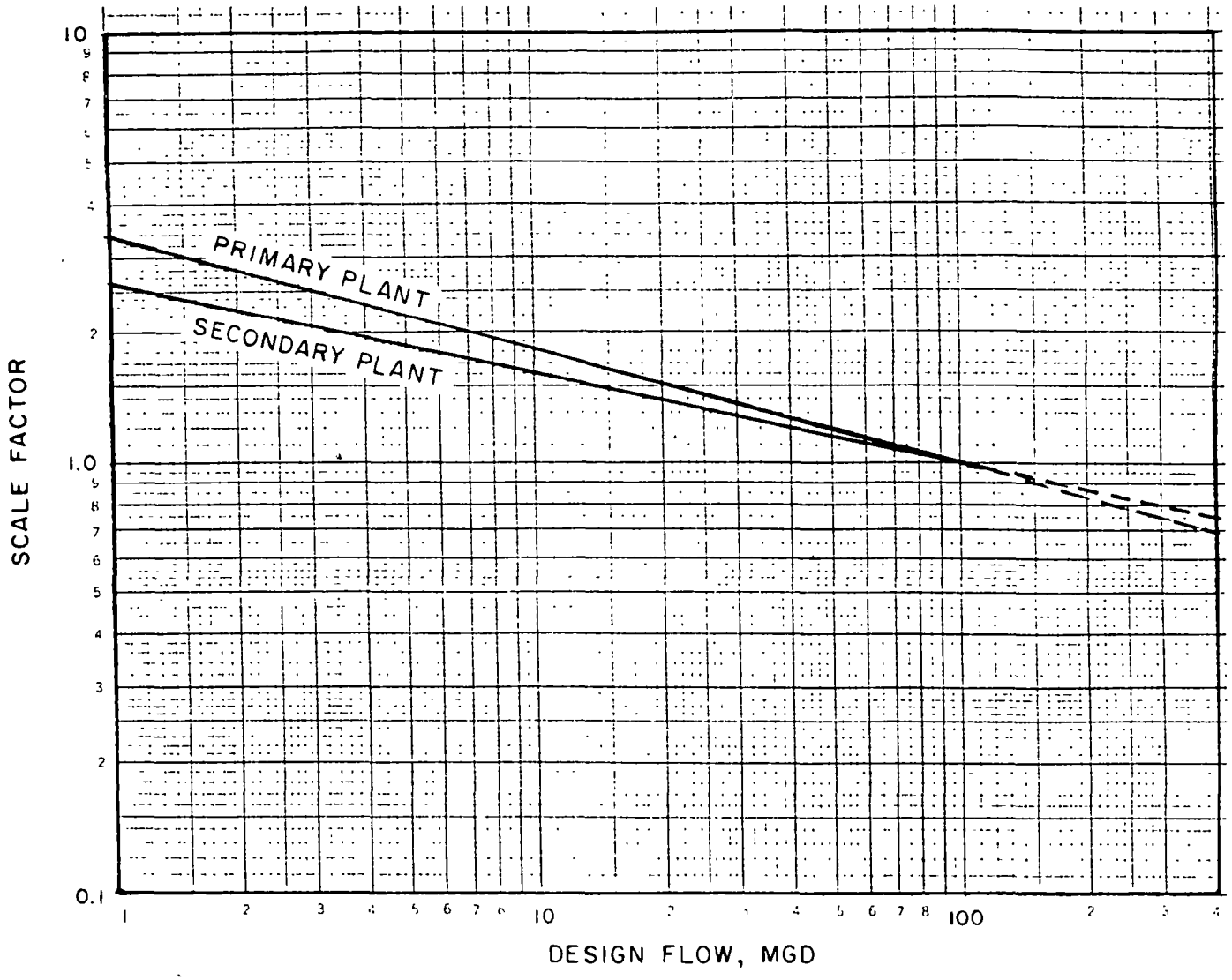

FIGURE 6-44. EFFECT OF PLANT DESIGN FLOW ON UNIT COST

TABLE 6-15

COMPARATIVE ECONOMICS OF VARIOUS PROCESSES[19]

	Costs/1,000 gallons (Dollars)				
Activated Sludge	1 mgd	5 mgd	10 mgd	25 mgd	50 mgd
Conventional	1.02	0.49	0.38	0.29	0.24
Single Stage Nitrification	1.10	0.51	0.41	0.31	0.26
Two Stage Nitrification	1.21	0.59	0.46	0.35	0.29
Conventional with Coagulation & Filtration*	1.49	0.71	0.55	0.44	0.37
Granular Carbon Systems*					
1,500 lbs carbon/mg	1.84	0.73	0.58	0.46	0.40
750 lbs carbon/mg	1.75	0.66	0.52	0.40	0.35
200 lbs carbon/mg	1.72	0.64	0.48	0.36	0.31
Powdered Carbon Systems					
Eimco* - "PAC"					
Basic Process	2.08	0.94	0.77	0.62	0.56
Single Stage	1.96	0.89	0.73	0.60	0.54
Two Stage with 100 mg/l Carbon	1.89	0.72	0.57	0.42	0.37
Two Stage with 300 mg/l Throwaway (5¢/lb) Carbon	1.68	0.81	0.68	0.53	0.48
Battelle* - "PAC"					
Basic Process	1.70	0.97	0.87	0.78	0.71
200 mg/l Carbon, 125 mg/l alum	1.18	0.55	0.46	0.39	0.35
200 mg/l Carbon without Filtration	0.96	0.48	0.41	0.36	0.33
Bio-Physical - "PACT"					
Basic Process	1.46	0.55	0.43	0.33	0.29
Carbonaceous Criteria	1.43	0.52	0.39	0.30	0.26
Effect of 50% Reduction in Carbon Price on Basic Process					
Eimco	2.02	0.88	0.71	0.56	0.50
Battelle	1.58	0.85	0.75	0.66	0.59
Bio-Physical - "PACT"	1.44	0.53	0.41	0.31	0.27
Effect of Multiple Hearth Regeneration on Basic Process					
Eimco	2.21	1.00	0.81	0.65	0.60
Battelle	1.66	0.91	0.78	0.72	0.67
Bio-Physical - "PACT"	1.66	0.63	0.50	0.38	0.33
Filtration	0.22	0.07	0.05	0.034	0.024

*These processes include effluent filtration.

TABLE 6-16

ESTIMATES PROCESS EFFLUENT QUALITY CHARACTERISTICS

	Primary Treatment	Activated Sludge	Activated Sludge Nitrification	Activated Sludge and Coagulation and Filtration	Physical-Chemical Processes			
					Granular Carbon System	"PAC" Eimco Process	"PAC" Battelle Process	"PACT" Bio-Pysical Process
BOD (mg/l)	140	25	15	15	20	20	20	20
Suspended Solids (mg/l)	70	25	15	0.5	7	10	10	20
Total P (mg/l)	9.8	6.7	6.7	0.1	0.3	6.7	6.7	6.7
Total N (mg/l)	32	25	25	25	25	25	25	28
NH_3-N (mg/l)	25	23	1	23	23	23	23	3
NO_3-N	-	-	23	-	-	-	-	18

O&M Costs have been extracted from the I&A Technology Manual to show approximate costs for nitrification, denitrification and phosphorus removal. Approximate adjustments for 1981 costs are shown allowing for increased power (2-3), labor (1.5) and chemical costs (2). Figure 6-45 presents this information.

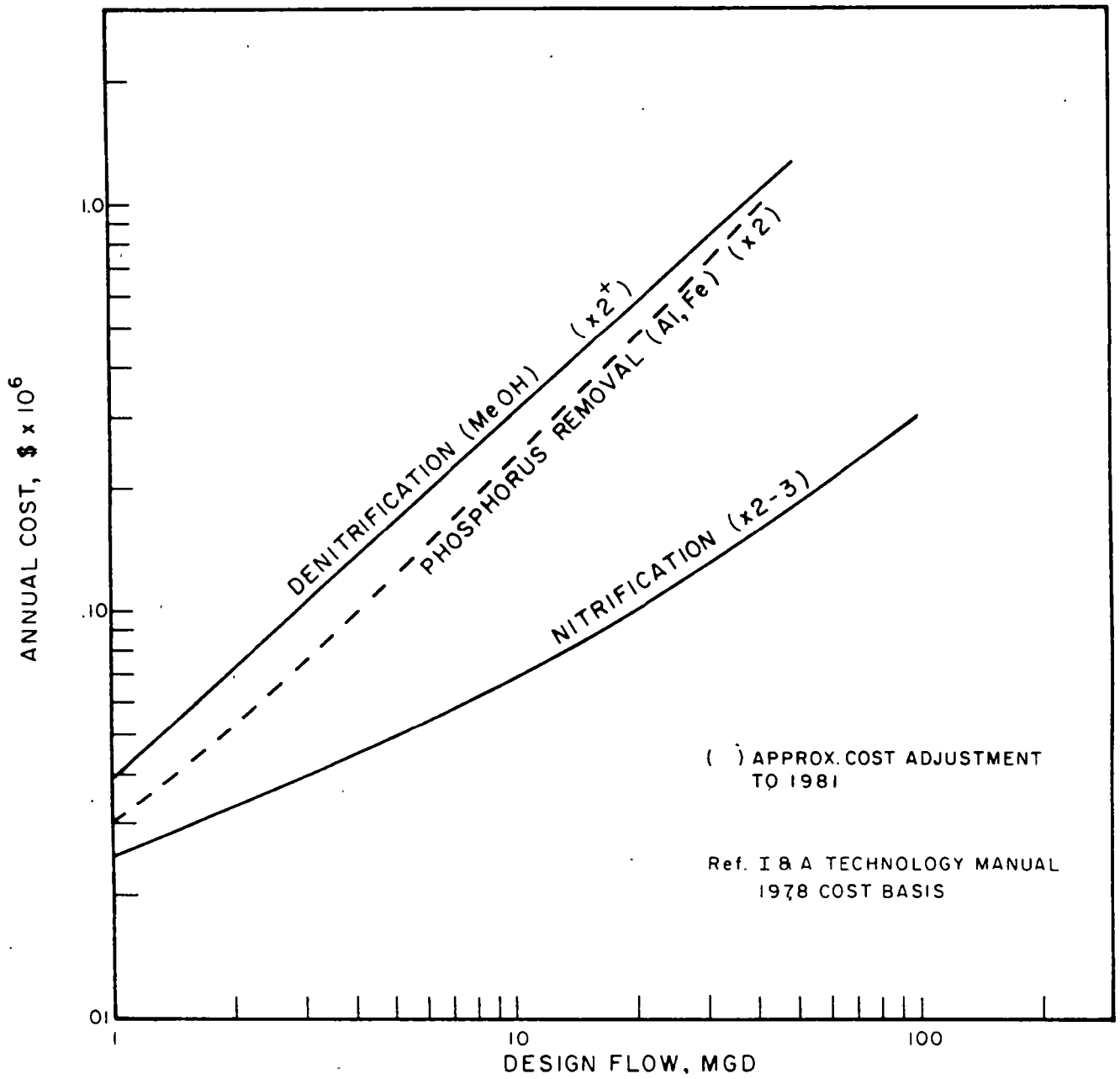

FIGURE 6-45

NUTRIENT REMOVAL
O & M COST

REFERENCES

1. Process Design Manual for Nitrogen Control - EPA Technology Transfer.

2. Process Design Manual for Phosphorus Removal - EPA Technology Transfer.

3. PACT Process State of Art Review - HydroQual internal document.

4. Biological Waste Treatment - Manhattan College 1981 Summer Institute in Water Pollution Control.

5. Performance of Activated Sludge Processes and Reliability Based Design - Niku, et. al., Journal of Water Pollution Control, December 1979.

6. Stability of Activated Sludge Processes Based on Statistical Measures - Niku, et. al., Journal of Water Pollution Control, April 1981.

7. Innovative and Alternative Technology Assessment Manual, EPA 430/9-78-009.

8. Results of Various Industrial & Municipal Wastewater Treatment Studies - HydroQual, Inc.

9. Florida Sewage Treatment Plant First to Remove Nutrients with Bacteria Alone, Burdick, et. al., October 1978. Civil Engineering - ASCE.

10. Biological Nutrient Removal Without the Addition of Chemicals, Barnard, J. L., Envirotech.

11. Grieves, G. G., Stenstrom, M. R., Walk, J. D., and Grutsch, J. F., "Powdered Carbon Improved Activated Sludge Treatment," Hydrocarbon Processing, Vol. 56, 125-120, Oct. 1977.

12. Crame, L., "Activated Sludge Enhancement: A Viable Alternative to Tertiary Carbon Adsorption," presented at 2nd EPA-API-NPRA-UT Forum, Tulsa, Oklahoma, June 6-9, 1977.

13. Kehrberger, G., "Nitrification Study for LaPorte, Texas Plant, E. I. Dupont de Nemours & Co., Inc.," Hydroscience, DUPO0600, May 1978.

14. Mulligan T., "Process Evaluation Studies of the Cone Mills Dye Waste Disposal Plant, Greensboro, N. C.," Hydroscience, Inc., June 1976.

15. Shuckrow, A. J. and Culp, G. L., "Appraisal of Powdered Activated Carbon Processes for Municipal Wastewater Treatment," EPA-600/2-77-156.

16. Zimpro, Inc., "Carbon Impacts Vernon," REACTOR, publication of Zimpro, Inc., August 1979.

17. Singley, J. Beaudet, B., Ervin, A., and Zegel, W., "Use of Powdered Activated Carbon to Reduce Organic Contaminant levels," from Environmental Science & Engr., Inc., May 10, 1979.

18. Grutsch, J. F. and Kloeckner, D. C., "Application of Industrial Treatment Technology to Municipal Wastewater," presented at the 52nd Annual WPCF Conference, Houston, October 1979.

19. Hutton, D. and Temple, S., "Priority Pollutant Removal: Comparison of Dupont PACT PROCESS and Activated Sludge," 52nd WPCF Convention, Houston, Texas, October 1979.

TREATMENT OF TOXIC WASTEWATERS[a]

By Thomas J. Mulligan,[1] M.ASCE, James A. Mueller,[2] M. ASCE, O. Karl Scheible,[3] A.M. ASCE

INTRODUCTION

Congress has enacted more than two dozen statutes regulating potential routes by which certain chemicals or chemical usages can threaten human health and environment. The Clean Water Amendments of 1977 address in particular the control of toxic material discharge to natural water systems. Section 304 stipulates that technology-based effluent limitations are required for all pollutants, including toxic substances, from point source discharges. Although past effluent standards dealing with broad, non-specific parameters such as biochemical oxygen demand (BOD_5) and suspended solids will continue to be important measures, limits are now being promulgated for specific chemical compounds. This will place new and complex demands on pollution control technology since removals of priority pollutants will be required to much higher levels than have generally been accomplished by conventional treatment systems.

Toxic pollutants are presently defined as the priority pollutants identified in the National Resource Defense Council (NRDC) vs. Train Consent Decree. There are a total of 129 substances presently on the list, including 114 organics, 13 metals, cyanide, and asbestos. The following presents a discussion of alternate treatment processes capable of removing these priority pollutants from wastewater. No attempt is made here to be all inclusive, but those processes that have in general the widest potential application have been selected for inclusion in this discussion.

a. Presentation at the May 11-15, 1981, ASCE International Convention and Exposition, held in New York City, N.Y.

1. President, HydroQual, Inc., Mahwah, N.J.
2. Staff Consultant, HydroQual, Inc., Mahwah, N.J.; Associate Professor Environmental Engineering and Science Program, Manhattan College, Bronx, New York, N.Y.
3. Principal Engineer, HydroQual, Inc., Mahwah, N.J.

ACTIVATED CARBON

The ability of activated carbon to function effectively as a practical adsorbent is due to an extremely large active surface per unit mass. Carbon adsorption is generally favored for compounds of a hydrophobic nature, i.e., low water solubility. Since the solubility of organics will typically decrease with increasing chain length, adsorption is greater for higher molecular weight compounds.

The quantity of sorbate that can be adsorbed by a given weight of activated carbon is related to the concentration of the sorbate in the external liquid phase. Adsorptive capacity increases with liquid-phase concentration. An adsorption isotherm is the relationship (at constant temperature) between the equilibrium concentration of sorbate in solution and the quantity adsorbed per unit weight of carbon.

Dobbs et. al.,(1) have computed data on carbon adsorption isotherms for a number of toxic organics. Carbon adsorption capacities were determined at an equilibrium concentration of 1 mg/l and neutral pH utilizing pulverized Filtrasorb 300. When considering the priority pollutants, the pesticides, acid extractable phenolic compounds, and most of the base/neutral extractable organics were found to adsorb reasonably well on activated carbon. The purgeable organics are typically poorly adsorbed. The nitrosamines and haloethers, depending on the particular compound, may or may not exhibit good adsorption onto carbon.

The influence of pH depends on the physico-chemical properties of the individual organic. Adsorption decreases with increasing ionization and with increasing polarity of compounds. Adsorption will generally be enhanced at pH levels below the pk values of the compounds. Non-destructive regeneration of activated carbon has been practiced using an acid or alkaline as the regenerant and is applicable when the adsorbed chemical is ionized by a change in pH. This method is particularly attractive when considering chemical recovery.

Interaction between components in a mixture can reduce the adsorption of some components well below that which would exist in a single solute waste stream. As an example, consider a wastewater mixture of two compounds, p-nitrophenol and phenol. Of the two compounds, p-nitropenol is the more favorably adsorbed. As schematically illustrated on the upper display of Figure 1, phenol is prevented (time = t_1) from adsorbing onto the carbon at the influent end of the column due to competition from the favored p-nitrophenol for adsorption sites. But it adsorbs without inhibition at downstream positions. As the bed becomes

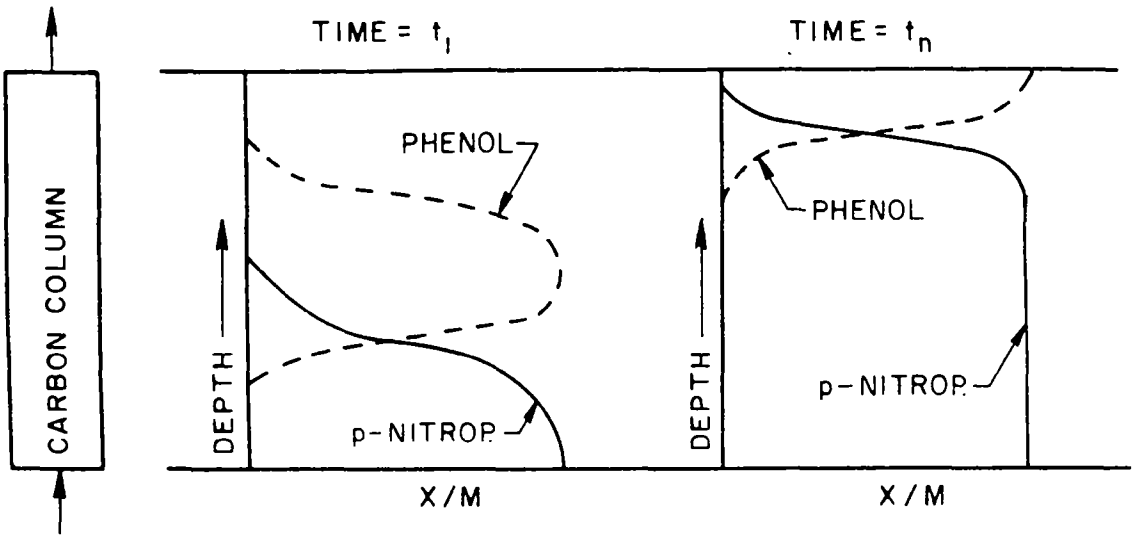

Schematic of solid phase loading with depth.

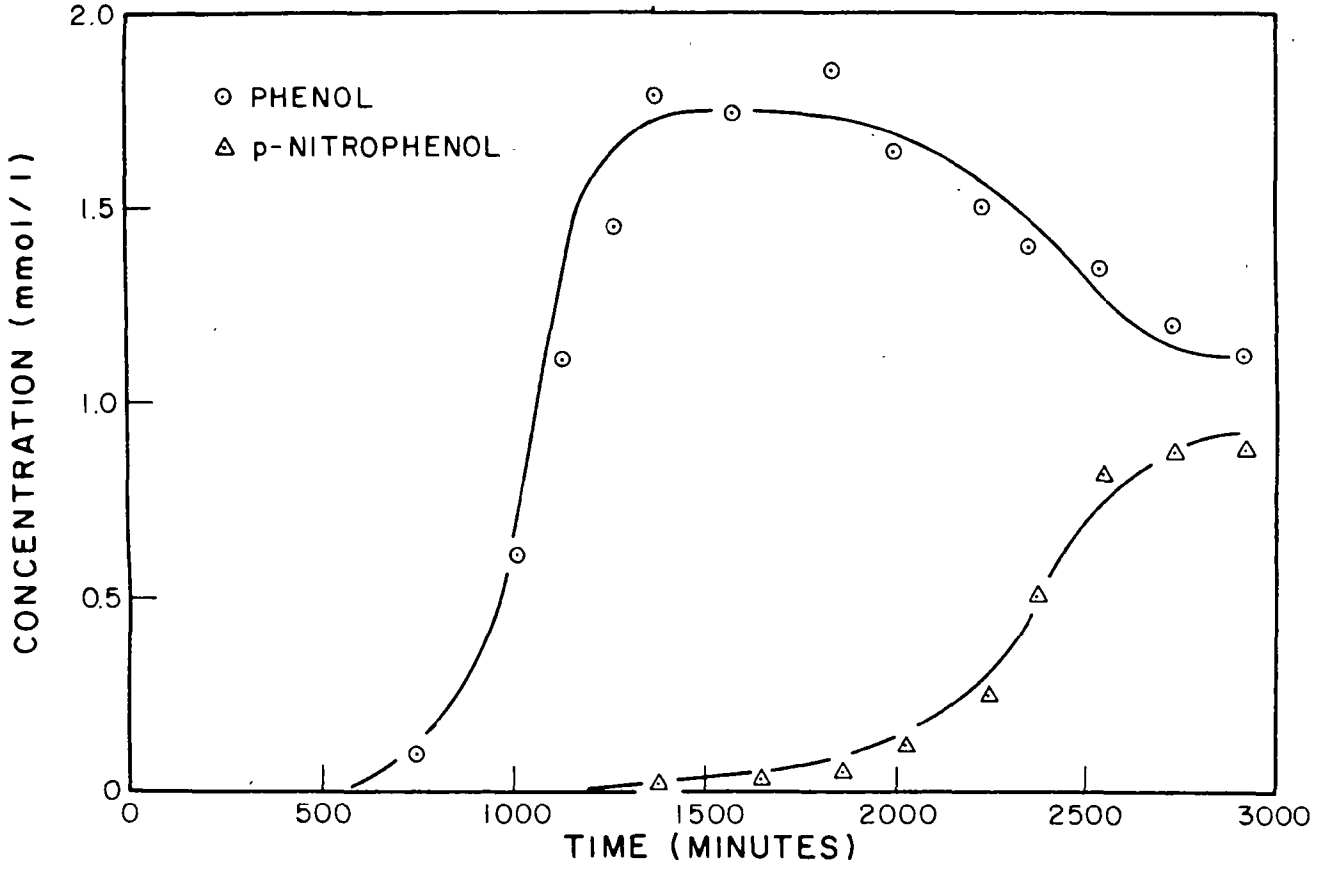

Figure 1. Breakthrough curves illustrating competitive adsorption of organics.

saturated (time = t_n), p-nitrophenol advances through the column and contacts carbon which had been exposed only to phenol. Displacement of the phenol by p-nitrophenol then occurs. This can result in the effluent concentration of the displaced organic actually rising above the raw waste concentration.

This phenomenon is confirmed in the lower display of Figure 3, which presents actual breakthrough curves for the binary system of phenol and p-nitrophenol (2). The feed solution contained equal molar concentrations of each compound (1 mmol/l) and was pumped at a constant rate to a system with a large inventory of carbon. The system was able to accumulate a significant amount of phenol. As the more readily adsorbed material (p-nitrophenol) saturates the carbon, phenol displacement occurs and effluent phenol concentrations actually increase to levels well above feed concentrations.

Thus although solute isotherm analyses are important and provide information on the potential of activated carbon as a treatment process for the removal of a specific compound, compound interactions are an important element in defining carbon adsorption capacities for the priority pollutants. Continuous flow laboratory or pilot studies should be performed in order to develop design criteria. The use of mathematical models to simulate the competitive adsorption of organics in carbon columns can effectively reduce the amount of pilot study required to evaluate and design an activated carbon adsorption system for a given wastewater.

CHEMICAL OXIDATION

Classifying the chemical oxidizability of organic compounds is difficult because of the interaction of many variables. Large molecule organics, such as the PCB's, pesticides and other cyclic organics are generally not amenable to chemical oxidation, except under certain catalyzed conditions. Polar, low molecular weight organics such as acetic acid are also generally resistant. Process selection for chemical oxidation is usually based on economics, which in turn rely on waste volume and characterics, reaction stoichiometry, and kinetics. The completeness of the oxidation reactions and the formation of by-products are also being addressed now with increasing importance.

The oxidants in wide use today are chlorine, ozone, and hydrogen peroxide. Permanganate and chlorine dioxide have had limited applications. Chlorine dioxide has been shown to be a selective oxidant with particular application to cyanide, phenol, sulfides and mercaptons.

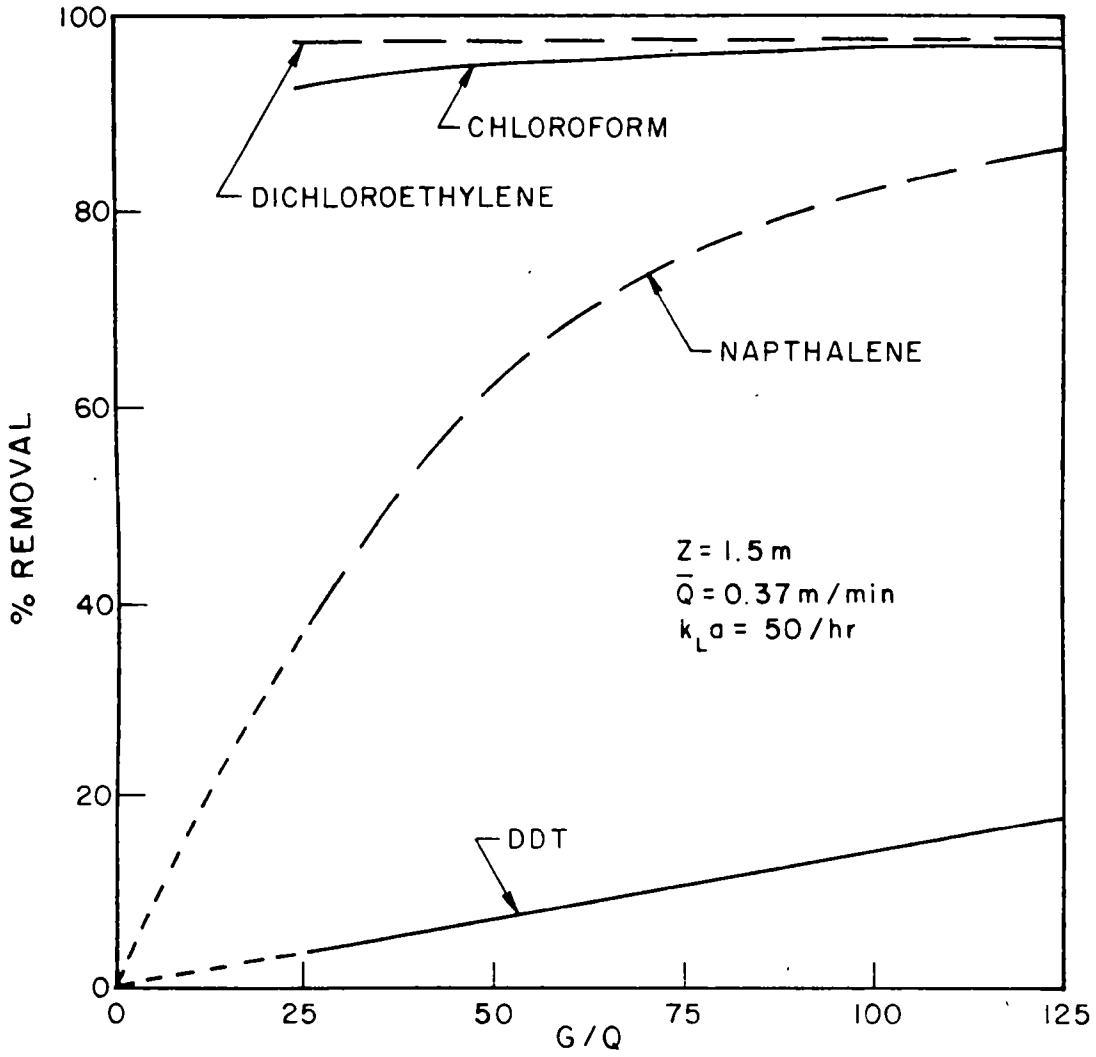

Figure 2. Effect of gas to liquid flow ratio on air stripping of priority pollutants in packed towers.

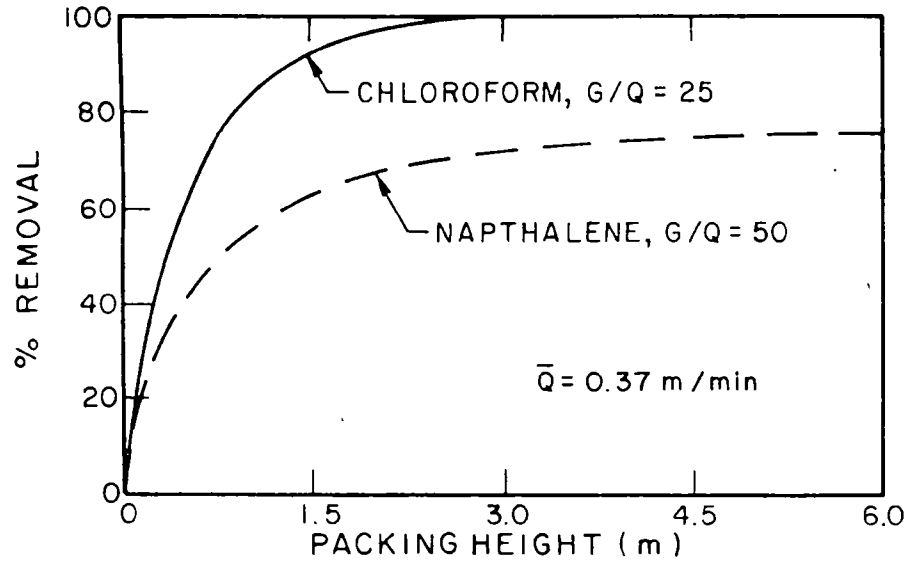

Figure 3. Effect of packing height on stripping efficiency.

Optimization of chlorination often requires strict control pH, since the aqueous chemistry of chlorine is pH dependent. The pH dependence of the organics to be oxidized is also a critical element in control of the reactions. Generally, oxidation rates are highest when the organic compound is present as the disassociated species.

Chlorination under alkaline conditions has long been an accepted practice for the destruction of cyanides and is an effective oxidant of phenols at high pH, where the hypochlorite ion is favored. Recent work has also centered on the control of the chlorination process to allow step-wise oxidation of mixtures by manipulation of pH. A study reported the chlorination of methylamine, emphasizing the importance of pH control for optimum reaction rate and selective reaction pathways (3).

Hydrogen peroxide has had little direct application to the destruction of priority pollutant organics. It is effective in oxidizing phenols and cyanides (alkaline pH) and has the advantage of adding minimally to the dissolved solids of the solution. Generally, peroxide has been used in conjunction with a catalyst.

Ozone is an allotropic state of oxygen and is significantly more active because it delivers elemental oxygen. As with chlorination, care must be exercised in controlling the pH at which ozonation reactions occur. Ozone is typically ineffective under acidic conditions.

Fochtman and Eisenberg(4) reported on the treatability of several priority (or similar) pollutants by ozonation. Compounds which were found to readily react with ozone were 1,1-diphenylhydrazine, beta-naphthylamine, and 4,4-methylene-bis(2-chloroaniline). Naphthalene was found to react slowly with ozone, while dimethylnitrosamine was resistant to ozone oxidation. Nebel, et. al. (5) reported the application of ozone oxidation to phenolic effluents and indicated that high pH (optimum pH = 11.8) values favored oxidation of phenol by ozone.

ULTRAVIOLET PHOTOLYSIS AND CATALYZATION

Chemical oxidation utilizing the primary oxidants described above can be significantly enhanced by employing the synergistic and/or catalytic effects of ultraviolet light energy. Ultraviolet photolysis can in itself provide pretreatment by detoxifying certain compounds, particularly chlorinated organics. This is accomplished by cleavage of the chlorine-carbon bond. The altered compounds may subsequently be amenable to biological treatment. Banerjee, et. al., (6) reported the photodegradation of 3,3-dichlorobenzidine utilizing ultraviolet energy in a pure

solute. The decomposition of TCDD was reported by Batre, et. al. (7) Ultraviolet photolysis was also utilized to destroy dioxin contained in a waste sludge by-product. (8)

Prober, et. al., (9) reported the impact of ultraviolet energy on the ozone oxidation of ferricyanide. The synergistic effects of ozone and ultraviolet caused the rate of reaction to increase by an order of magnitude over what would result with either one individually. Meiners, et. al., (10) studied the effect of ultraviolet radiation on the rate and extent of chlorine oxidation of organic material in a highly nitrified effluent. They determined that ultraviolet increased the rate of oxidation by a factor of 3 to 10, with maximum rates occurring at pH 5.

AIR STRIPPING

Since approximately 35% of the organic priority pollutants are volatile to some extent, air stripping is a viable process for significant organic removal. A number of equipment configurations can be utilized for this purpose. Conventional aeration tanks used in activated sludge wastewater treatment, employing either diffused or mechanical aeration, can obtain significant stripping of volatile organics. The most effective type of air stripper for the highly volatile compounds are countercurrent packed towers. Cross flow towers can be utilized when high gas to liquid flow ratios are required for the less volatile compounds.

A quantitative evaluation of air stripping may be obtained by applying basic gas transfer principles. The rate of air stripping across a liquid-gas interface can be simplistically related to resistance in two films; one on the gas side of the interface and the other on the liquid side. Gases with high Henry's Constant values, such as oxygen, are relatively insoluble, and liquid film controls the transfer rate. Gases with low H values, such as ammonia, are highly soluble and the gas film controls the transfer rate. For the toxic organics, both phases can be important depending on the compound. The more volatile compounds, where liquid film controls, can be easily removed by stripping.

Mass balance equations for both liquid and gaseous phases can be solved at steady state to evaluate the capabilities of specific air stripping systems for removal of toxics. For countercurrent packed tower strippers, the height of a packed tower is related to the chacteristics of the packing medium and hydraulic loading rate. Both affect the gas transfer coefficient and Henry's constant for a particular toxicant. The height is also related to the ratio of the gas and liquid flow rates, a major design parameter.

Figure 2 shows the results of a packed tower air stripping analysis using a 2.5 cm Raschig ring packing medium. Four toxic organics were chosen representing a range of volatilities. Those compounds more volatile than chloroform will have greater than 90% removal at relatively low G/Q values of 25. Intermediate volatile compounds such as napthalene will be markedly affected by the G/Q ratios, requiring values of 50 or greater for substantial removals. The low volatility compounds such as DDT will require extremely high G/Q values for significant removals. The DDT curve is linear, indicating that removal is completely controlled by G/Q and not markedly affected by transfer coefficient. Thus, gas phase saturation for the low volatility compounds is reached quickly, requiring high gas flow rates for significant removal. Further analysis (Figure 3) would demonstrate that the height of packing has a slight effect on removals in the range of 1.5 to 3.0 meters and substantially no effect when greater than 3 meters. Detention time (total tower volume) varies from 4 to 8 minutes for the 1.5 to 3.0 meter column.

Upper limits of G/Q exist for countercurrent flow columns to prevent flooding the column. In this situation, the liquid cannot flow downward but is pushed out the top of the column due to an excessive gas flow rate. To attain significant removals for the low volatility compounds, either cross flow stripping towers or surface aeration with high G/Q values must be used.

Figure 4 presents the expected removal efficiencies by air stripping in aeration tanks. Diffused aeration systems have the lowest removal efficiencies due to the gas flow limitation per diffuser. The lower gas flow (G/Q = 2 - 5) range would be typical of fine bubble dome or disc type diffusers having transfer efficiency (E_o) values near 20%, while the higher gas flow range would be typical of the coarse bubble units with lower transfer efficiencies (6 - 10%). The higher removal efficiencies attained by the surface aerators are due to the capability of blowing relatively large amounts of air across the surface. Significant removals of the low volatility compounds such as DDT can be attained at these high gas flow rates. These rates are similar to those used in ammonia stripping.

An important design parameter for the surface aeration system is the power per unit flow rate, hp/Q. Analysis indicates that at hp/Q levels above 0.08 kWh/m^3 (400 hp-hr/MG), little additional removal capability is attained. Staging the reactors to attain more of a plug flow system may improve removals. At intermediate removal efficiencies for the volatile compounds (chloroform, G/Q = 25), removals may be increased by 10 to 20% by using 3 to 4 stages instead of 1. There is little impact from staging for the low volatility compounds since the major effect is the G/Q ratio.

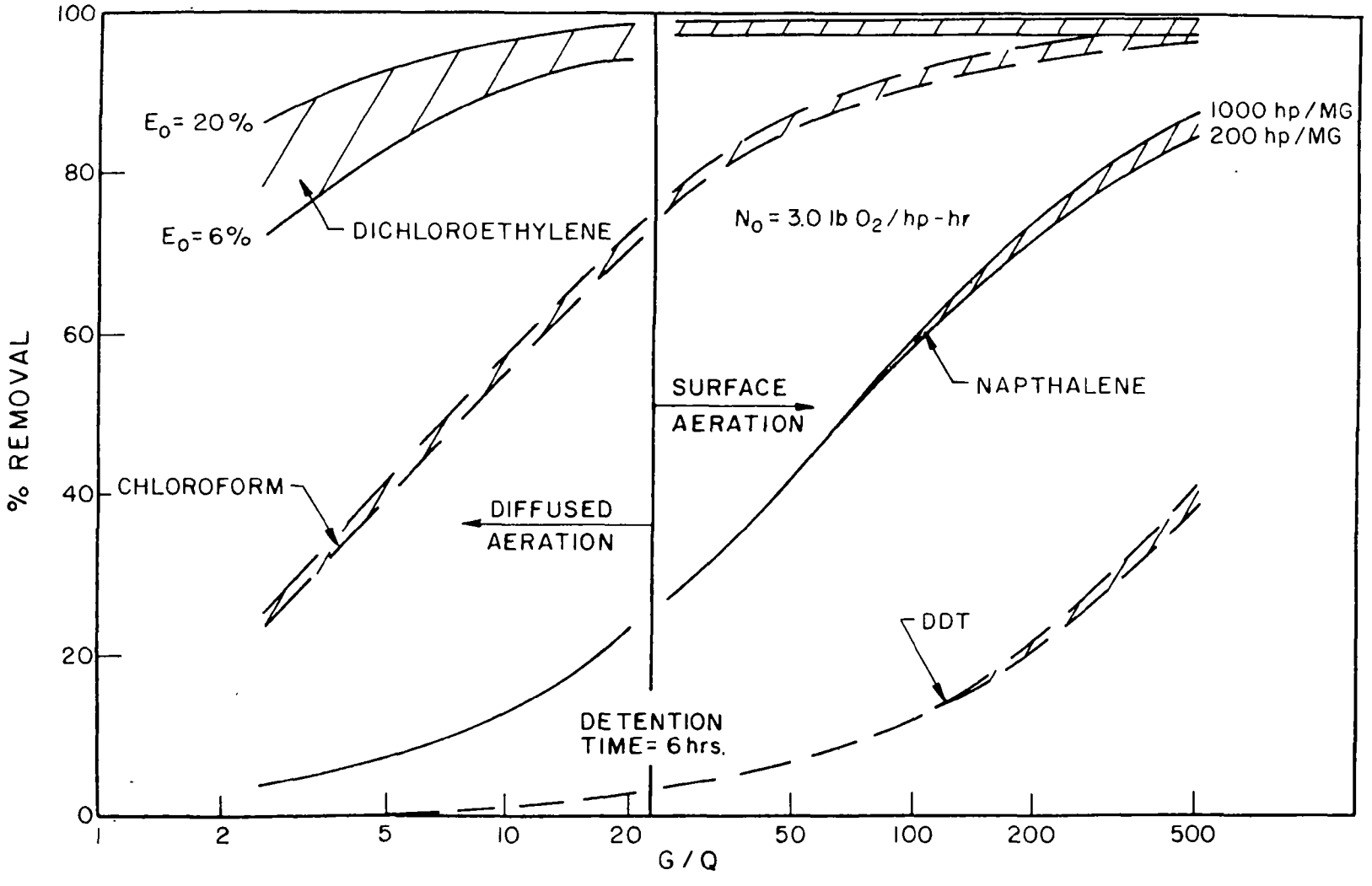

Figure 4. Effect of gas to liquid ratio on air stripping of priority pollutants in aeration basins.

Table 1 summarizes the characteristics of field air stripping systems and their measured organic removal efficiencies (11, 12). The field systems were designed for decarbonation and ammonia stripping at Water Factory 21 in Orange County, California, and ammonia stripping at Palo Alto.

TABLE 1. CHARACTERISTICS OF FIELD AIR STRIPPING SYSTEMS

	Packed Towers			
	Countercurrent Flow	Cross Flow		Mechanical Aeration
		Fans On	Fans Off	
Location Design Purpose	Orange Cty, Ca. Decarbonation	Orange Cty, Ca. Ammonia Stripping		Palo Alto, Ca. Ammonia Stripping
G/Q	22	2700	225	430
hp/Q hp-hr/MG	69	690	140	2770
t_o, min_{-1}	1.5	50	50	340
$K_L^o a$, hr^{-1}	89 ($CHCl_3$)	3.2(NH_3)	--	2.5($CHCL_3$)
	Removal Efficiencies, %			
Tetrachloroethylene	--	--	95	99
Trichloroethylene	--	--	--	99
Chlorobenzene	--	96	--	--
1,1,1-Trichloroethane	--	--	91	--
Chloroform	79	83	79	92
Bromodichloromethane	85	--	--	94
Dibromochloromethane	71	--	82	82
1,3-Dichlorobenzene	--	--	83	94
1,4-Dichlorobenzene	--	97	92	92
1,2-Dichlorobenzene	--	--	88	91
1,2,4-Trichlorobenzene	--	--	--	92
NH_3	--	81	25	--

BIOLOGICAL TREATMENT

Given the prevalence of biological systems for wastewater treatment, they must be regarded as a critical element in the control of priority pollutants. This would be relative to direct applications for the removal of priority pollutants, or to the

impact of priority pollutants on subsequent biological processes. Design of biological systems for specific industrial wastewater applications requires a high degree of process evaluation, especially for wastewaters containing compounds toxic to the organisms, or compounds generally resistant to biodegradation. Process modifications to minimize these impacts have been successfully applied, notably the completely mixed activated sludge and extended aeration processes. Microbial populations may also be successfully adapted to specific wastewaters and achieve efficient oxidation.

Three mechanisms can describe the removal of priority pollutants in a biological process: biodegradation, adsorption, and volatilization. Biodegradation is the only true treatment mechanism, resulting in a decomposition of the material to stable by-products. Adsorption and stripping remove the material from the wastewater to the solid and gas phase, respectively. These are legitimate mechanisms, but it must be understood that the subsequent impact of the compounds on the plant sludges and air quality need to be fully understood and properly accounted for. Should these removal mechanisms result in an environmentally incompatible sludge or in unsafe air quality conditions, alternative processes would be required to remove and/or treat the material.

Results on the biodegradability of ninety-six priority pollutant compounds have been presented (13). Of the ninety-six tested, twenty-three were found to be resistant to degradation. All but four of these are halogenated, with a significant degree of halogen substitution. Generally, the results imply that the majority of the priority pollutants are treatable by biodegradation. Such results, however, must be used with caution. Acclimation often entails concentration levels which are high enough to be available in the organic matrix. Low levels in certain systems render the compound non-competitive to more degradable material and may never be amenable to adaptation, thus passing through the plant.

A survey of 40 POTW's for the removal of priority pollutants has been an ongoing EPA sponsored study. In an interim report (14) on 20 plants, preliminary analysis indicates the POTW's to be capable of significant organics removal. Net losses for total priority organics in 5 plants ranged from 26 to 76%. These losses were attributed to both volatilization and biodegradation.

System design for the biological treatment of the biodegradable priority pollutants can generally follow normal process evaluation procedures and analysis. Laboratory investigations should be carried out which evaluate loading rates to achieve a desired effluent quality to determine maximum

permissible concentrations before inhibition sets in; and to assess the degree of variability which would be acceptable to the process. Generally, in systems which must achieve removal of substances which are resistant to biodegradation, the design incorporates low loadings and extended sludge ages.

The "PACT" process (duPont patent) is an activated sludge process employing powdered activated carbon (PAC) addition to the aeration tanks for adsorption of non-degradable organics. Hutton (15,16) described removals in the duPont Chambers Works "PACT" plant which treats 136,000 m^3/day (36 mgd) of chemical plant wastewater, using an average PAC dosage of 126 mg/l (37 percent regenerated). Of 36 organic priority pollutants found in the feed to the wastewater treatment plant, 90% removal or greater was achieved for 28. The overall removal of dissolved organic carbon at the plant was 81% while color removal was 64%. Thus most of the priority pollutants were removed to a greater extent than the overall organic carbon or color.

1. Dobbs, Richard A., Cohen, Jesse M., Carbon Adsorption Isotherms for Toxic Organics, EPA-600/8-80-023, April 1980.

2. Famularo, J., "Binary Characterization of Wastewater Adsorption," presented at the 52nd Annual WPCF Conference, Houston, Texas. October 1979.

3. Exner, Jurgen H., Fox, Robert D., Parmili, Charles S., and Mayer, John R., "Chlorination Effects on Typical Organic Chemical Plant Effluents," Presentation at the Conference on Water Chlorination, Gatlinburg, Tenn. October 31, 1977.

4. Fochtman, Edward G. and Eisenberg, Walter, Treatability of Carcinogenic and Other Hazardous Organic Compounds, Municipal Environmental Research Laboratory, U.S.E.P.A. EPA-600/2-79-097, Cincinnati, OH, August 1979.

5. Nebel, Carl, Gottschling, Ronald G., Holmes, John L., Unangst, Paul C., "Ozone Oxidation of Phenolic Effluents" 31st Industrial Waste Conference, Purdue University, Ann Arbor Science, 1976.

6. Banerjee, S., et. al., "Photodegradation of 3,3-dichlorobenzidine, Environmental Science and Technology, V12, No. 13, December 1978.

7. Batre, C., et. al., "TCDD Solubilization and Photodecomposition in Aqueous Solutions," Environmental Science and Technology, Vol 12, No. 3, March 1978.

8. IT Enviroscience, "Destroying Dioxin; A Unique Approach," Waste Age, October 1980.

9. Prober, Richard, Melnik, Peter B., Mansfield, Lee A., "Ozone-Ultraviolet Treatment of Coke Oven and Blast Furnace Effluents for Destruction of Ferricyanides" 32nd Industrial Waste Conference, Purdue University, Ann Arbor Science, 1977.

10. Meiners, A.F., Lawler, E.A., Whitehead, M.E., and Morrison, J.I., An Investigation of Light-Catalyzed Chlorine Oxidation for Treatment of Wastewater, NTIS PB-187757, December 1968.

11. McCarty, P.L., Sutherland, K.H., Graydon, J., and Reinhard, M., "Volatile Organic Contaminants Removed by Air Stripping", presented at AWWA Conference, San Francisco, Ca., June 1979.

12. McCarty, P.L., "Removal of Organic Substances From Water by Air Stripping," submitted to EPA, October 1980.

13. Tabak, J., Quave, S.A., Mashini, C.I., and Barth, E.F., "Biodegradability Studies with Organic Priority Pollutant Compounds" U.S.E.P.A., Office of Research and Development, Cincinnati, OH., April 1980.

14. Feiler, H. Fate of Priority Pollutants in Publicly-Owned Treatment Works, Interim Report, U.S.E.P.A., EPA-440/1-80-301, October 1980.

15. Hutton, D.G., "Removal of Priority Pollutants by the DePont PACT Process," presented at the 7th Annual Industrial Pollution conference, WW MA, Philadelphia, June 1979.

16. Hutton, D.G., "Removal of Priority Pollutants with a Combined Powdered Activated Carbon-Activated Sludge Process," presented at the 179th ACS meeting, Houston, Texas, March, 1980.

PRIORITY POLLUTANTS

I PURGEABLE ORGANICS

II BASE NEUTRAL

HALOETHERS
POLYNUCLEAR AROMATICS
PHTHALATE ESTERS
NITROSAMINES

CHLORINATED HYDROCARBON
NITROBENZENES
BENZIDINES

III ACID EXTRACTABLES

PHENOLS

IV PESTICIDES & PCB

V METALS

VI MISCELLANEOUS

ACTIVATED CARBON

FACTORS AFFECTING ADSORPTION

SOLUBILITY
IONIZATION & POLARITY
SURFACE TENSION
pH
TEMPERATURE

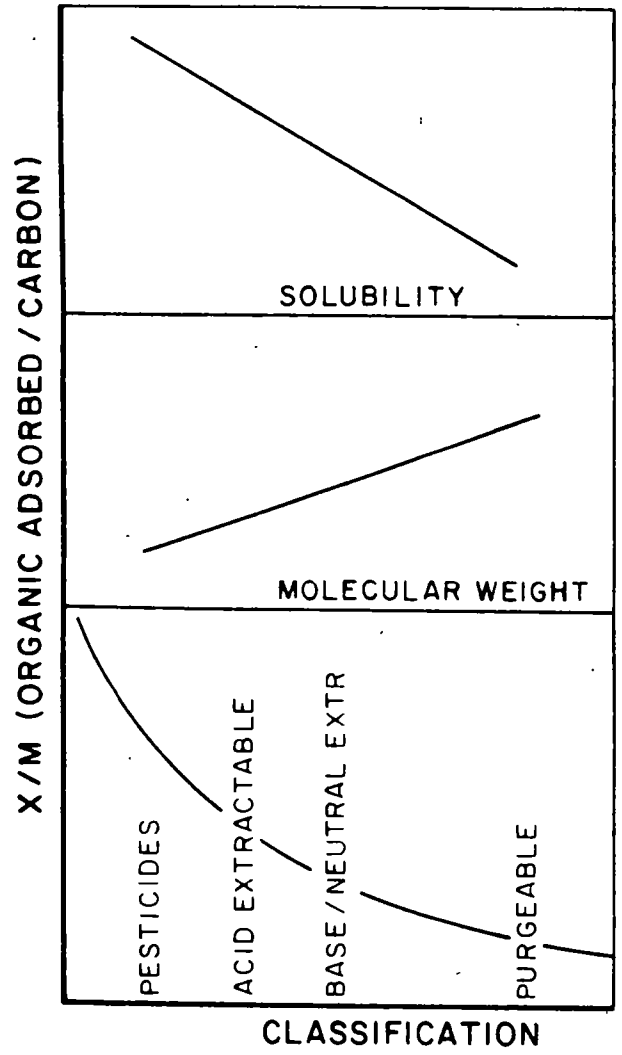

Figure I. General adsorption characteristics of priority pollutants.

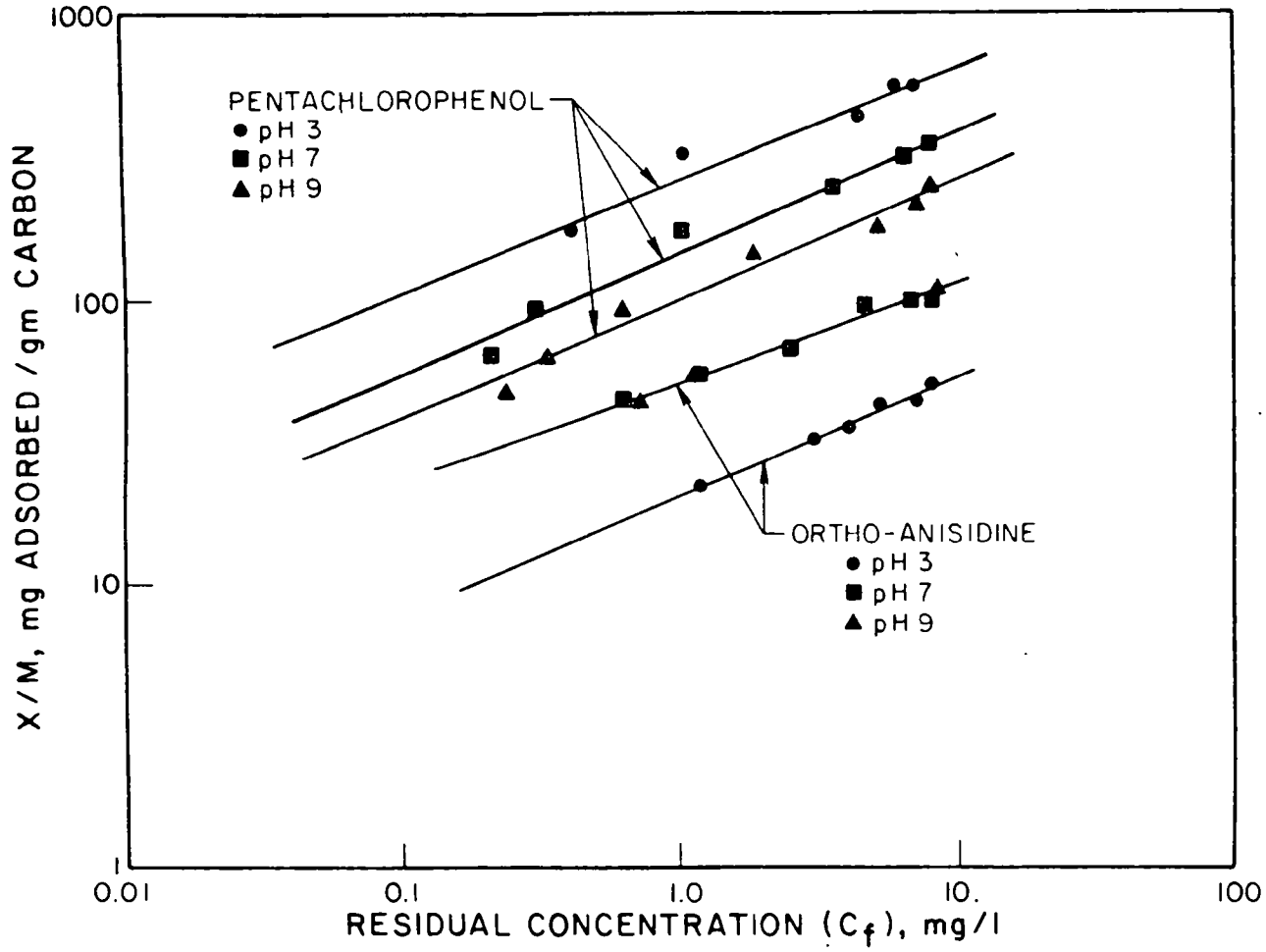

Figure 2. pH effect on activated carbon adsorption.

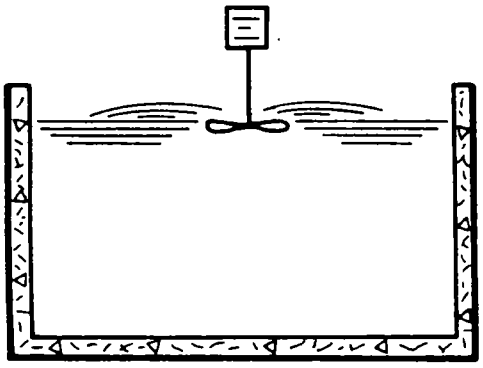

MECHANICAL AERATION

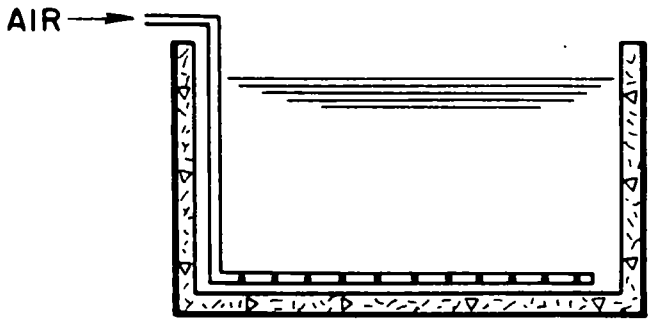

DIFFUSED AERATION

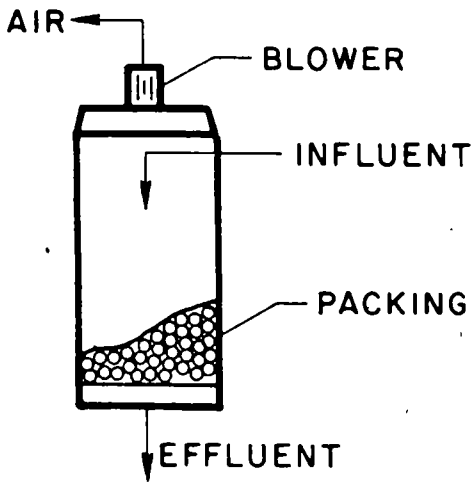

PACKED TOWER

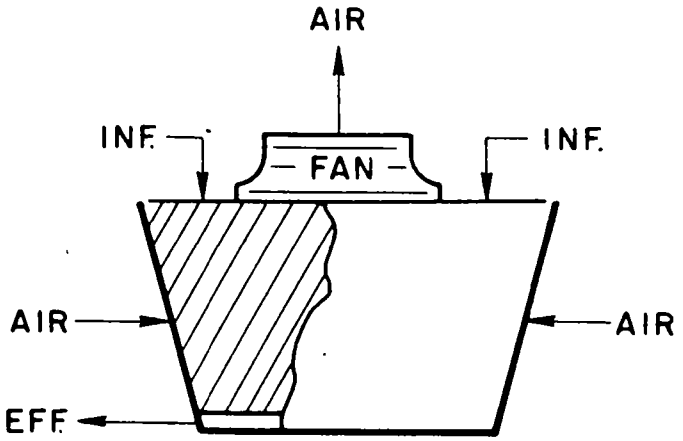

CROSS FLOW TOWER

Figure 6. Air stripping process configurations.

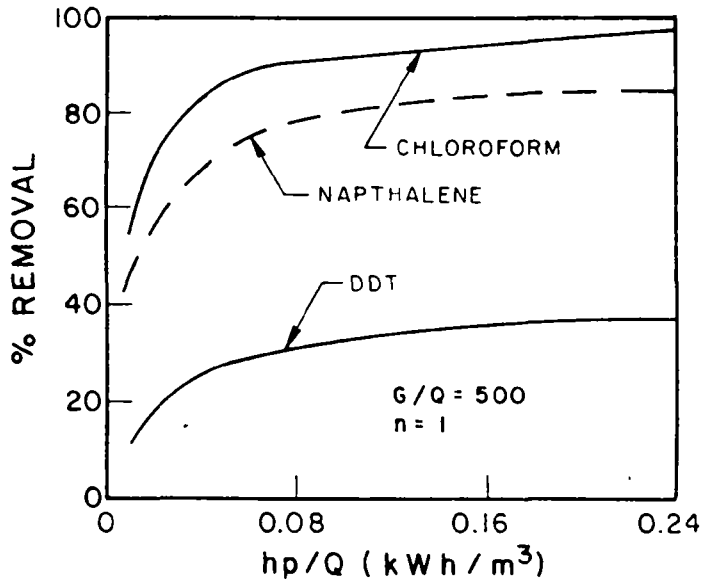

Figure 13. Effect of aerator mixer power in closed tank.

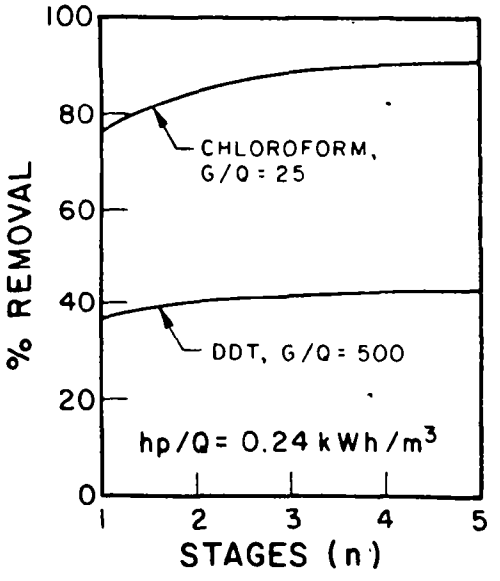

Figure 14. Effect of staging on stripping efficiency in closed tank.

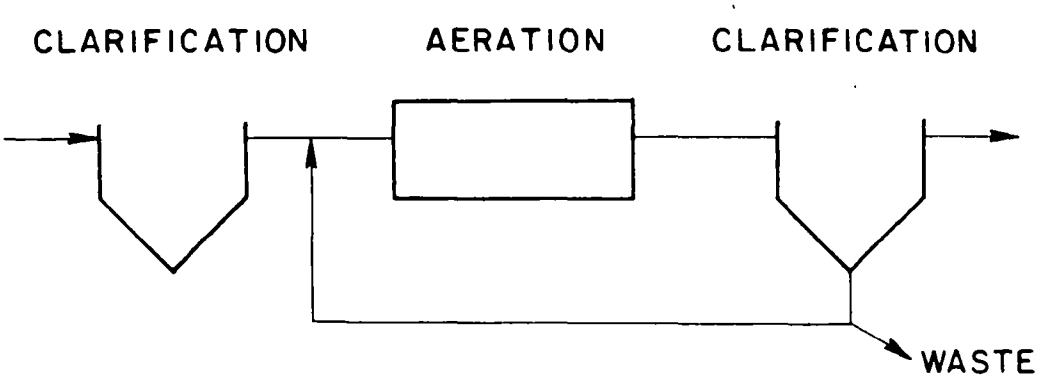

ACTIVATED SLUDGE

BIOCONCENTRATION ON ACTIVATED SLUDGE

COMPOUND	FACTOR
ACENAPHTHENE	24
1, 2 DICHLOROBENZENE	7-8
1, 3 DICHLOROBENZENE	5-28
FLUORANTHENE	15-45
NAPHTHALENE	8-29
N-nitrosodi-n-PROPYLAMINE	100
Bis (2-ETHYLHEXYL) phthalate	30-76
BUTYL BENZYL PHTHALATE	172
Di-n-butyl PHTHALATE	15-21
Di-n-octyl PHTHALATE	22
DIMETHYL PHTHALATE	6
BENZO (a) pyrene	48
BENZO (k) fluoranthene	20
CHRYSENE	20
ACENAPHTHYLENE	100
FLUORENE	9-30
PHENANTHRENE	23-31
TETRACHLOROETHYLENE	6
TOLUENE	48
PYRENE	31

CHARACTERISTICS STRIPPING SYSTEMS

PACKED TOWERS

	COUNTERCURRENT FLOW	CROSS FLOW FAN ON	CROSS FLOW FAN OFF	MECH. AERATION
LOCATION	ORANGE CITY[1]	ORANGE CITY[2]		PALO ALTO[2]
G/Q	22	2700	225	430
HP/Q HP-HR/MG	69	690	140	2770
T_0, MIN	1.5	50	50	340
REMOVAL EFFICIENCIES %				
TETRACHLOROETHYLENE	—	—	95	99
TRICHLOROETHYLENE	—	—	—	99
CHLOROBENZENE	—	96	—	—
1,1,1-TRICHLOROETHANE	—	—	91	—
CHLOROFORM	79	83	79	92
BROMODICHLOROMETHANE	85	—	—	94
DIBROMOCHLOROMETHANE	71	—	82	82
1,3-DICHLOROBENZENE	—	—	83	94
1,4-DICHLOROBENZENE	—	97	92	92
1,2-DICHLOROBENZENE	—	—	88	91
1,2,4-TRICHLOROBENZENE	—	—	—	92
NH_3	—	81	25	—

DESIGN POSPOSE:

(1) DECARBONATION

(2) AMMONIA STRIPPING

APPENDIX A

Simplified Analytical Method for Determining NPDES Effluent Limitations for POTWs Discharging into Low-Flow Streams

---------- o ----------

NATIONAL GUIDANCE

Monitoring Branch

Monitoring and Data Support Division

Office of Water Regulations and Standards

September 26, 1980

I. INTRODUCTION

A. General

A simplified analytical method for determining effluent limitations for publicly-owned treatment works (POTWs) discharging into low-flow streams has been developed for nationwide use. This method should help ensure that proposed construction grant projects have adequate water quality justifications based on technically sound water quality analyses, and that construction grant funds are used in a cost-effective manner.

The analytical techniques which are used in water quality modeling should be the simplest possible that will still allow the

water quality manager to make confident and defensible water pollution control decisions. In many cases, where similar and relatively simple conditions exist, simplified modeling efforts that have less extensive manpower and data requirements (than normal, more comprehensive efforts) are often adequate to make such decisions. Use of simplified efforts, when appropriate, can result in both substantial savings in State and EPA resources and cost-effective and technically sound effluent limitations that will protect designated water uses and allow water quality standards to be achieved.

This simplified analytical method has been developed because of the large number of relatively small municipal sewage treatment facilities discharging into low-flow streams, and the need for more cost-effective yet technically sound water quality analyses for these cases. For example, this simplified method may be applicable to over 50 percent of the existing construction grant projections in Region V. Additionally, this method will help ensure that similar dischargers in similar situations will receive consistent consideration.

It should be noted that the analytical techniques described below are intended to represent minimum levels of analysis acceptable to EPA as justification for treatment beyond secondary. Water quality analysts may, of course, employ more rigorous techniques incorporating detailed intensive surveys and more complex models. EPA, however, will not accept further simplification of the methods described below.

unless such simplifying assumptions are adequately supported by a technical justification.

B. Modifications to the Region V Technology

The simplified method discussed below is based on the approach originally proposed by Region V, and on comments and suggestions received in response to the Region V proposal. Though generally supportive of the overall approach, comments revealed some concern regarding some details on calculating rate constants, DO targets, and permit conditions. Consequently, several modifications have been made to the Region V proposal.

C. Needs for Additional Data and Future Modifications

The simplified method described below is based on the information and data available to date. The data bases for many of the recommendations are quite limited, and should be expanded. Users of this method (as well as others) are strongly encouraged to develop their own specific rates and other factors, and to submit this additional data and other information, along with suggested improvements for the method, to:

Chief, Wasteload Allocations Section
Monitoring Branch
MDSD/OWRS (WH-553)
U.S. Environmental Protection Agency
401 M Street, SW
Washington, DC 20460
(202) 426-7778

This additional data and other information is needed so that appropriate improvements to the Method can be made periodically.

Areas in the method that require additional research and/or data include:

- K-rates (reaeration, CBOD, NBOD), including relating them to waterbody characteristics, levels of treatment, etc.
- $CBOD_u/BOD_5$ ratio
- diurnal fluctuation factors
- methods for performing the sensitivity analysis
- sediment oxygen demand rates, including relating them to stream bottom characteristics, levels of treatment, etc.

II. APPLICATION AND CONSTRAINTS

This method may be applied only if all of the following conditions are met:

1) The discharger must be a publicly-owned treatment works (POTW) receiving predominantly sanitary wastewaters. Any nonsanitary wastewaters in the treatment plant's influent must exhibit essentially the same characteristics (e.g., reactions) as sanitary wastes.

2) The discharge must be to a free-flowing stream in which the design low flow (usually the 7-day, 10-year low flow) is approximately equal to or less than the design discharge flow from the POTW.

3) The design discharge flow from the treatment plant must be 10 MGD (15.5 cfs) or less.

4) There is no significant interaction between the discharger being analyzed and any other upstream or downstream discharger.

Water quality in this type of system is highly dependent on effluent quality. Hence, upstream quality is less significant here than in systems where the upstream design flow is much greater than design effluent flows. This method can also be applied to simple systems where the upstream flow is greater than the POTW's discharge flow, provided the upstream water quality and reaction kinetics are well documented.

III. PROCEDURE

In order to determine the level of treatment required for a POTW, the following analytical steps are recommended:

(a) gather necessary data

(b) perform an ammonia toxicity analysis

(c) perform a dissolved oxygen analysis

(d) perform a sensitivity analysis

(e) interpret the results, and determine the final effluent limitations.

These five steps of the Simplified Method are discussed below.

A. Data Requirements

The data required for the Simplified Method, and some of their possible sources are listed below:

1) stream design flow-sources include USGS low-flow publications; drainage area yields; measurements during low-flow periods.

2) upstream water quality-including the necessary DO, BOD, ammonia, pH, alkalinity, temperature and other data needed for this Method. Sources include historical data (e.g., in STORET); State, EPA, or other water quality monitoring; sewage treatment plant monitoring; transferable data from similar streams.

3) stream physical characteristics-including stream slope, depth, etc. Sources include field measurements; USGS topographic maps; special Corps of Engineers or county project maps; stream gazetteers.

4) time of travel/velocity-sources include dye studies; direct velocity measurements; calculations based on field measurements of widths, depths, etc.; estimates based on slope/velocity relationships.

5) effluent design flow-sources include State or local agency population projections; Step 1 applications.

6) characteristics of design effluent-including the necessary pH, alkalinity, temperature, and other data needed for this Method. Sources include treatment capabilities for different levels of treatment, presented herein; other data can be obtained from State, EPA, or other water quality/effluent monitoring; sewage treatment plant monitoring; transferable data from similar treatment plants.

Direct field measurements of time-of-travel/velocity, upstream quality, stream physical characteristics (such as depth, type of bottom, benthic deposits, etc.), and other data should be employed for each segment studied, most notably for those where post-filtration of the sewage treatment plant effluent is considered. Since these data are readily obtainable by means of short duration, low resource surveys, efforts should be made to obtain the data through State agency monitoring programs or as part of the 201 grant process. When such data are not available, estimates can be made from some of the suggested sources listed above. The impact of less site-specific data

should be considered in the sensitivity anlysis. Time-of-travel studies provide the most useful data when the upstream flow and existing sewage treatment plant flow are equivalent to the sum of the upstream $_7Q_{10}$ and the treatment plant design flow. If flows in the immediate range of the design flow are not encountered during the time-of-travel studies, a second study at a different flow will permit extrapolation of the data to the design flow.

As a minimum, all modeling efforts must include: (1) a search for all applicable historical data and information (e.g., in STORET, old modeling or water quality study reports, treatment plant records, etc.) to support the current modeling work, and (2) a general on-site reconnaissance visit to visually observe the system to be modeled (to gain a better intuitive understanding of the system).

B. Ammonia Toxicity Analysis

A mass balance analysis will be used to determine whether the nitrification unit process is required on the basis of instream ammonia toxicity. The total ammonia-N limitation for the proposed discharge will be determined by using the applicable water quality standards (WQS), upstream flow and background concentration, and design effluent flow as follows (2):

$$C_D = (C_{WQS}(Q_D+Q_U) - C_UQ_U)/Q_D \qquad \text{(Eq. 1)}$$

where C_D = allowable design discharge concentration of total ammonia-N for POTW,

C_{WQS} = water quality standard limit of total ammonia-N (usually based on un-ionized ammonia-N standard and selected pH and temperature),

C_U = upstream or background concentration of total ammonia-N,

Q_D = design POTW discharge flow rate,

Q_U = upstream design low-flow.

The allowable instream total ammonia-N concentration (C_{WQS}) will normally be based on the water quality standard for un-ionized ammonia-N and the expected values of pH and temperature downstream of the discharge (if an applicable total ammonia-N standard is specified, C_{WQS} will equal that standard). The value of C_{WQS} can be determined from a table or graph which relates the toxicity of un-ionized ammonia-N to pH and temperature (such a table and graph is presented in Exhibit 1). When selecting C_{WQS}, one should be sure to use appropriate values for the expected downstream pH and temperature conditions during the design season, <u>after</u> mixing of the discharge and the receiving stream. If no un-ionized or total ammonia-N standards are available for use, the following criteria are recommended:

- 0.02 mg/l un-ionized ammonia for freshwater cold water habitat
- 0.05 mg/l un-ionized ammonia for freshwater warm water habitat.

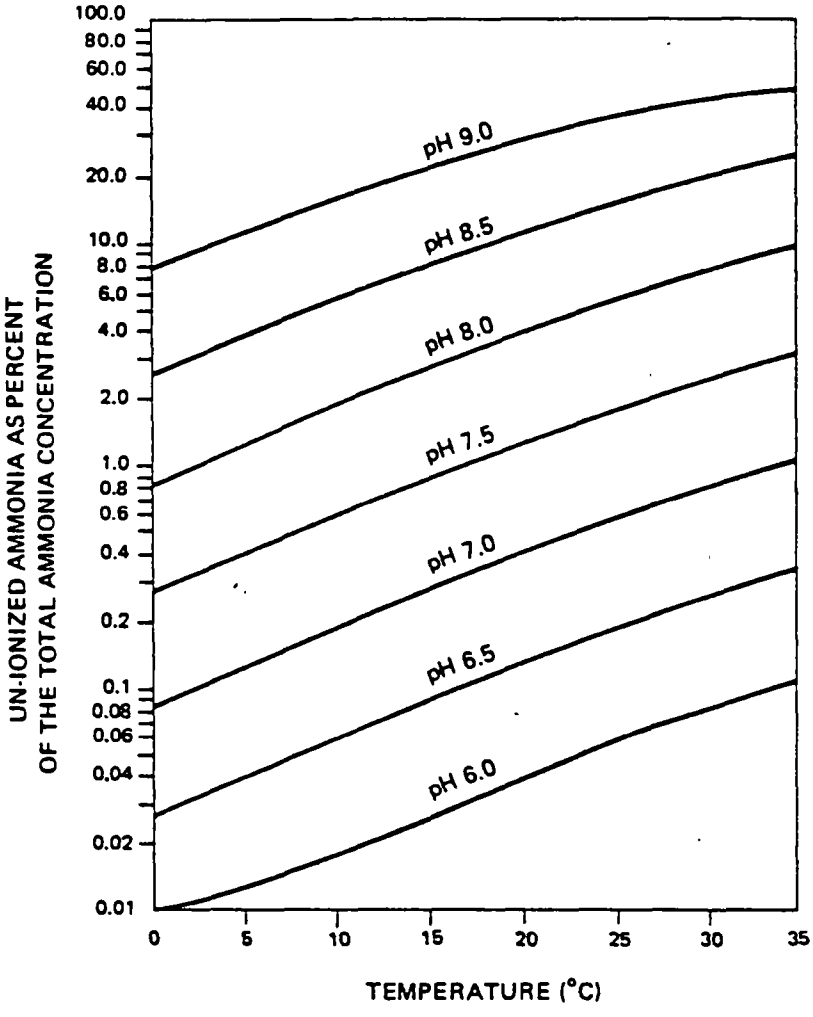

Note: Redrawn from William T. Willingham, Ammonia Toxicity, USEPA 908/3-76-001, Feb. 1976

Percent un-ionized ammonia in aqueous ammonia solutions*									
Temperature (°C)	pH Value								
	6.0	6.5	7.0	7.5	8.0	8.5	9.0	9.5	10.0
5	0.013	0.040	0.12	0.39	1.2	3.8	11.	28.	56.
10	0.019	0.059	0.19	0.59	1.8	5.6	16.	37.	65.
15	0.027	0.087	0.27	0.86	2.7	8.0	21.	46.	73.
20	0.040	0.13	0.40	1.2	3.8	11.	28.	56.	80.
25	0.057	0.18	0.57	1.8	5.4	15.	36.	64.	85.
30	0.080	0.25	0.80	2.5	7.5	20.	45.	72.	89.

*[Thurston, et al. (1974)]

Exhibit 1. Percentage of un-ionized ammonia in ammonia-water solution at various pH and temperature values.

The expected values of pH and temperature downstream of the discharge should be based on the pH and temperature of the POTW effluent and of the upstream waters. If sufficient temperature data are available or can be estimated for the POTW and for the stream (upstream of the discharge point), the expected downstream temperature can be calculated as follows:

$$T_R = (Q_U T_U + Q_D T_D)/(Q_U + Q_D) \qquad \text{(Eq. 2)}$$

where T_R = resultant water temperature downstream of discharge after mixing,

Q_v = upstream design low-flow,

Q_D = design (POTW) discharge flow rate,

T_U = upstream water temperature,

T_D = temperature of POTW effluent.

Also, if sufficient pH data is available or can be estimated for the POTW and for upstream, the method outlined in Appendix A1 can be used to determine the expected downstream pH.

When sufficient data is available for pH and temperature, use of the maximum pH and temperature values ever recorded is generally not realistic. It is more appropriate to use pH and temperature values which are exceeded 25 percent of the time during the critical low-flow season. It appears that the likelihood of having simultaneous "worst case" occurrences of both pH and temperature significantly greater than their respective 25 percent exceedence values along with design low-flow conditions is not very great; however, additional research

should be conducted in this area. When actual stream or POTW data are limited or not available, data from similar nearby streams and POTWs, or equilibrium water temperature data, may be used as design conditions and to help establish the range for a sensitivity analysis. In this analysis, the pH and temperature values which are used should be supported by one or more of the means described above. Any deviations must be supported by a sound technical justification.

This mass balance analysis should be used to determine whether the nitrification unit process is required solely on the basis of instream ammonia toxicity. Since nitrification in sewage treatment plants is generally an "all or nothing" process, the water quality analyst should be aware that, in terms of treatment capital costs, there may be no difference between an ammonia effluent limitation of, say, 2 mg/l, and 8 mg/l. For example, the cost of building a treatment plant to produce an effluent quality of 2 mg/l ammonia-N, may not be substantially different from that for a treatment plant designed to produce an effluent quality of 8 mg/l. For further details see the discussion below on treatment capabilities.

In light of the above discussion, this mass balance approach should be used to estimate instream un-ionized ammonia concentrations with and without nitrificaiton at the treatment plant. In cases where it appears that only marginal violations of the instream ammonia standard will result without nitrification at the plant, the decision to provide nitrification can be deferred until the dissolved oxygen

(DO) analysis (Step C, below) has been completed. The DO analysis may indicate the need for a reduction of ultimate oxygen demand (UOD), which would also support the need for the nitrification unit process at the plant (a process known to be more economical than filtration) for UOD removal. However, the latter conclusion is based on the implicit assumption that all of the instream ammonia will exert an oxygen demand in the stream segment under consideration, i.e., that nitrification occurs instream.

In situations where the DO analysis does not indicate a need for advanced treatment levels, but the ammonia toxicity analysis predicts toxicity problems, consideration shall be given to using pH adjustments (i.e., pH reductions) of the effluent during critical conditions to control ammonia toxicity in lieu of requiring nitrification. This consideration should include a determination of whether the temporary lowering of pH and increase in total dissolved solids (TDS) concentration would have any significant instream ecological or other effects.

In addition to this mass balance analysis, a qualitative if not quantitative assessment of nonpoint source contributions of ammonia must be made. This assessment may reveal that nonpoint source pollution may be of sufficient magnitude to preclude attainment of water quality objectives in terms of ammonia concentrations. An example which illustrates this point would be a treatment plant discharge located in a predominatly agricultural watershed that has significant

nonpoint source problems. Because nitrification alone may not solve an ammonia toxicity problem, nonpoint source controls must also be considered before nitrification is chosen. National guidance for nonpoint source analysis related to facility planning is presently being developed and is expected in the near future.

C. Dissolved Oxygen Analysis

A simplified Streeter-Phelps (3) analysis will be used to determine the effluent dissolved oxygen (DO) and BOD limitations for the POTW. This approach incorporates both carbonaceous (CBOD) and nitrogenous (NBOD) oxygen demands in the analysis. The equation used to calculate the DO deficit downstream from the point source is shown below:

$$D = D_o \exp(-K_2 t) + [K_1\ CBOD_o]/[K_2-K_1][\exp(-K_1 t)-\exp(-K_2 t)] + [K_3\ NBOD_o]/[K_2-K_3][\exp(-K_3 t)-\exp(-K_2 t)] + S/HK_2[1-\exp(-K_2 t)] \quad \text{(Eq. 3)}$$

where D = the DO deficit (mg/l),

D_o = mixed initial DO deficit (at discharge point) (mg/l)

$CBOD_o$ = mixed ultimate CBOD concentration at discharge point (mg/l),

$NBOD_o$ = mixed NBOD concentration at dischage point (mg/l). The magnitude of the NBOD should be based on the total ammonia concentration, and can be estimated using the following stoichiometric relationship: NBOD = 4.57 (NH_3-N),

K_1 = CBOD reaction (decay) rate (base e) (1/day),

K_2 = reaeration rate (base e) (1/day)

K_3 = NBOD reaction (decay) rate (base e) (1/day),

t = travel time below discharge (days),

S = sediment (benthic) oxygen demand ($gm/m^2/day$),

H = stream depth (meters).

The instream average DO concentration at a given point downstream of the discharge point is calculated by using the following equation:

$$DO_{AVG} = DO_{SAT} - D \qquad \text{(Eq. 4)}$$

where DO_{AVG} = instream average DO concentration (mg/1),

DO_{SAT} = saturation DO concentration at specified water temperature (mg/1). This can be determined from Exhibit 2,

D = as defined above.

Calculations using the above equations and a specified set of coefficients and assumptions apply for a given uniform stream reach. It is important to subdivide the stream into individual uniform reaches wherever any significant system changes occur (e.g., changes in channel geometry, significant tributary inflows, etc.) so that appropriate coefficients and assumptions that adequately represent each reach can be applied to the respective stream reaches when the model calculations are made.

Exhibit 2. SOLUBILITY OF OXYGEN IN FRESHWATER (AFTER STREETER)

T (°C)	Dissolved Oxygen (mg/l) (at normal atmospheric pressure, 760 mm Hg)									
	0.0	0.1	0.2	0.3	0.4	0.5	0.6	0.7	0.8	0.9
0	14.62	14.58	14.54	14.50	14.46	14.42	14.39	14.35	14.31	14.27
1	14.23	14.19	14.15	14.11	14.07	14.03	14.00	13.96	13.92	13.88
2	13.84	13.80	13.77	13.73	13.70	13.66	13.62	13.59	13.55	13.52
3	13.48	13.44	13.41	13.38	13.34	13.30	13.27	13.24	13.20	13.16
4	13.13	13.10	13.06	13.03	13.00	12.97	12.93	12.90	12.87	12.83
5	12.80	12.77	12.74	12.70	12.67	12.64	12.61	12.58	12.54	12.51
6	12.48	12.45	12.42	12.39	12.36	12.32	12.29	12.26	12.23	12.20
7	12.17	12.14	12.11	12.08	12.05	12.02	11.99	11.96	11.93	11.90
8	11.87	11.84	11.81	11.79	11.76	11.73	11.70	11.67	11.65	11.62
9	11.59	11.56	11.54	11.51	11.49	11.46	11.43	11.41	11.38	11.36
10	11.33	11.31	11.28	11.25	11.23	11.21	11.18	11.15	11.13	11.11
11	11.08	11.06	11.03	11.00	10.98	10.96	10.93	10.90	10.88	10.86
12	10.83	10.81	10.78	10.76	10.74	10.71	10.69	10.67	10.65	10.62
13	10.60	10.58	10.55	10.53	10.51	10.48	10.46	10.44	10.42	10.39
14	10.37	10.35	10.33	10.30	10.28	10.26	10.24	10.22	10.19	10.17
15	10.15	10.13	10.11	10.09	10.07	10.05	10.03	10.01	9.99	9.97
16	9.95	9.93	9.91	9.89	9.87	9.85	9.82	9.80	9.78	9.76
17	9.74	9.72	9.70	9.68	9.66	9.64	9.62	9.60	9.58	9.56
18	9.54	9.52	9.50	9.48	9.46	9.44	9.43	9.41	9.39	9.37
19	9.35	9.33	9.31	9.30	9.28	9.26	9.24	9.22	9.21	9.19
20	9.17	9.15	9.13	9.12	9.10	9.08	9.06	9.04	9.03	9.01
21	8.99	8.98	8.96	8.94	8.93	8.91	8.89	8.88	8.86	8.85
22	8.83	8.81	8.80	8.78	8.77	8.75	8.74	8.72	8.71	8.69
23	8.68	8.66	8.65	8.63	8.62	8.60	8.59	8.57	8.56	8.54
24	8.53	8.51	8.50	8.48	8.47	8.45	8.44	8.42	8.41	8.39
25	8.38	8.36	8.35	8.33	8.32	8.30	8.28	8.27	8.25	8.24
26	8.22	8.20	8.19	8.17	8.16	8.14	8.13	8.11	8.10	8.08
27	8.07	8.05	8.04	8.02	8.01	7.99	7.98	7.96	7.95	7.93
28	7.92	7.90	7.89	7.87	7.86	7.84	7.83	7.81	7.80	7.78
29	7.77	7.75	7.74	7.73	7.71	7.70	7.69	7.67	7.66	7.64
30	7.63	7.61	7.60	7.59	7.57	7.56	7.55	7.54		

T (°C)	Dissolved Oxygen (mg/l)	T (°C)	Dissolved Oxygen (mg/l)
31	7.5	41	6.5
32	7.4	42	6.4
33	7.3	43	6.3
34	7.2	44	6.2
35	7.1	45	6.1
36	7.0	46	6.0
37	6.9	47	5.9
38	6.8	48	5.8
39	6.7	49	5.7
40	6.6		

Note: correction for barometric pressure B (mm Hg) multiply by B/760; correction for salinity S (chloride, mg/l) multiply by [1 - (S/100,000)].

The universe of possible coefficients and assumptions that can be used in the model may vary over a wide range, and can result in significantly different predictions of instream DO. It is extremely important that the best possible estimate of these parameters be obtained for each case to ensure that they adequately represent the stream system to be modeled. Site-specific data should be used whenever possible. When a comprehensive field survey is not feasible, appropriate data described in the literature or available transfer data may be used. However, if literature data or transfer data are used, it is strongly encouraged that a general reconnaissance visit of the site to be modeled be made in order to qualitatively evaluate the applicability and reasonableness of the data being used. The coefficients and assumptions to be used and minimum site-specific data requirements for this Method are discussed further, in the next section. It is important to ensure that the coefficients and assumptions which are used in the model do adequately represent the conditions in each uniform stream reach, and that they are changed in the model, as appropriate, between the stream reaches being modeled to reflect any system changes between the reaches (e.g., make appropriate changes in coefficients, travel time, etc., to reflect significant changes in slope, channel geometry, benthic characteristics, etc.)

After the appropriate assumptions are made and coefficients selected, the location of minimum DO concentration (i.e., the sag point) is to be determined. This can be accomplished by applying

incremental time periods in Equations 3 and 4 and noting where the minimum DO concentration occurs. The number of trial-and-error iterations can be minimized by first using the following equation to determine the approximate location of the sag point:

$$t_c = [1/(K_2-K_{BOD})] \quad [\ln(K_2/K_{BOD})] \quad [1-D_o(K_2-K_{BOD})/(K_{BOD}\ UBOD_o)] \qquad \text{(Eq. 5)}$$

where t_c = approximate time (and, hence, distance) to the sag (critical) point,

K_2 = reaeration rate,

K_{BOD} = BOD reaction rate (for CBOD, NBOD, or average of two rates; see text, below),

D_o = mixed initial DO deficit (at discharge point),

$UBOD_o$ = initial ultimate BOD concentration (at discharge point).

Where CBOD and NBOD have different rates, the sag point can be bounded by assigning first the lower and then the higher rate to the total ultimate BOD, or approximated by averaging the two rates.

The next overall step in this Method is to establish the allowable loading rates needed in order to meet the water quality standards at the critical sag point. This can be accomplished by applying, in an iterative manner, successively lower CBOD and NBOD values until the DO standards are met at the sag point. An alternative to this "trial and error" method for dissolved oxygen is to separately calculate the dissolved oxygen deficit due to each BOD source (e.g., upstream BOD, sediment demand, plant carbonaceous BOD, and plant nitrogenous BOD).

By knowing the relative contribution of each BOD source to the total deficit when using this alternative approach, and since the various oxygen deficits are additive (see Equation 3), it is an easy task to identify the combinations of wastewater BOD reductions that will achieve water quality standards and to select the combination that will be the most cost-effective.

As stated above, it is extremely important that the best possible estimate of the parameters used in the model be obtained for each case, and that they adequately represent the system being modeled. The next several subsections discuss recommended parameter values and assumptions to be used with the Simplified Method. The following points are addressed:

- flow regime
- target DO
- treatment capabilities
- rate constants
- inital deficit determination
- conversion from $CBOD_u$ to BOD_5
- post-aeration
- nonpoint sources.

The recommendations made below are intended to help the Simplified Method user to develop modeling results that are consistent with the applicable water quality standards.

1) Flow Regime. Both low-flow and high-flow conditions should be assessed to determine the critical conditions. In some cases, severe non-point source pollutant contributions during high-flows might

preclude attainment of desired water quality objectives. If the high-flow condition is found to be critical, further analyses of nonpoint sources should be conducted.

The flow regime to be used in the Simplified Method is the design low-flow specified in the applicable water quality standards. This flow will, in most cases, be the 7-day, 10-year low-flow ($_7Q_{10}$). If no design flow is specified, the $_7Q_{10}$ should be used for design purposes. If any flow value other than those specified above is used in the analysis, a sound justification must be provided to support the use of this value.

2) Target Dissolved Oxygen. DO standards are often presented as a minimum at all times; some States include an average value along with the minimum. Outputs (the DO simulation) from steady-state models are based on the averaging period for input loadings; they, therefore, represent the average DO conditions likely to prevail at the flow condition being simulated. The two major factors that can cause the actual minimum DO to be considerably lower than the average predicted by steady-state model computations are: (1) diurnal variations in loadings to and from the contributing waste treatment plant, and (2) diurnal variations of instream DO caused by algal photosynthesis and respiration. The magnitude of these variations is likely to differ from plant to plant and from stream to stream. The problem is further complicated by the fact that prevailing fluctuations in a

stream may be radically altered under construction of a larger treatment plant with higher levels of treatment, and that quantification of these fluctuations through intensive field investigations may not accurately define these future conditions. For this reason, users of this Method are urged to obtain additional field data so that instream responses can be better correlated with different levels of treatment, and that better estimates under projected conditions can be made.

When modeling, the following DO targets should be used:

(a) If the DO standard is expressed as an average and a minimum requirement (e.g., an average of 5 mg/l and a minimum of 4 mg/l), the average number (e.g., 5 mg/l) should be used as the target.

(b) If the DO standard is expressed only as a minimum (e.g., a minimum of 5 mg/l at all times), the target DO may be obtained by adding one-half of the diurnal variation to the DO standard (e.g., for a total diurnal variation of 1 mg/l, then the target is 5 mg/l + 0.5 mg/l = 5.5 mg/l). In the absence of adequate site-specific or transferable data, 0.5 mg/l should be added to the DO standard. If any other values (either lesser or greater than 0.5) are used, they must be supported by adequate data.

There is not a strong quantitative basis for using the recommended value of 0.5 mg/l to compensate for diurnal variations; the choice is based in part on the acknowledgement of the existence of such variations and on the need to allow some reasonable compensation in the absence of an adequate data base. However, Thomann (19) feels that there is a basis for using the 0.5 mg/l value, but this value is associated more with random, rather than just photosythesis/respiration, fluctuations. Additional field studies should be conducted to either support or modify this value.

3) Treatment Capabilities. For typical domestic wastewaters, the following effluent concentrations should ordinarily be assumed for modeling purposes. These values are 30-day averages that would be expected during warm summer months (i.e., during conditions similar to those being modeled).

Treatment	Effluent Concentration (mg/l)	
	BOD_5	NH_3-N
Influent	100 - 300	12 - 35
Secondary	30 (or 85% removal)	10% less than raw concentration
Nitrification (single stage or two stage)	5 - 8**	1.0 - 1.5
Oxidation Ditch	10 - 15	1.0 - 1.5
Nitrification plus Tertiary Filtration	3 - 5**	1.0 - 1.5

**(See Appendix A2 for clarification.)

The values selected from the ranges given above should depend on the influent concentrations (e.g., lower values should be used for lower influent concentrations).

4) Rate Constants

(a) Reaeration Rate(K_2). The critical values in DO analyses of small streams are the reaeration rate, and to a lesser extent, the CBOD and NBOD decay rates and effluent DO levels. Many formulations have been developed for predicting stream reaeration rates based on

physical characteristics such as stream width, depth, velocity, and slope (4,5). Recent work by Rathbun (6) and by Grant and Skavroneck (8) indicates that the Tsivoglou formula (7,20), in which K_2 is calculated by Equation 6, tends to most accurately predict stream reaertion. Presently, the data base on which most reaeration equations and recommendations are based is quite limited. Additional data collection efforts and research are needed in this area.

The Tsivoglou formula, presented below, should be used for computing reaeration rates on small, shallow streams:

$$K_2 = CVS \quad \text{at } 20^{\circ}C \qquad \text{(Eq. 6)}$$

where K_2 = reaeration rate (1/day)

V = stream velocity (ft/sec)

S = stream slope (ft/mi)

C = proportionality constant with the values shown below:

$C = 1.8$ for $1 \leq Q \leq 10$ cfs
$= 1.3$ for $10 < Q < 25$ cfs
$= 0.88$ for $25 \leq Q \leq 300$ cfs.

According to Tsivoglou (9), there is no evidence to support restricting the use of Equation 6 based on minimum slope. It should be pointed out that the values of the proportionality constant (C) given above for flows between 1-10 cfs and 25 - 300 cfs were determined by Tsivoglou (20) using data in these flow ranges. The value of C for the flow range between 10 and 25 cfs appears to be basically an estimated value only, since a paucity of data exists in this flow range. However, this C value has been recommended by Neal (22). When the streamflow (Q) is near either 10 or 25 cfs (the points at which the value of C changes), it is recommended that a sensitivity analysis be performed by doing

separate DO calculations using both the higher and lower C values so that lower and upper limits of predicted DO can be established. If this range of predicted DO is found to be relatively large, it is recommended that additional work, including field measurements, be performed to help reduce the uncertainty in the reaeration rate to be used.

O'Conner's reaeration formula, presented below, may be used for larger, deeper streams with more uniform channel geometry or those with significant pooling (4):

$$K_2 = 12.9\ v^{0.5}/H^{1.5} \qquad \text{at } 20^{\circ}C \qquad \text{(Eq. 7)}$$

where V = stream velocity (ft/sec),
H = average stream depth (ft).

The values of V and H used in the above equations should be based on actual field measurements so that the uncertainty in the rate can be reduced. The value of S can be determined from field measurements or from appropriate maps.

Any other applicable reaeration prediction methods may be used in lieu of the above methods only if these alternative methods are supported by an adequate technical justification that includes sufficient field data collected from the area.

(b) CBOD Decay Rate(K_1). A review of reaction rates measured on low flow streams with similar characteristics showed that CBOD rates generally range from about 0.2 to around 3.0 or more (10, 11, 12, 13, 21,), depending in part on depth and degree of treatment (see

Exhibit 3). The minimal data available for small, low flow streams with treatment greater than secondary suggest that the CBOD rates under these conditions typically fall between about 0.2 and 0.5 (at 20°C). Adjusting CBOD rates by depth as proposed by Hydroscience (13) suggests 0.3 to be a representative value for these low flow streams with a mostly stable fairly rocky bottom, and about 0.2 for streams with a primarily unstable sediment bottom.

Using this approach, CBOD then becomes (14):

$$K_1 = C\,(H/8)^{-0.434} \qquad \text{for } H < 8 \text{ ft.} \qquad \text{(Eq. 8)}$$

$$= C \qquad \text{for } H \geq 8 \text{ ft.}$$

where K_1 = CBOD decay rate (1/day),

H = average stream depth (ft),

C = 0.3 for streams with mostly stable fairly rocky bottoms,

C = 0.2 for streams with primarily unstable sediment bottoms.

It should be noted that Equation 8 generally represents an average of a range of possible values at any given depth. Based on limited data presented in the literature (11, 13, 21) and elsewhere (10, 12; also see Exhibit 3), the following ranges of the CBOD rate are presently being suggested:

Exhibit 3. REACTION RATES MEASURED ON LOW FLOW STREAMS**

River	CBOD Rate		NBOD* Rate	Treatment Level	Flow (cfs)		Depth (ft)
	Measured	Depth Adjusted			River	STP	
Upper Olentangy, Ohio (7)	1.24	0.43	--	AST - No nitrification	2.3	3.0	0.7
Patuxent River, (8) Maryland	0.30	0.3	.27-.50	AWT - Nitrification with microscreens	31	6.8	--
West Fork of Blue River, Indiana (9)	0.5-0.79	0.2-.32	0.5	AST - Secondary with rapid sand filters	4	1.4	0.9-1.2
Hydroscience (10)	.37-.96	.19-.42		Highly treated effluent nitrification			1-3
Recommended Values		0.3	.42				
Depth Adjustment $K = K\ (Measured)\ (D/8)^{.434}$			$D < 8$ ft				

*Reaction rates are at 20°C.
**Submitted by EPA Region V.

Exhibit 4. CBOD/BOD_5 DATA*

State	Plant	Type	Flow (MGD)	Percent Industrial Flow	Number of Samples	Ultimate CBOD BOD_5
Ohio	Lakewood	Activated Sludge	11.7	0%	1	3.27
Ohio	Mansfield	Activated Sludge	10.6	32%	1	3.43
Ohio	Shelby	Activated Sludge	1.2	0%	3	3.21
Ohio	Lorain	Activated Sludge	14.1	14%	4	3.13
Ohio	Coshocton	Activated Sludge	2.3	39%	1	4.34
Ohio	Conneaut	Activated Sludge	2.6	0%	1	2.61
Ohio	CRSD Easterly	Activated Sludge	136.0	12%	2	5.10
Minnesota	Minneapolis-St. Paul	Activated Sludge		27%	13	3.18
Wisconsin	Fall Creek	Trickling Filter			2	3.40
Wisconsin	Neenah-Menasha	Activated Sludge		40%	2	3.20
Wisconsin	Town Menasha East	Activated Sludge		22%	1	1.80
Wisconsin	Town Menasha West	Activated Sludge		42%	2	3.10
Wisconsin	Heart of the Valley	Act. and filters	5	< 10%	2	2.75
Wisconsin	Depere	Activated Sludge		20%	1	3.00
Average						3.2

*Submitted by EPA Region V.

Level of Treatment	CBOD Rate (K_1)** Minimum	Maximum
Secondary treatment	0.3	1.5
Greater than secondary		
• streams with mostly stable fairly rocky bottoms.	0.3	0.5
• streams with primarily unstable sediment bottoms.	0.2	0.4

(Note: These ranges are based on a very limited data set; they are subject to modification, as necessary, as additional rate data are submitted to EPA Headquarters. Users are urged to collect site-specific rate data whenever possible.)

**-(1/day, base e, at 20°C)

Equation 8 may be used to estimate the CBOD rate within the ranges specified above. Users of this approach should note that, at best, the above equation is a crude, though rational, empiricism, based on a limited data set. A much larger data set consisting of accurate K_1 measurements for different levels of treatment and types of streams is needed before a more precise empirical correlation equation can be developed. Towards this end, States and EPA Regions are urged to expand relevant data bases, and to submit these data and suggestions to EPA Headquarters to assist in the refinement of the above approach and ranges. Post-construction intensive surveys to measure K_1 (and K_3) below AST and AWT plants would aid this

effort significantly. Users are encouraged to collect site-specific data or to use transferable data to help reduce the uncertainty in the CBOD rate to be selected. Any deviations from the above approach must be supported by an adequate technical justification.

(c) NBOD Decay Rate (K_3). Several environmental factors have been shown to influence the rate at which nitrification occurs. Among them are pH, temperature, suspended particle concentration, hydraulic parameters, other pollutants that inhibit the nitrification process (e.g., some toxics), and the benthos of the receiving waters. While no attempt is made in this Method to quantify the effects of these factors on K_3, users are expected to determine qualitatively whether or not nitrification is likely to occur in the subject stream. If so, users must determine whether or not conditions are optimal for nitrification. For example, several researchers have shown that a pH in the range of 8.4 to 8.6 is optimal for nitrification, with a rapid decrease in nitrification outside the range of 7.0 to 9.0. Because most State water quality standards require a pH in the range of between 6.5 or 7.0 and 9.0, it is unlikely that the pH factor greatly influences the occurrence of nitrification. However, consistent pH observations in the range of 8.4 to 8.6 indicate that this factor is conducive to maximum nitrification. Nitrification is also a function of available benthic surface area for nitrifying organisms to attach themselves. For example, if a stream bottom is completely devoid of

surfaces (such as rocks, etc.) on which nitrifiers can attach themselves, it is likely that nitrification will not be a significant factor in the DO analysis. Conversely, a shallow stream with a rocky bottom is likely to have a high nitrification rate.

A site inspection will indicate the likelihood of nitrification, and should be conducted. Based on the observations which are made during the inspection, the user must estimate the applicable NBOD rate value. In view of the tenuous nature of this rate selection procedure, particular care should be taken in evaluating the effects through sensitivity analyses. Another point to consider is the outcome of the ammonia toxicity analysis. If it was determined previously that ammonia removal is required on the basis of ammonia toxicity considerations, then the role of K_3 in the overall DO analysis becomes somewhat less critical. On the other hand, if the ammonia toxicity analysis does not clearly indicate the need for ammonia removal, then the decision to provide nitrification at the treatment plant will hinge solely on the DO analysis. This makes the determination of the K_3 value much more critical. The water quality analyst must then carefully assess stream conditions, and assign reasonable rate coefficients, accordingly.

Based on limited observations of NBOD decay rate (2; also see Exhibit 3), it appears that, where instream nitrification is found to occur, most K_3 values range between about 0.1 and 0.6. In the

absence of applicable site-specific data, a K_3 value within the range of 0 to 0.6 is to be selected. This selection should be based part on a site inspection (as stated above), and on any appropriate available transfer data. Generally, a K_3 value of around zero should be selected only if strong evidence suggests a lack of instream nitrification occurring under the projected conditions. Otherwise, the K_3 values which are selected might be roughly 0.2-0.3 for deeper streams with a primarily sediment bottom, around 0.4 for shallower streams with a moderately rocky bottom, and about 0.6 for shallow, rocky streams. The user is strongly encouraged to collect site-specific data, and data from similar sites, whenever possible to support the selection of the NBOD decay rate.

(d) Sediment (Benthic) Oxygen Demand (S). Sediment oxygen is a factor that is often significant in the DO analysis. For the types of situations applicable to this Method, Thomann (19) suggests that the following benthic demand rates be used when simulating stream DO response to various treatment levels:

	S(gm/m^2/day of O_2 at 20°C)	
Treatment Level	Vicinity of Outfall	Downstream of Outfall
Poor Secondary Trt	2 - 4	0.5 - 1
Secondary Trt	1 - 2	0.3 - 0.7
Greater than Secondary	0.2 - 0.5	0.1 - 0.2*

*(Even with high levels of treatment at the point source, there will usually be at least a minimal benthic demand present, e.g., due to "background" or other sources).

For the purpose of this analysis, the benthic demands should be considered to be at a minimum under future conditions, unless site-specific circumstances indicate a continued presence of substantial benthic deposits in the future (e.g., from nonpoint sources). The applicable rates suggested above should be used in the analysis, unless site inspections indicate that higher or lower values should be used.

When selecting the benthic demand rate for future conditions, consideration should be given to the fact that there might be continued other sources of benthic demand, such as from nonpoint sources. Therefore, a site inspection should be conducted to determine the characteristics of the stream bottom and the areal extent and magnitude of the benthic demand, and to reveal any possible continuing benthic demand problems.

(e) Temperature Corrections of Reaction Rates. Temperature effects on the various reaction rates can be approximated by the following equations:

- for the Sediment Oxygen Demand Rate:

$$(SB)_T = (SB)_{20}(1.065)^{T-20} \qquad \text{(Eq. 9)}$$

where $(SB)_T$ = adjusted benthic demand rate for specified stream temperature,

$(SB)_{20}$ = selected benthic demand rate (for stream temperature of 20°C),

T = specified stream temperature (°C),

for K_1, K_2, and K_3: $K_T = K_{20}\ \theta^{T-20}$ (Eq. 10)

where K_T = adjusted K-rate for specified stream temperature.

K_{20} = selected K-rate (for stream temperature of 20°C),

T = specified stream temperature (°C),

θ = 1.047 for K_1,

= 1.024 for K_2,

= 1.1 for K_3.

(5) Initial Deficit (D_o) Determination. When performing a DO analysis, the initial dissolved oxygen deficit (D_o) must be known (see Equation 3). In order to calculate D_o, the resultant mixed DO concentration at the discharge point must first be calculated. This can be accomplished by performing the following mass balance:

$$DO_o = [DO_u Q_u + DO_D Q_D]/[Q_u + Q_D] \quad \text{(Eq. 11)}$$

where DO_o = mixed instream dissolved oxygen concentration at discharge point (mg/l),

DO_u = upstream dissolved oxygen concentration (mg/l),

DO_D = POTW discharge dissolved oxygen concentration (mg/l),

Q_u = upstream design low flow,

Q_D = POTW design discharge flow rate.

Then the saturation DO (DO_{SAT}) concentration must be determined using the resultant water temperature downstream of the discharge

(T_R) which was calculated using Equation 2 (in the "Ammonia Toxicity Analysis" section). This can be determined from Exhibit 2. By using DO_o and DO_{SAT}, the initial mixed dissolved oxygen deficit (D_o) can be calculated as follows:

$$D_o = DO_{SAT} - DO_o \qquad \text{(Eq. 12)}$$

(6) Conversion from $CBOD_u$ to BOD_5. Data submitted by Region V (see Exhibit 4) indicate that the ratio of $CBOD_u$ to BOD_5 should be about 3.0. Other limited data presented in the literature suggest that this ratio is about 1.5 to 2.0. It is suspected that many of the lower ratio values were established using older data from older, less efficient treatment plants, and that the Region V data is generally from newer, more efficient plants.

When evaluating secondary treatment discharges, water quality analysts should use a ratio in the range of 1.5 to 2.0, unless applicable long-term BOD tests indicate some other value. The value of 1.5 should generally be applied to "poorer" secondary plants, and 2.0 should probably be applied to the "better", more efficient secondary treatment plants. A ratio in the range of 2.5 to 3.0 should be used for plants with treatment levels greater than secondary, unless applicable plant-specific data indicate some other value. These higher ratios resulting from greater levels of treatment are also consistent with intuitive expectations. Site-specific or transferable data should be collected whenever possible to help support the selected value.

All EPA Regions, the States, and others are strongly urged to participate in a nationwide data gathering effort so that more accurate ratios can be developed. Such an effort would not be very resource intensive, and the results would be extremely useful. Care should be taken to ensure that only the carbonaceous demand is measured. This data collection effort should include information on the type of treatment and type of influent, and the sampling should, to the extent possible, only be performed on sanitary wastewaters that are unchlorinated. This data should be submitted to EPA Headquarters for compilation and analysis.

(7) Post-Aeration. Post-aeration of the effluent to a DO concentration of 7 mg/l should always be evaluated as an alternative to higher levels of treatment, unless there is a site-specific constraint that precludes the use of post-aeration equipment. This technique can be particularly useful in cases where dilution is low and reaeration rates are also low.

(8) Nonpoint Sources. In some cases, nonpoint sources may preclude attainment of dissolved oxygen water quality objectives even with stringent advanced treatment. For example, streams with extensive wetlands may contribute low DO water in sufficient quantities to cause standards violations, and agricultural or urban runoff in the vicinity of a plant discharge may also nullify the benefits of advanced treatment. In cases such as these, nonpoint

source control tradeoffs must be considered before advanced treatment is chosen. Site-specific evaluations should be made to identify possible nonpoint source problems.

D. Sensitivity Analysis

The sensitivity of computed stream responses to changes in estimated input variables must be determined before a final decision of treatment levels is made. A sensitivity analysis combined with judgement is essential to help establish greater confidence in the results that are obtained.

The sensitivity of computed (predicted) instream responses to the various input values should be determined by repeating the analyses described above with changes (increases and decreases) in the input variables. The following steps should be followed:

1) Initially, three sets of calculations should be made to reflect a "worst," "best," and "average" case for each alternative treatment level. This can be accomplished by using model input values that represent, respectively, the "worst" and "best" ends of their sensitivity ranges and the values actually selected for the model. The outputs of these computations should be plotted as DO profiles. If all three cases indicate a violation of the water quality standard with the given level of treatment, then the next level of treatment is needed, and no further justification is necessary. If all three cases do not indicate a violation, then the next step must be taken.

2) Next, each input variable to each equation above should be individually increased and decreased, so that the magnitude of the differences in predicted instream responses can be assessed. Each input variable (including rate coefficients, travel time, physical characteristics, etc.) should be varied over a range of values that reflects the uncertainty in the particular variable. If direct measurements of certain input variables are made, then the uncertainty in the variable would tend to be relatively small and, therefore, the range to be used in the sensitivity analysis would generally be relatively small. Very close scrutiny should be given to those input variables which have no site-specific or transferable data to support their having been selected. If rates (or rate formulations) other than those suggested in the above analyses are used, then the sensitivity analysis should be used as part of the justification for the alternative rates (or formulations).

The results of these sensitivity analyses (in step 2) should be reviewed within the context of the effluent quality expected for various treatment levels. Therefore, if the effluent requirements determined using the range of inputs for each variable fall within the expected effluent quality from a single treatment level (e.g., AST or AWT), then additional analyses would generally not be required for that variable since the need for that level of treatment is obvious. However, if the required treatment level is heavily sensitive to, and dependent on, the selection of an input value(s) <u>especially</u> where existing data are inadequate to characterize the variable(s), <u>then a</u>

sufficient amount of additional data shall be obtained to more accurately define that model variable(s) (thus increasing the confidence in that variable) so that the selection of the treatment alternative can be clarified. For even further confirmation of the selected effluent limitations, the sensitivity analysis can also be rerun for the individual input variables at a less stringent level of treatment and the results analyzed to determine if the desired water quality objectives could possibly be met at that lesser treatment level within the range of individual inputs being utilized. It must be emphasized that the use of sound professional judgment is essential when evaluating the confidence in the model input variables used and in the modeling results obtained.

To further assist in evaluating the results of the sensitivity analyses, the incremental present worth cost (construction and O&M) of the proposed improved treatment process may also be considered when deciding the necessary level of treatment. For example, if oversizing the clarifiers, providing additional aeration and clarifiers for nitrification, or seasonal chemical addition could provide the level of treatment in question, such treatment could be partly justified based on best judgment due to the relatively low cost of such additional treatment. On the other hand, filters (as an add-on to nitrification), due to their high incremental cost, could be justified by this Simplified Method only if the results of these sensitivity analyses indicate sufficient confidence in the results. Otherwise, additional data (including for calibrating and verifying the model) would be required.

Generally, the variables to be analyzed in the sensitivity anlaysis should include those listed below, and should generally be varied by sensitivity ranges in the order of those which are suggested below (especially if little or no data is available to support the variable's selection):

- CBOD rate - vary by about ±50 to 100% (and appropriate increments in between), depending on the uncertainty in the estimated value.
- NBOD rate - vary by about ±25 to 75% or more (and appropriate increments in between), depending on the uncertainty in the estimated value.
- Reaeration rate - vary by about ±25% to ±100% or more (depending on the uncertainty in the estimated value), and by intermediate increments. An appropriate sensitivity analysis should also be performed on the variables used in the respective reaeration equations (i.e., velocity, and slope or depth).
- Benthic demand - generally should use the suggested ranges presented in Section III(C)(4)(d).
- Temperature, pH - use ranges appropriate for the situation.

E. Results

1) Permit Conditions. After determining the final effluent limitations necessary for the maintenance of water quality standards, these limitations should be entered into the NPDES permit. Municipal effluent limitations are often specified as 30-day and 7-day average values for BOD_5, ammonia-N, and suspended solids. For streams with zero flow at the critical conditions, the results of the DO analysis shall be used as 7-day average effluent limits rather than 30-day averages, since these small streams are often very reactive to variable waste inputs. For streams with nonzero flow at the critical

conditions, the currently adopted and applicable State or EPA Regional procedures for applying modeling results to POTW discharge permit effluent limitations shall be used.***

The CBOD and NBOD outputs from the DO analysis should be converted to BOD_5 and ammonia-N NPDES permit limitations using the following relationships (established earlier):

(a) $BOD_5 = CBOD/r$

(where r = the UCBOD:BOD_5 ratio, for the appropriate level of treatment, selected in section III(C)(6).)

(b) NH_3 -N= NBOD/4.57

2) Seasonal Effluent Limitations. The effects of variations in temperature and flow should be evaluated to determine whether or not operating costs can be reduced through seasonal relaxation of effluent limitations. For example, it is conceivable that in winter, higher flows and lower temperatures would allow for a relaxation of BOD and ammonia limitations from a toxicity and DO standpoint.

EXAMPLE PROBLEM

(An example problem will be prepared and provided to the users of this Method in the near future.)

***-NOTE: This issue is currently being analyzed and will be addressed in the forthcoming regulation on wasteload allocations/total maximum daily loads. The Agency is presently leaning towards using modeling results as 7-day averages. Comments are welcomed on this issue.

APPENDIX A1

METHOD FOR DETERMINING EXPECTED DOWNSTREAM pH

Calculating the pH of the stream after mixing of upstream flow with wastewater discharge is straightforward - provided there is some minimal water quality information available on each.

It can be done with information on different combinations of alkalinity, acidity and pH. The most direct method, and simplest to present for a simplified methodology, requires information on pH and alkalinity. If no pH or alkalinity data is presently available for the POTW and/or for upstream, then a short-term program of collecting the needed pH and/or alkalinity data should be initiated. Assuming generally average conditions exist at the POTW and upstream during the data collection program, then a fairly accurate determination of their average pH and alkalinity conditions can be made in several days or a few weeks. The tests for pH and alkalinity are easy and inexpensive:

- pH - is easily (and commonly) measured by pH meter.
- Alkalinity - is also commonly measured. Standard Methods specifies titration with strong acid (0.02 N H_2SO_4) - in which case alkalinity is reported as mg/l as Ca CO_3.

  The ionic forms comprising alkalinity (HCO_3^-, $CO_3^=$ and OH^- be calculated from the relative amounts of acid

required to reach the two end points (Phenolphthalein at pH 8.3, and Methyl Orange at about pH 4.5). For natural waters between pH 4.5 and 8.3 (essentially all we need be concerned with for this exercise), there will be no phenolphthalein end point -- and <u>all</u> of the alkalinity will be present as bicarbonate ion (HCO_3^-).

Note that the procedure presented, and the chart used, will apply for any situation. The instructions for its use are much simpler to present if it is assumed that the only waters being dealt with will be in the pH 4.5 to 8.3 range (which will usually be the case).

There are a number of techniques, methods, etc., for calculating pH. The one presented here seems to be best suited for these purposes. The chart is taken from "Aquatic Chemistry" by Stumm & Morgan (Wiley Interscience, 1970), and the approach is a portion of the overall approach they describe - which for simplicity is limited to the usual case which was selected.

The calculation is illustrated by the following example:

- In a natural water system (or wastewater) with a pH in the range of 4.5 to 8.3, the alkalinity measured is all bicarbonate ion (HCO_3^-) reported as mg/l as $CaCO_3$. The Total Inorganic Carbon (C_T) will consist of both HCO_3^- and soluble CO_2 which coexist in water in this pH range. (NOTE: The Standard Methods test for acidity would measure soluble CO_2.)

- The chart requires that alkalinity be reported in terms of milliequivalents/liter (meq/l). The conversion is as follows:

  Alkalinity-mg/l as $CaCO_3$ X 1/50 = Alk.-meq/l

- Total Inorganic Carbon (C_T) must be in terms of millimoles/liter (mM/l). However, if we are working with pH and alkalinity, we need not worry about this conversion, nor about determining the acidity or CO_2 concentration.

- In a situation like the one being addressed, both alkalinity and C_T are conservative (pH is not). Thus, when two waters with different concentrations of alkalinity and C_T are mixed - the final concentration in the blend can be determined by simple mass balance.

- The steps are:

  1. From alkalinity and pH, determine C_T for stream and waste.

  2. Calculate concentration of alkalinity and C_T in blend.

  3. Determine pH of blend from blend alkalinity and C_T.

- An example problem and a calculation sheet are given in Exhibit 5. A blank calculation sheet, with chart, is also attached (Exhibit 6).

EXHIBIT 5. EXAMPLE CALCULATION.

1. GIVEN

	POTW Discharge	Upstream Flow
Flow =	6 MGD = 3.86 CFS	3.0 CFS
pH =	7.2	7.5
ALK =	150 mg/ℓ = 3.0 mg/ℓ as $CaCo_3$	50 mg/ℓ = 1.0 mg/ℓ as $CaCo_3$

2. DETERMINE C_T FROM CHART

POTW Discharge	Upstream Flow
ALK = 3.0, pH = 7.2 → C_T = 3.55	ALK = 1.0, pH = 7.5 → C_T = 1.1

3. CALCULATE BLENDED ALK AND C_T

B = Blend S = Stream D = Discharge

$$C_T \text{ or } ALK_B = \frac{C_{T_S} \quad C_{T_D}}{\frac{(ALK_S \cdot Q_S) + (ALK_D \cdot Q_D)}{(Q_s + Q_D)}}$$

$$ALK_B = \frac{(1.0 \cdot 3.0) + (3.0 \cdot 3.86)}{(3.0 + 3.86)} = \frac{14.58}{6.86} = 2.12$$

$$C_{T_B} = \frac{(1.1 \cdot 3.0) + (3.55 \cdot 3.86)}{(3.0 + 3.86)} = \frac{17.00}{6.86} = 2.48$$

4. DETERMINE pH OF BLEND FROM CHART

ALK = 2.12, C_T = 2.48 → pH = 7.2

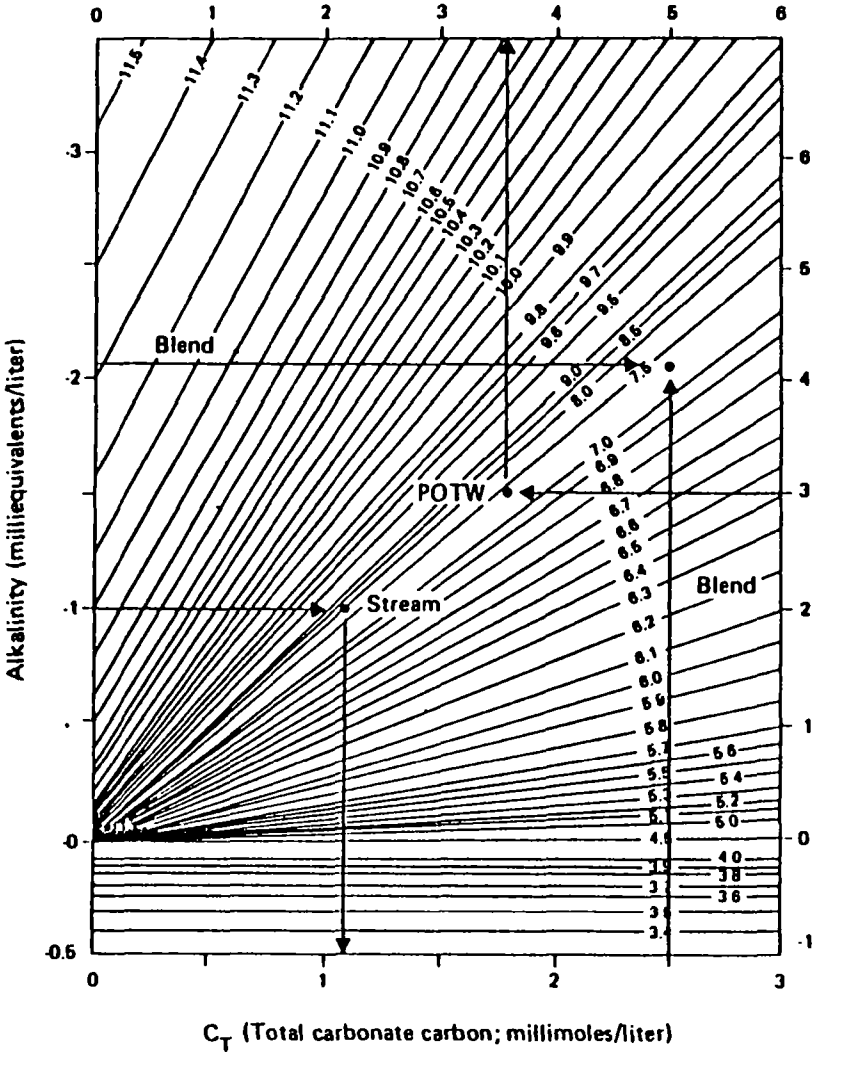

Note: Doubled scales apply if pH line goes through origin.

EXHIBIT 6. BLANK CALCULATION SHEET.

1. GIVEN

	POTW Discharge	Upstream Flow
Flow =		
pH =		
ALK =		

2. DETERMINE C_T FROM CHART

POTW Discharge			Upstream Flow	
ALK =	}	C_T =	ALK =	}
pH =	}		pH =	}

3. CALCULATE BLENDED ALK AND C_T

B = Blend S = Stream D = Discharge

$$C_T \text{ or } ALK_B = \frac{(ALK_S \cdot Q_S) + (ALK_D \cdot Q_D)}{(Q_S + Q_D)}$$

$$ALK_B = \frac{(\quad) + (\quad)}{\quad} = \quad =$$

$$C_{T_B} = \frac{(\quad) + (\quad)}{\quad} = \quad =$$

4. DETERMINE pH OF BLEND FROM CHART

ALK =	}	pH =
C_T =	}	

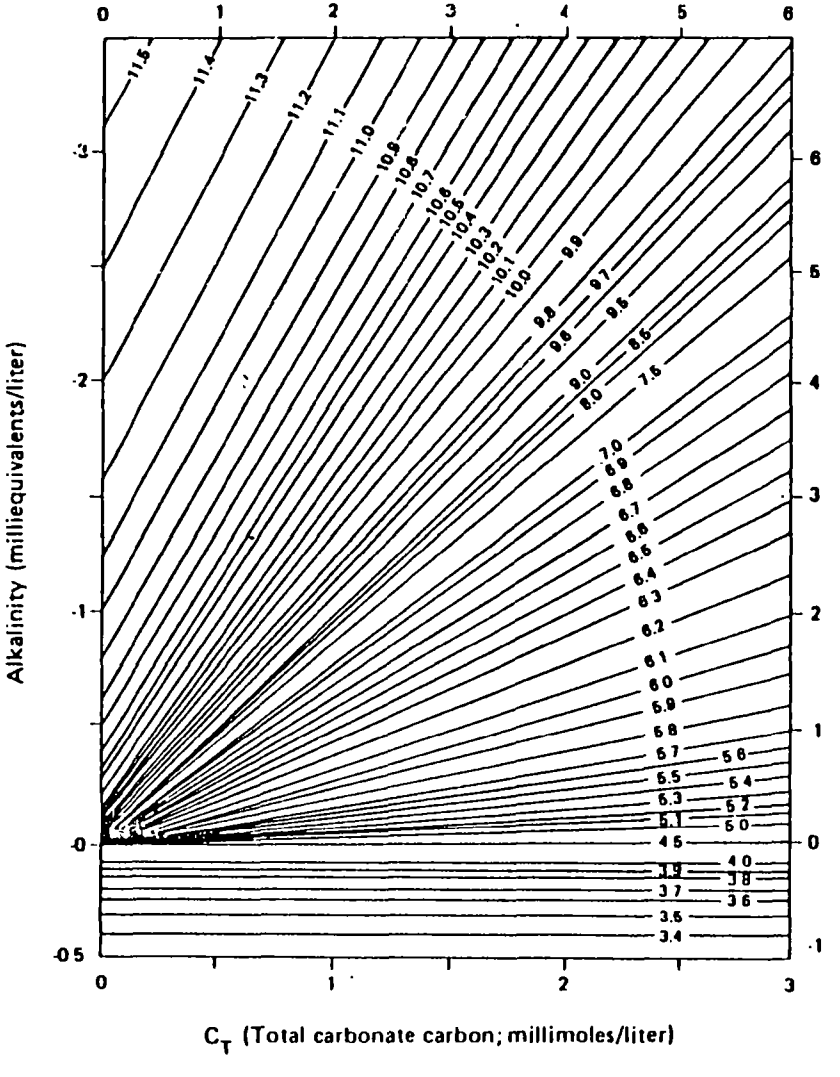

Note: Doubled scales apply if pH line goes through origin.

APPENDIX A2

The results of new data supplied by EPA EMSL-Cincinnati show that BOD_5 levels in nitrification system effluents range from BOD_5 5 - 8 mg/l. Tests run on typical nitrified effluents using the Standard Methods BOD_5 test consistently exhibited higher than actual carbonaceous BOD_5 due to nitrification occurring during the CBOD test. The reason for the high BOD_5 result is that aqueous solutions containing ammonium salts are used in the standard BOD_5 test. These ammonium salts in the presence of nitrifying organisms in the nitrified effluent create an additional apparent BOD_5 demand in the effluent. For this reason, data from plants with nitrification cannot be used to predict treatment capabilities unless nitrification inhibitors are used.

The Agency has proposed (December 3, 1979 Federal Register) an inhibitory BOD_5 test for nitrified effluents. Early work at the Washington, D.C.—Pilot Plant used allyl thiourea as the inhibitory chemical. These tests show that the BOD_5 measured for uninhibited nitrified effluents is two to three times greater than for inhibited effluents (See Exhibit 7).

It is advised that all treatment plants with nitrification use the inhibiting chemical and report the BOD_5 values that are determined from this method to expand the data base of plant operational capabilities.

REFERENCES

1. Tetra Tech Inc. 1977. Water Quality Assessment; A Screening Method for Nondesignated 208 Areas, EPA Publication No. EPA-600/9-77-023, August.

2. Thomann, R.V. 1972. Systems Analysis and Water Quality Management. McGraw Hill Book Co., pp 65-122.

3. Streeter, H.W. and E.B. Phelps. "A Study of the Pollution and Natural Purification of the Ohio River, III, Factors Concerned in the Phenomena of Oxidation and Reaeration", U.S. Public Health Service, Public Health Bulletin No. 146.

4. Covar, A.P. 1976. "Selecting the Proper Reaeration Coefficient for use in Water Quality Models", presented at the EPA Conference on Environmental Modeling and Simulation, April.

5. Bennett, J.P. and R.E. Rathbun. 1972. "Reaeration in Open-Channel Flow, Geological Survey Professional Paper 737".

6. Rathbun, R.E. 1977. "Reaeration Coefficients of Streams, State-of-the-Art", Journal of the Hydraulics Division, ASCE, Vol. 103 No. HY4, April.

7. Tsivoglou, E.C. and J.R. Wallace. 1972. "Characterization of Stream Reaeration Capacity", U.S. Environmental Protection Agency, Report No. EPA-R3-72-012. October.

8. Grant, R.S. and Skavroneck. 1980. Comparison of Tracer Methods and Predictive Equations for Determination of Stream Reaeration Coefficients on Three Small Streams in Wisconsin. U.S. Geological Survey, Water Resources Investigation 80-19, March.

9. Personal Communication with Dr. Ernest Tsivoglou, March 26, 1980.

10. Personal Communication with Maan Osman, Upper Oletangy Water Quality Survey, Ohio EPA, September 1979.

11. Pheiffer, T.H., L.J. Clark, and N.L. Lovelace. 1976. "Patuxent River Basin Model, Rates Study", Presented at EPA Conference on Environmental Modeling and Simulations, April.

12. Personal Communication with Dr. T.P. Chang. 1979. West Fork of Blue River Water Quality Survey, Indiana State Board of Health, September.

13. Hydroscience Inc. 1971. Simplified Mathematical Modeling of Water Quality. EPA, March.

14. Raytheon Co. 1974. Oceanographic and Environmental Services, Expanded Development of BEBAM-A Mathematical Model of Water Quality for the Beaver River Basin. EPA Contract No. 68-01-1836, May.

15. Tetra Tech Inc. 1978. Rates, Constants, and Kinetic Formulations in Surface Water Quality Modeling. EPA Publication No. EPA-600/3-78-105, December.

16. EPA, Region V, Eastern District Office, Dischargers Files.

17. Personal Communication with Mark Tusler, Water Quality Evaluation Section, Wisconsin Department of Natural Resources, October 17, 1979.

18. Upper Mississippi River 208 Grant Water Quality Modeling Study. Hydroscience Inc., January 1979.

19. Personal Communication between E.D. Driscoll and R.V. Thomann, August 1980.

20. Tsivoglou, E.C. and L.A. Neal. 1976. "Tracer Measurements of Reaeration: III. Predicting the Reaeration Capacity of Inland Streams". Journal WPCF, December.

21. Wright, R.M. and A.J. McDonnell. 1979. "In-Stream Deoxygenation Rate Prediction", ASCE Journal of the Environmental Engineering Division, April.

22. Personal Communication with R.F. McGhee, EPA Region IV, August 1980.